Modern Molecular Photochemistry

Nicholas J. Turro

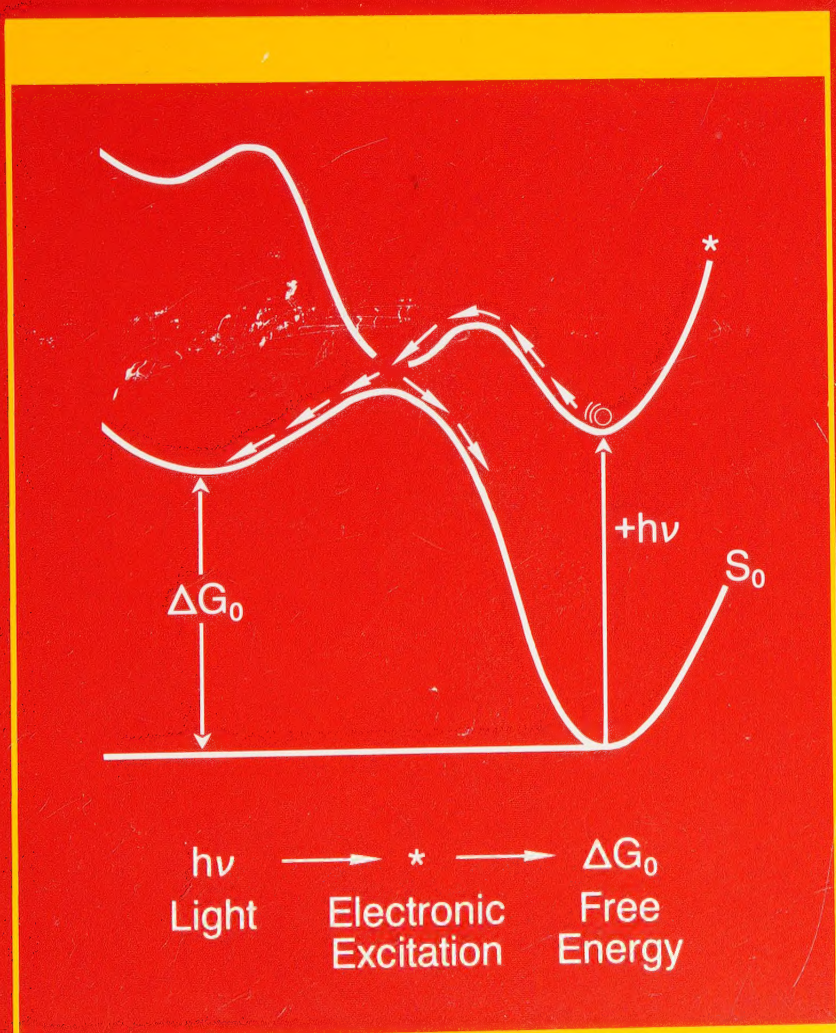

Modern Molecular Photochemistry

Nicholas J. Turro
Columbia University

UNIVERSITY SCIENCE BOOKS
Mill Valley, California

University Science Books
20 Edgehill Road
Mill Valley, CA 94941
Fax: (415) 383-3167

Printed in the United States of America

10 9 8 7 6 5 4 3 2 1

ISBN 0-935702-71-7

Library of Congress Catalog Card Number: 91-65267

Preface

During the last two decades the photochemistry of organic molecules has grown into an important and pervasive branch of organic chemistry. Since the publication of the text *Molecular Photochemistry* over a decade ago, tremendous progress has been made in the development of the theory of photoreactions, the utilization of photoreactions in synthetic sequences, and the advancement of powerful laser techniques to study the mechanisms of photoreactions. *Modern Molecular Photochemistry* brings students up to date with these exciting advances. The author has attempted to maintain the style and philosophy of the earlier text while expanding the concepts and experimental data to include current information.

Level and Approach: My goal in writing the text was to familiarize students and researchers with the important concepts and methodology involved in studying organic photoreactions. Following the development of each general principle, a number of representative examples are given to help readers understand the principle. Students with two years of college chemistry and a year of college physics should be readily able to handle the material.

All important concepts are presented in terms of a *geometric representation.* This approach is coupled with the use of *topological concepts* to emphasize the very general and ubiquitous features of theoretical organic photochemistry. In this way students are provided with a vivid graphical approach to assist in visualization and understanding of molecular organic photochemistry.

The pedagogical approach employed in *Modern Molecular Photochemistry* is, I believe, unique. A complete and general theory that ties together the ideas of light absorption, light emission, radiationless processes, and photoreaction is developed within a common conceptual framework. This is done in a manner that is nonmathematical yet precise.

For example, the crucial concept of energy surfaces is presented in a fashion that can be grasped by students who have had only a conventional course in general chemistry. The energy surface concept, together with simple molecular

orbital theory, is used to show the remarkable and beautiful analogies that exist among many of the processes involved in the photochemistry of organic molecules. A basic model for understanding singlet-triplet interconversions (spin-flips) is presented in a way that allows students to recognize the correlation between electronic structure and the rates of processes that involve spin-flips.

Arrangement and Presentation of Topics: The method of presentation of material in chapters 1–9 will be useful to students interested in a qualitative, pictorial interpretation of spectroscopic processes involving the absorption and emission of light. Thus a large portion of the text can be used in introductory courses in physical chemistry for nonmajors and in courses in biochemistry when a qualitative appreciation of the physical basis of light absorption and emission is desired. The numerous examples of photoreactions and their interpretation given in chapters 10–13 is appropriate material for discussion in courses in advanced organic chemistry or physical organic chemistry. A variety of examples of the utilization of organic photochemistry as a synthetic tool are presented in chapters 10–13. Chapter 14 is a thorough introduction and examination of chemiluminescent organic reactions. Numerous references to the primary literature and to review articles are provided throughout the text. Tables, schemes, and figures are used liberally to summarize and systematize data and to calibrate theoretical concepts.

Acknowledgments: The text is an outgrowth of courses and lectures on organic photochemistry given at Columbia University, in industry, and at other universities. I am indebted to the many students who helped me by posing important questions concerning mechanistic interpretations and their relation to experimental data and concerning the models required to visualize phenomena at the molecular level. I owe special thanks to many colleagues who enabled me—by "picking their brains" or by reading their publications—to gain an understanding of how to translate theoretical concepts into concrete pictures. In particular, professors Lionel Salem, Alain Devaquet, Richard Bersohn, Phil Pechukas, and Josef Michl must be singled out in this regard. Sandy Turro, my constant source of pride and inspiration, requires a special acknowledgment for providing patient and unfaltering encouragement during the long travail of producing and editing the manuscript. Several generations of excellent secretarial assistance were involved in bringing the manuscript to the point of acceptability for submission for publication. Lastly, I am grateful to Sandie Rose, Janet Stowell, Edward Freuh, and Diane Welch for their indispensable assistance and good spirit in bringing the enterprise to completion, and to Gregory Weed and Michael Blaustein for careful reading and editing of the page proofs. John Choi receives a special acknowledgment for his fine craftsmanship in preparing most of the illustrations in the text. Finally the author is indebted to the Schusters, both: Gary and Dave for their critical, thorough, and extremely helpful review of the manuscript.

Nicholas J. Turro
Columbia University
July 1978

To my three foxes:
For the songs they sing,
For the joys they bring.

Contents

1

Organic Photochemistry—An Overview

1.1 Molecular Photochemistry of Organic Molecules

What is "molecular photochemistry"? The definition which suits the meaning intended in this book is: "Molecular photochemistry is a science concerned with description of physical and chemical processes induced by the absorption of photons, in terms of a concrete mechanistic model based on molecular structures and their implied properties." In this book we shall be concerned with the molecular photochemistry of *organic compounds*. Molecular photochemistry is a very broad discipline, embracing an extensive range of energetic, structural, and dynamic processes. The "molecular" part of molecular photochemistry emphasizes the use of the molecule as a crucial and unifying intellectual unit, which is utilized to parameterize, systematize, and visualize photochemical processes at the microscopic level from their very start (absorption of a photon) to their termination (isolation of products). The "photo" part of molecular photochemistry is a historical prefix and is now too restrictive. It is now clear that *electronically excited* states of molecules are at the heart of all "photoprocesses." Although photons are a most convenient means of initiating photochemistry, the absorption of light is not *required* to produce electronically excited states, i.e., thermal pathways may produce excited states efficiently and can therefore cause photoreactions to occur "in the dark."

In this chapter we shall present a brief outline of the plan of the book. The notions of structure, energetics, and dynamics are crucial for understanding molecular photochemistry. By *structure* we mean the composition, constitution, and configuration of a molecule. Each stable configuration of electrons and electron spins corresponds to a stable nuclear geometry and possesses an associated energy. The enumeration, classification, and visualization of these structures in terms of *molecular states* is the topic of Chapter 2.

Given the existence of various possible structures, we next consider the problem of the interconversion of an initial structure into a different final structure. This

problem is approached in Chapter 3 using the concepts of *molecular dynamics* in terms of transitions between molecular states. In Chapter 4 the concepts of structure, dynamics, and energetics are tied together in terms of potential-energy surfaces, which allow an effective visualization of the pathways by which molecular states may be interconverted.

With the notions of potential-energy surfaces, Chapter 5 reviews how the rates of radiative transitions (absorption and emission) can be qualitatively and quantitatively related to molecular structure. Chapter 6 reviews the rates of radiationless transitions. The transitions considered in Chapters 5 and 6 are called "photophysical" because they occur between initial and final molecular states of very similar *nuclear geometry*. In Chapter 7, we consider the theory of radiationless transitions that correspond to chemical reactions, and we develop a theory for the visualization of photochemical reactions in terms of energy surfaces.

Chapters 8 and 9 describe the experimental methods for studying photoreaction mechanisms and electronic energy transfer. The next four chapters (10, 11, 12, and 13) survey the important classes of organic photoreactions. Finally, in Chapter 14, we review the concept of *chemiexcitation*, i.e., generation of electronically excited states by thermal reactions or so-called "photochemistry in the dark."

1.2 Photochemical Reactions

Photochemical reactions differ from thermal reactions in several important respects:

1. The initiating activation of a photoreaction is mainly provided by the absorption of light; activation of a thermal reaction is mainly provided by heat.

2. The electronic distribution and nuclear configuration of a photochemically activated molecule generally differ substantially from those of a thermally activated molecule so that the excited molecule is really an *electronic isomer* of the corresponding ground-state molecule.

3. The thermodynamically favorable products accessible to a photoexcited molecule are far greater than those accessible to a ground-state molecule, since the excited molecule possesses an excess energy content as a result of photon absorption.

The fact that light absorption, rather than heat, activates a photoreaction allows for selectivity of activation (since only light-absorbing molecules are excited) and also allows for the ability to initiate reactions even at very low temperatures in all three phases. In fact, certain photoreactions are known to occur even at temperatures near 0 K!

The chronology of photoreactions may be conveniently divided into three stages:

1. The *absorptive act*, which consists of the interaction of a photon and molecule, resulting in absorption of the photon and formation of an *electronically excited molecule*.

2. The *primary photochemical processes*, which involve electronically excited molecules.

3. The *secondary* or "*dark*" *processes*, which occur from the intermediates produced by primary photochemical processes.

A "complete" understanding of a photoreaction requires knowing what happens at the molecular level from the absorptive act to the isolation or identification of products. Molecular photochemistry is concerned with defining, via the interplay of theory and experiment, the spatiotemporal choreography of molecular structure (electrons, nuclei, and spins) that occurs during steps (1), (2), and (3).

1.3 The Electronic Excitation and Deexcitation of Organic Molecules

The absorption of ultraviolet or visible light by an organic molecule causes the excitation of an electron from an initially occupied, low energy orbital to a high energy, previously unoccupied orbital. The process may be visualized quite simply, as shown in Figure 1.1. The energy of the absorbed photon is used to energize an

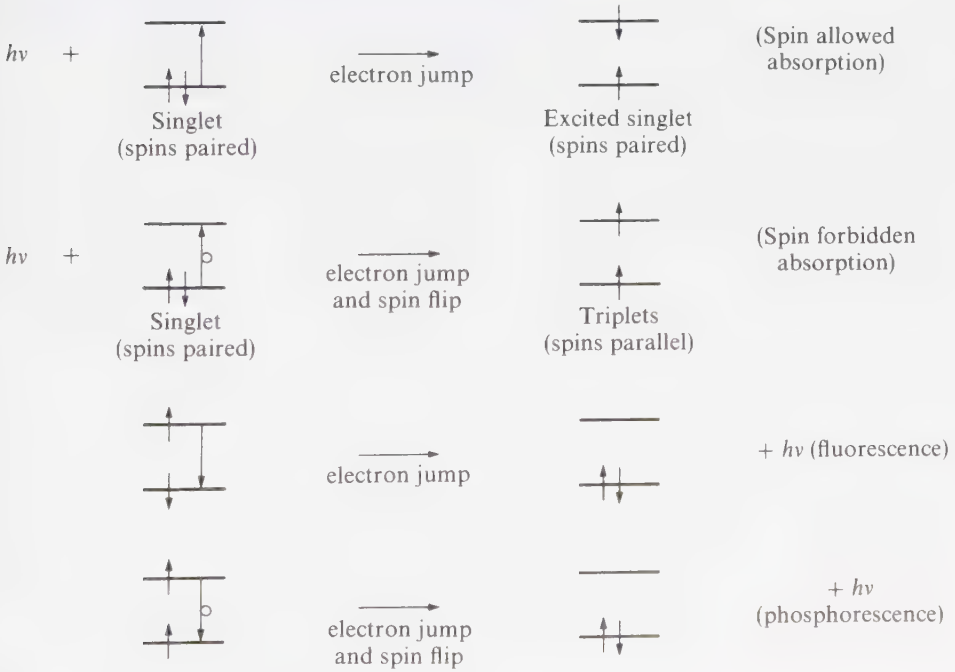

Figure 1.1

Orbital energy level description of absorption and emission. The arrows intersected by the levels represent electrons. The direction of the arrow represents the orientation of the electron spin.

electron and cause it to "jump" to a higher energy orbital. Two excited electronic *states* derive from the *electronic orbital configuration* produced by light absorption. In one state, the electron spins are paired (antiparallel) and in the other state the electron spins are unpaired (parallel). The state with paired spins has no resultant spin magnetic moment, but the state with unpaired spins possesses a net spin magnetic moment. A state with paired spins remains a single state in the presence of a (laboratory) magnetic field, and is termed a *singlet state*. A state with unpaired spins interacts with a (laboratory) magnetic field and splits into *three* quantized states, and is termed a *triplet state*.

Throughout this text we shall use the following notation to describe the three states which are most crucial to an understanding of organic photoreactions:

1. S_0 = ground, singlet state
2. S_1 = lowest energy excited, singlet state
3. T_1 = lowest triplet state

The photochemistry of most organic molecules is conveniently discussed with reference to these three states in terms of a *state energy diagram.*

1.4 State Energy Diagrams: Electronic and Spin Isomers

An energy diagram is a display of the relative energies of the ground state, the excited singlet states, and triplet states of a molecule for a given, fixed nuclear geometry (Figure 1.2). It is generally assumed that the nuclear geometries of all states displayed in a single state diagram are not very different from the equilibrium nuclear geometry of the ground state. Each excited state is different from the ground state even though their molecular constitution are identical, i.e., all the states in an energy diagram are *isomeric*. What is the basis of the isomerism? It is the *electronic* differences or the *spin* differences between the displayed states. Thus, the S_n states are electronic isomers of each other and the T_n states are electronic isomers of each other. The S_n and T_n state are related as spin-electronic isomers.

Photophysical processes may be defined as transitions which interconvert excited states with each other or excited states with the ground state. The important photophysical processes, in turn, are classified as *radiative* and *radiationless* processes.

The commonly encountered photophysical radiative processes, as shown in Figure 1.2, are:

1. "Allowed" or singlet-singlet absorption ($S_0 + h\nu \rightarrow S_1$), characterized experimentally by an extinction coefficient $\varepsilon(S_0 \rightarrow S_1)$;

2. "Forbidden" or singlet-triplet absorption ($S_0 + h\nu \rightarrow T_1$), characterized experimentally by an extinction coefficient $\varepsilon(S_0 \rightarrow T_1)$;

3. "Allowed" or singlet-singlet emission, called *fluorescence* ($S_1 \rightarrow S_0 + h\nu$), characterized by a radiative rate constant k_f;

4. "Forbidden" or triplet-singlet emission, called *phosphorescence* ($T_1 \rightarrow S_0 + h\nu$), characterized by radiative rate constant k_p.

The commonly encountered photophysical *radiationless* processes are:

5. "Allowed" transitions between states of the same spin, called *internal conversion* (e.g., $S_1 \rightarrow S_0$ + heat), characterized by a rate constant k_{IC};

6. "Forbidden" transitions between excited states of different spin, called *intersystem crossing* (e.g., $S_1 \rightarrow T_1$ + heat), characterized by a rate constant, k_{ST};

7. "Forbidden" transitions between triplet states and the ground state—also called intersystem crossing (e.g., $T_1 \rightarrow S_0$ + heat)—and characterized by a rate constant, k_{TS}.

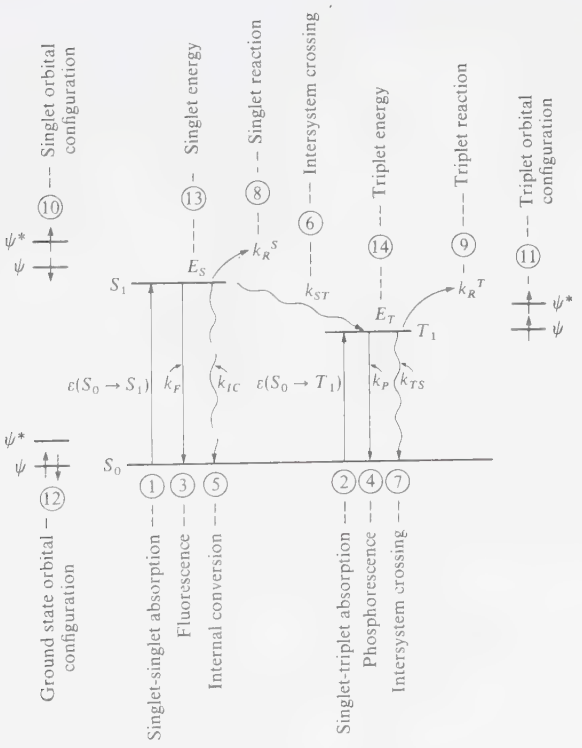

Figure 1.2
State energy diagram. A standard paradigm.

Photochemical processes may be defined as transitions from an electronically excited state to yield structures of different constitution or configuration than S_0. The commonly encountered photochemical processes are relatively few in number and will be discussed in later chapters. In general, these reactions will be initiated by molecules in (8) S_1, or (9) T_1, and these reactions will be characterized by rate constants k_R^S and k_R^T, respectively.

1.5 Calibration Points for Molecular Dimensions and Molecular Motions

If we consider the atoms or groups involved in absorption or photoreactions, the "size" of these groups generally are of the order of 2 Å to 10 Å. A particle (photon) travelling at the speed of light, moves 3×10^{10} cm/sec $= 3 \times 10^{18}$ Å/sec. If we associate the *wavelength* of light with the *size* of a photon, then photons corresponding to blue light have a "size" of the order of 4000 Å. We may interpret the "size" of photons in terms of their ability to collide with a molecule. Thus, the time it takes a "blue" photon to pass a point in space is $t = d/v = 4000$ Å$/3 \times 10^{18}$ Å sec $\sim 10^{-15}$ sec. Crudely, this corresponds to the maximum "interaction time" available for absorption of such a photon by a molecule.

Can an electron make an orbital jump in this period of time? The velocity of an electron making one complete circuit in a Bohr orbit is $\sim 10^{16}$ Å/sec. Thus, an electron may move on the order of 10 Å in 10^{-15} sec. Since 10 Å is the order of size of many commonly encountered groups of atoms (*chromophores*) responsible for absorption of light, we deduce that the time scales of photon interaction and electron motion are of the same order of magnitude.

In terms of a wave model of light and electrons, we would say that the frequency of the oscillation of a light wave overlaps that of the electron wave. Thus, if the resonance condition is met, the energy may be absorbed from the oscillating light wave by electrons which are simultaneously sent into oscillation.

The time period of $\sim 10^{-16}$ sec sets a lower limit to the scale of chemical events, since no chemistry can occur before electron motion has occurred. It thus serves as a calibration point for the fastest events of chemical or photochemical interest.

What are calibration points for the *slowest* processes of direct photochemical interest? The latter are limited by the radiative lifetimes of electronically excited molecules. The *longest* fluorescence (S_1) lifetimes known for organic molecules are $\sim 10^{-6}$ sec, and the longest phosphorescence (T_1) lifetimes are of the order of 30 sec. Let us compare these times to those for nuclear motions such as vibrations, collisions, diffusion, and reaction. The fastest vibrations of organic molecules occur with a frequency of $\sim 10^{13}$ sec^{-1} (e.g., a C—H stretching motion) and the slowest occur with a frequency of $\sim 10^{12}$ sec^{-1} (e.g., a C—C bending motion). This means that it takes $\sim 10^{-12}$ to 10^{-13} sec to complete a typical vibration. In 10^{-6} sec (the longest fluorescence periods) an organic molecule will have executed $\sim 10^6$–10^7 vibrations and in 30 sec an organic molecule will have executed $\sim 10^{13}$–10^{14}

vibrations. The point of this comparison is to show that there is plenty of time for extensive nuclear motion during the lifetime of an electronically excited molecule. Figure 1.3 compares the spread of events of photochemical interest (from 10^{-15} sec to 1 sec) with the same spread of time ranging from 1 sec to 10^{15} sec. When compared in this manner, the history of a photoreaction passes through as many "decades" of time as the "history" of the universe!

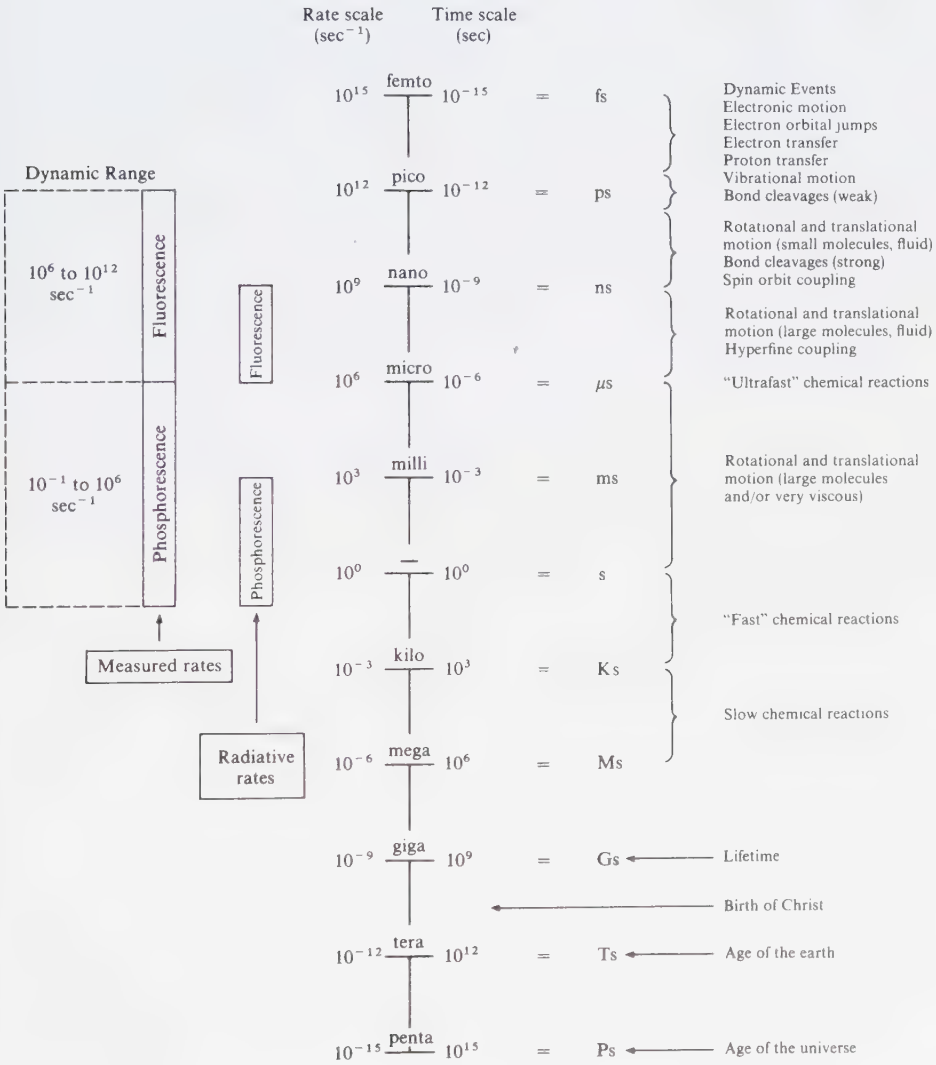

Figure 1.3

Comparison of time scales of events of photochemical interest (from $\sim 10^{-15}$ sec to ~ 1 sec) with macroscopic events (~ 1 sec to $\sim 10^{15}$ sec).

The rates of photoreactions (k_R, Fig. 1.2) vary from $\sim 10^{13}$ sec^{-1} to $\gg 0.1$ sec.$^{-1}$ Whether or not photoreaction occurs from S_1 or T_1 depends on *both* k_R and $\sum k$, where the latter represents the sum of all deactivating pathways of the excited state.

1.6 Calibration Points for Molecular Energetics and Reaction Dynamics

Absorption of a photon by a molecule transforms light energy into electronic excitation energy. Table 1.1 shows how the energy of a mole of photons is related to the corresponding wavelength of light. Since different energy units are commonly employed, values are given in terms of Å, nm, kcal/mole, cm^{-1}, and sec^{-1}. In the text we shall generally employ kcal/mole and cm^{-1} units only.

The *minimum* energy required for electronic excitation of organic molecules is $\sim$30–40 kcal/mole and corresponds to "red light" (700–800 nm). The *maximum* energy commonly employed by organic photochemists corresponds to $\sim$140 kcal/mole and corresponds to for ultraviolet light ($\sim$200 nm).

The energy required to produce an excited state is obtained by inspection of the *absorption* or *emission spectrum* of the molecule in question, together with the application of Eq. (1.1)

$$\Delta E = E_2 - E_1 = h\nu \tag{1.1}$$

where h is Planck's constant, ν is the frequency (sec^{-1}) at which absorption occurs, and E_2 and E_1 are the energies of a single molecule in the final and initial states.

Table 1.1 Energy Conversion Table

Region	λ (Å)	λ (nm)	$\bar{\nu}$ (cm^{-1})	ΔE (kcal/mole)	ν (sec^{-1})	Structure and motion involved in absorption or emission
↑	2,000	200	50,000	143.0	15×10^{15}	↑
Ultraviolet	2,500	250	40,000	114.4	12×10^{15}	
↓	3,000	300	33,333	95.3	1.0×10^{15}	
	3,500	350	28,571	81.7	8.7×10^{14}	
↑	4,000	400	25,000	71.5	7.5×10^{14}	Electrons-orbital motion
	4,500	450	22,222	63.5	6.6×10^{14}	
Visible	5,000	500	20,000	57.2	6.0×10^{14}	
	5,500	550	18,182	52.0	5.4×10^{14}	
	6,000	600	16,666	47.7	5.0×10^{14}	
	6,500	650	15,385	44.0	4.6×10^{14}	
↓	7,000	700	14,286	40.8	4.2×10^{14}	↓
↑	10,000	1,000	10,000	28.6	3×10^{14}	
Infrared	50,000	5,000	2,000	5.8	6×10^{13}	Nuclei-vibrational motion
↓	100,000	10,000	1,000	2.86	3×10^{13}	
Microwave	10^8	10^7	10	3×10^{-2}	3×10^{11}	Electron spin-precessional motion
	10^{10}	10^9	0.1	3×10^{-4}	3×10^9	
Radiowave	10^{12}	10^{11}	0.001	3×10^{-6}	3×10^7	Nuclear spin-precessional motion

The position of an absorption band is often expressed by its wavelength (λ) in nanometers or its wave number ($\bar{\nu} = 1/\lambda$) in reciprocal centimeters or frequency in sec.$^{-1}$ For example, 300 nm is equivalent in wave numbers to

$$\text{wave number: } \bar{\nu} = \frac{1}{300 \text{ nm}} = \frac{1}{3 \times 10^{-5} \text{ cm}} = 3.33 \times 10^{4} \text{ cm}^{-1} \tag{1.2}$$

or in frequency to

$$\text{frequency: } \nu = \frac{c}{\lambda} = \frac{3 \times 10^{10} \text{ cm sec}^{-1}}{3 \times 10^{-5} \text{ cm}} = 10^{15} \text{ sec}^{-1} \tag{1.3}$$

Equation 1.1 may be rewritten as

$$\text{kcal/mole: } E_2 - E_1 = h\bar{\nu}c = 2.86 \times 10^{-3}\bar{\nu} \text{ cm}^{-1} \tag{1.4}$$

or

$$\text{kcal/mole: } E_2 - E_1 = \frac{2.86 \times 10^{4}}{\lambda \text{ nm}} \tag{1.5}$$

where $E_2 - E_1$ is the energy difference between the final and initial states in kcal/mole, and $\bar{\nu}$ and λ are the position of absorption expressed in wave numbers (reciprocal centimeters) and nm, respectively.

The amount of energy produced through the absorption of one mole of photons by a compound at a given wavelength is equivalent to the energy of 6.02×10^{23} photons. This energy is called an *einstein*. Thus an einstein of 700 nm (14,300 cm^{-1}) light is equal to

$$E_2 - E_1 = \frac{2.86 \times 10^{4}}{700 \text{ nm}} = 40.8 \text{ kcal/mole} \leftarrow \begin{cases} \text{one mole of} \\ \text{“700 nm” photons} \end{cases} \tag{1.6}$$

while an einstein of 200 nm light is

$$E_2 - E_1 = \frac{2.86 \times 10^{4}}{200 \text{ nm}} = 143 \text{ kcal/mole} \leftarrow \begin{cases} \text{one mole of} \\ \text{“200 nm” photons} \end{cases} \tag{1.7}$$

For comparison with photochemical excitation energies, some typical bond energies are shown in Figure 1.4. The weakest single bonds commonly encountered in organic molecules have strengths of $\sim$35 kcal/mole (e.g., an O—O bond) and the strongest single bonds have strengths of the order of $\sim$100 kcal/mole (e.g., a C—H bond). We might ask whether absorption of 250 nm light (114 kcal/mole) leads to random rupture of all the single bonds of an organic molecule? The answer is negative. In fact, many photoreactions proceed with remarkable *selectivity*, i.e., only certain bonds are made or broken. The reason for this selectivity is due to the localization of electronic excitation and the specificity

with which this electronic excitation is employed to make or break bonds. In other words, specific mechanisms exist for the conversion of electronic excitation energy into nuclear motion that results in a net chemical reaction. In this text we shall seek an understanding of these mechanisms in order to understand photoreactions.

We are generally concerned not only with reaction feasibility but also with reaction dynamics, i.e., the rates at which feasible reactions occur. In this regard, the *energy of activation* E_a is the quantity of interest. It is often possible to represent rates in terms of two factors: A (units sec^{-1}) which is the measure of the probability of reaction from a state which possesses the minimum energy for reaction, and E_a (units kcal/mole) which is a measure of the minimum energy required for reaction. The expression relating these quantities and rate is

$$\text{rate} = A \exp - E_a/RT = A \times 10^{-E_a/(0.0046T)} \tag{1.8}$$

This expression may be treated strictly as an empirical relation between rate and temperature. In practice, maximal values of A are of the order of 10^{12} to 10^{15} sec^{-1}. These large values of A usually correspond to structurally uncomplicated *unimolecular* reactions. Minimum values of A are of the order of 10^6 to 10^8 sec^{-1}. These

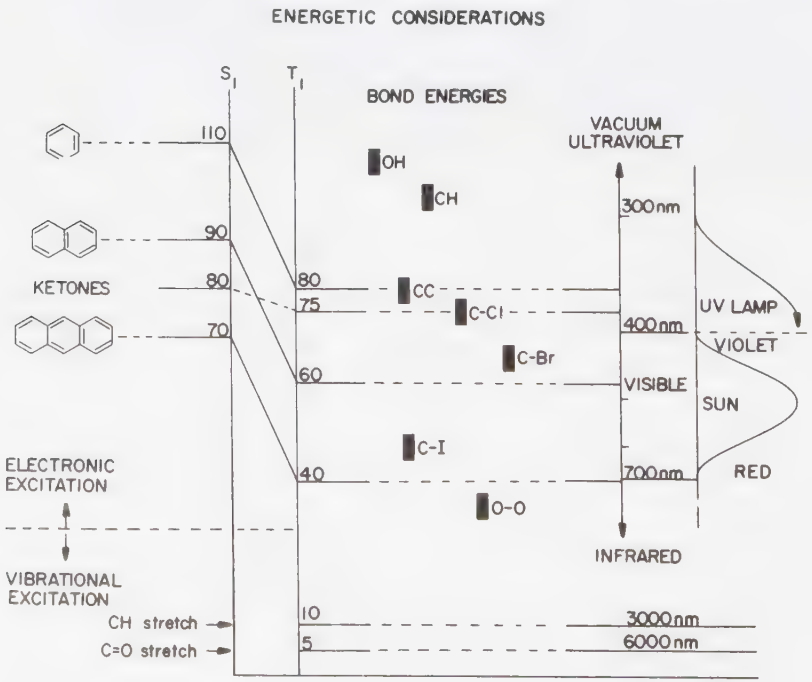

Figure 1.4

Some energetic considerations. The "energy spread" of conventional photochemistry is compared to the emission spectrum of the sun. Vibrational energies are shown for comparison.

small values of A usually correspond to *bimolecular* reactions which require specific structural orientations for a reaction to occur. We may view A as a reflection of the entropy requirements for a reaction. If the entropy of reaction is highly positive (increase in freedom of the particles of the system) then A is very large ($\sim 10^{12}$ to 10^{15} sec^{-1}). If the entropy of reaction is highly negative (decrease in freedom of the particles of the system) then A is small ($\sim 10^{6}$ to 10^{8} sec^{-1}).

The values of E_a may range from a few kcal/mole to values approaching bond dissociation energy (>40 kcal/mole). If we confine our discussion to reactions occurring near room temperature then we can evaluate the *maximum* value of E_a which we are likely to encounter. As an example, let us consider a reaction which proceeds in the order of minutes. The activation energy for such a reaction will be of the order of 20–30 kcal/mole, depending on the value of the A factor.

Recall that photoreactions must always occur in competition with radiationless and radiative processes, which limit excited state lifetimes to values which are generally much less than one second. It can be appreciated that as the lifetime of an excited state becomes shorter, the amount of activation energy which can be accumulated decreases.

Consider a photoreaction for which $A = 10^{13}$ sec^{-1} and a second for which $A = 10^{8}$ sec^{-1}. The former is representative of a unimolecular photoreaction and the latter is representative of a bimolecular photoreaction, at room temperature. A rate of 10^{8}–10^{9} sec^{-1} would be feasible if $E_a \leq 6$ kcal/mole and $A = 10^{13}$ sec^{-1}, but a reaction with $E_a = 6$ kcal/mole and an A factor of 10^{8} sec^{-1} would proceed with a rate of only 10^{3}–10^{4} sec^{-1}. Since lifetimes of excited states are generally *much less* than a second, activation energies for photoreactions generally must be less than 20 kcal/mole. Furthermore, photoreactions of singlet states will rarely be able to compete with fluorescence if they possess E_a values larger than 10 kcal/mole.

1.7 The Nuclear Geometry of Electronically Excited States

The *nuclear shape* or *geometry* of an electronically excited state, like its energy, electronic configuration, and possibly its electronic spin, may be quite different from that of the ground state. For example, in the case of formaldehyde (Eq. 1.9) both S_1 and T_1 have significantly different physical properties from S_0. We note the equilibrium shapes of S_1 and T_1 are both pyramidal whereas S_0 is planar. A difference in nuclear configuration is usually associated with a difference in electronic configuration. If we consider only the half-occupied orbitals, both S_1 and T_1 are n, π^* states, i.e., in a simple two electron configuration approximation S_1 and T_1 both possess half-filled n and π^* orbitals. The presence of a π^* electron in S_1 and T_1 causes the sp^2 hybridization at carbon to change from sp^2 to a hybridization (more like) sp^3. Such a hybridization change is expected to be accompanied by changes in bond lengths and molecular shape, as is found. The C—O bond

lengths of S_1 and T_1 are considerably longer (less double-bond character) than is the C=O bond length of S_0 and the molecule prefers a pyramidal shape. The dipole moments of S_1 and T_1 are smaller than that of S_0 (the dipole vector is still oriented in the same direction as that for S_0). This is due to the partial transfer of electric charge from the n orbital (localized on oxygen) to the π^* orbital (delocalized on carbon and oxygen).

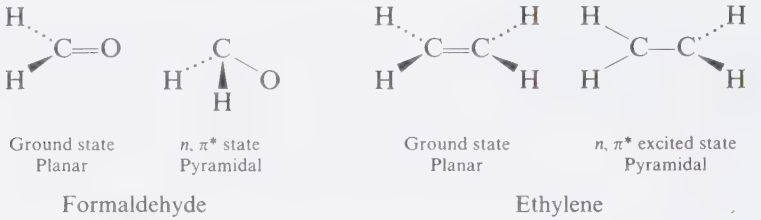

(1.9)

In the case of ethylene the equilibrium shapes of S_1 and T_1 are also very different from that of S_0. Both excited states are twisted substantially. The basis for the twisted shape is related, as with formaldehyde, to the electronic configuration of S_1 and T_1, which may be classified as π, π^* states, i.e., both S_1 and T_1 possess half-filled π and π^* orbitals. In effect, the π and π^* electrons can best avoid each other (and thereby minimize their mutual repulsion) when the nuclear configuration is twisted such that the two CH_2 groups of ethylene are in mutually perpendicular planes. The C–C bond lengths in S_1 and T_1 are much longer than that of S_0. Because of such differences in nuclear and electronic structure, we expect the chemical properties of S_1 and T_1 to be very different from those of S_0.

A number of interesting questions concerning photochemical reactions arise from the above analysis:

1. Are the photochemical properties of S_1 and T_1 the same if they possess the same two electron configurations?

2. Do the photochemical properties of states of the same spin but different two electron configurations differ?

3. What are the photochemical reactions expected for different electronic spin isomers?

1.8 An Energy Surface Description of Molecular Photochemistry

A particularly effective means of understanding photochemical processes is possible by considering potential energy surfaces or the more readily visualized potential energy curves (Fig. 1.5). It is assumed that a potential energy curve completely controls nuclear motion, except for situations for which two surfaces come

close together. Each point on a potential energy curve represents a specific nuclear geometry (horizontal axis) and a specific energy (vertical axis). For a given nuclear geometry, the energy of the molecule is determined mainly by its electronic orbital configuration. A unique molecular state or structure is defined at all points on an energy surface except for those nuclear geometries for which two surfaces "come close together." We shall see (Chapter 4) that situations of this type are of utmost importance in understanding photoreactions which require such geometries for facile radiationless passage ("jumps") from one surface to another.

Suppose it is known that the following overall photoreaction occurs:

$$R + h\nu \rightarrow P \qquad \text{Net reaction} \tag{1.10}$$

Figure 1.5 shows two potential energy curves for the overall $R \rightarrow P$ nuclear geometry change. The *possible pathways* to proceed from R to P are "mapped out" by these two curves.

One possibility is that R* will proceed along the excited surface to region ① which happens to be close in energy to the ground state surface for a certain nuclear geometry. Such a situation turns out to be very favorable for a jump from the excited surface to the ground surface and vice versa (we shall see why in Chapters

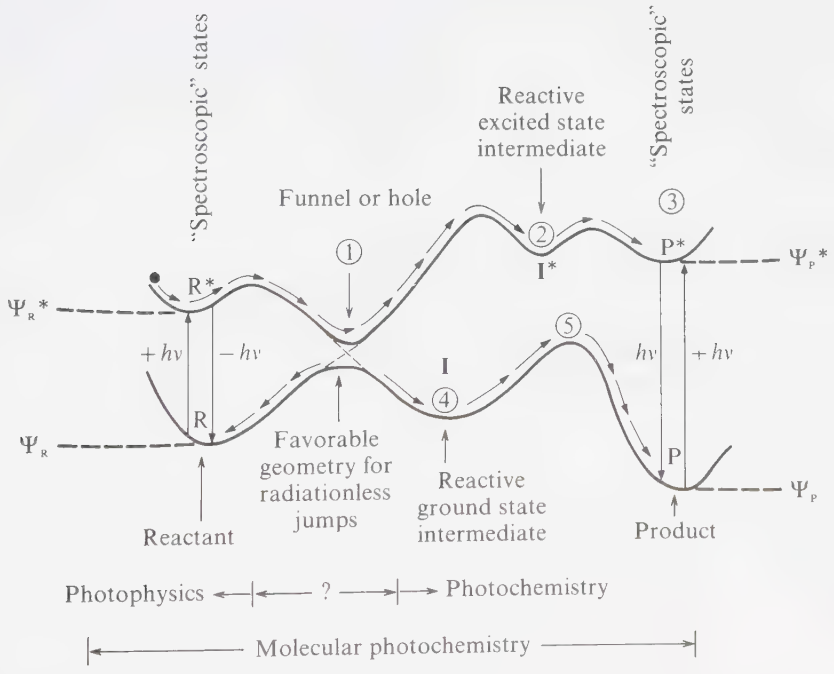

Figure 1.5

Schematic representation of a ground-state and excited-state surface. The arrows on the surface indicate the motion of a point which represents a molecule whose nuclear geometry is moving along the reaction coordinate.

4 and 6). Some molecules may thus "jump" to the ground surface and "spill" into the R minimum (resulting in a net photophysical cycle $R + h\nu \rightarrow R^* \rightarrow R$). Others may be able to overcome the energy barrier on the excited surface and proceed to region ② and eventually reach region ③.

It is possible that some molecules may jump from region ① to the ground surface and arrive at ④, which is a geometry corresponding to a minimum on the lower surface. Since this minimum corresponds to a new molecular structure, **I**, a photochemical reaction has occurred. **I** may be an isolable molecule, or may be a reactive intermediate. For instance, **I** may be able to gather thermal activation and proceed over barrier ⑤ to yield P. If the "jump" generates **I** on the ground surface with sufficient energy, and if this energy is not rapidly removed, the molecule may move past ④ and over ⑤ and finally come to rest at P before thermally equilibrating with its environment. Such a reaction is termed a "hot ground state" reaction. For the pathway $R^* \rightarrow ① \rightarrow ④ \rightarrow ⑤ \rightarrow P$ the nuclear motion was controlled by the excited-state curve for part of the reaction and by the ground-state curve for another part of the reaction. Indeed, such a situation appears to be typical of many photoreactions.

From Figure 1.5, we note some important generalizations: (a) absorption and emission of light tends to occur at nuclear geometries which correspond to minima in both the ground and in the excited surface; (b) radiationless jumps are most facile for geometries for which two surfaces come close together in energy; (c) the location and heights of energy barriers on *both* the excited and ground state surface may determine the specific pathway of a photoreaction; (d) some minima on excited surfaces may not be readily detected by conventional absorption and emission techniques; (e) the course of a photoreaction depends on competing photophysical as well as photochemical processes.

1.9 Organic Photoreactions

From the brief introduction to photochemical processes discussed in this chapter, it should be apparent that the favored nuclear motions explored by an electronically excited molecule may be completely different from those of the more familiar ground state molecule. It is also apparent that an excited molecule must leave the upper surface at some point and jump to the ground state. The nuclear geometry at which this jump occurs may be crucial in determining the structure of the *primary photoproduct*. Because access to the ground surface is best achieved when the excited and ground surface get close in energy, we can understand why many photoreactions produce primary products which possess structures of high energy content. The delivery of the excited molecule to the ground state will tend to occur near geometries which have high energies on the ground-state surface, since for these geometries the ground and excited states will tend to come close in energy. These "high energy" points on the S_0 surface commonly correspond to extreme stretching of a σ-bond, extreme twisting of a π-bond and to orbitally forbidden ground state reactions.

Thus, photoreactions for which a strong σ or π bond is broken, or for which a highly strained structure is produced are commonly encountered (Eqs. 1.11–1.13):

$$R_2C{=}O + R'H \xrightarrow{h\nu} R_2\dot{C}OH + \dot{R}' \rightarrow \text{products} \tag{1.11}$$

$$R_2C{=}CR_2 \xrightarrow{h\nu} R_2\dot{C}{-}\dot{C}R_2 \rightarrow \text{products} \tag{1.12}$$

(1.13)

1.10 Summary

Scheme 1.1 represents an overview of molecular photochemistry and systemitizes many of the processes we shall encounter in the following chapters. The science of molecular photochemistry has been viewed in its broad outline. Hopefully, the

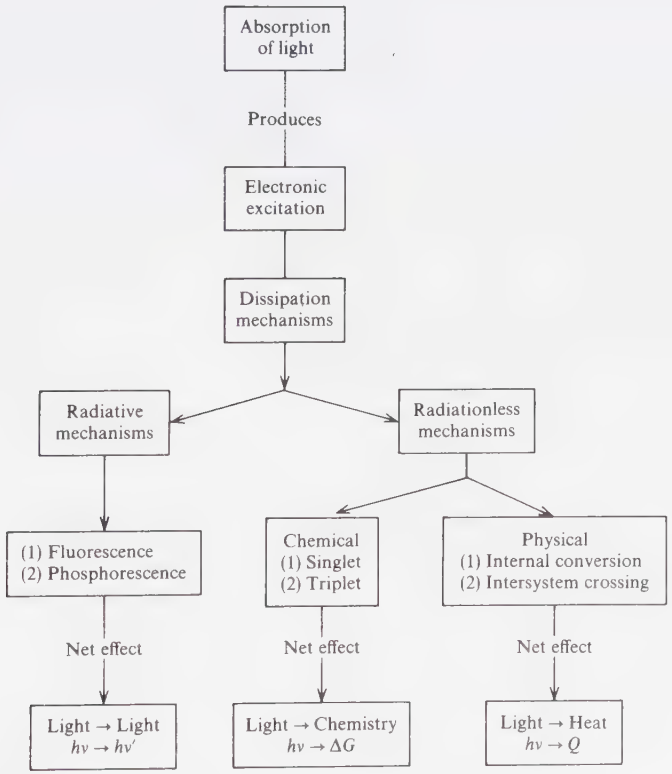

Scheme 1.1

Schematic of the network of processes of interest to a molecular photochemist.

reader has had his curiosity piqued by the allusions to the numerous structural, dynamic, and energetic concepts which are required to understand and interpret photoreactions, and has been intrigued by the promise of a simple means of visualizing photochemical processes.

References

Up until the early 1960s only a handful of textbooks on photochemistry were available. The most authoritative dealt completely with vapor phase photochemistry: Noyes, W. A., Jr., and Leighton, P. A., *Photochemistry of Gases*. New York: Reinhold, 1941.

About 1960 a number of reviews and textbooks began to reveal the synthetic promise of photochemical methods:

1. De Mayo, P., *Adv. In Organic Chem.*, *2*, 367 (1960).
2. De Mayo, P., and Reid, S. T., *Quart. Revs.*, *14*, 393 (1961).
3. Masson, C. R., Boekelheide, V., and Noyes, W. A., Jr., in *Techniques of Organic Chemistry*, ed. Weissberger, A., New York: Interscience, 1956. Vol. 2, p. 257.
4. Schonberg, A., *Preparative Organic Photochemistry*, Berlin: Springer-Verlag, 1968.
5. Schenck, G. O., and Steinmetz, R., *Bull. Soc. Chim. Belges*, *71*, 781 (1962).
6. Hammond, G. S., and Turro, N. J., *Science*, *142*, 1541 (1964).
7. Leermakers, P. A., and Vesley, G. F., *J. Chem. Ed.*, *41*, 535 (1964).
8. Schaffner, K., *Fortschr. Chem. Org. Naturstoffe*, *22*, 1 (1964).

In the early sixties mechanistic organic photochemistry began to develop. For some early reviews see:

9. References 1, 2, and 3 above.
10. Saltiel, J., in *Survey of Progress in Chemistry*, ed. Scott, A. F., New York: Academic Press, 1964. Vol. 2, p. 239.
11. Turro, N. J., *Molecular Photochemistry*, San Francisco: W. A. Benjamin, 1965.
12. Barltrop, J. A., and Coyle, J. D., *Excited State in Organic Chemistry*, New York: John Wiley, 1975.
13. Cowan, D. O., and Drisko, R. L., *Elements of Organic Photochemistry*, New York: Plenum, 1976.
14. For a comprehensive review starting from 1969 and continuing to the present see *Photochemistry—Specialist Periodical Reports*, London: The Chemical Society.
15. Lamola, A A., and Turro, N. J., *Organic Photochemistry and Energy Transfer*, New York: Interscience, 1969.
16. Calvert, J., and Pitts, J., *Photochemistry*, New York: John Wiley, 1965.

2

Electronic Orbitals, Configurations and States

2.1 Molecular Wavefunctions and Molecular Structure

Quantum mechanics provides an understanding of molecular structure, energetics and dynamics on the basis of *molecular wavefunctions*, Ψ. If Ψ is known for a molecular system, it is possible *in principle* to calculate the average value of any experimental observable for an assumed set of initial conditions and interactions. More practically speaking, Ψ is not known in a precise manner for even the simplest organic molecules. Furthermore, initial conditions and or interactions are often not precisely known or are ill-defined. As a result, one must resort to approximations — and severe approximations at that — in order to actually employ wave functions to achieve quantitative comparisons with experiments.

Because of the intractable mathematical complexity of the "true" or "exact" molecular wave function Ψ, a means of developing approximate wave functions must be sought. A useful, but qualitative use of quantum mechanics, fortunately, is possible.

2.2 The Born-Oppenheimer Approximation

An important method for approximating molecular wave functions was proposed by Born and Oppenheimer.[1] They suggested, in essence, that since the motions of electrons in orbitals are much more rapid than nuclear motions, electronic and nuclear motions could be treated separately in terms of an approximate wave function. Furthermore, since electron "spin" motion is due to a magnetic interaction, and since magnetic and electronic interactions interact only weakly for most organic molecules, the spin motion of electrons may be treated separately from both the motion of electrons in orbitals and the motion of nuclei in space.

If we let Ψ_0 represent an *approximate* wave function for electron position and orbital motion, let χ represent the approximate wave function for nuclear position and motion and let $\mathscr{S}$ represent the approximate wave function for spin direction and motion, then

$$\underset{\text{"true" molecular wave function}}{\Psi} \sim \underset{\substack{\text{orbital nuclear spin} \\ \text{approximate wave functions}}}{\Psi_0 \quad \chi \quad \mathscr{S}} \tag{2.1}$$

A useful feature of the Born-Oppenheimer approximation is that it allows visualization of the positions and motions of electrons, nuclei, and spins in space and in time. The specific nature of Ψ_0 depends on the level of sophistication desired. For many qualitative analyses of molecular phenomena Ψ_0 is further approximated as a composite of "one electron" molecular orbitals,

$$\Psi_0 \sim \psi_1 \psi_2 \cdots \psi_n = \prod_i \psi_i \tag{2.2}$$

where ψ_i is a solution of the Schrödinger equation for a "one electron" molecule, i.e., a fictitious molecule that possesses only one electron and therefore does not experience any electron-electron repulsions. For a discussion of these approximations the reader is referred to any one of a number of elementary texts.[2] For our purposes, it is only necessary to point out that ψ is at the level of approximation for orbitals that is conventionally given in introductory texts (the so-called Hückel orbitals).

The following qualitative and topological characteristics of the approximate molecular wave function are of concern to us: (a) the quantities Ψ_0^2, χ^2 and $\mathscr{S}^2$ relate to the probability of finding the electrons, nuclei, and spins at particular points in space; (b) the functions Ψ_0 (and ψ), χ, and $\mathscr{S}$ may be visualized with respect to a molecular framework; (c) for molecules possessing local or overall symmetry elements, Ψ_0 (and ψ), χ, and $\mathscr{S}$ will possess useful symmetry properties that can be related to the motion and position of the electrons, nuclei, and spin.

In this chapter we are concerned with how knowledge of Ψ can lead to a qualitative estimate of two important equilibrium (static) properties of molecular states: (a) state energy, and (b) state electronic, nuclear, and spin configurations. From knowledge of (a) and (b) we can readily construct energy diagrams.

According to the postulates of quantum mechanics, the average value, P, of any observable state property can be evaluated in terms of a *matrix element*:

$$P = \underset{\substack{\text{Average value} \\ \text{of observable} \\ \text{quantity}}}{} = \frac{\int_0^\infty \Psi |H| \Psi \, d\tau}{\int_0^\infty \Psi \Psi \, d\tau} \equiv \underset{\text{"Matrix element"}}{\langle \Psi | H | \Psi \rangle} \tag{2.3}$$

where H represents forces or interactions that operate on Ψ. H is called a "Hamiltonian operator." The quantitative evaluation of matrix elements is an

important procedure in theoretical chemistry. We shall attempt to visualize the components of the matrix element (i.e., Ψ and H) by attributing to them concrete properties that can be associated with classical mechanics, and by then seeking qualitative conclusions based on these oversimplified but useful models.

Combining Eq. 2.1 and Eq. 2.3, the value of P is given by

$$P \sim \langle \Psi_0 \chi \mathscr{S} | H | \Psi_0 \chi \mathscr{S} \rangle \tag{2.4}$$

We need to visualize Ψ_0, χ, $\mathscr{S}$, and H in order to "understand" the factors that determine the magnitude of P and to be able to qualitatively evaluate its magnitude.

From Eqs. 2.2 and 2.4 the value of P is given by

$$P \approx \langle \psi_1 \psi_2 \cdots \psi_n \chi \mathscr{S} | H | \psi_1 \psi_2 \cdots \psi_n \chi \mathscr{S} \rangle \tag{2.5}$$

We term this level of evaluation of P as the *Zeroth-Order approximation.* By this we understand that we are within the Born-Oppenheimer approximation (separation of electronic, nuclear, and spin motion) and that we are dealing with one electron orbital wave function (Hückel theory). In the First Order approximation we challenge some aspect of the Zeroth-Order approximation and note its effect on the magnitude of P. For example, we might let the electron's orbital motion couple with its magnetic spin motion (spin-orbit coupling), or we might introduce the idea of electron-electron repulsion (electron correlation or configuration interaction) and note how the magnitude of P is influenced as a result of these "First Order" interactions.

2.3 The Spirit of the Use of Quantum Mechanical Operators

In the previous section the wave function of a molecule, Ψ, was defined in terms of a solution of a wave equation. The spirit of the meaning of the "true molecular wave function" is similar to the spirit of the conservation laws, which we assume to be correct in detail, *if we knew all the details.* Similarly, *if* Ψ were known, all of the observable properties of a system (state) could be evaluated by performing an appropriate mathematical operation dictated by Eq. 2.3 (at some level of approximation).

Classical mechanics deals with observables such as position and momentum as functions. Newton's laws of motion enable these functions to be displayed in a mathematical form. Quantum mechanics supposes that all the information about the system is contained in its wave function, Ψ, and that in order to extract the information about the value of an observable, some mathematical operation, H, must be performed on the function. This is analogous to the necessity of doing an act—an experiment—on the system in order to make a measurement of its

state. Problems in quantum mechanics often boil down to making the correct selection of the operation (H) which corresponds to the appropriate interaction leading to the observable or to the selection of the proper qualitative form of Ψ. Thus, the selection of the "operators" (mathematical operations) which correspond to observable properties is as crucial to the explicit solution of a problem in quantum mechanics as is knowledge of the form of Ψ. Two of the key "operators" of quantum mechanics are related to the classical dynamical quantities of the *momentum* and *position* of a particle. Once the operators for these dynamical variables have been selected, it usually turns out that operators for many observables can be set up in terms of these two fundamental variables. In the same manner that Zero Order wave functions are employed to approximate Ψ, in a quantitative evaluation of a matrix element we almost always begin with a Zero Order Hamiltonian or operator, H_0. In the First Order approximation we consider interactions that are "weak" relative to those described by H_0.

2.4 Atomic Orbitals, Molecular Orbitals, Electronic Configuration, and Electronic States

It is assumed that the reader is familiar with the manner in which a molecular orbital is approximated as a sum (or superposition) of atomic orbitals.[2] The primary goal of this chapter is to develop a protocol for generating a *state energy diagram* for a given (stable) ground state nuclear geometry of an organic molecule.

The general procedure is as follows. For a given nuclear geometry, it is assumed that appropriate one-electron (Hückel) molecular orbitals (MO's) can be constructed from atomic orbitals (AO's). By this we mean that we build up the wave function corresponding to an MO from a set of AO's. The MO's are then filled with the available electrons in various ways to generate a set of molecular *electronic configurations*. Only the lowest energy configuration (ground configuration) and the first or second low-energy excited configuration generated are considered explicitly. This corresponds to a *Zero Order molecular electronic configuration* (Born-Oppenheimer approximation, one-electron orbitals). In order to generate proper *molecular electronic states* we must take into account electron-correlation in some manner.

An electronic configuration in which the Pauli principle has been employed to handle electron correlation is termed a (First Order) *molecular electronic state*. A display of such molecular electronic states as a function of energy for a *fixed nuclear geometry* is called a *state energy diagram*.

The "recipe" for construction of Zero Order electronic configurations is as follows.

1. Start with the assumption that "one electron" AOs (ϕ) can serve as a basic set of wave functions:

2. Generate MO's by the Linear Combination of Atomic Orbitals (LCAO) method;

3. Generate molecular electronic configurations by adding electrons to each MO, two at most in each MO (Pauli principle);

4. Generate the lowest energy electronic configuration (the *ground electronic configuration*) by adding electron pairs to only the lowest energy orbitals (Aufbau principle) in accordance with (3);

5. Generate excited electronic configurations by adding electrons to antibonding orbitals.

Organic molecules generally possess ground (lowest energy) "closed shell" configurations, i.e., all the bonding and nonbonding orbitals are filled with a pair of electrons.

2.5 The Ground State Configuration

As an example of the procedure for constructing electronic configuration, consider the formaldehyde molecule H_2CO. The energies of the MO's for this molecule increase in the order $1s_o < 1s_c < 2s_o < \sigma_{CH} < \sigma_{CO} < \pi_{CO} < n_o$ where $1s_o$, $2s_o$, and $1s_c$ refer to the essentially atomic MO's localized on oxygen and carbon, and the other MO's refer to the conventional representations.

In the ground state, each of the orbitals in this configuration contains two electrons. The configuration of the ground state is represented in Eq. 2.6, in which the superscripts designate the number of electrons in each orbital:

$$\Psi(CH_2{=}O) = (1s_o)^2(1s_c)^2(2s_o)^2(\sigma_{CH})^2(\sigma'_{CH})^2(\sigma_{CO})^2(\pi_{CO})^2(n_o)^2(\pi^*_{CO})^0 \qquad (2.6)$$

In general, the energetic order of the molecular orbitals, the number of available electrons, and the Pauli and Aufbau principles are employed to designate the ground-electronic configuration of a molecule. Physically, the total electronic distribution of a configuration may be approximated as a superposition of each of the occupied MO's which make up the configuration. Usually, only the highest occupied MO or the two highest energy MO's need be explicitly considered for an electronic orbital interpretation of ground state properties. Thus, a shorthand notation for the ground state configuration is:

$$\Psi(CH_2{=}O) = K(\pi_{CO})^2(n_o)^2 \quad \text{Ground state} \qquad (2.7)$$

In Eq. 2.7, K represents the "core" electrons which are "tightly bound" to the molecular framework, i.e., are close to and are stabilized by the positive nuclear charge. For nearly all qualitative purposes to be discussed in this text, the electrons symbolized by K are not "perturbable" during photophysical and photochemical processes.

Similarly, *if we ignore the σ and lower energy MO's*, we may describe the ground state configuration of ethylene ($CH_2{=}CH_2$) as:

$$\Psi(CH_2{=}CH_2) = K(\pi_{cc})^2 \tag{2.8}$$

The use of electron orbital configurations allows us to enumerate, to visualize, and to conveniently classify electronic transitions and electronically excited configurations. For example, we expect that formaldehyde (Fig. 2.1) will have two relatively low-energy electronic transitions ($n \rightarrow \pi^*$ and $\pi \rightarrow \pi^*$) and two corresponding electronic configurations (n, π^* and π, π^*). On the other hand, ethylene will have only one low-energy electronic transition ($\pi \rightarrow \pi^*$) and one corresponding electronic configuration (π, π^*).

In the above discussion we have initiated an abbreviation scheme which shall be employed throughout the text. In general we shall describe ground configuration of molecules in terms of the highest energy filled MO, or when appropriate and useful, in terms of the two highest energy filled MO's. Electronically excited configurations shall be described in terms of the two singly occupied MO's. Transitions shall be described only in terms of the orbitals undergoing a change in electronic occupancy.

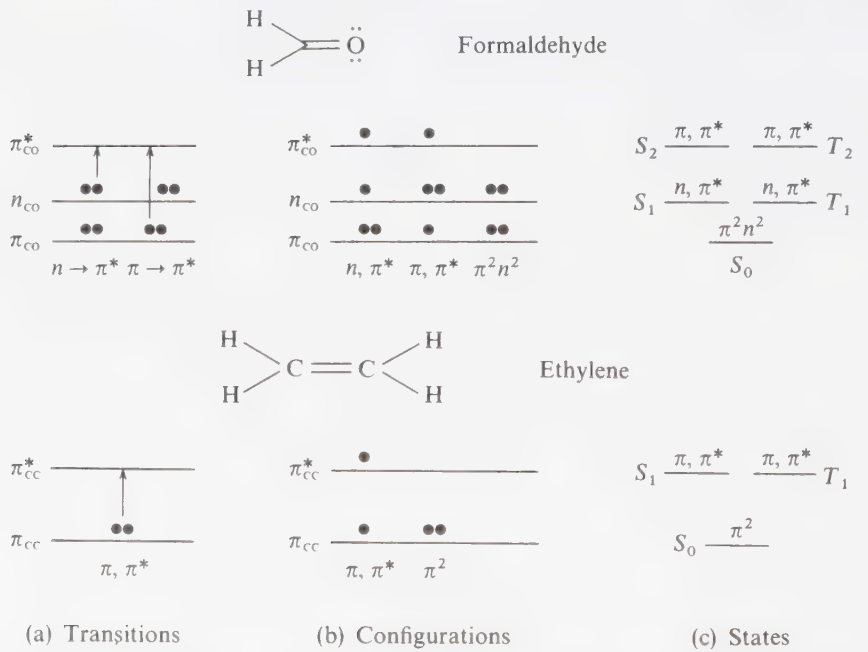

Figure 2.1

Schematic representation of (a) electron transitions, (b) electronic configurations and (c) electronic states for the lowest excited states of formaldehyde (top) and ethylene (bottom).

2.6 The Construction of Electronic States from Electronic Configurations

The goal of this chapter was to be able to enumerate, classify, and qualitatively understand the electronic nature of molecular states. We are very close to that goal. We must distinguish the singlet and triplet states that may be derived from the same electronic orbital configuration if two orbitals are half-occupied.

Construction of Singlet and Triplet States from Electronically Excited Configurations and the Pauli Principle[3]

The Pauli principle demands that any ground state configuration—such as that for formaldehyde in which the electrons are all paired in orbitals—must be a ground state singlet, i.e., the spins of the two electrons in each orbital are paired. In the excited state two electrons are orbitally unpaired, i.e., each electron is in a different orbital. As a result, the Pauli principle does not require the spin of these two electrons to be paired. As a result, a singlet excited state in which there is no net spin (i.e., electron spins are paired as in the ground state) or a triplet excited state (the two electrons which are orbitally unpaired now possess parallel spins) may result from the same electronic configuration of half-occupied orbitals. This means that each of the *excited configurations* given in Figure 2.1 refer to either a singlet or to a triplet *state.*

Thus, *four states*, not two, result from the two lowest energy electronic excited configurations of formaldehyde. The n, π^* state may be either a singlet or a triplet configuration, and the π, π^* state may be either a singlet or triplet configuration.

Characteristic Configurations of Singlet and Triplet States: A Shorthand Notation

Let us employ the following convention to serve as a shorthand MO notation to describe electronic configurations and molecular states. We call the ground electronic singlet state S_0, where S indicates there is no net electronic spin associated with the state (i.e., each spin up is matched by a spin down) and the subscript zero refers to the *ground* electronic *state.* We label electronically *excited* singlet states S_1, S_2, etc, where the subscript refers to the *energy ranking* of the state relative to the ground state (arbitrarily given the rank of zero). Thus S_1 is the *first* electronically excited singlet state located energetically above S_0, and S_2 is the *second* electronically excited singlet state located energetically above S_0.

We reserve the subscript zero for the ground electronic ground state. Thus, for triplet states we label the *first* triplet level located energetically above S_0 as T_1, where T indicates a *threefold* degeneracy of the state due to the three possible alignments of two unpaired spins (to be discussed in Section 2.8) and the subscript 1 refers to the energy ranking among triplet states relative to S_0.

The terms "singlet" and "triplet" derive historically from an *empirical* finding. Atoms and molecules in certain electronic configuration can be resolved into

three distinct states when a molecular beam is passed through a strong magnetic field. These molecules were said to be in "a triplet state." If the magnetic field does not resolve the beam, the molecules were said to be in "a singlet state."

In many cases a single electron configuration is adequate to approximate a state. In some cases, however, a combination of two or more electronic configurations will be required to achieve a good approximation of a state. As a shorthand, we describe *configurations* in terms of the key molecular *orbitals* which are expected to dominate the energy and/or chemistry of the configuration. Thus, for formaldehyde we explicitly consider the π_{co}, n_o, and π^*_{co} orbitals only in discussing configurations, and hence in discussing states. As a result of the above discussion we may state the following rule: Each electronic state may be described (a) in terms of a *characteristic electronic configuration*, which in turn may be described in terms of two or three *characteristic orbitals*, and (b) in terms of a characteristic spin configuration.

For example, the S_0, S_1, S_2, T_1, and T_2 states of formaldehyde may be described as follows:

State	Characteristic Orbitals	Characteristic Spin-Electronic Configuration	Shorthand Description of State
S_2	π, π^*	$(\pi\uparrow)(n\uparrow\downarrow)(\pi^*\downarrow)$	$^1(\pi, \pi^*)$
T_2	π, π^*	$(\pi\uparrow)(n\uparrow\downarrow)(\pi^*\uparrow)$	$^3(\pi, \pi^*)$
S_1	n, π^*	$(\pi\uparrow\downarrow)(n\uparrow)(\pi^*\downarrow)$	$^1(n, \pi^*)$
T_1	n, π^*	$(\pi\uparrow\downarrow)(n\uparrow)(\pi^*\uparrow)$	$^3(n, \pi^*)$
S_0	π, n	$(\pi\uparrow\downarrow)(n\uparrow\downarrow)$	$\pi^2 n^2$

We shall see in Section 2.9 that the triplet state derived from a given electronic configuration possessing two half-filled orbitals is *always* of lower energy than the singlet state derived from the *same* configuration, i.e., $E^1(n, \pi^*) > E^3(n, \pi^*)$ and $E^1(\pi, \pi^*) > E^3(\pi, \pi^*)$.

2.7 Visualization of Electron Spin: A Simple Vectoral Model

The electron may be viewed as an electrically charged particle that generates a magnetic angular momentum as a result of rotation or *spin* about an axis.[3] This angular momentum is termed *electronic spin*, $\mathscr{S}$. The behavior of the electronic spin may be qualitatively understood by referring to the properties of magnets and gyroscopes. Consider a magnet as a *dipole* (it possesses north and south poles). The idea of a vector along the dipole axis serves to represent most of the important

properties of a magnet. The vector representing a classical magnet may "sit still" (i.e., remain motionless in space) and may "point" in any of an infinite number of directions in space (i.e., may take up any arbitrary orientations in space) even in the presence of other magnetic fields. In contrast, the vector representing the electron spin ($\mathscr{S}$) is not allowed to either "sit still" or to "point anywhere." The uncertainty principle requires the electron spin vector to possess some type of endless motion (lest the vector be defined too precisely in space). We may view this motion as precession of the magnetic moment vector along an axis of spin. Thus, the *quantum electron spin vector is imagined to precess like a gyroscope while the electron spins like a top* (Fig. 2.2). The orientation of the vector may be defined relative to some reference structure, such as a molecular nuclear framework or a laboratory magnetic field. However, quantum mechanics requires that only two measurable orientations of the vector are allowed to occur: the two allowed orientations may be described in terms of the component of the spin angular momentum on an arbitrary axis. The familiar values of $\frac{1}{2}\hbar$ and $-\frac{1}{2}\hbar$ are associated

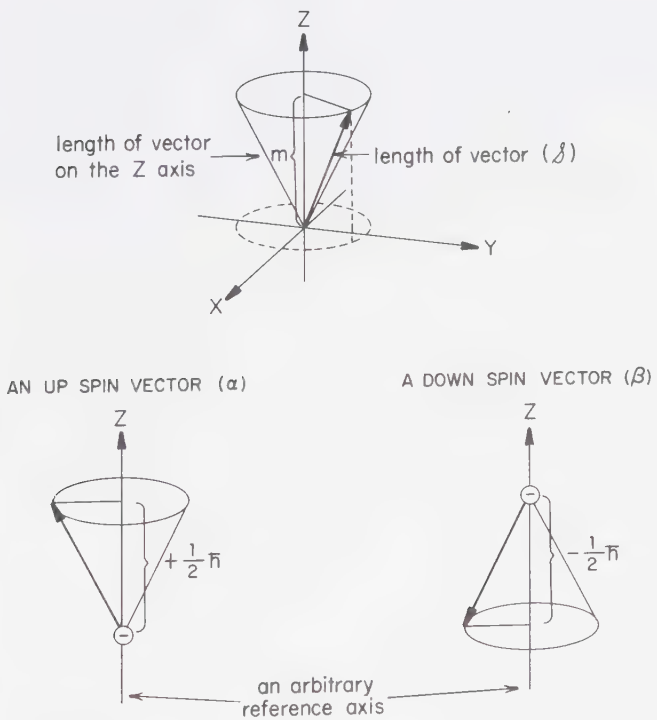

Figure 2.2

Vector representation of an electron's spin magnet moment. The vector is viewed as precessing about the Z-axis. The projection of the vector on the *z*-axis possesses a length *m*. Only two orientations of the spin vector are stable: an up (α) orientation and a down (β) orientation.

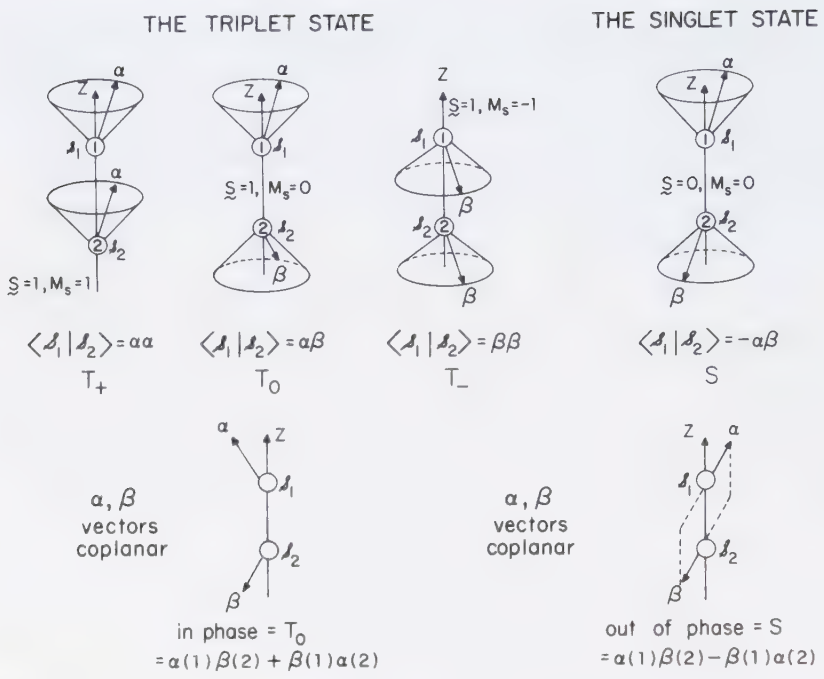

Figure 2.3

Vector representation of the triplet state and the singlet state. An "up" spin vector is represented by α and a "down" spin vector is represented by β.

---

with the two allowed components. We may thus visualize some arbitrary axis for which the component of the spin vector on the axis is "up" and "down". We may refer to the "up" spin vector as α-spin and the "down" spin vector as β-spin. *The axis of precession of the spin vector is determined by the magnetic fields it experiences. It will tend to precess about the strongest magnetic field to which it can couple.* This fact is crucial for an understanding of the mechanisms by which singlet (spin paired) and triplet (spin unpaired) states may interconvert.

2.8 Vectorial Representation of Singlet and Triplet States Derived from a Single Configuration

Consider a system of electron configuration $\psi_i\psi_j$ where the one-electron MO $\psi_i \neq \psi_j$ (e.g., an n, π^* configuration or a π, π^* configuration). Since the spin vectors $\mathscr{S}_i$ and $\mathscr{S}_j$ (which correspond to the spinning electron in ψ_i and ψ_j, respectively) may only take on values of α ("up" spin) or β ("down" spin), it follows that *four*

possible spin vector representations may characterize the two spin system $\mathscr{S}_i\mathscr{S}_j$, (schematically shown in Fig. 2.3). According to the postulates of quantum mechanics, the only *stable* configuration of the spin vectors correspond to two situations: (a) $\mathscr{S}_i$ and $\mathscr{S}_j$ are completely *in phase* (they precess at the same rate and such that they are always pointing "in the same direction"), or (b) $\mathscr{S}_i$ and $\mathscr{S}_j$ are completely *out of phase* (they precess at the same rate and are always pointing in opposite directions.)

These situations may be visualized by reference to Figure 2.3. Let the two electrons in ψ_i and ψ_j be labeled 1 and 2, and let $\mathscr{S}_1$ and $\mathscr{S}_2$ be their corresponding spin vectors. We note that the spin quantum number S, equals 1 in the triplet state and S equals zero in the singlet state. The three components $(1, 0, -1)$ of the triplet state correspond to three different possibilities for the magnetic quantum number M_s. Each of these possibilities corresponds to a *stable state*, i.e., one of the three components of a triplet. We define the three components of the triplet as $T_+ \equiv \alpha_1\alpha_2$, $T_- \equiv \beta_1\beta_2$, and $T_0 \equiv \alpha_1\beta_2$, for $M_s = 1, -1$, and 0, respectively.

It is absolutely essential to note that there are *two* states for which the spins are $\alpha\beta$.[4] If the vectors corresponding to α and β are in phase (Fig. 2.3), a resultant vector exists perpendicular to the z-axis but *no* resultant spin occurs along this axis. This state corresponds to one of the components of the triplet state ($S = 1$, $M_s = 0$). If the vectors corresponding to α and β are 180° out of phase, their *resultant* on the z-axis is *zero* and corresponds to a singlet state ($S = 0$) $M_s = 0$. Thus, if one $M_s = 0$ state has *paired spins* (i.e., is a singlet state) this means not only that one electron has α spin and the other has β spin but also that they are oriented so that they point in opposite directions. In the $M_s = 0$ state of the triplet one electron has α spin and the other has β spin. Their resultant along the z-axis is zero, but is non-zero in the xy plane.

Since the triplet state has two spin-parallel electrons, it must be paramagnetic. Indeed, the observation that irradiation of a solution of fluorescein (and other molecules) in boric acid induces a transient paramagnetic susceptibility provided early evidence for the existence of triplet states.[5,6] Later it was shown the decay of the light-induced paramagnetism and the decay of phosphorescence were identical.[7] This result implied the identity of the paramagnetic and phosphorescent state of molecules.

In the case of a triplet organic molecule in the absence of an external magnetic field, the interaction between spins will be anisotropic, i.e., the interaction energy will be different in different directions.[8] In effect, the spins are "coupled" to the molecular framework and this is equivalent to quantization of spin along some arbitrarily defined x, y, and z axes due to a local magnetic field within the molecule due to spin-spin interactions. In practice this molecular magnetic field amounts to $\sim$2000 gauss (~ 0.2 cm^{-1}). Thus, in zero *external* magnetic field, the magnetic energy levels of the triplet state are determined by the "effective molecular magnetic field." The separation of the triplet sublevels (termed T_x, T_y, and T_z for the molecular case) is termed the *Zero Field Splitting* and is shown schematically in Figure 2.4. Since external magnetic fields of the order of 1000 to 10,000 gauss are routinely available, one may experimentally "switch" the coupling of the paired electron spins from the molecular frame ("low fields") to the direction of the external mag-

netic field ("high fields"), i.e., at appropriate field strengths there may be a competition between the molecular axes and the external field for spin quantization.

Electron spin resonance (ESR) spectroscopy (discussed in Chapter 8) allows direct observation of transitions between the magnetic sublevels T_x, T_y, and T_z of the triplet states of organic molecules.[8] In addition, the energy separation of the magnetic sublevels increases with the application of an increasing external magnetic field.

In summary, "the triplet state" of organic molecules is a real, if metastable, species. In later chapters we shall discuss the physical and chemical properties of these important photochemical intermediates.

2.9 Electronic Energy Difference between Singlet and Triplet States

The difference in *electronic energy* between singlet and triplet states (that are derived from the same electron orbital configuration) results from the "better" correlation of electron motions in a triplet state. The Pauli principle operates as a sort of quantum mechanical force which "instructs" the two key orbitally unpaired electrons in triplet states how to "avoid" one another and thereby *correlate* their motions to minimize electronic "collisions" (i.e., minimize electron-electron repulsions). In order to understand how this singlet-triplet energy separation (ΔE_{ST}) arises and to gain an appreciation of how the magnitude of the ΔE_{ST} depends upon the orbitals comprising the characteristic configuration, we must investigate

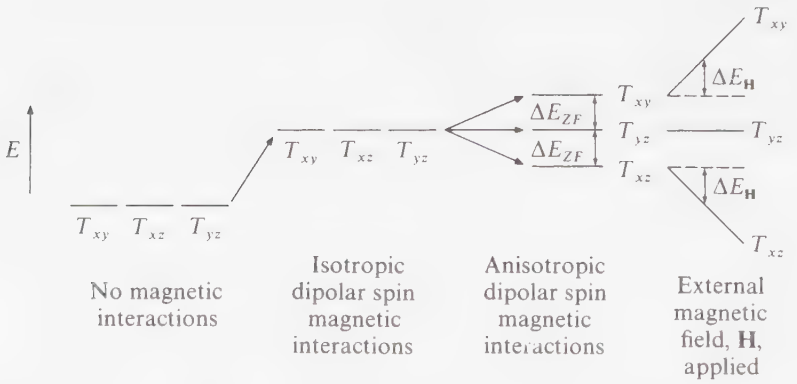

Figure 2.4

The effect of spin-spin dipolar interactions on the triplet sublevels. The anisotropic interaction results in a "zero field splitting" of the magnetic sublevels of the triplet state even at zero *external* magnetic field. Application of an external magnetic field, **H**, causes further separation of the magnetic sublevels. It is assumed that T_{xy} corresponds to a state for which $M_S = 0$, for simplicity.

the nature of the *matrix elements* which evaluate the electronic energy of orbitals, configurations, and states.

Qualitative Evaluation of the Electronic Energies of States

We may now consider a means of qualitatively evaluating the magnitude of ΔE_{ST}, the electronic energy splitting of singlet and triplet states derived from the same electronic configuration.[9] We shall identify a state energy as the summation of a Zero Order (one-electron orbital) energy plus electron repulsion energies. For example, the energetics of the ground state and the lowest excited states of formaldehyde are given by:

$$E(S_0) = 0 \qquad \text{by definition} \tag{2.9}$$

$$E(S_1) = E(n, \pi^*) + K(n, \pi^*) + J(n, \pi^*) \tag{2.10}$$

$$E(T_1) = E(n, \pi^*) + K(n, \pi^*) - J(n, \pi^*) \tag{2.11}$$

where J is the matrix element that measures electron repulsion due to electron exchange and K is the matrix element that measures electron repulsion due to Coulombic interactions. Both J and K are positive (energy enhancing) quantities. Note that

$$\Delta E_{ST} = E(S_1) - E(T_1) = 2J(n, \pi^*) > 0 \tag{2.12}$$

and since J must be positive we conclude that $E(S_1) > E(T_1)$ *in general.*

The Zero Order energy (one-electron configuration) of both S_1 and T_1 is $E(n, \pi^*)$, i.e., the energy required for an orbital jump from an n-orbital to a π^*-orbital (in the one-electron orbital approximation) *plus* a correction for Coulombic repulsion of electrons. The repulsion does not split S_1 and T_1 but raises the energies of both states. The S_1 and T_1 states are then split in energy by the exchange term, J, which stabilizes the triplet relative to the Zero Order states and destabilizes the singlet relative to the Zero Order states (Fig. 2.5). The *state energy*

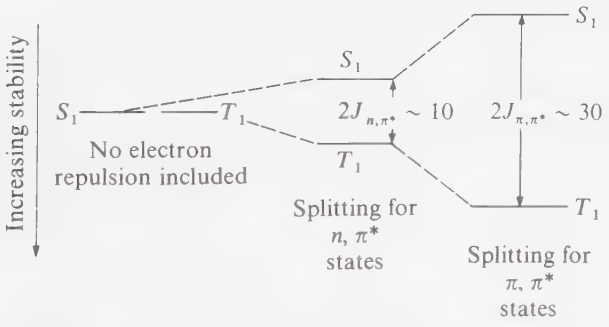

Figure 2.5

Singlet-triplet separation for n, π^* and π, π^* states. Energies in kcal/mole.

diagram for formaldehyde may now be modified to take singlet-triplet energy splittings into account (Fig. 2.6). We term this the *working* state energy diagram. All state diagrams from this point on will be at this level of approximation.

Examples of Singlet-Triplet Splittings[9]

Let us consider a qualitative picture which will give a feeling for the magnitude of J, the electron exchange integral. The lowest S_1 and T_1 states of many carbonyl compounds are n, π^* states. The value of J represents the electrostatic repulsion between the electrons in an n orbital and in a π^* orbital.

The magnitude of J is given by a matrix element shown in Eq. 2.13, in which n and π^* represent the wavefunctions for the n and π^* orbitals, respectively. The numbers refer to the electrons occupying these orbitals and e/r_{12} represents the repulsion between the exchanging electrons. The latter term may be factored out of Eq. 2.13 so that the value of J can be seen to be proportional (Eq. 2.14) to the *overlap* of the n orbital with the π^* orbital.

$$J_{n,\pi^*} = \langle n(1)\pi^*(2)|e/r_{12}|n(2)\pi^*(1)\rangle \tag{2.13}$$

or

$$J_{n,\pi^*} \sim \langle n(1)\pi^*(2)|n(2)\pi^*(1)\rangle \sim \langle n|\pi^*\rangle \tag{2.14}$$

In words, the magnitude of J_{n,π^*} will be proportional to the overlap integral $\langle n|\pi^*\rangle$. We may visualize the overlap integral $\langle n|\pi^*\rangle$ if we replace the symbol n with a picture of the n-orbital and the symbol π^* with a picture of the π^*-orbital (Eq. 2.15). We then estimate the degree of overlap between the n and π^* orbital. In fact we note that the overlap integral is small because these orbitals do not occupy very much of the same region of space.

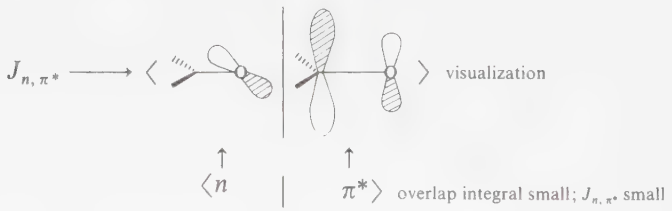

(2.15)

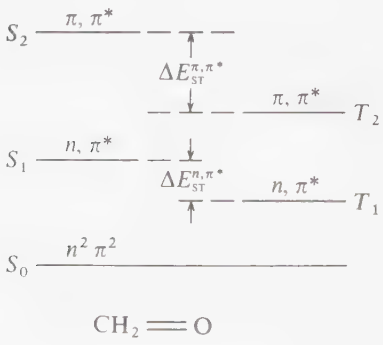

Figure 2.6
The working state energy diagram of formaldehyde. Singlet-triplet energy differences are included.

Now let us compare this result to that for a π, π^* configuration. Employing the ideas leading to Eqs. 2.14 and 2.15 for a π, π^* configuration we obtain Eqs. 2.16 and 2.17.

$$J_{\pi,\pi^*} \sim \langle \pi | \pi^* \rangle \tag{2.16}$$

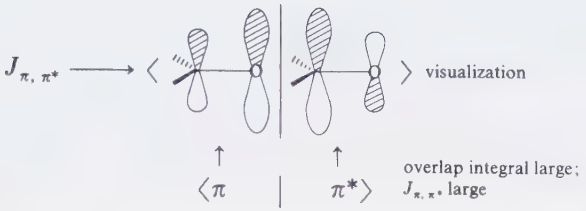

(2.17)

It is clear that J_{π,π^*} will be greater, *in general*, than J_{n,π^*} because the overlap integral $\langle \pi | \pi^* \rangle$ will generally be greater than the overlap integral $\langle n | \pi^* \rangle$.

Experimentally, $S_1 - T_1$ splittings of the n, π^* states for ketones are 8–10 kcal/mole, while for molecules with π, π^* $S_1 - T_1$ splittings, such as benzene, values of 30–40 kcal/mole for J_{π,π^*} are common. Table 2.1 lists some experimental values of singlet-triplet energy splittings.

The table shows that states derived from n, π^* configurations consistently have smaller singlet-triplet splitting energies than states derived from π, π^* configurations. Notice that typical values of $S_1 - T_1$ splittings are high relative to even

Table 2.1 Singlet-Triplet Splittings

Molecule	Configuration ($S_1 - T_1$)	ΔE ($S_1 - T_1$) in kcal/mole
$CH_2{=}CH_2$	π, π^*	70
	π, π^*	40
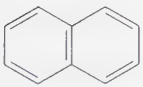	π, π^*	35
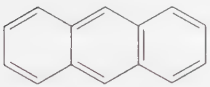	π, π^*	30
$CH_2{=}O$	n, π^*	10
$(CH_3)_2C{=}O$	n, π^*	7
$Ph_2C{=}O$	n, π^*	7

the largest zero field splittings ($\sim 10^{-3}$ kcal/mole). For nearly all chemical processes the three sublevels of T_1 are rapidly equilibrated and behave as a common "pool" of molecules. Hence the term "triplet state" even though *three states* actually exist. In Chapter 8 we shall see how the "three state" character of T_1 may be observed directly by the technique of electron spin resonance.

The energy diagram for formaldehyde (Fig. 2.6) is appropriate for a molecule possessing the following electronic configuration: $S_1 = n, \pi^*$; $S_2 = \pi, \pi^*$; $T_1 = n, \pi^*$; and $T_2 = \pi, \pi^*$. This situation is common for unsaturated chromophores possessing heteroatoms, i.e., ketones.

From Atomic Orbitals to a "Working" (First Order) State Energy Diagram

Scheme 2.1 summarizes the pathway from "one electron" atomic orbitals (ϕ), to "one electron" molecular orbitals (ψ), to one electron configurations $\Pi_i\psi_i$, to Zero Order States, to First Order States, and finally to First Order or "working" states and state energy diagrams. The working state, it should be emphasized, is at the level of a "two orbital configuration approximation," i.e., we take only two orbitals into account, and characterize a state in terms of the orbital configuration of the two highest-energy electrons.

2.10 The Experimental Measurement of Orbital Energies: Photoelectron Spectroscopy

A basic premise of this chapter is that we may approximate molecular states in terms of a model involving molecular orbitals. Is there any direct experimental means of checking the concept of molecular orbitals? Although no truly direct means exists, it is possible to provide evidence for the validity of the idea that MO's exist by means of a technique called *photoelectron spectroscopy* (PES).[10] The key idea of PES is the notion that *the energy of a molecular orbital is characterized by the amount of energy required to completely remove an electron from that molecular orbital, i.e., the energy to ionize the molecule.* Thus, PES is concerned with the measurement of ionization potentials of molecules and the association of measured ionization potentials with the extraction of electrons from specific molecular orbitals. The power of the technique is the relative ease and accuracy with which ionization potentials may be measured.

Use of PES to Measure Orbital Energies

The idea of PES measurements (which are made on molecules in the vapor phase) is as follows. A photon of very high energy ($E = h\nu$) is absorbed by a mol-

ecule. If the value of $h\nu$ is greater than the ionization potential, IP (energy required to completely remove an electron from a molecule), then an electron is ejected from the molecule. In general there will be an energy balance to be accounted for. For example, if

$$\Delta E = (h\nu - IP) \neq 0 \tag{2.18}$$

then the difference in energy, ΔE appears experimentally as an increase in the energy of either the ejected electron or the positive molecular ion left behind, i.e., as kinetic energy of the molecular ion or expelled electron. Because the electron is so much lighter than the molecular ion, essentially *all* of ΔE goes into kinetic energy of the electron. The key measurement of PES is the kinetic energy of ionized electrons. Knowledge of this kinetic energy (KE) allows evaluation of ΔE

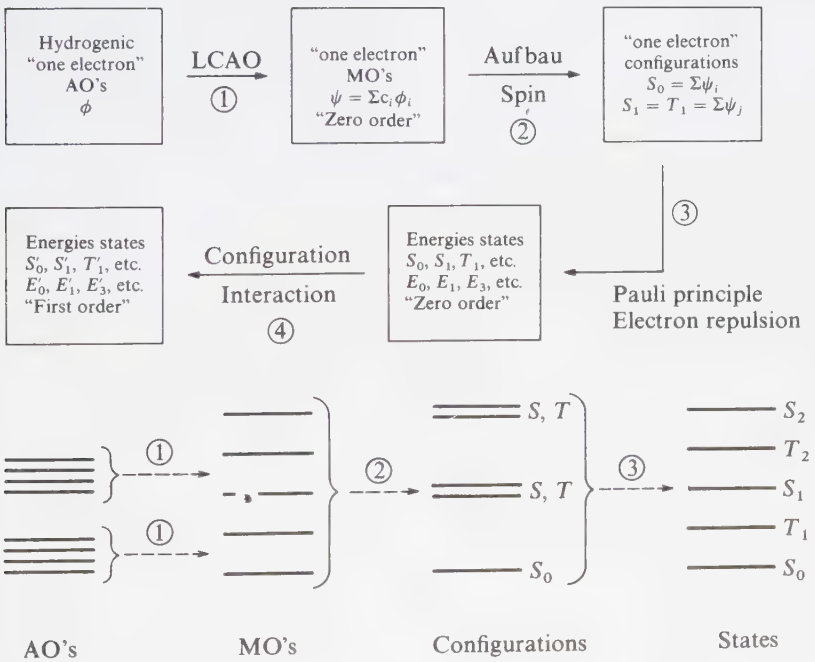

Scheme 2.1

Schematic of the method of building an energy diagram from theory. Each of the final states in the "Zeroth order" is derived from a distinct configuration. At a high level of approximation (configuration interaction) more than one configuration is required to describe each state.

(Fig. 2.7). Since the value of $h\nu$ is known, then IP may be evaluated as:

$$KE = \Delta E \quad \text{and} \quad IP = h\nu - KE \tag{2.19}$$

The minimum energy required to eject any electron from a molecule is termed the *first ionization potential* of a molecule. In the molecular orbital view of molecules, this energy corresponds to that needed to remove an electron from the highest energy occupied MO. To a Zero Approximation, the orbital energy may be defined as being equal to the negative of the corresponding ionization potential. Thus, PES provides an experimental check of the orbital picture.

Information about Orbitals from PES

Let a molecule M be ionized as a result of absorption of a photon, i.e.,

$$M + h\nu \rightarrow M^{+} + e^{-} \tag{2.20}$$

Since PES measures only the KE of the electron, the fate of M^{+} is not of interest. Consider now formaldehyde, a molecule whose higher energy MO's are now familiar to us. What do we expect from a PES experiment if the MO picture is valid? Since the first ionization potential (IP_1) corresponds to ejection of the highest energy (least bonded) electron in a molecule we would expect that IP_1 corresponds to ionization of an electron in the n orbital on oxygen. From Eq. 2.6 we predict that IP_2 should correspond to ejection of a π_{CO} electron, IP_3 should correspond to ejection of a σ electron, etc. The actual PES spectrum of formaldehyde is shown in Figure 2.8. The vertical axis is a measure of the probability that an ejected electron will possess the kinetic energy plotted on the horizontal axis. At the extreme right of the figure is a set of bands corresponding to IP_1 10.88 ev (= 250 kcal/mole). A second set of bands maximizing near 14.1 ev (= 330 kcal/mole) corresponds to IP_2. Finally the bands corresponding to IP_3 maximize at 16 ev (= 368 kcal/mole). The "fine structure" associated with each IP is interpreted as

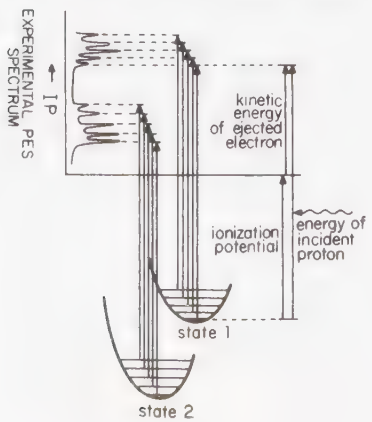

Figure 2.7
Schematic representation of how a photoelectron spectrum occurs.

due to *formation of different vibrational levels of* M^+. Since the kind of vibration "left behind" in M^+ should be related to the nature of the orbital from which the electron is ejected, analysis of the fine structure leads to clues concerning the kind of orbital corresponding to each *IP*. For example, IP_1 mainly shows one vibrational band, meaning that many vibrations are not excited during ionization and the lowest vibrational state of M^+ is formed *selectively* upon ejection of the electron responsible for IP_1. This means that the ejected electron did not participate in bonding, i.e., if it did, its removal would have significantly affected (i.e., excited) the vibrations of the atoms which it was binding. Thus, we conclude that IP_1 corresponds to removal of a nonbonding electron, as expected from our simple MO picture of formaldehyde.

The vibrational structure of IP_2 indicates that an electron has been ejected from a strongly bonding orbital (many vibrations excited). Since $D_2C{=}O$ shows the same vibrational structure for IP_2 as does $H_2C{=}O$ and since a large difference between the photoelectronic spectra of D_2CO and H_2CO is expected if a σ_{CH} (or σ_{CD}) electron is removed, we conclude that the bonding orbital responsible for IP_2 is *not* associated with a σ_{CH} orbital. The logical choice is the π_{CO} orbital. Furthermore, the vibrational spacing of IP_2 shows a repeating value of $\sim 1200\ cm^{-1}$ which corresponds to the value expected of a carbon-oxygen double bond stretching frequency in H_2CO^+.

There are now many examples of the validity of the assumption that

$$E(\psi) = -IP \tag{2.21}$$

i.e., that the orbital energy may be equated to the negative of *IP* as measured by PES. This useful approximation has become known as *Koopmans' theorem.*

Relationship of PES to Electron Affinities, Excitation Energies, and the *HO-LU* Concept

In addition to serving as a pretty experimental check of simple MO theory, PES provides us with a handy means of obtaining a highly useful and important

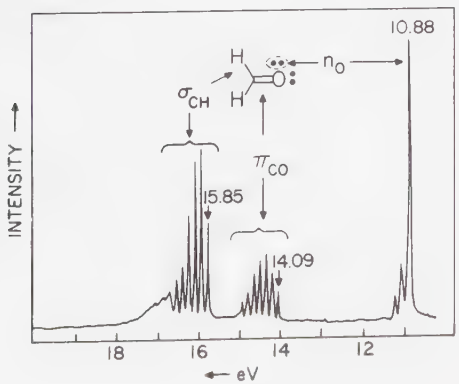

Figure 2.8
Photoelectron spectrum of formaldehyde.

property of molecules, namely their lowest ionization potential, IP_1. Chemical reactivity is mainly due to the behavior of valence electrons, and the highest occupied (HO) orbital often determines the lowest-energy electronic pathways available for reaction. We may associate $-IP_1$ with the energy of the HO orbital. Furthermore, we may identify (Fig. 2.9) the energy of the lowest unoccupied (LU) orbital in the groundstate with the value of a molecule's electron affinity, EA. If we know the value of IP_1 *and* the energy of the lowest-energy electronically excited states (E_*) we may estimate the energy of the LU orbital as $-IP + E_*$, where $h\nu$ is the energy required for the lowest energy electronic transition. As a result, knowledge of both IP_1 *and* electronic excitation energies will help us to locate the energies of orbitals and to establish a qualitative energetic disposition of a molecule's LU and HO orbitals. This energetic ordering, in turn, will be of great value in our qualitative analysis of photoreactivity.

2.11 Summary

The state diagram of a typical chromophore is of enormous importance in understanding of photoreactions. What is a state diagram and what information does it provide the photochemist?

The state diagram relates the energies of the lowest excited singlet state and the lowest triplet of a molecule to the energy of the ground state of the molecule. The state diagram is only concerned with energies relative to the ground state, since these energy differences represent the maximum electronic energy available for processes such as energy transfer and energy storage in intermediates. The state energy diagram provides a general and systematic *structure* for the analysis of the molecular photophysics (radiative and radiationless processes that correspond to electronic transitions between states displayed in the state energy diagram).

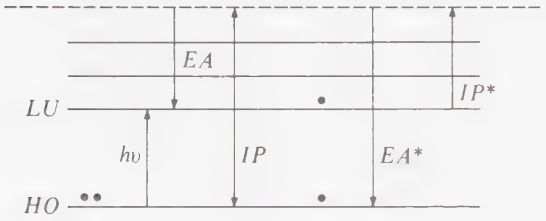

$$EA^* = EA + h\upsilon$$
$$IP^* = IP - h\upsilon$$

Figure 2.9
Relationships between *HO*, *LU*, *EA*, and *IP*.

It also provides an excellent starting point for the analysis of molecular photochemistry. In the latter case, the connectivity relationships between the state energy diagrams of reactants and the state energy diagram of products are considered.

The combination of the MO approximations with energy diagrams allows us to plot the lowest energy states of simple chromophores, note the energetic proximity of states, and deduce their fundamental electronic character. We shall see in Chapter 3 that the energetic separation of states (ΔE) and their electronic structure (approximated by a singlet configuration) will be of importance in deducing rates of transitions and reactions.

References

1. Born, M., and Oppenheimer, J. R., *Ann. Phys.*, *84*, 457 (1927).
2. Dewar, M. J. S., and Dougherty, R. C., *The PMO Theory of Organic Chemistry*, Englewood Cliffs, N.J.: Prentice-Hall, 1975.
3. Atkins, P. W., *Quanta. A Handbook of Concepts*, Oxford: Clarendon Press, 1974, pp. 217, 223.
4. Strictly speaking $\alpha\beta$ and $-\alpha\beta$ are improper representations of the mathematic functions representing the spin part T_0 and S, although this fact does not affect the qualitative points of the discussion. See: McGlynn, S. P., Azumi, T., and Kinoshita, M., *Molecular Spectroscopy of The Triple State*, Englewood Cliffs, N.J.: Prentice-Hall, 1969, p. 73.
5. Lewis, G. N., and Calvin, M., *J. Am. Chem. Soc.*, *67*, 1232 (1945).
6. Joussot-Dubien, J. and Lesclaux, J., *J. Chem. Phys.*, *61*, 1147, 1631 (1964).
7. Evans, D. F., *Nature*, *176*, 777 (1955).
8. El-Sayed, M., *Excited States*, ed. Lim, E. C., New York: Academic Press, p. 35; El-Sayed, M., *Pure Appl. Chem.*, *24*, 475 (1970).
9. McGlynn, S. P., Smith, F. J., and Cilento, G., *Photochem. Photobio.*, *3*, 269 (1964).
10. Turner, R. B., *Photoelectron Spectroscopy*, New York: John Wiley, 1972.

3

Transitions Between States—Chemical Dynamics

3.1 Chemical Dynamics as Transitions between States

The purpose of this chapter is to provide a basis for visualizing the factors that determine the *rates* of photochemical processes. In Chapter 2 we were mainly concerned with the enumeration, chemical nature, and energetic ranking of states associated with a given "spatially frozen" nuclear geometry. In effect, we artificially separated electronic motion from nuclear motion and spin motion and concentrated on *energetics* and *structure* which were "time independent," or so-called "average," "static," or "equilibrium" properties of isolated molecules. Now we will consider what happens when we take into consideration nuclear and spin motion, and what happens when these two motions interact with electron motion. We shall regard the *rates* of chemical processes as being associated with and determined by the probabilities of *transitions between states*. We call the systematic study of transitions between states the science of *chemical dynamics*.

As a general strategy, we suppose that all changes of structure (electronic, nuclear, or spin) are resisted if conservation laws are not obeyed. When conservation laws are fully obeyed, then changes of structure which correspond to an extension of the natural motions of the particles (orbital, vibrational, and spin) and which correspond to small displacements in space (good overlap) occur at a maximal rate and are termed "fully allowed." Even if conservation laws are obeyed, changes of structures which correspond to unnatural motion (jumps between orbitals of different symmetry or spin flips), or which correspond to large displacements in space (poor overlap), are slow (relative to "allowed" structural changes).

3.2 Classical Dynamics: Some Preliminary Comments[1]

The classical theory of dynamics derived from Newton's laws is based on two principles:

1. The central problem in understanding dynamic processes is the identification of interactions (the *forces*, *energies*, or *work*) involved in changing the motion of the particles in the system.

2. Deviations from original motions result from interactions and occur reciprocally, i.e., to each action there is an equal and opposite reaction.

In addition to these two principles, two *laws* apply when analyzing the dynamics of any classical system:

1. *The Law of Conservation of Energy*. In any isolated system energy may be transformed from one kind to another but cannot be created or destroyed.

2. *The Law of Conservation of Momentum*. In any isolated system, momentum may be transformed from one kind to another but cannot be created or destroyed. (For example, angular momentum may be transformed into linear momentum and vice versa, but the total angular plus linear moment is conserved.)

The first law refers to a quantity we call *energy* and the second law refers to a quantity we call *motion*.

The combination of the Newtonian *ideas* and the energy-motion conservation *laws* provides a powerful basis for the qualitative and quantitative analysis of dynamic processes even at the molecular level. For instance, suppose we wish to analyze transitions between electronic states which are given in a known state energy diagram. The protocol of the analysis based on classical dynamics would be as follows. Identify (a) the *energetic and structural* differences between the initial and final states, (b) any implied *momentum* differences between the two states, and (c) any *forces* which will operate in such a manner as to convert the initial structure into the final structure.

If we succeed in steps 1, 2, and 3, we say that we have identified a *mechanism* for conversion of the initial state into the final state. Next we must ascertain whether the mechanism we have generated violates the conservation laws.

If the law of conservation of energy is violated, the transition is *strictly forbidden* in an isolated system. We must introduce into the mechanism an *external energy source* or *energy sink* in order to obey the energy conservation law:

> For a molecular assembly of particles the energy source or sink is provided either by molecular collisions (we may include vibrations

as "collisions" between bound atoms or groups) or by the absorption and emission of radiation (collision with, or ejection of, a photon).

If the law of conservation of momentum is violated, the transition is *strictly forbidden* in an isolated system. In order to make the mechanism acceptable, we must introduce a previously ignored internal or external force which causes momentum exchange to occur so that the total momentum remains constant.

We might note that the spirit of the conservation laws is to tell us what *cannot* be done, i.e., these laws provide us with selection rules for rapidly identifying acceptable and unacceptable mechanisms. In the Zero Order, selection rules provide us with a basis for *elimination* of possibilities which are forbidden by a a selection rule. A process which proceeds in violation of a selection rule *always* proceeds at a slower rate than a corresponding process which proceeds in compliance with a selection rule. We understand "allowed" and "forbidden" to be relative terms and not to imply finite versus zero.

3.3 Quantum Dynamics: The Golden Rule for Transitions between States

We noted in Chapter 2 that a general formulation of rate processes is possible in terms of *quantum dynamics*, i.e., the analysis and evaluation of the rate of transitions between Zero Order states in terms of matrix elements. A "Golden Rule" expression is available for understanding rate processes in terms of quantum dynamics: *the rate of transitions between two states is proportional to the square of the matrix element corresponding to the (weak) first order perturbation coupling the Zero Order states.*[2] A more exact expression of the Golden Rule of dynamics has the form:

$$\text{rate } (\text{sec}^{-1}) = \frac{2\pi}{h} \rho \langle H' \rangle^2 \tag{3.1}$$

where ρ corresponds to the "density" or number of final states capable of coupling with the initial state, and $\langle H' \rangle$ represents the matrix element for the (weak) perturbation coupling the initial and final states.

The spirit of the Golden Rule is that the rate of transitions between two states is related to the magnitude of a perturbation or force which changes the positions or motions of the particles of the initial state and "reshapes" the initial state so that it looks like the final state. The same matrix elements that cause energy splittings of states are "plugged into" Eq. 3.1 in the case of radiationless transitions. The situation is analogous for radiative transitions except that in this case an electromagnetic field provides the perturbation which changes the position or motion of the particles.

3.4 Transitions between States: Evaluation of Transition Probabilities

Let us now consider a useful modification of the "Golden Rule" (Eq. 3.1). The idea is as follows. We start off with a Zero Order approximation to describe the system of our interest. If in the first approximation the interactions between states are large (i.e., the first order splittings of the Zero Order states are as large or larger than the initial separations in state energy before the first order interaction) the transition probability is maximal and in the extreme is limited by the zero point motion of the particles.

In structural terms this means that in the range of large interactions, the rate of "fully electronically allowed" transitions is limited by electronic motion only for the transition (provided the nuclear and spin configurations remain constant). On the other hand, if the nuclear and/or spin configurations change during a "fully allowed" electronic transition, the transition may be "rate limited" by the time it takes to change nuclear or spin configuration. Such a view creates limit points for the maximal rates of various "allowed" transitions, and indicates that structural changes may serve as "bottlenecks" in determining transition rates. We may associate a prohibition factor (f) for each abrupt structural change (in the sense of spatial position or motion) involved in a transition between states. Thus, the *observed experimental rate constant*, k may be decomposed into components:

Observed rate constant ⟶ Zero point motion limited rate constant ⟵ "Fully allowed" rate

$$k(\text{obs}) = k^{\circ}_{\text{max}} \times \underbrace{f_e \times f_v \times f_s}_{\uparrow} \tag{3.2}$$

Prohibition to maximal rate caused by "selection rules" ⟶ Prohibition factors due to changes in electronic, nuclear, or spin configuration

where f_e is the prohibition factor associated with the electronic change (orbital configuration change), f_v is the prohibition factor associated with the nuclear configuration change (usually describable as a vibrational change) and f_s is the prohibition factor associated with a spin configurational change (equal to unity for total spin conserving transitions and usually determined by spin orbit coupling for transitions which do not conserve total spin).

For a spin conserving *unimolecular* radiationless transition from ψ_i to ψ_f, k°_{max} is of the order of 10^{13}–10^{14} sec^{-1} and is limited by the time it takes nuclei to execute zero point motions. The value of k(obs) is in general much smaller than 10^{13} 10^{14} sec^{-1}. Thus, f_e, f_v, or f_s (or some combination) usually contrive to place a prohibition on the maximum transition rate. For example, if the transition involves an orbital configuration change which corresponds to a substantial change in electronic distribution or motion along the nuclear framework, f_e may be very

much less than 1.00. Similarly, if the transition involves a drastic change in nuclear configuration or motion, f_v may be very much smaller than 1.00. Finally, if the transition does not conserve total electronic spin, f_s may be much smaller than 1.00.

How do we evaluate f_e, f_v, and f_s? For large, favorable interactions between zero order states $f_e \sim f_v \sim f_s \sim 1.00$ and $k(\text{obs}) \sim k^\circ_{\text{max}}$. Since $k(\text{obs})$ is generally much smaller than k°_{max}, we are generally concerned with *small* interactions between zero order states. From perturbation theory, the magnitude of the f factors, for small interactions, is given by

$$f \sim \left|\frac{\langle H\rangle}{\Delta E}\right|^2 \tag{3.3}$$

where $\langle H\rangle$ is the matrix element for the ψ_i° to ψ_f° transition, i.e., $\langle\psi_i|H|\psi_f\rangle$, and ΔE is the energy gap between the zero order states ψ_i° and ψ_f°.

We may rewrite Eq. 3.2 as:

$$k(\text{obs}) = \underbrace{\frac{k^\circ_{\text{max}}\langle\psi_i|H_e|\psi_f\rangle^2}{\Delta E^2}}_{\substack{\uparrow \\ \text{Orbital} \\ \text{interactions}}} \times \underbrace{\frac{\langle\psi_i|H_{so}|\psi_f\rangle^2}{\Delta E^2}}_{\substack{\uparrow \\ \text{Spin-orbit} \\ \text{interactions}}} \times \underbrace{\langle\chi_i|\chi_f\rangle^2}_{\substack{\uparrow \\ \text{Franck-Condon} \\ \text{factors}}} \tag{3.4}$$

In summary, from the form of the rate constant for radiationless transitions we expect that there will be three major (unimolecular) features which will determine the probability of transition from the initial state ψ_i to the final state ψ_f:

1. The structure and motion of electrons in ψ_i relative to those in ψ_f
2. The structure and motion of the nuclei in ψ_i relative to those in ψ_f
3. The structure and motion of spins in ψ_i relative to ψ_f

The Spirit of Selection Rules for Transition Probabilities

The spirit of the great *conservation laws* is that they work no matter what the details of the physical system under study. They provide an economy of mathematical expressions and possess sweeping universality.

The spirit of a *selection rule* is that within a certain set of assumptions which assign an initial idealized geometry or symmetry for a molecular state and a set of quantum numbers for the electrons, nuclei, and spins (ψ, χ, $\mathcal{S}$), a transition probability to a final state may be calculated. If the transition probability equals zero, the transition is said to be "strictly forbidden" within the given level of approximation. When a more realistic nonideal symmetry or when previously ignored forces have been included, a *new* calculation may yield a nonzero value for the transition probability. If this probability is still small (say less than 1% of the maximal transition probability) the process is said to be "weakly allowed" or "strongly forbidden." It can be seen that such qualitative descriptions can only

provide a "rough" feeling for transition probabilities. Indeed, sometimes the breakdown of selection rules is so severe that the magnitude of "forbidden" transition probability approaches that of the "allowed" transition probability. When this occurs, we have selected a poor Zero Order starting point for our evaluation of the transition probability.

Visualization of the Mechanisms of Transitions between States. The Breakdown of Selection Rules

In any theory of molecular behavior we should consider (a) conservation laws as fundamental and always applicable, and (b) selection rules as artificial and approximate. Since selection rules are approximate they "break down" when mechanisms for coupling momenta exchanges occur or when external perturbations become possible. For our purposes, we shall consider only the angular momenta of electrons (due to orbital motion), the vibrational momenta of nuclei, and the spin momenta of electrons. It is important to note that although quantization of states and zero point motions are quantum mechanical effects, nearly all quantum mechanical selection rules are derived from conservation laws for *classical particles.* In effect, quantum mechanics assumes that the classical systems serve as an appropriate and useful starting point for the description of molecular dynamics.

3.5 Nuclear Motion; Vibronic States

Up to this point, we have considered electronic states in terms of electronic configurations for fixed nuclear geometries. This approximation allowed us to generate a Zero Order description of *electronic structure* and *electronic energy*, based on an assumed fixed and rigid nuclear geometry. Since the uncertainty principle requires that vibrational "zero point" motion occurs at all temperatures, we must consider the effect of nuclear motion on the electronic structure and electronic energy of a molecule. Our goal is to replace the "pure" vibrationless molecule with a vibrating molecule and to be able to visualize how this motion will modify our Zero Order model. We call the states of a vibrating molecule *vibronic* states rather than "pure" electronic states.

The Effect of Nuclear Motion on Electronic Energy and Electronic Structure

If the inclusion of nuclear motion causes only a small change in the electronic energy of our Zero Order model, then we can use perturbation theory to evaluate the "splitting" energy E_v of the electronic energy of the Zero Order *electronic* states into the First Order *vibronic* states. According to perturbation theory

$$E_v = \pm \frac{\langle \Psi_1^0 | H_v | \Psi_2^0 \rangle^2}{\Delta E_{12}} \tag{3.5}$$

where Ψ_1^0 and Ψ_2^0 are two "pure" electronic states "mixed" or "split" by the motion of nuclei, H_v is the operator which describes how the electronic energy depends on nuclear motion and ΔE_{12} is the energy difference between the Zero Order states.

In general, the value of E_v is commonly less than 5 kcal/mole (2000 cm^{-1}), so that vibronic interactions do not change significantly the Zero Order description of electronic states whose Zero Order energies differ by, say, 50 kcal/mole (20,000 cm^{-1}). However, vibronic interactions are much more likely to be significant in mixing Zero Order electronically *excited* states since the electron energy difference between Zero Order electronic states is sometimes of the order of 5 kcal/mole. In such cases, the electronic energy and electronic structure may vary considerably during a vibration.

As a simple example of the effect of nuclear motion on electronic energy, consider the effect of vibrations of a carbon atom which is bound to three other atoms (e.g., a methyl group as a radical, anion, or carbonium ion). When the system is planar and the angles between the atoms are 120°, the "free valence" orbital may be described as "pure" *p*. What happens to the shape of this orbital as the molecule vibrates? (See Fig. 3.1) If the vibrations do not destroy the planar geometry (angles between the atoms change but system remains planar) the spatial distribution of the free valence orbital above and below the plane must be *identical* because of the

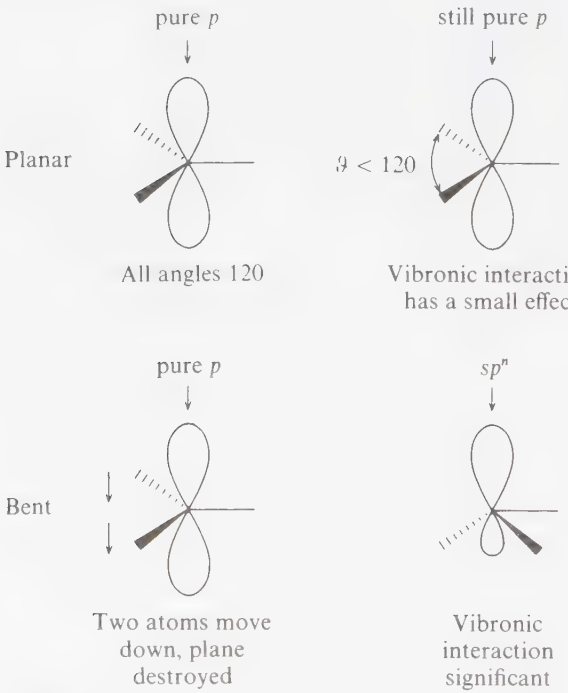

Figure 3.1

The effect of vibronic motion on the hybridization of a *p* orbital.

symmetry plane. In other words, if we put electrons into the free valence orbital the electron density would have to be the same above and below the symmetry plane, since all conceivable interactions on one side of the plane are identical to those on the other side. In effect, *the p orbital remains essentially "pure p" during the planar vibration.* We say negligible vibronic coupling of electronic and nuclear motions occurs during this vibration. Now consider a vibration which *breaks* the planar symmetry of the molecule. Intuitively we expect the "pure p" orbital to change its shape in response to the fact that more electron density (due to the bonds) are on one side of the plane. We say that a *rehybridization* occurs and imagine that the "pure p" orbital begins to take on *s-character*, i.e., *the out-of-plane vibration converts the p orbital into a* sp^n *orbital*, where n is a measure of the "p character" remaining. In the extreme situation $n = 3$, we imagine that the out-of-plane vibration causes a continual $p(\text{planar}) \leftrightarrow sp^3$ (pyramidal) electronic change. We say that a significant vibronic coupling of electronic and nuclear motion occurs due to this vibration.

Although the energy difference of the Zero Order electronic levels and vibronic levels may be small relative to the total electronic energy, the matrix element $\langle H_v \rangle$ may provide a means or a *mechanism* for transition from one vibronic state to another, even though the transition is strictly forbidden in the Zero Order approximation. In other words, from the Golden Rule expression, if $\langle \Psi_1^0 | H_0 | \Psi_2^0 \rangle = 0$ the transition rate equals zero. If, however, $\langle \Psi_1^0 | H_v | \Psi_2^0 \rangle \neq 0$ then according to the "Golden Rule" the transition rate is given by:

$$\text{rate } (\text{sec}^{-1}) = \frac{2\pi}{h} \rho \langle \Psi_1^0 | H_v | \Psi_2^0 \rangle^2 \tag{3.6}$$

Thus, the transition probability would be due entirely to the vibronic coupling of the Zero Order states. We say that vibronic coupling "provides a mechanism" for transition between Ψ_1^0 and Ψ_2^0.

In summary, we have deduced that some, but not all, vibrations are capable of changing the electronic energy of Zero Order "vibrationless" electronic states. From a classical viewpoint, momentum must be transferred from nuclear motion to electronic motion in order for vibronic coupling to occur. In the example discussed above, the "pure p" orbital did *not* undergo a momentum change during the in-plane vibration, but the nonplanar vibration allowed a change in nuclear motion to be accompanied by an exchange of momentum between nuclear and electronic motion. An electron in a "pure p" orbital has different momentum than an electron in a sp^3 orbital, so that conservation of momentum is achievable by coupling the planar $\rightleftarrows$ nonplanar nuclear momentum with the $p \leftrightarrow sp^3$ orbital momentum change.

The Effect of Nuclear Shape and Motion on Transitions between States; The Franck-Condon Principle

Intuitively, we expect that the rate of transitions between vibronic states not only must depend on the similarity of the electronic distributions of the initial and

final state but also on the similarity of the nuclear configuration and motion in the initial and final states. Classically, a transition between two electronic states of different nuclear configuration is viewed in the following terms. Suppose an electron in a diatomic molecule makes a jump from one orbital to another as a result of some external perturbation such as absorption of light or an energetic collision. If the equilibrium separation of the nuclei is the same in the initial (r_i) and final state (r_f), the electron "jump" (which corresponds to an electronic transition) may occur with no restriction with respect to nuclear motion.

Suppose, however, that the final state possesses a much different value for the equilibrium separation of the nuclei, i.e., $r_i \neq r_f$. In order to change r_i to r_f, some type of nuclear motion must occur. Thus, the transition rate depends on the ability of the system to change its nuclear motion. Since the electron jump generally takes of the order of 10^{-16}–10^{-14} sec to occur whereas nuclear motion takes of the order of 10^{-13} 10^{-12} sec to occur, we see that the electron jump is usually *not* rate determining, but nuclear motion change is.

The Franck-Cordon principle states that for the classical electronic transition of a vibrating molecule:

> Since electronic motions are much faster than nuclear motion, electronic transitions occur most favorably when the nuclear structure of the initial and final states are most similar.

An expression of the same idea in classical terms is that electrons, being light particles, have difficulty transferring their angular momentum (due to orbital motion) into linear momentum of the heavier nuclei, i.e., the conversion of electronic energy into vibrational energy may be the rate determining step in an electronic transition between states of different nuclear geometry.

A sharp description of the Franck-Condon would be that (a) for radiative transitions, nuclei *geometries* do not change during the time it takes for a photon to "hit", "be absorbed," and cause an electron to jump; and (b) for radiationless transitions, nuclear *motions* do not change during the time it takes an electron to jump from one orbital to another. We shall see in Chapter 4 that surface crossings remove the Franck-Condon restrictions somewhat for radiationless processes, but that for radiative processes, the principle holds firmly, in the sense of restricting transition probabilities.

3.6 Singlet-Triplet Interconversions[3]

When immersed in a magnetic field $\mathbf{H}$ the magnetic moment due to an electron spin tends to precess about a field of strength $\mathbf{H}_0$ (along a z-axis) with a frequency ω given by:

$$\text{RATE OF PRECESSION} \quad \omega = \pm\tfrac{1}{2}\beta\mathbf{H}_0/h \sim 10^7\,\mathbf{H}_0\,(\text{in gauss}) \tag{3.7}$$

The spin state is represented pictorially as a vector that precesses about a z-axis (direction of $\mathbf{H}_0$) with frequency ω. (see Fig. 3.2). As the field $\mathbf{H}_0$ is made weaker, the precession frequency slows down. *The rate of precession about an axis is directly proportional to the strength of coupling to that axis.* Thus, the magnetic spin vector will "search" for the strongest magnetic field in its sphere of influence and then "associate" with that field by precessing about it. The most important magnetic fields influencing electron spin, from the standpoint of photoreactions, are the magnetic fields which result from the orbital motion of an electron (strength for systems containing C, H, N, and O atoms the field generated is ~ 10–$100\ \text{cm}^{-1}$). From the vector model it is apparent that intersystem crossing from a singlet state to a triplet state and vice versa may result from the occurrence of magnetic torques that either "rephase" one of the spin vectors or "flip" one of the spin vectors.

Visualization of Singlet-Triplet Interconversions: The Vector Model

Figure 3.2 describes a singlet-triplet intersystem crossing in terms of the precessing vector model. First, assume we start in a "pure" singlet state (i.e., $\mathscr{S}_1 = \alpha$, $\mathscr{S}_2 = \beta$ and the vectors are 180° out of phase so that $S = 0$ and $M_s = 0$.) Suppose that $\mathscr{S}_1$ experiences a slightly different magnetic torque about the z-axis than $\mathscr{S}_2$. As a result, $\mathscr{S}_1$ begins to precess faster about the z-axis of some arbitrarily defined

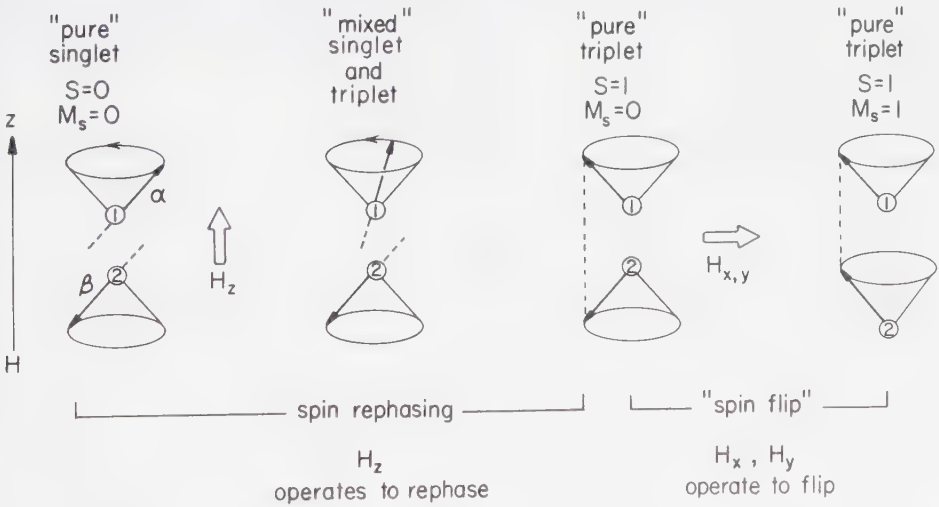

Figure 3.2

Schematic representation of spin rephasing resulting from a different precessional rate of the spin of electron 1 relative to electron 2 about the axis defined by H_z. A magnetic component at right angles (H_x or H_y) to H_z will produce a torque which can flip an electron spin (say, of electron 2) when the "mixed" state has the 0° orientation of spin.

magnetic field **H**. The out-of-phase orientation ("pure" singlet, $-\alpha\beta$) is gradually turned into an in-phase orientation ("pure" triplet, $\alpha\beta$). In other words, the undefined magnetic torque that operates on $\mathscr{S}_1$ causes a "mixing" of $S(M_s = 0)$ and the $T_0(M_s = 0)$ component of the triplet. If now a torque along the x- or y-axis is applied to one or the other of the spin vectors, a "spin flip" can occur to produce either the T_- or T_+ components of the triplet state.

A field from a laboratory magnet cannot effect such an interconversion because it affects both spins equally (i.e., a laboratory magnetic field is homogeneous on a molecular scale). However, a field arising from within the molecule may be able to provide the magnetic torque required to rephase and/or to flip the electron's spin vector, for example, the magnetic torque generated by an electron's orbital motion or the magnetic torques due to other magnetic spins. The former is called *spin-orbit coupling* and the latter *spin-spin coupling*. We shall consider only spin-orbit coupling here, since it is the dominant mechanism for intersystem crossing of organic molecules. We shall consider the spin-spin coupling, which is important as an intersystem crossing mechanism in diradicals, in Chapter 8.

A Primitive Model of Spin-Orbit Coupling[3]

The problem in determining a spin-orbit mechanism for flipping an electron's spin angular momentum is to identify a magnetic torque which can "flip" the magnetic moment vector. In addition, a means of conserving the total angular momentum of the system must be available. The magnitude of the magnetic torque (force) generated by a charged particle will depend on the charge of the particle and its velocity. The strength of a magnetic field caused by an accelerating charged particle has the form

$$\begin{matrix}\text{MAGNETIC FIELD}\\ \text{GENERATED BY AN}\\ \text{ACCELERATING CHARGE}\end{matrix} \rightarrow \mathbf{H}_e = \frac{E\mathbf{X}v}{c} \tag{3.8}$$

where E is the electric field due to the charged particle, v is the velocity of the charged particle, c is the speed of light, and **X** is the vector multiplication.

Since the velocity of motion of the electron is a thousand times faster than that of nuclei, we surmise from Eq. 3.8 that electron *orbital* motion is much more likely to build up a significant magnetic field than is nuclear vibrational motion. The coupling of the motion of one electron spin to another electron spin is not expected to lead to a net change in spin since the total spin momentum apparently must remain constant when this mechanism is operative. We can conclude therefore, that spin-orbit coupling is the most probable *general* mechanism available for intersystem crossing. Spin-orbit coupling provides a magnetic torque (generated by the electron's orbital motion) capable of "flipping" the electron's spin magnetic moment and can also provide a means of conserving total momentum by coupling a spin-flip with a compensating orbital jump. In other words, the momentum change due to the change in spin momentum can be exactly balanced by a change in orbital momentum.

A primitive model for spin-orbit coupling, yet one which provides a rather remarkable amount of physical insight, is available from a consideration of the electron's motion in Bohr-like orbits, each of which has an associated value for orbital momentum.

A classical electron in a Bohr orbit executes two important kinds of motion: it makes circuits about nuclei and it spins about an axis of its own. A moving charged particle generates a magnetic field $\mathbf{H}_e$. Thus, both the orbital motion and the spin motion of the electron generate magnetic fields which pervade the space about the electron. We thus imagine that both the orbital and spin motion of the electron generate *magnetic moments*, which may be visualized in terms of *vectors*. Suppose an electron moves about a nucleus in a Bohr *s* orbit. Such an electron has an associated angular momentum of *zero*. Since the "coupling" of orbital and spin motions requires *exchange* of angular momentum, we do not expect a significant spin-orbit related spin flipping mechanism due to spin-orbit interaction to be available to an electron in an *s* orbit.

Imagine an electron whose trajectory is a "figure-eight" about the nucleus (Fig. 3.3). For simplicity, let us consider a planar analogue. The situation is reminiscent of the harmonic oscillator model for vibrations, i.e., the electron is executing

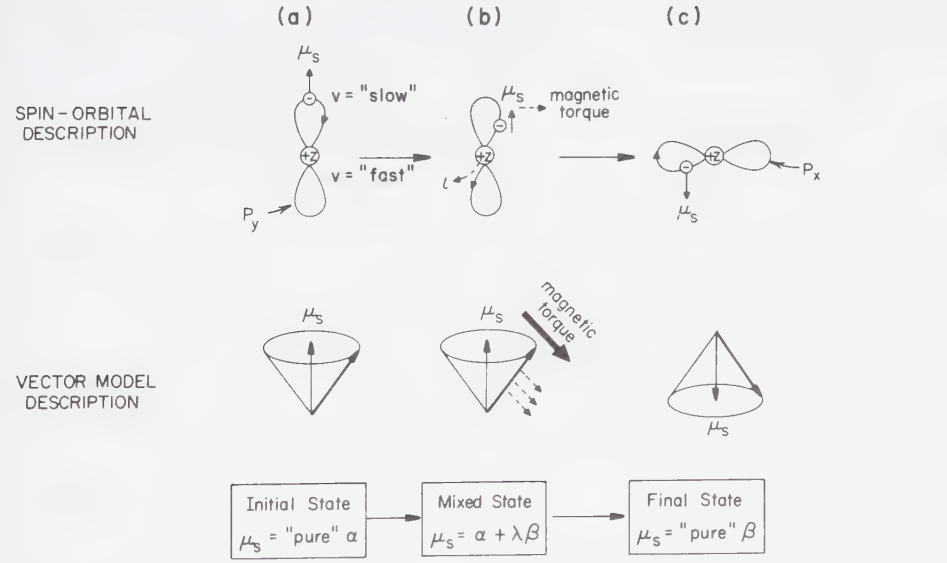

Figure 3.3

An (oversimplified planar) model of an electron in a *p* orbital. We imagine the electron to execute a "figure-8" trajectory about the nucleus. Many of the topological features of a *p* orbital are carried over in this simple representation. An electron executing a "figure-8" trajectory generates a magnetic torque, and a spin flip can occur with a simultaneous orbital momentum change. The lower half of the figure compares the "figure-8" (spin-orbital) model to the vector model.

periodic motion about the nucleus. The turning point (Fig. 3.3a) is evidently the "top" of the orbit when the distance of the electron from the nucleus is greatest. At this point the electron is moving relatively slowly because the restoring force (attraction to the nucleus) is minimal. When the electron approaches the nucleus it must be going at a very high speed since a restoring force accelerates the electron toward the nucleus (Fig. 3.3b). Apparently, the speed of the electron must begin to approach the speed of light (at relativistic velocities) in order to avoid being "sucked" into the nucleus. From Eq. 3.8 it is evident that $\mathbf{H}_e$ is maximal when the electron approaches the nucleus (v is maximal). Since $\mathbf{H}_e$ is a vector quantity, the possibility now exists that $\mathbf{H}_e$ will serve as a *magnetic torque* on μ_s (the electron spin magnetic moment) and tend to flip the electron's magnetic moment vector (Fig. 3.3c). We expect that $\mathbf{H}_e$ will exert a maximum torque on μ_s when the electron is in the region of its orbit close to the nucleus. However, a torque on μ_s is not sufficient to cause the spin flip; total angular momentum in the system must be conserved. This can happen if as the spin momentum μ_s begins to change (dotted line Fig. 3.3b), the orbital angular momentum l begins to change, i.e., the electron jumps from one p orbit to another. In other words, if the initial orbit (p_y, Fig. 3.3a) is orthogonal to the final p orbit (p_x, Fig. 3.3c) there has been a change in the associated angular momentum from l_y to l_x. The *coupling* of the spin angular moment $\mathcal{S}$ to the orbital angular momentum saves the day by allowing the total angular momentum of the system to be unchanged. The change in l exactly compensates the change in $\mathcal{S}$ (i.e., $\mathcal{S}$ goes from α to β and l goes from p_x to p_y).

The following conclusions, relating the magnitude spin-orbit coupling to atomic parameters, are readily drawn from the primitive model given above:

1. The magnitude of energy associated with spin-orbit coupling is given by:

$$E_{SO} = \pm \mathbf{H}_e \mu_s \tag{3.9}$$

i.e., the energy of the magnetic moment μ_s times the magnetic field $\mathbf{H}_e$, generated by orbital motion.

2. The magnitude of E_{SO} should increase, for a given orbit, as Z, the charge on the nucleus, increases, i.e., the accelerating force is proportional to Z.

3. The magnitude of E_{SO} should depend mainly on the atom of highest Z that the electron (whose spin is to be flipped) sees, i.e., the maximal value of $\mathbf{H}_e$ occurs only near the nucleus.

4. Irrespective of the magnitude of E_{SO}, for the spin flip to occur, another angular momentum change must couple with the spin flip, i.e., a $p_x \rightarrow p_y$ transition or its equivalent must occur.

We may generalize these conclusions in terms of spin-orbit rules:

> **Rule 1:** A "$p_x \rightarrow p_y$" effect should be observed (meaning that spin-orbit coupling is most effective) when a p_x to p_y orbital jump is possible during the intersystem crossing.

Rule 2: A "*heavy atom*" effect should occur such that spin flips are most probable if the system contains a "heavy atom" (atom of high value of Z) which is accessible to the electron whose spin is to be flipped.

Rule 3: A "*one-center*" effect should occur such that spin flips are most probable if an atom is available which can accommodate a $p_x \rightarrow p_y$ transition simultaneous with the spin flip.

Examples of the operation of these important rules will be given in later chapters.

References

1. Halliday, D., and Resnick, R., *Physics*, New York: John Wiley, 1967.
2. Robinson, G. W., *Excited States*, ed., Lim, E. C., New York: Academic Press, 1974, p. 1.
3. McGlynn, S. P., Azumi, T., and Kinoshita, M., *Molecular Spectroscopy of the Triplet State*, Englewood Cliffs: Prentice-Hall, 1969, p. 183.

4

Potential Energy Surfaces

4.1 Potential Energy Curves and Potential Energy Surfaces

A molecule in a particular electronic state may exist with various configurations of its nuclei, each configuration in space corresponding to a particular potential energy of the system. A map of the potential energy versus nuclear configuration for a given electronic state is called a *potential energy surface.*[1]

The notion of a surface as a geometrical form (or graph) allows a visualization and provides a method for handling many problems of chemical interest. The goal of this chapter is to show how potential energy surfaces can provide a general basis for a qualitative visualization of molecular energetics, dynamics, and structure.

A two-dimensional energy curve is more readily visualized than an energy surface. The important topological (i.e., qualitative geometric) features of a curve may be generalized to deduce the topological features of surfaces. Thus, we will first discuss *potential energy curves* for a diatomic molecule and then extrapolate the concepts and apply them to energy surfaces. We shall show how the simple notion of potential energy curves may be used to unify the ideas of structure, energetics, and dynamics. In particular, transitions between states (radiative and radiationless) and photochemical reactions can all be visualized under the systematizing and unifying framework of energy surfaces.

4.2 Movement of a Classical Particle on a Surface[2]

An analogy exists between a marble rolling along a curved surface and a "representative point" sliding along a hypothetical potential energy surface. The point represents a specific nuclear configuration. We shall assume that like the marble, which is "held" onto a surface by the force of Earth's gravitational field, the representative point is also "held" onto the potential energy surface by some sort

of force. If the marble leaves the surface as the result of an impulse from some external force, it is always a momentary departure only, because gravity provides a restoring force which quickly attracts the particle back onto the surface. For the analogy to be complete, the same must be true for our hypothetical representative point, i.e., a restoring force must keep attracting it to the energy surface. Before we consider the nature of this restoring force, let us review the behavior of a classical particle (e.g., a marble) on an idealized smooth (frictionless) surface, and then consider the more realistic case of a rough (friction-producing) surface.

The Trajectory of a Marble on a Surface

Figure 4.1 reviews the important features of the trajectory of a classical particle, such as a marble, on a frictionless surface. First, the conservation of energy requires that if the particle is moving on the surface, then only energy exchanges occur. Energy in the form of motion of the particle (kinetic energy, KE) is shuttled into and out of energy in the form of the position of the particle (potential energy, PE). For all points on the surface E (the total energy) equals $PE + KE$. If the particle is motionless at any point on the surface, then for this position $E = PE$, i.e.,

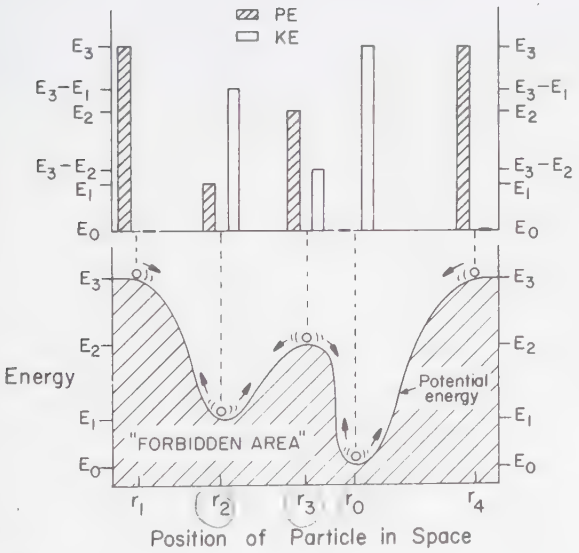

Figure 4.1

Schematic representation of a particle rolling over a surface (bottom). The interchanging kinetic and potential energies (at constant total energy) are shown at the top for different positions of the particle on the surface. The minima r_2 and r_0 correspond to stable (or metastable) "configurations" of the systems, i.e., the $v = 0$ and $v = 1$ vibrational levels. The maxima at r_1, r_3, and r_4 correspond to unstable "configurations" of the system. The minima serve as "attractors" for the particle. Similarly, minima are "attractors" for the representative point traveling over the surface.

$KE = 0$. In Figure 4.1, a schematic representation of the *PE-KE* interchange is shown.

Suppose the marble is placed at a point r on the surface. Gravity operates as a driving force which can "attract" the particle toward the minima at r_2 and r_0. From elementary physics,[2] the magnitude of this force is given by:

$$\begin{matrix}\text{Force acting} \\ \text{on the particle} \\ \text{at } r\end{matrix} \quad F = -dPE/dr \quad \begin{matrix}\text{Slope of the} \\ \text{curve at } r\end{matrix} \tag{4.1}$$

At points r_3, r_2 and r_0, $F = 0$, and at all other points $F < 0$.

We now can see clearly the analogy between a marble sliding along a frictionless surface in the earth's gravitational field and our hypothetical representative point sliding along a frictionless potential energy surface. *The undefined restoring force of our representative point that keeps it "sticking" to the surface is analogous to the force of gravity which "holds" the particle on a surface.* In a molecule, the restoring forces will be associated with the attractive force between electrons and nuclei. The potential energy of our hypothetical point is analogous to the height of a mass above the earth's surface. Points r_2 and r_0 correspond to a mass in a valley, point r_3 corresponds to a mass teetering on the top of a mountain, and points to the left of r_1, and to the right of r_4 correspond to a mass which has left the earth's gravitational field. Because of the physical requirement that $E - PE > 0$, the representative point is not allowed to "drop" below the lowest energy surface. Thus, in Figure 4.1, the shaded region of space *forbidden* to the representative point

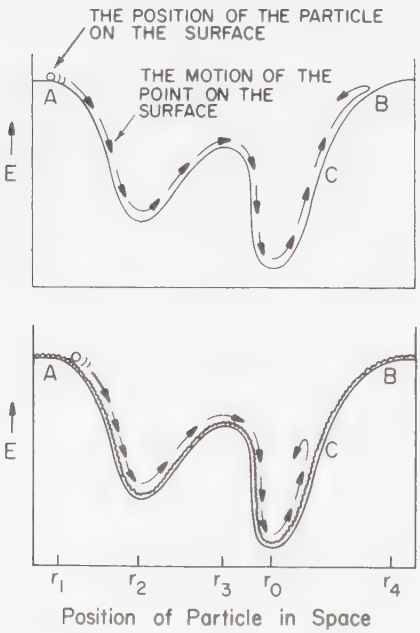

Figure 4.2

The trajectory of a particle on a surface without friction (top) and with friction (bottom). If no energy loss (friction) occurs, the particle will roll back and forth between points A and B (r_1 and r_4) forever. The occurrence of friction ("rough" surface) removes energy from the particle so that it cannot reach point B. Depending on the rate of loss of energy, the particle will be trapped in the first minimum (r_2) or the second minimum (r_0).

corresponds to *negative* potential energy on the earth. This impenetrability would then be analogous to a mass moving along a hard crust on the earth.

Once started on its trajectory, our idealized classical particle would oscillate back and forth over the surface between points r_1 and r_4, i.e., its energy trajectory is completely described as periodic horizontal motion between two end points. A more realistic picture of the motion of the particle considers *frictional forces* which remove energy from the molecule. Since PE is dependent only on position, apparently frictional forces can only remove kinetic energy as the particle travels over the surface, i.e., the particle will slow down.

Energy Sinks and Energy Sources: The Trajectory of a Classical Particle on a Surface with Friction

Suppose now that we obey the law of conservation of energy by means other than shuttling energy back and forth between PE and KE, or that we allow the particle to leave the surface. Imagine for example, that some undefined force sets the particle into a horizontal motion starting from r_1, i.e., the initial force holding the particle at r_1 is removed and motion will start from r_1 (see Fig. 4.2a). In the absence of any other external forces the particle will obey the law of conservation of energy by moving from r_1 to r_4 and then by reflecting off the right-hand portion of the curve back to r_1. As another possibility, imagine that the particle starts its descent *on* the surface, but experiences friction of some sort (Fig. 4.2b). The particle's speed and acceleration are less than they would be if its motion were determined by a frictionless surface. In effect, the friction is an *energy sink* for some of the particle's kinetic energy. *In the case of a molecule, this "friction" or energy sink will correspond to molecular collisions or to molecular vibrations* (Fig. 4.3). If the friction is sufficiently

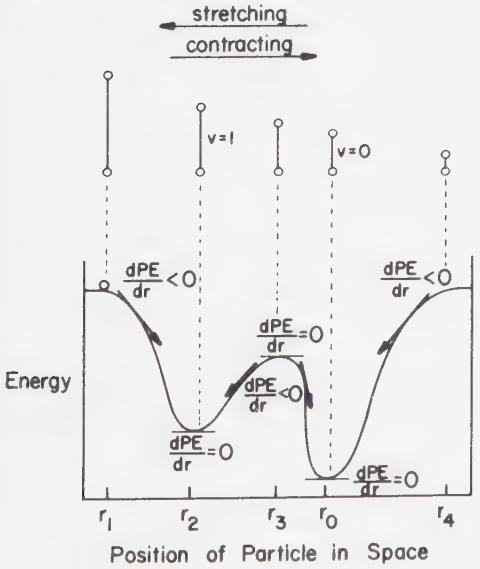

Figure 4.3
Schematic comparison of a particle on a frictional surface and a vibrating molecule.

great, the particle may reach r_2 with insufficient KE (or momentum) to carry it up to and past r_3, i.e., the particle will get "stuck" in the well associated with r_2. The particle will roll back and forth past r_2, continuously losing KE to friction, and eventually come to rest at r_2.

After coming to rest, the particle requires an *energy source* in order to proceed from r_2 to other regions of the energy surface. In the case of a molecule this energy source, like the energy sink, will be associated with molecular collisions and molecular vibrations. If sufficient kinetic energy is available, the particle will pass over point r_3 and eventually come to rest at r_0, the point of lowest potential energy.

The notion of friction allows the law of conservation of energy to be satisfied, even though we do not know in detail to what the friction is due. For molecules, vibrations and collisions (i.e., nuclear motions) often provide the "friction" which allows the total energy of an individual molecule to be conserved.

4.3 Potential Energy Curves and Surfaces for Visualization of Molecular Behavior[3]

We may now extend the ideas derived from considering a classical particle on a surface to assist in visualization of molecular behavior. First we shall consider the classical description of potential energy *curves* for vibrating diatomic molecules. Then we shall introduce the quantum mechanical concepts of *quantization* and vibrational wave functions. We will then be at a level of approximation suitable for qualitative visualization of radiative and radiationless transitions. In Chapters 5, 6, and 7 we will consider radiative and radiationless transitions, and photochemical reactions, respectively, in terms of potential-energy surfaces, but in a quantitative fashion.

4.4 The Quantum Mechanical Version of the Harmonic Oscillator[4]

Solution of the wave equation for a harmonic oscillator yields a set of vibrational wave functions χ. Examination of the properties of these wave functions leads to a picture of the vibrating diatomic molecule —a picture which is strikingly different from the classical harmonic oscillator for low-energy vibrations but which is quite analogous to the classical harmonic oscillator for high-energy vibrations.

The most important results can be conveniently compared by starting with a *classical* potential energy curve and showing how the quantum mechanical model handles the problem of establishing the positions and motion of a pair of bonded atoms X and Y.

For a given electronic configuration (or state) the nuclear wave function χ describes the shape (position in space relative to the electron cloud) and motion of the nuclei, just as Ψ describes the shape (position in space relative to the nuclei) and motion of the electrons. We have discussed the orbital model for visualizing

the electronic portion of a wave function. How can we visualize χ, the vibrational wave function?

Let us consider a diatomic molecule, XY, which is approximated as a *harmonic oscillator*, i.e., the motion of X and Y relative to one another is a periodic function of time. For purposes of visualization we may consider X as being attached to Y by a spring (representing the bond between X and Y) and that both nuclei vibrate back and forth with respect to one another along the bond axis (Diagram a). If one of the two atoms is much lighter than the other (e.g., HCl) nearly all of the motion in space is due to the lighter mass. In this case we can assume the heavier mass to be stationary. In effect, we can consider it to be a "wall" to which the lighter mass is attached by a spring (Diagram b).

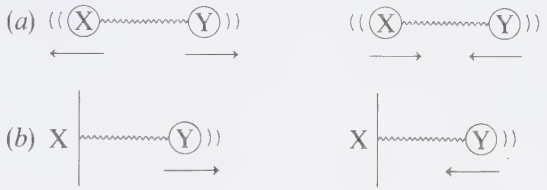

Stretching Contracting

A plot of the potential energy of a vibrating diatomic molecule as a function of internuclear separation is given by the familiar *classical potential-energy curve* (Fig. 4.4). At some particular internuclear separation r_e the potential energy of the system is at a minimum, i.e., at r_e *the nuclei possess their equilibrium configuration.* If the separation is decreased to a value less than r_e, the potential energy of

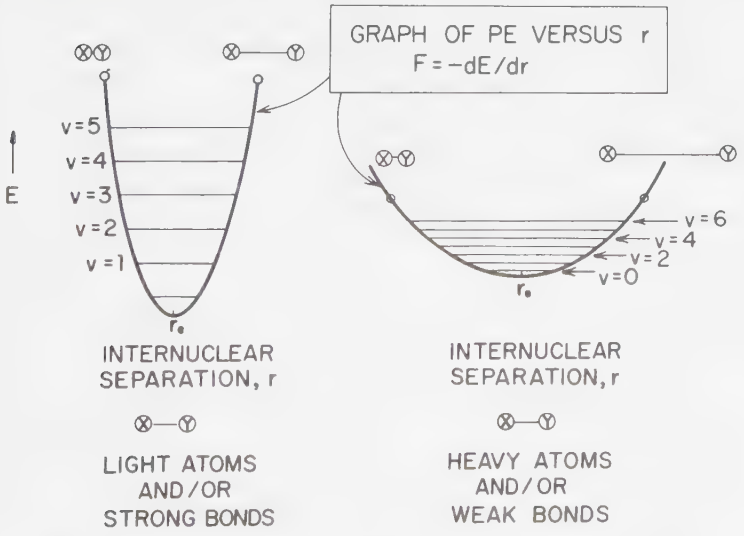

Figure 4.4

Comparison of vibrational spacings for a strong bond (or light atoms) to those for a weak bond (or heavy atoms).

the system increases rapidly as a result of internuclear and electronic repulsions. On the other hand, if the internuclear separation is increased to a value greater than r_e, the potential energy also increases due to the stretching of the X—Y bond (see Fig. 4.4). At the equilibrium position there is no net restoring force operating on the atoms, but at any displacement from r_e a restoring force exists. The restoring force thus varies in *magnitude* and in *direction* in a periodic fashion in equal intervals of times. We see that particles undergoing harmonic motion pass back and forth through a point at which the potential energy of the system is a minimum. Since we will generally be interested in *energy differences* we may arbitrarily define the potential energy minimum as E_0 with $E_0 \equiv 0$.

At any point on the potential-energy curve the molecule experiences a restoring force F which tries to attract the system into the equilibrium geometry. The magnitude of this force, is given by $F = dPE/dr$, i.e., the force is the ratio of the potential energy of the system at any point to the displacement from equilibrium $\Delta r = |r - r_e|$. Notice that this is precisely analogous to the form of the force law operating for the marble on the surface (Eq. 4.1).

The meaning of the term "representative point" may now be more sharply defined. We refer to a particular point on the curve as a "*representative point*" which "follows" the motion, configuration, and energy of the pair of atoms XY. For example, when the point is at r_e, the molecule possesses zero PE (by definition). At any other points on the PE curve for a motionless representative point, the molecule possesses excess potential energy. The molecular structures corresponding to such points are kinetically unstable, i.e., they are attracted toward r_e by restoring forces, just as the classical particle on a downward-sloping surface is attracted toward a potential energy minimum. We expect an initially motionless representative point to spontaneously move toward r_e.

Solution of the Schrödinger equation for a harmonic oscillator obeying Hooke's law ($E = \frac{1}{2}kr^2$) reveals that the energy levels are quantized and given by

$$E_v = h\nu(v + \tfrac{1}{2}) \tag{4.2}$$

where v is the vibrational quantum number (which can take only integral values, 0, 1, 2, . . .), ν is the vibrational frequency of the classical oscillator, and h is Planck's constant.

The important results derived from the quantum mechanical solution for the harmonic oscillator are:

1. Only the *quantized* energy values given by Eq. 4.2 for integral values of v are allowed for the harmonically vibrating molecule.

2. The potential energy of the lowest possible vibration is not zero (as it would be classically) but equal to $\frac{1}{2}h\nu$.

3. The vibrational energy levels are equally spaced above the $v = 0$ level in units of $h\nu$.

4. The mathematical forms of the eigenfunctions, χ_j, which are solutions to Eq. 4.2 for the harmonic oscillator, are useful for determining transition probabilities between vibronic states.

5. Nuclear motion cannot be made to cease, i.e., the nuclei never stops fluctuating about the equilibrium position, so that their average KE can never equal zero.

The amplitude of the corresponding classical vibrational motion is obtained in Figure 4.4 from the intersection of the potential-energy curve with the corresponding energy level. The classical turning points are the positions which define the potential energy—i.e., *at the turning points the total energy of the oscillator is potential energy, because the kinetic energy is zero.* This results from the fact that the total vibrational energy, E, is constant during the stretching and compression motions of the nuclei, but the kinetic energy, KE, and potential energy, PE, are continually changing such that:

$$E_v = PE + KE \tag{4.3}$$

When the nuclei are close to their equilibrium distance, the potential energy of the system is minimal for the vibration; the kinetic energy must therefore be maximal. At points on the curve which correspond to extreme stretching or compression $KE = 0$, since the atoms pause momentarily as the turning point in a vibration is reached, and PE is thus maximal.

The Vibrational Wave Functions for a Harmonic Oscillator[4]

The form of the *vibrational wave functions* for a harmonic oscillator near the geometry of equilibrium separation are very nonclassical and therefore nonintuitive. However, as one goes up the vibrational ladder the behavior of the wave mechanical harmonic oscillator becomes increasingly classical. The mathematical form of the vibrational eigenfunctions χ_v for $v = 0, 1, 2, 3, 4$, and 10 are plotted qualitatively in Figure 4.5 on the permitted (quantitized) energy levels, which are indicated by horizontal lines. The (mathematical) value of χ_v *above* the horizontal line is arbitrarily considered to be positive, the value of χ_v *below* the horizontal line is negative, and the value of χ_v *on* the line is zero. The number of times that χ_v passes through zero equals v, the vibrational quantum number. Although the (mathematical) sign of χ_v is arbitrary, the sign is crucial when we consider that χ_v, a wave function, is not directly related to laboratory observation, but that a *product* of two wave functions is related to laboratory observation, i.e., the *vibrational overlap integral* $\langle\chi\rangle$ is related to the probability of transition between two different vibrational states.

$$\int \chi_i \chi_j \, d\tau = \langle \chi_i | \chi_j \rangle \equiv \langle \chi \rangle \tag{4.4}$$

The *probability* function χ_v^2 where $i = j$ represents the probability of finding the nuclei at a given value of r during vibration in a given level. By examining Figure 4.5 it can be seen that there is a finite, non-negligible probability that the atoms will vibrate outside of the region defined by the classical potential-energy curve. The probability of finding the nuclei at a given separation is peculiar for upper vibrational levels in that, in addition to the broad maxima of the probability distribution in the vicinity of the classical turning points, a number of maxima

(for $v > 1$) exist in between. Although the behavior of the harmonic oscillator is "peculiar" relative to the classical model for small values of v, as we go to higher and higher values of v, the quantum mechanical situation approximates the classical situation more closely (Bohr's correspondence principle)—i.e., the atoms tend to spend more time near the turning points of vibration and very little time in the region about $r = r_e$.

The probability distribution curve for the $v = 0$ level in Figure 4.5 contrasts dramatically with the classical picture. Instead of two turning points, one broad probability maximum at $r = r_e$ exists. Classically, the vibrational state of lowest energy corresponds to the state of rest (point r_e in Fig. 4.5), which is *impossible* for the quantum mechanical model, since the position and velocity of this state would then be exactly defined (a violation of the uncertainty principle). *Most radiative and radiationless transitions in condensed phases originate from thermally equilibrated vibrational states, which means that the $v = 0$ level will be of great importance in organic spectroscopy and photochemistry.*

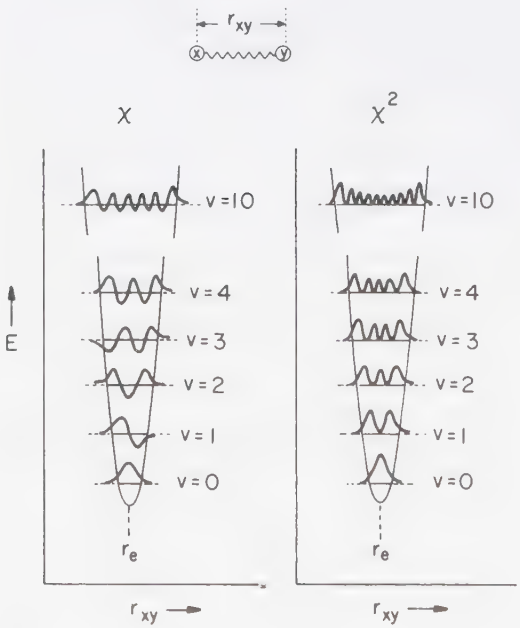

Figure 4.5

Quantum mechanical description of a vibrating molecule. Superimposed on the various levels ($v = 0, 1, 2, \ldots$) are the vibrational eigenfunction (χ)—left-hand curves—and the square of the vibrational eigenfunctions (χ^2). The mathematical sign of the function oscillates from positive to negative values except for the χ of $v = 0$, which is positive everywhere. The positive portions of χ are indicated as portions of the curve above the line representing the energy of the vibrational level. The greater the number of nodes in χ, the greater the kinetic energy of the vibrational level. The values of χ^2 are proportional to the probability of finding the nuclei XY at a corresponding separation r_{xy}.

We can now transfer reversibly and smoothly from the classical description of a "dynamic" representative point moving on the surface to the quantum description of a "static" probability of finding the nuclei in a certain region of space with a given motion.

The Anharmonic Oscillator[4]

The harmonic oscillator approximation fails for nuclear geometries corresponding to severe compressions or severe elongations of the XY bond. For example, when a bond has been extended to, say, 2 or 3 times its normal length (from 1–2 Å to 5–6 Å) the atoms X and Y experience very little "restoring" force, i.e., the bond is essentially broken. For an ideal harmonic oscillator, the restoring force increases indefinitely and smoothly with increasing or decreasing distance from the equilibrium position (see Figs. 4.4 and 4.5). In a real molecule the potential energy will rise more gradually than predicted by $PE = \frac{1}{2}kr^2$, because of weakening of the X—Y bond at large r, as is shown in Figure 4.6 for the HCl molecule. Eventually the potential energy reaches a limiting value as the restoring force disappears, and the bond breaks. This corresponds to the dissociation energy of the molecule and is represented by the asymptote in Figure 4.6. If the energy of the system just corresponds to the asymptote, the atoms at a great distance from one another will have zero velocity. Above the asymptote their kinetic energy (which is essentially continuous) is increased. On the other hand, compression of the nuclei results in a more rapid increase in potential energy than is predicted, because of the sudden rise of coulombic repulsions with decreasing nuclear separation.

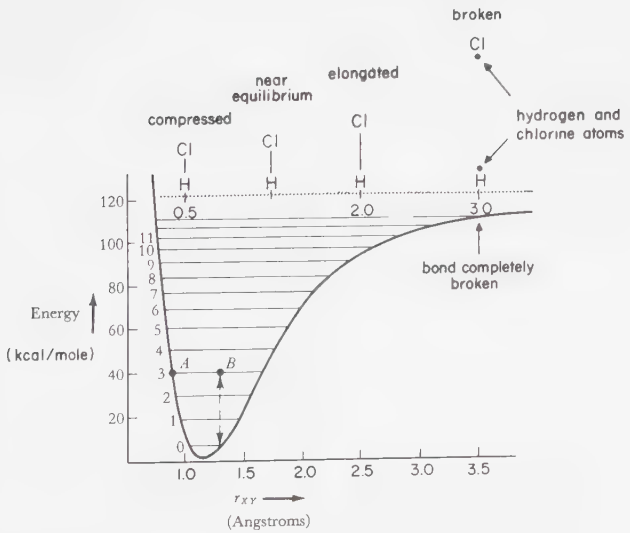

Figure 4.6

Potential curve for the ground state of HCl.

Recall that the sum total energy of the system equals the sum of the kinetic and potential energy. For example, in the $v = 3$ vibration level, the anharmonic oscillator shown in Figure 4.6 possesses 40 kcal/mole^{-1} at a point A (all potential energy), while at point B the system possesses about 35 kcal/mole^{-1} of kinetic energy and 5 kcal/mole^{-1} of potential energy (relative to an arbitrary energy of zero for the lowest point in the curve).

The vibrational levels, although quantitized, are not equally separated for the anharmonic oscillator. Their separation *decreases* slowly with increasing v, as shown in Figure 4.6. For example, for HCl the energy separation between $v = 0$ and $v = 1$ is about 12 kcal mole^{-1}, while the energy separation between $v = 10$ and $v = 11$ is only about 5 kcal mole^{-1}.

Extension of the Ideas of Potential-Energy Curves to Potential-Energy Surfaces[3]

For a two-atom system, we speak of a potential-energy *curve* rather than *surface* because the nuclear coordinate is simply a vibration. For a polyatomic molecule, the situation is very much more complicated and a polydimensional surface would be required to describe even the rather elementary organic molecules. Simplifying assumptions are therefore required, e.g., we can replace the concept of a group of nuclei with the notion of a *center of mass*, a representative point that moves with the same characteristics as a single particle. The center of mass of a system is known, from elementary physics, to depend only on the masses of the particles of the system and their positions *relative* to one another. When a complicated array of bound particles (the nuclei of a molecule) moves under the influence of external forces, the center of mass moves in the same way that a single particle subject to the same external forces would move. The concept of the center of mass point allows us to visualize in a simple way an energy trajectory of a complex system of particles executing very complicated motions.

For the remainder of this text we shall assume that the qualitative (topological) features of potential-energy curves may be generalized to include potential-energy surfaces.

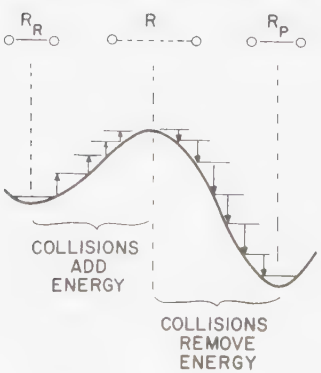

Figure 4.7
The effect of collisions on the motions of a molecule. Collisions provide an energy source and an energy sink to move the representative point along an energy surface.

4.5 The Influence of Collisions and Vibrations on the Motion of the Representative Point

Consider the effect of collisions on a molecule in solution. Such collisions may be considered as impacts which a molecule experiences as a result of being in a solvent. The magnitude of these impacts depends on temperature, varies over a wide distribution of energies, and follows a Boltzman distribution—i.e., near room temperature the average energy per impact is $\sim RT = 0.6$ kcal/mole. The separation between individual available energies associated with collision is nearly continuous. Thus, near room temperature, collisions can be considered to provide a reservoir of energy which will match, without much difficulty, vibrational energy gaps.

Figure 4.7 schematizes the effects of collisions on movement along a potential-energy surface from one minimum to another. Suppose the reactant starts with a nuclear configuration in which a reacting bond has an internuclear separation equal to R_R. Collisions serve as an energy source and move the reactant along the energy surface to a maximum (transition state). Further movement along the surface toward the product requires *removal* of energy, i.e., the collisions serve as an energy sink as the system moves from R_R to R_P.

As a prototype system, let us consider the effect of collisions on the nuclear motion of a diatomic molecule. Consider Figure 4.8, which shows how the tra-

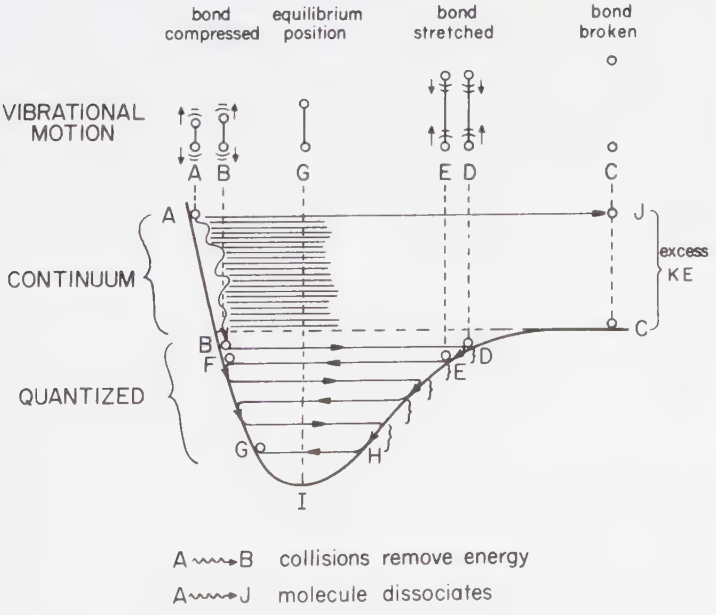

Figure 4.8
Schematic representation of the effect of collisions on a diatomic molecule.

jectory of the center of mass is affected by the occurrence of *quantized* vibrations. We suppose that an anharmonic *PE* curve describes the vibration. If the molecule starts at point A, it experiences a restoring force which spontaneously begins to move the center of mass toward point I, the position of minimum *PE* at which $F = dPE/dr = 0$. Along the curve between points A and B, the vibrational states are essentially *continuous* and the system behaves *classically*. Collisions act like frictional forces which rapidly remove the excess vibrational energy from the molecule; this allows the center of mass to follow a trajectory close to that defined by the *PE* curve. In Figure 4.8 this path is schematized as a curved line leading from A to B. Near point B, vibrations become quantized and it is now possible to take up energy from the environment as quantized packets of vibrational energy. In the absence of energy-removing collisions, the center of mass of the molecule thus may proceed from near point A to J rather than continue downward toward F. If this is the case, the molecule will have *dissociated* into fragments.

Suppose that from near point B the molecule proceeds to point D, which corresponds to a *bound* portion of the *PE* curve. A collision could drive the molecule up the curve toward C or down the curve to E. If the latter occurs we might expect the molecule to begin its vibratory motion toward F. Since the motion between E and F is correlated by a chemical bond, we would expect that motion to be more probable than the motion induced by external random collisions. The process of collisions and energy removal is imagined to continue as shown in Figure 4.8 until the center of mass reaches point H. The molecule will then begin to execute zero point motion about the equilibrium separation I.

For simplicity, an energy-conserving vibration is shown as a horizontal arrow (say, connecting B and D, E and F, H and G). This picture is related to the quantum mechanical description of a vibration in terms of χ^2, i.e., only the probability of finding the nuclei at a given position of r for a given total energy is defined. In terms of a classical description, we would imagine the representative point *oscillating* on the surface between B and D (E and F, H and G, etc.). There would be an *implied KE* associated with the point. Referring back to Figure 4.1, if the point started at r_1 and then accelerated along the frictionless surface to r_2, when the point reached r_2 it would possess *KE* equal to $E_3 - E_1$. This *KE* would be sufficient to carry the point over the maximum at r_3 to r_0. When it arrived at r_0 it would have its maximum $KE = E_3 \quad E_0$. This *KE* would be just sufficient to carry it to r_4. Upon reaching r_4 it would pause momentarily and start to slide down the surface toward r_0 and so on.

4.6 Transitions between Potential-Energy Surfaces[3]

In principle, some reactions cannot be interpreted in terms of the motion of the system along *one* fixed potential-energy surface. A *nonadiabatic* reaction is a reaction in which a transition from one electronic potential-energy surface to

another occurs during the reaction. All photoreactions which lead to stable ground-state molecules are nonadiabatic reactions, since light absorption places them on an excited-state surface. But since a product on a ground-state surface is observed, a transition between two electronic surfaces must have occurred at some point.

In terms of photochemical systems, nonadiabatic transitions may be discussed in terms of two broad, distinct classes:

1. *Radiative nonadiabatic transitions*, e.g., fluorescence and phosphorescence.

2. *Radiationless nonadiabatic transitions*, e.g., internal conversion, intersystem crossing, and most photoreactions.

Nonadiabatic transitions must obey the Franck-Condon principle, such that the initial and final nuclear geometries must be very similar. In effect, a "chemical reaction" (in the sense of drastic change in nuclear configuration) never occurs via a radiative nonadiabatic transition. However, many, if not most, photochemical reactions involve radiationless nonadiabatic transitions as a key step, which affects either the reactivity and/or efficiency of the reaction.

In the following section we shall show how radiative and radiationless transitions may be visualized in terms of "jumps" between energy surfaces and how the probabilities of these jumps may be related to molecular structure via classical or quantum mechanical models.

4.7 The Franck-Condon Principle and Radiative Transitions: A Classical Model[5]

A readily visualized classical model of the Franck-Condon principle during a radiative transition between two states is this: suppose that the potential-energy curves for the ground and excited states of a diatomic molecule occur as shown in Figure 4.9. Let the molecule be represented as a vibrating ball attached to a string, which in turn is affixed to a wall. This would be analogous to a light atom bound to a much heavier one. Most of the motion of the two atoms is due to the movement in space of the lighter particle.

The geometry produced on the upper surface by the transition is governed by the relative positions of the upper and lower energy curves. If the curves were of the same shape, and one lay directly over the other (Fig. 4.9a), the transition would be from the minimum of the ground surface to the minimum of the excited surface, i.e., electronic transition would occur without vibrational excitation. In general, we may regard the transition as occurring from the *most probable* nuclear configuration of the ground state —which is the static, equilibrium arrangement of the nuclei. The electronic transition occurs, and during it the nuclei do not change their arrangement. At the completion of the electronic transition the nuclei are static, but in a new force field because of the new electronic distribution. They

therefore begin to move, and vibrate away from and back to their initial arrangement (Figs. 4.9b and 4.9c). *It follows that the original arrangement is a turning point of the new motion, and that vibrational energy is stored by the molecule.*

This new motion of the molecule may be described in terms of a *representative point*, which follows the potential-energy curve from its initial point of formation to another point, which is the other vibrational extreme. The *velocity* of motion of the point depends on its excess kinetic energy.

A line drawn vertically from the initial ground state intersects the upper potential-energy curve at the point which will be the turning point in the excited state. The line also shows how much energy is absorbed in the transition, since the energy of a harmonic oscillation is constant; what potential energy is lost as the spring decompresses is turned into kinetic energy, which is used to recompress the spring. Therefore the potential energy at the turning points, E_{vib}, determines the energy at all displacements for that mode of oscillation.

Let us now consider the effect of quantization on the classical model for radiative transition.

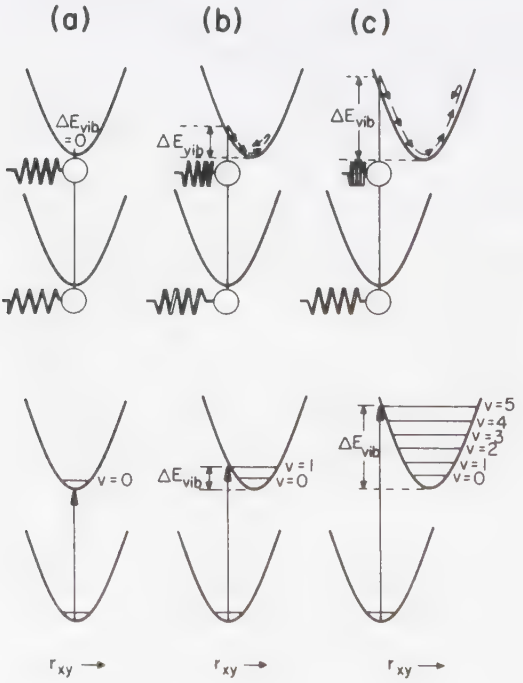

Figure 4.9

A mechanical analogue to the Franck-Condon principle for radiative transitions. The motion of a point representing the motion of the vibrating atoms is shown as a sequence of arrows. These arrows indicate the motion of the representative point on the curve.

A Classical but Quantized Model of Radiative Transitions

The major difference between the classical system and the quantum system is that the quantum system cannot possess an energy of 0 but must possess an energy of E_v or larger, due to the irrepressible zero-point motion imposed on microscopic systems by the uncertainty principle and by quantization. The *trajectory* of the point representing the molecule on the curve is imagined to oscillate back and forth between A and B. Everywhere along the trajectory $E_v = PE + KE$. Near r_0, the classical equilibrium position, $E_v \cong KE$ and $PE \cong 0$. Near A and B, $E_v \cong PE$ and $KE \cong 0$ (Fig. 4.10).

Without specific consideration of spin type, let ψ^0 represent a ground-state surface and ψ^* represent an excited-state surface. In ψ^0 the zero-point motion is between points A and B, whereas in ψ^* the zero-point motion is between points J and K. If we consider the zero-point motion of ψ^0 only, we see that for a semiclassical system (i.e., a classical system except for quantization), absorption *must* occur when the molecule possesses internuclear separations whose values vary between A and B. From a classical standpoint, the nuclei are most likely to be found near points A and B since these correspond to classical turning points for the vibration, and the nuclei are either at rest or moving very slowly near A and B.

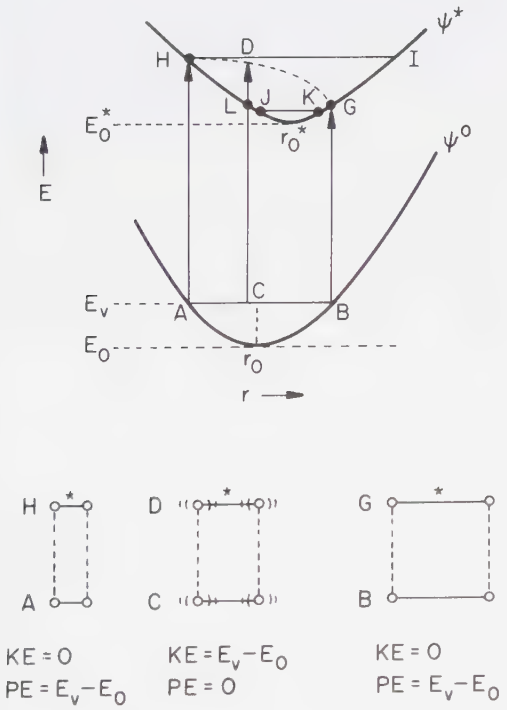

Figure 4.10

Two-surface semiclassical representation of a radiative transition and the Franck-Condon principle.

A radiative transition is an abrupt event in which a collision of a photon with the electrons of a molecule causes a sudden electron jump, leaving the nuclei behind as *spectators* to the event, i.e., the Franck-Condon principle operates. This means that the magnitude KE of the nuclei should be the same just before and just after the electron jump. In other words, the action of light in the act of absorption is to raise the electronic energy without changing the position or velocities of the nuclei relative to one another. In Figure 4.10 there are two points for which $KE = 0$ on the ψ^0 curve, namely points A and B. The corresponding vertical points H and G would be reached by absorption which originated from A or B respectively. If a transition were to occur when the molecule had an equilibrium geometry near r_0, absorption would carry the system to point D, whose energy is slightly lower than point H. The reason for this is that, since $E_v \sim KE$ near r_o and since when the molecule is excited it arrives on the ψ^* surface with the same kinetic energy it had in ψ^0, the energy gap LD must equal the zero-point energy E_v. At any point associated with the energy curve the kinetic energy of the nuclei is given by the difference between the ordinate of the point and the curve. Thus, the distance LD equals the distance from r_o to the horizontal line AB. The dotted line from H to G indicates the locus of the "allowed" radiative transitions based on the Franck-Condon principle, i.e., KE is exactly the same just before and just after excitation (lower half of Fig. 4.10).

In terms of absorption probability, the strictly classical picture with zero-point motion between A and B would allow for absorption to occur from ψ^0 to any point on the upper surface along the dotted line HDG. However, quantum mechanics requires that the transition must generate ψ^* in a quantized vibrational level. Thus, only transition A → H is possible, since a vertical transition from the ground state at all other points either requires a change in KE or produces a nonquantized state.

In practice, the vibrational level HI is not very sharply defined for a typical organic molecule in solution. The vibration typically will interact with other vibrations and be subject to interactions with colliding molecules. The net effect is to replace a sharp absorption between A and H with a spread of absorptions. We would expect, however, that a *maximum* in absorption will occur and correspond to the sharp line absorption expected in the idealized model.

If the molecule becomes thermally equilibrated in ψ^*, the nuclei find themselves acted upon by electronic forces other than in ψ^0. As a result their frequency of vibration (ν) and equilibrium positions r_0^* of ψ^* will be different from that in ψ^0. In general ν will be *slower* and r_0^* will be *longer*. The bond lengthening is expected from the occurrence of an antibonding electron in ψ^*, and the lower frequency of vibration results from the weaker bonding force which holds the atoms together. Usually, the *shape* of the excited-state curve will be flatter than that of the ground-state curve, again because looser bonding implies smaller values of ν and longer stretches are possible in ψ^* relative to ψ^0.

The zero-point motion of ψ^* is defined by the level between points J and K. Notice that a smaller zero-point energy is indicated for ψ^* than for ψ^0. The smaller zero point energy is often associated with a shallower potential energy (see also Fig. 4.4). By arguments similar to those discussed above we expect absorption to

be most probable from points near A or B, and emission to be most probable from points near J or K.

A Quantum Mechanical Interpretation of Radiative Transitions: The Overlap Principle

In quantum mechanics, the classical concept of the precise position of nuclei in space and associated motion is replaced by the concept of a nuclear or *vibrational wave function*, χ, which "codes" the nuclear configuration and momentum but is not as restrictive in confining the nuclear configurations to the regions of space bound by the classical potential-energy curves. In classical mechanics we considered that electronic transitions require a similar nuclear configuration and momentum in the initial and final states at the instant of transition. In quantum mechanics the requirement becomes the *net positive overlap* of the wave functions in the initial and final states at the instant of transition. This overlap is given by the *Franck-Condon integral* $\langle \chi_i | \chi_f \rangle$. The probability of any electronic transition is directly related to the *square* of the vibrational overlap integral, i.e., $\langle \chi_i | \chi_f \rangle^2$, which is called the *Franck-Condon factor*.

The Franck-Condon factor *governs* the relative intensities of vibrational bands in electronic absorption and emission spectra. In radiationless transitions the Franck-Condon factor is also important in the determination of the rates of transitions. Since the value of $\langle \chi_i | \chi_f \rangle^2$ parallels that of $\langle \chi_i | \chi_f \rangle$, we will generally consider the integral itself rather than its square. The larger the difference in the vibrational quantum numbers i and f, the more likely it is that the *shape* and *momentum* of the initial and the final state are different, and the more difficult is the transition. Indeed, this is exactly the result anticipated from the Franck-Condon principle. In other words, the product $\langle \chi_i | \chi_f \rangle$ is related to the probability that a state ψ_i will have the same shape and momentum as ψ_f. The Franck-Condon overlap integral is analogous to the electronic overlap integral $\langle \psi_i | \psi_f \rangle$, i.e., poor overlap means weak interactions and slow transition rates.

Consider Figure 4.11, which is a schematic representation of the quantum mechanical basis of the Franck-Condon principle for radiative transitions. Ab-

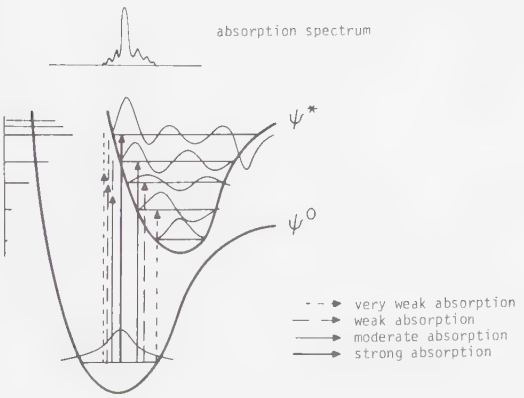

Figure 4.11
Quantum mechanical interpretation of the Franck-Condon principle.

sorption is assumed to initiate from the $v = 0$ level of ψ^0. The most likely radiative transition from $v = 0$ of ψ^0 to a vibrational level of ψ^* will correspond to the transition for which χ_0 and χ_i^* is maximal. As shown, this corresponds to the $v = 0$ to $v = 4$ transition. Other transitions from $v = 0$ to vibrational levels of ψ^* will occur, but with lower probability, as shown. A possible resulting absorption spectrum is shown.

The same general ideas will apply to emission, except the important overlap is then between χ_0 of ψ^* and the various vibrational levels of ψ^0.

4.8 The Franck-Condon Principle and Radiationless Transitions: Analogy to a Vibrating Spring[5]

The Franck-Condon principle induces a preference for "vertical" jumps between surfaces for the representative point of a molecular system. The same principle *prohibits* certain vertical jumps in radiationless processes (between surfaces separated by large energy gaps) and favors other vertical jumps (at Zero Order surface crossings). The connection between the quantum mechanical interpretation of radiationless transitions in terms of $\langle \chi_i | \chi_f \rangle$ and the motion of the representative point of a potential-energy surface may now be made.

Consider Figure 4.12. Suppose a molecule starts off on an excited surface ψ^* and during its zero-point motion it makes the trajectory from A to B on the

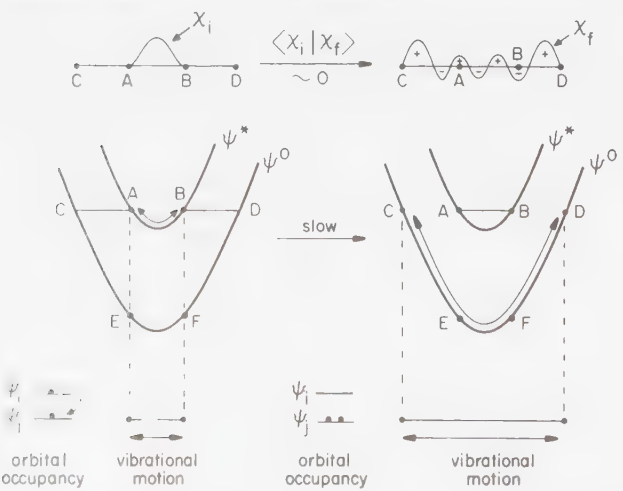

Figure 4.12

Visualization of the quantum mechanical basis for a slow rate of radiationless transitions.

surface. Classically, a "jump" to the lower surface will require an abrupt change in geometry (i.e., a horizontal "jump" from B → D or A → B) or an abrupt change in kinetic energy (a "vertical" jump from A → E or B → F). The net result of either jump is that the vibration of the molecule will abruptly change from a placid, low-energy vibration between points A and B to a violent, high-energy vibration between points C and D. Both the positional and momentum characteristics of the vibration have suffered drastic change. Electrons resist drastic changes in orbital motion or spatial location; nuclei resist drastic changes in their vibrational motion of spatial geometries. Visually, the wave function χ_i (plotted above the classical curve representing the initial excited state, ψ^*) is drastically different in form (positive everywhere, no node) from that of ψ^0 (highly oscillatory).

The vertical jump from ψ^* to ψ^0 may be thought of as one for which a rate-limiting electron perturbation occurs first and *promotes* the transition from ψ^* to ψ^0. Nuclear motion is now suddenly controlled by the ψ^0 surface rather than ψ^* and *acceptor* vibrations must now be found to soak up the excess potential energy associated with the jump. The horizontal jump may be regarded as one for which a rate-limiting nuclear geometry perturbation occurs first and *promotes* the transition from geometry A → C (or B → D). Electronic motion then suddenly switches from that of ψ^* to that of ψ^0. The vibration which brings ψ^* from A → C (or B → D) may also act as an acceptor of the excess energy. The horizontal jump is related to quantum mechanical "tunneling," and can be interpreted as being due to the very small overlap of χ_i and χ_f outside the regions of the classical potential-energy surfaces.

In Figure 4.13, the situation for surface noncrossing and crossing are compared. The poor overlap of the vibrational wave functions of ψ^0 and ψ^* for a molecule

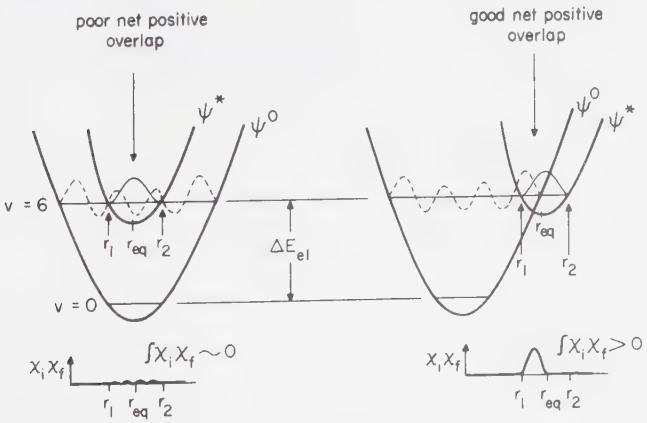

Figure 4.13

Schematic representation of situations for poor (left) and good (right) net positive overlap of vibrational wave functions. The value of the integral $\chi_i\chi_f$ as a function of r is shown at the bottom of the figure.

in the lowest vibrational level of ψ^* for the noncrossing situation contrasts with the significant overlap for the crossing situation.

In both cases, χ_i corresponds to the $v = 0$ level of ψ^* and χ_f corresponds to the $v = 6$ level of ψ^0. The *amount* of electronic energy (ΔE_{el}) that must be converted into vibration energy and the vibrational quantum number (v) of the state produced by the transition are the same for both transitions. Nevertheless, the radiationless transition on the right will occur much faster than the radiationless transition on the left because $\int \chi_i \chi_j$ (right) $\gg \int \chi_i \chi_j$ (left). We say that the radiationless transition on the left (no surface crossing) is *Franck-Condon forbidden* (i.e., the Franck-Condon factor $\langle \chi_i \chi_j \rangle$ is ~ 0), whereas the radiationless transition on the right (surface crossing) is *Franck-Condon allowed* (i.e., the Franck-Condon factor $\langle \chi_i \chi_j \rangle > 0$).

We conclude that, with respect to the Franck-Condon factors, a radiationless transition from ψ^* to ψ^0 will be very slow for the disposition of curves shown on the left of Figure 4.13 relative to the disposition on the right.

4.9 Visualization of "Chemical" versus "Physical" Mechanisms of Radiationless Transitions[6]

Generally, the occurrence of unimolecular radiationless transitions such as internal conversion and intersystem crossing may be inferred from quantum yield measurements (Chapter 6, Section 6.) The observation of *no net reaction* after absorption of a photon is a common experimental observation. It is possible, however, that reversible photochemistry, rather than photophysical radiationless transitions is responsible for the reaction inefficiency. By *photophysical radiationless transitions* we mean the more or less *vertical* jumps which occur from minima on excited surfaces to minima in S_0. Often the same minima are involved in spectroscopic transitions, and correspond to the Zero Order equilibrium nuclear geometry of the ground state, S_0. By *photochemical radiationless transitions* we mean the horizontal pathways which lead to a primary photoproduct. The photoproduct then finds a pathway to return to S_0.

The distinction between "physical" and "chemical" radiationless transitions can become blurred, but the pathways followed on the energy surfaces can still remain sharply defined. Consider the three surface situations shown in Figure 4.14. Below each pair of surfaces an energy diagram is shown for comparison.

In case (a), light is employed to take the representative point from the ground state of S_0 surface (equilibrium geometry) to the excited state surface (postulated to have an equilibrium geometry similar to R). Thermal energy then propels the representative point (which follows the dotted line) over an energy barrier to a new minimum, which corresponds to the equilibrium geometry of P^*. Emission then occurs from P^* to P. Because the two surfaces are "far apart" for all geome-

tries experienced by the representative point, radiationless transition to S_0 is unlikely everywhere along the reaction coordinate. Commonly, energy barriers separating reactant geometry from product geometry are *smaller* on the excited surface for the *same reaction coordinate*. In case (a), if the excited-state barrier is too high for the representative point, emission from R^* to R would occur instead of emission from P^* to P.

In case (b) an excited surface and a ground surface approach one another at some geometry intermediate between that of R and P. Near this geometry, radiationless jumps to S_0 are favored. However, with respect to the maximum on the S_0 surface we can imagine jumps leading to geometries "to the left" (return to R and a net *photophysical* process) or "to the right" (formation of P and a net *photochemical* process. For case (b), it is clear that the terms photophysical and photochemical may become blurred when one is discussing processes occurring for the nuclear geometries in which the two surfaces *come close*.

As a third example, in case (c) we suppose that the jump from the excited surface puts the representative on the ground surface with a *large excess of thermal energy*. As a result the minimum on the ground surface (corresponding to an intermediate on the ground surface) cannot "hold" onto the representative point and the latter escapes from the minimum (corresponding to the vertical jump) to a second minimum corresponding to P. We suppose that by the time the representative point reaches P its excess energy has been removed (say, by collisions with atoms in its environment) and eventually settles into the $v = 0$ level of P.

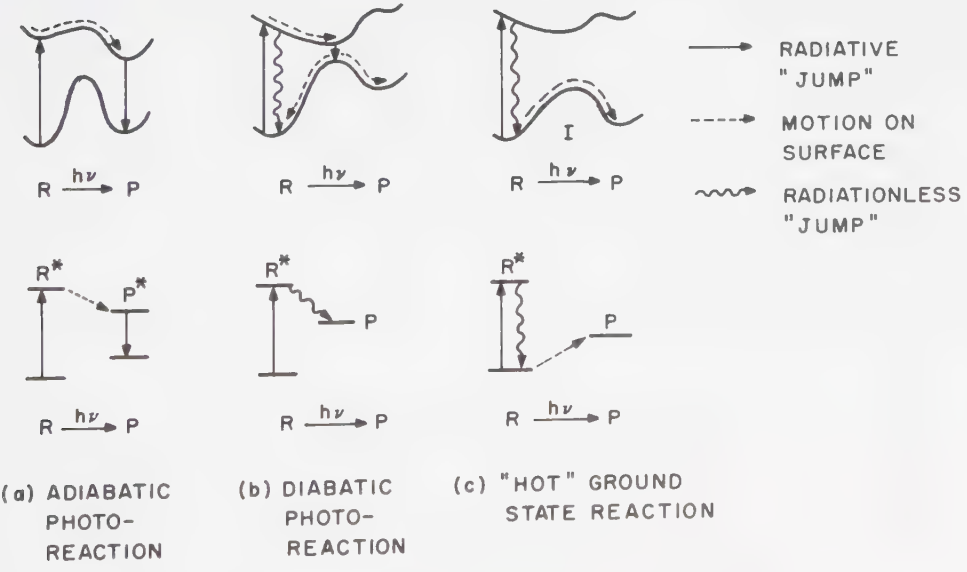

Figure 4.14

Classifications of photoreactions in terms of surfaces: (a) adiabatic photoreaction; (b) diabatic photoreaction, and (c) "hot" ground-state reaction.

Cases (a), (b), and (c) are respectively termed *adiabatic* photoreactions, *diabatic* photoreactions, and "*hot*" *ground-state* reactions. The terms adiabatic and diabatic refer to whether reactions occur *completely* on an excited surface or *partly* on a ground surface. Thus, a hot ground-state reaction is a special case of a diabatic photoreaction.

It appears that most organic photoreactions conform to case (b). As a result, a knowledge of both photophysical and photochemical radiationless processes is crucial for an understanding of the molecular photochemistry of organic compounds. Of special importance is knowing when surfaces "get close" and what mechanisms are available to allow the representative point to make its jump to another surface.

Classically, we may view radiationless transitions as occurring from a "hole" or "funnel" in an upper surface at critical molecular geometries. When the representative point must search for a considerable time for the correct geometry required for a surface jump (thermal equilibrium), we speak of a "hole" on the excited surface at that geometry. When the representative point makes a surface jump nearly every time it achieves a certain geometry, we speak of a "funnel" on the excited surface at that geometry.[3]

How does one predict where "holes" and "funnels" are likely to occur on excited surfaces? Since this topic is discussed in detail in Chapters 6 and 7, we simply note here that radiationless surface jumps are favored at geometries for which (a) the initial and final surfaces come "close" to one another, (b) the initial and final states have similar electronic characteristics, and (c) the initial and final states experience strong spin-orbital coupling to one another (for jumps involving a change in electronic spin).

In summary, the following features of the surfaces are of particular interest to a photochemist:

1. The location of the minima in S_0, S_1, and T_1.
2. The location of maxima in S_0, S_1, and T_1.
3. The interactions (relative to the zeroth-order model) which cause the separation of the surfaces.
4. The geometries for which two surfaces come "close together."

4.10 Summary and Prospectus

The goal of this chapter has been to provide a qualitative understanding of the concept and use of potential-energy surfaces. We have seen both how reactions on a single surface and how radiationless transitions between surfaces can be visualized. We can usually approximate an electronic state in terms of a single configuration for nuclear geometries near the minima of an energy surface which is well separated from other surfaces. When two surfaces come close together, cross,

or touch, the one-configuration approximation of an electronic state may break down. If it does, radiationless transitions from one electronic state to another (jumps between surfaces) may occur. Radiative transitions between surfaces allow us to visualize the factors related to molecular shape which might influence the probability of radiative transitions.

Our next task is to proceed from this qualitative description of transitions to a more quantitative one. We shall first discuss the highly developed theory of radiative electronic transitions in Chapter 5, and then the theory of radiationless transitions in Chapter 6. In both cases we shall not be concerned with deviations of nuclear geometry which are too far from the equilibrium nuclear configuration. In Chapter 7 we shall outline how the more drastic nuclear motions which occur in chemical reactions may be correlated to electronic states via potential energy surfaces.

References

1. For an elementary discussion of energy surfaces, see: Dewar, M. J. S., and Dougherty, R. C., *The PMO Theory of Organic Chemistry*, New York: Plenum, 1975.
2. For an elementary discussion, see: Halliday, D., and Resnick, R., *Physics*, New York: John Wiley, 1967.
3. For a discussion of surfaces in photochemical reactions, see: Michl, J., *Molec. Photochem.*, *4*, 243 (1972); *Photochem. Photobio.*, *25*, 141 (1977); *Topics in Current Chemistry*, *46*, 1 (1974); *Pure Applied Chem.*, *41*, 507 (1975); Devaquet, A., *ibid.*, *41*, 535 (1975); *Topics in Current Chemistry*, *54*, 1 (1975); Salem, L., et al., *J. Am. Chem. Soc.*, *97*, 479 (1975); Dauben, W., Salem, L., and Turro, N. J., *Acc. Chem. Research*, *8*, 41 (1975); Salem, L., *J. Am. Chem. Soc.*, *96*, 3486 (1974).
4. Herzberg, G., *Spectra of Diatomic Molecules*, Princeton, N.J.: van Nostrand, 1950.
5. Atkins, P., *Quanta: A Handbook of Concepts*, Oxford: Clarendon Press, 1974, p. 78.
6. Förster, T., *Pure Appl. Chem.*, *24*, 443 (1970).

5

Radiative Transitions—The Absorption and Emission of Light

5.1 Absorption and Emission Spectra of Organic Molecules

The electronic absorption and electronic emission spectra of a molecule provide important information concerning the structure, energetics, and dynamics of electronically excited states. From knowledge of the $S_0 + h\nu \rightarrow S_1$ and $S_0 + h\nu \rightarrow T_1$ absorption processes, and of the $S_1 \rightarrow S_0 + h\nu$ and $T_1 \rightarrow S_0 + h\nu$ emission processes, a fairly complete "static" state-energy diagram can often be deduced. From measurements of the lifetimes of S_1 and T_1 and of the efficiencies of emission, the dynamics of the photophysical and photochemical pathways available to S_1 and T_1 can be deduced.

The organic photochemist is generally not interested in rigorous mathematical interpretations of spectroscopic data. He more commonly seeks a pictorial standpoint from which to understand light absorption and emission so that he can relate spectroscopic measurements to state properties via correlations of observations and molecular structure. He would like to derive state electronic configurations, state nuclear geometries, state multiplicities, and state energies by setting up rules or a protocol that translates spectral data into "pictures" of structures. In order to do this, he must employ a theory relating state properties to observables. We shall see that the state electronic configuration and state multiplicity are often readily inferred from measurements of the absorption (or emission) probabilities. State nuclear geometries are more difficult to obtain, but in favorable cases they can be derived from analysis of the vibrational structure of absorption and emission spectra. State energies are readily derived from the onset of absorption (lowest energy transition observed) or emission (highest energy transition observed).

5.2 Typical Experimental Absorption and Emission Spectra of Organic Molecules

In initiating a photochemical study of an organic molecule, the photochemist usually will first measure the electronic absorption and emission spectra of the starting materials (solutes, solvents, reaction vessels). Typically, unsaturated organic molecules possess several absorption bands in the "photochemical" region, 200 - 700 nm. Saturated organic compounds are generally "transparent" in the region 200 - 700 nm. These limits of the photochemical region are set at the short wavelength extreme by technical considerations (quartz glass and organic solvents transmit little light of wavelength less than 200 nm) and at the long wavelength extreme by theoretical considerations (electronic excitation of organic molecules usually requires light of wavelengths shorter than 700 nm).

Although absorption of light resulting in electronic excitation is a completely general experimental observation, the observation of emission of light is not. The efficiency of light emission (Section 5.7) may be too low to be detected experimentally. For example, most saturated organic molecules and polyenes do not display efficient emission.

A *chromophore* is defined as an atom or group of atoms that serve as a unit in light absorption. A *lumophore* is an atom or group of atoms that serve as a unit in light emission. Typical organic chromophores and lumophores are C=C, C–O, and aromatic groups.

Table 5.1 lists the longest-wavelength absorption bands (maximum) and extinction maxima of some typical organic chromophores, and assigns an electronic transition to the band. We shall postpone discussion of emission parameters until Section 5.7, but wish to point out here that the latter vary widely as a function of molecular structure.

Table 5.1 Long-Wavelength Absorption Bands of Some Typical Organic Chromophores

Chromophore	λ_{max} (nm)	ε_{max}	Transition type
C—C	<180	1000	σ, σ^*
C—H	<180	1000	σ, σ^*
C=C	180	10,000	π, π^*
C=C—C=C	220	20,000	π, π^*
Benzene	260	200	π, π^*
Napththalene	310	200	π, π^*
Anthracene	380	10,000	π, π^*
C=O	280	20	n, π^*
N=N	350	100	n, π^*
N=O	660	200	n, π^*
C=C—C=O	350	30	n, π^*
C=C—C=O	220	20,000	π, π^*

Why is there such a variation in absorption and emission parameters? How is an orbital configuration assigned to a given absorption or emission band? How are experimental absorption and emission parameters related to theoretical quantities? Are the processes of absorption and emission related mechanistically?

In order to answer these questions we shall devise a pictorial model of light absorption and emission that relates molecular structure (electronic, nuclear, and spin configurations) to spectroscopic parameters. We shall start by developing a simple model of light and its interaction with the electrons of molecules.

5.3 The Nature of Light: Electromagnetic Waves and Oscillating Electric Dipoles[1,2]

A common pictorial description of light is that of an electromagnetic wave (Fig. 5.1). This wave may exert electric and magnetic forces on charged particles (e.g., electrons and nuclei) and on magnetic dipoles (e.g., electron and nuclear spins). We can view light as mapping an electric and magnetic force field into the neighborhood of space about its direction of propagation. In this neighborhood of space, two vectors can be drawn: an electric vector, $\mathscr{E}$, which represents an *electro-*

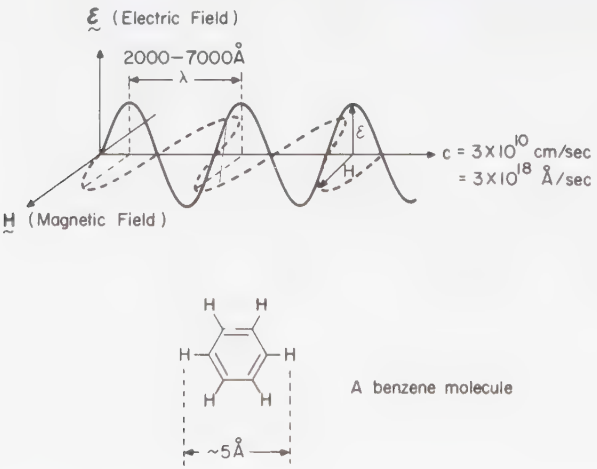

Figure 5.1

An electromagnetic wave. The electric field ($\mathscr{E}$) is imagined to be in the plane of the page and the magnetic field (**H**) is imagined to be perpendicular to the plane of the page. The wave front is propagated at c, the velocity of light (3×10^{10} cm/sec). The value of $\mathscr{E}$ varies with time according to the expression $\mathscr{E} = \mathscr{E}_0 \cos 2\pi\nu t$, where t = time, $\mathscr{E}_0$ is some fixed value of the electric field, and ν is the frequency of the wave (the number of oscillations made past a single point per second). Note that the "size" of a small organic molecule (e.g., benzene) is much smaller than one wavelength.

static force, and a magnetic vector, **H**, from which a *magnetic force* can be evaluated. The magnitudes of $\mathscr{E}$ and **H** at any point in space vary as a function of time from positive (attractive) to negative (repulsive) values. A stationary spectator measuring the magnitude of $\mathscr{E}$ (or **H**), as the wave passes, would thus record oscillating values as a function of time. A test electric charge in space would be set into "oscillation" by the oscillating values of $\mathscr{E}$. To both the spectator and the test charge, the light wave appears to have the characteristics of an *oscillating electric dipole.*

Like an oscillating electric dipole, a light wave generates a time-dependent *force field* **F**, whose frequency of oscillation is related to that of dipole oscillation. An oscillating dipole generates an electromagnetic wave, and this wave (a pattern of electric forces) can set other dipoles into oscillation at the same frequency. *The key idea in understanding the interaction of light with molecules is that electrons may be set into motion by the oscillating electric field of light, i.e., the excited electron behaves as if it were an oscillating dipole.* As an oscillating dipole, an electron may emit energy as radiation. We can thus visualize the interaction of light by molecules as a process in which energy is exchanged between a collection of oscillating dipoles (electrons) and a radiation field (an oscillating electric field). *The oscillation of the dipoles corresponds to the movements of electrons in bonds relative to positively charged nuclei in matter, i.e., electrons oscillate about the nuclear framework of molecules.*

A Mechanistic View of the Interaction of Light with Molecules

The interaction between light and a molecule depends on *resonance*, in which the oscillations of one system (i.e., an undulating light wave) are coupled by some mutual interaction which causes the oscillation of a second system (e.g., the electrons of a molecule). Strict requirements exist for the attainment of effective resonance. They are: that the systems interact, and that the law of energy conservation is satisfied:

$$\Delta E = h\nu \tag{5.1}$$

Here, ΔE is an energy gap between two electronic states of a molecule, h is Planck's constant, and ν is the frequency of oscillation of the light wave. This condition is imposed on molecules by the *quantized* nature of electronic states. In the classical model of light absorption, the *maximum* rate of energy absorption from a light wave occurs at resonance. Light absorption by a molecule is an "all or nothing" proposition.

According to Equation 5.1, the possible interactions of light and a molecule will depend on the *energy gap* (or *frequency*) of oscillations possible for the electrons of the molecule. Typically, the frequencies at which electrons in bonds oscillate back and forth between various nuclei fall in the range 10^{15}–10^{16} sec^{-1} (see Section 1.5). These frequencies correspond to those of light with wavelength in the "photochemical" range of 200–700 nm, i.e., in the ultraviolet and visible regions of the spectrum. Therefore, we expect that a resonance interaction of light whose

wavelength is 200 to 700 nm with molecules is possible and if it occurs it will tend to set the electrons of the molecules into oscillation. How does the light wave do this?

Imagine a light wave passing a stationary molecule.[3] The wave causes electrical and magnetic disturbances in the region of space through which it passes (Fig. 5.2). The force **F** exerted on an electron in a molecule by the light wave is given by:

$$\begin{matrix}\text{Total force exerted on an electron by a light wave}\end{matrix} \rightarrow \mathbf{F} = \underset{\substack{\uparrow \\ \text{Electrical force}}}{e\mathscr{E}} + \underset{\substack{\uparrow \\ \text{Magnetic force}}}{\frac{e[\mathbf{H}v]}{c}} \tag{5.2}$$

where, e is the charge of an electron, $\mathscr{E}$ the electric field strength, **H** the magnetic field strength, v the velocity of an electron, and c the speed of light. From this equation it can be seen that since the speed of light (3×10^{10} cm/sec) is much greater than the possible speed of a moving electron ($v_{max} \sim 10^8$ cm/sec), the magnitude of $e\mathscr{E}$, in general, will be considerably greater than that of $(e/c)[\mathbf{H}v]$ so that the force on an electron (ignoring magnetic interactions) may be approximated by:

$$\begin{matrix}\text{Force on electron ignoring magnetic interactions}\end{matrix} \mathbf{F} \cong e\mathscr{E} \tag{5.3}$$

In other words, *the major force operating on the electrons of a molecule in consequence of a passing light wave is that due to the undulating electric field* $\mathscr{E}$. *The interaction of electrons with the undulating magnetic interaction,* **H**, *is negligible.* Consider the electric force, $\mathscr{E}$, as it interacts with the electrons bound to the nuclear framework of a stationary molecule. As the light wave passes, the electrons of the molecule experience an electrical disturbance, caused by the repulsive and attractive forces of the undulating electric field of the light wave. At any given point in the

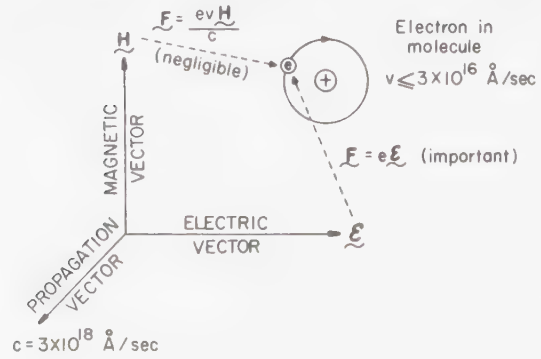

Figure 5.2
Interaction of the electric field **E** and the magnetic field **H** of an electromagnetic wave on an electron in an orbit about a nucleus.

electron cloud of the molecule, the electric field strength due to the light wave will vary as a function of time, i.e., it may start at a value of zero, build up to an (attractive) maximum, decrease to a value of zero and then begin to produce a field opposite to the previous one, build to a (repulsive) maximum, decrease to a value of zero, then start the cycle all over again. The net effect of these interactions is to generate a transitory dipole moment in the molecule due to the interaction of $\mathscr{E}$ and the electrons. The situation is analogous to changing the charge on two electrical plates and noting the effect of this oscillation of electrical potential on charged particles between the plates. To understand this analogy we must briefly introduce the concept of polarizability.

Polarizability and the Transition Moment[4]

Polarizability (α) is defined as the magnitude of the induced dipole moment (μ_i) generated in a molecule by an electric field $\mathscr{E}$ of unit intensity, i.e.,

$$\alpha = \mu_i/\mathscr{E} \tag{5.4}$$

Suppose that a field $\mathscr{E}$ is imposed on a molecule and that the electrons behave as an elastic fluid which is constrained spatially by the positive charge of the fixed nuclear framework of the molecule. For simplicity let us consider the interaction of one electron and $\mathscr{E}$. Initially ($\mathscr{E} = 0$), the electron is held, on the average, at some distance r from the center of "electrical gravity" of the molecule. When $\mathscr{E} > 0$, a displacing force $\mathscr{E}e$ will cause the electron to select a new equilibrium distance different from the original distance by the amount $\delta\mathbf{r}$. The new electronic distribution is related to the induced dipole moment (also called *transition dipole*) by:

$$\mu_i = e\delta\mathbf{r} \tag{5.5}$$

We are now in a position to see how the effect of the $\mathscr{E}$ vector of the light wave may be compared to the effect of two charged plates on an electronic cloud. Consider the behavior of a molecule under the influence of an external electric field between two charged plates, such that the centers of positive and negative charge (which are assumed to coincide in the absence of a field) are displaced (Fig. 5.3). The molecule is said to become polarized by the electric field; and a

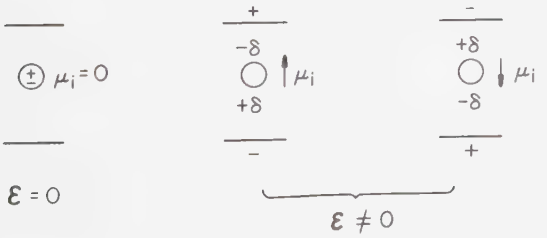

Figure 5.3
Induction of a dipole moment by an electric field.

transitory dipole moment, μ_i, is *induced* by the external field. An important general relation between μ_i and $\mathscr{E}$ is that *the direction of the induced dipole is always parallel to the direction of the external field.* We shall now develop an analogy between an induced or transition dipole moment generated by two charged plates and an induced or transition dipole moment generated by a light wave.

A Pictorial Representation of Light Absorption and Emission[5]

As an example of the absorption of light, let us consider two simple chemical species, namely an atom and a diatomic molecule. The lowest energy state of a *hydrogen atom* is the 1*s* state, which is spherically symmetrical about the nucleus. A higher-energy electronic state is the 2*p* state, which possesses a nodal surface containing the nucleus. We can represent the absorption of light by a hydrogen atom as shown in Figure 5.4. The oscillating electric field of the light wave operates as a vector force on the electron. Its interaction with the electron cloud "reshapes" the electron distribution and causes the conversion of the 1*s* state to the 2*p* state. Note that the latter state is usually represented as the *time average* of the oscillating state.

An electron in a *p* orbital possesses an average electronic distribution above and below a nodal plane. A topological view of an electron in a *p* orbital is available via a representation that views the electron as rapidly oscillating from side to side across the nodal plane (Fig. 5.4). This model brings to mind a *vibration* of a particle. Thus, when a light wave interacts with a hydrogen atom in its 1*s* state (no node, therefore no vibration) absorption sends the electron into vibratory motion (one node, corresponding to the lowest excited vibration).

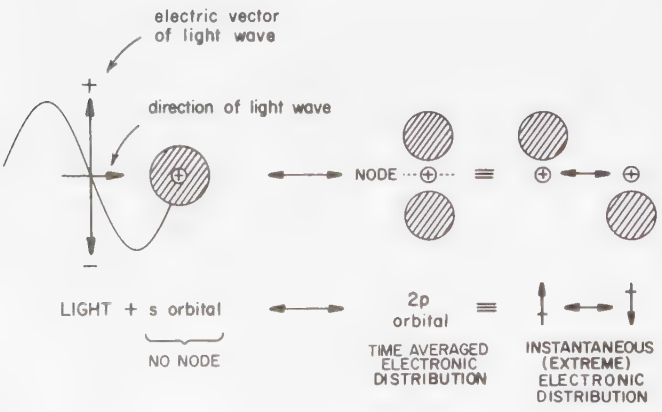

Figure 5.4

Pictorial representation of light absorption by a hydrogen atom. The light wave and the 1*s* state of hydrogen are in resonance with the 2*p* state. The latter may be represented as time-averaged (in which case the electron cloud is dumbbell-shaped) or as an oscillating dipole.

In Figure 5.4, a light wave is shown (assumed to be polarized with its $\mathscr{E}$ vector in the plane of the paper). Suppose this wave is of the proper frequency to interact with the hydrogen molecule in its $1s$ state. This interaction can lead to absorption of energy from the light wave and accompanying excitation of the atom. The excited atom possesses an electron in a p orbital, the nodal plane of the p orbital being at right angles to the electric vector direction. This picture suggests that the electron is set into vibration selectively along the electric vector direction. Absorption of polarized light initially leads to an atom with a polarized (anisotropic) electron distribution, i.e., only one of the three p orbitals is selectively excited.[5]

According to Figure 5.4 the electron cloud of a $2p$ electron is imagined to be an oscillating dipole whose time-average spatial distribution is the same as that of the electronic shape of the $2p$ orbital. The node of the newly generated p orbital is parallel to the propagation vector of the light wave. The p orbital may be viewed as a wave form which vibrates up and down through a plane containing the nucleus—i.e., an electron in a p orbital may be viewed as an oscillating charge. The conversion of the s orbital shape to a p orbital shape develops a node in the electron's wave form (s has no nodes, p has one). *An increase in the number of nodes describing an electron's orbital is an essential part of light absorption. A decrease in the number of nodes of an electron's orbital is an essential part of light emission.* The requirement that light absorption must occur with the generation of a node and that light emission must occur with the disappearance of a node in the electron cloud may be viewed as a symmetry selection rule. The light wave (or loosely speaking, a photon contained in the light wave) possesses a node since the values of $\mathscr{E}$ and **H** oscillate from negative to positive values. The essence of this property must be preserved during and after light absorption or emission. The detailed manner in which it is accomplished is to generate or destroy nodes in the electron cloud.

The *strength* of the interaction between an electron and $\mathscr{E}$ (when the resonance condition is satisfied) is related directly to the ability of the electron to "follow" the light wave and to the magnitude of the maximal charge separation effected by the interaction of $\mathscr{E}$ and e. The magnitude of development of charge separation as one proceeds from the s orbital to the p orbital is related to the *transition dipole moment*, μ_i (Eqs. 5.4 and 5.5). The fundamental requirement for absorption or emission of light may now be given in terms of the simple model discussed above:

1. The transition between orbitals must generate a node (absorption) or destroy a node (emission).
2. The transition dipole moment, μ_i, must be finite.

In diatomic molecules, the notion of s and p orbitals is replaced with that of σ and π orbitals. In the simple case of H_2 the absorption of light converts an electron in a σ orbital, which is cylindrically symmetric about the bond axis and possesses no node, into a π orbital, which possesses a node along the bond axis (Figure 5.5), or into a σ^* orbital, which possesses a node perpendicular to the bond axis.

In the ground state the hydrogen molecule possesses an electron in a 1σ orbital. The latter orbital is cylindrically symmetric about the internuclear axis. The nuclear

axis imbues the molecule with an inherent polarity and one can imagine electronic oscillations of two types:

1. Parallel to the bond axis.
2. Perpendicular to the bond axis.

Notice that both of these oscillations are analogous to the $1s \rightarrow 2p$ transformation of atoms. The major difference is that two symmetry-distinct oscillations are possible for the molecule. Generation of an electric oscillation parallel to but above and below the bond axis corresponds to a $\sigma \rightarrow \pi$ transition (Fig. 5.5, upper drawing). During the oscillation there is always a low probability of finding the electron between the nuclei (we say that a "nodal" plane contains the bond axis). Generation of an electric oscillation along the bond axis (Fig. 5.5, lower drawing) corresponds to a $\sigma \rightarrow \sigma^*$ transition, and during a vibration there is always a low probability of finding the electron midway between the nuclei (we say that there is a nodal plane *perpendicular* to the bond).

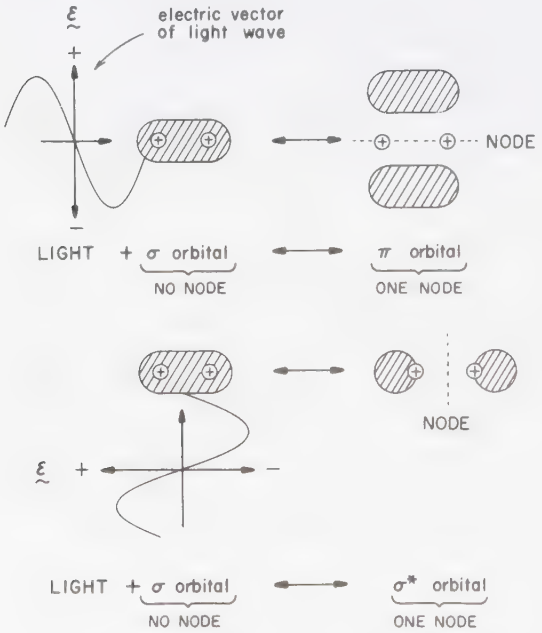

Figure 5.5

Pictorial representation of light absorption by a hydrogen molecule positive ion. The light wave and the 1σ state have two possible resonances. One interaction of the electric field (upper drawing) drives the electron into oscillations perpendicular to the bond axis; the other interaction (lower drawing) drives the electron into oscillations along the bond axis.

5.4 Light as a Stream of Particles: Photons[5]

For a number of qualitative aspects of the interaction of light with molecules, we can consider a pictorial representation of light as a stream of particles (photons), rather than as an electromagnetic wave. A "hybrid" model of light in which the flight of a photon is *guided by a wave motion* is also possible. The concept of a photon as a particle implies the possibility of considering the photon as a "reagent." This reagent may "collide" and "react" (be absorbed) with molecules. We may consider a beam of light of frequency ν and energy $N h\nu$ (N = Avogadro's number, $h\nu$ = energy) as being composed of N photons, each of which possesses the energy $h\nu$. Each photon of wavelength $\lambda = c/\nu$ carries an energy $h\nu$, and a linear momentum $h\nu/c$. *Low frequency (long wavelength) photons carry little energy and momentum; high frequency (short wavelength) photons carry a great deal of both.*

Photons may be viewed as *chiral* reagents in that they may possess a "handedness" analogous to that of optically active molecules. A photon possesses angular momentum. *The existence of left-and-right-circularly polarized light is a manifestation of this angular momentum.* A beam of circularly polarized light passing through a quartz crystal (which itself has a right or left "chirality") causes the crystal to acquire an angular momentum and turn. In any absorption or emission process, the photon and the molecule "exchange" angular momentum and the total system of photon-plus-molecule experiences no net change in angular momentum. The fact that a photon possesses an angular momentum is the basis of the selection rule for creating or destroying nodes in the electron cloud of a molecule as the result of absorption or emission of light. Perhaps the most convincing evidence for the chirality of photons is the observation that racemic mixtures may be resolved if one enantiomer of a d, ℓ pair absorbs circularly polarized light more efficiently than the other enantiomer, and if a reaction follows the act of absorption.[6]

It is possible to evaluate the "cross section" which a molecule presents for being "struck" by the photon. By "cross section" we mean the volume of space around a molecule which is accessible to being struck by the photon. If we view the molecule as a target of a given area, then the extinction coefficient ε (units cm^{-1}/M) for absorption is given by:[5,7]

$$\varepsilon \cong 10^{20} a = 10^{20} d^2 \tag{5.6}$$

where a (or d^2) is the area or cross section of the molecule in cm^2. Experimentally the maximal value of $\varepsilon_{\max} \sim 10^5\ \text{cm}^{-1}/\text{M}$, we calculate $a_{\max}$ to be

$$a_{\max} \sim \frac{10^5}{10^{20}} = 10 \times 10^{-16}\ \text{cm}^2 \sim 10\ \text{Å}^2 \tag{5.7}$$

According to this evaluation, *the largest cross section of an individual chromophore is of the order of one or two bond lengths.*

If we view light as a photon we can calculate the "flight time" of the photon past a molecule. Let us suppose that the molecule has an effective cross sectional diameter of ~ 3 Å. The "flight time" of the photon past the molecule will be

$$\tau \sim 3 \times 10^{-8} \text{ cm}/3 \times 10^{10} \text{ cm/sec} \sim 10^{-17} \text{ sec} \tag{5.8}$$

The fastest nuclear motions commonly encountered in organic molecules are C—H stretching vibrations, which occur at a rate of $\sim 10^{14}$ sec^{-1}. Thus, only 10^{14} sec$^{-1} \times 10^{-17}$ sec, or 10^{-3}, of a vibration is experienced as the photon flies past. Although no quantitative exactitude can be drawn from this calculation, it serves to show that the nuclei are effectively stationary in space as the photon passes.

Relationship of Experimental Spectroscopic Quantities to Theoretical Quantities[4]

Two key experimental quantities related to absorption and emission of light are the extinction coefficient for absorption (ε) and the rate of decay of emission (k_e^0). For simplicity, let us assume that emission is the only pathway for excited state deactivation. How do these experimental quantities relate to theoretical qualities of light?

According to the laws of quantum mechanics (Section 2.2) any experimental quantity may be considered in terms of a theoretical quantity, a matrix element (i.e., for transitions between states):

$$\underset{\text{transition rate}}{\text{Experimental quantity:}} \quad P \rightarrow \langle \Psi_i | H | \Psi_f \rangle^2 \quad \underset{\text{matrix element}}{\text{Theoretical quantity:}} \tag{5.9}$$

Our question may now be rephrased as: to what states of a molecule do Ψ_i and Ψ_f correspond, and what is the nature of the operator H? If we know Ψ_i, Ψ_f and have identified an appropriate operator H, we can then proceed to evaluate the matrix element given in Eq. 5.9. We may set up the calculation of a matrix element such that the result allows us to evaluate ε or k_e^0. If we let $k_e^0 \equiv 1\ \tau_e^0$, we immediately know the decay time of emission τ_e^0 if we know k_e^0, the rate of decay of emission, and vice versa.

The results of the classical theory of light absorption,[4] which considers electrons as charges which can oscillate in specified ways along the molecular framework,[4c,8] can be related to Eq. 5.9. The important terms we need in this connection are *oscillator strength*, f, transition dipole moments, μ_i, and *transition probabilities*, P. First we shall show the connection between the oscillator strength and transition probability, and then we shall connect the concept of transition probability to an explicit form of Eq. 5.9.

The Oscillator Strength Concept[4,5]

If an electron bound to a nuclear framework possessed "perfect" oscillating properties, then according to classical theory the excitation probability of this

electron would be said to have an oscillator strength, f, of unity. Suppose that the excited electron is approximated as a one-dimensional oscillator,[4c] i.e., an oscillating dipole. For this simple case, from classical theory, the *theoretical quantity* of the oscillator strength f in the classical theory of light absorption is related to the *experimental* quantity (the extinction coefficient ε of absorption) by the expression:[4]

$$\underset{\text{strength}}{\text{Theoretical oscillator}} \quad f \equiv 4.3 \times 10^{-9} \int \varepsilon \, d\bar{\nu} \quad \underset{\text{absorption}}{\text{Experimental}} \tag{5.10}$$

where ε is the experimental extinction coefficient and $\bar{\nu}$ is the energy (in wavenumbers) of the absorption in question.

Experimentally, $\int \varepsilon \, d\bar{\nu}$ is the quantity of area under a curve of the molecular extinction coefficient plotted against wavenumber (e.g., Fig. 5.14). Values of f calculated from Eq. 5.10 are found to vary greatly (from values near 1 to 10^{-10}). One of the major failings of the classical theory of light absorption was its inability to provide an adequate basis for understanding the wide observed variation in f.

The rate constant, k_e^0, for emission (probability per unit time), according to classical theory, is related to the extinction coefficient for absorption[8] by:

$$\underset{\text{constant}}{\text{Radiative rate}} \quad k_e^0 = 3 \times 10^{-9} \, \bar{\nu}_0^2 \int \varepsilon \, d\bar{\nu} \cong \bar{\nu}_0^2 f \tag{5.11}$$

where $\bar{\nu}_0$ is the energy corresponding to the maximum wavelength of absorption, and the integral $\int \varepsilon \, d\bar{\nu}$ is the same as that given in Eq. 5.10. We can see that the probability of light absorption as measured by f is directly related to the experimental extinction coefficient, ε.

The Relationship between the Classical Concept of Oscillator Strength and the Quantum Mechanical Concept of Transition Dipole Moment Integral

According to classical theory,[4,5] f is related to the square of the induced dipole moment μ_i produced by action of a light wave on an electric dipole:

$$\underset{\text{strength}}{\text{Oscillator}} \quad f \propto \mu_i^2 = \langle e\mathbf{r} \rangle^2 \quad \underset{\text{dipole moment}}{\text{Transition}} \tag{5.12}$$

where μ_i is the induced transition dipole moment or *dipole strength* corresponding to the electronic transition. The latter quantity may be set equal to $e\mathbf{r}$, where $\mathbf{r}$ is the dipole length. Quantitatively the expression relating f and μ_i is given by

$$f = \left(\frac{8\pi m_e \bar{\nu}}{3he^2} \right) \mu_i^2 \cong 10^{-5} \, \bar{\nu} |e\mathbf{r}_i|^2 \tag{5.13}$$

where m_e is the mass of the electron, $\bar{\nu}$ is the energy of the transition (in cm^{-1}), h is Planck's constant, and $\mathbf{r}$ is the length (in cm) of the transition dipole (i.e., $e\mathbf{r}$ is the transition dipole moment).

We can now identify μ_i with an observable quantity related to the quantum mechanical transition moment matrix element or integral, i.e., $\mu \equiv \langle H \rangle$, and produce:

$$\text{Classical} \rightarrow f = \left(\frac{8\pi m_e \bar{\nu}}{3he^2}\right)\langle H \rangle^2 \leftarrow \text{Quantum mechanical} \tag{5.14}$$

From this expression, which bridges the gap between classical and quantum mechanical theory, we can derive the relationship between the quantum mechanical quantity, $\langle H \rangle$ and experimental quantities, since classical theory may be directly related to experimental quantities via Eq. 5.10.

Examples of the Relationships of ε, k_e^0, τ_e^0, $\langle H \rangle$, and f

It should be emphasized that the expressions given above to relate theory and experiment are oversimplified and are given only to provide insight into the nature of radiative transitions. The use of these equations provides only a *qualitative order-of-magnitude agreement* with experiment. With these qualifications in mind let us evaluate some numerical examples in order to acquire a "feel" for the orders and limits of magnitude of quantities associated with various radiative transitions.

Since at this point we are concerned only with qualitative conclusions, let us simplify an integration problem and assume that the absorption spectrum is a smooth Gaussian curve which can be approximated by an isosceles triangle. With this assumption, we have:

$$\int \varepsilon \, d\bar{\nu} \sim \varepsilon_{\max} \Delta\bar{\nu}_{\frac{1}{2}} \tag{5.15}$$

where $\varepsilon_{\max}$ is the value of ε at the absorption maximum and $\Delta\bar{\nu}_{\frac{1}{2}}$ is the width of the absorption band at $\frac{1}{2}\varepsilon_{\max}$.

Let us take as an example the absorption spectrum of a molecule with $\varepsilon_{\max} = 5 \times 10^4$ at 20,000 cm^{-1} (500 nm, 5000 Å) and half-width of 5000 cm^{-1}. Such a half-width for an absorption band is common for organic molecules and the extinction of maximum absorption is as high as is commonly found. In other words, *this example is a prototype for a fully-allowed electronic absorption.*

It is helpful to relate these experimental quantities to their theoretical counterparts, namely f and $\langle H \rangle^2$. $\langle H \rangle$ equals $e\langle \mathbf{r} \rangle$ and approximate expressions relating f and $\langle \mathbf{r} \rangle^2$ are given by:

$$f \sim \frac{\varepsilon_{\max} \Delta\bar{\nu}_{\frac{1}{2}}}{2.5 \times 10^8} \qquad \text{(unitless)} \tag{5.16}$$

$$\langle \mathbf{r} \rangle^2 \sim \frac{\varepsilon_{\max} \Delta\bar{\nu}_{\frac{1}{2}}}{2.5 \times 10^{19}\nu} \qquad \text{(units cm}^2\text{)} \tag{5.17}$$

Evaluating for $\varepsilon_{max} = 5 \times 10^4$ at 20,000 cm^{-1} with $\Delta\bar{\nu}_{\frac{1}{2}} = 5000\ cm^{-1}$ we find:

$$f \sim \frac{(5 \times 10^4)(5 \times 10^3)}{2.5 \times 10^8} = 1.0 \tag{5.18}$$

$$\langle \mathbf{r} \rangle^2 \sim \frac{(5 \times 10^4)(5 \times 10^3)}{(2.5 \times 10^{19})(2 \times 10^4)} = 5 \times 10^{-16}\ (\text{units cm}^2) \tag{5.19}$$

Thus, we see that such a strong absorption corresponds to an *oscillator strength of unity*.

In classical theory such a prototype system would correspond to an ideal isotropic electron oscillator.[4c] As we mentioned earlier, we may identify $\langle H \rangle$ with a transition dipole moment $e\mathbf{r}$. The transition dipole length $\mathbf{r}$ for the example under discussion is 2.2×10^{-8} cm. According to quantum theory, our prototype system would have a transition dipole moment length of 2.2 Å, corresponding to a transition dipole moment of 2.2×10^{-8} cm $\times$ $4.8 \times 10^{-10} \sim 10 \times 10^{-18}$ cm $\times$ esu = 10 D. Thus, the electronic transition has associated with it a transition dipole moment of about 10 Debyes. In other words, during the interaction of the lightwave and the molecule, the electron cloud is distorted enough to produce a transitory induced dipole moment of 10 D.

Now let us evaluate the inherent radiative rate constant k_e^0 associated with emission of light from the state producing the absorption spectrum we have just discussed. From our calculation of f and with the use of Eq. 5.11 we have:

$$k_e^0 \sim \nu_0^2 f \sim (2 \times 10^4)^2 \sim 4 \times 10^8\ \text{sec}^{-1} \tag{5.20}$$

In the calculation of k_e^0 we have to take a theoretical relationship of absorption to emission and make a prediction of the relationship between *experimental* quantities, i.e., the integrated absorption spectrum and the inherent emission lifetime τ^0 (which is defined as $1/k_e^0$) for a corresponding radiative transition.

Consider now a second example of a molecule whose absorption spectrum is identical in shape and position to our first case, but whose ε_{max} is only ~ 10. We find that

$$\begin{aligned} f &= 2 \times 10^{-4} \\ \mathbf{r} &= 0.3\ \text{Å} \\ k_e^0 &\sim 10^5\ \text{sec}^{-1} \end{aligned} \tag{5.21}$$

These order-of-magnitude calculations allow us to make "ball park" estimates of the most intense (measured by ε_{max}) or the fastest (measured to k_e^0) radiative transitions which we expect to encounter experimentally.

How large can ε_{max} be for an organic molecule? If one uses arguments derived from the classical theory of light absorption, the largest value of ε_{max} is associated with an oscillator strength of 1.0. For absorptions occurring near 400 nm

(20,000 cm^{-1}), a limiting value of $\varepsilon_{max} \sim 100{,}000$ is predicted. The corresponding radiative rate is $\sim 10^9$ sec^{-1}, and thus we have:

$$\begin{aligned} &\text{Absorption: } \varepsilon_{max} \rightarrow 10^5 \text{ cm}^2 \text{ M}^{-1} \quad \text{(limit)} \\ &\text{Emission: } \quad k_e^0 \rightarrow 10^9 \text{ sec}^{-1} \quad \text{(limit)} \end{aligned} \tag{5.22}$$

Thus, the effective half-band widths ($\Delta\bar{\nu}$) of many absorption bands in the visible and near ultraviolet region are (at room temperature) on the average of the order 3000 cm^{-1}, so that a convenient approximate relationship between the rate of emission and ε_{max} is given by:

$$k_e^0 \equiv 1/\tau^0 \sim 10^4 \varepsilon_{max} \tag{5.23}$$

It should be noted that lifetimes calculated in this way are *radiative* lifetimes τ^0, that is, lifetimes which would be observed in the absence of all other processes by which the molecule could return to the ground state. The observed lifetimes τ are nearly always less than the calculated values because of competing radiationless processes. How small can ε_{max} be for a spin-forbidden absorption of an organic molecule? Of course the theoretical limit is precisely zero. The experimental limit for organic molecules seems to be in the range of $\varepsilon_{max} \sim 10^{-4}$. This corresponds to a radiative rate $k_e^0 \sim 10^{-1} - 10^{-2}$ sec.

Table 5.2 Experimental and Calculated Radiative Lifetimes for Singlet-Singlet Transitions

Compound	τ^0 ($\times 10^9$)[a] (calculated)	τ ($\times 10^9$)[b] (experimental)
Rubrene[c]	22.5	16.0
Anthracene[d]	13.5	16.7
Perylene[c]	5.1	5.6
9,10-Diphenylanthracene[d]	8.9	8.8
9,10-Dichloroanthracene[d]	11.0	15.4
Acridone[e]	15.9	15.1
Fluorescein[e]	4.7	5.0
9-Aminoacridine[e]	15.6	15.3
Rhodamine B[e]	6.0	6.0
Acetone[e]	10,000	1000
Diaza[2.2.2.]bicyclooctane[f]	4000	1000
Perfluoroacetone[g]	10,000	5000
Benzene[h]	140	600

[a] Calculated from the lowest energy singlet-singlet absorption band and use of a modified form of Eq. 5.11.
[b] Evaluated from experimental measurements of τ_S and Φ_F via Eq. 5.42. Note that τ_F is defined as being equal to k_F^{-1}.
[c] Data from Reference 9a.
[d] Data from Reference 9b.
[e] Data from Reference 11b.
[f] Data from Reference 11a.
[g] Data from Reference 9f.
[h] Data from Reference 11c.

Experimental Tests of the Quantitative Theory Relating Emission and Absorption to Spectroscopic Quantities

Experimental tests[9] of a slightly modified form of Eq. 5.11 have been made for singlet-singlet transitions; the results are given in Table 5.2. Little comment on this data is needed except to note that the agreement between the calculated and experimental values is excellent.

Although application of Eq. 5.11 to electronically-forbidden singlet-singlet and spin-forbidden singlet-triplet radiative transitions is not theoretically justified,[10] it appears that *relative* values of k_e^0 may be safely derived from absorption data.[11]

5.5 The Shape of Absorption and Emission Spectra[12]

From the equation $\Delta E = h\nu$ and the postulate that only one electron is excited or deexcited in an individual absorption or emission event, we may well ask ourselves why all absorption and emission spectra are not "sharp lines" with respect to the frequency ν of the absorbed or emitted light. In fact, only the absorption and emission spectra of atoms come close to being "sharp lines" (see Fig. 5.6a). This sharpness is due to the fact that the electronic states of atoms can be accurately described by specifying the orbits of their valence electrons. This statement applies to vapors of atoms at very low pressures. Thus, an atomic electronic transition from the ground state to an excited state requires a quantum of well-defined

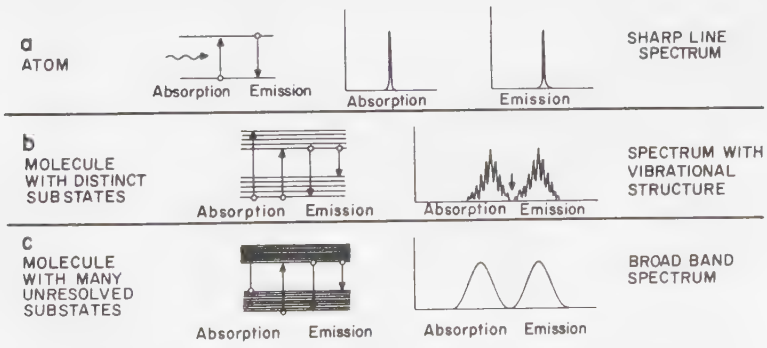

Figure 5.6

(a) Sharp-line absorption and emission spectrum typical of atoms at low pressure in the vapor phase. (b) Broad-band absorption and emission spectrum typical of certain rigid molecules at low pressure in the vapor phase. (c) Structureless broad absorption and emission spectrum typical of molecules in solvents. Each absorption and emission corresponds to a single electronic transition.

energy, and its absorption or emission spectrum is a very narrow band of frequencies.

In a molecule, an electronic transition is not as "pure" as it is in an atom. This is because of the fact that, in order to describe the electronic states of a molecule, the motions of nuclei relative to one another (e.g., vibrations, rotations, collisions) must be considered. A molecular electronic transition does not correspond to a well-defined quantum of energy because an *ensemble* of different nuclear shapes may correspond to the initial or to the final states. As a result, the absorption (and emission) spectrum of a molecule may involve transitions over a range of energies even in the vapor phase at low pressures (Fig. 5.6b). The sharp line or band which characterized atomic transitions is replaced in molecular absorption by a set of closely spaced lines which may be only partially resolved or even completely unresolved. For organic molecules in solution, this latter situation is common (Fig. 5.6c). In certain cases some vibrational structure is apparent in a band corresponding to an electronic transition. The most prominent vibrational progression of an electronic absorption or emission band is often associated with a vibration whose equilibrium position is most greatly changed by the radiative electronic transition.[12b] Thus, a prominent vibrational progression reveals the most important nuclear distortion which occurs during a transition. For "weak" spin-allowed

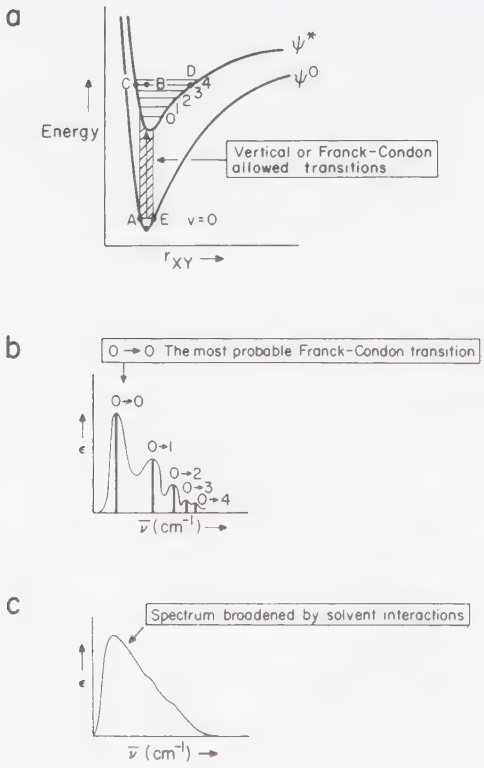

Figure 5.7

(a) Depicts the potential-energy curves. (b) Shows the form of the observed absorption spectrum. For an example of such a situation see Figure 5.8. (c) Shows the effect of solvent broadening on the vibrational structure of the absorption spectrum.

electronic transitions ($f < 10^{-2}$), often the vibration in question is the one that destroys the molecular symmetry to such an extent that a forbidden transition (in idealized perfect molecular symmetry) is caused to become partially allowed via electronic-vibrational interaction.

For example, during the n, π^* radiative transitions of a ketone, the C=O vibration is selectively excited. The vibrational structure of the C=O vibration of the excited state dominates the vibrational progression absorption spectrum, whereas the C=O vibration of the ground state dominates the emission spectrum.

As an illustration, in Figure 5.15 the separation of the vibrational bands in the n, π^* absorption of benzophenone and a cyclic ketone are weakly resolved. The vibrational separation of $\sim 1200\ \text{cm}^{-1}$ corresponds to the C=O stretch in $S_1(n, \pi^*)$. In Figure 5.18 the separation of well-resolved vibration bands in the (phosphorescence) emission spectrum of benzophenone is $\sim 1700\ \text{cm}^{-1}$. This value is in good agreement with the energy of the C=O stretching vibration of ground state benzophenone (as measured by infrared spectroscopy). We shall now see how vibration intensities are related to the Franck-Condon principle.

The Franck-Condon Principle and Absorption Spectra[13]

In Chapter 4 (Section 4.7, especially Fig. 4.10) we pointed out that because of the Franck-Condon principle, both the classical and quantum mechanical interpretations of radiative transitions lead to the conclusion that there will be a difference in the probability of vibrational transitions between ψ^0 and ψ^* of a diatomic molecule XY. Here let us present examples in terms of a *semi*classical model. In Figure 5.7, a situation is shown for which the two potential curves for ψ^0 and ψ^* are similar and more or less vertically displaced i.e., the equilibrium separation r_{xy} is the same for ψ^0 and ψ^*. This situation corresponds to an electronic orbital jump for which the overall bonding is similar in ψ^0 and ψ^*. As a result, the equilibrium geometries should be similar. A typical example[14] would be a rigid aromatic hydrocarbon (Fig. 5.8). In such a situation a relatively strong 0–0 and/or 0–1 transition is observed for both absorption and emission.

Figures 5.9 and 5.10 depict situations for which the excited curve ψ^* is displaced relative to ψ^0 (r_{eq} is assumed to be larger in ψ^* than in ψ^0). In Figure 5.9, the 0–2 and 0–3 bonds are relatively intense and the 0–0 and 0–1 bonds relatively weak. In Figure 5.10, excitation of ψ^* to produce geometries more contracted than point C in the figure results in dissociation of the diatomic XY molecule into X + Y.

The Franck-Condon Principle and Emission Spectra

In condensed phases the rate of vibrational- and electronic-energy relaxation among excited states is very rapid compared to the rate of emission. As a result, emission will occur from the $v = 0$ vibrational level of the lowest excited states. Let us apply the Franck-Condon principle to emission (Fig. 5.11).

In analogy to absorption, the most probable emissions will be those which occur vertically. In contrast to absorption, the equilibrium separation of the ground-state potential-energy curve minimum is smaller than that of the excited state

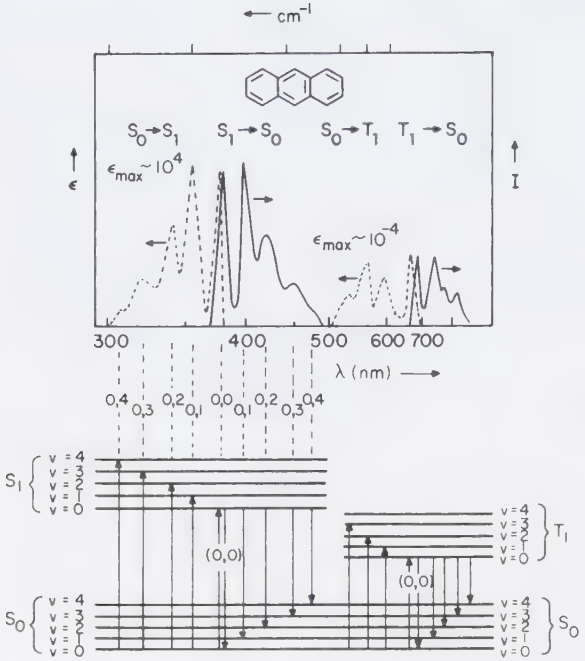

Figure 5.8

Absorption (dotted lines) and emission (solid lines) of anthracene in solution. The lower portion displays the basis for vibrational assignments.

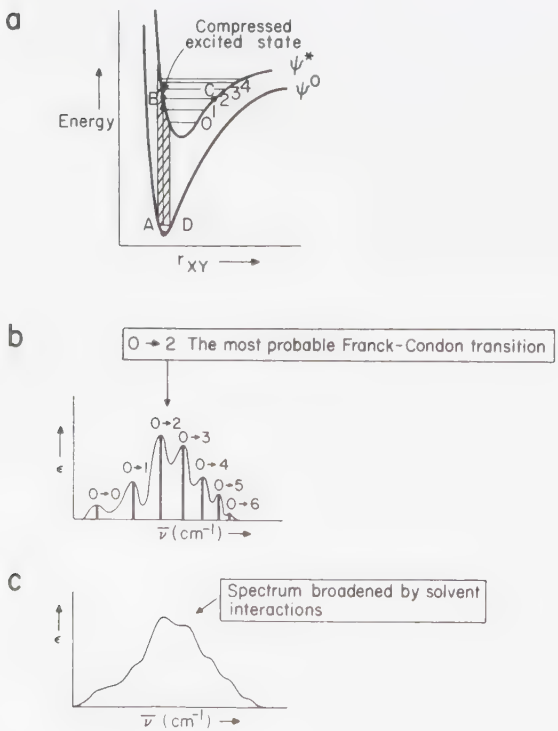

Figure 5.9

(a) depicts the potential-energy curves, (b) the form of the observed absorption spectrum, and (c) the effect of solvent broadening on the vibration structure of the absorption spectrum. A typical example is an aromatic ketone undergoing n, π^* absorption (see Fig. 5.15).

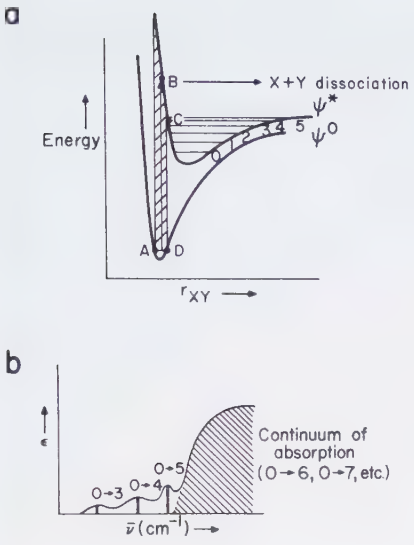

Figure 5.10

(a) Depicts the potential-energy curves and (b) depicts the absorption curve spectrum. A typical example is a molecule possessing a weak σ bond, e.g., CH_3I.

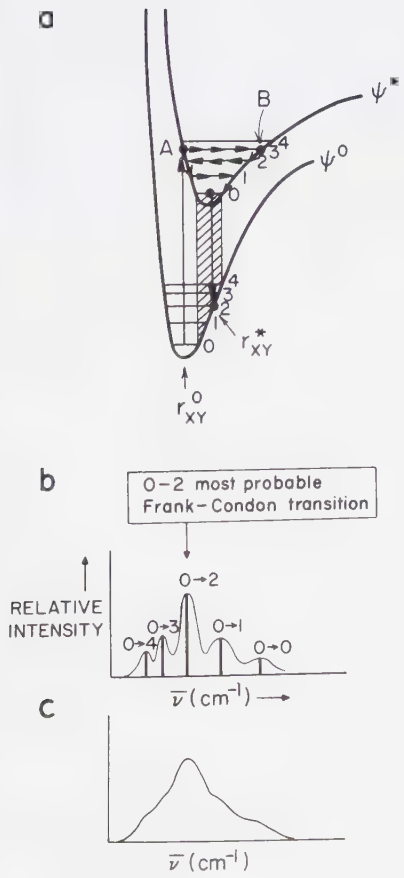

Figure 5.11

(a) Depicts potential-energy curves (b) emission spectrum (c) solvent broadened emission spectrum. As shown, the 0 → 2 emission is the most probable Franck-Condon transition. The most probable absorption is from r_{XY} and the most probable emission is from r^*_{XY}. Emission from ψ^* produces an elongated ground state.

curve, so that the most probable vertical transitions produce an elongated ground state, while absorption produces a compressed excited state immediately after transition. The frequency of emission cannot be greater than the frequency of the 0–0 emission, since the 0–1, 0–2, etc., emissions correspond to smaller energies than the 0–0 emission. The emission spectrum expected from a molecule whose potential-energy curves are similar to those in Figure 5.9 is shown in Figure 5.11.

Let us suppose that absorption occurs vertically from the ground-state surface and the excited state is "born" near point A, a turning point for the compressed vibration in $v = 3$. The molecule will begin to vibrate in the $v = 3$ state and, in the absence of any external perturbation, the atoms XY would continue to persist in the $v = 3$ state. In solution, however, there are many perturbations induced by collisions. In a polyatomic molecule, vibrations in one part of the molecule may act as a perturbation to vibrations in another part of the same molecule. In any case, energy is generally removed very rapidly from upper vibrational levels and transitions between vibrational levels seem to occur about as fast as vibrational energy can either be removed by the environment or redistribute itself within a molecule. In Figure 5.11, this decrease in vibrational energy from $v = 3$ to $v = 0$ is shown as a sequence of arrows.

5.6 State Mixing: Breakdown of the Single Orbital Configuration and Pure Multiplicity Approximations[14]

The notion that S_1 or T_1 is a "pure" state in the sense of being derived from either a single electronic orbital configuration or from a single spin multiplicity allows for a simple and reliable Zero Order classification of the lowest electronic states of many organic molecules. However, the approximation begins to break down when significant state mixing occurs. *State mixing is the first-order or higher-order corrections to an original Zero Order approximation.*

Consider an initial Zero Order approximation in which S_1 is viewed as a "pure" n, π^* state. In "real ty" the wave function of S_1 has a finite amount of π, π^* character mixed into it. For simplicity, we assume that only the mixing of a Zero Order π, π^* state with a Zero Order n, π^* state is significant. Thus, in the First Order we must describe the wavefunction for S_1 as:

$$\underset{n,\,\pi^*}{\text{First order}} \rightarrow \psi(S_1) = \underset{\substack{\uparrow \\ \text{Zero order} \\ n,\,\pi^*}}{\psi(n, \pi^*)} + \lambda \underset{\substack{\uparrow \\ \text{Zero order} \\ \pi,\,\pi^*}}{\psi(\pi, \pi^*)} \tag{5.24}$$

where λ is the "mixing" coefficient or the amount of π, π^* character mixed into S_1, and $\psi(n, \pi^*)$ and $\psi(\pi, \pi^*)$ are the *Zero Order* (single configuration) wave

functions of the system. How can λ be estimated? According to perturbation theory (Chapter 3), for a weak perturbation, i.e., a good Zero Order approximation, λ is given by:[12]

$$\text{Mixing coefficient} \rightarrow \lambda = \left| \frac{\langle \psi_a | H | \psi_b \rangle}{E_a - E_b} \right| \begin{matrix} \leftarrow \text{Matrix element} \\ \leftarrow \text{Energy separation} \end{matrix} \tag{5.25}$$

where ψ_a and ψ_b are the states which are mixed in First Order by the interaction H, and $E_a - E_b$ is the energy difference between the Zero Order states ψ_a and ψ_b.

Thus, from Eqs. 5.24 and 5.25 for the mixing of n, π^* and π, π^*, we have (in a condensed form):

$$\text{First Order } n, \pi^* \rightarrow S_1 = n, \pi^* + \left| \frac{\langle n, \pi^* | H | \pi, \pi^* \rangle}{E_{\pi, \pi^*} - E_{n, \pi^*}} \right| \pi, \pi^* \tag{5.26}$$

We can now deduce the qualitative features which will be important to a state mixing of n, π^* and π, π^* configurations:

1. The energy gap between the Zero Order configurations.
2. The magnitude of the matrix element which mixes the states.

The spatial *overlap* of the mixing states, their symmetry properties, and the nature and symmetry of H will be crucial in the determination of the extent of mixing.

The matrix element for mixing may be approximated by considering only the *orbitals which are occupied differently* in two states, i.e.,

$$\underset{\substack{\uparrow \quad \uparrow \\ \text{Occupied in} \\ \text{both states}}}{\langle n, \pi^* |} \underset{\substack{\uparrow \\ \text{Involved} \\ \text{in mixing}}}{H} \underset{\substack{\uparrow \\ \text{Involved} \\ \text{in mixing}}}{| \pi} \underset{\substack{\uparrow \\ \text{Occupied in} \\ \text{both states}}}{, \pi^* \rangle} \sim \langle n | H | \pi \rangle \tag{5.27}$$

For purely planar molecules the integral in Eq. 5.27 equals zero because the n and π orbitals are defined as orthogonal to one another for an idealized planar geometry. However, as the molecule undergoes vibrations which destroy the planar symmetry of the molecule, the n and π orbitals begin to mix, i.e., if H represents electronic interactions which occur during nonplanar vibrations the integral $\langle n | H | \pi \rangle$ does not equal zero. In other words, the n and π orbitals are no longer "pure," and therefore they are no longer orthogonal.

From these qualitative considerations we can deduce that the mixing of n, π^* and π, π^* states may depend upon the occurrence of certain vibrations which generates the nonorthogonality of the n and π orbitals. The extent of mixing, in turn, depends on the overlap of the Zero Order n, π^* and π, π^* functions and their energetic separation.

State mixing has important spectroscopic as well as important photochemical

consequences. It is mixing which provides a mechanism for the breakdown of Zero Order selection rules (Fig. 5.12).

Mechanisms for the Mixing of Singlet and Triplet States; Multiplicity Mixing[14]

All singlet-triplet transitions (whether radiative or radiationless) are strictly forbidden in the Zero Order approximation, which ignores spin-orbit and other electron spin interactions. Spin-orbit coupling "mixes" singlet and triplet states so that transitions become allowed to an extent which depends on the magnitude of the mixing coefficient λ (Eq. 5.25). We may consider the specific matrix elements, which represent different methods of mixing S and T states, as "mechanisms" which break down the Zero Order selection rule which states that the probability of *all* $S \rightleftarrows T$ transitions is *zero.*

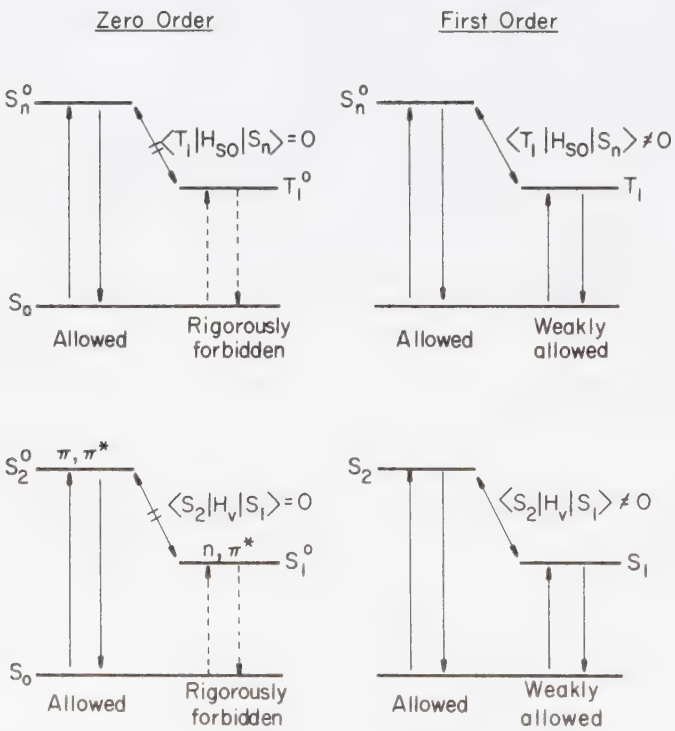

Figure 5.12

The transition from Zero Order to First Order involves "turning on" a mechanism for "mixing" states. Top: in Zero Order $S_0 \rightleftarrows T_1^0$ transitions are strictly forbidden. In First Order $S_0 \rightleftarrows T_1$ transitions become weakly allowed via spin-orbit coupling. Bottom: In Zero Order $S_0 \rightleftarrows S_1$ (n, π^*) transitions are strictly forbidden. In First Order $S_0 \rightleftarrows S_1$ (n, π^*) transitions become weakly allowed via orbital configuration mixing.

Figure 5.12 shows the Zero Order and First Order approximations in terms of a state energy diagram. Transitions between S_0 to T_1 are *defined* as being *rigorously forbidden* in Zero Order. In this approximation the observation of $S_0 \rightarrow T_1$ absorption, $T_1 \rightarrow S_0$ emission, or $S_1 \rightarrow T_1$ intersystem crossing cannot be understood because no mechanism for inverting spins is available, i.e., spin flipping mechanisms have been postulated not to exist.

In the First Order we allow spin-orbit mixing of states, i.e., T_1 takes on the character of one or more singlet states, S_n. Several mechanisms are possible for this interaction:[14,15]

1. Direct electronic coupling of T_1 with S_n, i.e.,

$$\langle T_1|H_{so}|S_n\rangle \neq 0 \tag{5.28}$$

2. Indirect electronic coupling of T_1 and S_n via an intermediate triplet T_n, i.e.,

$$\langle T_1|H_{so}|S_n\rangle = 0 \tag{5.29}$$

$$\langle T_n|H_{so}|S_n\rangle \neq 0 \quad \text{and} \quad \langle T_n|H_e|T_1\rangle \neq 0 \tag{5.30}$$

3. The "turning on" of mechanisms (1) and (2) via vibrational motions of the molecule, i.e.,

$$\langle T_1|H_{so}|S_n\rangle = 0 \quad \text{but} \quad \langle T_1^v|H_{so}|S_n\rangle \neq 0 \tag{5.31}$$

$$\langle T_n|H_e|T_1\rangle = 0 \quad \text{but} \quad \langle T_n^v|H_e|T_1^n\rangle \neq 0 \tag{5.32}$$

The mixing coefficients, λ, for mechanisms (1) and (2) are:

$$\lambda(1) = \frac{\langle T_1|H_{so}|S_n\rangle}{E_{S_n} - E_{T_1}} \tag{5.33}$$

$$\lambda(2) = \frac{\langle T_n|H_e|T_1\rangle\langle T_n|H_{so}|S_n\rangle}{|E_{T_n} - E_{T_1}|\,|E_{T_n} - E_{S_n}|} \tag{5.34}$$

In summary, two major mechanisms generally account for the radiative strength of phosphorescence of organic molecules: (a) direct First Order spin-orbit interaction between T_1 and S_n, and (b) indirect or Second Order spin-orbit interaction of T_1 and S_n via vibrational mixing of T_1 with upper triplets. The T_1 state will normally be classified in terms of a Zero Order electronic orbital configuration. However, it will be better approximated in terms of a mixture of other triplet and singlet configurations.

In the case of aromatic hydrocarbons T_1 is a well-classified Zero Order π, π^* state. The only singlet states capable of mixing with T_1 and capable of inducing spin-orbit coupling are σ, π^* and π, σ^* states, i.e., these states have the "$p_x \rightarrow p_y$" feature that is crucial for conserving total angular momentum in a singlet triplet mixing. However, the energy gap corresponding to $E(\sigma, \pi^*) - E(\pi, \pi^*)$ or

$E(\pi, \sigma^*) - E(\pi, \pi^*)$ is very large. From Eqs. 5.33 and 5.34 we see that this large energy gap serves to inhibit spin-orbit coupling. In fact, vibrational perturbation is probably required for effective mixing of singlet states with T_1. As a result, the phosphorescence radiative strength of aromatic hydrocarbons is among the weakest of any organic molecule ($f \sim 10^{-9}$–10^{-8}, $k_p^0 \sim 10^{-1}$–10^{-2} $\sec^{-1}$).

For compounds possessing n, π^* and π, π^* states (e.g., ketones), the dominant mixing mechanisms are expected to be direct ${}^3n, \pi^* \leftrightarrow {}^1\pi, \pi^*$ or ${}^1n, \pi^* \leftrightarrow {}^3\pi, \pi^*$. Thus, for benzophenone, whose T_2 state is ${}^3\pi, \pi^*$ in Zero Order, mixing with the close lying $S_1(n, \pi^*)$ state is favored. The phosphorescence radiative strength of the $T_1(n, \pi^*)$ states of aryl ketones is among the strongest of any organic molecule ($f \sim 10^{-5}$–10^{-6}, $k_P^0 \sim 10^3$–10^2 $\sec^{-1}$).

The Effect of Orbital Configuration Mixing and Multiplicity Mixing on Radiative Transitions[8]

A basic result of state mixing is to imbue a Zero Order state originally described in terms of a single electronic orbital configuration (or spin multiplicity) with characteristics of a second electronic orbital configuration (or spin multiplicity). We may, of course, consider the mixing of many orbital configurations. Often, however, mixing of a single second-orbital configuration suffices to interpret a great deal of experimental data. How does mixing affect Zero Order predictions? For radiative (and radiationless) transitions, First Order mixing is generally the significant mechanism which "allows" processes which are strictly forbidden in Zero Order to occur with measurable probability (Fig. 5.12).

Consider the magnitude of f, the oscillator strength in Eq. 5.14, which is directly related to the probability of absorption and of emission involving an n, π^* state. In Zero Order, $f = 0$ for $S_0 \rightleftarrows S_1$ (pure) radiative transitions, if the n and π^* orbitals undergoing transition are strictly orthogonal, i.e., $\langle H \rangle$ in Eq. 5.14 $= 0$. In First Order, we consider that vibrations or electron-electron interactions may "mix" n, π^* and π, π^* configurations by deorthogonalizing the n and π^* orbitals; thus, we assume Eq. 5.35 is valid:

$$S_1 = n, \pi^* + \lambda(\pi, \pi^*) \tag{5.35}$$

The $S_0 \rightarrow \pi, \pi^*$ transition is generally "allowed" (i.e., $\langle H \rangle$ in Eq. 5.14 is not generally $= 0$) and therefore a transition is possible. We may now calculate the value of f for Eq. 5.36:

$$S_0 \underset{h\nu}{\overset{h\nu}{\rightleftharpoons}} S_1 \quad \text{(mixed)} \tag{5.36}$$

The expression for f becomes:

$$f(S_0 \rightleftarrows S_1) = \lambda^2 f(S_0 \rightleftarrows S_2) \tag{5.37}$$

In other words, the First Order $S_0 \rightleftarrows S_1$ transitions are allowed only to the extent that S_2 is mixed into S_1 (amount of mixing given by λ). Thus, the *observed*

value of $f(S_0 \rightleftarrows S_1)$ may be evaluated in terms of the *theoretical* value of f for the Zero Order $S_0 \rightarrow S_2$ transition. Replacing λ by its equivalent from Eq. 5.25, we produce Eq. 5.38:

$$\underset{\text{mixed state}}{\text{Observed}} \quad f(S_0 \rightleftarrows S_1) = \underbrace{\left|\frac{\langle n, \pi^* | H | \pi, \pi^* \rangle}{E_{\pi,\pi^*} - E_{n,\pi^*}}\right|^2}_{\text{Mixing coefficient}} \underbrace{f(S_0 \rightleftarrows \pi, \pi^*)}_{\text{Zero Order}} \qquad S_2 = \pi, \pi^* \tag{5.38}$$

where n, π^* and π, π^* refer to the Zero Order states, and H corresponds to the interaction that mixes S_1 and S_2.

The *measured* $f(S_0 \rightleftarrows S_1)$ reflects both λ and $f(S_0 \rightleftarrows \pi, \pi^*)$. Thus, the *magnitude* of $f(S_0 \rightleftarrows S_1)$ depends on three factors:

1. The magnitude of the matrix element $\langle n, \pi^* | H | \pi, \pi^* \rangle$,
2. The energy gap $E_{\pi,\pi^*} - E_{n,\pi^*}$,
3. The *Zero Order* oscillator strength $f(S_0 \rightleftarrows \pi, \pi^*)$.

In effect, theory predicts that $f(S_0 \rightleftarrows S_1)$ will possess all of the characteristic properties of $S_0 \rightleftarrows \pi, \pi^*$ transitions *except* that the probability of the observed transitions will be *decreased* by the factor λ^2. For example, the *polarization* of the $S_0 \rightleftarrows S_1$ transitions will be derived from the polarization of the $S_0 \rightleftarrows S_2(\pi, \pi^*)$ transitions. For aromatic molecules, $S_0 \rightleftarrows S_2(\pi, \pi^*)$ transitions are *in-plane* polarized.[14] Thus, if S_1 is a mixture of n, π^* and π, π^* states, the $S_0 \rightleftarrows S_1$ transitions will be *in-plane* polarized.

We may now straightforwardly apply the same ideas to the qualitative evaluation of $f(S_0 \rightleftarrows T_1)$. If we assume that a $^3(n, \pi^*)$ and $^1(\pi, \pi^*)$ mixing is dominant for a $S_0(n^2) \rightarrow T_1(n, \pi^*)$ transition, then we have:

$$f(S_0 \rightleftarrows T_1) = \left|\frac{\langle {}^3(n, \pi^*) | H_{SO} | {}^1(\pi, \pi^*) \rangle}{E_{\pi,\pi^*} - E_{n,\pi^*}}\right|^2 f(S_0 \rightleftarrows \pi, \pi^*) \tag{5.39}$$

We see that the "forbidden" $S_0 \rightleftarrows T_1$ transitions pick up finite oscillator strength via a mechanism which mixes the states. The magnitude of f for $S_0 \rightarrow T_1(n, \pi^*)$ depends on the value of the matrix element and the oscillator strength of the "pure" spin allowed $S_0 \rightleftarrows \pi, \pi^*$ transitions. Both the $S_0 \rightarrow T_1(n, \pi^*)$ absorption and $T_1(n, \pi^*) \rightarrow S_0$ emission are predicted to be in-plane polarized, because the oscillator strength of the "real" transition is due to the π, π^* state mixed into T_1, and because π, π^* states are generally in-plane polarized.

From the above, it is clear that measurement of "forbidden" absorptions and emissions provide evidence of the identity of the mixing state which provides a mechanism that makes a Zero Order forbidden transition allowed in First Order. A study of the vibrational structure of an absorption or emission also provides clues as to which molecular motions are most effective in mixing states. As an

illustration, the vibrational structure of the $S_0 \rightarrow S_1(n, \pi^*)$ absorptions of benzophenone and hydrindanone (Fig. 5.15) show a regular progression of bands separated by $\sim 1200\ cm^{-1}$.[16] This separation corresponds to the energy required to stretch the C—O bond in S_1. In other words, the C=O stretching vibrations are important in mixing allowed π, π^* character into S_1, which is a nominal n, π^* state.

The phosphorescence of acetophenone shows a vibrational pattern that is characteristic of the C—O vibrational stretch in S_0 (see Fig. 5.13).[16] Such a vibrational pattern is expected for emission from a n, π^* state if the transition is localized on the C=O group, i.e., the $\pi^* \rightarrow n$ electron jump leaves excess vibrational energy on the C and O atoms specifically because an antibonding node between these atoms disappears. The phosphorescence of acetonaphthone does *not* show the characteristic C=O vibrational pattern. Instead, a complicated pattern of C—C vibrations characteristic of the aromatic ring in S_0 is observed. This is expected for emission from a π, π^* state since the $\pi^* \rightarrow \pi$ electron jump leaves excess vibrational energy between certain C atoms of the aromatic ring as the result of the destruction of a node.

In summary, numerous spectroscopic criteria for the assignment of configuration to S_1 and T_1 are available. In later Chapters we shall see how photochemical reactivity can also serve to classify S_1 and T_1 in terms of electronic configurations. Because of the two correlations, (a) spectroscopic parameters ↔ orbital configura-

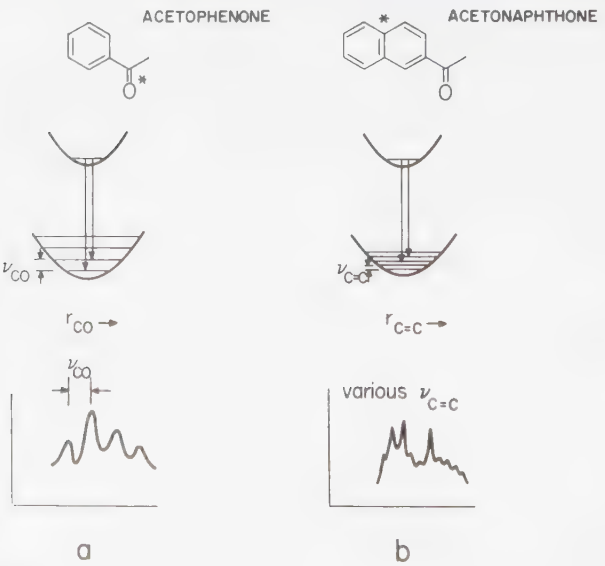

Figure 5.13

(a) Emission of acetophenone possesses a C=O vibrational pattern. (b) Emission of acetonaphthone possesses a C=C vibrational pattern.

tions, and (b) orbital configuration ↔ photoreactivity, we expect (and will find) correlations between spectroscopic parameters and photoreactivity. The theoretical basis for this relationship will be made via state correlations (Chapter 7).

5.7 Experimental Measurements of the Absorption and Emission of Light: Molecular Electronic Spectroscopy[16]

For most photochemical reactions we need consider only the lowest excited singlet state (S_1) or the lowest triplet state (T_1) as likely candidates for the initiation of a reaction (Kasha's rule).[17] This generalization results from the experimental observation that the majority of reactions which have been studied do not appear to involve higher-order electronic states (S_2, T_2, etc.), because rapid radiationless conversion to S_1 and/or T_1 competes favorably with higher-order processes. Thus it is the spectroscopy of S_1 and T_1 which is of the greatest interest to the organic photochemist. Accordingly, we shall consider:

1. $S_0 \rightarrow S_1$ absorption (singlet-singlet absorption),
2. $S_0 \rightarrow T_1$ absorption (singlet-triplet absorption),
3. $S_1 \rightarrow S_0$ emission (fluorescence),
4. $T_1 \rightarrow S_0$ emission (phosphorescence).

A case example of these four key radiative transitions is shown for anthracene in Figure 5.8. The $S_0 \rightarrow S_1$ absorption occurs at the highest energies ($\sim$300 nm to $\sim$380 nm), and $S_1 \rightarrow S_0$ fluorescence emission occurs at lower energies ($\sim$380 nm to $\sim$480 nm). The bands which nearly overlap in $S_0 \rightarrow S_1$ absorption and in $S_1 \rightarrow S_0$ emission are called 0, 0 *bands for absorption and emission* (see level diagram below spectrum in Figure 5.8). At still lower energies, the $S_0 \rightarrow T_1$ absorption ($\sim$500 nm to $\sim$700 nm) appears. Notice that the probability of this absorption is $\sim 10^8$ *times smaller*, as measured by ε, than is $S_0 \rightarrow S_1$ absorption. Finally, at lowest energies, $T_1 \rightarrow S_0$ phosphorescence emission is observed.

Absorption, Emission, and Excitation Spectra

The practical measurement of an *absorption spectrum* is based on two important principles: Lambert's law and Beer's law.[16b] Lambert's law states that the proportion of light absorbed by a medium is independent of the initial intensity I_0. Beer's law states that the amount of light absorbed is proportional to the concentration of absorbing molecules in the light path. The quantity related to absorption that is conventionally measured is called the *optical density* (OD) and is defined as being equal to $\log(I_0/I_t)$ where I_0 is the intensity of incident light

and I_t is the intensity of transmitted light, i.e., an optical density of 2.0 corresponds to $\sim 1\%$ transmittance or $\sim 99\%$ absorbance. An OD of 0.01 corresponds to $\sim 98\%$ transmittance or $\sim 2\%$ absorbance.

An absorption spectrum is completely described by a graph of absorption intensity as the ordinate and the wavelength of absorbed light as the abscissa (Examples: Figs. 5.14, 5.15). Conventionally, the molar extinction coefficient, ε, is employed in such graphs rather than absorption intensity, and is given by:

$$\varepsilon \equiv [\log(I_0/I_t)]/\ell c$$

where I_0 and I_t are the intensity of the incident and transmitted light, respectively, ℓ is the optical path length and c is the concentration of absorbing material. The molecular extinction coefficient is a fundamental molecular property and is independent of concentration and path length if Lambert's and Beer's laws hold. Note that the units of ε are $cm^{-1}\ M^{-1}$ (usually not given explicitly). It is interesting to note that ε has the dimensions of area per mole, i.e., $cm^{-1}\ M^{-1} = cm^{-1}\ mole^{-1}\ \ell = cm^2/mole$.

A "true" *emission spectrum* is a plot of emission intensity, I_e (at a fixed absorption intensity) as a function of frequency ν or wavelength λ of absorbed light (examples Figs. 5.16 -5.20). Most reported spectra are not "true" emission spectra because of certain instrumental problems.[16b] The key parameters of an emission spectrum are its "shape" (I_e versus λ), its quantum efficiency Φ_e (I_e relative to I_a, the absorbed intensity) and its lifetime, τ_e (I_e as a function of time, Section 8.6).

An *excitation spectrum* is a plot of emission intensity, I_e (at a fixed emission wavelength and constant exciting intensity I_0) as a function of frequency (or wavelength) of exciting light. For a weakly absorbing solution of a luminescent

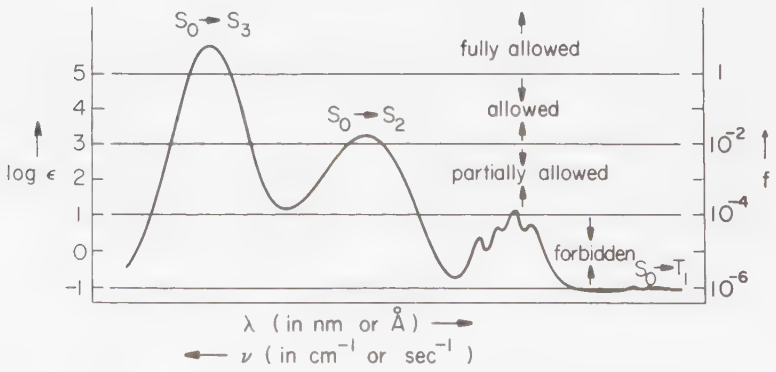

Figure 5.14

Schematic representation of the absorption spectrum of a simple organic molecule. Often the first ($S_0 \rightarrow S_1$) transition is relatively weak compared to $S_0 \rightarrow S_2$ and $S_0 \rightarrow S_3$ transitions. The $S_0 \rightarrow T_1$ transition, while always present, is often too weak to measure experimentally. Note that the ordinate is a log scale, each entry specifying a power of 10.

molecule A, I_e is given by

$$I_e = 2.3\, I_0 \varepsilon_A \ell \Phi_e^A [A]$$

where ε_A is the extinction coefficient of the absorbing molecule, ℓ is the optical path length, Φ_e^A is the quantum yield of emission of A and $[A]$ is the concentration of A. From the Kasha-Valivov rule,[16] Φ_e^A is independent of exciting wavelength. Thus, at fixed $[A]$, I_0 and ℓ, $I_e \propto \varepsilon_A$. In other words, the observed *excitation spectrum* (I_e as a function of varying wavelength of exciting light) will vary as ε_A. In such cases, the excitation spectrum has the *same* spectral appearance as the absorption spectrum. An advantage of excitation spectroscopy over standard absorption spectroscopy is the greater sensitivity of luminescence techniques which allow observation of excitation spectra at $[A]$ too low to be directly measured by absorption spectroscopy.

Experimental Examples of Spin-Allowed Electronic Radiative Transitions: $S_0 \rightarrow S_1$ Absorption and $S_1 \rightarrow S_0$ Fluorescence[16]

By the term *spin-allowed electronic radiative transition*, we mean any radiative transition which does not involve a spin inversion.

For organic molecules only singlet-singlet and triplet-triplet transitions need be considered. The probability of such "allowed" transitions ranges over four orders of magnitude (Fig. 5.14 and Table 5.3). Thus, we must accept the fact that there are "degrees of allowedness" in radiative transitions, even when a spin inversion is not required so that the terms "allowed" and "forbidden" are relative. According to the classical theory of the interaction of light with molecules, the "allowedness" is measured by a quantity called the *oscillator strength*, f. Recall from Eqs. 5.10 and 5.11 that

$$f \propto \int \varepsilon \, d\nu \sim \varepsilon_{\max} \Delta\nu \qquad \text{and} \qquad f \propto k_e^0 (\bar{\nu}^2)^{-1} \tag{5.40}$$

Table 5.3 Some Representative Examples of ε_{max} and f Values for Prototype Transitions. These Values Represent Orders of Magnitude Only

	k_e (sec^{-1})	Example	Transition type	ε_{max}	f	$\bar{\nu}_{max}$ (cm^{-1})
Spin allowed	10^9	p-Terphenyl	$S_1(\pi,\pi^*) \rightarrow S_0$	3×10^4	1	30,000
	10^8	Perylene	$S_1(\pi,\pi^*) \rightarrow S_0$	4×10^4	10^{-1}	22,850
	10^7	1,4-Dimethylbenzene	$S_1(\pi,\pi^*) \rightarrow S_0$	7×10^2	10^{-2}	36,000
	10^6	Pyrene	$S_1(\pi,\pi^*) \rightarrow S_0$	5×10^2	10^{-3}	26,850
	10^5	Acetone	$S_1(n,\pi^*) \rightarrow S_0$	10	10^{-4}	~30,000
Spin forbidden	10^4	Xanthione	$T_1(n,\pi^*) \rightarrow S_0$	1	10^{-5}	~15,000
	10^3	Acetone	$T_1(n,\pi^*) \rightarrow S_0$	10^{-1}	10^{-6}	~27,000
	10^2	1-Bromonaphthalene	$T_1(\pi,\pi^*) \rightarrow S_0$	10^{-2}	10^{-7}	20,600
	10	1-Chloronaphthalene	$T_1(\pi,\pi^*) \rightarrow S_0$	10^{-3}	10^{-8}	20,600
	10^{-1}	Naphthalene	$T_1(\pi,\pi^*) \rightarrow S_0$	10^{-4}	10^{-9}	21,300

For order-of-magnitude estimates we may assume that $\Delta\bar{\nu}$ is roughly constant for commonly encountered transitions, so that $f \propto \varepsilon_{max}$ (Eq. 5.16). Thus, a qualitative relationship between the commonly measured experimental quantity ε_{max} and the theoretical quantity f is available. Table 5.3 lists this relationship. "Fully allowed" transitions ($f = 1$) correspond to values of ε_{max} on the order of 10^4–10^5. The weakest "allowed" transitions possess $\varepsilon_{max} \sim 10$ and therefore correspond to $f \sim 10^{-4}$. Figure 5.14 compares ε_{max} and f in terms of absorption spectra.

Note that the relationship between f and k_e^0 also depends on the frequency of the emission. Thus, while 1,4-dimethylbenzene and pyrene possess similar values of ε_{max}, they emit at very different frequencies. As a result, they possess quite different oscillator strengths for fluorescence. Similarly, perylene possesses a larger ε_{max} than p-terphenyl, but the latter possesses a larger f because of the different values of $\bar{\nu}_{max}$ for the two compounds.

If we think of a perfectly allowed transition as having an oscillator strength f equal to 1.0, then we may think of a measured f value in terms of individual forbiddeness factors f_i, which *reduce* the value of f_{max} from that of the ideal system:

$$f = (f_e \times f_v \times f_s) f_{max} \tag{5.41}$$

where f_e is the prohibition due to electronic factors, f_v is the prohibition due to Franck-Condon factors, and f_s is the prohibition due to spin factors. For a spin-allowed transition $f_s = 1$ and for a spin-forbidden transition f_s depends on spin-orbit coupling (typical values of f_s from 10^{-6} to 10^{-11}).

The electronic factor f_e may be subclassified in terms of different *kinds* of forbiddeness:

1. *Overlap* forbiddeness, which results from poor spatial overlap of the orbitals involved in the electronic transition, for example, n, π^* transitions in ketones.

2. *Orbital* forbiddeness, which results from orbital wave functions (involved in transition) which overlap in space but cancel because of the symmetry of the wave functions, for example, the lowest π, π^* transition in pyrene.

Generally, for allowed transitions the electronic factor f_e is the major factor in the determination of the observed value of f. From Table 5.3 we note that perylene and p-terphenyl possess "strong" $S_0 \rightarrow S_1$ absorptions ($f \sim 1$–10^{-1}, $\varepsilon_{max} \sim 10^5$–$10^4$). These absorptions correspond to essentially fully-allowed ($\pi \rightarrow \pi^*$) transitions. For pyrene the $S_0 \rightarrow S_1(\pi, \pi^*)$ transition is *orbitally forbidden* and an electronic "forbiddenness factor" of $\sim 10^{-3}$ results in a relatively weak ε_{max} of $\sim 10^2$. For acetone the $S_0 \rightarrow S_1$ transition corresponds to an $n \rightarrow \pi^*$ transition. This transition is both *orbital overlap and orbital symmetry forbidden* and would be predicted to have $f = 0$ if the n orbital were a pure p orbital and if the molecules were strictly planar. Experimentally, $\varepsilon_{max} \sim 10$ for this $n \rightarrow \pi^*$ transition.

However, out-of-plane vibrations allow the n orbital to pick up s "character." In the case of benzophenone, "mixing" of the n, π^* state with nearby π, π^* states make S_1 a hybrid of these two transition types (see Section 5.7). As a result, the

$S_0 \rightarrow S_1$ transition has more oscillator strength because of the π, π^* character "mixed" into S_1. In a manner of speaking, the S_1 state picks up absorption intensity from its acquired π, π^* character. In the case of acetone, S_1 is more nearly "pure" n, π^* because of the poorer mixing (ΔE is much larger in the denominator of Eq. 5.39), and the absorption intensity is correspondingly lower.

Because of the direct relationship between f and the fluorescence rate constant k_F^0, (Eq. 5.11 $k_e^0 \equiv k_F^0$), *the factors determining the magnitude of f automatically are related to those determining* k_F^0. This approximation is a good one if we can ignore f_v as a major factor determining the value of f or k_F^0. If the nuclear geometry of the equilibrated excited state is very different from that of the initial ground state, then the value of k_F^0 for the $S_1 \rightarrow S_0$ transition will be determined by f_e and by different Franck-Condon factors that relate to f for the $S_0 \rightarrow S_1$ transition. In the special cases for which the equilibrium geometry and predominant vibrational progressions of S_0 and S_1 are similar, a "mirror image" relationship is sometimes observed for the absorption and related emission spectra (see Fig. 5.8), i.e., $S_0 \rightarrow S_1$ "mirrors" $S_1 \rightarrow S_0$ and $S_0 \rightarrow T_1$ "mirrors" $T_1 \rightarrow S_0$.

Based on information from absorption spectra an orbital configuration may be assigned to the electronic transition responsible for an absorption band. For anthracene (Fig. 5.8), the entire π system behaves as a chromophore and only $\pi \rightarrow \pi^*$ transitions are energetically feasible in the region 200–700 nm. For benzophenone, both $n \rightarrow \pi^*$ and $\pi \rightarrow \pi^*$ transitions are possible (Fig. 5.15). Empirically a number of criteria have been developed which allow an orbital configuration change to be associated with a given absorption band (Table 5.4).

Table 5.4 Empirical Criteria for the Assignment of Orbital Configurations of Ketones

Property	n-π^*		π-π^*	
	$S_0 \rightarrow S_1$	$S_0 \rightarrow T_1$	$S_0 \rightarrow S_1$	$S_0 \rightarrow T_1$
ε_{max}	<200	$>10^{-2}$	>1000	$<10^{-3}$
k_e (sec^{-1})	10^5–10^6	10^3–10^2	10^7–10^8	1–10^{-1}
Solvent shift	Shorter wavelengths with increasing solvent polarity		Longer wavelengths with increasing solvent polarity	
Vibrational Structure	Localized vibrations		Delocalized vibrations	
Heavy atom effect	None		Increases probability of all $S \rightarrow T$ transitions	
ΔE_{ST}	Small (<10 kcal)		Large (>20 kcal/mole)	
D(spin-spin)	~ 0.3–0.4 cm^{-1}		~ 0.1 cm^{-1}	
Polarization of transition moment	Perpendicular to molecular plane	Parallel to molecular plane	Parallel to molecular plane	Perpendicular to molecular plane
Φ_e^{77K}	<0.01	~ 0.5	1.0 to 0.05	<0.5
E_T	<75	<65	Variable	

As an example, in Figure 5.15 the spin-allowed absorption spectrum of benzophenone consists of two major bands, one maximizing at ~350 nm (in cyclohexane) and the other maximizing at ~250 nm (in cyclohexane). The low value of ε_{max} (~100) for the longer wavelength band allows assignment of a $n \rightarrow \pi^*$ orbital transition to this band (see Table 5.4). This assignment is consistent with the "blue shift" of the maximum upon going from cyclohexane to ethanol (Fig. 5.15). The value of ε_{max} (~10,000) of the short wavelength band allows assignment of a $\pi \rightarrow \pi^*$ orbital transition to this band. This assignment is consistent with the "red shift" of the maximum upon going from cyclohexane to ethanol. Notice

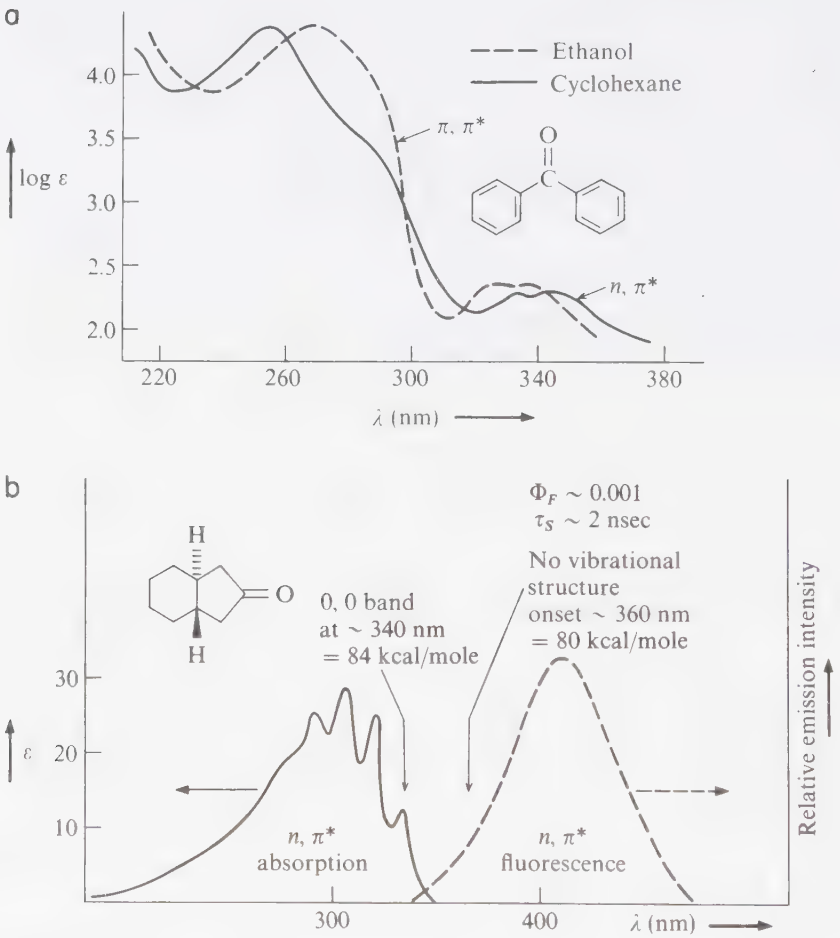

Figure 5.15

(a) Absorption spectrum of benzophenone in ethanol (dotted line) and cyclohexane (solid line). (b) Absorption and emission spectrum of trans-β-hydrindanone in isooctane at room temperature. The emission is nearly pure fluorescence. At low temperatures (77K) phosphorescence becomes significant.

that the n, π^* absorption of an alkanone (Fig. 5.15b) occurs in a similar region to that for benzophenone.

To the photochemist, the limiting values of k_F^0 are important to calibrate the maximum time allowed for reaction in S_1, i.e., if a reaction from S_1 is to occur efficiently, its rate must be competitive with k_F^0. From Table 5.3 we note that for organic molecules the "world's record" for the largest k_F^0 is $\sim 10^9$ sec^{-1} (fully allowed $\pi \rightarrow \pi^*$ transition, example p-terphenyl) and the "world's record" for the smallest k_F^0 is $\sim 10^5$ sec^{-1} (weakly allowed $n \rightarrow \pi^*$ transition, example acetone).

Quantum Yields for Allowed $S_1 \rightarrow S_0$ Fluorescence

Examples of the total (fluorescence and phosphorescence) emission spectra of different types of organic molecules are given in Figures 5.16–5.20.

Whether or not emission is observed for an organic molecule is determined by the experimental quantum yield for emission (Φ_F for fluorescence and Φ_P for phosphorescence). Recall that Φ is a measure of the efficiency of an emission process (photons out versus photons in). Although all excited states emit a certain number of photons *in principle*, it is found *in practice* that quantum yields of less than 10^{-4} (i.e., 0.01% efficiency based on absorbed light) are difficult to measure experimentally and are prone to ambiguities.

A general expression for a quantum yield of emission is given by:

$$\Phi_e = \Phi_* k_e^0 (k_e^0 + \Sigma k_i)^{-1} = \Phi_* k_e^0 \tau \tag{5.42}$$

where Φ_* is the formation efficiency of the emitting state, k_e^0 is the rate constant for emission, Σk_i is the sum of all rate constants (unimolecular or pseudo-unimolecular) that deactivate the emitting state, and τ is the measured experimental lifetime of the emitting state; i.e., $\tau \equiv (k_e^0 + \Sigma k_i)^{-1}$. The experimental lifetime τ, and therefore the experimental quantum yield of emission Φ_e, depend crucially on the magnitude Σk_i, which in turn is very sensitive to experimental conditions for measurement.

For example, in fluid solution at room temperature bimolecular, diffusional quenching processes and thermally activated chemical reactions may compete with radiative decay of an excited state. Thus Φ_e may be very small even if Φ_* is close to unity. Thus, in order to routinely observe an electronic emission spectrum it is usually necessary to minimize Σk_i. This is routinely accomplished by cooling the sample to a very low temperature (77 K, the boiling point of liquid nitrogen, is an experimentally convenient temperature) and by making the sample rigid (most organic solvents are solids at 77 K). The low temperature causes terms in Σk_i which correspond to the rate constants of processes that are activated by several kcal mole or more, to become small relative to k_e^0. The rigidity of the sample eliminates terms in Σk_i which are due to bimolecular quenching processes, since diffusion is essentially eliminated in solid solution. In addition to preventing diffusional quenching, a rigid solvent matrix may restrict certain molecular motions (e.g., twisting of C=C bonds or extensive stretching of C—C bonds), which are particularly effective at promoting radiationless transitions. Numerous

solvents form optically clear solid solutions at 77 K and are called *glasses* at this temperature.

Even when fluorescence and phosphorescence spectra of organic molecules are measured at 77 K in organic glasses, the total quantum yields of emission ($\Phi_F + \Phi_P$) are *generally* less than 1.00. Evidently, radiationless processes occur even at 77 K in rigid glasses, i.e.,

$$\Phi_F + \Phi_P + \Sigma\Phi_R \equiv 1 \tag{5.43}$$

where $\Sigma\Phi_R$ is the sum of quantum yields for photochemical and photophysical radiationless transitions from S_1 and T_1. Identification and evaluation of the photophysical sources of Φ_R will be discussed in Chapter 6. For our purposes we simply note here that radiationless processes can compete with k_F for deactivation of S_1 and with k_P for deactivation of T_1, even at 77 K.

Data derived from fluorescence and phosphorescence spectra are best interpreted in terms of Eq. 5.44 which is a specific form of Eq. 5.42 ($\Phi_* = 1.00$, since the emitting state is the absorbing state, $k_e = k_F$, and $\Sigma k_i = k_{ST}$).

$$\Phi_F = k_F(k_F + k_{ST})^{-1} = k_F\tau_S \tag{5.44}$$

where $\tau \equiv (k_F + k_{ST})^{-1}$.

Equation 5.44 has two limiting situations: (a) $k_F \gg k_{ST}$, in which case $\Phi_F \sim 1.00$, and (b) $k_{ST} \gg k_F$ in which case $\Phi_F \equiv k_F/k_{ST}$.

In terms of these limits we note that Φ_F will $\to 1$ when k_F is very large or if k_{ST} is very small. Also $\Phi_F \to 0$ when k_F is very small or k_{ST} is very large. From the limits of ε_{max} for $S_0 \to S_1$ absorption, the *limits* of the rate constant of fluorescence for organic molecules are (from Eq. 5.19):

$$10^9 \text{ sec}^{-1} \gtrsim k_F \gtrsim 10^5 \text{ sec}^{-1} \tag{5.45}$$

The *limits* of k_{ST} turn out to be

$$10^{11} \text{ sec}^{-1} \gtrsim k_{ST} \gtrsim 10^5 \text{ sec}^{-1} \tag{5.46}$$

Experimental Examples of Fluorescence Quantum Yields

Some data for fluorescence quantum yields (77 K, rigid organic glass) are given in Table 5.5. The following "generalizations" may be made:[16]

1. Most rigid aromatic hydrocarbons (e.g., benzene, naphthalene, etc.) are measurably fluorescent ($1 \geq \Phi_F > 0.01$).

2. Low values of Φ_F for rigid aromatic hydrocarbons are usually the result of competing $S_1 \to T_1$ intersystem crossing (to be discussed in detail in Chapter 6).

3. Substitution of Cl, Br, or I for H generally results in a decrease in Φ_F such that $\Phi_F^H > \Phi_F^{Cl} > \Phi_F^{Br} > \Phi_F^I$ (e.g., compare naphthalene with the halonaphthalenes).

4. Substitution of C=O for H generally results in a substantial decrease in Φ_F. (e.g., compare benzene with benzophenone).

5. Molecular rigidity (due to structural or environmental constraints) enhance Φ_F (compare rigid aromatics to stilbene).

Starting with aromatic hydrocarbons, let us now determine how specific values of k_F and k_{ST} contrive to determine Φ_F.

For naphthalene the $S_0 \rightarrow S_1$ transition is "orbital symmetry forbidden." The molecule is so symmetrical that the electric vector of the light cannot easily find an axis along which to oscillate an electron. As a result $\varepsilon_{max} \sim 10^2$ and $k_F \sim 10^6$ sec^{-1}. The rate of intersystem crossing from $S_1 \rightarrow T_1$ is also $\sim 10^6$ sec^{-1} for naphthalene. Thus, naphthalene fluoresces with a moderate quantum yield

Table 5.5 Some Examples of Fluorescence Quantum Yields and Other Emission Parameters

Compound	Φ_F[a]	ε_{max}	k_F^0	k_{ST}	Configuration of S_1
Benzene	~0.2	250	2×10^6	10^7	π, π^*
Naphthalene	~0.2	270	2×10^6	5×10^6	π, π^*
Anthracene	~0.4	8500	5×10^7	$\sim 5 \times 10^7$	π, π^*
Tetracene	~0.2	14000	2×10^7	$\sim 10^8$	π, π^*
9,10-Diphenylanthracene	~1.0	12600	$\sim 5 \times 10^8$	$< 10^7$	π, π^*
Pyrene	~0.7	510	$\sim 10^6$	$< 10^5$	π, π^*
Triphenylene	~0.1	355	$\sim 2 \times 10^6$	$\sim 10^7$	π, π^*
Perylene	~1.0	39500	$\sim 10^8$	$< 10^7$	π, π^*
Stilbene[b]	~0.05	24000	$\sim 10^8$	$\sim 10^9$	π, π^*
1-Chloronaphthalene	~0.05	~300	$\sim 10^6$	5×10^8	π, π^*
1-Bromonaphthalene	~0.002	~300	$\sim 10^6$	$\sim 10^9$	π, π^*
1-Iodonaphthalene	~0.000	~300	$\sim 10^6$	$\sim 10^{10}$	π, π^*
Benzophenone[c]	~0.000	~200	$\sim 10^6$	$\sim 10^{11}$	n, π^*
Biacetyl[d]	~0.002	~20	$\sim 10^5$	$\sim 10^8$	n, π^*
Diaza[2.2.2]bicyclooctane[e]	~1.0	~200	$\sim 10^6$	$< 10^5$	n, π^*
Acetone[f]	~0.001	~20	$\sim 10^5$	$\sim 10^9$	n, π^*
Perfluoroacetone[g]	~0.1	~20	$\sim 10^5$	$\sim 10^7$	n, π^*
3-Bromoperylene[h]	~1.0	~40,000	$\sim 10^8$	$< 10^6$	π, π^*
Pyrene-3-carboxaldehyde[i]	~0.25	~70,000	$\sim 10^8$	$\sim 10^8$	π, π^* (?)
Cyclobutanone[j]	~0.0001	~20	$\sim 10^5$	$\sim 10^9$	n, π^*
Diaza[2.2.1]bicycloheptane[e]	~0.0001	400	$\sim 10^6$	$\sim 10^6$	n, π^*

[a] Values refer to fluid solutions at room temperature. Data extracted from reference 17a unless otherwise specified
[b] Reference 23.
[c] References 38 and 53.
[d] Almgren, M., *Photochem. and Photobio.*, *6*, 829 (1967); Yekta, A., Ph.D. Dissertation, Columbia University, 1973
[e] Solomon, B. S., Thomas, T. F., and Steel, C., *J. Am. Chem. Soc.*, *90*, 2249 (1968).
[f] Reference 11b.
[g] Halpern, A. M., and Ware, W. R., *J. Chem. Phys.*, *53*, 1969 (1970)
[h] Dreeskamp, H., Koch, E., and Zander, M., *Chem. Phys. Letters*, *31*, 251 (1975).
[i] Bredereck, K., Forster, T., and Osterlin, H. G., *Luminescence of Organic and Inorganic Materials*, eds. Kallman, H. P., and Spruch, G. M., New York: John Wiley, 1962, p. 161.
[j] O'Sullivan, M., and Testa, T., *J. Phys. Chem.*, *77*, 1830 (1973); see also Shortridge, R. G., Rusbult, C. F., and Lee, E. K. C., *J. Am. Chem. Soc.*, *93*, 1863 (1971).

($\Phi_F \sim 0.20$). The (80 of 100) nonfluorescing naphthalene S_1 molecules intersystem cross to T_1.

For anthracene the $S_0 \rightarrow S_1$ transition is symmetry-allowed (the electric vector recognizes the long axis of anthracene as an excellent axis for induction of electron oscillation). As a result, $\varepsilon_{max} \sim 10^4$ and $k_F \sim 10^8$ sec^{-1}. In the case of diphenyl anthracene $\Phi_F \sim 1.00$, i.e., essentially every singlet state fluoresces.

Now consider the decrease in Φ_F which generally (but not universally) accompanies the replacement of H with halogen or C=O functions. The small value of Φ_F (within the framework of our assumption) means that $k_{ST} \gg k_F$. For halogenated naphthalenes, the substitution of halogen for H affects ε_{max} by a factor of only ~ 2 whereas Φ_F varies over several orders of magnitude. From the constancy of ε_{max} we conclude that k_F does not vary much in this series, so that k_{ST} must be the changing variable leading to the radical variation in Φ_F. The enhancement of probability of spin-forbidden transitions which result from the replacement of H by halogen has become known as the "heavy atom effect." The theoretical basis of this effect is due to enhanced spin-orbit coupling, and is discussed in Section 5.9.

A general feature of the emission of ketones possessing $S_1(n, \pi^*)$ states (Figs. 5.19 and 5.20) is the small value of the fluorescence quantum yield ($\Phi_F \sim 0.01$ to 0.0001). Since the radiative rate of $S_1(n, \pi^*) \rightarrow S_0$ fluorescence is relatively slow ($\sim 10^5$ from Table 5.3), the magnitude of k_{ST} need not be much larger than it is for aromatic hydrocarbons. However, it is found that k_{ST} may reach values of 10^{11} sec^{-1} for certain ketones (benzophenone, for example), implying an *enhanced* value of k_{ST} relative to aromatic hydrocarbons (see the discussion in Section 5.6 for an explanation of this effect). Thus, a small value of k_F and a large value of k_{ST} combine to make Φ_{ST} very small.

In certain cases (e.g., cyclic azoalkanes) a small k_F is accompanied by an even *smaller* value of k_{ST}, so that Φ_F is still ~ 1.0.

Exceptions to the general rule that Φ_F is small for halogenated compounds and carbonyl compounds exist and are informative to analyze. From Table 5.5, bromoperylene ($\Phi_F \sim 1.0$) and pyrene-3-aldehydes ($\Phi_F \sim 0.70$) are examples. For these compounds, k_{ST} is exceptionally slow because T_2 lies well above S_1. $S_1 \rightarrow T_1$ intersystem crossing is inhibited by Franck-Condon factors (Section 6.9). Of course, if photochemistry occurs in S_1, the value of Φ_F may be small. For example, cyclobutanone ($\Phi_F \sim 0.0001$) undergoes an efficient cleavage reaction in S_1 (Chap. 13) that competes effectively with both fluorescence and intersystem crossing.

The lesson to be learned from these examples of the experimental values of Φ_F is that this quantity represents an *efficiency* which compares *relative* transition probabilities and does *not* relate directly to *rates*, i.e., $\Phi_F \sim 1.0$ for 9,10-diphenylanthracene for which $k_F \sim 5 \times 10^8$ sec^{-1} and $\Phi_F \sim 1.0$ for diaza[2.2.2]bicyclooctane for which $k_F \sim 10^6$ sec^{-1}. Furthermore, quenching processes (oxygen, impurities, solvent, etc.) may determine the value of Φ_F.

Saturated compounds,[18] ethylenes,[19] and polyenes[20] generally do not fluoresce efficiently (exception: some aliphatic amines[21] fluoresce strongly). For example, tetramethylethylene shows a very broad weak fluorescence ($\lambda^F_{max} \sim 265$ nm) with

$\Phi_F \sim 10^{-4}$ and $\tau \sim 10^{-11}$ sec. Such short lifetimes and low emission efficiencies are typical of "flexible" molecules for which a rapid radiationless deactivation may occur via a stretching motion along a C—C (or C—H) bond or via a twisting motion about a C=C bond.

As an illustration of the role of stretching and twisting motions in determining Φ_F, consider[22] the aromatic hydrocarbons toluene (**1**) and t-butyl benzene (**2**). The latter possesses a "looser" side chain vibration and lower value of Φ_F than the former:

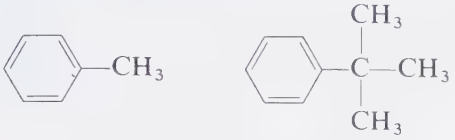

1, $\Phi_F = 0.14$ **2**, $\Phi_F = 0.032$

The flexible stilbenes **3**[23a] and **4**[23b] and their rigid cyclic derivatives **5**[23c,d] provide a nice example of how both structure or environmental rigidity enhance Φ_F:

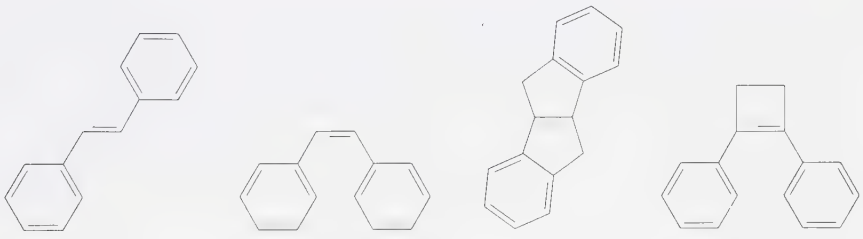

		3	**4**	**5***t*	**5***c*
Φ_F	25°C	0.05	0.00	1.0	1.0
	77 K	0.75	0.75	1.0	1.0

Although trans-stilbene (**3**) is only weakly fluorescent ($\Phi_F = 0.05$) and cis-stilbene (**4**) is nonfluorescent in fluid solution at room temperature, in a rigid environment both compounds are strongly fluorescent ($\Phi_F \sim 0.75$). Both temperature and environmental rigidity contribute to this enhancement. For example,[23] the fluorescence efficiency of trans-stilbene increases by a factor of 3 in going from fluid organic solvents ($\Phi_F \sim 0.05$) to viscous glycerol ($\Phi_F \sim 0.15$). Presumably, twisting about the C=C bond is inhibited in the more viscous solvent. In contrast, the fluorescence yields [23c,d] of the structurally rigid analogues **5***t* and **5***c* are ~1.0 at both 25°C and 77 K.

In several exceptional cases,[20] structured fluorescence emission has been reported. For example, the rigid steroidal dienes **6** and **7** show emission sufficiently structured to allow an assignment of the 0,0 transition. Presumably, structural rigidity enhances the efficiency of light by inhibiting radiationless processes that

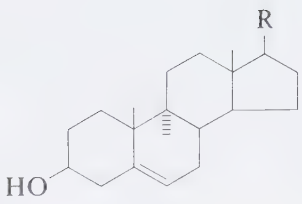

6

$\lambda_F^0 = 305$ nm
$E_S \sim 95$ kcal/mole

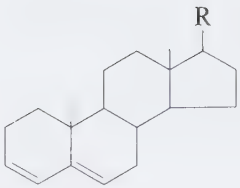

7

$\lambda_F^{0,0} = 312$ nm
$E_S \sim 92$ kcal/mole

compete with fluorescence and by enhancing k_F by preventing a large Franck-Condon geometry difference between S_1 and S_0.

The Relationship of Fluorescence Parameters to Molecular Structure

In the previous section we learned that three important experimental fluorescence parameters are, (a) the radiative fluorescence rate constant, k_F^0, (b) the quantum yield for fluorescence, Φ_F, and (c) the measured experimental fluorescence or excited singlet state lifetime, τ_S.

The theoretical relationship of molecular structure and k_F^0 follows from examination of Eqs. 5.11, 5.14, and 5.42 ($\Phi_e \equiv \Phi_F$, $k_e^0 \equiv k_F^0$, $\tau \equiv \tau_S$). The magnitude of $\langle H_F \rangle$ and the value of k_F^0 depends on the orbitals involved in the electronic transition, the nuclear shape of the initial and final states. Thus, there is a direct theoretical connection between k_F^0 and electronic structure and symmetry.

The theoretical relationship between Φ_F or τ_S and $\langle H_F \rangle$ is not generally direct since (Eq. 5.42), Φ_F and τ_S depend on k_F^0 *and* the radiationless rates Σk_i. Thus, a small value of Φ_F or short fluorescence lifetime τ_S may reflect fast radiationless processes, and be relatively unaffected by the magnitude of k_F^0.

Determination of "State Energies" from Emission Spectra

The *highest* energy vibrational band in an emission spectrum corresponds to the 0,0 transition (Fig. 5.8). The energy gap corresponding to this 0,0 transition characterizes the energy of the excited state responsible for the emission. It is the *maximum* energy derivable from the excited state if S_0 is regenerated. The singlet state energy, E_S, and the triplet state energy, E_T, are defined as the 0,0 energy gap for fluorescence, $S_1(v = 0) \rightarrow S_0(v = 0)$, and phosphorescence, $T_1(v = 0) \rightarrow S_0(v = 0)$, respectively.

Sometimes an emission spectrum does not show resolved fine structure (Fig. 5.15b). In this case, the "onset" of emission must be used to guess the upper limit of E_S or E_T. If vibrational structure appears in the absorption spectrum, the 0,0 band of absorption (Fig. 5.15b) serves as a safe guide for an upper limit to state energies. In Figures 5.16 to 5.20 the 0,0 bands of fluorescence and or phosphorescence are noted and the values of E_S or E_T are given.

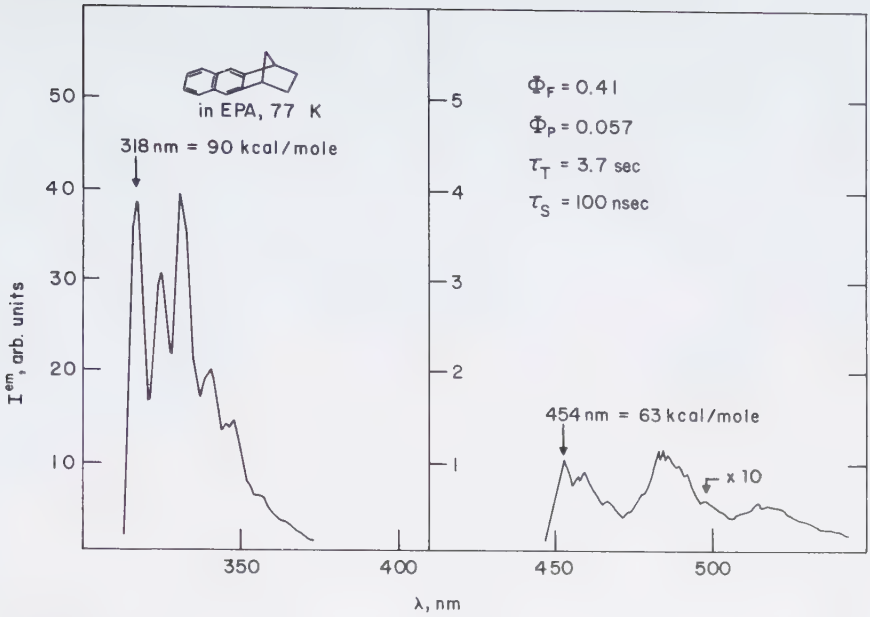

Figure 5.16
Total emission spectrum of naphthonorbornene at 77 K.

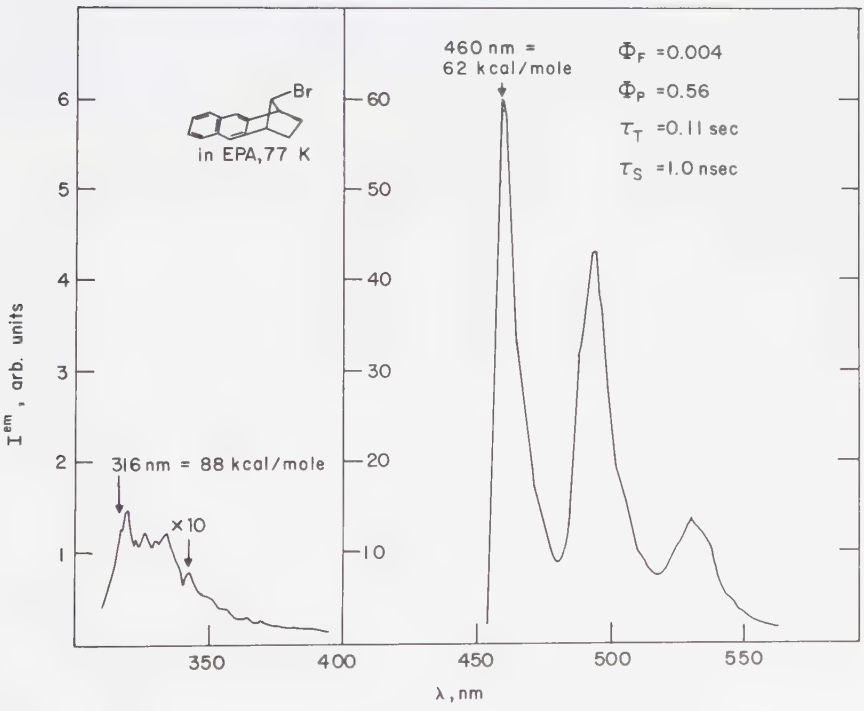

Figure 5.17
Total emission spectrum of 7-anti-bromonaphthonorbornene at 77 K.

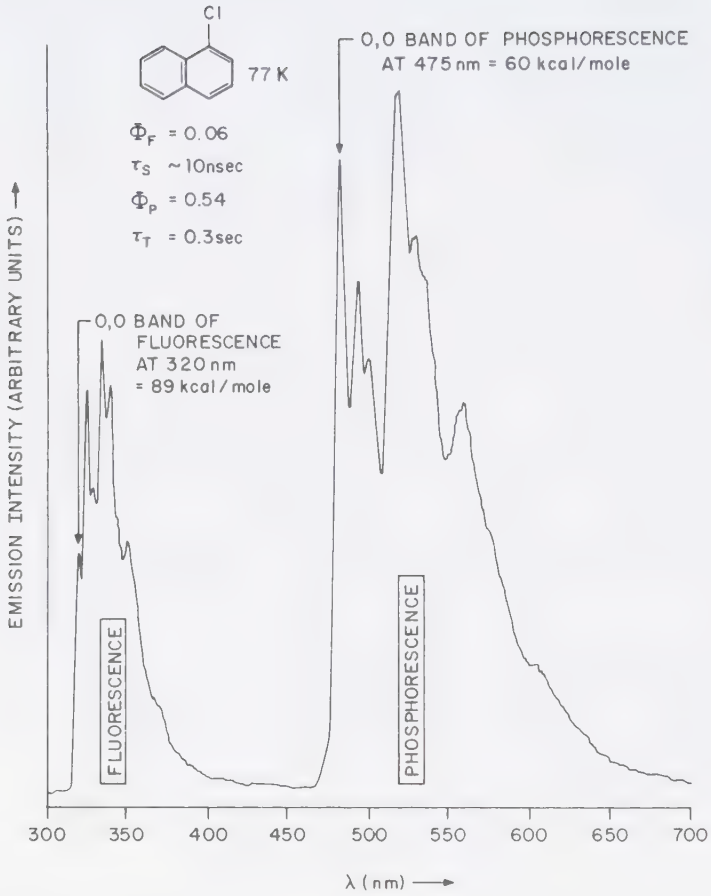

Figure 5.18

Total emission spectrum of 1-chloronaphthalene at 77 K in EPA (mixture of ether-isopentane-ethanol).

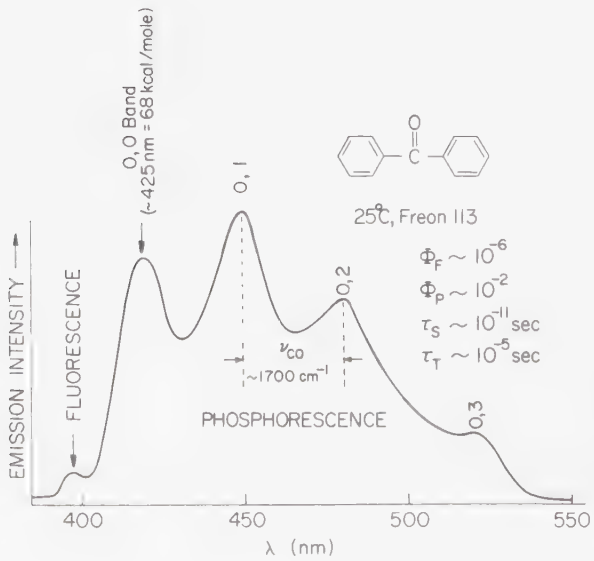

Figure 5.19

Total emission of benzophenone at room temperature in Freon 113 solvent. The fluorescence band is due mainly to "delayed" fluorescence (see Section 5.14).

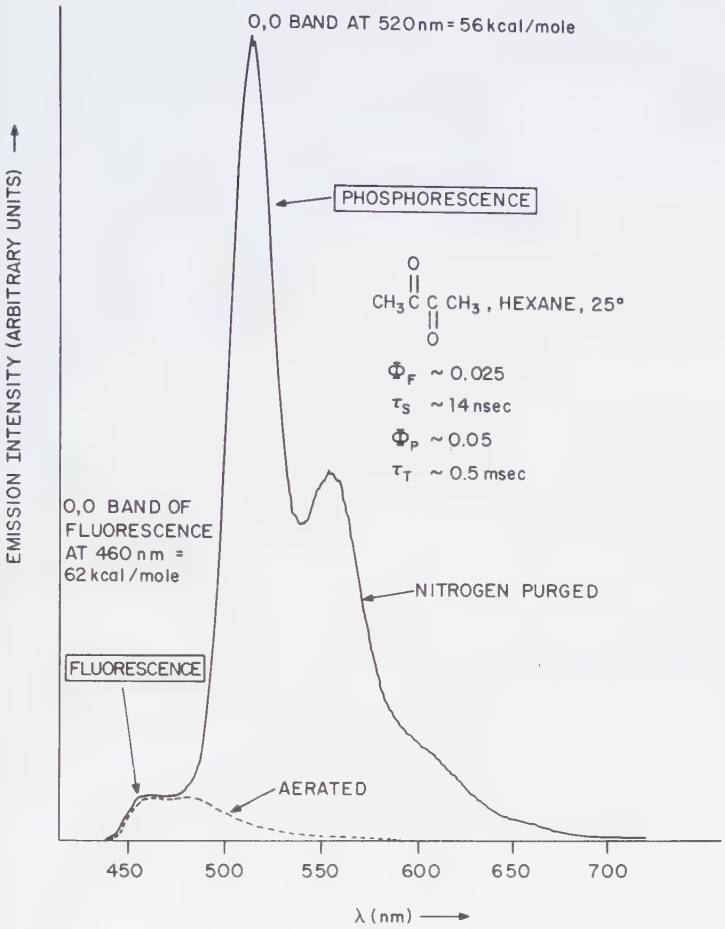

Figure 5.20

Emission of biacetyl in de-aerated hexane solution at room temperature. The fluorescence (left) is relatively insensitive to impurities, oxygen, temperature, etc., but the phosphorescence (right) is extremely sensitive to impurities. In aerated solutions *no* phosphorescence is observed.

5.8 Spin-Orbit Coupling and Spin-Forbidden Radiative Transitions

The value of $\varepsilon(S_0 \rightarrow T)$ or of $k_P^0(T \rightarrow S_0)$ is directly related to the degree of spin-orbit coupling between S_0 and T. From Section 3.6 the degree of spin-orbit coupling was shown to depend strongly on (a) nuclear charge, (b) the availability of transitions between orthogonal (or nearly orthogonal) orbitals, and (c) the availability of a "one atom center" transition.[8]

The degree of spin-orbit coupling between states of an atom is related to ζ, a fine structure or spin-orbit coupling constant available from atomic spectra.[24]

The correlation of the magnitude of spin-orbit coupling within a molecule (as judged from the magnitude of fine structure constants of atoms) and the magnitude of $\varepsilon(S_0 \rightarrow T)$ absorption and $k_P^0(T \rightarrow S_0)$ emission played a decisive role in establishing the triplet state as an important photochemical entity.[25] The oscillator strength of a radiative transition is related to ζ, the spin-orbit coupling constant for *atoms*.[24] This means the $\varepsilon(S_0 \rightarrow T)$ and $k_P^0(T \rightarrow S_0)$ will increase as ζ increases if the *orbital factors are similar*. The magnitude of ζ depends on the orbital configurations of the states involved (Table 5.6). The important points to be derived from this table are: (a) the rapid increase in the magnitude of spin-orbit coupling as the atomic number increases, (b) for first-row atoms such as C, N, and O, the magnitude of spin-orbit coupling is smaller than the energy of vibrational couplings ($\sim$1–5 kcal/mole), and (c) for very heavy atoms (Pb, Xe) the magnitude of spin-orbit coupling begins to approach the value of electronic energy gaps and strong electronic interactions ($\sim$20–30 kcal/mole). For the latter molecules spin inversion can occur on a time scale comparable to electronic motions.

Radiative Transitions Involving a Change in Multiplicity: $S_0 \rightleftarrows T(n,\pi^*)$ and $S_0 \rightleftarrows T(\pi,\pi^*)$ Transitions

The oscillator strengths for spin-forbidden transitions in organic molecules range from $\sim 10^{-5}$ to $\sim 10^{-9}$ (Table 5.3). This means that radiative $S_0 \leftrightarrows T$ transitions are strongly forbidden relative to spin-allowed $S_0 \leftrightarrows S$ transitions ($f \sim 1$–10^{-4}). We could say that the light wave must "catch" the molecule in a situation such that spin-orbit coupling is operating on the electron spins at the same time that the electric vector of the light wave is operating on the electron cloud, which is a situation of low probability.

Table 5.6 Spin-Orbit Coupling in Atoms. Values are only representative and depend on electron configuration; they are intended here to show only trends

Atom	Atomic number	ζ kcal/mole	Atom	Atomic number	ζ kcal/mole
C[b]	6	0.1	I	53	15.0
N[b]	7	0.2	Kr	36	15
O[b]	8	0.4	Xe	54	28
F[b]	9	0.7	Pb	82	21
Si[b]	14	0.4	Hg	80	18
P[b]	15	0.7	Na	11	0.1
S[b]	16	1.0	K	19	0.2
Cl[b]	17	1.7	Rb	37	1.0
Br	35	7.0	Cs	55	2.4

[a] Values adapted from McClure, D. S., *J. Phys. Chem.*, *17* (1949) 905. The values are in kcal/mole and are rounded off, and, strictly speaking, apply to the radical part of ζ. In effect, the angular part of ζ is considered to be close to unity. Values of ζ are for the lowest-energy atomic configurations.

[b] Because of substantial configuration interaction for these atoms, the values given are extrapolated from nearby atoms in the periodic table by assuming that ζ varies with Z^4.

In general, $n^2 \leftrightarrows n, \pi^*$ transitions possess a much greater oscillator strength than $\pi^2 \leftrightarrows \pi, \pi^*$ transitions for a spin-forbidden transition, i.e.,

$$f[S_0 \rightleftarrows T(n, \pi^*)] \gg f[S_0 \rightleftarrows T(\pi, \pi^*)] \tag{5.47}$$

This is exactly the opposite of the situation for $S_0 \leftrightarrows S_n$ transitions, for which $f(\pi, \pi^*) > f(n, \pi^*)$. The reason for this turnaround in behavior is that the spin-orbit force is much more effective when $n^2 \rightleftarrows n, \pi^*$ transitions occur than when $\pi^2 \rightleftarrows \pi, \pi^*$ transitions occur.

The situation may be viewed schematically as follows. The f values of the $S_0(n^2) \rightleftarrows T(n, \pi^*)$ and $S_0(\pi^2) \rightleftarrows T(\pi, \pi^*)$ transitions are composed of three parts: the electronic, vibrational, and spin factors. We know that in general $f_{el} f_v(\pi, \pi^*) > f_{el} f_v(n, \pi^*)$ because $\varepsilon(\pi, \pi^*) > \varepsilon(n, \pi^*)$ for singlet-singlet transitions for which spin is *not* a factor. This implies that for spin-forbidden radiative transitions, $f_s(n, \pi^*) \gg f_s(\pi, \pi^*)$.

Consider a radiative $S_0(n^2) \rightarrow T(n, \pi^*)$ transition absorption for formaldehyde and a $S_0(\pi^2) \rightarrow T(\pi, \pi^*)$ transition of ethylene. The spin-flip in the first case (Fig. 5.21a) is due to a $n \rightarrow \pi^*$ transition, which may be viewed as a jump from a p orbital (say, p_X) in the plane of the molecule to a p orbital (say, p_y) perpendicular to the plane of the molecule (i.e., the atomic p orbital on oxygen which makes up half of the π^* orbital). The simultaneous $p_x \rightarrow p_y$ orbital jump is thus a *one-center* jump involving a momentum change. *This is precisely the type of situation which favors strong spin-orbit coupling*, i.e., the orbital momentum change associated with the $p_x \rightarrow p_y$ jump is matched exactly by the spin momentum change associated with the $\alpha\beta \rightarrow \alpha\alpha$ (or $\alpha\beta \rightarrow \beta\beta$) spin flip.

Let us now compare this qualitative picture to the situation for a radiative $S_0(\pi^2) \leftrightarrows T(\pi, \pi^*)$ transition, e.g., for ethylene (Fig. 5.21b). It is immediately seen that for a planar ground state there is no low-energy orbital in the molecular

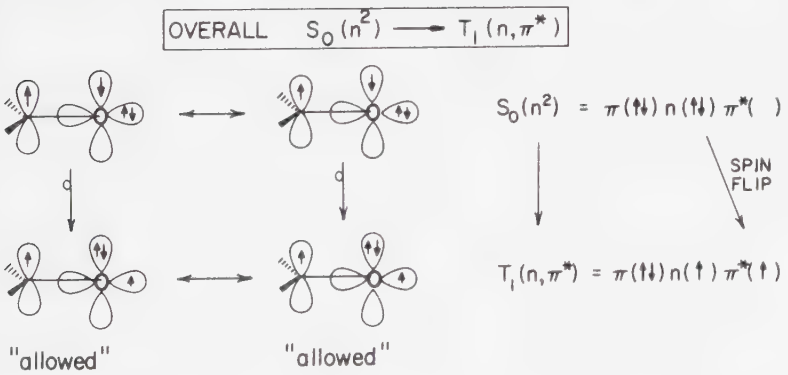

Figure 5.21a

Orbital description of the spin-orbit selection rules for a radiative transition involving a spin flip. The $n^2 \rightarrow n, \pi^*$ transition involves an orbital angular momentum change that can be coupled with a spin momentum charge, and is spin-orbit "allowed."

plane into which the π electron can jump, i.e., the analogue of the $p_x \rightarrow p_y$ jump of ketones does not exist for ethylene. As a result, there are no "one-center" spin-orbit interactions to help flip spins when a light wave interacts with the π electrons of the ethylene.

This means that the matrix element for spin-orbit coupling is much larger for $n^2 \rightleftarrows n, \pi^*$ transitions than for $\pi^2 \rightleftarrows \pi, \pi^*$ transitions. Since the oscillator strength of a spin-forbidden transition depends directly on the square of the matrix element (Eq. 5.38) corresponding to the perturbation (spin-orbit coupling) which mixes the states undergoing transition, we can conclude

$$f[S_0(n^2) \rightleftarrows T(n, \pi^*)] \gg f[S_0(\pi^2) \rightarrow T(\pi, \pi^*)] \tag{5.48}$$

An aromatic hydrocarbon such as benzene cannot invoke an $n \leftrightarrow \pi^*$ mixing to generate a spin-orbital coupling mechanism.[14] The analogous mixing is $\sigma \leftrightarrow \pi^*$ or $\pi \leftrightarrow \sigma^*$. There is a theoretical connection between the out-of-plane vibrations, the observation of *spin-forbidden* phosphorescence emission, and the allowed transitions involving σ or σ^* orbitals. Consider Figure 5.22 which shows (a) a planar benzene molecule and (b) another benzene molecule undergoing out-of-plane C—H vibrations. As long as the molecule is planar, the π, π^* states and, say, the π, σ^* states do not mix. An out-of-plane C—H vibration destroys the planar symmetry and then allows mixing of the π, π^* and π, σ^* states. In the extreme case, a violent out-of-plane C—H vibration would cause a p orbital (originally symmetric above and below the molecular plane) to be transformed into an sp^n orbital which possesses an assymmetric electronic distribution relative to the plane of the molecule.

This mechanism is not expected to be particularly effective because of the large amount of energy required to deform the aromatic π electron cloud in this manner. However, no better mechanism for spin-orbit coupling exists. Indeed, the radiative phosphorescence lifetimes of aromatic hydrocarbons such as benzene and naphthalene are of the order of 30 *seconds* ($f \sim 10^{-9}$!).

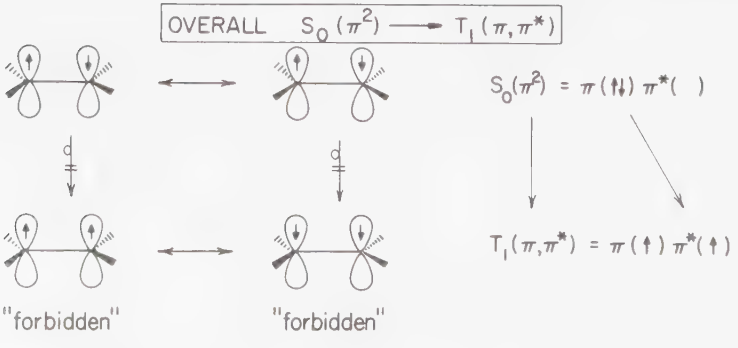

Figure 5.21b

Orbital description of the spin-orbit selection rules for a radiative transition involving a spin flip. The $\pi^2 \rightarrow \pi, \pi^*$ transition does not involve an orbital angular momentum change and is spin-orbit "forbidden."

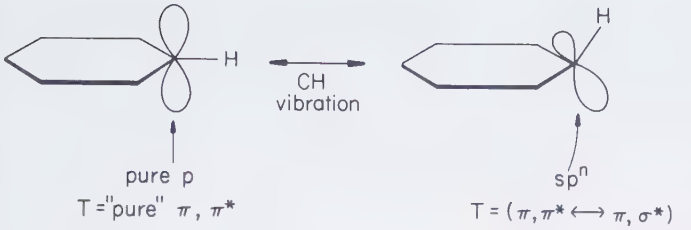

Figure 5.22

Schematic of the effect of an out-of-plane C—H vibration on the hybridization of a carbon atom in benzene. The vibration induces "s character" in the carbon atom and provides a "weak" mechanism for spin-orbit coupling.

5.9 Experimental Examples of Spin-Forbidden Radiative Transitions: $S_0 \rightarrow T$ Absorption and Phosphorescence

Some experimental data for radiative $S_0 \rightleftarrows T_1$ transitions were given in Table 5.3. (We give more below in Table 5.7). The following points may be derived from the data. As expected, the oscillator strengths of $S_0(\pi^2) \rightleftarrows T_1(\pi, \pi^*)$ are very small ($\sim 10^{-7}$ to 10^{-9}). Indeed, the values of $\varepsilon_{max}(S_0 \rightarrow T_1)$ and k_P for $S_0 \rightleftarrows T_1(\pi, \pi^*)$ are the smallest ever observed for organic molecules, i.e., $\varepsilon_{max} \sim 10^{-5}$ to 10^{-6} and $k_P^0 \sim 1$ to 10^{-1} sec^{-1}. The largest values of $\varepsilon_{max}(S_0 \rightarrow T_1)$ and k_P^0 are found

Table 5.7 Quantum Yields for Phosphorescence and Other Triplet Emission Parameters.[a]

Compound	Φ_P 77 K	Φ_P 25 C	Φ_{ST}	k_P^0	Configuration of T_1
Benzene	~0.2	($<10^{-4}$)	~0.7	$\sim 10^{-1}$	π, π^*
Naphthalene	~0.05	($<10^{-4}$)	~0.7	$\sim 10^{-1}$	π, π^*
1-Fluoronaphthalene	~0.05	($<10^{-4}$)		~0.3	π, π^*
1-Chloronaphthalene	~0.3	($<10^{-4}$)	~1.0	~2	π, π^*
1-Bromonaphthalene	~0.3	($\sim 10^{-4}$)	~1.0	~30	π, π^*
1-Iodonaphthalene	~0.4	—	~1.0	~300	π, π^*
Triphenylene	~0.5	($<10^{-4}$)	~0.9	$\sim 10^{-1}$	π, π^*
Benzophenone	~0.9	(~0.1)[b]	~1.0	$\sim 10^2$	n, π^*
Biacetyl	~0.3	(~0.1)[c]	~1.0	$\sim 10^2$	n, π^*
Acetone	~0.03	(~0.01)[c]	~1.0	$\sim 10^2$	n, π^*
4-Phenylbenzophenone	—	—	~1.0	1.0	π, π^*
Acetophenone	~0.7	(~0.03)[b]	~1.0	$\sim 10^2$	n, π^*
Cyclobutanone	0.0	0.0	0.0	—	n, π^*

[a] Data gathered from references 14 and 16.
[b] In deaerated perfluoromethylcyclohexane.
[c] In deaerated acetonitrile.

for $T_1(n, \pi^*)$ states or for $T_1(\pi, \pi^*)$ states which possess a heavy atom (e.g., Br or I) conjugated to the π systems, i.e., $\varepsilon_{max} \sim 10^{-1}$–$10^{-2}$ and $k_P \sim 10$ to 10^2 sec^{-1}. For some organometallic compounds (e.g., tetraphenyl lead), ε_{max} values of the order of 10 have been claimed.[26a] The wide variation in Φ_P in going from 77 K to 25°C is usually the result of diffusional quenching of triplets at the higher temperature (in fluid solution). The fact that triplet lifetimes at 25°C in plastics (rigid medium which prevents diffusional quenching) are comparable to those at 77 K is strong support for this conclusion. For example, the lifetime of triphenylene is 16 sec at 77 K and is 12 sec at 25°C in a plastic.[26c]

The substantial difference between the values of ε_{max} (and k_P^0) for π, π^* relative to n, π^* triplet states gives us an experimental means of classifying molecules in terms of the orbital configuration of T_1. The postulate is as follows: for nonheavy-atom-containing molecules possessing "pure" π, π^* configurations the value of $\varepsilon_{max}(S_0 \rightarrow T_1)$ and k_P^0 will be on the order of 10^{-5} to 10^{-6}, and 10^2 to 10^{-1} sec^{-1}, respectively. For molecules possessing "pure" n, π^* configurations, the value of $\varepsilon_{max}(S_0 \rightarrow T_1)$ and k_P^0 will be on the order of 10^{-1} to 10^{-2}, and 10^2 to 10 sec^{-1} respectively.

An example of an *unperturbed* $S_0 \rightarrow T$ absorption is shown in Figure 5.23.[26b] The value of ε_{max} is $\sim 10^{-2}$ and corresponds to k_P^0 of $\sim 10^2$ sec^{-1}, a value expected for phosphorescence from $T_1(n, \pi^*)$ states (Table 5.7). In general, it is easier to measure k_P^0 than ε_{max}, so the former is more commonly measured.

Some examples of the relation of k_P^0 and orbital configuration (see Table 5.4 and 5.7) are available for aromatic ketones. For these molecules, T_1 may be

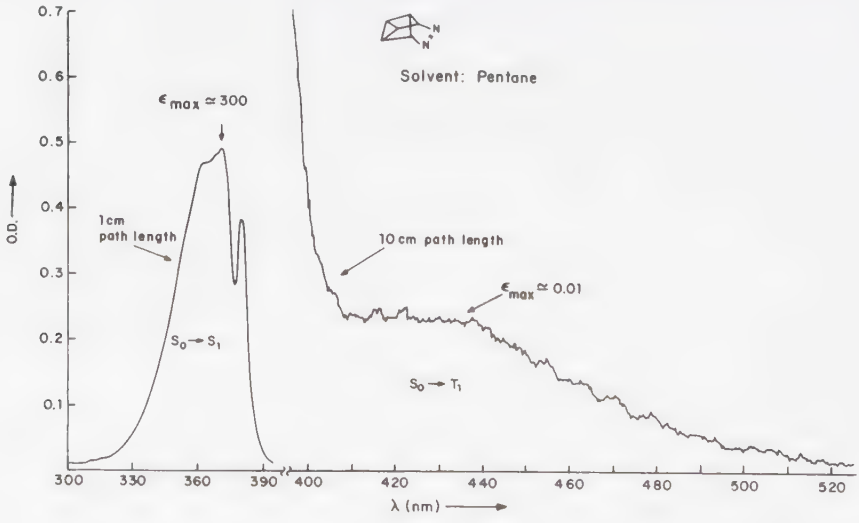

Figure 5.23

Singlet-singlet and singlet-triplet absorption of a polycyclic azoalkane. A long path-length and enhanced instrumental sensitivity are required to observe the weak $S_0 \rightarrow T$ absorption.

either n, π^*, π, π^*, or a hybrid. A model for a "pure" $T_1(n, \pi^*)$ state is acetone, for which $k_P = 60\ \text{sec}^{-1}$; a model for a "pure" $T_1(\pi, \pi^*)$ state is naphthalene, for which $k_P = 0.1\ \text{sec}^{-1}$. Examination of Table 5.4 shows that the structures may be classified as "acetone-like" (k_P within an order of magnitude of $60\ \text{sec}^{-1}$), or "naphthalene-like" (k_P within an order of magnitude of 0.1 sec ^{1}). For example, we may assign an n, π^* configuration to T_1 of benzophenone ($k_P = 20\ \text{sec}^{-1}$) and a π, π^* configuration to T_1 of 4-phenyl benzophenone ($k_P \sim 1\ \text{sec}^{-1}$).

Absorption and Emission from Triplet Sublevels

The "triplet state" of a molecule at room temperature is a rapidly equilibrating mixture of *three* states, i.e., the triplet sublevels T_x, T_y, and T_z. Absorption by an individual molecule produces only one of the three sublevels initially. In normal $S_0 \rightarrow T_1$ absorption (Fig. 5.23), absorption to the three sublevels is not resolved. At low temperatures in favorable cases, however, resolved absorption and magnetic field effects involving the three sublevels are observed.[27a]

The "mechanism" of phosphorescence is spin-orbit coupling between T_1 and various singlet states (Section 5.8). The strongest mixing occurs between T_1 and singlets which possess the correct electronic symmetry to maximize matrix elements of the type $\langle T_1|H_{so}|S_n\rangle$. Molecules in different spin sublevels may be viewed as having their electrons in different planes.[27b] The electronic symmetry of the three magnetic spin components of T_1 (i.e., T_x, T_y, and T_z, Section 2.8) are different. Thus, k_P^x, k_P^y, and k_P^z (the radiative rates from sublevels T_x, T_y, and T_z, respectively) will be different. The mechanism of *populating* the sublevels from S_1 will also lead to different rates of population of T_x, T_y, and T_z. The net result of these theoretical considerations is the expectation that if T_x, T_y, and T_z are not rapidly equilibrated in a time comparable to phosphorescence lifetimes, different phosphorescence parameters will be observed for T_x, T_y, and T_z.

The energetic separation of these sublevels is $\sim 1\ \text{cm}^{-1}$ or less. If sublevel interconversion requires no thermal activation, the dynamic equilibrium interconverting T_x, T_y, and T_z is rapid relative to the triplet lifetime until temperatures < 10 K are achieved. As a result, at 77 K "the triplet state" may be treated as a single state, i.e., an equilibrium mixture of $\frac{1}{3}T_x$, $\frac{1}{3}T_y$, and $\frac{1}{3}T_z$. Below 10 K magnetic sublevel interconversion is slow relative to the triplet lifetime. Under these conditions, the phosphorescence spectrum, lifetime, and polarization depend on the emission properties of each sublevel. In other words, the observed phosphorescence parameters correspond to a populated weighted average of the properties of the T_x, T_y, and T_z states.

As an experimental example,[27c] the phosphorescence rates of the T_x, T_y, and T_z levels of naphthalene are $\sim 0.9\ \text{sec}^{-1}$, $\sim 0.5\ \text{sec}^{-1}$, and $\sim 0.07\ \text{sec}^{-1}$, respectively ($T_x$ and T_y are taken as being in the plane of the molecule and T_z as perpendicular to the molecular plane). The shape of the emission spectrum of each sublevel is different since the vibrational perturbations which induce spin-orbit coupling are different for each sublevel. This results in a different vibrational pattern for emission from each sublevel. For biacetyl,[27d] the values of k_P^x, k_P^y, and k_P^z are $\sim 100\ \text{sec}^{-1}$, $\sim 25\ \text{sec}^{-1}$, and $\sim 1000\ \text{sec}^{-1}$, respectively.

Examples of Perturbation of $S_0 \rightarrow T$ Absorption

The extremely weak inherent spin-orbit coupling of aromatic hydrocarbons makes them prime candidates for spin-orbit perturbation studies. Compounds possessing lowest energy (n, π^*) states or heavy atoms are generally not sensitive to spin-orbit perturbations, because they already possess substantial *internal* spin-orbit interactions. These expectations are confirmed by the experimental observations that:

1. The $S_0 \rightarrow T_1(\pi, \pi^*)$ absorption of aromatic hydrocarbons is generally enhanced by spin-orbit perturbation.

2. The $S_0 \rightarrow T_1(n, \pi^*)$ absorption of ketons is insensitive to spin-orbit perturbation.

The following molecules or classes of molecules have been commonly employed to enhance the $S_0 \rightarrow T_1$ absorption of aromatic hydrocarbons:

1. Molecular oxygen.[28]
2. Organic halides[29] and organometallic compounds.[30]
3. Heavy atom rare gases, e.g., xenon.[31]

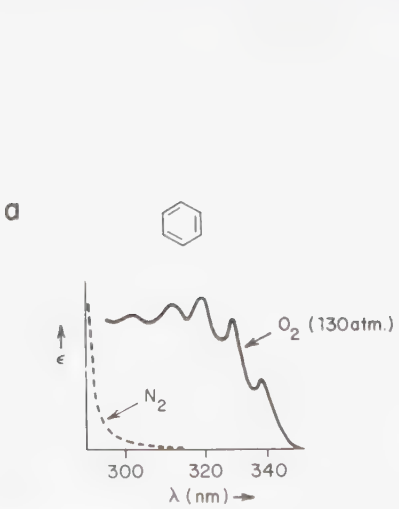

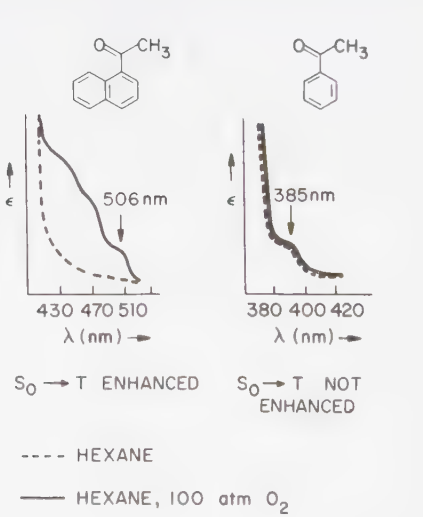

Figure 5.24a

Oxygen perturbation of the $S_0 \rightarrow T_1$ absorption spectrum of benzene.

Figure 5.24b

Examples of the O_2 perturbation of a $S_0 \rightarrow T_1$ (π, π^*) absorption (left, 1-acetonaphthone) and lack of O_2 perturbation on a $S_0 \rightarrow T_1$ (n, π^*) absorption (right, acetophenone).

An example of the effect of O_2 on $S_0 \rightarrow T_1$ of benzene is shown in Figure 5.24. The first resolved band (presumably a vibrational band) occurs at ~ 340 nm (29,400 cm^{-1}, 84 kcal/mole). Since the O, O band of benzene phosphorescence ($T_1 \rightarrow S_0$) occurs at nearly the same energy, the intensity (probability) of the $T_1 \rightarrow S_0$ transition is enhanced, but the energy of the transition is unaffected by oxygen perturbation.[28a]

Perturbation methods offer a means of determining whether T_1 is an n, π^* or a π, π^* state.[32] For example, the absorption spectrum of acetophenone shows a very weak absorption band at ~ 385 nm in n-hexane (Fig. 5.24b). The intensity of this band does not increase significantly even under 100 atm of O_2. The O, O band of acetophenone phosphorescence also occurs at ~ 385 nm. On the other hand, the absorption spectrum of 1-acetonaphthone, which shows negligible absorption near 510 nm in n-hexane, shows several new bands under 100 atm of O_2. The O-O band of 1-acetonaphthone phosphorescence occurs at ~ 506 nm. These results are interpreted to mean that T_1 for acetophenone is n, π^* and therefore not subjected to significant oxygen perturbation, but that T_1 for 1-acetonaphthone is π, π^* and is therefore sensitive to oxygen perturbation.

A second important method for enhancing $S_0 \rightarrow T_1$ absorption is *heavy atom perturbation*. The heavy atom may be directly affixed to the molecule being studied (*internal* heavy atom effect)[33] or may be located in the solvent (*external* heavy atom effect).[34] An example of the *internal* heavy atom effect is shown for β-iodonaphthalene, α-iodonaphthalene, and β-chloronaphthalene in Figure 5.25a[33]. The position of the O, O band for absorption corresponds to that found for the

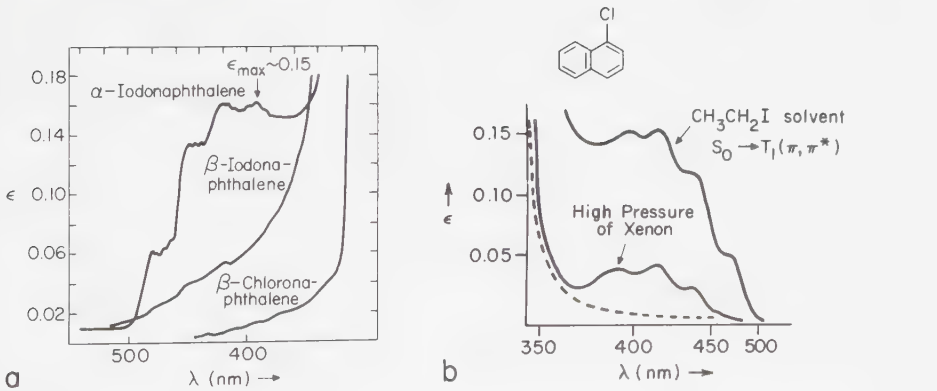

Figure 5.25a

Experimental examples of the internal "heavy atom effect" on $S_0 \rightarrow T_1$ absorption. Notice that the "heavy atom effect" is *different* for different positions for the same molecule.

Figure 5.25b

Heavy atom perturbation of the $S_0 \rightarrow T_1$ absorption of 1-chloronaphthalene. The dotted line indicates the absorption spectrum in a "light atom" solvent.

O, O band of phosphorescence (at 77 K). Furthermore, the shape of the $S_0 \rightarrow T_1$ absorption is nearly the mirror image of the $T_1 \rightarrow S_0$ phosphorescence. The intensity of the $S_0 \rightarrow S_1$ transition is not significantly affected by the heavy atom substitution.

As an example of the *internal* heavy-atom effect, consider 2-bromonaphthalene undergoing a $T_1 \rightarrow S_0$ transition. The triplet state may be represented as a set of resonance structures of diradical character, several of which will place the odd electron on the 1-carbon atom. Since bromine is capable of expanding its valence octet, some delocalization of the odd electron onto the bromine atom is possible. This finite amount of delocalization produces a good mechanism for spin inversion because of the strong spin-orbit coupling the electron experiences when it is on the bromine atom. Presumably, the odd electron which undergoes the spin inversion does so by simultaneously jumping from one orbital to another in order to satisfy the requirement of conservation of total angular momentum.

Examples of the *external* heavy atom effect are shown for a bromonorbornane (**9**)[35] and for 1-chloronaphthalene[34] in Figures 5.18 and 5.25b.

The heavy-atom effect on absorption spectra is to strongly enhance[17] $\varepsilon(S_0 \rightarrow T_1)$ but not $\varepsilon(S_0 \rightarrow S_1)$. Because of the relationship between $\varepsilon(S_0 \rightarrow T_1)$ and k_P^0 and between $\varepsilon(S_0 \rightarrow S_1)$ and k_F^0 (Eq. 5.23), we expect that k_P^0 but not k_F^0 will be influenced by heavy-atom perturbation. For example, the fluorescence and phosphorescence spectra of **8** (Fig. 5.16), **9** (Fig. 5.17), and **10** are very similar in appearance:[35]

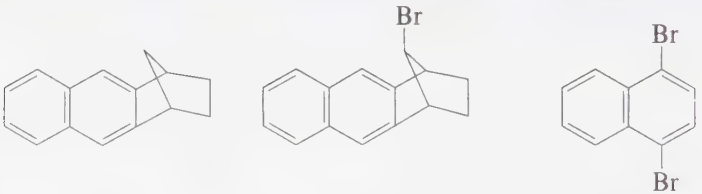

	8	**9**	**10**
k_F^0	1×10^6 sec^{-1}	1×10^6 sec^{-1}	1×10^6 sec^{-1}
k_P^0	3×10^{-2} sec^{-1}	500×10^{-2} sec^{-1}	1000×10^{-2} sec^{-1}

On the other hand, the fluorescence and phosphorescence yields for the "light atom" molecule **8** are $\Phi_F \sim 0.5$ and $\Phi_P \sim 0.06$, and for **9**, $\Phi_F \sim 10^{-3}$ and $\Phi_P \sim 0.6$. The values of k_F^0 are essentially constant in this series, but the values of k_P^0 are greatly enhanced in the bromine-containing molecules. The much higher values of Φ_P reflect both a greater efficiency of population of T_1 (k_{st} is enhanced, see Section 6.11) and a greater efficiency of emission from T_1 (k_P^0 is enhanced *more* than k_{ts}).

For the case of 1-chloronaphthalene (Fig. 5.25b), the pure liquid exhibits a number of weak absorption bands near 470 nm. A 1:2 (by volume) mixture of 1-chloronaphthalene in ethyl iodide shows that the weak bands are greatly enhanced in intensity.[29c] The O, O band of the enhanced absorption (58 kcal/mole) occurs at nearly the same energy as that of the O, O band of phosphorescence.

A phosphorescence excitation spectrum (observation of phosphorescence as a

function of changing excitation wavelength) provides a means of distinguishing whether the triplet produced in $S_0 \rightarrow T_1$ absorption is an n, π^* or π, π^* state.[36] This is done by examining the intensity of the phosphorescence excitation spectrum in the presence and absence of heavy atoms. If T_1 is n, π^* then *no* heavy atom enhancement is expected, since the inherent spin-orbit coupling in n, π^* states is stronger than that which can be induced by external effects.[32] However, if T_1 is π, π^*, a significant heavy atom effect is expected. For example,[36a] the phosphorescence excitation spectrum of benzophenone ($T_1 = n, \pi^*$) is not significantly affected by changing from a "light" to "heavy" atom (e.g., C_2H_5Br or C_2H_5I) solvent (Fig. 5.26a). The phosphorescence excitation spectrum of naphthalene (Fig. 5.26b) ($T_1 = \pi, \pi^*$), however, is significantly affected by such a change in solvent.

The phosphorescence ($T_1 \rightarrow S_0$) and phosphorescence excitation ($S_0 \rightarrow T_1$) spectra of acetophenone (77 K) is analogous to that of benzophenone. No heavy atom effect is noted in either spectrum. The phosphorescence and phosphorescence excitation spectra of p-methoxyacetophenone is shown in Figure 5.26c. Two bands are observed: a weak $S_0 \rightarrow T_1(\pi, \pi^*)$ band and a more intense $S_0 \rightarrow T_1(n, \pi^*)$ band. Only the former is enhanced by the inclusion of heavy atoms in the solvent. In

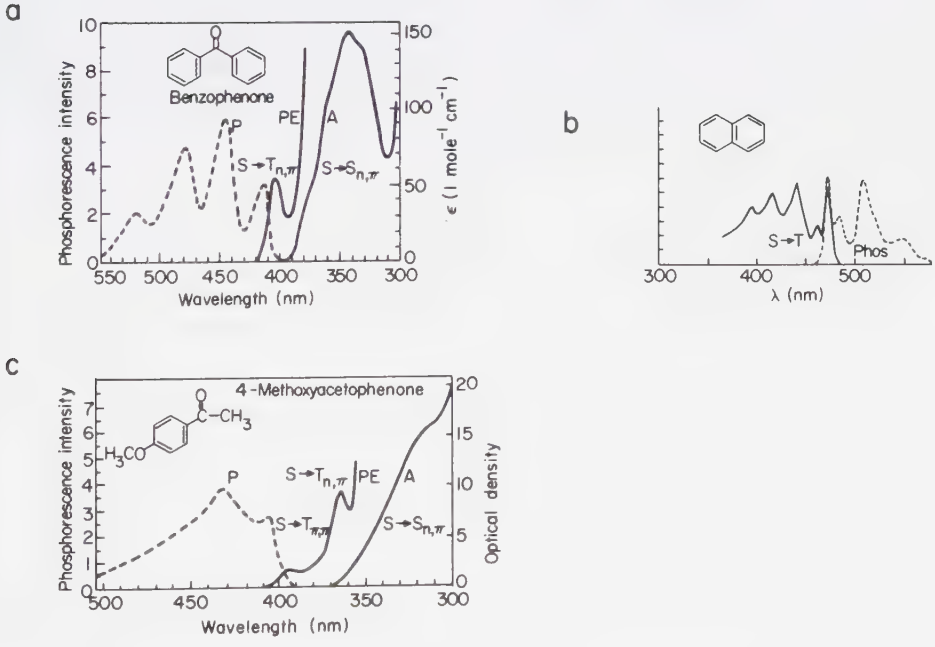

Figure 5.26

Phosphorescence emission (dotted curve *P*, left) and phosphorescence excitation spectrum (solid curve *PE*, right) of (a) benzophenone (b) naphthalene and (c) p-methoxyacetophenone. The conventional singlet-singlet absorption spectrum is also shown (solid curve *A*, right).

agreement with the $T_1(\pi, \pi^*)$ assignment, the phosphorescent lifetime of p-methoxyacetophenone is ~ 100 ms and its phosphorescence spectrum does not display the characteristic C=O stretching progression. Notice the significant overlap of the O, O bands of the phosphorescence spectrum and the phosphorescence excitation spectrum.

Quantum Yields of Phosphorescence

The quantum yield of phosphorescence is given by

$$\Phi_P = \Phi_{ST} k_P^0 (k_P^0 + \Sigma k_D + \Sigma k_q[Q]^{-1}) = \Phi_{ST} k_P^0 \tau_T \tag{5.49}$$

where Φ_{ST} is the quantum yield for intersystem crossing, $S_1 \rightarrow T_1$, k_P^0 is the radiative rate of phosphorescence, Σk_d is the sum of the rate constants of *all* unimolecular radiationless deactivations of T_1 (including reactions), and $\Sigma k_q[Q]$ is the sum of *all* bimolecular deactivations of T_1 (including reactions). By definition the experimental lifetime of T_1 is given by $\tau_T = (k_P^0 + \Sigma k_d + \Sigma k_q[Q])^{-1}$. From Eq. 5.49 we see that the quantum yield of phosphorescence is the product of a number of factors. Unless these factors can be experimentally identified and controlled, Φ_P is not a reliable parameter for characterizing T_1, although it may be a useful parameter in certain kinetic analyses (see Chap. 8).

In Table 5.7 we were given data for Φ_P for molecules at 77 K in rigid glasses (optically clear frozen solvents). Experimentally, a wide range of values of Φ_P are found for organic molecules. High values of Φ_P (~ 1) require that $\Phi_{ST} \sim 1$ and $k_P^0 > (\Sigma k_d + \Sigma k_q[Q])$. At 77 K, it appears that the major deactivation process competing with phosphorescence for the deactivation of T_1 is $T_1 \rightarrow S_0$ intersystem crossing. Thus, the quantum yield of phosphorescence is given by

$$\Phi_P \cong \Phi_{ST} k_P^0 (k_P^0 + k_{TS})^{-1} \text{ (at 77 K)} \tag{5.50}$$

The Phosphorescence of Nonaromatic Hydrocarbons

There are no convincing, authenticated reports of phosphorescence from simple nonaromatic hydrocarbons (e.g., alkanes, ethylenes, polyenes, etc.). In other words, $\Phi_P < 10^{-6}$ for these molecules. This low value of Φ_P results from (a) a generally low value of Φ_{ST}, since $S_1 \rightarrow T_1$ intersystem crossing is very inefficient for flexible hydrocarbons; (b) a very small value of k_P^0, since $T_1 \rightarrow S_0$ emission is both spin-forbidden (very weak spin-orbit coupling) and Franck–Condon-forbidden (from twisted triplet), and (c) a large k_D due to a surface touching between T_1 and S_0.

Although rigidity (to eliminate "free rotor" effects), triplet sensitization, and heavy-atom perturbation (to overcome a small Φ_{ST}) should enhance Φ_P to the point that phosphorescence is observable, to date no successful examples have been reported.

The lack of phosphorescence data means that the "triplet energies" E_T of ethylenes and polyenes are not available from photoluminescence techniques. However, in favorable cases, perturbed $S_0 \rightarrow T$ absorption allows evaluation of E_T (Section 5.10).

Because ethylenes and polyenes do not phosphoresce, their triplet state parameters (lifetimes, energies, etc.) must be measured by other techniques. $S_0 \rightarrow T_1$ perturbation spectroscopy (heavy atoms[37] and oxygen[28a] as perturbers) has been very useful as a method of evaluating E_T.

The Relationship between Phosphorescence Parameters and Molecular Structure

The important experimental parameters relating to phosphorescence are (a) the radiative phosphorescence lifetime k_P^0, (b) the quantum yield for intersystem crossing Φ_{ST}, (c) the phosphorescence quantum yield Φ_P, and (d) the measured experimental phosphorescence or triplet lifetime τ_T.

The theoretical relationship between molecular structure and k_P^0 follows from an examination of Eqs. 5.11, 5.14, and 5.40. The magnitude of the pertinent matrix element $\langle H_P \rangle$ and the magnitude of k_P^0 depends on the orbitals involved in the electronic transition, the nuclear configuration of the initial and final states, and the extent of spin-orbit coupling in the triplet state (Eq. 5.39). The major factor is generally the spin-orbit term.

The theoretical relationship between Φ_P or τ_T (Eq. 5.49) and molecular structure is not direct. Small values of Φ_P may result either from small probability of populating T_1 from S_1 (Φ_{ST} small), or from radiationless processes from T_1 that compete effectively with emission from $T_1 (k_D > k_P^0)$. In Section 6.10, we shall see examples of the remarkable influence of substitution of D for H on Φ_P. These effects will be shown to result from changes in k_D and not k_P^0 or Φ_{ST}.

Phosphorescence in Fluid Solution at Room Temperature[38]

Until recently, the observation of phosphorescence in fluid solution at room temperature was considered to be a rare and unusual phenomenon.[20] The common observation of phosphorescence at 77 K contrasted sharply with the rarity of its observation at room temperature. It is now clear that if phosphorescence is observed at 77 K it can also *generally* be observed at room temperature in fluid solution if two conditions can be met:

1. Impurities capable of quenching triplets are rigorously excluded,

2. The triplet does not undergo an activated unimolecular deactivation which possesses a rate of $\gtrsim 10^4 k_P^0$ at room temperature.

The *observation* of measurable phosphorescence requires a value of $\Phi_P \sim 10^{-4}$. The value of Φ_P may be expressed in terms of the rate of phosphorescence and all processes which deactivate T_1. From 5.49, in the case for which triplet formation from S_1 is efficient; Φ_P is given by

$$\Phi_P \sim \frac{k_P^0}{k_D + k_Q[Q] + k_P} \sim \frac{k_P^0}{k_D + k_Q[Q]} \text{ (in most fluid solutions)} \qquad (5.51)$$

where k_d represents the sum of *all* unimolecular deactivations of T_1 and $k_Q[Q]$ represents the sum of *all* bimolecular deactivations of T_1.

A typical value of k_P^0 for $T_1(n, \pi^*)$ is 10^2 sec^{-1}, and a typical value of k_P^0 for $T_1(\pi, \pi^*)$ is 10^{-1} sec^{-1}. For $\Phi_P \sim 10^{-4}$ we find:

$$k_d + k_q[Q] \sim 10^6 \text{ sec}^{-1} \text{ for } T_1(n, \pi^*) \tag{5.52}$$

$$k_d + k_q[Q] \sim 10^3 \text{ sec}^{-1} \text{ for } T_1(\pi, \pi^*) \tag{5.53}$$

Let us calculate the maximum value of $[Q]$ tolerable for observation of phosphorescence if Q is a diffusional quencher. For a nonviscous organic solvent $k_{dif} \sim 10^{10}$ M^{-1} sec^{-1}. Therefore,

$$\text{if } k_{dif}[Q] < 10^6 \text{ sec, then } [Q] < 10^{-4} \text{ M} \tag{5.54a}$$

and

$$\text{if } k_{dif}[Q] < 10^3 \text{ sec, then } [Q] < 10^{-7} \text{ M} \tag{5.54b}$$

The limit of 10^{-4} M for $[Q]$ is relatively easily obtained, but the limit of 10^{-7} M is more difficult to achieve. These qualitative considerations allow us to understand why compounds with phosphorescence from $T_1(n, \pi^*)$ states are commonly observed in fluid solutions but phosphorescence from $T_1(\pi, \pi^*)$ are rarely observed, unless extraordinary care is taken to eliminate bimolecular quenching.

The value of k_P^0 may be increased for aromatic hydrocarbons by external or internal heavy atom perturbation. In certain heavy atom solvents, the value of k_P^0 is increased to values approaching $10-10^2$ sec^{-1}. In these cases, phosphorescence is observed even for aromatic hydrocarbons if the heavy atom solvent is not itself a triplet quencher.[38e] Examples of phosphorescence data in fluid solutions were given in Table 5.7 and Figures 5.19 and 5.20. In very favorable or contrived circumstances phosphorescence from aromatic hydrocarbons occurs even in the vapor phase.[38f]

5.10 Flash Spectroscopy[39]

The development of flash lamps and lasers as sources of pulsed excitation has allowed the study of excited states and transient intermediates whose lifetimes are exceedingly short. The idea of flash spectroscopy is to "very quickly" introduce an intense pulse of light into an absorbing system and then "very quickly" analyze the time evolution of the system by absorption or emission spectroscopy. The high intensity produces a large number of photons, which in turn can produce a large number of electronically excited molecules. If the latter are produced in

sufficiently large concentrations, they may be monitored spectroscopically, and the decay of concentration with time (decay kinetics) may be measured.

What is "very quick" in flash spectroscopy? Experimentally, intense pulses (10^{16}–10^{18} photons) may be delivered in time periods as short as 10^{-12} sec (a *pico*second)! In order to gain an appreciation of the time scale implied by a picosecond, consider the following. A bullet travelling 1000 m/s takes 10^6 picosec to travel 1 mm and light travels 0.3 mm in one picosecond.

Flash spectroscopy enables us to study $T_1 \rightarrow T_n$ absorption.[23] The relatively long lifetime of triplets allows the buildup of substantial concentrations of T_1. If the $T_1 \rightarrow T_n$ transition is moderately or strongly allowed ($\varepsilon \sim$ 10,000–1,000,000) it is generally possible to detect T_1 by the measurement of its absorption spectrum. Once the absorption spectrum is established, the decay kinetics of T_1 may be

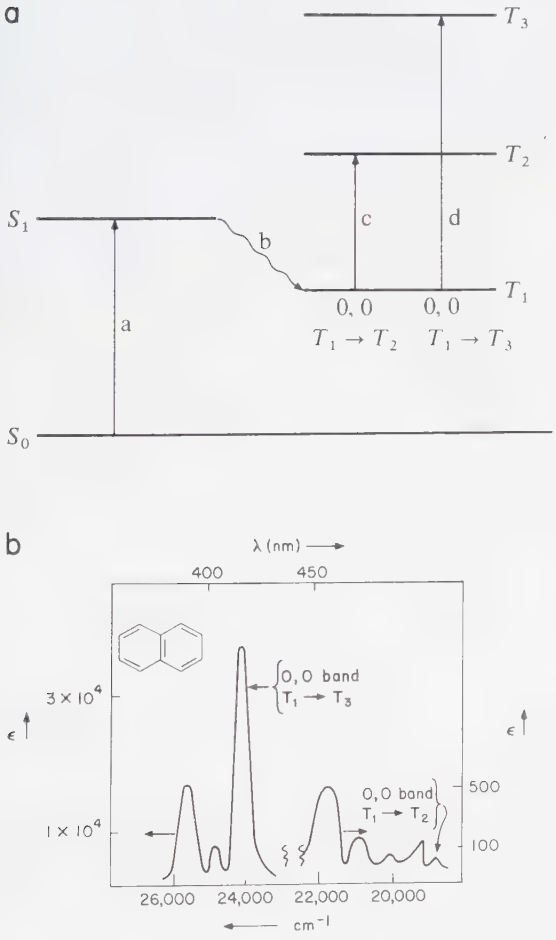

Figure 5.27

The triplet-triplet (*T-T*) absorption spectrum of naphthalene. At the top of the figure is a state diagram showing the pathway leading to *T-T* absorption. Absorption (a) is followed by intersystem crossing (b) to populate T_1. The latter is capable of absorbing photons and undergoing $T_1 \rightarrow T_2$ and $T_1 \rightarrow T_3$ transitions.

measured. $T_1 \rightarrow T_n$ absorption is feasible in vapors, liquids, and solids. An experimental example of a triplet-triplet absorption spectrum is shown for naphthalene in Figure 5.27.

In practice, if $k_T \equiv \tau_T^{-1}$ is of the order of 10^6 sec^{-1} or less and if $\varepsilon_{max}(T_1 \rightarrow T_n) \sim 10^4$ 10^5, it is generally possible to detect triplet states by triplet-triplet absorption if no competing absorption occurs in the region of the $T_1 \rightarrow T_n$ absorption.

5.11 Excited State Structures and Dipole Moments

In favorable cases, analyses of absorption and emission spectra allow us to deduce the equilibrium nuclear geometry of S_1 and T_1 as well as their dipole moments.

Some examples[40] of the nuclear shapes of prototype electronically excited states are given in Scheme 5.1. Notice that the geometry of ethylene (a planar

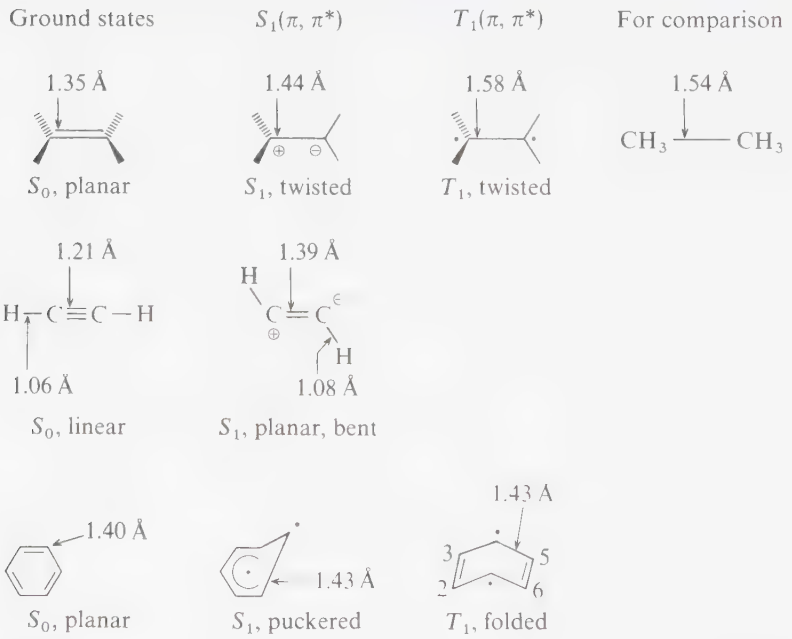

Scheme 5.1

Shapes of ground and excited states.

Table 5.8 Dipole Moments of the Excited and Ground States of Some Organic Molecules[a]

Molecule	Permanent dipole (in Debye units) S_0	T_1	S_1
$H_2C{=}O$	2.33[b]	1.29[b]	1.56[b]
$Ph_2C{=}O$	2.98[c]	1.72[c]	1.23[c]
$H{-}C{\equiv}C{-}CHO$	2.39[d]	—	0.7[d]
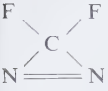	0		1.5
	6		1.5
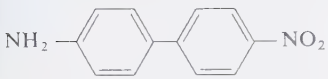	6		16
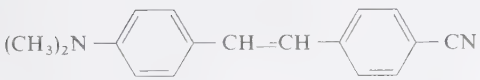	7		20
	2.2[e]	—	−1.0[e]
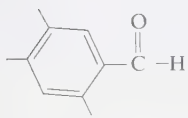	3.5[f]	4.2[f]	2.1[f]
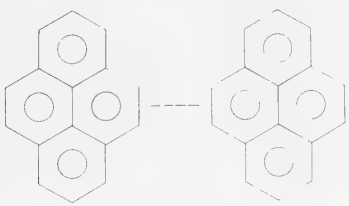 (Excimer)	—	—	2.5[g]
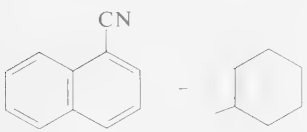 (Exciplex)			10.8[h]

[a] Unless specified, these data are extracted from reference 41a. The direction of dipole moment is the same for excited state, except for pyridine for which the dipole is reversed (indicated by negative value).
[b] Freeman, D. E., and Klemperer, W., *J. Chem. Phys.*, *40*, 604 (1954); *45*, 52 (1966). Buckingham, A. D., Ramsay, D. A., and Tyrrell, J., *Can. J. Phys.*, *48*, 1242 (1970).
[c] Gore, P. H., Hoskins, J. A., LeFevre, R. J. W., Radom, L., and Ritchie, G. L. D., *J. Chem. Soc. B*, 1967, 741. Hochstrasser, R. M., and Noe, L. J., *J. Mol. Spectrosc.*, *38*, 175 (1971).
[d] Freeman, D., Klemperer, W., and Lombardi, J., *J. Chem. Phys.*, *45*, 58 (1966).
[e] Hochstrasser, R. M., and Michaluk, J. W., *ibid.*, *55*, 4668 (1971).
[f] Sheng, J. J., and Hanson, M., *ibid.*, *60*, 368 (1974).
[g] Ghosh and Basu, S., *J. Photochem.*, *3*, 247 (1974).
[h] Taylor, G. N., *Chem. Phys. Letters*, *3*, 71 (1969).

molecule in S_0) becomes severely twisted in S_1 and T_1. Similar extensive geometry changes occur for acetylene, ethane, and benzene in their electronically excited states. Formaldehyde, a planar molecule in S_0, becomes pyramidal in S_1 and T_1. In addition, the C—O bond length becomes more like that of a single bond upon electronic excitation. Clearly, the S_1 and T_1 states of molecules are *electronic isomers* of S_0.

Some examples[41] of the dipole moments of selected electronically excited states are given in Table 5.8. For formaldehyde and benzophenone the dipole moment undergoes a substantial decrease in S_1 and T_1 relative to S_0. This result is nicely consistent with the n, π^* character of the excited states. The configuration of $S_0 = n^2$ puts more negative charge on the oxygen atom than the n, π^* configuration (for which some negative charge has been moved from the oxygen atom to the π^* system and therefore partially onto the carbon atom). Such a charge transfer clearly should lead to a decrease in the dipole moment of an n, π^* state relative to a ground state. Note also that some molecules undergo enormous dipole moment increases in their excited states.

The substantial differences in nuclear geometry and dipole moment of S_0 relative to S_1 and T_1 imply very different chemistry of these states. In Chapters 10–13 we shall see that this implication is experimentally confirmed.

An important photochemical consequence of the change in molecular nuclear structure and electronic distribution which occurs upon electronic excitation is

Table 5.9. Acid and Base Strengths of Singlet and Triplet States of Some Organic Molecules

Reaction	Example	$pK_a(S_0)$[b]	$pK_a(S_1)$[c]	$pK_a(T_1)$[d]
$OH \rightleftarrows -O^{\ominus} + H^{\oplus}$	2-Naphthol	9	3	8
$-\overset{\oplus}{N}H_3 \rightleftarrows -NH_2 + H^{\oplus}$	2-Naphthylamine	4	−2	3
$C{=}\overset{\oplus}{O}H \rightleftarrows {>}C{=}O + H^{\oplus}$	Xanthone	−4	1	—
$C(=O)-OH \rightleftarrows -C(=O)-\overset{\ominus}{O} + H^{\oplus}$	2-Naphthoic acid	4	11	4
$C(=\overset{\oplus}{O}H)-OH \rightleftarrows -C(=O)-OH + H^{\oplus}$	1-Naphthoic acid	−8	2	—
$R_3CH \rightleftarrows R_3\overset{\ominus}{C} + H^{\oplus}$	Fluorene	21	−8	5
$\overset{\oplus}{C}-CH \rightleftarrows {>}C{=}C{<} + H^{\oplus}$	Naphthalene	−4	12	-
$N{=}\overset{\oplus}{N}H- \rightleftarrows -N{=}N- + H^{\oplus}$	Azobenzene	−3	14	—

[a] Data gathered from Ireland, J. F., and Wyaat, P. A. H., *Adv. Phys. Org. Chem.*, *12*, 131 (1976).
[b] pK_a of ground state. $pK_a \equiv -\log K_{eq}$ where K_{eq} refers to reaction shown in extreme left-hand column.
[c] pK_a of lowest excited singlet state
[d] pK_a of lowest triplet state

the qualitative and quantitative changes in chemical properties of S_1 and T_1. Although these changes will be discussed in detail in later chapters, we mention one example briefly here.

Excited molecules may undergo acid-base reactions without simultaneous electronic deactivation.[42] The acid and base strengths of excited molecules may therefore be evaluated by spectral measurement of the concentrations of protonated excited molecules as a function of pH. Some results of experiments are summarized in Table 5.9. Commonly, the pK of the triplet state is remarkably close to that of the ground state. However, the excited singlet state often possesses a substantially different pK than S_0 or T_1.[43] These results serve to emphasize the large difference in chemical reactivity which may exist between a singlet and triplet state. This difference is a reflection of the fundamental zwitterionic character of S_1 and the fundamental diradical character of T_1 for many organic molecules (Section 7.8).

5.12 Radiative Transitions Involving more than One Molecule: Absorption Complexes and Exciplexes[44]

Thus far we have considered absorption and emission processes which involve just one molecule. In certain cases, two or more molecules may participate in *cooperative* absorption or emission, i.e., the absorption or emission can only be understood as arising from *molecular complexes*. Most commonly, two molecules are involved in such phenomena. When two molecules act cooperatively to absorb a photon, we say that an *absorption complex* exists. If two molecules act cooperatively to emit a photon, we say an *exciplex* exists. The absorption complex need not form an exciplex upon excitation and the exciplex need not emit to produce a ground state complex.

The important experimental spectroscopic characteristics of absorption complexes and exciplexes are:

1. The observation of a new absorption band which is characteristic of the absorption complex but not of either of the components of the complex.

2. The observation of a new emission band which is characteristic of the exciplex but not of the components of the exciplex.

3. A concentration dependence of the new absorption or emission intensity.

A molecular aggregate may be dissociated or only weakly associated (van der Waals interactions $E \sim 1$–3 kcal/mole) in the ground state, but more strongly associated in its excited states ($E \sim 3$–10 kcal/mole). An excited molecular complex of definite stoichiometry that is dissociated or only weakly associated in its ground state is called an *exciplex*. In further discussions we will assume that the stoichiometry conforms to a 1:1 complex. In the special case that components of the complex are of the same type, the excited molecular complex is termed an *excimer*.

The notion of a specific stoichiometry is included in our definitions of exciplex and excimer because we wish to distinguish these species from those solvated excited molecules for which an indefinite number of unexcited solvent molecules provide an environment.

Charge Transfer Absorption[45]

Mixtures of molecules which possess a low ionization potential (electron donors), or a high electron affinity (electron acceptors) often exhibit absorption bands which are not separately shown by either component. Generally, the new band is due to an EDA (Electron Donor Acceptor) or charge-transfer complex. A typical example is shown in Figure 5.28. Generally, the absorption band is broad and devoid of vibrational structure. This breadth is explained by the fact that the rather small binding energies of EDA complexes allows many different structural con-

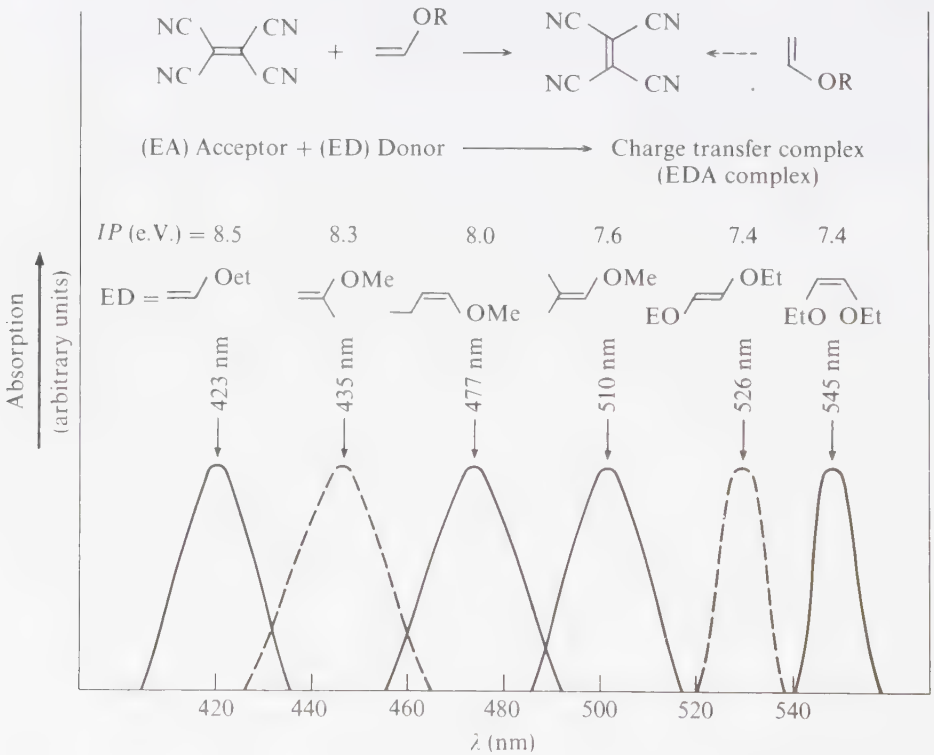

Figure 5.28

The absorption spectra of some EDA complexes of tetracyanoethylene and a variety of enol ethers. Neither tetracyanoethylene nor the enol ethers possess significant absorption above 400 nm. The maxima are experimentally meaningful, the extinction is not. The maxima increase steadily along with the decreasing ionization potential *IP* (greater electron *donor* character) of the enol ether component.

figurations of the complex to exist in equilibrium with one another. The absorption energy for each configuration will differ and cause a broadening of the band.

An important experimental characteristic of an EDA absorption band is its sensitivity to solvent polarity. For example, the maxima of the EDA absorption band of enol ethers (donors) and tetracyanoethylene (acceptor) vary substantially as solvent polarity is varied. The energy required for absorption decreases as the solvent polarity increases. This effect is understood as follows. The ground state wave function of an EDA complex is described by

$$\Psi = \alpha D, A + \beta D^+ A^- \tag{5.55}$$

where D, A is a "no-bond" electronic configuration of the complex and D^+A is a "charge-transfer" electronic configuration of the complex. The coefficients α and β indicate the contribution of each representation to the true wave function Ψ.

The excited state wave function may also be described in terms of no-bond and charge-transfer configurations as:

$$\Psi^* = \gamma D, A + \delta D^+ A^- \tag{5.56}$$

If the charge transfer is *weak* in the ground state and *dominant* in the excited state we may assume that

$$\Psi \sim D, A \tag{5.57}$$

$$\Psi^* \sim D^+ A^- \tag{5.58}$$

Thus, the transition $\Psi \rightarrow \Psi^*$ corresponds to the configurational change $D, A \rightarrow D^+ A^-$.

Excimers and Exciplexes[44]

An electronically excited state may be a very polarizable species and, because of the occurrence of an electrophilic half-filled HO and a nucleophilic half-filled LU, may participate in charge-transfer interactions with other polar or polarizable species. As a result, a collision complex between an electronically excited species, M*, with any polar or polarizable ground state molecule, N, will generally be stabilized by some charge-transfer interaction. This stabilization will in turn cause the M*N collision complex to possess a longer lifetime than the corresponding MN (ground state) collision complex. Quite often the M*N collision complex possesses observable properties distinct from those of M*. When this is the case, the M*N collision complex can be considered as a metastable species in its own right, i.e., the M*N collision complex is a new electronically excited species. Such an electronically excited species is termed an *exciplex*. If M and N are the same, then the excited complex M*N is termed an *excimer*:

$$\mathrm{M}^* + \mathrm{N} \rightarrow \mathrm{M}\text{---}\overset{*}{\text{---}}\text{---}\mathrm{N} \quad \text{(exciplex)} \tag{5.59}$$

$$\left.\begin{aligned} \mathrm{M}^* + \mathrm{M} &\rightarrow \mathrm{M}\text{---}\overset{*}{\text{---}}\text{---}\mathrm{M} \\ \mathrm{N}^* + \mathrm{N} &\rightarrow \mathrm{N}\text{---}\overset{*}{\text{---}}\text{---}\mathrm{N} \end{aligned}\right\} \text{(excimer)} \tag{5.60, 5.61}$$

What are the typical properties of exciplexes? Perhaps the most general distinguishing characteristic of an electronically excited state is its emission to produce a ground state and light. Thus, if exciplexes exist, they should in principle exhibit fluorescence (singlet exciplexes) or phosphorescence (triplet exciplexes). The emission from M*N will in general be different from that of the M*. Furthermore, since the ground state collision complex MN will generally be less bound than M*N, emission from the exciplex will usually occur to a weakly bound or dissociative ground state.

A simple theoretical basis for the enhanced stabilization of a M*N collision pair relative to a MN collision pair is available from the simple theory of MO interactions (Fig. 5.29). If we consider M and N colliding, then the major electronic interactions will be among their highest-energy filled (HO) and lowest-energy unfilled (LU) orbitals. According to the rules of perturbation theory the HO of M will interact with the HO of N to yield two new HO's of the collision complex or exciplex. Similarly the LU of M will interact with that of N to produce two new LU's of the collision complex or exciplex. Recall that the new HO's and LU's are split in energy relative to the original HO's and LU's of M and N. This means that in the collision complex and exciplex one of the new HO's is lower in energy and one higher in energy than the original HO's. Similarly, the LU's of the collision complex and exciplex split in energy above and below the original LU's.

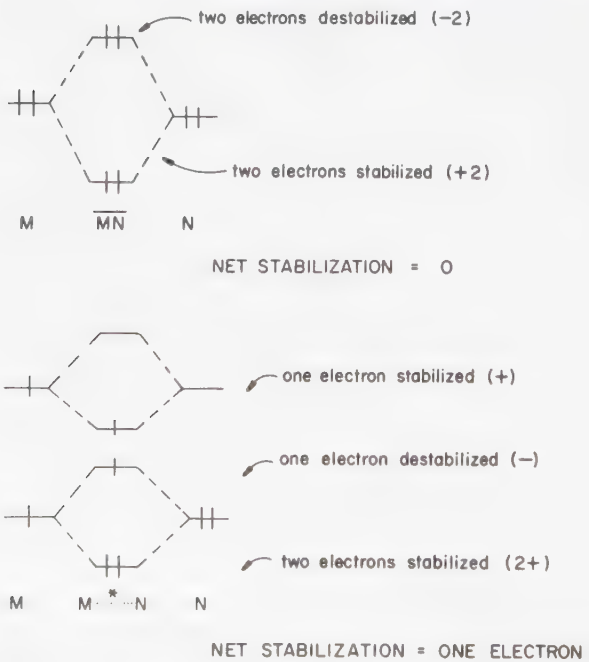

Figure 5.29

Orbital interactions of MN collision pairs and M---*---N exciplexes.

In the collision complex of M and N, the four electrons which occupied the HO's of M and N occupy the new set of HO's. Two electrons are stabilized and two electrons are destabilized; thus no gain in energy is achieved by interaction of M and N during their collisions. In the exciplex, however, since one of the partners (say M) is electronically excited, *three* electrons are stabilized and only one electron is destabilized as the electrons redistribute themselves from their original noninteracting orbitals to the new orbitals of the exciplex.

Consider now the *states* corresponding to the collision complex and the exciplex. If there is no interaction between M* and N the emission of the M*N collision complex will be that of the monomer M* and the energy of the emission will correspond to that for the $M^* \rightarrow M + h\nu$ process. If the collision complex M*N becomes an exciplex ($M{-}{-}\overset{*}{-}{-}N$), then the energy of the latter *decreases*. Emission from ($M{-}{-}\overset{*}{-}{-}N$) is to MN, the ground state collision complex. The latter is essentially the same state in which a noninteracting M*N collision complex would emit.

Figure 5.30 shows a potential-energy surface description of excimer (or exciplex) emission and relates it to absorption. Let us now identify M and N as a pair of molecules to which donor and acceptor properties may be associated, since most exciplexes appear to be stabilized mainly by charge-transfer interactions. Thus

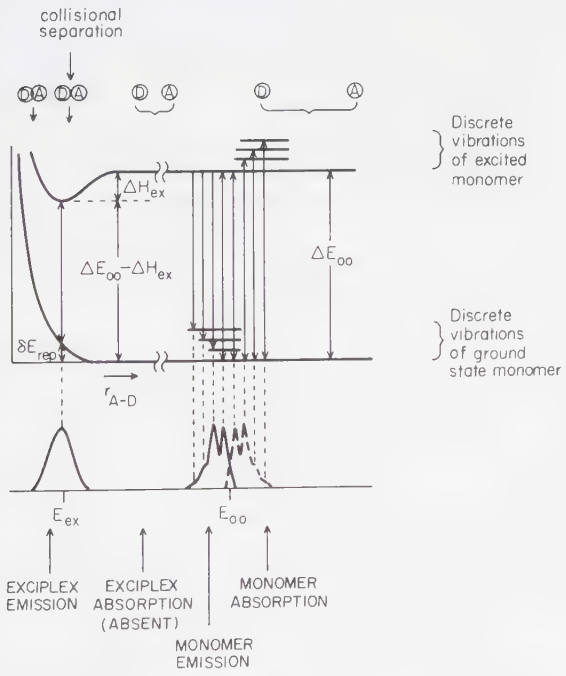

Figure 5.30
Surface interpretation of excimer emission.

we use the labels D and A for the donor and acceptor, respectively. At large separations of D and A, the absorption spectrum of either component would be identical to that of each monomer, i.e., neither component would influence the other. As D and A approach, the absorption spectrum remains constant. Eventually, D and A undergo collisions. If there are no substantial attractions between D and A in their ground states (lower surface), collisions will raise the energy of the system and very few collision complexes will exist at any given time. As a result, their concentrations will be quite low and *no new absorption due to the collision complex will be observed.* The "instability" of the ground state complex is a somewhat arbitrary feature of the excimer and exciplex definition. The essential idea is that the ground state DA collision complexes are *unstable*, low-structured species, *not* that they lack a measurable absorption spectrum.

Consider the situation for the approach and collision of D* and A (or A* and D) on the excited surface. At a large separation of D* and A, the emission spectrum is that of the monomer, D*. As the two molecules approach, the bonding between them may increase due to charge transfer or excitation exchange interactions. This will cause a minimum to occur in the potential-energy curve and if this enthalpy decrease is not offset by an entropy increase, an excited state complex — an exciplex — will form. Emission from the exciplex will occur according to the Franck-Condon principle, i.e., vertically from the excited state minimum. If the separation of D and A in the excited state minimum corresponds to a point on the repulsive part of the ground-state potential curve, Franck-Condon emission will lead exclusively to repulsive states on the ground surface. Within a few collisions, D and A will fly apart rapidly. This process is the emission analogue of predissociative or directly dissociative absorption. The short lifetime and indefinite character of the "vibrations" of the final state (D + A) result in a total absence of *vibrational structure* in the emission spectra of excimers and exciplexes.

We are now in a position to appreciate the single most definitive kind of direct spectroscopic evidence for the formation of an excimer or exciplex: the observation of a concentration-dependent, vibrationally unstructured emission spectrum which occurs on the red (lower energy) end of the absorption spectrum of both D and A, but which does not correspond to the monomer emission spectrum of either D or A.

From Figure 5.30 we also notice how the important quantities ΔE_{00}, ΔE_{ex}, and ΔH^* are related. ΔE_{00} is either the excitation energy required to raise the monomer from $v = 0$ of the ground state to $v = 0$ of the excited state, or is the excitation energy released when the monomer excited state ($v = 0$) emits a photon and produces the ground state ($v = 0$).

Triplet excimers and exciplexes, while less often directly observed by their emission, are well established excited state species.[46,47] They tend to be more weakly bound and to possess different structures[33] than singlet excimers and exciplexes, probably because of the generally decreased charge-transfer character of triplets.

Our theoretical analysis of exciplexes indicates that D−−*−−A should possess the typical properties of electronically excited states, e.g., emission, radiationless transitions, photochemistry. The exciplex may be treated as a stoichiometric

species and its reactions considered as *unimolecular*, although its formation is bimolecular.

The important operational experimental tests for exciplexes can be derived from the general scheme

$$D^* + A \underset{k_2}{\overset{k_1}{\rightleftharpoons}} D\text{--}^*\text{--}A \xrightarrow{k_3} \begin{cases} 1. \text{ Emission} \\ 2. \text{ Radiationless transitions} \\ 3. \text{ Photochemistry} \end{cases} \tag{5.62}$$

Examples of Excimers: Pyrene and Aromatic Compounds[44]

The pyrene excimer serves as a classic example of this class of photochemical intermediates.[48] Figure 5.31 shows the fluorescence of pyrene in *n*-heptane as a function of pyrene concentration. At concentrations of about 10^{-5} M or less the fluorescence is concentration-independent and is composed of pure pyrene monomer fluorescence. As the pyrene concentration increases two effects are observed: (a) the monomer emission decreases in intensity, and (b) a new fluorescent emission, due to the pyrene excimer, appears on the red (i.e., longer wavelengths or lower energies) side of the monomer emission and increases in intensity. The

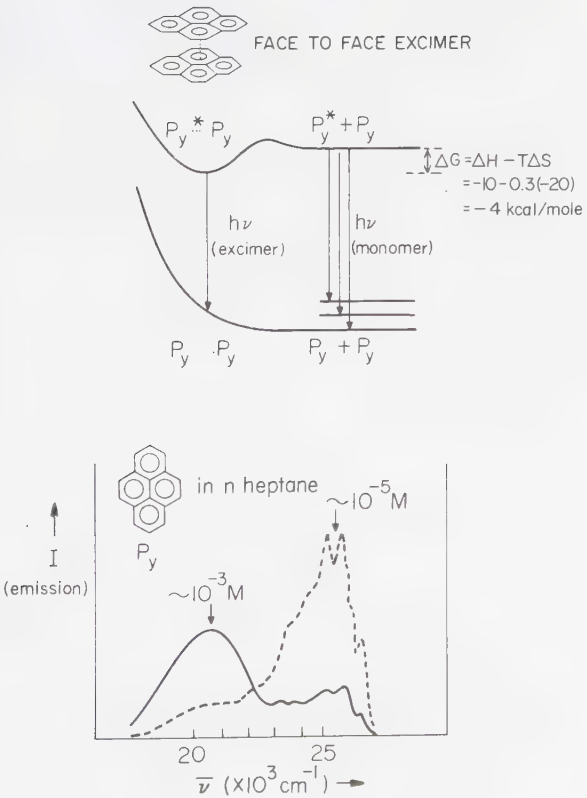

Figure 5.31
Experimental example of the excimer emission of pyrene and surface interpretation.

occurrence of an isoemissive point is consistent with the involvement of two and only two species in the observed fluorescence.

A potential-energy diagram for the formation of pyrene excimer is also shown in Figure 5.31. The diagram indicates how the energy of two pyrene molecules varies as a function of their internuclear separation. For the ground-state pair at large distances of separation (~ 10 Å) the energy of the pair is constant, since intermolecular interactions are weak at this separation distance. At a separation of about 4 Å, which is close to the equilibrium separation of the excimer, the energy of the ground state PyPy pair rises rapidly due to occupied π orbital repulsions. From the figure it is easy to see why the pyrene excimer emission is structureless and why no absorption is observed which corresponds to PyPy $\rightarrow$ Py$\cdots$Py absorption, i.e., the emission is to an unstable dissociative state (the molecule dissociates before it can complete a vibrational cycle and too few PyPy molecules are in a collision complex at a close enough distance for significant amounts of Franck-Condon excitation of the excimer to occur).

From a spectroscopic analysis of pyrene excimer emission, and a correlation of this with the emission of pyrene crystals, it has been concluded that the structure of the "face to face" pyrene singlet excimer is favored. This structure is in agreement with expectations based on maximal overlap of π orbitals.

The electronic stabilization energy of the pyrene excimer is substantial ($\Delta H \cong -10$ kcal/mole), but the entropy of formation is quite negative ($\Delta S = -20$eu; $T\Delta S = 6$ kcal/mole at room temperature).[44b] Thus, at ambient temperatures, formation of the excimer is favorable, and $\Delta G \sim -4$ kcal/mole.

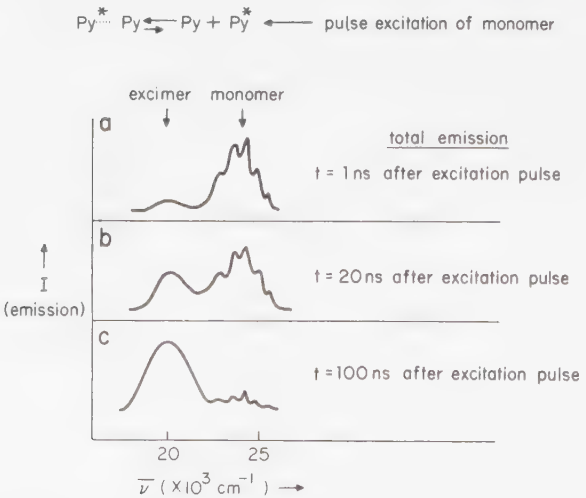

Figure 5.32

The dynamic behavior of pyrene monomer and excimer emission. After 1 ns most of the excited pyrene exists as the monomer. After 20 ms comparable amounts of excimer and monomer are observed. After 100 ns most of the excited pyrene molecules exist in the excimer form.

In contrast to the large solvent shifts observed for exciplex emission (Section 5.13), the emission frequency of excimers is usually not very solvent-dependent. This suggests that charge transfer interactions are not as pronounced for excimers as for exciplexes—as is to be expected from the inherently less-polar nature of excimers.

The time dependence of emission from pyrene solutions (*time-resolved emission spectroscopy*) provides an excellent confirmation of the *dynamic* nature of excimer formation.[49] If a solution of pyrene in cyclohexane ($\sim 10^{-3}$ M) is excited with a brief pulse of light, only the excited monomer is produced (the excimer possesses no absorption). If the *total* emission spectrum is taken after $\sim 1 \times 10^{-9}$ sec (~ 1 ns), it is found that the spectrum is mainly that of the *monomer* (Fig. 5.32a), i.e., the diffusion of an excited monomer toward a ground state pyrene and the formation of an excimer is required for excimer emission, and pyrene molecules can only move a few angstroms in 10^{-9} sec. The small amount of excimer emission results from the formation of excimers by excited pyrene monomers which happened to be close to pyrene ground-state molecules. After ~ 20 ns substantial diffusional displacements have occurred and the concentrations of excimer and monomer are becoming comparable (Fig. 5.32b). After ~ 100 ns the emission spectrum (Fig. 5.32c) is that which is normally seen under steady-state conditions. (Compare with Fig. 5.31, in which the excited monomer and excimer are essentially equilibrated.)

Exciplexes and Exciplex Emission[50]

As in the case of excimer emission, exciplex emission is usually observed as a broad structureless band to the red of the monomer emission. For example, the fluorescence of aromatic hydrocarbons is quenched often at the diffusional rate by electron donors such as anilines. The quenching is accompanied by the appearance of a broad structureless band which occurs about 5000 cm^{-1} (~ 15 kcal/mole) to the red of the fluorescence of the hydrocarbon monomer. This new fluorescence (Fig. 5.33) increases in intensity as the electron donor concentration is increased. There is no corresponding change in the absorption spectrum.

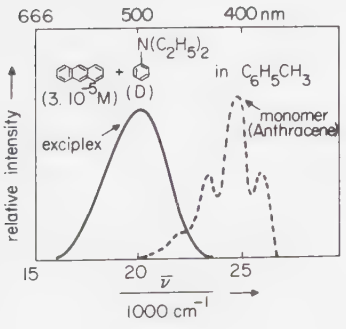

Figure 5.33
Exciplex and monomer emission of the anthracene-diethyl aniline system. The anthracene monomer is the light-absorbing species in this system.

For exciplexes of similar type in the same solvent:

$$E^{max} = h\nu^{max} \sim IP_D - EA_A + C \tag{5.63}$$

where E^{max} refers to either an absorption or emission maximum. IP_D is the ionization potential of the donor, EA_A is the electron affinity of the acceptor, and C is the coulombic attraction between the components of the ion pair D^+A^-. Thus, for a constant donor E_{CT}^{max} will be proportional to EA_A or for a constant acceptor E_{CT}^{max} will be proportional to IP_D, i.e.,

$$E_{CT}^{max} \propto EA_A \qquad \text{if } IP_D \text{ is held constant in a given solvent} \tag{5.64}$$

$$E_{CT}^{max} \propto IP_D \qquad \text{if } EA_A \text{ is held constant in a given solvent} \tag{5.65}$$

Thus, if a plot of E_{CT}^{max} versus EA_A or IP_D yields a straight line, the relationship may be used as evidence for similiar, charge-transfer bonding in the complex. Furthermore, no corresponding change is observed in the absorption spectrum (i.e., Beer's law is strictly followed). As a result, it can be concluded that to explain the concentration effect the new fluorescence must be ascribed to an associate of excited- and ground-state pyrene molecules, which, to explain the observation that Beer's law of absorption is followed, is formed after light absorption.

The term $IP_D - EA_A$ is related to the experimental quantities $E(D/D^+)$, the oxidation potential of the donor (in an appropriate solvent), and $E(A \quad A)$, the reduction potential of the acceptor (in an appropriate solvent). Under the proper conditions

$$(IP_D - EA_A) \propto E(D/D^+) - E(A^-/A) \tag{5.66}$$

When this is the case, from Eq. 5.63 we conclude

$$E^{max} = h\nu^{max} \propto E(D/D^+) - E(A^-/A) \tag{5.67}$$

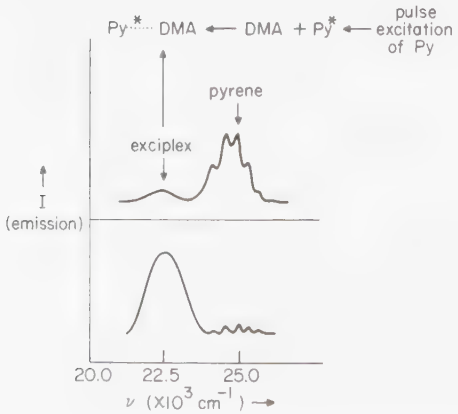

Figure 5.34
Dynamic behavior of the pyrene-dimethylaniline exciplex.

Experimental examples confirm Eq. 5.67. For instance, if the fluorescence maxima of some exciplexes are plotted against $E(D/D^+) - E(A/A^-)$ an excellent linear agreement is found.[50]

The dynamic behavior of exciplex formation is also nicely demonstrated by time-resolved emission spectroscopy.[49] Figure 5.34 shows the total emission of pyrene-plus-dimethylaniline in cyclohexane: (a) ~1 ns after an excitation of the pyrene chromophore, and (b) ~100 ns after the excitation. It is evident that immediately after the excitation, emission is mainly from the pyrene monomer, but as time goes on the exciplex begins to increase its contribution to the total.

Intramolecular Excimers and Exciplexes[51]

Incorporation of two chromophores into a single molecule separated by a certain number of atoms (in such a way that there are no important interactions in the ground state) can substantially modify the observed emission parameters. As far as "excimer" or "exciplex" formation is concerned, the requirement of intramolecularity may assist or inhibit complexation in the excited state. For example, in compounds of the type A-$(CH_2)_n$-X, the efficiency of intramolecular exciplex (or, if A = X, excimer) formation is a function of n. Often for $n = 3$ an optimal situation is obtained.[51] For example,[51d] even intramolecular *triplet* excimers (Fig. 5.35) are observed in the case of compound **11**.

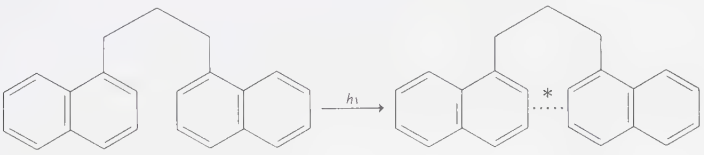

(5.68)

11 Singlet and triplet excimers

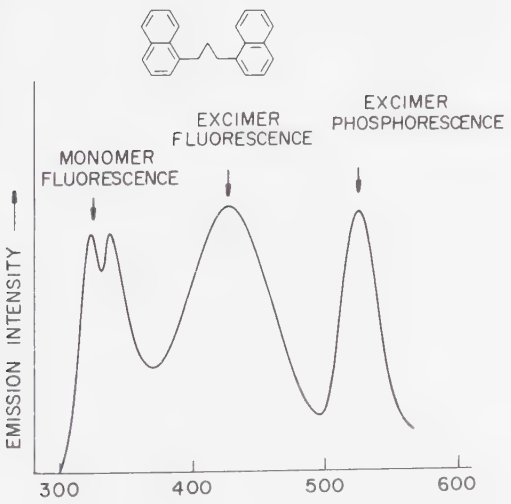

Figure 5.35
Intramolecular *triplet* excimers are observed in the case of compound **11**.

In certain cases an exciplex may associate with a ground state molecule to form a "tripliplex," or excited state aggregate consisting of three weakly interacting species.[51c]

5.13 Delayed Fluorescence and Phosphorescence[52]

It is possible that the observed lifetime of fluorescence from S_1 or phosphorescence from T_1 is *longer* than that expected based on "prompt" emission from these states. "Delayed emission," sometimes of a much longer lifetime, is observed whenever a process leading to formation of S_1 or T_1 is kinetically limiting for emission. By "prompt" fluorescence we mean the $S_0 + h\nu \rightarrow S_1 \rightarrow S_0 + h\nu'$ sequence. "Delayed fluorescence" may arise if after a fast intersystem crossing, T_1 is thermally popped back into S_1. Thus, for the sequence $S_0 + h\nu \rightarrow S_1 \rightarrow T_1 \rightarrow S_1 \rightarrow S_0 + h\nu'$, it may take a "long time" for the emission to occur from S_1. In a limit, the lifetime of fluorescence would be nearly equal to the lifetime of T_1, if the decay of the latter were rate-determining. A second type of delayed emission is known to occur when *two* excited states interact and "annihilate" to produce an emitting state. In this case, the time it takes for the annihilating states to diffuse together may be rate-determining. Delayed fluorescence is commonly observed to result from *triplet-triplet* annihilation (Section 9.16).

Thermally induced delayed fluorescence (via a $T_1 \rightarrow S_1$ mechanism) is favored in molecules possessing small singlet-triplet energy gaps (Section 2.9), i.e., ketones.

"Prompt" fluorescence: path a → d
"Delayed" fluorescence: path a → b → c → d

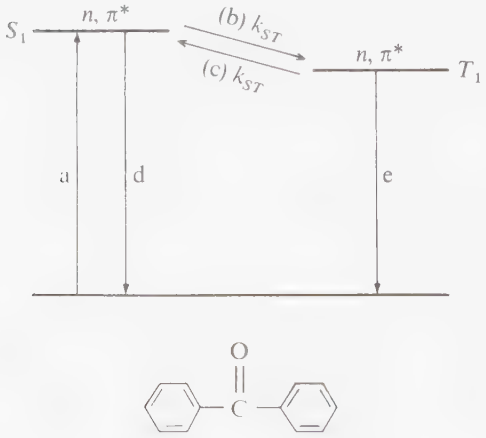

Figure 5.36

State energy diagram of the "prompt" and "delayed" fluorescence of benzophenone at room temperature: (a) absorption to form S_1, (b) $S_1 \rightarrow T$ intersystem crossing, (c) $T_1 \rightarrow S_1$ intersystem crossing, (d) fluorescence, (e) phosphorescence. The lifetime of the delayed fluorescence is approximately the same as that of the triplet, showing that triplet decay is rate limiting.

Benzophenone at room temperature provides a specific case of delayed fluorescence via thermal repopulation of S_1 via T_1.

The emission spectrum of benzophenone at room temperature in fluid solution (Fig. 5.18) consists of "prompt" fluorescence (emission from S_1 molecules that have been directly excited by absorbed photons), "delayed" fluorescence (emission from S_1 molecules that have undergone intersystem crossing to T_1 and are then thermally activated back to S_1), and phosphorescence.[53] The "prompt" fluorescence has a lifetime of $\sim 10^{-10}$–10^{-11} sec and is limited by intersystem crossing $S_1 \rightarrow T$. The delayed fluorescence has a lifetime of $\sim 10^{-6}$ sec. Its lifetime is temperature-dependent and may be limited by k_F^0 or k_{-ST}, whichever is slower at a given temperature.

The "delayed fluorescence" of benzophenone is readily differentiated from the prompt fluorescence by observation of the influence of decreasing temperature.[38c] Since the $T_1 \rightarrow S_1$ process is activated, at low temperatures, k_{-ST} (Fig. 5.37) is too slow to compete with k_P^0 and pure phosphorescence is observed. The activation energy ΔE_{DF} for delayed fluorescence can be obtained via an Arrhenius plot

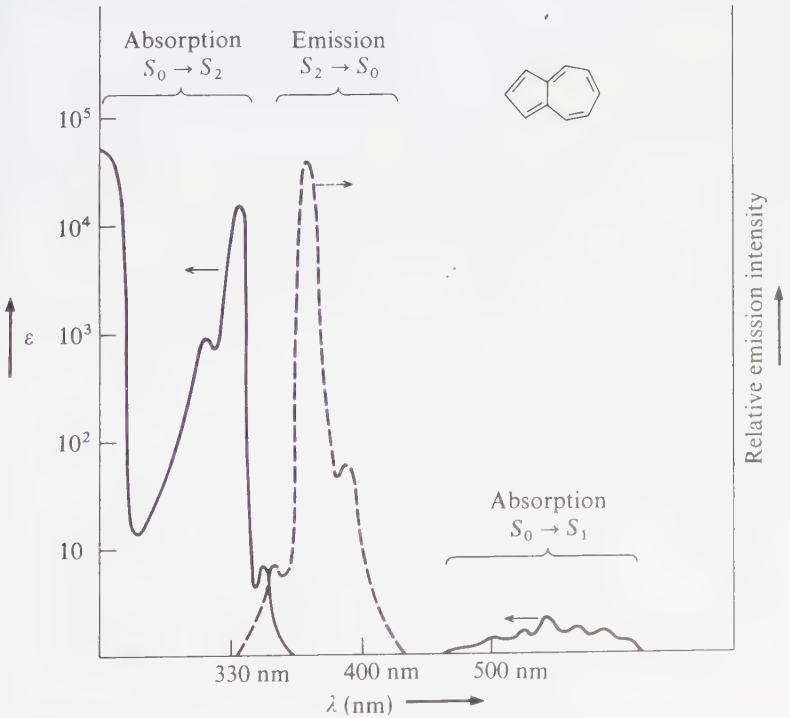

Figure 5.37

The anomolous $S_2 \rightarrow S_0$ fluorescence of azulene. The solid curve shows the $S_0 \rightarrow S_2$ (UV) and $S_0 \rightarrow S_1$ (VIS) absorption of azulene. The fluorescence of azulene (dotted curve) is an approximate mirror image of the $S_0 \rightarrow S_2$ absorption.

of $\ln k_{DF}$ versus $1/T$. In the cases studied, $\Delta E_{DF} \sim \Delta E_{ST}$, i.e., the value of the activation from $T_1 \rightarrow S_1$ is identical to the spectroscopic singlet-triplet energy gap. This implies that there is no activation required beyond reaching the energy of S_1.

5.14 Emission from "Upper" Excited Singlets and Triplets; The Azulene Anomaly

Because of the large number of organic molecules known to obey Kasha's rule (in condensed phases fluorescence is only observed from S_1, phosphorescence is only observed from T_1),[17] claims of "anomalous" emission from the S_2, S_3, etc., and the T_2, T_3, etc., states of molecules should be viewed with suspicion. To data, examples of emission from T_n $(n > 1)$ are extremely rare.[54] However, well-documented cases of $S_2 \rightarrow S_0 + h\nu$ fluorescence are found for azulene (**12**) and its derivatives.[55] The fluorescence spectrum of **12** maximizes at $\sim$374 nm,

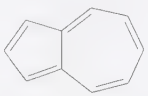

12, Azulene

$\Phi_F^{S_2} = 0.02$
$\tau_F \leqq 10^{-9}$ sec

$Cl_2C{=}S$

$\Phi_F^{S_2} \sim 1.0$
$\tau_F \sim 10^{-6}$ sec

13, Thiophosgene

whereas its $S_0 \rightarrow S_1$ absorption maximizes at 585 nm (azulene is a blue organic compound). The O, O band of the fluorescence, the O, O band of $S_0 \rightarrow S_2$ absorption overlap and display an approximate mirror image relationship to one another (Fig. 5.37). The reason for the observation of $S_2 \rightarrow S_0$ fluorescence in azulene is the relatively large $S_2 - S_1$ energy gap, which slows down the normally very rapid rate of $S_2 \rightarrow S_1$ internal conversion (Section 6.8) by decreasing the Franck-Condon factor for radiationless transitions. Examples of S_2 emission are known which can be ascribed to thermal population of S_2 from S_1, followed by emission from S_2. These cases are similar mechanistically to those proposed for delayed fluorescence (Section 5.13).

In the vapor phase, internal conversion may be quite slow from upper singlets, again because of poor Franck-Condon factors for internal conversion. For example, thiophosgene[56] fluoresces from S_2 with a quantum yield of $\sim$1.0 at low pressures. Thioketones,[57] even in solution, generally show weak emission from S_2. Again the basis for "upper singlet" emission is a large energy gap between S_2 and S_1.

Interestingly, $S_1 \rightarrow S_0$ fluorescence from azulene is extremely weak ($\phi_F < 10^{-4}$) and can be obtained only under special conditions.[58]

References

1. For excellent nonmathematical discussions of light and its interaction with molecules see:
   (a) Clayton, R. K., *Light and Living Matter, The Physical Part*, New York: McGraw-Hill, 1970.

For more rigorous treatments see:
(b) Jaffe, H. H., and Orchin, M., *Theory and Applications of Ultraviolet Spectroscopy*, New York: Wiley, 1962.

2. For a more detailed discussion the reader is referred to any elementary textbook of physics, e.g., Halliday, D., and Resnick, R., *Physics*, New York: Wiley, 1967.

3. For an excellent discussion see Kauzman, W., *Quantum Chemistry*, New York: Academic Press, 1957, p. 546ff.

4. (a) Robinson, G. W., in *Experimental Methods of Physics, Vol. 3*, eds. Marton, L., and Williams, D., New York: Academic Press, 1962, p. 155.
(b) Heitler, W., *Quantum Theory of Radiation*, Oxford: Clarendon Press, 1944.
(c) Lewis, G. N., and Calvin, M., *Chem. Rev.*, *25*, 273 (1939).

5. (a) Bowen, E. J., *Quart. Rev.*, *4*, 236 (1950); *Chemical Aspects of Light*, Oxford: Clarendon Press, 1946.
(b) Maccoll, A., *Quart. Rev.*, *1*, 16 (1947).
(c) McMillin, D. R., *J. Chem. Ed.*, *55*, 7 (1978).

6. (a) Balavoine, G., Moradpour, A., and Kagan, H. B., *J. Am. Chem. Soc.*, *96*, 5152 (1974).
(b) Kuhn, W., and Knoph, E., *Z. Phys. Chem.*, *7B*, 292 (1930).

7. Braude, E. A., *J. Chem. Soc.*, 379 (1950).

8. (a) Perrin, F., *J. Phys. Radium*, *7*, 390 (1962).
(b) Berlman, I. B., *Molec. Crystals*, *4*, 157 (1968).

9. (a) Strickler, S. J., and Berg, R. A., *J. Chem. Phys.*, *37*, 814 (1962).
(b) Ware, W. R., and Baldwin, B. A., *ibid.*, *40*, 1703 (1964).
(c) Birks, J. B., and Dyson, D. J., *Proc. Royal Soc.*, *A275*, 135 (1963).
(d) Melhuish, W. H., *J. Phys. Chem.*, *65*, 229 (1961).
(e) Bennett, R. G., *Rev. Sci. Instr.*, *31*, 1275 (1960).
(f) Lewis, R. S., and Lee, K. C., *J. Chem. Phys.*, *61*, 3434 (1974); Phillips, D., *J. Phys. Chem.*, *70*, 1235 (1966).

10. (a) Lewis, G. N., and Kasha, M., *J. Am. Chem. Soc.*, *67*, 994 (1945).
(b) Kasha, M., *Chem. Rev.*, *41*, 401 (1948).
(c) Lewis, G. N., and Kasha, M., *J. Am. Chem. Soc.*, *66*, 2100 (1944).
(d) McGlynn, S. P., Azumi, T., and Kasha, M., *J. Chem. Phys.*, *40*, 507 (1964).

11. (a) Solomon, B. S., Thomas, T. F., and Steel, C., *J. Am. Chem. Soc.*, *90*, 2449 (1968).
(b) Hansen, D. A., and Lee, E. K. C., *J. Chem. Phys.*, *62*, 183 (1975).
(c) Condall, R. B., and Ogilvie, S., *Organic Molecular Photophysics*, ed. Birks, J. B., Vol. 2. New York: Wiley, 1975, p. 33.

12. (a) Neporent, B. S., *Pure Appl. Chem.*, *37*, 111 (1976); *Opt. Spectr.*, *32*, 133 (1972).
(b) Suzuki, H., *Electronic Absorption Spectra and the Geometry of Organic Molecules*, New York: Academic Press, 1967, p. 79.

13. For a more rigorous discussion, see Herzberg. G., *Spectra of Diatomic Molecules*. Princeton, N.J.: van Nostrand, 1950.

14. (a) McGlynn, S. P., Azumi, T., and Kinoshita, M., *Molecular Spectroscopy of the Triplet State*, Englewood Cliffs, N.J.: Prentice Hall, 1969.
(b) Dewar, M. J. S., and Dougherty, R. C., *The PMO Theory of Organic Chemistry*, New York: Plenum, 1975.

15. Hochstrasser, R. M., and Marzzallo, *Molecular Luminescence*, ed. Lim, E., New York: W. A. Benjamin, 1969, p. 631.

16. For detailed compilations of data the interested reader is referred to
(a) Birks, J. B., *Photophysics of Aromatic Molecules*, New York: Wiley, 1970.
(b) Parker, C. A., *Adv. Photochem.*, *2*, 305 (1964).
(c) Turro, N. J., *Molecular Photochemistry*, New York: Benjamin, 1967.
(d) Becker, R., *Theory and Interpretation of Fluorescence and Phosphorescence*, New York: Wiley, 1969.

17. Kasha, M., *Disc. Faraday Soc.*, *9*, 14 (1950).

18. (a) Hirayama, F., and Lipsky, S., *J. Chem. Phys.*, *51*, 3616 (1969).
(b) Henry, M. S., and Helman, W. P., *ibid.*, *56*, 5734 (1972).

19. Hirayama, F., and Lipsky, S., *ibid.*, *62*, 576 (1975).

20. (a) Havinga, E., *Chimia*, *16*, 145 (1962).
(b) Pusset, J., and Bengelmans, R., *Chem. Comm.*, 448 (1974).

21. (a) Henry, M. S., and Helman, W. P., *J. Chem. Phys.*, *56*, 5734 (1972).
(b) Halpern, A. M., and Danziger, R. M., *Chem. Phys. Letters*, 72 (1972).

22. Schloman, W. W., and Morrison, H., *J. Am. Chem. Soc.*, *99*, 3342 (1977).

23. (a) Sharafy, S., and Muszkat, K. A., *J. Am. Chem. Soc.*, *93*, 4119 (1971).
(b) Gegion, D., Muszkat, K. A., and Fischer, E., *ibid.*, *90*, 12, 3097 (1968).
(c) Saltiel, J., Zafirion, O. C., Megarity, E. D., and Lamola, A. A., *J. Am. Chem. Soc.*, *90*, 4759 (1968).
(d) De Boer, C. D., and Schlessinger, R. H., *ibid.*, *90*, 803 (1968).

24. (a) Hochstrasser, R., *Electrons in Atoms*, San Francisco: W. A. Benjamin, 1966;
(b) McClure, D. S., *J. Phys. Chem.*, *17*, 905 (1949).

25. (a) Lewis, G. N., and Kasha, M., *J. Am. Chem. Soc.*, *67*, 994 (1945); *ibid.*, *66*, 2100 (1944).
(b) Terenin, A., *Acta Physicochim., USSR*, *18*, 210 (1943).

26. (a) LaPaglia, S. R., *Spectrochim. Acta.*, *18*, 1295 (1962).
(b) Turro, N. J., et al., *Tetrahedron Letters*, 555 (1978).
(c) Kellogg, R. E., and Wyeth, N. C., *J. Chem. Phys.*, *45*, 3156 (1966).

27. (a) Hochstrasser, R. M., *J. Chem. Phys.*, *60*, 1258 (1974); *ibid.*, *48*, 646 (1968).
(b) El-Sayed, M. A., *Pure Appl. Chem.*, *24*, 475 (1970).
(c) Sixl, H., and Schwoerer, M., *Chem. Phys. Letters*, *6*, 21 (1970).
(d) Chan, I. Y., and Clarke, R. H., *ibid.*, *19*, 53 (1973).

28. (a) Evans, D., *J. Chem. Soc.*, 1351 (1957); *ibid.*, 2753 (1959); *ibid.*, 1735 (1960); *ibid.*, 1987 (1961).
(b) Grabowsha, A., *Spectrochim. Acta.*, *20*, 96 (1966).
(c) Tsubomura, H., and Mulliken, R. S., *J. Am. Chem. Soc.*, *82*, 5966 (1960).

29. (a) McGlynn, S. P., et al., *J. Phys. Chem.*, *66*, 2499 (1962); *J. Chem. Phys.*, *39*, 675 (1963).
(b) Giachino, G. G., and Kearns, D. R., *J. Chem. Phys.*, *52*, 2964 (1970); *53*, 3886 (1970).
(c) Kasha, M., *J. Chem. Phys.*, *20*, 71 (1952).
(d) Christodonleas, N., and McGlynn, S. P., *J. Chem. Phys.*, *40*, 166 (1964).
(e) McClure, D. S., *J. Chem. Phys.*, *17*, 905 (1949).

30. Vander Donckt, E., and Vogels, C., *Spectrochim. Acta.*, *27A*, 2157 (1971).

31. (a) Wright, M. R., Frosch, R. P., and Robinson, G. W., *J. Chem. Phys.*, *33*, 934 (1960).
(b) Grabowska, A., *Spectrochim. Acta.*, *19*, 307 (1963).

32. Warwick, D. A., and Wells, C. H. J., *Spectrochim. Acta*, *24A*, 589 (1968).

33. (a) McClure, D. S., Blake, N. W., and Hanst, P. L., *J. Chem. Phys.*, *22*, 255 (1954).
(b) Ermolaev, V. L., and Svitashev, K. J., *Opt. Spect.*, *7*, 399 (1959).

34. Kasha, M., *J. Chem. Phys.*, *20*, 71 (1952).

35. Karvanos, G., Cole, T., Scribe, P., Dalton, J. C., and Turro, N. J., *J. Am. Chem. Soc.*, *93*, 1032 (1971).

36. (a) Kearns, D. R., and Case, W. A., *J. Am. Chem. Soc.*, *88*, 5087 (1966).
(b) Marchetti, A. P., and Kearns, D. R., *J. Am. Chem. Soc.*, *89*, 768 (1967).

37. Kellogg, R. E., and Simpson, W. T., *J. Am. Chem. Soc.*, *87*, 4230 (1965).

38. (a) Parker, C. A., and Joyce, T. A., *Trans. Farad. Soc.*, *65*, 2823 (1969).
(b) Clark, W. D. K., Litt, A. D., and Steel, C., *Chem. Comm.*, 1087 (1969).
(c) Saltiel, J., Curtis, H. C., Metts, L., Miley, J. W., Winterle, J., and Wrighton, M., *J. Am. Chem. Soc.*, *92*, 410 (1970).
(d) For a review of the factors allowing the observation of phosphoresence in fluid solution see: Turro, N. J., Liu, K. C., Chow, M. F., and Lee, P., *Photochem. Photobio.*, *27*, 500 (1978).
(e) Kalyanasundaram, K., Grieser, and Thomas, J. K., *Chem. Phys. Letters*, *51*, 501 (1977).
(f) Gatterman, H., and Stockburger, M., *J. Chem. Phys.*, *63*, 4541 (1975).

39. (a) For a review of the method of flash spectroscopy, see Porter, G., *Techniques of Organic Chemistry*, *8*, New York: Wiley, 1963, p. 1055.
(b) For a review of T-T absorption, see Labhart, H., and Heinzelmann, W., in *Photophysics of Organic Molecules*, *1*, ed. Birks, J. B., New York: Wiley, 1973, p. 297.

40. Brand, J. C. D., and Williamson, D. G., *Adv. Phys. Org. Chem.*, *1*, 365 (1963); Arnold, D. R., et al., *Photochemistry*, New York: Academic Press, 1974, pp. 91–93.

41. (a) Bakhsliev, N. G., et al. *Russ. Chem. Rev.*, *38*, 740 (1969).
(b) Labhart, H., *Experientia*, *15*, 65 (1966).
(c) Liptay, W., *Excited States*, ed. Lim, E. C., Vol. 1, New York: Academic Press, 1974, p. 129.

42. (a) Martnov, U. Y., Demyashkevich, A. B., Uzhinov, B. M., and Kuzamin, M. G., *Russ. Chem. Rev.*, *46*, 1 (1977).
(b) Ireland, J. F., and Wyatt, P. A. H., *Adv. Phys. Org. Chem.*, *12*, 131 (1976).
(c) Klöpffer, W., *Adv. Photochem.*, *10*, 311 (1977).

43. Exceptions to this rule: Bonneau, R., Pereyre, J., and Joussot-Dubien, J., *Molec. Photochem.*, *6*, 245 (1974).

44. For reviews, see:
(a) Forster, T., *Angew. Chem. Int. Ed. Eng.*, *8*, 333 (1969).
(b) Birks, J. B., *Photophysics of Aromatic Molecules*, New York: Wiley, 1970, p. 301.
(c) Beens, H., and Weller, A., *Organic Molecular Photophysics*, ed. Birks, J. B., Vol. 2, New York: Wiley, 1975, p. 159.

45. For a survey of charge transfer phenomena, including absorption and emission, see Birks, J. B., *Photophysics of Aromatic Molecules*, New York, N.Y.: Wiley, 1970, p. 403.

46. (a) Subudhi, P. C., and Lim, E. C., *J. Chem. Phys.*, *63*, 5491 (1975).
(b) Takemura, T., Aikawa, M., Baba, H., and Shindo, Y., *J. Am. Chem. Soc.*, *98*, 2205 (1976).

47. Kajima, S. O., Subudhi, P. C., and Lim, E. C., *J. Chem. Phys.*, *67*, 4611 (1977).

48. Forster, T., and Kasper, K., *Z. Physik. Chem., N.F., 1*, 275 (1954).

49. Yoshihara, K., Kasuya, T., Inoue, A., Nagakura, S., *Chem. Phys. Letters, 9*, 469 (1971).

50. (a) Weller, A., *Pure Appl. Chem., 16*, 115 (1968).
(b) Knibbe, H., Rehm, D., and Weller, A., *Ber. Bunsen. Gesell., 73*, 839 (1969); (c) *ibid., 72*, 257 (1968); *ibid., 73*, 834 (1969).

51. (a) Review: DeSchryver, F., *Adv. Photochem., 10*, 359 (1977).
(b) Hirayama, F., *J. Chem. Phys., 42*, 3163 (1965).
(c) Mimura, T., and Itoh, M., *J. Am. Chem. Soc., 98*, 1095 (1976).
(d) Okajima, S., Subudhi, P. C., and Lim, E. C., *J. Chem. Phys., 67*, 4611 (1977).

52. Birks, J. B., *Photophysics of Aromatic Molecules*, New York: Wiley, 1970, p. 372.

53. Brown, R. E., Singer, L. A., and Parks, J. H., *Chem. Phys., 14*, 193 (1972).

54. For example, triplet-triplet fluorescence of carbenes (ground state triplets) is known: Trozzolo, A. M., and Gibbons, W. A., *J. Am. Chem. Soc., 89*, 239 (1967).

55. (a) Beer, M., and Longuet-Higgins, H. C., *J. Chem. Phys., 23*, 1390 (1955).
(b) Viswath, G., and Kasha, M., *ibid., 24*, 757 (1956).
(c) Birks, J. B., *Chem. Phys. Letters, 17*, 370 (1972).
(d) Murata, S., Iwanga, C., Toda, T., and Kohubun, H., *Ber. Bunsen. Gesell., 76*, 1176 (1972).

56. Oka, T., Knight, A. R., and Steen, R. P., *J. Chem. Phys., 66*, 699 (1977).

57. Hui, M. H., DeMayo, R., Suau, R., and Ware, W. R., *Chem. Phys. Letters, 31*, 257 (1975).

58. (a) Rentzepis, P. M., *Chem. Phys. Letters, 3*, 717 (1969).
(b) Gillispie, G. D., and Lim, E. C., *J. Chem. Phys., 65*, 4314 (1976).

6

Photophysical Radiationless Transitions

6.1 Photophysical Radiationless Transitions as a Form of Electronic Relaxation

Radiationless transitions between electronic states may be considered as a form of electronic relaxation by which electronic energy is converted into the kinetic energy associated with nuclear motion.[1] In Chapter 4 it was shown that photophysical and photochemical radiationless transitions may not always be sharply distinguished. In this chapter we will be concerned with photophysical radiationless transitions, which occur (a) without a change in spin multiplicity (internal conversions: $S_n \rightarrow S_1$, $S_1 \rightarrow S_0$, $T_n \rightarrow T_1$, etc.), and (b) with a change in spin-multiplicity (intersystem crossing: $S_1 \rightarrow T_1$ and $T_1 \rightarrow S_0$).

Photophysical radiationless transitions generally start from a minimum on an excited state surface and terminate with the molecule back in its original minimum on the ground state surface. What factors determine the rates and efficiencies of internal conversions and intersystem crossings? How can these radiationless processes be visualized in terms of molecular mechanisms and representative points on energy surfaces? Are there relationships between the rates and probabilities of radiationless processes and molecular structure?

This chapter provides a basis for answering these questions. The conclusions and generalities we make can be extended to photochemical radiationless transitions. The latter can be treated as being analogous to photophysical processes, except that the conversion of electronic energy into nuclear energy causes such a distortion of the original ground state structure that the molecule does not return to its original ground state minimum, i.e., a photoproduct is formed.

6.2 A Classical Interpretation of Radiationless Electronic Transitions as Jumps between Surfaces

A classical interpretation[2] of radiationless electronic transitions treats them in terms of jumps of a representative point between energy surfaces. The representative point will make a radiationless "jump" from one surface to another at "critical" nuclear configurations, r_c. These critical geometries will generally correspond to minima on excited surfaces. According to classical theory[2] the probability P that the representative point will make a jump as r_c is approached can be deduced from the expression:

$$P(\text{Probability of surface jump at } r_c) \sim \exp\text{-}\Delta E/v\,\delta s \tag{6.1}$$

where ΔE is the energy separation between the surfaces involved in the transition at r_c, v is related to the velocity of the nuclei as they approach r_c, and δs is related to the difference in slopes of the two surfaces in the region near r_c (dE/dr, the slope of an energy curve, is directly related to the forces acting on the nuclei).

Consider a simple situation involving two surfaces (Fig. 6.1). We can identify three important situations: (a) a Zero Order crossing, for which ΔE is 0 at r_c, (b) a "weakly avoided" crossing, for which ΔE is "small" at r_c, and (c) a "strongly avoided" crossing, for which ΔE is "large" at r_c. This terminology and the use of

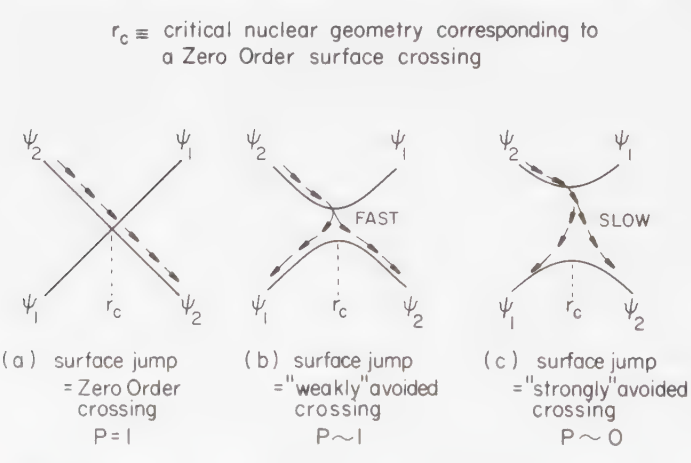

Figure 6.1

Representation of the dynamics of a representative point (motion represented by arrows) on an energy surface.

Ψ to identify surfaces are used to indicate the correspondence between the classical and wave mechanical interpretations.

The classical interpretation of radiationless transitions uses the simplicity of the classical description of the motion of the representative point in the regions where the surfaces are well separated. This motion (symbolized by the arrows in Fig. 6.1) continues on a single initial surface until the nuclei attain a critical geometry, r_c, corresponding to a region of strong electronic coupling to a lower surface. In this region the representative point may execute a jump from the initial surface to a second neighboring surface with a probability P, which depends on certain parameters such as nuclear velocity as the system approaches r_c, the slopes of the potential energy curves near r_c, and the energy separating the states near r_c. The motion of the representative point on the second surface continues until a second region corresponding to a second critical geometry r_c' is reached. Thus, the classical picture of radiationless transitions is: (a) motion along an upper surface, (b) jump to a lower energy surface at critical geometry, (c) motion along the lower surface, (d) jump to a lower energy surface at a critical geometry, r_c', until a stable minimum on the ground surface is achieved. Although the classical interpretation reveals that nuclear kinetic energy (e.g., velocity of representative point) can promote surface jumps, it does not clearly reveal the nature of the "electronic coupling" that can promote surface jumps. We shall see in the following section that a wave mechanical interpretation of surface jumps will form a basis for correlating the rates and efficiencies of radiationless transitions with molecular structure.

6.3 Wave Mechanical Interpretation of Radiationless Transitions between States

Wave mechanics also treats the problem of radiationless transitions in terms of energy surfaces.[3] In order to calculate energy surfaces from theory, a number of simplifying assumptions are necessary. One of the most important of these excludes electron motion and formulates the problem in terms of the motion of *nuclei* only. This is called *the adiabatic (or Born-Oppenheimer) approximation*, and energy surfaces generated under such assumptions are termed *adiabatic* surfaces. Further, the dynamics of nuclear motion are treated in terms of the motion of a "representative point."

If the changes in the electronic energy of a molecule brought about by nuclear motions are essentially adiabatic, then the behavior of the motions of the electrons may be treated by solution of the wave equation for stationary nuclei. The problem of evaluating electron motion as a function of nuclear motion is then the same as for vibrations or for chemical reactions. The differences between vibrations and reactions are only in the amount of nuclear motion and the occurrence of different equilibria positions for nuclear motions of the reactants and products. If the electron motions are treated as *adiabatic* (i.e., completely and continuously adjusting to

changes in nuclear structure), and if the nuclear motions are treated as *classical*, one can in principle evaluate the electronic potential energy for all nuclear configurations. This is how one generates adiabatic electronic potential-energy surfaces. *In such a situation, the actual motions of the nuclei follow the rules of classical mechanics, and are completely subject to the control of the adiabatic surface.* Thus, the motions of nuclei are wholly determined by the potential-energy surfaces "on which" the *representative point* (or more loosely speaking, the *molecule*) happens to be.

Suppose the change in nuclear configuration brings the molecule from an initial state into a region corresponding to a Zero Order crossing at geometry r_c. This situation is optimal for mixing of Zero Order states, i.e., near r_c

$$\text{Initial state} \qquad \psi_2 \rightarrow \psi_2 \pm \psi_1 \rightarrow \psi_1 \qquad \text{Final state} \tag{6.2}$$
$$\text{mixing}$$

We say that in the crossing region the Zero Order states ψ_2 and ψ_1 are capable of being in resonance near r_c. If resonance should occur the electron motion is no longer adequately defined in terms of one Zero Order function alone. The nuclear motion is no longer unambiguously controlled by a single surface. What happens when the system which is initially prepared in state ψ_1 enters the crossing region,[4] i.e., when the representative point of an initial electronic state approaches the "critical" geometry r_c (see Fig. 6.2)?

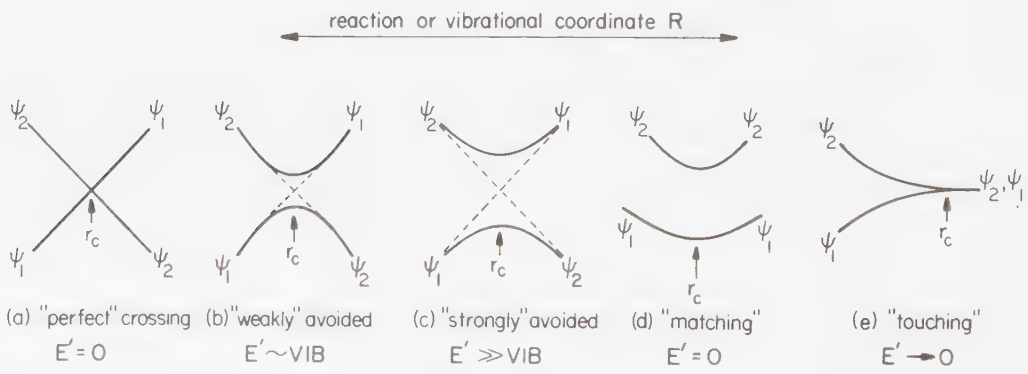

Figure 6.2

The archetype *adiabatic* surface topologies for a two-surface system: (a) "perfect" crossing for which $\psi_1 \leftrightarrows \psi_2$ transitions are strictly forbidden; (b) and (c) "weakly" and "strongly" avoided crossings for which $\psi_1 \leftrightarrows \psi_2$ transitions are possible near r_c (see text); (d) "matching" for which $\psi_1 \leftrightarrows \psi_2$ transitions are very improbable; and (e) "touching" for which $\psi_1 \leftrightarrows \psi_2$ transitions are possible near r_c, (see text).

The situations expected with respect to the probable trajectory of a representative point are summarized in Figure 6.3. If the system corresponds to Zero Order (fast passage through nuclear geometries near r_c or weak mixing of ψ_2 and ψ_1 near r_c), a representative point starting in ψ_2 will remain on ψ_2 throughout its trajectory, i.e., the process will be completely adiabatic (all on one surface). A similar situation will occur if the mixing of ψ_1 and ψ_2 is small near r_c, i.e., a formal "jump" or nonadiabatic transition will occur between the adiabatic surfaces. In the case where there is a large electronic interaction between ψ_1 and ψ_2 near r_c, a representative point starting on ψ_2 will "switch" over to ψ_1 near r_c, but will remain on the same adiabatic surface. For most practical purposes, this situation is indistinguishable from the case in Figure 6.2, if the representative point moves well beyond r_c. If the representative point gets "stuck" in an excited state minimum for a long enough period of time, an interaction may occur to cause a radiationless transition to the lower surface. This may be viewed as occurring via the dynamic link (dotted lines) provided by the Zero Order crossing. In other words, as the molecule is vibrating in the excited state, a small perturbation may couple the excited and ground states and the representative point may be thought to follow the trajectory of the Zero Order surfaces (dotted lines in Fig. 6.3c). Whether the representative point falls to the ground state and proceeds to ψ_1 or to ψ_2 will depend on the particulars of the perturbation and the dynamics of the system.

In the region near r_c, an oscillation (resonance) or electronic motion occurs such that the electron motion may be described by either $\psi_1 + \psi_2$ or $\psi_1 - \psi_2$, i.e., the two electronic states are strongly mixed. The frequency of these imaginary oscillations back and forth is called *electronic tautomerism.*[4b] In the limit of perfect

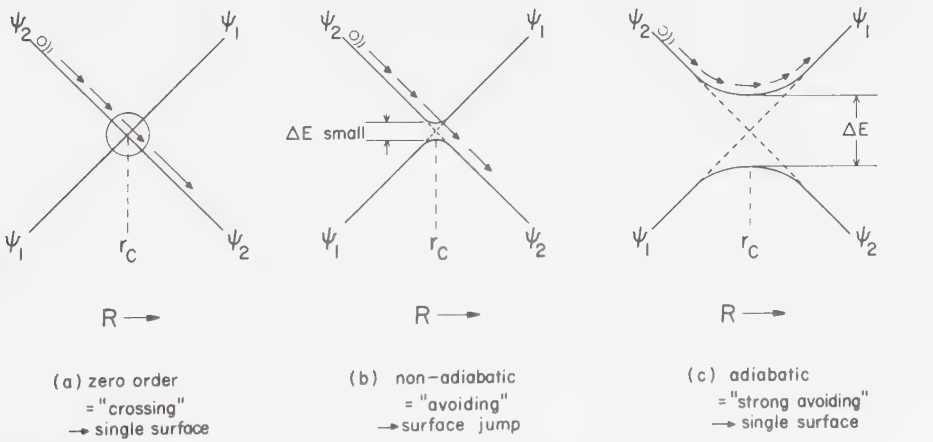

Figure 6.3

Schematic representations of the trajectories of a representative point: (a) $\psi_2 \rightarrow \psi_2$ via an adiabatic (no surface jump) pathway along a Zero Order crossing, (b) $\psi_2 \rightarrow \psi_2$ via a nonadiabatic (surface jump) pathway including a weak "avoiding", (c) $\psi_2 \rightarrow \psi_1$ via an adiabatic pathway (no surface jump).

resonance the "lifetime" τ that the molecule spends in a tautomeric form is of the order of

$$\tau(\text{"lifetime" of an electronic tautomer}) \cong \hbar/\Delta E \sim 10^{-13}/\Delta E \text{ sec} \qquad (6.3)$$

where ΔE is the resonance energy in kcal/mole. Clearly, if a switch from one tautomer to another is to occur it must happen within the time $\Delta\tau$ that the molecule is in the region of crossing of surfaces, i.e., $\tau < \Delta\tau$.

Strong resonance interactions (e.g., crossings of states of the same electronic and spin symmetries) are of the order of >30 kcal/mole. This corresponds to a lifetime (Eq. 6.3) of an individual electronic tautomer (resonance structure) of $\tau \cong 10^{-15}$–10^{-14} sec via nuclear perturbations occurring at a rate of $1/\tau$.

If the relative velocity of the nuclei moving through the crossing region is $\sim 10^4$–10^5 cm/sec $= 10^{12}$–10^{13} Å/sec (typical values for light atoms), then the *time* $\Delta\tau$ the nuclei spend in a given region (say, along a line of length of ~ 3 Å) is $\sim 10^{-12}$–10^{-13} sec. This rough calculation shows that the lifetime of the tautomer is *shorter* than the time it takes to cross the interaction region. Thus, the tautomerization is complete before the nuclei can move out of the interaction region. In the case of "weak" resonance interaction (<1 kcal/mole), the lifetime of the tautomer is $\sim 10^{-13}$ or longer. Thus, tautomerizeration may or may not occur in the interaction region, depending on the velocity of the representative point and the precise value of τ.

$$\begin{matrix}\text{Frequency of} \\ \text{electronic} \\ \text{tautomerization}\end{matrix} \quad \nu = 1/\tau \cong \Delta E/\hbar \cong 10^{13}\,\Delta E \text{ (in kcal/mole)} \qquad (6.4)$$

Radiationless Transitions and the Breakdown of the Born-Oppenheimer Approximation

Radiationless transitions between surfaces are difficult at geometries for which the B-O surfaces are far apart (more than several vibrational quanta) in energy.[3,5] On the other hand, *radiationless transitions are most probable at geometries, r_c, corresponding to crossings of the Zero Order B-O surfaces.* These geometries correspond to "leaks" in surfaces, and radiationless "jumps" are expected to occur with their highest probability when the representative point corresponds to a geometry "in the region" of a Zero Order B-O crossing.[3] These are precisely the regions in which the electronic wavefunction is a rapidly changing (orbital and/or spin) function of nuclear geometry. As the representative point passes through such a region, the nuclear motion has a certain probability of being controlled by *either* electronic surface.

Some Archetype Surface Situations Near Critical Nuclear Geometries

There are a number of possible surface classifications.[6] For simplicity we shall define five which are relatively common (see Fig. 6.2). The main idea of a classifica-

tion of surfaces is to provide some insight into possible radiationless transitions at certain "crucial" molecular geometries which correspond to a region near r_c along the reaction coordinate. Suppose that two potential-energy surfaces cross in Zero Order for a "critical nuclear geometry," r_c. The five "archetype surface topologies" of the two surfaces at r_c may be classified as: (a) "perfect" crossing, (b) "weakly" avoiding, (c) "strongly" avoiding, (d) "matching," and (e) "touching."

For the "perfect crossing" situation, the electronic interaction energy E' between the initial and final states is precisely zero at r_c. A representative point on ψ_2 would have no "knowledge" of the existence of ψ_1 and would pass through the "crossing region" (geometries close to that of r_c) completely unperturbed. Such a situation is idealized, i.e., rigorously valid only for certain highly symmetric geometries. It is postulated that small distortions from the idealized geometries do not significantly modify the conclusions based on the Zero Order crossing. As a rule, if the coupling between ψ_1 and ψ_2 in the region near r_c is much less than the energy of vibrational couplings ($< 100\ \text{cm}^{-1}$), we may consider $E' \sim 0$. A close approximation to a "perfect crossing" is one for which the two states differ in spin multiplicity and for which spin-orbit coupling is weak, i.e., most singlet-triplet surface crossings involving aromatic hydrocarbons.

For the "weakly avoiding" situation, the electronic coupling (in First Order) between ψ_1 and ψ_2 at r_c is of the order of vibrational energies but not much greater. In Figures 6.2 and 6.3, dotted lines are drawn to serve as a reminder of the Zero Order crossing. For the "strongly avoiding" situation, the electronic coupling (in First Order) between ψ_1 and ψ_2 at r_c is much larger than vibrational energies. In the "matching" situation as in the Zero Order crossing situation, ψ_1 and ψ_2 do not possess any electron coupling even in First Order. Thus, one must proceed to a Second or higher order perturbation if ψ_1 and ψ_2 are to be coupled.

Although all Zero Order crossings are "avoided" to a greater or lesser extent (see Fig. 6.1), for weakly avoided crossings the molecule may readily jump from one adiabatic (First Order) surface to another, i.e., the representative point may behave as if there is no avoiding at all and follows the Zero Order surface (for which electronic configuration or multiplicity is preserved). Such crossings may be called "holes" or "funnels" in the surface.[3b] As the crossing becomes more strongly avoided (Fig. 6.3c), the probability of jumps between adiabatic surfaces in the region of the geometry corresponding to Zero Order surface crossing decreases. In the limit a "funnel" becomes a true excited state "minimum," which is detectable by conventional flash spectroscopic and/or chemical trapping methods.

"Leaks" or "jumps" from one surface to another occur most readily when they can occur "vertically," (i.e., with very little nuclear geometry change) and with little change in nuclear momentum. The greater the change in nuclear geometry or in nuclear momentum which results from a surface jump, the more strongly the leak or jump is resisted, i.e., the slower the rate of the radiationless transition from one surface to another.

An essential difference between the "strongly" avoiding and "matching" topologies is the occurrence of a "Zero Order" linkage (dotted lines) between the upper and lower surfaces in the former, which does not occur in the latter. The importance of this distinction is that for an avoided crossing the representative point may jump

from ψ_2 to ψ_1 in the region near r_c, because the dotted line (Zero Order connectivity) provides a "dynamic" link between the upper and lower surfaces. When surfaces are "matched" near r_c, there is no dynamic link coupling them at the purely electronic level. The "strongly avoiding" topology occurs typically near geometries which correspond to transition states for "allowed" pericyclic reactions.

A final surface situation is termed "touching". In this case, the two electronic surfaces approach each other asymptotically, and at or near r_c they become very close in energy, i.e., they essentially "touch" each other. Such a surface topology near r_c would be typical for certain states during the breaking of a σ bond or a π bond (see Section 6.5, especially Fig. 6.12).

6.4 Formulation of a Parameterized Model of Radiationless Transitions

Only a few parameters are necessary for a qualitative evaluation of the probabilities (or relative probabilities) of radiationless transitions to be made. As was done for radiative transitions in Section 5.8 we may consider the *experimental* probability of a radiationless transition (usually expressed in terms of a rate constant, k_{OB}) as the product of the rate constant for a hypothetical "fully allowed" (k_0) process; and *prohibition factors* (f) which contrive to reduce k_0 to the observed k_{OB}. Recall the concept of oscillator strength and the various selection rules which lead to a decrease in observed oscillator strengths from an ideal, maximal value of 1.0. In the same spirit we can suppose that k_{OB} may be parameterized as[7]

$$\text{Observed rate } k_{OB} = \underset{\text{Maximal rate}}{k_0} \times \underset{\text{time prohibition}}{f_E \times f_v \times f_S} \quad \begin{matrix}\\ \text{factors}\end{matrix} \tag{6.5}$$

where f_E, f_v, and f_S represent the "prohibition factors" due to the electronic, nuclear, and spin configurational changes which occur during the radiationless transitions.

As discussed in detail in sections 5.8ff, the magnitude of term f_E is related to the magnitude of the matrix element for the *pure electronic part* of the radiationless transition. The magnitude of f_E may be qualitatively evaluated by inspection of the positive overlap of the *orbitals which change* during the radiationless transition. The magnitude of f_v is related to the magnitude of the overlap of the nuclear wave functions for the initial and final states. We may identify f_v with the *Franck-Condon factor* or the prohibition to the probability of transition due to change in nuclear configuration or motion. Finally, f_S is related to the similarity of the total electron spin in the initial and final states. The magnitude of f_S will depend on the spin-orbit coupling (or in special cases to the hyperfine coupling) interactions which occur during an intersystem crossing.

Each one of the factors, f, may act as the promotor of an electronic perturbation (f_E), vibrational perturbation (f_v), or a spin perturbation (f_S), which may be rate-limiting. Such a situation implicitly assumes that the excess electronic energy

released by the radiationless transition is "accepted" somehow and that this energy release is not rate-determining. The "acceptors" of the excess electronic energy may be either the vibrations of the molecule undergoing the transition or the vibrations and translation motions of solvent molecules. Thus, intramolecular vibrations and intermolecular collisions typically serve as a "heat bath" that eventually soaks up the excess electronic energy originally localized in the molecule undergoing the radiationless transition.

Visualization of Radiationless Transitions Promoted by Vibrational Motion; Vibronic Mixing

In the Zero Approximation we assume that for a given, fixed nuclear geometry the electronic states may be classified in terms of a single electronic orbital configuration and a single spin type (multiplicity). We consider these Zero Order states as "electronically pure," e.g., "pure" n, π^* or π, π^* and "pure" singlet or triplet. In the First Approximation we consider various mechanisms for "mixing" of the states. Vibrations, collisions, electron-electron interactions, and spin-orbit interactions all serve to "mix" the Zero Order states.[8]

In terms of orbitals, a $n, \pi^* \rightarrow \pi, \pi^*$ radiationless transition corresponds to a one-electron jump of a π electron into an n orbital (we assume that π^* electron does not change during the transition), i.e., we consider a $\pi \rightarrow n$ orbital jump (Fig. 6.4). For the process to be *isoenergetic*, vibrational motion must cause a "switching" of the energetic ordering of the n and π levels. It is not absolutely necessary that the π, π^* be lower in energy than the n, π^* state, but only that a crossing point can be reached and that the system then deactivates along the π, π^* surface. In some cases energy must be provided to the system in order for

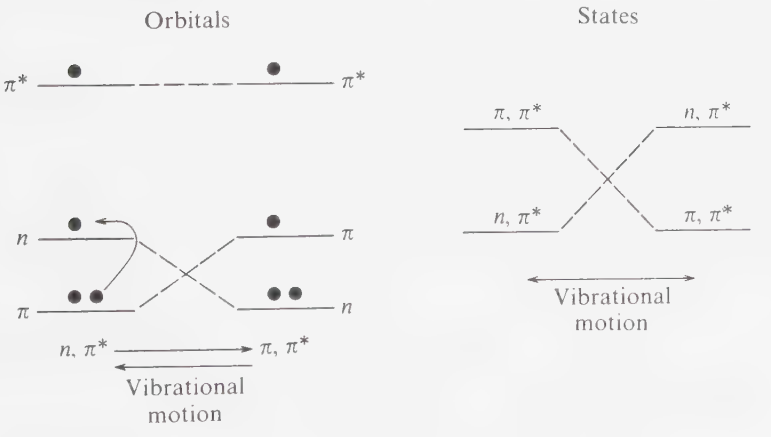

Figure 6.4

Orbital and state descriptions of $n, \pi^* \leftrightarrows \pi, \pi^*$ state switching as a result of vibrational motion.

the crossing point to be reached, i.e., the radiationless process will require an activation energy. Of course, the reverse situation of a $\pi, \pi^* \rightarrow n, \pi^*$ transition can easily be imagined. In this case the system starts off in a π, π^* configuration and a $n \rightarrow \pi$ orbital transition occurs.

From the standpoint of theory,[9] the largest matrix elements for vibronic interactions are those which generate electric dipoles in the same region of space as the transition dipoles for the states undergoing transition. Thus, the "best" vibrations for causing mixture of the n, π^* and π, π^* states are those nuclear motions which cause displacement of atoms possessing substantial *n and* π density, i.e., the O atom.

Vibrations which do not disrupt planarity are not effective in generating electric dipoles near the oxygen atom because the n and π orbitals are *orthogonal* as long as the system is planar. Therefore $\langle n|\pi\rangle = 0$. Nonplanar vibrations, on the other hand, cause the p orbitals on oxygen to rehybridize (Fig. 6.5). As a result, $\langle n|\pi\rangle$ is not equal to zero for nonplanar geometries. However, it is to be expected that the avoiding of surfaces due to nonplanar vibrations will be weak. The occurrence of a crossing for a planar vibration and of an avoiding for a nonplanar vibration is shown in Figure 6.6. It is important to notice that the states are strongly mixed *only* for those geometries near the crossing point. Thus for geometries near the energy minima on the lower surface, the *Zero Order approximation* of a "pure" n, π^* and "pure" π, π^* state is still quite valid.

Let us consider how "mixing" of states is viewed in terms of energy surfaces (Fig. 6.6). Suppose a Zero Order crossing of an n, π^* and a π, π^* state of a ketone occurs as a result of a certain nuclear motion (vibration). If that motion causes the nuclear structure to change from a strictly planar shape (for which the assumption of purity of n, π^* and π, π^* states is a good approximation) to a nonplanar shape (for which the n, π^* and π, π^* states are allowed to mix), then the Zero Order crossing is removed and replaced by First Order avoided crossing. The magnitude of the avoiding is given by a matrix element of the type:[9]

$$\langle n, \pi^*|H_{\text{VIB}}|\pi, \pi^*\rangle \tag{6.6}$$

where H_{VIB} is an operator representing the nuclear motion which causes the mixing. The magnitude of this matrix element may be estimated from the overlap integral $\langle n, \pi^*|\pi, \pi^*\rangle \sim \langle n|\pi\rangle \neq 0$. This integral is nonzero for nonplanar vibrations. The effects of state mixing of any type are to cause photophysical parameters (e.g., rate constants for radiative or radiationless transitions) to deviate from those expected for a Zero Order configurational or multiplicity model.

Figure 6.5
Schematic of the "mixing" of *s* character into a *p*-orbital as the result of nonplanar vibrations.

It is useful and important to have calibration points for the frequency of vibrational motion of pairs of atoms that commonly occur in organic molecules.

The oscillation *frequency* of a harmonic oscillator is related to the restoring force ($-kr$) and the masses of the particles involved in the oscillation by the expression

$$\nu(\text{frequency of vibration}) = \frac{1}{2\pi}\sqrt{\frac{k}{\mu}} \tag{6.7}$$

where k is the *force constant* (a measure of the "stiffness" of the restoring force, or for a molecule, of the bond strength), and μ is the reduced mass. When the mass of X is much larger than the mass of Y, μ is approximately equal to the mass of Y, i.e., $\mu \sim$ mass of the lighter nucleus.

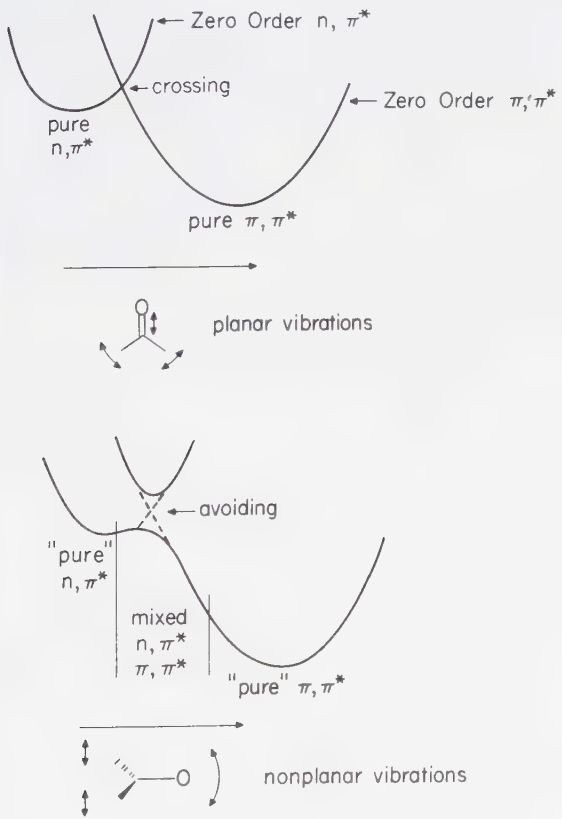

Figure 6.6

The effect of planar (top) and nonplanar (bottom) vibrations on a Zero Order crossing of n, π^* and π, π^* surfaces.

Table 6.1 lists some frequencies of vibrations for pairs of diatomic groups. Even in molecules, strongly bonded pairs of atoms may often be treated as an independently vibrating pair. From Eq. 6.7 we expect and find that ν will *increase* with increasing bond strength at constant μ, e.g., ν(C C) > ν(C=C) > ν(C C). We also expect for comparable bond strength that ν will *decrease* with increasing μ, e.g., ν(C—H) > ν(C—D) and ν(C—C) > ν(C—Cl).

Visualization of Radiationless Transitions Promoted by Spin-Orbit Coupling

From the vector model for electronic spin (Sections 2.7 and 3.6) it was deduced that two possible mechanisms exist for intersystem crossing, a spin "flip" and a spin "rephasing." For organic molecules, spin-orbit interactions usually provide the major mechanism for intersystem crossing, whereas spin-spin interactions provide an alternate mechanism for diradicals.[10]

Consider Figure 6.7 for a general, schematic interpretation of intersystem crossing in terms of surfaces.[10] In the Zero Order approximation we assume we do not have a mechanism for intersystem crossing, resulting from our artificial separation of electronic and spin motions. In this approximation (top of Fig. 6.6) if a molecule is in an initial singlet state it will forever stay in the singlet state, or if it is in an initial triplet state it will remain forever in the triplet state, even if a reaction coordinate exists such that a crossing of the singlet and triplet state occurs.

When we introduce spin-orbit coupling (or for diradicals, hyperfine coupling, laboratory magnetic fields, etc.) it becomes possible that as a representative point moves along an initially "pure" singlet or triplet surface, intersystem crossing may occur near the nuclear geometry corresponding to r_c, *if certain conditions are met.* These conditions are that the interaction that mixes the spin states must be "turned on" and must be effective when the representative point is near r_c. Thus, there is a requirement not only that a force capable of changing the spin multiplicity must exist but also that it must operate effectively during the period when the repre-

Table 6.1 Some Common Bond Types and Associated Stretching Frequencies and Bond Strengths

Bond Type	Vibrational Type	Oscillation period	Bond Strength (kcal/mole)
C=C	stretch	2200 cm ^{1} = 6.6 × 10^{13} sec^{-1}	100
C=O	stretch	1700 cm ^{1} = 5.1 × 10^{13} sec^{-1}	180
C—C	stretch	1600 cm ^{1} = 4.2 × 10^{13} sec^{-1}	165
N=N	stretch	1500 cm^{-1} = 4.0 × 10^{13} sec^{-1}	110
C—H	bend	1000 cm^{-1} = 3 × 10^{13} sec^{-1}	100
C—C	stretch	1000 cm^{-1} = 3 × 10^{13} sec^{-1}	85
C—C	bend	500 cm^{-1} = 1.5 × 10^{12} sec^{-1}	85
C—H	stretch	3000 cm^{-1} = 9 × 10^{13} sec^{-1}	100

sentative point is in the region near r_c (i.e., the molecule has a nuclear geometry corresponding to r_c and an energy close to that of the Zero Order crossing point).

Selection Rules for Intersystem Crossing

In Section 3.6 we learned that spin-orbit interactions are effective in promoting intersystem crossing if: (a) the orbital transition involved possesses the character of a $p_x \rightarrow p_y$ orbital jump, and (b) the orbital transition is localized on a single atom.

Let us consider an unsaturated system containing a heteroatom. From the standpoint of spin-orbit coupling, such a system introduces a crucial difference relative to an unsaturated hydrocarbon, namely the occurrence of low-energy n, π^* configurations. Let us take a carbonyl group as a prototype for our qualitative analysis of spin-orbit coupling in such systems. The singlet state of a carbonyl

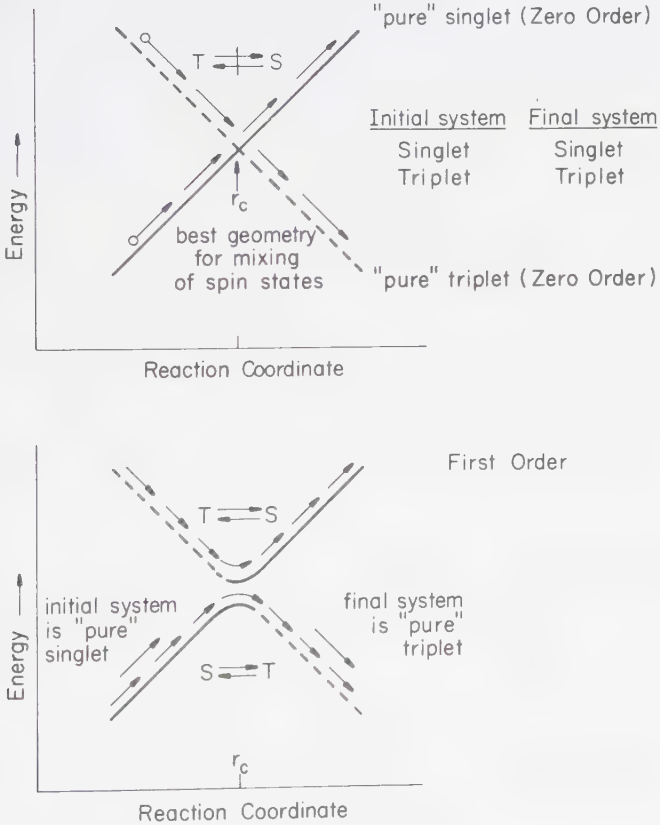

Figure 6.7

Intersystem crossing is strictly forbidden in the Zero Order approximation (top figure) but becomes partially allowed when a spin mixing mechanism is available (lower figure).

group may be derived from an n, π^* or a π, π^* configuration. Consider the four possible intersystem crossings from S_1 of a carbonyl group:

1. $^1n, \pi^* \rightarrow {}^3\pi, \pi^*$ (6.8) } Figure 6.8
2. $^1n, \pi^* \rightarrow {}^3n, \pi^*$ (6.9) }
3. $^1\pi, \pi^* \rightarrow {}^3n, \pi^*$ (6.10) } Figure 6.9
4. $^1\pi, \pi^* \rightarrow {}^3\pi, \pi^*$ (6.11) }

If we assume that the rate of intersystem crossing is directly related to the magnitude of spin-orbit coupling, then we can estimate the magnitude by inspection of the several configurations of the initial state to determine if there is finite First-Order interaction with any of the configurations of the final state, i.e., if a one-center $p_x \rightarrow p_y$ orbital jump occurs.[10] Two center $p_x \rightarrow p_y$ orbital jumps are less effective in promoting spin-orbital coupling.

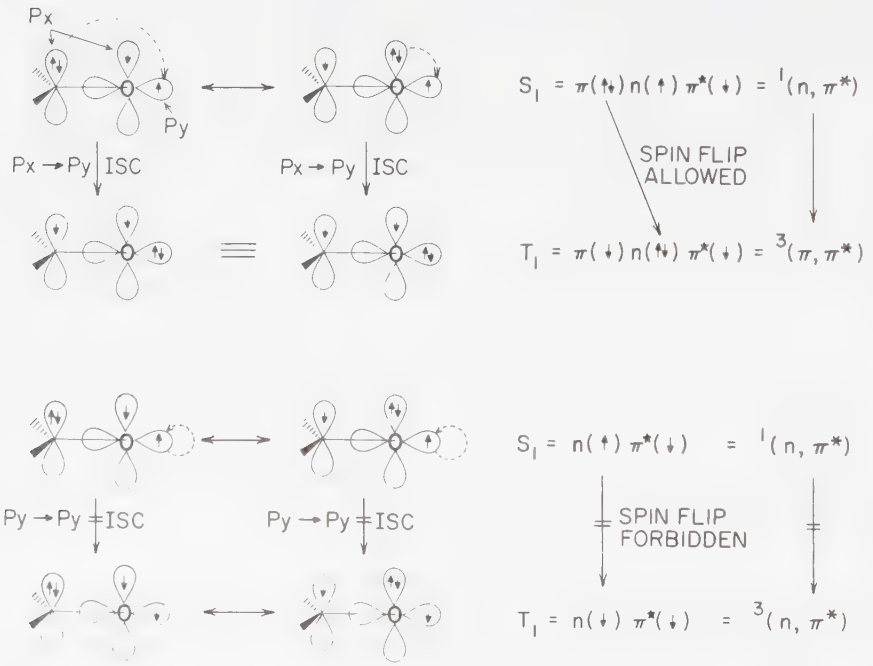

Figure 6.8

Qualitative orbital description of the basis for the allowed $^1(n, \pi^*) \rightarrow {}^3(\pi, \pi^*)$ and the forbidden $^1(n, \pi^*) \rightarrow {}^3(n, \pi^*)$ intersystem crossings.

Consider a $^1n, \pi^* \rightarrow {}^3n, \pi^*$ intersystem crossing. Two major atomic orbital representations of the $^1n, \pi^*$ state are shown in Figure 6.8a. Intersystem crossing must involve either an n or a π^* electron spin flip. In neither configuration is a First-Order spin-orbit coupling possible because neither the $n(\uparrow) \rightarrow n(\downarrow)$ nor the $\pi^*(\downarrow) \rightarrow \pi^*(\uparrow)$ electronic transitions generate orbital angular momentum along the bond axis; i.e., no $p_x \rightarrow p_y$ single atomic orbital jump is involved. Thus, there is no First-Order spin-orbit coupling for the $^1n, \pi^* \rightarrow {}^3n, \pi^*$ transition.

In contrast, the $^1n, \pi^* \rightarrow {}^3\pi, \pi^*$ transition has a First-Order spin-orbit coupling in one of its major atomic orbital configurations (Fig. 6.8b). As a result, intersystem crossing can be triggered via a one-center $p_x \rightarrow p_y$ interaction. In addition, the highly electrophilic, half-filled n orbital provides a substantial "driving force" for the electronic transition.[10]

Starting from a $^1\pi, \pi^*$ state we must consider three atomic orbital configurations (Fig. 6.9). By inspection, two of the atomic orbital configurations have a First Order coupling with a configuration of the $^3n, \pi^*$ state. Thus a $^1\pi, \pi^*$ to $^3n, \pi^*$ transition is "allowed" to occur by spin-orbit coupling. By inspection of the $^1\pi, \pi^* \rightarrow {}^3\pi, \pi^*$ transition, there is no First Order spin-orbit coupling between any of the singlet configurations and the triplet configuration (Fig. 6.9).

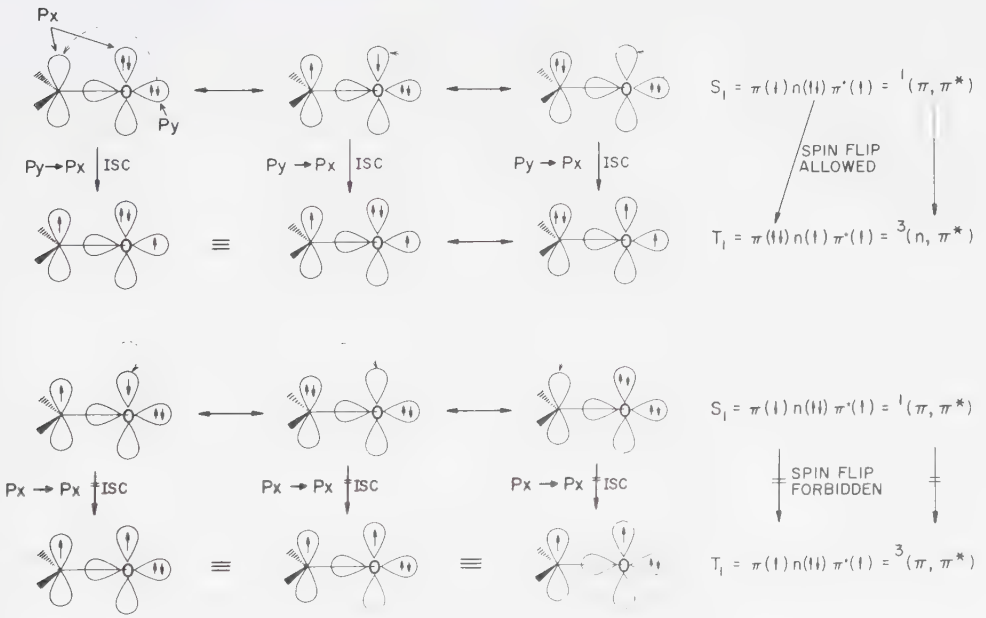

Figure 6.9

Qualitative orbital description of the allowed $^1(\pi, \pi^*) \rightarrow {}^3(n, \pi^*)$ and the forbidden $^1(\pi, \pi^*) \rightarrow {}^3(\pi, \pi^*)$ intersystem crossings.

As a result of our analysis we deduce the following *selection rules* (commonly termed El-Sayed's rules)[11] for intersystem crossing of carbonyl groups:

	$n, \pi^* \rightleftarrows n, \pi^*$	Forbidden	(6.12)
$S_1 \leftrightarrows T$ Transitions	$n, \pi^* \rightleftarrows \pi, \pi^*$	Allowed	(6.13)
	$\pi, \pi^* \rightleftarrows \pi, \pi^*$	Forbidden	(6.14)

The rules should be general for n, π^* and π, π^* states and are not restricted to carbonyl compounds.

Although more quantitative data is listed in Table 6.4, here we will give examples of an alkyl ketone,[12] benzophenone,[13] and pyrenaldehyde[14] for which the values of k_{ST} are $\sim 10^8\ \text{sec}^{-1}$, $\sim 10^{11}\ \text{sec}^{-1}$, and $\sim 10^7\ \text{sec}^{-1}$ respectively. Figure 6.10 summarizes the transitions involved.

Extending the logic, we deduce that a $p_x \rightarrow p_y$ transition is also required for an allowed $T_1 \rightarrow S_0$ intersystem crossing transition, so that

$T_1 \leftrightarrows S_0$ Transitions	$n, \pi^* \rightarrow n^2$	Allowed	(6.15)
	$\pi, \pi^* \rightarrow \pi^2$	Forbidden	(6.16)

The $T_1 \rightarrow S_0$ transitions of benzophenone and acetone ($k_{TS} \sim$ 10–100 sec^{-1}) are much faster than that for pyrenaldehyde ($k_{TS} \lesssim 1\ \text{sec}^{-1}$), which is in agreement with the above selection rules. It should be noted that the actual magnitude of spin-orbit

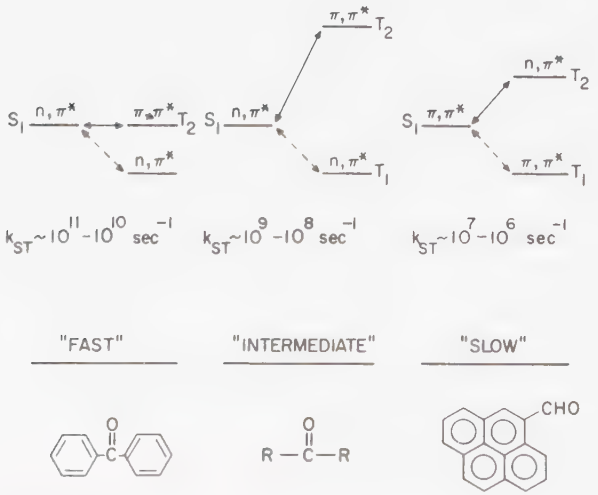

Figure 6.10

Examples of different rates of intersystem crossing for $S_1(n, \pi^*) \rightarrow T(\pi, \pi^*)$, $S_1(n, \pi^*) \rightarrow T(n, \pi^*)$, and $S_1(\pi, \pi^*) \rightarrow T(\pi, \pi^*)$, of carbonyl compounds.

coupling for the excited states of organic molecules is on the order of 0.3–0.001 kcal/mole, i.e., spin-orbit coupling is a very weak perturbation.[10]

For example of the effect of *vibrations* on spin orbit coupling,[15] consider a surface crossing between a π, π^* singlet and a π, π^* triplet state of ethylene or of benzene. In this case the strong electronic coupling inherent when two states of the same orbital configuration cross is suppressed because the crossing states possess different spin multiplicity. Spin-orbit coupling is required to cause surface avoiding. Since spin-orbit interactions are generally very weak for organic molecules which do not possess heavy atoms, the avoiding will be very weak.

It can be shown that in-plane vibrations generally do not cause significant mixing of singlet and triplet states of planar hydrocarbons, but out-of-plane vibrations are capable of mixing singlet and triplet states.[16] Figure 6.11 shows the surface situation for in-plane and out of plane vibrations. In executing planar vibrations the molecule may pass through a surface crossing geometry, but will not be able to "turn on" a spin-orbit interaction because the planar vibration is an ineffective promoter for coupling spin and orbital motion. If the molecule is brought into a crossing geometry by an out-of-plane vibration, a finite but very weak spin-orbit

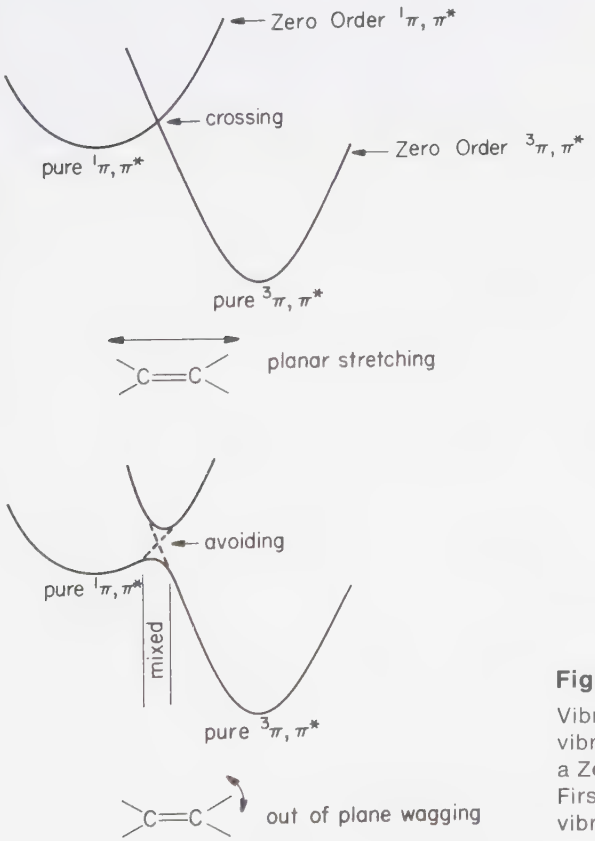

Figure 6.11

Vibronic interactions. Top: planar vibrations do not mix states, so that a Zero Order crossing persists in First Order. Bottom: out-of-plane vibrations cause an avoiding.

interaction occurs, the surfaces avoid, and a $^1\pi, \pi^* \rightarrow {}^3\pi, \pi^*$ conversion is possible ($k_{s_1} < 10^7$ sec $^{-1}$). In effect, the "door is open" at a crossing geometry only if the molecule is conducted to the crossing region by an appropriate vibration or nuclear motion.

6.5 The Relationship of Rates and Efficiencies of Radiationless Transitions to Molecular Structure

The photochemist needs a theory that reveals the relationship of the probability of radiationless transitions to molecular structure. From the discussions of Sections 6.2 and 6.3, it is clear that an important feature of such a relationship is the idea of "critical geometries," r_c, from which radiationless transitions are particularly favored. Thus, a theory relating radiationless processes to molecular structure must be able to relate critical geometries to molecular structure.[3] Surface crossings, surface touchings, and relatively deep excited state minima all correspond to critical geometries (Fig. 6.2). In Chapter 7 we shall consider how one may relate the occurrence of Zero Order surface crossings as a function of molecular structure. In this section we consider how "surface touchings" can be related to molecular structure. In Section 6.8 we shall see how radiationless transitions from excited state minima that correspond to "surface matchings" may be related to molecular structure.

The "Loose Bolt" and "Free Rotor" Effects: Promoter and Acceptor Vibrations

It is possible for certain vibrations to act as *promoters* of radiationless transitions if specific vibrations "carry" the representative point to r_c. However, since energy must be conserved in detail after a radiationless transition, some vibrations (or collisions) must act as acceptors of the energy difference between the electronic states involved in the transition. *If a vibration is at once a promotor and an acceptor it should be particularly effective in triggering radiationless transitions.*[17]

Consider two examples of a "touching" of surfaces induced by stretching a single bond and by twisting a double bond respectively (Fig. 6.12). The stretching or twisting vibration may escort the representative point on ψ^* to r_c. If this vibration also mixes ψ^* and ψ^0, a radiationless transition to ψ^0 can then occur. The stretching vibration is analogous to a "loose bolt" in some moving part of a machine. The "loose bolt" tends to be set in motion by other moving parts of the machine[17a] and thereby "takes up" kinetic energy produced by other moving parts of the machine. In the case of the twisting motion of a double bond (Fig. 6.12b) an analogy to a "free rotor" seems more apt.

Examples of the free rotor effect on radiationless transitions such as internal conversion are available from fluorescence analysis of conjugated aromatic compounds. For example, at 25 C trans-stilbene (**1**) is weakly fluorescent and cis-

stilbene (**2**) is nonfluorescent.[18] On the other hand, the structurally constrained derivatives **3** and **4** are strongly fluorescent.[19]

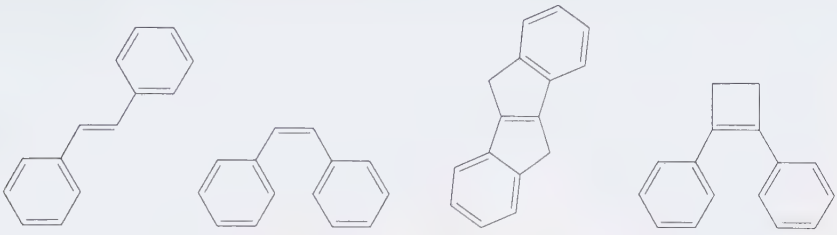

1, $\Phi_F = 0.05$ **2**, $\Phi_F = 0.00$ **3**, $\Phi_F \cong 1.0$ **4**, $\Phi_F \cong 1.0$

Presumably, steric interactions between the phenyl groups of cis-stilbene provide the molecule with an inherent torque and tendency to twist about the central C—C bond. In S_1 the state energy is rapidly lowered by twisting (See Fig. 6.12b. For a more rigorous discussion, see Section 7.7.) The twisting motion brings S_1 to a geometry which is favorable for radiationless conversion to S_0. Although **1** can also twist about the C=C bond in S_1, the lack of a torque due to steric interactions makes the twisting motion *slower* than it is for **2**. Fluorescence now competes with internal conversion.

For compounds **3** and **4** the twisting motion about the C=C bond is severely hindered by structural constraints. As a result, these molecules are unable to adopt nuclear geometries that differ substantially from the initial geometry of S_0. The representative point on the S_1 surface cannot move to regions on the S_1 surface that correspond to nuclear geometries favorable for radiationless conversions. As a result, fluorescence dominates. In addition to structural constraints, low temperature and rigid environment can inhibit twisting motions that promote radiationless conversions. If small energy barriers (~ 3–5 kcal/mole) separate the representative point from the lower energy twisted geometries, at low temperatures (~ 77 K) these barriers may not be surmounted during the excited state lifetime and efficient

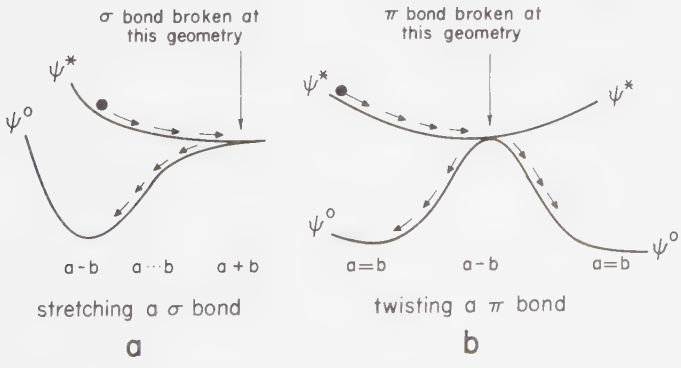

Figure 6.12

Schematic representation of (a) the stretching of a σ bond and (b) the bending of a π bond.

emission results. A rigid environment may be viewed as perturbing the potential energy surface corresponding to rotation by introducing an energy barrier to twisting.[20] These environment (e.g., solvent) imposed barriers are due to the requirement that molecules in the neighborhood of the twisting C—C bond must be displaced if the twisting is to be substantial.

The free rotor effect may also operate to facilitate radiationless transitions of triplets (intersystem crossing). As an illustration,[21] the triplet state of 1-phenylcycloheptene (**5**) undergoes a very rapid intersystem crossing at room temperature relative to 1-phenylcyclobutene (**6**). This result may be interpreted to be due to a surface touching (Fig. 6.12b; see Section 7.7 for discussion) which results from twisting about the C=C bond. Since **5** is much more flexible than **6** with respect to this motion, in T_1 it may move toward the twisted geometry at a faster rate:

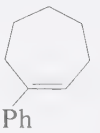

5, $k_{TS} \cong 4 \times 10^9\ \text{sec}^{-1}$

6, $k_{TS} \cong 6 \times 10^7\ \text{sec}^{-1}$

An example of a "loose bolt" effect[17a] on internal conversion is available from data on the radiationless decay of alkyl benzenes.[22] The fluorescence yield of toluene (**7**) is ~ 0.14, whereas the fluorescence yield of tert-butyl benzene (**8**) is ~ 0.032.

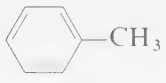

7

$k_{IC} \sim 10^7\ \text{sec}^{-1}$

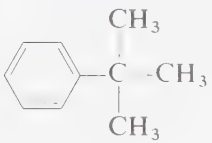

8

$k_{IC} \sim 10^8\ \text{sec}^{-1}$

It was shown that the mechanism for decrease in Φ_f was neither intersystem crossing nor permanent photoreaction. It appears that the σ-bonds of the tert-butyl group serves as a "loose bolt" to accelerate internal conversion by a factor of ~ 10 (possibly via a mechanism related to Fig. 6.12a).

The observation that **7** is much more strongly phosphorescent ($\Phi_p^{REL} = 1.0$) than **8** ($\Phi_p^{REL} = 0.00$) at 77 K is probably a manifestation of the "loose bolt" effect on $T_1 \rightarrow S_0$ intersystem crossing.[23]

Radiationless Transitions between "Matching" Surfaces

In Figure 6.2d, a "matching" of surfaces is shown. Suppose two surfaces are not related by a Zero Order surface crossing at r_c. Can a radiationless transition at r_c still occur? A positive answer may be given, but with the qualification that such radiationless transitions are expected to be much slower than those at critical geometries corresponding to situations (a), (b), (c), and (e) in Figure 6.2.

From theory,[24] the rate of such transitions will be related to the *Franck-Condon factor* $f_v = \langle \chi_i | \chi_f \rangle^2$. The value of f_v in general follows an energy gap law

$$f_v = \alpha \exp - \Delta E \tag{6.17}$$

i.e., the rate of a radiationless transition from r_e (for a "matching") will fall exponentially as ΔE increases, if f_e and f_s are not rate-determining.

As an example of how the Franck-Condon factor operates to control the rate of spin-allowed processes corresponding to Figure 6.2d, consider internal conversion ($f_s = 1$). Suppose that two excited states S_2 and S_1 possess potential curves which undergo a Zero Order intersection at point F, but that the ground–state-potential curve is "matching" with (i.e., does not intersect) S_1 and S_2 (Fig. 6.13). A transition from S_2 to S_1 can occur without an appreciable alteration of position

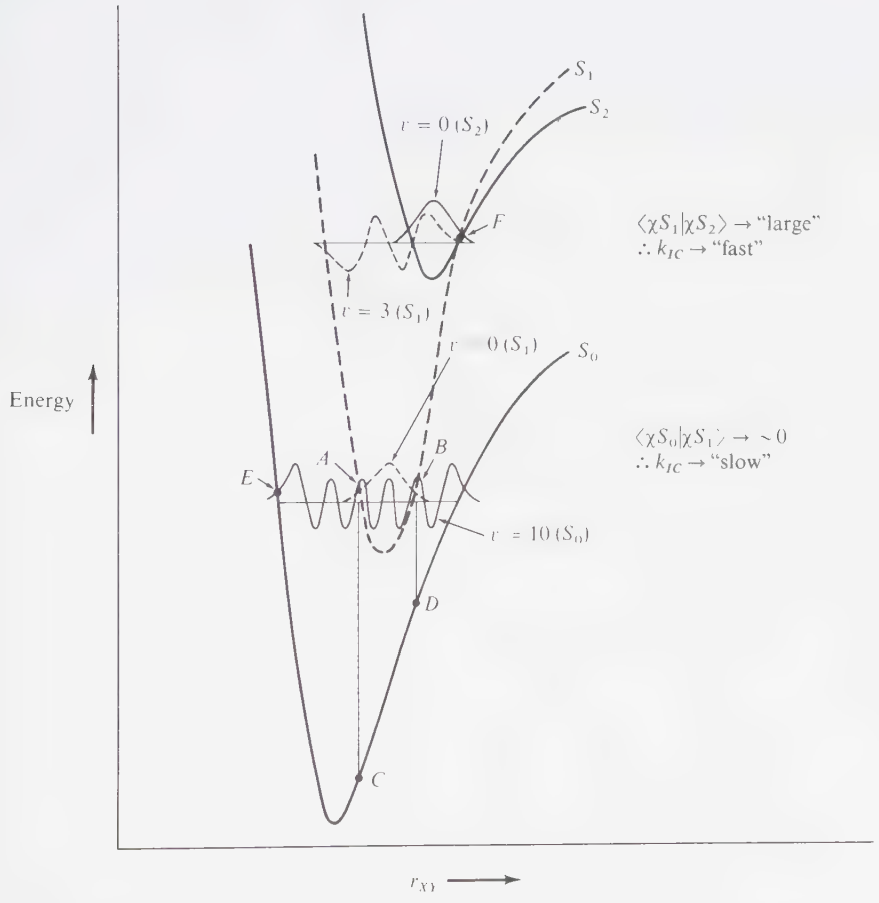

Figure 6.13
Representation of internal conversion between S_2 and S_1 and between S_1 and S_0.

or momentum of the nuclei if the transition occurs at geometries near F. Such an internal conversion is expected to occur rapidly. The direct radiationless transition $S_2 \rightarrow S_0$, however, is highly improbable.

Now consider what happens when the molecule reaches the lowest vibrational levels of S_1. From Figure 6.13 it can be seen that if the vibrational eigenfunctions for χS_0 (a high-energy vibrational level of S_0) oscillates from negative to positive values rapidly in the region where χS_1 (assumed to be in the $v = 0$ state) is always positive, then the integral $\chi S_1 \chi S_0 \, dr_1$ will always be very small making the $S_1 \rightarrow S_0$ probability very low. This contrasts with the situation in the region of interaction about point F, χS_1, and since χS_2 (assumed to be in the $v = 0$ state) are situated so $\chi S_2 \chi S_1 \, dr_1$ has a considerable value. (The reader is referred to Sections 4.8, 4.12, and 4.13 for a review.) The $S_2 \rightsquigarrow S_1$ transition is therefore more probable than the $S_1 \rightarrow S_0$ transition, if the electronic part of the molecular wave functions for the two transitions are comparable.

It has long been known that many organic compounds which possess rigid cyclic structures and or long conjugated systems of π electrons tend to fluoresce strongly (e.g., structures **3** and **4** discussed above). We may now theoretically rationalize this result from the standpoint of the Franck-Condon principle for radiationless transitions. The Franck-Condon principle tells us that for rigid structures the conversions $S_1 \rightsquigarrow S_0$ and $T_1 \rightsquigarrow S_0$ will be difficult, because the restraints placed on the molecule tend to hold the nuclei together. In effect, the S_1 states of such systems possess no "loose bolts," "free rotors," or intersystem crossing mechanisms. Thus, they fluoresce with high efficiency (e.g., **3** and **4**). If a long conjugated system tends to have intense transitions to S_1, it will also tend to have a *short* fluorescence lifetime. All other factors being equal, rigidity in general will inhibit radiationless processes relative to radiative processes.

6.6 Factors that Influence the Rate of Vibrational Relaxation

The advent of picosecond laser spectroscopy has allowed the direct measurement of vibrational relaxation processes in fluid solutions. For organic molecules[25] values of k_{vib} (rate constant for vibrational relaxation) are typically $\sim 10^{12}$ sec^{-1}. Why is the transfer of excess vibrational energy to the environment so rapid? The answer is that the environment, since it may take up the energy of nuclear motion of a molecule and convert it into many different degrees of vibrational motion, behaves like a classical heat bath. Because the number of energy levels of the environment is for all intents and purposes continuous, any amount of vibrational energy may be taken up by the environment.[26]

Is the transfer of electronic energy into excess vibrational energy always relatively slow? The answer to this is that the rate of electronic vibrational energy may be rapid only *if* it can occur via a surface crossing near the zero vibrational level of the initial state or via a photoreaction.

This situation is shown in Figure 6.14. In the excited state, the electron motion and position are responsible for the excess energy of the molecule. The vibrations

are not excited and the local solvent molecules are "cool," i.e., their translational and vibrational motion is average in relation to the macroscopic temperature. Imagine that the *e*lectronic motion and position change ($e \rightarrow e$) and the C—O vibration is excited. This corresponds to an *e*lectronic-*v*ibrational ($e \rightarrow v$) radiationless transition (e.g., $S_1 \rightarrow S_0$, $T_1 \rightarrow S_0$). Where does the energy go after the isoenergetic electronic transition has occurred? We imagine it to be dissipated as follows (Fig. 6.14): The vibrationally excited nuclei collide with the solvent and take on translational energy. The vibrations "cool down" and the local microscopic temperature "heats up," i.e., the solvent molecules in the immediate vicinity of the formerly excited molecule have a higher *t*ranslational and *v*ibrational energy ($v \rightarrow t$) than the average for the macroscopic temperature.

It appears that in fluid solution or in rigid matrices, the take-up of energy by the solvent is rarely if ever rate-determining for a radiationless transition.[26] One might ask at this point if emission of infra-red radiation is a significant path for transitions between the rotational and vibrational levels. Experimentally, infrared emission (loss of a few quanta at a time) does not compete with radiationless deactivation, but ultraviolet and visible emission do. This result follows theoretically from the relationship:[27]

$$k = \frac{64\pi^4}{3h} \bar{\nu}^3 |H_{21}|^2 \propto \langle H_{21} \rangle^2 \tag{6.18}$$

where $\bar{\nu}$ is the wave number of the photon which is emitted upon passing from state 2 to state 1, H_{21} is the electric dipole matrix element for the transition, (Section 5.3), and k is the rate constant for spontaneous emission.

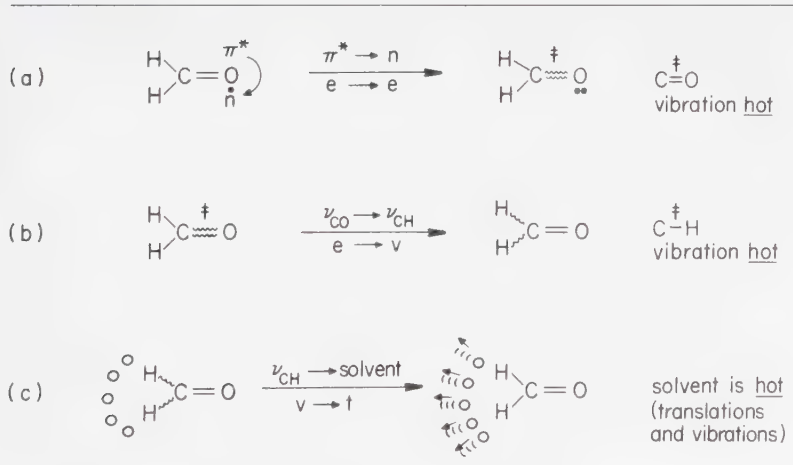

Figure 6.14

Schematic description of energy dissipation for formaldehyde. (a) the conversion of electronic excitation into vibration for formaldehyde, initially localized as excitation (wiggly lines) between the C and O atoms, followed by (b) vibrational energy transfer to the CH bonds, and (c) transfer to translational motion of the solvent.

Since $\bar{\nu}$ is usually 1,000 to 3,000 cm^{-1} for infrared transitions, while $\bar{\nu} \sim 30{,}000$ cm^{-1} for ultraviolet transitions, the $\bar{\nu}^3$ term places a prohibition factor of about 10^{-3} or greater on the relative rate of infrared emission as compared to ultraviolet-visible emission. Furthermore, the dipole-moment changes involved in pure vibrational transitions are usually small compared to those which occur upon passing from one electronic state to another. This factor may apply another order of magnitude prohibition on the rate of infrared emission.

In any case, the inherent rate constants for infrared emission are typically of the order of 10^2 sec^{-1} or *smaller*. For example,[28] an *infrared* emission of CO_2 occurs at ~ 1000 cm^{-1} and possesses a transition dipole of ~ 0.1 Debyes. This results in a k value of $\sim 10^2$ sec^{-1}. Since the rates of vibrational deactivation of molecules in solution[25] are of the order of 10^{12} sec^{-1}, we see that vibrational fluorescence will generally be a minor pathway for vibrational deactivation in condensed phases.

6.7 The Evaluation of Rate Constants for Radiationless Processes from Quantitative Emission Parameters

In general, a combination of experimental emission lifetimes τ_e and emission quantum yields Φ_e provides a convenient means of measuring the unimolecular rate constants of internal conversion and intersystem crossing. Knowledge of the rates of interconversions and lifetimes of excited states is of great importance in analyzing photochemical problems. The following scheme will help us estimate these rates from spectral data alone. In the absence of irreversible photochemical reaction and specific bimolecular quenching the following reaction steps describe the important paths of deactivation of a molecule which is excited to its lowest singlet S_1.

	Step	Rate	
$h\nu + S_0 \rightarrow S_1$	Excitation	I	(6.19)
$S_1 \rightsquigarrow S_0 + \text{heat}$	Internal conversion	$k_{IC}[S_1]$	(6.20)
$S_1 \rightsquigarrow T_1 + \text{heat}$	Intersystem crossing	$k_{ST}[S_1]$	(6.21)
$T_1 \rightsquigarrow S_0 + \text{heat}$	Intersystem crossing	$k_{TS}[T_1]$	(6.22)
$T_1 \rightarrow S_0 + h\nu$	Phosphorescence	$k_P^0[T_1]$	(6.23)
$S_1 \rightarrow S_0 + h\nu$	Fluorescence	$k_F^0[S_1]$	(6.24)

The steady-state approximation in excited singlet states leads to

$$I = (k_{ST} + k_F^0 + k_{IC})[S_1] \tag{6.25}$$

where I is the rate of absorption of light in einsteins/liter sec, and $[S_1]$ is the concentration of excited singlets. Similarly, for triplets we have

$$k_{ST}[S_1] = (k_{TS} + k_P^0)[T_1] \tag{6.26}$$

or

$$[T_1] = \frac{k_{ST}[S_1]}{(k_P^0 + k_{TS})} \tag{6.27}$$

Under the conditions of steady-state excitation, the efficiency of a process from S_1 or T_1 is simply the ratio of the rates of the process of interest to the total deactivation rate of the state.

From the conventional state-energy diagram we note that in general:

$$\Phi_F = k_F^0/(k_F^0 + k_{ST} + k_{IC}) \tag{6.28}$$

$$\Phi_{IC} = k_{IC}/(k_F^0 + k_{ST} + k_{IC}) \tag{6.29}$$

$$\Phi_{ST} = k_{ST}/(k_F^0 + k_{ST} + k_{IC}) \tag{6.30}$$

$$\Phi_P = \Phi_{ST} \times k_P^0/(k_P^0 + k_{TS}) \tag{6.31}$$

$$\Phi_{TS} = \Phi_{ST} \times k_{TS}/(k_P^0 + k_{TS}) \tag{6.32}$$

In other words, the fluorescence efficiency is equal to the ratio of the rate of fluorescence to the total rate of deactivation of the S_1 state. Similarly, the efficiency of intersystem crossing from S_1 to T_1 is equal to the ratio of the rate of intersystem crossing to the total rate of deactivation of S_1. The phosphorescence efficiency depends directly not only on the ratio of the rate of phosphorescence to the total deactivation rate of T_1, but also depends directly on Φ_{ST}, the probability that T_1 is formed from S_1.

The singlet lifetime τ_S is equal to the inverse of the sum of all rates that deactivate S_1 and the triplet lifetime τ_T is equal to the inverse of the sum of all rates that deactivate T_1, i.e.,

$$\tau_S = 1/(k_F^0 + k_{ST} + k_{IC}) \qquad \text{experimental } S_1 \text{ lifetime} \tag{6.33}$$

$$\tau_T = 1/(k_P^0 + k_{TS}) \qquad \text{experimental } T_1 \text{ lifetime} \tag{6.34}$$

Thus with the definition of the radiative lifetimes $\tau_F^0 \equiv (k_F^0)^{-1}$ and $\tau_P^0 \equiv (k_P^0)^{-1}$ the expressions for quantum yields may be written as:

$$\Phi_F = k_F^0 \tau_S \tag{6.35}$$

$$\Phi_{IC} = k_{IC} \tau_S \tag{6.36}$$

$$\Phi_{ST} = k_{ST} \tau_S \tag{6.37}$$

$$\Phi_P = \Phi_{ST} k_P^0 \tau_T \tag{6.38}$$

$$\Phi_{TS} = \Phi_{ST} k_{TS} \tau_T \tag{6.39}$$

Experimentally, values of τ_S and τ_T may be evaluated directly by measurement of the decay of S_1 and T_1 as a function of time. In the case of S_1, the most convenient method to monitor $[S_1]$ is usually by measuring the fluorescence intensity emitted from S_1. Thus, τ_S is generally the same as the *measured* fluorescence lifetime, τ_F (not the radiative lifetime, τ_F^0). Similarly, measurement of the phosphorescence lifetime, τ_P, provides a direct measure of τ_T. In the case of triplet states, T_1 may be measured also by flash absorption spectroscopy or (in the solid state) by electron spin resonance.

Measurement of Φ_F, Φ_P, Φ_{ST}, τ_S, and τ_T allow evaluation of the rate constants k_F^0, k_P^0, k_{IC}, k , and k_{TS}. The measurement of Φ_{ST} sometimes requires special methods.[29] For certain systems such as rigid aromatic hydrocarbons internal conversion from S_1 can be neglected $\Phi \cong 1 - \Phi_F$, i.e., every singlet which does not fluoresce is assumed to undergo intersystem crossing. The validity of this assumption depends on the absence of photoreactions surface crossings or other quenching processes of S_1.

As an example[30] of the calculation of radiationless rate constants, consider the state diagram for 1-chloronaphthalene (Fig. 6.15). At 77 K this molecule shows a weak ($\Phi_F = 0.06$) fluorescence but a strong ($\Phi_P = 0.54$) phosphorescence. The measured fluorescence and phosphorescence lifetimes are $\sim 10 \times 10^{-9}$ and 0.3 sec respectively.[30] Notice that 40% of the absorbed photons are not accounted for by emission ($\Phi_F + \Phi_P = 0.60$). We shall see in Section 6.9 that internal conversion ($S_1 \rightsquigarrow S_0$) is not likely to compete with intersystem crossing ($S_1 \rightsquigarrow T_1$) for naphthalene. As a result, $\Phi_{ST} \cong 1 - 0.06 = 0.94$. Since $\Phi_{ST} = 0.94$ but Φ_P is only 0.54 we deduce that $\Phi_{TS} = \Phi_{ST} - \Phi_P = 0.40$.

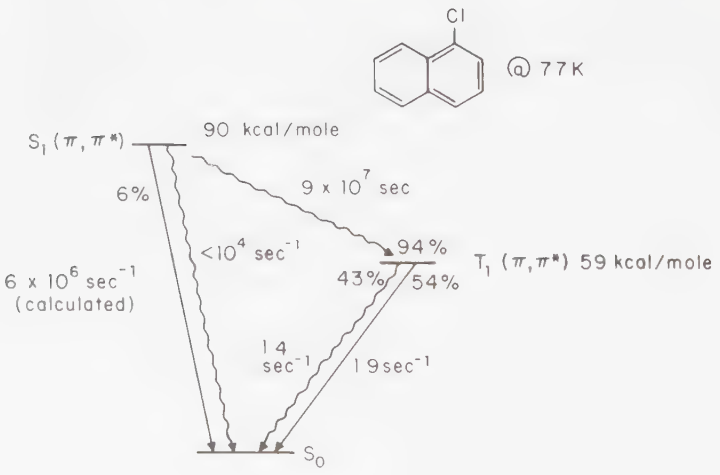

Figure 6.15

Energy diagram for 1-chloronaphthalene at 77 K, at 25 C° $k_t \sim 10^4$ sec^{-1}.

From these data and use of Eqs. 6.37 and 6.39 we find:

$$k_{ST} = \Phi_{ST}/\tau_S = 0.94/10^{-8} = 9.4 \times 10^7 \text{ sec}^{-1} \tag{6.40}$$

and,

$$k_{TS} = \Phi_{TS}/\Phi_{ST}\tau_T = 0.40/(0.94)(0.3) = 1.4 \text{ sec}^{-1} \tag{6.41}$$

If k_{IC} is at least ten times smaller than the major rate determining deactivation pathway of S_1 (i.e., k_{ST}) we may estimate an upper limit to k_{IC} as:

$$k_{IC} < 0.1k_{ST} \quad \text{or} \quad k_{IC} < 0.1k_F \tag{6.42}$$

The *inherent* or radiative rate constants for emission k_F^0 and k_P^0 may be calculated from Eqs. 6.35 and 6.38, i.e.,

$$k_F^0 = \Phi_F/\tau_S = 0.06/10^{-8} = 6 \times 10^6 \text{ sec}^{-1} \tag{6.43}$$

$$k_P^0 = \Phi_P/\Phi_{ST}\tau_P = 0.54/(0.94)(0.3) = 1.9 \text{ sec}^{-1} \tag{6.44}$$

As a second example, consider benzophenone (Fig. 6.16). This molecule is essentially nonfluorescent ($\Phi_F < 10^{-4}$) and possesses a very short singlet lifetime ($\tau_S \sim 10^{-11}$ sec). At 77 K, benzophenone[31] shows a strong phosphorescence

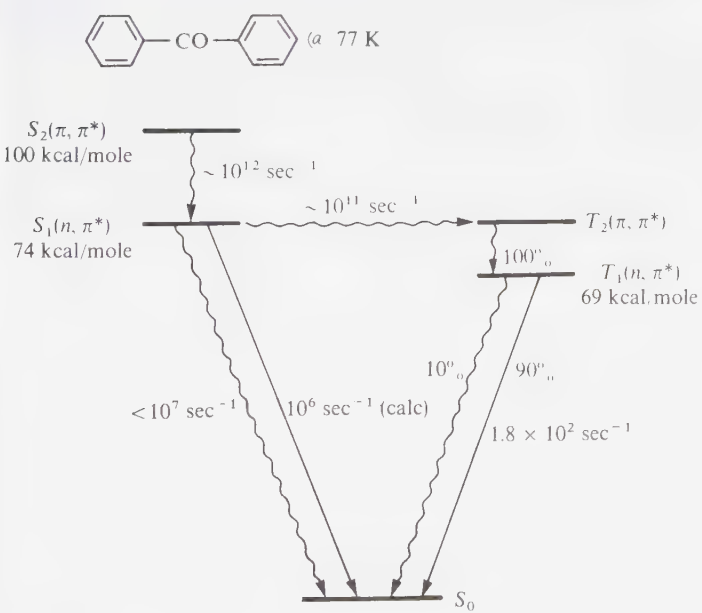

Figure 6.16
State diagram for benzophenone at 77 K.

($\Phi_P = 0.90$) with a lifetime of 6×10^{-3} sec. Since 90% of the photons absorbed by benzophenone are accounted for by phosphorescence, a maximum of 10% of the S_1 molecules can be undergoing $S_1 \rightarrow S_0$ internal conversion. In fact, it appears that *nearly every molecule* in S_1 undergoes intersystem crossing to T_1. In other words,

$$k_{ST} = \Phi_{ST}/\tau_S = 10^{11} \text{ sec}^{-1} \tag{6.45}$$

This remarkably fast intersystem crossing rate is typical of certain carbonyl compounds possessing $S_1(n, \pi^*)$ states with a close lying $T(\pi, \pi^*)$ state.

The value of k_{TS} and k_P for benzophenone are given by:

$$k_{TS} = \Phi_{TS}/\Phi_{ST}\tau_T = 1.7 \times 10 \text{ sec}^{-1} \tag{6.46}$$

$$k_P = \Phi_P/\Phi_{ST}\tau_T = 1.5 \times 10^2 \text{ sec}^{-1} \tag{6.47}$$

If Φ_f is too weak to measure accurately, k_f may be determined indirectly, i.e., by application of the equation relating ε_{max} to τ_f (Eq. 5.23). The value of $\tau_f = 10^{-6}$ sec is obtained in this manner.

Empirically, the unimolecular rate constant for a radiationless transition k_{OB} may be considered to be composed of temperature-independent and temperature-dependent components, i.e.

$$k_{OB} = k_{OB}^0(T \text{ independent}) + k_{OB}(T \text{ dependent}) \tag{6.48}$$

The temperature-independent part of k_{OB} may be viewed as due to radiationless transitions that occur during the zero point motion of the molecule. Such transitions occur even at temperatures approaching 0 K! The temperature dependent part of k_{OB} may be viewed as due to radiationless transitions that require an activation energy. Such transitions usually obey an Arrhenius relationship (See Section 6.9 for examples).

6.8 Internal Conversion ($S_n \rightarrow S_1$, $S_1 \rightarrow S_0$)

The three most important classes of internal conversion commonly encountered for organic molecules are:

1. Radiationless transition from an upper *excited* singlet state to the lowest excited singlet state, $S_n \rightarrow S_1$ (rate constant $\equiv k_{IC}^{SS}$);

2. Radiationless transition from an upper excited triplet state to the lowest lying triplet state, $T_n \rightarrow T_1$ (rate constant $\equiv k_{IC}^{TT}$);

3. Radiationless transitions from the lowest energy singlet state to the ground singlet state, $S_1 \rightarrow S_0$ (rate constant $\equiv k_{IC}$).

The Relationship of Internal Conversion to Molecular Structure

Let us consider some experimental information concerning internal conversion in aromatic hydrocarbons. We begin with data taken at 77 K in a rigid glass matrix. Under these conditions photoreactions may generally be avoided and fluorescence and phosphorescence are readily observed. Table 6.2 summarizes some pertinent data. The following generalizations have been noted for rigid aromatic hydrocarbons and serve as a basis for discussion:[32]

1. Fluorescence occurs from S_1 to S_0; phosphorescence occurs from T_1 to S_0; S_n and T_n emissions are rare (Kasha's rule).

2. The quantum yield of fluorescence and the quantum yield of phosphorescence are independent of initial excitation energy (Vavilov's rule).

3. The sum of $\Phi_F + \Phi_{ST} \cong 1$ (Ermolev's rule).

These data are consistent with very rapid internal conversion from $S_n \rightarrow S_1$ and $T_n \rightarrow T_1$, and with a much slower internal conversion from $S_1 \rightarrow S_0$ that cannot compete with fluorescence and intersystem crossing. Let us now see how such a conclusion may be deduced from experimental data. The lack of measurable fluorescence from $S_n (n > 1)$ means that emission yields from these states are less

Table 6.2 Quantum Yields for Fluorescence and Intersystem Crossing of Organic Molecules[a]

Molecule (Configuration of S_1)	Φ_F	Φ_{ST}	$1 - (\Phi_F + \Phi_{ST})$[b]	E_{S_1}[c]
Benzene (π, π^*)	0.05	0.25	0.70	110
1,4-Dimethylbenzene (π, π^*)[d]	0.35	0.65	<0.05	100
Naphthalene (π, π^*)	0.20	0.80	<0.05	92
Anthracene (π, π^*)	0.70	0.30	<0.05	76
Tetracene (π, π^*)	0.15	0.65	0.20	60
Pentacene (π, π^*)	0.10	0.15	0.75	50
Azulene (π, π^*)	0.000	—	Low	50
Acetone (n, π^*)	0.001	~ 1.0	0.05	85
Biacetyl (n, π^*)	0.002	~ 1.0	0.05	65
Benzophenone (n, π^*)	0.000	~ 1.0	0.05	75
5-Methyl-2-heptanone (n, π^*)[e]	0.000	0.10	0.90	85
Cyclobutanone (n, π^*)[f]	0.000	0.00	1.0	80
1,3-Pentadiene (n, π^*)[g]	0.000	0.00	1.0	100

[a] Except where noted, data for molecules in fluid solution at room temperature from Wilkinson, F., *Organic Molecular Photophysics*, ed. Birks, J. B., New York: Wiley, 1975, p. 95.

[b] A lower limit of 5% is placed on the experimental uncertainty of measurements of Φ. This quantity sets an upper limit to Φ_{IC}.

[c] Singlet energy (0,0 energy) in kcal mole.

[d] Carroll, F. A., and Quinta, F. H., *J. Am. Chem. Soc.*, *98*, 1 (1976).

[e] Yang, N. C., and Elliott, S. P., *J. Am. Chem. Soc.*, *91*, 7550 (1969). Reaction ($\Phi \sim 0.05$) occurs in S_1. See Chapters 8 and 10.

[f] Morton, D. R., and Turro, N. J., *Adv. Photochem.*, *9*, 197 (1074). A cleavage reaction occurs with an efficiency of ~ 0.3 from S_1.

[g] Srinivasan, R., *J. Am. Chem. Soc.*, *84*, 4141 (1962). In Chapters 11 and 12, it will be shown that $\Phi_{ST} \sim 0$ in general for simple ethylenes and polyenes. An isomerization reaction of efficiency ~ 0.1 occurs from S_1.

than 10^{-4}. From the value of the extinction coefficient $S_0 \rightarrow S_n$ we may estimate the radiative rate constant for $S_n \rightarrow S_0$. Knowledge of this rate and a limit on Φ_F allow us to calculate a limit for the radiationless rate $S_n \rightarrow S_1$.

Consider anthracene as an example. The $S_0 \rightarrow S_3$ absorption maximizes at 39,700 cm^{-1} (252 nm) with $\varepsilon_{max} \sim 2 \times 10^5$. From Eq. 5.23:

$$k_F^0 \sim 2 \times 10^9 \tag{6.49}$$

Since

$$\Phi_F^{S_2} = k_F^0/k_D < 10^{-4} \tag{6.50}$$

$$k_D > 10^4 k_F \sim 2 \times 10^{13}\ \text{sec}^{-1} \tag{6.51}$$

In other words, S_2 deactivates with a rate constant of the order of that for vibrational motion. Since *emission* from S_1 is observed when S_3 of anthracene is excited, we must conclude that $k_{IC}(S_3 \rightarrow S_1) \sim 10^{13}\ \text{sec}^{-1}$. It appears that for most organic molecules $k_{IC}(S_n \rightarrow S_1)$ falls in the range 10^{11}–$10^{13}\ \text{sec}^{-1}$. Evidently, electronic relaxation by internal conversion from upper levels is rate-limited by only nuclear motion. This in turn suggests that Zero Order crossings are common for $S_n (n > 1)$ states and that critical geometries may be readily achieved during vibrational motion of S_n in its $v = 0$ level.

Because many molecules fluoresce from S_1, the $S_1 \rightarrow S_0$ internal conversion must, at best, be competitive only with other modes of decay from S_1. In Table 6.2 we noted that $\Phi_F + \Phi_{ST} \sim 1$ for many aromatic hydrocarbons. As a result, the internal conversion $S_1 \rightarrow S_0$ cannot occur to more than a few percent (the experimental error of measuring Φ) for these compounds.

For example,[32] since the singlet decay of pyrene is $\sim 10^6\ \text{sec}^{-1}$ and since $\Phi_F + \Phi_{ST} \sim 1.00$, we must conclude that $k_{IC}(S_1 \rightarrow S_0) < 10^6\ \text{sec}^{-1}$. A factor of $\sim 10^6$ separates the typical rate of a $S_n \rightarrow S_1$ internal conversion from a typical $S_1 \rightarrow S_0$ internal conversion.

Relatively little data exists on the rates of $T_n \rightarrow T_1$ internal conversions. The reason for this lack of data may be technical rather than theoretical in nature. One would expect that $T_2 \rightarrow T_1$ *fluorescence* should occur with a *range* of efficiencies, as does $S_1 \rightarrow S_0$ fluorescence. However, $T_2 \rightarrow T_1$ energy gaps generally are on the order of 30 kcal mole or *smaller*. This means that $T_2 \rightarrow T_1$ fluorescence, even if it occurs efficiently, would appear at wavelengths greater than ~ 800 nm. Experimentally, however, equipment capable of measuring light at these wavelengths with high sensitivity is not available.

In favorable cases, however, $T_2 \rightarrow T_1$ fluorescence has been observed. For example,[33] 9,10-dibromoanthrocene displays a weak ($\Phi_f \sim 10^{-6}$) $T_2 \rightarrow T_1$ fluorescence. From the extinction coefficient for $T_1 \rightarrow T_2$ *absorption*, $k_t (T_2 \rightarrow T_1)$ can be derived and it is found that $k_t \sim 10^5\ \text{sec}^{-1}$. From the value of Φ_f and Eq. 6.27 we deduce that $k_{IC}(T_2 \rightarrow T_1) \sim 10^{11}\ \text{sec}^{-1}$, a very reasonable value considering the rather large energy gap between the interconverting states. Indirect evidence also supports a value of k_{IC} of $\sim 10^{11}\ \text{sec}^{-1}$ for 9,10-dibromoanthracene.[34]

The Energy Gap Law for Internal Conversion ($S_1 \rightarrow S_0$)

In the absence of a Zero Order surface crossing between S_1 and S_0 a $S_1 \rightarrow S_0$ internal conversion must occur via a "Franck-Condon forbidden" mechanism, i.e., the nuclei in one state must undergo a rather drastic change in position and momentum as a result of the transition, since the net overlap of vibrational wavefunctions in both states is small.[24,35] For such situations the $S_1 \rightarrow S_0$ internal conversion is often rate limited by the Franck-Condon factor, $\langle \chi | \chi \rangle^2 \equiv f_v$. If we take 10^{13} sec^{-1} as an order-of-magnitude estimate of the maximum rate of internal conversion, then from Eq. 6.5

$$k_{IC} \sim 10^{13} f_v \tag{6.52}$$

It is possible to calculate or estimate f_v from spectral data.[36] Both theoretical and experimental evidence demonstrate that f_v is a very sensitive function of the *energy gap*, ΔE, between the zero point vibrational levels of the states undergoing internal conversion.[35] From Eq. 6.17 and Eq. 6.52:

$$k_{IC} \sim 10^{13} \exp - \alpha \Delta E \tag{6.53}$$

where α is a proportionality constant. The energy gap law can be attributed to the changes in the Franck-Condon overlaps of the nuclear wavefunctions, which become increasingly unfavorable with increasing energy separation.

Experimentally, $S_1 \rightarrow S_0$ internal conversion is usually negligible relative to fluorescence or intersystem crossing for nonphotoreactive relatively rigid molecules if $\Delta E(S_1 \rightarrow S_0)$ is larger than ~ 50 kcal/mole. For example, at $\Delta E \sim 100$ kcal/mole, $f_v \sim 10^{-8}$, so that $k_{IC} \sim 10^5$ sec^{-1}. Even for $\Delta E \sim 50$–60 kcal/mole, $f_v \sim 10^{-5}$ so that $k_{IC} \sim 10^8$ sec^{-1}. Since the *slowest* rates of $S_1 \rightarrow S_0$ fluorescence are generally $> 10^5$ sec^{-1}, and since the slowest rates of $S_1 \rightarrow T_1$ intersystem crossing are generally $> 10^6$ sec^{-1}, we see that internal conversion is unlikely to compete favorably with fluorescence or intersystem crossing if $\Delta E(S_1 \rightarrow S_0)$ is > 50 kcal/mole. Thus we have a theoretical rationale for Ermolev's Rule that:[37]

$$\Phi_F + \Phi_{ST} = 1 \qquad \text{or more properly} \qquad 1 - (\Phi_F + \Phi_{ST}) \sim \Phi_{IC} \tag{6.54}$$

We anticipate a breakdown of Ermolev's rule (a) if S_1 and S_0 undergo a surface crossing at a nuclear geometry accessible to the molecule as it executes low-energy vibrations, (b) if S_1 undergoes a photochemical deactivation, and (c) when ΔE becomes less than ~ 50–60 kcal/mole.

For example, tetracene and pentacene (Table 6.2) possess relatively low singlet energies (~ 60 and ~ 50 kcal/mole, respectively) and undergo significant internal conversion from S_1 ($\Phi_{IC} = 0.20$ and 0.75, respectively). The large value of Φ_{IC} for benzene (0.80) is probably due to a reversible photoreaction or a surface crossing of the S_1 and S_0 surfaces. In the case of the last three entries of Table 6.2 (5-methyl-2-heptanone, cyclobutanone, and 1,3-pentadiene) reversible photochemical reaction from S_1 probably accounts for a significant fraction of Φ_{IC}.

The Deuterium Isotope Test for Internal Conversion

An "isotope test" for the origin of the energy gap law of Eq. 6.51 is available. The Franck-Condon factors are generally *greatest* for high frequency vibrations.[24,35] This is because the higher the energy of a vibration the fewer the number of quanta required to match an electronic gap with vibrational energy. The highest frequency vibrations in organic molecules (Table 6.1) often correspond to C-H stretching motions ($\sim 3000\ cm^{-1}$). We thus expect that electronic-vibrational energy transfer will be fastest for "leakage" through C-H vibrations. If C-H vibrations are replaced by lower energy C-D vibrations ($\sim 2200\ cm^{-1}$) the rate of electronic to vibrational energy transfer should be slowed down substantially. Thus, we predict that if $S_1 \rightarrow S_0$ occurs via an electronic-vibronic mechanism, the lifetime of $S_1(\tau_s)$ will be *increased* by the substitution of C-D for C-H, because k_{ic} will decrease (Eq. 6.33). Thus, we have an *isotope test* for internal conversion.

Experimentally, the replacement of C-H bonds by C-D bonds in aromatic hydrocarbons[38] generally *does not change the singlet state lifetime or the fluorescence yield.* For example,[3,3c] at 77 K both pyrene-h_{10} and pyrene-d_{10} possess a fluorescence yield of 0.90, and singlet lifetimes (τ_s) of 450 ns. Since $\tau_s = (k_r + k_{sT} + k_{ic})^{-1}$ and since $\tau_s(\text{pyrene-h}_{10}) = \tau_s(\text{pyrene-d}_{10})$, we may conclude $k_F + k_{sT} \gg k_{ic}$, because a large decrease in k_{ic} is expected upon going from the h_{10} to d_{10} compound. The important point to be made here is that since there is *no* significant deuterium isotope effect on τ_s or Φ_f, internal conversion ($S_1 \rightarrow S_0$) cannot contribute significantly to the decay of S_1. In Section 6.10 we shall see that a large deuterium effect does operate on $T_1 \rightarrow S_0$ intersystem crossing.

In contrast to the small influence of the substitution of D for H on τ_s and Φ_f for aromatic hydrocarbons, this substitution may cause a significant enhancement for ketones and aldehydes. The effect of deuteration on Φ_f is most dramatic for aldehydes, especially in the vapor phase.[39]

For example,[39] the fluorescence quantum yield of formaldehyde increases by a factor of ~ 20 upon going from $H_2C{=}O$ to $D_2C{=}O$.

$H_2C{=}O$	$D_2C{=}O$	Low pressure vapor phase
	Φ_f	~ 0.4
	τ_s	$\sim 0.08\ \mu s$

Evidently, the substitution of D for H greatly decreases the magnitude of k_{sT} or k_{ic}. It is not yet clear whether a spin-orbit or Franck-Condon inhibition is involved.

The effect of deuteration on acetone[40] is less striking (τ_s acetone-h_6 is 1.7 ns, acetone-d_6 is 2.3 ns) it is nonetheless significant. In this case it appears that intersystem crossing may be specifically slowed down by deuteration, possibly because of a decrease of f_v upon deuteration.

Examples of Unusually Slow $S_n \rightarrow S_1$ Internal Conversion

Azulene[41] and its derivatives provide a striking exception to the general rule that $S_2 \rightarrow S_1$ internal conversion completely dominates fluorescence (in condensed

phases). For azulene (**9**), Φ_F is ~ 0.03 (see Section 5.14). The rate of internal conversion ($S_2 \rightarrow S_1$) is exceptionally slow ($k_{IC} \sim 7 \times 10^8$ sec^{-1}) for **9**. This fact is consistent with the exceptionally large energy gap of ~ 40 kcal/mole between the 0,0 levels of S_2 and S_1 of azulene (Eq. 6.51), i.e., the $S_2 \rightarrow S_1$ internal conversion possesses a poor Franck-Condon factor (Eq. 6.50).

In the vapor phase at low pressures, such that collisions are rare, internal conversion may be exceptionally slow. For small molecules possessing few internal vibrations, the Franck-Condon factors may be very unfavorable. For example,[42] $\Phi_F \sim 1.0$ from S_2 of the thiophosgene (**10**) at low pressure. The internal conversion rate constant $k_{IC}(S_2 \rightarrow S_1)$ is calculated to be $< 10^7$ sec^{-1}.

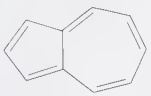

9 (azulene, solution)

$\Phi_F(S_2 \rightarrow S_0) \sim 0.03$

$k_{IC}(S_2 \rightarrow S_1) \sim 7 \times 10^8$ sec^{-1}

$Cl_2C{=}S$

10 (thiophosgene, vapor)

$\Phi_F(S_2 \rightarrow S_0) \sim 1.0$

$k_{IC}(S_2 \rightarrow S_1) < 10^7$ sec^{-1}

Azulene is also remarkable for its exceptionally rapid rate of $S_1 \rightarrow S_0$ internal conversion (Table 6.2). Direct measurements[43] indicate that $k_{IC}(S_1 \rightarrow S_0)$ is $\sim 10^{12}$ sec^{-1}. Such a large rate constant is consistent with a small value of E_{S_1} and/or a surface crossing of the S_1 and S_0 surfaces near the $v = 0$ level of S_1.

6.9 Intersystem Crossing from S_1 to T_1

Table 6.3 gives some examples of the "spread" of measured values of k_{ST}, the rate constant for intersystem crossing from S_1 to T_1. First it should be noted that the smallest values of k_{ST} ($\sim 10^6$ sec^{-1}) occur for aromatic hydrocarbons, and the largest values ($\sim 10^{10}$–10^{11} sec^{-1}) occur for molecules containing "heavy atoms", such as bromonaphthalene, or possessing $S_1(n, \pi^*)$ states such as benzophenone. However, it is clear that other factors in addition to the "heavy atom" or "n, π^*" effects must also influence the value of k_{ST}. These factors are:

1. The energy gap, ΔE_{ST}, between S_1 and the state to which intersystem crossing actually occurs (i.e., T_1 or some *upper* triplet, T_n),

2. The electronic configurations of the states undergoing intersystem crossing.

The $S_1 \rightarrow T_1$ transition may occur via (a) direct spin-orbit coupling of S_1 to the upper vibrational levels of T_1, or (b) via spin-orbit coupling of S_1 to an upper T_n state followed by rapid $T_n \rightarrow T_1$ internal conversion.

For case 1 we expect the measured value of k_{ST} to depend on the energy gap between S_1 and T_1, whereas for case 2 the energy gap between S_1 and T_1 should

not be significant. In addition to the singlet-triplet energy gap we expect that nuclear motion in the S_1 state is required to allow the molecule to explore different shapes as it searches for an effective spin-orbit coupling mechanism.

The Relationship of $S_1 \rightarrow T$ Intersystem Crossing to Molecular Structure

An important empirical observation (Table 6.3) is that nearly *all* measured values of k_{ST} for aromatic hydrocarbons fall in the range $\sim 10^8$–10^6 sec^{-1}. This range is comparable to that of fluorescence, i.e., k_F^0 from aromatic hydrocarbons, $\sim 10^6$–10^9 sec. As a result, most aromatic hydrocarbons exhibit a measurable amount of fluorescence, and undergo significant intersystem crossing if k_F^0 is not maximal.

To exemplify how these factors operate, let us compare the values of k_{ST} for the aromatic hydrocarbons anthracene[44] and pyrene.[45] In each case, an $S_1(\pi, \pi^*) \rightarrow T_n(\pi, \pi^*)$ process occurs. However, a variation factor of ~ 100 is noted in the rate of k_{ST}. The possibilities for this variation are: (a) differing degrees of electronic coupling between S_1 and the triplet state to which crossing occurs, (b) differing energy gaps between S_1 and the triplet state to which crossing occurs, and (c) differing degrees of spin-orbit coupling between S_1 and the triplet state to which crossing occurs. The variation may be qualitatively explained on the basis

Table 6.3 Representative Values of Intersystem Crossing Rates ($S_1 \rightarrow T_1$), Singlet-Triplet Energy Gaps.[a]

Molecule	k_{ST} (sec^{-1})[a]	ΔE_{ST} (kcal/mole)[a]	
Naphthalene	10^6	30	$S_1(\pi, \pi^*) \rightarrow T_1(\pi, \pi^*)$
Anthracene	10^8	2–3	$S_1(\pi, \pi^*) \rightarrow T_2(\pi, \pi^*)$
Pyrene	10^6	30	$S_1(\pi, \pi^*) \rightarrow T_1(\pi, \pi^*)$
Triphenylene	5×10^7	20	$S_1(\pi, \pi^*) \rightarrow T_1(\pi, \pi^*)$
1-Bromonaphthalene	10^9	30	$S_1(\pi, \pi^*) \rightarrow T_1(\pi, \pi^*)$
9-Acetoanthracene[b]	$\sim 10^{10}$	~ 5	$S_1(\pi, \pi^*) \rightarrow T_2(n, \pi^*)$
Perylene	$< 10^8$	~ 30	$S_1(\pi, \pi^*) \rightarrow T_1(\pi, \pi^*)$
3-Bromoperylene[c]	$< 10^8$	30	$S_1(\pi, \pi^*) \rightarrow T_1(\pi, \pi^*)$
Acetone[d]	5×10^8	5	$S_1(n, \pi^*) \rightarrow T_1(n, \pi^*)$
Benzophenone[e]	10^{11}	5	$S_1(n, \pi^*) \rightarrow T_2(\pi, \pi^*)$
Benzil	5×10^8	5	$S_1(n, \pi^*) \rightarrow T_1(n, \pi^*)$
Biacetyl	7×10^7	5	$S_1(n, \pi^*) \rightarrow T_1(n, \pi^*)$
9,10-Dibromoanthracene[f]	$\sim 10^8$	30	$S_1(\pi, \pi^*) \rightarrow T_1(\pi, \pi^*)$
		5	$S_1(\pi, \pi^*) \rightarrow T_2(\pi, \pi^*)$
[2.2.2]-diaza-bicyclooctane[g]	$\sim 10^6$	25	$S_1(n, \pi^*) \rightarrow T_1(n, \pi^*)$

[a] Unless specified, data from Birks, J. B., *Photophysics of Aromatic Molecules*, New York: Wiley, 1970; or Wilkinson, F., *Organic Molecular Photophysics*, vol. 2, ed. Birks, J. B., New York: Wiley, 1975, p. 95. The values ΔE_{ST} (kcal/mole) refer to the energy gaps between S_1 and the triplet to which intersystem crossing occurs.
[b] Reference 42.
[c] Reference 36b.
[d] Reference 32a.
[e] Reference 12b.
[f] Reference 37.
[g] Reference 40.

of (c) alone. In the case of pyrene[45] it appears that S_1 crosses *directly* to an excited vibrational level of T_1. The energy gap $\Delta E_{ST} \sim 30$ kcal/mole. In the case of anthracene and substituted anthracenes,[46] S_1 may cross to T_2, which is nearly isoenergetic[49] with S_1. Thus, in anthracene a small energy gap and consequently a favorable Franck-Condon factor exists for intersystem crossing.

According to theory,[47] mixing of π, σ^* and σ, π^* triplet states with $S_1(\pi, \pi^*)$ is required to imbue S_1 with "triplet character." This mixing must be vibronically induced so that mixing is relatively ineffective for molecules possessing a rigid structure in S_1.

With respect to n, π^* states, a similar situation appears to hold with respect to k_{ST} and the energy gap when $S_1(n, \pi^*) \rightarrow T_1(n, \pi^*)$ transitions are involved. Thus, both acetone ($k_{ST} = 5 \times 10^8$ sec^{-1})[48] and biacetyl ($k_{ST} = 1 \times 10^8$ sec^{-1})[49] involve "forbidden" spin-orbit mechanisms but enjoy a small (~ 6 kcal/mole) ΔE_{ST} and (presumably) a favorable Franck-Condon factor. The net result is typically that $k_{ST} \gg k_F$ and as a result $\Phi_{ST} \sim 1$ for compounds possessing $S_1(n, \pi^*)$ states (Table 6.3). However, cyclic azoalkanes[50] which possess a large energy gap between S_1 and T_1 ($\Delta E_{ST} \sim 25$ kcal/mole) encounter a poorer Franck Condon factor and k_{ST} is thereby considerably slower. As a result, some cyclic azoalkanes exhibit a very high Φ_F because of a very small value of k_{ST}.

The largest values of k_{ST} for organic molecules not possessing "heavy atoms" are found for systems undergoing $n, \pi^* \rightarrow \pi, \pi^*$ transitions with small energy gaps, e.g., benzophenone[13,51] ($k_{ST} = 10^{11}$ sec^{-1}, $^1n, \pi^* \rightarrow {}^3\pi, \pi^*$) and 9-benzoyl anthracene[52] ($k_{ST} = 10^{10}$ sec^{-1}, $^1\pi, \pi^* \rightarrow {}^3n, \pi^*$).

The magnitudes of k_{ST} for alkyl ketones is sensitive to molecular structure. For acetone[48] $k_{ST} \sim 5 \times 10^8$ sec^{-1}, whereas for di-tert-butyl ketone[53] $k_{ST} \sim 10^8$ sec^{-1} and for perfluoracetone[48] $k_{ST} \sim 10^7$ sec^{-1}. This variation suggests a decreasing amount of spin-orbit coupling or decreasing Franck-Condon factor as one proceeds from acetone to tert-butyl ketone to perfluoroacetone. The observation of a deuterium isotope effect[40] on k_{ST} and the rather large influence of substitution of fluorine are consistent with reduced Franck-Condon factors. The effect of "heavy atoms" on $S_1 \rightarrow T$ intersystem crossing is discussed in Section 6.11.

Temperature Dependence of $S_1 \rightarrow T$ Intersystem Crossing

The fluorescence yield Φ_f and singlet lifetimes τ_s of organic molecules are sometimes found to vary with temperature. Since k_r^0 is generally temperature independent,[32] some radiationless process from S_1 is temperature dependent. Indeed, photoreactions from S_1 commonly have small energy barriers and therefore will possess temperature dependent rate constants. Intersystem crossing ($S_1 \rightarrow T$) or internal conversion ($S_1 \rightarrow S_0$) may be temperature dependent if upper vibrational levels of S_1 possess a different mechanism for radiationless transition than the $v = 0$ level.

For example, the rate constant for intersystem crossing can be expressed as

$$k_{ST}^{OB} = k_{ST}^0 + A \exp - E/RT \tag{6.55}$$

Experimentally, k_{ST}^{OB}, the observed rate constant, is sometimes found to be essentially temperature independent *below* a certain temperature and to follow Eq. 6.55 above that temperature. A common mechanism for this temperature dependence is thermally activated $S_1 \rightarrow T_n (n \neq 1)$ intersystem crossing.

The rate of intersystem crossing in certain anthracene derivatives is temperature dependent.[46] This observation has been explained in terms of a temperature dependent rate of intersystem crossing from S_1 to T_2. For example, the value of k_{ST} for 9,10-dibromoanthracene may be expressed as $k_{ST} \sim 10^{12} \exp - E_a/RT$ where $E_a \sim 4.5$ kcal mole. A large energy gap between S_1 and T_1 serves to slow down the direct $S_1 \rightarrow T_1$ intersystem crossing because of an unfavorable Franck-Condon factor. That T_2 is populated, rather than an upper vibration level of T_1, is supported by triplet-triplet absorption measurements, which demonstrate that T_2 lies about 4–5 kcal mole above S_1. Since the value of E_a is ~ 4.5 kcal mole, it is logical to suppose that an activated $S_1 \rightarrow T_2$ process is involved in the temperature dependent intersystem crossing of 9,10-dibromoanthracene.

It is interesting to note that Φ_f and τ_s are usually *not* very temperature dependent below ~ 100 K. For example,[54] Φ_f of naphthalene is ~ 0.3 at 77 K and at 4 K. This implies that $k_{ST}(S_1 \rightarrow T)$ is temperature independent in the range 4 K to 77 K. This result suggests, that the energy term in Eq. 6.55 becomes small relative to k_{ST}^0 at temperatures below 100 K.

Intersystem Crossing to Individual Triplet Sublevels ($S_1 \rightarrow T_x, T_y, T_z$)

An interesting detail of intersystem crossing is the requirement that an individual molecule undergoing a $S_1 \rightarrow T$ process does so by selecting one of the three magnetic sublevels (T_x, T_y, T_z, Section 2.8)[55] of the triplet state. Likewise, for an individual molecule $T_1 \rightarrow S_0$ intersystem crossing (Section 6.10) occurs specifically from an individual magnetic sublevel. Radiationless processes (as was the case for radiative processes, Section 5.9) involving different sublevels will possess different rate constants for each sublevel. For example, it can be shown that the T_z level of aromatic compounds is predominantly populated by $S_1(n, \pi^*) \rightarrow T$ intersystem crossing. The T_z level is symmetry-related[55] to the $^3\pi, \pi^*$ state. Thus, the observation that T_z is dominantly populated by intersystem crossing from $S_1(n, \pi^*)$ indicates that a matrix element of the type $\langle {}^1n, \pi^* | \mathbf{H}_{SO} | {}^3\pi, \pi^* \rangle$ provides the spin-orbit mechanism for the $S_1 \rightarrow T$ process.

6.10 Intersystem Crossing ($T_1 \rightarrow S_0$)

Of the three important radiationless processes, $S_1 \rightarrow S_0$, $S_1 \rightarrow T_1$, and $T_1 \rightarrow S_0$, only in the latter case no electronic states lie between T_1 and S_0. Thus, phosphores-

scence and intersystem crossing are directly relatable to a common electronic $T_1 \rightarrow S_0$ transition.

The Relationship between $T_1 \rightarrow S_0$ Intersystem Crossing and Molecular Structure

As in the case of $S_1 \rightarrow S_0$ internal conversion, we expect an energy gap law (Eq. 6.17) and isotope effect if $T_1 \rightarrow S_0$ occurs via an electronic-vibrational (matching) mechanism. In addition, spin-orbit coupling may be important. It is not a priori obvious whether Franck-Condon factors (f_v) or spin-orbit factors (f_s) will determine the ultimate k_{TS} value.

For *aromatic hydrocarbons*, a clearcut relationship between k_{ST} and $E(T_1)$ is found.[35] As for the $S_1 \rightarrow S_0$ process, we expect the high-energy C-H vibrations to serve as the major "acceptor" vibrations for leakage of electronic into vibrational energy.[24] Indeed, a plot of log k_{ST} versus $E(T_1)$ (corrected for the number of C-H vibrations) is linear.[35] This result provides strong evidence that the electronic energy of T_1 "leaks out" via C-H vibrations for rigid aromatic hydrocarbons.

Factors other than Franck-Condon factors can influence the value of k_{ST} (Table 6.4). For example, increased spin-orbit coupling due to the heavy atom effect or the occurrence of an $^3n, \pi^* \rightarrow S_0$ transition will enhance the value of k_{TS}. Thus, for naphthalene, $k_{TS} \sim 0.4\ \text{sec}^{-1}$, while for 1-bromonaphthalene $k_{TS} \sim 100\ \text{sec}^{-1}$. Ketones possessing $T_1(n, \pi^*)$ undergo the fastest $T_1 \rightarrow S_0$ crossings which have yet been measured ($k_{TS} \sim 10^3\ \text{sec}^{-1}$).

Deuterium Isotope Effects on $T_1 \rightarrow S_0$ Intersystem Crossing

Dramatic deuterium isotope effects are found for radiationless $T_1 \rightarrow S_0$ transitions,[24,35] results which contrast sharply with those for $S_1 \rightarrow T_1$ transitions. Presumably, the difference lies in the much smaller energy gap required for

Table 6.4 Some Representative Values of Triplet Energies, Phosphorescence Radiative Rates, Intersystem Crossing Rates ($T_1 \rightarrow S_0$), and Phosphorescence Yields[a]

Molecule[b]	E_T	k_p^0	k_{TS}	Φ_P
Benzene-h_6	85	~0.03	0.03	0.20
Benzene-d_6	85	~0.03	<0.001	~0.80
Naphthalene-h_8	60	~0.03	0.4	0.05
Naphthalene-d_8	60	~0.03	<0.01	~0.80
$(CH_3)_2C{=}O$	78	~50	1.8×10^3	0.043
$(CD_3)_2C{=}O$	78	~50	0.6×10^3	0.10

[a] In organic solvents at 77 K. E_T in kcal/mole, k in sec^{-1}.
[b] Data for benzene and naphthalene from reference 24. Data for acetone from Borkman, R. F., *Molec. Photochem.*, *4*, 453 (1972).

$S_1 \rightarrow T_1$ transitions and the greater probability of surface crossings between S_1 and T_1. For example, (Table 6.4) the lifetimes of naphthalene triplets increase from ~ 2 seconds to ~ 20 sec upon substitution of C-H for C-D and the lifetime of acetone triplets increase from 0.56 ms to 1.7 ms upon substitution of C-H for C-D.

The radiative lifetime of the deuterated hydrocarbons nearly equals the maximum radiative lifetime—i.e., in the deuterated materials nearly every triplet emits, whereas only a small fraction of the perprotio-benzene triplets emit.[56] This striking result derives from Franck-Condon factors, in other words, f_r is much smaller for C-D vibrations than for C-H vibrations. However, f_r for C-D vibrations is ~ 20-30 times smaller than f_r for C-H vibrations.[8b] For example, the triplet states of both perprotio- and perdeuterobenzene lie at 85 kcal/mole above S_0. This corresponds to about ten vibrational quanta for C-H vibrations. The lower amplitude of the C-D vibrations requires a larger number of vibrational quanta to equal 85 kcal/mole. Therefore, the vibrational level of S_0 that is reached when the deuterated material converts from T_1 to S_0 possesses a large vibrational amplitude and intersystem crossing from T_1 to S_0 is inhibited.

In the vapor phase, for small molecules, the effect of deuterium substitution on triplet lifetimes may be dramatic. For example,[40b] $H_2C{=}O$ possesses $\tau_T < 0.4 \times 10^{-6}$ sec, whereas for $D_2C{=}O$, $\tau_T \sim 17 \times 10^{-6}$ sec.

Temperature Effects on $T_1 \rightarrow S_0$ Intersystem Crossing

The magnitude of k_{IS} is expected to be relatively temperature independent if $T_1 \rightarrow S_0$ intersystem crossing occurs via a unimolecular photophysical mechanism. In fact, the phosphorescence lifetimes of aromatic hydrocarbons and aromatic ketones are very similar at temperatures from 4 K to 300 K (room temperature), if bimolecular quenching mechanisms or photoreactions do not occur.[57] For example, the phosphorescence lifetime of naphthalene (**11**) in solid *matrices* is mainly determined by intersystem crossing $T_1 \rightarrow S_0$. Since τ_p varies[54,57] by less than a factor of 2 upon going from 4 K to 300 K, k_{IS} is clearly undergoing at most small changes as a function of temperature. In fluid solution,[58] however, the lifetime of naphthalene triplets is determined mainly by bimolecular quenching and τ_T is generally < 1 ms. For benzophenone (**12**), τ_T is mainly determined by phosphorescence from $T_1(\Phi_P \sim 0.9)$ at 77 K. At 300 K in an inert, nonquenching solvent,[59] phosphorescence is still the major pathway for T_1 deactivation.

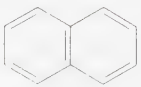

11

$Ph_2C{=}O$

12

	τ_T	τ_T
4 K	2.4 sec.	—
77 K	2.4 sec.	1.0
300 K	1.5 sec.	0.7

Intersystem Crossing from Individual Spin Levels (T_x, T_y, $T_z \rightarrow S_0$)

In Chapter 5 we learned that under appropriate conditions three *phosphorescences* are observed, one from each of the triplet magnetic sublevels T_x, T_y, and T_z. Similarly, intersystem crossing to S_0 from each of these levels occurs at a different rate. At temperatures near 4 K, the thermal equilibrium is slow relative to k_{TS} and the individual contributions to phosphorescence of the sublevels may be evaluated.[60]

6.11 Perturbation of Spin-Forbidden Radiationless Transitions

The "heavy atom effect" is a term which has been coined to describe the influence of "heavy atom" substitution on spin-forbidden transitions.[19] For example, the substitution of Br for H usually enhances the probability of radiationless processes such as $S_1 \rightarrow T_n$ and $T_1 \rightarrow S_0$ intersystem crossings. It is usually assumed that the dominant influence of the heavy atom is to enhance spin-orbit coupling. In order to understand how the heavy atom effect measurably influences properties, let us assume that it influences all spin-forbidden transitions (intersystem crossings, $S_1 \rightarrow T_1$, $T_1 \rightarrow S$, and phosphorescence $T_1 \rightarrow S_0$) but does not influence spin-allowed transitions (internal conversion $S_1 \rightarrow S_0$ and fluorescence $S_1 \rightarrow S_0$). In this approximation the rate constants k_{ST}, k_{TS}, and k_P should be *increased* by the heavy atom effect but k_F and k_{IC} should not.

From Eqs. 6.31–6.37, we predict that the heavy atom effect will generally:

1. Decrease Φ_F (when k_{ST} is comparable to k_F compared to the "light atom" analogue)

2. Increase Φ_{ST} (when k_{ST} is comparable to k_F compared to the "light atom" analogue)

However, Φ_P and Φ_{TS} may either increase or decrease with heavy atom substitution, depending on whether it is k_P or k_{TS} which is influenced to the greater extent.

From this analysis we deduce that heavy atom effects will *not* be universal. They will occur only when the heavy atom increases k_{ST} (k_P or k_{TS}) to a value which alters τ_S (or τ_T).

Empirically, the *maximum* heavy atom effect that can be induced on k_{ST} by bromine atom substitution corresponds to a rate of the order of 10^8 10^9 sec^{-1}. As a result, if k_F or k_{ST} are of the order of 10^9 sec^{-1}, a bromine atom may not produce a significant effect on the fluorescence lifetime or yield. In practice, this means that heavy atom effects on $S_1 \rightarrow T$ intersystem crossing tend to be minimal for states which already possess substantial spin-orbit coupling (n, π^* states) or very fast fluorescence rates.

Internal Perturbation of Intersystem Crossing

As an example of the heavy atom effect on k_{S1}^0, k_{TS}, and k_P^0 consider the data in Table 6.5. The effect is most pronounced when the parent structure possesses inherently weak intersystem crossing and a slow rate of fluorescence deactivation. A classical example is given by naphthalene and its halo derivatives. Both k_F^0 and k_{ST} are $\sim 10^6$ sec^{-1} for naphthalene. Substitution of F for H has relatively little effect on the emission efficiencies or rate constants of fluoro-naphthalene relative to naphthalene. However, substitution of Cl, then Br, then I leads to an ever-increasing decrease in Φ_f, and an accompanying increase in k_{S1} and k_P^0. The effect on Φ_P is not readily predictable (both k_P^0 and k_{TS} are influenced by the heavy atom).

As a final example, perylene[45] possesses a very fast and efficient fluorescence ($\Phi_f \sim 0.98$, $k_F^0 \sim 10^9$ sec^{-1}). If the heavy atom effect were the same for naphthalene and for perylene, then substitution of Br for H would increase k_{S1} to $\sim 10^8$ sec^{-1}. The lack of a heavy atom effect on k_F^0 when going from perylene to bromoperylene can be understood in terms of a very fast inherent fluorescence.

In the case of anthracence → 9-bromoanthracence, a dramatic decrease in ϕ_F and k_{ST} is noted. However, substitution of a second bromine atom (9-bromo-anthracence → 9,10-dibromoanthracene) results in an *increase* in Φ_f and decrease in k_{ST}. This "inverse" heavy atom effect is explained in terms of the influence of halogen substitution on the position of T_2. In anthracence k_{S1} occurs via a $S_1 \rightarrow T_1^{\ddagger}$ mechanism but in 9-bromoanthracene T_2 is lowered in energy so that it falls *below* S_1. Thus, a $S_1 \rightarrow T_2$ mechanism for intersystem crossing becomes available. Thus, $S_1 \rightarrow T_1^{\ddagger}$ or an *activated* $S_1 \rightarrow T_2$ intersystem crossing occurs. The net effect is to decrease k_{S1} relative to 9-bromoanthracene, although it is still large relative to anthracene.

9,10-Dibromoanthracene offers an interesting example of how the energetic relationship of S_1 and T_n affects the value of k_{ST}.[46] In spite of the presence of two bromine atoms, 9,10-dibromoanthracene (DBA) possesses a modest fluorescence yield ($\phi_F \sim 0.05$). This implies that the "heavy atom" effect does not dominate and bring about very rapid intersystem crossing. Furthermore, the fluorescence yield of DBA is found to be extremely solvent-dependent. This peculiar behavior is understandable when it is realized that T_2 lies about 5 kcal/mole *above* S_1 for DBA. The energetic spacing of S_1 and T_2 requires that DBA either (a) undergoes

Table 6.5 The Internal Heavy Atom Effect on Transitions between States[a]

Molecule	k_F^0	k_{ST}	k_P^0	k_{TS}	Φ_f	Φ_P
Naphthalene	10^6	10^6	10^{-1}	10^{-1}	0.55	0.05
1-Fluoronaphthalene	10^6	10^6	10^{-1}	10^{-1}	0.84	0.06
1-Chloronaphthalene	10^6	10^8	10	10	0.06	0.54
1-Bromonaphthalene	10^6	10^9	50	50	0.002	0.55
1-Endonaphthalene	10^6	10^{10}	500	100	0.000	0.70
Perylene	2×10^8	10^7	—	—	0.98	
3-Bromoperylene	2×10^8	10^7	—	—	0.98	

[a] Data for rigid solution at 77 K. At room temperature k_{TS} is often dominated by bimolecular deactivation of T_1 or by reactions of T_1. Rate constants are approximate

activated intersystem crossing from S_1 to T_2, or (b) undergoes direct intersystem crossing from S_1 to an upper vibrational level of T_1. Either mechanism will cause k_{ST} to be slowed down. The solvent effect is due to the shifting of the position of S_1 and T_2 as a function of solvent. In solvents such that $\Delta E(S_1 - T_2)$ is maximal, ϕ_F is maximal.

External Perturbation of Intersystem Crossing

Examples of enhancement of the overall $S_1 \rightarrow T_1$ process by molecular oxygen,[61] xenon,[62] organic halides,[63] and organometallics[64] are known. In the case of oxygen several mechanisms are possible, including enhancement of spin-orbit coupling and energy transfer (to produce a simultaneous $S_1 \rightarrow T_1$ transition in the perturbed molecule and a $T \rightarrow S$ transition in the oxygen molecule). The *efficiency* of the oxygen effect depends on the oxygen concentration and may be expressed as $k_{ST}^{O_2}[O_2]$, where $k_{ST}^{O_2}$ is a bimolecular rate constant for oxygen perturbation and $[O_2]$ is the concentration of oxygen in the sample. The *overall* or observed rate of intersystem crossing (k_{ST}^{OB}) becomes

$$k_{ST}^{OB} = k_{ST} + k_{ST}^{O_2}[O_2] \tag{6.56}$$

Typical values of $k_{ST}^{O_2}$ are $\sim 10^{10}$–10^9 M^{-1} sec^{-1}.[61] The solubility of O_2 in many organic solvents (under 1 atm of O_2) is $\sim 10^{-2}$ M. Thus, $k_{ST}^{O_2}[O_2] \sim 10^8$ 10^7 sec^{-1}. Thus, the effect will be noticeable only if $k_{ST} \sim 10^8$ sec or less. For example, $\Phi_{ST} \sim 0.3$ for pyrene ($k_{ST} \sim 10^7$ sec^{-1}) in the absence of O_2, and increases to ~ 1.0 under 1 atm of O_2. Similar effects are noted for xenon as a $S_1 \rightarrow T$ perturber.[62]

Although O_2 and Xe are known to be efficient quenchers of T_1 states, it is clear that not only enhancement of $T_1 \rightarrow S_0$ occurs, but other quenching pathways (including reaction) may occur.

External heavy atom (e.g., organic halides) effects on k_{ST} and k_{TS} are well established. As an illustration, consider the naphthalene derivatives **13** and **14**.[65]

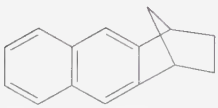

13

$k_{ST} = 2 \times 10^6$ sec^{-1}
$k_{TS} = 2 \times 10^{-1}$ sec^{-1}

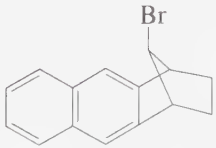

14

$k_{ST} = 300 \times 10^6$ sec^{-1}
$k_{TS} = 40 \times 10^{-1}$ sec^{-1}

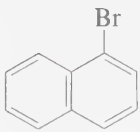

15

$k_{ST} = 500 \times 10^6$ sec^{-1}
$k_{TS} = 600 \times 10^{-1}$ sec^{-1}

The effect of the "external" bromine in **14** is to enhance both k_{ST} and k_{TS}. The enhancement of k_{ST} is comparable to the "internal" effect of bromine on **15.** Note however, that k_{TS} is much higher for **15** than **14.** This may result from the somewhat different surface situation in **15** which may result in better Franck-Condon factors or better intersystem crossing.

6.12 The Relationship between Photophysical Radiationless Transitions and Photochemical Processes

In this chapter we have considered the photophysical radiationless pathways by which an electronically excited molecule can "find its way" back to its original ground state. If we view radiationless transitions in the general sense as a conversion of electronic energy into nuclear motion, then the distinction between "photophysical" and "photochemical" processes becomes blurred.[66] Indeed, we can imagine (Fig. 6.17) that they differ only in the degree of nuclear geometry change. If the distortion from an original ground state geometry is not too severe, return to the original geometry via radiationless transition(s) is possible. Suppose this transition takes place via the funnel on the excited surface shown in Figure 6.17. Relatively small changes in nuclear shape ("to the right" of the minimum) of the funnel will tend to deliver the molecule back to the ground state in a nuclear configuration that will favor formation of products rather than reactants. Thus, a photophysical transition which takes place through the funnel via transitions "to the left" of the minimum and returns the excited molecule to its original ground

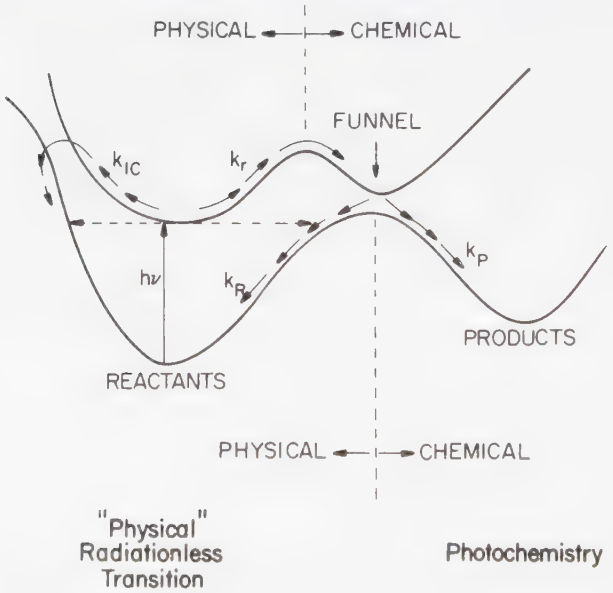

Figure 6.17

Schematic surface description of a possible relationship between "photophysical" and photochemical radiationless processes.

state may not differ qualitatively from photochemical transitions which produce products.

In Chapters 10 -14, we shall see that the notions of photophysical radiationless transitions and photochemical reactions are intimately related, via the common theory of energy surfaces.

References

1. For a discussion of the theory of radiationless processes with a historical perspective, see:
   (a) Robinson, G. W., *Excited States*, ed. Lim, E., *Vol. I*, New York: Academic Press, 1974, p. 1.
   (b) Kasha, M., *Light and Life*, ed. McElroy, W. D., and Gloss, B., Baltimore: Johns Hopkins Press, 1961, p. 31.
   (c) Kasha, M., *Comparative Effects of Radiation*, ed. Burton, M., Kirby-Smith, J. S., and Magee, J. J., New York: Wiley, 1960, p. 72.
   (d) Kasha, M., *Radiation Research*, Supl. 2., 243 (1960).
   (e) Birks, J. B., *Photophysics of Aromatic Molecules*, New York: Wiley, 1970, p. 142.
   (f) Kasha, M., *Disc. Faraday Soc.*, *9*, 14 (1950).
   (g) Henry, B. R., and Kasha, M., *Annu. Rev. Phys. Chem.*, *19*, 163 (1968).
2. (a) Zener, C., *Proc. Royal Soc.*, *A137*, 696 (1939); *ibid.*, *A140*, 660 (1933).
   (b) Bernstein, R. B., *Molecular Reaction Dynamics*, Oxford: Clarendon, 1974.
   (c) Nikitin, E. E., *Russ. Chem. Rev.*, *43*, 905 (1974).
3. (a) Dewar, M. J. S., and Dougherty, R. C., *The PMO Theory of Organic Chemistry*, Englewood Cliffs, New Jersey: Prentice-Hall, 1975.
   (b) Michl, J., *Molec. Photochem.*, *4*, 253 (1972).
   (c) Salem, L., Leforestier, C., Segal, G., and Wetmore, R., *J. Am. Chem. Soc.*, *97*, 479 (1975).
   (d) Salem, L., *ibid.*, *96*, 3486 (1974).
4. (a) Kauzman, W., *Quantum Chemistry*, New York: Academic Press, 1957, p. 534.
   (b) Teller, E., *Israel J. Chem. 7*, 227 (1969).
5. (a) Devaquet, A., *Pure Appl. Chem.*, *41*, 535 (1975); *Topics in Chemistry*, *54*, 1 (1975).
6. Dauben, W. G., Salem, L., and Turro, N. J., *Acc. Chem. Research*, *8*, 41 (1975).
7. Ting, C. H., *Photochem. Photobio.*, *9*, 17 (1969).
8. (a) Azumi, T., and Matsuzaki, K., *Photochem. Photobio.*, *25*, 315 (1977).
   (b) Schlag, E. W., Schneider, S., and Fischer, S. F., *Annu. Rev. Phys. Chem.*, *22*, 465 (1971).
   (c) Henry, B. R., and Sisbrand, W., *Organic Molecular Photophysics*, ed. Birks, J. B., New York: Wiley, 1973, p. 153.
   (d) Becker, R. S., *Theory and Interpretation of Fluorescence and Phosphorescence*, New York: Wiley, 1969.
9. (a) Lim, E. C., Li, Y. H., and Li, R., *J. Chem. Phys.*, *53*, 2443 (1970).
   (b) Kanamaru, N., and Lim, E. C., *ibid.*, *62*, 3252 (1975).
10. For excellent reviews of spin-orbit coupling see:
    (a) McGlynn, S. P., Azumi, T., and Kinoshita, M., *Molecular Spectroscopy of the Triplet State*, Englewood Cliffs, New Jersey: Prentice-Hall, 1969, p. 183;

(b) Salem, L., and Rowland, C., *Angew. Chem. Intern. ed. Eng.*, *11*, 92 (1972);
(c) Salem, L., *Pure Appl. Chem.*, *33*, 317 (1973).

11. El-Sayed, M. A., *J. Chem. Phys.*, *38*, 2834 (1963); *ibid.*, *36*, 573 (1962); *ibid.*, *41*, 2462 (1964).

12. Halpern, A., and Ware, W. R., *J. Chem. Phys.*, *53*, 1969 (1970).

13. Anderson, R. W., Hochstrasser, R. M., Lutz, H., and Scott, G. W., *J. Chem. Phys.*, *61*, 2500 (1974).

14. Bredereck, K., Förster, T., and Oesterlin, H. G., *Luminescence of Organic and Inorganic Materials*, New York: Wiley, 1962, p. 161.

15. Henry, B. R., and Siebrand, W., *J. Chem. Phys.*, *54*, 1072 (1971).

16. Madej, S. L., Okajima, S., and Lim, E. C., *ibid.*, *65*, 1219 (1976).

17. (a) Lewis, G. N., and Calvin, M., *Chem. Rev.*, *25*, 272 (1939).
(b) Lin, S. H., and Bersohn, R., *J. Chem. Phys.*, *48*, 2732 (1968).
(c) Calzaferri, G., Gugger, H., and Leutwyler, S., *Helv. Chim. Acta*, *59*, 1969 (1976).
(d) Lin, S. H., *J. Chem. Phys.*, *44*, 3759 (1969).

18. (a) Sharafy, S., and Muskat, K. A., *J. Am. Chem. Soc.*, *93*, 4119 (1971).
(b) Gegion, D., Muskat, K. A., and Fischer, E., *ibid.*, *90*, 12, 3097 (1968).

19. (a) DeBoer, C. D., and Schlessinger, R. H., *J. Am. Chem. Soc.*, *90*, 803 (1968).
(b) Saltiel, J., Zafirious, O. C., Megarity, E. D., and Lamola, A. A.,*ibid.*, *90*, *4759* (1968).

20. Dellinger, D., and Kasha, M., *Chem. Phys. Letters*, *38*, 9 (1976).

21. Zimmerman, H. E., Kamm, K. S., and Werthemann, D. P., *J. Am. Chem. Soc.*, *97*, 3718 (1975).

22. Schloman, W. W., and Morrison, H., *J. Am. Chem. Soc.*, *99*, 3342 (1977).

23. Froehlich, P. M., and Morrison, H., *J. Phys. Chem.*, *76*, 3566 (1972).

24. (a) Robinson, G. W., and Frosch, R. P., *J. Chem. Phys.*, *38*, 1187 (1963); *ibid.*, *37*, 1962 (1962).
(b) Dexter, D. L., and Fowler, W. B., *ibid.*, *47*, 1379 (1967).

25. Some experimental examples:
(a) Coumarin derivative: Maier, J. P., Seilmeier, A., Loubereau, A., and Kaiser, W., *Chem. Phys. Letters*, *46*, 527 (1977).
(b) Rhoamine GG: Ricard, D., and Ducuing, J., *J. Chem. Phys.*, *62*, 3616 (1975).
(c) Coronene: Shank, C. V., Ippen, E. P., and Teschke, O., *Chem. Phys. Letters*, *45*, 291 (1977).

26. Goutermann, M., *J. Chem. Phys.*, *36*, 2846 (1962).

27. Herzberg, G., *Spectra of Diatomic Molecules*, 2nd ed. Princeton: Van Nostrand, 1950.

28. Statz, H., Tang, C. L., and Foster, G. F., *J. Appl. Phys.*, *37*, 4278 (1966).

29. Wilkinson, F., *Organic Molecular Photophysics*, ed. Birks, J. B., New York: Wiley 1975, p. 95.

30. Ermolaev, V. L., and Svitaskev, K. J., *Opt. Spectr.*, *7*, 399 (1959).

31. Gilmore, E. H., Gibson, G E., and McClure, D. S., *J. Chem. Phys.*, *20*, 829 (1952); correction, *ibid.*, *23*, 399 (1955).

32. Birks, J. B., *Photophysics of Aromatic Molecules*, New York: Wiley, 1970.

33. Gillispie, G. D., and Lim, E. C., *J. Chem. Phys.*, *65*, 2022 (1976).

34. Campbell, R. O., and Lin, R. S. H., *J. Am. Chem. Soc.*, *95*, 6560 (1973).

35. Siebrand, W., *J. Chem. Phys.*, *46*, 440 (1967); *ibid.*, *47*, 2411 (1967).

36. Byrne, J. P., McCoy, E. F., and Ross, I. G., *Aus. J. Chem.*, *18*, 1589 (1965).

37. Ermolaev, V. L., *Soviet Physics, Uspekhi*, *80*, 333 (1963).

38. (a) Laposa, J. D., Lim, E. C., and Kellogg, R. E., *J. Chem. Phys.*, *42*, 3025 (1965).
(b) Birks, J. B., *Photophysics of Aromatic Molecules*, New York: Wiley, 1970, p. 122.
(c) Kanamaru, N., Bhattacharjic, H. R., and Lim, E. C., *Chem. Phys. Letters*, *26*, 174 (1974).

39. Miller, R. C., and Lee, E. K. C., *Chem. Phys. Letters*, *41*, 52 (1976).

40. (a) Halpern, A. M., and Ware, W. R., *J. Chem. Phys.*, *54*. 1271 (1971).
(b) Luntz, A. C., and Maxson, V. T., *J. Chem. Phys.*, *26*, 553 (1974).

41. Murata, S., Iwanga, C., Toda, T., and Kokubun, H., *Chem. Phys. Letters*, *15*, 152 (1972).

42. Oka, I., Knight, A. R., and Steen, R. P., *J. Chem. Phys.*, *66*, 699 (1977).

43. (a) Heritage, J. P., and Penzkofer, A., *Chem. Phys. Letters*, *44*, 76 (1976).
(b) Ippen, E. P., Shank, C. V., and Woerner, R. L., *ibid.*, *46*, 20 (1977).

44. Bennett, R. G., and McCartin, P. J., *J. Chem. Phys.*, *44*, 1969 (1966).

45. Dreekamp, H., Koch, E., and Zander, M., *Chem. Phys. Letters*, *31*, 251 (1975).

46. Kearvill, A., and Wilkinson, F., *J. Chim. Phys.*, *125* (1969); *Molec. Crystals*, *4*, 69 (1968).

47. Henry, R. B., and Siebrand, W., *Chem. Phys. Letters*, *54*, 1072 (1971).

48. Halpern, A., and Ware, W. R., *J. Chem. Phys.*, *53*, 1969 (1970).

49. Almgren, M., *Mol. Photochem.*, *4*, 327 (1972).

50. Solomon, B. S., Thomas, T. F., and Steel, C., *J. Am. Chem. Soc.*, *90*, 2449 (1968).

51. (a) Morris, J. M., and Williams, D. F., *Chem. Phys. Letters*, *25*, 312 (1974).
(b) El-Sayed, M. A., and Leyerle, R., *J. Chem. Phys.*, *62*, 1579 (1975).
(c) Batley, M., and Kearns, D. R., *Chem. Phys. Letters*, *2*, 423 (1968).

52. Matsumoto, T., Sato, M., and Hiroyama, S., *Chem. Phys. Letters*, *13*, 13 (1972).

53. Hansen, D. A., and Lee, K. C., *J. Chem. Phys.*, *62*, 183 (1975).

54. Hunter, T. F., *Photochem. Photobio.*, *10*, 147 (1969).

55. (a) Cheng, T. N., and Robinson, G. W., *J. Chem. Phys.*, *49*, 3184 (1968).
(b) Dym, S., and Hochstrasser, R. M., *J. Chem. Phys.*, *51*, 2458 (1969).

56. (a) Birks, J. B., Hamilton, T. D. S., and Najbar, J., *Chem. Phys. Letters*, *39*, 445 (1976).
(b) Clark, R. H., and Frank, H. A., *J. Chem. Phys.*, *65*, 39 (1976).

57. Kellogg, R. E., and Schwenker, R. P., *J. Chem. Phys.*, *41*, 2860 (1964).

58. Tsai, S. C., and Robinson, G. W., *J. Chem. Phys.*, *49*, 3184 (1968).

59. Parker, C. A., and Joyce, T. A., *Trans. Faraday Soc.*, *65*, 2823 (1969).

60. (a) Antheunis, D. A., Schmidt, J., and van der Waals, J. H., *Molec. Phys.*, *27*, 1521 (1974).
(b) Winscom, C. J., and Maki, A. H., *Chem. Phys. Letters*, *12*, 264 (1971).

61. Stevens, B., and Algar, B. E., *J. Phys. Chem.*, *72*, 3468 (1968); *Chem. Phys. Letters*, *1*, 58, 219 (1967).

62. Horrocks, A. R., Kearvill, A., Tickle, K., and Wilkinson, F., *Trans. Faraday Soc.*, *62*, 3393 (1966).

63. Quina, F. H., and Carroll, F. A., *J. Am. Chem. Soc.*, *98*, 6 (1976).

64. Vander Donckt, E., and Vogels, C., *Spectrochim. Acta*, *27A*, 2157 (1971).

65. Karvanos, G., Cole, T., Scribe, P., Dalton, J. C., and Turro, N. J., *J. Am. Chem. Soc.*, *93*, 1032 (1970).

66. (a) Phillips, D., Lemaire, J., Burton, C. S., and Noyes, W. A., *Adv. Photochem.*, *5*, 329 (1968).
    (b) Hammond, G. S., *ibid.*, *7*, 373 (1969).

7

Theoretical Organic Photochemistry

7.1 A Qualitative Theory of Organic Photoreactions

A proper qualitative theory of photoreactions should provide useful answers to the questions: (a) What are the *possible* products of a photoreaction which starts from a particular electronic state? (b) What are the *probable* products of a photoreaction which starts from a particular electronic state?

These questions can be answered qualitatively if we can visualize the energy surfaces which connect the starting molecular structures (reactants) to the possible final molecular structures (products). If we could "see" these energy surfaces, they would serve as maps or networks of possible pathways which would allow us to immediately recognize the following important features of organic photoreactions:

1. The energy barriers which must be overcome in proceeding from reactant to product on various energy surfaces.

2. The minima on the excited and ground surfaces.

3. The "critical" nuclear geometries for which excited surfaces come close together, and for which an excited surface comes close to the ground state.

For most photoreactions in solution we need consider only the S_1, T_1, and S_0 surfaces in detail. Thus, the task of a useful theory of photoreactions is to provide procedures for qualitatively predicting the maxima and minima and the critical geometries on the S_0, T_1, and S_1 surfaces. Theory should also allow an evaluation of the electronic nature of minima and maxima on the various surfaces, e.g., whether or not they are the results of avoided crossings.

State Correlation Imposed Energy Barriers along Reaction Coordinates

A qualitative, a priori "feeling" for the occurrence of energy barriers may be obtained by employing either the concepts of *orbital interactions*[1] or the concepts

of *state correlation diagrams*.[2,3] For example, significant positive overlap of the highest occupied (HO) and lowest unoccupied (LU) orbitals of reactants usually signals a small energy barrier to reaction, whereas negative (or zero) net overlap of the HO and LU orbitals usually signals a large energy barrier. If we start on a given surface from a reactant (or reactants) along which there are two reaction choices, we call the pathway with the smaller energy barrier "allowed" and the pathway with the larger energy barrier "forbidden." In effect, we postulate that reactions prefer to proceed via transition structures that have obtained the most favorable positive orbital overlap.

Within the framework of correlation diagrams, if an initial state makes an endothermic ("uphill") correlation with a high-energy product state along one reaction coordinate but an exothermic ("downhill") correlation with a low-energy product state along another coordinate, we may say that the former experiences a *state correlation-imposed energy barrier*, whereas the latter does not. We postulate that movement of the representative point along a surface that corresponds to a reaction coordinate which possesses a state correlation-imposed energy barrier will be less probable (forbidden reaction) than movement along a surface which does not possess correlation-imposed barriers (allowed reaction).

Relationship between Molecular Structure, Minima, and Crucial Geometries on S_1 and T_1 Surfaces

For which geometries can one expect minima on S_1 and T_1? Are there general situations for predicting minima based on simple structural considerations? The answer is affirmative. For example, minima are expected on S_1 or T_1 at geometries which correspond to minima on S_0 when S_1 and T_1 possess an electronic configuration which corresponds to only a small change in the overall bonding of the ground state, e.g., π, π^* states of aromatic molecules or n, π^* states of ketones. Molecules which reach such minima may generally be treated as being in pseudo-equilibrium with their environment, i.e., vibrational equilibrium to the $v = 0$ level is achieved. From such minima the photophysical processes of fluorescence, phosphorescence, intersystem crossing, and internal conversion occur. Vertical radiationless jumps from such minima are not generally directly relevant to photoreactions unless a "hot" ground state (or triplet) is produced which can overcome energy barriers which ordinarily cannot be surmounted by molecules in equilibrium at the reaction temperature (Fig. 4.14).

A second structural type which commonly possesses an excited state minimum is termed the *diradicaloid* geometry.[4,5] In many photoreactions a bond is broken in a molecule and a "critical" geometry is produced such that two half-occupied atomic orbitals (or molecular orbitals) are generated in such a way that they interact with each other very weakly. The energy gaps between S_0, S_1, and T_1 are relatively small for such diradical geometries.

In Sections 7.6 and 7.7 we shall discuss three prototype "critical" geometries which serve as a basis for unifying ideas concerning the required radiationless jumps which must occur during a photoreaction:

1. The geometry (pericyclic minimum) of a transition for a "ground state forbidden" pericyclic reaction.

2. The geometry (stretched σ bond minimum) at which a severely stretched σ bond is essentially broken.

3. The geometry (twisted π bond minimum) for which a severely twisted π bond is essentially broken.

It is through the above minima that access to S_0 is commonly achieved. After this point the "photo" part of a photoreaction is effectively over.

7.2 The Principle of Maximum Positive Orbital Overlap[1]

According to quantum theory, molecular orbitals generally have spatial directiveness associated with them. As a result, if a reaction is to be initiated by orbital overlap, certain spatial positions of nuclei (with their associated electron clouds) will be favored over others. The principle of stereoelectronic control of reaction pathways postulates that reaction rates are controlled by the overlap of orbitals in space. Certain nuclear geometries are easier to achieve than others during a reaction because of the greater positive orbital overlap accompanying one nuclear motion relative to another. The principle of maximum positive overlap postulates that the reaction rates are proportional to the degree of positive (bonding) overlap of orbitals. Although qualitative in nature, these two principles are a powerful basis for analyzing photochemical reactions and for quickly sorting out plausible and implausible reaction pathways.

In the application of these two principles we must also consider the *energies* of the orbitals involved, since only the higher-energy filled orbitals (i.e., valence orbitals) and lower-energy (vacant) orbitals are likely to be involved in reactions at ordinary temperatures. We shall employ the frontier molecular orbital approximation[1] in analyzing orbital interactions. This approximation postulates that chemical reactivity may be gauged by the overlap behavior of "frontier molecular orbitals" (FMO's), which the orbitals correspond to the highest-energy orbital filled in the ground state (the HO orbital) and the lowest-energy orbital unfilled in the ground state (the LU orbital). This assumption is justified since the HO is usually furthest from the nuclei of all the orbitals that are occupied in the ground state. As a result, nuclear attraction of an electron in an HO is relatively weak and the HO is more readily deformed, and most readily gives up electron density to electrophilic sites in the environment, i.e., the HO generally possesses the highest polarizability and the smallest ionization potential of any orbital that is occupied in the ground state. The LU, which is unoccupied in the ground state, is most capable of accepting electron density with minimum increase in the total molecular energy.

The fundamental underlying principle of HO-LU interactions as a means of understanding chemical reactivity is the assumption that a majority of chemical reactions should take place most easily (lowest activation enthalpy) at the position of and in the direction of maximum positive overlap of the HO and the LU of the

interacting species. A singly occupied molecular orbital (SO) produced by electronic excitation may play the role of HO or LU, or both.

The key physical idea in this theory of chemical reactivity is that *charge transfer* interactions will occur between HO and LU. Chemists appreciate the fact that HO contains the valence electrons of the molecules. These are the electrons which are the easiest to perturb during the initiation of a reaction. If this initial perturbation is assisted by movement of the HO electrons toward a LU, we can readily visualize how the transfer of charge from one orbital to another actually occurs.

7.3 Orbital Interactions[1]

The "stabilization" energy E due to overlap of frontier orbitals (FMO's) is given qualitatively by

$$E \sim \frac{\text{overlap of FMO's}}{\Delta E} \tag{7.1}$$

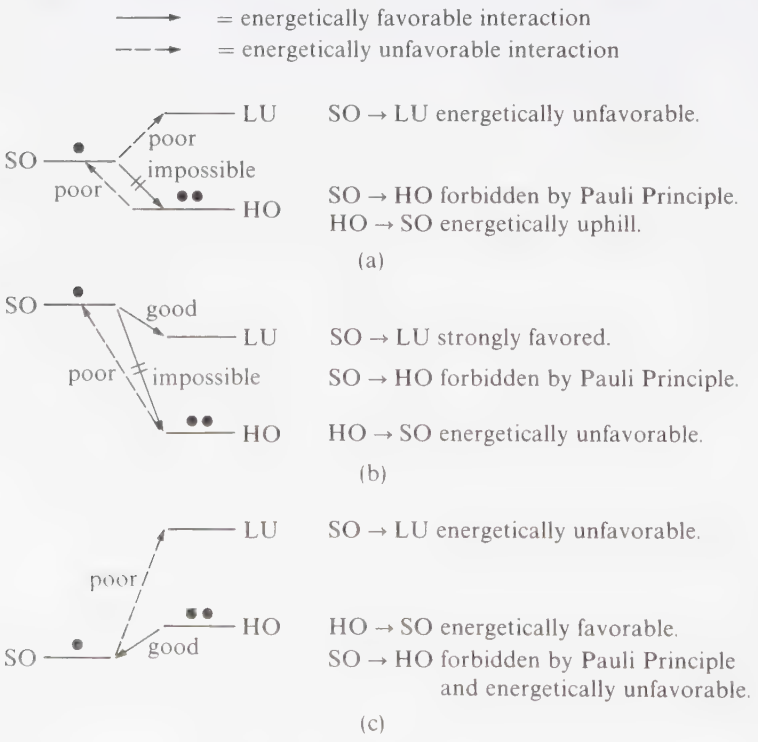

Figure 7.1

Some examples of possible SO ↔ HO and SO ↔ LU interactions. The solid circles represent electrons in orbitals.

The magnitude of E in the stabilizing sense will depend on the magnitude of the *net* positive overlap of the FMO's and of the term ΔE, which measures the energy difference between the pertinent interacting FMO's.

Consider Figure 7.1 which schematically shows possible SO ↔ HO and SO ↔ LU interactions. Whether charge flows from or to a SO, a LU (or HO) will depend to a large extent on the energy differences between the interactions SO and LU (or HO). In the case of flow to the SO, the charge flow from HO → SO is the most energetically feasible pathway. In the case of flow from the SO, charge flow from SO → LU is preferred.

Commonly Encountered Orbital Interactions in Organic Photoreactions

Figure 7.2 shows two commonly encountered photochemical situations. From an energetic standpoint, in case (a) the D*(LU) → A(LU) orbital interaction dominates, whereas in case (b) the D(HO) → A*(HO) orbital interaction dominates.

From Figures 7.1 and 7.2 and the criteria of maximum positive overlap, we can postulate the following recipe for deciding how orbital interactions will determine the favored nuclear motions for a given set of photochemical reaction pathways:

1. After setting up the molecular orbitals of the reactants according to their relative energies, identify the FMO's and the half-filled MO's of the electronically excited moiety.

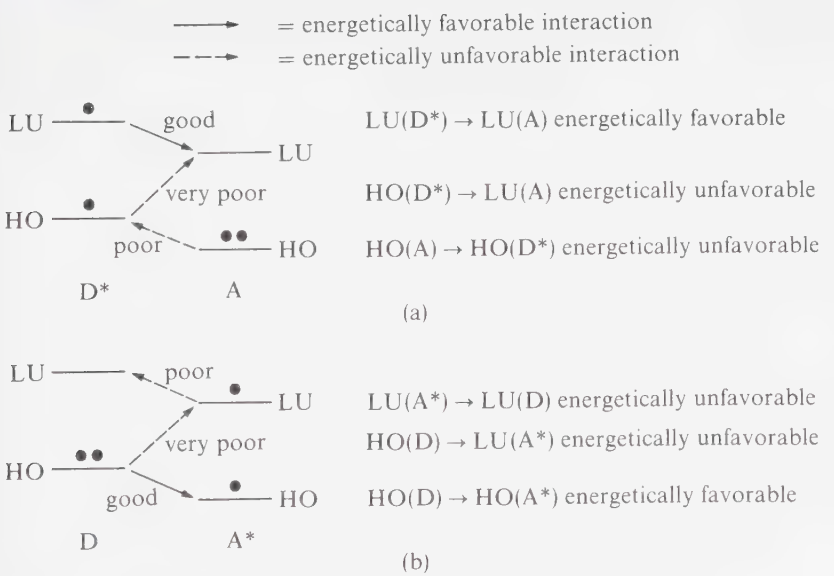

Figure 7.2

Schematic representation of two important orbital interaction types: (a) Dominant D*(LU) → A(LU) interaction and secondary A(HO) → D*(HO) and D*(HO) → A(LU) interactions and (b) Dominant D(HO) → A*(HO) and secondary D(HO) → A*(LU) and A*(LU) → D(LU) interactions.

2. Draw the possible orbital interactions between an SO and an HO or LU.

3. Determine whether the orbital interactions lead to positive overlap and whether the interaction arrow points up (thermodynamically unfavorable) or down (thermodynamically favorable).

4. Evaluate the positive orbital overlap and thermodynamic factors to determine qualitatively the more favorable reaction pathways.

Selection of Reaction Coordinates from Orbital Interactions

In analyzing a photochemical reaction theoretically, one must select the particular reaction coordinate or coordinates which describe the nuclear geometry changes accompanying the transformation of reactants to products. In principle, all possible reaction coordinates might be analyzed. In practice, we seek to select only the lowest-energy reaction pathways from a given initial excited state. These pathways may be qualitatively identified by the use of orbital interactions.

For theoretical analysis, we will consider the following photoreactions, which will serve as prototypes for many other photoreactions (see Equations 7.2 through 7.6).

Consideration of orbital interactions leads to the well-known selection rules for pericyclic reactions.[3] For example (see Fig. 7.3), from consideration of orbital interactions and according to the rules of orbital interactions, we are led to the prediction that from the π, π^* states of cyclobutene both $\sigma \rightarrow \pi$ and $\pi^* \rightarrow \sigma^*$ charge transfers should contribute significantly.

Inspection of the orbital symmetry for disrotatory and conrotatory processes[3] shows that the former is favored by the rule of maximum positive overlap:

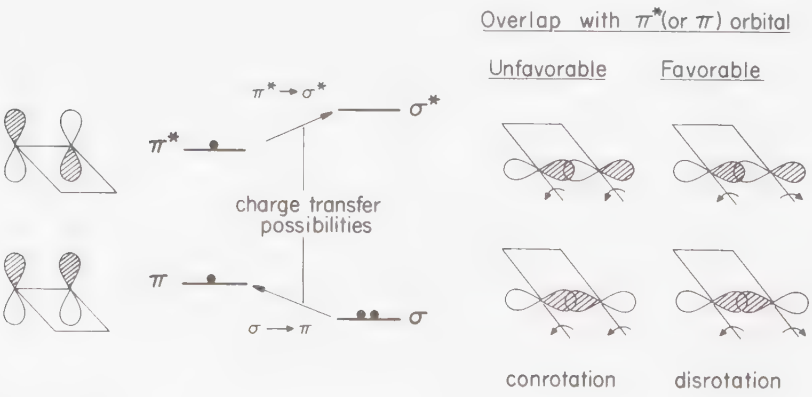

Figure 7.3

Orbital interactions for the conrotatory and disrotatory ring opening of the π, π^* state of cyclobutene to form 1,3-butadiene.

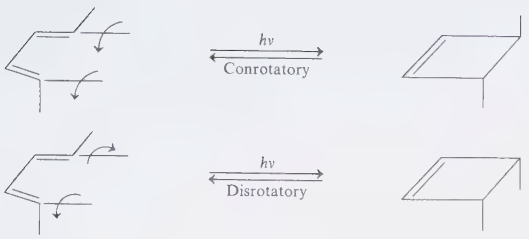

"Forbidden" by orbital interactions (7.2)

"Allowed" by orbital interactions (7.3)

Thus, from a consideration of orbital interactions we expect that for this four-electron system the *disrotatory interconversions are photochemically allowed* (favorable orbital interactions), whereas the *conrotatory interconversions are photochemically forbidden* (unfavorable orbital interactions). We shall see in a later section that the same conclusions may be reached by considering a state correlation diagram for the complete reaction coordinate.

As a second example, consider the typical bimolecular reactions of an excited ketone in its n, π^* state:

1. Abstraction of a hydrogen atom from a hydrocarbon (HX) to produce a ketyl-alkyl radical pair:

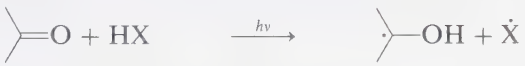

(7.4)

2. Addition to an ethylene to produce a diradical:

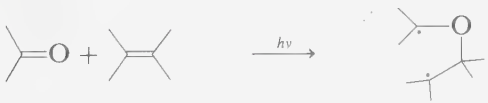

(7.5)

3. Abstraction of an electron from an amine to produce a radical ion pair:

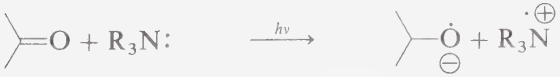

(7.6)

An orbital interaction analysis (Fig. 7.4) reveals that each of these reactions possesses an important similarity: *the most stabilizing orbital interaction is expected to result from charge transfer to the half-filled n orbital of the n, π* state of the ketone*, i.e., $\sigma_{CH} \rightarrow n_O$, $\pi_{CC} \rightarrow n_O$, and $n_N \rightarrow n_O$ respectively. We shall see that a result of this similarity is that these reactions possess state correlation diagrams which are topologically equivalent (qualitatively equivalent connectivity relationships between reactants and products). Because of the dominant interaction of σ_{CH}, π_{CC}, and n_N electrons with the half-filled orbital, we expect the preferred reaction coordinate to be one for which these orbitals are best able to achieve positive overlap

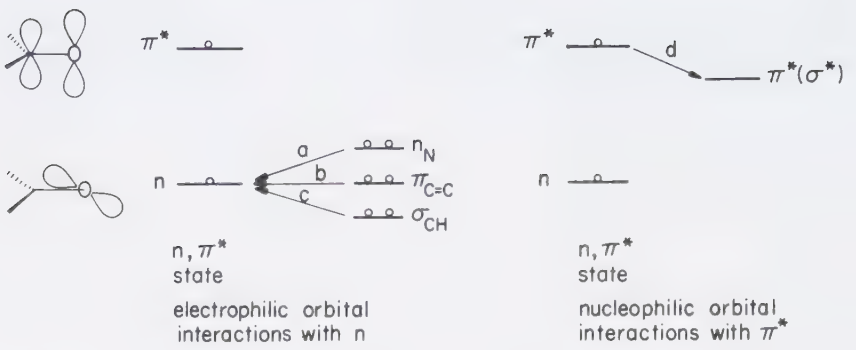

Figure 7.4
Orbital interactions of the n, π^* state with substrates.

with one lobe of the n_0 orbital. This interaction should be important whenever an n, π^* state interacts with a molecule possessing a low ionization potential (i.e., a high-energy HO).

It is also possible that the π^* orbital of the n, π^* state will be important in terms of orbital interactions if the reaction partner possesses a high electron affinity (i.e., a low energy LU).

7.4 Orbital and State Correlation Diagrams

After orbital interactions have been utilized to allow us to postulate the lowest-energy reaction coordinates, we can then employ orbital and state correlation diagrams to deduce the nature of the energy surfaces which connect reactants to primary photochemical products (i.e., deduce the surface topology).

The protocol for the generation of orbital and state correlation diagrams depends heavily on the concept of *molecular and electronic symmetry* (either for the complete molecule or a portion of it). The reader is assumed to be somewhat familiar with this concept, and only a brief review will be given here.[2,3]

Consider the symmetry properties of orbitals which are possible with respect to a plane.[6] If a molecule possesses a plane of symmetry, all of its MO's must be either symmetric (**s**) or antisymmetric (**a**) with respect to reflection through the symmetry plane. For example, for the formaldehyde molecule (Fig. 7.5), the n orbital has **s** symmetry (contained by the molecular plane) and the π (and π^*) orbital has **a** symmetry (above and below the molecular plane) with respect to reflection through the plane. In other words, reflection of the n orbital through the plane does not change the sign of the wave function (**s** symmetry) but reflection of the π (or π^*) orbital through the plane does change the sign of the wave function (**a** symmetry).

Electronic *state* symmetry is a composite or *product* of orbital symmetries.[2] If we know the orbital symmetries relative to a symmetry element and if we know the orbital electron occupations, we can immediately deduce the state symmetries. The protocol for classification of state symmetries is as follows:

1. If only doubly occupied orbitals occur in a configuration, the state symmetry is automatically **S** (totally symmetric).

2. If two (and only two) half-occupied orbitals ϕ_i and ϕ_j occur in a configuration, the state symmetry is given by the following rules:

Orbital symmetry		State symmetry
ϕ_i	ϕ_j	$\Psi_{ij} = \text{---} \phi_i \phi_j$
a	**a**	**S**
a	**s**	**A**
s	**a**	**A**
s	**s**	**S**

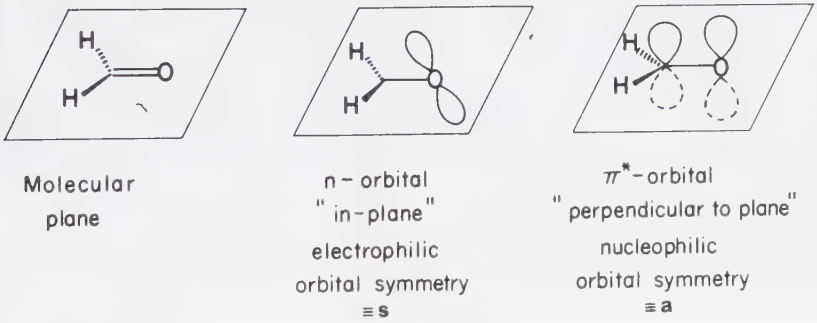

Figure 7.5
The symmetry plane of formaldehyde. The n_0 orbital lies in the symmetry plane and is termed *symmetric* (**s**) with respect to reflection through the symmetry plane. The π^* (and the π) orbital lies above and below the symmetry plane and is termed *antisymmetric* (**a**) with respect to reflection through the symmetry plane.

7.5 The Construction of Electron Orbital and State Correlation Diagrams for a Selected Reaction Coordinate

The construction of electronic state correlation diagrams starts with the selection of a chemical reaction coordinate. This coordinate is based on orbital interactions or experimental data, and describes the nuclear motions of the initial reactant into

a primary product. First a Zero Order correlation of the orbitals of the reactant with the orbitals of the primary product is made.[6,7] Next the noncrossing rule is applied in order to set up the First Order *adiabatic* orbital correlation diagram. The state correlation diagram is then generated by connecting the states of reactants to the states of the primary product. This First Order state correlation diagram is considered to be a *working* set of surfaces, which should have the correct general topology for discussion of the possible mechanisms. Now let us list a specific protocol, or set of general rules, for the construction of an electronic state correlation diagram for a given reaction coordinate:

1. Enumerate and rank energetically the reactant and primary product electronic states (generate a reactant and primary product state energy diagram), using any pertinent theoretical, semi-empirical, or experimental evidence available. A basic goal of the correlation diagram is to determine the connectivity relations of the S_0, S_1, and T_1 states of the reactant to the states of the primary product, and to determine the connectivity relations of the corresponding lowest states of the primary product with the appropriate states of the reactant.

2. Determine the symmetry elements common to the reactant and primary product. Deduce the molecular symmetry in terms of the implied reaction coordinate. Search for symmetry elements which persist throughout the course of the reaction and bisect or contain the bonds being made or broken during reaction. To each orbital assign a symmetry type (symmetric, **s**, or antisymmetric **a**).

3. In order to be useful, a symmetry element selected for correlation must be relevant to the actual chemistry which is occurring. Therefore, the appropriate elements must relate to the bonds being made or broken during the course of reaction. If no such symmetry element exists, it will usually not be possible to construct a meaningful correlation diagram.

4. The *orbitals* of the reactant are now correlated in Zero Order (crossings ignored) with the orbitals of the primary product. The correlation proceeds by the rule that the lowest-energy orbital of reactant of a given symmetry is connected directly to the corresponding orbital of the product.

5. The orbital correlation diagram is inspected for orbital crossings in Zero Order. If these crossings correspond to orbitals of the same symmetry, the crossing is replaced by an avoiding (i.e., the noncrossing rule is applied). The resulting diagram is a First Order (working) *adiabatic* orbital correlation diagram.

6. One now returns to the state energy diagram which displays the electronic configurations and relative energetic rankings of the reactant and product states. To each reactant and product state (usually only the lowest-energy states need be considered explicitly) a characteristic electronic orbital configuration is assigned.

7. Based on the orbital correlation diagram, an orbital symmetry is associated with each orbital of a characteristic orbital configuration, and the state

symmetry is deduced for each electronic state. Corresponding states of the same symmetry are now connected. The connections are continued until the lowest lying states of reactants and the lowest lying states of the primary products have all been correlated. An important rule of making connections between states is that only one connection may be made between any given individual reactant state and any product state. In other words, two product states may not correlate with the same reactant state and vice versa.

8. The *noncrossing rule* is now applied to the state correlation diagram. All curve crossings of states of the same symmetry are replaced by avoidings. The resulting diagram is a First Order adiabatic state correlation diagram.

With the First Order state correlation diagram in hand we have a means of quickly enumerating possibilities of reaction pathways, and by using the theory of radiationless transitions we can judge reactivities and probabilities (efficiencies) of various reaction pathways.

To summarize, first an orbital correlation diagram is generated (orbital symmetry determines connectivity relationships), then orbital configurations are assigned to the lowest energy reactant and product states in the state energy diagram. Finally, a state correlation diagram is generated.

7.6 Typical State Correlation Diagrams for Concerted Photochemical Pericyclic Reactions[3,8]

Let us demonstrate the construction of electronic state energy diagrams for an important type of concerted pericyclic reaction: electrocyclic reactions.[3,8] The ideas presented here are readily extendable to other types of concerted pericyclic reactions, such as sigmatropic rearrangements, cycloadditions, and cheleotropic reactions.[3a]

First let us consider a well-established prototype concerted electrocycle reaction, the rearrangement of cyclobutenes and 1,3-butadienes.

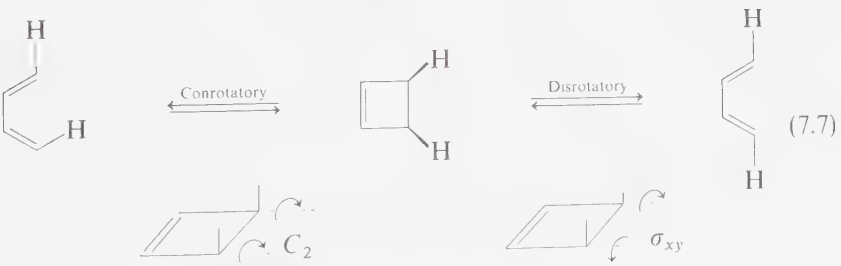

(7.7)

Under the three assumptions that the carbon framework of both molecules is planar, that the carbon framework is still planar in the transition state and that the 1,3-butadiene is formed as a *primary product* in the s-cis-conformation, we deduce two main symmetry elements for the reaction:

1. A twofold axis which bisects the cyclobutene 1,2 and 3,4 bonds and the butadiene 1,2 bond. We call this a C_2-axis. A ring opening or closing which preserves this symmetry element is termed conrotation.

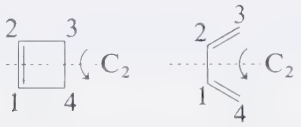

C_2-axes (7.8)

2. A mirror plane of symmetry perpendicular to the molecular plane and bisecting the cyclobutene 1,2 and 3,4 bonds. We call this plane σ_{xy}. A ring opening or closing which preserves this symmetry element is called a *disrotation.*

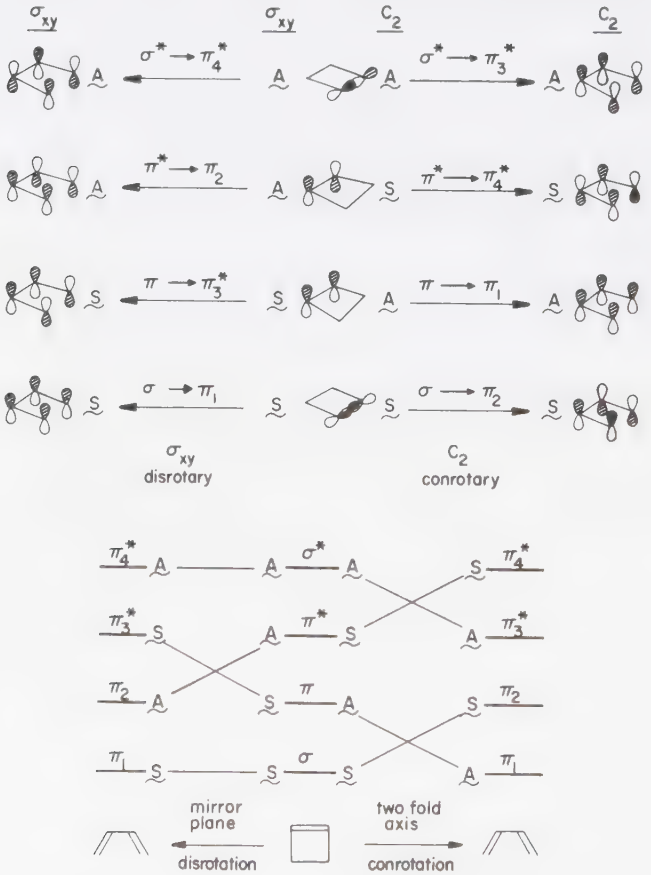

Figure 7.6

Transformation of the four key orbitals of cyclobutene into those of butadiene (top) and orbital correlation diagram (bottom) for the C_2 operation (conrotation) and σ_{xy} operation (disrotation).

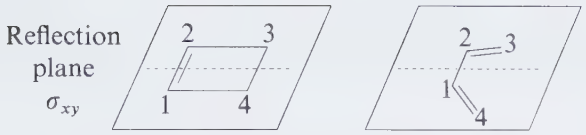

(7.9)

If the cyclobutene to butadiene process occurs with the maintenance of a C_2 or σ_{xy} symmetry element, we can construct a state correlation diagram for both reaction pathways.

Classification of Orbitals and States for the Electrocyclic Ring Opening of Cyclobutene to 1,3 Butadiene

The orbitals of 1,3-butadiene and cyclobutene may now be classified as **a** or **s** for the conrotatory and disrotatory reactions. The results are given in Figure 7.6.[3] From the information in Figure 7.6, the state correlations for the conrotatory and disrotatory reactions can be deduced and used to generate the Zero Order surface correlation diagram shown in Figure 7.7. For example, S_0 (cyclobutene) $= \sigma^2\pi^2$. From Figure 7.6, for a conrotatory motion, σ(cyclobutene) $\rightarrow \pi_2$(butadiene) and π(cyclobutene) $\rightarrow \pi_1$(butadiene). Thus, S_0(cyclobutene) $= \sigma^2\pi^2$ correlates with a

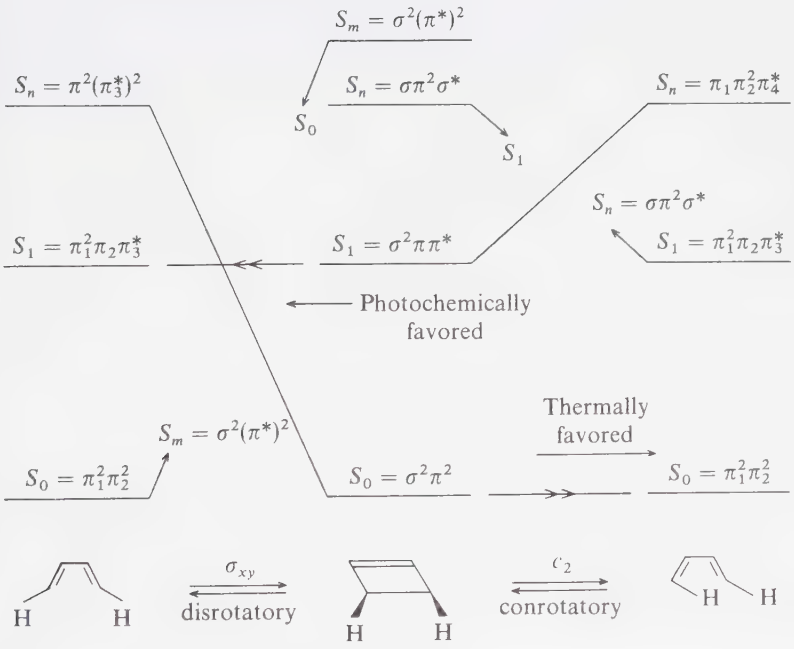

Figure 7.7

Preliminary state correlation diagram for the concerted ring opening of cyclobutene to 1,3-butadiene. Only singlet states are shown. The state correlations are based on the orbital correlations of Figure 7.6.

$(\pi_1)^2(\pi_2)^2$ configuration of butadiene. The latter corresponds to S_0 of butadiene. For a disrotatory motion, S_0(cyclobutene) $= \sigma^2\pi^2$ correlates with a $(\pi_1)^2(\pi_3^*)^2$ configuration of butadiene. The latter corresponds to doubly excited state of butadiene. Similarly, the S_1(cyclobutene) $= \sigma^2\pi, \pi^*$ correlates with a $(\pi_1)(\pi_2)^2(\pi_4^*)$ configuration of butadiene for a conrotatory motion but correlates with a $(\pi_1)^2(\pi_2)(\pi_3^*)$ configuration for a disrotatory motion.

Thus, S_0(cyclobutene) goes uphill in energy during a disrotatory motion but downhill in energy during a conrotatory motion.[9] The reverse is true for a conrotatory motion. A qualitative and preliminary state correlation diagram is given in Figure 7.7. It appears that this diagram predicts zero activation energy for the thermal conversion of S_0(cyclobutene) to butadiene via the conrotatory pathway. In fact, an activation energy[10] of 33 kcal/mole is observed for this reaction. A more proper interpretation of Figure 7.7 is that there is no state–correlation-imposed barrier for the thermal conrotatory reaction but there is a state correlation-imposed barrier for the thermal disrotatory reaction. Recall that the spirit of "allowed" and "forbidden" is really "faster" and "slower" in the sense of reaction rate or probability. In this sense, to the extent that both conrotatory and disrotatory reaction paths are otherwise comparable, the thermal disrotatory pathway is slower ("forbidden") relative to the faster thermal conrotatory pathway ("allowed") because the former automatically experiences a state–correlation-imposed energy barrier. It should be remembered that this discussion presumes *concerted* reactions.

By a similar line of reasoning, it follows that S_1(cyclobutene) should follow the disrotatory pathway preferentially to the conrotatory pathway. It should also be noted that butadienes should undergo favored conrotatory ring closure on S_0 and favored disrotatory ring closure on S_1.

We can complete the diagram (for the singlet states) by adding the correlations of butadiene: for the disrotatory motion $S_0(\pi_1^2\pi_2^2) \rightarrow S_m(\sigma^2(\pi^*)^2)$, and for the conrotatory motion $S_1(\pi_1^2\pi_2\pi_3^*) \rightarrow S_n(\sigma\pi^2\sigma^*)$. The important conclusion is that for both processes a symmetry-imposed barrier occurs along the reaction coordinate (the actual correlation is not shown in order to keep Fig. 7.7 simple and clear).

If we assume that the T_1 surface parallels the S_1 surface, we produce a working *adiabatic* (appropriate crossings are avoided) state correlation diagram as shown in Figure 7.8.

The topology of these surfaces, derived for the specific example of an electrocyclic reaction, has been shown to be general for concerted pericyclic reactions.[3,6] Thus, *all* ground state *forbidden* pericyclic reactions can be expected to have a surface topology qualitatively equivalent to the *disrotatory* ring opening of cyclobutene to butadiene; all ground-state-allowed pericyclic reactions may be expected to have a surface topology qualitatively equivalent to the conrotatory ring opening of cyclobutene to butadiene.

The important features of these surfaces are: (a) the occurrence of a maximum on the S_0 surface (for the forbidden ground-state reaction) which comes close in energy to the S_1 surface and T_1 surface; and (b) the occurrence of a barrier on the S_1 surface (for the allowed ground-state reaction) and (c) the absence of close approach of the excited surfaces and S_0 at any point along the reaction pathway.[9]

The transition state for a *forbidden* ground-state reaction is known to correspond to a diradicaloid structure.[5,6] From the general rules for radiationless transitions such a structure corresponds to a "critical" geometry so that a jump from the S_1 surface to S_0 should be favored from the minimum on the S_1 surface, because the S_1 and S_0 surfaces are very close at this geometry (Fig. 7.9).

To a first approximation the topology state correlation diagram shown in Figure 7.9 below may be extended to all concerted pericyclic reactions. For four (or more generally 4N) electron concerted pericyclic reactions the disrotatory (or stereochemically equivalent) pathway corresponds to motion from the center of the diagram to the right and the conrotatory (or stereochemically equivalent) pathway corresponds to motion from the center of the diagram to the left. We see that this means that four (or 4N) electron concerted pericyclic reactions are generally photochemically allowed.

For six (or more generally 4N + 2) electron concerted pericyclic reactions the disrotatory (or stereochemically equivalent) pathway corresponds to motion from the center of the diagram to the left and the conrotatory (or stereochemically equivalent) pathway corresponds to motion from the center of the diagram to the right. Thus, 4N + 2 electron concerted photoreactions are forbidden.

These ideas are illustrated in Figure 7.9 for the electrocyclic reactions of cyclobutene-1,3-butadiene and 1,3-cyclohexadiene-1,3,5-hexatriene. For example, the disrotatory four electron ring closure of 1,3-butadiene to cyclobutene (and the reverse ring opening) is photochemically *allowed* and the analogous conrotatory electrocyclic reaction is photochemically *forbidden*. In contrast, the conrotatory six electron closure of 1,3,5-hexatriene to 1,3-cyclohexadiene is photochemically *allowed*.

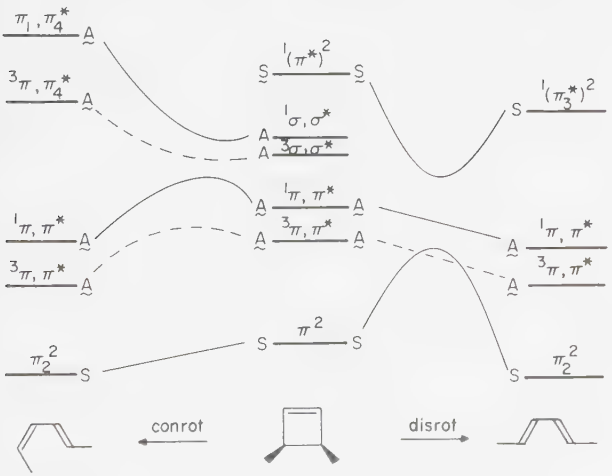

Figure 7.8

Simplified state correlation diagram for the concerted ring opening of cyclobutene to 1,3-butadiene.

In Chapter 12 we shall show how photochemical pericyclic reactions are conveniently and generally analyzed in terms of Figure 7.9.

In summary, pericyclic reactions which are ground–state-forbidden are generally excited–state-allowed in S_1 because the surface topology of S_1 will generally possess a minimum which corresponds to a diradicaloid structure which possesses the geometry of the "antiaromatic" transition state on S_0. By contrast, pericyclic reactions which are ground state-allowed will generally be forbidden on the S_1 surface because of the existence of a barrier to conversion to product structure and the lack of a suitable surface crossing to allow for the occurrence of a radiationless jump from S_1 to S_0.

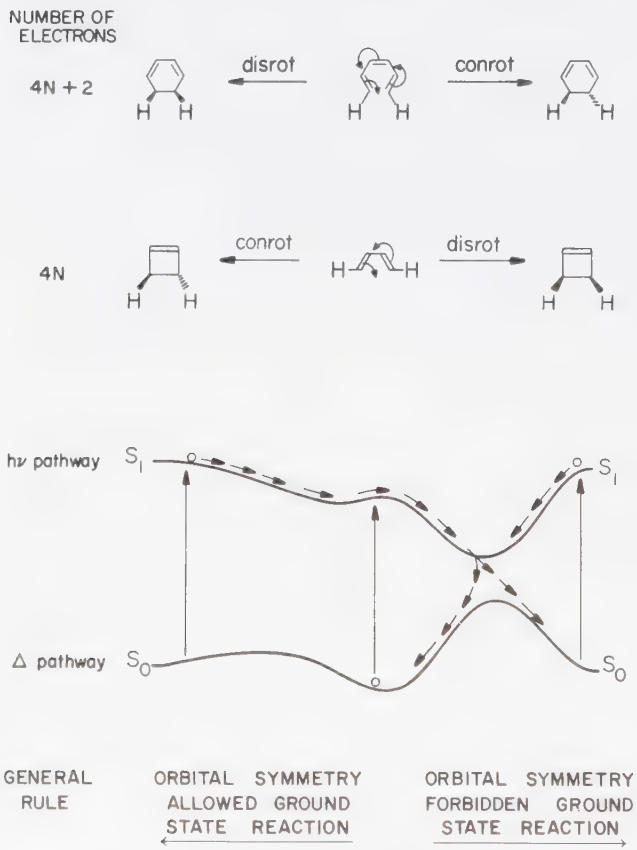

Figure 7.9

A simplified, general schematic description of the two lowest singlet surfaces for a concerted pericyclic reaction. The selection rules are shown for 4N electron and for 4N + 2 electron reactions (N = 0 or an integer and 4N or 4N + 2 is the number of electrons involved in bond making or bond breaking).

7.7 State Correlation Diagrams for Photoreactions Involving Diradical Intermediates

Relatively few photochemical reactions conform to the type of energy diagram indicated in Figure 7.9, i.e., few photoreactions proceed directly to a fully bonded ground-state product via a pericyclic minimum on an excited surface. More commonly, photoreactions produce diradicals or "diradicaloid" structures as primary photochemical products. In order to obtain some insight into the nature of energy surfaces when diradicaloid structures are produced along a reaction coordinate, we shall discuss the surfaces for two prototype reactions which produce diradical structures: (a) the stretching and breaking of a σ bond, and (b) the twisting and breaking of a π bond.

The Stretching and Breaking of a σ Bond

Imagine the chemical bond of a diatomic molecule (a-a) as it is being stretched and eventually broken. As the bond stretches we anticipate that it will take on diradical character, and that when the bond is completely cleaved a diradical (or radical) pair will be produced:[5,6,7]

$$a\text{——}a \xrightarrow[\text{stretch}]{} \underset{\text{diradicaloid}}{a^{\cdot\delta}\text{---}^{\cdot\delta}a} \xrightarrow{\text{cleave}} \underset{\text{diradical}}{\dot{a} + \dot{a}} \qquad (7.10)$$

In fact, four electronic states which correspond to the product nuclear geometry are possible when a σ-bond cleaves. A simple description of the process is shown in Figure 7.10.

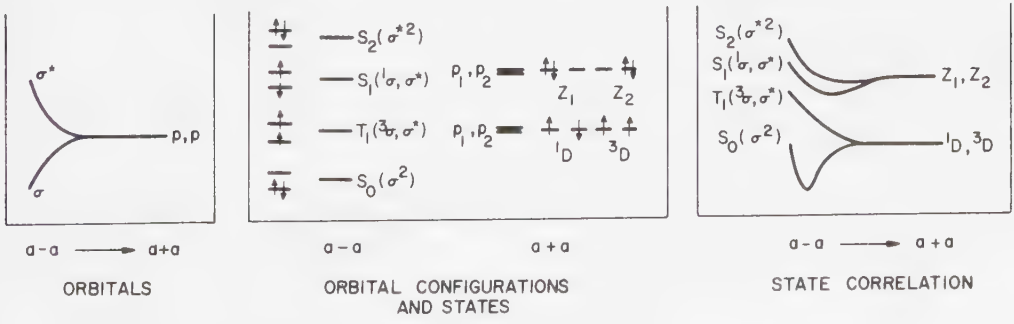

Figure 7.10

Orbitals, orbital configurations, and state correlation diagrams for stretching and breaking of a σ bond.

First let us consider the orbital behavior as the bond stretches. When the nuclei a are close together (close to their equilibrium separation) the σ orbital is very low in energy relative to the σ^* orbital. The electronic states which can be derived for this nuclear geometry are $S_0(\sigma)^2$, $T_1(\sigma, \sigma^*)$, $S_1(\sigma, \sigma^*)$, and $S_2(\sigma^*)^2$. When the nuclei a are far apart, both the σ and σ^* orbitals will correlate with a pair of nonbonding orbitals (say, a p orbital), one on each a atom (Fig. 7.10a). The electronic states which can be derived from completely separated atoms $a + a$ are $^1D(p_1, p_2)$, $^3D(p_1, p_2)$, $Z_1(p_1)^2$, and $Z_2(p_2)^2$. In the terminology employed here, D stands for *diradical* and will always refer to a state in which two orbitals of comparable energy are half-filled, Z stands for *zwitterion* and will always refer to a state in which two orbitals of comparable energy have their electrons all *spin-paired* and all orbitals are doubly occupied (Fig. 7.10b). There are two possible D states, a singlet and a triplet. The Z states are always singlets. Although in the example given, the two Z states would be of identical energy, for any asymmetric bond (a-b) cleavage, one Z state (defined as Z_1) will be lower in energy than the other Z state (defined as Z_2) because one of the possibilities $a(\uparrow\downarrow) + b$ or $a + b(\uparrow\downarrow)$ will generally be of lower energy if a and b are different.

Without making a detailed argument,[5] we expect the state correlation diagram to be as shown in Figure 7.10c. For example, it is clear that the σ orbital will correlate with a p orbital on each of the atoms and lead to a $D(p_1, p_2)$ state in the product. Since S_0 is a singlet, it must correlate with the $^1D(p_1, p_2)$ state. The $T_1(\sigma, \sigma^*)$ state must correlate with $^3D(p_1, p_2)$ since the latter is the only triplet state of the product. By exclusion, *both* $S_1(\sigma, \sigma^*)$ and $S_2(\sigma^*)^2$ must correlate with Z_1 or Z_2.

The state correlation diagram shown is a prototype for cleavage of a σ bond and in fact corresponds closely to the actual surfaces for the hydrogen molecule. This molecule is known to possess shallow minima along the S_1 and S_2 surfaces and these are assumed in the figure to be general for a simple bond cleavage. On the other hand, the triplet state does not possess a minimum for any a-a geometry, but eventually "flattens out" energetically for large separations of the atoms, and for large separations the triplet surface essentially "touches" the ground-state surface. S_0, of course, possesses a deep minimum corresponding to the stable ground state of the molecule.

In summary, a simple σ bond cleavage possesses the following surface characteristics:

1. Along the ground surface the bond is stable and a large activation energy is required for cleavage.

2. Along the triplet surface the bond is unstable and little or no activation energy is required for cleavage.

3. The products of cleavage along S_0 or T_1 are *diradicals*.

4. Along the S_1 and S_2 surfaces the bond is metastable and requires only a small amount of energy for cleavage.

5. The products of cleavage along S_1 or S_2 are *zwitterions*.

The Twisting and Breaking of a π Bond

Imagine an ethylene molecule which is twisted and which eventually arrives at a nuclear geometry for which the two methylene groups are mutually perpendicular:

Both CH_2 groups in the same plane  CH_2 groups perpendicular (7.11)

At this geometry we would guess that the π bond is broken and that a 1,2-diradical is produced. In terms of a standard structure equation we might write:

$$CH_2{=}CH_2 \rightarrow \dot{C}H_2{-}\dot{C}H_2 \qquad (7.12)$$

In fact, as in the case of σ bond cleavage, four electronic states which correspond to the twisted product nuclear geometry are possible when we break a π bond by twisting about the bond axis. Again, two diradicals and two zwitterions result (Fig. 7.11). As the π bond twists, the energy of the π orbital sharply increases, and the energy of the π^* orbital sharply decreases. At 90° of twist (the perpendicular configuration) the π and π^* orbitals have transformed into two p orbitals, one on each carbon. In wave-mechanical terms, the wave function of the π orbital is given by $p_1 + p_2$ and the wave function of the π^* orbital is given by $p_1 - p_2$. As the molecule is twisted, the molecular orbitals transform into a pair of nonbonding p orbitals (Fig. 7.11a).

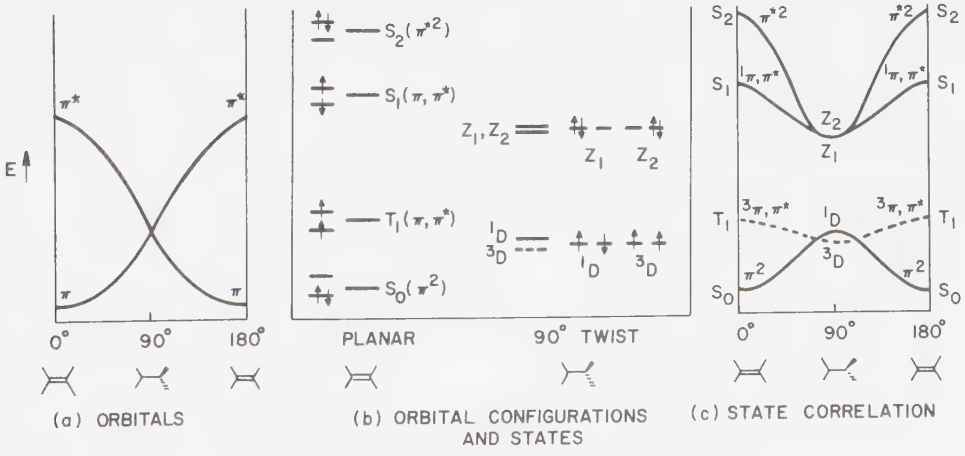

Figure 7.11
Orbitals, orbital configurations, and state correlation diagrams for twisting a π bond.

The electronic states derived from the possible π and π^* orbital configurations are:[4]

$$\begin{aligned} &\text{Planar ethylene:} \quad S_0(\pi)^2,\ T_1(\pi, \pi^*),\ S_1(\pi, \pi^*), \text{ and } S_2(\pi^*)^2 \\ &90^\circ \text{ Twisted ethylene:}\ {}^3D(p_1, p_2),\ {}^1D(p_1, p_2),\ Z_1(p_1)^2, \text{ and } Z_2(p_2)^2 \end{aligned} \tag{7.13}$$

Twisting about the carbon-carbon bond of excited ethylene sharply relieves electron-electron repulsion and will thereby tend to lower the energy of any ethylene state for which π bonding is not important. Thus, the electronic energies of S_2, S_1, and T_1 *drop* rapidly as a function of the ethylene twisting, because electronic excitation has effectively broken the π bond. However, the electronic energy of S_0 *increases* as the molecule is twisted because the π bond is being broken.

The correlation of $S_0 \rightarrow {}^1D$, $T_1 \rightarrow {}^3D$, $S_1 \rightarrow Z_1$, and $S_2 \rightarrow Z_2$ may be made on the basis of orbital symmetry considerations. The symmetry element which brings the starting planar geometry into the twisted (diradicaloid) geometry is a rotation of one CH_2 group.[4] The overall state symmetries must be definable in terms of this symmetry element. Although the state correlation is best done by use of group theory and point-group analysis, the following qualitative description will indicate the basis of the correlation.

The wave function for the π^2 configuration (Fig. 7.11b) at the planar geometry is essentially *covalent* in character,[5] i.e., there is very little ionic character to planar ethylene, and the wave function for π^2 has (in terms of atomic orbitals) the form $p_1(\uparrow)p_2(\downarrow)$. This means that at all times there is only one p electron near carbon 1 and one near carbon 2, and these electrons have paired spins. For the ${}^3(\pi, \pi^*)$ configuration at the planar geometry there can *never* be two electrons on one carbon in the same p orbital (violation of the Pauli principle), since the electrons have parallel spins. The T_1 state is purely covalent and has no ionic character, and its wave function has the form ${}^3(\pi, \pi^*) = p_1(\uparrow)p_2(\uparrow)$.

The wave functions for ${}^1(\pi, \pi^*)$ and ${}^1(\pi^*)^2$ must differ from that of π^2 and must reflect the basis for the high energy content of the state. It is found that the former two states are best described by zwitterionic wave functions.

The important qualitative features of the state correlation diagram for a twist about the ethylene double bond (Fig. 7.11c) are:

1. The occurrence of minima in the S_2, S_1, and T_1 surfaces which correspond to Z_2, Z_1, and ${}^3D$ respectively.

2. The avoided crossing nature of the minimum at Z_2, i.e., the Zero Order $\pi^2 \rightarrow (\pi^*)^2$ correlation is strongly avoided and the adiabatic surfaces show a minimum in S_1 and a maximum in S_0.

3. The occurrence of a maximum in the S_0 surface which corresponds to ${}^1D$.

4. The absence of any avoided crossings with small energy gaps.

5. The zwitterionic (closed shell) behavior of S_2 and S_1.

6. The diradical behavior of T_1.

Note that the state correlation diagrams for *thermally forbidden* ground-state pericyclic reactions have the general form of those for twist about the double bond of ethylene (see Fig. 7.11).

7.8 Typical State Correlation Diagrams for Nonconcerted Photoreactions: Reactions Involving Intermediates (Diradicals and Zwitterions)[4,5]

The majority of known photoreactions of organic molecules are probably not *concerted* in nature; i.e., they tend to involve intermediates along the reaction pathway between reactant (photoexcited molecule) and product. The most common photochemical intermediates are species which are not fully bonded, i.e., diradicals and zwitterions. Consider Figure 7.12, which shows the relationships among electronically excited molecules, diradicals, zwitterions, and high-energy-content ground state molecules. An electronically excited state may generally be viewed in terms of two characteristic half-filled orbitals. Motion along a reaction coordinate due to stretching a σ-bond or due to twisting a π-bond may bring the representative point to a geometry for which the two half-filled orbitals are nearly degenerate. In this geometry[5] the molecule is termed a "diradicaloid." Interactions between the orbitally unpaired electrons of the diradicaloid generate *four* states: a diradical singlet ^1D; a diradical triplet ^3D; and, two zwitterionic singlets, Z_1 and Z_2. The postulate that an electronically excited state tends toward a D or Z primary product as a reaction proceeds is an exceedingly powerful device for interpreting the photoreactions of organic molecules.

It is not uncommon for the representative point, while moving along an excited surface, to achieve a geometry similar to a "strained ground state molecule." Radiationless transitions to such structures may produce very strained species which are, nonetheless, stable on the ground state surface. Indeed, we shall see that photoreactions often produce strained ground state molecules as products.

Photochemical Hydrogen Abstraction

The photoreaction of excited ketones with alcohols (Eq. 7.4) to produce pinacols involves a radical pair intermediate.[11] The state correlation diagram for this reaction is typical of a large class of photoreactions which involve diradical intermediates (compare Eqs. 7.4, 7.5 and 7.6). As a result we shall treat it in some detail. For most alkanones, $S_1 = n, \pi^*$ and $T_1 = n, \pi^*$. Thus, our correlation diagram will seek to connect these states, and $S_0 = \pi^2 n^2$ with the appropriate states of the product (diradicals and zwitterions). What is a proper and probable reaction coordinate for hydrogen abstraction? To determine the most likely reaction coordinate we must select the most favorable orbital interactions, search for elements

of symmetry in the geometry of the reactants that lead to the most favorable orbital interactions, and then relate that symmetry element to establish a correlation along the reaction coordinate of the reactant to the primary product transformation.

Recall that orbital interactions suggested that the charge transfer to the half-filled n orbital from the H-X σ bond should serve as a reasonable Zero Order description of the most favorable initial interactions of $R_2C{=}O^*$ and H-X (Fig. 7.4). The most symmetrical geometry of approach of $R_2C{=}O^*$ and H-X which allows the $n \leftarrow \sigma$ interaction is one in which the C=O and H-X groups are coplanar (Fig. 7.13). Since the energy of this geometry should be comparable to other nonplanar geometries in which the $n \leftarrow \sigma$ interaction is occurring, we shall

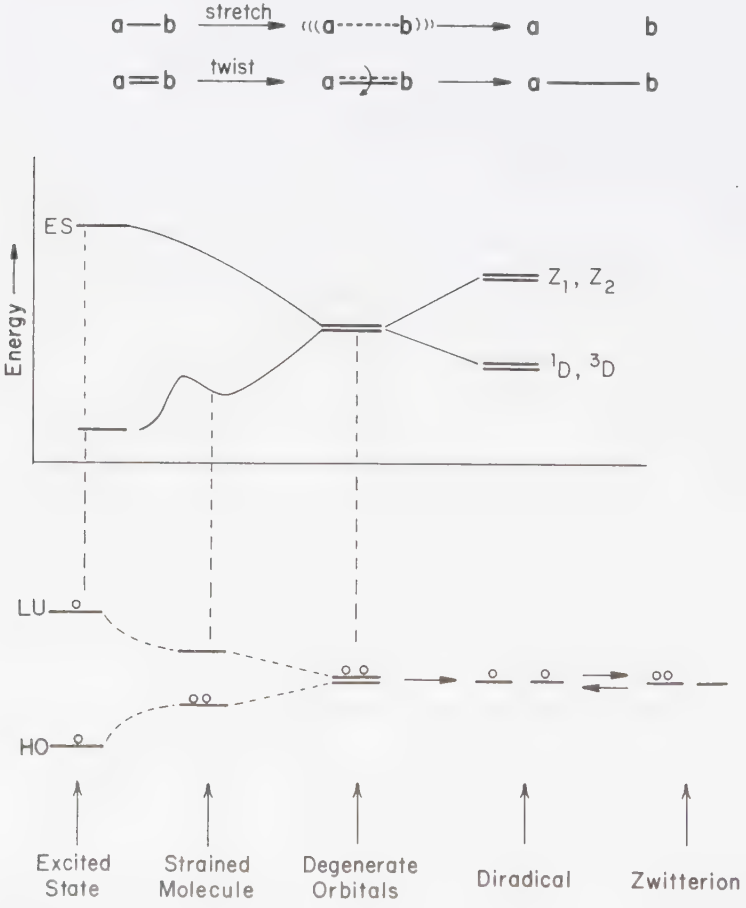

Figure 7.12

Schematic description of the surface relationships of excited states, strained ground state molecules, diradicals, and zwitterions.

generate a state correlation diagram *assuming* that the strictly planar approach represents the reaction coordinate. This assumption of an idealized coplanar reaction should provide a reasonable, qualitative Zero Order description of the surfaces. In general, the *plane* containing the pertinent reaction centers will be a *discriminating symmetry element* for selecting the reaction coordinates of n, π^* states which lead to diradicaloid geometries. Let us now consider this assumption in greater detail.

The Symmetry Plane Assumption: Salem Diagrams[6]

Qualitative state correlation diagrams for photochemical reactions may sometimes be generated by inspection and without resort to detailed computation if the reactions are postulated to possess an (idealized) symmetry element such as a plane. This is a commonly encountered situation for reactions involving n, π^* states. If the symmetry element is the molecular plane, the analysis is particularly straightforward under certain conditions. An idealized symmetry plane refers only to the plane containing the nuclei *directly* involved in the electronic excitation. These nuclei, in turn, are identified under the single characteristic configuration approximation, i.e., the electronic symmetry of each low-lying excited state is postulated to be determined by a single electronic orbital configuration. Under these assumptions the correlation between states of the same symmetry

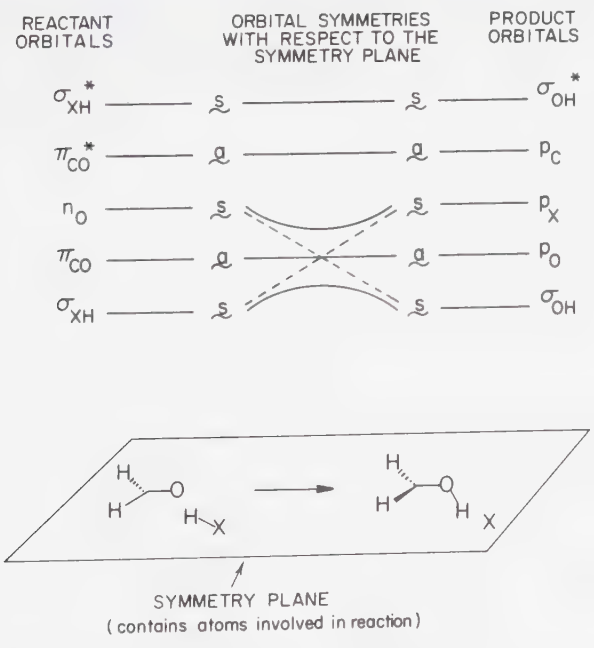

Figure 7.13
Orbital correlation diagram for coplanar hydrogen abstraction by formaldehyde.

may be made by a simple electron classification and counting procedure. In turn, this classification and count may be simplified by using classical resonance structures for describing the electronic states involved. These resonance structures can only possess electrons in orbitals which are either symmetric, **s** (do not change sign upon idealized reflection in the symmetry plane), or antisymmetric, **a** (change sign upon idealized reflection in the symmetry plane). The postulate of an idealized symmetry plane demands that orbitals possess either **a** or **s** symmetry.

State Correlation Diagram for Photochemical Hydrogen Abstraction

The pertinent orbitals for analysis of coplanar hydrogen abstraction are shown in Figure 7.13. The orbitals of the reactants are classified relative to the symmetry plane in a conventional notation. Any orbital which lies "in the plane" must be of **s** symmetry (i.e., σ_{XH}, n_O, and σ^*_{XH}). Any orbital that exists "above and below" the plane must be of **a** symmetry (i.e., π_{CO} and π^*_{CO}).

The pertinent product orbitals are σ_{OH} and σ^*_{OH} (both of **s** symmetry) and the p orbitals on carbon (p_C "above and below," **a**), the p orbital on X (p_X "in the plane," **s**), and the p orbital on O (p_O "above and below," **a**). From Figure 7.13, the initial (Zero Order) orbital correlations are maintained during reaction, except for the $\sigma_{XH} \leftrightarrow p_X$ and $n_O \leftrightarrow \sigma_{OH}$ correlations which are avoided (noncrossing rule for orbitals of the same symmetry).

Remember that completely filled orbitals are always totally symmetric (**S**) with respect to a symmetry element (i.e., $\mathbf{A} \times \mathbf{A} = \mathbf{S}$ and $\mathbf{S} \times \mathbf{S} = \mathbf{S}$), but half-filled orbitals *may* be **A** (i.e., $\mathbf{A} \times \mathbf{S} = \mathbf{A}$). Since the state symmetry is the composite of all filled and unfilled orbitals, we can deduce the state symmetry of reactants by evaluating the product of the symmetry of appropriate reactant and primary product orbitals.

From Figure 7.13, the state symmetries of the reactants and products are easily deduced. For example, S_0 must be of **S** symmetry because it possesses only doubly occupied orbitals. The symmetry of the n, π^* state is $\mathbf{s} \times \mathbf{a} = \mathbf{A}$, the symmetry of the π, π^* state is $\mathbf{a} \times \mathbf{a} = \mathbf{S}$, the symmetry of the $D(p_C, p_X)$ state is $\mathbf{s} \times \mathbf{a} = \mathbf{A}$, and the symmetry of a Z state must be **S** because it possesses only doubly occupied orbitals.

We may now proceed to the Zero Order state correlation diagram or *Salem diagram* (Fig. 7.14) by connecting states of the same symmetry. We need consider only the number of states necessary to correlate S_1 and T_1 with product states. From Figure 7.14 we see that both S_1 and T_1 states correlate directly with the lowest states of the product, i.e., $S_1 = {}^1n, \pi^*$ correlates with ${}^1D$ and $T_1 = {}^3n, \pi^*$ correlates directly with ${}^3D$. We say that coplanar hydrogen abstraction to form ketyl radicals from $S_1(n, \pi^*)$ or $T_1(n, \pi^*)$ is symmetry-allowed. By this we mean that in Zero Order, there is no electronic symmetry-imposed energy barrier on the surface connecting the initial excited state n, π^* of a given spin and the lowest energy primary (diradical) product of the same spin.

On the other hand, the S_2 and T_2 states (both π, π^*) correlate with excited states of the zwitterion forms of the product. These excited zwitterionic states

are expected to have very high energies relative to S_2 and T_2. As a result, if S_2 or T_2 were to attempt to participate in coplanar hydrogen abstraction, a symmetry-imposed energy barrier would have to be overcome. We say that coplanar hydrogen abstraction to form ketyl radicals is *symmetry-forbidden* from $S_2(\pi, \pi^*)$ or $T_2(\pi, \pi^*)$.

We may now propose how a First Order surface description of the hydrogen abstraction reaction may be derived from Figure 7.14. Destruction of the perfect coplanar geometry will result in a weakly avoided crossing between the $S_1 \rightarrow {}^1D$ and $S_0 \rightarrow Z$ surfaces. However, the $T_1 \rightarrow {}^3D$ and $S_0 \rightarrow Z$ crossing will remain, since the multiplicity (spin symmetry) of the crossing surfaces is still different. The result of the avoided crossing is to put a minimum along the S_1 surface.

From Figure 7.14 we conclude that there are two low-energy pathways from n, π^* states for the representative point in coplanar hydrogen abstraction reactions. These two pathways are:

1. From the ${}^1n, \pi^*$ state the representative point may proceed to decrease its energy until it reaches the geometry corresponding to the avoided crossing (AC)

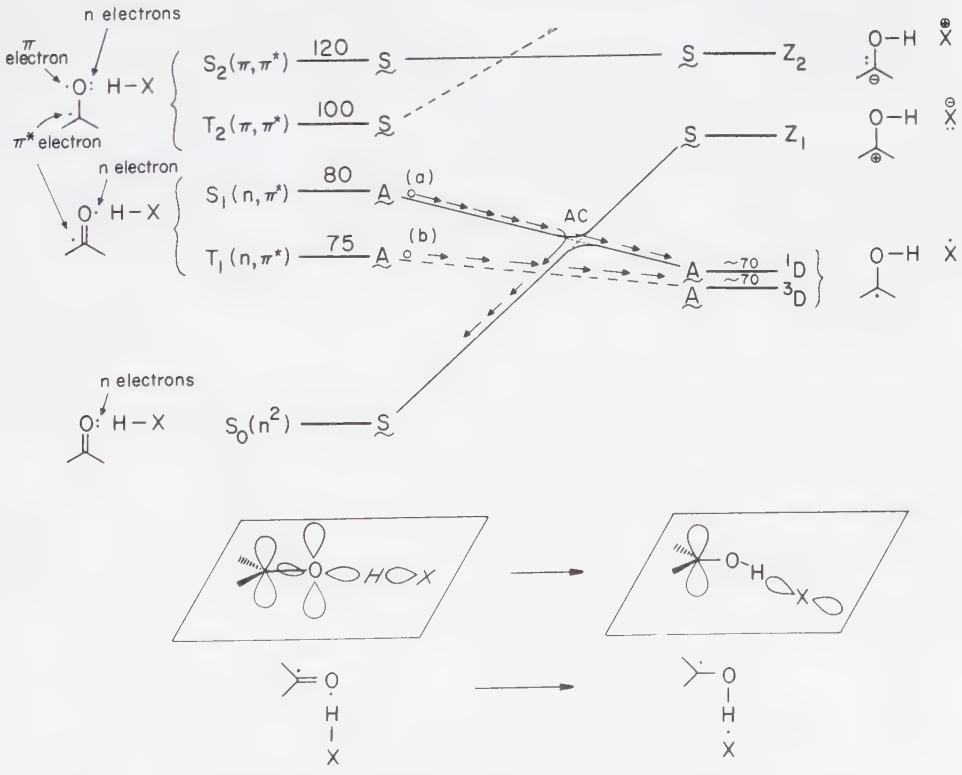

Figure 7.14

First Order correlation diagram for coplanar hydrogen abstraction. State energies in kcal/mole.

minimum. What are the consequences of this avoided crossing? We note that the occurrence of AC has no effect on *reactivity*, i.e., the rate of reaction is determined by the energy barriers near the S_1 minimum. These small activation energies are not due to correlation effects. However, the *efficiency* of reaction from S_1 may be decreased since the AC minimum allows partitioning from the excited surface to either S_0 or ^1D (by providing a "Born-Oppenheimer hole" for radiationless transition from S_1 to S_0 or D_1), whereas in the Zero Order only passage from S_1 to ^1D was allowed.

2. From the $^3n, \pi^*$ state the representative point may decrease its energy by moving directly to ^3D, i.e., proceeding through the crossing of T_1 and S_0 surfaces. Of importance is the fact that the reactivity and efficiency of T_1 are the same in both First and Second Order. In Second Order (avoidance between electronic states of different spatial symmetry *and* of different spin multiplicity), we generate a small splitting near the intersection of S_0 and T_1. In this Second Order, very weak avoidance will allow various intersystem crossings to occur, but such processes are not expected to be important in general.

In Chapter 10, we shall see that all of the qualitative features (reactivity, efficiency, and primary product structures) expected from Figure 7.13 have experimental support.

Extension of a Given State Correlation Diagram to New Situations

A combination of the methods of orbital interactions and state correlation diagrams allows us to generalize the correlation diagram for hydrogen abstraction. At the orbital level, the key electronic features of hydrogen abstraction are the withdrawal of electronic charge from a H-X σ orbital by the half-filled n orbital. We may postulate that any reaction whose electronic mechanism is dominated by electrophilic attack by the n orbital will have the same surface topology as that deduced for hydrogen abstraction (Fig. 7.14).

For example, n, π^* states of ketones are known to (a) abstract electrons from amines (and other electron donors), (b) add to electron-rich ethylenes, and (c) transfer energy to electron-rich unsaturated compounds. On the basis of orbital interactions, each of these reactions is expected to be dominated by electrophilic attack by the n orbital of the n, π^* state. In each case a diradical intermediate is possible and the same generalizations and expectations as were made for hydrogen abstraction are possible. In other words, the topology of Figure 7.14 may be employed for the three reactions discussed above.

7.9 State Correlation Diagrams for α-Cleavage of Ketones[10]

A commonly observed fragmentation reaction of n, π^* states of carbonyl compounds is the cleavage of a σ bond which is α to the excited carbonyl group.[11]

For example, the n, π^* states of acetone undergoes α-cleavage to acyl and methyl radicals:

$$CH_3COCH_3 \xrightarrow{h\nu} \underset{n,\,\pi^*}{CH_3COCH_3} \longrightarrow CH_3\dot{C}O + \dot{C}H_3 \qquad (7.14)$$

This reaction is a prototype for the second major reaction type of n, π^* states. The reaction coordinate in this case is essentially the distance separating the carbonyl carbon and methyl carbon atoms (some motion of the CH_3-CO moiety may also occur). S_1 and T_1 are n, π^* and both are **A** with respect to the characteristic symmetry plane associated with the reaction. The primary product states at the diradicaloid geometry are of two types: (a) those corresponding to a bent $CH_3\dot{C}O$ group, and (b) those corresponding to a linear $CH_3\dot{C}O$ group. The two lowest energy electronic states of these structures have different electronic symmetries relative to the characteristic symmetry plane. This result occurs because the bent form of $CH_3\dot{C}O$ will be sp^2 hybridized at the carbonyl carbon, whereas the linear $CH_3\dot{C}O$ will be sp hybridized at the carbonyl carbon (Fig. 7.15). The radical site (sp^2 orbital) generated in the bent acyl group remains in the symmetry plane, and is therefore **s** with respect to coplanar cleavage. The linear acyl group possesses a π_s orbital which is in the symmetry plane and a π_a orbital which is perpendicular to the symmetry plane. Thus, the π_s orbital is **s** and the π_a orbital is **A** with respect

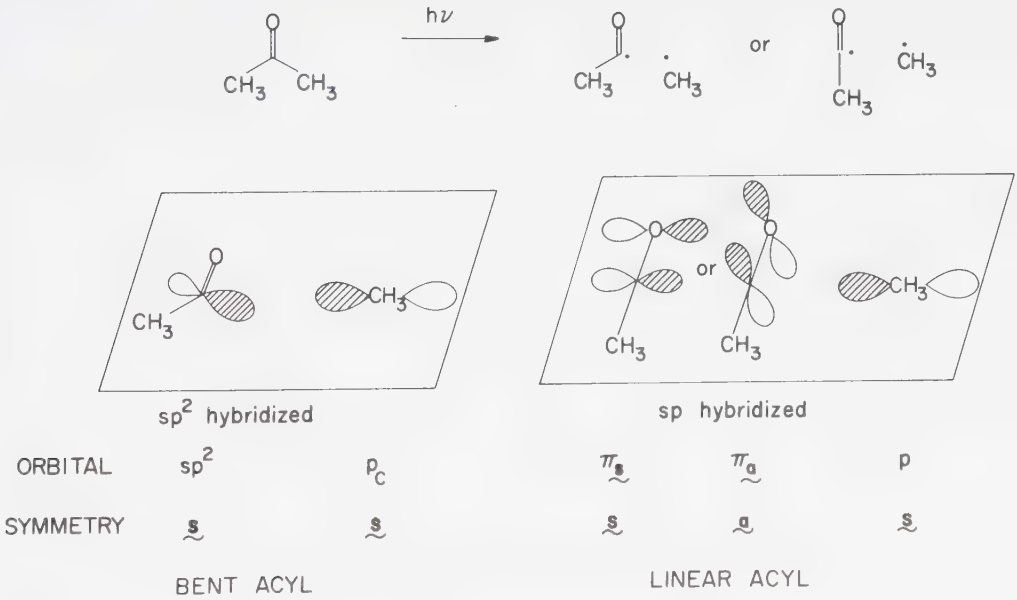

Figure 7.15
Two pathways of α-cleavage of acetone. Either a bent acyl or a linear acyl fragment may be formed.

to coplanar cleavage. Thus, two degenerate electronic states correspond to the linear acyl-methyl radical pair. One state (π_s, p) is **S** and the other state (π_A, p) is **A**. The number of distinct radical sites developed during a reaction is termed the *reaction topicity*.[6] Since α-cleavage to produce a bent acyl radical and alkyl radical produces two distinct radical sites, it is said to have a topicity equal to two. On the other hand, α-cleavage to produce a linear acyl radical and alkyl radical produces three distinct radical sites and is said to have a topicity of three. In the latter case, an odd electron may be in the π_s or π_a orbital, leading to two different diradical pairs.

Topicity can have a major influence on the topology of a correlation diagram. Let us construct the correlation diagram for α-cleavage by proceeding in the usual manner. First we identify the symmetry of the key orbitals involved in the transformation. The orbital correlation is given in Figure 7.16. Notice that the half-filled orbital on CH_3 is assumed to be a p orbital contained by the discriminating reaction plane, i.e., this orbital is of **s** symmetry.

We may now construct the Zero Order state correlation diagram (Fig. 7.17). In the case of cleavage to form a linear acyl fragment, the lowest excited states $S_1(n, \pi^*)$ and $T_1(n, \pi^*)$ correlate directly to low-lying $^1D(\pi_a, p_c)$ and $^3D(\pi_a, p_c)$ states. However, for the cleavage to form bent acyl, $S_1(n, \pi^*)$ and $T_1(n, \pi^*)$ correlate with excited forms of D, namely $D^*(sp^2, \pi^*_{co})$. As a result, the initial slope of the surface for cleavage from an n, π^* state to a bent acyl rises steeply as this state tries to correlate with D^*.

From the Zero Order diagram (Fig. 7.17) we deduce that α-cleavage of n, π^* states to yield a linear acyl fragment is symmetry-allowed, but that α-cleavage of n, π^* states to yield a bent acyl fragment is symmetry-forbidden.[12] Thus, the pathway of higher topicity is allowed, whereas the pathway of lower topicity is forbidden.

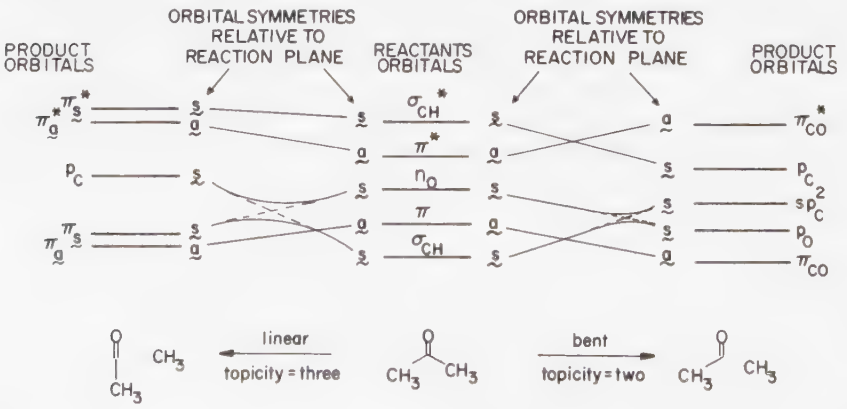

Figure 7.16
Orbital correlation diagrams for bent (right) and linear (left) α-cleavage of acetone.

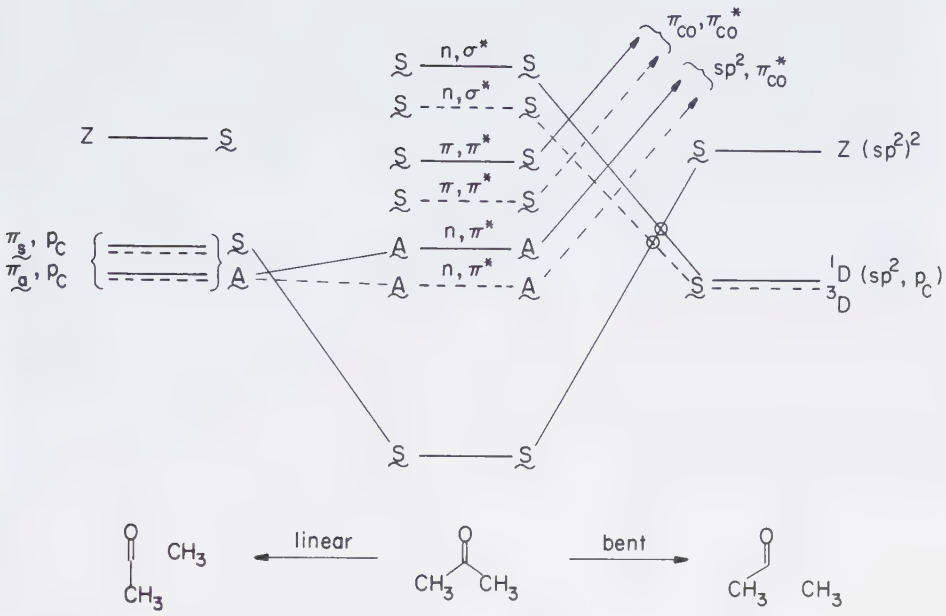

Figure 7.17

Zero Order state correlation diagram for bent (right) and linear (left) α-cleavage. Circled crossings are weakly avoided.

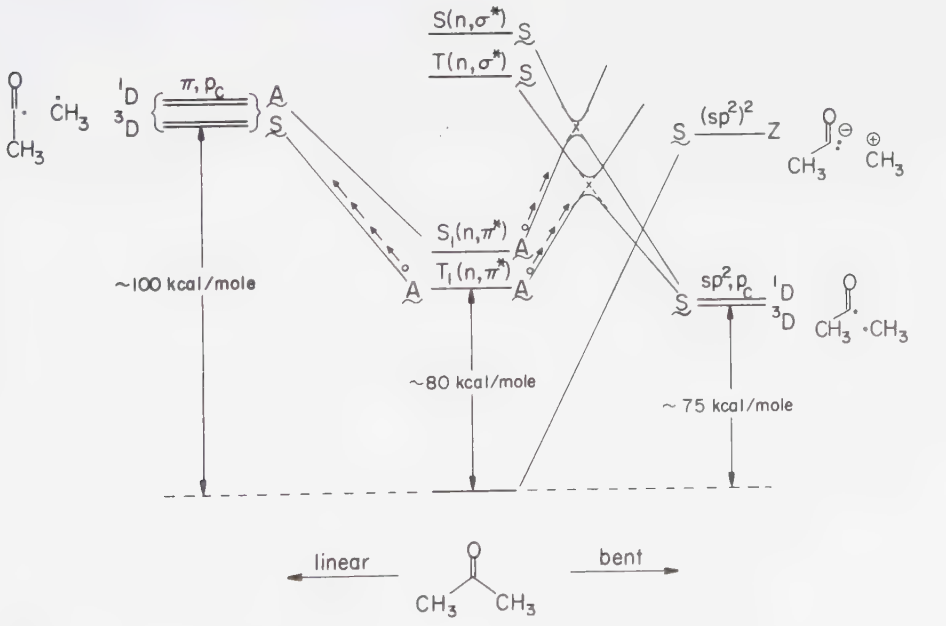

Figure 7.18

First Order correlation diagram for α-cleavage.

Now let us consider a more realistic First Order correlation diagram (Fig. 7.18) which depicts α-cleavage for acetone. The state and diradical energies are also shown. The situation for cleavage to the linear fragment is essentially the same. However, weakly avoided crossings occur along the surfaces for cleavage to the bent acyl fragment (circled in the Zero Order diagram, Fig. 7.17). Notice, however, that the $T_1(n, \pi^*)$ surface is subject to a First Order crossing at an earlier point than $S_1(n, \pi^*)$. This earlier crossing may lead to a lower energy symmetry-imposed energy barrier for cleavage of $T_1(n, \pi^*)$ relative to $S_1(n, \pi^*)$.

From Figure 7.18 we expect that α-cleavage of acetone will be an activated process no matter which pathway is followed. Furthermore, if the energy of the linear diradical pair is lowered by structural effects (e.g., release of ring strain in a cyclic enone or stabilization of the acyl or alkyl radical sites), the linear pathway may be specifically favored, since a symmetry-imposed barrier does not occur along this reaction coordinate. In Chapter 13 we shall see that all of the important qualitative features of Figure 7.18 have experimental support.

7.10 A Standard Set of Primary Photoreactions for π, π^* and n, π^* States

We have noted that the most commonly encountered lowest-energy excited states of organic molecules may be classified as $S_1(\pi, \pi^*)$, $T_1(\pi, \pi^*)$, $S_1(n, \pi^*)$, or $T_1(n, \pi^*)$. In this chapter we have seen how theory can lead (a) to a prediction of the possible (i.e., low-energy) primary photochemical processes via the consideration of orbital interactions, and (b) to the generation of the network of surface (reaction) pathways via the maps which result from state correlation diagrams. Now we can list the possible primary photoreactions of S_1 and T_1 based on the above theoretical considerations.

The Characteristic Primary Photochemical Process of π, π^* States

We expect $S_1(\pi, \pi^*)$ states to undergo concerted pericyclic photoreactions such as:

1. Electrocyclic rearrangements.
2. Cycloadditions and Cycloeliminations.
3. Sigmatropic rearrangements.

The favored stereochemical pathways of these reactions can be predicted by considering orbital interactions, and the prototype surface topology for such reactions will be analogous to Figures 7.7 and 7.8.

$S_1(\pi, \pi^*)$ states will often possess a substantial zwitterionic character, which will result in proton or electron transfer reactions, nucleophilic or electrophilic

additions, or rearrangements to produce intermediates which will then proceed to isolated products.

Finally, $S_1(\pi, \pi^*)$ of ethylenes and polyenes will often possess an inherent tendency to twist its double bonds, which is a process that leads to twisted zwitterionic intermediates and/or cis-trans isomerization.

Granted that $S_1(\pi, \pi^*)$ has the *possibility* of the above set of characteristic reactions, the rate of any one of these reactions will depend on the reactant structure and the reaction conditions. The probability of any reaction from $S_1(\pi, \pi^*)$ will depend on a competition between the rate of reaction and the rate of other photophysical or photochemical pathways from $S_1(\pi, \pi^*)$.

$T_1(\pi, \pi^*)$ is not expected to undergo concerted pericyclic reactions unless the product can be produced in a triplet state or if a good spin-orbit coupling mechanism is available. More commonly, $T_1(\pi, \pi^*)$ will generate a primary diradical product, ^3D, which will then proceed to initiate reactions leading to the eventual isolated products. For example, we expect $T_1(\pi, \pi^*)$ to undergo primary photoreactions characteristic of radicals such as:

1. Hydrogen atom or electron abstractions.
2. Addition to unsaturated bonds.
3. Radicaloid rearrangements.
4. Homolytic fragmentations.

In addition, $T_1(\pi, \pi^*)$ will generally possess an inherent driving force to twist about double bonds, a process that could lead to cis-trans isomerization or twisted diradical intermediates.

The Characteristic Primary Photochemical Processes of n, π^* States

The photochemistry of n, π^* states can be expected to contrast with that for π, π^* states in two major respects: (a) the photochemistry of $S_1(n, \pi^*)$ and $T_1(n, \pi^*)$ for a given molecule should be qualitatively identical and differ only quantitatively. Reactions expected from $S_1(\pi, \pi^*)$ and $T_1(\pi, \pi^*)$ differ qualitatively, i.e., zwitterionic and/or concerted versus radicaloid, respectively; and (b) the photochemistry of n, π^* states is completely diradicaloid to a good approximation, i.e., $n, \pi^* \rightarrow D$ processes are typical.

Based on an orbital interaction analysis (Fig. 7.4), and the postulate that all n, π^* reactions proceed preferentially via D states (Fig. 7.14), we can conclude that the primary photochemical processes of n, π^* will produce radicals and that the overall photoreactions will mimic radical chemistry. Let us consider that the plausible primary processes expected from a theoretical standpoint are:

n-Orbital Initiated	π^*-Orbital Initiated
Atom abstraction	Atom abstraction
Radical addition	Radical addition
Electron abstraction	Electron donation
α-Cleavage	β-Cleavage

Although both atom abstraction and radical addition are expected in theory to be initiated by either the n or by the π^* orbitals, the former will exhibit *electrophilic* and the latter will exhibit *nucleophilic* characteristics. Furthermore, the stereoelectronic dispositions of the reactions will differ, depending on which orbital dominates the electronic interactions with the substrate. For example, if the n orbital initiates the interaction, the reaction will be sensitive to steric factors influencing the approach of the substrate in the plane of the molecule and near the "edges" of the carbonyl oxygen. On the other hand, if the π^* orbital initiates the reaction, the reaction will be sensitive to steric factors which influence the approach of the substrate above and below the "faces" of the carbonyl function. Convincing experimental support for this prediction is given in Chapter 11.

Since the π^* orbital is delocalized, attack may be initiated predominantly at the carbon atom or at the oxygen atom. Ignoring the specifics of the substrate (which is either an atom donor or an electron abstractor), we note that if the reaction is initiated by the π^* electron, only the addition to carbon produces a low-energy diradical state. Attack of the π^* orbital to produce a bond to oxygen produces an electronically excited diradical and will therefore encounter a symmetry-imposed energy barrier.

7.11 Conclusion: Energy Surfaces as Reaction Maps or Graphs

Orbital interactions and state correlation diagrams provide the basic elements of a qualitative theory of photoreactions. The *possible* products of a photoreaction which starts from a particular state may be deduced from state correlation diagram maps. The *probable* products may also be deduced from consideration of (a) symmetry-imposed barriers, and (b) minima which facilitate pathways from an excited surface to the ground state.

The difficulties in establishing a *quantitative* theory of photoreactions are substantial. Photoreactions are at once blessed with richness of chemistry and cursed by the profound complexity which results from the multidimensionality of excited-state surfaces. The omnipresent competition between photochemical and photophysical processes requires a knowledge of the dynamics of both electronic relaxation routes before a quantitative theoretical prediction can be made. Furthermore, the role of Franck-Condon factors (f_i) and spin-orbit coupling (f_s) must be considered in any quantitative formulation of photoreactivity and or efficiency.

Despite the formidable difficulties demanded by a quantitative theory, the qualitative factors discussed in this chapter serve as a useful systematizing, unifying framework in the consideration of photoreactions.

The state correlation diagram may be viewed as a *reaction graph* which displays the possible pathways for interconverting reactants to products. The vertices of the reaction graph correspond to structures corresponding to maxima or minima

on the various energy surfaces. A major goal of mechanistic organic photochemistry is to provide experimental support for the occurrence or nonoccurrence of "transition structures" (maxima or minima) along the reaction pathway. Once the structures along a reaction pathway have been established, the dynamics of the reaction (rate constants for conversion of one structure into a second structure) can be determined. The theoretical reaction graph given by energy surfaces provide mechanistic photochemistry with a framework for thinking about experiments, i.e., transition structures are suggested and are subject to experimental verification. Chapter 8 discusses the experimental methods available to test the mechanisms suggested by state correlation diagrams.

References

1. For reviews and discussions of the theory of orbital interactions, see:
   (a) Fukui, K., *Topics in Current Chemistry*, *15*, 1 (1970); *Acc. Chem. Res.*, *4*, 57 (1971).
   (b) Hudson, R. F., *Angew. Chem. Intern. Ed. Eng.*, *12*, 36 (1973).
   (c) Epiotis, N. D., *ibid.*, *13*, 751 (1974).
   (d) Dewar, N. J. S., *ibid.*, *10*, 761 (1971).
   (e) Salem, L., *J. Am. Chem. Soc.*, *90*, 3251–3255 (1968).
2. (a) For discussions of symmetry in chemistry, see Pearson, R. G., *Symmetry Rules for Chemical Reactions*, New York: John Wiley, 1976.
   (b) For an elementary discussion of commonly encountered symmetry operations, see Cotton, F. A., *Chemical Applications of Group Theory*, New York: John Wiley, 1971.
3. For reviews of orbital symmetry control of chemical reactions, see:
   (a) Woodward, R. B., and Hoffmann, R., *The Conservation of Orbital Symmetry*, New York: Academic Press, 1970.
   (b) Zimmerman, H. E., *Acc. Chem. Research*, *4*, 272 (1971).
   (c) Dewar, M. J. S., *Angew. Chem. Int. Ed. Eng.*, *10*, 761 (1971).
4. For a discussion of the role of diradicals and zwitterions in photoreactions, see Salem, L., and Rowland, C., *Angew. Chem. Int. Ed. Eng.*, *11*, 92 (1971); Salem, L., *Pure Appl. Chem.*, *33*, 317 (1973).
5. Michl, J., *Molec. Photochem.*, *4*, 243, 257, 287 (1972); *Topics in Current Chemistry*, *46*, 1 (1974).
6. (a) Salem, L., *J. Am. Chem. Soc.*, *96*, 3486 (1974).
   (b) Dauben, W. G., Salem, L., and Turro, N. J., *Acc. Chem. Research*, *8*, 41 (1975) and references therein.
7. Devaquet, A., *Topics in Current Chemistry*, *54*, 1 (1975); *Pure Appl. Chem.*, *41*, 535 (1975).
8. Longuet-Higgins, H. C., and Abrahamson, E. W., *J. Am. Chem. Soc.*, *87*, 2046 (1965).
9. Van der Lugt, W. T. A. M., and Oosterhoff, L. J., *J. Am. Chem. Soc.*, *91*, 6042 (1969).
10. Carr, R. W., and Walters, W. D., *J. Phys. Chem.*, *69*, 1073 (1965).
11. For a discussion, see Turro, N. J., et al., *Acc. Chem. Research*, *5*, 92 (1972) and references therein.
12. Turro, N. J., Farneth, W. E., and Devaquet, A., *J. Am. Chem. Soc.*, *98*, 7425 (1976).

8

Mechanistic Organic Photochemistry

8.1 Mechanisms

The term "mechanism" is derived from the notion of a "machine" or "contrivance" and evokes the image of forms or structures (parts) operating in a collective and connected sense, i.e., the machine possesses certain components, connectivity, and spatial relationships. If we saw the "guts" of a machine that is not operating (i.e., a machine in a "static" state), we might deduce from the configuration of the parts how the machine works; that is, we might imagine, given the "static" forms and their perceived relationships, how the motions of the components could create the dynamics of the machine when operating. We could then attempt to visualize the forces capable of producing the dynamics of the machine, i.e., the motion sequences of the parts in time. Next we might test our conjectures on the interplay of the parts of the machine by getting it to work and beholding the process of operation. We could then determine the forces which provide the energy to operate the machine. If at this stage everything seemed quite natural (i.e., the parts moved as expected and the machine operated as expected), we could say that we "understand" the mechanism.

A similar approach can be applied to the investigation of photochemical mechanisms. The "components" of such a mechanism are the significant *structures* along the reaction pathway, i.e., structures which correspond to maxima and minima on energy surfaces. The "connectivity" of a mechanism refers to the relationships of the transition structures, one to another, i.e., how they are connected through radiative transitions, radiationless transitions, or chemical transformations. The "configuration" of a mechanism is the detailed surface pathway which is followed starting from an initial excited state. Dynamics tell us how forces operating on transition structures determine the relative probabilities that a specific configuration or pathway will be followed.

Thus, a "complete" photochemical mechanism must include a knowledge of (a) all significant transition structures along the reaction pathway, (b) the rate

constants for converting one intermediate structure to its successor structure, and (c) the forces responsible for interconverting structures.

Chemical Mechanisms; The Standard Mechanistic Set

The conventional mechanism of a chemical reaction is a finite sequence of elementary physical and chemical steps which adequately accounts for the conversion of reactant structures to product structures. All mechanisms are *provisional* and *incomplete*. They are provisional because we can never conclusively *prove* a statement with the inferential logic required in scientific inquiry, i.e., an alternate mechanism (possibly not yet thought of) may also be consistent with all *known* data. Mechanisms are incomplete because experimental data is incomplete and is constantly in various stages of refinement, and because to write *all* of the physical and chemical steps would be impossible in principle and unnecessary in practice. In writing a chemical mechanism we can only hope to put forth the "highlights" of a reaction sequence. Since energy is a general property of all chemical systems, we might suppose that we can always describe the conversion of reactants to products in terms of the change in energy of the system as the reaction develops. These highlights should include descriptions of all energy *minima* which correspond to the structures of reaction intermediates (or to funnels which lead to the ground-state surface) and all energy *maxima* which correspond to the structure of transition states. If possible, the electronic, nuclear, and spin structure of these minima and maxima (and of all important forces which cause structural interconversions) should be clearly identified.

Although many mechanisms can be written a priori, we usually find that few or only one are consistent with the known relevant data and theories of chemistry. The protocol of establishing or validating (not "proving") a mechanism for a *known* reaction is the following:

One must decide in a general way the highlights one wishes to cover, i.e., select those features of the reaction sequence which are of greatest particular interest. Next, one must enumerate all plausible mechanisms which involve *commonly* encountered reactions. This group of mechanisms is called the *standard mechanistic set*, and is selected to be analogous to the one under study. Data or theory is then sought to eliminate each of the members of the standard mechanistic set. After this elimination, three possibilities generally will result (see Scheme 8.1):

1. If every member but one is eliminated, that remaining member provides a provisional *working* mechanism.

2. If more than one member of the standard mechanistic set remains after the elimination, then more than one provisional working mechanism must be considered as validly describing the reaction.

3. If no members of the standard mechanistic set remain, then we must conclude that the reaction involves a "novel" or previously unencountered mechanistic pathway.

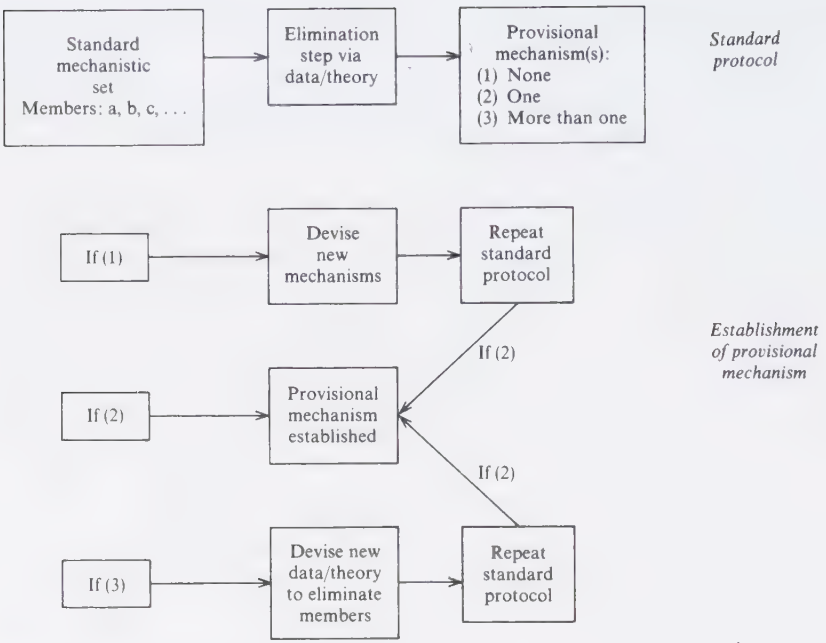

Scheme 8.1

Flow sheet of the steps involved in establishing a provisional mechanism. The members a, b, c, . . . represent complete, distinct mechanisms.

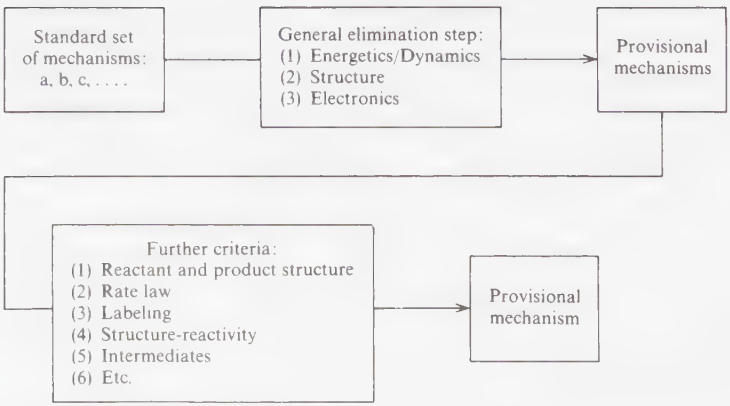

Scheme 8.2

Flow sheet of the steps involved in employing theoretical and experimental criteria to establish a reaction mechanism.

The Criterion of Experimental Denial; Empirical Methods for the Elimination of Members of a Standard Mechanistic Set

In order to eliminate a member of the standard mechanistic set, we must establish a logical inconsistency between a premise of the set member and experimental data or theoretical laws. For example, we may eliminate a set member if it incorrectly predicts or is inconsistent with the observed product types, the stereochemical pathway, or the empirical form of the observed reaction kinetics. We may also eliminate a set member if it implies a violation of a conservation law (total energy, momentum, spin, etc.). Clearly, in eliminating members of the standard set, we should first apply the most general criteria possible (energetics, structure, and dynamics) in order to quickly reduce the number of remaining members (see Scheme 8.2).

After application of the general energetic, structural, and dynamic implausibility criteria, we may use *specific* experimental data to eliminate remaining members of the standard set. For example, any or all of the following consistency criteria are commonly used:

1. Reactant and Product structure
2. Structure of intermediates on the pathway from reactant to product
3. Kinetic rate law
4. Labeling experiments
5. Structure-reactivity relationships

8.2 Use of Kinetic Feasibility in Quantitative Mechanistic Analyses

The question of kinetic feasibility can be formulated as: *Can an excited molecule acquire sufficient activation energy during its lifetime to react at a rate competitive with other modes of excited-state deactivation?* In order to acquire an idea of the relationship of lifetime to energy we can employ the Arrhenius expression:

$$k\,(\text{sec}^{-1}) = A \exp - E_a/RT \tag{8.1}$$

which relates the rate constants for reaction to the activation energy for reaction and a probability factor. In terms of the more familiar Base 10 units, Eq. 8.1 becomes:

$$k\,(\text{in sec}^{-1}) = A \times 10^{-Ea/2.3RT} \tag{8.2}$$

Typical values of A are $\sim 10^{15}$ to 10^{12} sec^{-1} for unimolecular reactions and $\sim 10^{8}$ sec^{-1} for bimolecular reactions (at 1 M reactants).[5] Table 8.1 lists the relationship of k to E_a at three temperatures: 77 K (−126°C)—; 300 K (27°C)—;

and 400 K (127 C—somewhat above the temperature of boiling water) for $A = 10^{15}$ sec^{-1} and $A = 10^{8}$ sec^{-1}.

Consider the column corresponding to reaction near room temperature. If an excited-state possesses a lifetime of 10^{-12} sec, a reaction possessing E_a of 4 kcal/mole can compete with excited-state deactivation if $A = 10^{15}$ sec^{-1}, i.e., $k = 10^{15} \times 10^{-4/1.4} \sim 10^{12}$ sec^{-1}, but not if $A = 10^{8}$ sec^{-1}, i.e., even if $E_a = 0$ kcal/mole, $k = 10^{8}$ sec^{-1} and the reaction is too slow to compete with other deactivation pathways. If the excited-state lifetime is 10^{-3} sec, a reaction possessing E_a of ~ 16 kcal mole can compete with excited-state deactivation if $A = 10^{15}$ sec^{-1}. On the other hand, a bimolecular reaction ($A \sim 10^{8}$ sec^{-1}) will require a much lower E_a (~ 7 kcal/mole) in order to compete with excited-state deactivation.

Typical activation energies for "thermal reactions" which proceed at convenient rates ($\sim$ hours) near room temperature are of the order of 25–35 kcal/mole. For example, the ring opening of cyclobutene to butadiene (reaction exothermic by ~ 10 kcal mole) requires an activation energy of 33 kcal/mole and possesses an A factor of $\sim 10^{13}$. At 300 K (near room temperature) the ring opening rate of cyclobutene is $\sim 10^{-10}$ sec^{-1}. (This corresponds to a half-life of hundreds of years!) On the other hand, the photochemical ring closure of 1,3-butadiene to cyclobutene (endothermic by 10 kcal mole in the ground state) occurs with negligible activation energy in about 10^{-10} sec or less.

Rate constants depend on both energetic ($\Delta H^{\ddagger}$ or E_a) and entropic ($\Delta S^{\ddagger}$ or A) factors. Restriction of conformational freedom in *reactants* can increase the rate of reaction if the restriction also favors the formation of the reaction transition state. This corresponds to an *entropic* enhancement of the rate constant for reaction, since the entropy change upon going from reactant to transition state is more positive (less ordering is required to achieve the transition state).

As an example of the information which is available from E_a and A but not available from k, consider the data in Table 8.2 for an intramolecular hydrogen abstraction reaction called the "Type II" hydrogen abstraction (which we shall

Table 8.1 Relationship Between Rate Constants, Activation Energies, Frequency Factors, and Temperature[a]

	$T = 77$ K		$T = 300$ K		$T = 400$ K	
k	$A = 10^{15}$, $A = 10^{8}$		$A = 10^{15}$, $A = 10^{8}$		$A = 10^{15}$, $A = 10^{8}$	
	E_a		E_a		E_a	
10^{15}		-	0	—	0	—
10^{12}	1	—	4	—	5	—
10^{9}	2	0	8	0	11	0
10^{6}	3	1	12	3	16	3.5
10^{3}	4	2	16	7	22	9
1	5	3	21	11	27	15
10^{-3}	6	4	25	15	33	20
10^{-6}	7.5	5	29	19	38	25
10^{-9}	8.5	6	33	23	44	31

[a] Units of K are sec^{-1}. Units of E_a are kcal/mole.

discuss in detail in Chapter 10). This reaction occurs exclusively from T_1:

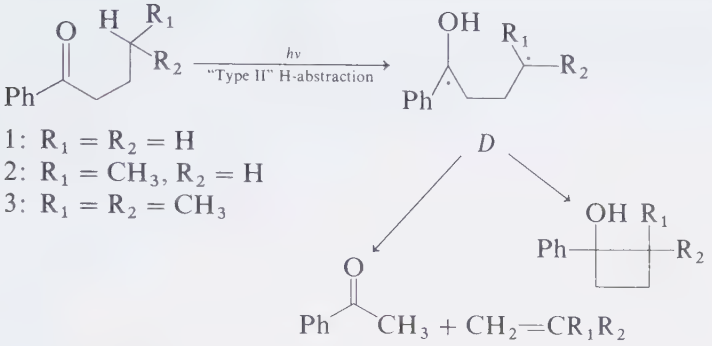

(8.3)

Table 8.2 Rate Constants and Activation Parameters for Some Hydrogen Abstraction Reactions of Ketones. (Reactions at room temperature.)

Ketone[a]	k_r[b]	E_a[c] (kcal/mole)	A[c] (sec^{-1})	Ref
1. $PhCOCH_2CH_2C\underline{H}_3$	8×10^6	~7	$\sim 10^{12}$	(d)
2. $PhCOCH_2CH_2C\underline{H}_2CH_3$	1×10^8	~5	$\sim 10^{12}$	(d)
3. $PhCOCH_2CH_2C\underline{H}(CH_3)_2$	5×10^8	~4.5	$\sim 10^{12}$	(d)
4. $CH_3COCH_2CH(C\underline{H}_3)_2$	1×10^7	~7	$\sim 10^{12}$	(e)
5. $CH_3COCH_2CH_2C\underline{H}_2CH_3$	6×10^8	~4.5	$\sim 10^{12}$	(e)
6. $CH_3COCH_2CH_2CH(CH_3)_2$	2×10^9	~3.5	$\sim 10^{12}$	(e)
7. $Ph_2CO + RC\underline{H}_3$	3×10^4	~4.5	$\sim 10^8$	(f)
8. $Ph_2CO + RC\underline{H}_2R$	7×10^5	~2.8	$\sim 10^8$	(f)
9. $Ph_2CO + R_3C\underline{H}$	9×10^5	~2.2	$\sim 10^8$	(f)
10. $Ph_2CO + PhC\underline{H}_3$	4×10^5	~2.5	$\sim 10^8$	(f)
11. $Ph_2CO + C\underline{H}_3OH$	3×10^5	~3.5	$\sim 10^9$	(g)
12. $Ph_2CO + CH_3C\underline{H}_2OH$	8×10^5	~2.8	$\sim 10^9$	(g)
13. $Ph_2CO + (CH_3)_2C\underline{H}OH$	1×10^6	~2.6	$\sim 10^9$	(g)
14. 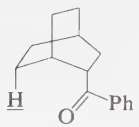	3×10^9	~4	$\sim 10^{13}$	(h)
15. 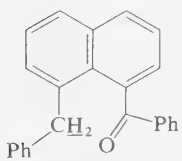	7×10^3	~4.7	$\sim 10^4$	(i)

[a] Underlined hydrogen is involved in the hydrogen abstraction process.
[b] Rate constant for hydrogen abstraction. Values are representative only. Absolute, accurate values depend on solvent, temperature, and other experimental conditions. Units are sec^{-1} for compounds 1, 2, 3, 4, 5, 6, 11, and 12 (intramolecular hydrogen abstraction) and M^{-1} sec^{-1} for systems 7, 8, 9, and 10 (intermolecular hydrogen abstraction).
[c] E_a is the activation energy for hydrogen abstraction and A is the frequency factor. Values are rounded off and approximated for simplicity and consistency.
[d] Grotewald, J., Previtali, C. M., and Scaiano, J. C., *J. Photochem.*, *1*, 471 (1972/73).
[e] Encina, M. V., and Lissi, E. A., *J. Photochem.*, *6*, 173 (1976); *4*, 321 (1975).
[f] Giering, L., Berger, M., and Steel, C., *J. Am. Chem. Soc.*, *96*, 953 (1974).
[g] Topp, M. R., *Chem. Phys. Letters*, *32*, 144 (1975).
[h] Lewis, F. D., Johnson, R. W., and Kory, D. R., *J. Am. Chem. Soc.*, *96*, 6100 (1974).
[i] DeBoer, C. D., et al., *J. Am. Chem. Soc.*, *95*, 3963 (1973).

There is a variation in *rate constant* of a factor of ~ 60 in proceeding from $1(k_r \sim 8 \times 10^6\ \text{sec}^{-1})$ to $2(k_r \sim 1 \times 10^8\ \text{sec}^{-1})$ to $3(k_r \sim 5 \times 10^8\ \text{sec}^{-1})$. From the activation parameters it is seen that the increase in k going from 1 to 2 to 3 is due mainly to a decrease in E_a; i.e., the A-factor is more or less constant for the series.[1]

On the other hand in Table 8.2, the bicyclic ketone 14 undergoes reaction nearly 100 times faster than 2 (a secondary hydrogen is abstracted when both 2 and 14 react).[2] The increase in k on going from 2 to 14 is due mainly to an increase in the A-factor. These results are reasonable when we identify A with $\Delta S^{\ddagger}$, the activation entropy. As A increases, $\Delta S^{\ddagger}$ becomes more positive, i.e., the reaction requires *less* organization. Ketones 1, 2, and 3 require similar organization on proceeding from the starting excited state to the transition state; therefore, $\Delta S^{\ddagger}$ (and A) should be similar. It is thus expected, and found that the differences in k result from differences in E_a (primary hydrogen is abstracted slower than secondary hydrogen which, in turn, is abstracted slower than tertiary hydrogen).

On the other hand, in comparing 2 and 14 the same type of hydrogen atom (secondary) is abstracted, so that comparable values of E_a are expected. However, because of its structure, 14 is locked into a conformation particularly favorable for hydrogen abstraction. As a result, a smaller price in activation entropy must be paid (less organization required) to reach the transition state for hydrogen abstraction. This results in a more positive $\Delta S^{\ddagger}$ (larger A) for 14 than for 2 and, because of the comparable E_a values, a larger value of k for 14 than for 2.

A comparison of 14 and 15 is informative. The latter can undergo an intramolecular hydrogen abstraction only via a seven-membered cyclic transition state. The entropy requirements for achieving such a structure are much more difficult than those for a six-membered cyclic transition state. As a result, the A factor drops from $\sim 10^{13}\ \text{sec}^{-1}$ in 14 to $\sim 10^{4}\ \text{sec}^{-1}$ in 15. This nearly million-fold larger rate constant for 14 is due mainly to the A-factor differences.

Finally, note that the A-factor for intermolecular hydrogen abstraction is $10^8 - 10^9\ \text{sec}^{-1}$. Such values are typical of bimolecular reactions requiring a modest amount of structural organization in the transition state.[5]

8.3 The Use of Structural Criteria and the Role of Reactive Intermediates in Mechanistic Analysis

The most definitive information concerning photoreactions is knowledge of the *structure* of the reactants, products, and intermediates. Important qualitative arguments concerning photochemical reaction mechanisms can be made based on structural considerations alone. It is convenient to consider the structures in terms of two classifications:

1. Initial reactants and isolated products
2. Transient structures or *reactive intermediates*

Since all photochemical reactions start with a ground-state structure, proceed to an excited-state structure, and end in a ground-state structure, photochemical mechanisms are inherently multistep, i.e., they require the occurrence of intermediates between reactants and products.

What can we deduce about the mechanism of a reaction solely from the structure of the ground-state reactants or products? The answer is quite a bit *qualitatively* but very little quantitatively. More can be deduced if the nature (e.g., electronic configuration) of the S_1 and T_1 states is known. Still more can be deduced if it is known whether S_1 or T_1 (or both) undergo the reaction under study, and whether reactive intermediates in addition to S_1 and T_1 are involved (including upper excited states, diradicals, zwitterions, excited states of products, and ground-state intermediates).

Molecular structure is the "glue" of reaction mechanisms: i.e., structures hold everything together. In a mechanism, the chemist tries to develop the constitution of a mechanism by employing the idea of spatiotemporal objects (chemical structures) to define a system of forms or structures in temporal evolution. The possible evolutions may not occur in any arbitrary manner but rather are subject to a formalizable protocol (Scheme 8.2) which restricts the "allowed" sequence of structural transformations in time.

In effect, the chemist parameterizes the state of a chemical system in terms of structures. He implicitly assumes that each state may be parameterized in terms of a distinct structure. He understands that not all structural interconversions are allowed under a given set of reaction conditions. Therefore, his mechanism takes the initial structures, and via the logic of the mechanistic protocol maps the *logical* succession of structures into a *temporal* succession, i.e., he generates an a priori acceptable mechanism.

The Use of Reaction Types and Structural Relationships in Mechanistic Analyses

The relationships of product structure to reactant structure usually provide a valuable set of clues to the reaction mechanism. The following questions should be answered before proceeding in a mechanistic analysis:

1. Does the overall reaction correspond to a standard reaction type or to a sequence of standard reaction types?

2. How does the product atomic composition and connectivity relate to the reactant atomic composition and connectivity?

3. How does the product stereochemistry relate to the reactant stereochemistry?

If the answers to these questions are available, a basis for guessing at the most plausible mechanisms is at hand. This procedure is based on the postulate that *there are very few fundamentally different reaction mechanism types for an elementary chemical step.* In effect, we postulate that many reactions are more or less the same

with respect to the fundamental chemistry which occurs at a reactive site, and differ in quantitative detail rather than in their qualitative nature.

A corollary of the above postulate is that *reactions can be classified in terms of mechanistic types, and for any given class of reactions only a small set of mechanistic types is likely to be required for a detailed analysis.*

In ground-state chemistry, most of the fundamental reaction types can be viewed as proceeding via shifts of *pairs* of electrons toward or away from carbon as one passes from reactant to product. An exception occurs when one (and only one) of the reagents possesses an odd number of electrons, i.e., reactions of monoradicals. In this case, the reaction is usually viewed in terms of single-electron shifts toward or away from carbon.

Most, but not all, photoreactions are closer in nature to the one-electron shifts characteristic of radical chemistry than to two-electron shifts. This is understandable in terms of electronic excitation, which may be thought of as orbital decoupling of an electron pair to produce a species which possesses two half-filled orbitals. The one-electron behavior is a natural consequence of the high one-electron affinity of the lower-energy half-filled orbital and the low one-electron ionization potential of the higher-energy half-filled orbital.

The point of these classifications is that each reaction type has been established to occur via a relatively small and well-defined set of mechanisms. If a reaction falls into one of the above categories, one automatically has a standard set of mechanisms available to consider. If a reaction does not fall into one of the above categories, we may assume that the reaction is complex (i.e., involves a sequence of two or more of the above reaction types) or that one has encountered a novel mechanism.

An Example of the Use of Structural Relationships in Mechanistic Analysis

The photolysis of aryl alkyl ketones generally results in the formation of products of the type shown in Eq. 8.3, i.e., methyl aryl ketones, ethylenes, and cyclobutanols (Type II products).[6] These product structures may be used as a basis to surmise precursor structures. When more than one product is observed from photoreactions of a single excited state, it is commonly observed that these products are logically derived from competing pathways for reaction of an intermediate. For example, all the Type II products are derivable from the common diradical *D*, shown in Eq. 8.4. In other words, two "natural" and logical reactions of *D* are (a) cleavage of bond *a*, or (b) cyclization (Eq. 8.4). Note that cleavage does not produce the methyl aryl ketone that is isolated directly, but rather an enol. The latter, however, is known to be generally unstable both kinetically and thermodynamically with respect to its corresponding ketone.

Thus, the product structures may be said to "imply" the diradical *D* as a predecessor structure. The diradical, in turn, "implies" a precursor structure capable of abstracting a hydrogen from the side chain. The n, π^* state of the aryl alkyl ketone is such a predecessor. Importantly, the enol and diradicals indicated in Eq. 8.4 were detected spectroscopically (Chapter 10) long after their existence was inferred via product-reactant relationships.

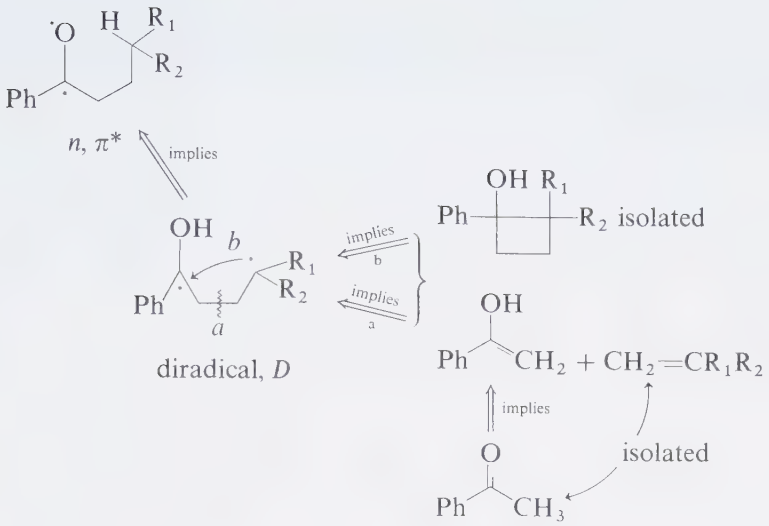

(8.4)

8.4 Rules for Proceeding from Rate Laws to Photochemical Reaction Mechanisms[3]

The *theoretical rate law* for any elementary chemical step is the product of the rate constant for that step times the concentrations of its reactants. The *empirical rate law* is an algebraic expression which relates measured concentrations to the rate of reaction.

If we assume that a mechanism has only one rate-determining step (i.e., has one molecular configuration of highest energy along a reaction coordinate) then a useful working rule is possible which allows the establishment of guidelines on how to proceed from empirical rate law data to inferences of steps in a reaction mechanism.

For an empirical rate law whose orders in concentrations are integers,

> The molecular formula of the transition state for the rate-determining step is directly related to the empirical molecular composition of the species whose concentrations appear in the empirical rate law.

In photochemical kinetics we interpret "rate-determining step" to mean that step which determines the overall rate of reaction or the rate of deactivation of a given electronically excited state. This step may or may not be the slowest step in the overall sequence from reactants to products.

As an example, consider the photoreduction of acetone to pinacol by isopropanol:[1]

$$(CH_3)_2CO + (CH_3)_2CHOH \xrightarrow{h\nu} (CH_3)_2\overset{OH}{\underset{|}{C}}\!\!-\!\!\overset{OH}{\underset{|}{C}}(CH_3)_2 \qquad (8.5)$$

The key photochemical step in the reaction involves abstraction of a hydrogen atom from the tertiary carbon of isopropanol by either S_1 or T_1 of acetone (Eq. 8.6). This is followed by the formation of a pair of ketyl radicals, which then couple to yield the product (Eq. 8.7):

$$(CH_3)_2CO^* \ (S_1 \text{ or } T_1) + (CH_3)_2CHOH \longrightarrow \underset{\text{ketyl radicals}}{2(CH_3)_2\dot{C}OH} \tag{8.6}$$

$$2(CH_3)_2\dot{C}OH \longrightarrow (CH_3)_2\overset{OH}{\overset{|}{C}}\!\!-\!\!\overset{OH}{\overset{|}{C}}(CH_3)_2 \tag{8.7}$$

How can we decide on the basis of empirical rate law data whether this assumed mechanism is provisionally acceptable? Experimentally, both the fluorescence and the phosphorescence of acetone are measurable. The intensity and lifetime of each emission can be related to the concentrations of S_1 and T_1. It is found that the measured rate of product formation is expressed by:

$$\underset{\text{formation}}{\text{Rate of product}} \ dP/dt = k[(CH_3)_2CHOH][T_1] \tag{8.8}$$

From our rule, we can conclude that (a) acetone triplets and isopropanol are involved in the photochemical rate-determining step for reaction, and (b) S_1 of acetone is *not* involved in the photochemical rate-determining step, i.e., since the concentration of S_1 does not appear in the empirical rate law S_1 cannot be directly involved in the product-determining step. Thus, we can associate the measured k with the theoretical rate-constant for the reaction:

$$(CH_3)_2CO(T_1) + (CH_3)_2CHOH \xrightarrow{k} 2(CH_3)_2\dot{C}OH \tag{8.9}$$

A second useful rule is related to the principle that chemical species of similar energy and structure possess similar chemical properties. Using this principle, we may make the following statement concerning the structure of transition states, known as the Hammond postulate:[4]

> If a transition state and an intermediate possess comparable energies and occur consecutively along a reaction coordinate, the chemical composition, the chemical constitution (structures) and chemical properties of the transition state will be similar to those of the intermediate.

Extending this idea to photochemical reactions, if E_a is small (a few kcal/mole) for reaction from an excited state, then we may postulate that the transition state "looks like" the initial excited state in most important chemical aspects. This in turn leads to the corollary that *the excited-state configuration is a guide to excited-*

state reactivity; i.e., if the transition state "looks like" the initial excited state, the orbital interactions should relate to the initial excited-state electronic configuration.

8.5 Rules for Proceeding from Efficiency Laws to Inferring Photochemical Reaction Mechanisms

The efficiency of a photochemical reaction can be expressed in two ways:

1. The quantum yield or efficiency of formation or destruction of a given species can be based on the number of photons absorbed by the system.

2. The state efficiency of formation or destruction of a given species can be determined from molecules in a given state.

It is important to distinguish these terms. We shall call Φ (the efficiency based on photons absorbed) the *quantum yield*, and ϕ (the efficiency based on a given state) the *state efficiency*.

The efficiency based on (1) is given by

$$\text{QUANTUM YIELD } \Phi = \frac{\text{moles of given species formed or destroyed}}{\text{moles of photons absorbed by the system}} \tag{8.10}$$

The efficiency based on (2) is given by

$$\phi = \frac{\text{moles of a given species formed or destroyed}}{\text{moles of a given state formed by absorption of a mole of photons}} \tag{8.11}$$

In a practical sense, quantum yield is the more interesting quantity because it relates the effectiveness with which absorbed photons can form products. The magnitude of Φ may vary from 0 to very large values ($> 10^4$). From the theoretical standpoint, in order to understand the factors determining Φ, an "overall" quantity of a reaction, we must understand the factors determining ϕ, a quantity which relates to individual steps from states along the reaction pathway.

All quantum yields may be considered as the product of ϕ_{A^*}, the probability that light absorption will produce the reactive state A^*; ϕ_R, the probability that A^* will undergo a particular reaction to yield P; and ϕ_I, the probability that any metastable intermediate which exists between A^* and R will lead to P. (See Eq. 8.12.)

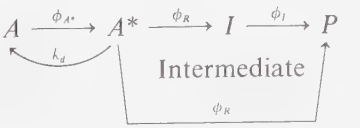

(8.12)

If P is formed from only one excited state, A^*, then in general:

$$\Phi_R = \phi_{A^*}\phi_R \qquad \text{or} \qquad \Phi_R = \phi_{A^*}\phi'_R\phi_I \tag{8.13}$$

In direct excitation experiments in solution, ϕ_{A^*} is generally unity if $A^* = A_1$ (i.e., a singlet state is produced). This generalization and its limitations derive from consideration of Eq. 8.14 where k_{IC} is the rate of internal conversion from any upper level of A_1 to the thermally equilibrated state, and k_x is the rate of any process which competes with internal conversion:

$$\phi_{A^*} = \frac{k_{IC}}{k_{IC} + k_X} \tag{8.14}$$

Generally, $k_{IC} \sim 10^{12}\ \text{sec}^{-1} \gg k_x$, so that $\phi_{A^*} \sim 1$. Thus, it is clear that only extremely rapid unimolecular reactions and "diffusion controlled" reactions with solvents have a real chance of competing with k_{IC}.

When a triplet state A_3 is involved, then ϕ_{A_3} is generally identical to Φ_{ST} (intersystem crossing quantum yield) and is given by:

$$\Phi_{ST} = \frac{k_{ST}}{k_{ST} + k'_d + k_q[Q]} = k_{ST}\tau_S \tag{8.15}$$

In determining photochemical reactivities, the efficiency ϕ_R is often crucial. This efficiency is given by:

$$\phi_R = \frac{k_D}{k_D + k_d} = k_D\tau_{A^*} \tag{8.16}$$

where k_D is the rate constant for reaction of A^* to form I or P and k_d represents the rate of major decay of A^*.

We are now in a position to formulate a rule of the relationship between quantum yields and state efficiencies.

> **Rule 1.** The quantum yield for reaction from a given state equals the state efficiency for reaction times the quantum yield for formation of the reacting state (Eq. 8.17):
>
> $$\phi\ (\text{given state}) = \phi_R \times \Phi\ (\text{formation of state}) \tag{8.17}$$

Now we can understand how a high state efficiency for reaction can be consistent with a low quantum yield for reaction from the state. This is the situation if the *state* is inefficiently produced after the absorption of the photon.

The following rules relate the magnitude of the quantum yield to mechanistic conclusions:

> **Rule 2.** If $\Phi > 1$ (for reasons not trivially associated with reaction stoichiometry), then a chain reaction must be involved in the mechanism.

This rule derives from the generalization that one photon excites only one molecule.

> **Rule 3.** If $\Phi < 1$ then the provisional mechanism must account for the reaction inefficiency by some specific cyclic pathway which degrades the energy of the absorbed photon and returns the system back to its original ground state without net reaction.

8.6 Experimental Methods for Determining Rate Constants of Photoreactions

In this section we will discuss the common experimental methods for determining k, the reaction rate constant of a photochemical process.

The term "instantaneous" applied to a reaction rate once meant "less than a second," or a time of the order of reagent mixing. It is now possible to study reactions whose rates are of the order 10^{12} moles/l-sec, i.e., reactions which are well on their way to completion in 10^{-12} sec. The mechanical problem of "mixing" reagents and the time limitation required before measurement is overcome by a method based on the rapid perturbation of a system from its equilibrium and then following the rate of return of the system to equilibrium. In photochemistry the perturbation is usually applied by subjecting the system to a very short pulse of light which causes a number of molecules to suddenly find themselves in electronically excited states, then measuring their reactions. Some fast analytical method, usually flash absorption or emission spectroscopy, is used to monitor the concentration of excited molecules as they return to equilibrium.

A second method of studying very fast reactions is based on *kinetic competition* between two reaction pathways, under conditions in which the rate of one of the pathways is known or calculable. From knowledge of the rate of one pathway and the ratio of partitioning between the pathways, the rates of the other pathway can be evaluated. This method depends on the establishment of a fixed time-independent concentration of reactive intermediates and is known as a *steady-state* or *continuous excitation* method.

Pulsed Excitation

Figure 8.1 depicts the results of the pulsed excitation of a system. A "very fast" absorption of light by a molecule D produces a high concentration of excited states D^* (represented as a "filled box"). The excited state D^* will generally decay (the "box" empties) according to a unimolecular (or pseudo-unimolecular) rate law:

$$[D^*]_t = [D^*]_0 \exp t/\tau_D \equiv [D^*]_0 \exp k_D t \tag{8.18}$$

where τ_D is the experimental lifetime of D^*, and $[D^*]_t$ and $[D^*]_0$ are the concentrations of D^* at time t and time $t = 0$, respectively. Typically, the absorption or

emission of D^* are monitored to "track" the concentration of D^* as a function of time.

Stern-Volmer Analysis of Photochemical Kinetics; Lifetime-Concentration Measurements

A Stern-Volmer analysis[7] of photochemical kinetics postulates a reaction mechanism which involves a competition between an inherent unimolecular decay of A^* and a bimolecular quenching by Q:

unimolecular decay of A^* $\quad A^* \xrightarrow{k_1} \text{product}$ (8.19)

quenching of A^* by Q $\quad A^* + Q \xrightarrow{k_q} \text{quenching of } A^*$ (8.20)

The simplest situation is one in which these are the only two processes that occur. The lifetimes of A^* in the absence and presence of Q are given by:

Lifetime of A^*, No Q, $\quad 1/\tau_1 = k_1$ (8.21)

Lifetime of A^*, Q present, $\quad 1/\tau_2 = k_1 + k_q[Q] = 1/\tau_1 + k_q[Q]$ (8.22)

Since *both* experimental lifetimes τ_2 and τ_1 are measurable, as is $[Q]$, we can determine k_q from Eqs. 8.21 and 8.22. Experimentally, this is done by plotting $1/\tau_2$ as a function of $[Q]$. The slope of such a plot is equal to k_q in units of M^{-1} sec; i.e., the units of a bimolecular rate constant.

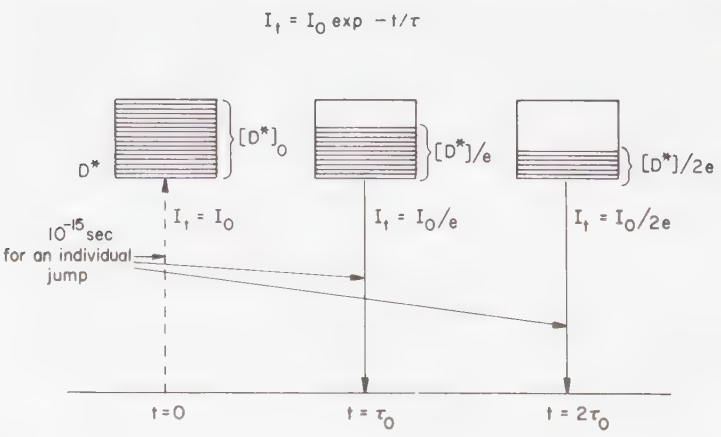

Figure 8.1

Schematic representation of the depletion of molecules in an excited state. The shaded area represents the concentration of excited states, D^*.

Stern-Volmer Quenching; Efficiency versus Concentration Measurements

If an excited state undergoes a unimolecular reaction in competition with emission, *both* the emission efficiency and the reaction efficiency can be measured. Often the emission lifetime can also be measured. From the expressions for reaction efficiency under steady-state excitation (Eqs. 8.23 and 8.24), we note that measurement of ϕ_e, ϕ_R, and τ_A allow evaluation of k_e and k_1.

$$A^* \xrightarrow{k_e} A + \text{light} \qquad \phi_e = \frac{k_e}{k_e + k_1} = k_e \tau_A \tag{8.23}$$

$$A^* \xrightarrow{k_1} \text{products} \qquad \phi_R = \frac{k_1}{k_e + k_1} = k_1 \tau_A \tag{8.24}$$

If $\tau_A \equiv 1/(k_e + k_1)$ cannot be measured directly, indirect methods of determining k_1 are possible. For example, since the value of k_e may be approximated from the theoretical relationship (Eq. 5.11) between a radiative rate constant and the absorption spectrum, τ_A may be estimated from a measured value of ϕ_e and a calculated (theoretical) value of k_e. From the measured value of ϕ_R and estimated value of τ_A, k_1 can be determined.

A second indirect method of evaluating k_1 employs specific bimolecular quenching. Either ϕ_e or ϕ_R may be determined as a function of quencher concentration. Assuming a simple competition between emission, reaction, and quenching, Eqs.8.25 and 8.26 hold for emission and reaction in the presence of quencher Q:

$$\phi_e = \frac{k_e}{k_1 + k_e + k_q[Q]} \begin{array}{l} \longleftarrow \text{rate of emission of } A^* \\ \longleftarrow \text{total rate of deactivation of } A^* \end{array} \tag{8.25}$$

$$\phi_R = \frac{k_1}{k_1 + k_e + k_q[Q]} \begin{array}{l} \longleftarrow \text{rate of reaction of } A^* \\ \longleftarrow \text{total rate of deactivation of } A^* \end{array} \tag{8.26}$$

If we define the quantum yields of emission or reaction in the *absence* of Q as ϕ_e^0 and ϕ_R^0 then:

Stern-Volmer equations

$$\frac{\Phi_e^0}{\Phi_e} = \left(\frac{k_e}{k_e + k_1}\right)\left(\frac{k_1 + k_e + k_q[Q]}{k_e}\right) = 1 + k_q \tau_A [Q] \tag{8.27}$$

$$\frac{\Phi_R^0}{\Phi_R} = \left(\frac{k_1}{k_e + k_1}\right)\left(\frac{k_1 + k_e + k_q[Q]}{k_1}\right) = 1 + k_q \tau_A [Q] \tag{8.28}$$

Thus, a plot of the *relative* efficiencies of emission in the presence or absence of a quencher (or of reaction in the presence or absence of quencher) versus $[Q]$ is

predicted to yield a straight line of slope equal to $k_q\tau_A$ and intercept equal to 1 (see Fig. 8.2 for an example).

It is sometimes possible to employ a quencher whose rate constant k_q can be estimated (Section 8.7). In such cases, a value of τ_A is available from the experimental values of $k_q\tau_A$ and the estimated k_q. From independent measurement of Φ_R, a value of k_1 is available.

If the photochemical reaction of A^* is bimolecular, the same general situation holds, except that k_1 is replaced throughout by $k_2[B]$, where k_2 is the bimolecular rate constant for reaction of A^* and $[B]$ is the concentration of substrate B reacting with A^*. In this analysis for low conversion to products we assume that $[B]$ does not change significantly during the measurement; accordingly, this concentration is treated as a constant.

8.7 Experimental Examples of the Measurements of Photochemical Rate Constants

As typical examples of the use of Stern-Volmer analysis to determine rate constants, we shall discuss (a) a unimolecular photoreaction for which the excited state does not emit measurably, and (b) a bimolecular photoreaction for which emission of the reactive excited state is measurable.

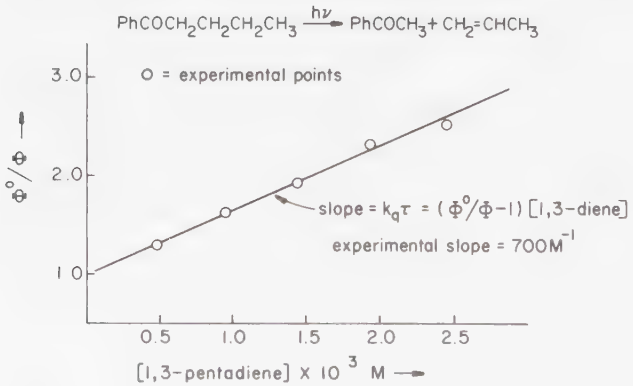

Figure 8.2

Experimental plot of Φ^0/Φ_R versus [1,3-pentadiene] for the Type II reaction of triplet butyrophenone (Eq. 8.3, $R_1 = R_2 = H$). The data follows Eq. 8.28 within experimental error. The intercept is 1.0 and the slope is 700 M^{-1}. Data taken from Kochevar, I. E. H., PhD Dissertation, Michigan State University, 1970. See also Reference 6b.

An example of case (a) is the so-called Type II intramolecular hydrogen abstraction reaction of phenyl alkyl ketones (Eq. 8.3). The mechanism of this reaction involves intramolecular hydrogen abstraction by the $T_1(n, \pi^*)$ state of the ketone.[6] This state may be specifically quenched by 1,3-dienes.[6c] The details of the quenching mechanism are not of direct interest in a Stern-Volmer analysis as long as the quenching products do not interfere with the analysis (e.g., by competing with the reactive state for light absorption, by being quenchers themselves, etc.). The quantum yield for a Type II reaction may be measured in terms of the efficiency of disappearance of reactant or appearance of products. Let Φ^0 be the quantum yield of Type II reaction measured in the absence of 1,3-diene, and Φ_q be the quantum yield measured in the presence of 1,3-diene. A typical plot of Φ^0/Φ versus [1,3-diene] was shown in Figure 8.2. If only one state is quenched by the diene, then the intercept of the plot will be 1.0 and the slope of the plot will be linear and equal to $k_q\tau$, according to Eq. 8.28.

Experimentally,[6b] the slope *is* linear and the intercept is 1.0, thereby confirming the assumed mechanism. The value of $k_q\tau$ for the specific case of butyrophenone (Eq. 8.3, $R_1 = R_2 = H$) in acetonitrile is 700 M^{-1}. The maximum value of k_q for quenching of a $T_1(n, \pi^*)$ state is equal to the rate constant for diffusion and is equal to 1×10^{10} M^{-1} sec^{-1} for diffusion in acetonitrile. Thus, if $k_q = 10^{10}$ M^{-1} sec^{-1} (a maximum value), then $\tau = 700/k_q = 7 \times 10^{-8}$ sec (minimum value). The minimum value for the rate constant k_1 is equal to $1/\tau$. Therefore:

$$k_1^{\min} = 1/\tau = 1.4 \times 10^7 \text{ sec}^{-1} \tag{8.29}$$

The confidence that can be placed in the value of k_1 depends on the confidence that can be assigned to the selection of a value of k_q. In this case the confidence level is high because for $T_1(n, \pi^*)$ states such as acetophenone, acetone, or benzophenone the value of k_q for a 1,3-diene as quencher may be measured by *direct* quenching of phosphorescence and the experimental values are of the order of 10^{10} M^{-1} sec^{-1}.

As a second example,[8] consider the reaction of $S_1(n, \pi^*)$ of acetone and 1,2-dicyanoethylene (DCE). The fluorescence of acetone is quenched by DCE and an oxetane (**1**) is formed as product:

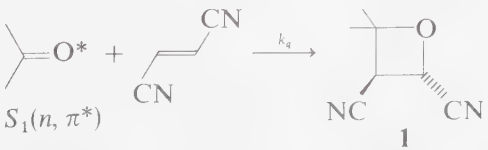

$S_1(n, \pi^*)$ **1** (8.30)

A plot of Φ_f^0/Φ_f versus [DCE] is linear (see Fig. 8.3) with intercept equal to 1.0 and slope equal to 7 M^{-1}. Thus, the value of $k_q\tau$ is equal to 7 M^{-1}. The lifetime of the acetone singlet state is readily measured from the decay of its fluorescence and equals 2×10^{-9} sec. Thus, k_q is given by:

$$k_q = 7/(2 \times 10^{-9}) = 3.5 \times 10^9 \text{ M}^{-1} \text{ sec}^{-1} \tag{8.31}$$

Measurement of Absolute Efficiencies in Determining Kinetic Parameters

In a Stern-Volmer analysis in which relative efficiency is measured, information concerning absolute efficiencies is lost. Although the maximum rate constant for quenching or unimolecular reaction is established by this type of analysis, the absolute rate of the process is not established unless the absolute efficiency is known. For example,[8] the limiting *absolute quantum yield* Φ for addition of acetone to DCE is about 0.10. This means that even if each $S_1(n,\pi^*)$ state is *quenched* by DCE, only 10% of the quenched singlets proceed to product. This conclusion, in turn, requires a bimolecular quenching pathway which does not lead to oxetane.

Experimentally, a plot of Φ versus quencher concentration will yield a limiting value of Φ, since

$$\underset{\text{yield}}{\text{Quantum}} \rightarrow \Phi = a\frac{k_2[B]}{k_q[B] + k_D} \leftarrow \underset{\text{parameters}}{\text{Kinetic}} \tag{8.32}$$

where a = efficiency of formation of A^*, k_2 is the rate constant for bimolecular reaction, k_q is the rate constant for all bimolecular quenching (i.e., reaction and other bimolecular deactivation of A^*), and k_D is the rate constant for inherent rate of unimolecular deactivation of A^*. A plot of Φ versus $[B]$ yields a curve which flattens out to a limiting value when $k_q[B] \gg k_D$. The value of Φ for the plateau is related to a, k_2, and k_q by:

$$\Phi = a\frac{k_2[B]}{k_q[B] \gg k_D} = ak_2/k_q \tag{8.33}$$

Thus, measurement or evaluation of Φ, a, and k_q are necessary to evaluate k_2. In the case of acetone and DCE, since the reactive state is $S_1(n,\pi^*)$, we may

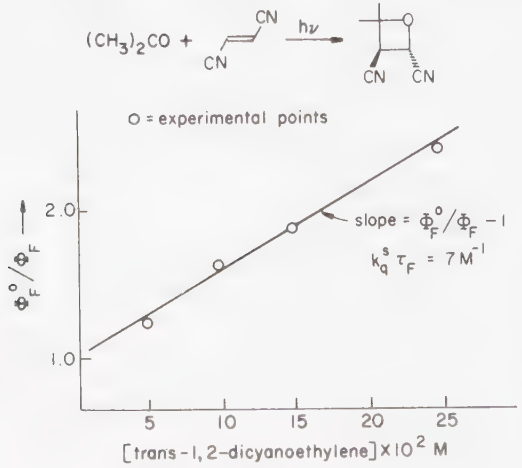

Figure 8.3

Experimental plot of Φ_F^0/Φ_F versus [trans-1,2-dicyanoethylene] for the cycloaddition of acetone singlets to the ethylene (Eq. 8.30). The data follows Eq. 8.27 within experimental error. The intercept is 1.0 and the slope is 7 $M^{-1} = k_q\tau_F$.

assume that $a = 1.0$ (Kasha's rule). From the Stern-Volmer quenching analysis we found that $k_q = 3.5 \times 10^9\ M^{-1}\ sec^{-1}$. Since Φ in the limit equals 0.1 we calculate $k_2 = 3.5 \times 10^8\ M^{-1}\ sec^{-1}$.

A second method may be used to handle the quantum yield data. There is "kinetic information" in the curved plot of Φ versus $[B]$. To extract this information it is convenient to invert the expression for Φ as follows:

$$\frac{1}{\Phi} = \frac{k_q[B] + k_D}{ak_2[B]} = \frac{1}{a}\left(\frac{k_q}{k_2} + \frac{k_D}{k_2[B]}\right) \tag{8.34}$$

Now a plot of $1/\Phi$ versus $1/[B]$ is predicted by Eq. 8.34 to yield a straight line with slope equal to $s = k_D/ak_2$ and intercept of $i = k_q/(ak_2)$. Notice that:

$$\frac{i}{s} = \left(\frac{k_q}{ak_2}\right)\left(\frac{ak_2}{k_D}\right) = k_q/k_D \tag{8.35}$$

or,

$$\frac{i}{s} = k_q\tau \tag{8.36}$$

In the case of reaction from S_1, this product, $k_q\tau$, is the same product we derive from a Stern-Volmer analysis employing relative *fluorescence* efficiencies (Eq. 8.27). Thus, in the case of oxetane formation between acetone and DCE, we predict that the mechanism of fluorescence quenching is the same as that for oxetane formation. The value of i/s from a plot of $1/\Phi$ versus $1/[\text{DCE}]$ will equal $\sim 7\ M^{-1}$.

The experimental value of i is 13.2 and the value of the slope is 2.6 M (Fig. 8.4). Thus, the limiting quantum yield is equal to $1/i = 1/13.2$ or 0.076. The ratio k_q/k_d is given by $i/s = 13.2/2.6\ M = 5.0\ M^{-1}$. This value of k_q/k_d may be compared

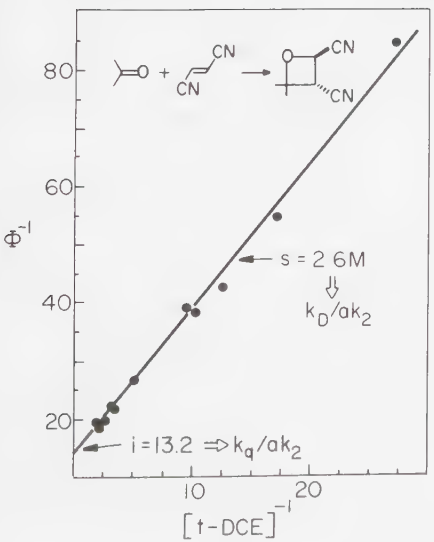

Figure 8.4

Experimental plot of Eq. 8.34 for addition of acetone singlet to DCE (Eq. 8.30).

to that obtained independently from fluorescence quenching, e.g., k_q/k_d (fluorescence) = 7.0 M^{-1}. The agreement between the values is within the experimental error ($\pm 20\%$) and is therefore a check of the consistency of the kinetic analysis.

Kinetics of Reactions Involving More than One Excited State

In some photoreactions both S_1 and T_1 undergo the same chemical transformation. In such cases consideration of *differential quenching* of the two states is necessary if kinetic information is to be extracted. For example, both S_1 and T_1 of alkanones (e.g., 2-hexanone) undergo Type II reactions:[5]

$$\begin{array}{l} \mathrm{CH_3\overset{\displaystyle O}{\overset{\|}{C}}CH_2CH_2CH_2CH_3} \longrightarrow S_1 \longrightarrow T_1 \\ \qquad\qquad\qquad\qquad\qquad\qquad \searrow \quad \swarrow \\ \text{Type II reaction} \quad \mathrm{CH_3COCH_3 + CH_2{=}CHCH_3} \\ \qquad\qquad\qquad\quad \text{Product formed from both } S_1 \text{ and } T_1 \end{array} \tag{8.37}$$

Experimentally, 1,3-dienes are found to quench $T_1(n, \pi^*)$ states of alkanones with rate constants approaching those for diffusion ($k_q^T \sim 10^9$ 10^{10} M^{-1} sec^{-1}), but the values of rate constants for quenching of $S_1(n, \pi^*)$ states of alkanones are much smaller ($k_q^S \sim 10^7$ M^{-1} sec^{-1}).[7] Thus, given a concentration of diene, the *relative* rates of quenching of S_1 and of T_1 are:

$$\frac{\text{rate of } S_1 \text{ quenching}}{\text{rate of } T_1 \text{ quenching}} = \frac{k_q^S[\text{Diene}]}{k_q^T[\text{Diene}]} = \frac{k_q^S}{k_q^T} \tag{8.38}$$

The *efficiency* of quenching of S_1 relative to T_1 is given by:

$$\frac{\Phi_q^S}{\Phi_q^T} = \frac{k_q^S \tau_s}{k_q^T \tau_t} \tag{8.39}$$

Since τ_t is generally larger in value than τ_s, $\Phi_q^T \gg \Phi_q^S$, i.e., S_1 is less efficiently quenched than T_1.

The kinetic expressions for systems in which more than one state reacts are quite complicated and will not be derived here.[7b] However, the form of the experimental Stern-Volmer plot may be intuitively derived (Fig. 8.5). Suppose differential quenching of the Type II reaction of an alkanone may be achieved with a 1,3-diene as quencher. To the first approximation we can assume that at high concentrations of diene *all* the triplets will be selectively quenched and that *none* of the singlets will be quenched. If this is the case the value of $\Phi^0 \Phi_q$ will not vary with $[Q]$ at sufficiently high concentrations of Q. On the other hand, at low $[Q]$, both S_1 and

T_1 will react, but T_1 will be quenched. Thus, we expect that the form of the experimental plot of Φ^0/Φ_q versus $[Q]$ will be a curve for low $[Q]$ which then plateaus at high $[Q]$.

The intercept along the plateau should equal Φ_0/Φ_q for an S_1 reaction. This value, when subtracted from the total Φ_0/Φ_q along the curved region of the plot, should provide Φ_0^T/Φ_q^T for the triplet portion of the reaction:

$$\begin{array}{l} (\Phi_0/\Phi_q) - i \quad = \Phi_o^T/\Phi_q^T \\ \text{Reacting state } \overbrace{S_1 + T_1}^{\uparrow} - S_1 = T_1 \end{array} \qquad (8.40)$$

Thus, a plot of $\Phi_o^T\ \Phi_q^T$ versus $[Q]$ for low $[Q]$ should yield a normal Stern-Volmer plot with intercept of 1.0 and slope of $k_q\tau$ for the triplet reaction alone.

An experimental example of the specific quenching of one of two excited states is given in Figure 8.5 for the quenching of Type II hydrogen abstraction of 2-*n*-propylcyclohexanone (Eq. 8.41).[9] Extrapolation of the plateau to the Φ_0, Φ coordinate yields 1.37. Assuming that this unquenchable reaction is due to Type II reaction from S_1, the contribution of T_1 reaction to the slope may be determined by subtracting 1.37 from the experimental values of Φ^0/Φ. A plot of Φ_0^T, Φ^T, i.e., the "pure" triplet component of the reaction,' may now be plotted. A straight line results, allowing identification of the slope with $k_q\tau_T$, i.e., the Stern-Volmer quenching constant for triplet alone. A value of $\tau_T = 9 \times 10^{-8}$ sec is obtained from this analysis. The rate of reaction is therefore $k_R = 1/\tau_T = 1.1 \times 10^9\ \text{sec}^{-1}$.

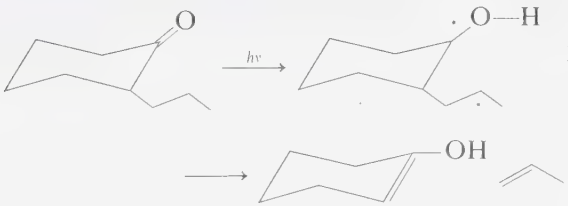

Reaction occurs from both S_1 and T_1

(8.41)

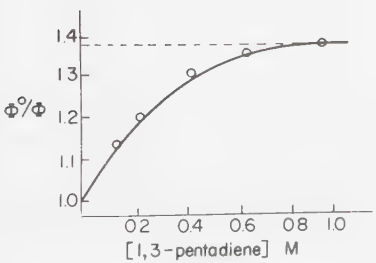

Figure 8.5

Experimental example of selective quenching—a situation in which both S_1 and T_1 undergo the same reaction. The quenching of the Type II reaction of 2-*n*-propylcyclohexanone is by 1,3-pentadiene (Eq. 8.41).

A second experimental example involves the specific T_1 sensitized isomerization of trans-dicyanoethylene (t-DCE) to cis-dicyanoethylene by triplet acetone:[6]

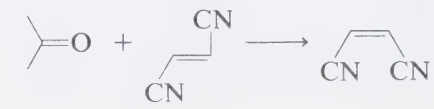

(8.42)

$T_1(n, \pi^*)$ t-DCE c-DCE

The S_1 state of acetone does not cause isomerization of t-DCE. The only reaction of S_1 and t-DCE leads only to oxetane formation (Eq. 8.30). As a result, at high concentrations of t-DCE, reaction 8.42 is *quenched* by t-DCE. Thus, a plot of $1/\Phi_{tc}$ versus $1/[\text{t-DCE}]$ does not yield a straight line, i.e., does not extrapolate to infinite concentration. Instead $1/\Phi_{tc} \to \infty$ at "infinite" concentration of t-DCE, i.e., $\Phi_{tc} \to 0$ as [t-DCE] approaches infinity. The experimental plot of $1/\Phi_{tc}$ versus $1/[\text{t-DCE}]$ is shown in Figure 8.6.

8.8 Reactive Intermediates: Experimental Detection and Characterization

Three general types of experimental methods are commonly employed for identification and characterization of nonisolable or transient intermediates that cannot be isolated by "conventional" techniques: (a) *spectroscopic* methods, which employ the absorption or emission of light; (b) *chemical* methods, which employ some characteristic chemical reaction; and (c) *kinetic* methods, which employ some characteristic behavior of concentration as a function of time.

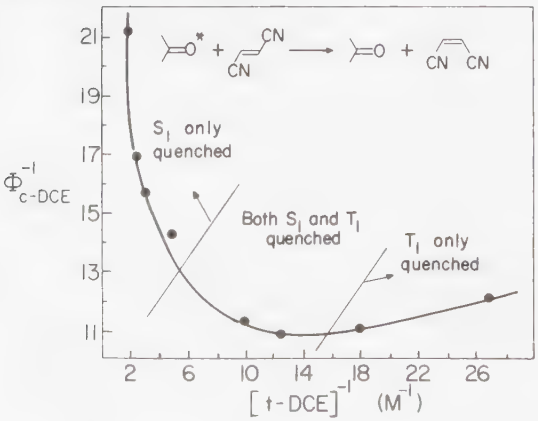

Figure 8.6

Plot of the reciprocal quantum yield for acetone sensitized trans cis isomerization of DCE (Eq. 8.42) versus reciprocal [DCE].

The most important types of *spectroscopic* techniques available for the detection of organic reaction intermediates are:

1. *Electronic spectroscopy*, which involves the absorption or emission of UV or visible light as the result of electronic transitions.

2. *Vibrational spectroscopy*, which involves the absorption of infrared light as the result of vibrational transitions.

3. *Magnetic resonance spectroscopy*, which involves the absorption of microwave radiation as the result of electronic spin transitions or the absorption of radio frequency radiation as the result of nuclear spin transitions. Table 8.3 elaborates on these three types of reaction-intermediates detection.

8.9 Experimental Tests for Reactive Intermediates

In order to qualify as a nonisolable reactive intermediate, we shall require that such a species possess a molecular structure sufficiently stable such that its existence is subject to experimental confirmation such as spectroscopic or chemical trapping. This means that the structures of "true" reactive intermediates must imply an experimental test that "confirms" the structure: i.e., a potentially measureable experimental quantity which relates to the structure must exist. For

Table 8.3 Experimental Methods for Detection of Intermediates

Intermediate	Direct Methods	Indirect Methods
S_1	F, A	CIDNP, kinetics, products
T_1	P, A, ESR	CIDNP, kinetics, products
S_n	none	λ-effect, kinetics, products
T_n	none	λ-effect, kinetics, products
R_3C+	A, F, P	MI, CT, products
R_3C-	A, F, P	MI, CT, products
$R_3C\cdot$	F, A, ESR	MI, CT, products
Z	A, F, P	MI, CT, products
D	ESR, F, P	CIDNP, MI, CT, products
$R_2\dot{C}$	ESR, A, F, P	MI, CIDNP, products
R_2C:	A, F, P, ESR(T)	CIDNP, products

F = Fluorescence
P = Phosphorescence
A = Absorption
ESR = Electron Spin Resonance
CT = Chemical Trapping
MI = Matrix Isolation
CIDNP = Chemically Induced Nuclear Polarization
Products = Structure and distribution, stereochemistry, regiochemistry, labeling, etc.

convenience we shall classify the observation employed for detection and characterization of reactive intermediates in terms of (a) chemical measurements or (b) physical measurements (Table 8.3).

Experimental Tests for the Involvement of Electronically Excited States: Qualitative Aspects

Although the most definitive experimental test for the occurrence of an electronically excited state is the observation of its emission spectrum, many excited states emit too weakly for experimental detection. For example, with rare exception, only the S_1 and T_1 states of organic molecules emit measurably. This means that S_2, S_3, etc., and T_2, T_3, etc., in general cannot be detected by conventional emission spectroscopy. How does one decide if "upper excited states" are involved in photoreactions?

If a photoreaction is wavelength-independent, i.e., it occurs with the same efficiency and or rate and yields the same products irrespective of whether S_1, S_2, S_3, etc., is excited, then we conclude that a common structure is responsible for the result. Since only S_1 is energetically allowed as a common structure we conclude that reaction does not occur from S_2, S_3, etc. Can we conclude that reaction occurs from S_1 based solely on these results? The answer is no. The lack of a wavelength-dependence would only eliminate upper singlet levels as candidates for reaction. It would be possible that S_1 or some triplet derived from it might be the reactive state.

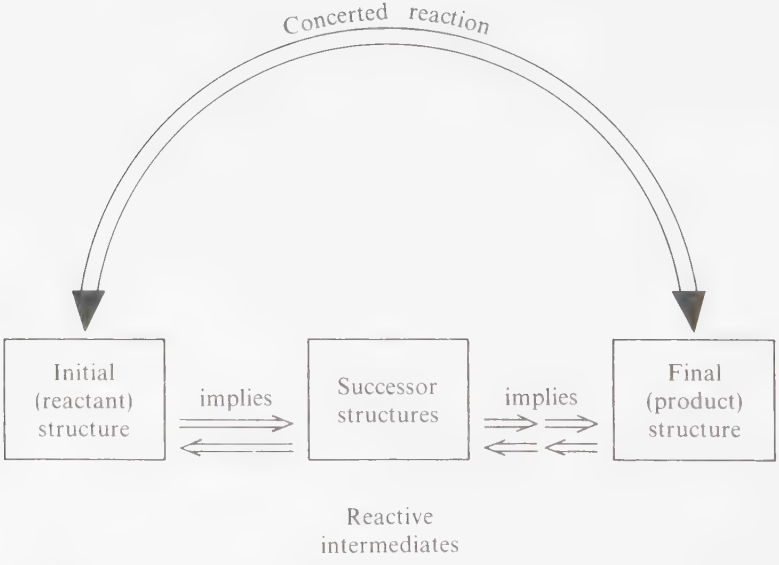

Scheme 8.3

The role of structures in mechanistic analyses.

Suppose a reaction, $R + h\nu \rightarrow P$ has been found to be wavelength-independent. For simplicity let us assume that only one triplet (T_1) lies lower in energy than S_1 and that S_1 and T_1 exhibit different photoreactivities. How does one decide experimentally whether reaction occurs from S_1 or T_1 (or both)? Since T_1 is formed from S_1, quenching of S_1 will not prove much, since reaction from both S_1 and from T_1 will be inhibited.

Two general procedures have been developed to decide whether S_1 or T_1 is the reactive state in a photoreaction:

1. Selective photosensitization of formation of T_1 via an energy-transfer process.
2. Selective quenching of T_1.

The mechanism of energy transfer and selective triplet quenching is discussed in Chapter 9. For our purposes here, we accept that specific triplet sensitizers and quenchers can be found. The logic of triplet photosensitization (see Fig. 8.7) is that if, upon triplet photosensitization, the same products are formed as occur during direct excitation; since S_1 is not produced in the triplet sensitized process, T_1 must be the reactive state under both direct and sensitized excitation. A negative result implies that T_1 is *not* involved in the direct excitation process, i.e., reaction occurs from S_1.

By a related logic, if a *selective* quencher of T_1 inhibits the reaction, then reaction is deduced to occur from T_1. A negative result implies that reaction occurs from S_1.

Although these procedures are commonly employed in mechanistic studies, they are only qualitative. The conclusions become convincing if they are made *quantitative*. For example, the failure to observe a reaction undergo "triplet photosensitizing conditions" may result from failure to efficiently cause production of T_1 by triplet energy transfer.[10] This failure may be due simply to improper experimental conditions, i.e., the concentrations and sensitizer-acceptor pair must be selected to optimize energy transfer. Similarly, the failure to observe quenching of reaction in the presence of a "selective triplet quencher" may result from too low a concentration of quencher or too short a lifetime of T_1. Knowledge of rate constants for energy transfer and triplet lifetimes removes these ambiguities. It is good practice to attempt to observe *directly* both sensitization of triplet reactant phosphorescence and quenching of triplet reactant phosphorescence.

Experimental Tests for the Involvement of Electronically Excited States: Quantitative Aspects

Although triplet photosensitization and quenching provide useful qualitative tools for deciding whether a given excited state (S_1, T_1, etc.) is involved along a reaction pathway, mechanistic tests are more convincing when they can be applied quantitatively. The basic idea behind a quantitative application of sensitization and quenching is the notion that if all of the appropriate rates are known, the probabilities of various reaction pathways are known.

For example, the notion of a "selective" triplet quencher is made quantitative by the measurement of k_q for quenching S_1 and T_1. The reason that 1,3-dienes have been commonly employed as specific triplet quenchers of ketones[8c] is the large differential between k_q^S and k_q^T, the rate constants for quenching of S_1 and T_1 of alkanones, respectively.[7] In the case of acetone with 1,3-pentadiene as quencher, the value of k_q^S is $\sim 10^8\ M^{-1}\ sec^{-1}$ whereas k_q^T is $\sim 5 \times 10^9\ M^{-1}\ sec^{-1}$. This factor of ~ 50 means that at a given concentration of 1,3-pentadiene and excited states, acetone triplets are quenched 50 times faster than acetone singlets. However, the actual rate of quenching of S_1 and T_1 depends on the steady-state concentrations of S_1 and T_1:

General Idea:
(1) $R^* \rightarrow I \rightarrow P$ if I is trapped, No P.
(2) $I \leftarrow R^* \rightarrow P$ if I is trapped, P still formed.

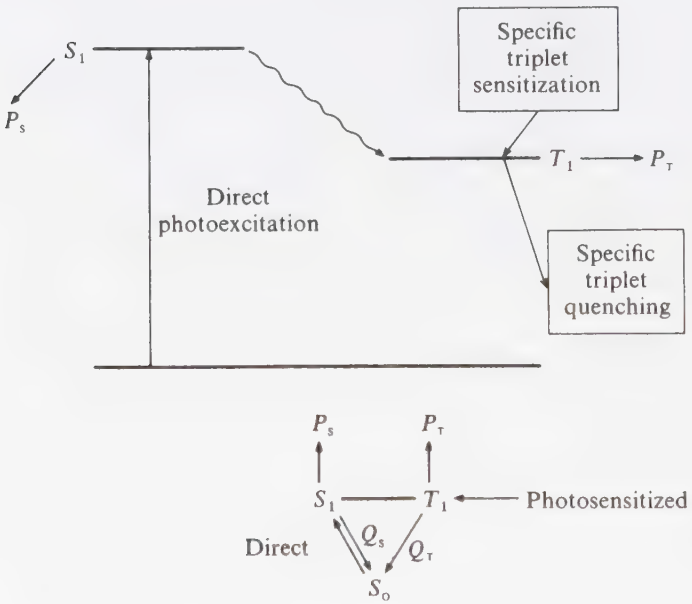

Result	Conclusion
Only S_1 quenched, reaction inhibited	None
Only T_1 quenched, reaction inhibited	T_1 reacts
Only T_1 quenched, reaction uninhibited	S_1 reacts
Only T_1 sensitized, reaction does not occur	S_1 reacts
Only T_1 sensitized, reaction occurs	None

Figure 8.7

Paradigm for specific sensitization and quenching of T_1 for a wavelength-independent reaction.

$$\text{rate of quenching of } S_1 = k_q^S[S_1][Q] \tag{8.43}$$

$$\text{rate of quenching of } T_1 = k_q^T[T_1][Q] \tag{8.44}$$

At the steady state $[S_1] \propto \tau_S$ and $[T_1] \propto \tau_T$ so that:

$$\text{rate of quenching of } S_1 = k_q^S\tau_s[Q] \tag{8.45}$$

$$\text{rate of quenching of } T_1 = k_q^T\tau_T[Q] \tag{8.46}$$

For acetone at room temperature (in acetonitrile as a typical "inert solvent") $\tau_s \sim 2 \times 10^{-9}$ sec and $\tau_T \sim 50 \times 10^{-6}$ sec. Thus:

$$\frac{\text{quenching of } S_1}{\text{quenching of } T_1} = \frac{k_q^S\tau_s[Q]}{k_q^T\tau_T[Q]} = \frac{(10^8) \times (2 \times 10^{-9})}{(5 \times 10^9) \times (50 \times 10^{-6})} \cong \frac{1}{10^6} \tag{8.47}$$

From Eq. 8.47 we learn that at the steady state the ratio of *effective* quenching of T_1 relative to S_1 is about 1 million to one.

From the above analysis a long triplet lifetime can be seen to be useful in selective quenching. Even if $k_q^S \sim k_q^T$, the effective ratio of quenching of S_1 relative to T_1 goes as τ_s/τ_T, so if S_1 is short-lived and T_1 is long-lived, selective triplet quenching can still be achieved.

Without quantitative information about quenching constants, many tests for the involvement of S_1 and T_1 become ambiguous. We have seen that if S_1 is quenched, then *no* information is revealed about whether S_1 or T_1 is involved along the reaction pathway because T_1 is generally derived from S_1. Thus, if a quencher is observed to be effective, *it must be established that S_1 is not quenched.* Experimentally, knowledge of k_q, τ_s, and $[Q]$ allow the adjustment of concentrations so that S_1 will not be quenched.

For example, for S_1 of acetone, a concentration of 10^{-3} M of 1,3-pentadiene leads to a rate of quenching of $k_q[Q][S_1] = 10^5[S_1]$ sec^{-1}. From the lifetime of S_1, its rate of decay is $(1/\tau_s)[S_1] = 5 \times 10^8[S_1]$. Thus:

$$\frac{\text{rate of quenching of } S_1}{\text{rate of decay of } S_1} = \frac{10^5[S_1]}{5 \times 10^8[S_1]} = \frac{1}{5 \times 10^3}$$

$$= 2 \times 10^{-3} \text{ at } 10^{-3} \text{ M of } Q \tag{8.48}$$

A similar analysis for the quenching of T_1 leads to:

$$\frac{\text{rate of quenching of } T_1}{\text{rate of decay of } T_1} = \frac{4 \times 10^6[T_1]}{2 \times 10^4[T_1]} = 200 \text{ at } 10^{-3} \text{ M of } Q \tag{8.49}$$

Clearly, T_1 is nearly completely quenched at 10^{-3} M of 1,3-pentadiene (200 triplets quenched for every one not quenched), whereas S_1 is essentially unaffected by 10^{-3} M of 1,3-pentadiene.

It is possible that quenchers may inhibit a reaction without deactivating S_1 or T_1. This can occur when a reactive intermediate produced from S_1 or T_1 is intercepted by the quencher. Since the lifetime of such a reactive intermediate will generally be different from that of S_1 and T_1, the occurrence of such a situation may be revealed from a Stern-Volmer analysis which indicates a $k_q\tau$ value inconsistent with that expected for quenching of S_1 or T_1 as measured by fluorescence and/or phosphorescence quenching.

As an illustration, the ketyl radicals produced via hydrogen abstraction of the n, π^* states of ketones may be intercepted by the commonly employed triplet ketone quencher 1,3-pentadiene (Eq. 8.50).[11] Thus, if product analysis is monitored experimentally, the hydrogen abstraction reaction will be quenched. The Stern-Volmer analysis might yield a linear plot in such a case. However, $k_q\tau$ (from the slope of the plot) would refer to the rate constant for addition of ketyl radical to the 1,3-diene (k_q) and the lifetime of the ketyl radical (τ):

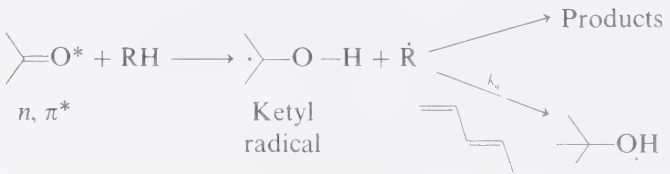

(8.50)

An upper limit to the magnitude of the bimolecular quenching constant k_q is usually set by the rate of diffusion (k_{DIF}) of the excited state and quencher into a *solvent cage* (discussed in more detail in Section 9.7). It is informative to examine the relationship of the rate of bimolecular quenching to the decay rate (k_D) or lifetime (τ_D) of an excited state D^*. Let k_q be the bimolecular rate constant for bimolecular quenching of D^* by a quencher Q. Table 8.4 shows how the quencher concentration $[Q]$, k_q, τ_D, and k_D are related. The quencher concentrations $[Q]_{0.50}$ and $[Q]_{0.99}$ denote the concentrations required to quench 50% and 99% of the D^* molecules.

Taking $k_q = 10^{10}\ \text{M}^{-1}\ \text{sec}^{-1}$ as typical of diffusion-controlled quenching, it is clear from the Table that if $[Q] < 10^{-3}$ M then virtually no quenching will occur if $\tau_D < 10^{-8}$ sec ($k_D > 10^8\ \text{sec}^{-1}$). However, if $\tau_D > 10^{-3}$ sec ($k_D < 10^3\ \text{sec}^{-1}$), at $[Q] = 10^{-5}$ M more than 99% of the D^* molecules will be quenched.

In general, since k_r is usually greater than $10^6\ \text{sec}^{-1}$ (Table 5.3), most *fluorescent* molecules are not quenched efficiently by any quencher whose concentration is $< 10^{-3}$ M, since k_q rarely exceeds $10^{10}\ \text{M}^{-1}\ \text{sec}^{-1}$. However, since k_r is rarely larger than $10^2\ \text{sec}^{-1}$, most *phosphorescent molecules* will be strongly quenched at concentrations $> 10^{-4}$ M if Q is a diffusional quencher. Finally, if $[Q] > 0.1$ M, both fluorescence and phosphorescence will generally be quenched if $k_q = 10^{10}$ $\text{M}^{-1}\ \text{sec}^{-1}$.

The Use of Kinetic Methods to Detect and to Identify Intermediates

The experimental observation of a Stern-Volmer quenching of a photochemical reaction is in itself evidence for an intermediate, i.e., *something* is being intercepted by the quencher. The *Stern-Volmer constant* $k_q\tau$ (the slope of the Stern-Volmer quenching plot) is a reaction constant characteristic of that intermediate for a given solvent and temperature. Thus, the value of $k_q\tau$ may serve to characterize the intermediate being quenched. Because k_q is limited by the rate of diffusion, we can calculate the *minimum lifetime* of the species being quenched if we calculate τ under the assumption $k_q = k_{\text{DIF}}$.

A relevant example of the application of the above principles is found in a "classic" argument[12] for the involvement of $T_1(n, \pi^*)$ of benzophenone as the chemically reactive agent in the photoreduction of benzophenone by benzhydrol:

$$\mathrm{Ph_2CO} + \mathrm{Ph_2CHOH} \xrightarrow{h\nu} \mathrm{Ph_2C(OH)CPh_2(OH)} \qquad (8.51)$$

Table 8.4 Relationships Between Concentrations, Lifetimes, and Quenching Constants

τ_{X^*} (sec)	Values of $[Q]_{0.50}$ (moles/liter) if $k_q = 10^8$	10^{10}	10^{12} M^{-1} sec^{-1}	Values of $[Q]_{0.99}$ (moles/liter) if $k_q = 10^9$	10^{10}	10^{11} M^{-1} sec^{-1}
10^{-11}		10	10^{1}			
10^{-10}		1	10^{2}			10
10^{-9}	10	10^{1}	10^{3}		10	1
10^{-8}	1	10^{-2}	10^{4}	10	1	10^{-1}
10^{-7}	10^{-1}	10^{-3}	10^{5}	1	10^{1}	10^{2}
10^{-6}	10^{-2}	10^{-4}	10^{6}	10^{-1}	10^{2}	10^{3}
10^{-5}	10^{-3}	10^{-5}	10^{7}	10^{-2}	10^{-3}	10^{-4}
10^{-4}	10^{-4}	10^{-6}	10^{8}	10^{-3}	10^{4}	10^{-5}
10^{-3}	10^{-5}	10^{-7}	10^{9}	10^{-4}	10^{-5}	10^{6}

$[Q]_{0.50}$ (moles/liter)	Values of k_q (M^{-1} sec^{-1}) if $\tau_{X^*} = 10^{-9}$	10^{-8}	10^{-7}	10^{-6}	10^{-5}	10^{-4}	10^{-3}
10	10^{8}	10^{7}	10^{6}	10^{5}	10^{4}	10^{3}	10^{2}
1	10^{9}	10^{8}	10^{7}	10^{6}	10^{5}	10^{4}	10^{3}
10^{-1}	10^{10}	10^{9}	10^{8}	10^{7}	10^{6}	10^{5}	10^{4}
10^{-2}	10^{11}	10^{10}	10^{9}	10^{8}	10^{7}	10^{6}	10^{5}
10^{-3}	10^{12}	10^{11}	10^{10}	10^{9}	10^{8}	10^{7}	10^{6}
10^{-4}		10^{12}	10^{11}	10^{10}	10^{9}	10^{8}	10^{7}
10^{-5}			10^{12}	10^{11}	10^{10}	10^{9}	10^{8}
10^{-6}				10^{12}	10^{11}	10^{10}	10^{9}
10^{-7}					10^{12}	10^{11}	10^{10}

This argument was proposed before emission spectroscopy and flash spectroscopy were widely available for direct detection of excited states. The "chemical mechanism" assumed for the reaction is:

$$\underset{\text{B}}{Ph_2CO} \xrightarrow{h\nu} \underset{\text{B}^*}{Ph_2CO^*} \qquad \textit{rate } aI \tag{8.52}$$

$$B^* \longrightarrow B_0 \qquad k_d[B^*] \tag{8.53}$$

$$B^* + \underset{\text{BH}_2}{Ph_2CHOH} \longrightarrow BH\,(Ph_2\dot{C}OH) \qquad k_r[B^*][BH_2] \tag{8.54}$$

$$2BH \longrightarrow \text{pinacol} \qquad k_p[BH]^2 \tag{8.55}$$

$$B^* + Q \longrightarrow Q^* + B_0 \qquad k_q[B^*][Q] \tag{8.56}$$

The question is whether $S_1(n, \pi^*)$ or $T_1(n, \pi^*)$ is involved in the abstraction step. We have seen that if a photoreaction involves the competition between a bimolecular reaction and a unimolecular decay of B^*, then an efficiency-rate law of the following form should exist:

$$1/\Phi = 1/a + k_d/ak_r[BH_2] \tag{8.57}$$

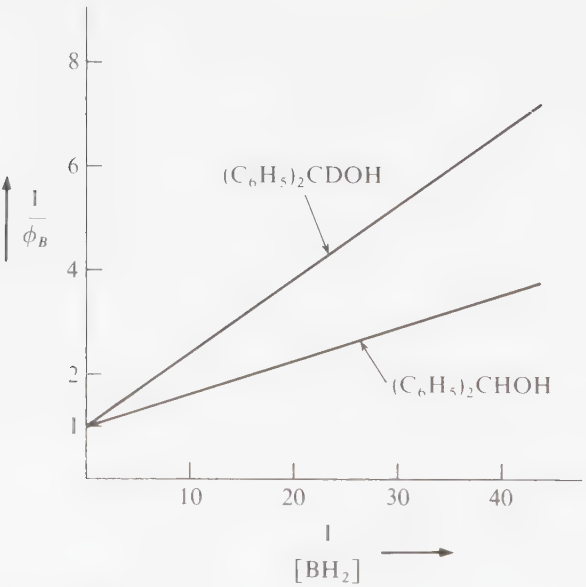

Figure 8.8

Schematic representation of the plot of Eq. 8.57 for the photoreduction of benzophenone to benzpinacol by $(C_6H_5)_2CDOH$ and $(C_6H_5)_2CHOH$ (Eq. 8.51).

where a = the efficiency of formation of B^*. A plot of $1/\Phi$ (where Φ = the quantum efficiency for disappearance of benzophenone *or* the formation of benzpinacol) versus $1/[BH_2]$ is predicted to yield a straight line of slope = k_d/ak_r and an intercept of $1/a$. Such a plot is shown in Figure 8.8.

First, the linearity of the plot confirms the assumed mechanisms and allows us to identify the value of slope with the ratio k_d/ak_r and the intercept with $1/a$. The value of the intercept for *both* reducing agents is equal to 1.0. Therefore the value of the slope equals k_d/k_r. The measured value of 0.05 means that $k_d = 0.05k_r$.

If known concentrations of such a bimolecular quencher, Q, are added to benzene solutions of benzhydrol and benzophenone, the following rate law is predicted:

$$\frac{1}{\Phi} = \frac{1}{a} + \frac{k_d}{ak_r[BH_2]} + \frac{k_q[Q]}{ak_r[BH_2]} \tag{8.58}$$

Since k_d/k_r and a are known from treatment of data for $[Q] = 0$, a plot of $1/\Phi$ versus $[Q]$, a fixed initial concentration of $[BH_2]$ will yield a slope equal to $k_q/k_r[BH_2]$ since as we already have seen, $a = 1$. Figure 8.9 shows such a plot for Q = 1,3-pentadiene, for which $k_q/k_r = 500$. The same ratio should be derivable from variation of $[BH_2]$ at constant $[Q]$, as in fact it is.

From the experimental ratios of k_d/k_r and k_q/k_r, an upper limit for the value of k_d, the inherent decay rate of B^*, can be evaluated. The maximum value of k_q is $k_{DIF} = 5 \times 10^9\ M^{-1}\ sec^{-1}$, i.e., the rate constant for diffusion in benzene. Thus, $k_r(max) = 5 \times 10^9/500 = 1 \times 10^7\ M^{-1}\ sec^{-1}$ and

$$k_d(max) = 0.05k_r(max) = 5 \times 10^5\ sec^{-1} \tag{8.59}$$

Only very weak fluorescence ($\Phi_f < 10^{-4}$) is observed from benzophenone. Based on its absorption spectrum, the inherent radiative lifetime of $S_1(n, \pi^*)$ of

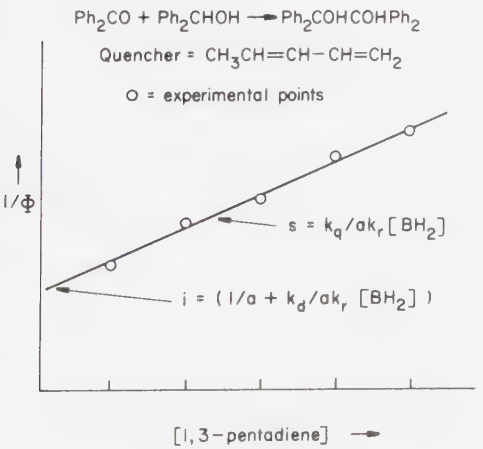

Figure 8.9

Example of the quenching of a bimolecular reaction. The concentration of reactant, $Ph_2CHOH(BH_2)$, is held fixed, and the concentration of quencher (1,3-pentadiene) is varied. It is important to note that Eq. 8.58 is valid only if $[BH_2]$ does not change significantly during the reaction, and that $[Q]$ also remains constant.

benzophenone is theoretically (Eq. 5.11) expected to be of the order of 10^5 10^6 sec^{-1}. Thus, the rate constant for deactivation of $S_1(n, \pi^*)$ must be greater than 10^9–10^{10} sec^{-1} in order to account for the very weak fluorescence efficiency. However, Eq. 8.59 requires that the reactive state is deactivated at a maximum rate of 5×10^5 sec^{-1}.

Under the premise that B^* must be $S_1(n, \pi^*)$ *or* $T_1(n, \pi^*)$, $S_1(n, \pi^*)$ is excluded as a plausible reactive intermediate.

This conclusion has since been completely vindicated by measurements of quenching of $T_1(n, \pi^*)$[13] monitored by triplet-triplet absorption and phosphorescence.[14]

8.10 Experimental Tests for the Involvement of Radicals and Diradicals

Radicals, diradicals, and radical pairs are extremely common intermediates in organic photoreactions. In Chapter 7, we found that $n, \pi^* \rightarrow D$ transformations are the general rule for both singlet and triplet states and that $^1\pi, \pi^* \rightarrow Z$ and $^3\pi, \pi^* \rightarrow {}^3D$ transformations are common.

All of the experimental criteria (Table 8.3) for detecting and characterizing intermediates may be employed to detect radicaloid species as transients in photochemical reactions. In this section we shall discuss product structure criteria and in the next section we shall discuss the powerful method of *magnetic resonance*. The latter may be used to unambiguously identify radicaloid species.

Reactions of Diradicals ^1D and ^3D

The notion that a diradical (^1D = a singlet diradical and ^3D = a triplet diradical) exhibits chemistry consistent with that expected of two independent odd-electron centers allows us to anticipate the following behavior:[15]

1. ^1D will yield singlet products only.

2. ^3D will yield triplet products only.

3. Intersystem crossing $^1D \rightleftarrows {}^3D$ will potentially compete with reactions of ^1D and ^3D.

$$\underset{\text{products}}{\text{Singlet}} \longleftarrow {}^1D \rightleftarrows {}^3D \longrightarrow \underset{\text{products}}{\text{Triplet}} \tag{8.60}$$

Given these preliminary rules of behavior we next suppose:

4. Reactions of ^1D and ^3D are precisely those known and expected of the individual radical centers, consistent with 1, 2, and 3 listed above. (Exceptions may be those processes of a diradical which can directly produce molecular products).

Let us take as an example a 1,4 biradical. Such species are commonly implicated in intramolecular hydrogen abstraction (Type II) reactions and cycloadditions. Of the various *unimolecular* processes which are probable, the singlet diradical ^1D can generally undergo several *general* processes which lead directly to molecular products: (a) coupling, (b) disproportionation or intramolecular hydrogen transfer, and (c) fragmentation. In addition, ^1D can proceed to other diradicals via (d) internal rearrangements, and (e) undergoing electron transfer to produce zwitterions. In competition with these chemical reactions of ^1D are the physical processes of (f) conformational changes, and (g) intersystem crossing. Finally, ^1D may undergo bimolecular reactions which serve to "trap" the species. These trapping processes are usually hydrogen abstraction and/or addition to unsaturated systems.

The reactions of ^3D are much more limited because of Rule 2 above, i.e., ^3D must proceed directly to triplet products. As a result, $^3D \rightarrow$ coupling, disproportionation, and fragmentation are unlikely (unless an exceptionally facile mechanism for intersystem crossing exists) since the immediate products must be molecular triplet states which usually possess a higher energy content than ^3D. As an example (Eq. 8.61), fragmentation of a 1,4-diradical to a triplet ethylene and ground-state is unfavorable energetically and is not expected to be efficient:

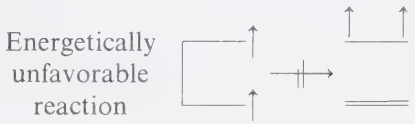

(8.61)

As a result:

5. We expect ^3D to undergo only physical processes, trapping, and rearrangement to different triplet diradicals.

A final rule for triplet diradicals postulates that:

6. Structures in which odd electrons are of the same spin are more stable the further apart are the location of the odd electrons.[16]

Examples of Rule 6 are the conversion of a di-π-methane triplet into a cyclized cyclopropyl carbinyl diradical (Eq. 8.62), and the cyclization of a bis-allylic triplet to a cyclized cyclopentyl carbinyl diradical (Eq. 8.63):

(8.62)

bis-allylic triplet (1,2-diradical) — cyclopropyl carbinyl (1,4-diradical) (8.63)

8.11 Magnetic Resonance Methods for Detecting Radicals, Radical Pairs, and Diradicals

Magnetic resonance is a powerful experimental tool for the detection and characterization of radicaloid structures.[17,18] The technique of magnetic resonance is a form of spectroscopy which measures from the absorption or emission of light due to change in electronic or nuclear magnetic *spin* states. *Monoradicals* may be *directly* detected and characterized by the form of magnetic resonance known as (ESR) Electron Spin Resonance. This form of spin spectroscopy is applicable to the liquid, solid, and gaseous phases. In the solid phase ESR may be employed to characterize the electronic configuration of triplet states.

A rather recent type of magnetic resonance employs an indirect method to detect and characterize *radical pairs* and *diradicals*. This is known as *Chemically Induced Dynamic Nuclear Polarization* (CIDNP).[19] In the following sections a brief theoretical discussion of the ESR and CIDNP methods will be given, along with experimental applications to the detection and characterization of monoradicals, radical pairs, and diradicals.

Magnetic Resonance: Electron Spin Spectroscopy Applied to Monoradicals and Triplets

The spin motion of an electron generates a magnetic moment, and since the orientation of this moment can be quantized in the presence of any arbitrary magnetic field, electronic spin "sublevels" are produced. We expect that transitions between these quantized states may occur by radiationless and radiative mechanisms. The study of absorption of electromagnetic radiation which causes transitions from one spin sublevel to another is called *magnetic resonance spectroscopy*.[18] When applied to electrons it is termed *Electron Paramagnetic Resonance* (EPR) or *Electron Spin Resonance* (ESR). When applied to nuclear spins, it is termed *Nuclear Magnetic Resonance* (NMR). The theories of ESR and NMR are very similar in form. The major experimental differences are the energy gap between sublevels and the frequency of radiation required for resonance. Typically, the energy gap between electron spin sublevels is of the order of 1 to 10^{-1} cm^{-1} (3×10^{-3} to 3×10^{-4} kcal mole) in a strong external magnetic field ($\sim$10,000 gauss). This corresponds to electromagnetic radiation in the microwave region ($\sim 10^{10}$ sec^{-1}). On the other hand, the energy gap between nuclear spin sublevels

is of the order of 10^{-2} to 10^{-3} cm^{-1} (3×10^{-5} to 3×10^{-6} kcal/mole) in a strong external magnetic field ($\sim$10,000 gauss). This corresponds to electromagnetic radiation in the radio frequency range.

The technique of electron spin resonance has been profitably applied to the study of photochemical problems involving species that possess one or more unpaired electrons. The most extensive studies are concerned with monoradicals which are common photoproducts produced from reactions of triplet excited states and with triplet states themselves. Practically speaking, the latter studies must be performed in a rigid, solid solution, because the rotational motions of molecules which occur in fluids cause substantial "line broadening" and loss of sensitivity. As a result, most ESR studies of triplets are performed with solid samples at very low temperatures. Monoradicals, on the other hand, may be studied in the solid, liquid, or vapor phase, with the major limitation generally being that a proper analysis requires a steady-state free radical concentration of about 10^{-8} M. In summary, some important points to keep in mind are:

1. The ESR of monoradicals may be studied in all three phases.
2. The ESR of triplets may be studied only in the solid phase.
3. Minimum steady-state concentrations of about 10^{-8} M are required for proper analysis.
4. Steady-state concentrations may be controlled to a certain degree by variation of the intensity of the exciting incident radiation.
5. The ESR transitions are between very closely spaced (<1 cm^{-1} or $<10^{-3}$ kcal/mole) spin sublevels of a triplet and not between electronic levels, i.e., each of the triplet sublevels corresponds to the same electronic configuration.
6. Triplet ESR provides information such as spin-spin interaction energies, of both electron-electron and electron-nuclear origin.

ESR of an Idealized Single Electron System

For simplicity, let us consider the behavior of an idealized system, namely an isolated electron with only spin motion (i.e., spin angular momentum). The simultaneous occurrence of a charge and spin motion imbues this electron with a magnetic moment μ which can interact with molecular or laboratory magnetic fields. In units of Planck's constant, μ can only have values of $+\frac{1}{2}$ or $-\frac{1}{2}$, corresponding to two *spin states*, parallel (lowest energy) or antiparallel (higher energy), with a defined magnetic field (Fig. 8.10). In the absence of a magnetic field, the energy of the two spin states is degenerate. These two states will separate in energy when a magnetic field interacts with μ, the electron's magnetic moment. Let us suppose that an external magnetic field $\mathbf{H}_0$ is applied to our free electron. The electron spin moment will now tend to align with the magnetic field. The energy separation, ΔE, corresponding to the parallel and antiparallel alignment,

will depend upon the magnitude of the applied field;

$$E = g\beta \mathbf{H}_o \mu = \mu h\nu \tag{8.64}$$

$$\Delta E = g\beta \mathbf{H}_o = h\nu \tag{8.65}$$

where g is called the "g factor," a proportionality constant for a given electron and equal to 2.00023 for a hypothetical "free" electron, and β is called the "Bohr magneton," and is also a proportionality constant. Figure 8.10 indicates the energy of separation of the electron spin levels as a function of H_o. A typical value of $\mathbf{H}_o$ is 3000 gauss, for which $\Delta E \cong 1$ to 0.1 cm $^{1} = 3$ to 0.3×10^{-3} kcal mole. In terms of frequency, $\nu \cong 10^{10}$ to 10^{9} sec^{-1}.

Because of the uncertainty principle, we imagine electrons of spin of $+\frac{1}{2}$ and $-\frac{1}{2}$ to precess about the principal axis of $\mathbf{H}_o$. Experimentally, we can only measure the average value of the spin magnetic moment, namely the value corresponding to the resultant value of the precessing spin moment on the $\mathbf{H}_o$ axis. We call this average value α and β for the $+\frac{1}{2}$ and $-\frac{1}{2}$ states, respectively. We expect that when $h\nu$, the energy of impinging radiation, equals the energy separation between the $+\frac{1}{2}$ and $-\frac{1}{2}$ spin states transition from the $-\frac{1}{2}$ to the $+\frac{1}{2}$ state will occur, with

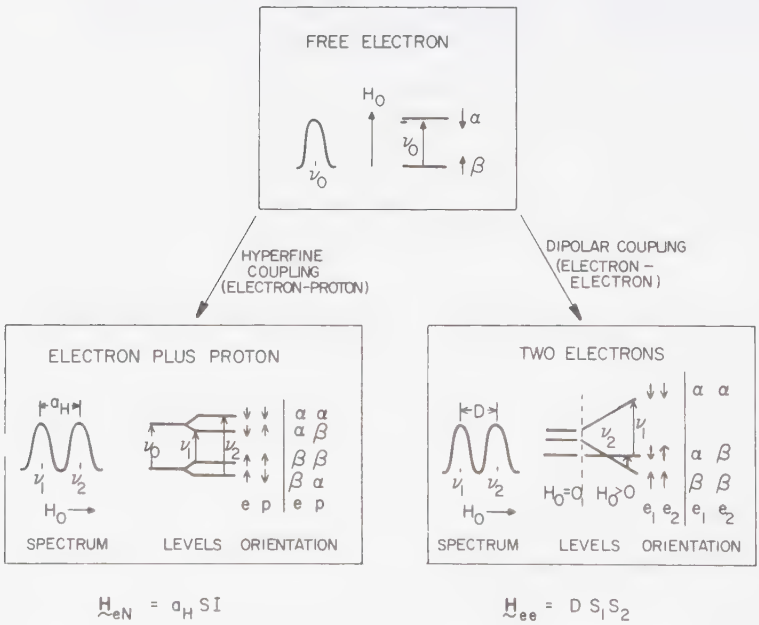

$$\underset{\sim}{H}_{eN} = a_H \, S I \qquad \underset{\sim}{H}_{ee} = D \, S_1 S_2$$

Figure 8.10

Simplified schematic description of the effect of interaction of "free" electron spin with (1) a proton spin (lower left, hyperfine coupling constant termed a_H or a), and (2) another electron spin (lower right, coupling constant given approximately by D).

the simultaneous absorption of radiation. Experimentally, an absorption curve will result, with its maximum corresponding to the average energy for the transition.

Interaction of Electron Spin with Nuclear Spin: Hyperfine Coupling

An electron in an actual molecule does not behave exactly like our idealized free electron. The most important differences are: (a) spin-orbit coupling will cause the value of g to vary somewhat from the "ideal" value of 2.00023 for a "free" electron due to *spin-orbit* coupling, and (b) interactions between the electron spin magnetic moment and the nuclear spin magnetic moment will occur via electron-spin–nuclear-spin hyperfine coupling. The latter coupling leads to a splitting in the single absorption line of the idealized free electron.

For example, if a proton (nuclear spin $= +\frac{1}{2}$ or $-\frac{1}{2}$) couples with the electron, four states instead of two states result, and two absorption lines are possible.

The situation for a one (unpaired) electron–one (coupled) proton system is shown in Figure 8.10, on the left. Absorption will involve transitions from the lower two levels ($\beta\alpha \equiv$ electron spin β, proton spin α; $\beta\beta \equiv$ electron spin β and proton spin β, etc). A relatively large number of transitions are possible.

Those transitions which involve changing the orientation of only the nuclear spin are NMR transitions (e.g., $\beta\alpha \rightarrow \beta\beta$), and are not of direct interest to us here. Those which involve changing both the electron and proton spin orientations may be described as forbidden transitions and may be neglected. The remaining transitions are those in which the electron spin orientation changes but the nuclear spin orientation is conserved. There are two such transitions and we therefore observe two resonance absorption lines. Since the spectrum is recorded by varying the magnetic field, these two lines will be observed at different values of the applied field, and the separation between them (called the hyperfine splitting constant, a_H) is usually expressed in gauss. Similarly, if two electrons of parallel spin interact, then a triplet state is possible and two absorptions are observed (Fig. 8.10, on the right). Selection rules dictate that only $\beta(1)\beta(2) \rightarrow \alpha(1)\beta(2)$ and $\alpha(1)\beta(2) \rightarrow \alpha(1)\alpha(2)$ transitions are "allowed," i.e., only one "spin flip" at a time may occur. In practice, a weaker double flip transition may also be observed.

For our purposes it will be sufficient to know that ESR-spectra free radicals and triplets provide information concerning *electronic* and nuclear structure. In the case of organic free radicals, the ESR spectrum will generally appear as a pattern of absorption bands which will be related to the number of protons coupled to the odd electron and to the positions and stereochemical relationships of the protons to the odd electrons.

A key information parameter which is extracted from the ESR of organic free radicals is the proton-electron hyperfine coupling constant a_H. Most commonly encountered organic free radicals will possess the odd electron in a localized p-orbital or delocalized π-orbital. An important point (amply confirmed by both theory and experiment) is that the *magnitude of the electron proton hyperfine interaction, a_H, is directly related to the electron density of the unpaired electron*

on the atom bearing the proton which is coupled to the electron. Thus, experimental measurement of the value of a_H yields information on the unpaired electron density at various sites in the organic free radical and therefore allows conclusions to be drawn concerning the *electronic structure* of the free radical. In the following sections on CIDNP we shall see how the hyperfine coupling can provide a mechanism for intersystem crossing and actually determine the *rates* of chemical processes.

For triplet states, the most important parameters derived from ESR spectroscopy are the D and E values, and of these the D parameter (which provides a rough measure of the average separation of the unpaired electrons) usually provides the most valuable information. Values of D for organic triplet states commonly vary over the range 0–1 cm^{-1}.

Although we will go no further into the theory of electron-spin–nuclear-spin interaction, we will summarize the important results which allow structural and dynamic information to be extracted from the ESR spectra of free monoradicals.

Experimental Examples of ESR Spectra; Free Radicals and Triplet States

An ESR spectrometer measures the absorption of electromagnetic energy which occurs when $\Delta E = g\beta\mathbf{H}_0 = h\nu$, i.e., when the resonance condition is satisfied. The interaction causes the transitions to occur between the magnetic dipole of the electron and the oscillating field accompanying an electromagnetic wave. One must "search" for resonance absorption by placing the sample in the magnetic field of the spectrometer and illuminating the sample with microwave radiation. Experimentally, for reasons of technical convenience, derivative curves rather than absorption curves are usually employed. Also, although either $\mathbf{H}_0$ (magnetic field strength) or ν (frequency of impinging radiation) can be varied to bring about the resonance condition, it is usually more convenient to vary $\mathbf{H}_0$.

The ESR spectrum of the $(CH_3)_2COH$ radical, produced by irradiating acetone in isopropanol, is shown in Figure 8.11.[17] The various lines in the spectrum are due to hyperfine splitting, and the hyperfine coupling constant (a_H) of the electron spin to the proton spins is equal to the separation between adjacent lines. Experimental values of a_H are useful as a parameter to characterize the structure of free radicals. Values of a_H generally range from 25 gauss to less than 1 gauss ($\sim 2.5 \times 10^{-3}$ cm^{-1} to $\sim 10^{-4}$ cm^{-1}, or $\sim 10^{-6}$ kcal/mole).

Because free radicals, radical pairs, and diradicals are produced in many photoreactions, one might expect that ESR would be used extensively as an experimental tool in the study of reactive intermediates of organic photoreactions. Unfortunately, this is not the case. The sensitivity of the technique does not allow detection of short-lived free radicals. In particular, for fluid solution, radical pairs and diradicals are generally not detectable by ESR. The reason for this failure is the low steady-state concentration of free radicals. Reactive free radicals have very short lifetimes which are reaction-limited.

However, it is possible to generate many free radicals in a solid matrix (e.g., a solvent in which diffusion is inhibited) and study their ESR properties. For

example, monoradicals, radical pairs, and even diradicals have been "matrix isolated" under conditions such that these "reactive intermediates" are stable indefinitely.

Triplet states possess ESR spectra distinctly different from the ESR spectra of monoradicals. In general, triplet ESR spectra can only be observed in solid solution. (The tumbling of molecules in fluid solution causes interaction averaging and line broadening, and the triplet spectrum is smeared to the point that it becomes unobservable.) Thus, triplet ESR spectroscopy cannot be applied directly to the observation of triplets produced by photoreactions in solution. However, from triplet ESR spectra at low temperatures a quantity called the "D parameter" may be evaluated. The D parameter is a measure of the Zero Field splitting (Section 2.8) of the triplet sublevels.

A Time-and-Distance Scale Derived from ESR Parameters

It is possible to derive a qualitative "order of magnitude" estimate of the rate of electronic changes and of distances of electron separation of radicals from the ESR parameters a_H and D, respectively. In general, the precessional rate of a spin moment $\mathscr{S}$ about any arbitrary magnetic axis is given by:

$$\text{Rate of precession of } \mathscr{S} \quad \omega = \gamma g \mathbf{H}_0 = 3 \times 10^6 \mathbf{H}_0 \text{ for electrons} \tag{8.66}$$

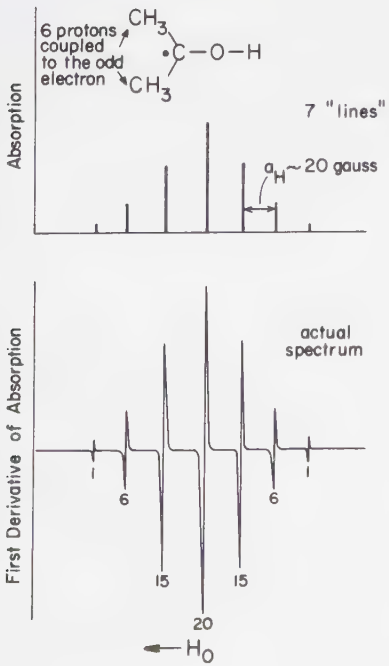

Figure 8.11

ESR spectrum of the $(CH_3)_2\dot{C}OH$ radical, produced by the irradiation of acetone in isopropanol. The six protons of the methyl groups are equally coupled to the odd electron, causing a split into seven lines. The separation between any two adjacent lines is equal to a_H. The experimental absorption spectrum (bottom) is usually displayed as a derivative. The numbers under the bands refer to the relative intensities.

where ω is the precessional rate of $\mathscr{S}$ in radians sec if $\mathbf{H}_0$ is in gauss. Since the *strongest* external magnetic fields correspond to $\sim$10,000 gauss, $\omega_{max} \sim 3 \times 10^8$ rad sec if the precessional rate is determined by an external magnetic field. The magnitude of magnetic fields generated by electron orbital motion may exceed 10^6 gauss (e.g., the magnetic field near the nucleus due to orbital motion of an electron in an innermost Bohr orbit of a hydrogen atom is calculated to be $\sim 10^6$ gauss). As a result, the value of ω due to "internal" magnetic fields may exceed 10^{10} radians/sec^{-1}.

For most hydrogen containing carbon-free radicals, either hyperfine coupling or an external magnetic field will determine the precessional rate of the electron spin moment. We shall see in Section 8.12 that for certain diradicals and diradical pairs, $\mathbf{H}_0$ and a_H may play a crucial role in determining the observation of CIDNP.

The g factor of an unpaired electron may also be evaluated from ESR data. For hydrocarbon radicals the measured value of the g factor is very close to that predicted for a "free electron" in a carbon p-orbital, i.e., 2.00023. However, as the amount of spin-orbit coupling increases the magnitude of g deviates from the free-electron value. For example, if a $p_x \rightarrow p_y$ orbital exchange is possible, its measured value may be approximated by:

$$g(\text{measured}) - g_e \sim |2\zeta/\Delta E| \qquad (8.67)$$

where ζ is the spin-orbit coupling constant for the atom on which the odd electron has density, and ΔE is the energy difference between p_x and p_y orbitals.[18,20]

For a methyl radical, no $p_x \rightarrow p_y$ jump is energetically feasible and ζ is small so that $2\zeta/\Delta E \sim 0$ and $g(\text{measured}) \sim g_e$. However, for peroxy radicals, alkoxy radicals, carbon radicals attached to heavy atoms, etc., the magnitude of $2\zeta\ \Delta E$ may be significant relative to g_e. In fact, the g (measured) values of peroxy radicals differ substantially from those for hydrocarbon radicals.[21]

Finally, from the value of D, an estimation of the separation of the electron spin dipoles (and by inference the average separation of electrons) may be derived.[22] It can be shown that

$$D \sim \tfrac{3}{2}g^2\beta^2 R_{12}^{-3} \rightarrow D \sim 10^{-24} R_{12}^{-3} \qquad (8.68)$$

where R_{12} is the average separation of the electron spins (in Å) and D is the measured ESR parameter in cm^{-1}. As a result, D is sensitive to the "average separation" between electrons 1 and 2, and experimental values of D may be used as a probe to analyze the spatial separations of the triplet electrons. Basically, we may view the two electron spins as being confined to a "box," because the spins are fixed with respect to their limiting spatial separation by the molecular framework. As the "size" of the "box" increases, the value of $\langle R_{12} \rangle^{-3}$ will decrease, as will D.

For example, in the case of a carbene triplet (Eq. 8.69), values of $D \sim 1$ cm^{-1} are common and correspond to $R_{12} \sim 1$ Å, i.e., the electrons on the average are close to one another because they are essentially confined to one atom.[23] In contrast, the triplet diradical pair (Eq. 8.70) produced by photolysis of azo compounds (in a frozen matrix) show a D value of 0.01 cm^{-1}, corresponding to an average separation of the two unpaired electrons of $\sim$6–7 Å.[24]

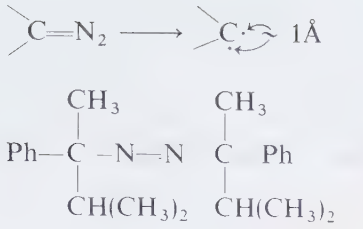

(8.69)

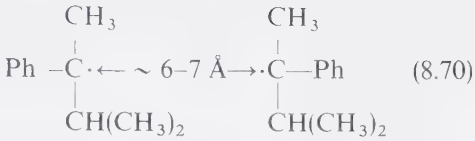

(8.70)

Since the magnitude of D is related to the average distance of separation of the two unpaired spins, it seems reasonable to expect that the value of D may be correlated with the orbital configuration of the triplet state.[22c] Inspection of the data in Table 8.5 shows that this is the case. To the extent that data obtained under matrix conditions is applicable in fluid solutions, D parameters may be used to infer the electron configuration of T_1. We expect that the average distance of separation of electrons in n, π^* states should be different from that of electrons in π, π^* states. By extension of this reasoning, the values of $D(n, \pi^*)$ and $D(\pi, \pi^*)$ should be different. Inspection of Table 8.5 shows that this is the case, so that the value of D may be used as diagnostic of the configuration of T_1.

8.12 Chemically Induced Nuclear Polarization and the Experimental Detection of Radical Pairs

The Electron Spin Resonance (ESR) and Nuclear Magnetic Resonance (NMR) Spectra of molecules provide important structural information concerning (a) chemical structure, (b) frequency of spin motion, and (c) energies of electron-electron and electron-nuclear *magnetic* interactions. Usually ESR and NMR spectra are recorded as *absorption* spectra of the thermally equilibrated populations of electron and nuclear spins in their lower Zeeman levels (the two possible quantized levels of a magnetic dipole in an external magnetic field). It is possible to produce radicals and molecules such that nonequilibrium population of *either* the upper or lower Zeeman levels occurs. This possibility occurs when a chemical reaction generates radicals or molecules such that there is a selection of electron or nuclear spin states. When such processes occur the ESR or NMR spectra are not the conventional spectra corresponding to equilibria populations of the Zeeman levels. Instead, an "anomalously" strong *enhanced* NMR absorption or even an NMR *emission* spectrum may be observed.

The method of Chemically Induced Dynamic Nuclear Polarization (CIDNP) has been coined to define systems for which the *dynamic* chemical reactions lead

to nonequilibrium concentrations of nuclear sublevels.[19] The observation of enhanced absorption or of emission in an NMR experiment is prima facie evidence for the occurrence of a CIDNP phenomenon.

Experimentally, the NMR of the species observed in CIDNP is exactly the same as the normal NMR with respect to the number and chemical shifts of all observed

Table 8.5 Values of D from ESR Spectra and Associated Average Separation of Unpaired Electron Spins

Molecule	D (cm^{-1})[a]	R_{12} (Å)[b]	Triplet Configuration
Benzene[c]	0.160	~1–2	π,π^*
Naphthalene[c]	0.100	~2	π,π^*
Anthracene[c]	0.072	~3	π,π^*
Cyclopentanone[d]	0.140	~2	n,π^*
$Ph_2C{=}O$[e]	0.150	~1–2	n,π^*
PhCOCOPh[f]	0.090	~2–3	n,π^*
$CH_3COCOCH_3$[g]	0.070	~2–3	n,π^*
2-Acetonaphthone[h]	0.095	~2–3	π,π^*
Cyclohexenones[i]	~0.2–0.3	~1	n,π^*

Diradicals	D (cm^{-1})[a]	R_{12} (Å)[b]	Diradical Type
$\cdot\dot{C}H_2$[j]	0.96	~1	1,1
$\cdot\dot{N}H$[k]	1.86	~0.8	1,1
$\underline{Ph_2}\dot{C}\cdot$[l]	0.40	~1–2	1,1
$\overline{R\dot{R}}$[m]	~0.01	~5	
	0.084	~2–3	1,3
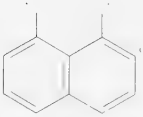	~0.020	~4–5	1,5
$\dot{O}{-}\dot{O}$[p]	~2	~0.5	1,2

[a] Zero field splitting parameter in cm^{-1}.
[b] Average separation of spins evaluated from Eq. 8.68.
[c] Birks, J. B., *Photophysics of Aromatic Molecules*, New York: Wiley, 1970; Thomson, C., *Quart. Rev.*, 45 (1970).
[d] Shain, A. L., Chiang, W. T., and Sharnoff, M., *Chem. Phys. Letters*, *16*, 206 (1972).
[e] Sharnoff, M. J., *Chem. Phys.*, *51*, 451 (1969).
[f] Hayashi, H., Morigaki, K., and Nagkura, S., *Chem. Phys. Letters*, *9*, 119 (1971).
[g] Chan, I. Y., and Clark, R. H., *Chem. Phys. Letters*, *19*, 53 (1973).
[h] Wells, C. H., Horsfield, A., and Paxton, *J. Chem. Comm.*, 393 (1969).
[i] Jones, C. R., Maki, A. H., and Kearns, D. R., *J. Chem. Phys.*, *54*, 873 (1973).
[j] Wasserman, E., Kuck, V. J., Hutton, R. S., and Yager, W. A., *J. Am. Chem. Soc.*, *92*, 7491 (1970).
[k] Wasserman, E., Smolinsky, G., and Yager, W. A., *J. Am. Chem. Soc.*, *86*, 3166 (1964).
[l] Trozzolo, A. M., Murray, R. W., and Wasserman, E., *J. Am. Chem. Soc.*, *84*, 4990, 3213 (1962).
[m] Bartlett, P. D., and McBride, J. M., *Pure Appl. Chem.*, *15*, 89 (1967).
[n] Buchwalter, S. L., and Closs, G. L., *J. Am. Chem. Soc.*, 97, 3857 (1975).
[o] Pagni, R. M., Burnett, M., and Dodd, J. R., *J. Am. Chem. Soc.*, *99*, 1972 (1977).
[p] Tinkhan, M., and Stranderg, M. W. P., *Phys. Rev.*, *97*, 951 (1955); Langhoff, S. R., *J. Chem. Phys.*, *61*, 1208 (1974).

peaks. However, some peaks display an *enhanced* absorption intensity or display an emission (called *polarization* of NMR bands). The importance of CIDNP studies to photochemistry is:

1. The observation of a CIDNP spectrum during photoreactions requires a radical pair (or in favorable cases a diradical) *precursor* to the species responsible for the polarized NMR bands.

2. The details of the CIDNP spectrum allow deduction of the singlet or triplet nature and structural type of the radical pair.

3. Study of magnetic field effects on CIDNP signals allows deduction of the rates of intersystem crossing.

4. Polarization effects (deviations from Boltzmann populations) can be very strong, thus enhancing the sensitivity of NMR as a technique for identifying short-lived transients in low concentrations.

The theory of CIDNP is based on the concept of a *radical pair*. The radical pair mechanism of CIDNP may be broken down into two parts: (a) the spin mechanics and spin dynamics (time evolution of "singlet character" in triplet states and the development of "triplet character" in singlet states), and (2) the fluctual behavior of the relative motion of the radical pair.

The Radical-Pair Theory of CIDNP[19]

A basic premise of the radical-pair theory of CIDNP is the postulate that the reactivity of a radical pair in solution depends upon the spin states of the nuclei present in the radical pair. This is a rather remarkable premise since the interactions between electrons and nuclei (e.g., protons) are given by the electron-nuclear hyperfine couplings and amount to exceedingly small energies. Typical hyperfine couplings (a_n) are of the order of 10–20 gauss ($\sim 10^{-3}$ cm^{-1}; $\sim 10^{-6}$ kcal/mole). Clearly, such tiny interaction energies cannot significantly influence equilibrium properties, electronic distributions, or energy barriers. Then how is it possible for nuclear spins to influence the rates of reactions of radical pairs and thereby cause nonequilibrium nuclear spin populations of radical pair products, when the chemical reactions involve *activation* energies of at least the order of 5–50 kcal/mole?

The answer lies in the fact that nuclear spin may influence rate constants by influencing the A-factor of reactions of radical pairs but not by influencing the energy factor, E_a (Eq. 8.1). The small interactions of nuclear spins with the electron spin provide mechanisms for "flipping" the direction of the electron spin vector and for "rephasing" the rate of precession of the electron spin vector about an external field. In other words, the interaction of electron spins with the spins of the nuclei may determine the *rates* of intersystem crossing of singlets to triplets and vice-versa. If reactions of the radical pair are spin-dependent (i.e., if triplet reactions occur at a different rate than singlet reactions) then the nuclear spin *may* exert an influence on the rates of product formation.

For example, if a radical pair approach each other when their electron spins correspond to a triplet state, such a pair cannot form *singlet* products in a solvent cage until intersystem crossing via a spin flip or spin rephasing occurs. Since a singlet radical pair can form singlet products directly, the rate of formation of singlet products from triplet and singlet diradical precursors will generally be different, i.e., the A-factor of Eq. 8.1 will be different for reactions of the singlet and triplet pair.

On the other hand, the rates of diffusion of triplet and singlet radical pairs do not depend on spin multiplicity. Thus, depending on the spin state of a radical pair, the competition between cage reaction and escape (via diffusion) of the radical pair into solution will depend on the spin state of the diradical pair. Within a solvent cage, the singlet radical pair will tend to react faster and more efficiently than the triplet radical pair.

The Mechanism of Nuclear Spin-Dependent Mixing of Singlet and Triplet States of Radical Pairs

What is the mechanism by which nuclear spins (via hyperfine coupling) can influence the rate of interconversion ("mixing") of singlet and triplet states of radical pairs, thereby causing CIDNP to be observed? The vector model of electron spin provides a simple theoretical model by which CIDNP effects can be qualitatively understood.

Figure 8.12 reviews the vector model of the singlet and triplet states. In the singlet state let the spin vectors of electrons (1) and (2) be $\mathscr{S}_1$ and $\mathscr{S}_2$. We suppose that these spin vectors possess values of $\beta(-\frac{1}{2})$ and $\alpha(+\frac{1}{2})$ along some magnetic spin axis $\mathbf{H}_0$, about which the vectors precess. In the singlet state $\mathscr{S}_1$ and $\mathscr{S}_2$ point in opposite directions and are always 180° out of phase. We may label the singlet state as $S = -\alpha\beta$, where the minus sign indicates the out-of-phase property of the α and β species.

Recall that the three components of the triplet state may be described in terms of three vectorial situations: $T_+ = \alpha\alpha$, $T_- = \beta\beta$, and $T_0 = \alpha\beta$. In each case the vectors $\mathscr{S}_1$ and $\mathscr{S}_2$ are *in phase*, i.e., they are coplanar with each other and with the magnetic axis. Of the three triplet levels (T_+, T_-, T_0) only T_0 will be degenerate with S when the radical pair is well separated ($\gtrsim 6$–10 Å). Let us therefore consider only the mixing of the T_0 and S states (Fig. 8.12). Recall that T_0 possesses a net spin-momentum ($S = 1$), but its projection on the magnetic field is equal to zero ($M_s = 0$). The S state also possesses a zero net magnetic moment in all directions in space ($S = 0$, $M_s = 0$). Thus, there is *no* change in spin momentum along the magnetic field axis when S and T_0 interconvert.

A transition between $S = -\alpha\beta$ and $T_0 = \alpha\beta$ may occur if the precessional rates of $\mathscr{S}_1$ and $\mathscr{S}_2$ are slightly different. This will occur when the magnetic fields experienced by $\mathscr{S}_1$ and $\mathscr{S}_2$ are different. It is important to realize that the vectors $\mathscr{S}_1$ and $\mathscr{S}_2$, once prepared in S or T_0, would remain in these states "forever," if the magnetic fields operating on them were identical. What are the magnetic fields that act on $\mathscr{S}_1$ and $\mathscr{S}_2$? The most important are those associated with (a) an external laboratory magnetic field, (b) spin-orbit induced magnetic fields,

(c) magnetic fields associated with an electron spin, and (d) magnetic fields associated with a nuclear spin. An external magnetic field ($\mathbf{H}_0$) will influence $\mathscr{S}_1$ and $\mathscr{S}_2$ *identically* and therefore cannot cause a mixing of S and T_0 by rephasing the spin's precessional rates. When $\mathscr{S}_1$ and $\mathscr{S}_2$ are close together in space (as in the case of two orbitally unpaired electrons of a molecular triplet state) the two electron spins subject each other to a magnetic field of the order of 1000–3000 gauss, but again, the magnetic field influences each electron's spin to the same extent and therefore does not affect the relative precessional rate of vectors $\mathscr{S}_1$ and $\mathscr{S}_2$.

The local magnetic fields due to spin-orbit coupling and hyperfine coupling at the different radical centers may be different. Consider a radical pair $\dot{A}\ \dot{B}$ separated by a distance of 5–6 Å such that electron exchange is very slow relative to spin precessional motion. Under such a condition the spin vectors associated with the odd electrons on $\dot{A}$ and $\dot{B}$ may begin to precess at different rates if either the spin-orbit magnetic fields at $\dot{A}$ or $\dot{B}$ are different or if $\dot{A}$ and $\dot{B}$ experience different magnetic fields due to nuclear spins via hyperfine coupling. The "g-factor" available from ESR spectra is directly related to the amount of spin-orbit coupling experienced by an odd electron (Eq. 8.67) and different "g-factors" are therefore directly related to the different magnetic fields associated with *different* spin-orbit

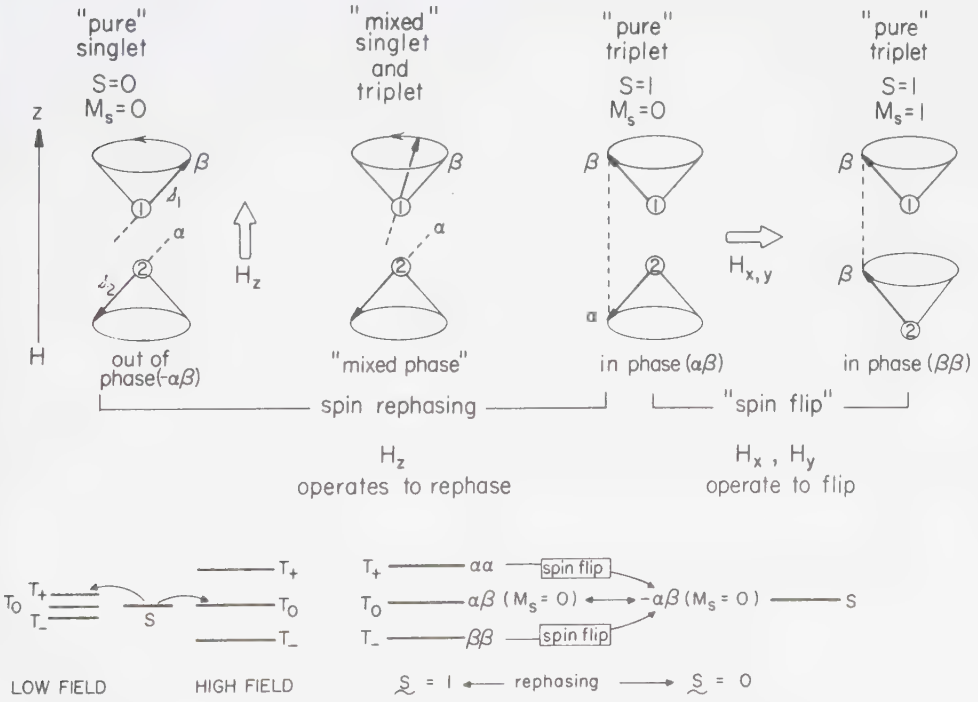

Figure 8.12

Review of the vector model for singlet-triplet mixing and intersystem crossing by a spin-flip.

coupling at sites $\dot{A}$ and $\dot{B}$. Thus, knowledge of the value of "g-factors" of radicals $\dot{A}$ and $\dot{B}$ and of the hyperfine constants a_H of nuclei coupled to the odd electrons on $\dot{A}$ and $\dot{B}$ allows evaluation of the difference in precessional frequencies of the spin vectors $\mathscr{S}_1$ and $\mathscr{S}_2$. If electrons 1 and 2 possess different g-factors and hyperfine couplings, then the difference in precessional rates $\Delta\omega$ of vectors $\mathscr{S}_1$ and $\mathscr{S}_2$ is given by:

$$\begin{matrix}\text{Difference in precessional} \\ \text{rates of } \mathscr{S}_1 \text{ and } \mathscr{S}_2\end{matrix} \qquad \Delta\omega = \underset{g\text{-factor effect}}{\Delta g \beta \mathbf{H}_o h^{-1}} \pm \underset{\text{hyperfine effect}}{(a_1 - a_2)I} \tag{8.71}$$

where $\Delta g = |g_1 - g_2|$ and the labels refer to electron 1 and electron 2.

In the case of ordinary organic radicals $\Delta g \sim 10^{-3}$ or larger. In an external field of 10,000 gauss, $\Delta\omega \sim 10^{11}\ \Delta g\ \text{sec}^{-1}$, so that if $\Delta g \sim 10^{-3}$, $\Delta\omega \sim 10^{8}\ \text{sec}^{-1}$. In other words, spin mixing of diradicals via different g-factors can occur at rates of the order of $10^8\ \text{sec}^{-1}$ or larger in a strong magnetic field.

Let the axis of the external magnetic field be in the z direction. We say that the *local* magnetic fields due to different g-factors cause rephasing of the two spin vectors $\mathscr{S}_1$ and $\mathscr{S}_2$ (assumed to be initially completely out of phase, i.e., $S = -\alpha\beta$) about the z-axis (see Fig. 8.12).

If the local magnetic fields ($\mathbf{H}_z$) acting in the z direction differ for electron 1 and electron 2, a relative rephasing of the spin vectors will occur, but the orientation (α or β) of the spin vectors relative to the z-axis is not influenced, i.e., electron 1 remains "up" (remains β) and electron 2 remains "down" (remains α). As a result, the singlet ($-\alpha\beta$) will switch into the $M_s = 0$ ($T_0 = \alpha\beta$) state of the triplet. We say the singlet and triplet states are "mixed." The triplet will tend to rephase back into the singlet and a pseudo-equilibrium between S and T_0 will be set up until a perturbation (e.g., chemical reaction or diffusion out of the cage) removes S or T_0 from the equilibrium.

Local magnetic fields ($\mathbf{H}_x$ and $\mathbf{H}_y$) in the x,y plane may also cause rephasing, but also may provide a torque to twist one of the spins (say the α spin of electron 1) and cause it to "flip" (say into a β state) and also cause reorientation relative to the z-axis. In other words, local magnetic fields $\mathbf{H}_x$ and $\mathbf{H}_z$ can "flip" the electron spin and cause transitions into either T_- or T_+ (see Fig. 8.12).

We shall now see how nuclear spin can provide the local magnetic fields $\mathbf{H}_x$ and $\mathbf{H}_y$ via hyperfine coupling and that total spin-conserving double spin flip will cause nuclear spin "polarization," e.g., a non-Boltzmann distribution of nuclear spins in the α or in the β state.

The Mechanism of Nuclear Spin Polarization via Hyperfine Coupling in Radical Pairs

The coupling of electron spins to nuclear spins or to external magnetic fields will determine the rates of intersystem crossing when all other important mechanisms for intersystem crossing (e.g., spin-orbital coupling) are inoperative. In addition, the triplet state (T) and singlet state (S) undergoing intersystem crossing must be equal in energy during the time period during which mixing occurs. In practical

terms, this means that the two unpaired electrons must be part of a radical pair which is well separated (~6–10 Å); otherwise the singlet-triplet splitting, which depends on the electron overlap integral J, will cause the T and S states to be separated by a relatively large energy gap. Finally, in order to observe nuclear polarization experimentally, a nonequilibrium distribution of nuclear spin states must be produced in the products.

The basic features of the hyperfine coupling mechanism for intersystem crossing in a radical pair may be recognized by reference to a simple example. Suppose a singlet radical pair $\overline{\dot{A}\ \dot{B}H}$ is formed in a solvent cage as a result of a rapid bond cleavage of $A—BH$, i.e., the homolysis step occurs so rapidly that the electron spin vectors remain in the same relative, paired orientation in $\overline{\uparrow A\ \downarrow BH}$ as they were in $A{\uparrow\downarrow}BH$, but the spin vectors are now centered on two different radicals (Eq. 8.72). In the absence of an external magnetic field, the two separated spins will maintain some indefinite overall spatial orientation but will possess a definite and well-defined orientation relative to one another. The exchange force, J_e, which preserves electron indistinguishability, will initially compel the relative spin orientations to stay fixed, i.e., the radical pair is "locked" into a singlet state.

For simplicity we assume that only the electron on radical $\dot{B}H$ experiences proton hyperfine coupling. When radicals $\dot{A}$ and $\dot{B}H$ begin to diffuse apart, the electron exchange interaction J falls off rapidly as the separation of $\dot{A}$ and $\dot{B}H$ increases (Fig. 8.13). At some point in their separation (~10 Å), the electron

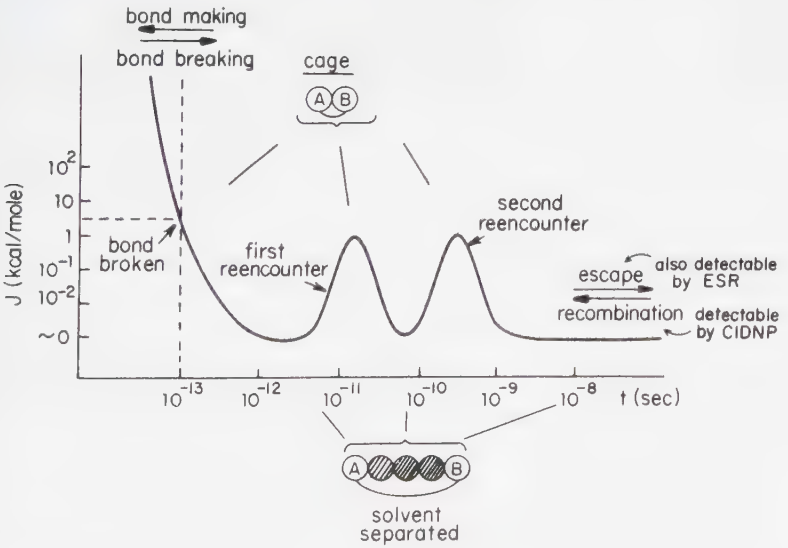

Figure 8.13

Schematic representation of the value of J_e, the electron exchange integral, as a function of time for a radical $\dot{A}—\dot{B}H$ generated by a sudden homolysis. The bond-breaking step is assumed to be essentially "instantaneous," i.e., ~ 10^{-13} sec.

exchange interaction which couples the precessional motion of the spins together becomes

$$A\text{-}B \xrightarrow[\text{fast}]{} \overset{\uparrow}{A}\ \overset{\downarrow}{B}H \longrightarrow \overset{\uparrow}{A}\ \overset{\downarrow}{B}H \qquad (8.72)$$

cage free

negligible relative to interactions with external fields, orbital-motion—induced fields, and hyperfine nuclear spin fields. This means that instead of precessing strictly in phase (i.e., instead of being "pure" S and "pure" T states) as when they were coupled by J, each electron spin now can precess at a different rate, determined by the magnetic fields to which it is most strongly coupled.

For the case in question, the important magnetic fields are (a) that of an external laboratory magnet, and (b) that of nearby molecular nuclear magnets. For such a situation, the magnitudes of the external fields are deducible from the spin Hamiltonian of the electron for negligible electron exchange:

$$\mathbf{H}\,(\text{spin}) \Longrightarrow \beta H_0(g_A\mathcal{S}_A + g_B\mathcal{S}_B) + \mathcal{A}_H\mathcal{S}_B I_B \qquad (8.73)$$

where $g_A\mathcal{S}_B$ and $g_B\mathcal{S}_B$ represent the inherent coupling of electron spin $\mathcal{S}_A$ (which may be α or β) and electron spin $\mathcal{S}_B$ (which may be α or β) to an external field $\mathbf{H}_0$, and $a_H\mathcal{S}_B I$ represents the hyperfine coupling between the electron spin on B–H with the proton spin I (which may be α or β).

If radical A possessed a proton a term of $a_H\mathcal{S}_A I$ would be added to Eq. 8.73. In other words, $\mathbf{H}$ tells us that the dominant interaction operating on $\mathcal{S}_A$ and $\mathcal{S}_B$ is determined by the magnitude of $\beta\mathbf{H}_0 g$ relative to a_H, that the rate of rephasing of $\mathcal{S}_A$ depends on $\mathbf{H}_0$ and g_A, and that the rate of rephasing of $\mathcal{S}_B$ depends on $\mathbf{H}_0$, g_B, and a_H. $\mathbf{H}$ also tells us that if a_H couples $\mathcal{S}_B$ with I, a simultaneous double spin flip is possible, e.g., $\mathcal{S}_B(\alpha \to \beta)$ simultaneous with $I_B(\alpha \to \beta)$, as are other combinations for which total (electron spin plus nuclear spin) momentum is conserved.

The situation for a coupled simultaneous electron-nuclear "flip-flop" spin flip is shown schematically in Figure 8.14 in terms of a "figure 8" model of an electron.

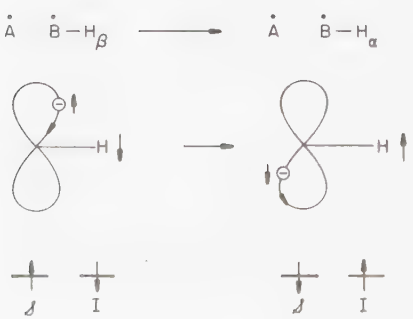

Figure 8.14

Schematic representation of a coupled, simultaneous electron-nuclear spin flip. The electron, in passing near the nucleus has its spin weakly coupled to the nuclear spin. If a simultaneous "flip-flop" of spins occurs, then the electron spin flips from $\alpha \to \beta$ at the same time that the nuclear spin flips from $\beta \to \alpha$. In this way, the total spin momentum is preserved and the overall process may cause intersystem crossing in the radical pair $\dot{A}$ $\dot{B}H$.

A spin vector precesses faster as the magnetic axis to which it is coupled gets stronger (Eq. 8.66). Thus, different values of $\mathbf{H}_z$ at $\dot{A}$ and $\dot{B}H$ will cause two electrons which are initially out of phase (say as a singlet state) to undergo a spin rephasing and will eventually cause $\mathscr{S}_A$ and $\mathscr{S}_B$ to come into phase (as the $M_s = 0$ component of the triplet). At this point, if a magnetic field in the x or y direction ($\mathbf{H}_x$ or $\mathbf{H}_y$) operates on one of the spins, and if the total spin angular momentum can be conserved, an electron spin flip can occur. For example, hyperfine couplings with protons can supply such an $\mathbf{H}_x$ or $\mathbf{H}_y$ field. The operation of an electron spin flip requires a simultaneous proton nuclear spin flip in order to conserve the total spin momentum of the system. Hence, the nuclear spins may become *polarized* as a result of the simultaneous electron spin-nuclear spin flip, i.e., the population of nuclear spin states on $\dot{B}$ H no longer corresponds to a Boltzmann distribution and the nuclear spin states are said to be polarized.

In a strong magnetic field ($\beta\mathbf{H}_0 g > a_H$) the rate of precession about $\mathbf{H}_0$ depends on the value of g (Eq. 8.66). Although the electron spins on $\dot{A}$ and $\dot{B}H$ will precess independently when they are separated by ~ 6 10 Å, their common origin imposed a specific vector orientation (180 opposed) and phase relation between the spin vectors $\mathscr{S}_A$ and $\mathscr{S}_B$. No matter what the distance of separation of A and BH, the directional and phase relationships of $\mathscr{S}_A$ and $\mathscr{S}_B$ would persist as long as the magnetic fields acting on them were identical.

In fact, because of the presence of hyperfine coupling, the spin $\mathscr{S}_B$ associated with the radical $\dot{B}$-H will precess with different rates depending on whether the proton's nuclear spin is in the $+\frac{1}{2}$ state (say, $\mathscr{S}_B$ precesses faster) or in the $-\frac{1}{2}$ state (say, $\mathscr{S}_B$ precesses slower). Let τ_+ be the time it takes the $\dot{A} + \dot{B}$-$H_{+\frac{1}{2}}$ radical pair to undergo intersystem crossing to T_0 and let τ_- be the time it takes the $\dot{A} + \dot{B}$-$H_{-\frac{1}{2}}$ radical pair to undergo intersystem crossing to T_0. If $\tau_- \gg \tau_+$ all of the $\dot{B}$-$H_{+\frac{1}{2}}$ radicals will be associated with *triplet* radical pairs, while the $\dot{B}$-$H_{-\frac{1}{2}}$ radicals will remain associated with singlet radical pairs. Clearly, recombination reactions of the $\dot{A} + \dot{B}$-$H_{-\frac{1}{2}}$ singlet pairs are more likely than recombination reactions of $\dot{A} + \dot{B}$-$H_{+\frac{1}{2}}$ triplet radical pairs. A mechanism for "sorting" the radical pairs with proton spins $H_{-\frac{1}{2}}$ and $H_{+\frac{1}{2}}$ thus exists. The products of singlet recombination AB-$H_{-\frac{1}{2}}$ will possess more protons in the $H_{-\frac{1}{2}}$ state. The triplet $\dot{A} + \dot{B}$-$H_{+\frac{1}{2}}$ pairs will have a higher probability of diffusing completely away from one another and becoming "free" radicals in solution. In the extreme case, all the cage recombination products derived from the $\dot{B}$-H radicals would be completely in the $H_{-\frac{1}{2}}$ state and all cage escape products from $\dot{B}$-$H_{+\frac{1}{2}}$ would be in the $H_{+\frac{1}{2}}$ state. Since it takes typically 1 to 50 sec for relaxation from $H_{-\frac{1}{2}}$ to $H_{+\frac{1}{2}}$ to occur, while radical reactions take place within 10^{-3}–10^{-6} sec, the spin polarization is passed along to the products of $\dot{B}$-$H_{-\frac{1}{2}}$, i.e., the polarization lasts for the order of seconds in the product and therefore can be detected by NMR spectroscopy which requires seconds for an analysis.

The situation is reviewed in Figure 8.15. The radical pairs with $H_{-\frac{1}{2}}$ are assumed to keep their singlet phasing longer, and therefore have a higher probability of producing recombination products possessing a population of $H_{-\frac{1}{2}}$ states in excess of the equilibrium population. The NMR of the proton in the recombination products will appear as an *emission*, i.e., the radio frequency field of the NMR spectrometer will stimulate emission of radiation associated with the conversion

of $H_{-\frac{1}{2}}$ to $H_{+\frac{1}{2}}$ states. Eventually, of course, equilibrium will be achieved and the NMR will be a normal absorption.

The excess $\dot{B}\text{-}H_{+\frac{1}{2}}$ radicals which do not form cage recombination products may react with a scavenger, X, to form a product $XBH_{+\frac{1}{2}}$. This product will have an excess population of protons in the lower spin level and result in an enhanced absorption. This means that for the actual concentration of XBH a much stronger absorption signal is observed by the NMR spectrometer, since the absorption signal strength is related to the excess of spins in the lower state.

Although this simple description predicts equal absolute intensities, different relaxation rates cause one type of polarization (emission or absorption) to predominate in practice. It is important to remember that the observation of polarization is very dependent on the time scales of certain interactions, the most important being: (a) initial bond cleavage, (b) primary recombination in the solvent cage, (c) secondary recombination after a brief escape from the cage, (d) complete escape to generate free radicals in the bulk solvent, and (e) spin rephasing or spin flipping in the radical pair.

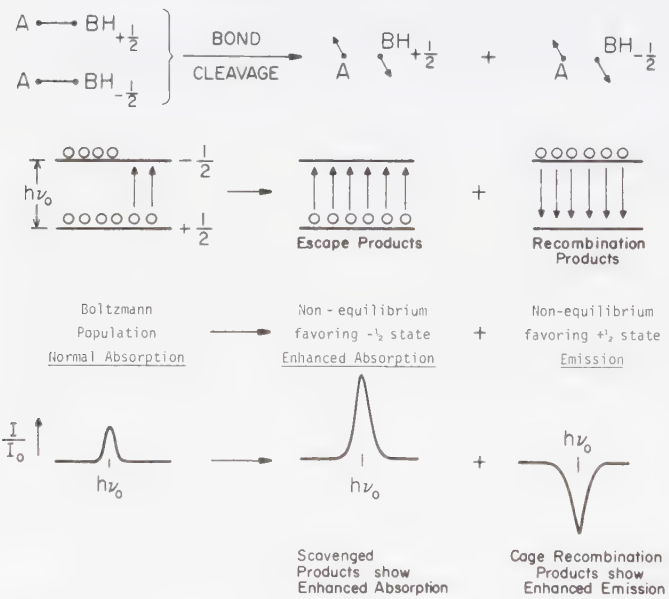

Figure 8.15

Schematic representation of the relationship between normal ("unpolarized", or Boltzmann distribution) NMR and CIDNP NMR (polarized or non-Boltzmann distribution). In normal NMR, the excess of protons in the lower level is very small (about 1 part per million). This tiny excess, however, is responsible for conventional NMR absorption. As a result of CIDNP interactions, it is possible that cage escape products may be formed with most of the protons in the lower level whereas the cage recombination products are formed with protons mostly in the upper level. This leads to an enhanced absorption and enhanced emission NMR respectively.

Generalizations Concerning CIDNP. Use in the Analysis of Photochemical Mechanisms. Kaptein's Rules

Without going into detail of how they come about (the reader is referred to several excellent reviews)[19] there are a number of features of CIDNP spectra:

1. The observation of CIDNP effects require the involvement of free radical pairs for which cage recombination and cage escape are competitive (an exception to this rule is discussed in Section 8.10).

2. The CIDNP effects arise from magnetic hyperfine couplings of nuclei (usually protons, for organic molecules) to the spin of unpaired electrons.

3. Net polarization effects require that $\Delta\omega \neq 0$. This in turn requires that $\Delta g \neq 0$ and/or $a_{\text{H}} \neq 0$.

4. The type of polarization observed experimentally depends on the nature of Δg and a_{H} and is related to the "absolute mathematical signs" of these parameters.

5. Cage recombination and scavenged escape products show opposite polarization.

6. Triplet and singlet precursors to the same radical pair give rise to opposite polarizations.

CIDNP has been used in studying numerous photochemical mechanisms. When it is observed, conclusive evidence thus exists that a radical or radical pair precursor occurs prior to a product. Since triplet and singlet precursors give different polarizations (i.e., one gives emission and the other absorption, or vice-versa) and since rules allow one to predict beforehand the associated polarizations, CIDNP can be used to determine whether a product possesses a singlet or triplet precursor. When the polarization is strong, very small concentrations of products may be determined. As a result, low concentrations of unstable transients (which are eventually converted to products) may be detected.

With respect to this last point, it is important to realize that NMR spectra observed under CIDNP conditions are identical to those expected under "normal" conditions *except* for the intensities of bands, i.e., the chemical shift and coupling constants do not change as a result of CIDNP.

A set of rules has been formulated (Kaptein's rules)[19b] which allows the prediction of the singlet or triplet nature of the precursor of a product if the net polarization, the nature of the product (i.e., recombination or escape products), the value of $\Delta g = g_{\text{BH}} - g_{\text{BH}}$, and the hyperfine coupling constant of the proton to the electron are known. Thus, if CIDNP is observed during a photoreaction and if the above parameters are known experimentally, the singlet or triplet nature of the radical pair precursor to products showing CIDNP may be deduced. In addition, because time scales are very important in determining whether or not CIDNP is observed, the dynamic behavior of precursor diradical pairs may often be deduced from CIDNP experiments.

Kaptein's rules are summarized by:

$$\Gamma \text{ (net polarization)} = \mu\varepsilon\,\Delta g a_{\text{H}} = \underset{\substack{\text{enhanced}\\\text{absorption}}}{+(A)} \text{ or } \underset{\substack{\text{enhanced}\\\text{emission}}}{-(E)} \tag{8.74}$$

where μ is defined as positive for a triplet precursor or free radical pair and negative for a singlet precursor, and ε is defined as positive for recombination products and negative for escape products. Δg and a_{H} are derived from experimental measurements ($\Delta g \equiv g_{\text{BH}} - g_{\text{A}}$). Thus, for each term in Eq. 8.74 a "+" or "−" value may be assigned. If the product of the ensemble is positive, then *net enhanced absorption* (A) is predicted, whereas if the product of the ensemble is negative, then *net emission* (E) is predicted.

If a specific polarization is observed experimentally (from prior knowledge of Δg or a_{H}), the nature of μ and or ε may be deduced. For example, if products are known to arise via an escape from the solvent cage, then μ (triplet or singlet precursor) may be deduced from experimental quantities Γ, Δg, and a_{H}.

From Eq. 8.74, a number of features of the vector model for CIDNP via the radical pair theory may be expressed in terms of Kaptein's rules. First of all, *net* polarization effects arise only when $\Delta g \neq 0$, because the absolute value of $\Delta\omega$ determines the amount of $S - T_0$ mixing, and if $\Delta g = 0$ then $|\Delta\omega_+| = |\Delta\omega_-|$ for $+a_{\text{H}}$ and $-a_{\text{H}}$, respectively, and there would be no rephasing (mixing) of S and T_0. Next, the "sign" of the polarization (net emission versus net enhanced absorption) depends on the *relative* signs of Δg and a_{H}. From the above discussion we expect that recombination products will show an opposite polarization relative to escape products (Fig. 8.15). Finally, singlet and triplet precursors should give rise to opposite polarizations.

For example, application of CIDNP to the formation of 1,1,2-triphenylethane produced by three different methods allowed a distinction to be made concerning whether the product ethane was formed via singlet or triplet precursors and whether it was formed via cage combination or combination of free radicals:[25]

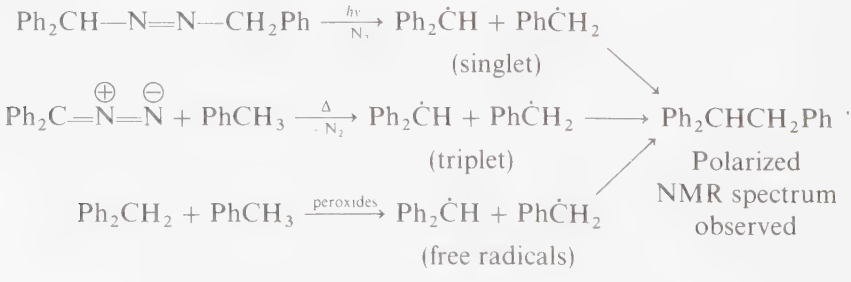

(8.75)

CIDNP Detection of Diradicals

In special cases, CIDNP may be employed to "observe" diradical intermediates by the polarized NMR spectra of products derived from the diradical. Recall that

the usual mechanism for CIDNP is a $T_0 - S$ mixing in a radical pair which occurs via the hyperfine interaction and g-factor differences. For effective mixing, the energy difference between T_0 and S must be very close to the value of the hyperfine coupling (usually $\gtrsim 10^{-2}$ cm^{-1} $\sim 3 \times 10^{-5}$ kcal/mole). Recall that the hyperfine interactions can cause the spin vector to "lock on" to nuclear magnetic fields only when J, the electron exchange interaction, is *smaller* than the hyperfine coupling, i.e., $J < 10^{-2}$ cm^{-1} for CIDNP. The same mechanism is possible in principle for diradicals. However, since the magnitude of J falls off as exp-R where R is the average separation of the two electrons, it is unlikely that $J < 10^{-2}$ cm^{-1} for 1,n diradicals where n is small, because the electrons will be too close in space. When J is $\gg 10^{-2}$ cm^{-1}, CIDNP by the radical pair mechanism will not be possible. Furthermore, for the $T_0 - S$ mechanism to cause measurable net polarization there must be an escape pathway which competes with self-reaction of the diradical. Thus, CIDNP does not show promise as a general method for detecting 1,n diradicals where n is small.

There are certain cases, however, for which CIDNP of medium to large diradicals ($n = 6$) can be observed.[26] This situation occurs when the Zeeman (magnetic-field-dependent) splitting of the T_+, T_0, and T_- states is such that mixing of $T_\pm$ with S becomes possible. Since the Zeeman splittings may be controlled by adjusting the magnetic field strength of an *external* laboratory magnet, CIDNP induced by $T_\pm - S$ mixing is magnetic-field-strength dependent.

According to the above, CIDNP can be observed in diradicals if an external magnetic field can adjust the energy of $T_\pm$ so that they match that of S. At some length of a diradical this should be possible. As an example of CIDNP for a diradical, consider the intramolecular hydrogen abstraction:

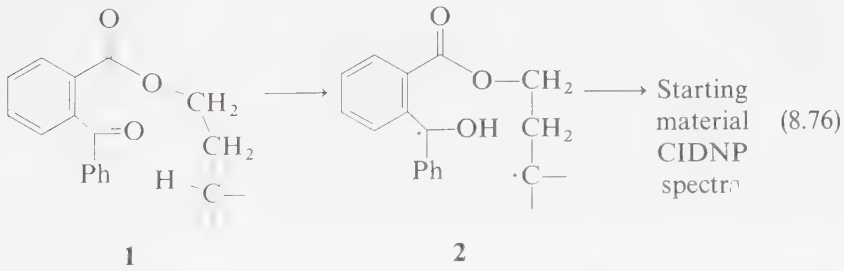

(8.76)

1 **2**

The fact that a CIDNP spectrum of the starting material appears upon irradiation of **1** (Eq. 8.76) suggests that a 1,n diradical is formed, which then reverts back to the starting ketones. Since the mechanism of polarization in such diradicals is due to a spin flip rather than hyperfine coupling, the CIDNP spectrum is independent of the proton hyperfine interactions, and turns out to be entirely *emission*.[27] It is important to realize that *no net competition* for reaction of the diradical is required when the $T_\pm - S$ mechanism operates, i.e., the polarization comes about because of coupled electron-nuclear spin flips, not hyperfine modulated dephasing.

A very nice example of diradical polarization due to $S - T_-$ mixing is found in the photolysis of cycloalkanones (Eq. 8.77).[29] The primary photochemical process

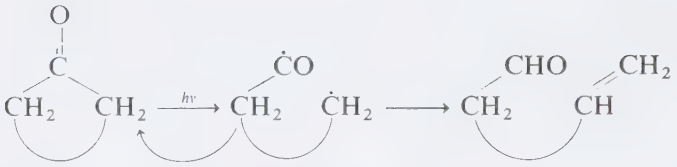

(8.77)

occurs in $T_1(n, \pi^*)$ to yield a triplet diradical. Figure 8.16 shows a surface diagram for the $T_{\pm,0}$ levels as a function of the α—CO C bond length. At a certain separation (just before the bond breaks), T_- is exactly degenerate with S_0, i.e., $J \sim \Delta E(T_0 - T_-)$. When the bond is completely broken and the —ĊO Ċ radicals separate by 6–10 Å, $J \sim 0$ and S_0 is degenerate with T_0 and not T_-. However, since no "escape" mechanism is available to small 1,*n* diradicals, only self-reaction occurs and no CIDNP is expected. However, the energies of $T_\pm$ may be altered by an external magnetic field, and T_- may be brought into degeneracy with S by varying an external magnetic field H_0. When this happens T_- mixes with S_0 and

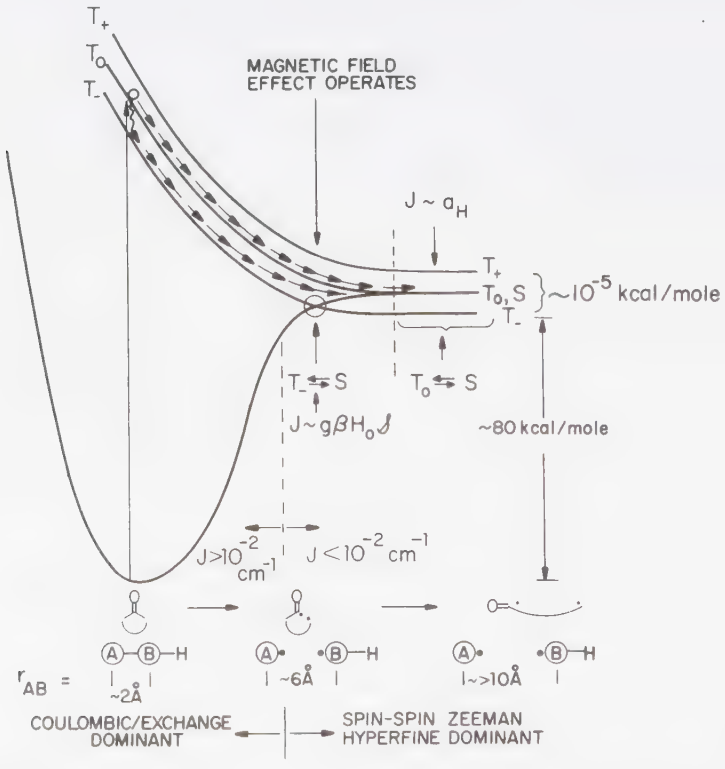

Figure 8.16

Schematic representation of the effect of radical separation on mixing of *S* with *T* and with T_0. See text for discussion.

CIDNP is observed. If T_- flips to S while a proton coupled to one of the electrons flips from its α (lower) to β (upper) state, intersystem crossing and polarization are simultaneous and coupled. The T_- to S flip corresponds to a $\Delta M_s = +1$ transition and must be coupled to a $\Delta M_I = -1$ transition in order to preserve momentum (total ΔM must $= 0$). Thus, there is a net flow of nuclear spins from the lower $+\frac{1}{2}$ spin state to the upper $-\frac{1}{2}$ spin state. The products from such biradicals will clearly possess an excess of nuclei with higher energy $-\frac{1}{2}$ spins, i.e., a net CIDNP *emission* will be observed.

The measurement of CIDNP of 1,*n*-diradicals derived from cycloheptanone and large-size cyclanones show an emissive CIDNP spectrum for the aldehyde protons derived from the enal products.[30] No signal was found for cyclohexanone and smaller ring cyclanones. The intensities of the CIDNP polarization was found, as expected from a $T_1 - S$ polarization mechanism, to be magnetic-field-dependent. The greatest intensity is expected when T_- and S are exactly degenerate, i.e., when $g\beta H_0 = 2J_{av}$, where $2J_{av}$ refers to an *average* value over the various conformations of the diradical. For $\dot{C}H_2(CH_2)_5\dot{C}O$ a value of $\sim 2\ cm^{-1}$ is found for $2J_{av}$ whereas for $\dot{C}H_2(CH_2)_8\dot{C}O$ a value of $\sim 0.03\ cm^{-1}$ is found for $2J_{av}$.

These values may be compared to $2J = 0.003\ cm^{-1}$, found for stable diradicals separated by 15 Å. For $\dot{C}H_2(CH_2)_8\dot{C}O$ the radical centers are separated by 13 Å in the *most* extended form. Thus, the values of $2J$, as expected, seem to drop off rapidly as the separation between the radical sites increases. Figure 8.17 shows an example of biradical CIDNP in the photolysis of cycloheptanone. The same arguments hold for ^{13}C NMR as for ^1H NMR.[29]

A striking example of hyperfine coupling on chemical reactions is available from the observation of *isotope effect* in radical recombinations.[30] It was found that photolysis of aliphatic ketones results in enrichment of the recovered starting material in ^{13}C. This remarkable result is explained by the postulates that (a)

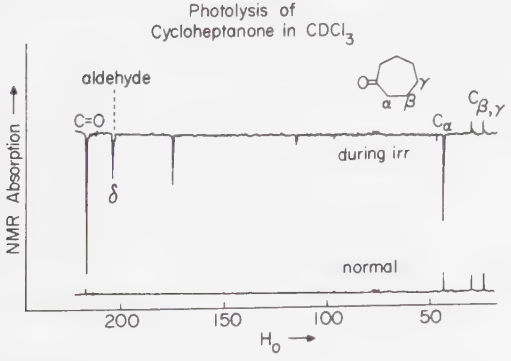

Figure 8.17

CIDNP spectrum (above) and normal ^{13}C NMR spectrum (below) of irradiated cycloheptanone.

photolysis results in a homolytic cleavage of the CO—C bond in T_1, leading to a triplet diradical pair, ^3D; (b) faster intersystem crossing to singlets in the triplet radical pairs which possess a ^{13}C atom at the radical center; and (c) rapid recombination of the singlet radical pairs to regenerate ^{13}C-enriched starting material:

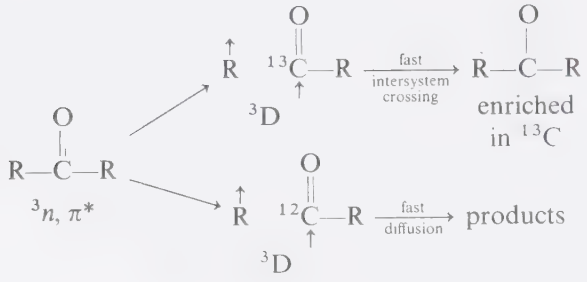

(8.78)

8.13 Chemical Spectroscopy: The Use of Photochemical Reactions to Measure Excited-State Energetics and Dynamics

The term *chemical spectroscopy* has been coined to define a principle which involves the use of photochemical reactions to measure properties of electronically excited molecules which are normally determined directly by spectroscopic means. One must employ an alternative to ordinary spectroscopy—to measure triplet energies, for example—if a molecule does not show measurable phosphorescence or singlet-triplet absorption under the reaction conditions being studied.

Chemical spectroscopy has been successfully employed in the estimation of triplet energies and in the measurement of intersystem crossing efficiencies. Great care must be made in the selection of systems and in the interpretation of results of experiments because the method is based on the assumption of a very simple scheme, an assumption which may not apply under the conditions of a particular experiment.

The concepts behind the principle of chemical spectroscopy are given by the following scheme for determining intersystem crossing yields (ϕ_{ST}), triplet energies (E_T), and triplet lifetimes (τ_T):

	STEP	
$S_0 \longrightarrow S_1$	Excitation	(8.79)
$S_1 \xrightarrow{k_{ST}} T_1$	Intersystem crossing	(8.80)
$T_1 + A_0 \xrightarrow{k_T} S_0 + A_T$	Energy transfer	(8.81)
$T_1 \xrightarrow{k_1} S_0$	Triplet decay	(8.82)
$A_T \xrightarrow{k_R}$ characteristic reaction	Reaction of acceptor	(8.83)

The *substrate* molecule of interest is assumed to possess standard decay pathways from S_1 and T_1. Addition of an acceptor molecule, A_0, introduces a step that quenches T_1 of the substrate and produces the acceptor triplet A_T, which then undergoes a characteristic reaction. This analysis assumes:

1. That S_1 is not quenched by A_0.
2. That T_1 produces A_T quantitatively for each quenching of T_1.
3. The reaction of A_T is independent of the reaction conditions.

If these conditions are met, then Φ_{ST} is measured by completely quenching T_1 and measuring the quantum yield of reaction from A_1 based on absorption to produce $S_1(\Phi_R)$. If the quantum yield of reaction from A_T is Φ_A, then

$$\Phi_R = \Phi_{ST}\Phi_A \quad \text{or} \quad \Phi_{ST} = \Phi_R/\Phi_A \tag{8.84}$$

i.e., the efficiency of sensitized reaction of A, under conditions of complete quenching of T_1, is the product of the efficiency of formation of $T_1(\Phi_{ST})$ and the inherent reaction efficiency of A_T. Since both Φ_R and Φ_A are measurable, Φ_{ST} may be evaluated from photochemical data, namely by quantum yield measurements. A Stern-Volmer analysis of the sensitized reaction of A will yield the ratio k_q/k_T which is equal to $k_q\tau_T$. If k_q is assumed to be the value of diffusion-controlled quenching, τ_T can be evaluated if k_{DIF} is known. This assumption is questionable in the absence of independent evidence that the quenching step is diffusion-controlled.

The scheme discussed above, with its numerous assumptions, does appear to work in carefully selected systems. The energy levels of the acceptor usually can be chosen so that triplet-triplet energy transfer is exothermic and singlet-singlet energy transfer is endothermic. In fluid solutions, the majority of directly measured quenching constants for the reactions involving an acceptor whose triplet energy is lower than that of the donor are generally close to the rate constant for diffusion. However, the scheme is not universally true.

An interesting application of chemical spectroscopy involves the determination of *triplet energies*. The key idea here is that if a pair of molecules or conformers possess different triplet energies, then

1. Donor triplets will excite each molecule equally effectively as long as energy transfer is exothermic (i.e., transfer to each molecule is assumed to be diffusion-controlled).
2. Donor triplets will excite the lower energy molecule more effectively when the donor triplet energy "brackets" the triplet energies of the two molecules.
3. Donor triplets will be ineffective in exciting either molecule when energy transfer becomes endothermic to both.

Experimental examples of this principle have been found in the dimerization of dienes and in the cis-trans isomerization of dienes (see Fig. 8.18).

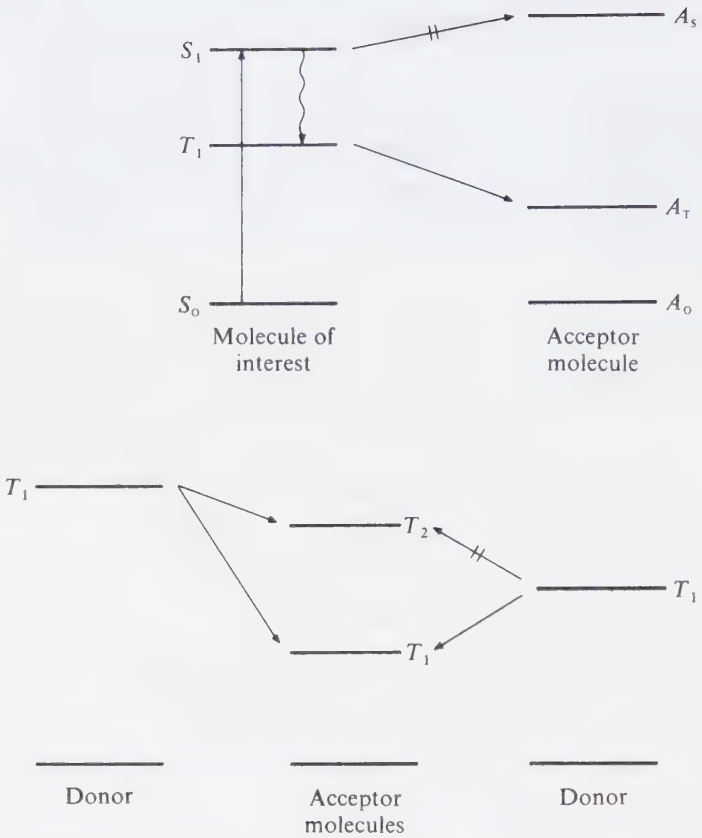

Figure 8.18

State-energy diagram relevant to "chemical spectroscopy." See text for discussion.

Table 8.6 Energetics and Dynamics of Carbonyl Compounds

Molecule	E_1[a]	E_3[a]	k_s[b]	k_{ST}[b]	k_T[b]	ϕ_{ST}
Acetone	84	78	10^9	10^9	10^6	1.0
2-Pentanone	84	78	10^9	10^9	10^7	0.9
2-Hexanone	84	78	10^{10}	10^9	10^8	0.5
Cyclobutanone	84	78	10^{11}	10^9	—	0.0
Cyclopentanone	84	78	10^9	10^9	10^8	1.0
Cyclohexanone	84	78	10^9	10^9	10^7	1.0
Acetophenone	80	74	10^{10}	10^{10}	10^5	1.0
Benzophenone	76	69	10^{11}	10^{11}	10^5	1.0
2-Acetophenone	77	59	10^{10}	10^{10}	10^3	0.8
4-Phenylbenzophenone	75	62	10^{10}	10^{10}	10^3	1.0
Fluorenone	65	53	10^9	10^9	10^4	0.9
2-Acetylnaphthalene	75	58	10^9	10^{10}	10^4	0.9
Biacetyl	62	55	10^8	10^8	10^4	1.0
Camphorquinone	57	51	10^8	10^8	10^5	1.0

[a] Energies in kcal/mole.

[b] Rate constants are in sec^{-1}. k_s = measured singlet lifetime, k_{ST} = measured rate of $S_1 \rightarrow T$ intersystem crossing, k_T = measured triplet lifetimes. Values are order-of-magnitude only and refer to measurements in "inert" solvents under deaerated conditions.

8.14 Some Archetype State-Energy Diagrams

It is useful to calibrate one's expectations of the behavior of electronically excited states in terms of archetype models. In the case of electronically excited states, the state-energy diagrams of many molecules are derivable from a combination of absorption and emission data. In this section we present briefly some archetype state-energy diagrams, e.g., for some ketones, alkenes, aromatic compounds, and enones. The archetype state-energy diagrams serve as a paradigm which may be the basis for deciding on reaction or mechanistic feasibilities. These diagrams are readily constructed if the energies of S_1, T_1, and the dynamics of deactivation of these states are known.

Ketones

The state energies and configurational assignments of some typical organic ketones are given in Table 8.6.

In proceeding from acetone to benzophenone to methyl naphthyl ketone, the energy diagrams present some interesting contrasts. The first big contrast is the rate constant of intersystem crossing for acetone relative to benzophenone ($\sim 5 \times 10^8$ sec^{-1} and $\sim 10^{11}$ sec^{-1}, respectively). As a result of these relatively rapid intersystem crossing rate constants and relatively slow fluorescence rates, ketones generally possess a low fluorescence yield. Although both molecules possess lowest n, π^* singlet and triplet states, the $S_1 \rightarrow T_1$ crossing in benzophenone is of the $^1n, \pi^* \rightarrow {}^3(\pi, \pi^*) \rightarrow {}^3(n, \pi^*)$ type, whereas acetone is of the $^1(n, \pi^*) \rightarrow {}^3(n, \pi^*)$ type. The former is always much faster than the latter. Alkanones tend to possess relatively "pure" n, π^*, S_1, and T_1 states. Benzophenones possess "mixed" n, π^* and π, π^* states. Naphthyl ketones may possess mixed $n, \pi^* \leftrightarrow \pi, \pi^*$ singlet states but tend to possess pure π, π^* triplet states.

Alkenes and Polyenes

Direct dynamic information on k_s, k_{st}, k_t, etc. is almost nonexistent for alkenes and polyenes. However, values of singlet and triplet energies are usually available (Table 8.7). An important feature of these molecules is the general lack of (or very weak) fluorescence and phosphorescence. Evidently, based on chemical evidence (to be discussed in Chapter 12), $S_1 \rightarrow T_1$ intersystem crossing is also inefficient. The state-energy of alkenes and polyenes generally decreases with increasing conjugation.

Aromatic Hydrocarbons

A list of the energies of some commonly encountered aromatic hydrocarbons is given in Table 8.8. Aromatic hydrocarbons generally exhibit both fluorescence and phosphorescence at low temperatures, so that their state-energy diagrams can be well established. In the case of anthracenes, an interesting feature occurs in

Table 8.7 Singlet and Triplet Energies for Some Ethylenes and Conjugated Polyenes

Molecule	E_1[a]	E_3[b]
$CH_2{=}CH_2$	120	82
$CH_2{=}C(CH_3)_2$	95	81
trans-$CH_3CH{=}CHCH_3$	95	81
cis-$CH_3CH{=}CHCH_3$	95	78
$(CH_3)_2C{=}C(CH_3)_2$	86	76
cis-CHCl=CHCl	—	76
Norbornene	—	74
trans-CHCl=CHCl	—	72
$CH_2{=}CH{-}CH{=}CH_2$	80	60
$CH_2{=}CCH_3{-}CCH_3{=}CH_2$	80	60
1,3-Cyclohexadiene	75	54
1,3,5-Hexatriene	70	48

[a] Energy of S_1 in kcal/mole.
[b] Energy of T_1 in kcal/mole.

the accidental closeness of T_2 to S_1. Depending on the substitution pattern of an anthracene, T_2 may lie somewhat above or below S_1. Thus, either $S_1 \rightarrow T_2 \rightarrow T_1$ or $S_1 \rightarrow T_1$ intersystem crossing mechanisms can operate. Both S_1 and T_1 energies decrease monotonically with increasing condensation of rings in a linear manner (benzene → naphthalene → anthracene).

Conjugated Enones and Dienones

Enones and dienones are similar to alkenes and polyenes in that they exhibit only weak emission at best. An interesting feature of both enones and dienones

Table 8.8 Energetics and Dynamics of Aromatic Hydrocarbons

Molecule	E_1[b]	E_3[b]	k_s[c]	k_{st}[c]	k_i[c,d]	Φ_{st}[e]
Benzene	115	85	$\sim 10^7$	$\sim 10^7$	$\sim 10^6$	~0.2
Naphthalene	90	61	$\sim 10^7$	$\sim 10^7$	$\sim 10^3$	~0.7
1-Fluoronaphthalene	89	60	$\sim 10^7$	$\sim 10^7$	$\sim 10^3$	~0.7
1-Chloronaphthalene	89	59	$\sim 10^8$	$\sim 10^7$	$\sim 10^3$	~1.0
1-Bromonaphthalene	89	59	$\sim 10^9$	$\sim 10^7$	$\sim 10^3$	~1.0
1-Iodonaphthalene	89	59	$\sim 10^{10}$	$\sim 10^7$	$\sim 10^3$	~0.7
Anthracene	76	42	$\sim 2 \times 10^8$	$\sim 10^7$	$\sim 10^3$	~0.7
Pyrene	83	48	$\sim 2 \times 10^7$	$\sim 10^6$	$\sim 10^3$	~0.3
Triphenylene	81	67	$\sim 3 \times 10^7$	$\sim 10^7$	$\sim 10^3$	~0.9

[a] Data from Birk, J. B., *Photophysics of Aromatic Molecules*, New York: Wiley, 1970.
[b] Energies in kcal/mole and correspond to 0,0 emission.
[c] Rates in sec^{-1} from decay of fluorescence or phosphorescence in fluid solution near room temperature in the absence of oxygen.
[d] This rate constant is only approximate because impurities or other bimolecular quenching usually determines the observed value (except for benzene).
[e] Intersystem crossing quantum yield.

is the occurrence of two energetically similar T states, one n, π^* and the other π, π^*. Dynamic information on S_1 and T_1 of enones and dienones is relatively scarce. However, values of singlet and triplet energies are available. The state energies of some selected enones and dienones are given in Table 8.9. The electronic configuration of T_1 of a number of enones has been probed and spectroscopic evidence is available in some cases which allows a configurational assignment.

The important feature to be noticed, from the standpoint of enone and dienone photochemistry, is that the lowest T_1 state may be n, π^* or π, π^* depending on substituents, and that these two configurations will commonly be comparable in energy. As a result, the solvent may have a major influence on which configuration best corresponds to the lowest triplet.

Table 8.9 The singlet and triplet energies of some conjugated and related compounds.

Molecule	E_1	E_3
CH_2—CH CHO	74	70
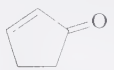	83	74
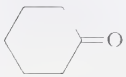	80	75(n, π^*) 74(π, π^*)
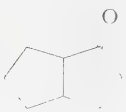	81	75
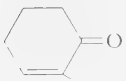	~76	76(n, π^*) 68(π, π^*)
	~78	69(n, π^*)
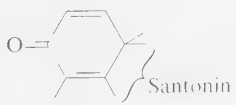 Santonin		70(π, π^*)
$CH_3(CH$ $CH)_3CHO$ $CH_3(CH$—$CH)_4CHO$ $CH_3(CH$ $CH)_5CHO$	—	44(π, π^*) 36(π, π^*) 32(π, π^*)
	56	50(n, π^*)

References

1. Grotewald, J., et al., *J. Photochem.*, *1*, 471 (1972/73).
2. Lewis, F. D., Johnson, R. W., and Ruden, R. A., *J. Am. Chem. Soc.*, *94*, 4292 (1972); Lewis, F. D., *Molec. Photochem. 4*, 501 (1972).
3. For a discussion of reaction kinetics and rate laws and their use in mechanistic analysis, see:
   (a) Benson, S. W., *The Foundation of Chemical Kinetics*, New York: McGraw-Hill, 1960.
   (b) Lewis, E. S., *Technique of Organic Chemistry*, vol. VIII, Part I, New York: Interscience, 1961, p. 1.
4. Hammond, G. S., *J. Am. Chem. Soc.*, *77*, 334 (1955). For a discussion, see Farcasir, D., *J. Chem. Ed.*, *52*, 76 (1975).
5. For extensive compilations of experimental values of A and E_a see:
   (a) Nazin, G. M., *Russian Chem. Rev.*, *41*, 711 (1972).
   (b) Benson, S. W., and O'Neal, H. E., *Kinetic Data on Gas Phase Unimolecular Reactions*, Washington, D.C.: NSRDS, 1970.
   (c) Reference 3.
   (d) Bazilevskii, M. V., and Trosman, E. A., *Russ. Chem. Rev.*, *41*, 1 (1972).
6. (a) Wagner, P. J., *Acc. Chem. Research*, *4*, 168 (1971).
   (b) Wagner, P. J., and Kochevar, I., *J. Am. Chem. Soc.*, *90*, 2232 (1969).
   (c) Wettack, F. S., Renkes, G. D., Renkly, M. G., Turro, N. J., and Dalton, J. E., *J. Am. Chem. Soc.*, *92*, 1318 (1970).
7. (a) Stern, O., and Volmer, M., *Physik. Z.*, *20*, 183 (1919);
   (b) For more detailed kinetic expressions the interested reader is referred to Wagner, P. J., *Creation and Detection of the Excited State*, Vol. I, Part A, New York: Marcel Dekker, 1971, p. 173.
8. Dalton, J. C., Wriede, P. A., and Turro, N. J., *J. Am. Chem. Soc.*, *92*, 1318 (1970).
9. Dalton, J. C., Dawes, K., Turro, N. J., Weiss, D. S., Barltrop, J. A., and Coyle, J. D., *J. Am. Chem. Soc.*, *93*, 7213 (1971).
10. For a review of complications that can occur in photosensitized reactions, see Engel, P., and Monroe, B., *Adv. Photochem.*, *8*, 245 (1971).
11. Turro, N. J., and McDaniel, D. M., *Molec. Photochem.*, *2*, 98 (1970).
12. Moore, W. M., Hammond, G. S., and Foss, R. P., *J. Am. Chem. Soc.*, *83*, 2789 (1961).
13. Bell, J. A., and Linschitz, H., *J. Am. Chem. Soc.*, *85*, 528 (1963).
14. Cohen, S. G., and Litt, A. D., *Tetrahedron Letters*, 837 (1970).
15. For a discussion of radical reactions and rearrangements, see Monkebel, D. C., and Walton, J. C., *Free Radical Chemistry*, Cambridge: 1974, Chapters 8, 12, and 13.
16. Kita, S., and Fukui, K., *Bull. Chem. Soc., Japan*, *42*, 66 (1969).
17. For excellent elementary discussions of the chemical applications of magnetic resonance, see Forrester, A. R., et al., *Organic Chemistry of Stable Free Radicals*, New York: Academic Press, 1968.
18. Carrington, A., and McLachlan, A., *Introduction to Magnetic Resonance*, New York: Harper & Row, 1967, p. 132 ff.
19. For an excellent and lucid discussion of CIDNP, see:
   (a) Buchachenko, A. L., and Zhidomov, F. M., *Russ. Chem. Rev.*, *40*, 801 (1971).

(b) Kaptein, R., *Adv. Free Radical Chem.*, *5*, 381 (1975).
(c) Lawler, R. G., *Acc. Chem. Research*, *5*, 25 (1972).

20. Zeldes, H., and Livingston, R., *J. Phys. Chem.*, *45*, 1946 (1966).

21. Kochi, J., in *Free Radicals*, ed. Kochi, J., Vol. 2, New York: John Wiley, 1973, p. 665.

22. (a) Zuchik, J., *J. Chem. Phys.*, *52*, 3592 (1970).
(b) Ikegami, Y., et al., *J. Am. Chem. Soc.*, *94*, 3274 (1972).
(c) Hayashi, H., and Nagakura, S., *Molec. Physics*, *27*, 969 (1974).

23. Wasserman, E., and Hutton, R. S., *Acc. Chem. Research*, *10*, 27 (1977).

24. Bartlett, P. D., and McBride, J. M., *Pure. Appl. Chem.*, *15*, 89 (1967).

25. Closs, G. L., and Trifunac, A. D., *J. Am. Chem. Soc.*, *92*, 7227 (1970).

26. Kaptein, R., Frater-Schroder, F., and Oosterhoff, L. J., *Chem. Phys. Letters*, *12*, 16 (1971); *41*, 26 [illegible] 6).

27. Closs, G. L., *Chemically Induced Magnetic Polarization*, ed. Lepley, A. R., and Closs, G. L., New York: Academic Press, 1973, p. 95; *Ind. Chim. Belg.*, *36*, 1064 (1971).

28. Closs, G. L., and Doubleday, C. E., *J. Am. Chem. Soc.*, *95*, 2735 (1973).

29. DeKanter, F. J. J., Kaptein, R., and van Santen, R. A., *Chem. Phys. Letters*, *45*, 575 (1977).

30. Buchachenko, A. L., *Russ. Chem. Rev.*, *45*, 761 (1976); Turro, N. J., and Kraeutler, B. *J. Am. Chem. Soc.*, *100*, 7432 (1978).

9

Energy Transfer

9.1 An Energy-Surface Description of Electronic Energy Transfer and Energy Degradation[1,2]

It is possible to visualize the electronic energy transfer process $M^* + Q \rightarrow M + Q^*$ in terms of potential-energy surfaces. For example, let us consider a collisional mechanism for energy transfer.

A simplified energy-surface description of a collisional energy-transfer complex is shown in Figure 9.1. As $M + Q$ approach each other in their ground states, their interactions are repulsive, and the energy of the ground state surface rapidly rises as M and Q come to within collisional distance. If either M or Q is excited as they approach, however, the energy of a collision pair M^*Q or MQ^* will generally be lower than that of the separated pairs $M^* + Q$ and $M + Q^*$ (see Section

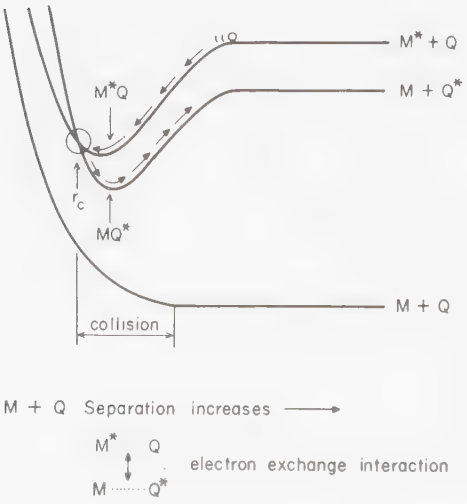

Figure 9.1
Schematic surface representation of collisional energy transfer.

5.13 on exciplexes). At some geometry, r_c, the surface of $M^* + Q$ is imagined to intersect with that of $M + Q^*$ and an internal conversion (or intersystem crossing if a triplet is involved) to the lower surface may occur. At the crossing point, r_c, some interaction between M^* and Q allows a transfer of electronic excitation. After relaxation to the minimum of the lower excited surface, thermal energy must now be provided to pop the MQ^* collision pair back to the upper surface. In general, there will be competition between a return to the upper surface and a separation of the collision complex MQ^* into separated monomers $M + Q^*$. Should the latter result, *a net electronic energy transfer from M^* to produce Q^* has been effected.*

If the minima corresponding to M^*Q and MQ^* are sufficiently deep, we then say that exciplex formation has occurred. In such a case, there is the possibility of observing exciplex emission or absorption.

It should be noticed that the description of energy transfer given above is analogous to the radiationless transitions of internal conversion or intersystem crossing within a molecule. In the same way that the "electronic energy sink" principle causes the electronic excitation energy to rapidly degrade to the lowest excited levels intramolecularly, an analogous process can be proposed to occur between two molecules. The energy degradation process $M^* + Q \rightarrow M + Q +$ heat can be visualized if we imagine that a crossing occurs between the ground surface for interaction of M and Q and the excited surface for interaction of M^* and Q. A pathway is then available for efficient intermolecular internal conversion or intersystem crossing to the ground surface.

An energy transfer induced via a very different mechanism is shown schematically in Figure 9.2. In this case, a surface crossing does *not* occur. The surfaces which correspond to M^*, M, Q, and Q^* are considered to be separate and distinct.

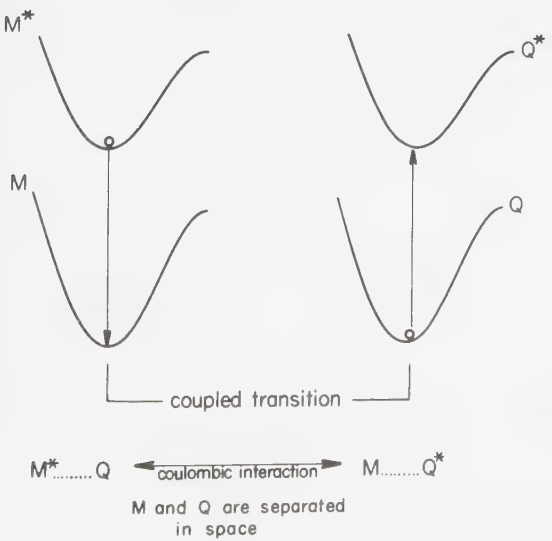

Figure 9.2
Schematic surface description of energy transfer by the Coulombic mechanism.

However, if through some interaction M^* is caused to jump to M (a vertical transition) simultaneously with the jump of Q to Q^* (also a vertical transition), energy transfer can occur. In fact, the transition moment (Section 5.5) which corresponds to the $M^* \rightarrow M$ jump can "trigger" the $Q \rightarrow Q^*$ transition. The molecule Q is excited to Q^* by a mechanism analogous to the radiative excitation of Q to Q^* via interaction with the electric vector of a light wave. Indeed, we shall see that most of the ideas developed to visualize the interaction of light with molecules (Chapter 5) are transferable to energy-transfer processes which occur via Coulombic (dipole-dipole) interaction.

9.2 The "Trivial" or Radiative Mechanism for Electronic Energy Transfer: The Spectral Overlap Integral

Excitation transfer may occur in a "trivial" case, which consists of the emission of a quantum of light by one molecule which is followed by absorption of the emitted photon by a second molecule.[3] While complicated in practice to analyze quantitatively, this mechanism is readily understandable in terms of the laws of optics and of light absorption and emission. The second molecule does not at all influence the emission ability of the first molecule, but merely intercepts the emitted photon before the latter can be observed.

The mechanism of "trivial" radiative energy transfer is the two-step sequence given below, in which D^* is an excitation *donor* and A is an excitation *acceptor*.

Radiative	$D^* \rightarrow D + h\nu$	(9.1)
emission-absorption energy transfer	$h\nu + A \rightarrow A^*$	(9.2)

The "trivial" mechanism requires that the excited-energy donor molecule D^* emit photons which are then absorbed by the energy acceptor molecule A. Thus, the rate or probability per unit time of energy transfer from D^* to produce A^* will depend (1) on the quantum yield (Φ_e^D) of emission by D^*, (2) the number of A molecules (the concentration of A) in the path of photons emitted by D^*, (3) the light-absorbing ability of A, and (4) the overlap of the emission spectrum of D^* and the absorption spectrum of A.

It is clear that trivial transfer is favored when each of these four factors is maximized, i.e., $\Phi_e^D \sim 1$, high concentration of A, high extinction coefficient of A, and good overlap between the emission of D^* and absorption of A. The last factor may be quantified in terms of the spectral overlap integral, J, which is the *integrated* overlap of the experimental absorption and emission curves (Fig. 9.3).[1a]

Mathematically, J is given by

$$J \equiv \int_0^\infty I_D \varepsilon_A \, d\bar{\nu} \tag{9.3}$$

where I_D is a graph of the experimental emission of D^*, and ε_A is a graph of the experimental absorption spectrum of A, both plotted on an energy scale (usually cm^{-1}), and normalized so that complete overlap would correspond to $J = 1.00$.

9.3 Theory of Radiationless Energy Transfer: A General Formulation

In Chapter 3 we noted that all transitions between states (e.g., $D^*A \rightarrow DA^*$) due to weak perturbations can be formulated in terms of a "Golden Rule":

$$\text{Probability}\,(D^*A \rightarrow DA^*) \rightarrow \frac{2\pi}{h}(\rho)\langle\psi_i|H|\psi_f\rangle^2 \qquad \text{"Golden Rule"} \quad (9.4)$$

where ψ_i is the wave function of the initial state, ψ_f is the wave function of the final state, ρ is a measure of the number or density of initial and final states capable of interaction, and H is the specific interaction capable of coupling ψ_i and ψ_f. For the electron energy transfer $D^* + A \rightarrow D + {}^*A^*$, ψ_i corresponds to $\psi(D^*)\psi(A)$ and ψ_f corresponds to $\psi(D)\psi(A^*)$. Since there are two electronic mechanisms by which ψ_i can undergo transition to ψ_f, we can break H up into two types of interactions, i.e., H_e, the exchange interaction, and H_c, the Coulombic interaction.

We may relate the probability P of Eq. 9.4 to an experimental quantity, the *rate constant of energy transfer*, k_{ET}. From this interpretation of probability and Eq. 9.4, we have a relationship of the form

$$k_{ET}(\text{total}) \rightarrow \Big[\langle\Psi(D^*)\Psi(A)|\underbrace{H_e}_{\text{Exchange}}|\Psi(D)\Psi(A^*)\rangle^2 + \langle\Psi(D^*)\Psi(A)|\underbrace{H_c}_{\text{Coulombic}}|\Psi(D)\Psi(A^*)\rangle^2\Big] \quad (9.5)$$

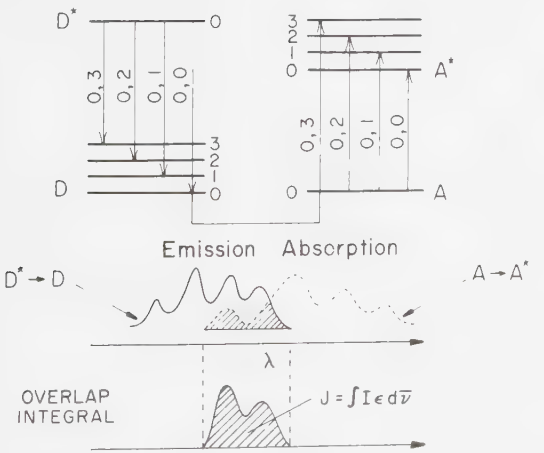

Figure 9.3

Schematic description of the spectral overlap integral J (Eq. 9.3) and its relation to an experimental absorption and emission spectrum. The shaded region corresponds to the overlap of the emission spectrum of D^* and the absorption spectrum of A.

The matrix element for Coulombic interaction represents the electrostatic (repulsive) interactions of the electronic charge clouds $Q_i^e = \phi_{D^*}(1)\phi_A(2)$ and $Q_f^e = \phi_D(1)\phi_{A^*}(2)$, whereas the matrix element for exchange interaction represents the electronic (repulsive) interactions of the charge clouds $Q_i^e = \phi_{D^*}(1)\phi_A(2)$ and $Q_f^e = \phi_D(2)\phi_{A^*}(1)$. Let us consider Figure 9.4 in order to visualize the meaning of these ideas in terms of orbital interactions.

We are assuming that interactions between two electrons (represented by open circles in Figure 9.4) can provide qualitatively significant information on the mechanism of energy transfer. In the figure, the solid circles represent "passive" electrons whose interaction with other electrons are assumed to be roughly constant during the energy transfer step. In Figure 9.4 (top) the nature of the Coulombic perturbation (corresponding to H_c in Eq. 9.5) is represented in terms of interactions (dotted line) between electron 1 in the *LU* of the excited donor D^* and electron 2 in the HO of the ground state acceptor A. The orbital motions (oscillations) of electron 1 cause perturbation of the orbital motions (oscillations) of electron 2. If resonance occurs, energy transfer may occur whereby electron 2 is set into oscillatory motion (is excited) and electron 1 relaxes its motion (is deexcited), i.e., $D^* + A \rightarrow D + A^*$ occurs. The reverse process $D + A^* \rightarrow D^* + A$ is represented at the top right of Figure 9.4.

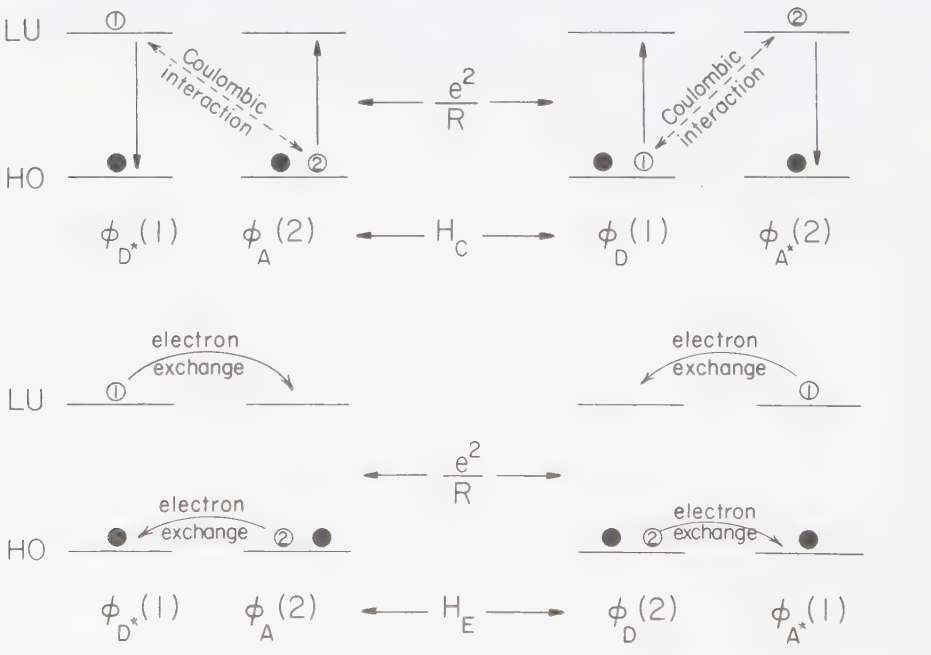

Figure 9.4

Orbital comparison of the Coulombic and exchange mechanisms of electronic energy transfer.

In Figure 9.4 (bottom left) the nature of the exchange perturbation (corresponding to H_e in Eq. 9.5) is represented in terms (a) of overlap (arrow) of electron 1 in the LU of D^* with the LU of the ground state A, and (b) of overlap (arrow) of electron 2 in the HO of A with the HO of the excited donor D^*. These overlaps may be viewed as charge transfers. In the extreme case, electron 1 is completely transferred to the LU of A and electron 2 is completely transferred to the HO of D. The net result is a collisionally induced energy transfer $D^* + A \rightarrow D + A^*$, and is analogous to a moving particle transferring energy to other particles by way of collisions. The reverse process $D + A^* \rightarrow D^* + A$ is represented in the bottom right of Figure 9.4. We can see that the following differences between H_c and H_e, (the Coulombic and exchange matrix elements respectively) are apparent:

1. The Coulombic interaction (dotted double arrow) represents an "action at a distance," i.e., the electrons initially on D^* *stay* on D while the electrons initially on A *stay* on A^*. In other words, the Coulombic resonance interaction $D^*A \rightarrow H_c \rightarrow DA^*$ (dotted arrows) occurs via the electromagnetic field and does not require physical contact of the interacting partners. The basic mechanism involves the induction of a dipole oscillation in A by D^*.

2. The exchange interaction (double solid arrows) represents a "double" electron substitution reaction, i.e., the electron initially on D^* "jumps" to A simultaneously with the jump of an electron on A to D^*. In other words, the exchange resonance interaction of $D^*A \rightarrow H_e \rightarrow DA^*$ (solid arrows) occurs via overlap of electron clouds and requires physical contact between the interaction partners.

A major distinction between the exchange concept (also called the *collisional mechanism*) and the Coulombic concept (called the *induced dipole mechanism*) is that in the former electrons exchange and therefore collisions are *required*, whereas in the latter collisions are *not required*. In other words, in exchange energy transfer, excitation is transferred from one system to another analogous to a moving particle which transfers momentum to other particles with which it collides. In the induced dipole mechanism, the excitation is transferred through *space*, analogous to a radio transmitter acting on a radio receiver.

9.4 Visualization of Energy Transfer by Coulombic Interactions: A Transmitter-Antenna Mechanism

The Coulombic interaction represents a classical interaction between charged particles, and as such a classical analogy is possible.[4] The electric field near an electronically excited molecule is assumed to behave like a field generated by a

classical oscillating dipole whose frequency of oscillation is ν and whose *instantaneous* dipole moment is μ. If $|\mu_o|$ is the *maximal* value of the induced dipole that can be achieved, we apply

$$\mu = \mu_o \cos 2\pi\nu t \tag{9.6}$$

In molecular terms we can identify this oscillating dipole moment as the result of the back-and-forth motion along the molecular framework of the excited electron on D^*. The resulting electric charge oscillation causes electrostatic forces to be exerted on the electronic systems of nearby molecules.

In the Coulombic mechanism an excited molecule (an oscillating dipole) may cause the electrons of a given ground state molecule to oscillate in much the same way as does the electric field of a light wave. For A^* to be produced, a resonance condition and a coupling must occur in each case. For light absorption, the resonance condition is $\Delta E(A \rightarrow A^*) = h\nu$, and for energy transfer the resonance condition is $\Delta E(D^* \rightarrow D) = \Delta E(A \rightarrow A^*)$. In the case of light, the coupling occurs between the electrons of A and the oscillating electronic field of the light wave. In the case of energy transfer, the coupling occurs between the oscillating electron of D^* and the electrons of A.

Relationship Between k_{ET} and Theoretical and Experimental Quantities. Förster Theory of Coulombic Energy Transfer

What are the factors which determine the magnitude of the Coulombic interaction that leads to energy transfer from D^* to A, and how does the magnitude of this interaction relate to k_{ET}? According to classical theory[4] the interaction energy, E, between two *electric dipoles* is directly related to the magnitude of the two dipoles (μ_D and μ_A) and the distance between them (R_{DA}) as follows:

$$\underset{\text{energy}}{\text{Interaction}} \quad E(\text{dipole-dipole}) \propto \frac{\mu_D \mu_A}{R_{DA}^3} \tag{9.7}$$

Förster[4] identified μ_D and μ_A with the oscillator strengths for *radiative* $D^* \rightleftarrows D$ and $A \rightleftarrows A^*$ transitions. He was thus able to quantify the dipole-dipole interaction energy in terms of f_D and f_A, the *measured* oscillator strengths for the radiative transitions of D and A, which, being properties of real systems, include vibrational and spin factors. Thus, a poor vibrational or Franck-Condon factor or a change in multiplicity will lead to small values of f and an associated small interaction energy. Recall that oscillator strength is related to the inherent radiative lifetime and the extinction coefficient of a given transition (Eqs. 5.10 and 5.11). Förster showed that, since the rate of energy transfer k_{ET} by the dipole-dipole mechanism is related to E^2, and since E^2 is related to experimental properties, then k_{ET} can be related to E^2 as follows:

$$k_{ET}(\text{Coulombic}) \rightarrow E^2 \sim \left(\frac{\mu_D \mu_A}{R_{DA}^3}\right)^2 = \frac{\mu_D^2 \mu_A^2}{R_{DA}^6} \tag{9.8}$$

Thus, Förster's theory predicts that k_{ET} for an energy transfer via a Coulombic interaction will be proportional to: (1) the square of the transition dipole moment μ_D, (2) the square of the transition dipole moment μ_A, and (3) the inverse sixth power of the separation of D^* and A.

In Chapter 5, the relationships between the transition moments and experimental quantities were derived (Section 5.5 ff). Thus,

$$\mu_D^2(D^* \rightleftarrows D) \rightarrow \int \varepsilon_D \text{ or } k_D^\circ \tag{9.9}$$

$$\mu_A^2(A^* \rightleftarrows A) \rightarrow \int \varepsilon_A \text{ or } k_A^\circ \tag{9.10}$$

where $\int\varepsilon$ is the integrated extinction coefficient of an absorption bond and k° is the pure radiative rate.

Since we are specifically considering the $D^* \rightarrow D$ and $A \rightarrow A^*$ process in an energy transfer, we select k_D and $\int\varepsilon_A$ as the experimental terms to replace the square of the transition dipole moments:

$$k_{ET}(\text{Coulombic}) \rightarrow \frac{k_D^\circ \int \varepsilon_A}{R_{DA}^6} \tag{9.11}$$

Finally, we must recognize the spectral overlap requirement and consider the overlap of D^* emission with A absorption. Forster[4] showed that:

$$k_{ET}(\text{Coulombic}) = k \frac{\kappa^2 k_D^\circ}{R_{DA}^6} J(\varepsilon_A) \tag{9.12}$$

The term k is a constant determined by experimental conditions such as the solvent index of refraction and concentration. The term κ^2 takes into account the fact that the interaction between two oscillating dipoles depends on the orientation of the dipoles in space. For a random distribution of interacting dipoles, κ^2 is a constant and equal to $\frac{2}{3}$. The term $J(\varepsilon_A)$ is similar to the spectral overlap integral of Eq. 9.3 except that the extinction coefficient of the acceptor is included in the integration.

The Relationship of k_{ET} to Energy-Transfer Efficiency and Separation of Donor and Acceptor

From Eq. 9.12 the major factors which influence the rate constant for energy transfer are: (1) the magnitude of J, the spectral overlap integral, which is theoretically related to the density and probability of isoenergetic resonances from various vibrational levels for the $D^* + A \rightarrow D + A^*$ process, (2) the magnitude of k_D°, the pure radiative rate of D, which is theoretically related to the oscillator strength of the $D^* \rightarrow D$ transition, (3) the magnitude of ε_A, the extinction coefficient for the $A \rightarrow A^*$ transition integrated over the absorption band, and (4) R_{DA}, the separation of D^* and A.

Thus, we anticipate that the *rate* of energy transfer induced by a Coulombic mechanism will be most favored for D^* and A pairs, such that: (1) the $D^* \rightarrow D$ and $A \rightarrow A^*$ processes correspond to a large overlap integral J, (2) the radiative rate constant k_D is large as possible, (3) the magnitude of ε_A is large as possible (for qualitative purposes we may consider ε_A^{max} which is generally proportional to ε_A), (4) there is a small spatial separation between D^* and A.

Experimentally, the *efficiency* rather than the *rate constant* of energy transfer by the dipole-dipole mechanism is often measured, since the latter depends on the *spatial* separation R of D^* and A (recall that $k_{ET} \propto R^{-6}$). It is convenient to define an efficiency for which the *rate* of energy transfer equals the sum of the rates of deactivation of D^*:

$$k_{ET}[D^*][A] = k_D[D^*] \quad \text{at} \quad R = R_0 \tag{9.13}$$

or,

$$k_{ET}[A] = k_D = 1/\tau_D \tag{9.14}$$

Here k_D is the experimental lifetime of D^*, not the pure radiative lifetime. When $[A]$ is such that this equality holds experimentally we may calculate a value of R_0, for the *average* separation of D and A. R_0 is termed the "critical separation," for which the rate of energy transfer and inherent rate of deactivation of D^* are equal.

The *rate constant* and the *efficiency* for energy transfer by the dipole-dipole mechanism may be related to any actual separation R of D^* and A by the

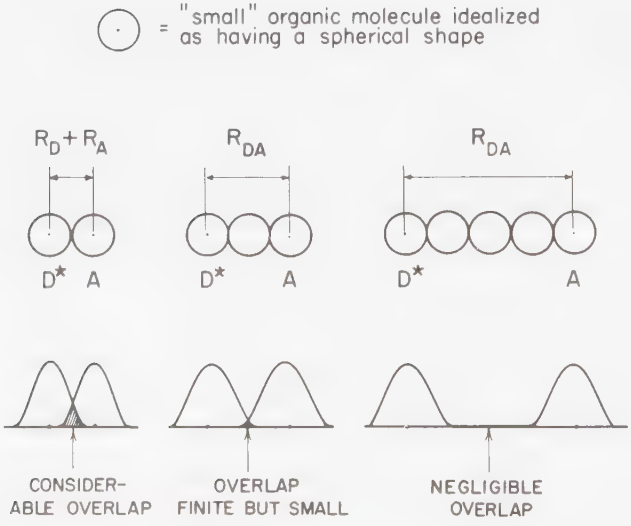

Figure 9.5

Schematic description of electronic overlap between an electronically excited donor, D^*, and a ground-state acceptor, A, as a function of separation.

expressions:[4]

$$\text{Rate:}\quad k_{ET}(\text{for any separation } R) \propto k_D\left(\frac{R_o}{R}\right)^6 = \left(\frac{1}{\tau_D}\right)\left(\frac{R_o}{R}\right)^6 \tag{9.15}$$

$$\text{Efficiency:}\quad \Phi_{ET}(\text{for any separation } R) \propto \left(\frac{R_o}{R}\right)^6$$

where τ_D is the actual mean lifetime of D^*, R is the separation between the centers of D^* and A, R_o is the critical separation of donor and acceptor for which energy transfer from D^* to A and emission from D^* are equally probable and Φ_{ET} is the quantum yield of energy transfer. Thus, since the rate of energy transfer at $R_o = R$ is equal to $1/\tau_D$, if $R < R_o$, energy transfer dominates, and if $R > R_o$, deactivation of D^* dominates.

The *theoretical* "critical" transfer distance R_o may also be calculated from an approximate equation, where the emission spectrum of the donor is expressed in terms of the absorption spectrum of the donor by using the assumed mirror-image symmetry of these spectra.[4]

9.5 Energy Transfer by Electron Exchange: An Overlap or Collision Mechanism

We normally view bimolecular chemical interactions as occurring via *collisions* between the reacting partners. By collisions we mean that the electron clouds of the reacting species overlap significantly in space. In the region of overlap, electron exchange may occur. This situation is shown qualitatively in Figure 9.5.

If we ignore the stereoelectronic details of orbital overlap, then the rate constant for energy transfer by electron exchange is expected to fall off *exponentially* as the separation between D^* and A increases because electron densities usually fall off exponentially as the distance between the electron and the nucleus is increased. Of course, the rate of energy transfer will also be directly related to J, the spectral overlap integral. A theory for energy transfer by electron exchange was worked out by D. L. Dexter, who proposed that for the rate constant of energy transfer:[6]

$$k_{ET}(\text{exchange}) = KJ\exp(-2R_{DA}/L) \tag{9.16}$$

where K is related to the *specific* orbital interactions, J is a spectral overlap integral normalized for the extinction coefficient of the acceptor (cf. Eq. 9.5), and R_{DA} is the donor-acceptor separation relative to their van der Waals radii, L. It is important to note that J, by being normalized for ε_A, does not depend on the magnitude of ε_A. Thus, k_{ET} is predicted to be independent of the absorption characteristics of A. This result contrasts with the prediction of k_{ET}(Coulombic), as can be seen from comparison with Eq. 9.12.

The *electron exchange interaction* is a purely quantum-mechanical effect which does not have a classical analogy. This concept was introduced in order to preserve the notion of electron indistinguishability and to generate proper wave functions. Since there is no classical analogy for exchange we might expect that the connections between the predictions of a theory based on exchange interactions and observable quantities will be indirect. From Eq. 9.5, we can infer the relationship between Eq. 9.16 and theoretical quantities, i.e., Eq. 9.5 must equal 9.16 as shown by:

$$k_{ET}(\text{exchange}) \rightarrow J\langle H'_e\rangle^2\langle \mathcal{S}\rangle^2 = KJ\exp(-2R_{DA}/L) \tag{9.17}$$

In comparing the Förster equation (Eq. 9.12) with the Dexter equation (Eq. 9.16), we note the following contrast in predictions:

1. The rate of dipole-induced energy transfer decreases as R^{-6} whereas the rate of exchange-induced transfer decreases as exp-$2R/L$. (We will discuss this further in Section 9.9.) This means that k_{ET}(exchange) drops to negligibly small values (relative to the donor lifetime) as R increases more than on the order of one or two molecular diameters (5–10 Å).

2. The rate of dipole-induced transfer depends on the oscillator strength of the $D^* \rightarrow D$ and $A \rightarrow A^*$ radiative transitions, but the rate of the exchange-induced transfer is *independent* of the oscillator strength of the $D^* \rightarrow D$ and $A \rightarrow A^*$ transitions.

3. The efficiency of energy transfer (fraction of transfers per donor lifetime $\sim k_{ET}/k_D$) by the dipole mechanism depends mainly on the oscillator strength of the $A \rightarrow A^*$ transition (since a smaller oscillator strength for $D^* \rightarrow D$ is compensated by a *slower* radiative rate) and is directly related to Φ_D, whereas the efficiency of energy transfer by the exchange interaction cannot be directly related to an experimental quantity.

Although these theories have contrasting features, they both predict a direct dependence of k_{ET} on J, a spectral overlap integral.

Visualization of Energy Transfer by Electron Exchange

Energy transfer by an exchange of electrons can occur in one step or several steps. Therefore, it is helpful to consider these possibilities according to the following classification:

1. *Concerted* exchange of electrons, i.e., the electrons of the donor and acceptor are exchanged *simultaneously*.

2. *Charge transfer* exchange of electrons, i.e., the electrons of the donor and acceptor exchange in a stepwise manner via a radical ion pair.

3. *Chemical or covalent bonding exchange of electrons*, i.e., the electrons of donor and acceptor exchange as the result of a chemical bonding to form an intermediate diradical or zwitterion.

Let us use a four-orbital description of the above possibilities in order to illustrate these ideas (Fig. 9.6). In the case of concerted and charge transfer exchange we imagine that the electrons of D^* and A exchange to eventually produce the *same* final state DA^*. The concerted exchange is imagined to occur by overlap of the HO of D^* with the HO of A and of the LU of D^* with the LU of A. *If both of these overlaps are favorable*, then a simultaneous *jump* of the electron in the LU of D^* to the LU of A and the electron in the HO of A to the HO of D^* occurs. The result of this electron exchange is the formation of D and A^*. There is, of course, no experimental way to label the electrons, but if a concerted exchange mechanism were to operate, its effectiveness should depend on the ability of the donor and acceptor to have favorable and simultaneous overlap of the appropriate orbitals. Indeed, the same factors responsible for determining the rates of concerted *chemical* reactions, which proceed mainly by an exchange mechanism (i.e., orbital symmetry factors) should also apply to the rates of energy transfer by a concerted exchange mechanism.

In the extreme case of two-step charge-transfer exchange of electrons, we may imagine (Fig. 9.6) that either (a) the $D^*(LU)$ electron jumps first to the vacant $A^*(LU)$ and then the HO electron of $A\cdot$ jumps to the HO of $D^{\cdot+}$, or (b) an $A(HO)$

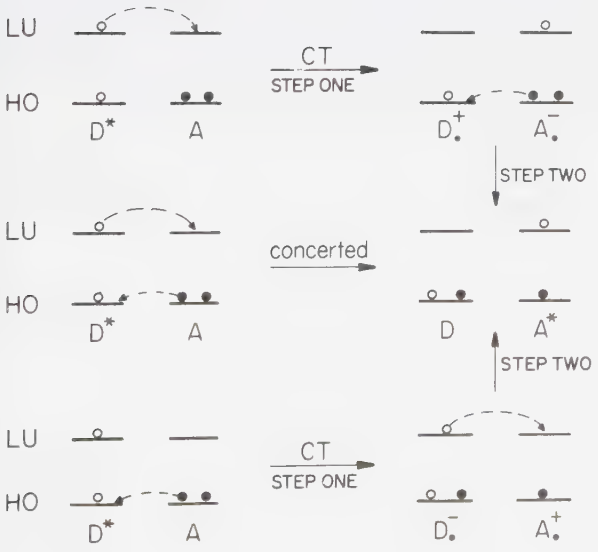

Figure 9.6

Schematic orbital description of different energy transfers. Extreme situations are represented for step one: Bottom—$HO \rightarrow HO$ charge-transfer interaction. Middle—concerted $HO \rightarrow HO$ and $LU \rightarrow LU$ interactions. Top—$LU \rightarrow LU$ charge-transfer interaction.

electron jumps first to the half-occupied $D^*(HO)$ orbital and then the $D^-(LU)$ electron jumps to the LU of A^+. Since the conversion of the radical ion pair to $D + A$ is highly exothermic, it would not be surprising if this *quenching* mechanism were competitive with the much less energetically favorable conversion to $D + A^*$.

In the case of a chemical bonding mechanism for exchange of electrons, we imagine that some two-center interaction occurs between the half-filled orbitals of D^* with the highest filled and lowest unfilled orbitals of A, and that this interaction leads to formation of a full bond between D and A to form a biradical ($\dot{D}$-$\dot{A}$) or zwitterion $\dot{D}$—A or D—$\dot{A}$. These reactive intermediates may produce $D + A$ or $D + A^*$.

Energy Profiles for Energy-Transfer Processes which Occur by Electron Exchange

In order to visualize the exchange energy-transfer process in a general way we shall discuss two situations: (1) a "concerted" electronic energy-transfer process in which an overlap of electron clouds of the donor and acceptor is required for excitation transfer to occur, and (2) formation of an excited-state complex (ăn *exciplex*) which then dissociates into an excited acceptor and ground-state donor. In each case we imagine that the donor and acceptor, originally free molecules in solution, approach each other until they are within each other's sphere of influence and surrounded by a solvent cage, i.e., the donor and acceptor form an *encounter complex*. While donor and acceptor are in the encounter complex, they undergo a number of collisions with one another. By a *collision* we mean that the peripheries of the electron clouds of donor and acceptor overlap and interpenetrate with one another. The *collision complex* (i.e., situation for which the electron clouds of donor and acceptor overlap) is imagined to be higher in energy than the encounter complex, and thereby serves as a transition state for "changing direction" of the translational motions of the colliding donor and acceptor.

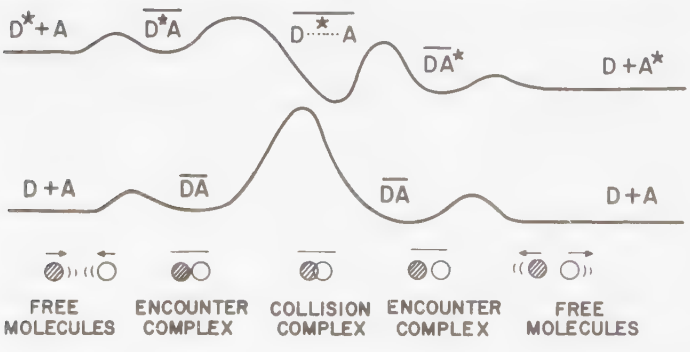

Figure 9.7

Schematic surface description of the formation of encounter and collision complexes of $D + A$ and $D^* + A$, under conditions such that D^* and A are stabilized by collisions but D and A are destabilized by collisions.

Thus, on the ground-state surface we imagine that D and A approach, form an encounter complex, bounce off one another a few times, and then eventually separate from the encounter complex as free molecules in solution (Fig. 9.7).

On the excited-state surface (Fig. 9.7), however, it often happens that the collision complexes ($\overline{D^*A}$) are more energetically stable relative to the free molecules because of the greater polarizability of excited states, which leads to stronger bonding van der Waals interactions. (If they become substantially more stable than the free molecules, we say that an *exciplex* has formed.) Upon collision of D^* and A, the excited electron has penetrated the electron cloud of A and, in the region of overlap, the excited electron cannot be said to belong to either the donor or the acceptor molecule. Thus, after a collision, if the electronic energy of $\overline{DA^*}$ is lower than that of $\overline{D^*A}$, the collision complexes will prefer to spill down toward the lower energy minimum (to the right of Figure 9.7). As a result, molecules initially in a $\overline{D^*A}$ encounter complex can be drained off to the lower-energy encounter complex $\overline{DA^*}$. If the energy gap between $\overline{D^*A}$ and $\overline{DA^*}$ is sufficiently large, the conversion $\overline{D^*A} \rightarrow \overline{DA^*}$ will be irreversible. The *probability* of reversibility will depend not only on the energy gap between the encounter complexes but also on the lifetime of $\overline{DA^*}$ and A^*.

The actual *rate* of energy transfer is limited first by the rate of molecular diffusion of D^* and A into an encounter complex, and second by the rate of energy transfer within an encounter complex.

9.6 The Role of Energetics in Energy-Transfer Mechanisms

Energetics provide important "selection rules" for energy-transfer processes by any mechanism. If a pair of molecules D^* and A are in the state of collision in solution, in general it is found that:

1. *Energy-transfer processes which are endothermic by more than several kcal/mole are generally inefficient, even if they are spin-allowed.*

2. *Spin-allowed energy-transfer processes which are exothermic are generally efficient.*

No general statement can be made for exothermics *spin-forbidden* energy-transfer processes.

The basis of the first rule above is the idea that the *event* of energy transfer requires an exact (resonant) energy which matches the levels of D^* and A. The rate of vibrational relaxation is usually fast compared to the rate of energy transfer. The transfer probability is then usually independent of the wavelength of the exciting radiation, and increases, for a given donor molecule, as the extinction coefficient of the acceptor and the overlap of the donor emission spectrum and acceptor absorption spectrum increase (increasing number of interacting resonant states possible, see Figure 9.3).

Figure 9.8 indicates the reason for the latter result. The emission spectrum of the donor will result from transitions from the $v = 0$ vibrational level of D^* to the $v = 0, 1, 2$, etc. levels of the ground state, whereas the absorption spectrum of A will be from its $v = 0$ level to the $v = 0, 1, 2, 3$, etc. levels of A^*. A coupled transition which spontaneously deactivates D^* and produces A^* requires an energy match in the levels of the two molecules. If D^* undergoes a 0-0 emissive transition, A must undergo an *isoenergetic* 0-4 absorption i.e., at the instant of energy transfer, the overall energy of the system must be conserved so that the energy gap $D^*(v = 0) \rightarrow D(v = 0)$ must equal that for $A(v = 0) \rightarrow A^*(v = 4)$. Clearly, the greater the amount of overlap of the D^* emission spectrum with the absorption spectrum of A, the greater the number of possibilities of energy matchings for coupled transitions. This is the general situation for *exothermic* energy transfer, i.e.,

$$\underset{\text{efficient}}{\text{Transfer}} \quad D^* + A \rightarrow D + A^* \; \Delta E_{DA} < 0 \quad \text{exothermic} \tag{9.18}$$

Consider now (Figure 9.9) the situation for which the 0-0 transition energy for the $D^* \rightarrow D$ process is of lower energy than the 0-0 transition energy for the $A \rightarrow A^*$ process, i.e.,

$$\underset{\text{inefficient}}{\text{Transfer}} \quad D^* \rightarrow A \not\rightarrow D + A^* \; \Delta E_{DA} < 0 \quad \text{endothermic} \tag{9.19}$$

In this case there is no *overlap* of the two spectra and no chance for energy matching (compare Figure 9.9 and Figure 9.3). The rate of transfer from D^* to A

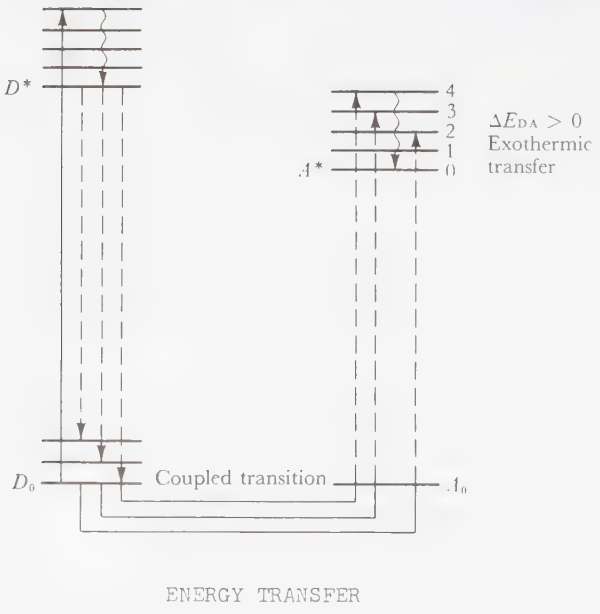

Figure 9.8

Energetically favorable conditions for the energy transfer process $D^* + A \rightarrow D + A^*$.

will be zero because the overlap integral J of common electronic states is zero. The overlap restriction is obviously related to the energy of transitions available from D^* and A, so that for efficient energy transfer molecule A must possess an excited state of lower energy than D^*.

As a rule of thumb, each 1.4 kcal/mole of endothermicity in an energy-transfer step occurring near 25°C slows down the rate by a factor of 10. For example, suppose $\Delta E_{DA} = 6$–8 kcal/mole i.e., energy transfer is now exothermic. The *fastest* rate possible for energy transfer would be slower by at least a factor of 10^4 to 10^5 relative to an exothermic energy transfer of the same type.

Rule (2) above is based on the empirical observation that if $E(D^*) > E(A^*)$ the rate constant of spin-allowed reactions is generally close to the rate constant for diffusion of D^* and A. In the case of the electron exchange mechanism, this generalization may stem from a general tendency of D^* and A to form exciplexes whose rate of formation is close to that for diffusion and which persist for sufficient time to allow efficient energy transfer to occur during the lifetime of the exciplex.

9.7 The Role of Molecular Diffusion in Energy-Transfer Processes in Fluid Solution; "Diffusion Controlled" Quenching[7]

Many energy-transfer processes in fluid solution occur via an electron exchange mechanism and *require* molecular diffusion of D^* and A to within collision

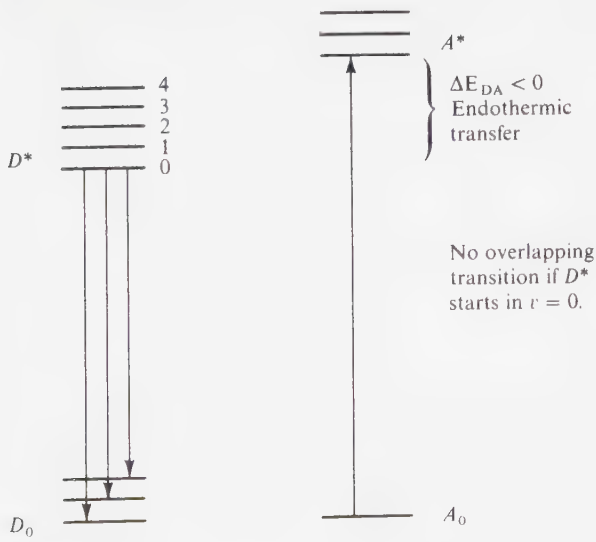

Figure 9.9
Energetically unfavorable conditions for the energy transfer process $D^* + A \rightarrow D + A^*$.

separations as a rate limiting feature of energy transfer. We shall here discuss the process of molecular diffusion in some detail in order to gain some insight into how the process affects the parameter k_{ET} as measured by a *Stern-Volmer* analysis of energy transfer data.[7]

Let us suppose that an energy transfer which occurs via the collisional mechanism proceeds in the following manner (Fig. 9.10):[8]

1. The energy donor D^* first diffuses through the solution until it encounters an acceptor molecule A, and both become collision partners in an encounter complex $\overline{D^*A}$.

2. Collisions occur between D^* and A and eventually one of the collisions leads to energy transfer and generation of a new encounter complex $\overline{DA^*}$.

3. The encounter complex $\overline{DA^*}$ breaks up into free $D + A^*$.

Consider the following description of the net reaction $D + A^*$:

$$\begin{array}{ccccccc} D^* + A & \xrightarrow{k_{DIF}} & \overline{D^*A} & \xrightarrow{k_{ET}} & \overline{DA^*} & \xrightarrow{k_{-DIF}} & D + A^* \\ \Big\downarrow k_D & & \Big\downarrow k_q & & \Big\downarrow k_{-ET} & & \\ D & & \overline{DA} & & \overline{D^*A} & & \end{array} \tag{9.20}$$

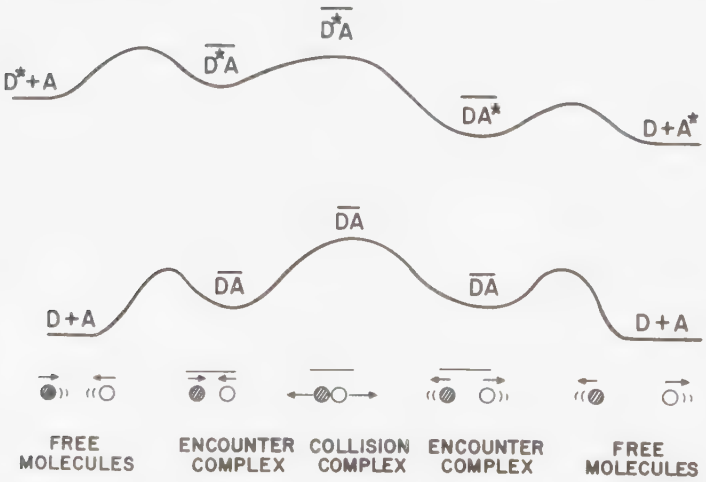

Figure 9.10

Schematic surface description of the formation of encounter and collision complexes of $D + A$ and of $D^* + A$, where little stabilization occurs in the complex.

If energy transfer is to be efficient, the following inequalities must obtain:

$$k_{DIF}[A] \gg k_D \tag{9.21}$$

$$k_{ET} \gg k_q \tag{9.22}$$

$$k_{-DIF} \gg k_{-ET} \tag{9.23}$$

In other words, the rates of proceeding forward must be greater, at each stage, than the rates of competing processes.

If energy transfer and breakup of the collision complex are the only processes available to $\overline{D^*A}$, we may formulate the relationship between the *observed* rate constant for quenching of D^* by A and the rate constant for energy transfer as:[7b]

$$k_{ET}^{OB} = \underbrace{k_{DIF}}_{\text{Rate constant of diffusion}} \underbrace{[k_{ET}/(k_{ET} + k_{-DIF})]}_{\text{Probability of energy transfer}} = \underbrace{\alpha k_{DIF}}_{\text{"Observed" rate constant from Stern-Volmer analysis}} \tag{9.24}$$

In other words, the observed rate constant (k_{ET}^{OB}) for quenching of D^* depends on the rate constant (k_{DIF}) for diffusion of D^* and A together and the probability (α) that energy transfer will occur during the lifetime of the exciplex or encounter complex.

Consider two extreme situations:

1. The rate of dissociation of the exciplex or encounter complex is very fast relative to energy transfer ($k_{-DIF} \gg k_{ET}$).

2. The rate of dissociation of the exciplex or encounter complex is slow compared to energy transfer ($k_{ET} \gg k_{-DIF}$). Under these conditions the observed rate constant for quenching of D^* becomes:

$$\text{Case (1):} \quad k_{OB} = \frac{k_{DIF}}{k_{-DIF}} k_{ET} \quad \text{if} \quad k_{-DIF} \gg k_{ET} \tag{9.25}$$

$$\text{Case (2):} \quad k_{OB} = k_{DIF} \quad \text{if} \quad k_{ET} \gg k_{-DIF} \tag{9.26}$$

We are led to the conclusion that the observed rate constant does not directly reflect k_{ET} in *either* case. In case (1) the observed rate constant is a composite of the (pseudo) equilibrium constant (k_{DIF}/k_{-DIF}) for exciplex or encounter complex formation and the rate constant for energy transfer. In case (2) the observed rate constant is a measure of the rate of diffusion of D^* and A together and is unrelated to k_{ET} except for the implication that $k_{ET} \gg k_{-DIF}$.

In the more general case,[10] α (Eq. 9.24) will contain a bimolecular quenching rate constant, k_q, i.e., $\alpha = (k_{ET} + k_q)/(k_{ET} + k_q + k_{-DIF})$. The Stern-Volmer expression for quenching by energy transfer may now be formulated as:

$$\Phi^o/\Phi = 1 + k_{ET}^{OB}\tau_D[A] \tag{9.27}$$

or

$$\Phi^o/\Phi = 1 + \alpha k_{ET}\tau_D[A] \tag{9.28}$$

Due consideration must be given to α, the "probability factor" for energy transfer, when data on energy-transfer rates are extracted from Stern-Volmer analysis.

The relationship between k_{DIF} and temperature and viscosity[8,9] becomes (with the proper constant evaluated):

$$k_{DIF}\,(M^{-1}\,sec^{-1}) = 2 \times 10^5 T/\eta \tag{9.29}$$

where T is in °K and η is in Poise.

Values of **D**, the molecular diffusion constant for small organic molecules in common nonviscuous solvents (benzene, acetonitrile, etc.) are in the range of 10^{-5} cm^2 sec^{-1}. This corresponds to a value of $k_{DIF} \sim 10^{10}$–10^9 M^{-1} sec^{-1}.

Some viscosity values of commonly encountered organic solvents near room temperature are given in Table 9.1. In general, a nonviscous fluid solvent like hexane possesses a viscosity, η, ~0.01–0.002 Poise. Note (Eq. 9.29) that k_{DIF} depends on both temperature and η. There is an activation energy associated with diffusion through a solvent. The value of E_a for a fluid solvent is ~2–3 kcal/mole. In Table 9.1 some experimental values of k_{DIF} are listed. The agreement between the value calculated from Eq. 9.29 and experiment is quite remarkable, considering the simple assumptions which were employed to derive the equation. The "A-factor" asso-

Table 9.1 Experimental Values of Viscosity and Calculated Values of k_{DIF} at 25°C*

Solvent	Viscosity (Poise)	k_{DIF} (M^{-1} sec^{-1})[a]
n-pentane	0.002	3×10^{10}
n-hexane	0.003	2×10^{10}
acetonitrile	0.003	2×10^{10}
benzene	0.006	1×10^{10}
cyclohexane	0.009	0.7×10^{10}
ethanol	0.010	0.5×10^{10}
acetophenone	0.016	0.4×10^{10}
cyclohexanone	0.020	0.3×10^{10}
1-chloronaphthalene	0.029	0.2×10^{10}
1,2-ethanediol	0.20	0.03×10^{10}
glycerol	15	0.0004×10^{10}

[a] Values predicted by Eq. 9.29 for $T = 25$ C.
* Data from Reference 10.

ciated with diffusion in nonviscous solvents[7a] is generally of the order of 10^{10}–10^{12} sec^{-1}.

Experimental criteria for diffusion-controlled energy transfer processes usually fall into one of the following categories:

1. The measured value of k_{OB}, the bimolecular rate constant for reaction or quenching, is close to that calculated from Eq. 9.29.

2. The experimental value of k_{OB} is a function of η/T, i.e., k_r depends on η at a given temperature and varies with $1/T$ for constant viscosity.

3. The experimental value of k_{OB} is essentially invariant for quenchers of widely varying structure, i.e., a mechanical, not a molecular structural feature is rate-limiting.

4. The experimental value of k_{OB} for different quenchers reaches a limiting value which corresponds to the fastest bimolecular rate measured for that solvent.

If energy transfer is truly diffusion-controlled, then measured values of k_{ET} should behave exactly as k_{DIF}. Thus, we expect that $k_{ET} = \alpha T/\eta$ (Eq. 9.29), so that at constant temperature, k_{ET} should be inversely proportional to the solvent viscosity. In the case of quenching of the valerophenone triplet ($E_T \sim 73$ kcal mole) by 2,5-dimethyl-2,4-hexadiene, the measured value of k_{TT} (for triplet-triplet energy transfer) is *not* a linear function of viscosity for a series of inert solvents (Fig. 9.11).[9] For example, a 15-fold decrease in viscosity (hexadecane to pentane) causes less than a fourfold increase in the transfer rate. It seems clear that in nonviscous (very fluid) solvents such as pentane, the transfer of triplet excitation is not completely efficient and an excited donor-acceptor can separate before energy transfer occurs, i.e., $\alpha < 1.0$.

On the other hand, the rate parameters for quenching of naphthalene fluorescence by biacetyl in solvents of viscosity ranging from $\eta = 0.0034$ poise (hexane) to 0.172 poise (liquid paraffin) are strictly proportional to η^{-1}.[10] The quenching

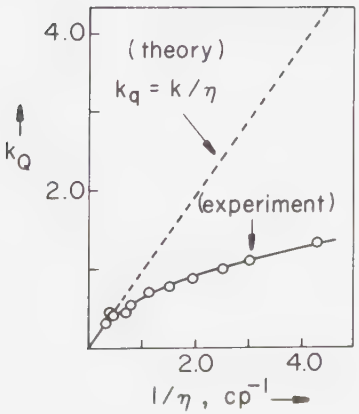

Figure 9.11
Comparison of theoretical (dotted line) and experimental relationships between k_q and $1/\eta$.

is probably due to singlet-singlet energy transfer via a simple overlap electron-exchange mechanism. The data is consistent with a quenching range of ~11 Å for effective transfer.

9.8 Distance-Time Relationships for Diffusion

How long does it take a molecule in a fluid solvent to diffuse a given distance from an initial location? In Eq. 9.29 we note that at any given temperature T, the rate of diffusion depends inversely on the solvent viscosity η.

From diffusion theory it is found that the average distance of displacement x of a diffusing particle during a time t is related to the diffusion coefficient **D** of the particle by:[10]

$$x = \sqrt{2\mathbf{D}t} \tag{9.30}$$

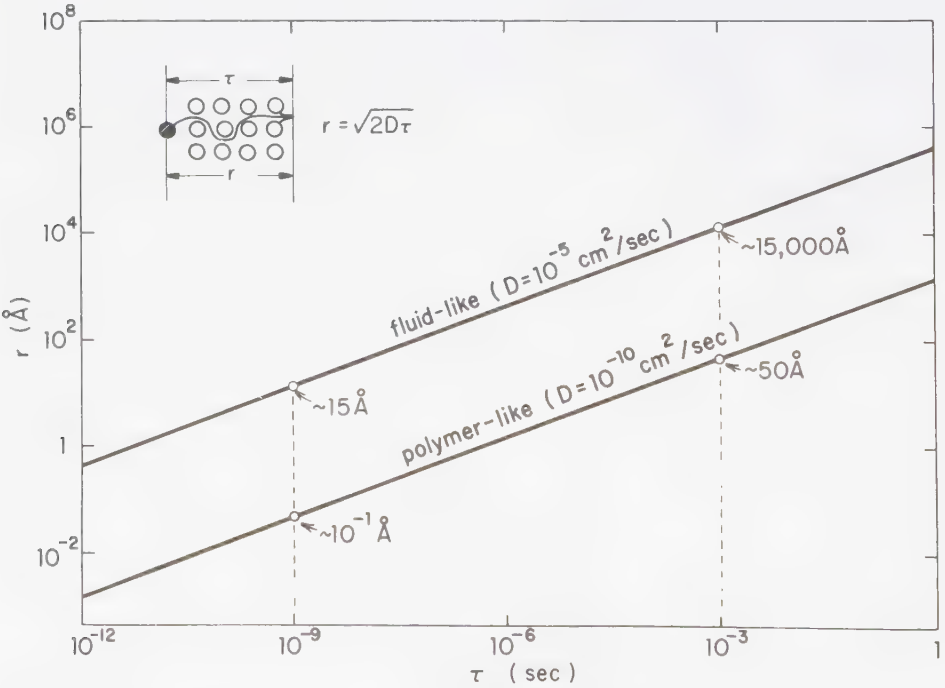

Figure 9.12

Graphs of the relationship between diffusional distance and time for a small organic molecule in a fluid (nonviscous) and polymer-like (viscous) solvent.

In a solution, even a displacement over a distance of only several molecular diameters (say $x = 10 \times 10^{-8}$ cm = 10 Å), is usually achieved by a complicated zig-zag path. How long is the duration of a "collision" in a liquid, according to this model? Since for small, uncharged molecules in fluid organic solvents $\mathbf{D} \sim 5 \times 10^{-5}$ cm^2/sec, then for $x = 2$ Å $= 2 \times 10^{-8}$ cm (considered to be typical separation between organic molecules) we have $t = 8 \times 10^{-10}$ sec.[10] During this interval, the colliding partners are essentially in a state of collision, i.e., they are jiggling back and forth without separating far enough apart for a solvent molecule to slip through them. If we apply a "vibrational" period of about 10^{-12} sec, then we expect about 10 vibrations or "collisions" during the time period that two molecules are 2 Å apart. Thus it can be seen that when two solute molecules get close together in solution, the collisions occur in sets, i.e., the two molecules collide a number of times before separating. The idea that collisions of two particles in a space densely populated with other particles occur in sets is the basis of the notion of "cage effects".

A plot of x, the average displacement of a molecule (in Å) versus time, is given in Figure 9.12 for a nonviscous ($\mathbf{D} \sim 10^{-5}$ cm^2/sec) and a viscous ($\mathbf{D} \sim 10^{-10}$ cm^2/sec) solvent. Notice that in a nonviscous medium a molecule diffuses ~ 15 Å in 10^{-9} sec and 15,000 Å in 10^{-3} sec, whereas in a viscous medium the same molecule hardly moves in 10^{-9} sec and only travels ~ 50 Å in 10^{-3} sec.

9.9 Energy Transfer in the Absence of Diffusion: The Perrin Formulation[12]

Energy transfer may occur in solid solutions under conditions such that molecular diffusion is impossible or may occur also between donor-acceptor components of a rigid molecule that cannot change their positions in space relative to one another. In such a case the Stern-Volmer formulation,[13] which assumes statistical mixing of D^* and A, is no longer valid. *The Perrin formulation* (Eq. 9.31), which assumes that an effective "quenching sphere" exists about D^*, may be used to analyze experimental data in such situations.

The Perrin model (Fig. 9.13) assumes

1. The donor and acceptor cannot undergo displacements in space during the lifetime of D^*.

2. There exists a volume in space—or more precisely a "quenching sphere" about D^* whose radius is R and if a quencher molecule is within this quenching sphere, then D^* is deactivated with unit efficiency.

3. If a quencher molecule is outside of the quenching sphere, it does not quench D^* at all.

The situation is schematized in Figure 9.13. In effect, this assumption is equivalent to stating that there is a "sphere of effective quenching"—a volume of space of radius R in which effective quenching may occur about the excited molecule. If this quenching sphere contains a quencher molecule, the excited molecule is quenched with 100% efficiency. On the other hand, if the quencher is located outside of the quenching sphere, no quenching of the excited molecule occurs.

The Perrin model predicts the following relationship

$$\ln(\Phi^{\circ}/\Phi_{D}) = VN[Q] \tag{9.31}$$

Where Φ° and Φ_{D} are the quantum yields for donor emission in the absence and presence of quencher, respectively, V is the volume of the active sphere of quenching (in cm^3), N is Avogadro's number, and $[Q]$ is the concentration of quencher in M. A plot of $\ln(\Phi^{\circ}\ \Phi_{D})$ versus C yields NV, and since N is known from the concentration, V may be directly evaluated.

Conventionally, the radius R of the quenching sphere rather than its volume V is employed to parameterize experimental data. By expressing R in Å, the common unit of molecule dimensions, one can obtain a feeling for the short-range ($R \sim$ molecular diameters) or long-range ($R \gg$ molecular diameters) nature of the energy-transfer process.

A useful relationship between the radius of the quenching sphere, R and the concentration of acceptor is given by:[12b]

$$R = \left(\frac{3V}{4\pi}\right)^{1/3} = 6.5[A]^{1/3} \tag{9.32}$$

where R is the radius (in Å) of the quenching sphere and $[A]$ is the concentration of acceptor (in moles liter). A plot of R versus $[A]^{1/3}$ is shown in Figure 9.14.

Figure 9.14 emphasizes that for samples which are less concentrated than 10^{-2} M, D^* and A are *on the average* quite far apart. Only for very concentrated

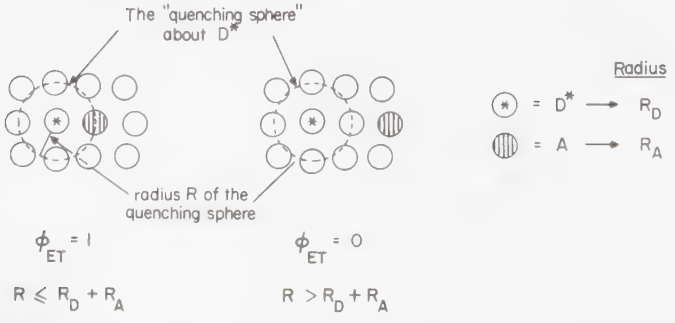

Figure 9.13

Two-dimensional representation of the Perrin formulation of a "quenching sphere" about an electronically excited molecule D^*.

solutions (~ 1 M in A) is there a high probability that D^* will on the average have a molecule of A nearby.

9.10 Comparison of the Theoretical Distance Dependencies of Energy-Transfer Rates and Efficiencies

For qualitative purposes, we may consider the rate constant of energy transfer by the electron exchange mechanism to be written in the form[14]

$$k_{ET} = k_0 \exp - R \tag{9.33}$$

where k_0 is the maximum rate constant for energy transfer which occurs when D^* and A are in the state of a "classical" collision ($R_D + R_A = R_{DA}$) and R is the separation between the peripheries of D^* and A when they are further apart than the sum of their classical radii, i.e., $R = R_{DA} - (R_A + R_D)$. The *maximum* value of k_0 is expected to be on the order of 10^{13} sec^{-1} i.e., the order of collisions. Figure 9.15

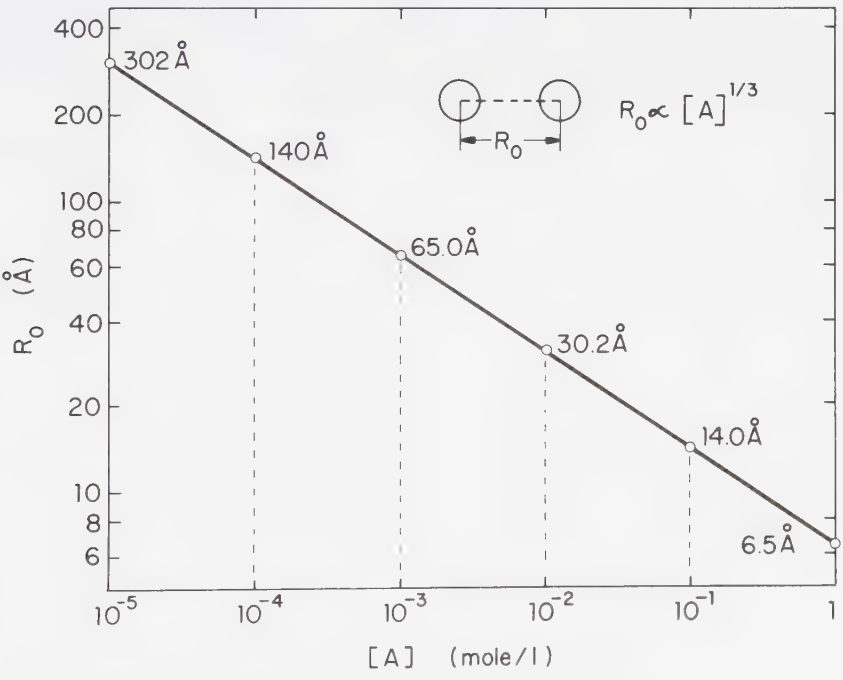

Figure 9.14

Graph of the relationship between concentration and average separation in a rigid solution (Eq. 9.32).

shows a plot of log k versus R. The value of k_{ET} falls from 10^{13} sec^{-1} when D^* and A collide ($R = 0$) to $\sim 10^4$ sec^{-1} when R equals 10 Å. Although these calculations are not intended to be accurate, they indicate the sharp fall of k_{ET} by exchange mechanisms as D^* and A are separated by more than one or two classical collisional diameters.

We should emphasize the crudeness of this model and the fact that it is intended to serve only as a qualitative guide to the falloff in k_{ET} as a function of distance. Since organic molecules are not spheres but have shapes, we expect *stereoelectronic* effects to enter into the detailed determination of the form of the dropoff in k_{ET} as a function of donor-acceptor separation. For a given decay rate k_D of D^*, the value of k_{ET} k_D (a measure of energy-transfer efficiency) drops off much more

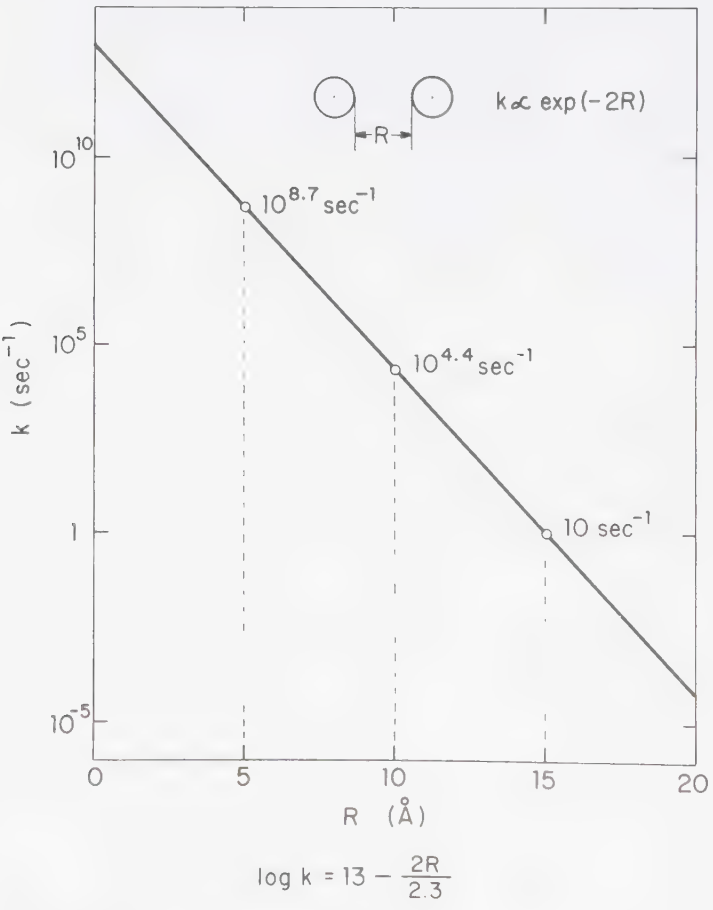

Figure 9.15

Graph of the distance dependence of energy transfer by the exchange mechanism as a function of distance (Eq. 9.33) where k_0 is taken as 10^{13} sec^{-1}.

rapidly for the exchange mechanism than for the dipole-dipole mechanism. Figure 9.16 shows a plot of ln k_{ET}/k_D versus R_{DA} (in Å).[14] For small organic molecules in fluid solvents, the falloff of ln k_{ET}/k_D for the exchange is quite drastic for separation distances greater than ~ 10 Å. Beyond this distance, the falloff in ln k_{ET}/k_D is roughly a factor of 6 10 per Å *increase* in separation. For the dipole-dipole mechanism, the falloff is much more gradual, so that k_{ET} and k_D may have comparable values for distances of R_{DA} exceeding 20–30 Å.

9.11 Experimental Examples of Singlet-Singlet Energy Transfer

Singlet-singlet energy transfer (Eq. 9.34) is "spin-allowed" for both the Coulombic and exchange interactions:

$$\underset{\text{energy transfer}}{\text{Singlet-singlet}} \quad D^*(S_1) + A(S_0) \rightarrow D(S_0) + A^*(S_1) \tag{9.34}$$

As a result, donor (singlet) to acceptor (singlet) electronic energy transfer may occur either by a long-range Coulombic (*dipole-dipole*) mechanism or by a short-range *electron exchange* mechanism.

Some experimental data for singlet-singlet energy transfer are given in Table 9.2. For each case the energy sufficiency requirement is met, i.e., E(donor) > E(acceptor), an overlap of donor emission and acceptor absorption occurs, and the donor fluorescence is quenched and the acceptor fluorescence is sensitized. In the case of ketones and 1-chloroanthracene as donors, the trivial donor emission-acceptor reabsorption mechanism is ruled out because the quantum yield for

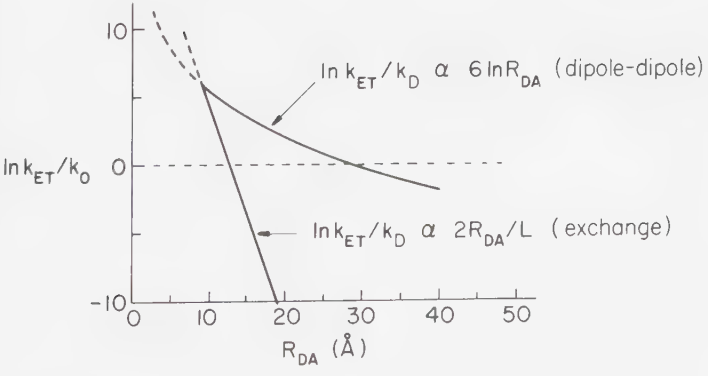

Figure 9.16

Graphs of the rate ratio of energy transfer to D^* decay plotted as ln k_{ET}/k_0 versus 6 ln R_{DA} for Förster-energy transfer (Eq. 9.15) and $2R_{DA}/L$ for exchange-energy transfer (Eq. 9.33).

Table 9.2 Singlet-Singlet Energy Transfer

Entry	Donor	Acceptor	Solvent	ε_A^{max}	k_{ET}(exp)	R_{DA}	Ref
(1)	$(CH_3)_2CO$	$CH_3COCOCH_3$	Cyclohexane	30	9×10^9	–	(a)
(2)	Norcamphor	$(CH_3)_3CCOCOC(CH_3)_3$	Polymer	30	$< 10^8$	< 15 Å	(d)
	Norcamphor	$(CH_3)_3CCOCOC(CH_3)_3$	Cyclohexane	10	7×10^9	—	(a)
(3)	1-Chloroanthracene	perylene	Benzene	5×10^4	1×10^{11}	—	(b)
	1-Chloroanthracene		Liquid paraffin		1×10^{11}	—	(b)
(4)	Naphthalene	$CH_3COCOCH_3$	Cyclohexane	30	1×10^{10}	—	(c)
	Naphthalene		Liquid paraffin	30	5×10^8	—	(e)
(5)	$(CH_3)_2CO$	9,10-Diphenylanthracene	Benzene	10^4	1×10^{11}	~25 Å	(d)
	$(CH_3)_2CO$		Polymer	10^4	5×10^{11}		(h)
(6)	Rhodamine 6B	Malachite Green			3×10^{11}		(f)
(7)	Pyrene	Sevron Yellow L	Polymer		4×10^6	40 Å	(g)
(8)	Pyrene	Perylene	Solid			36 Å	(g)

[a] Yekta, A., and Turro, N. J., *Chem. Phys. Letters*, *17*, 31 (1972).
[b] Bowen, E. J., and Livingston, R., *J. Am. Chem. Soc.*, *76*, 6300 (1954).
[c] Dubois, J. T., and Cox, M., *J. Chem. Phys. 38*, 2538 (1963).
[d] Steinmetzer, H. C., Lechtken, P., and Turro, N. J., *Liebigs. Ann. Chem.*, 1984 (1973).
[e] Birks, J. B., and Leite, M., *J. Phys. B. Atom Molec. Phys.*, *3*, 417 (1970).
[f] Rehm, D., and Eisenthal, K. B., *Chem. Phys. Letters*, *9*, 389 (1971).
[g] Bennett, R. G., Schwenker, R. P., and Kellogg, R. E., *J. Chem. Phys.*, *41*, 3040 (1964).
[h] Steinmetzer, H. C., and Turro, N. J., *J. Am. Chem. Soc.*, *96*, 4677, 4697 (1974).

sensitized fluorescence is much *greater* than the total quantum yield for unquenched donor fluorescence.[15] This means that the product of the efficiency of energy transfer times the fluorescence efficiency of the acceptor is greater than the fluorescence efficiency of the donors. For example, although the quantum yield of fluorescence of 1-chloroanthracene is 0.05 under the conditions of measurement (benzene, room temperature), the limiting sensitized quantum yield of perylene fluorescence is nearly 0.5. Thus, the *maximum* contribution from the trivial mechanism would account for only 10% of the observed effect. Clearly, energy transfer from singlet 1-chloroanthracene to perylene occurs *before* fluorescence, i.e., a *radiationless* transfer of singlet energy is occurring. The examples selected were chosen so that "trivial" reabsorption would be minimized. Experimentally, the contribution of trivial emission reabsorption is minimized by using small pathlengths for analysis of the sensitized emission, since the absorption of light depends on the pathlength available for absorption.

From theory we have seen that two possible mechanisms for radiationless transfer of singlet to singlet energy exist: exchange and dipole-dipole mechanisms. Experimentally, these two mechanisms may be distinguished by measurements of the rate constants for energy transfer (k_{ET}), comparing them to the rate constant for diffusion (k_{DIF}), and then measuring the rate constant for energy transfer as a function of solvent viscosity. If k_{ET} is significantly greater than k_{DIF} and if k_{ET} is insensitive to solvent viscosity, then a mechanism which requires diffusional encounters is ruled out and the dipole-dipole mechanism is confirmed. If, on the other hand, k_{ET} is comparable to, or less than, k_{DIF} and k_{ET} is sensitive to viscosity, then a rate-limiting diffusional encounter is implied and the exchange mechanism, which requires close contact (i.e., collisions) of donor and acceptor, is confirmed. k_{DIF} for the fluid solvents listed in Table 9.2 are on the order of 10^{10} M^{-1} sec^{-1} (viscosity of cyclohexane = 0.9 cP), k_{DIF} (calc) = 7×10^9 M^{-1} sec^{-1}, viscosity of benzene = 0.6 cP, k_{DIF} (calc) = 1×10^{10} M^{-1} sec^{-1}), whereas for "liquid paraffin" (a viscous oil, viscosity ~ 200 cP, k_{DIF} (calc) $\cong 3 \times 10^8$ M^{-1} sec^{-1}). Inspection of Table 9.2 indicates that for the donor-acceptor pairs listed, acetone-biacetyl,[16] norcamphor-dipivolyl,[16] and naphthalene-biacetyl[17] all have $k_{ET} \sim k_{DIF}$, suggesting that an exchange mechanism operates for these pairs. Furthermore, in the case of the naphthalene-biacetyl pair, k_{ET} varies from 1×10^{10} M^{-1} sec^{-1} to 5×10^8 M^{-1} sec^{-1} upon changing from a fluid to a viscous solvent, a result which strongly supports the exchange mechanism. The 1-chloronaphthalene-perylene[15c] and acetone-9,10-diphenylanthracene systems,[18] on the other hand, have values of $k_{ET} \gg k_{DIF}$ and the magnitude of k_{ET} for these pairs is insensitive to solvent viscosity. Indeed, the value of k_{ET} for the acetone-9,10-diphenylanthracene system[18] is about 5×10^{10} M^{-1} sec^{-1} even when this donor-acceptor is embedded in a *rigid* polymer[19] for which the normal diffusional processes are severly inhibited. Thus, the long-range dipole-dipole energy transfer mechanism apparently operates for the acetone-9,10-diphenyl anthracene and 1-chloroanthracene-perylene pairs.

For the latter pair from the "half-quenching" concentration of perylene, a value of R_0 (the average separation of donor and acceptor when donor decay and energy transfer occur at equal rates) may be evaluated. Experimentally,[15] a 6.2×10^{-3} M concentration of perylene quenches half of the fluorescent 1-chloronaphthalene

molecules. The value of R_0 is given by

$$R_0\,(\text{Å}) = 7.3 \times [A]^{1/3}_{1/2} = 7.3 \times [6.2 \times 10^{-3}]^{1/3}$$
$$R_0\,(\text{Å}) = \sim 40\ \text{Å} \tag{9.35}$$

Thus, the separation for which energy transfer and donor decay occur at equal rates is much larger than the molecular diameter of donor or acceptor (~ 8 Å). Notice that Eq. 9.35 differs slightly from Eq. 9.32. In the latter, R refers to the Perrin quenching sphere (every D^* with a Q molecule within distance R is quenched). In the case of R_0 only half of the D^* molecules with a Q molecule with distance R_0 are quenched.

Importantly, for the systems which appear to proceed via an exchange mechanism, the *acceptor* possesses a low absorption coefficient corresponding to its lowest $S_0 \rightarrow S_1$ radiative transition, whereas for the systems which appear to proceed via a dipole-dipole mechanism, the acceptor possesses a rather large extinction coefficient for its $S_0 \rightarrow S_1$ radiative transition.

In contrast to the lack of a viscosity effect on k_{ET} for the 1-chloroanthracene (donor)–perylene (acceptor) system,[15] it is found (see Table 9.2) that for the naphthalene-biacetyl system, k_{ET} is much slower in liquid paraffin ($5 \times 10^8\ M^{-1}\ sec^{-1}$, $\eta = 1.7$ Poise) than in hexane ($k_{ET} = 2 \times 10^{10}\ M^{-1}\ sec^{-1}$, $\eta = 0.03$ Poise).[20] In fact, it is found that for this system $k_{ET} \propto t/\eta$ is expected from theory if $k_{ET} \propto k_{DIF}$. The data are consistent with an R value of ~ 10 Å. From Förster theory, the value of R_0 is calculated to be only ~ 4–5 Å for the singlet-singlet energy transfer in the naphthalene biacetyl system (Eq. 9.36). The "molecular radii" of naphthalene and biacetyl are both of the order of 3 Å, thereby yielding a "collisional radius" of ~ 6 Å. Thus, since $R(\text{exp}) \sim 10$ Å, the data are consistent with an electron exchange mechanism, i.e., the interactions which lead to energy transfer do not require substantial bonding but merely a peripheral overlap of electron clouds.

Evidence for the insensitivity of the rate constant for exothermic singlet-singlet energy transfer by the electron-exchange mechanism to structural effects is revealed by the observation that ketone donors **1** and **2** transfer energy to biacetyl with essentially the same rate constant ($\sim 7 \times 10^9\ M^{-1}\ sec^{-1}$), even though **2** possesses much greater steric bulk around the carbonyl function:[16]

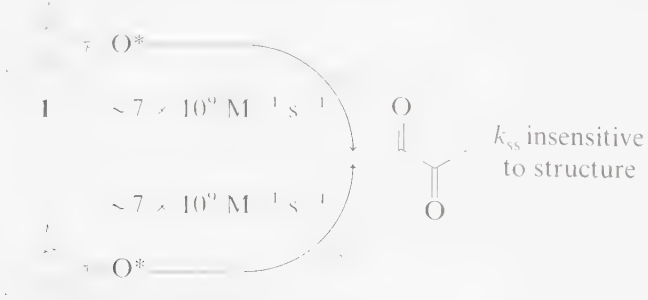

(9.36)

The spectral overlap function J is expected to be a factor in determining k_{ET} if overlap of the donor emission and acceptor absorption is very small, even for *exothermic* energy transfer. However, it is generally the case that substantial overlap exists for *any* exothermic singlet-singlet energy transfer, because the acceptor absorption rarely decreases to very small values for energies greater than the spectroscopic O,O energy. This means that acceptor absorption is generally continuous, albeit with varying probability, from the O,O band to higher energies.

Azo compounds represent a classic exception to this rule.[21] The absorption spectrum of 2,3-diazoocetene shows that the value of ε drops from ~ 200 at 375 nm to ~ 1 at 280 nm. Thus, according to theory the spectral overlap term should tend to *decrease* k_{ET} as the donor energy *increases* if the increase in energy for the $D^* \rightarrow D$ transition causes it to fall in the region where $A \rightarrow A^*$ absorption is very weak. This expectation is verified for singlet-singlet energy transfer from various donors to alkyl azo acceptors. For example, the rate constant for energy transfer from benzene singlets ($E_s \sim 110$ kcal mole) to azo singlets is considerably smaller than that for transfer from aromatic hydrocarbon singlets whose energies are less than ~ 90 kcal/mole.

Experimental Tests of the Förster (Coulombic) Theory of Electronic Energy Transfer

The Förster formulation of Coulombic energy transfer is cast in a form particularly well suited to experimental confirmation or denial.[5] As such it is "vulnerable" to the assaults of the experimentalist seeking data which might reveal inadequacies in the theory. In fact, the theory has held up exceedingly well under many searching experimental examinations.

For example, various forms of Equation 9.12 (repeated below) have been tested by measuring k_{ET} as a function of k_D, of R_{DA}, and of $J(\varepsilon_A)$. In each case

$$k_{ET}(\text{Coulombic}) = k \frac{\kappa^2 k_D}{R_{DA}^6} J(\varepsilon_A) \tag{9.12}$$

the agreement between theory and experiment was excellent.[1]

Tests of the Förster Theory: Donor-Acceptor Separation and Spectral Overlap Integrals

We shall consider three experimental tests of the Förster theory for allowed singlet-singlet energy-transfer processes between donors and acceptors whose separation is fixed by a molecular skeleton or by "molecular spacers." The first example[22] is a "bis-steroid" structure which keeps the donor and acceptor at a fixed and well-defined distance of separation. The second example involves a study of the efficiency of energy transfer for a given donor-acceptor pair as a function of varying the separation between D^* and A. The third example involves the use of monolayers to space the donor-acceptor pair.

Consider the bis-steroid **3** (Fig. 9.17). From measurement of the quantum yield of emission and the spectral overlap integral, a value of R_0 could be calculated, and from the assumed R^{-6} dependence of energy transfer (Eq. 9.12) a value of R_{DA} for the bis-steroid system **3** could be evaluated. Experimentally, the *calculated* value of R_{DA} was 19 ± 2 A and the value of R_{DA} from molecular models was 21 ± 2 A. Thus, there is agreement within the experimental error of the value calculated from the Förster theory and experimental data, and from the separation of D^* and A based on molecular models.[22]

A particularly revealing example of the dependence of *singlet-singlet* energy transfer on distance is given by the results derived from a series of oligomers of poly-L-proline (**4**, Fig. 9.18) for which the donor group (α-naphthyl) and acceptor group (dansyl) were separated by distances ranging from 12 to 46 Å.[23]

This system allows an important test of the Forster equation to be made, namely it allows evaluation of the efficiency of energy transfer as a function of distance, and comparison of the latter with theory. The singlet-singlet transfer efficiency for **4** is ~100% for $n = 1, 2, 3$, and 4 ($R \sim 10$–20 A). The efficiency then drops off and reaches a value of ~15% when $n = 12$. 50% transfer occurs when $R \sim 35$ A, i.e., R_0 for this system is 35 A. The *distance-dependence* of the efficiency of energy transfer by the dipole-dipole mechanism is predicted to be $\phi_{ET} \propto R^{-6}$. This prediction is found to hold for energy transfer in the proline oligomers. Since ϕ_{ET} is expected to fall off *exponentially*, not as R^{-6}, for an exchange mechanism, it is evident that singlet-singlet energy transfer occurs via a dipole-dipole mechanism for the proline oligomers.[23]

From the above studies it is clear that the distances between chromophores which have a fixed but unknown separation can be estimated from the energy

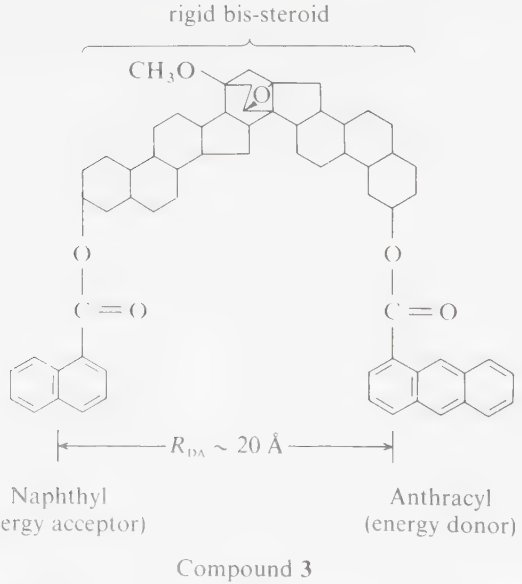

Compound **3**

Figure 9.17

The bis-steroid used to test the distance dependence of Coulombic energy transfer.

transfer studies. If the transfer occurs by the dipole-dipole mechanism, the energy transfer process serves as a *spectroscopic ruler* since transfer efficiency depends on inverse sixth power of the distance between chromophores.

A particularly impressive and elegant example of the verification of the Förster theory has been provided by the use of "molecular spacers" to hold the donor and acceptor at *fixed* and *known* distances of separation.[24] In this case the molecular spacers are long linear soap molecules of the general structure $CH_3(CH_2)_nX$, where n is usually 10 or greater and X is a polar group. The technique of constructing monolayers of molecules with soap molecules as molecular spacers allows one to hold a donor and acceptor at various fixed and known distances, R_{DA}. From the experimental efficiency of energy transfer as a function of R_{DA}, the Förster equation can be tested.

Monolayers of soap molecules can be constructed on a glass slide by simply dipping a glass slide into a soap solution and then slowly withdrawing it.[25] A monolayer of soap molecules is transferred from the surface of the water to the slide. Numerous variations of this technique are available, and as a result it is possible to construct an arbitrary number of different monolayers laid one upon the other.

An experimental demonstration of the effect of monolayer separation on the emission properties of a donor-acceptor pair is shown in Figure 9.19. For the pair shown, only acceptor emission is observed when the two chromophores are in direct contact, i.e., $R_{DA} = 0$.[25] At a separation of $R_{DA} \sim 27$ Å, the sensitizer emission is clearly visible. At a separation of $R_{DA} \sim 54$ Å, the sensitizer emission is dominant.

From Eq. 9.12, it is clear that for a *fixed value* of R_{DA} and k_F, k_{ET} should be proportional to the magnitude of J. A particularly interesting test[26] of the predicted

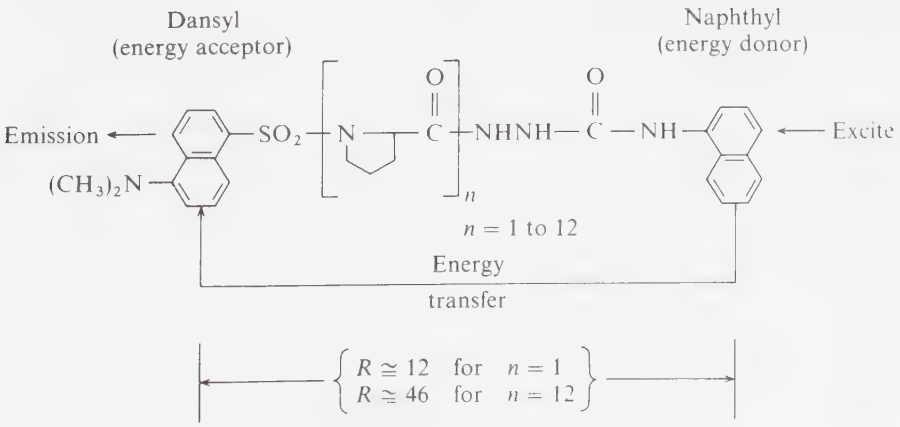

Figure 9.18

Series of oligomers used to test the distance dependence of singlet-singlet energy transfer by the Förster mechanism.

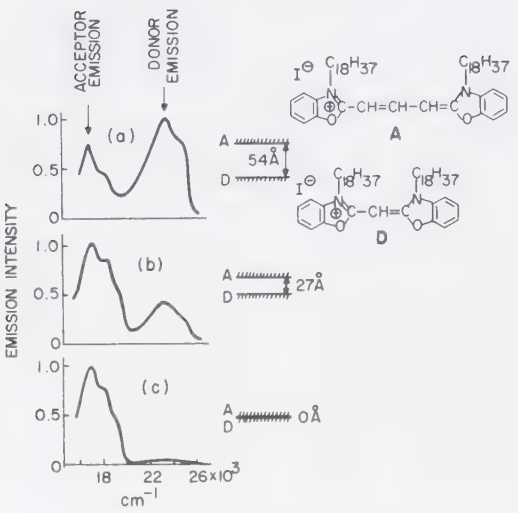

Figure 9.19

Experimental example of the effect of separation on the emission properties of *D* and *A*. In (a) the donor and acceptor are separated by 54 Å and the observed emission is a comparable mixture of donor and acceptor fluorescence. In (b) *D* and *A* are separated by ~ 27 Å and the observed emission is mainly the fluorescence of *A* (i.e., the fluorescence of *D* is quenched more efficiently). In (c) *A* completely quenches the emission of *D*. In all cases *D* is the light-absorbing species.

dependence of the rate constant for resonance energy transfer on J was possible for the steroid structures **5** and **6** (Fig. 9.20). The energy donor was the N-methylindole moiety and the energy acceptor was the ketone function.[26] The value of R is about 10 A for **5** and is, of course, fixed. However, the donor emission spectrum of **5** depends strongly on solvent, and J could be varied by a factor of 40 by simply altering the solvent (Fig. 9.21). The rate constant, k_t, for **5** was measured and then compared to that for **6**, which cannot undergo intramolecular energy transfer. The transfer rate was found to be proportional to the magnitude of J as predicted by Förster's theory.

For example, the rate constant for intramolecular energy transfer varied from 1×10^7 sec^{-1} (methanol solvent) to 55×10^7 sec^{-1} (heptane solvent).[26] The values of J in these solvents were found from spectral data to be much smaller in methanol than in heptane.

9.12 Triplet-Triplet Energy Transfer

By triplet-triplet energy transfer we mean that an *electronically excited donor in its triplet state produces an electronically excited acceptor in its triplet state:*

$$\text{Triplet-triplet energy transfer} \quad D^*(T_1) + A(S_0) \rightarrow D(S_0) + A^*(T_1) \tag{9.37}$$

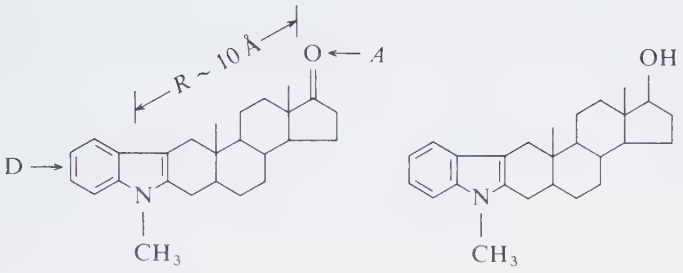

Compound **5** Compound **6**

Figure 9.20

Steroids **5** and **6** used to test the dependence of energy transfer by the Coulombic mechanism on J, the overlap integral.

Triplet-triplet energy transfer is "forbidden" by the dipole-dipole mechanism (exceedingly low ε_A, Eq. 9.12). However, triplet-triplet energy transfer is "spin-allowed" by the exchange mechanism[14].

We expect therefore that triplet-triplet transfer will generally occur only via the exchange mechanism. Values of R_0^{DA} of the order of 10 15 Å are expected for triplet-triplet energy transfer, since close approach of donor and acceptor are required for effective exchange interaction.

Triplet-triplet energy transfer (Eq. 9.37) is the most common and most important type of energy transfer involved in organic photochemistry.[27] The longer a molecule remains in an excited state the greater the probability that it will transfer electronic excitation energy to a suitable neighbor which happens to be in its vicinity. In general, the lowest triplet state of a molecule is longer-lived than the

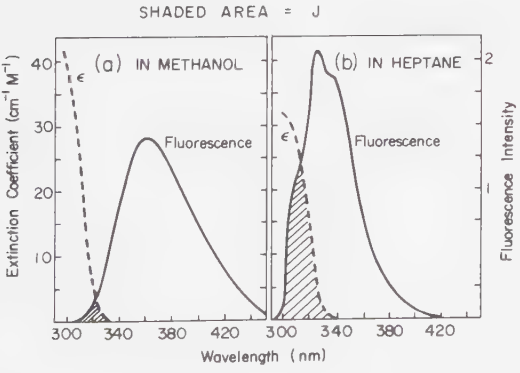

Figure 9.21

Overlap of the emission spectrum of N-methylindole energy donor (**5**) and the absorption spectrum of the ketone energy acceptor (**6**) in (a) methanol and (b) heptane.

corresponding lowest excited singlet state of the same molecule. This means that, all other factors being equal, the triplet of a molecule is a more likely candidate to participate in energy-transfer processes than the singlet.

Convenient experimental conditions for the detection of the triplet-triplet transfer can be deduced from a consideration of Figure 9.22. If the lowest singlet state of the donor D_1 lies below that of the acceptor A_1 but the lowest triplet level of the donor D_3 lies *above* that of the acceptor A_3, the selective excitation of the donor in the presence of the acceptor is possible by employing exciting radiation which is totally absorbed by the donor. The donor is selected to have a high intersystem crossing efficiency and rate. (The $S_0 \rightarrow T$ absorptions of donor and acceptor are negligible.) Under such conditions, singlet-singlet transfer is unlikely because of the unfavorable energetic positions of the D_1 and A_1. Triplet-triplet transfer, which is unlikely by a resonance mechanism since forbidden transitions in both the donor and acceptor are involved, may occur efficiently by an exchange mechanism if the molecules D_3 and A_0 are within collisional diameters of one another. The advantage of selectively exciting the donor is that any process which occurs through the triplet acceptor (which does not pass through S_1) arises from the energy-transfer process in Eq. 9.37.

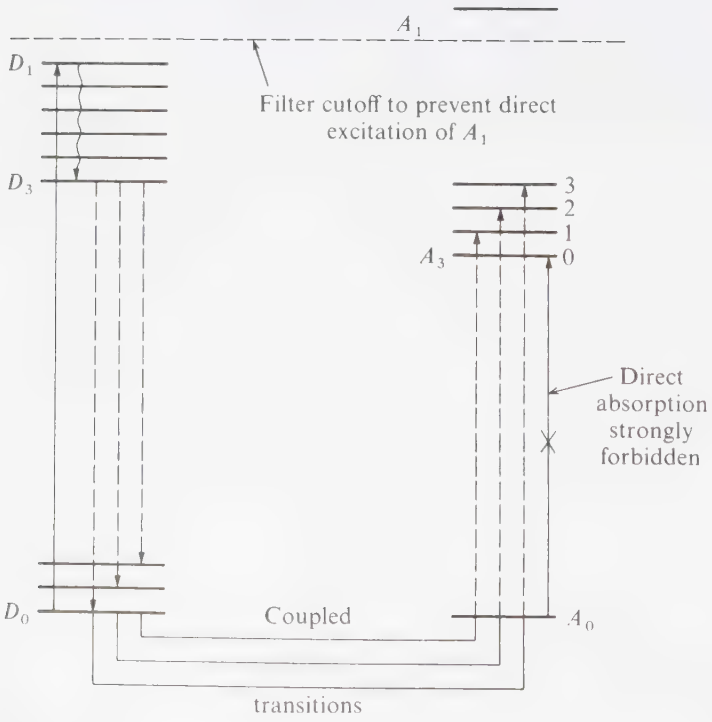

Figure 9.22
Triplet-triplet excitation transfer.

Experimental Examples of Triplet-Triplet Transfer in Fluid Solution

Triplet-triplet energy transfer in fluid solution is of great importance in both mechanistic and synthetic organic photochemistry.[27] "Triplet sensitization" (i.e., the generation of T_1 of an acceptor via energy transfer from a triplet sensitizer) is useful to populate T_1 states that are not efficiently populated by intersystem crossing. "Triplet quenching" (i.e., the specific quenching of T_1 of a donor via energy transfer to an acceptor) is useful as a mechanistic probe and as a means of avoiding the T_1 reactions of the donor.

It is expected from theory and confirmed by the data in Table 9.3 that energetically *favorable* exothermic energy transfers, i.e., $\Delta E(D - A) < 0$, do not occur with values of k_{ET} greater than k_{DIF}. An interesting generalization of the data is the fact that when triplet-triplet energy transfer is exothermic, k_{ET} is within an order of magnitude of k_{DIF}. This "rule" of exothermic triplet-triplet energy transfer is generally independent of donor-acceptor types. Examples of exothermic energy transfers such as $D_3(\pi, \pi^*) \rightarrow A_3(\pi, \pi^*)$; $D_3(\pi, \pi^*) \rightarrow A_3(n, \pi^*)$; $D_3(n, \pi^*) \rightarrow A_3(\pi, \pi^*)$; and $D_3(n, \pi^*) \rightarrow A_3(n, \pi^*)$ are to be found in Table 9.3, i.e., triphenylene-naphthalene,[28] naphthalene-biacetyl,[29] biacetyl-naphthalene,[29] and acetone-biacetyl,[30] respectively. The range of values of k_{ET} for these donor-acceptor pairs is only a factor of five or so. Thus, the rate constant for exothermic energy transfer appears to be relatively insensitive to the electronic configurational change which occurs in the donor and acceptor during triplet-triplet energy transfer.

The measurement of "diffusion controlled" quenching of benzophenone by 1,3-pentadiene and by 1-methylnaphthalene has been measured directly by picosecond flash spectroscopy.[31] The build up and decay rate (k_{ST} and k_q respectively) of benzophenone triplet-triplet absorption in 1,3-pentadiene or 1-methylnaphthalene solvent were measured after picosecond excitation of the first excited singlet state of the ketone. The picosecond technique allows both *direct* measurement of the $S_1 - T_1$ intersystem crossing of benzophenone ($k_{ST} \sim 1 \times 10^{11}$ sec^{-1}) and the true rate of quenching of T_1 ($k_q \sim 10^{11}$ sec^{-1}), i.e., triplet benzophenone need not diffuse in order to be quenched.

Exothermic Energy Transfers which Occur by the Exchange Mechanism but Do Not Proceed at the Diffusional Rate

There are many reports in the literature which demonstrate that triplet-triplet excitation transfer is nearly diffusion-controlled when the donor triplet's energy is higher than the acceptor triplet's by 3–5 kcal mole (see Table 9.3). From theory, although the activation energy for exothermic energy transfer is not *required* to be equal to zero, there is also no reason to expect that an energy transfer overlap which occurs via an energy exchange mechanism will possess a substantial activation energy. However, if *orbital interactions* are required for effective electron exchange, then energy barriers to energy *transfer* may exist for the same reasons that energy barriers exist in bimolecular photochemical *reactions*, i.e., a direct surface pathway from the D^*A complex to the lower energy DA^* may not exist

Table 9.3 Experimental Examples of Triplet-Triplet Energy Transfer

Entry	Donor	Acceptor	Solvent	k_{diff} (calc)	k_{ET}	k_{-ET}	$\Delta E(D\text{-}A)^a$	Ref.
(1)	Triphenylene	Naphthalene	n-hexane	$\sim 10^{10}$	2×10^9	—	−6	b
(2)	Naphthalene	Triphenylene	n-hexane	$\sim 10^{10}$	—	$<10^4$	+6	b
(3)	Naphthalene	Biacetyl	benzene	$\sim 10^{10}$	9×10^9	—	−5	c
(4)	Biacetyl	Naphthalene	benzene	$\sim 10^{10}$	—	2×10^6	+5	c
(5)	1-Bromonaphthalene	Biacetyl	benzene	$\sim 10^{10}$	3×10^9	—	−3	c
(6)	Biacetyl	1-Bromonaphthalene	benzene	$\sim 10^{10}$	—	3×10^7	+3	c
(7)	Benzophenone	Naphthalene	benzene	$\sim 10^{10}$	1×10^{10}	—	−8	b
(8)	Naphthalene	Benzophenone	benzene	$\sim 10^{10}$	—	$<10^4$	+8	b
(9)	Acetophenone	Naphthalene	isooctane	$\sim 10^{10}$	1×10^{10}	—	−12	d
(10)	Acetone	1,4-di-Bromonaphthalene	acetonitrile	$\sim 10^{10}$	3×10^9	—	−18	e
(11)	Acetone	Biacetyl	acetonitrile	$\sim 10^{10}$	5×10^9	—	−23	e
(12)	Acetone	Acetone	acetonitrile	$\sim 10^{10}$	10^6	10^6	0	f

[a] Difference in energy between D_1 and A_1. Positive values mean the overall energy transfer is endothermic, i.e., requires thermal energy input. Negative values mean that overall energy transfer is exothermic.

[b] Porter, G., and Wilkinson, F., *Proc. Royal Soc. 264A*, (1966).

[c] Sandros, K., *Acta Chem. Scand.*, *18*, 2355 (1964).

[d] Makemura, T., Baba, H., and Fujita, M., *Bull. Chem. Soc. Japan. 46*, 2625 (1973).

[e] Turro, N. J., Schore, N. E., Steinmetzer, H. C., and Yekta, A., *J. Am. Chem. Soc. 96*, 1936 (1974).

[f] Lechtken, P. and Turro, N. J., *Angew. Chem. Intern. Ed. Eng. 12*, 314 (1973).

as revealed by the state correlation diagram.[21c] Thus, the initial slope of the surface leading toward DA^* will be upward and continue upward until a surface crossing occurs. Activation energies are also expected if activated vibronic interactions are required to make the energy transfer electronically favorable. For instance, one expects that if Franck-Condon factors (spectral overlap) are not favorable vibronic activation may become significant. Finally, steric effects may prevent the required favorable electronic interactions and as a result activation may be necessary.

A steric effect has been observed for triplet-triplet energy transfer involving alkyl azo compounds.[32] The values of E_t for several alkyl azo compounds have been estimated by means of energy transfer experiments, and fall in the range 50–60 kcal mole.[21a] Thus, triplet energy transfer from alkanones ($E_t \gtrsim 75$ kcal mole) or aryl ketones ($E_T \gtrsim 68$ kcal/mole) to alkyl azo compounds is expected to be substantially exothermic.

Quenching of ketone phosphorescence by alkyl azo compounds is found to depend on the structure of the azo compound, and appears to be related to steric hindrance to approach by the donor.[32] For instance, azo-n-butane is a much better quencher of ketone phosphorescence than is azo-tert-butane (see Table 9.4). When phosphorescence emission from an acceptor is not observed, there is no guarantee that the triplet of the azo compound is produced. The observed rate constants for quenching of ketone phosphorescence thereby represents *maximum* values for triplet-triplet energy transfer. As a specific example, the rate constant for quenching of acetone phosphorescence by azo-tert-butane is $\sim 6 \times 10^8\ M^{-1}\ sec^{-1}$ whereas for azo-n-butane as quencher a value of $\sim 3 \times 10^9\ M^{-1}\ sec^{-1}$ is found.

More work is required before the factors which determine when exothermic energy transfer will not occur efficiently are completely understood. It seems likely that electronic factors (orbital symmetry considerations) and Franck-Condon factors (donor-acceptor spectral overlap) will play a role in certain cases.

Table 9.4 Exothermic Triplet-Triplet Energy Transfers which Occur at less than the Diffusional Rate

Donor Triplet	E_T^D	Acceptor	E_T^Q	k_q	Transfer Type	Ref.
$Ph_2C{=}O$	69	n-BA	~55	3×10^9	$n, \pi^* \rightarrow n, \pi^*$	1
$Ph_2C{=}O$	69	t-BA	~55	0.8×10^9	$n, \pi^* \rightarrow n, \pi^*$	1
Triphenylene	67	n-BA	~55	3×10^9	$\pi, \pi^* \rightarrow n, \pi^*$	1
Triphenylene	67	t-BA	~55	0.3×10^9	$\pi, \pi^* \rightarrow n, \pi^*$	1
$(CH_3)_2C{=}O$	78	p-CH_3V	~72	0.5×10^9	$n, \pi^* \rightarrow n, \pi^*$	2
$(CH_3)_2C{=}O$	89	$CH_2{=}CHCN$	~65	0.5×10^9	$n, \pi^* \rightarrow \pi, \pi^*$	2

n-BA = $CH_3CH_2CH_2CH_2N{=}NCH_2CH_2CH_2CH_3$
t-BA = $(CH_3)_3CN{=}NC(CH_3)_3$
p-CH_3V = p-$CH_3C_6H_4COCH_1CH_2CH_2CH_3$

[1] Wamser, C. C. et al. *J. Am. Chem. Soc.* *97*, 4864 (1975).
[2] Unpublished results: Schore, N., and Mirbach, M. Columbia University.

Conclusions from Triplet-Triplet Transfer Experiments in Fluid Solution

The important conclusions derived from studies of triplet-triplet transfer in condensed phases are:

1. If E_T^D, the triplet energy of the donor is greater than E_T^A, the triplet energy of the acceptor, the rate constant for energy transfer from donor to acceptor equals the rate constant for encounters.

2. If E_T^D is similar or equal to E_T^A, the net rate of energy transfer may be less than the encounter rate because of reversible energy transfer (if A possesses a triplet lifetime greater than about 10^{-6} sec).

3. If E_T^D is less than E_T^A by more than several kilocalories per mole, essentially no quenching of donor triplets occurs.

4. There is no evidence for a *decrease* in quenching efficiency as $E_T^D - E_T^A$ increases.

5. The exchange (*collisional*) mechanism operates in triplet-triplet energy transfer.

6. Triplets are formed in high yield when organic molecules are excited in fluid solution at room temperature.

7. The triplet state of A may be produced *without* the intermediacy of the excited singlet state of A.

Triplet-Triplet Energy Transfer in Rigid Solution

Table 9.5 lists some values of R_0 which have been evaluated from experimental data in solid solution at low temperatures, and which follow the Perrin efficiency law.[1b] In addition,[1c] a "formal rate constant" for energy transfer may be calculated from such data, assuming a *linear* relationship (i.e., Stern-Volmer relationship Eq. 9.27), between the rate of energy transfer and $[A]$. The important results

Table 9.5 Triplet-Triplet transfer in rigid media at 77 k*

Donor[a]	E_T[b]	E_S[c]	R_0	Acceptor[a]	E_T[b]	E_S[c]	k_{ET}[d]
Benzophenone	69	74	13	Naphthalene	61	89	2×10^2
Benzaldehyde	72	76	12	Naphthalene	61	89	2×10^2
Carbazole	70	84	15	Naphthalene	61	89	3×10^{-1}
Diphenylamine	72	89	13	Biphenyl	65	97	—

[a] Donor and acceptor concentration about 1.0 M in ethanol and ether solvent. Excitation provided by 3660 Å light.
[b] Energy of lowest triplet level in kcal mole^{-1}
[c] Energy of lowest singlet level in kcal mole^{-1}
[d] Pseudo-unimolecular rate constants (in sec^{-1}) for the rate of excitation transfer.
* Ermolaev, V. L., *Soviet Physics, Doklady*, 6, 600 (1967).

from these data are:

1. The values of R_o are generally less than 15 Å, as expected for an electron exchange mechanism.

2. The "rate constants" for energy transfer are $\sim 10^{10}$ to 10^8 times *slower* than those found for singlet-singlet energy transfer (Table 9.2).

Clearly, triplet-triplet energy transfer under these conditions is short-range in nature and does not occur with a large rate constant for separations greater than 10 Å or so. It is the long lifetime of triplets in rigid media at low temperatures which allow triplet-triplet transfer to be observed at all.

A study of the relationship of the strength of $\varepsilon(S_0 \rightarrow T)$ absorption of the acceptor on the efficiency of quenching donor phosphorescence reveals that triplet-triplet energy transfer is insensitive to this variable.[33] For example, the efficiency of quenching donor phosphorescence showed that there is no difference in the efficiency of transfer in the series naphthalene, 1-chloronaphthalene, 1-bromonaphthalene, and 1-iodonaphthalene as quenchers of biacetyl phosphorescence. It is found that $k_q \sim 5 \times 10^9\ M^{-1}\ sec^{-1}$ for each of these quenchers.[29] However, judging from their radiative phosphorescence lifetimes, $\varepsilon(S_0 \rightarrow T)$ differs by a factor of 1000 for these compounds. These results imply that resonance-excitation transfer is negligible, and that exchange transfer, since it is already fully allowed when the donor and acceptor are nearest neighbors, is unaffected by the $S_0 \rightarrow T_1$ transition probability of the acceptor.

Intramolecular Triplet-Triplet Energy Transfer[34]

Many examples of intramolecular triplet-triplet energy transfer have been reported. For example, the benzoyl (donor)-naphthyl (acceptor) system (**7**) (Fig. 9.23) shows only naphthalene-like phosphorescence when the benzoyl group is selectively excited with 350 nm light.[35] Control experiments indicate that the energy transfer from the initially excited benzoyl group is entirely *intramolecular* and, since singlet-singlet energy transfer is energetically prohibited, it can be concluded that triplet-triplet energy transfer is the major pathway.

The average separation of the benzoyl and naphthyl groups of **7** is about 7 Å. The Förster R_o for triplet-triplet transfer is calculated to be ~ 0.2 Å. (For such close distances, however, the underlying assumptions of the Förster theory that the molecules may be treated as point dipoles are vitiated.) It appears that either a through-space (electron overlap) or through-bond mechanism is needed to explain the result. From the practical standpoint, intramolecular experiments of this type (all of which lead to the same general conclusion) demonstrate that a nearest-neighbor collision is not *required* for efficient triplet-triplet transfer.

For the steroid **8** (Fig. 9.24), the phosphorescence of the benzophenone group is only partially quenched by the naphthalene group ($\Phi_{rr} \sim 35\%$). In this case, the rate constant for triplet-triplet energy transfer can be estimated by comparing the lifetime of the benzophenone-like phosphorescence of **8** to that of a model compound.[36] The result is that $k_{ET} \sim 25\ sec^{-1}$. The average separation between the benzophenone and naphthyl groups is ~ 15 Å for **8**. We note that this distance

is twice that for separation of donor and acceptor in **7** and that transfer is incomplete for **8**. A rate constant of the order of 25 sec^{-1} is not particularly fast, so that as the donor lifetime decreases, the separation between donor and acceptor will need to be small (i.e., less than about 10 Å) for efficient transfer to occur.

Interestingly[36], in compound **9** (for which the separation of carbazole (donor) and naphthalene (acceptor) is comparable to **8**) the rate of triplet-triplet (~ 0.04 sec^{-1}) energy transfer *is nearly 1000 times slower* than that found for **8** (see Fig. 9.24). This indicates that triplet-triplet transfer is not only distance-dependent but also structure-dependent. This is to be expected on the basis of any detailed Coulombic or exchange mechanism. From these results it appears that $\pi, \pi^* \rightarrow \pi, \pi^*$ triplet-triplet transfer is slower than $n, \pi^* \rightarrow \pi, \pi^*$ triplet-triplet transfer by

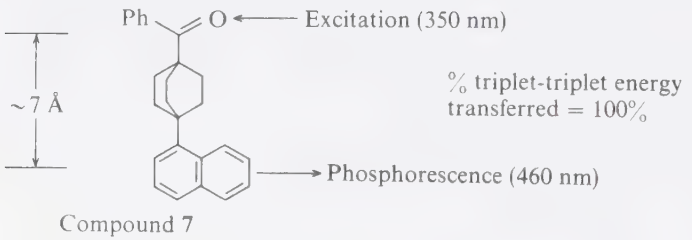

Compound 7

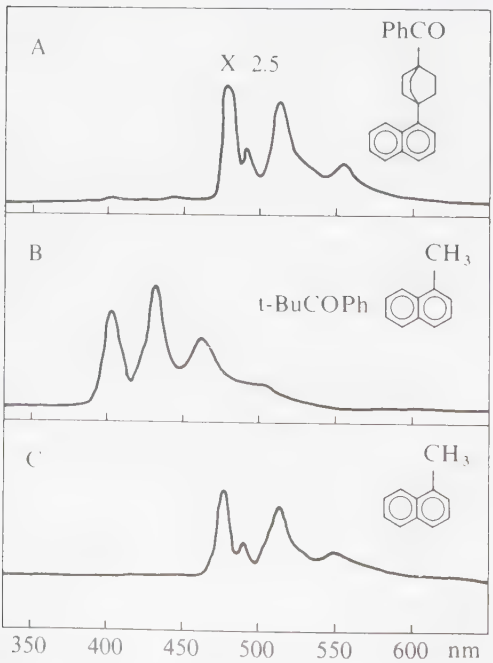

Figure 9.23

Phosphorescence spectra of 1-benzoyl-4-(α-naphthyl)-bicyclo-[2.2.2]octane (A), a mixture of 1-methylnaphthalene and pivalophenone (B), and 1-methylnaphthalene (C). Excitation of A and B is at 350 nm, while C is at 295 nm. Concentrations are 0.001 M.

a factor of about 1000 (for the same donor-acceptor separation). Singlet-singlet transfer rates may also be evaluated from studies of **8** and **9**. In these cases, the naphthyl group is the donor and the benzophenone or carbazole groups are acceptors. The results are that $\pi, \pi^* \rightarrow n, \pi^*$ singlet-singlet energy transfer is about one order of a magnitude slower than $\pi, \pi^* \rightarrow \pi, \pi^*$ singlet-singlet energy transfer for the same distance of separation.

The bisteroid **3** shown in Figure 9.17 was found to undergo singlet-naphthyl to singlet-anthracyl energy transfer with an efficiency accurately predicted by Förster theory. Measurement of the lifetime of the triplet naphthyl moiety of **3** was found to be 0.15 sec, the same value as for methyl-1-naphthoate.[37] It was therefore concluded that 20 Å is greater than the limit for energy transfer from one aromatic π, π^* triplet to another aromatic π, π^* triplet, even if the donor lifetime is of the order of tenths of seconds. The result requires that k_{ET} is less than $\sim 0.7\ \text{sec}^{-1}$, (the value required to reduce the triplet lifetime to about 10% of its initial value).

For molecules containing donor and acceptor groups separated by 1, 2, or 3 methylene groups, complete transfer of triplet excitation from donor to acceptor is observed, even when the molecules are studied in rigid glass solutions at low

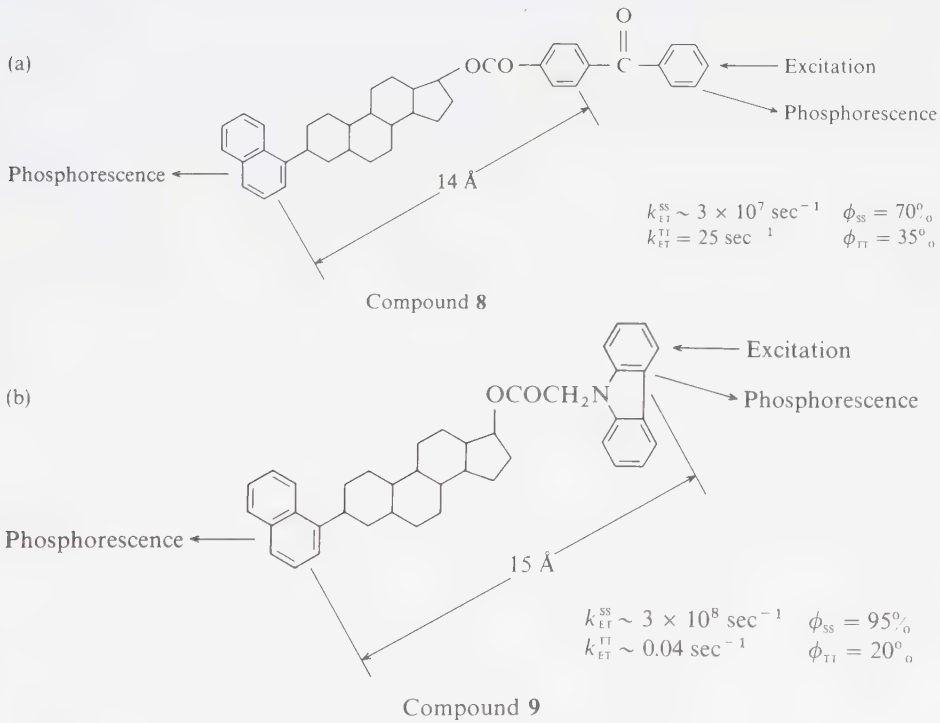

Figure 9.24

(a) Intramolecular singlet-singlet and triplet-triplet energy transfer in a rigid benzophenone-naphthalene donor-acceptor system (upper drawing). (b) Intramolecular singlet-singlet and triplet-triplet energy transfer in a rigid indole-naphthalene donor-acceptor system (lower drawing).

temperatures.[38] For example, for the molecule **10** (Figure 9.25), only the phosphorescence of the naphthalene moiety is observed when the benzophenone is selectively excited with 366 nm light.

From quenching studies[38] involving **10** it was estimated that the rate constant (k_{ET}^{TT}) for intramolecular energy transfer from the benzophenone triplet to the naphthalene triplet (k_{TT}^{TT}) was greater than 10^{10} sec^{-1}. This result should be contrasted with the relatively slow rate constant for singlet-singlet energy transfer ($k_{ET}^{SS} \sim 10^8$ sec^{-1}) from the naphthalene group of **10** to the benzophenone group. Since both energy transfers probably occur via an electron-exchange mechanism and since the distance of separation of the groups is the same for both types of energy transfer, the $n, \pi^* \rightarrow \pi, \pi^*$ triplet-triplet transfer is clearly favored over the $\pi, \pi^* \rightarrow n, \pi^*$ singlet-singlet transfer. This conclusion is consistent with the generally higher reactivity of carbonyl n, π^* states relative to π, π^* states in many comparable photoreactions, and with the result seen earlier for a rigid molecule, **8**. It would be interesting to measure the rate of *intermolecular* quenching of naphthalene singlets by benzophenone in order to check the basis for what may amount to be an unusually low value of k_{TT}^{SS}. This result contrasts with the observation that for **7**, more than 99% singlet-singlet energy transfer from the naphthalene moiety to benzoyl moiety occurs.

9.13 Triplet-Singlet Energy Transfer in Fluid Solution

Energy transfer from a triplet (donor) to a singlet (acceptor) to produce an *excited singlet* is a relatively rare process in fluid solutions. Experimentally, the selective photoexcitation of a triplet donor in the presence of an acceptor is difficult. An interesting means of circumventing this difficulty is available via chemilumines-

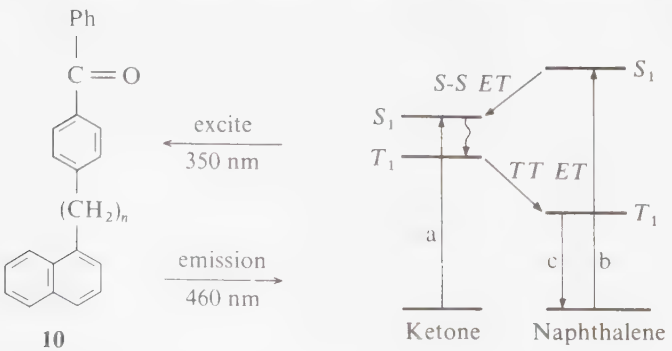

Figure 9.25

Intramolecular energy transfer between benzophenone and naphthalene moieties of **10** Direct excitation of the ketone moiety (a) or of the naphthalene moiety (b) leads to phosphorescent emission (c) from the naphthalene moiety only.

cence techniques.[39] This method employs the *thermal* generation of a triplet donor in the presence of an acceptor. For example, the thermolysis of tetramethyl-1,2-dioxetane yields triplet acetone.[28] This triplet phosphoresces measurably in the absence of acceptors and is capable of participating as a donor in triplet-singlet energy transfer processes.

$$\underset{\text{energy transfer}}{\text{Triplet-singlet}} \quad D^*(T_1) + A(S_0) \rightarrow D(S_0) + A^*(S_1) \tag{9.38}$$

Do triplet-singlet energy transfer processes occur via an exchange mechanism or via a dipole-dipole mechanism? Both processes are spin-forbidden and would therefore be expected to proceed at much slower rates than allowed energy transfers. However, the relatively long lifetime of the triplet state may compensate for a slow rate constant for energy transfer, and as a result the efficiency of triplet-singlet energy transfer may be substantial.

For example, in solid solution (in a solid polymer at room temperature or in a frozen organic solvent), the long-lived (~ 3 sec) phosphorescence of phenanthrene has been found to be quenched by Rhodamine B (a strongly fluorescent dye),[41] and the fluorescent state of the latter is produced, thereby establishing the occurrence of a triplet-singlet energy transfer. The process occurs with a very small rate constant, but is efficient because of the extraordinarily long lifetime of triplet phenanthrene. In this case, a dipole-dipole mechanism for triplet-singlet energy transfer is operating, since calculation of R_0 indicates that energy transfer occurs with 50% efficiency when the donor and acceptor are separated by 50 Å! The rate constant for triplet-singlet energy transfer at this separation is only $\sim 10^{-1}$ sec^{-1}. The rate constant for an *allowed* singlet-singlet dipole-dipole energy transfer would be about 10^7–10^8 sec^{-1} at a donor-acceptor separation of 50 Å.

Triplet-singlet energy transfer from *thermally* produced acetone triplets to appropriate acceptors has been observed.[40] The most effective acceptor known for this process is 9,10-dibromoanthracene. The limiting efficiency of triplet-singlet energy transfer from acetone triplet to 9,10-dibromoanthracene singlet is $\sim 20\%$, and the rate constant for the transfer in acetonitrile is $\sim 1 \times 10^9$ M^{-1} sec^{-1}, i.e., nearly that expected of a diffusion-controlled transfer.[42] An interesting feature of this donor-acceptor system is that triplet-singlet and triplet-triplet energy transfers are competitive. Furthermore, the mechanism of triplet-singlet energy transfer could occur, in principle, either by an exchange or by a dipole-dipole mechanism. A final, intriguing feature of this donor-acceptor pair is the fact that T_2 of 9,10-dibromoanthracene (DBA) is believed[43] to lie above S_1. Thus it is possible that the mechanism of this triplet-singlet energy transfer is T_1 of acetone to T_2 of DBA followed by competitive intersystem crossing of T_2 of DBA to S_1 and internal conversion of T_2 to T_1.

9.14 Singlet-Triplet Energy Transfer

The last, and rarest, of the four "spin types" of electron-energy transfer involves an excited *singlet* donor and ground-state singlet acceptor to produce an excited

triplet acceptor:

$$\text{Singlet-triplet energy transfer} \quad D^*(S_1) + A(S_0) \rightarrow D(S_0) + A^*(T_1) \tag{9.39}$$

An experimental example of this equation involves the fluorescence quenching of anthracene derivatives by the addition of naphthalene. A singlet-to-singlet energy transfer is extremely unlikely in this case because of the much higher singlet energy of naphthalene ($E_1 \simeq 85$) relative to anthracene ($E_1 \cong 72$). Importantly, the fluorescence of anthracenes containing "heavy atoms" was more efficiently quenched than the fluorescence of anthracenes not containing them.

For example, the fluorescence of 9,10-di-n-propyl-9,10-dichloro- and 9,10-dibromoanthracene (in toluene) is quenched by naphthalene at room temperature.[44] It was noted that the value of the rate constant is parallel to the sum of the square of the major spin-orbital coupling terms (assumed to be dominated by the halogen), a result consistent with a singlet-triplet energy transfer mechanism.

In the system 9,10-dicyanonaphthalene (singlet energy donor) and 1,4-disubstituted benzenes (triplet energy acceptors), the formation of the triplet of the acceptor and the quenching of the fluorescence of the donor could be directly monitored, providing strong support for the occurrence of a singlet-triplet energy transfer process.[46]

9.15 Excitation Transfer between Conjugated Chromophores

An interesting situation arises when one chromophore such as a carbonyl group is conjugated with another chromophore such as a benzene or naphthalene nucleus. If one chromophore can be excited selectively, is the excitation localized on the initially excited group, or may it be transferred to the other? From analogy with the intermolecular excitation transfers discussed above we might expect a general rule such as:

> The lowest excited states of a molecule possessing two independently absorbing but formally conjugated chromophores is determined by the chromophore moiety possessing the lowest excitation energy.[47]

In other words, the excitation will be passed on from one excited state to another until the lowest S_1 or T_1 states are reached. Lewis and Calvin proposed a similar theory in which electronic energy can be transferred within a molecule until it reaches a "loose-bolt" group which efficiently dissipates the energy.[48]

The rule given above can be tested by observing the nature of the emission spectrum of a molecule which emits from S_1 to T_1. If the fluorescence and phosphorescence can be shown to be characteristic of a particular group, then the extent of excitation transfer between the absorbing and emitting groups can be evaluated. We might expect that if energy transfer is possible because of the weak inter-

molecular interactions due to the peripheral parts of the electron clouds of different molecules, this process should take place more efficiently between two groups in the same molecule.

As an example, consider intermolecular excitation transfer between triplet levels for a molecule such as 4-phenylbenzophenone.[47] The absorption spectrum of this molecule in ethanol-ether at 77 K shows the long-wavelength absorption band due to an n, π^* excitation. Although the absorption spectrum of benzophenone and its 4-phenyl derivative look very similar, the emission spectrum of the latter compound is completely different in position, lifetime, and structure from the spectrum of benzophenone, and is more similar to the spectrum of biphenyl. The latter compound *must* possess a lowest $T_1(\pi, \pi^*)$ state, so that an intramolecular energy transfer has occurred from the $S_1(n, \pi^*)$ state localized on C=O to the $T_1(\pi, \pi^*)$ state localized on the biphenyl radical. This process is formally analogous to the intermolecular energy transfer between benzophenone and biphenyl. To understand these results let us use Figure 9.26, which is the energy-level diagram for 4-phenylbenzophenone. Excitation in the first absorption

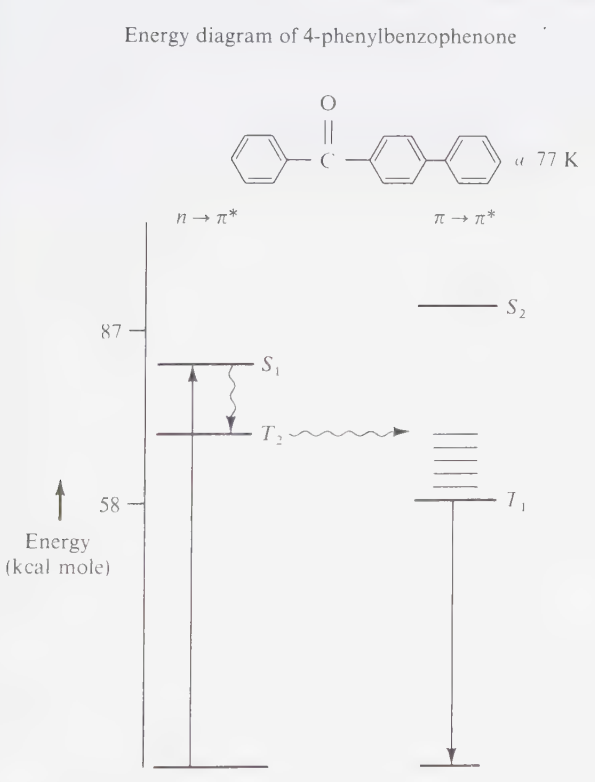

Figure 9.26

The electronic states of 4-phenylbenzophenone which participate in intramolecular energy transfer.

band produces a $S_1(n, \pi^*)$ state which, like benzophenone, undergoes efficient intersystem crossing to $T_2(n, \pi^*)$, since no fluorescence is observed from 4-phenylbenzophenone. This triplet in turn passes by intramolecular excitation transfer to $T_1(\pi, \pi^*)$ of the biphenyl group, which then phosphoresces.

Benzophenone does not phosphoresce from a benzene-like triplet because the lowest triplet of benzene is at 85 kcal mole ^{1} and $T_1(n, \pi^*)$ is at 69 kcal mole ^{1}. On the other hand, the lowest triplet in biphenyl is at 65 kcal mole^{-1}, which makes triplet-triplet excitation transfer energetically favorable.

If we assume that the triplet energies of all of simple carbonyl compounds are about 70 kcal mole^{-1}, then we predict that the attachment of a moiety (radical) whose triplet excitation energy E_t is much greater than 70 kcal mole^{-1} (e.g., alkyl groups and simple aryl groups) will result in a molecule whose lowest S_1 and T_1 are n, π^* states. Attachment of a moiety whose E_t is much lower than 70 kcal mole^{-1} results in intramolecular excitation transfer from the $^3(n, \pi^*)$ state to the triplet of attached group.

Another important point to remember in assigning the lowest triplet levels is that the singlet-triplet splittings of n, π^* states are smaller than those of π, π^* states. As a result,

$$\Delta E_{ST}^{\pi, \pi^*} > \Delta E_{ST}^{n, \pi^*}$$

if the $S_1(\pi, \pi^*)$ state is lowest in a molecule, the $T_1(\pi, \pi^*)$ state must be lowest also. We run into trouble only when the $S_1(n, \pi^*)$ state is lowest, and we need further information before we can make an assignment.

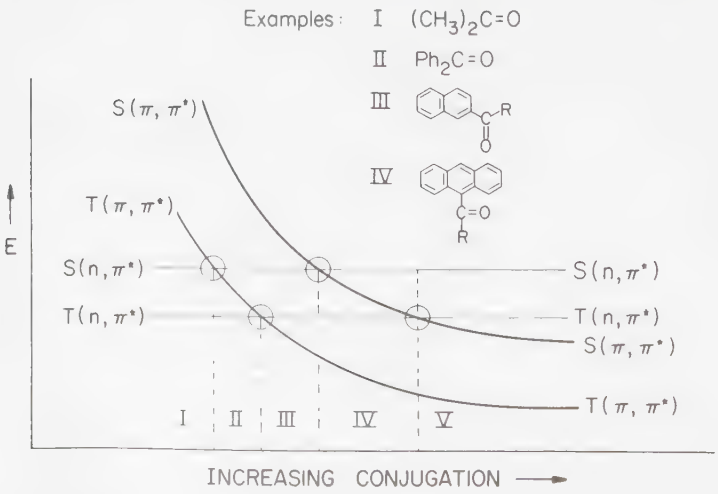

Figure 9.27

Variation of the energies of n, π^* and π, π^* states as a function of increasing conjugation of the π system.

Figure 9.27 shows how the disposition of n, π^* and π, π^* states of ketones varies with conjugation.[49] To a first approximation the energy of the n, π^* states does not change significantly with conjugation. With increasing conjugation the π, π^* states initially fall rapidly in energy, but then more slowly.

9.16 "Multiphoton" Energy Transfer Processes; Triplet-Triplet Annihilation;[50] Delayed Photoluminescence

Usually the concentration of excited states is so small that bimolecular interactions between two excited states are very improbable. For example, the rate of decay of D^* in general is equal to:

$$\text{Rate} = k_D[D^*] + k_q[D^*]^2 \tag{9.40}$$

where k_q is the rate of quenching of D^* by its interactions with another excited state, and k_D is the inherent unimolecular decay rate of D^*. If D^* possesses a very long lifetime and if k_q is large, it becomes feasible for bimolecular D^*-D^* quenching to occur. The most common example of this phenomena is the interaction of two triplet states. Under certain conditions two long-lived triplets D_T may collide with one another in solution and "annihilate" each other, simultaneously producing one molecule in the excited singlet state D_{S_1} and the other in a ground state D_{S_0}.

$$D_T + D_T \rightarrow D_{S_1} + D_{S_0} \tag{9.41}$$

$$D_{S_1} \rightarrow D_{S_0} + h\nu \tag{9.42}$$

The fluorescence emission of D_{S_1} then may be observed, but with a lifetime similar to that of the triplet because excitation has resided temporarily in D_T. The yield of this "delayed" fluorescence, since it results from a two-photon process, will depend upon the square of the intensity of the exciting light if T-T annihilation is rate-determining. This process is clearly different from the thermally activated "delayed" fluorescence which may occur, if the lowest singlet and triplet are so close in energy that thermal activation will occasionally promote triplets up to S_1, from which they fluoresce.

The rate constants of T-T annihilation are generally close to that for diffusion (Table 9.6). As a result, for very long-lived triplets in inert solvents, T-T annihilation may determine triplet lifetimes. For example, if $k_D = 10^2\ \text{sec}^{-1}$ then for $k_q^{TT}[T_1]$ to equal $10^2\ \text{sec}^{-1}$, the steady-state concentration of $[T_1]$ must equal $\sim 10^{-4}$ M. Such concentrations are readily achieved with routinely available sources of light.

The triplet-triplet annihilation mechanism requires that part of the energy from two separately absorbed photons be transferred to the same molecule. Energy

Table 9.6 Values of the Rate Constants for Triplet-Triplet Annihilation[a]

Annihilating Triplets	Solvent	$k_{TT}(M^{-1}\,sec^{-1})$	k_{DH}
Anthracene	n-hexane	1.6×10^{10}	$\sim 1 \times 10^{10}$
Naphthalene	n-hexane	2.1×10^{9}	$\sim 1 \times 10^{10}$
Biacetyl	benzene	$\sim 1 \times 10^{10}$	$\sim 1 \times 10^{10}$
Benzophenone	freon	2×10^{10}	2×10^{10}

[a] Data from Yekta, A., and Turro, N. J., *Molec. Photochem.*, *3*, 307 (1972).

transfer from donor triplets may therefore be used to produce acceptor triplets which, upon annihilation, will produce an excited singlet capable of emitting a photon of higher frequency (greater energy) than the absorbed light. The requirements for such a phenomenon are met if the donor has a S_1 state which lies below that of the acceptor but a T_1 state which lies above that of the acceptor.[35] The phenanthrene-naphthalene system fulfills this requirement, and the energy diagram for this system is shown in Figure 9.28.

The mechanism of sensitized naphthalene fluorescence is given by the following scheme:

$$P_0 \xrightarrow{3500\ \text{Å}} P_1 \rightsquigarrow P_3 \tag{9.43}$$

$$P_3 + N_0 \longrightarrow N_3 + P_0 \tag{9.44}$$

$$2N_3 \longrightarrow N_1 + N_0 \tag{9.45}$$

$$N_1 \longrightarrow N_0 + h\nu(3250\ \text{Å}) \tag{9.46}$$

where P and N refer to phenanthrene and naphthalene, and the subscripts 0, 1, and 3 refer to ground, lowest singlet, and triplet states, respectively. The quantum yield for delayed emission is about 1%, but an excess of about 6 kcal $mole^{-1}$ greater than that of the exciting light is produced.

9.17 Energy Transfer from Upper Excited States

Usually internal conversion from upper excited states ($S_3 \rightarrow S_2 \rightarrow S_1$ and $T_3 \rightarrow T_2 \rightarrow T_1$) occurs so fast ($\sim 10^{11}$–$10^{12}$ sec^{-1}) that bimolecular processes from S_3, S_2, T_3, T_2, etc., cannot compete. In certain cases, however, energy transfer from upper levels has been demonstrated.[51,52] For example, the $T_2 - T_1$ energy gap of anthracenes is sufficiently large (~ 30 kcal mole) so that Franck-Condon factors slow down the rate of T_2 to T_1 internal conversion to the point that energy transfer from T_2 can occur.

Evidence has been presented for energy transfer from T_2 of anthracenes.[52] The techniques employed to detect energy transfer from T_2 of anthracenes exemplify many of the general concepts that might be employed in any study which attempts to detect the involvement of an upper excited state in a reaction mechanism. It was found[52] that DBA is a photosensitizer of the rearrangement of norbornadiene to quadricyclene:

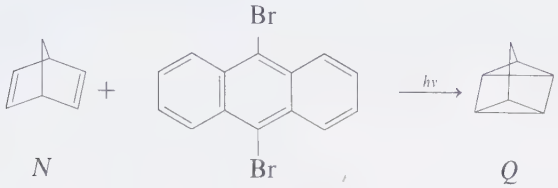

N DBA (Photosensitizer) from T_2 Q (9.47)

Since excitation of S_1 of DBA was employed, there are three candidates for the photosensitizing state: S_1, T_2, and T_1. The involvement of S_1 was ruled out by the observation that the fluorescence of DBA is not quenched by norbornadiene. The involvement of T_1 was ruled out by the observation that selective excitation of T_1 of DBA (via a specific energy transfer) did not result in photosensitized isomerization. From these data, only T_2 is left as a candidate for the photosensitizing state. A plot of 1 Φ versus 1 [norbornadiene], where Φ is the quantum yield of sensitized reaction, yields a straight line of intercept = 1.0 and slope =

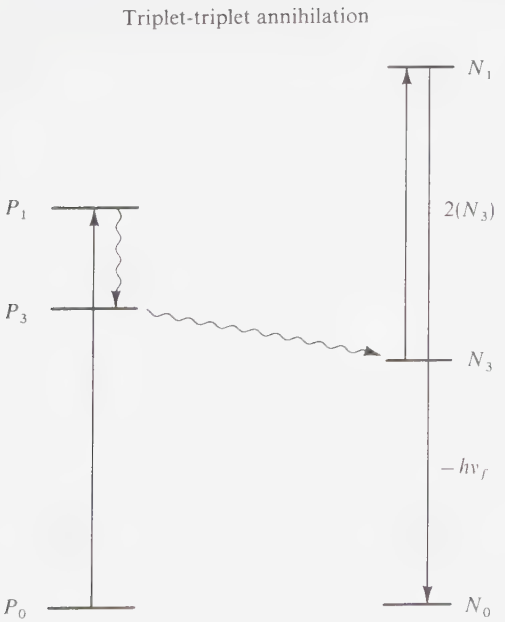

Figure 9.28
Energy diagram for triplet-triplet energy transfer from phenanthrene to naphthalene, then triplet-triplet annihilation by naphthalene, followed by fluorescence.

2.4 M^{-1}.[52c] Recall from Chapter 8 that in a Stern-Volmer analysis the ratio intercept/slope equals $k_q\tau$, where in this case k_q is the rate constant for quenching of T_2 and τ is the lifetime of T_2. The minimum lifetime of T_2 can be derived from the Stern-Volmer data, i.e., let k_q be maximal; then τ must be minimal. Assuming diffusional quenching, the largest value of k_q is $\sim 1 \times 10^{10}$ M^{-1} sec^{-1} for the solvent employed. Thus, $\tau \geq 2.4 \times 10^{-10}$ sec.

The conclusions from these indirect measurements have been confirmed[53] by the observation of $T_2 \rightarrow T_1$ *fluorescence* for DBA.[38] Since $T_1 \rightarrow S_0$ phosphorescence is also now measurable for DBA, it is possible to directly test the proposed mechanism.

9.18 Nonvertical Energy Transfer[54]

Occasionally energy transfer may occur between a donor and acceptor even though the acceptor does not possess a spectroscopically observable electronic state with a lower energy than D^*. In such cases the equilibrated excited state A^* may possess a very different nuclear geometry than A. As a result, spectroscopic observation of the transition $A \rightarrow A^*$ (equilibrium) may not be possible because the Franck-Condon principle inhibits radiative transitions that involve large changes in nuclear geometry. Nonetheless, the equilibrated state exists and may be populated by energy transfer if certain conditions are met.

First let us consider an example of "vertical" energy transfer and then contrast this with an example of "nonvertical" energy transfer. We shall then indicate a theoretical rationale of the latter process.

The rate constant for energy transfer (k_{ET}) from a variety of triplet donors to biacetyl (Eq. 9.48) follow the expressions:[55]

$$^3D + CH_3COCOCH_3 \rightarrow D + {}^3[CH_3COCOCH_3] \tag{9.48}$$

$$k_{ET} = k_{DIF} \quad \text{if} \quad \Delta E_{DA} > 0 \tag{9.49}$$

$$k_{ET} = k_{DIF} \exp(-\Delta E_{DA}/RT) \quad \text{if} \quad \Delta E_{DA} < 0 \tag{9.50}$$

where k_{DIF} is the rate constant for diffusion and ΔE_{DA} is the energy difference between the donor triplet and biacetyl. $\Delta E_{DA} > 0$ corresponds to *exothermic* energy transfer and $\Delta E < 0$ corresponds to *endothermic* energy transfer. The important point derived from these studies is that the rate constant for energy transfer decreases exponentially as the energy transfer becomes endothermic *if* the spectroscopic triplet energies are used to determine the reaction endothermicity.[28,29,55]

If the sensitizer triplet has insufficient energy to promote an acceptor to its triplets via an "allowed" energy transfer, one expects that the *energy* deficiency would be supplied as activation energy. The decrease in k_{ET} as a function of the

endothermicity would then be given by[29]

$$\frac{\Delta \log k}{\Delta E} = -1/(2.3RT) \tag{9.51}$$

The line of this equation is superimposed on the curve for endothermic energy transfer from triplet donors to biacetyl. Since the slope of the falloff of k_{ET} follows the equation precisely, we need not postulate any activation energy beyond that required for diffusion and the endothermicity of energy transfer. Since the energies of the spectroscopic or "vertical" excited states serve as a reliable guide to the rate constants for energy transfer, we may conclude that a "vertical" energy transfer from triplet donor to biacetyl is occurring. In other words, biacetyl accepts energy via a vertical $S_0 \rightarrow T_1$ transition.

Now consider the situation for trans- and cis-stilbenes as quenchers. If the log of the rate constants for quenching of a number of sensitizers is plotted against donor triplet energy, the falloff of k_q with transfer endothermicity is exponential for trans-stilbene ($S_0 \rightarrow T_1$ spectroscopic energy gap equal to 48 kcal/mole) but not for cis-stilbene.[56] For the latter compound, the measured k_q is *larger* than that expected from the transfer endothermicity based on the *spectroscopic* $S_0 \rightarrow T_1$ gap (57 kcal/mole) for cis-stilbene. That an energy transfer is occurring is demonstrated by the observation of cis-trans isomerization of the stilbenes. A comparison of the results of steady-state and quenching experiments leads to a correlation of the values of k_q for different donors and the quantum yields for cis-trans isomerizations.

From these data it is found that when the donor energy is 5 kcal/mole (i.e., ~43 kcal/mole) below the spectroscopic triplet energy of trans-stilbene $k_q \sim 10^5\ M^{-1}\ sec^{-1}$ but for the same transfer endothermicity (based on spectroscopic energies) for cis-stilbene $k_q \sim 1 \times 10^9\ M^{-1}\ sec^{-1}$, i.e., still close to the diffusional limit. The data for trans-stilbene is unexceptional since the falloff in k_q is expected from simple energetic considerations.

However, the data for cis-stilbene requires some special explanations. Because of the correlation of photostationary cis-trans isomerization compositions and k_q values, it is evident that donor quenching results in cis-trans isomerization. If we postulate that cis-trans isomerization occurs via population of stilbene triplets, an explanation of the contrasting behavior of trans- and cis-stilbenes as quenchers is available. The ground state and lowest triplet surfaces of stilbene are expected to be nearly isoenergetic at the 90 twisted geometry. As one twists about *triplet* cis-stilbene the energy of the system *decreases* faster than for an equivalent amount of twist of trans-stilbene. The basis of this postulate is the expectation that the steric interactions in cis-stilbene will cause a "torque" to be mutually exerted by the phenyl groups on one another, thereby facilitating the twisting mode in the cis molecule relative to the trans. Chemical interactions of the excited donor and cis-stilbene may also facilitate excitation stilbene i.e., an exciplex may be formed. The exciplex may now lower its energy by continuing the twisting motion and moving down the surface. The excitation energy has now become essentially

localized on the stilbene moiety. If the exciplex dissociates, then a twisted stilbene triplet will be produced. Evidently, trans-stilbene does not undergo as rapid a falloff in energy as a function of twist about the carbon-carbon bond. As a result, nonvertical transitions are less likely to occur during a collision complex, and the energy of a donor trans-stilbene exciplex is not expected to fall off rapidly as a function of twist.

An extreme situation for nonvertical energy transfer would correspond to full bond formation between donor and acceptor. This would be followed by changes in the acceptor nuclear configuration and fragmentation of the intermediate to produce a ground state donor and an acceptor which finds itself on one of its excited state surfaces far removed from its spectroscopic or vertical geometry.[57]

A generalized profile of nonvertical energy transfer which shows its possible connection with *reaction* between donor and acceptor and *quenching* without energy transfer is shown in Figure 9.29. We imagine that for some reaction coordinates a crossing occurs between the DA^* and D^*A surfaces. At the critical geometry of A the energy of $DA^* > D^*A$. As the nuclear geometry changes, a surface crossing occurs and the energy of DA^* becomes lower than that for D^*A. We may note that if a minimum in the D^*A surface occurs *before* the crossing, an exciplex is formed and may provide a channel for emission or radiationless deactivation. After the crossing point has been passed, excitation is localized mainly on A^*. Pathways may now exist for reactions of A^* or deactivation back to $D + A$.

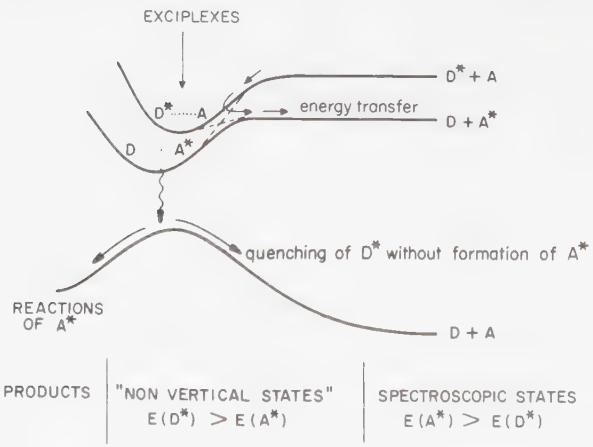

Figure 9.29

Qualitative description of nonvertical energy transfer. At large separations of D and A the surfaces which can be reached by vertical jumps are the spectroscopic states of the system. If the $D + A^*$ and $D^* + A$ surfaces cross for certain nuclear geometry changes, the minimum for $D + A^*$ species (excitation mainly associated with A^*) may drop below that of $D^* + A$.

9.19 Reversible Energy Transfer[29]

In principle, all energy transfer processes are reversible. In practice, the extent of reversibility depends on several factors, the most important of which are (a) the electronic energy gap between the donor and acceptor states participating in energy transfer, and (b) the lifetimes of the donor and acceptor states participating in energy transfer. In a reversible energy transfer, the concept of donor and acceptor depends upon the direction of the energy transfer. For clarity we shall define the donor as the initially excited partner.

Let us consider the following kinetic scheme:[13,29]

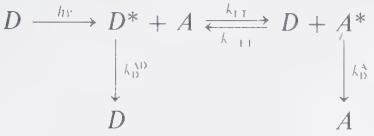

(9.52)

It can be seen that energy transfer in the direction $D^* \rightarrow A^*$ will become irreversible when $k_{ET}[D^*][A] \gg k_{-ET}[D][A^*]$ *or* $k_D^A[A^*] \gg k_{-ET}[D][A^*]$.

The *observed* rate constant, k_{ET}^{OB}, for energy transfer in the direction $D^* \rightarrow A^*$ may not be equal to the true rate constant k_{ET} when reversibility is significant. In general, the observed rate constant k_{ET}^{OB} will be *smaller* than k_{ET} by a factor equal to the efficiency of irreversible energy transfer, i.e.,

$$k_{ET}^{OB} = k_{ET}\Phi_{ET} = k_{ET}\frac{k_D^A}{k_D^A + k_{-ET}[D]} \tag{9.53}$$

where Φ_{ET} is the probability that an excited A^* will *not* transfer its energy back to D. According to the assumed scheme, this quantity depends on the ratio of rates $k_D^A[A^*]/(k_D^A[A^*] + k_{-ET}[D][A^*])$ or more simply $k_D^A/(k_D^A + k_{-ET}[D])$.

From the expression for k_{ET}^{OB} we see that the important parameters which determine whether reversibility is important or not are:

1. The magnitude of k_D^A
2. The magnitude of k_{-ET}
3. The value of $[D]$.

Experimentally, a simple test of reversibility is to study the effect of $[D]$ on k_{ET}^{OB}, i.e., if the observed rate constant for energy transfer *decreases* as $[D]$ *increases*, reversible energy transfer is indicated.

As an example of reversible energy transfer we shall consider the quenching of biacetyl phosphorescence by various quenchers. The rate of decay of biacetyl phosphorescence at room temperature in benzene solvent was measured as a function of the concentration of quencher. The observed quenching was found to

follow the relation:[40,41]

$$k_D = k_D^0 + k_q^{OB}[A] \tag{9.54}$$

where k_D is the measured decay rate of phosphorescence in the presence of acceptor at concentration equal to $[A]$, and k_D^0 is the measured decay rate of phosphorescence of biacetyl in the absence of acceptor. The slope of a plot of k_D versus $[A]$ yields k_q^{OB}.

From Table 9.7 it can be seen that the effectiveness of an energy transfer quencher is determined mainly by the position of its lowest triplet level and not by its molecular structure. This result and the fact that biacetyl fluorescence is negligibly affected by those quenchers which have an S_1 state at higher energy than biacetyl, demand that quenching involves only the triplet states of biacetyl and quencher. Furthermore, the strongest quenchers (E_T less than 50 kcal mole^{-1}) have nearly the same value of k_q^{OB} which in turn is close to that estimated from the Debye equation (Eq. 9.29) which yields $k_q = 1 \times 10^{10}$ liter mole^{-1} sec^{-1} for bimolecular diffusion in benzene solution at 25° C.

For quenchers with triplet levels higher than 55 kcal mole^{-1} there is a general trend toward a lowering of k_q^{OB} with increasing E_T. The scatter of the data observed for quenchers whose triplet energies are close to that of biacetyl is due to reversible energy transfer. This result is to be expected since at 20° C about one molecule in 100 will possess about 3 kcal mole^{-1} excess vibrational energy, so that coupled transitions between donor and acceptor (of slightly greater energy) may occur with reasonable probability. It may also be possible for transfer to be reversed if, during its lifetime, the triplet quencher molecule should encounter a ground-state biacetyl molecule. Reversible transfer, for quenchers with triplet levels slightly below or above that of biacetyl, is expected to be enhanced as the concentration

Table 9.7 Quenching Constant and E_T Values for Quenching of Biacetyl Phosphorescence in Benzene Solution at 20°C.*

Quencher	E_T	k_q (corrected)[a]	k_q^{OB} (observed)[b]
Phenanthrene	62	2×10^3	
Naphthalene	61	2×10^6	1×10^{10}
Nitrobenzene	61	1×10^4	—
2-Iodonaphthalene	60	6×10^6	—
1-Chloronaphthalene	59	3×10^7	4×10^9
1-Bromonaphthalene	59	3×10^7	3×10^9
1-Iodonaphthalene	59	3×10^7	—
2,2′-Dinaphthyl	56	3×10^9	1×10^9
Fluoranthene	54	5×10^9	2×10^7
1,2-Benzpyrene	54	6×10^9	5×10^7
Pyrene	49	8×10^9	2×10^2
Anthracene	42	8×10^9	—
Oxygen	23	$\sim 8 \times 10^9$	—

* Data from Reference 29.
[a] Quenching constant corrected for reversible energy transfer.
[b] Quenching constant directly from Stern-Volmer analysis.

of biacetyl increases—i.e., k_q^{OB} will decrease with increasing biacetyl concentration. This has been confirmed experimentally.[29]

Naphthalene and 1-iodonaphthalene (whose oscillator strengths for singlet-triplet absorption differ by a factor of 1000) are equally effective at quenching the phosphorescence of benzophenone in rigid solution at 77 K.[33] In this case the donor possesses a higher E_T than the quencher. A similar result was found for the quenching of biacetyl phosphorescence by naphthalene and iodonaphthalene in fluid solution when reversible energy transfer is taken into account.[29] It can be seen from Table 9.7 and in the next section that energy transfer from naphthalene to biacetyl occurs at a diffusion-controlled rate. If reverse transfer is ignored, k_q^{OB} is $4 \times 10^3\ M^{-1}\ sec^{-1}$ for energy transfer from biacetyl to naphthalene —lower than the true rate constant k_q by three orders of magnitude. On the other hand, 1- and 2-iodo-naphthalene possess such short triplet lifetimes that reverse transfer is negligible and no correction of k_q^{OB} is necessary. The results with biacetyl serve as further support of the generalization that (a) the exchange mechanism only operates when the partners involved in the energy transfer process collide, and (b) factors such as the oscillator strength of the $S_0 \rightarrow T_1$ transition of the acceptor are not important, even when the E_T of D^* lies below that of the acceptor.

9.20 Photosensitization and Quenching in Organic Photochemistry

Photosensitization and quenching play an important role in many aspects of organic photochemistry.[2,27] From the discussion given in this chapter, photosensitization and quenching processes which involve energy transfer of the type $D^* + A \rightarrow D + A^*$ may be used to control photochemical sequences and to study reaction mechanisms.[58]

For example, singlet-singlet and triplet-triplet energy transfer may be used to indirectly populate A^* states or to quench D^* states. Of special importance is triplet-triplet energy transfer, because the *quenching* of D_T^* by energy transfer often limits its lifetime. For example, a unimolecular typical triplet lifetime in a non-reactive organic solvent is $\sim 10^{-4}$ sec. This corresponds to a unimolecular decay rate constant, k_D, of $10^4\ sec^{-1}$. The *actual* rate constant of decay of the triplet is given by:

$$k_D^{OB} = \text{rate constant decay of } D_T^* = \underbrace{k_D}_{\text{True 1st order}} + \underbrace{k_q[Q]}_{\text{Pseudo 1st order}} \tag{9.55}$$

If $k_q = 10^{10}\ M^{-1}\ sec^{-1}$, then for $[Q] = 10^{-6}$ M, 50% of D_T^* molecules will be quenched by Q. Since exothermic energy-transfer rate constants, k_{ET}, are of the order of 10^9-$10^{10}\ M^{-1}\ sec^{-1}$, it is clear that very small amounts of impurities (which may serve as exothermic energy-transfer quenchers) can limit the lifetime of D_T^*.

On the other hand, numerous compounds possess inefficient intersystem crossing yields, so that T_1 is not easily produced by *direct* photoexcitation. Triplet-triplet energy transfer may allow for the efficient *indirect* production of such triplets. A *triplet photosensitizer* is one capable of transferring its triplet excitation to an acceptor.

Judicious selection of triplet photosensitizers is required in many specific cases in order to avoid the complications of singlet quenching of D_1^*, photoreactions of D_1^*, direct excitation of A_1^*, etc. An "*ideal*" triplet photosensitizer would possess the following characteristics:

1. A fast rate of intersystem crossing relative to other deactivation of S_1 (i.e., $k_{ST} \gg k_F$ so that $\phi_{ST} \sim 1.0$).

2. A high triplet energy, E_T, which would allow energy transfer to be exothermic with respect to a broad range of acceptors.

3. A long triplet lifetime, τ_T, in order to maximize the efficiency of the energy-transfer process (i.e., $k_{ET}[A] \gg k_T$ at accessible contractions of A).

4. A substantial absorption in a region of the spectrum where A does not significantly absorb.

5. A low chemical reactivity in order to avoid photochemical reactions with A.

Table 9.8 Important Parameters for Triplet Photosensitizers[a]

Compound	E_S	E_T	τ_S[b]	τ_T[b]	conf. T_1	Φ_{ST}
	kcal/mole		sec			
Benzene	110	84	$\sim 10^{-7}$	10^{-6}	π, π^*	0.2
Acetone	~85	~78	10^{-9}	10^{-5}	n, π^*	1.0
Xanthone		74	—	—	π, π^*	1.0
Acetophenone	~79	74	10^{-10}	10^{-4}	n, π^*	1.0
4-CF_3-Acetophenone		71	—		n, π^*	1.0
Benzophenone	~75	69	10^{-11}	10^{-4}	n, π^*	1.0
Triphenylene	83	67	$\sim 5 \times 10^{-8}$	10^{-4}	π, π^*	0.9
Thioxanthone	78	~65	—	—		—
Anthraquinone	—	62	-	—	n, π^*	1.0
4-Ph-benzophenone	77	61	—	10^{-4}	π, π^*	1.0
Michler's ketone	—	61	—	—	—	1.0
Naphthalene	92	61	10^{-7}	10^{-4}	π, π^*	0.7
2-Acetonaphthalene	78	59	—	10^{-4}	π, π^*	1.0
1-Acetonaphthalene	76	57	—	10^{-4}	π, π^*	1.0
Chrysene	79	57	5×10^{-8}	—	π, π^*	0.8
Biacetyl	~60	55	10^{-8}	10^{-3}	n, π^*	1.0
Benzil	~59	54	$\sim 10^{-8}$	10^{-4}	n, π^*	1.0
Camphorquinone	~55	50	$\sim 10^{-8}$	—	n, π^*	1.0
Pyrene	77	49	$\sim 10^{-6}$	—	π, π^*	0.3
Anthracene	76	47	$\sim 5 \times 10^{-9}$	10^{-4}	π, π^*	0.7
9,10-Dichloroanthracene	~74	40	$\sim 5 \times 10^{-9}$	10^{-4}	π, π^*	0.5
Perylene	66	~35	5×10^{-9}	-	π, π^*	0.005

[a] Data gathered from Birks, J., *Photophysics of Aromatic Molecules*, New York: John Wiley, 1970; and Wilkinson, F. *Organic Molecular Photophysics*, ed. J. Birks., New York: John Wiley, 1975, p. 95.
[b] *Maximum* lifetime for "inert" solvents. Order of magnitude only.

There is no "ideal" photosensitizer in a general sense. However, the rational choice of a photosensitizer can be made by examining the above characteristics for potential candidates. The most important single parameter in the selection of a triplet photosensitizer is the energy gap between D_T^* and A_T^*, since only if the energy transfer is exothermic can it possess a maximal value of k_{ET}. Thus, knowledge of $E_T(D^*)$ and $E_T(A^*)$ is of crucial importance in the selection of a triplet photosensitizer.

A list of triplet energies E_T (energy of the 0-0 transition, $T_1 \rightarrow S_0$) of selected compounds is given in Table 9.8, which also tabulates the configuration of T_1, singlet energies (E_S) and approximate experimental singlet and triplet lifetimes (τ_S and τ_T respectively). The values of E_S and E_T are usually only slightly solvent-dependent (± 1–2 kcal/mole). The tabulated data refer to *nonpolar*, chemically "inert," "oxygen-free" solvents. (The quotes refer to the relative nature of inertness and oxygen content.) In addition to the data given in Table 9.8 which allows one to rationally select a triplet sensitizer and appropriate concentration of quencher, the extinction coefficients of sensitizer become crucial if the quencher absorbs in the same region that the sensitizer absorbs.

In contrast to the desirability that τ_T be as long as possible for a triplet sensitizer, a desirable triplet *quencher* should have a very short lifetime and still be "chemically inert" to net reaction. The short lifetime is desirable to avoid participation of the triplet quencher (produced by energy transfer) in subsequent photoreactions. Table 9.9 lists some commonly employed "triplet" quenchers which are *not* acceptable as triplet photosensitizers (e.g., because of their poor absorption characteristics or short lifetimes). Of course, the compounds listed in Table 9.8 are potential triplet quenchers also. Other relevant data for energy transfer are listed in Tables 8.6–8.9.

Ketones often possess the best compromise of desirable characteristics of a triplet photosensitizer. For example, acetophenone possesses a relatively high triplet energy (~ 72 kcal/mole), a long inherent unimolecular lifetime (~ 100 μs),

Table 9.9 Energies of Some Common Triplet Quenchers*

Compound	E_S	E_T
$CH_3CH{=}CHCH_3$	~120	78
$PhC{\equiv}CH$	~100	72
Ph—Ph	~95	66
Ph—Ph—Ph (ortho-terphenyl)	~90	62
$CH_2{=}CH{-}CH{=}CH_2$	~90	60
$CH_3{-}CH{=}CH{-}CH{=}CH_2$	~90	59
Ph—Ph—Ph (para-terphenyl)	~105	58
Cyclopentadiene	~90	58
Cis-stilbene	~95	57
1,3-cyclohexadiene	~80	53
Trans-stilbene	~90	50
Azulene	~40	~30
Tetracene	~45	~29
Oxygen	—	23

* Data from Murov, S. L., *Handbook of Photochemistry*, New York: Dekker, 1973.

a high value of $\Phi_{s1}(\sim 1.0)$, and a short singlet lifetime. It has the disadvantages of not possessing a high absorption maximum ($\varepsilon_{max} \sim 100$) and of possessing a relatively reactive $T_1(n, \pi^*)$ state.

By use of the "energy sink" theorem (Section 9.15), the energy of T_1 may be predicted from the data in Tables 9.8 and 9.9. The procedure is simply to identify the various chromophores of a molecule and then check the table to determine the value of E_t for the closest analogue. The energy of T_1 will usually be within a few kcal/mole of the lowest-energy analogue.

9.21 Quenching by Molecular Oxygen

Molecular oxygen is a ground-state triplet (termed $^3\Sigma$ oxygen) possessing two very low-lying single states (termed $^1\Delta$ oxygen and $^1\Sigma$ oxygen), whose excitation energies are ~ 23 kcal/mole and ~ 38 kcal/mole, respectively. Thus, sensitizers possessing excitation energies as low as 23 kcal/mole may be quenched via energy transfer to produce $^1\Delta$ oxygen (Eq. 9.56). In addition, $^3\Sigma$ oxygen is a reactive species in its own right and tends to add to excited states or abstract an electron from an excited state. These processes may result in net quenching, reaction, or energy transfer.

$$\text{sens}^* + {}^3O_2({}^3\Sigma) \rightarrow \text{sens} + {}^1O_2({}^1\Delta) \tag{9.56}$$

Experimentally, both singlet[59] and triplet[60] states are quenched effectively by $^3O_2$. The mechanisms of these processes are discussed in Section 14.2. We point out here that the ubiquitous nature of $^3O_2$ as an effective "impurity" requires the suspicion that a pseudo-unimolecular quenching term, $k_q[O_2]$, may contribute to the pseudo-unimolecular decay of any excited state that possesses a fairly long lifetime. For example, if $k_q \sim 10^{10}\ M^{-1}\ sec^{-1}$ for $D^* + {}^3O_2 \rightarrow$ quench, then a concentration of $\sim 10^{-7}$ M of $^3O_2$ will *limit* the lifetime of D^* to $1/k_q[O_2] \sim 10^{-3}$ sec. At one atmosphere of air pressure, the concentration of $^3O_2$ in typical organic solvents is $\sim 10^{-3}$–10^{-4} M. Thus, if $k_q \sim 10^{10}\ M^{-1}\ sec^{-1}$, the lifetime of D^* cannot be longer than $\sim 10^{-7}$–10^{-6} sec in air-saturated solutions.

9.22 Energy Hopping or Energy Migration[7]

There are three distinct "mechanical" possibilities for energy to be transferred from one position in space (say, localized on a molecule D^*) to a different position in space (say, to a second molecule, A):

1. The relative diffusion of D^* and A through space (or through a solvent environment).

2. Long-range interactions of D^* and A not involving diffusional motions of either.

3. Translational movement of electronic excitation through space, in which the environment (the solvent molecules M) serves as an energy conductor.

We have discussed numerous examples of mechanisms 1 and 2 in this chapter. We now consider examples of mechanism 3, a process which is termed *energy migration* or *energy hopping.*

Excitons[61]

Complete localization of excitation on one particle in a system of identical particles is impossible in principle because such a situation does not constitute a stationary state of the system, i.e., there will always be a finite probability that the excitation will "hop" from one particle to another. In effect, identical particles with equal levels of electronic excitation perturb each other to a finite extent. This perturbation causes "energy hopping" from one particle to another and, in effect, an energy quantum is set in motion. The migrating quantum of electronic energy has been compared to a migrating particle and is termed an *exciton.*[61]

Imagine a situation in which an electronically excited solvent is capable of radiationlessly transferring its excitation energy to a ground-state solvent molecule. This process can continue and the electronic excitation can "hop" or migrate through the solvent until it is quenched by some unimolecular or bimolecular deactivation process. The situation is depicted schematically in Figure 9.30 for a short-range mechanism. Step 1 is a normal collisional energy transfer, followed by Step 2, Step 3, etc., until n hops have occurred and the excitation finds itself on an A^* which undergoes some form of deactivation. Notice that the result of excitation migration through the solvent M is the same as diffusion of the originally excited donor M to the site occupied by the final site at which M_n is deactivated by energy transfer from M_n^* to A. Energy migration may occur a number of times in favorable cases, i.e., the mechanism for the $D^* \rightarrow A^*$ process can be viewed as shown in Figure 9.30. An individual step of an energy migration may occur via either of the specific energy-transfer mechanisms we have already discussed, i.e., electronic, Coulombic, or exchange interactions. Energy migration is expected to be of particular importance when the solvent may serve as the energy-relaying agent and when the rate of energy migration through the solvent is faster than the rate of molecular diffusion.

When energy migration is important, the *net* rate of energy transfer will depend on the rates of molecular diffusion and energy migration. Experimentally, energy migration may be tested under two types of conditions:

1. In a fluid phase such that molecular diffusion is possible.

2. In a solid phase such that molecular diffusion is not possible.

For Case 1, energy migration will only be important in an overall energy transfer from D^* to A^* if $k_{vi}[M] > k_{11}^{DA}[A]$. Pictorially, we may view the situation

in terms of competing diffusional energy migration and diffusional molecular migration (Fig. 9.30) to achieve the same net energy transfer.

For Case 2, if D^* and A are separated in space by more than a few Å in excess of their collisional sizes, then the only mechanisms available to achieve a $D^* \rightarrow A^*$ transfer must be *long-range* in character, i.e.:

1. Energy migration via the intermediary molecules between D and A.
2. Through-space Coulombic interactions between D^* and A.
3. Emission by D^* followed by absorption by A.

Singlet and triplet energy migration is a well-documented process in molecular crystals.[7] For example, in benzene crystals at low temperature, singlet energy

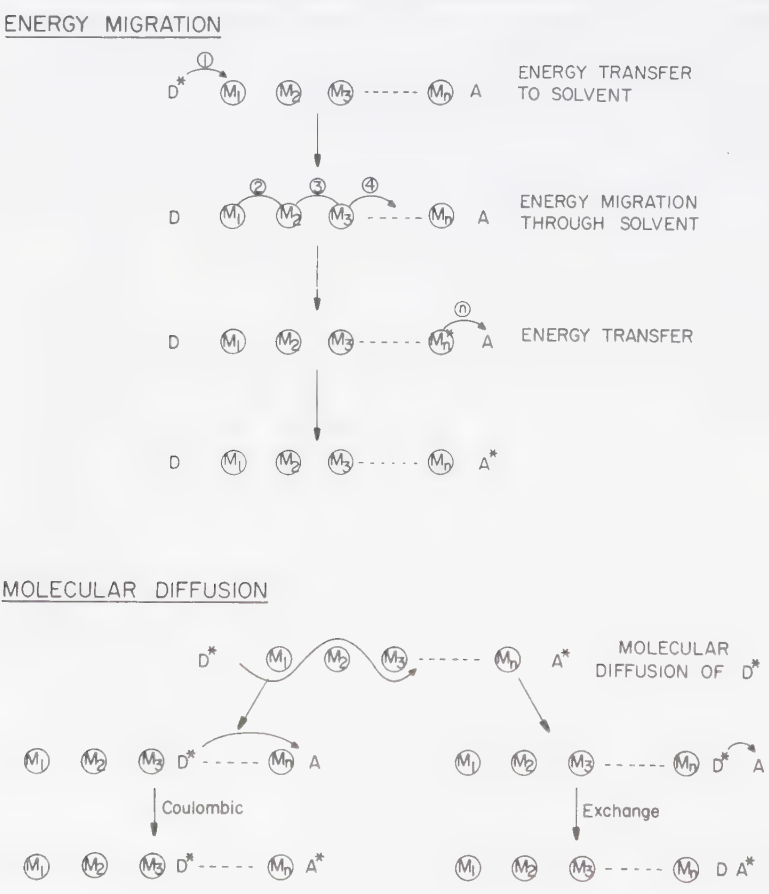

Figure 9.30

Comparison of energy transfer ($D^* + A \rightarrow D + A^*$) via energy migration or molecular diffusion.

"hops" $\sim 10^5$ times during the time period corresponding to the average lifetime τ_s of an isolated benzene molecule.[62] Triplet excitation undergoes $\sim 10^{11}$ hops during the time period (τ_T) corresponding to the average lifetime of a benzene triplet molecule. Translated into distances this means that a singlet "exciton" could travel up to $\sim 10^5 \times 2\,\text{Å} = 2 \times 10^5\,\text{Å}$ during τ_s and a triplet exciton could travel up to $\sim 10^{11} \times 2\,\text{Å} = 2 \times 10^{11}\,\text{Å}$ during τ_T. In fact, such large distances of travel are not actually achieved, because as it hops about, the exciton (excited benzene molecule) will occasionally reach a site in the crystal which serves to *quench* the exciton and terminate the hopping process.[62]

Triplet-Triplet Energy Migration; Self-Quenching of Triplets

Experimental examples of *triplet energy migration* in fluid solution are few, although such processes may be more common than suspected. Evidently *self-quenching* competes favorably with triplet energy migration, and as a result the triplet lifetime is shorted. *Self-quenching is defined as any interaction between an excited molecule D* and a ground-state molecule of the same type, D, which leads to net quenching of D* in competition with energy migration.*

$$D^* + D \xrightarrow{k_{EM}} D + D^* \quad \text{Energy migration} \tag{9.57}$$

$$D^* + D \xrightarrow{k_{SQ}} \text{No } D^* \quad \text{Self-quenching} \tag{9.58}$$

Measured self-quenching rate constants (see Table 9.10) vary over five orders of magnitude.[63] The detailed mechanism of self-quenching probably varies from

Table 9.10 Self-Quenching Rate Constants of Ketones

Compound	Solvent	$k_{sq}(M^{-1}\,sec^{-1})$	Reference
4-Hydroxybenzophenone	Benzene	6×10^7	(a)
4,4'-Dimethylaminobenzophenone	Benzene	3×10^8	(b)
Benzophenone	Acetonitrile	8×10^5	(c)
	Benzene	3×10^5	(d)
Acetophenone	Acetonitrile	2×10^7	(c)
	Benzene	8×10^5	(c)
Acetone	Acetonitrile	10^3	(e)
Methylnaphthylketone	Benzene	2×10^5	(f)
Thioxanthone	Benzene	2×10^9	(g)
Benzene	Hexane	$\sim 1 \times 10^6$	(h)
Naphthalene	Ethanol	$\sim 1 \times 10^6$	(h)

[a] Favaro, G., *Chem. Phys. Letters*, *23*, 592 (1973).
[b] Wolf, M. W., Brown, R. E., and Singer, L. A., *J. Am. Chem. Soc.* *99*, 526 (1977).
[c] Giering, L., Berger, M., and Steel, C., *J. Am. Chem. Soc*, *91*, 5390 (1969).
[d] Schuster, D. E., Weil, T. M., and Halpern, A. M., *J. Am. Chem. Soc.*, *94*, 8248 (1972).
[e] Yip, R. W., and Siebrand, W., *Chem. Phys. Letters*, *13*, 209 (1972).
[f] Schuster, D. I., and Goldstein, M. D., *Molec. Photochem.*, *7*, 209 (1976).
[g] DeBoer, C. D., and Schlessinger, R. H., *J. Am. Chem. Soc.*, *94*, 655 (1972).
[h] Reference 1c, p. 351.

system to system and both excimer formation and specific chemical interactions have been proposed in specific cases. In general, it appears the n, π^* states are less prone to self-quenching than π, π^* states. For compounds that possess a significant value of k_{ss} (i.e., $>10^7\ M^{-1}\ sec^{-1}$), concentration quenching of triplets can be a significant pathway for deactivation.

Energy hopping from acetone triplet to acetone triplet has been measured directly via a chemiexcitation technique.[64] The rate of energy migration ($\sim 3 \times 10^6\ M^{-1}\ sec^{-1}$) was found to be slow relative to the rate of diffusion ($\sim 1 \times 10^{10}\ M^{-1}\ sec^{-1}$). The rate of energy migration between aromatic hydrocarbon triplets was measured indirectly via CIDNP techniques.[65] In the case of anthracene a rate of $\sim 3 \times 10^4\ M^{-1}\ sec^{-1}$ was derived. It thus appears that the rate of energy migration between triplets may vary considerably in magnitude, depending on structural factors.

References

1. For reviews of electronic energy transfer the interested reader is referred to:
   (a) Lamola, A. A., *Energy Transfer and Organic Photochemistry*, New York: Interscience, 1969.
   (b) Turro, N. J., *Molecular Photochemistry*, San Francisco: W. A., Benjamin, 1967, Ch. 5.
   (c) Birks, J. B., *Photophysics of Aromatic Molecules*, New York: John Wiley, 1970, Ch. 11.
   (d) Wilkinson, F., *Adv. Photochem.*, *3*, 241 (1964); *Quart Rev.*, *Vol. 20*, 403 (1966).
   (e) Bennett, R. G., and Kellogg, R., *Prog. Reaction Kinetics*, *4*, 215 (1966); *J. Am. Chem. Soc.*, *90*, 1935 (1968).
2. For reviews of photosensitized organic reactions the interested reader is referred to Turro, N. J., Dalton, J. C., and Weiss, D. S., *Organic Photochemistry*, ed. Chapman, O. L., *2*, 1 (1969).
3. For a discussion of trivial (radiative) electronic energy transfer, see Birks, J. B., *Photochemistry of Aromatic Molecules*, New York: John Wiley, 1970, p. 522.
4. Förster, T., *Fluorenzenz Organische Verbindungen*, Gottingen: Vandenhoech and Ruprech, 1951.
5. (a) Förster, T., *Disc. Faraday Soc.*, *27*, 7 (1959).
   (b) Förster, T., *Ann. Physik*, *2*, 55 (1948).
6. Dexter, D. L., *J. Chem. Phys.*, *21*, 836 (1953).
7. (a) For reviews of energy migration and molecular diffusion see Birks, J. B., *Photophysics of Aromatic Molecules*, New York: John Wiley, 1970, p. 518.
   (b) Evans, T. R., *J. Am. Chem. Soc.*, *93*, 2081 (1970).
   (c) Alwattar, A. H., Lumb, M. D., and Birks, J. B., *Organic Molecular Photophysics*, *Vol. 1*, New York: Wiley, 1973, p. 403.
8. Smoluchowski, M., *Z. Phys. Chem.*, *92*, 129 (1917); Debye, P., *Trans. Electrochem. Soc.*, *82*, 265 (1942).
9. (a) Wagner, P. J., and Kochevar, I., *J. Am. Chem. Soc.*, *90*, 2232 (1969).
   (b) Reference 1c, Chap. 10.

10. (a) Reference 1c, Chap. 8.
(b) Birks, J. B., *Organic Molecular Photophysics, Vol. 1*, ed. Birks, J. B., New York: Wiley, 1973, p. 403.

11. (a) Gruska, E., and Kikta, E. J., *J. Am. Chem. Soc., 98*, 643 (1976).
(b) Miller, T. A., Prater, B., Lee, J. K., and Adams, R. N., *J. Am. Chem. Soc., 87*, 121 (1965).

12. (a) Perrin, J., *Comp. Rend. Acad. Sci. Paris, 184*, 1097 (1927); *178*, 1978 (1924).
(b) Perrin, F., *Ann. Chem. Phys., 17*, 283 (1932).
(c) Ermolaev, V. L., *Sov. Physics, Doklady, 6*, 600 (1962).

13. (a) Stern, O., and Mivolmer, H., *Z. Physik., 20*, 183 (1919).
(b) Valivov, S. I., *Z. Physik, 53*, 665 (1929).
For a discussion of generalized Stern-Volmer analyses, see Wagner, P. J., *Creation and Detection of the Excited State, 1A*, 174 (1971).

14. Ermolaev, V. L., *Sov. Physics, Doklady, 6*, 600 (1967).

15. (a) Bowen, E. J., and Brockelhurst, B., *Trans. Faraday Soc., 49*, 1131 (1953).
(b) *Ibid. 51*, 774 (1955).
(c) Bowen, E. J., and Livingston, R., *J. Am. Chem. Soc., 76*, 6300 (1954).

16. Yekta, A., and Turro, N. J., *Chem. Phys. Letters, 17*, 31 (1972).

17. Dubois, J. T., and Cox, M., *J. Chem. Phys., 38*, 2538 (1963).

18. Steinmetzer, H. C., Lechtken, P., and Turro, N. J., *Liebigs. Ann. Chem.*, 1984 (1973).

19. Steinmetzer, H. C., and Turro, N. J., *J. Am. Chem. Soc., 96*, 4677, 4697 (1974).

20. Birks, J. B., and Leite, M., *J. Phys. B. Atom, Molec. Phys., 3*, 417 (1970).

21. (a) Engel, P. S., and Steel, C., *Acc. Chem. Research, 6*, 275 (1973).
(b) Engel, P. S., Fogel, L. D., and Steel, C., *J. Am. Chem. Soc., 96*, 327 (1974).
(c) Evidence has been reported for orbital symmetry control of singlet-singlet energy transfer reactions; see Ullman, E. F., and Weinkam, R., *J. Am. Chem. Soc., 92*, 5256 (1970). However, it has been found that a trivial emission-absorption mechanism strongly complicates the systems studied, thereby calling the conclusion of orbital symmetry control into question. See Tokumaru, K., Sakuragi, H., and Takahashi, Y., *Chem. Letters*, 957 (1972); *Bull. Chem. Soc. Japan, 49*, 270 (1976).

22. Latt, S. A., Cheung, H. T., and Blout, E. R., *J. Am. Chem. Soc., 87*, 995 (1965).

23. Stryer, L., and Haugland, R. P., *Proc. Natl. Acad. Sci., 58*, 720 (1967).

24. For a review and leading references see Kuhn, H., and Mobius, D., *Angew. Chem., Inter. Ed. Eng., 10*, 620 (1971); Drexhage, K. H., *Sci. Amer., 222*, 108 (1970); Kuhn, H., Mobius, D., and Bucher, H., in *Techniques of Organic Chemistry*, eds. Weissberger, A., and Rossiter, B. W., Vol. 1, Part IIIB, 577 (1972); Bucher, H., et al. *Molec. Crystals, 2*, 199 (1967).

25. Kuhn, H., *Pure Applied Chem., 11*, 345 (1965).

26. Haugland, R. P., Yguerabide, J., and Stryer, L., *Proc. Natl. Acad. Sci., 63*, 23 (1969).

27. Turro, N. J., *J. Chem. Ed., 43*, 13 (1966).

28. Porter, G., and Wilkinson, F., *Proc. Royal Soc., 264A*, 1 (1961).

29. Sandros, K., *Acta Chem. Scand., 18*, 2355 (1964).

30. Turro, N. J., Schore, N. E., Steinmetzer, H. C., and Yekta, A., *J. Am. Chem. Soc., 96*, 1936 (1974).

31. Andersen, R. W., Hochstrasser, R. M., Lutz, H., and Scott, G. W., *J. Chem. Phys.*, *61*, 2500 (1974).

32. Wamser, C. C., Medary, R. T., Kochevar, I. E., Turro, N. J., and Chang, P. L., *J. Am. Chem. Soc.*, *97*, 4864 (1975).

33. (a) Ermolaev, V. L., *Opt. and Spec.*, *6*, 417 (1959); *Sov. Physics, Uspeckhi*, *80*, 333 (1963).
    (b) Terenin, A., and Ermolaev, V. L., *Trans. Faraday Soc.*, *52*, 1042 (1956); *Bull. Soc. Acad. Sci., U.S.S.R.*, Phys. Ser., *20*, 471 (1965); Terenin, A. N., and Ermolaev, V. L., *Bull. Acad. Sci. U.S.S.R. 26*, 21 (1962); Ermolaev, V. L., *Opt. and Spect.*, *13*, 49 (1962); Ermolaev, V. L., *Soviet Physics, Doklady*, *6*, 600 (1962).

34. For a review of intramolecular energy transfer, see De Schryver, F., and Boens, N., *Adv. Photochem.*, *10*, 359 (1977).

35. Zimmerman, H. E., and McKelvey, R. D., *J. Am. Chem. Soc.*, *93*, 3638 (1971).

36. Keller, R. A , and Dolby, L. J., *J. Am. Chem. Soc.*, *91*, 1293 (1969); Breen, D. E., and Keller, R. A., *ibid.*, *90*, 1935 (1968).

37. Rank, R. D., Evans, T. R., and Leermakers, P. A., *J. Am. Chem. Soc.*, *90*, 6897 (1968).

38. Lamola, A. A., Leermakers, P. A., Byers, G. W., and Hammond, G. S., *J. Am. Chem. Soc.*, *87*, 2322 (1965).

39. Vasilev, R. F., *Russ. Chem. Rev.*, *39*, 529 (1970).

40. Turro, N. J., Lechtken, P., Schore, N. E., Schuster, G., Steinmetzer, H. C., and Yekta, A., *Acc. Chem. Research*, *7*, 97 (1974).

41. Bennett, R. G., Schwenker, R. P., and Kellogg, R., *J. Chem. Phys.*, *41*, 3040 (1964).

42. Turro, N. J., Lechtken, P., Schuster, G., Orell, J., Steinmetzer, H. C., and Adam, W., *J. Am. Chem. Soc.*, *96*, 1627 (1974).

43. Kellogg, R., *J. Chem. Phys.*, *44*, 411 (1966); Bennett, R. B., and McCartin, P. J., *ibid.*, *44*, 1969 (1966).

44. Ermolaev, V. L., and Sveshnikova, E. B., *Opt. Spectro.*, *28*, 324 (1970).

45. Berlman, I. B., *J. Phys. Chem.*, *77*, 562 (1973).

46. Schulte-Frohlinde, D., and Hermann, H., *Ber. Bunsen. Ges.*, *81*, 562 (1977).

47. Ermolaev, V. L., and Terenin, A. N., *Soviet Physics, Uspekhi*, *3*, 423 (1960); *J. Chim. Phys.*, *55*, 698 (1958).

48. Lewis, G. N., and Calvin, N., *Chem. Rev.*, *25*, 273 (1939).

49. Plotnikov, V. G., *Opt. Spectro.*, *23*, 20 (1967).

50. For review of multiphoton processes, see:
    (a) Birks, J. B., *Photophysics of Organic Molecules*, New York: Wiley, 1970, p. 372;
    (b) Parker, C. A., *Adv. Photochem.*, *2*, 305 (1964).

51. Kaplan, I., and Jortner, J., *Chem. Phys. Letters*, *52*, 202 (1977).

52. (a) Liu, R. S. H., and Gale, D. M., *J. Am. Chem. Soc.*, *90*, 1897 (1968).
    (b) *J. Am. Chem. Soc.*, *90*, 213 (1968).
    (c) Liu, R. S. H., and Edman, J. R., *J. Am. Chem. Soc.*, *90*, 213 (1968).

53. Gillispie, G. D., and Lim, E. D., *J. Chem. Phys.*, *65*, 2022 (1976).

54. For a critical discussion of nonvertical energy transfer, see Ref. 1a, Ch. 1.

55. Wilkinson, F., and Dubois, J. T., *J. Chem. Phys.*, *39*, 377 (1963) and references therein.

56. Herkstroeter, W. G., and Hammond, G. S., *J. Am. Chem. Soc.*, *88*, 4769 (1966).

57. Such a mechanism is very similar to that proposed by Schenck to explain photosensitized reactions. See Schenck, G. O., and Steinmetz, R., *Bull. Soc. Chim. Belges*, *71*, 781 (1962).

58. For a review of the "complications" which may occur in photosensitized reactions, see Engel, P. S., and Monroe, B. C., *Adv. Photochem.*, *8*, 245 (1971).

59. Gijzman, O. L., et al., *Trans. Farad. Soc.*, II, *70*, 708 (1973).

60. Merkel, P. B., and Kearns, D., *J. Chem. Phys.*, *58*, 398 (1973).

61. Frenkel, J. I., *Phys. Rev.*, *37*, 1276 (1931).

62. Nieman, G. C., and Robinson, G. W., *J. Chem. Phys.*, *37*, 2150 (1962).

63. For a review, see Singer, L., et al., *J. Am. Chem. Soc.*, *99*, 526 (1977) and references therein.

64. Lechtken, P., and Turro, N. J., *Angew. Chem. Int. Ed. Eng.*, *12*, 314 (1973).

65. Boxer, S. G., and Closs, G. L., *J. Am. Chem. Soc.*, *97*, 3268 (1975).

10

Photoaddition and Photosubstitution Reactions

10.1 Classification of Photochemical Additions and Substitution Reactions

Many photochemical reactions may be classified as overall *linear* additions across an unsaturated linkage (cycloadditions are considered in Chapter 11). In general, these linear additions do not occur in a single step but generally proceed via diradical or zwitterionic intermediates. Photosubstitution reactions involving unsaturated systems occur by similar mechanisms. Photosubstitutions on saturated carbon atoms are very rare.

For example, the irradiation of ketones, ethylenes, conjugated enones, azo compounds, nitro-compounds, etc., in the presence of hydrogen-atom–donating substrates (alcohols, amines, hydrocarbons, etc.) commonly results in a photochemical primary process of hydrogen *abstraction*, followed by product formation via secondary thermal reactions:[1]

$$\underset{\substack{\text{hydrogen}\\\text{atom donor}}}{R_2C{=}O + X{-}H} \xrightarrow[\substack{\text{hydrogen}\\\text{abstraction}}]{h\nu} \underset{D\text{, radical pair}}{R_2\dot{C}OH + \dot{X}} \longrightarrow \text{products} \qquad (10.1)$$

In other cases, an electron transfer or proton transfer may result from primary interaction of an excited unsaturated chromophore with a substrate of low ionization potential or one possessing an acidic proton. The initially formed radical ion pair $D_{\pm}$ (Eq. 10.2) or zwitterion Z (Eq. 10.3) then proceed to yield products:

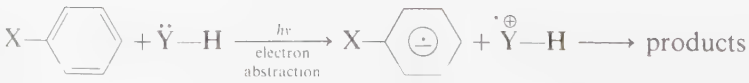

$D_{\pm}$, radical ion pair (10.2)

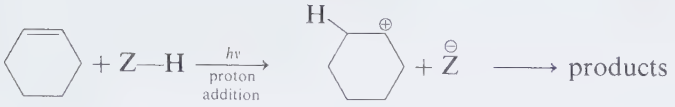

(10.3)

Z, zwitterionic pair

If we confine our discussion of photochemical additions and substitutions to n, π^* and π, π^* states we expect the following broad general behavior:

1. n, π^* states and π, π^* triplet states, being inherently diradical in nature, tend to undergo addition and substitution reactions via diradical mechanisms.

2. π, π^* singlet states, being polarizable and zwitterionic in nature, tend to undergo addition and substitution via zwitterionic mechanisms.

Scheme 10.1 shows a paradigm for the mechanistic analysis of addition reactions, based on knowledge of the initial-state configuration and multiplicity.

10.2 Photoreduction of Carbonyl Compounds and Ethylenes: Linear Addition Initiated by Hydrogen Abstraction Reactions

Of the various known classes of photoaddition reactions, photoreduction[1] (the reductive addition to a double bond, Eq. 10.1) is very commonly encountered. We shall discuss photoreduction of carbonyl and ethylene functions by H-atom–donating substrates as prototypes. The products isolated from these reactions are usually alcohols (Eq. 10.4) or alkanes (Eq. 10.5).

State	Primary photoreaction	Notation
$^1(n, \pi^*)$, $^3(n, \pi^*)$, $^3(\pi, \pi^*)$	Diradical additions	$n, \pi^* \rightarrow \mathrm{D}$ or $\mathrm{D}_{\pm}$ $\pi, \pi^* \rightarrow \mathrm{D}$ or $\mathrm{D}_{\pm}$
$^1(\pi, \pi^*)$	Zwitterionic additions	$\pi, \pi^* \rightarrow \mathrm{Z}$

Scheme 10.1

A paradigm for linear addition reactions initiated by n, π^* or π, π^* states.

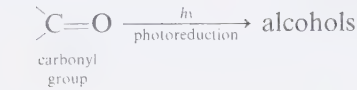

(10.4)

(10.5)

10.3 The Use of Radical Models for Hydrogen Abstraction from n, π^* and π, π^* States

Insight into the nature of photochemical hydrogen abstraction reactions can be obtained by considering the hydrogen abstraction reactions of alkoxy radicals and carbon radicals. The postulate that an n orbital of an n, π^* state or that a π orbital of a π, π^* state dominates the electronics of hydrogen abstraction suggests that $R\dot{O}$ and $R_3\dot{C}$ radicals (Eqs. 10.6 and 10.7) which possess half-filled p orbitals – may be suitable models to predict reactivity patterns for hydrogen abstraction reactions.[2,3]

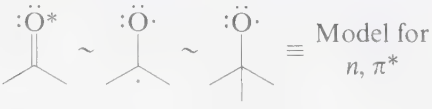

(10.6)

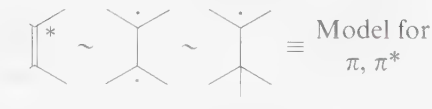

(10.7)

From kinetic data for abstraction of hydrogen atoms by $R_3\dot{C}$ and $R\dot{O}$ radicals, the below listed five factors are expected to influence the reaction rate constant, k_r, for the hydrogen abstraction step:[4,5]

(10.8)

1. The strength of the bond being broken (i.e., the bond dissociation energy D_{HX} for $HX \rightarrow \dot{H} + \dot{X}$).

2. The strength of the bond being formed (i.e., the bond formation energy D for the CH or OH bond being formed).

3. Polar or charge-transfer effects on the energy of the transition state relative to the energy of the reagents.

4. Steric effects on the approach of the reagent and substrate.

5. Solvent effects on the reagent, substrate, and transition state.

Each of these effects should have an analogy which will influence the rate constant k_r for the *net* abstraction of a hydrogen atom by a n, π^* state of a carbonyl compound:[6,7]

$$\underset{n,\pi^*}{\overset{\diagdown}{\underset{\diagup}{\text{C}}}}\text{—}\dot{\text{O}} + \text{X—H} \xrightarrow{k_r} \overset{\diagdown}{\underset{\diagup}{\text{C}}}\text{—}\overset{\prime}{\text{O}}\text{H} + \dot{\text{X}} \qquad (10.9)$$

Reactivity refers to the rate constant for an elementary chemical step. The reactivity for a given excited carbonyl-hydrogen donor pair is given by k_r, the rate constant for the primary photochemical process of hydrogen abstraction.[6] Thus, in discussing the reactivity of a state toward the primary process of hydrogen abstraction we direct our attention to k_r and how it depends on experimental variables. The relative reactivity of n, π^* states toward hydrogen abstraction from different hydrogen donors generally parallels that for hydrogen abstraction by tert-butoxy radicals.[2b,c] Indeed, the absolute rate constants are comparable for hydrogen abstraction from benzhydrol and cumene by benzophenone triplets ($10 \times 10^6\ M^{-1}\ sec^{-1}$ and $5 \times 10^5\ M^{-1}\ sec^{-1}$, respectively) or by tert-butoxy radicals ($7 \times 10^6\ M^{-1}\ sec^{-1}$ and $9 \times 10^5\ M^{-1}\ sec^{-1}$, respectively).[2e]

In Chapter 8 it was shown that the A factor for intermolecular hydrogen abstractions tends to be $\sim 10^8\ sec^{-1}$, whereas for unconstrained 6-membered-ring intramolecular abstractions the A factor is $\sim 10^{12}\ sec^{-1}$. The activation energies for intermolecular hydrogen abstraction range from $\sim$3-7 kcal/mole, when the formation of the primary radical pair (or diradical) is exothermic from the initial n, π^* state.[7]

It is important to remember that certain restrictions are imposed on reactivity (as measured by k_r or E_a) by energetics on reactions involving diradicals. Since the reverse reaction (radical recombination) generally requires little or no activation energy in the absence of major resonance or steric effects, and since E_a cannot be less than ΔH for an endothermic reaction, we may thus conclude that only *exothermic* reactions are likely to have E_a values small enough to allow reactions to be competitive with the other available, rapid modes of deactivation of excited states.[8]

Figure 10.1 is a qualitative diagram of the role of E_*, the excitation energy of the reacting state, and $D_{\diagdown\ \ \diagup}$ for hydrogen abstraction by a ketone. The contribution of the new OH bond to the overall reaction enthalpy, ΔH, will be constant, since for a given ketone the *same* ketyl radical is formed in all cases. In general, overall abstraction of a saturated alcohol OH, a benzene H, or a saturated alkane

CH will generally be endothermic, thereby automatically providing a contribution to E_a. On the other hand, abstraction of hydrogen from the carbon α to an alcohol, from a phenol OH, or from a tin hydride SnH is generally exothermic if $E_* \lesssim 70$ kcal/mole.[6]

From this analysis it is apparent from energetics alone why benzene and saturated hydrocarbons are not generally effective hydrogen donors in photoreductions and why isopropanol or tri-butyl tin hydride are generally employed as substrates in photoreductions.

This analysis allows a ready understanding of why, for isopropanol, the C—H ($D_{C-H} \sim 90$ kcal mole) bond and not the O—H bond ($D_{OH} \sim 100$ kcal/mole) will be abstracted by the n, π^* state of a ketone:

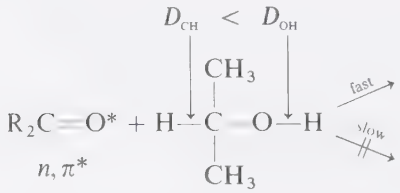

$$R_2\dot{C}OH + (CH_3)_2\dot{C}OH \qquad (10.10)$$

$$R_2\dot{C}OH + (CH_3)_2CH\dot{O} \qquad (10.11)$$

This analysis also explains why $T_1(n, \pi^*)$ of benzophenone ($E_* \sim 68$ kcal/mole) abstracts hydrogen atoms from isopropanol much faster than the $T_1(n, \pi^*)$ state of biacetyl ($E_* \sim 56$ kcal/mole). Thus, the bond strength of the hydrogen donor and the excitation energy of the excited state will be crucial factors in determining the feasibility of a hydrogen abstraction reaction. Other factors (generally less

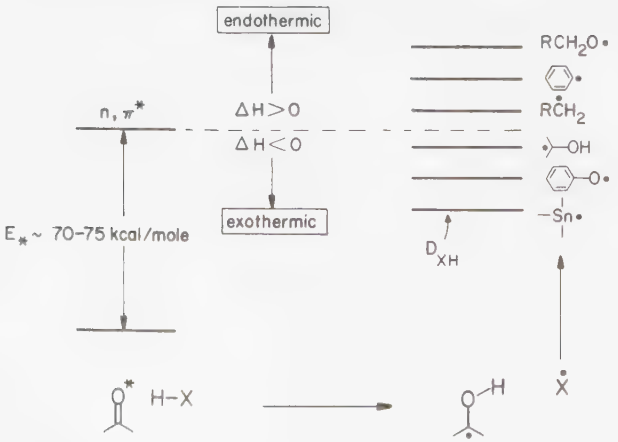

Figure 10.1

Qualitative comparison of the energetics for hydrogen abstraction from different hydrogen donors HX by the n, π states of simple alkyl or aryl ketones.

important) are: (1) polar effects ("electron poor" X—H bonds will react slower than "electron rich" X—H bonds for a comparable bond strength), (2) steric effects, and (3) solvent effects.

10.4 Theoretical Analysis of Hydrogen and Electron Abstraction Reactions of Ketones[9]

From Chapter 7 we saw that the *in-plane* hydrogen abstraction reaction is expected to be favored over the *perpendicular* abstraction (Fig. 10.2), based on orbital

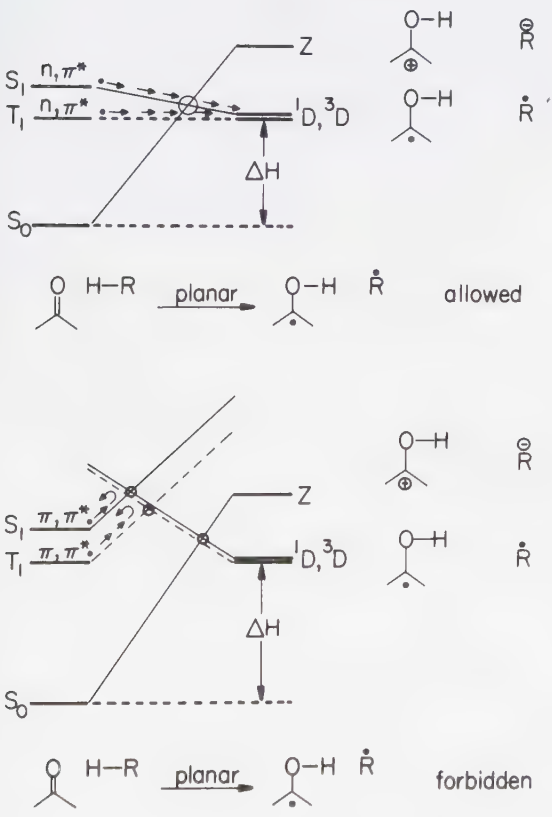

Figure 10.2
Summary of the surface correlation diagram for coplanar hydrogen abstraction by the n, π states (upper) and by the π, π^* states of a ketone. The circles indicate weakly avoided crossings.

interactions (Fig. 10.3). From correlation diagrams it was clear that for a given spin multiplicity we expect that $k_r(n, \pi^*) \gg k_r(\pi, \pi^*)$. Furthermore, it is expected that electron abstraction, a reaction which possesses a topologically equivalent correlation diagram, should follow the same behavior qualitatively as hydrogen abstraction.

10.5 Synthetic Applications of Photochemical Hydrogen Abstraction Reactions

The photoreduction of benzophenone by benzhydrol to form benzpinacol (Eq. 10.12) and the photoreduction of benzophenone to benzhydrol by alkaline isopropanol (Eq. 10.13) are examples of production of a carbon-carbon bond and a carbon-hydrogen bond as the result of initial formation of a ketyl radical followed by different secondary processes:

$$\begin{array}{ccc} Ph_2C{=}O + Ph_2CHOH & \xrightarrow[100°_n]{h\nu} & Ph_2COHCOHPh_2 \\ \Big\downarrow h\nu & & \Big\uparrow \\ Ph_2C{=}O^* + Ph_2CHOH & \xrightarrow{k_r} & Ph_2\dot{C}OH + Ph_2\dot{C}OH \\ & & \text{Ketyl radical pair} \end{array} \qquad (10.12)^{10}$$

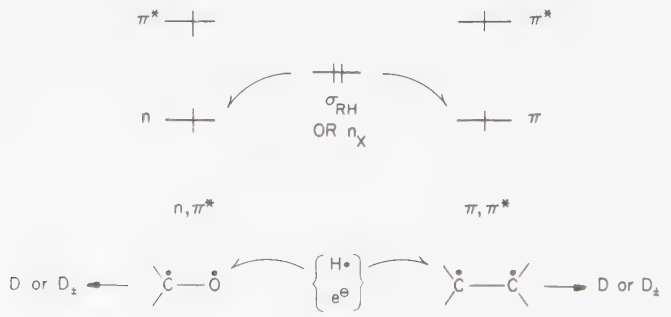

Figure 10.3

Summary of the orbital interactions for the *n*-orbital initiated abstraction of a hydrogen atom or electron by a n, π^* state of a ketone (left) and by a π, π^* state of an ethylene (right).

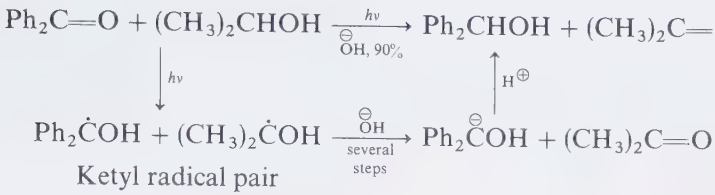

(10.13)[11]

Consider the complex appearance of a lactone derives from irradiation of benzophenone (light absorbing species), isopropanol, and maleic acid (Eq. 10.14). Benzophenone is formally a *photosensitizer* in this reaction because it is recovered. However, it initially abstracts a hydrogen atom (step *a*) to form $Ph_2\dot{C}OH$. The latter then donates a hydrogen atom (step *c*) to regenerate benzophenone.

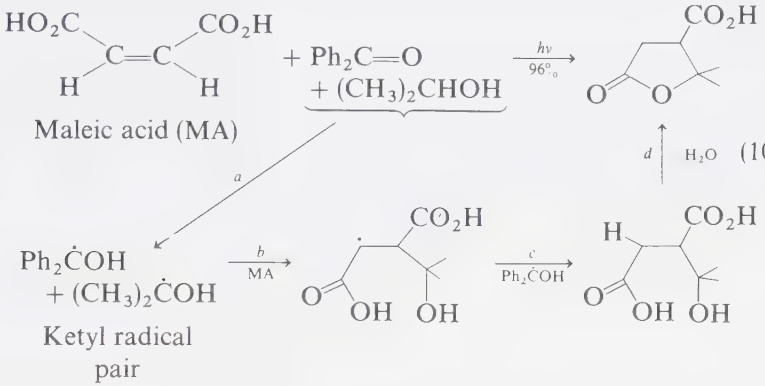

(10.14)[12]

An interesting extension of this trapping of radicals generated by hydrogen abstraction has been employed as a means of alkylating proteins (Eq. 10.15). Gylcine residues in proteins possess a particularly reactive CH bond. Abstraction of the hydrogen atom produces a carbon radical which is reactive toward addition to ethylenes or coupling with other radicals. Thus, Eq. 10.15 proves that a general sequence is available for modifying proteins by photoalkylation. Notice that a *net* substitution reaction ($H \rightarrow CH_2CH_2R$) has been effected:

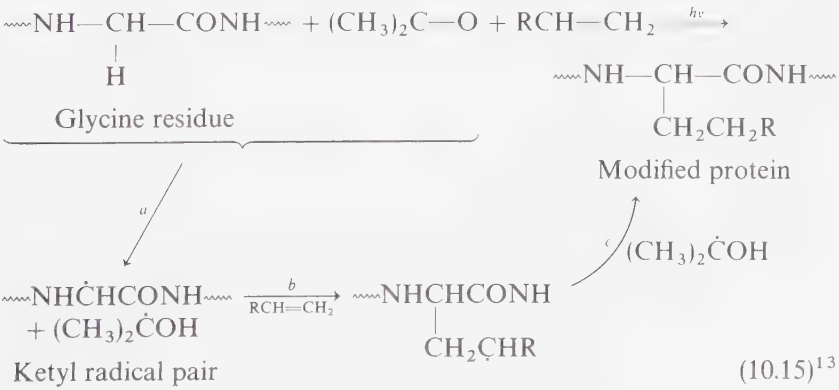

(10.15)[13]

The "Type II" reactions (γ-hydrogen abstraction via a six-membered transition state) of branched ketones result either in cyclizations that form four-membered rings or fragmentations that form unsaturated compounds. The ratio of the two processes depends on the structure of the diradical intermediate. Thus, if cleavage or cyclization is favored because of a structural restraint or structural acceleration of one of the processes, the reaction is synthetically useful. Some examples of this use of Type II reactions are:

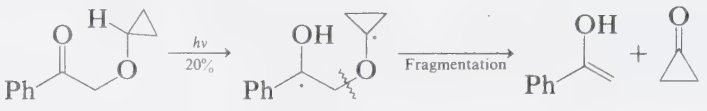

(10.16)[14]

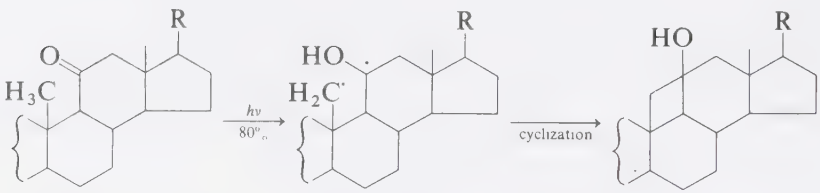

(10.17)[15a]

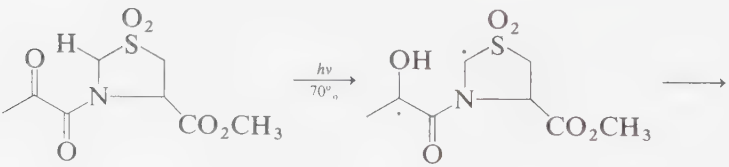

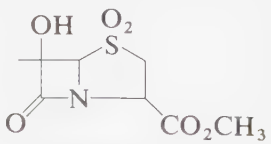

(10.18)[15b]

An interesting use of the Type II fragmentation has been employed to "protect" a $C{=}CH_2$ functionality which could be regenerated by photolysis (Eq. 10.19).

In the special case of an α,β-unsaturated enone, an enol may be formed as the result of intramolecular hydrogen abstraction.[1] The enol may be sufficiently stable to be isolated, may undergo a tautomeric [1,3] hydrogen shift to form a β,γ-unsaturated enone (Eq. 10.20) or may be trapped (say by a dienophile, Eq. 10.21).

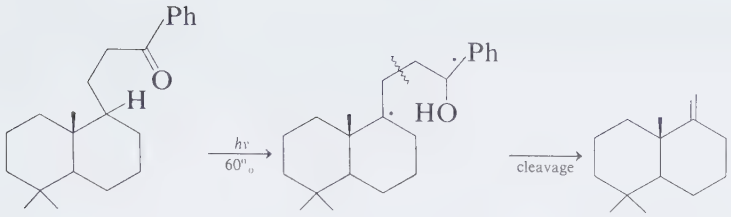

Diradical

(10.19)[16a]

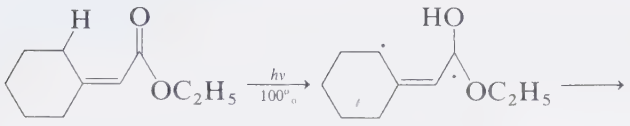

Diradical

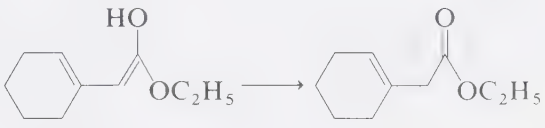

Unstable énol

(10.20)[16b]

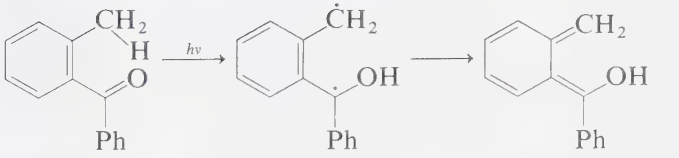

Diradical Unstable enol

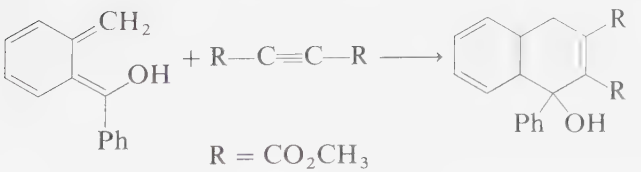

$R = CO_2CH_3$

(10.21)[16c]

For systems in which the abstraction of hydrogen is structurally determined by proximity, spectacular "remote but specific" hydrogen abstractions are possible (Eq. 10.22).[17]

The specific abstraction reaction given in Eq. 10.22 corresponds to a cyclic 15-membered transition state. The reaction occurs in a specific manner because the excited carbonyl can best "reach" H_1 and not any of the other tertiary (generally more reactive) hydrogen atoms.

As a final example of large ring synthesis by hydrogen abstraction, the activation of a specific hydrogen abstraction by sulfur has been utilized to achieve the

cyclization of large rings (Eq. 23):

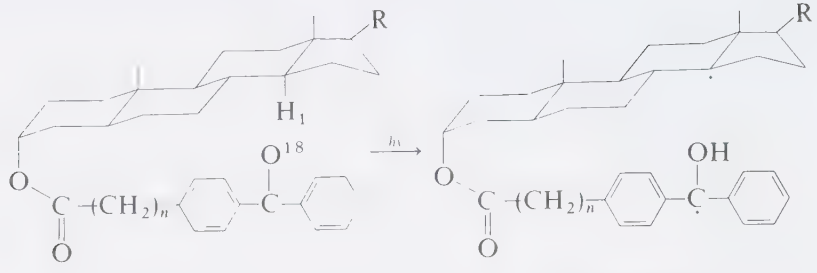

1 1,16-diradical

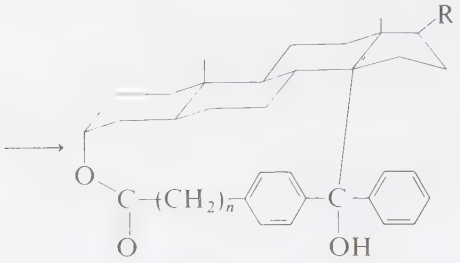

2, 16-membered ring

(10.22)[17]

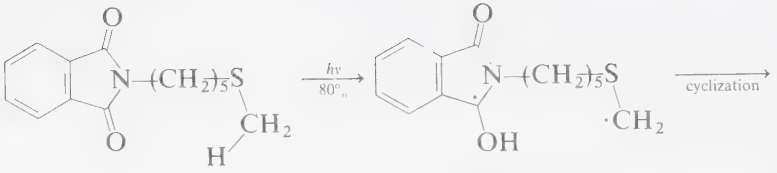

3 1,9-diradical

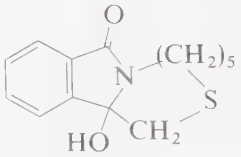

4, 9-membered ring

(10.23)[18]

10.6 Mechanistic Analysis of the Photoreduction of Ketones

The mechanisms of photoreduction of ketones have been so thoroughly investigated that this family of reactions is among the best understood of all photoreactions. As a result, the mechanistic analysis of this photoreduction will serve as a prototype for other mechanistic studies.

Product Structures and Intermediates in Photoreduction of Ketones: Evidence for Ketyl Radical and Ketyl Radical Ion Intermediates

The structure of the major products produced in the photoreduction of ketones are explained on the basis of *expected* secondary reactions of an initially produced $D_{\pm}$ or D pair, generally a ketyl radical anion and associated radical cation or a ketyl radical and associated radical partner. For example, the photoreduction of benzophenone to benzpinacol (Eq. 10.12) is readily understood in terms of the mechanism given by:[10]

$$Ph_2C{=}O^* + Ph_2CHOH \rightarrow \underset{\text{Ketyl radicals}}{2Ph_2\dot{C}OH} \tag{10.24}$$

$$2Ph_2\dot{C}OH \rightarrow Ph_2COHCOHPh_2 \tag{10.25}$$

Direct spectroscopic evidence for the intermediacy of ketyl radicals and ketyl radical ions in the photoreduction of ketones is available from ESR studies,[19a] absorption,[19b] and emission studies.[19c] Thus, for instance, $Ph_2\dot{C}OH$ generated from irradiation of Ph_2CO and Ph_2CHOH has been spectroscopically detected by ESR.[20a,b] The anion radical and cation radicals derived from electron abstraction by benzophenone from amines have also been detected by absorption spectroscopy:[21]

$$Ph_2CO^* + Ar_3N \rightarrow \underset{\lambda_{max} = 670\text{ nm}}{Ar_3\dot{N}^{\oplus}} + \underset{\lambda_{max} = 620\text{ nm}}{Ph_2\dot{C}O^{\ominus}} \tag{10.26}$$

The photoreduction of acetone by isopropanol represents an interesting example since the ketyl radicals produced disproportionate to generate acetone enol and acetone, in addition to coupling to produce pinacol.[20c] The occurrence of the disproportionation would not be apparent in analysis of the products of photoreduction, since the enol is unstable under the reaction conditions. However, the quantum yield of products and disappearance of acetone are reduced by this process.

$$(CH_3)_2CO + (CH_3)_2CHOH \xrightarrow{h\nu} 2(CH_3)_2\dot{C}OH \tag{10.27}$$

$$(CH_3)_2\dot{C}OH \longrightarrow \underset{\text{disproportionation}}{CH_3\overset{OH}{\overset{|}{\dot{C}}}{=}CH_2} + (CH_3)_2CHOH$$

$$+ \underset{\text{coupling}}{(CH_3)_2\overset{OH}{\overset{|}{C}}\,\overset{OH}{\overset{|}{C}}(CH_3)_2} \tag{10.28}$$

The occurrence of ketyl radicals in photoreduction has also been established by the principle of *alternate synthesis*; the same radical pair is produced by abstraction of triplet acetaldehyde from ground-state acetaldehyde or from cleavage of acetoin:[20d]

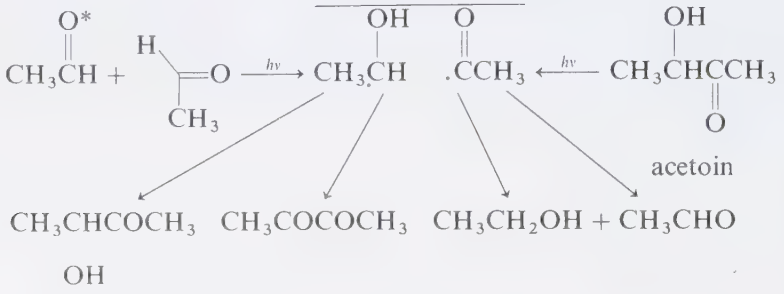

(10.29)

The Relationship between Substrate Structure and Reactivity in Photochemical Hydrogen Abstraction

Table 10.1 summarizes some data for the quenching of n, π^* triplets by hydrogen-atom and electron donors. The range of values of k_q spans six orders of magnitude.

Table 10.1 Reactivities for Quenching of Triplet n, π^* Ketones by Hydrogen and Electron Donors*

Hydrogen or electron donors	*IP* (eV)	k_q for triplet n, π^*		
		Acetone	Benzophenone	Biacetyl
$PhN(CH_3)_2$	7.1	2×10^9	3×10^9	3×10^8
$(CH_3CH_2)_3N$	7.5	3×10^8	2×10^9	5×10^7
PhSH	—	—	3×10^8	—
$(CH_3CH_2CH_2CH_2)_3SnH$	—	10^8	5×10^7	1×10^7
$(CH_3)_2C{=}C(CH_3)_2$	8.1	5×10^7	5×10^8	4×10^6
$CH_3(CH_2)_4CH_2NH_2$	8.7	1×10^7	10^8	3×10^7
$CH_3CH{=}CHCH_2CH_3$	9.1	1×10^7	5×10^7	—
RSH	—	—	1×10^7	—
Ph_2CHOH	—	—	1×10^7	7×10^4
$PhSCH_3$	—	—	6×10^7	—
$PhCH_3$	8.8	3×10^6	2×10^5	—
C_6H_6	9.3	2×10^6	10^4	—
$(CH_3)_3CNH_2$	8.5	1×10^6	—	—
$PhCH(CH_3)_2$	8.5	—	5×10^5	—
$(CH_3)_2CHOH$	10.1	1×10^6	1×10^6	10^4
CH_3CH_2OH	10.5	4×10^5	6×10^5	3×10^3
cyclo-C_6H_{12}	9.9	3×10^5	4×10^4	—
R-CH_2-R	10.2	2×10^5	5×10^5	—
CH_3OH	—	1×10^5	3×10^5	3×10^2
$(CH_3)_3COH$	—	4×10^3	—	—
CH_3CN	—	$< 10^3$	—	—
$(CH_3)_2CO$	—	$< 10^3$	—	—
H_2O	—	$< 10^3$	—	—

* Data from References 6 and 25.

It can be seen that there is a rough correlation between ionization potential (IP) and k_q for substrates possessing IP less than ~ 9 eV. It appears that saturated hydrocarbons and alcohols undergo quenching predominantly via a hydrogen-atom abstraction mechanism, whereas amines, sulfides, and unsaturated hydrocarbons undergo quenching via a charge-transfer interaction or full-electron transfer.[22] Thus, depending on the bond energy (DH) of the hydrogen donor and on its IP, there exists a continuum of mechanisms varying from an extreme of hydrogen transfer (high IP, moderate DH), to an extreme of electron transfer (low IP, strong DH). For substrates possessing *both* high IP and strong CH (e.g., acetone, acetonitrile), hydrogen abstraction is extremely inefficient.

The Effect of Excited-State Configuration and Reactivity

Both $^1(n, \pi^*)$ and $^3(n, \pi^*)$ states are expected to undergo *allowed* co-planar hydrogen (or electron) abstraction reactions. Thus, based on the simple orbital configurational model (pure single configurational states) both $S_1(n, \pi^*)$ and $T_1(n, \pi^*)$ should exhibit comparable reactivity. On occasion, the former may be more reactive because of energetic considerations ($E_{s_1} > E_{T_1}$). Thus, one expects that $^1k_r \sim {}^3k_r$ for n, π^* configurations; experimentally, this expectation is confirmed.[23]

If constrained to the coplanar geometry of Figure 10.3, both $^1\pi, \pi^*$ and $^3\pi, \pi^*$ states can undergo only forbidden coplanar hydrogen (or electron) abstraction reactions. Both $S_1(\pi, \pi^*)$ and $T_1(\pi, \pi^*)$ should be comparably reactive, but less reactive than their n, π^* counterparts.

Mixing and Switching of State Configurations

The model for the n, π^* state of ketones discussed above suffices for a description of the photochemistry of ketones possessing lowest n, π^* states. We would expect that although the primary processes should remain similar for aliphatic and aromatic carbonyl systems with lowest n, π^* states, the quantitative values of rate constants for these primary processes should vary with the nature of the aromatic moiety.

However, an important complication occurs if an excited state associated with the aromatic group is "mixed" into the lowest singlet or triplet. In such a case, the photochemistry typical of the n, π^* state will be modified or may disappear entirely. For example, if a π, π^* aromatic state is lower in energy than the carbonyl n, π^* state, reactivity may be more like that of a π, π^* state of a carbonyl function because of "coupling" or interaction of the π, π^* aromatic and n, π^* carbonyl states. We are dealing with approximate models when we discuss or classify electronically excited states in terms of a single electron configuration which makes the major contribution to that state. In principle, the n, π^* state of *all* ketones possesses some π, π^* character. Thus, the T_1 state of any ketone should be described by:

$$T_1 = a(n, \pi^*) + b(\pi, \pi^*) \tag{10.30}$$

where a and b are measures of the extent to which each configuration n, π^* or π, π^* contributes to the actual T_1 state of the molecule in question. For acetone, it

would seem that $a \gg b$, i.e., $T_1 \sim (n, \pi^*)$. The weighting of contributions of each configuration may be compared to the weighting of valence structures of ground-state molecules. According to perturbation theory, the magnitude of the contribution of a given state depends on several factors, such as the energetic separation (for which the contribution varies inversely as the square of the energy difference) of the configurations involved, and the symmetry of the states involved.

For aryl ketones the calculated energies of n, π^* and π, π^* configurations are much closer than for alkyl ketones, so that the corresponding S_1 or T_1 states may not be as clearly described in terms of either configuration. Indeed, for certain substituted benzophenones and all naphthyl ketones and aldehydes, the lowest triplet is generally best classified as π, π^*. This classification implies that: (a) the excited carbonyl oxygen is not as electron-deficient as it is in the n, π^* state, (b) the excitation energy is partially delocalized into the π-system and may therefore not be available to overcome activation energies for reaction at the carbonyl moiety, and (c) primary processes involving the π-system (or groups affixed to it) may occur.

In the case of certain aryl ketones and aldehydes which possess strong electron releasing groups, a configuration to describe the excited state is required which involves nearly complete transfer of an electron from a heteroatom on the substituent to the carbonyl group. This electron shift has the effect of reducing the electrophilicity of the carbonyl oxygen in the excited state and making it more nucleophilic. States which are best described by such a model are called *charge-transfer (CT) states*. Although both π, π^* and CT states involve mainly π-type orbitals, in the π, π^* state the π and π^* electrons are generally considered to occupy similar or the same regions of space, but in the CT state the π and π^* electrons may be located in different regions of space, thereby producing a charge separation. A key characteristic of CT transitions is often the excitation of a "lone pair" (ℓ-type) electron into the π^* system. Thus, ℓ, π^* transitions are identical is most cases to the so-called CT transitions.

Only in the case of n, π^* states is the triplet-excitation energy largely localized in the carbonyl group. In Eq. 10.31 the three common types of T_1 states of aryl ketones are exemplified for benzophenone (**5**), 2-acetonaphthone (**6**), and 4-aminobenzophenone (**7**) in terms of major contributing structures:

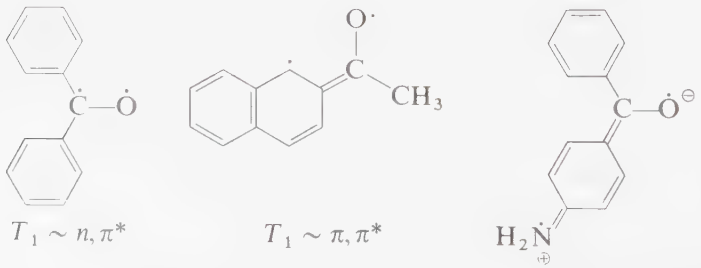

(10.31)

$T_1 \sim n, \pi^*$ $\quad$ $T_1 \sim \pi, \pi^*$ $\quad$ $T_1 \sim CT$

5 $\quad$ **6** $\quad$ **7**

Forms **5**, **6**, and **7** imply a decreasing order of reactivity of these excited states toward hydrogen abstraction. That is, on the basis of these structures only, one would predict that the order of reactivity of the excited states of substituted benzophenones toward hydrogen abstraction should be $n, \pi^* > \pi, \pi^* \gg CT$. (For examples of the verification of this expectation see Table 10.2.) This expectation is based on the premise that hydrogen abstraction is an electrophilic process, correctly interpreted in terms of the orbital interactions and correlation diagrams discussed in Chapter 7. In effect, the idea is that at the initial geometry of the reactants the *activation* energy for reaction with a given hydrogen donor is correlatable with the initial orbital configuration.

"State switching," the reversal of an initial state energetic disposition, can be achieved by variation of ketone structure, solvent, and other experimental variables. For example, acetophenone possesses a $T_1(n, \pi^*)$ and $T_2(\pi, \pi^*)$ state in nonpolar solvents but a $T_1(\pi, \pi^*)$ and a $T_2(n, \pi^*)$ state in polar solvents. State switching may occur as a reaction proceeds because of a surface crossing along the reaction coordinate. For example, a molecule initially in a $T_1(\pi, \pi^*)$ state may begin to participate in a (highly activated) hydrogen abstraction reaction, but as the reaction proceeds, a crossing with an n, π^* surface may occur and reduce the barrier for reaction.[9]

10.7 Quantitative Analysis of the Efficiency of Photoreduction

The expressions for the quantum yields for *net* photoreduction from S_1 and T_1 are given by Eqs. 10.32 and 10.33, respectively, where Φ_R^S and Φ_R^T are the quantum yields for photoreduction from S_1 and from T_1, k_R^S and k_R^T are the bimolecular rate constants for hydrogen abstraction from RH by S_1 and T_1, $\sum k_d^S$ and $\sum k_d^T$ are the sum of unimolecular (or pseudo-unimolecular) rates of decay of S_1 and T_1, and ϕ_P^S and ϕ_P^T are the efficiencies with which intermediates (primary radical products) go on to yield isolated photoreduction products from reaction of S_1 and T_1, respectively.

$$\text{Quantum yield of photoreduction from } S_1 \quad \Phi_R^S = \underbrace{\frac{k_R^S[RH]}{k_R^S[RH] + \sum k_d^S}}_{\phi_R^S} \phi_P^S \tag{10.32}$$

$$\text{Quantum yield of photoreduction from } T_1 \quad \Phi_R^T = \underbrace{\Phi_{ST} \frac{k_R^T[RH]}{k_R^T[RH] + \sum k_d^T}}_{\phi_R^T} \phi_P^T \tag{10.33}$$

The ratio of rates in Eqs. 10.32 and 10.33 are equal to the efficiencies ϕ_R^S and ϕ_R^T for formation of primary products from S_1 and T_1, respectively. The contribution of Φ_R^S is usually negligible relative to the contribution of $\Phi_{ST}\phi_R^T\phi_P^T$. When this

is the case (a good approximation for low concentrations of $[RH]$), Eq. 10.33 reduces to:

$$\Phi_P(\text{overall}) \sim \Phi_{ST}\phi_R^T\phi_P^T \tag{10.34}$$

Equation 10.34 reveals the crucial factors involved in determining the quantum efficiency of a "conventional" photoreduction. Under the assumption that only triplets react, the overall quantum efficiency depends on: (a) Φ_{ST}, the quantum yield of triplets, (b) ϕ_R^T, the efficiency with which the triplet, once formed, produces the primary products (ketyl radicals or ketyl radical ions), and (c) ϕ_P^T the efficiency with which the primary products proceed to isolated products.

In the case of the photoreduction of benzophenone by benzhydrol, $\Phi_P(\text{overall}) \rightarrow 1.0$ at high concentrations of benzhydrol.[10] Thus, in the limit of high concentration from Eq. 10.34, we concluded that Φ_{ST}, ϕ_P^T, and ϕ_P^T all equal 1.0 in the limit, i.e., each step (formation of T_1 from S_1, abstraction of a hydrogen atom to form a pair of ketyl radicals, and coupling of the ketyl radicals to form benzpinacol) is $\sim 100\%$ efficient at high concentrations of benzhydrol.

The Effect of Reactant Electronic Orbital Configuration and Substrate Structure on Efficiency of Photoreduction

Let us compare the photoreduction by isopropanol of benzophenone ($T_1 = n, \pi^*$) to that of 4-phenylbenzophenone ($T_1 = \pi, \pi^*$). (See Table 10.2.) The limiting

Table 10.2 Rate Constants for Quenching of Ketone Triplets by Isopropanol and Triethylamine*

Ketone	E_T[a]	Conf. T_1[b]	k_R Isopropanol[c]	k_R Triethylamine
$(CH_3)_2CO$	78	n, π^*	1×10^6	4×10^8 [a]
4-$CF_3C_6H_4COPh$	74	n, π^*	2×10^6	—
$PhCOCH_3$	72	n, π^*	1×10^6	7×10^7 [e]
4-$CH_3C_6H_4COPh$	70	π, π^*	1×10^5	—
PhCOPh	69	n, π^*	1×10^6	2×10^9 [e]
4-PhC_6H_4COPh	61	π, π^*	1×10^4	—
$CH_3COCOCH_3$	56	n, π^*	5×10^3	5×10^7 [e]
2-Acetylnaphthalene	56	π, π^*	—	$\sim 5 \times 10^5$ [d,e]
Fluorenone	~ 50(?)	π, π^*(?)	—	$\sim 10^7$ [f]
4,4′-Tetramethyldiamino-benzophenone (Michler's ketone)	~ 70	CT	$< 2 \times 10^3$ [g]	—

[a] Triplet energy in kcal/mole. Derived from phosphorescence spectroscopy.
[b] Triplet configuration. Derived from phosphorescence spectroscopy.
[c] Isopropanol as solvent.
[d] Acetonitrile as solvent.
[e] Benzene as solvent.
[f] Cyclohexane as solvent.
[g] Value for cyclohexane as hydrogen donor.
* Data from References 6, 25, and 30.

quantum yield (the quantum yield at infinite concentration of alcohol) for hydrogen abstraction is 1.0 for both ketones.[10,25] Thus, Φ_P^T and ϕ_P^T must both equal 1.0 in the limit of high concentration of isopropanol. However, the rate constants k_R for hydrogen abstraction by benzophenone ($T_1 = n, \pi^*$) versus 4-phenylbenzophenone ($T_1 = \pi, \pi^*$) differ by three orders of magnitude.[25] The limiting quantum yield of 1.0 arises because at very high concentrations of hydrogen donor all the triplets react, i.e., $k_R^T[RH] \gg \Sigma k_d^T$. At low concentration of RH, the situation is reversed. As an illustration, at $[RH] = 1\text{M}$, $\Phi_R = 1.0$ and 0.05 for benzophenone and 4-phenylbenzophenone, respectively.

Thus, benzophenone still yields pinacol efficiently when $[RH] = 1\text{M}$, but at this concentration 4-phenylbenzophenone is inefficient at producing pinacol. From the synthetic standpoint, good yields of pinacol are produced from *both* reactants because reactions of the initially produced ketyl radicals produce mainly pinacol products.

This example emphasizes the important difference between reactivity and efficiency and demonstrates the higher reactivity expected (as measured by k_R) for n, π^* states relative to π, π^* states.

Notice also from Table 10.2 that even n, π^* states may have a low reactivity when E_T is low. Thus, biacetyl ($E_T \sim 56$ kcal/mole) reacts efficiently ($\Phi_P \sim 1$) but relatively slowly ($k \sim 5 \times 10^3\ \text{M}^{-1}\ \text{sec}^{-1}$) with isopropanol.

Although π, π^* triplets of naphthyl ketones are generally unreactive toward photoreduction by alcohols and saturated hydrocarbons (presumably because of a slow rate constant for hydrogen abstraction), these same triplets are efficiently reduced by amines. For example, 2-acetonaphthone (inefficiently photoreduced by isopropanol) is efficiently photoreduced by triethylamine:[26]

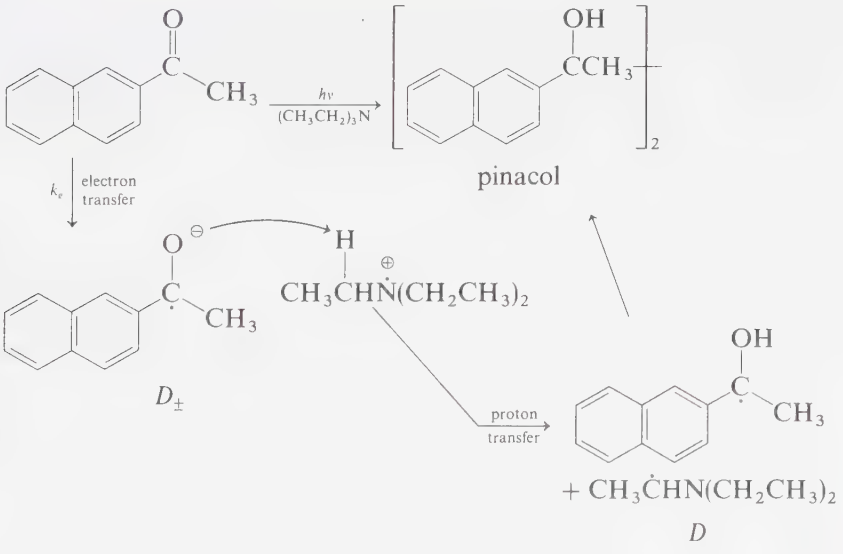

(10.35)

The details of the stereoelectronics of these photoreductions are not known, but it appears that an electron transfer (or formation of charge-transfer complex) followed by proton transfer from the radical ion $(CH_3CH_2)_3N^+$ produces ketyl radicals two of which then proceed to produce pinacol in the usual fashion.[27] The reason for the increase in efficiency is evidently due to a relatively large value of k_e, the rate constant for electron abstraction, relative to unimolecular decay of the $^3\pi, \pi^*$ states.

This example reveals an important point, namely that although π, π^* states are expected to be less reactive than n, π^* states, they may still undergo efficient photoreduction if k_e (or k_R) is comparable to k_D, i.e., the quantitative reactivity of a triplet toward photoreduction depends not only on the orbital configuration of T_1 but also on the substrate structure. For example, the rate constant for quenching of benzophenone triplets by $(CH_3CH_2)_3N$ is $\sim 2 \times 10^9\ M^{-1}\ sec^{-1}$, whereas the rate constant of quenching of naphthyl carbonyl triplets[27] by $(CH_3CH_2)_3N$ is $\sim 5 \times 10^5\ M^{-1}\ sec^{-1}$. Thus, a molecule with $T_1(n, \pi^*)$ may be quenched nearly four orders of magnitude faster than a molecule with $T_1(\pi, \pi^*)$. In this case, the crucial feature of the substrate structure is a low ionization potential, which facilitates the electron abstraction.

Can a substrate with a very weak bond to hydrogen cause the efficiency of a π, π^* state toward hydrogen abstraction to become substantial? The answer is positive. For example, naphthyl ketones are photoreduced efficiently by tin hydrides.[28a] The Sn—H bond is quite weak and therefore tin hydrides serve as substrates for photoreduction of even π, π^* triplets. In the case of 2-acetonaphthone, k_R is $\sim 10^6\ M^{-1}\ sec^{-1}$, i.e., of the order of that for benzophenone triplets with isopropanol as a substrate.[28b]

The Effect of Reactant Structure on Efficiency: State Switching[24]

Substituent or solvent effects may "switch" the electronic configuration of T_1 and T_2 states of aryl ketones, i.e., n, π^* and π, π^* may "flip-flop" energetically as a result of substituent effects on the energies of these states. In general, the energy of an n, π^* state increases with increasing solvent polarity, whereas the energy of a π, π^* state decreases with increasing solvent polarity.

In general, $k_R(n, \pi^*)$ is much larger than $k_R(\pi, \pi^*)$. In Chapter 5 it was shown that it is possible to alter the relative energetic positions of n, π^* and π, π^* states via solvent effects. Can the reactivity toward and efficiency of a photoreduction reaction also be varied by solvent-induced "state switching"? The answer is positive. Let us use the photoreduction of acetophenone to serve as a prototype of this phenomenon.

In a hydrocarbon glass at 77 K, acetophenone exhibits the short-lived, structured phosphorescence characteristic of n, π^* triplet aromatic carbonyl compounds.[24] However, in polar solvents the phosphorescence lifetime increases to ~ 1 sec, and the vibrational structure broadens significantly. It thus appears that a $^3\pi, \pi^*$ lies close enough in energy to the $^3n, \pi^*$ so that increasing solvent polarity can invert the two levels by blue-shifting the n, π^* state and by slightly red-shifting the π, π^* state.

The closeness of the n, π^* and π, π^* states of acetophenone allows both substituents and solvent to exert a dramatic influence on the reactivity and efficiency of photoreduction of acetophenone.

Acetophenone and its derivatives undergo photoreduction in isopropanol and other hydrogen-donating solvents.[29] In the case of the parent compound, the pinacol is the major product:

$$\mathrm{PhCOCH_3} + \mathrm{(CH_3)_2CHOH} \xrightarrow{h\nu} \underset{\mathrm{CH_3}}{\overset{}{\mathrm{PhCOHCOHPh}}} + \underset{\mathrm{CH_3}}{\overset{}{\mathrm{(CH_3)_2CO}}} \tag{10.36}$$

Figure 10.4 shows the triplet-triplet absorption spectrum of acetophenone in a polar and in a nonpolar solvent.[29a] The great difference in the spectra is associated with state switching. In a nonpolar solvent the spectrum is due to $T_1(n, \pi^*) \rightarrow T_n$ absorption. In a polar solvent the spectrum is due to $T_1(\pi, \pi^*) \rightarrow T_n$ absorption. The rate constant for hydrogen abstraction from isopropanol by acetophenone is $\sim 2 \times 10^6\ \mathrm{M^{-1}\ sec^{-1}}$ in benzene and $\sim 2 \times 10^5\ \mathrm{M^{-1}\ sec^{-1}}$ in acetonitrile, providing kinetic support for the state switching proposal, i.e., as T_1 takes on more π, π^* character, k_R decreases.

Notice that the T-T absorption spectrum of acetophenone in cyclohexane resembles that of 4-CF_3 acetophenone, a molecule for which T_1 is unambiguously n, π^*. Also note that the T-T absorption spectrum of 4-CH_3O acetophenone in cyclohexane ($T_1 = \pi, \pi^*$) is similar to that of acetophenone in acetonitrile. Evidently, the effect of the 4-CH_3O substituent is such that it lowers the π, π^* triplet so substantially that T_1 remains π, π^* (and unreactive) even in nonpolar solvents.

Hydroxy and amino benzophenones show substantial solvent effects on both their spectral characteristics and on their photochemical reactivities and effi-

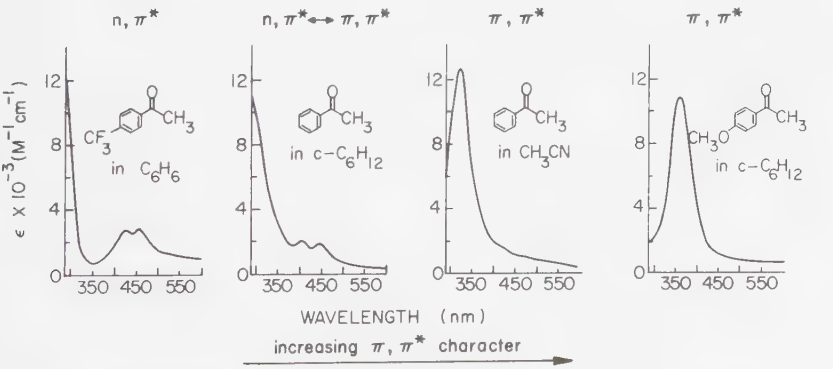

Figure 10.4
Triplet-triplet absorption spectra of some acetophenones as a function of solvent.

ciencies.[30] Table 10.3 summarizes some pertinent data. In Figure 10.5 the absorption spectrum and emission spectrum of 4-aminobenzophenone are shown.[31] Notice the large shift of the long-wavelength absorption to the red in the more polar solvent. It has been proposed that S_1 and T_1 of 4-aminobenzophenone is best classified as an n, π^* state in nonpolar solvents, and that in the polar solvents S_1 and T_1 are best classified as charge-transfer (CT) states.[30a] A charge-transfer state is one for which resonance forms such as **7** (Eq. 10.31) are a major contributor to the excited-state electronic distribution.

For example, the charge-transfer state of 4-aminobenzophenone presumably becomes the lowest-energy singlet or triplet in isopropyl alcohol.[30] Since an electron is donated from the electron-releasing group to the carbonyl group (an intramolecular electron abstraction) in the C-T state, the reactivity of the excited molecule is far less than that of an n, π^* state. On the other hand, in cyclohexane no particular stabilization of the C-T state occurs, and the n, π^* states remain lowest in energy. As a result, 4-amino[30]- and 4-hydroxybenzophenone[31] are reactive in hydrogen abstraction in cyclohexane but unreactive in isopropyl alcohol, as is shown in Table 10.3. In cyclohexane the reactive n, π^* triplet state is the lowest excited level, but in isopropanol not only is the n, π^* excitation energy raised but the energy of the charge-transfer state is lowered by solvation, so that this unreactive state becomes the triplet of lowest energy.[28b]

State switching may also occur as a hydrogen abstraction reaction proceeds, i.e., a $\pi, \pi^* \rightarrow n, \pi^*$ "state switch" is really a surface jump. An example of such a process is given in Section 10.9.

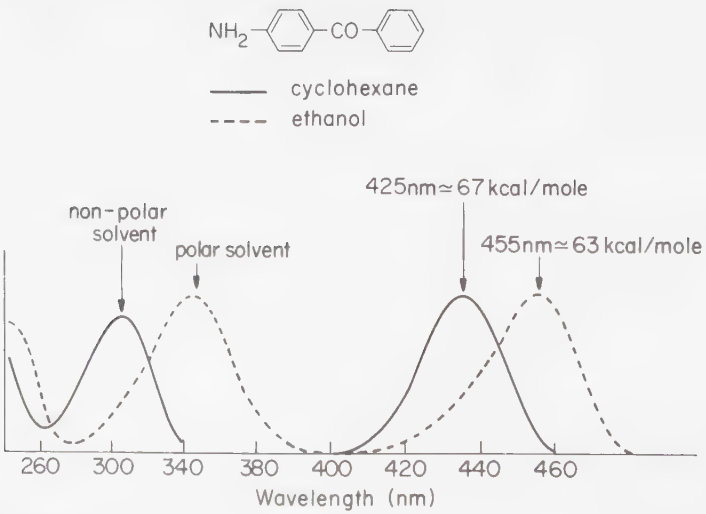

Figure 10.5

Absorption and emission spectra of 4-aminobenzophenone in polar and nonpolar solvents.

Miscellaneous Mechanisms for Suppression of Reaction Efficiency

In addition to structural- or solvent-induced "state switching" as a mechanism for suppressing the efficiency of photoreduction (basically via reduction of k_R^T in Eq. 10.33), many other possible mechanisms exist which result in a lowering of Φ_R. These may be classified as: (a) mechanisms for which Σk_d are increased relative to k_R^T, or (b) mechanisms for which ϕ_P^T is decreased. As examples of class (a) we have already noted in Eq. 10.21, a case for which a reversible intramolecular hydrogen abstraction serves to "cool off" T_1. Such a process explains why 2-methyl benzophenone is inefficiently photoreduced by isopropanol ($\Phi_R \sim 0.05$) whereas 2-tert-butyl benzophenone is reduced with nearly unit efficiency by isopropanol.[32] Self-quenching of ketone excited states is a more subtle mechanism for reducing Φ_R (see Chapter 9). Examples of class (b) might involve return of the initially formed radical pair to reactants or interception and diversion of the radical pair to other products. Inefficiencies from reactions initiated in S_1 may occur because of the surface crossing of S_0 and S_1 (Fig. 10.2) which provides a "leakage" mechanism along the reaction pathway.[9c]

10.8 Experimental Examples of the Competition between Hydrogen Abstraction and Electron Abstraction

The occurrence of *photoreduction* by an electron transfer rather than a hydrogen abstraction interaction is expected to be evidenced by the following:

1. The rate constants for photoreduction by charge-transfer are higher than those expected for radical-like hydrogen atom abstraction, based on an alkoxy radical model.

Table 10.3 Efficiencies of Photoreduction in Isopropanol and Cyclohexane Solvents[a]

Compound*	Φ_{IPA}	T_{IPA}^b	Φ_{CX}	T_{CX}^b
Benzophenone	1.0	n, π^*	0.5	n, π^*
4-Methoxybenzophenone	1.0	n, π^*	0.5	n, π^*
4-Hydroxybenzophenone	0.02	n, π^*	0.9	n, π^*
4-Aminobenzophenone	0.00	CT	0.02	π, π^*
4,4'-Tetramethyldiaminobenzophenone (Michler's ketone)	0.00	CT	0.03	π, π^*

[a] Quantum yields for disappearance of ketone. Excitation at 366 nm.
[b] Configuration of T_1 determined in isopropanol.
* Data from References 28–30.

2. The quantum yields are solvent-polarity dependent.

3. π, π^* states are more efficiently photoreduced by a hydrogen donor capable of reactivity via a charge-transfer mechanism than by hydrogen donors capable only of a hydrogen atom mechanism.

4. In favorable cases, direct spectroscopic evidence for radical cations, produced by a complete electron abstraction, is available.

Quite often, rate constants for photoreductions follow Eq. 10.37 or a related expression:[22,33]

$$\ln k_R \sim \Delta G \cong E_T + E(D/D^+) - E(A^-/A) + C \tag{10.37}$$

where ΔG is the Gibbs free energy for electron abstraction by an excited ketone, E_T is the triplet energy, $E(D\ D^+)$ is the oxidation potential of the electron donor, $E(A^-\ A)$ is the reduction potential of the ground-state ketone, and C is a measure of the Coulombic stabilization of the resultant radical ion pair. Observation of the correlation implied by Eq. 10.37 provides support for an electron-transfer mechanism. In general, $E(D\ D^+)$ correlates with ionization potential of the hydrogen or electron donor, so for a given ketone it is often found that $\ln k_R \propto IP$ (see Table 10.1, for example).

The charge-transfer interaction may assist in overcoming part of the barrier for hydrogen-atom abstraction, but may also provide alternate pathways for reaction or reversion to reactants.

In terms of surfaces, since hydrogen abstraction and electron abstraction are "topographically analogous" reactions,[9b] we expect similar substituent and environmental effects on the *reactivity* of an excited state toward either process. However, the efficiency of reaction and the types of products formed may vary.[9c] Let us suppose that photoreduction occurs and we wish to determine whether a hydrogen abstraction or an electron transfer mechanism is operating. An example of such a case occurs in the photoreduction of acetophenones by aromatic hydrocarbons.[34] The products evidently arise from radical coupling. An electron transfer or a hydrogen abstraction mechanism may be written to rationalize product formation:

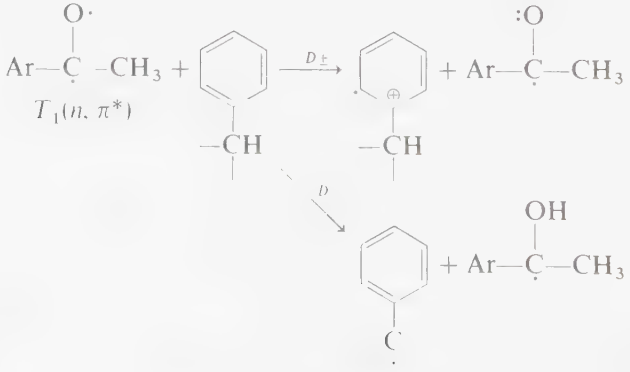

(10.38)

(10.39)

We anticipate that both the electron transfer and hydrogen abstraction processes will be favored by decreasing ionization potential of the hydrogen or electron donor.[33] However, only the hydrogen abstraction process should be sensitive to a deuterium isotope effect. Thus, if the reaction rate constant is not sensitive to replacement of C-H by C-D, the rate-determining step probably involves an electron rather than hydrogen abstraction. Furthermore, we expect that if an electron abstraction mechanism operates, the *sensitivity* of rate constants to ionization potential will be much greater than that expected for a hydrogen abstraction process.

Consider Table 10.4 which presents some data on the photoreduction of acetophenone and trifluoromethyl phenyl ketone by toluene and p-xylene.[34] The data is interpreted as follows: Hydrogen abstraction occurs when acetophenone is the reactive species and electron transfer occurs when trifluoromethyl phenyl ketone is the reactive species. This postulate is consistent with (a) the presence of a large isotope effect observed in the photoreduction of acetophenone by toluene and the absence of an isotope effect in the photoreduction of trifluoromethyl ketone, and (b) the much greater rate enhancement for the trifluoro ketone as one changes from toluene to p-xylene. The greater inefficiency of photoreduction in the case of the trifluoro ketone is interpreted to result from a rapid electron transfer (to generate ground states) in competition with proton transfer (to generate a radical pair).

Table 10.4 Deuterium isotope effects on quantum yields and quenching constants*

		Φ	k_q	
$PhCOCH_3$	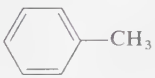	0.13	1×10^5	Small enhancement ∴ → hydrogen-abstraction mechanism
$PhCOCH_3$	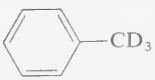	—	0.2×10^5	
$PhCOCH_3$	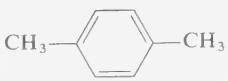	0.10	7×10^5	
$PhCOCF_3$	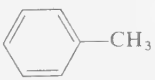	0.053	7.5×10^6	Large enhancement ∴ → electron-abstraction (*CT*) mechanism
$PhCOCF_3$	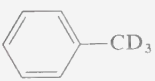	0.015	7.5×10^6	
$PhCOCF_3$	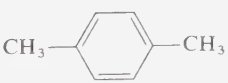	0.04	200×10^6	

* Data from Reference 31.

10.9 Intramolecular Hydrogen Abstraction: The Type II Family of Reactions

Based on the alkoxy model for n, π^* states it is expected that intramolecular hydrogen abstraction (or electron abstraction) should occur easily when achievement of a cyclic six-membered transition state is not precluded by structural constraints. Five- and seven-membered cyclic transition states are also expected to occur, but three- and four-membered transitions are highly unfavorable, based on analogy to alkoxy radical chemistry.[35]

The most commonly observed examples of photochemical intramolecular hydrogen abstractions of ketones do in fact involve cyclic six-membered transition states, and produce a 1,4-diradical (**8**) as the primary product.[36] To this stage

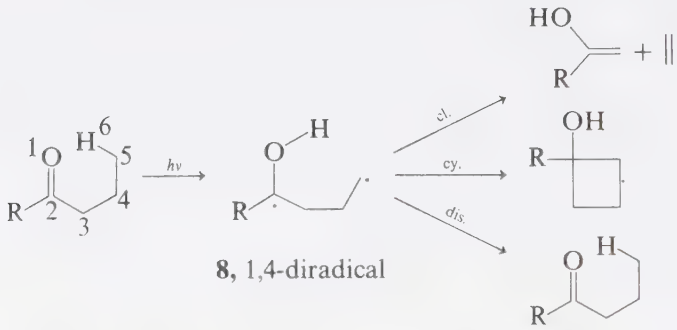

the chemistry is exactly analogous to intermolecular hydrogen abstraction. However, the *observed products* from **8** may differ substantially from those derived from intermolecular hydrogen abstraction, because of the specific chemistry available to a 1,4-diradical. The three most common reactions of a species such as **8** are *cleavage* (Eq. 10.40) to produce an enol (usually isolated as a ketone but detectable spectroscopically[36d]) and an ethylene, *cyclization* (Eq. 10.41), and *disproportionation* (Eq. 10.42) to regenerate the starting material or produce a rearranged structure. The reactions derived from **8** are termed "Type II reactions," and the formation of **8** by photoexcitation of a ketone is termed a "Type II process." The Type I process (the term was introduced by Norrish)[36b] is α-cleavage (see Chap. 13).

Intramolecular hydrogen abstraction by ketones is expected to manifest the preferred "in-plane" *n*-orbital–initiated mechanism.[37] An experimental test of this is available in the photochemistry of structurally rigid cyclohexanones. For example, irradiation of the 2,6-di-*n*-propyl cyclohexanone **9**, yields the less stable axial isomer **10**, which is relatively stable to further irradiation.[38] This result requires that the equitorial *n*-propyl side chain is more easily involved in a Type II reaction than is the axial side chain. The equitorial side chain, but not the axial side chain, is capable of achieving the required in-plane transition for hydrogen abstraction without producing severe molecular distortion.

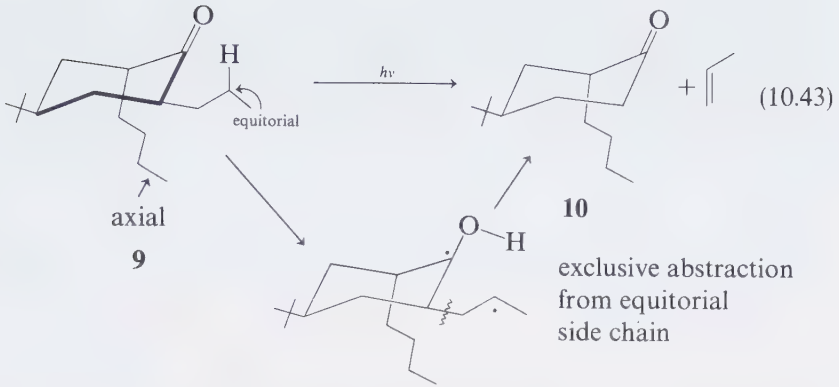

(10.43)

The six-membered transition state for hydrogen abstraction may be structurally "blocked," or non–six-membered transition states may be structurally favored. For example, irradiation of **11** (no γ-H) or of **13** (no γ-H but activated β-H) leads to formation of **12** and **14** via seven- and five-membered transition states for hydrogen abstraction.[39,40] A spectacular example is given in Eq. 10.46.

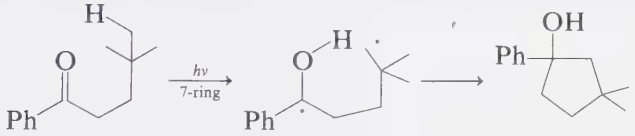

11 1,5-diradical **12**, 60%

(10.44)

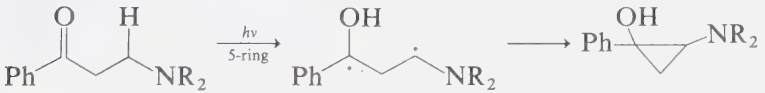

13 1,3-diradical **14**

(10.45)

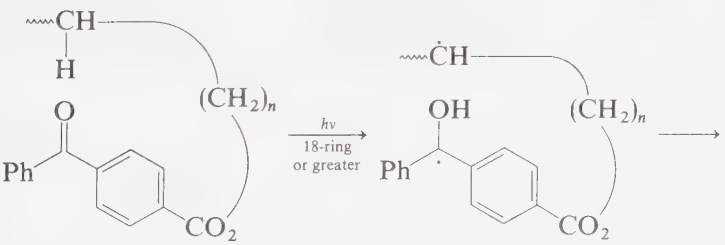

15 1,*n*-diradical

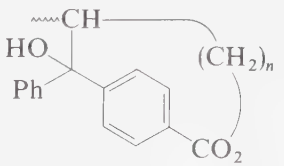

16

(10.46)

Consider the structures corresponding to **15**. For $n < 10$, the hydrogens on the hydrocarbon chain attached to the 4-carboxyl group cannot "reach" the *n*-orbital intramolecularly and achieve the required in-plane transition state. For $n \gtrsim 10$, the required transition state can be achieved and hydrogen abstraction occurs via transition states involving rings of *18 or more* atoms. For other examples of unusual ring sizes for intramolecular hydrogen abstraction, see Eqs. 10.22 and 10.23.

Structure-Reactivity and Structure-Efficiency Relationships in Type II Reactions

By analogy to the discussion of Section 10.7, the quantum yield for *net* Type II reaction from the triplet states of ketones is given by:

$$\Phi_{II} = \Phi_{ST}\left(\frac{k_R}{k_R + \sum k_d}\right)\phi_P^T \qquad (10.47)$$

Φ_{II}	Φ_{ST}	$\left(\frac{k_R}{k_R + \sum k_d}\right)$	ϕ_P^T
Quantum yield of Type II products	Intersystem crossing	Diradical formation from T_1	Efficiency of diradical to Type II products

Reactivity-structure relationships require correlation of k_R with the structure of T_1. Clearly, efficiency-structure relationships will be difficult to interpret because they reflect a product of three independent terms. From Table 10.5, it may be seen that observed values of Φ_{II} are sensitive to solvent effects[42] and not readily related to structural variations.[43] For example, for the first three ketones in Table 10.5, the value of $\Phi_{II} = 1.0$ in alcohol and ~ 0.3 to 0.4 in benzene. This lack of variation of efficiency with structure masks a large variation in k_R, which increases by nearly a factor of 10^2 in proceeding from the first to third entry. Furthermore, k_R is similar for each ketone in benzene and in alcohol solvents.

Table 10.5 Comparison of Quantum Yields and Reactivity Constants for Aryl Phenyl Ketones*

Ketone	Conf.	Φ_{II} (Type II)[a]	k_R ($\times 10^{-8}$ sec^{-1})[b]
$C_6H_5COCH_2CH_2C\underline{H}_3$	n, π^*	1.0 (0.36)	0.08
$C_6H_5COCH_2CH_2C\underline{H}_2CH_3$	n, π^*	1.0 (0.33)	1.0
$C_6H_5COCH_2CH_2C\underline{H}(CH_3)_2$	n, π^*	1.0 (0.25)	5
4-Cl—$C_6H_5COCH_2CH_2C\underline{H}_2CH_3$	n, π^*	0.8	0.3
4-CH_3O—C_6H_5—$COCH_2CH_2C\underline{H}_2CH_3$	π, π^*	0.3	0.06
4-CH_3O—C_6H_5—$COCH_2CH_2C\underline{H}(CH_3)_2$	π, π^*	—	0.03
4-CF_3—$C_6H_5COCH_2CH_2C\underline{H}_2CH_3$	n, π^*	1.0	3
$CH_3COCH_2CH_2CH_3$	$S_1(n, \pi^*)$	0.06 (0.06)	2
	$T_1(n, \pi^*)$	0.8 (0.4)	0.1
$CH_3COCH_2CH_2CH_2CH_3$	$S_1(n, \pi^*)$	0.1 (0.1)	10
	$T_1(n, \pi^*)$	0.1 (0.3)	1
$CH_3COCH_2CH_2CH(CH_3)_2$	$S_1(n, \pi^*)$	0.3 (0.3)	20
	$T_1(n, \pi^*)$	0.1 (0.9)	4

[a] Quantum yields for total Type II reactions in alcohol solvents. Values in parentheses refer to benzene solvent.
[b] Rate constants for Type II reactions. These values are roughly independent of solvent.
* Data from References 36a and 43.

These results are readily interpreted in terms of Eq. 10.47. In alcohol solvents ($\Phi_{II} = 1.0$) *all* triplets must form 1,4-diradicals, and the latter must proceed with unit efficiency to products. In benzene *all* triplets still react to form diradicals ($k_R \gg k_d$, assuming $\Sigma k_d \sim 10^5$ sec^{-1}, a value typical of phenyl alkyl ketones incapable of undergoing Type II reaction). However, ϕ_P^T must be less than unity, i.e., the diradical undergoes disproportionation to regenerate the parent ketone (Eq. 10.42) in competition with Type II reactions.

The effect of ring substituents is correlated with the "amount of n, π^* character" of T_1. For example, 4-methyoxyvalerophenone displays spectroscopic properties characteristic of a π, π^* configuration (e.g., $\tau_p \sim 100$ ms). We therefore expect that T_1 is predominantly π, π^* in character and therefore its reactivity toward hydrogen abstraction is reduced relative to valerophenone, which possesses a predominantly T_1 (n, π^*) state. From the data in Table 10.5 this is seen to be the case. On the other hand, 4-trifluoromethylvalerophenone displays spectroscopic properties typical of a predominant $T_1(n, \pi^*)$ state (e.g., $\tau_p \sim 10$ ms). We expect and find that the value of k_R should be comparable for 4-trifluoromethylvalerophenone and valerophenone itself.

This behavior is completely analogous to that discussed earlier for intermolecular hydrogen abstraction (see Section 10.7).

State Switching During Reaction

The naphthyl ketone **17** undergoes photochemical cyclization to **18** in good yield. This reaction is of interest because

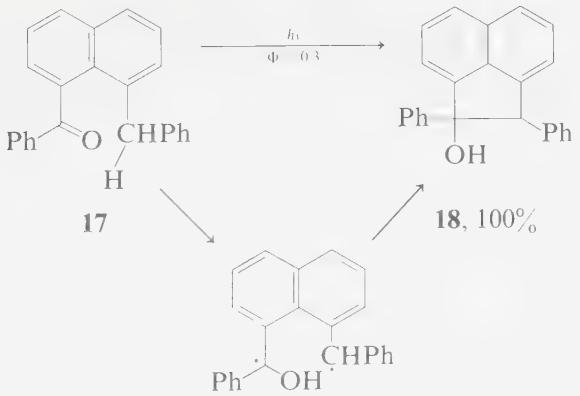

(10.48)

T_1 of **17** is shown by spectroscopy to be a typical π, π^* state and the reaction requires a seven-membered cyclic transition state for hydrogen abstraction.[44] The energy of $T_1(\pi, \pi^*)$ was found to be ~ 58 kcal/mole, while $T_2(n, \pi^*)$ was found to be ~ 67 kcal mole. Since the activation energy for reaction was found to be only ~ 5 kcal mole, the mechanism of reaction cannot involve the pathway $T_1(\pi, \pi^*) \rightarrow T_2(n, \pi^*) \rightarrow$ diradical, if we consider the spectroscopic (vertical) states. However, from correlation diagrams, the n, π^* state is expected to drop in energy and the π, π^* state is expected to rise in energy as the abstraction process proceeds.[9] Thus, at some geometry intermediate to that of reactants and diradical

product, a surface crossing (π, π^* with n, π^*) is expected. The "critical" geometry corresponding to this crossing probably represents the transition state for the reaction.

Experimental Support for 1,4-Diradicals in Type II Reactions

Analogous to the results of intermolecular hydrogen abstractions, a 1,4-diradical is expected to occur in Type II processes, and as we have seen, product structures, quantum yield data, and reactivity data are readily accommodated by postulating such a species.[45] This evidence is convincing but still quite indirect. More direct support for species such as **8** (Eq. 10.49) would rely on chemical trapping or spectroscopic observation. In other words, if a diradical such as **8** "exists," it should be capable of chemical interception and subject to observation by flash spectroscopy.

Indeed, the 1,4-diradical derived from several phenyl alkyl ketones has been intercepted chemically and has proven to be amenable to direct spectroscopic detection:

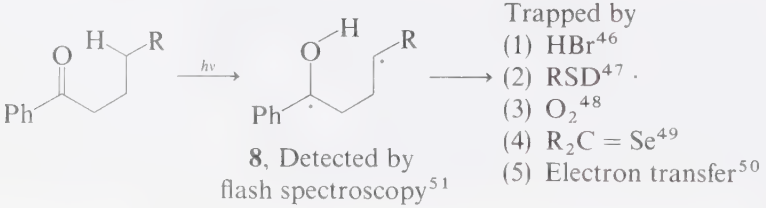

8, Detected by flash spectroscopy[51]

(10.49)

A lifetime on the order of 10^{-7}–10^{-8} sec^{-1} has been deduced for simple 1,4-diradicals of the type indicated in Eq. 10.49. This value is consistent with lifetimes determined by flash spectroscopy.[51]

Singlet and Triplet 1,4-Diradicals Derived from Type II Processes

The extremely rapid rate of intersystem crossing of aryl alkyl ketones ($k_{ST} \gtrsim 10^{10}$ sec^{-1}) precludes efficient hydrogen abstraction from S_1. Because of their longer inherent singlet lifetimes ($k_{ST} \sim 10^8$ sec^{-1}), dialkyl ketones undergo Type II processes from *both* $S_1(n, \pi^*)$ and $T_1(n, \pi^*)$ states. Such a situation allows for the generation and comparison of the chemistry of singlet and triplet diradicals.

Experimentally, it is found that the Type II products from dialkyl ketones are analogous to those found for aryl alkyl ketones. It appears that the overall chemistries of singlet and triplet 1,4-diradicals are qualitatively similar.[36a] There are quantitative differences, however. For example, a triplet 1,4-diradical usually is "stereopromiscuous" in the sense that its reactions involve a loss of initial stereochemical features. A singlet 1,4-diradical, on the other hand, reacts stereospecifically.

For example, analysis of the photochemistry of (+)-5-methyl-2-heptanone **19** suggests that both limiting cases occur for this molecule.[52] Thus, from S_1, Type

II products are observed and *no* racemization of unreacted starting material occurs. A quantitative analysis of the data reveals that more than 70% of excited S_1 states deactivate *without* the occurrence of a net observable reaction. Both the apparent S_1 inefficiency and the lack of racemization from S_1 are understandable in terms of a mechanism in which ^1D forms from S_1 and its major pathway for deactivation is reversal of the 1,5-hydrogen shift, with a minor competing pathway for ^1D deactivation being formation of Type II products.

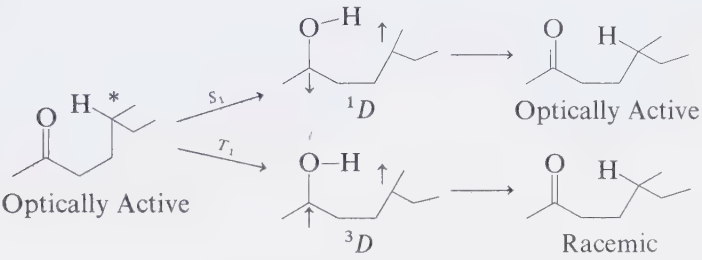

(10.50)

A model of the purely triplet diradical intermediate hypothesis is available from examination of the photochemistry of the optically active ketone (+) 4 methyl-1-phenyl-hexanone **20** (Fig. 10.6).[42a] If reversion of the diradical to the starting ketone occurs, then racemization will be expected to occur since the

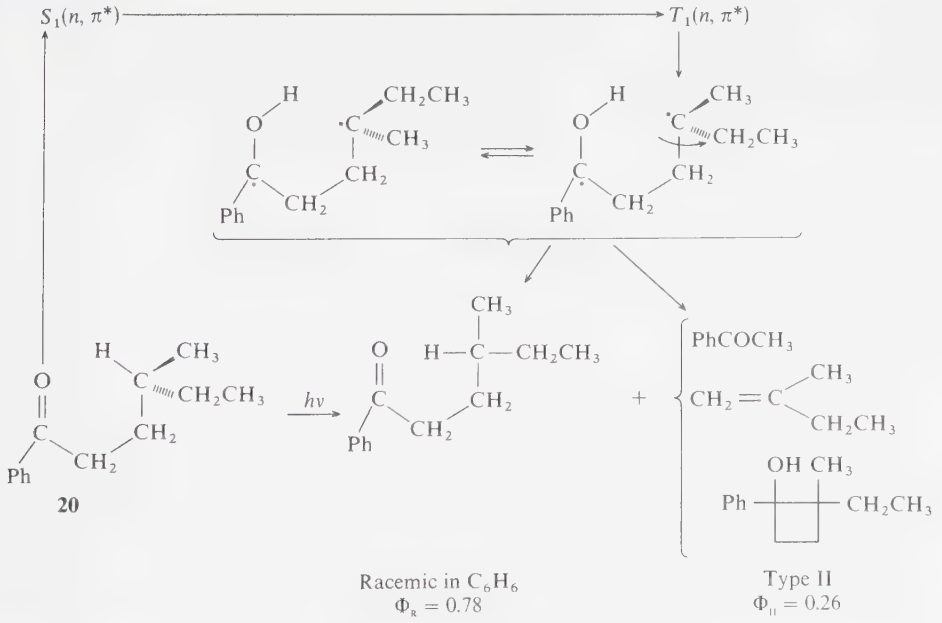

Figure 10.6

Type II and racemization reactions of 4-methyl-1-phenylhexanone.

initially produced triplet diradical should possess an appreciable lifetime during which bond rotations and racemization can occur. Indeed, when irradiated in benzene, both Type II reactions *and* racemization occur. Importantly, the sum of the quantum yield for Type II reactions plus racemization ($\Phi_{II} + \Phi_R$) is equal to 1.0. This is precisely what is expected if each diradical that forms either undergoes a Type II reaction or reverts back to its starting ketone. In the hydrogen-bonding solvent tert-butanol, the quantum yield of Type II reaction increases to 1.0. Apparently, solvation and/or hydrogen bonding slows down the reversal reaction relative to Type II processes, and every diradical formed proceeds to react to form products. In both solvents, quantum yields are determined by the reactions of the diradical and not the triplet precursor to the diradical. In other words, for Type II reactions of aryl alkyl ketones, quantum efficiency is given by $\Phi_{II} = \Phi_{ST}\phi_R^T\phi_P^T$, where Φ_{ST} = intersystem crossing quantum yield (= 1.0), ϕ_R^T = efficiency of forming the diradical from the triplet, and ϕ_P^T = efficiency of forming *products* from the diradical.

The situation for $T_1(n, \pi^*)$ of **19** is analogous. In this case, both Type II and racemization are competitive and $\Phi_{II}^T + \Phi_P^T$ (the sum of the quantum yields for triplet Type II reaction and triplet racemization) equals Φ_{ST}. Thus, as for 4-methyl-1-phenyl-1-hexanone **20**, all triplets formed react to yield ^3D and the latter (via ^1D) proceeds to both Type II and racemization products.[42a]

The diradical produced from $S_1(n, \pi^*)$ of **21** is found to lead to stereospecific ethylene formation in Type II elimination.[53] For example, the Type II elimination of the S_1 state of **21** (Eq. 10.51) is highly stereospecific, while the T_1 state of **21** shows much less stereospecificity with respect to ethylene formation:

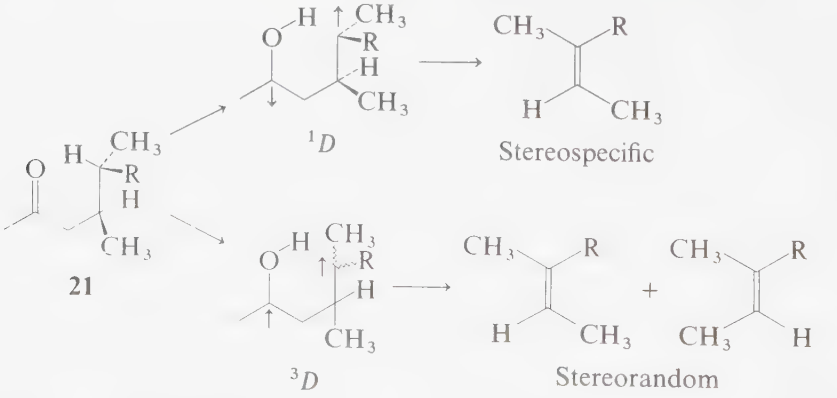

(10.51)[42]

The generalizations concerning ^1D and ^3D depend on the rates of bond rotations, spin inversion, and Type II processes. However, since a tertiary center is involved in the 1,4-diradical from **21**, its rate of rotation about its β-γ C-C bond should be as slow as any acyclic side chain, with a value of $\sim 10^7$ sec^{-1} or faster being expected.[54] We thus conclude that the rate of intersystem crossing must be of this order also.

10.10 Photochemical Hydrogen and Electron Abstraction of Carbonyl Derivatives and Unsaturated Nitrogen Compounds[55]

The general concepts developed for understanding hydrogen and electron abstraction reactions of ketones may be extended to the photochemistry of carbonyl derivatives (e.g., carboxylic acids, esters, amides, etc.) and to unsaturated nitrogen compounds (e.g., imines, azo compounds, pyridines, nitro compounds, etc.). We postulate that if T_1 may be classified as n, π^* for these compounds, then reactions derived from a primary process of hydrogen or electron abstraction should be observed. Depending on the pathways available to the primary diradicals, the *products* actually isolated may or may not appear to be analogous to the photoreduction products from ketones.

For example, azobenzene is photoreduced to **22**, and nitrobenzene is photoreduced to aniline by isopropyl alcohol (IPA):

$$\mathrm{PhN{=}NPh} \xrightarrow[\mathrm{IPA}]{h\nu} \mathrm{P\dot{N}{-}NHPh} + (\mathrm{CH_3})_2\mathrm{COH} \longrightarrow \underset{\mathbf{22}}{\mathrm{PhNHNHPh}} \qquad (10.52)^{56}$$

$$\mathrm{PhNO_2} \xrightarrow[\mathrm{IPA}]{h\nu} \mathrm{Ph{-}\dot{N}(O)(OH)} + (\mathrm{CH_3})_2\dot{\mathrm{C}}\mathrm{OH} \longrightarrow\longrightarrow \mathrm{PhNH_2} \qquad (10.53)^{57}$$

By contrast, irradiation of **23** in alcohol leads to a net substitution to yield **24**. The reaction course may be viewed as an initial hydrogen abstraction followed by coupling and elimination of HCN to yield **24**:

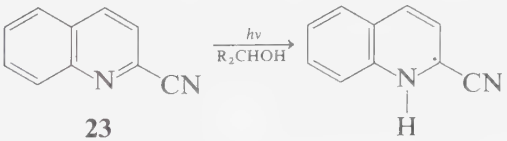

23

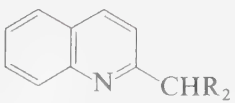

24

(10.54)[58]

Although aryl imines are reported to undergo photoreduction to amines in a reaction which looks analogous to the photoreduction of benzophenone, the excited states of the imines are *not* involved.[59] Instead, ketyl radicals (produced

by hydrogen abstraction by ketone impurities) cause a "chemical sensitization." Indeed, benzophenone is an excellent sensitizer for this reaction (Eq. 10.55).

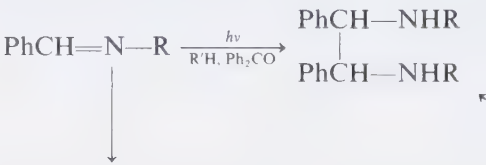

(10.55)

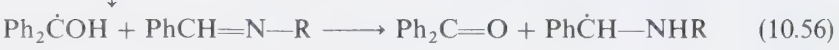

(10.56)

Intramolecular hydrogen abstraction reactions of carbonyl derivatives and unsaturated nitrogen compounds are well known. For example, irradiation of **25** yields **27**, presumably in a manner analogous to the Type II process via the intermediate species **26**:

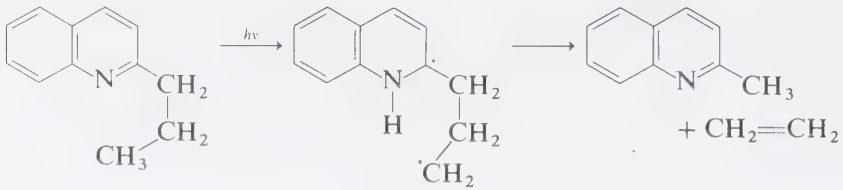

25 **26** **27**

(10.57)[60]

The intramolecular abstraction of hydrogen by nitrocompounds represents one of the earliest reported photoreactions:

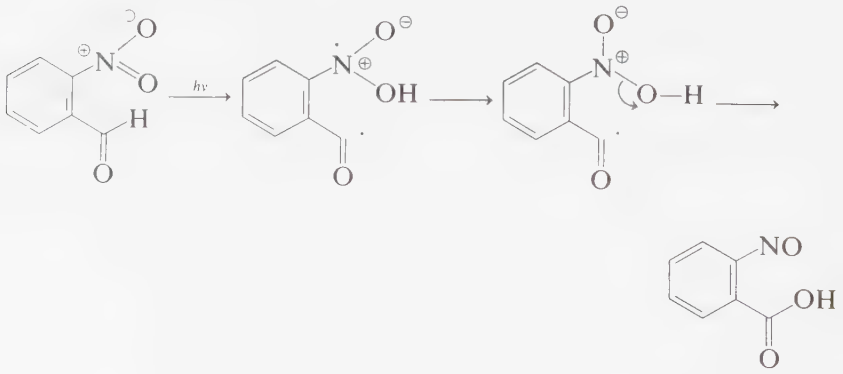

(10.58)[61]

This reaction has been usefully employed as a photosensitive blocking group for aldehydes and ketones.[62]

Reversible intramolecular hydrogen abstraction is the basis of the effectiveness of so-called "photostabilizers" which are added to plastics and polymers in order

to protect these substances from photodegradation.[63] These photostabilizers absorb light and undergo an intramolecular hydrogen abstraction to produce an unstable tautomer which then returns thermally to the original molecule:

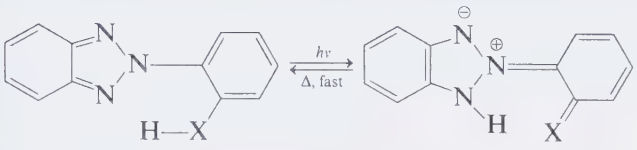

(10.59)

Reversible intramolecular hydrogen abstraction is also the basis for photochromic systems when the photoproduct possesses a different color (in the visible region) than the starting material:[64]

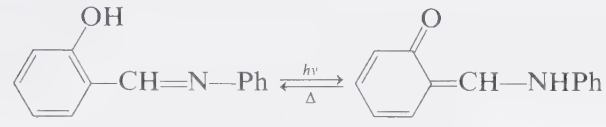

(10.60)

10.11 Addition Reactions of Acyclic Ethylenes

The photochemistry of systems involving an electronically excited ethylene is unified by the notions that: (a) for excited ethylenes, both S_1 and T_1 states possess a stabilizing twisting motion, and (b) the primary reactions of S_1 are zwitterionic or polar in nature, while those of T_1 are radicaloid in nature.[65] The ubiquitous competition of addition and cis-trans isomerization often favors the latter. In a later section we will see how structural restraints to cis-trans isomerization can tip the dynamics toward favoring addition.

Direct excitation of alkenes is expected from theory to result in a polarizable singlet, S_1, which may then convert via twisting to a metastable Z state.[65] Either of these species is anticipated to undergo ionic additions in competition with other polar reactions of S_1 and Z.

For instance, irradiation of tetramethyl ethylene in protonic solvents results in ionic addition products:[66]

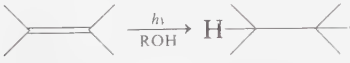

(10.61)

Although such products are expected to result from protonation or nucleophilic attack on S_1 or Z, several side products are formed which do not appear to be directly derived from the latter species. It has been proposed that an electron ejection leading to a $D_{\pm}$ species (the minus species being an electron) may occur

(Eq. 10.62). It has been proposed that the excited state involved in the direct photoexcitation of alkenes may be a "Rydberg state," rather than a π, π^* state. A Rydberg state is characterized by a very loosely bonded electron which would be expected to be easily ejected into polar solvents:[66]

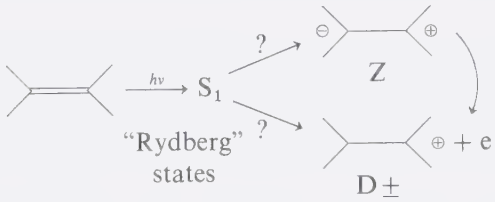

(10.62)

In addition to addition reactions, the Z species can undergo rearrangements (e.g., to carbenes). These reactions are discussed in Chapter 12.

Triplet photosensitization of acyclic ethylenes usually results in cis-trans isomerization as the major process. However, in favorable cases the expected radical addition reactions can be observed. As an illustration, direct irradiation or triplet sensitization of 1,1-diphenylethylene in isopropanol yields addition products derived from an initial hydrogen abstraction:[67]

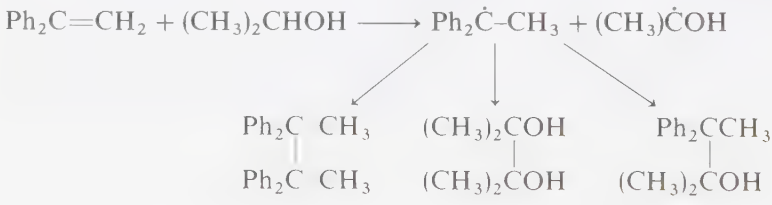

(10.63)

The zwitterionic singlet states of styrenes may be "trapped" with alcoholic solvents.[68] Thus, polar addition may be competitive with deactivation twisting of the $S_1(\pi, \pi^*)$ state, or the twisted Z species may itself add a polar trapping agent:

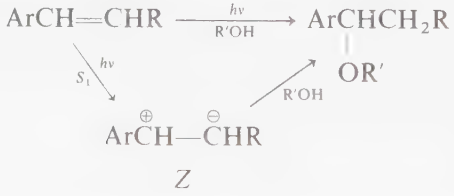

(10.64)

Ionic solvent addition analogous to Eq. 10.64 is also noted for cyclopropanes (discussed in Chap. 13).

Cyclic ethylenes undergo *both* ionic and radical addition reactions. The following generalizations have been noted:[69]

1. Three-, four-, and five-membered rings tend to undergo ionic additions upon direct excitation and radical additions upon triplet sensitized excitation.

2. Six- and seven-membered rings tend to undergo ionic additions upon direct excitation and upon triplet sensitized excitation.

3. Eight- and larger-membered rings tend to undergo ionic addition upon direct excitation and cis-trans isomerization upon triplet sensitized excitation.

A mechanistic basis for these generalizations—and a basis for understanding the scope and limitation of these reactions—is given in Figure 10.7. The primary reactions of S_1 and T_1 will always involve competition from twisting about the C=C bond and a tendency toward cis-trans isomerization.

From Figure 10.7 we see that there are five candidates for intermediates that might be involved in addition reactions: S_1, T_1, ^3D, Z, and strained trans-cycloalkene. The diradical ^1D is an energy maximum on the S_1 surface and therefore not considered to be a true intermediate of significant lifetime. We have already seen the types of chemistry expected of the excited-state species. The chemistry of strained trans-cycloalkenes is predictable from that of highly strained ethylenes.[70] Such species tend to behave as very reactive double bonds and are prone to undergo ionic reactions under mild conditions.

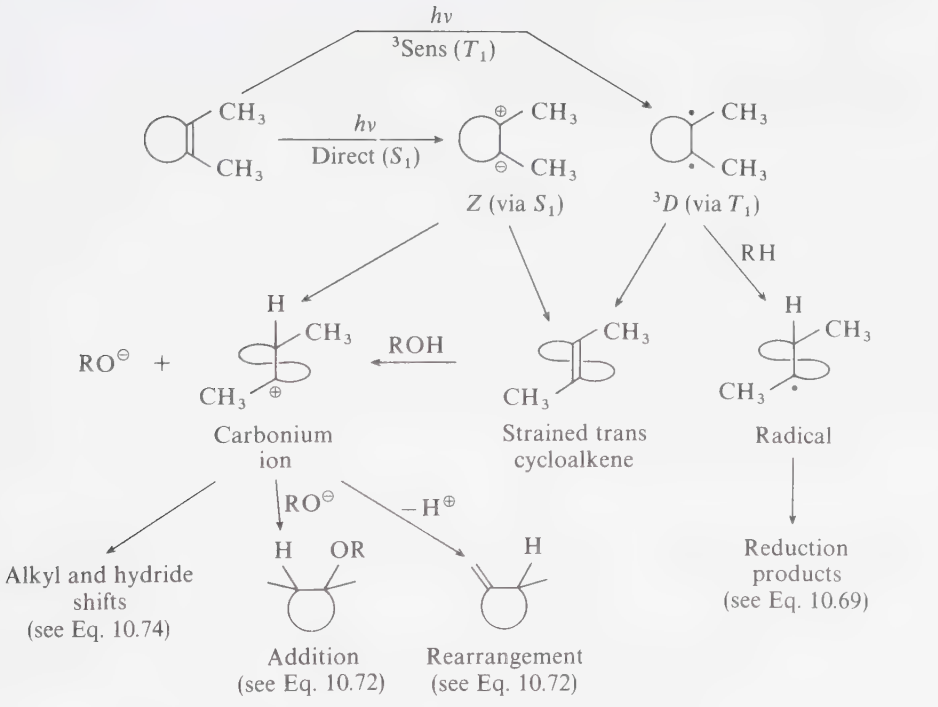

Figure 10.7

Paradigm for addition reactions of cyclic ethylenes.

If structural constraints such as ring size inhibit formation of Z or ^3D, we anticipate that trans-cyclic ethylenes will not be formed and S_1 (direct excitation) or T_1 (triplet sensitized) will be the reactive states in addition reactions. For example, the T_1 state of a small-ring ethylene will undergo radical additions to produce carbon radicals, which then go on to products.

Examples of Addition Reactions of Cyclic Ethylenes

Although cis-stilbene (**28**) shows only very weak emission, 1,2-diphenylcyclobutene (**29**) emits fluorescence with near unit efficiency in hydrocarbon solvents:[71]

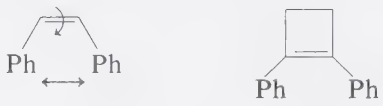

28 very weak emission

29 very strong fluorescence

(10.65)

The phenyl groups, which sterically interfere with each other in both molecules, may relieve this interference by twisting about the C=C bond of **28**, but twisting about the double bond of **29** is severely inhibited. Since $S_1 \rightarrow T_1$ crossing is generally slow for hydrocarbons, the S_1 of **29** has no dominant deactivation mode in hydrocarbon solvents, and strong fluorescence occurs.

Methanol quenches ($k_q \sim 10^8$ M^{-1} sec^{-1}) the fluorescence of **29** and ionic addition products **33** and **32** are formed:[72]

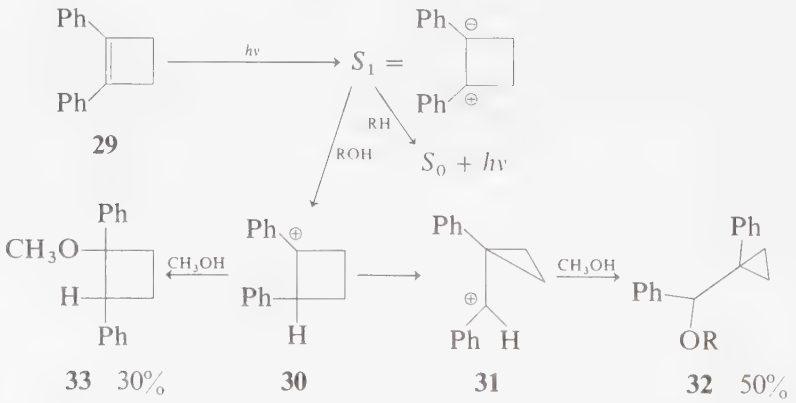

(10.66)

From our generalized scheme (Fig. 10.7) we may postulate that in methanol, S_1 (a polarizable species) is trapped as the carbonium ion, which then proceeds to yield the products **33** and **32**.

An example of contrasting singlet and triplet behavior [73] is given in Eqs. 10.67 and 10.68. Direct excitation of 1-phenylnorbornene in alcohol yields ionic adducts via attachment of a proton on S_1. Triplet sensitization of norbornenes yields a

T_1 state incapable of forming a "trans" double bond (or more strictly speaking, a trans double bond species of sufficient lifetime to be trapped). Instead, T_1 undergoes reactions expected of a radical reagent:

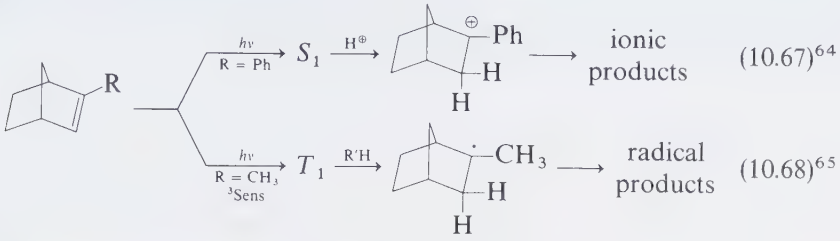

Triplet photosensitization offers a means of selectively populating the T_1 state of cyclic ethylenes. For example, by triplet sensitization xylene may be employed for the formation of triplet cyclic alkenes. Irradiation of norbornene in methanol, with xylene as sensitizer, results in radical addition products, and the expected radical coupling products and disproportionation:[74]

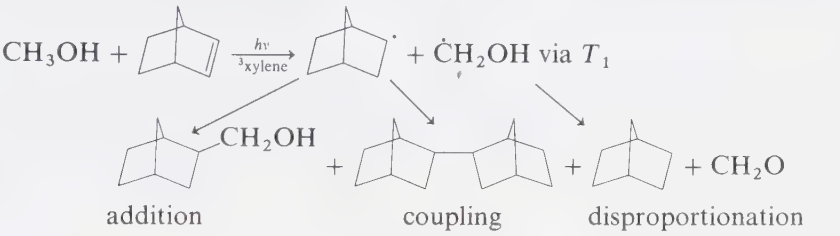

(10.69)

From our general scheme (Fig. 10.7) we may postulate that this reaction is initiated from T_1, which may be a slightly twisted species.

Irradiation of 2-phenyl cyclohexene in protonic solvents yields ionic adducts (Eq. 10.70).[74,75,76] However, the fluorescence of this compound is much weaker than that of diphenyl cyclobutene, attesting to the greater flexibility of the ring system. In the case of 2-phenyl cyclooctene,[75] no ionic adduct is formed under comparable conditions, presumably because *trans*-1-phenylcyclooctene is not sufficiently strained to provide driving force for the protonic addition of solvent (Eq. 10.70). Indeed, trans-cyclooctenes may be prepared by photosensitized excitation of cis-cyclooctenes:[76]

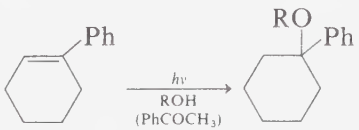

via S_1 or Z (10.70)

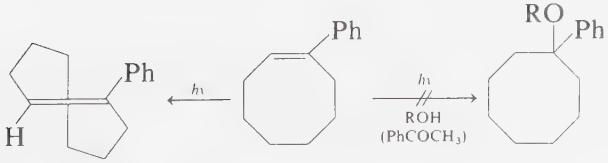

(10.71)

In contrast to the situation in which triplet sensitization produces radical-like chemistry of norbornenes,[74] triplet xylene sensitization in methanol solvent causes 1-methyl cyclohexene to undergo ionic rearrangement and solvent addition (Eq. 10.72). To explain this result we assume that a trans-cyclohexene is produced by sensitization and that this species is protonated by methanol:

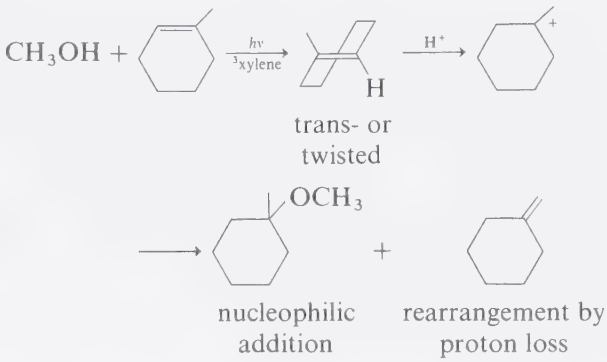

(10.72)

The triplet sensitized ionic additions are selective for cyclic six- and seven-membered rings.[74] For example, exocyclic double bonds deactivate by twisting and do not pause at a metastable trans- or twisted intermediate. Thus, the diene **34** yields only ionic addition products of the internal double bond:[78]

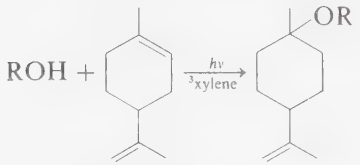

34

(10.73)

The trimethyloctalin **35** yields the *cis*-decalin **36** upon irradiation in xylene in the presence of a proton source.[79] Under the reaction conditions, **36** is irreversibly converted to the isomer **37**:

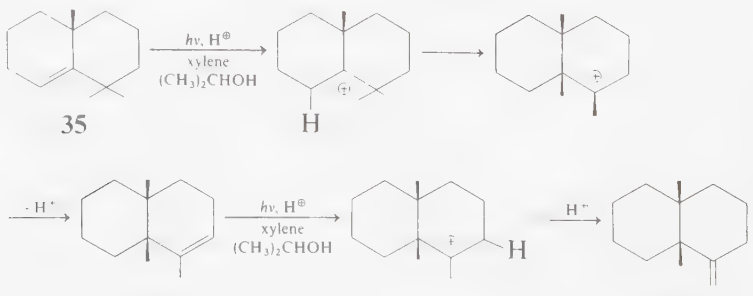

35 **36** **37**

(10.74)

An interesting example of an unusual sensitization effect has been reported in the 1-cyanonaphthalene–sensitized ionic additions to 1-phenylcycloalkenes. Direct irradiation without sensitizer did not produce significant amounts of the adducts:[80]

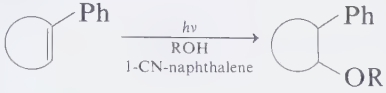

(10.75)

The proposed mechanism involves electron abstraction by the sensitizer to yield an exciplex or a radical cation of the ethylene. One of the latter species is then attacked by the solvent to yield the observed adduct.

Notice that the *orientation* of addition is in opposition to that expected on the basis of formation of the most stable carbonium ion. Formation of a radical ion pair ($D_{\pm}$) allows rationalization of these results if it is postulated that nucleophilic attack on $D_{\pm}$ occurs first, followed by electron abstraction by $D'_{\pm}$ and proton transfer:

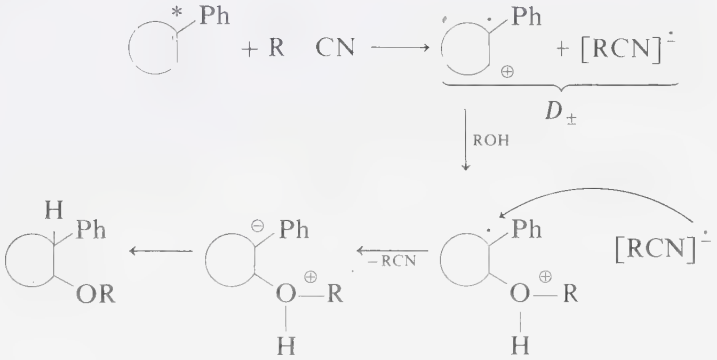

(10.76)

These reactions are examples of a novel method of *chemical* photosensitization, namely photosensitized electron transfer from an excited molecule to a ground-state "sensitizer," followed by reaction of a $D_{\pm}$ species and eventual regeneration of the sensitizer.

Addition Reactions of Cyclic Conjugated Enones

Addition reactions of conjugated enones may involve either the C—O or the C=C function. Cyclic enones may undergo an initial photoinduced isomerization to a strained trans- form, which then participates in ground-state addition reactions.

For example, irradiation of cis-2-cycloheptenone (**38**) at −160°C generates trans-2-cycloheptenone (**39**).[82,83] The latter is stable at low temperatures but reacts rapidly with alcohols at higher temperatures:[84]

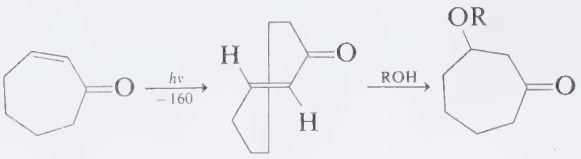

38 39 (10.77)

The overall photoreduction of the C=C bond of an enone may involve an initial hydrogen abstraction by the carbonyl oxygen of the n, π^* state, followed by a sequence analogous to that of Eq. 10.77.[85] In other cases, direct abstraction by the C=C group appears to be involved (Eq. 10.78 and 10.79). Which process occurs probably depends on whether the reactive state is n, π^* or π, π^* in nature.

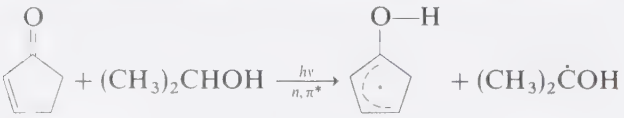

radical pair

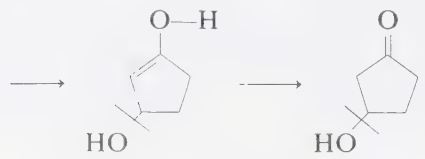

unstable enol (10.78)[86]

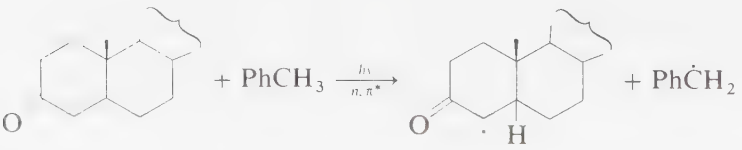

radical pair (10.79)[87]

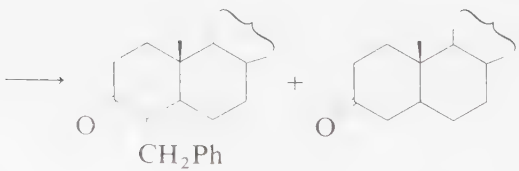

Intramolecular Hydrogen Abstraction and Protonation Reactions of Ethylenes and Enones

Intramolecular hydrogen abstraction and protonation reactions of ethylenes and enones are known. The former (but not the latter) reaction has analogy in the Type II reactions of ketones. For example, irradiation of **40** leads to **41** (a product of ionic addition) and **42** (a product of diradical fragmentation). Since **42** but not **41** is formed upon triplet sensitization, we may postulate the following mechanism for this reaction:

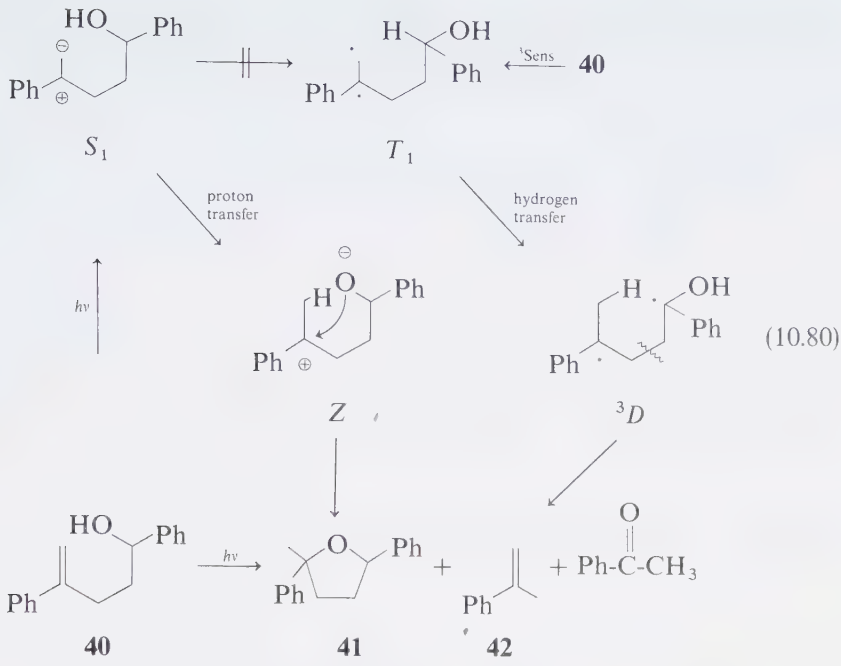

Many α,β-unsaturated enones undergo photochemical deconjugation to β,γ-enones via intramolecular hydrogen abstraction mechanisms.[89]

In certain cases, the enol produced by intramolecular hydrogen abstraction is sufficiently stable toward tautomerization that it may be isolated:[90]

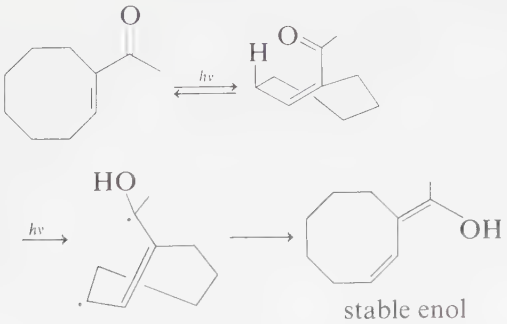

A "Type II" cyclization analogue also exists in the photochemistry of enones. For example, irradiation of the α-alkyl cyclopentenone **43** yields cyclized products **45** and **46**.[91]

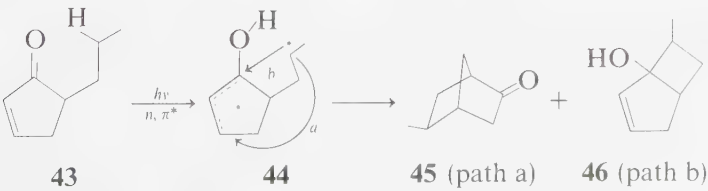

Even simple C–C bonds are capable of undergoing intramolecular hydrogen abstraction as evidenced by the photosensitized conversion of **47** to **48**.[92]

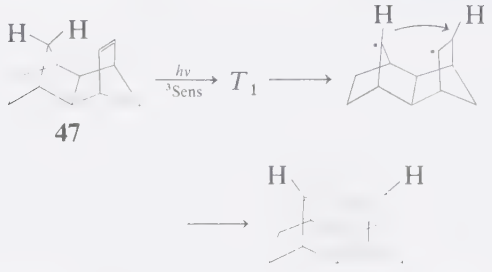

47 **48** (10.83)

10.12 Photochemical Aromatic Substitution

A number of examples of photoinduced aromatic substitution have been reported.[93] In general, nucleophilic aromatic substitutions have been more commonly observed than electrophilic aromatic substitutions. An interesting feature of photonucleophilic aromatic substitutions is the reversal of the "orientation" rules from those used to predict ground-state reactivity.

For example, strong electron-withdrawing groups (e.g., NO_2) orient incoming groups to ortho- and para- positions in thermal nucleophilic substitutions (e.g., Eq. 10.84).[93] In contrast, in photonucleophilic substitution, meta- orientation is the rule for electron-withdrawing substituents (e.g., Eq. 10.85).[94] A second contrasting feature of thermal versus photonucleophilic aromatic substitutions is the observation that strong electron-releasing substituents (e.g., CH_3O) may behave as "activating substituents" and direct incoming nucleophiles to the ortho- and para- positions (Eq. 10.86):[93]

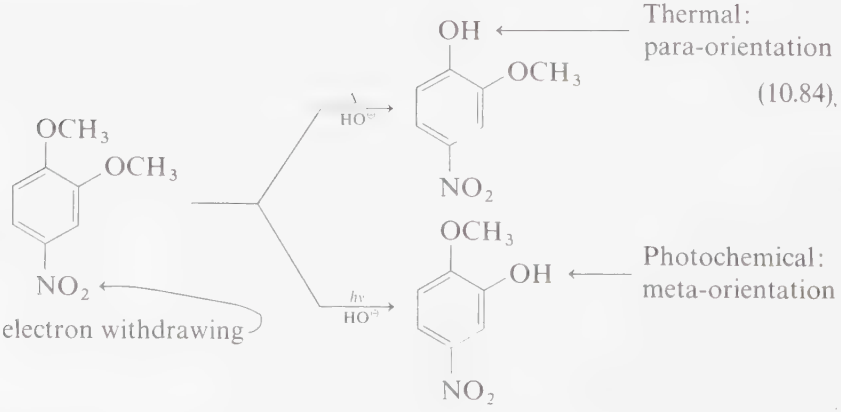

(10.85)

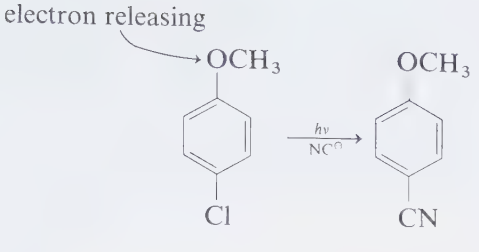

(10.86)

Moderate to weak electron-withdrawing or -releasing substituents (i.e., hydrogen) generally are not effective in promoting photonucleophilic substitutions.

In the case of naphthalenes, the 1- or α-position is strongly activated (Eq. 10.87) toward photonucleophilic substitution.[95] Indeed, even substitution of hydrogen may occur (Eq. 10.88):

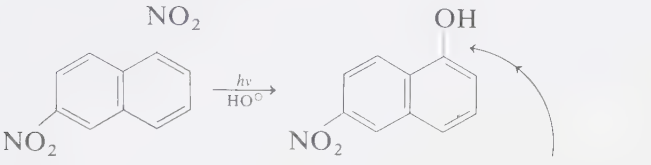

(10.87)

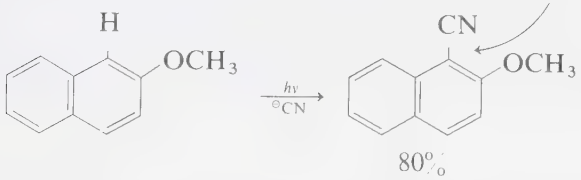

(10.88)

In summary, available experimental evidence indicates three rules for predicting the orientation of photonucleophilic aromatic substitution reactions: (a) meta-orientation of the incoming nucleophile by electron-withdrawing groups, i.e., nitro groups as in Eq. 10.85, (b) ortho-para- orientation of the incoming nucleophile by electron-releasing groups, i.e., methoxy groups as in Eq. 10.86, and (c) α orientation of the incoming nucleophile (with naphthalenes), as in Eqs. 10.87 and 10.88.

Theoretical Basis of the Orientation Rules for Photonucleophilic Aromatic Substitution

The orientation rules for photonucleophilic aromatic substitution do not explicitly consider factors that could be crucial in determining the efficiency of photosubstitution, i.e., intersystem crossing rates, specific rates of departure, leaving groups, etc. For example, in addition to being effective directing groups, alkoxy and nitro groups also serve well as leaving groups in aromatic photosubstitution.

In the case of haloaromatics, intersystem crossing followed by homolytic cleavage (especially for X = Br or I) often predominates over other mechanisms for photosubstitution (Eq. 10.89; see also 10.92).

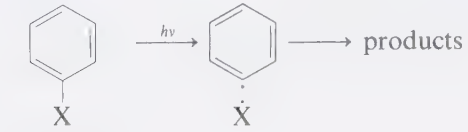

(10.89)

The meta-activation rule finds a simple rationalization in charge-density calculations which show that for both $^1\pi, \pi^*$ and $^3\pi, \pi^*$ states there is a greater positive charge meta to an electron-withdrawing group.[93,96] In valence bond language (Eq. 10.90), the excited state takes on the character of structure **49**. This probably happens directly for $^1(\pi, \pi^*)$ states and via a $D \rightarrow Z$ conversion for $^3\pi, \pi^*$ states.

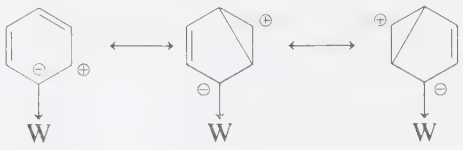

(10.90)

Mechanisms of Photonucleophilic Aromatic Substitution Reactions

Nucleophilic substitutions seem to generally involve an initiating interaction of the aromatic π, π^* triplet state and nucleophile. From a practical standpoint this suggests that when a choice exists, solvents favoring the π, π^* triplet as the T_1 state, should be employed.

From the theoretical standpoint, it is not yet clear whether a common mechanistic framework underlies these photonucleophilic substitutions.[93] In a general way, it would seem that true S_N^2 type substitutions probably occur only for aromatics substituted with electron-withdrawing groups. These reactions may proceed via a "σ-complex" of the excited aromatic and electron donor, which then ejects an originally bonded group in favor of the incoming nucleophile:

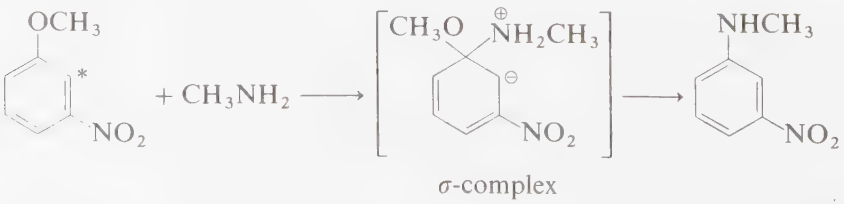

(10.91)

It is quite possible that mechanisms will exist which involve initial electron transfer followed by collapse of the radical ion pair and subsequent transformation to products. For example, the irradiation of halobenzenes in the presence of an electron source (liquid NH_3) and acetone enolate leads to good yields of phenylacetone.[97] The proposed mechanism involves the formation of the radical ion of the halobenzene, followed by unimolecular expulsion of X^- (an S_N^1 reaction) to form Ph·, which is then attacked by $CH_3\overset{\ominus}{C}OCH_2$ to form $[PhCH_2COCH_3]^{\cdot}$. The latter is a good electron donor and transfers an electron to PhX to set up a chain sequence:

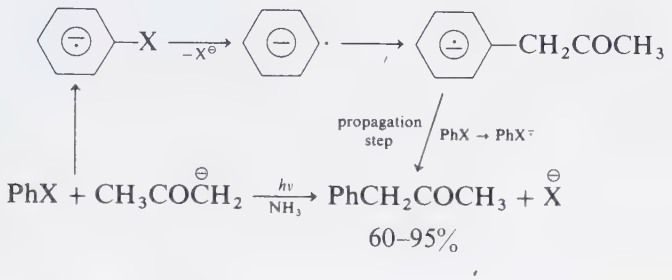

(10.92)

From such results, it seems likely that in the case of activation by electron-releasing groups, it is possible that *electron ejection* occurs, forming an aromatic radical cation which is subsequently attacked by a nucleophile. This mechanism also "explains" the general inefficiency of photoelectrophilic aromatic substitutions of aromatic molecules that possess electron-donating substituents. For example, irradiation of ortho-dimethoxybenzene in $tBuOH/H_2O$ in the presence of KCN yields 2-cyanoanisole:[93]

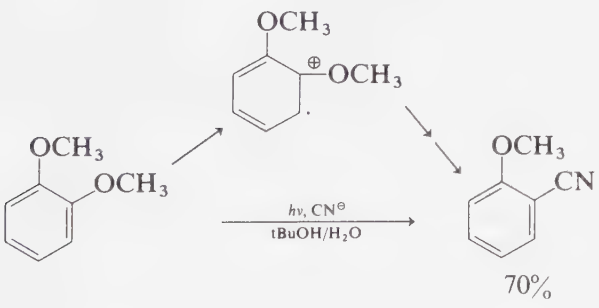

(10.93)

The mechanism may involve electron ejection to solvent, formation of the radical cation of ortho-dimethoxybenzene, which is then attacked by CN^-, followed by transformation to product.

The idea of photoinduced electron transfer followed by bond cleavage and a second electron transfer has been used to explain photoinduced nucleophilic

substitution at a *saturated* carbon atom:[98]

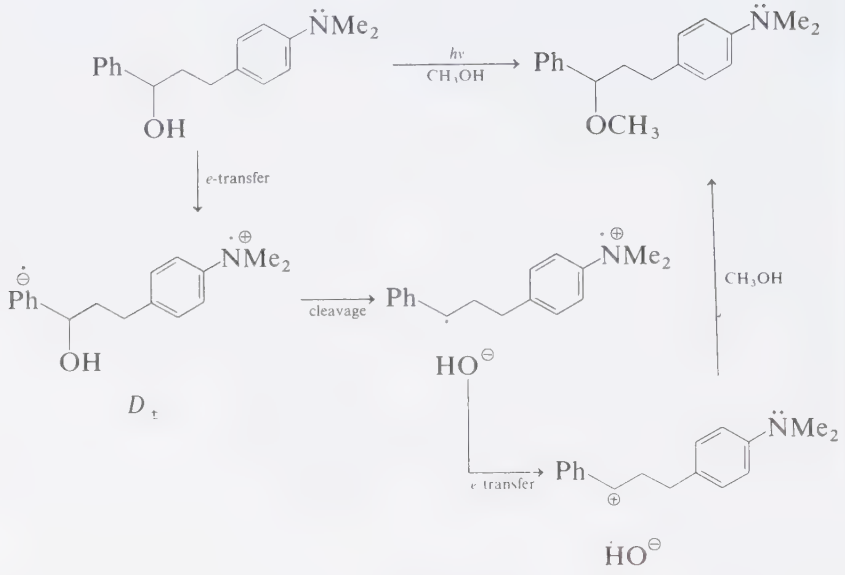

(10.94)

In Chapter 13, other mechanisms for such reactions will be discussed.

10.13 Summary

The primary process of hydrogen atom or electron abstraction occurs as an initial step in many photoreduction and photoaddition reactions. These reactions are related by the concept of an electronic charge transfer interaction that either occurs with full electron transfer (electron abstraction) or with electron abstraction concurrent with proton abstraction (net hydrogen atom abstraction). These reactions are typically diradicaloid in nature and are most commonly of the type $n, \pi^* \rightarrow D$ or $D_{\pm}$, or $\pi, \pi^* \rightarrow D$ or $D_{\pm}$. The observed products are derived from reactions of the primary products D and $D_{\pm}$.

Photoadditions may also occur via primary processes which generate a strained, reactive ground state molecule. In such cases zwitterionic (electron pair) reactions or rearrangements are often observed.

The mechanisms and theory of photoaddition reactions have been intensely investigated. As a single class of reactions, photochemical hydrogen abstraction is probably the best understood of all photoreactions. This reaction serves as a prototype for many reactions involving n, π^* states.

References

1. For a review of the synthetic applications of photoreductions, see: Schoenberg, A., *Preparative Organic Photochemistry*, New York: Springer-Verlag, 1968; Schoenberg, A., and Mustafa, A., *Chem. Rev.*, *40*, 181 (1947); Cowan, D. O., and Drisko, R. L., *Elements of Organic Photochemistry*, New York: Plenum Press, 1976, p. 75.

2. (a) Review of alkoxy radicals: Kochi, J., in *Free Radicals, Vol. II*, ed. Kochi, J., New York: John Wiley, 1973, p. 665 and references therein.
   (b) Walling, C., and Gibian, M., *J. Am. Chem. Soc.*, *86*, 3902 (1964).
   (c) Padwa, A., *Tetrahedron Letters*, 3465 (1964).
   (d) Hesse, R. H., *Adv. Free Radical Chem.*, *1*, 83 (1969).
   (e) Small, R. D., and Scaiano, J., *J. Am. Chem. Soc.*, *100*, 296 (1978).

3. Review of hydrogen abstraction by carbon radicals: Pryor, W. A., Fuller, D. L., and Stanley, J. P., *J. Am. Chem. Soc.*, *94*, 1632 (1972), and references therein.

4. Zavitsas, A. A., and Melikian, A. A., *J. Am. Chem. Soc.*, *97*, 2757 (1975). Nonhebel, D. C., and Walton, J. C., *Free Radical Chemistry*, Cambridge: Cambridge Univ. Press, 1974.

5. Bazilevskii, M. V., and Trosman, E. A., *Russ. Chem. Rev.*, *41*, 1 (1972); Nazin, G. M., *ibid.*, *41*, *711* (1972).

6. For a review of quantitative reactivity data on the intermolecular photoreduction of ketones, see: Scaiano, J. C., *J. Photochem.*, *2*, 81 (1973/74). For a general review of photoreduction mechanisms: Wagner, P. J., *Topics in Current Chemistry*, *66*, 1 (1976); Dalton, J. C., and Turro, N. J., *Ann. Rev. Phys. Chem.*, *21*, 499 (1970). General review of the photochemistry of alkanones: Turro, N. J., et al., *Acc. Chem. Research*, *5*, 92 (1972).

7. Giering, L., Berger, M., and Steel, C., *J. Am. Chem. Soc.*, *96*, 953 (1974).

8. Bennett, J. E., Eyre, J. A., Rimmer, C. P., and Summers, R., *Chem. Phys. Letters*, *26*, 69 (1974), and references therein.

9. (a) Salem, L., *J. Am. Chem. Soc.*, *96*, 3486 (1974).
   (b) Dauben, W. G., Salem, L., and Turro, N. J., *Acc. Chem. Research*, *8*, 41 (1975).
   (c) Turro, N. J., and Ramamurthy, V., *Molec. Photochem.*, *8*, 239 (1977).

10. Hammond, G. S., Moore, W. M., and Foss, R. D., *J. Am. Chem. Soc.*, *83*, 2798 (1961).

11. Bachmann, W. E., *J. Am. Chem. Soc.*, *55*, 391 (1933); Cohen, S. G., and Sherman, W. V., *ibid.*, *85*, 1642 (1963); Schenck, G. O., et al., *Ann.*, *719*, 80 (1968).

12. Schenck, G. O., and Steinmetz, R., *Naturwiss.*, *22*, 514 (1960).

13. Elad, D., *Fortschr. Chem. Forsch.*, *7*, 428 (1967); *The Chemistry of the Ether Linkage*, ed. Patai, S., New York: Wiley, 1967, p. 353.

14. Lewis, F. D., and Hirsch, R. H., *Molec. Photochem.*, *2*, 259 (1970); Darling, T. R., Turro, N. J., Hirsch, R. H., and Lewis, F. D., *J. Am. Chem. Soc.*, *96*, 434 (1974).

15. (a) Schaffner, K., and Jeger, O., *Helv. Chim. Acta.*, *46*, 1599 (1963).
   (b) Henry-Logan, K. R., and Chen, C. G., *Tetrahedron Letters*, 1103 (1973).

16. (a) Ohloff, G., et al., *Helv. Chim. Acta.*, *59*, 1140 (1976); Bernassau, J. M., and Fetizon, M., *Synthesis*, 795 (1975).
   (b) Jorgenson, M. J., and Patumtevapebal, *Tetrahedron Letters*, 489 (1970).
   (c) Yang, N. C., and Rivas, C., *J. Am. Chem. Soc.*, *83*, 2213 (1961).

17. Breslow, R., *Chem. Soc. Rev.*, *1*, 553 (1972); Breslow, R., and Baldwin, S. W., *J. Am. Chem. Soc.*, *92*, 732 (1970); Breslow, R., et al., *J. Am. Chem. Soc.*, *95*, 3251 (1973).

18. Sato, Y., et al., *J. Am. Chem. Soc.*, *98*, 2349 (1976).

19. (a) Zeldes, H., and Livingston, R., *J. Phys. Chem.*, *45*, 1946 (1966); 1465 (1967).
(b) Porter, G., and Topp, M. R., *Proc. Royal Soc.*, A315, 163 (1970).
(c) Topp, M. R., *Chem. Phys. Letters*, *39*, 423 (1976); Razi Naqvi, K., and Wild, U. P., *Chem. Phys. Letters*, *41*, 570 (1976).

20. (a) Paul, H., and Fischer, H., *Chem. Comm.*, 1038 (1971) and references therein.
(b) Hodgson, B. W., Keene, J. P., Land, E. J., and Swallow, A. J., *J. Chem. Phys.*, *63*, 3671 (1975).
(c) Laroff, G. P., and Fischer, H., *Helv. Chim. Acta.*, *56*, 2011 (1973); Henne, A., Fischer, H., *ibid. 58*, 1598 (1975).
(d) Blank, B., and Fischer, H., *Helv. Chim. Acta.*, *45*, 506 (1973).

21. Davidson, R. S., et al., *Chem. Comm.*, 732 (1969); *J. Chem. Soc.*, Perkin II, 1972 (1972); Pac, C., Mizuno, K., Tosa, T., Sakurai, H., *J. Chem. Soc.*, Perkin I, 561 (1974).

22. Gutenplan, J. B., and Cohen, S. G., *J. Am. Chem. Soc.*, *94*, 4040 (1972).

23. Charney, D. R., Dalton, J. C., Hautala, R. R., Snyder, J. J., and Turro, N. J., *J. Am. Chem. Soc. 96*, 1407 (1974); Henne, A., and Fischer, H., *J. Am. Chem. Soc.*, *99*, 300 (1977).

24. Lamola, A. A., *J. Chem. Phys.*, *47*, 4810 (1967).

25. Turro, N. J., and Lee, C. G., *Molec. Photochem.*, *4*, 427 (1972).

26. Cohen, S. G., Parola, A., and Parsons, G. H., *Chem. Rev.*, *73*, 141 (1973). For a review of photoreductions proceeding via *e*-transfer interactions, see: Davidson, R. S., *Molecular Association*, *Vol. 1*, ed. Forster, R., New York: Academic Press, 1975, p. 215.

27. Cohen, S. G., Davis, G. A., Clark, W. D. K., *J. Am. Chem. Soc.*, *94*, 869 (1972).

28. (a) Hammond, G. S., and Leermakers, P. A., *ibid.*, *84*, 207 (1962).
(b) Bell, J. A., and Linschitz, H., *J.* Am. *Chem. Soc.*, *85*, 528 (1963).

29. (a) Lutz, H., Breherdt, E., and Lindquist, L., *J. Phys. Chem.*, *77*, 1758 (1973), and references therein.
(b) Ciamician, G., and Silber, P., *Ber.*, *34*, 1530 (1901).
(c) Yang, N. C., and Dusenberg, R. L., *J. Am. Chem. Soc.*, *90*, 5899 (1968).

30. (a) Porter, G., and Suppan, P., *Trans. Faraday Soc.*, *61*, 1664 (1965); *Pure Appl. Chem.*, *9*, 499 (1964).
(b) Cohen, S. G., and Cohen, J. I., *J. Phys. Chem.*, *72*, 3782 (1968).
(c) Brown, R. G., and Porter, G., *J. Chem. Soc.*, Faraday Trans. I *73*, 1569 (1977).
(d) For an alternate interpretation of these reactions, see Schuster, D. I., Goldstein, M. D., and Bane, P., *J. Am. Chem. Soc.*, *99*, 187 (1977).
(e) Hoshino, M., and Koizumi, M., *Chem. Letters*, 189 (1972); *Bull. Chem. Soc. Japan*, *45*, 2731 (1972).
(f) Hoshino, M., and Koizumi, M., *Bull. Chem. Soc. Japan*, *45*, 3075 (1972).

31. (a) Godfrey, T. S., Porter, G., and Suppan, P., *Disc. Faraday Soc.*, *39*, 194 (1965).
(b) Hoshino, M., and Koizumi, M., *Chem. Letters*, 189 (1972).

32. (a) Becket, A., and Porter, G., *Trans. Faraday Soc.*, *59*, 2039, 2051 (1963).
(b) Review of photoenolization: Sammes, P. G., *Tetrahedron Letters*, *32*, 405 (1976).

33. Loutfy, R. O., and Loutfy, R. O., *J. Phys. Chem.*, *77*, 336 (1973); *Canad. J. Chem.*, *50*, 4052 (1972); *Canad. J. Chem.*, *50*, 3426 (1972).

34. Wagner, P. J., and Leavitt, R. A., *J. Am. Chem. Soc.*, *95*, 3669 (1973).

35. (a) Walling, C., *Pure Appl. Chem.*, *15*, 69 (1967).
(b) Barton, D. H. R., *Pure Appl. Chem.*, *16*, 1 (1968).
(c) Bazilevskii, M. V., and Trosman, E. A., *Russian Chem. Rev.*, *41*, 1 (1972).
(d) Howard, J. A., *Adv. Free Radical Chemistry*, *4*, 49 (1971).
(e) Wilt, J. W., *Free Radicals*, *Vol. I*, ed. Kochi, J., New York: Wiley, 1973, p. 333.

36. (a) Wagner, P. J., *Acc. Chem. Res.*, *4*, 1681 (1971).
(b) Norrish, R. G. W., *Trans. Faraday Soc.*, *33*, 1521 (1939).
(c) Wagner, P. J., and Hammond, G. S., *J. Am. Chem. Soc.*, *88*, 1245 (1966).
(d) Henne, A., and Fischer, H., *Angew. Chem., intern. ed. Eng.*, *15*, 435 (1976).

37. Turro, N. J., and Weiss, D. S., *J. Am. Chem. Soc.*, *90*, 2185 (1968).

38. Dawes, K., Dalton, J. C., and Turro, N. J., *Molec. Photochem.*, *3*, 71 (1971).

39. Wagner, P. J., Kelso, P. A., Kemppainen, A. E., and Zepp, R. G., *J. Am. Chem. Soc.*, *94*, 7500 (1972).

40. Roth, H. J., and El Raie, M. H., *Tetrahedron Letters*, 2445 (1970).

41. Breslow, R., Rothbard, J., Herman, F., and Rodriquez, M. L., *J. Am. Chem. Soc.*, *100*, 1213 (1978); Breslow, R., and Winnik, M., *ibid.*, *91*, 3083 (1969); Winnik, M. A., *Acc. Chem. Research*, *10*, 173 (1977); Winnik, M. A., *J. Am. Chem. Soc.*, *98*, 2929 (1976).

42. (a) Wagner, P. J., *J. Am. Chem. Soc.*, *89*, 5898 (1967).
(b) Barltrop, J. A., and Coyle, J. D., *Tetrahedron Letters*, 3235 (1968).

43. (a) Wagner, P. J., and Kemppainen, A. E., *J. Am. Chem. Soc.*, *90*, 5896, 5898 (1968).
(b) Pitts, J. N., Burley, D. R., Mani, J. C., and Broadbent, A. D., *J. Am. Chem. Soc.*, *90*, 5400 (1968).
(c) Wagner, P. J., Kemppainen, A. E., and Schott, H. N., *J. Am. Chem. Soc.*, *94*, 5604 (1973).

44. DeBoer, C. D., Herkstrocter, W. G., Marchetti, A. P., Schultz, A. G., and Schessinger, R. H., *J. Am. Chem. Soc.*, *95*, 3963 (1973).

45. Review of the chemistry of diradicals: Friedlina, R. K., and Terentev, A. B., *Russ. Chem. Rev.*, *43*, 129 (1974).

46. O'Neal, H. E., Miller, R. G., and Guderson, E., *J. Am. Chem. Soc.*, *96*, 3351 (1974).

47. Wagner, P. J., and Zepp, R. G., *J. Am. Chem. Soc.*, *94*, 287 (1972).

48. Small, R. D., and Scaiano, J. C., *Chem. Phys. Letters*, *50*, 431 (1977); *Chem. Phys. Letters*, *48*, 354 (1977).

49. Scaiano, J. C., *J. Am. Chem. Soc.*, *99*, 1494 (1977).

50. Small, R. D., and Scaiano, J. C., *J. Phys. Chem.*, *81*, 828 (1977); *J. Phys. Chem.*, *81*, 2126 (1977).

51. (a) Faure, J., Fouassier, J.-P., Lougnot, D.-J., and Salvin, R., *Nouv. J. Chim.*, *1*, 15 (1977); *J. Photochem.*, *5*, 13 (1976).
(b) Beck, G., Dobrowolski, Kiwi, J., and Schnabel, W., *Macromol.*, *8*, 9 (1975).

52. Yang, N. C., and Elliot, S. P., *J. Am. Chem. Soc.*, *91*, 7550 (1969); Yang, N. C., Elliott, S. P., and Kim, B., *J. Am. Chem. Soc.*, *91*, 7551 (1969).

53. Stephenson, L. M., Cavigli, P. R., and Parlett, J. L., *J. Am. Chem. Soc.*, *93*, 1984 (1971); Casey, C. P., and Boggs, R. A., *ibid.*, *95*, 2849 (1973); *ibid.*, *94*, 6457 (1972).

54. For a discussion of rates of rotation in radicals and diradicals: Firestone, R. A., *Tetrahedron Letters*, *33*, 3009 (1977).

55. Reviews: Frolor, A. N., Kuznetsova, N. A., and Eltsov, A. V., *Russ. Chem. Rev.*, *45*, 1024 (1976); Morrison, H., *The Chemistry of the Nitro and Nitroso Group*, ed. Feuer, H., New York: Interscience, 1969, p. 166; Dopp, D. O., *Topics in Current Chemistry*, *55*, 51 (1975).

56. Hashimota, S., and Kano, K., *Bull. Chem. Soc. Japan*, *45*, 852 (1972).

57. Ayscough, P., and Sargent, F., *Proc. Chem. Soc.*, (London), *94*, (1963); Ward, R., *J. Chem. Phys.*, *38*, 2488 (1963); Cu, A., and Testa, A. C., *J. Am. Chem. Soc.*, *96*, 1963 (1974); Capellos, C., and Porter, G., *J. Chem. Soc. Faraday Trans. II*, *70*, 1159 (1974).

58. Hata, N., and Saito, T., *Bull. Chem. Soc. Japan*, *47*, 942 (1974).

59. (a) Padwa, A., Bergmark, W., and Pashayan, D., *J. Am. Chem. Soc.*, *91*, 2653 (1969); (b) Fischer, M., *Chem. Ber.*, *100*, 3599 (1967).

60. Stermitz, F. R., and Wei, C. C., *J. Am. Chem. Soc.*, *91*, 3103 (1969).

61. Ciamician, G., and Silber, P., *Ber.*, *34*, 2040 (1901).

62. Herbert, J., and Gravel, D., *Can. J. Chem.*, *52*, 187 (1974); Zehavi, U., and Patchornik, A., *J. Am. Chem. Soc.*, *95*, 5673 (1973); Barltrop, J. A., Plant, P. J., and Schofield, R., *Chem. Comm.*, 822 (1966).

63. Morrill, J. R., and Bennett, R. G., *J. Chem. Phys.*, *43*, 1414 (1965).

64. (a) Becker, R. S., and Richey, W. F., *J. Am. Chem. Soc.*, *89*, 1298 (1967); (b) Toshima, N., Saeki, M., and Hirai, H., *Chem. Comm.*, 1424 (1971).

65. Salem, L., et al., *Angew. Chem., inter. ed. Eng.*, *14*, 575 (1975).

66. Kropp, P. J., et al., *J. Am. Chem. Soc.*, *95*, 7088 (1973).

67. Rosenberg, H. M., and Serve, P., *J. Am. Chem. Soc.*, *92*, 4746 (1970).

68. Hixson, S. S., *Tetrahedron Letters*, 277 (1973); Miyamoto, N., Kawanisi, M., and Nozaki, H., *ibid.*, 2565 (1971).

69. For reviews see: Kropp, P. J., *Pure Appl. Chem.*, *24*, 585 (1970); Marshall, J. A., *Science*, *170*, 137 (1970); Kropp, P. J., Duannes, C., and Beugelmanns, R., *Elements de Photochemie Avancée*, ed. Courtot, P., Paris: Hermann Press, 1972, p. 299.

70. Marshall, J. A., and Faubl, *J. Am. Chem. Soc.*, *89*, 5965 (1967); Wiseman, J. R., *ibid.*, *98*, 1564 (1976). Review of strained double bonds: Keese, R., *Angew. Chem., inter. ed. Eng.*, *14*, 528 (1974).

71. De Boer, C. D., and Schlessinger, R. J., *J. Am. Chem. Soc.*, *90*, 803 (1968).

72. Sakuragi, M., and Hasegawa, M., *Chem. Letters*, 29 (1974).

73. Kropp, P. J., *J. Am. Chem. Soc.*, *95*, 4611 (1973).

74. Kropp, P. J., *J. Am. Chem. Soc.*, *91*, 5783 (1969).

75. Tada, M., and Shinozaki, H., *Bull. Chem. Soc. Japan*, *43*, 1270 (1970).

76. Swenton, J. S., *J. Org. Chem.*, *34*, 3217 (1969).

77. Kropp, P. J., and Krauss, H. J., *J. Am. Chem. Soc.*, *89*, 5199 (1967).

78. Kropp, P. J., *J. Org. Chem.*, *35*, 2435 (1970).

79. Marshall, J. A., and Hochstettler, A. R., *J. Am. Chem. Soc.*, *91*, 648 (1969).

80. Shigemitsu, Y., and Arnold, D. R., *Chem. Comm.*, 407 (1975).

81. Arnold, D. R., and Maroulis, A. J., *J. Am. Chem. Soc.*, *98*, 5931 (1976).

82. Corey, E. J., Tada, M., Lamahieu, R., and Libit, L., *J. Am. Chem. Soc.*, *87*, 2051 (1965).

83. Eaton, P. E., and Lin, K., *J. Am. Chem. Soc.*, *87*, 2052 (1965).

84. Nozaki, H., M. Kurita, M., and Noyori, R., *Tetrahedron Letters*, 2025 (1968).

85. Noyori, R., Watanabe, A., and Kato, M., *Tetrahedron Letters*, 5443 (1968); Cantrell, T. S., and Solomon, J. S., *J. Am. Chem. Soc.*, *92*, 4656 (1970).

86. (a) De Mayo, P. J.-P., and Tchir, M., *Canad. J. Chem.*, *46*, 2535 (1968).
(b) Pfau, M., Dulou, R., and Vilkas, M., *Compt. Rend.*, *254*, 1817 (1962).

87. Bellus, D., and Schaffner, K., *Chimica*, *23*, 182 (1969).

88. Hornback, J. M., *J. Am. Chem. Soc.*, *96*, 6773 (1974); Reinfried, R., Bellus, D., and Schaffner, K., *Helv. Chim. Acta.*, *54*, 1517 (1971).

89. Yang, N. C., and Jorgenson, M. J., *Tetrahedron Letters*, 1203 (1964).

90. Noyori, R., Inoue, N., and Kato, M., *J. Am. Chem. Soc.*, *92*, 6699 (1970); Kropp, P. J., *J. Am. Chem. Soc.*, *89*, 3650 (1967).

91. Smith, A. B., and Agosta, W. A., *Chem. Comm.*, 343 (1971).

92. Scharf, H. D., *Tetrahedron*, *23*, 3057 (1967).

93. For reviews, see Havinga, E., and Cornelisse, J., *Pure Appl. Chem.*, *47*, 1 (1976); *Chem. Rev.*, *75*, 353 (1975); Cornelisse, J., de Grinst, G. P., and Havinga, E., *Adv. Phys. Org.*, *11*, 225 (1976); Cornelisse, J., *Pure Appl. Chem.*, *41*, 433 (1975).

94. Letsinger, R. T., and Colb, A. L., *J. Am. Chem. Soc.*, *94*, 3665 (1975).

95. Van Henegouven, G., and Havinga, E., *Rec. Trav. Chim.*, *89*, 907 (1970).

96. Zimmerman, H. E., and Sandel, V. R., *J. Am. Chem. Soc.*, *85*, 915, 922 (1963).

97. Rossi, R. A., and Bunnett, J. F., *J. Org. Chem.*, *38*, 1407 (1973). For a discussion of aromation substitutions via radical anion intermediates, see Kornblum, N., *Angew. Chem., inter. ed. Eng.*, *14*, 734 (1975).

98. Lim, C., Singh, P., and Ullman, E. F., *J. Am. Chem. Soc.*, *98*, 6711, 7848 (1976).

11

Cycloaddition Reactions

11.1 Classification of Cycloaddition Reactions[1]

A *cycloaddition* is a ring-forming addition of m atoms of one group to n atoms of another group. Thus, a *cycloadduct* is the *sum* of the individual components undergoing cycloaddition i.e., no groups are eliminated in the ring forming step:

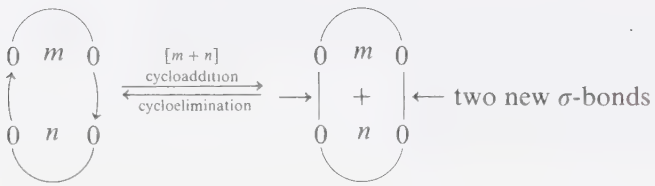

(11.1)

Most cycloaddition reactions are characterized by the formation of *two* new sigma bonds. A cycloaddition may be classified in terms of the number of atoms of each group which contribute to the final new ring that is formed. Thus, Eq. 11.1 represents a $[m + n]$ cycloaddition. The reverse reaction (a cycloelimination) is correspondingly characterized as a $[m + n]$ retrocycloaddition.

The most commonly encountered photochemical cycloadditions are of the $[2 + 2]$, $[4 + 4]$, and $[1 + 2]$ type; $[4 + 2]$ and $[3 + 2]$ types are also known but less frequently encountered.

A special group of cyclization reactions in which one new σ-bond is formed are called *electrocyclic reactions*. As an example, the photochemical electrocyclic ring closure of 1,3-butadiene to cyclobutene (Eq. 11.2) converts a $\pi^2 + \pi^2$ system into a $\pi + \sigma$ system; a net increase of one σ-bond. These reactions will be discussed in Chapter 12 as a special case of *pericyclic reactions*.

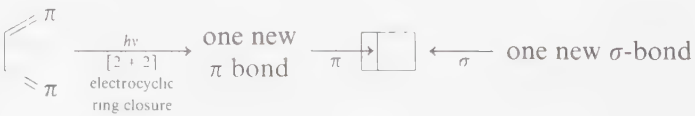

(11.2)

Cycloadditions which occur intramolecularly often generate more than one ring. Classification of these cycloadditions focuses on the atoms involved in the new ring formation. For example, Eq. 11.3 is a [2 + 2] cycloaddition and Eq. 11.4 is a [2 + 4] cycloaddition. Notice that although the cycloadditions represented in Eqs. 11.3 and 11.4 generate two rings, they still occur with formation of only two new σ-bonds (indicated by arrows in the structures).

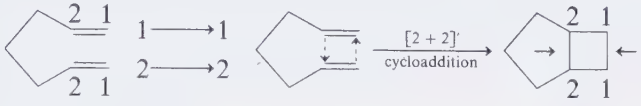

(11.3)

Two new
σ-bonds

(11.4)

Two new
σ-bonds

A special kind of stereochemistry is possible for intramolecular cycloadditions (cf. Eq. 11.3 to 11.5, and 11.4 to 11.6). In these cases the termini may bond to each other, or one terminus may bond to an internal atom. We classify the latter bonding as $x[m + n]$ because a "cross" bonding occurs. As an example, 11.5 is a $x[2 + 2]$ cycloaddition and 11.6 is a $x[2 + 4]$ cycloaddition:

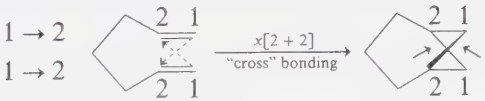

(11.5)

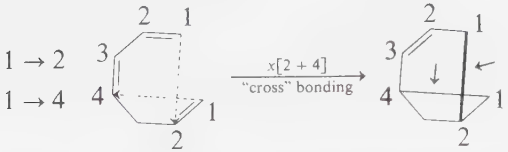

(11.6)

Note that the starting materials in Eqs. 11.3 and 11.5 (and in Eqs. 11.4 and 11.6) are identical, but that the products of [2 + 2] and $x[2 + 2]$ or of [2 + 4] and $x[2 + 4]$ cycloadditions are different.

An interesting example of the formation of two new σ-bonds is the rearrangement of 1,3-butadiene to bicyclobutane, a $x[2 + 2]$ cycloaddition (cf. Eq. 11.2). The analogous [2 + 2] reaction is in fact an electrocyclic ring closure (Eq. 11.2). Examples of $x[2 + 2]$ cycloadditions are given in Chapter 12.

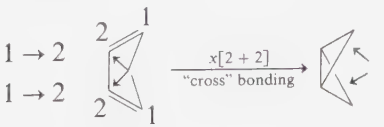

(11.7)

Stereospecificity. Suprafacial and Antarafacial Bonding. Selection Rules for Concerted Photochemical Cycloaddition Reactions

The *stereospecificity* of a cycloaddition refers to the configuration of the starting reactants relative to the possible isomeric cycloadducts. Usually one is dealing with unsaturated reactants that can possess a cis or trans configuration. In favorable cases (usually intramolecular) a strained σ bond may actively participate in a cycloaddition. If each pure configurational isomer of reactants produces a predominance of one configurational isomer of the cycloadduct, the cycloaddition is said to be *stereospecific*.

The terms *suprafacial* and *antarafacial* are employed to describe the nature of the overlap of orbitals during a cycloaddition reaction (or in general, during any pericyclic reaction). Although a detailed discussion of this point is beyond the scope of this text,[2] we note here that *suprafacial* addition refers to the situation in which both new bonds are being formed on the *same* "face" of the old bond, and *antarafacial* addition refers to the situation in which both new bonds are being formed on the *opposite* "faces" of the old bond (Eq. 11.8). For π bonds, these terms are analogous to syn (suprafacial) addition and anti (antarafacial) addition.

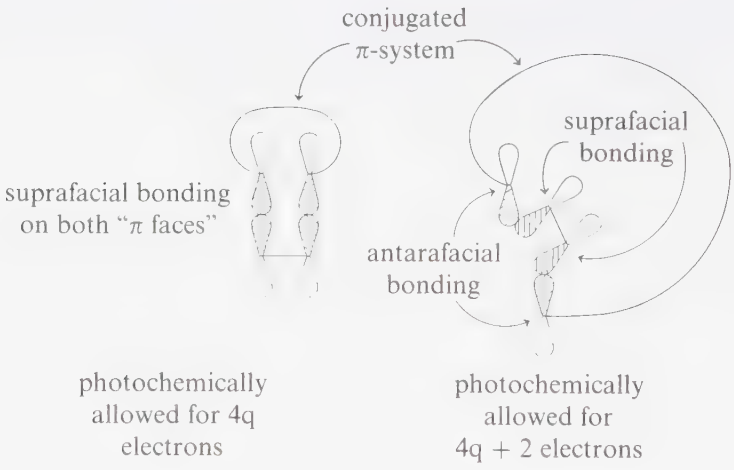

(11.8)

With respect to stereospecificity, *suprafacial* addition corresponds to *retention* of stereochemistry and *antarafacial* addition corresponds to *inversion* of stereochemistry.[2]

The notions of suprafacial and antarafacial bonding allow a general classification of the selection rules for a *concerted* cycloaddition reaction based on orbital symmetry considerations. The results are summarized in Table 11.1. The important information to be extracted from Table 11.1 is the fact that concerted photocyclo-

additions are allowed for supra-supra, supra-antara, and antara-antara cycloadditions, depending on the number of electrons involved. However, since excited singlet states generally possess very short lifetimes, it is likely that *concerted intermolecular* photocycloaddition reactions involving $4q + 2$ electrons will not be generally important for $^1\pi, \pi^*$ states (see Chapter 7 for review). It is unlikely that the geometry for an allowed reaction (the difficult achievement of supra-antara or antara-antara bonding (Eq. 11.8)) can occur during the very short singlet lifetimes of $^1\pi, \pi^*$ states. A corollary of this reasoning is that *only intermolecular photochemical concerted cycloadditions involving 4q electrons are expected to be observed, since only such cycloadditions involve the relatively easily achieved supra-supra bonding.*

In rigid, cyclic systems, if structural features are favorable, supra-antara or even antara-antara bonding may become feasible, so that the corollary must be applied carefully to such systems.[2]

11.2 Photocycloadditions via Intermediates: Diradicals, Zwitterions, and Exciplexes

Concerted photocycloaddition reactions are likely to be confined to reactions of short-lived $^1\pi, \pi^*$ states involving $4q$ electrons. Such reactions are not commonly encountered. Most photochemical cycloaddition reactions involve *intermediates* such as diradicals, zwitterions, and exciplexes.

The more generally encountered examples of photocycloadditions involve n, π^* states or a $^3\pi, \pi^*$ state as an immediate precursor to these intermediates. Three classes of diradical states may be produced from an excited state and a substrate prior to a cycloaddition:

1. A "locally excited" diradical or an exciplex (D_*), in which the structure of the diradical is best characterized by a single structure with local excitation on one partner (A*) and an unexcited substrate (B):

$$\mathrm{A}^* + \mathrm{B} \rightarrow \underset{D_*}{\dot{\mathrm{A}}\text{-----}\mathrm{B}} \qquad \text{exciplex} \tag{11.9}$$

Table 11.1 Selection Rules for Concerted Photochemical Cycloadditions

Number of electrons	Allowed	Forbidden
$4q$ ($q = 0, 1, 2, 3$, etc.)	supra-supra antara-antara	supra-antara
$4q + 2$	supra-antara	supra-supra antara-antara

An important feature of the exciplex D_* is the fact that it is an *electronically* excited state and, as such, possesses channels for electronic relaxation to lower electronic states (including emission) in addition to reaction pathways.

2. A "neutral" or conventional diradical (D) in which the structure of the diradical is best characterized by two half-filled orbitals and nonionic resonance structures. Usually D is formed by interaction of an excited molecule A* with the substrate B to produce one of the two new σ-bonds which must be made in the overall cycloaddition:

$$A^* + B \rightarrow \underset{D}{\dot{A}—\dot{B}} \qquad \text{a conventional diradical} \tag{11.10}$$

3. An "ionic" diradical or radical ion pair ($D_\pm$) in which the structure of the diradical is best characterized by two half-filled orbitals and an ion-resonance structure. Note that $D_\pm$ is *not* a zwitterion (Z) which is defined as possessing only orbitally paired electrons.

$$A^* + B \rightarrow \underset{D_\pm}{\overset{\ominus}{\dot{A}} + \overset{\oplus}{\dot{B}}} \qquad \text{radical ion pair} \tag{11.11}$$

In starting on a mechanistic analysis one should suppose that, (a) any one of the diradical pathways is possible and which one forms depends on the reaction conditions and reactant structure, and (b) the diradicals may all be reversibly interconvertible with each other and with A* + B.

For example, the reaction of n, π^* states of ketones and alkenes generally involves an initial interaction similar to Eqs. 11.9 or 11.11 followed by formation of a conventional diradical. The latter often yields a cycloadduct via cyclization or reverts to starting reagents in their ground states.

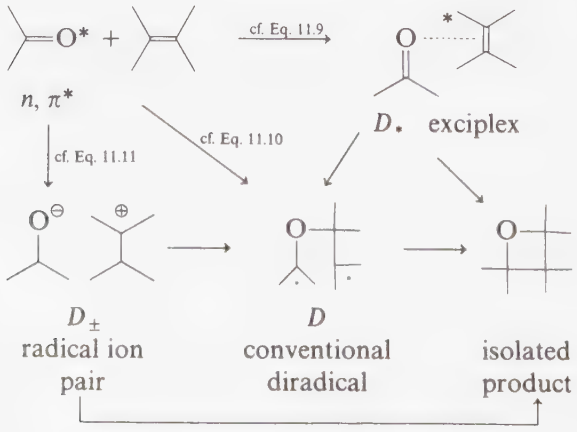

(11.12)

Intermolecular [2 + 2] Cycloaddition Reactions of Alkenes and Polyenes

Intermolecular [2 + 2] photocycloaddition reactions to form cyclobutanes typically result from attack of π, π^* states on unsaturated substrates. As a model for the type of photochemistry of π, π^* states we shall consider [2 + 2] reactions of alkenes and polyenes.[3] A paradigm for the photochemistry of alkenes and polyenes is shown in Scheme 11.1. Intersystem crossing is generally inefficient from S_1 so that triplet sensitization is required to form T_1. Both S_1 and T_1 are π, π^* in nature for alkenes and polyenes and both have a natural inclination to twist to form Z and ^3D intermediates, respectively.

The important features to remember are (a) the inherently short lifetime of S_1, its inefficient intersystem crossing to T_1, and its expected zwitterionic and/or concerted reactivity, and (b) the requirement for sensitization of T_1, its generally longer lifetime, and its expected radical-like reactivity.

Upon consideration of these points we expect that acyclic ethylenes and polyenes in general will not undergo efficient intermolecular photocycloaddition via direct excitation and that the efficiency of cycloaddition of triplet acyclic ethylenes and polyenes will depend upon both their triplet lifetimes and reactivity toward cycloaddition. Also, we expect that cyclic ethylenes and cyclic polyenes will have a better efficiency of cycloaddition than their acyclic counterparts if the ring size is small enough to inhibit twist about the C=C bond as an efficient deactivation pathway (see Sections 5.7 and 6.8).

Simple alkenes exhibit poor absorption in the spectral regions accessible to most common photochemical equipment. Since their triplet energies (see Table 8.7) are relatively high (ethylene: $E_T \sim 82$ kcal/mole, alkyl ethylenes: $E_T \sim 78$ kcal/mole), relatively few triplet sensitizers can be used to promote indirect triplet formation via triplet-triplet energy transfer. In general alkyl benzenes ($E_T \sim 80$ kcal/mole) and alkanones ($E_T \sim 78$ kcal/mole) have been employed to sensitize triplet formation

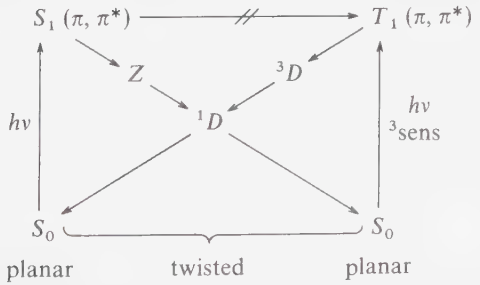

Rules:
(1) $S_1 \nrightarrow T_1$.
(2) T_1 formed from ^{3}sens.
(3) S_1 is zwitterionic.
(4) T_1 is diradicaloid.

Scheme 11.1

Paradigm for the photoreactions of alkenes and polyenes.

of alkenes. However, each type of sensitizer also tends to undergo photoreaction with the alkene in competition with energy transfer.

As an example, consider the photodimerization of 2-butene (Eqs. 11.13 and 11.14).[4] Direct irradiation ($\lambda_{ex} \sim 230$ nm) of liquid 2-butene at room temperature results mainly in cis-trans isomerization and (with a lower efficiency) cyclobutenes **1**, **2**, and **3** are formed. Irradiation of pure trans-2-butene yields only dimers **1** and **2**, while irradiation of pure cis-2-butene yields only dimers **2** and **3** (since cis-trans-isomerization is the major reaction pathway, this situation holds only for very low conversions, such that the initial stereoisomer is still present in very large excess).

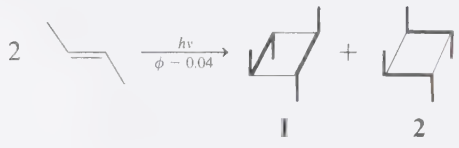

1 **2** (11.13)

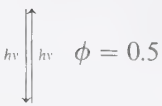

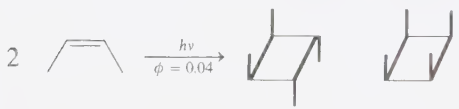

2 **3** (11.14)

Notice that **1** and **2** correspond to dimerization of two *trans*-2-butene molecules, while **2** and **3** correspond to dimerization of two *cis*-2-butene molecules. The dimerization reaction is therefore stereospecific. Of the possible mechanisms one can write for these [2 + 2] reactions, those involving long-lived Z or D intermediates directly derived from π, π^* states are unlikely because of the reaction stereospecificity. The reaction may proceed by one of the following pathways:

1. Concerted addition of $S_1(\pi, \pi^*)$ to 2-butene.

2. Formation of a singlet exciplex by interaction of $S_1(\pi, \pi^*)$ and 2-butene, followed by direct collapse to cycloadduct or by collapse to a singlet 1,4-diradical which collapses to cycloadduct faster than it loses memory of its initial stereochemistry.

In contrast to the few examples of photocycloadditions of acyclic alkenes, small- and medium-size cyclic alkenes *generally* undergo photosensitized [2 + 2] cycloadditions.[3] For example (Eq. 11.15), cyclopropenes, cyclobutenes, cyclopentenes, cyclohexenes, and cycloheptenes undergo photosensitized [2 + 2] cycloadditions and dimerizations.[3] Cyclooctenes, on the other hand, tend to

twist about the C=C bond and to undergo photosensitized cis-trans isomerization.[5]

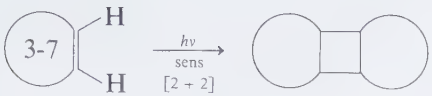

(11.15)

The mechanism of photosensitized cycloadditions generally involves triplet energy transfer from the sensitizer to form triplet cycloalkene, the latter being the reactive state in the cycloaddition. Sensitizers must be selected carefully, since few molecules possess a triplet energy comparable to simple alkenes ($E_T \sim 80$–75 kcal/mole) and reactions with photosensitizers may become significant.

As an example, consider the photosensitized dimerization of norbornene.[6] This reaction is readily effected by acetophenone as sensitizer (Eq. 11.16). However, with benzophenone as sensitizer, oxetane formation is the favored pathway (Eq. 11.17). These results are consistent with the postulate that the triplet excitation energy of norbornene is ≥ 74 kcal/mole, so that triplet energy transfer occurs with acetophenone ($E_T \sim 74$ kcal/mole) as sensitizer but not with benzophenone ($E_T \sim 69$ kcal mole) as sensitizer. In the latter case, a chemical interaction between triplet benzophenone and norbornene overrides the energy transfer process and the oxetane **4** is formed:

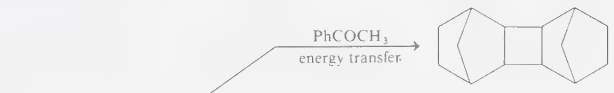

(11.16)

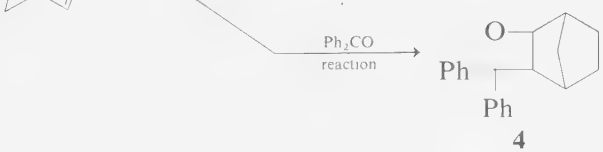

4

(11.17)

It is interesting to note that copper salts are capable of catalyzing the photodimerization of cyclic alkenes but not of acyclic alkenes.[7] It is thought that the mechanism of these reactions involves photoinduced cis-trans isomerization of a copper olefin complex to yield a highly strained and reactive trans-cyclooalkene (presumably stabilized somewhat as a copper complex). Remarkably the major [2 + 2] product, in the case of cyclohexene is a highly strained *doubly* transfused cyclobutane:

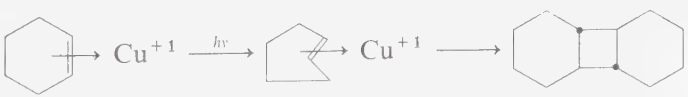

5, 50%

(11.18)

Photocycloadditions of Conjugated Polyenes

The photochemistry of conjugated polyenes (particularly 1,3-dienes) has been well studied.[8] In contrast to alkenes, the absorption spectra (max > 220 nm) of conjugated polyenes allow direct excitation to be conveniently effected and the triplet states of conjugated polyenes ($E_T < 60$ kcal/mole) are readily accessible via triplet-triplet energy transfer. Inefficient $S_1 \rightarrow T_1$ intersystem crossing (Scheme 11.1) is apparent in the photochemistry of conjugated polyenes, as it is in the photochemistry of alkenes. Different products are generally obtained via direct S_1 reaction and via triplet-photosensitized T_1 reaction excitation. In general, the S_1 states of conjugated polyenes tend to undergo intramolecular pericyclic reactions or cis-trans isomerization, while the T_1 states of conjugated dienes tend to undergo radical-like reactions.

Photosensitized Intermolecular Cycloadditions of Dienes

Because 1,3-diene triplet states are readily populated via energy transfer by a variety of photosensitizers, triplet-photosensitized excitation of dienes provides an important method for achieving the selective cycloaddition reactions of conjugated dienes.[8] Both *cyclodimerization* (Eqs. 11.19 and 11.20) and *cross-cycloaddition* (Eq. 11.21) reactions of dienes may be achieved via photosensitization:

trans + cis (11.19)[9]

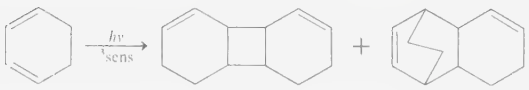

cis + anti endo + exo (11.20)[10]

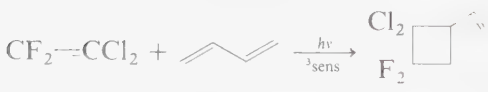

(11.21)[11]

Mechanisms of Photosensitized Cyclodimerization of 1,3-Dienes

The mechanism of photosensitized cyclodimerization of dienes is of special interest because of:

1. The important role that diene quenching of triplets played in the development of the theory of triplet-photosensitized reactions and triplet-triplet energy transfer.[9]

2. The insight into the reaction pathways and triplet structures provided by an analysis of sensitizer-energy effect on product ratios.

3. The use of photosensitized cyclodimerization as a useful synthetic reaction.

4. The use of photosensitized cyclodimerization as a method of "triplet counting" (see Chap. 8).

As an illustration of the mechanism of photosensitized cyclodimerization of 1,3-dienes, let us consider reactions 11.19 and 11.20, the photosensitized cyclodimerizations of 1,3-butadiene[9] and 1,3-cyclohexadiene,[10] respectively. A number of striking differences are observed for these two reactions:

1. The *limiting* quantum yields (e.g., the quantum yield derived from extrapolation to infinite concentration of diene) of both reactions approach a value of unity, but at lower concentrations, the quantum yield of cyclohexadiene dimerization remains at a value of unity while the quantum yield of 1,3-butadiene dimerization rapidly drops to a value much lower than unity.

2. The use of different sensitizers leads to wide variations in the relative amounts of butadiene dimers, but no corresponding variation is found in the composition of dimers from cyclohexadiene.

3. An increase in temperature produces a large (relative) increase in the amount of 4-vinylcyclohexene product formed in butadiene dimerization, but the same increase in temperature does not affect the relative yield of products from cyclohexadiene.

The data in Figure 11.1 can thus be explained as shown in Figure 11.2: Trans-diene triplets (**6**) are known to possess greater excitation energy than cis-diene triplets (**7**).[12] The trans triplets will react predominately with ground state *s*-trans-diene to yield cyclobutanes. The cis-triplet (**7**) reacts predominately with *s*-cis-butadiene to yield mainly vinylcyclohexene. All other factors being equal, both triplets are expected to react predominately with *s*-trans-butadiene because of the concentration advantage of the latter rotomer over *s*-cis-butadiene. The high-energy sensitizers transfer excitation to either *s*-cis- or *s*-trans-butadiene with comparable efficiency, and the ratio of trans- and cis-triplets produced reflects the relative concentrations of their precursors i.e., an overwhelming predominance of trans-triplets is produced and more than 95% of the dimers are cyclobutanes. However, when the energy of the sensitizer falls below 60 kcal transfer to *s*-trans-butadiene becomes measurably inefficient and relatively larger amounts of cis-triplets are formed as a result of the selective excitation of *s*-cis-butadiene molecules together with an increase of the relative yield of vinylcyclohexene. Finally, sensitizers having less than 53 kcal of excitation energy do not transfer efficiently to either isomer and non-Franck-Condon excitations (which may be governed by different rules) are possible.

In Fig. 11.1 a rather sharp cutoff in efficiency of dimerization occurs at about 54 kcal, which is also the energy reported for the $S_0 \rightarrow T$ transition of 1,3-cyclohexadiene.[12] Since butadiene exists as a mobile equilibrium mixture of s-cis- and s-trans-rotomers (the latter predominating at ordinary temperatures) the $S_0 \rightarrow T$ energy reported is that of the s-trans isomer. The value of the $S_0 \rightarrow T$

transition ($\sim$54 kcal/mole) reported for 1,3-cyclohexadiene[12] approximates the energy necessary to excite the triplet state of *s*-cis-butadiene. This situation is summarized in Figure 11.2.

Simple molecular orbital considerations for linear 1,3-butadiene predict that the first excited state of the molecule will result from excitation of an electron into an antibonding orbital between atoms 2 and 3 to an orbital which is bonding between these centers. Therefore, the lowest excited states of 1,3-butadiene are expected to have a larger barrier to rotation about the central bond in the excited state than in the ground state. The bond orders calculated for the simplest model are:[13]

$$\underset{\substack{\uparrow \quad \uparrow \\ 1.88 \quad 1.44}}{CH_2{=}CH{-}CH{=}CH_2} \xrightarrow{h\nu} \underset{\substack{\uparrow \quad \uparrow \\ 1.44 \quad 1.72}}{CH_2 \quad CH \quad CH \quad CH_2 \sim \dot{C}H_2{-}CH{=}CH \quad \dot{C}H_2} \qquad (11.22)$$

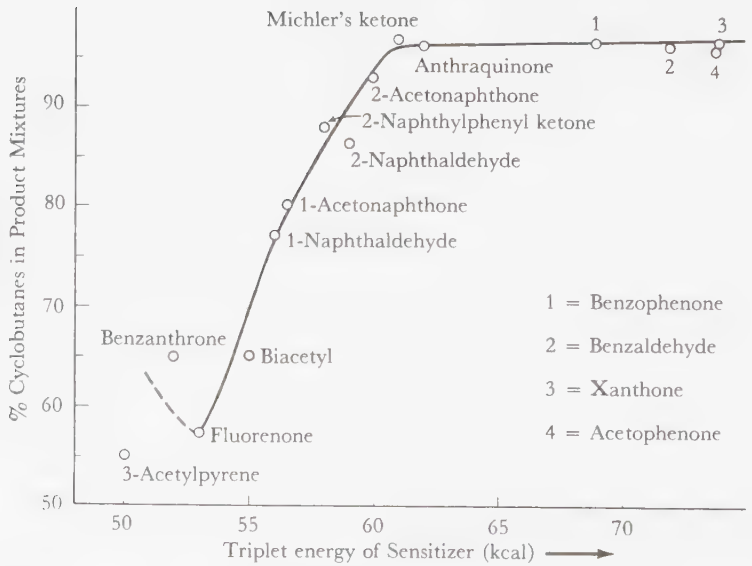

Figure 11.1

Variation of % cyclobutane products as a function of the triplet energy of the sensitizer.

Although these calculations are crude, more refined treatments also indicate that a substantial barrier to rotation about the 2-3 bond exists for the lowest excited states of butadiene.

Evidence for a barrier to rotation in allylic radicals is available from ESR studies.[4] The rate of rotation about the carbon-carbon bonds of the allyl radical $\dot{C}H_2—CH=CH_2$ was shown to be slower than $\sim 10^6$ sec^{-1} near room temperature. A free energy of activation >17 kcal/mole to rotation was found to exist.

Intramolecular Cycloaddition Reactions of Alkenes and Polyenes

From the patterns set by the intermolecular cycloadditions of alkenes and dienes, we expect that for intramolecular cycloadditions when structural constraints favor cycloaddition, reaction from both S_1 and T_1 should occur.[15]

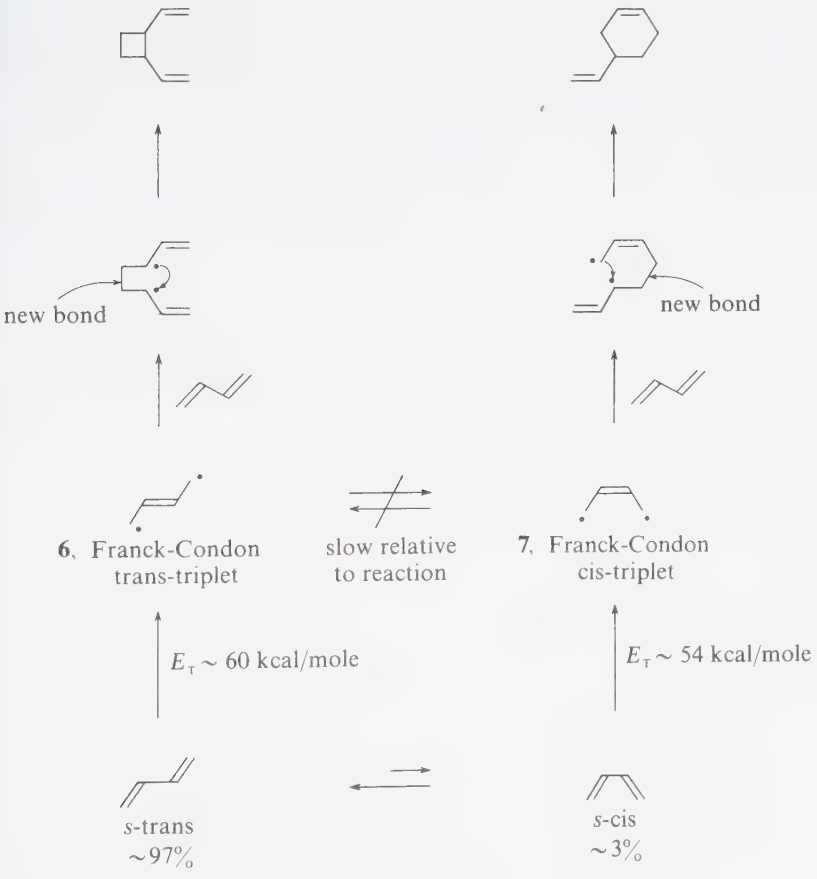

Figure 11.2
Schematic description of stereoisomeric forms of excited butadiene.

The use of an alkyl radical model provides an interesting prediction concerning intramolecular cyclizations.[16] For example, a general result of radical cyclization appears to be that if both 3- or 4-ring cyclizations are structurally possible (Eqs. 11.23 and 11.24: **8** → **9** and **8** → **10**) three-membered rings are formed faster (but reversibly).

In the case of 5 ring versus 6 ring, again the *formation of the smaller ring is kinetically favored* (Eqs. 11.25 and 11.26: **11** → **12** and **11** → **13**).

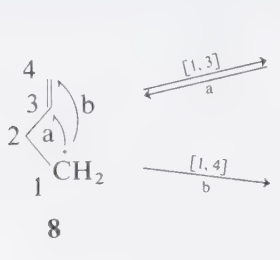

8

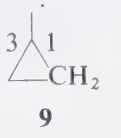

9

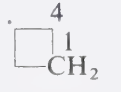

10

1,3-bonding
fast ($\sim 10^8$ sec^{-1})[16]
reversible (11.23)

1,4-bonding
slow-irreversible (11.24)

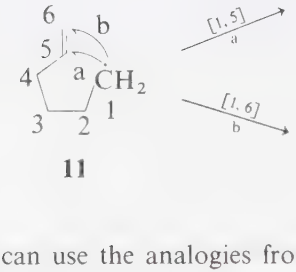

11

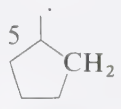

12

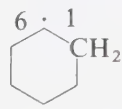

13

1,5-bonding
fast ($\sim 10^5$ sec^{-1})[16] (11.25)

1,6-bonding
slow (11.26)

We can use the analogies from radical cyclizations to anticipate the favored modes of intramolecular photocyclizations when a priori similar choices are available:

1. Formation of three-membered rings is favored to the formation of four-membered rings.

2. Formation of five-membered rings is favored to the formation of six-membered rings.

Of course, there may be special features of diradicaloid structures that result from S_1 and T_1 states which require modification of these two rules. The notion of "loose" and "tight" geometries of diradicals suggests a possible differentiation of the behavior of diradicals on excited singlet surfaces from those on triplet surfaces.[17] In Chapter 7 it was shown that on the excited singlet surface a diradicaloid structure is zwitterionic in its electronic structure, whereas the triplet is always covalent.[17] It follows that, all other factors being equal, a diradicaloid minimum on the S_1 surface will favor "tight" geometries for which the free (ionic) valences are close together in space, whereas a diradicaloid structure on the T_1 surface will favor a "loose" geometry for which the free (radical) valences are as far apart as possible:

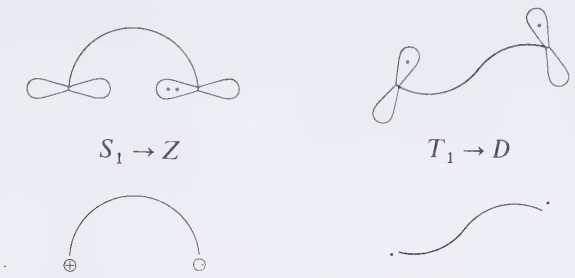

(11.27)

As an example, consider the intramolecular photocycloaddition of norbornadiene (**14** → **15**). The [2 + 2] photocycloaddition of norbornadiene to form quadricyclane may be effectively induced by *both* direct[18] and photosensitized excitation.[19] An interesting feature of this reaction is that it may be reversed by photosensitization.[20]

The diradicaloids **14** *D* and **15** *D* have been prepared by photolysis of the cyclic azoalkanes **16** and **17**.[21] It was found that S_1 of both **16** and **17** produced **14** as the major product (Eq. 11.28). These data may be interpreted in terms of qualitative surfaces for ground-state–forbidden $\pi^2 + \pi^2$ cycloadditions (Figure 11.3) since

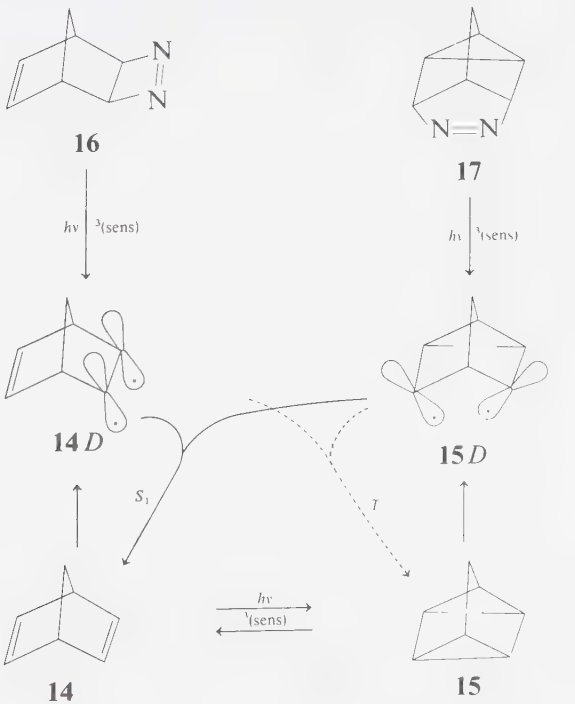

(11.28)

all forbidden ground state concerted reactions[17] have the same zero order topology as the surfaces for cis-trans-isomerization (see Section 7.7).

The minima on the S_1 and T_1 surfaces can be deduced from the notions of "tight" and "loose" geometries (Eq. 11.27). The diradicaloid **14** *D* can be better stabilized by zwitterionic contributions than the "1,3" diradicaloid **15** *D*. Conversely, a loose "1,3" diradicaloid **15** *D* will be energetically favored on T_1 (and therefore an energy minimum). Thus, placing a representative point on the S_1 surface leads to the minimum corresponding to the **14** *D* structure, irrespective of the starting geometry. From **14** *D*, internal conversion to S_0 will occur vertically and therefore favor formation of norbornadiene. Placement of a representative point on the T_1 surface leads to the minimum corresponding to the **15** *D* structure, irrespective of the intitial geometry. If intersystem crossing occurs from this geometry, formation of quadricyclene is clearly favored. The "cant" of the 1,3-orbitals in **15** *D* will also favor spin-orbit coupling and therefore facilitates intersystem crossing from the T_1 surface to the S_0.

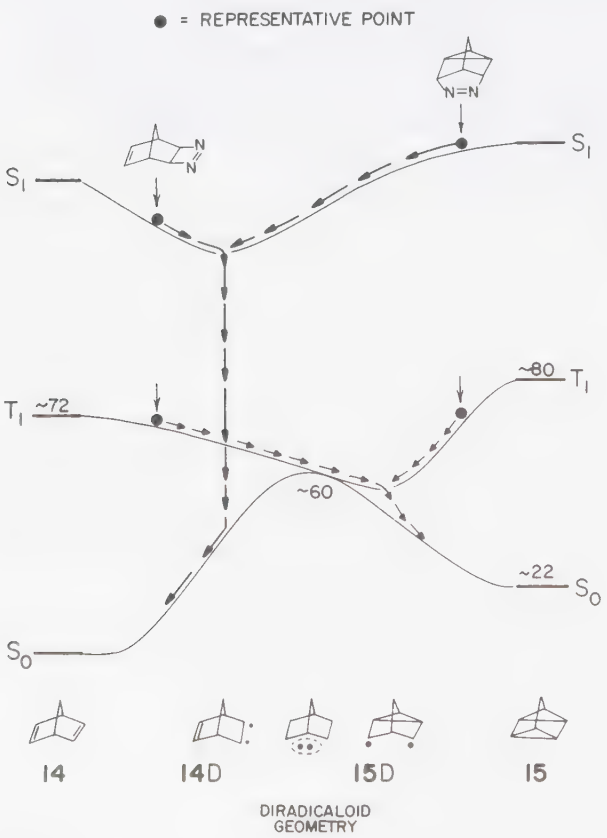

Figure 11.3

Energetics of the nonbornadiene-to-quadricyclane system.

This surface description provides a simple and accurate interpretation of the photochemistry of **16** and **17** and also allows an understanding of the low formation efficiency of **15** from **14** upon direct singlet excitation or sensitization by singlet sensitizers, and of the high efficiency of formation of **15** from **14** upon triplet photoexcitation.[21]

Among the more intriguing applications of [2 + 2] photocycloadditions are the photosensitized ring closures of **18** to **19**[23] (the latter is a precursor to basketene, **20**), and the direct closure of Dewar benzene and substituted Dewar benzenes to prismanes (**21** → **22**):[24]

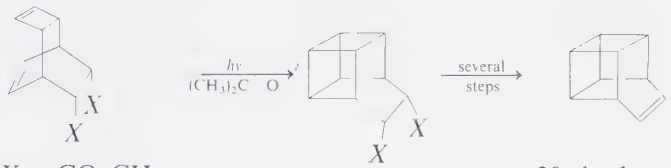

(11.29)

18, $X = CO_2CH_3$ **19**, 35% **20**, basketene

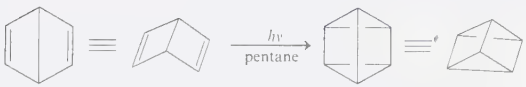

(11.30)

21, Dewar benzene **22**, prismane

Even $\sigma^2 + \pi^2$ photocycloadditions are possible if the starting molecule possesses appropriate structure features (e.g., **23** → **24**):[25]

(11.31)

23 **24**, 25%

Occasionally, cycloheptatriene derivatives are isolated from irradiation of 7-substituted norbornadienes. This situation is particularly common for norbornadienes which possess a 7-heteroatom substitutent.[26] A plausible mechanism for these rearrangements involves the sequence **25** → **26** → **27**:

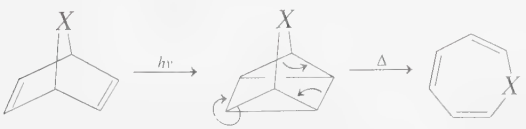

(11.32)

25 **26** **27**

A useful empirical "rule of five" has evolved for predicting the major product from triplet intramolecular photocyclizations which are free from structural constraints and which may form several sizes of rings.[27] In situations where rings

of various sizes may be formed via intramolecular triplet cyclization, in the absence of special constraints the favored ring system will be that derived from an initial 1,5 addition of the triplet to form a diradical possessing a five-membered ring. If a five-membered ring is not possible, a six-membered ring is next favored; then a four-membered ring.[28]

An example of the application of these rules is found in the photocycloaddition of the diene **28**, which undergoes quantitative cyclization to **29**:

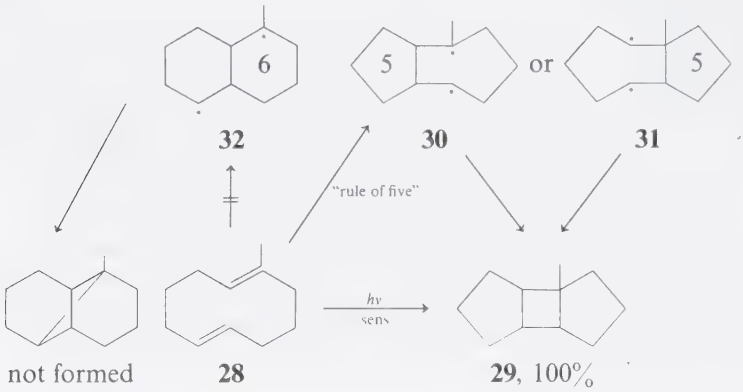

(11.33)

When two choices for five-membered rings are possible, the structure corresponding to the most stable biradical is expected to form preferentially (e.g., **30** should be preferred over **31**). This kinetic preference for formation of 5-membered rings is probably related to the known preference for cyclization of hexenyl radicals to cyclopentanes rather than cyclohexanes.[15]

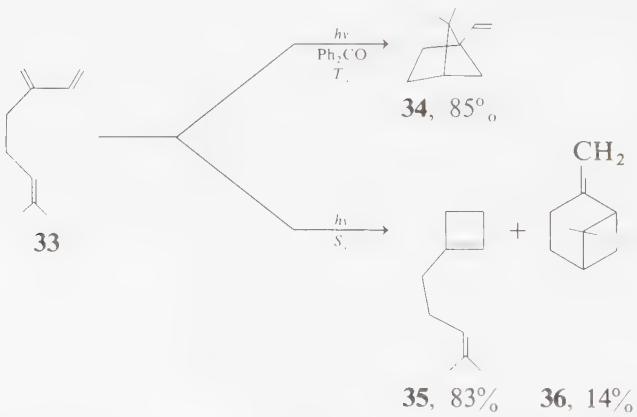

(11.34)

(11.35)

As another example of the operation of the "rule of five," consider the photoreactions of myrcene (**33**).[29] From the monoradical model we expect that, of the diradicals which might result from an attack of the diene triplet moiety on the

alkene moiety (structures **37**—**40**), five-membered rings will be formed faster.[30] This allows us to eliminate structures **39** and **40**.

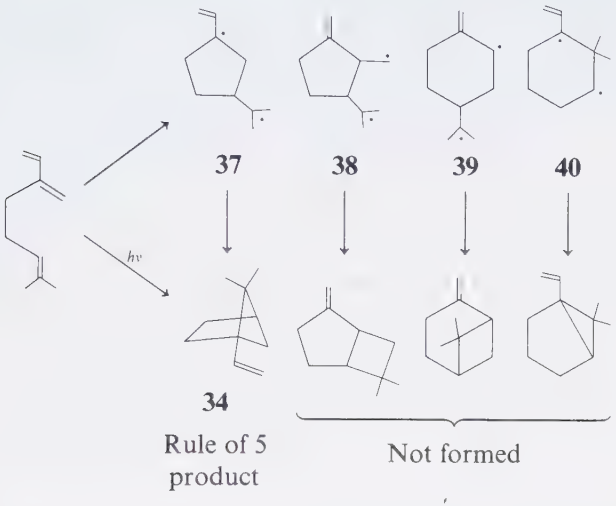

(11.36)

Next, we invoke radical stability to rank the five-membered ring diradicals and we eliminate **38** relative to **37**, since the latter enjoys both allylic and tertiary radical centers. Preferential formation of diradical **37** followed by cyclization to **34** leads to the observed product.

The constrasting behavior of S_1 and T_1 of alkenes and polyenes is also exemplified by the observation that direct excitation of myrcene (S_1 reaction) leads to entirely different products (Eq. 11.35). The major product results from electrocyclic ring closure and the minor product from an internal cyclization.[29] The mechanism of formation of the latter is not known, but from the zwitterionic model of S_1 we can speculate that a species such as **41** or **42** may be involved:

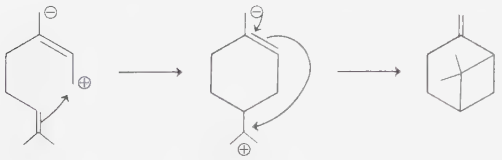

(11.37)

In this model, the difference between the favored five-ring cyclization of the triplet and the six-ring cyclization of the singlet is due to contrasting radical-versus-zwitterionic character of these states.[31] Ionic cyclizations are known to tend to favor six-ring formation.[16]

An interesting example (which provides strong support for a long-lived intermediate) is found in the observation that photosensitized triplet excitation of

either *trans*- or *cis*-3-methylene-1,5-heptadiene[43] results in a completely nonstereospecific $x[2 + 2]$ cycloaddition, i.e., the same mixture of adducts **44***a* and **44***b* is produced, irrespective of starting material (Eq. 11.38).[32] Since it was shown that the starting materials were interconverted very slowly relative to cyclization, the loss of stereospecificity must occur during the lifetime of some reactive intermediate. The mechanism shown in Eqs. 11.38–11.39 adequately explains these results and is fully consistent with our general theory of the expected behavior of $^3\pi, \pi^*$ states:

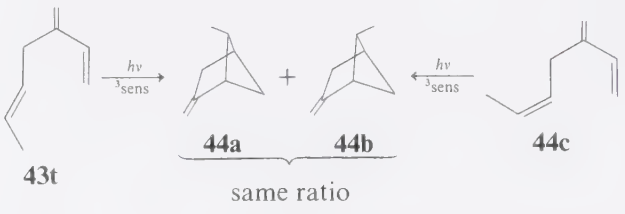

(11.38)

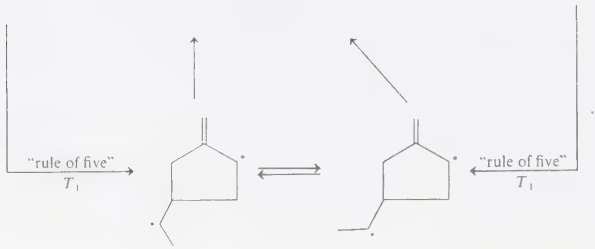

(11.39)

11.3 [2 + 2] Photocycloaddition Reactions of Carbonyl Compounds

[2 + 2] photocycloaddition of carbonyl compounds to ethylenes which yield *oxetanes* are reactions which are well known.[33] These reactions generally proceed from an attack of an n, π^* state of the carbonyl compound on an unsaturated substrate.[34] Concerted cycloaddition reactions of n, π^* states are unlikely because of the difficulty of obtaining proper cyclic overlap in the transition state.[35] As a result, [2 + 2] photocycloadditions of n, π^* states are generally expected to proceed via diradical intermediates. A simple paradigm for photochemical oxetane formation is shown in Eq. 11.12 and in Scheme 11.2. In general the following situations occur:

1. Both $S_1(n, \pi^*)$ and $T_1(n, \pi^*)$ may be involved in oxetane formation.

2. Diradical intermediates are produced either directly or indirectly from the n, π^* states and are the immediate precursors to oxetanes.

The occurrence of an exciplex or radical ion pair prior to diradical formation is possible under favorable circumstances. Also, if the unsaturated substrate possesses a lower excitation energy than the carbonyl compound, energy transfer to produce an electronically excited state of the substrate may occur. The latter process may occur via D, D_*, or $D_\pm$ states (Scheme 11.2).

Orbital Interactions and Correlation Diagrams for the Photocycloaddition of Ketones to Ethylenes

Figure 11.4 reviews the two major orbital interactions that can be expected to determine the low-energy pathways for photocycloaddition:[37]

1. An electrophilic attack initiated by the half-filled n orbital on the π electrons of the ethylene ($\pi \rightarrow n$), defined as the "perpendicular approach."

2. A nucleophilic attack initiated by the half-filled π^* orbital on the empty π^* orbital of the ethylene ($\pi^* \rightarrow \pi^*$), defined as the "parallel approach."

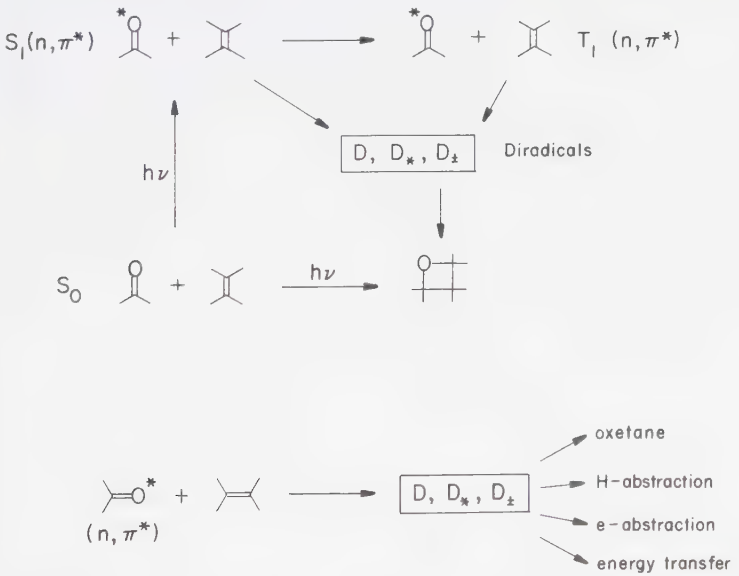

Scheme 11.2

Paradigm for interactions of n, π^* states and ethylenes. The top of the figure indicates that the interaction of $S_1(n, \pi^*)$ or $T_1(n, \pi^*)$ plus an ethylene will in general lead to a diradical intermediate (D, D_*, or $D_\pm$). The latter, which may be interconvertible, then lead to oxetane formation. The bottom of the figure indicates the connection between oxetane formation, H-abstraction, e-abstraction, and energy transfer, all of which may occur via similar orbital interactions.

Table 11.2 Quenching of Ketone n, π^* Excited States by Unsaturated Compounds

Quencher	*IP* (eV)	S_1	T_1		
		CH_3COCH_3	CH_3COCH_3	PhCOR	$CH_3COCOCH_3$
Dienes[a]					
$(CH_3)_2C{=}CH{-}\ CH{=}C(CH_3)_2$	7.5	1×10^9	5×10^9	5×10^9	5×10^8
$CH_3CH{=}CH{-}\ CH{=}\ CH_2$	8.4	1×10^8	4×10^9	5×10^9	2×10^6
Alkenes[b]					
$(CH_3)_2C{=}C(CH_3)_2$	8.1	1×10^8	5×10^7	5×10^8	4×10^6
$CH_3CH{=}CHCH_2CH_3$	9.1	4×10^7	1×10^7	5×10^7	$<10^6$
Enol ethers[c]					
$ROCH{=}CHOR$	7.4	1×10^9	1×10^9	4×10^9	2×10^9
$ROCH{=}CH_2$	8.5	3×10^7	2×10^7	8×10^7	$<1 \times 10^6$
Chloroethylenes[d]					
$CCl_2{=}CCl_2$	9.3	—	7×10^8	1×10^9	—
$CHCl{=}CHCl$	9.6	—	2×10^8	3×10^8	—
Cyanoethylenes[e]					
$CHCN{=}CHCN$	11.15	3×10^9	6×10^9	6×10^9	—
$CH_2{=}CHCN$	10.9	1×10^8	6×10^8	—	—
Benzenes[f]					
C_6H_6	9.14		2×10^6	2×10^4	$<10^3$
C_6F_6	10.0	—	2×10^7	—	—

[a] Data from References 61, 65, and 66.
[b] Data from Reference 61
[c] Data from Reference 49.
[d] Data from Reference 61.
[e] Data from References 51 and 52.
[f] Data from Reference 67.

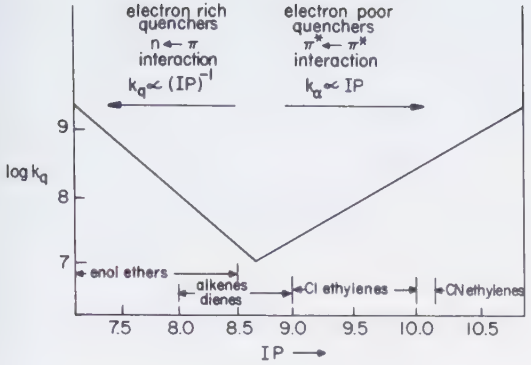

Figure 11.6

Quenching of n, π^* states of ketones by ethylenes. The terms "electron-rich" and "electron-poor" are qualitative and refer to the relative preference of an ethylene to interact with the n or with the π^* orbital of the n, π^* state.

Turning now to the structure of the *excited* state, we expect k_q to depend primarily on the configuration of the reacting state for a given ethylene quencher, i.e., in general, $k_q(n, \pi^*) > k_q(\pi, \pi^*)$. For a series of n, π^* states with the same substrate, we expect k_q to reflect the electron affinity of the n orbital if the reaction to form the primary diradical is exothermic, or to mainly reflect the reaction endothermicity. The data in Table 11.3 show that these trends are borne out for the quenching of n, π^* states by alkenes.

Oxetane Formation by Photocycloaddition of Excited Carbonyl Compounds with "Electron Rich" Substrates: Alkenes and Enol Ethers

The photocycloaddition of ketones to alkenes and to enol ethers will serve as representative of oxetane formation. Some examples are:

cis + trans oxetane

(11.42)[38]

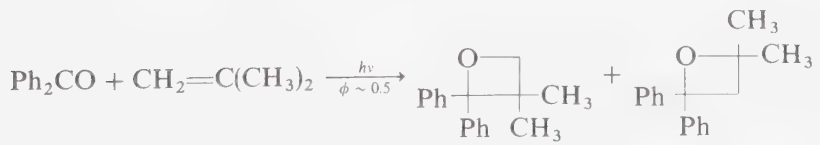

90% 10%

(11.43)[39]

The lack of stereospecificity in reaction 11.42 is explained in terms of a diradical intermediate of sufficient lifetime to allow substantial bond rotations:

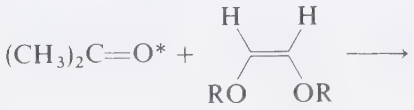

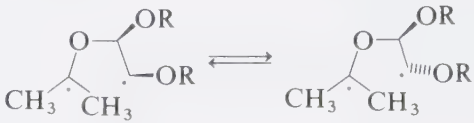

(11.44)

cis → cis-oxetane

trans → trans-oxetane

(11.45)

The side reaction of cis-trans isomerization may be understood in terms of cleavage of the diradical intermediate to generate ground-state ketones and (isomerized) ethylene.

The regiospecificity exhibited in Eq. 11.43 is explained in terms of a diradical intermediate, since diradical **45** should be more stable than diradical **46** in Eq. 11.46. Therefore, **45** is expected (on the basis of the diradical stability rule) to form faster:

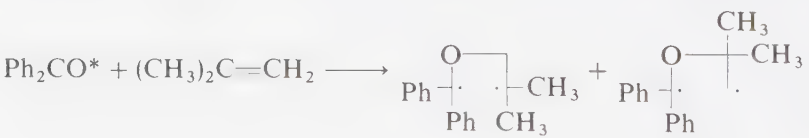

45 (more stable) **46** (less stable)

(11.46)

Table 11.3 Quenching of Unsaturated Ketone Triplets

		k_q (M^{-1} sec^{-1})	
	T_1	RCH=CHR	$R_2C=CR_2$
CH_3COCH_3	n, π^*	1×10^7	5×10^7
$PhCOCH_3$	n, π^*	5×10^7	5×10^8
4-$CF_3C_6H_4COPh$	n, π^*	2×10^8	—
PhCOPh	n, π^*	7×10^7	9×10^8
$(4\text{-}CH_3O\text{-}C_6H_4)_2CO$	π, π^*	4×10^6	—
4-Ph-C_6H_4COPh	π, π^*	—	5×10^6
2-Acetonaphthone	π, π^*	—	2×10^6
$CH_3COCOCH_3$	n, π^*	$\gtrsim 10^6$	4×10^6

We have not explicitly referred to the spin state in these cycloadditions. In the case of aryl ketones, intersystem crossing is generally too fast ($>10^{10}$ sec^{-1}) to allow significant reaction from S_1 to occur. In the case of dialkyl ketones such as acetone, however, $S_1(n, \pi^*)$ is sufficiently long-lived to be able to participate in oxetane formation.

It has been found that $S_1(n, \pi^*)$ and $T_1(n, \pi^*)$, although behaving *qualitatively* the same in oxetane formation, lead to *quantitatively* different results. For example, reaction of the n, π^*-states of acetone with enol ethers involves:

1. More stereospecificity in S_1 than in T_1;
2. Less competing cis-trans isomerization from S_1 than from T_1.[38]

These results are understandable in terms of the postulate that S_1 and an enol ether leads directly to a singlet diradical (^1D), whereas T_1 and an enol ether leads directly to a triplet diradical (^3D). The latter can neither cyclize nor cleave until a spin flip occurs. Since spin-orbit coupling is very weak for electrons in carbon p orbital, ^3D lasts a very long time, allowing many bond rotations to occur.[40] When intersystem crossing to ^1D does occur, cyclization or cleavage results. The ^1D formed from S_1 may cleave or cyclize more rapidly and more competitively with bond rotations.[40] As a result, oxetane formation is more stereospecific and less cis-trans isomerization occurs.

Evidence in support of a long-lived triplet diradical intermediate in the reaction of aryl ketones and ethylenes to form oxetanes is also provided by the observation that the same mixture of oxetanes is produced at low conversion by irradiating cis- or trans-2-butene with acetone or with benzophenone (Eq. 11.47), and that cis-trans isomerization occurs concomitantly.[33,41] Although the latter process could occur via a triplet energy transfer mechanism, the endothermicity of such a process ($\sim$8–10 kcal/mole) makes this possibility unlikely, so that the biradical mechanism is more plausible.

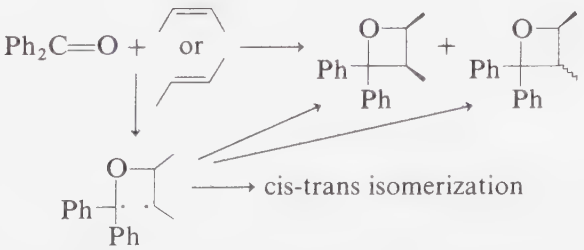

(11.47)

Finally, side products observed in oxetane formation often indicate the occurrence of a biradical intermediate which partitions to oxetane or other products. For example, one expects that disproportionation (a radical-radical reaction which often competes with radical-radical coupling) will compete with (and in some cases dominate) the net reaction of the diradical. In the case of acetone and tetramethylethylene, internal disproportionation products of the biradical are observed

in addition to oxetane:[42]

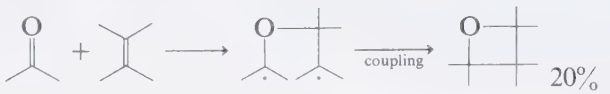

(11.48)

(11.49)

Although biacetyl undergoes [2 + 2] photocycloaddition to a number of olefines to form oxetanes, with α-methyl styrene[43] the major product is an enol ether **47**. The formation of **47** may be rationalized as occurring via (a) addition of triplet biacetyl to the styrene to form a 1,4-biradical which then undergoes intramolecular disproportionation, or (b) hydrogen abstraction followed by coupling of the radicals formed and tautomerization. From deuterium labeling experiments (Eqs. 11.50 and 11.51), path (b) is excluded, since path (b) predicts that the product (**47**) should have the label scrambled and this result is not observed.

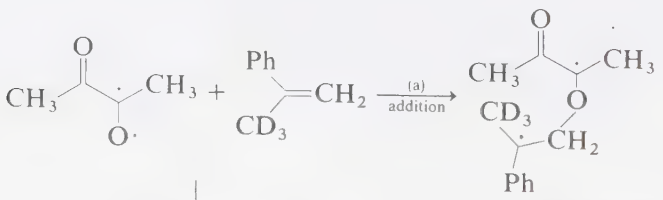

(11.50)

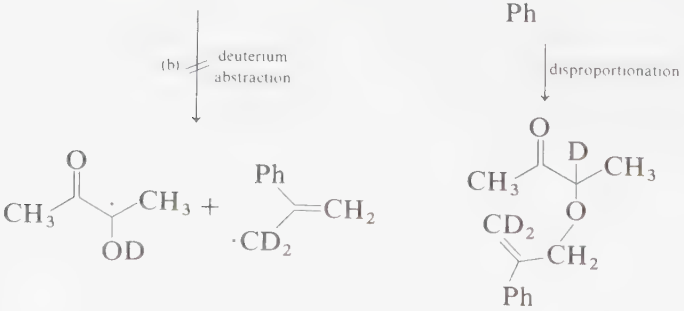

(11.51)

47, isolated

The addition of carbonyl compounds to acetylenes is expected to produce oxetenes. These products are prone to undergo electrocyclic ring opening to unsaturated carbonyl compounds.[44] In the case of benzaldehyde and 2-butyne, the oxetene **48** can be detected by NMR spectroscopy at −45 °.[45] Compound **48** undergoes rapid ring opening near room temperature:

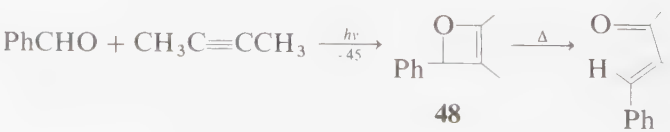

48

(11.52)

An interesting example of the addition of an n, π^* state to a σ-bond is given by the reaction of benzophenone and quadricyclene.[46] The major products may be formulated as arising from attack of the n, π^* state from the exo face to form a diradical which cyclizes to the observed products:

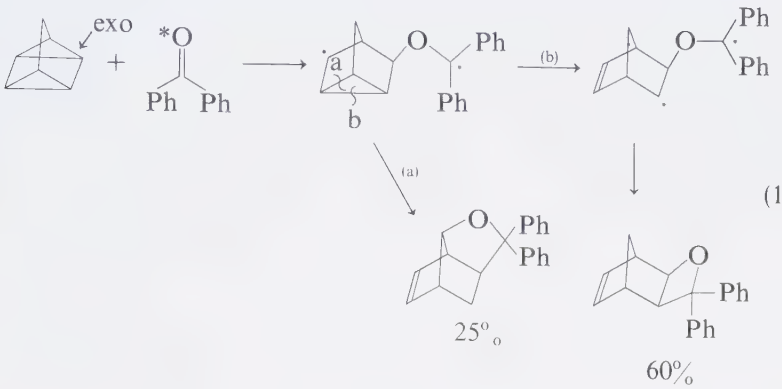

(11.53)

The photocycloaddition of benzophenone to cyclopropyl ethylenes is accompanied by formation of rearrangement products which evidently result from a cyclopropyl carbinyl-allylcarbinyl rearrangement of an intermediate diradical:[15,47]

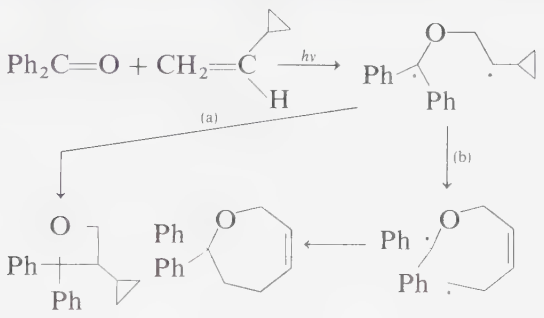

(11.54)

	49	**50**
T = 70°C	65%	15%
T = 160°C	30%	65%

It is important to note that the ratio of oxetane **49** to rearranged product **50** is temperature dependent. At relatively low temperatures the oxetane is the major product. Above 100 the rearrangement product **50** predominates. These results can be understood in terms of the intermediacy of a cyclopropyl carbinyl radical which undergoes ring opening (path b, Eq. 11.54). Ring opening will be favored as the temperature is increased.[15]

Attempts to trap the 1,4-diradical intermediates (derived from addition of the n, π^* states of ketones) with intermolecular substrates have been largely unsuccessful. An exception to this generalization is found in the photocycloaddition of benzoquinone to cyclooctatetraene and other ethylenes in the presence of oxygen.[48]

The product structure suggests that O_2 is capable of intercepting the 1,4-diradical **51**, to yield **52**:

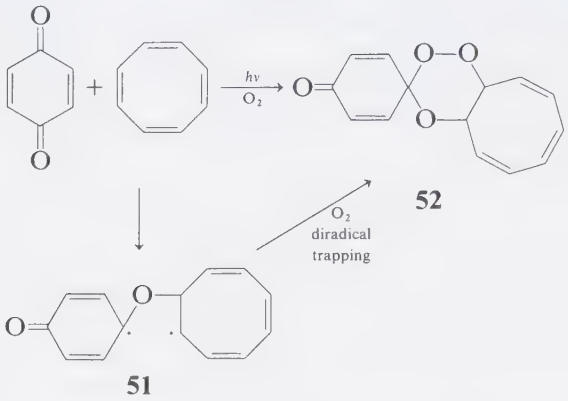

52 (11.55)

51

The diradical hypothesis does not always serve as a good guide to the prediction of the degree of regioselectivity in oxetane formation.[38,49] For example, the addition of acetone singlets and/or triplets to enol ethers is not very regiospecific although the diradical intermediates produced by one bond addition would be expected to result in a strong predominance of the 2-substituted oxetane, e.g.:

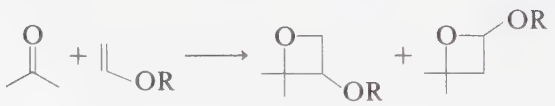

(11.56)

53, ~60% **54**, ~40%

Although isomer **53** usually predominates, the selectivity is less than might be expected. It has been proposed that a $D_{\pm}$ radical pair preceeds the diradical and the collapse of $D_{\pm}$ to D is not as regiospecific as the direct addition of an n, π^* state to the enol ether:[49]

n, π^* E $D_{\pm}$ D

(11.57)

Indirect routes to the diradical such as $n, \pi^* + E \rightarrow D_* \rightarrow D$ or $n, \pi^* + E \rightarrow D_{\pm} \rightarrow D$ are also consistent with quenching data and kinetic deuterium isotope effects.[50]

Oxetane Formation by Photocycloaddition of Excited Carbonyl Compounds with "Electron Poor" Substrates: Cyanoethylenes

The results from photocycloaddition of ketones to electron-poor ethylenes such as cyanoethylenes contrast sharply with those for photocycloaddition of ketones

to electron-rich ethylenes:

1. Only $S_1(n, \pi^*)$ forms oxetanes with cyanoethylenes (recall that *both* $S_1(n, \pi^*)$ and $T_1(n, \pi^*)$ formed oxetanes with electron-rich ethylenes).

2. Quenching of $S_1(n, \pi^*)$ does *not* effect cis-trans-isomerization as a side reaction.

3. Quenching of $T_1(n, \pi^*)$ sensitizes reactions of the cyanoethylene but does not lead to oxetane.

4. Oxetane formation from $S_1(n, \pi^*)$ is *completely* stereospecific (oxetane formation from S_1 was only modestly stereospecific with electron-rich ethylenes).

5. Oxetane formation from $S_1(n, \pi^*)$ is regiospecific, but the product structure does not conform to that expected from the most stable diradical rule.

As a specific example, we consider the photocycloaddition of acetone to cyanoethylenes (Eqs. 11.58–11.61):

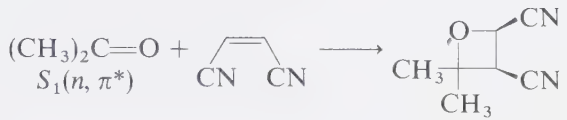

stereospecific (11.58)[51]

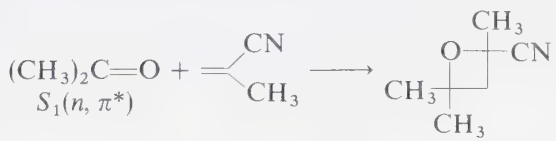

regiospecific (11.59)[52]

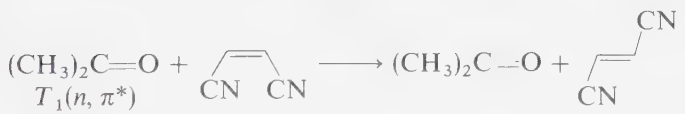

cis-trans-isomerization (11.60)[51]

dimerization (11.61)[53]

The quenching of $S_1(n, \pi^*)$ of acetone by cyanoethylenes may be quite efficient ($k_q \sim 3 \times 10^9\ M^{-1}\ sec^{-1}$ for CNCH=CHCN). $T_1(n, \pi^*)$ is also quenched efficiently by cyanoethylenes ($k_q \sim 10^9\ M^{-1}\ sec^{-1}$). However, the efficiency of oxetane formation from S_1 is only about 10^{-6}% (e.g., with 1,2-dicyanoethylene, Eq. 11.58). Since no other products result from the quenching of S_1 by 1,2-dicyanoethylene (DCE), a pathway for reaction inefficiency (i.e., a quenching pathway) from S_1 must exist.[51]

We may analyze these data in terms of a surface correlation diagram[37] (Fig. 11.7). It is expected that the best orbital interaction between an n, π^* state and an

electron-poor ethylene will occur via a parallel approach which allows a $\pi^*(n, \pi^*$ state) $\rightarrow \pi^*$ (electron-poor ethylene) interaction to occur.[35] Furthermore, only the *tritopic* pathway which occurs via a C—C bond formation is symmetry-allowed.[36] This pathway is shown in Figure 11.7. The stereospecificity of reaction 11.58 is easy to understand as a natural consequence of the geometry of approach and the spin-paired nature of the primary product. The reaction inefficiency may be explained, (a) as a consequence of formation of an exciplex ($^1D_*$) due to a weak avoiding of the $S_0 \rightarrow Z$ and $S_1(n, \pi^*) \rightarrow {}^1D$ surfaces, or (b) as a consequence of formation of ^1D followed by competing collapse of ^1D to oxetane or ground-state ketone and ethylene.[54]

The reaction regiospecificity is explained quite nicely by the tritopic approach (see Fig. 11.7), which also reveals the reason why the conventional most-stable-diradical rule completely fails (Eq. 11.59). Since only the tritopic pathway is electronically allowed, we should *not* consider the diradicals produced by C—O bond formation (Eq. 11.62) as was the case for electron-rich ethylenes; rather, we must consider the stability of diradicals formed by formation of a C—C bond.

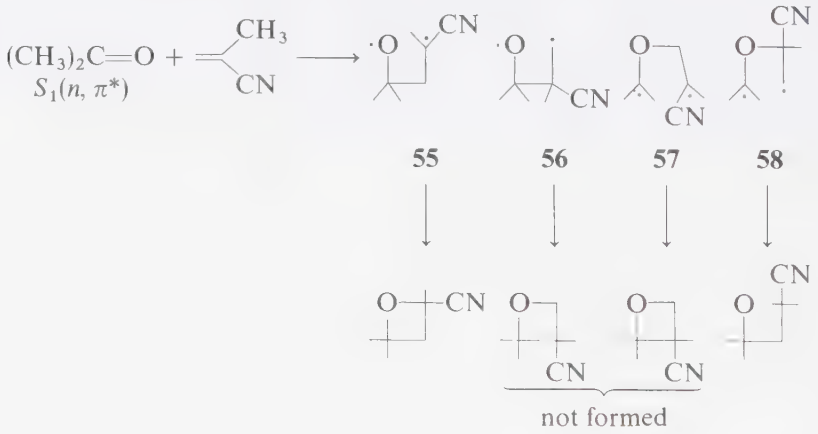

(11.62)

In other words, neither **57** nor **58** are pertinent to the analysis. If they were we would have to predict the formation of a product that is *not* observed. However, if we postulate that diradicals **55** and **56** are the pertinent radicals for analysis then we immediately perceive that **55** is favored by both radical stability considerations and steric effects.

Finally let us consider the basis for the failure of $T_1(n, \pi^*)$ to undergo efficient oxetane formation. From the surface diagram (Fig. 11.8) for the tritopic, parallel approach of $T_1(n, \pi^*)$ and DCE, we expect the connection $T_1(n, \pi^*) \rightarrow {}^3D$ to be direct. However, ^3D cannot close to oxetane before intersystem crossing to D. If the spin flip is slow compared to either bond rotations and/or energy transfer to the ethylene, oxetane formation becomes noncompetitive as a reaction pathway. Evidently, energy transfer *is* preferred over the $^3D \rightarrow {}^1D \rightarrow$ oxetane pathway.

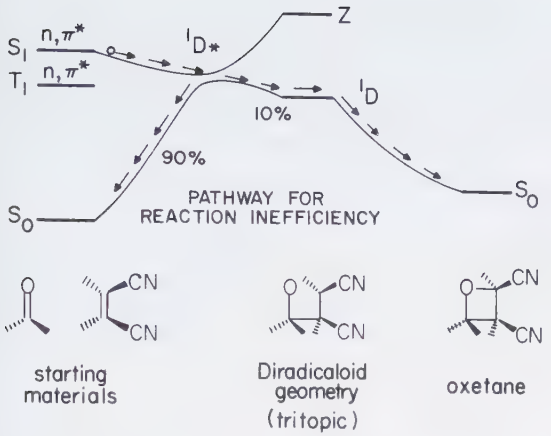

Figure 11.7

Surface description of the addition of acetone to cis-dicyanoethylene. Near the diradicaloid geometry a weak complex or a "hole" in the singlet surface occurs. About 90% of the "quenched" singlet acetone molecules fall through.

Stereoelectronic Requirements for Oxetane Formation

Simple theory (see Fig. 11.4) predicts a preferred "edge-to-face" interaction between n, π^* states and electron-rich ethylenes as substrates and a preferred "face-to-face" interaction for electron-poor ethylenes as substrates.[35]

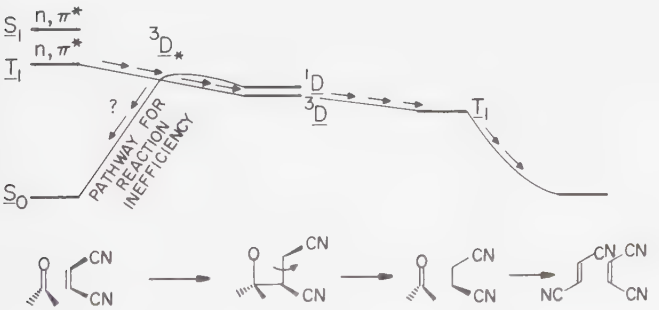

Figure 11.8

Surface description of the acetone-triplet-sensitized cis-trans isomerization of trans-dicyanoethylene. The conversion of $^3(n, \pi^*)$ to ^3D goes by a surface crossing which is very weakly avoided because it involves a singlet/triplet crossing. Unless spin-orbit coupling is effective, most of the quenched T_1 states will proceed to ^3D, which cannot close to oxetane but must either intersystem cross to ^1D or proceed via an adiabatic photocleavage to T_1 of the cyanoethylene. The latter then decays to cis- and trans-dicyanoethylene.

A test of this prediction is possible from a study of steric effects on the rates of quenching of n, π^* states. The premise is that n-orbital interactions will be sensitive to steric effects near the "edges" of the carbonyl function, whereas π^*-orbital interactions will be sensitive to steric effects near the "faces" of the carbonyl function.

Figure 11.9 summarizes an experimental system which tested these ideas. The rigid norcamphor framework can be modified to provide steric hindrance to approach of the "edges" (the n-orbital) or to the "faces" (the π^*-orbital) of the carbonyl function.[55] The qualitative results are that steric blocking of the "faces" retards attack by cyanoethylenes but not attack by enol ethers (as measured by quenching constants). By contrast, steric blocking of the "edges" retards attack by enol ethers but not by cyanoethylenes.

Intramolecular Oxetane Formation

Based on an alkoxy model,[56] intramolecular oxetane formation, like intramolecular cycloadditions of ethylenes,[27] is expected to obey a "rule of five." Experimentally, examples are known (Eq. 11.63) which confirm this expectation,[57] but exceptions (Eq. 11.64) are not uncommon.[58] It may be that primary addition is reversible. In this case product structure would not be a valid guide to the preferred ring size in the primary step of cyclization. The formation of **60** in addition to oxetane upon photoexcitation of **59** is evidence in support of a diradical intermediate in these

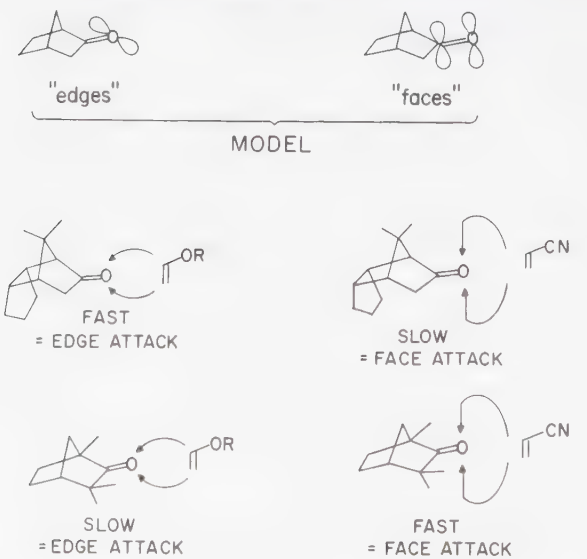

Figure 11.9

Schematic of the use of substituent effects on the rate of quenching of fluorescence of norcamphor and its derivatives by electron-rich (enol ethers) and electron-poor (cyanoethylenes) to demonstrate "edge" ($n - \pi$ interaction) versus "face" ($\pi^* - \pi^*$) interactions of the n, π^* state and ethylenes.

cyclizations.[58] Thus, the diradical *D* can (1) revert to **59** (path a) and cause reaction inefficiency, break bond b and lead to **60**, a rearrangement product of **59**, or (2) cyclize to oxetane (path c). $T_1(\pi, \pi^*)$ states, which are generally inefficient in reacting with ethylenes to form oxetanes intermolecularly[6,33] may undergo efficient *intra*molecular oxetane formation.[59]

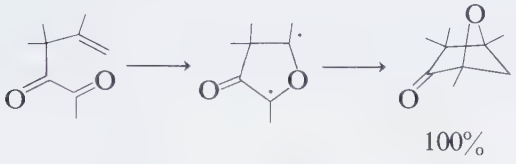

(11.63)

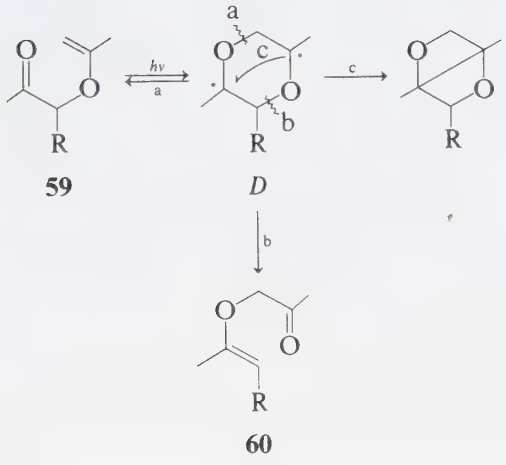

59 *D* **60**

(11.64)

Although intramolecular oxetane formation is normally thought of as a small-ring synthesis, large-ring formations employing this [2 + 2] cycloaddition are plausible. A striking application of this idea is found in the intramolecular photocycloaddition of **61** to yield the paracyclophane **62**:[60]

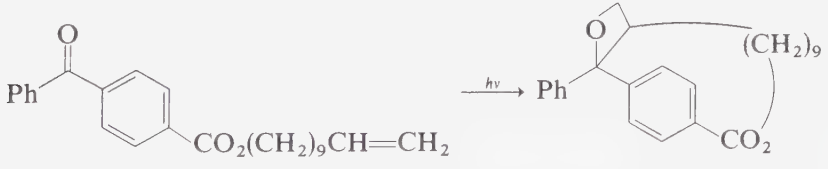

61 **62**, 83%

(11.65)

Interestingly, for short chain analogues of **61**, the phosphorescence lifetime τ_p in dilute solution is relatively constant (~ 70 μs). For **61**, τ_p drops to 2μs, because of the quenching interaction of the $CH{=}CH_2$ group on the side chain.[60]

Evidence for the Intermediacy of Exciplexes in the Formation of Oxetanes

From a number of indirect lines of evidence, exciplexes have been suggested as intermediates in oxetane formation:[49,50]

1. *Reaction inefficiency.* The fact that n, π^* states may be completely quenched by ethylenes, but generally lead to products with much less than 100% efficiency is consistent with a deactivation channel (via an exciplex) to ground state along the reaction coordinate.

2. *Reaction kinetics.* The fact that the rate constants for quenching are much faster than those predicted from simple radical additions is inconsistent with the *direct* primary formation of a diradical intermediate in the quenching step.

3. *Reaction products.* The fact that certain product structures cannot be explained by the most stable diradical hypothesis is consistent with a precursor to the diradical.

Taken as a whole, these data suggest that some precursor may preceed the diradical intermediate (D) in oxetane formation. Theoretically, this intermediate may be a $D_\pm$ or D_* species (see Scheme 11.2). Differentiation between the two has not been possible, so we shall refer to the precursor as an *exciplex*, possibly one with strong charge-transfer characteristics.

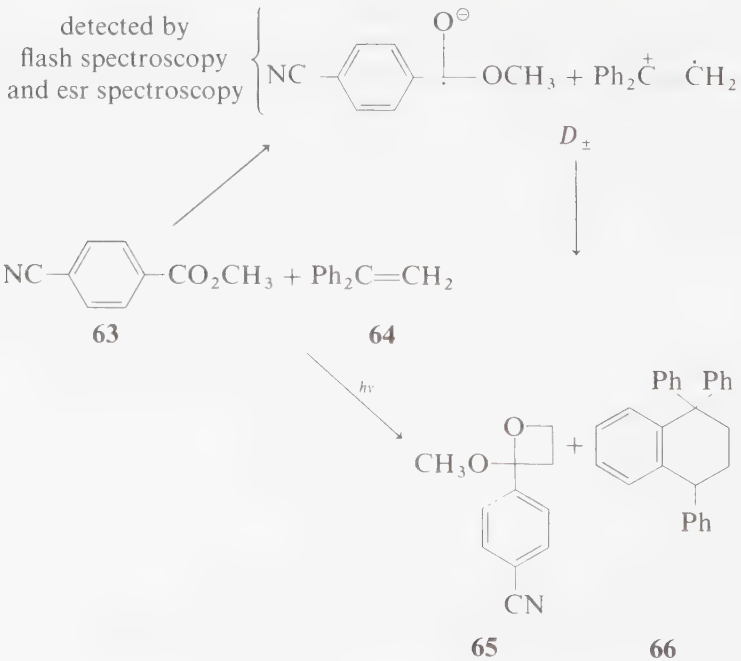

(11.66)

The question arises as to the extent of charge transfer in the quenching step. Is a full electron transferred, forming a radical ion pair, or does the interaction only lead to a polarized charge transfer complex? Experimentally it is likely that both situations occur, depending on the electron-donor or electron-acceptor characteristics of the n, π^* state and the ethylene.[49,61] It is expected that under favorable circumstances, full electron transfer will be achieved to produce a radical ion pair which will then be the precursor to the cycloadducts.

For example, irradiation of **63** and **64** in acetonitrile solvent results in formation of the oxetane **65** and the dimer **66**. Both flash absorption spectroscopy and ESR indicate the occurrence of radical ions in the reaction.[62] Support for the occurrence of a $D_{\pm}$ pair is provided by solvent effects. In benzene **65** becomes the major product, consistent with the fast collapse of $D_{\pm}$ to oxetane than dissociation to free ions. In methanol, low yields of **65** and **66** are formed and ionic addition to $Ph_2\overset{+}{C}—\dot{C}H_2$ predominates. An exciplex has been proposed as a precursor to $D_{\pm}$, but direct spectroscopic evidence for its involvement has not yet been produced.

A more quantitative confirmation of the charge-transfer nature of quenching of excited states is provided by the observation that a plot of Eq. 11.67 has been found to yield a straight line for a wide variety of singlet quenching processes, such as the quenching of n, π^* and π, π^* states by dienes and the quenching of n, π^* states by electron donors.[49,61,63]

$$\ln[k_q/(k_{\text{DIF}} - k_q)] = \alpha[IP] + b \tag{11.67}$$

The slope of such a plot is equal to α and possesses the units of (energy)$^{-1}$ or sec^{-1}. The magnitude of the slope may be considered to be related to the *degree* of charge transfer associated with the quenching step.[63] A "full" electron transfer has been associated with a slope equal to $-17\ \text{eV}^{-1} = 390\ (\text{kcal/mole})^{-1}$. Plots for the quenching of acetone singlets, acetone triplets, benzophenone triplets, and biacetyl singlet and triplets yield similar slopes of ~ 1.5 to $2\ \text{eV}^{-1}$ [46 (kcal/mole)$^{-1}$].[49] This similarity in slopes indicates that *all* n, π^* states, singlets, and triplets show similar sensitivities to ionization potential or charge-transfer energy differences. If we compare the slopes of the line corresponding to Eq. 11.67 for quenching of n, π^* states by ethylenes ($\sim 1.7\ \text{eV}^{-1}$) to the slope for "complete" electron transfer ($\sim 17\ \text{eV}^{-1}$), it is evident that about 10% electron transfer is present in the quenching step.

Since only a small total percent charge transfer occurs in the quenching step, solvent polarity effects on k_q are not expected. Whereas $k_q(CH_3CH)\ k_q(C_6H_6) = 13$ for *full* charge transfer only a small effect is found for quenching of n, π^* states by ethylenes, i.e., $k_q(CH_3CN)/k_q(C_6H_6) \sim 1$.

Competition between Oxetane Formation and Energy Transfer: Photocycloaddition to 1,3-Dienes

Since an exciplex may be involved in some oxetane-forming reactions, it is anticipated that net energy transfer (Eq. 11.69) to produce an excited ethylene or

polyene may compete with oxetane formation (Eq. 11.68):

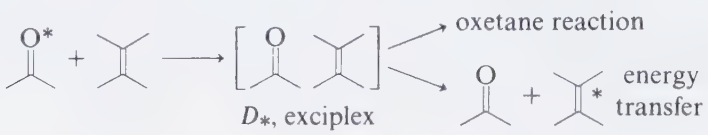

(11.68)

(11.69)

A simple rule of thumb allows us to anticipate when energy transfer to ethylenes will compete with oxetane formation: If the ethylene possesses an electronically excited state of *lower energy* and of the same *multiplicity* as the interacting n, π^* state, energy transfer to the ethylene is competitive with oxetane formation.[6] This rule is based on the generalization that the rate constant for spin-allowed exothermic energy transfer is often close in value to that for diffusional quenching. By inspection of the energetics and by estimation of rates of interaction to form oxetanes we can reliably predict the competition between energy transfer and oxetane formation.

In general, most simple ethylenes and conjugated dienes possess singlet states of higher energy than n, π^* states of ketones. Thus, we expect that energy transfer will not be competitive with oxetane formation in the case of $S_1(n, \pi^*)$-ethylene interactions. Nonconjugated ethylenes possess (vertical) triplet states whose energies are higher than those of the triplet n, π^* states. However, conjugation and ring strain lower the ethylene triplet energy and cause the conjugated ethylene to possess a lower triplet energy than $T_1(n, \pi^*)$.

Since $S_1(n, \pi^*)$ possesses an energy (~ 80 kcal/mole) considerably less than that of $S_1(\pi, \pi^*)$ of 1,3-dienes (> 100 kcal/mole) energy transfer to dienes will not compete with oxetane formation.[64] Irradiation of acetone in trans-2-methyl-2,4-hexadiene yields the oxetanes **67** and **68** and the cis-isomer, **69**. The oxetanes, which are formed stereospecifically, result from attack of the $S_1(n, \pi^*)$ state on

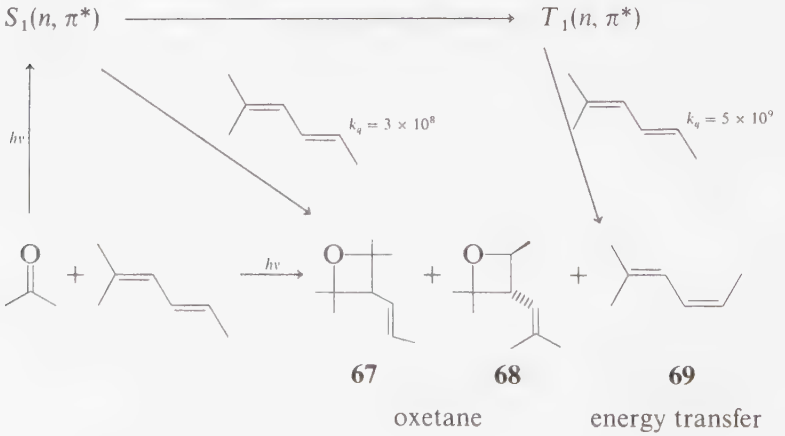

(11.70)

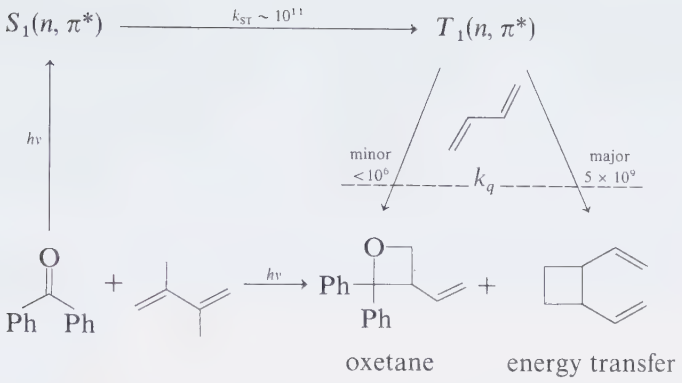

(11.71)

the ethylene, while the cis-isomer results from attack of the $T_1(n, \pi^*)$ state ($E_T \sim 78$ kcal/mole) to yield the diene triplet ($E_T \sim 60$ kcal/mole) which undergoes trans-cis isomerization.[64,65] The mechanism of reaction is quite analogous to the addition of n, π^* states to electron rich ethylenes.[65]

Benzophenone is a good photosensitizer of the formation of 1,3-diene triplets because its $S_1(n, \pi^*)$ is too short-lived to add to dienes, and its triplet energy, being higher than that of dienes, allows for very rapid energy transfer (Eq. 11.71).[9]

For example, benzophenone photosensitizes the dimerization of dienes, and oxetane formation is a minor competing pathway.[66] In the case of 1,3-butadiene, the quantum yield of diene dimers is about 10^3 that of oxetane formation.

It is informative to compare the rate constants for quenching of triplet acetone and triplet benzophenone by a series of benzenes.[67] The data reveal that acetone triplets are quenched approximately 100 times faster than benzophenone triplets. The results of such studies suggest that acetone triplet ($E_T \sim 78$ kcal/mole) is quenched by a charge-transfer interaction which leads to slightly endothermic energy transfer to the benzene triplet ($E_T \sim 80$ kcal/mole). The benzophenone triplet ($E_T \sim 69$ kcal/mole) cannot be quenched by energy transfer because of the large endothermicity of the process.

(11.72)

(11.73)

In benzene solvent, the lifetimes of the acetone and benzophenone triplets are limited by solvent quenching.[68] We may estimate that $\tau \sim (k_q[B])^{-1}$ where k_q is the solvent-quenching constant and $[B]$ is the benzene concentration (~ 10 M in pure benzene). Thus for acetone and benzophenone triplets, τ_T is $\sim 3 \times 10^{-8}$ sec and $\sim 10^{-5}$ sec, respectively. It is clear from this estimation that benzene is a suitable solvent for photoreaction of benzophenone, but not for acetone.

Competition between Photocycloaddition and Photoreduction

We saw in Chapter 10 that the rate constant for *direct* hydrogen abstraction by an n, π^* state reaches a limit of $\sim 10^6\ M^{-1}\ sec^{-1}$ and then *electron* abstraction or exciplex formation begins to dominate the quenching process. Thus, we expect that hydrogen abstraction will not compete favorably with oxetane formation when the ethylene is a "good" quencher ($k_q > 10^7\ sec^{-1}$) of n, π^* states, but hydrogen abstraction may be competitive when $k_q < 10^6\ sec^{-1}$.

For example, the photocycloaddition of acetone triplet to cyclohexene is accompanied by extensive hydrogen abstraction, as evidenced by photoreduction products:[69]

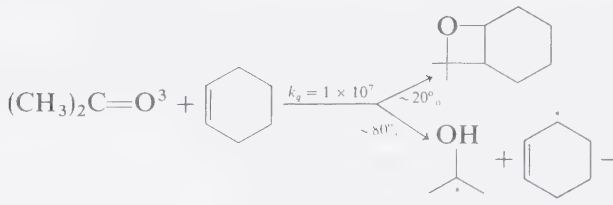

(11.74)

(11.75)

The rate constant for hydrogen abstraction from toluene by benzophenone triplets is $\sim 2 \times 10^5\ sec^{-1}$, a value which is expected to be typical for hydrogen abstraction by a $^3(n, \pi^*)$ state (Table 10.3). The actual value of k_q by ethylenes is much larger than 2×10^5. Thus, for cyclohexene it is not likely that a direct hydrogen abstraction mechanism is occurring.

In general, intramolecular addition to C=C bonds (e.g., reactions shown in Eqs. 11.63 and 11.64) competes effectively with intramolecular hydrogen abstraction. This result is consistent with results for the analogous intramolecular reactions of alkoxy radicals.[56,70]

11.4 Photocycloadditions of Benzene

Benzene, a molecule known for its special ground-state stability, undergoes a variety of photoreactions, including cycloadditions. Benzene is known to undergo [2 + 2], [2 + 4], [3 + 2], and [4 + 4] photocycloadditions.[71] For example, irradiation of tetramethyl ethylene and benzene results in formation of a [2 + 2] adduct:

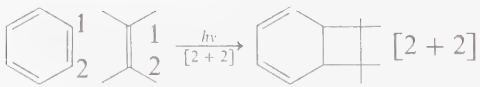

(11.76)

Cyclopentene and benzene, on the other hand, yield mainly a [3 + 2] adduct:

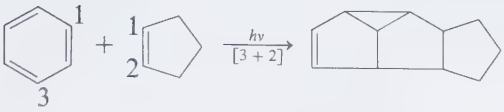

(11.77)

The [3 + 2] photocycloaddition of benzene and ethylenes is stereospecific.[72b] With other substrates [4 + 2] and [4 + 4] adducts are observed:

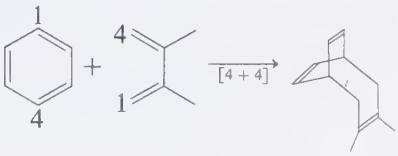

(11.78)

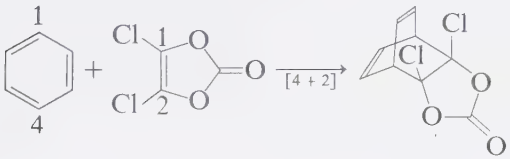

(11.79)

With maleic anhydride a 2:1 adduct **70** is formed that involves a [2 + 2] photoaddition followed by a [4 + 2] thermal addition:[76,77]

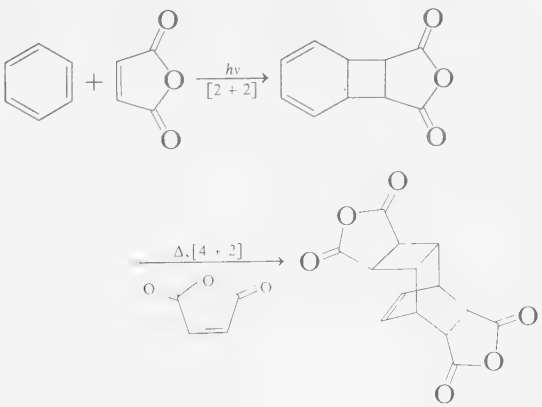

(11.80)

70

No single mechanism has been proposed which is capable of explaining all of the observed results for photocycloadditions involving benzene. However, the reactions of benzenes with alkenes and polyenes appear to more commonly involve S_1 of benzene[72b] and not T_1. In some cases (Eq. 11.76) a charge-transfer complex is involved.[78]

Exciplexes as Intermediates in the Photocycloaddition Reactions of Aromatic Compounds

The photocycloaddition reactions of many aromatic compounds proceed via exciplexes.[79] Although the exciplex mechanism may be very general, experimental evidence for an exciplex intermediate is rarely direct, since fast radiationless process (reaction or dissociation) usually compete with exciplex emission. In favorable cases, however, confirming exciplex emission is observed.

The $\pi^4 + \pi^4$ cycloaddition of two diene systems is photochemically allowed. We might expect however that the unfavorable entropy of activation ($\Delta S^{\ddagger}$) will slow down the rate of a concerted [4 + 4] cycloaddition relative to multistep processes that involve formation of only one bond in the primary photochemical process.

Exciplexes may predispose a pair of molecules toward cycloaddition, because formation of such loose excited state aggregates keeps two potentially reactive partners in close proximity such that orientations of the partners which are favorable for bond formation may exist.

Many exciplexes between aromatic compounds and substrates which possess moderate or low ionization potentials appear to have strong charge-transfer characteristics. In polar solvents a complete electron transfer may occur and thereby alter the course of cycloaddition reactions.

[2 + 2] cycloadditions of aromatic ethylenes may occur via a radical ion mechanism. For example, irradiation of acetonitrile solutions of indene and alkyl vinyl ethers in the presence of 1-naphthonitrile yields [2 + 2] cycloadducts (Eq. 11.81). In the absence of alkyl vinyl ethers, [2 + 2] cyclodimers of indene are formed. It appears that these reactions are "sensitized" by the 1-naphthonitrile via initial electron abstraction reaction which is later reversed.[80]

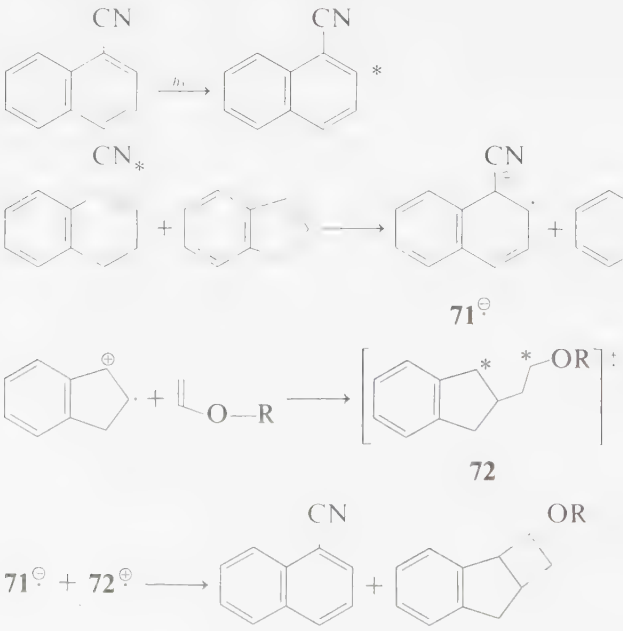

An analogous mechanism for [2 + 2] cycloaddition occurs with indenes and electron-rich ethylenes in polar solvents.[81] If an exciplex is formed and if the binding in the exciplex brings the 1,4-1,4 positions together, then both the exciplex lifetime and preordered reactant structure will favor [4 + 4] concerted cycloaddition relative to the direct interaction of an excited diene with a ground-state diene. Similar arguments would apply to $\pi^2 + \pi^2$ photocycloadditions. We may generalize these ideas in the rule that formation of singlet exciplexes favors concerted and stereoselective cycloaddition reactions.

As an example, irradiation of naphthalene and 1,3-dienes results in formation of either the *trans*- [4 + 4] adduct **73** (Eq. 11.82) or the *cis*- [4 + 4] adduct **74** (Eq. 11.83), apparently depending on the configuration of the diene in the exciplex.[82] Thus, 2,5-trans-trans-hexadiene (which exists mainly as the *s*-trans conformer) yields **73**, whereas 2,4-dimethyl-1,3-pentadiene (which exists substantially as the *s*-cis conformer) yields **74**.

Spectroscopic and kinetic evidence implicate exciplexes in the quenching of napththalene fluorescence by 1,3-dienes and the product type and structure are consistent with either a concerted $\pi^4 + \pi^4$ exciplex cycloaddition or formation of an intermediate from the exciplex which collapses stereospecifically to the [4 + 4] adduct.[83]

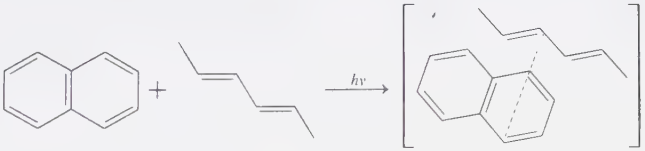

singlet exciplex (11.82)

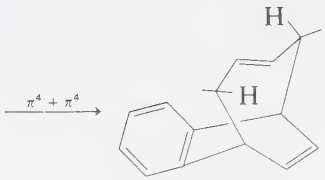

73

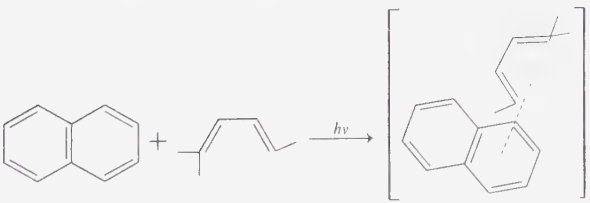

singlet exciplex (11.83)

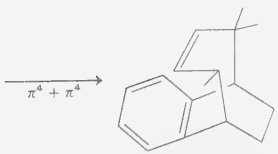

74, 60%

The observation of cycloadducts (often formed in high quantum and chemical yields and with high regiospecificity and stereospecificity e.g., Eq. 11.84) from irradiation of aromatic hydrocarbons and ethylenes or dienes demonstrates that product formation is an important deactivation pathway for the corresponding exciplexes. In a few cases exciplex emission has been detected (e.g., 9-cyanoanthracene and 2,5-dimethyl-2,4-hexadiene).[84,85]

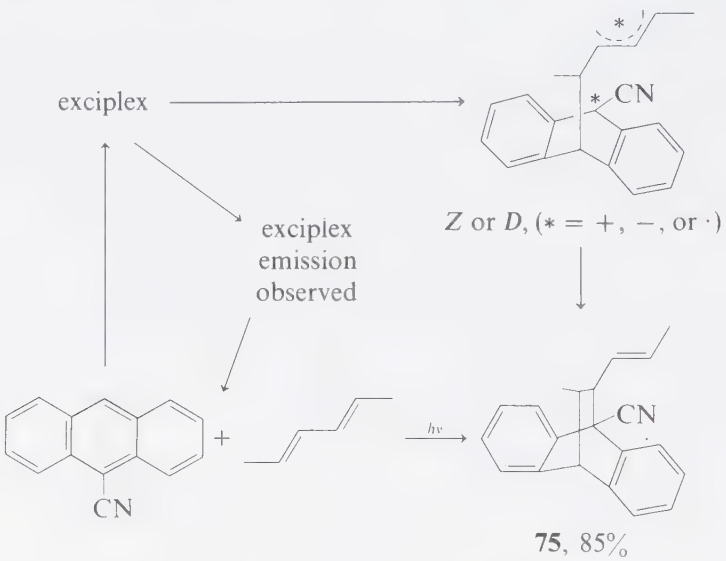

(11.84)

75, 85%

In addition to the above lines of evidence for the occurrence of exciplexes, "negative temperature dependences" of rate constants for photoreactions provides an indirect means of "detecting" exciplexes.[86] The basic idea is that if an exciplex is formed reversibly but goes on to product irreversibly, increasing temperature may cause an apparent slowing down of the observed rate constant.

Photocyclodimerization of Aromatic Compounds

The photochemical cyclodimerization of aromatic compounds is a well-established photoreaction that falls into two categories: (a) cyclodimerizations involving the aromatic nucleus, and (b) cyclodimerizations involving an ethylene conjugated to the aromatic nucleus. The most common type of reaction in class a is the [4 + 4] cyclodimerization of arenes.[87] Although the photocyclodimerization of benzene has not been reported, examples of both inter- and intramolecular [4 + 4] cycloadditions of naphthalenes and anthracenes are known:

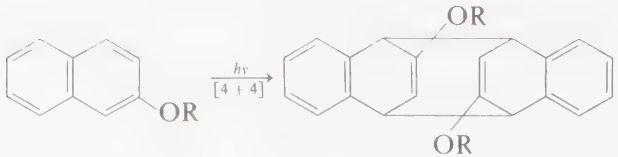

(11.85)[88]

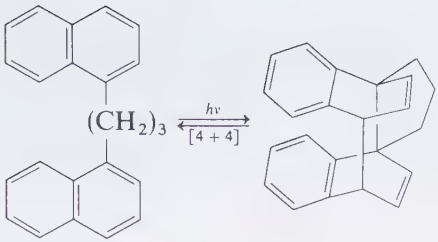

(11.86)[89]

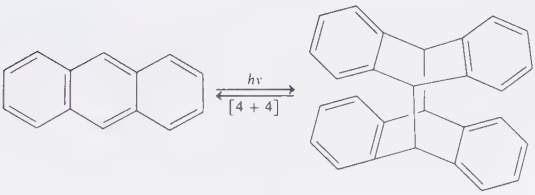

(11.87)[90]

The most common types of photocyclodimerization of aromatic compounds involve [2 + 2] cycloadditions (class b reactions, Eq. 11.88) of an excited conjugated ethylene to a ground-state ethylene. For example, styrene, indene, and stilbene undergo [2 + 2] photocyclodimerization of this type.[3] The following paradigm serves to correlate the photocyclodimerization of aromatic compounds:

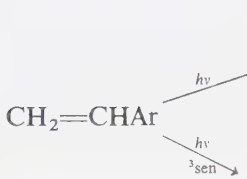

	Class a	Class b	Comment
hν	[4 + 4]	[2 + 2]	Exciplex Syn, head-to-head
hν, ^{3}sen	no reaction	[2 + 2]	Diradical Anti, head-to-tail
	Aromatic nucleus	Double bond conjugated to nucleus	

(11.88)

Thus, for direct excitation both class a and class b photocycloadditions appear in general to proceed via singlet exciplex intermediates. Triplets do not undergo class a dimerization, but do undergo class b dimerization. The regiospecificities of both direct and triplet [2 + 2] reactions are head-to-head, for an asymmetric ethylene, i.e., the cyclobutane is generally formed with a plane, but not with a center of symmetry. These cycloadditions occasionally proceed via radical ions (e.g., Eq. 11.81).[81]

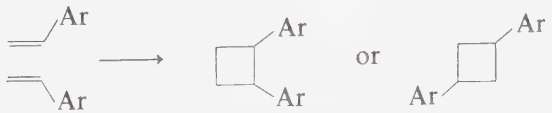

head-to-head singlet reaction | head-to-tail triplet reaction

(11.89)

Photoaddition of *trans*-stilbene to tetramethylethylene gives a *trans*-1,2-diphenylcyclobutane in high yield (Eq. 11.90). Reversible formation of an exciplex is invoked as an intermediate in this reaction, because of the strong temperature-dependence of the quantum yield and the rate constant for cycloaddition, i.e., lower temperature favors exciplex formation. The reaction cannot be triplet-sensitized, thus suggesting that S_1 of *trans*-stilbene is involved.[91]

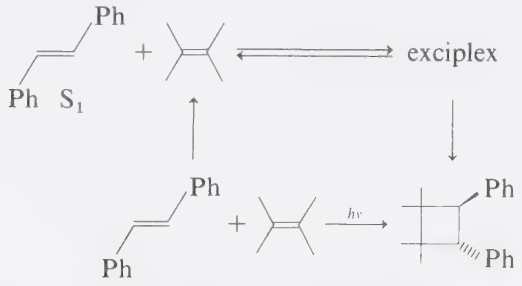

(11.90)

The photocyclodimerization of acenaphthylene (**76**) represents an example of class b photocyclodimerization which may be subjected to a heavy-atom effect. Acenaphthylene dimerizes under direct and triplet photosensitized conditions to form a [2 + 2] syn dimer **77** (major product upon direct photoexcitation) and a [2 + 2] anti dimer **78** (major product upon triplet photosensitization). Heavy atoms such as bromine or iodine in the solvent catalyze $S_1 \rightarrow T_1$ conversion of acenaphthylene and thereby more antiisomer is formed. Evidently, the singlet exciplex favors overlap of the naphthalene rings but in the triplet reaction a diradical is formed in which the naphthalene rings are kept far apart.[92]

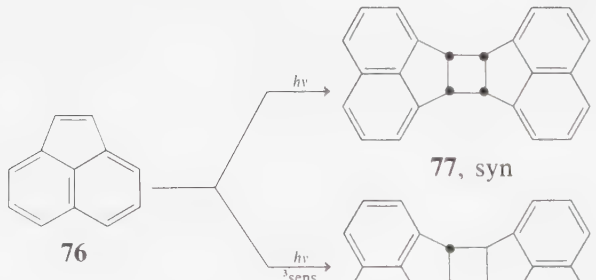

(11.91)

(11.92)

11.5 Photocycloaddition Reactions of Conjugated Enones

The photocycloaddition of conjugated enones is of interest because either n, π^* or π, π^* states may be involved.[93] In fact, experimental evidence indicates that either or both states may be active under certain conditions. A complicating

feature in interpretation of the photocycloaddition reactions of enones is the lack of a definitive means of assigning an appropriate configuration to their lowest excited states. It appears that although the n, π^* state is usually lowest in the singlet manifold, either the n, π^* or π, π^* state may be lowest in the triplet manifold.

If we postulate that the n, π^* state of enones will behave analogously to the n, π^* states of ketones and that the π, π^* states of enones will behave analogously to the π, π^* states of conjugated ethylenes, then we can generate a paradigm for the photocycloaddition reactions of enones (Scheme 11.3). It appears that intersystem crossing is efficient for conjugated enones, so that T_1 is a likely candidate for the active excited state in photocycloadditions. According to our postulate, the $T_1(\pi, \pi^*)$ state should possess a tendency to twist about the C=C bond of the enone, but it is not so clear how great this tendency will be in the $T_1(n, \pi^*)$ state.

Photocycloaddition of Cyclic Enones and Related Compounds

Photocycloaddition reactions of conjugated cyclic enones have been known since the early 1900s. In the most commonly studied cases, an ethylene is added to the cyclic enone to form a cyclobutane. For example, the photochemical [2 + 2] cycloaddition of ethylene to cyclohexenone yields a bicyclo [4.2.0] octanone (Eq. 11.93) in good yield. Cyclohexenone may also undergo photochemical [2 + 2] *dimerization* (Eq. 11.94):

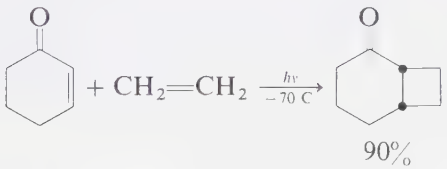

(11.93)[94]

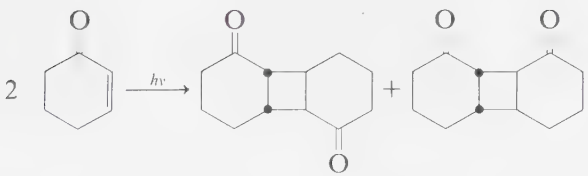

(11.94)[95]

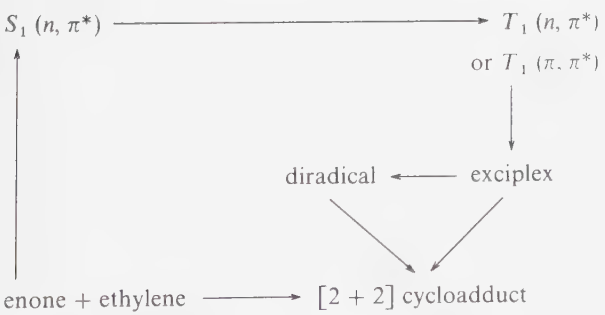

Scheme 11.3

Reaction diagram for the [2 + 2] photocycloaddition of enones to ethylenes.

If structural limitations are not present, intramolecular photocycloaddition of enones to ethylenes offers an attractive synthetic route to polycyclic molecules (Eq. 11.95). Such a reaction provided a route to the "cage" molecule **79**, a key intermediate in the synthesis of the remarkable molecule *cubane*.

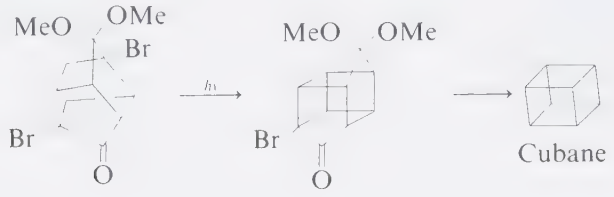

(11.95)

79

Mechanisms of Photocycloaddition of Cyclic Enones to Ethylenes

The mechanisms of photocycloaddition of ethylenes to cyclic enones has been extensively studied and number of generalizations are possible:

1. The reactive state is T_1 of the enone and may be either of n, π^* or π, π^* character.
2. Electron-rich ethylenes react more rapidly than electron-poor ethylenes.[95]
3. Cycloaddition occurs regiospecifically for electron-rich ethylenes.[97]
4. Cycloaddition occurs with loss of stereochemistry of the ethylene fragment.[98]

Some other interesting features of these reactions are the occasional formation of strained trans- ring-fused products (especially with electron-rich substrates) preferentially to the less strained cis- ring-fused products (Eq. 11.96) and the occurrence of side products which are expected from biradical intermediates (Eq. 11.97).

The occurrence of side products characteristic of diradicals and the loss of stereochemistry of the ethylene component suggest a diradical intermediate. If a diradical intermediate is involved, then we should be able to predict the orientational preference of addition of an unsymmetrical ethylene to a cyclic enone. However, a problem arises when we attempt to decide whether a radical α to a carbonyl group is "more stable" than a secondary carbon radical. These stabilities would have to be evaluated in the case of simple enones. If we assume that a radical site adjacent to a carbonyl group is *less* stable than an ordinary secondary radical site, we can correctly predict the preferred orientation of addition for electron rich ethylenes. The preferred orientation is also predictable if it is assumed that a complex between T_1 of the enone and the ground-state ethylene is formed and that the geometry of this complex determines the orientation in the product, whatever the details of sequential steps.[95] This complex was proposed to possess electrophilic character at the carbon α to the carbonyl. To predict the preferred

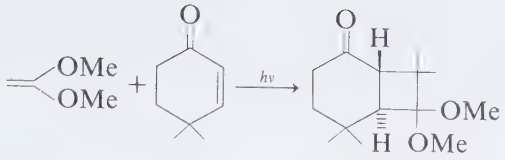

42%

(11.96)

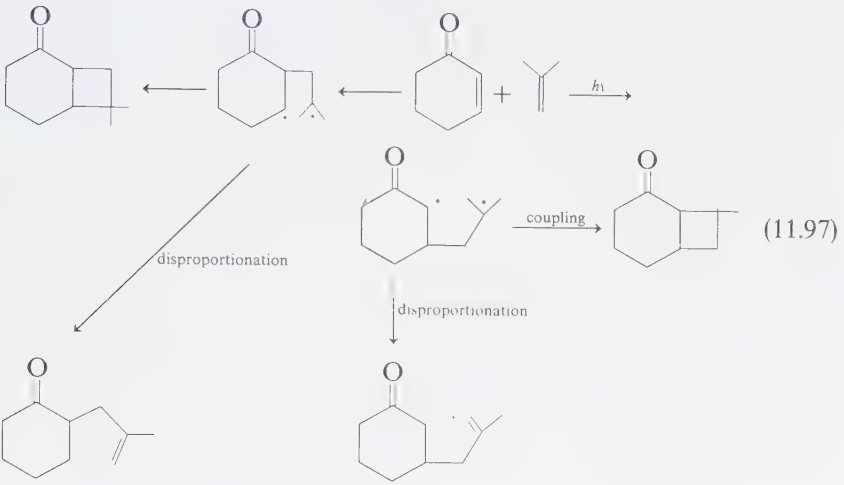

(11.97)

orientation of cycloaddition a single bond is made between the more negative carbon of the ethylene and the α-carbon of the enone and then the ring is closed.

As an example consider the [2 + 2] photocycloaddition of 1,1-dimethoxyethylene to cyclohexenone.[95] The charge-transfer complex hypothesis says to line up the more negative CH_2 terminus of the ethylene with the α-carbon of T_1 of the enone. The diradical mechanism (assuming a radical α to a carbonyl is less stable than a secondary carbon radical) says that the biradical which is stabilized by the two MeO groups should be favored. Both predictions are consistent with experiment.

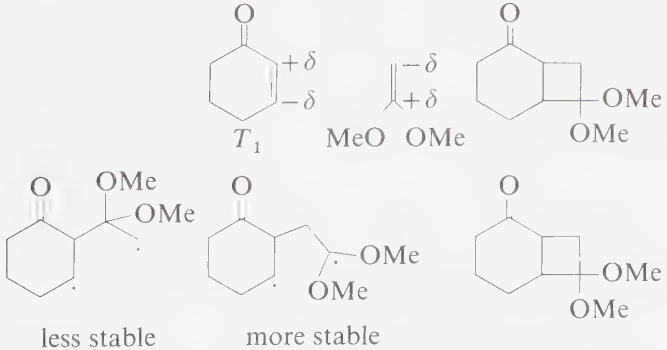

(11.98)

A wide variety of data can be accomodated by combining the charge-transfer and complex diradical mechanisms. In this case we assume that either a complex

may be formed which can then collapse directly to a product or biradical, or that a diradical is formed directly. In this mechanism, the extent of formation of complex and/or diradical will depend on the electronic properties of the ethylene.

The formation of trans ring-fused products is not an obvious expectation from either the exciplex or the diradical mechanism. However, it may be accomodated by either, if we allow that the exciplex possesses a highly twisted double bond which approaches a trans configuration. Collapse of the exciplex then leads to a triplet diradical. The latter undergoes conversion to a singlet diradical that kinetically prefers closure to trans product rather than bond rotation.

Although a trans cyclic enone might be considered as a reactive intermediate in some of these cycloadditions, it is observed that isolable or detectable trans cyclic enones (i.e., cyclooctenones, Eq. 11.99)[98] add to electron-rich ethylenes with the opposite orientation observed for photocycloaddition of cyclohexenone and cyclopentenone. Thus, for the latter enones, an electronically excited intermediate is more likely to be involved.

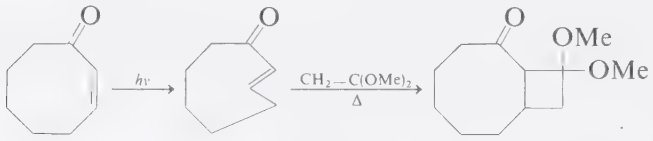

(11.99)

The photodimerization of coumarin (**80**) in ethanol yields the head-to-head cis- dimer (**81**) as the major product.[99] Furthermore, the reaction does not go in benzene solution. The dimerization of compound **80** is sensitized by benzophenone, in benzene solution, and the predominant product is the head-to-head trans- dimer (**82**):

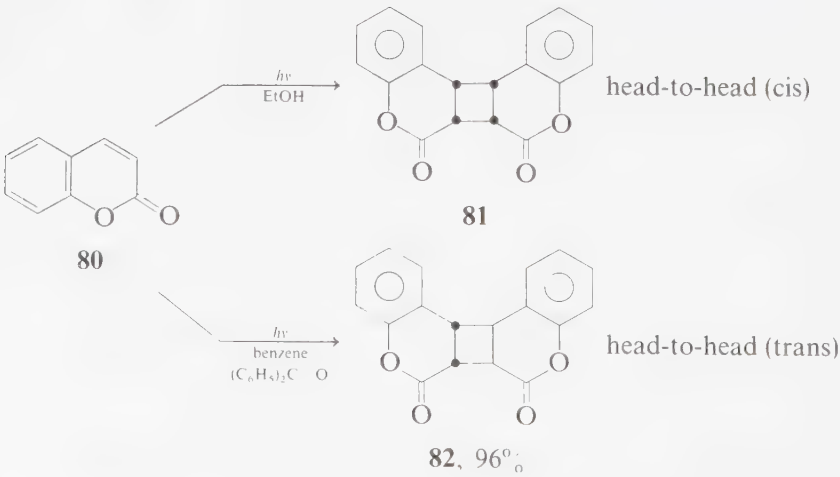

(11.100)

The difference in the course of the direct and sensitized reactions is the result of the involvement of different excited states in the two cases. The mechanism is

probably the following:

$$C_0 \xrightarrow{h\nu} C_1 \tag{11.101}$$

$$C_1 \longrightarrow C_3 \tag{11.102}$$

$$B_3 + C_0 \longrightarrow C_3 + B_0 \tag{11.103}$$

$$C_1 + C_0 \longrightarrow \mathbf{81} \tag{11.104}$$

$$C_3 + C_0 \longrightarrow \mathbf{82} \tag{11.105}$$

where C_0, C_1, and C_3 are the coumarin ground state, lowest excited singlet state, and lowest triplet state, respectively, and B_0 and B_3 are benzophenone ground and triplet states (produced quantitatively by intersystem crossing from the singlet), respectively. In nonpolar solvents such as benzene, C_1 is deactivated by "self-quenching." In polar solvents such as ethanol, C_1 reacts with C_0 to produce **81**. In the presence of B_3, C_3 is produced by triplet-energy transfer in both polar and nonpolar solvents. The reaction of C_3 with C_0 produces **82** predominately. Spectroscopic data yield the energy diagram shown in Figure 11.10. It is seen that singlet-singlet excitation transfer from C_1 to benzophenone is also possible—i.e., the C_1 molecules which absorb in the presence of benzophenone can be quenched by the latter compound, which in turn undergoes intersystem crossing to B_3. An elegant vindication of these hypotheses is the fact that in dilute

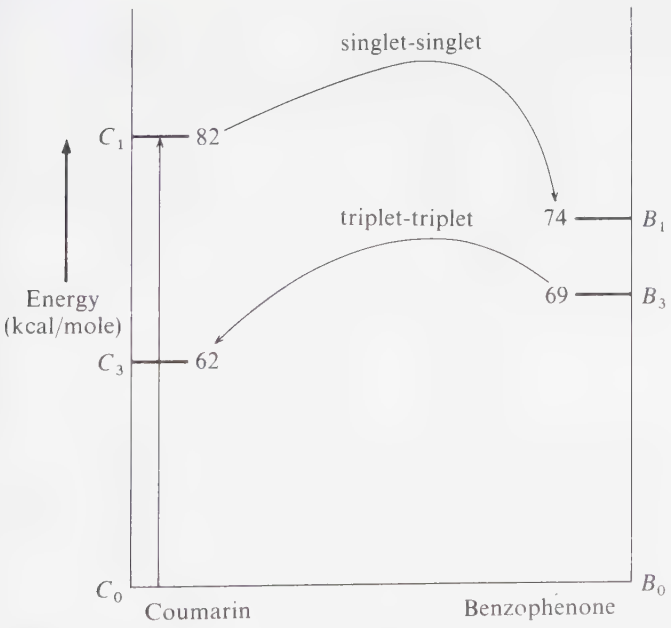

Figure 11.10
State-energy diagram for the benzophenone-coumarin system.

concentration, coumarin yields **82** under direct excitation.[99] Thus, coumarin singlets either cross over to C_3 or are deactivated to C_0 under these conditions—i.e., dimerization, a bimolecular reaction, does not compete efficiently with rapid unimolecular processes in dilute solution. The coumarin triplets thus produced react in exactly the manner as those produced by energy transfer, and **82** is produced by energy transfer, and **82** is produced by reaction of C_3 and C_0.

Synthetic Applications of the [2 + 2] Photochemical Cycloadditions of Enones

The [2 + 2] photocycloaddition of ethylenes to enones and related compounds has provided the synthetic chemist with a powerful tool for the construction of four-membered rings.[3,100] In a number of cases both a remarkably high stereospecificity and/or regiospecificity are observed:

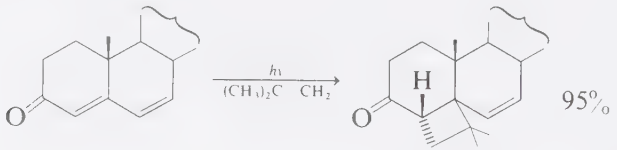

transfused

(11.106)[101]

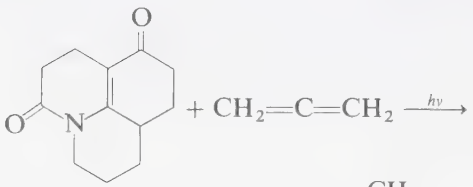

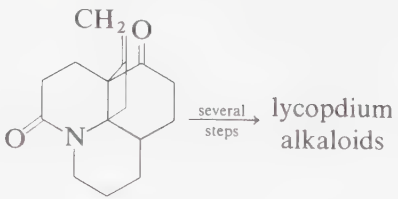

100%

(11.107)[102]

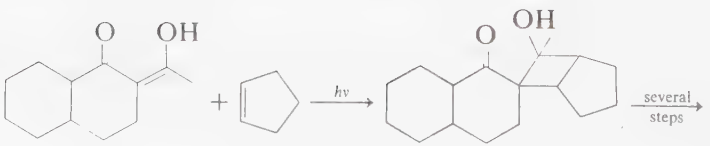

(11.108)[103]

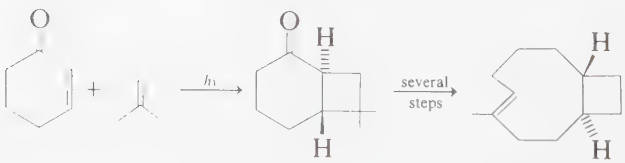

caryophylene

(11.109)[95]

An interesting use of multiple annelations and photochemical steps has been employed to synthesize the unusual [2.2.2] propellane, **83**:

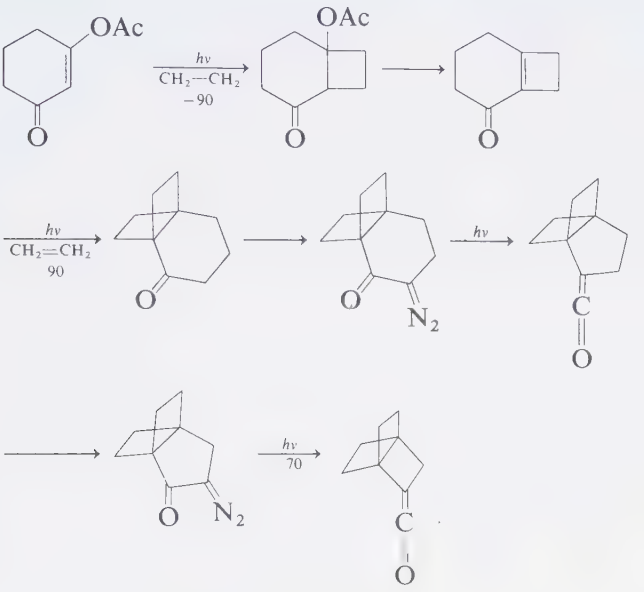

(11.110)[104]

83

The photochemical [2 + 2] cycloaddition of a special enone, thymine, **83**, and its derivatives,[105] is of great importance in the photoreactions of biological systems containing DNA.[106] It appears that a related photoreaction occurs between thymine base pairs in DNA.[107]

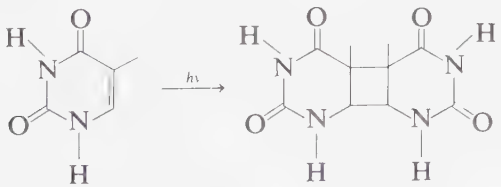

(11.111)

Thymine

11.6 Photocycloadditions Involving Unsaturated Nitrogen Compounds and Thioketones

In analogy to the reactions of n, π^* states with ethylenes, it is expected that the $T_1(n, \pi^*)$ states of other functional groups will also enter into photocycloaddition reactions. In Chapter 10, we noted that an analogy exists between the hydrogen and electron abstraction reactions of *all* n, π^* states, e.g., ketones, nitro compounds,

imines, etc. In cycloaddition reactions this analogy still holds. For example, aromatic nitro compounds react with alkenes to yield 1,3,2-dioxazolidines (Eq. 11.111).[108] These substances decompose readily at room temperature but are isolable at low temperature.

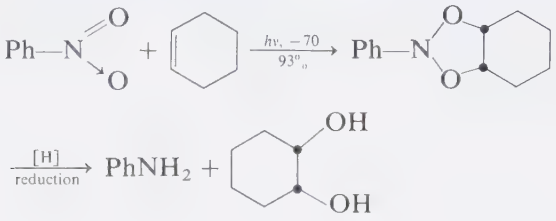

(11.112)

Hydrogenation yields an aniline plus a 1,2-cis-diol.

The imine **84**, like its enone counterpart undergoes [2 + 2] photocycloaddition to electron rich ethylenes:[109]

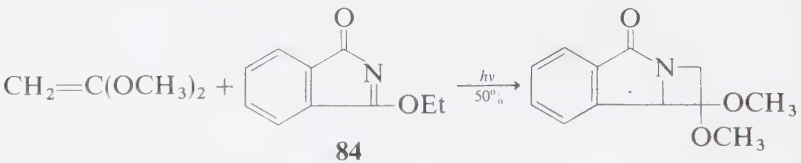

84

(11.113)

Thioketones undergo photoreactions analogous to ketones, e.g., photoreduction, cycloaddition, etc. A special feature of these systems is that reactions from *upper* electronic states are common. For example, adamantanethione undergoes cycloaddition to ethylenes.[110] Reaction is initiated from $S_2(\pi, \pi^*)$ and $T_1(n, \pi^*)$. Interestingly, S_2 also forms an excimer which collapses to a 1,4-dithietane dimer.

via excimer Ad = Adamantane nucleus

(11.114)

The cycloaddition reaction from S_2 is stereospecific but not regiospecific, whereas the cycloaddition reaction from T_1 is regiospecific but not stereospecific.

Because of the reactivity of S_2, the cycloaddition reactions of thiocarbonyl compounds are wavelength-dependent. Electron-deficient ethylenes appear to react more readily with $S_2(\pi, \pi^*)$ to yield thietanes, whereas $T_1(n, \pi^*)$ generally yields thietanes and 1,4-dithianes.[111] The formation of the thiadioxanes may be viewed as resulting from trapping of a 1,4-diradical intermediate by a ground-state thioketone:

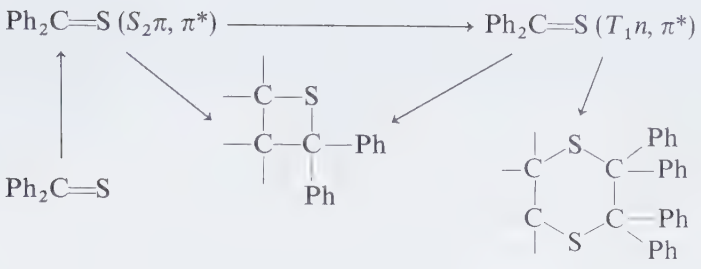

(11.115)

The reactivity of T_1 seems to derive entirely from an n orbital interaction with ethylene in contrast to ketones where the π^*-ethylene interaction becomes manifest when the ethylene possesses a high electron affinity.[112]

11.7 Summary

Photochemical cycloaddition reactions, especially those leading to formation of four membered rings, provide an important tool for organic synthesis. Most intermolecular photocycloadditions proceed via triplet states and diradical intermediates. The relatively few intermolecular photocycloadditions which occur via singlet states appear to involve initial formation of exciplexes. The photocycloaddition of ketones to ethylenes is reasonably well understood and serves as a prototype for all photocycloadditions involving n, π^* states. Three primary product types occur: (1) conventional diradicals, D; (2) exciplexes, D_*; and (3) radical ion pairs, $D_\pm$. Which species is formed first and the extent of the interconversion of these diradicaloids depends on the specific reaction conditions.

Alkenes and conjugated polyenes serve as prototypes for photocycloadditions of π, π^* states. S_1 states may react via Z intermediates or produce strained ground state species which undergo thermal cycloaddition. T_1 states generally react via D, D^* or $D_\pm$ intermediates or produce strained ground state species which then undergo thermal cycloaddition. Aromatic hydrocarbons behave similarly except that they are prone to form exciplexes prior to Z or diradicaloid intermediates.

References

1. Huisgen, R., Grashey, R., and Sauer, J., *The Chemistry of Alkenes*, ed. Patai, S., New York: John Wiley, 1964, p. 739; Huisgen, R., *Angew. Chem., Inter. Ed. Eng.*, *7*, 321 (1968).

2. Woodward, R. B., and Hoffman, R., *The Conservation of Orbital Symmetry*, New York: Academic Press, 1970.

3. For reviews of [2 + 2] photocycloaddition, see Chapman, O. L., *Organic Photochemistry*, *1*, 333 (1967). For reviews of cycloaddition in the reactions of polyenes, see Seebach, D., *Fortschritt, Chem. Forschung*, *11*, 177 (1969); Scharf, H. D., *ibid.*, *11*, 216

(1969); Steinmetz, R., *ibid.*, *7*, 445 (1967); Meyer, H., *Photochemie II*, in *Methoden der Organischen Chemie*, Stuttgart: Houben-Weyl, Georg Thieme, 1976, p. 898 ff; Kaupp, G., *Photochemie I*, *Methoden der Organische Chemie*, Stuttgart: Houben-Weyl, 415a, 278 (1975).

4. Yamazaki, H., and Cvetanovic, R. J., *J. Am. Chem. Soc.*, *91*, 520 (1969); Yamazaki, H., Cvetanovic, R. J., and Irwin, R. S., *ibid.*, *98*, 2198 (1976).
5. Swenton, J. S., *J. Org. Chem.*, *34*, 3217 (1969).
6. Arnold, D. R., Hinman, R. L., and Glick, A. H., *Tetrahedron Lett.*, 1724 (1964); Scharf, D., and Korte, F., *ibid.*, 821 (1963); Arnold, D. R., Trecker, D. J., and Whipple, *J. Am. Chem. Soc.*, *87*, 2596 (1965).
7. Salomon, R. G., Folting, K., Streib, W. E., and Kochi, J. K., *J. Am. Chem. Soc.*, *96*, 1133, 11455 (1975).
8. Dilling, W. L., *Chem. Rev. 69*, 845 (1969).
9. Liu, R. S. H., Turro, N. J., and Hammond, G. S., *J. Am. Chem. Soc.*, *87*, 3406 (1965); Liu, R. S. H., and Hammond, G. S., *ibid.*, *89*, 4936 (1967); Hammond, G. S., Turro, N. J., and Liu, R. S. H., *J. Org. Chem.*, *28*, 3297 (1963).
10. Valentine, D. H., Turro, N. J., and Hammond, G. S., *J. Am. Chem. Soc.*, *86*, 5202 (1964).
11. Turro, N. J., and Bartlett, P. D., *J. Org. Chem.*, *30*, 1849 (1965); Dilling, W. L., Kroening, R. D., and Little, J. C., *J. Am. Chem. Soc.*, *92*, 928 (1970).
12. Kellogg, R. E., and Simpson, W. T., *J. Am. Chem. Soc.*, *87*, 4230 (1965).
13. Roberts, J. D., *Molecular Orbital Calculations*, New York: Benjamin, 1962, p. 48.
14. Krusic, P. J., Meakin, P., and Smart, B. E., *J. Am. Chem. Soc.*, *96*, 6212 (1974).
15. Review of intramolecular ring closures via photocycloadditions: Dilling, W., *Chem. Rev.*, *67*, 373 (1967).
16. Carlsson, D. J., and Ingold, K. U., *J. Am. Chem. Soc.*, *90*, 7047 (1968); Maillard, B., Forrest, D., and Ingold, K. U., *J. Am. Chem. Soc.*, *98*, 7024 (1976); Sheldon, R. A., and Kochi, J. K., *J. Am. Chem. Soc.*, *92*, 4395 (1970); Walling, C., and Cioffari, A., *ibid.*, *94*, 6059 (1972); Julia, M., *Acc. Chem. Research*, *4*, 386 (1971).
17. Michl, J., *Molec. Photochem.*, *4*, 243 (1972).
18. Dauben, W. G., and Cargill, R. L., *Tetrahedron*, *15*, 197 (1961); Ivanoff, N., et al., *J. Photochem.*, *2*, 199 (1973).
19. Hammond, G. S., Turro, N. J., and Fischer, A., *J. Am. Chem. Soc.*, *83*, 4674 (1961).
20. Hammond, G. S., Wyatt, P., De Boer, C. D., and Turro, N. J., *ibid.*, *86*, 2533 (1964); Murov, S., and Hammond, G. S., *J. Phys. Chem.*, *72*, 3797 (1968).
21. Turro, N. J., Cherry, W. R., Mirbach, M. F., and Mirbach, M. J., *J. Am. Chem. Soc.*, *99*, 7388 (1977).
22. Salem, L., and Rowland, C., *Angew. Chem. Int. Ed. Eng.*, *11*, 92 (1971).
23. Dauben, W. G., and Whalen, P. L., *Tetrahedron Letters*, 3743 (1966); Masamune, S., Cuts, H., and Hogben, M. G., *ibid.*, 1017 (1966).
24. Turro, N. J., Ramamurthy, V., and Katz, T. J., *Nouv. J. Chim.*, *1*, 363 (1977).
25. Freeman, P. K., and Balls, M., *J. Org. Chem.*, *32*, 2354 (1967).

26. Bausal, R. C., McCulloch, A. W., and Innes, A. G., *Canad. J. Chem.*, *47*, 2391 (1969).
27. Srinivasan, R., and Carlough, K. H., *J. Am. Chem. Soc.*, *89*, 4933 (1967).
28. Heathcock, C. H., Badger, R. A., and Starkey, R. A., *J. Org. Chem.*, *37*, 231 (1972).
29. Saltiel, J., and Zofiriou, O. C., *Mol. Photochem.*, *1*, 319 (1969); Liu, R. S. H., and Hammond, G. S., *J. Am. Chem. Soc.*, *86*, 1892 (1964); *ibid.*, *89*, 4936 (1967); Crowley, K. J., *Proc. Chem. Soc.*, *245*, 334 (1962).
30. Pryor, W. A., Fuller, D. L., Stanley, J. P., *J. Am. Chem. Soc.*, *94*, 1632 (1972); Hay, J. M., *Reactive Free Radicals*, New York: Academic Press, 1974, p. 112 ff; and Nonhebel, D. C., and Walton, J. C., *Free Radical Chemistry*, Cambridge: Cambridge Press, 1974, p. 210 ff.
31. Salem, L., et al., *Angew. Chem., Inter. Ed. Eng.*, *14*, 575 (1975).
32. Liu, R. H. S., *Tetrahedron Letters*, 2159 (1966).
33. For reviews of oxetane formation, see Arnold, D. R., *Adv. Photochem.*, *6*, 301 (1968); Meier, H., *Photochemie II*, in *Methoden der Organische Chemie*, Stuttgart: Houben-Weyl, Georg Thieme, 1976, p. 838.
34. For theoretical discussion of oxetane formation, see Herndon, W., *Tetrahedron Letters*, 125 (1971); *Molec. Photochem.*, *2*, 277 (1970).
35. For a discussion of the mechanism of oxetane formation see: Turro, N. J., *Pure Appl. Chem.*, *27*, 697 (1972); Dalton, J. C., and Turro, N. J., *Ann. Rev. Phys. Chem.*, *71*, 499 (1970).
36. Dauben, W. G., Salem, L., and Turro, N. J., *Acc. Chem. Research*, *8*, 41 (1975).
37. Turro, N. J., et al., *Acc. Chem. Research*, *5*, 92 (1972).
38. Turro, N. J., and Wriede, P. A., *J. Am. Chem. Soc.*, *92*, 320 (1970); Schrocter, S. H., and Orlando, C. M., *J. Org. Chem.*, *34*, 1181 (1969); Niemczyk, M., Ph.D. Dissertation, Columbia University, 1972.
39. Yang, N. C., et al., *Tetrahedron Letters*, 3657 (1964).
40. Firestone, R. A., *Tetrahedron*, *33*, 3009 (1977); Bennett, J. E., et al., *Chem. Phys. Letters*, *26*, 69 (1974).
41. Carless, H. A. J., *Tetrahedron Letters*, 3173 (1973).
42. Carless, H. A. J., *J. Chem. Soc., Perkin II*, 834 (1974).
43. Ryang, H. S., Shima, K., and Sakura, H., *J. Am. Chem. Soc.*, *93*, 5270 (1971); *J. Org. Chem.*, 2860 (1973); *Bull. Chem. Soc. Japan*, *50*, 7611 (1977).
44. Buchi, G., et al., *J. Am. Chem. Soc.*, *78*, 876 (1956); Bryce-Smith, D., Fray, G. I., and Gilbert, A., *Tetrahedron Letters*, 2137 (1964); Zimmerman, H. E., and Craft, L., *ibid.*, 2131 (1964).
45. Friedrich, L. E., and Bower, N. D., *J. Am. Chem. Soc.*, *95*, 6869 (1973).
46. Gorman, A. A., and Leyland, P. L., *Tetrahedron Lett.*, 5345 (1972); *ibid.*, 5085 (1973); Kubota, T., Shima, K., and Sakurai, H., *Chem. Letters*, 343 (1972).
47. Shimizu, N., et al., *J. Am. Chem. Soc.*, *96*, 6456 (1974).
48. Wilson, R. M., et al., *J. Am. Chem. Soc.*, *96*, 2955 (1974); *Chem. Comm.*, 461 (1974).
49. For a discussion, see Schore, N. E., and Turro, N. J., *J. Am. Chem. Soc.*, *97*, 2482 (1975); *ibid.*, 3079 (1971).

50. For a review of the evidence, see Caldwell, R. A., Sovocool, G. W., and Gajewski, R. P., *J. Am. Chem. Soc.*, *95*, 2549 (1973), and previous papers in this series.

51. Dalton, J. C., Wriede, P. A., and Turro, N. J., *J. Am. Chem. Soc.*, *92*, 1318 (1970).

52. Barltrop, J. A., and Carless, H. A. J., *J. Am. Chem. Soc.*, *94*, 1951 (1972).

53. Gale, D. M., *J. Org. Chem.*, *35*, 970 (1970).

54. Turro, N. J., and Ramamurthy, V., *Molec. Photochem.*, *8*, 239 (1977).

55. Turro, N. J., et al., *J. Am. Chem. Soc.*, *92*, 6978 (1970).

56. Surzur, J. M., and Bertrand, M. P., *Bull. Soc. Chim. France*, *5b*, 1861 (1973).

57. Bishop, R., and Hamer, N. K., *J. Chem. Soc.*, *C*, 1197 (1970).

58. Dalton, J. C., and Tremont, S. J., *Tetrahedron Letters*, 4025 (1973); *J. Am. Chem. Soc.*, *97*, 6916 (1975).

59. Sauers, R. R., and Rousseau, A. D., *J. Am. Chem. Soc.*, *94*, 1776 (1972).

60. Bichan, D., and Winnik, M., *Tetrahedron Letters*, 3857 (1974); Winnik, M. A., and Hsiao, C. K., *Chem. Phys. Letters*, *33*, 518 (1975).

61. Loutfy, R. O., Yip, R. W., and Dogra, S. K., *Tetrahedron Letters*, 2843 (1977); Niemczyk, M., Schore, N. E., and Turro, N. J., *Mol. Photochem.*, *5*, 69 (1973); Monroe, B. M., Lee C. G., and Turro, N. J., *ibid.*, *6*, 271 (1974).

62. Neunteufel, R. A., and Arnold, D. R., *J. Am. Chem. Soc.*, *95*, 4080 (1973); Shigemitsu, Y., Nakai, H., and Odaira, Y., *Tetrahedron Letters*, 2887 (1971).

63. Rehm, D., and Weller, A., *Ber. Bunsenges. Phys. Chem.*, *73*, 834 (1969).

64. Hautala, R. R., Dawes, K., and Turro, N. J., *Tetrahedron Letters*, 1229 (1972); Shima, K., Sakai, Y., and Sakurai, H., *Bull. Chem. Soc. Japan*, *44*, 215 (1971).

65. Hautala, R. R., and Turro, N. J., *J. Am. Chem. Soc.*, *93*, 5595 (1971); Yang, N. C., Hui, M. H., and Bellard, S. A., *ibid.*, *93*, 4056 (1971); Yang, N. C., Hui, M. H., Shold, D. M., Turro, N. J., Hautala, R. R., Dawes, K., and Dalton, J. C., *ibid.*, *99*, 3023 (1977); Sattiel, J., Coates, R. M., and Dauben, W. G., *ibid.*, *88*, 2745 (1966).

66. Barltrop, J. A., and Carless, H. A. J., *J. Am. Chem. Soc.*, *94*, 8761 (1972).

67. Loutfy, R. O., and Yip, R. W., *Can. J. Chem.*, *41*, 1881 (1973).

68. Schuster, D. E., Weil, T. M., and Halpern, A. M., *J. Am. Chem. Soc.*, *94*, 8248 (1972); Wolf, M. W., Brown, R. E., and Singer, L. A., *ibid.*, *99*, 526 (1977).

69. Borrell, P., and Sedlar, J., *Trans. Faraday Soc.*, *66*, 1670 (1970).

70. Suzur, J. M., Bertrand, M. P., and Nougier, R., *Tetrahedron Letters*, 4197 (1969); Rieke, R. D., and Cooke, B. J. N., *J. Org. Chem.*, *36*, 2674 (1971).

71. For reviews of the photocycloaddition reactions of benzenes, see Bryce-Smith, D., *Pure Appl. Chem.*, *16*, 47 (1968); *ibid.*, *34*, 193 (1973).

72. (a) Wilzbach, W. E., and Kaplan, L., *J. Am. Chem. Soc.*, *93*, 2073 (1971).
    (b) *Ibid.*, *90*, 3291 (1968); *ibid.*, *88*, 2066 (1966); Morikawa, A., Brownstein, and Cvetanovic, R. J., *ibid.*, *92*, 1471 (1970).

73. Merritt, V. Y., Cornelisse, J., and Srinivasan, R., *J. Am. Chem. Soc.*, *95*, 8250 (1973).

74. Yang, N. C., Neywick, C. V., and Srinivasachar, K., *Tetrahedron Letters*, 4313 (1975).

75. Hesse, G., and Lechtken, P., *Angew. Chem.*, *83*, 143 (1971); *Annalen.*, *754*, 1 (1972); Scharf, H. D., and Klar, R., *Tetrahedron Letters*, *517* (1971); *Chem. Ber.*, *105*, 575 (1972).

76. Bryce-Smith, D., Deshpande, R. R., and Gilbert, A., *Tetrahedron Letters*, 1627 (1975) and references therein.

77. Hartman, T. W., Heine, H.-G., and Schrader, L., *ibid.*, 3101 (1974).

78. Bryce-Smith, D., Gilbert, A., Orger, B., and Tyrrell, H., *Chem. Comm.*, 334 (1974).

79. For a general discussion of exciplexes see Section 5.11 ff.

80. Mizuno, K., Kaji, R., Otsuji, Y., *Chem. Letters*, 1027 (1977).

81. Farid, S., and Shealer, *Chem. Comm.*, 677 (1973); Yamamoto, M., Asanuma, T., and Nishijima, Y., *Chem. Comm.*, 53 (1975).

82. Yang, N. C., Libman, J., and Savitzky, M., *J. Am. Chem. Soc.*, *94*, 9226 (1972).

83. Taylor, G. N., and Hammond, G. S., *J. Am. Chem. Soc.*, *94*, 3687 (1972), and references therein.

84. Yang, N. C., Shold, D. M., and McVey, J. K., *J. Am. Chem. Soc.*, *97*, 5004 (1975).

85. Yang, N. C., Srinivasachar, K., Kim, B., and Libman, J., *J. Am. Chem. Soc.*, *97*, 5006 (1975).

86. Pac, C., Sugioka, T., and Sakurai, H., *Chem. Letters*, *39*, 667 (1972); Sugioka, T., Pac, C., and Sakurai, H., *Chem. Letters*, 791 (1972); Saltiel, J., D'Agostino, J. T., Chapman, O. L., and Lura, R. D., *J. Am. Chem. Soc.*, *93*, 2804 (1971).

87. For a review, see Cowan, D. O., and Dresko, R. L., *Elements of Organic Photochemistry*, New York: Plenum, 1976, p. 36 ff.

88. Selinger, B. K., and Sterns, M., *Chem. Comm.*, 978 (1969).

89. Chandross, E. A., and Dempster, C. J., *J. Am. Chem. Soc.*, *93*, 703 (1970).

90. Linebarger, C., *Amer. Chem. J.*, *14*, 597 (1892).

91. Chapman, O. L., and Adams, W. R., *J. Am. Chem. Soc.*, *90*, 2333 (1968); Chapman, O. L., and Lura, R. D., *ibid.*, *92*, 6352 (1970).

92. Cowan, D. O., and Drisko, R. L. E., *J. Am. Chem. Soc.*, *92*, 6281, 6286 (1970); Hartmann, I., Hartmann, W., and Schenck, G. O., *Ber.*, *100*, 3146 (1967).

93. For a review of photocycloadditions of cyclic enones, see Weiss, D. S., and Chapman, O. L., *Organic Photochemistry*, *3*, 197 (1973); Bauslaugh, P. G., *Synthesis*, 287 (1970).

94. Yamada, Y., Uda, H., and Nakanishi, K., *Chem. Comm.*, 423 (1966).

95. Corey, E. J., et al., *J. Am. Chem. Soc.*, *86*, 485, 5570 (1964).

96. Eaton, P., and Cole, T. W., *J. Am. Chem. Soc.*, *86*, 963 (1964).

97. Nelson, P. J., Ostrem, D., Lassila, J. D., and Chapman, O. L., *J. Org. Chem.*, *34*, 811 (1969).

98. Dilling, W. L., Tabor, T. E., Boer, F. P., and North, P. P., *J. Am. Chem. Soc.*, *92*, 1399 (1970).

99. Hammond, G. S., Stout, D. A., and Lamola, A. A., *J. Am. Chem. Soc.*, *86*, 3103 (1964); Krauch, H., Farid, S., and Schenck, G. O., *Chem. Ber.*, *99*, 625 (1966); Hoffman, R., Wells, P., and Morrison, H., *J. Am. Chem. Soc.*, *36*, 102 (1971).

100. Reviews of [2 + 2] photoadditions to enone: Bauslaugh, P. G., *Synthesis*, 287 (1970); de Mayo, P., *Acc. Chem. Research*, *4*, 41 (1971); Eaton, P. E., *ibid.*, *1*, 50 (1968).

101. Lenz, G. R., *Tetrahedron*, *28*, 2195, 2211 (1972).

102. Wiesner, K., et al., *Canad. J. Chem.*, *47*, 43 (1969).

103. de Mayo, P., et al., *Tetrahedron*, *24*, 1821 (1968).

104. Eaton, P. E., and Temme, G. H., *J. Am. Chem. Soc.*, *95*, 7508 (1973).

105. Reviews: Burr, J. G., *Adv. Photochem.*, *6*, 193 (1968).

106. Eisenger, J., and Lamola, A. A., *Mol. Photochem.*, *1*, 209 (1969).

107. Lamola, A. A., *Photochem. Photobio.*, *7*, 619 (1968); Lamola, A. A., *Pure Appl. Chem.*, *24*, 599 (1970).

108. Charlton, J. L., Liao, C. C., and de Mayo, P., *J. Am. Chem. Soc.*, *93*, 2403 (1971).

109. Koch, T. H., and Howard, K. H., *Tetrahedron Letters*, 4035 (1972).

110. Lawrence, A. H., Liao, C. C., de Mayo, P., and Ramamurthy, V., *J. Am. Chem. Soc.*, *89*, 2219, 3572 (1976).

111. Ohno, A., Ohnishi, Y., and Tschihashi, *J. Am. Chem. Soc.*, *91*, 5038 (1969); de Mayo, P., and Shizuka, H., *ibid.*, *95*, 3942 (1973).

112. Turro, N. J., and Ramamurthy, V., *Tetrahedron Letters*, 2423 (1976); Gotthardt, H., and Nieberl, S., *ibid.*, 3999 (1976).

12

Isomerizations and Rearrangements

12.1 Classification of Photochemical Rearrangements

Many photoreactions are known to interconvert isomeric compounds. The term "rearrangement" is more general than "isomerization," but for the reactions discussed in this chapter we will not be concerned with a distinction between these terms.

For convenience, we shall classify *primary* photochemical rearrangements as the following reaction types:

1. Cis-trans isomerization.
2. Sigmatropic rearrangements.
3. Electrocyclic rearrangements.
4. Structural rearrangements which result from intramolecular cycloadditions.

In a broad sense all four of these classes are special cases of *pericyclic* rearrangements and, for concerted reactions, they all may be treated under a unifying framework guided by the rules derived from orbital-symmetry considerations.[1]

12.2 Cis-trans Isomerization of Unsaturated Compounds

Absorption of a photon by a compound containing an olefinic link often results in cis-trans geometrical isomerization.[2] Cis-trans isomerization may also be effected by photosensitization and is one of the most general photoreactions of

ethylenes and other unsaturated linkages capable of geometrical isomerization, (e.g., C=N, N=N, etc.).

It is important to note that numerous photoreactions of compounds containing cyclic double bonds which are overall linear additions, cycloadditions, electrocyclic reactions, rearrangements, etc., are, in fact, photoinduced cis-trans isomerizations followed by reaction of a reactive trans-cyclic isomer (Section 10.11). For example, the solvent addition reaction (Eq. 12.1) and the fragmentation reaction (Eq. 12.2) both involve an initial photochemical cis-trans isomerization to form highly reactive trans-cyclic ethylenes (**1** and **2**) which proceed to products via secondary thermal reactions.

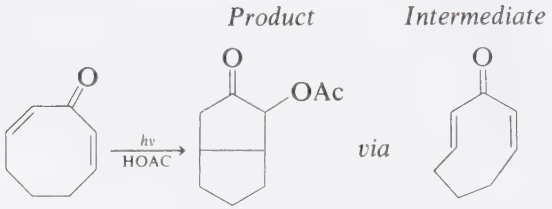

(12.1)[3]

1

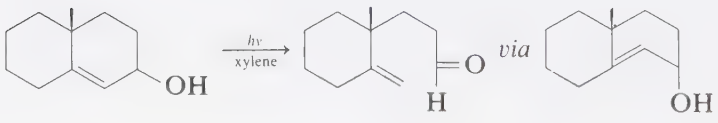

(12.2)[4]

2

Mechanisms of Photosensitized cis-trans Isomerization

There are two general mechanisms of photosensitized cis-trans isomerizations of ethylenes:[5]

1. Energy transfer in which an electronically excited state of the ethylene is produced. The S_1 or T_1 state produced then undergoes a twisting motion about the C=C bond until a critical geometry is reached and radiationless transition to S_0 occurs (Fig. 12.1).

2. Chemical sensitization in which the sensitizer effects cis-trans isomerization but an electronically excited ethylene is not formed.

In class 1 there are two convenient subclassifications:

1a. "Vertical" energy transfer, in which the ethylene excited state formed initially has a nuclear shape similar to that of *vertical* transitions achieved by light absorption of the equilibrium ground state shape (Eq. 12.3).

1b. "Nonvertical" energy transfer, in which the ethylene excited state formed is significantly different from that involved in probable spectroscopic ("vertical") radiative transitions (Eq. 12.4).

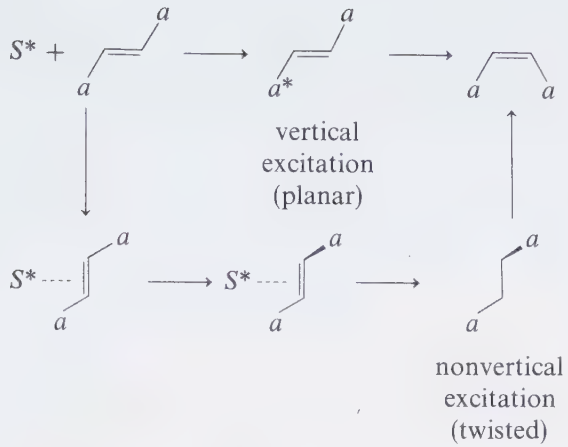

(12.3)

(12.4)

Experimentally, we expect "nonvertical" energy transfers[6] to be possible whenever the energy acceptor ethylene is unusually flexible with respect to twist about its C=C bond and when sens-ethylene electronic interactions are significant (Section 9.18). The cis-trans isomerization of the excited sensitizer-ethylene complex on an excited state surface may be considered as essentially the same as that of the free ethylene (weak excited sensitizer-ethylene interactions) or as one which is significantly different from that of the pure ethylene (strong excited sensitizer-ethylene interactions). The latter corresponds to a strong electronic interaction or strong spin-orbit interaction between the sensitizer and ethylene. Such mechanisms can be termed *Schenck mechanisms*[7] for photosensitization.

Photochemical cis-trans Isomerization of Ethylenes and Conjugated Polyenes

The photochemical cis-trans isomerizations of ethylenes—and especially 1,3-dienes—hold a special place in the theoretical development and practice of

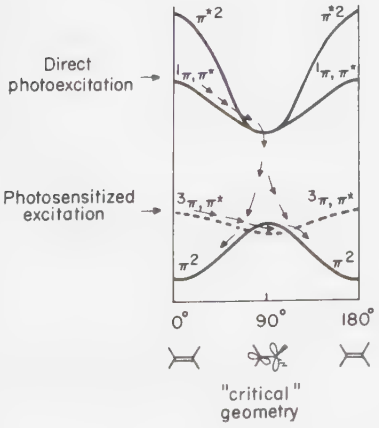

Figure 12.1
Prototype surface diagram for twisting about a C=C bond.

mechanistic organic photochemistry. 1,3-dienes are commonly employed as probes of photoreaction mechanisms by serving as triplet energy acceptors.[8] Since the triplets of 1,3-dienes undergo efficient cis-trans isomerization, the observation of photosensitized cis-trans isomerization has often been employed as diagnostic of triplet energy transfer. However, as mentioned above, numerous mechanisms for cis-trans isomerization exist and many do not require involvement of an ethylene or diene triplet. Nevertheless, 1,3-dienes are often useful as specific triplet quenchers (Section 8.7). An ideal triplet quencher would have a high selectivity toward triplet (relative to singlet) quenching (say $>10^3$ to 1). Also an ideal quencher should not undergo irreversible reactions with the sensitizer it is quenching. Finally, an ideal quencher should undergo some specific reaction or emit a characteristic emission.

Dienes are nearly ideal triplet quenchers of a number of triplet sensitizers. For alkyl ketones, for example, 1,3-dienes usually quench T_1 from 10^2 to 10^4 times faster than they quench S_1.[9] Adducts of ketones and dienes derived from triplet quenching are only formed with low quantum yield.[10] Finally, cis-trans-isomerization of the diene serves as a chemical manifestation of the quenching event.

Experimental Examples of cis-trans Isomerization of Ethylenes

Cis-trans isomerization of acyclic ethylenes and polyenes is a very general photoreaction which can be effected by direct or sensitized excitation.[2] One of the simplest ethylenes, 2-butene, undergoes cis-trans isomerization upon direct excitation or upon triplet sensitization.

Both benzene triplets and ketone triplets sensitize the cis-trans isomerization of the 2-butenes.[11] The mechanisms for these sensitizations probably differ. The triplet energy of benzene is somewhat higher ($\sim$84 kcal mole) than that for 2-butene ($\sim$80 kcal mole). Thus, triplet energy transfer from benzene triplet to the butene triplet is likely. Sensitizers whose triplet energy is less than 70 kcal mole (e.g., benzophenone) are also capable of effecting sensitization of cis-trans isomerization, presumably via a Schenck mechanism. Reaction of the ketone triplet with the butene to form an intermediate, capable of executing rotations about the CC bond, probably occurs.[12] A 1,4-diradical intermediate is a likely candidate. This species can also collapse to form oxetanes, products which commonly accompany the ketone photosensitized cis-trans isomerization of ethylenes (see Section 11.3).

Photosensitized cis-trans Isomerization of Polyenes

The rates of conversion of trans to cis and cis to trans isomers are equal at the "photostationary state." Stilbene and 1,3-pentadiene are isomerized to photostationary mixtures by various triplet sensitizers.[2] A most remarkable feature of these photostationary mixtures is that the ratio of cis to trans isomers depends on the sensitizer employed (Fig. 12.2).

As an example, consider the triplet photosensitized isomerization of 1,3-pentadiene.[8] It was found that dibenzalacetone, acetylpyrene, and benzanthrone (sensitizers whose triplet states are less than 53 kcal mole^{-1} above their ground

states) are extremely inefficient as sensitizers. This is in marked contrast to the high efficiency exhibited by other carbonyl compounds, whose triplet energies were greater than ~55 kcal/mole. Sensitizers whose triplet-excitation energies are above 60 kcal mole^{-1} give the same photostationary mixtures (a cis-trans mixture containing 55% of the trans isomer); while sensitizers whose triplet excitation energies are below 60 kcal mole^{-1} give a variety of results (photostationary cis-trans mixtures varying from 65 to 80% trans), and are markedly less efficient in effecting cis-trans isomerization.

Postulates which easily accommodate these results are that

1. All the sensitizers whose E_T is greater than 60 kcal mole^{-1} transfer triplet energy to either cis- or trans-1,3-pentadiene in a diffusion controlled process, so that the composition of the photostationary mixtures depends only on the unimolecular decay processes of the pentadiene triplets.

2. If the energy of the sensitizer is less than 60 kcal mole^{-1}, transfer to trans-1,3-pentadiene becomes measurably inefficient, and the photostationary mixture becomes richer in trans, because the system is preferentially "pumped" to produce the cis-diene triplet which may decay to either the cis or trans isomer.

3. A point is reached at which transfer to both isomers becomes somewhat inefficient and energetics are no longer the controlling factor in the energy transfer step.

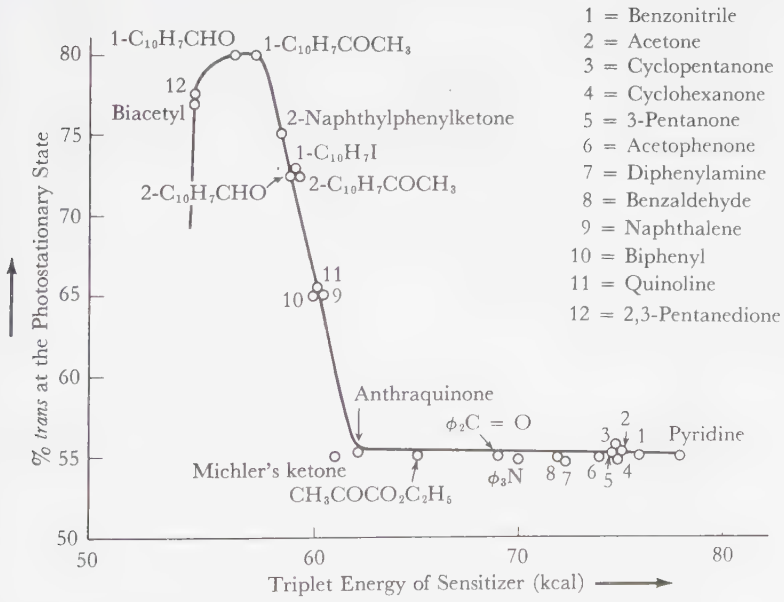

Figure 12.2
Photosensitized isomerization of the piperylenes.

4. Sensitizers with E_T less than 53 kcal mole^{-1} are inefficient at exciting either isomer because they possess insufficient excitation energy to transfer efficiently to either the cis or trans isomer.

From a simple mechanism which assumes that a common triplet is produced in sensitized cis-trans isomerizations and that energetics are the controlling factor in the energy transfer step, we predict that at the photostationary (PSS) state:

$$\frac{[\text{cis}]_{\text{PSS}}}{[\text{trans}]_{\text{PSS}}} = \frac{k_{qt}}{k_{qc}} \times \frac{k_c}{k_t} \tag{12.5}$$

where k_{qt} and k_{qc} are the rate constants for quenching of the sensitizer excited state by the trans and cis isomers, respectively, and k_c and k_t are the rate constants for decay of triplet diene to cis and trans ground states, respectively. For high-energy sensitizers $k_{qt}/k_{qc} = 1$, i.e., energy transfer occurs at close to the diffusion-controlled rate to each isomer, and the equation simplifies to

$$\frac{(\text{cis})_{\text{PSS}}}{(\text{trans})_{\text{PSS}}} = \frac{k_c}{k_t} \tag{12.6}$$

i.e., for "high"-energy sensitizers the composition of the isomer mixture depends only on the rate of decay of triplet 1,3-pentadiene to cis- or trans-1,3-pentadiene. When transfer to trans-1,3-pentadiene becomes inefficient $k_{qc} > k_{qt}$ and the relative yield of trans isomer in the photostationary mixture increases.

An interesting contrast has been noted between the direct cis-trans isomerization of dienes and triplet-sensitized cis-trans isomerization.[13] The singlet reaction proceeds with just *one* terminal double bond rotation, whereas the triplet proceeds with "double" double bond rotation. Experimentally the conversion of a trans-trans diene into a cis-trans diene occurs exclusively in direct excitation, but the formation of some cis-cis diene occurs in sensitized excitation:

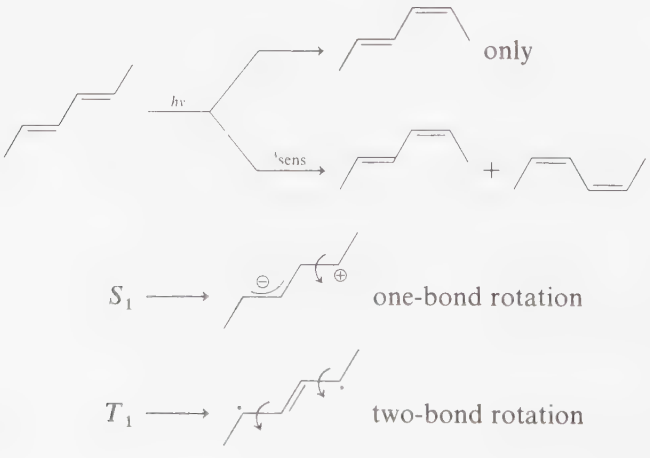

(12.7)

From the standpoint of syntheses, it is often possible to photochemically "drive" a reaction exclusively toward the formation of the cis or trans isomer. In this regard, if one of the isomers absorbs strongly in a region of the spectrum where the other isomer does not, the absorbing isomer will be driven to the nonabsorbing isomer. It is also possible to use photosensitizers to drive the specific formation of one isomer. This technique works best when the sensitizer transfers energy specifically to one of the two cis/trans isomers. An example of the use of photosensitized excitation in synthesis is found in the photosensitized trans-cis isomerization of β-ionol (Eq. 12.8).[14] Low-energy triplet sensitizers ($E_T \gtrsim 65$ kcal/mole) selectively excite trans-ionol, driving the photostationary mixture completely to the less stable cis-ionol (Fig. 12.3).

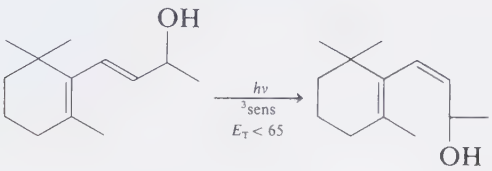

(12.8)

trans-ionol

Linear polyenes related to ionol are involved in the mechanism of vision, which is believed to be triggered by a photochemical cis-trans isomerization.[15] The cis-

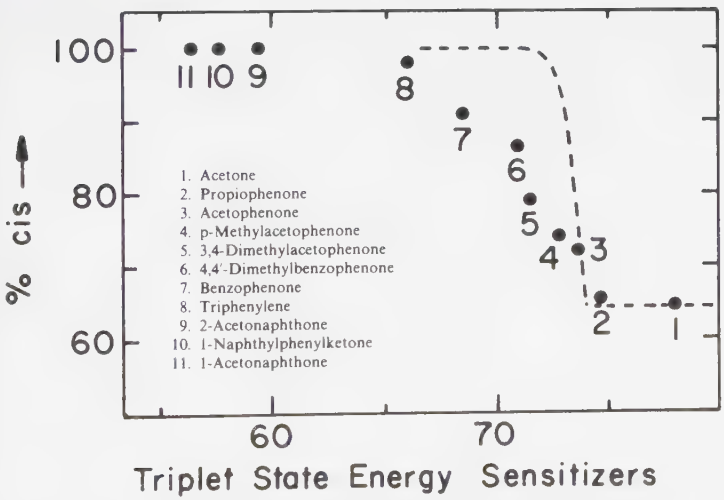

Figure 12.3

Photostationary state compositions of β-ionol as a function of sensitizer excitation energy. The dashed line is that of calculated compositions based on excitation involving ground state activation only (see text).

trans isomerization of the stilbenes has received considerable mechanistic attention and appears to proceed in both S_1 and T_1 states.[2]

Uses of cis-trans Isomerization

Compilation of data such as that shown in Figures 12.2 and 12.3 allows an estimation of the E_t of sensitizers. This may be important if no method is available for direct measurement of this quantity. Photochemical reactions may be studied by including isomerizable ethylenes in the photolysis mixture. If quenching of the photoreaction and cis-trans isomerization occur concurrently, this gives presumptive evidence for a triplet intermediate in the direct photolysis. Dienes are especially suited for such studies because of their large S_1-T_1 energy split, which puts S_1 at close to 125 kcal mole^{-1} (which is higher than the singlet excitation energy of many organic molecules), and T_1 at about 55 to 60 kcal mole^{-1} (which is lower than the triplet excitation energy of many other organic molecules). This allows the use of many sensitizers for which only energy transfer to diene triplets is energetically possible.

Cis-trans Isomerization of Cycloalkenes

The relationship between reactivity toward cis-trans isomerization and ring size can be inferred from an extension of the ideas presented earlier in the discussion of acyclic ethylenes. Both S_1 and T_1 energetically prefer a rotation about the C=C bond to achieve the 90° twist angle which minimizes the π and π^* electron repulsions (see Fig. 12.1)

The concept of strain is a valuable guide to the understanding of photochemical cis-trans isomerization of cycloalkenes. Strain may be defined as a general destabilizing feature of a molecule which is introduced along with deviation of valence angles from optimal values as a result of molecular structural constraints.[16] Strain raises the energy of a strained molecule relative to an unstrained model and affects the physical and chemical properties of the molecule.

A 90° twisted conformation of S_1 and T_1 should be possible and a severely twisted ground-state isomer with a finite kinetic stability can occur. We shall refer to such species as a "trans" isomer. The following rules are an empirical classification of the possibility of achieving "trans" isomers of cycloalkenes by photoexcitation:

1. 3 or 4 rings—"impossible."
2. 5 rings—"difficult." reactive cycloalkene produced.
3. 6 or 7 rings—"facile", reactive cycloalkene produced.
4. 8 and more rings—"facile", stable cycloalkene produced.

The smallest carbocyclic trans double bond which has been synthesized and matrix isolated is trans-2-cycloheptenone, prepared by photoexcitation of cis-2-

cycloheptenone.[17] This species has also been detected at room temperature in fluid solid by flash spectroscopy:[18]

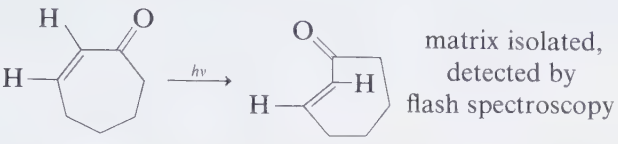

(12.9)

In Section 10.11 we noted that formation of trans-cycloalkenes (especially cyclohexenes and cycloheptenes)[19] could result in protonation of the strained cycloalkene to produce a carbonium ion and to result in ionic additions to the strained cycloalkene. It was also noted in Section 12.2 that strained cycloalkenes may undergo other net reactions (Eqs. 12.1 and 12.2).

The decay rates of the S_1 and T_1 states of 1-phenylcycloalkenes are consistent with a ring size dependent deactivation via rotation about the ring C=C bond.[20a] Irradiation of 1-phenylcyclohexene in methanol (Eq. 12.10) produces a transient ($\tau \sim 10 \times 10^{-6}$ sec) which has been identified as trans-1-phenylcyclohexene:[20b]

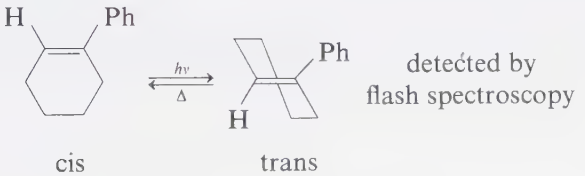

(12.10)

Photochemical cis-trans Isomerization of Unsaturated Groups other than Ethylenes

Unsaturated groups other than ethylenes undergo photochemically induced cis-trans isomerizations. For example, alkyl and aryl trans-azo compounds are photoisomerized into the less stable cis-azo (Eq. 12.11) compounds by both direct and photosensitized excitation.[21]

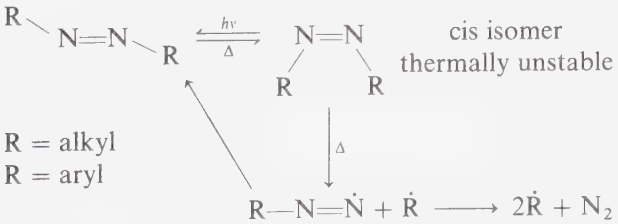

(12.11)

The cis-azo alkanes are frequently unstable with respect to thermal reaction[22] such as reisomerization to the trans isomer or fragmentation into radicals (this process is discussed in detail in Section 13.4).

The singlet and triplet states of azo compounds may exhibit different photochemistry.[23] For example, direct irradiation of the diazacyclooctene **1** (Eq. 12.12)

results in loss of nitrogen and fragmentation products **2** and **3**. Sensitized excitation results mainly in cis-trans isomerization (Eq. 12.13). The latter thermally reverts to the more stable cis-isomer.[24]

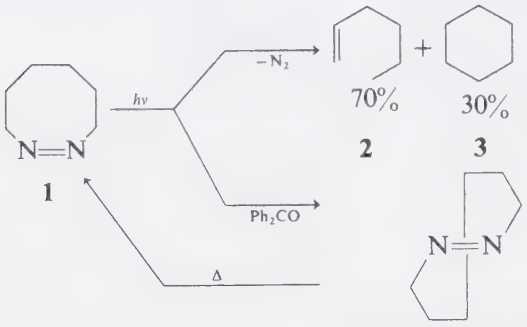

(12.12)

(12.13)

trans-diazacyclooctene

The smallest size for which a trans-azo double bond has been isolated or detected spectroscopically is a seven-membered ring.[25]

The photoisomerization of other unsaturated groups (imines, oximes, etc.) is known but has not been the subject of extensive mechanistic studies.[26]

12.3 Skeletal and Positional Photoisomerizations: Sigmatropic Rearrangements

A commonly encountered structural photoisomerization involves rearrangement of the carbon skeleton or position of a substitutent in such a way that a sigma-bond shift occurs from a given position along a chain of carbon atoms to a new position.[1] Such isomerizations are termed *sigmatropic rearrangements* when a sigma bond moves from one position to another along a conjugated π system. The most important sigmatropic rearrangements involve carbon skeletal shifts or hydrogen shifts. Examples of carbon skeletal and hydrogen sigmatropic rearrangements are given in Scheme 12.1.

Sigmatropic rearrangements are classified by convention in terms of the number of atoms involved in the rearrangement. One identifies the sigma bond being broken in the reactant ("starred" atoms in the Scheme) and assigns each of these atoms the number 1. Then one counts along the carbon-connected atoms until the two positions of the *new* sigma bonds of the product are located. These positions are assigned the numbers i and j, which correspond to the number of carbon atoms intervening between the old and new sigma bonds. The rearrangement is classified as $[i,j]$. If a hydrogen undergoes migration, there are no carbon atoms intervening

the old and new sigma bond for half of the rearrangement. Thus, sigmatropic rearrangements of hydrogen are necessarily of the [1,*j*] variety.

Since sigmatropic reactions are pericyclic reactions, a set of selection rules are available for predicting which sigmatropic reactions are likely to be concerted. In concerted sigmatropic rearrangements, as in other concerted pericyclic reactions, the nature of bonding in the transition state determines whether the reaction pathway is allowed or forbidden in terms of orbital symmetry (Table 12.1).

Suprafacial and antarafacial bonding refer specifically to the atoms undergoing breaking and making of the new sigma bond. *Suprafacial* bonding implies retention at both reaction termini whereas *antarafacial* bonding implies inversion at one of the reaction termini. In open-chain systems, antarafacial bonding may be difficult to achieve, and in certain cyclic systems antarafacial interaction is structurally impossible, thereby militating against any "allowed" process requiring an antara-

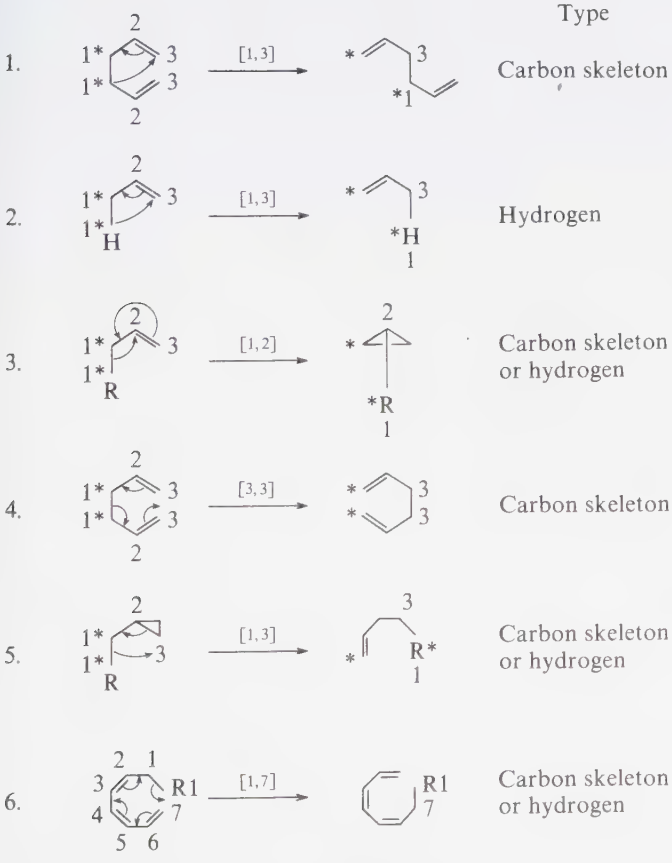

Scheme 12.1

Examples of sigmatropic rearrangements.

Table 12.1 Orbital Symmetry Rules for Concerted Sigmatropic Rearrangements

	Allowed	
	Ground state	Excited state
Number of electrons	Δ	$h\nu$
$4q$ ($q = 1, 2$, etc.) → 4e, 8e, etc.	(supra-antara)	supra-supra (antara-antara)
$4q + 2$ ($q = 1, 2$, etc.) → 2e, 6e, etc.	supra-supra (antara-antara)	(supra-antara)

facial interaction (Fig. 12.4). As a result, (except in special structural situations, *vide infra*) we anticipate that concerted photochemical sigmatropic rearrangements should occur preferentially if $4q$ electrons are involved, because orbital symmetry allowed and structurally facile supra-supra bonding is involved in such situations. An easy bookkeeping procedure for deciding on the number of electrons involved in a sigmatropic rearrangement is to use the "curved arrow" convention to transform reactant to product (see Scheme 12.1). Two times the number of curved arrows equals the number of electrons.

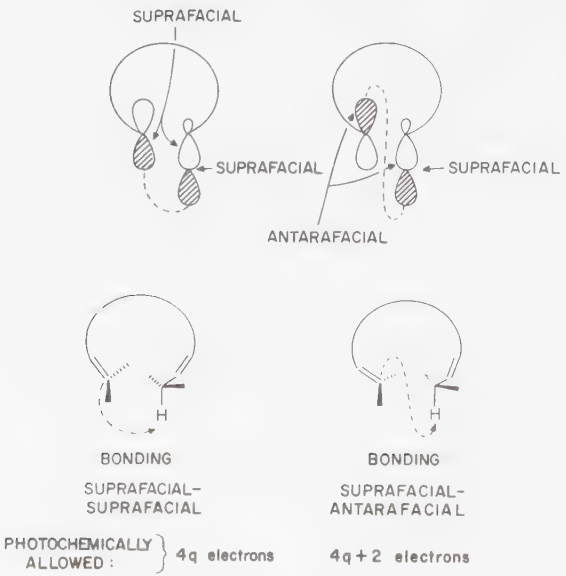

Figure 12.4

Schematic representation of suprafacial bonding during a [1, *n*] rearrangement involving a hydrogen atom. Suprafacial bonding is generally more accessible to acyclic, nonconstrained systems than is antarafacial bonding.

In general, since suprafacial-suprafacial bonding is generally structurally more feasible than suprafacial-antarafacial bonding, it is expected that $4q$ electron processes will be the more frequently encountered photochemical sigmatropic rearrangements (e.g., the [1,3], [1,2], and [1,7] isomerizations in Scheme 12.1). In certain rigid cyclic systems, suprafacial-suprafacial bonding may become very difficult but because of molecular structure antara-antara bonding is feasible. For these systems $4q$ processes may also occur photochemically. In terms of "electron bookkeeping," if a sigmatropic rearrangement (without structural constraints) can be written with a formal "two-arrow" or four-electron mechanism or a formal "four-arrow" or eight-electron mechanism, the reaction is "photochemically" allowed, i.e., assuming that suprafacial-suprafacial bonding is not restrained, the reaction can proceed concertedly with a low-energy barrier in S_1.

[1,3], [1,5] and [1,7] Sigmatropic Rearrangements of Alkenes and Polyenes and Related Molecules

On the basis of the orbital symmetry selection rules in Table 12.1, we expect that $^1\pi, \pi^*$ states will possess a tendency to undergo 4- or 8-electron sigmatropic rearrangements, since these isomerizations are allowed to occur supra-supra via the readily attainable bonding. Experimentally, many examples confirm this expectation. For example, direct irradiation of **4** results in a [1,3] sigmatropic rearrangement to **5** (Eq. 12.14).[27] Since the triplet-sensitized reaction follows a completely different course to form the $\chi[2 + 2]$ adduct **7** (Eq. 12.16), the **4** → **5** transformation is a singlet reaction, possibly via a concerted reaction. Interestingly, thermolysis of **4** results in different, but still "allowed" thermal sigmatropic rearrangement, the six-electron [3,3] sigmatropic shift (*Cope rearrangement*) to **6** (Eq. 12.15).

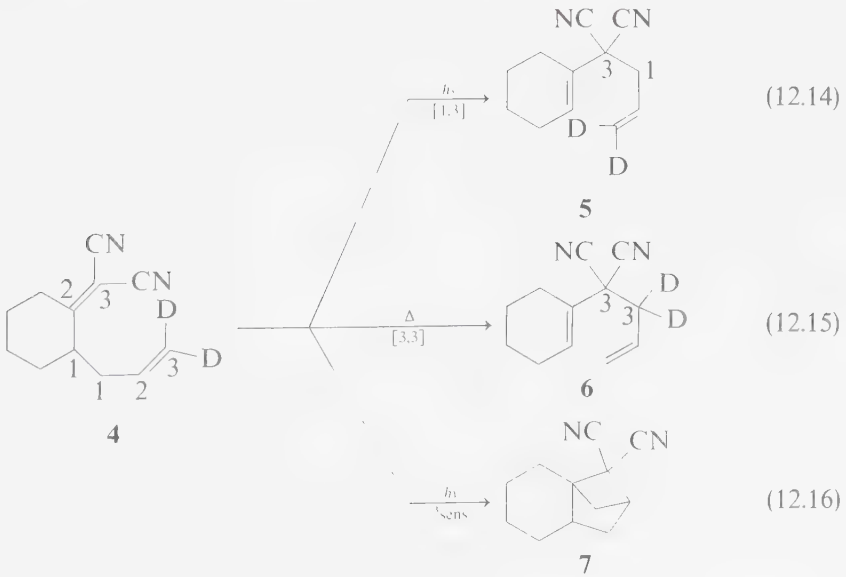

(12.14)

(12.15)

(12.16)

Irradiation of many cycloheptatrienes results in an eight-electron [1,7] sigmatropic rearrangement of a hydrogen or alkyl group (e.g., **8** → **9**). The specificity of this reaction contrasts with the occurrence of a specific six electron [1,5] sigmatropic rearrangement when cycloheptatrienes are heated.[28] Although a *four*-electron [1,3] sigmatropic rearrangement is photochemically "allowed," the formation of the transition state for this isomerization does not compete favorably with the more accessible transition state for "equally allowed" eight electron [1,7] rearrangement.[29] In general, [1,3] and [1,7] sigmatropic shifts *do not occur upon triplet photosensitization*, so reactions such as these are assumed to occur exclusively via S_1 and are probably concerted.

The conversion of **10** to **11** may involve an allowed supra-antara [1,5] shift.[30]

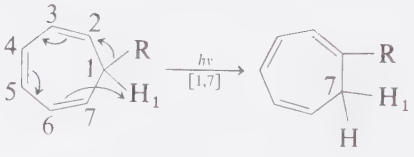

(12.17)

8 **9**

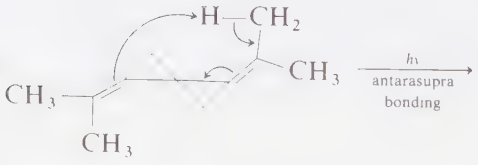

10

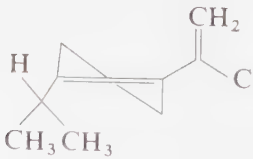

(12.18)

11

Direct irradiation of tetrasubstituted alkenes (e.g., Eq. 12.19) results in sigmatropic rearrangements.[31] The product structures suggest a carbene intermediate

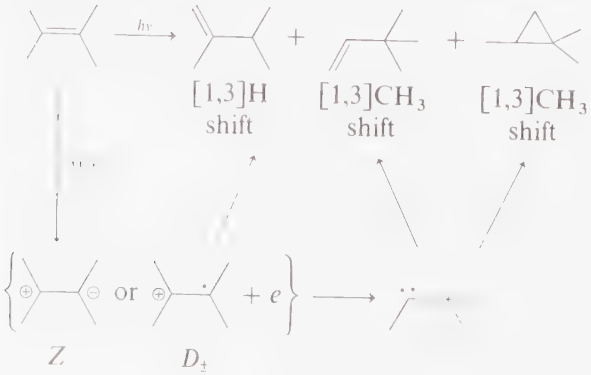

(12.19)

rather than a concerted reaction from S_1. In protonic solvents, ionic adducts are also produced (Section 10.11). These reactions may be explained in terms of a Z intermediate produced from S_1 of the ethylene or in terms of an electron ejection to yield a $D_{\pm}$ intermediate (radical cation plus an electron) from S_1. As expected, these reactions are not achievable via triplet photosensitization.

Carbene intermediates have also been invoked to explain the [1,2] or [1,3] rearragnements of styrenes and related compounds.[32] Indenes, on the other hand, undergo [1,5] sigmatropic rearrangements to isoindenes [(Eq. 12.20) which have been trapped chemically and detected spectroscopically.[33]

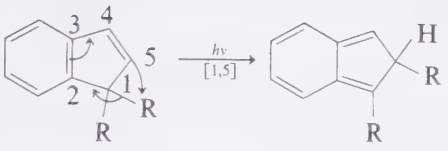

(12.20)

indene isoindene

[1,2] Rearrangements of Hydrocarbons: The Di-π-Methane Rearrangement

The di-π-methane reaction is a [1,2] sigmatropic rearrangement of 1,4-dienes (or equivalent structures) to vinyl cyclopropanes (Eq. 12.21).[34] Although the second

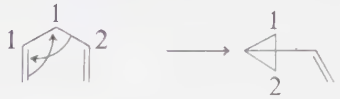

(12.21)

1,4-diene
("di-π-methane")

double bond is not formally required for the occurrence of an overall [1,2] sigmatropic rearrangement, it is clear that 1,4-dienes employ the second bond in the rearrangement. In this regard, the reaction is most effective when structural factors allow for interaction of the 2,4-centers of a 1,4-diene. As a rule, only singlet states of acyclic ethylenes and/or triplet states of rigid cycloalkenes are involved as the reactive states in di-π-methane rearrangements, i.e., acyclic triplet and cyclic singlet systems generally undergo the reaction only inefficiently.[35] These rules are summarized in Table 12.2.

Table 12.2 Structure-Efficiency Rules for the Di-π-methane Rearrangement of Hydrocarbons

Reactive state	Acyclic	Rigid cyclic
S_1	Efficient	Inefficient
T_1	Inefficient	Efficient

A formal mechanistic scheme for the di-π-methane reactions is shown in Scheme 12.2. The mechanism is an extreme situation in which discrete diradical intermediates are shown. In any actual case some or all of the steps may merge into one step, i.e., the reaction may tend toward a concerted reaction.

As some examples of the rules given in Table 12.2, the compounds **12** (Eq. 12.22) and **13** (Eq. 12.23) undergo [1,2] shifts upon direct excitation, but only cis-trans isomerization occurs upon triplet sensitized excitation.[36] Note that upon direct excitation the [1,2] shift is both regiospecific and stereospecific.

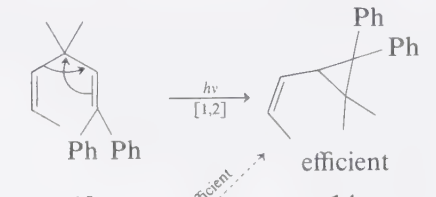

(12.22)

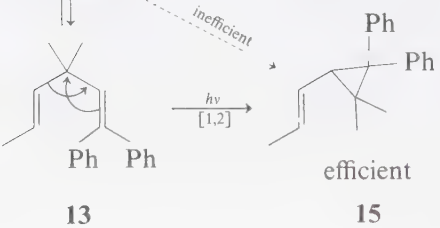
^{3}sens
via T_1
inefficient
Ph
Ph
hν
[1,2]
via S_1
Ph Ph
efficient
13
15

(12.23)

In contrast to the results of the above acyclic systems, the cyclohexadiene **16** undergoes a [6] electrocyclic ring opening from its $S_1(\pi, \pi^*)$ state to form **17** (see

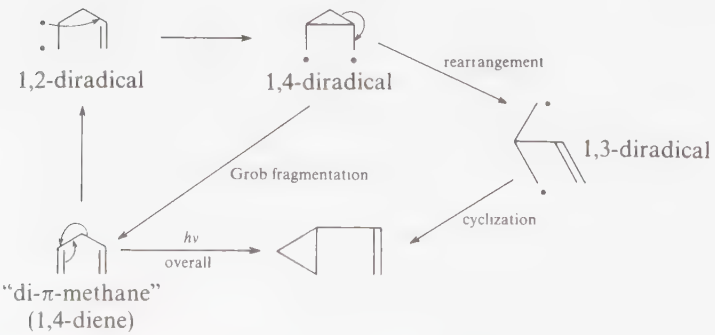

Scheme 12.2

Paradigm for the di-π-methane reaction. Usually the initial 1,2-diradical is derived from a triplet. It is not known at which step intersystem crossing occurs. In certain cases some or all of the steps may merge into a concerted mechanism.

Section 12.4 for a discussion of photoinduced electrocyclic reactions). In contrast, the T_1 state of **16** undergoes di-π-methane rearrangement to **18**.[37] Note that Eqs. 12.22–12.25 exemplify the rules summarized in Table 12.2 and that in Eq. 12.25 a double bond of a phenyl group serves as one of the di-π-methane components.

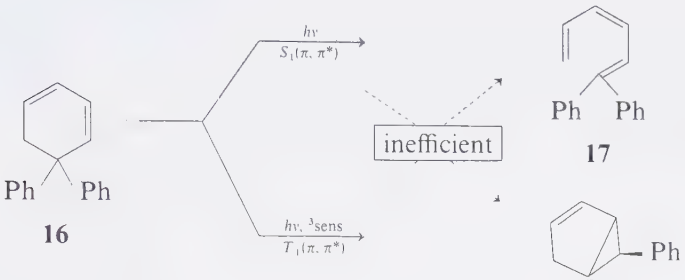

(12.24)

(12.25)

These reactions exemplify several other points concerning the di-π-methane reaction.

When an asymmetric diene is employed, the three-membered ring is usually derived from rearrangement of the lowest energy chromophore. Another rule which yields the same predictions is: to predict the product, consider the 1,4-diradical intermediate (Scheme 12.2) and cleave the bond adjacent to the least stable radical (Eq. 12.26). These rules are based on the theoretical notion of maximum π-delocalization in the bond- making or breaking steps. Thus to predict the product from **12** or **13** we (a) note either that the diphenylethylene chromophore is lower in energy than the alkene chromophore, or (b) cleave the cyclopropane bond adjacent to the alkyl radical in the diradical intermediate (Eq. 12.26).

The reason for the inefficiency of [1,2] shifts from T_1 in acyclic systems may be simply a result of a faster deactivation to the ground state by twisting about double bonds in the triplet state.[20] This would constitute an example of the "free-rotor"

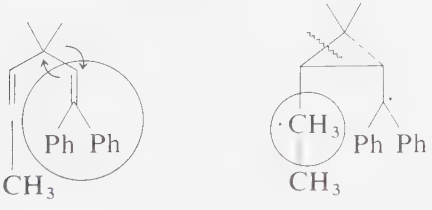

19a, lower energy

19b, less stable radical

(12.26)

effect,[6] in which radiationless decay to ground state occurs via the twisting mechanism $T_1 \rightarrow {}^3D \rightarrow {}^1D \rightarrow S_0$.

In contrast to the behavior of **12** and **13**, the bicyclic molecule **20** (trivial name "barrelene") undergoes [1,2] shift (Eq. 12.27) to **21** when triplet sensitized, but upon direct irradiation reaction leads to cyclooctatetraene (**22**):[38]

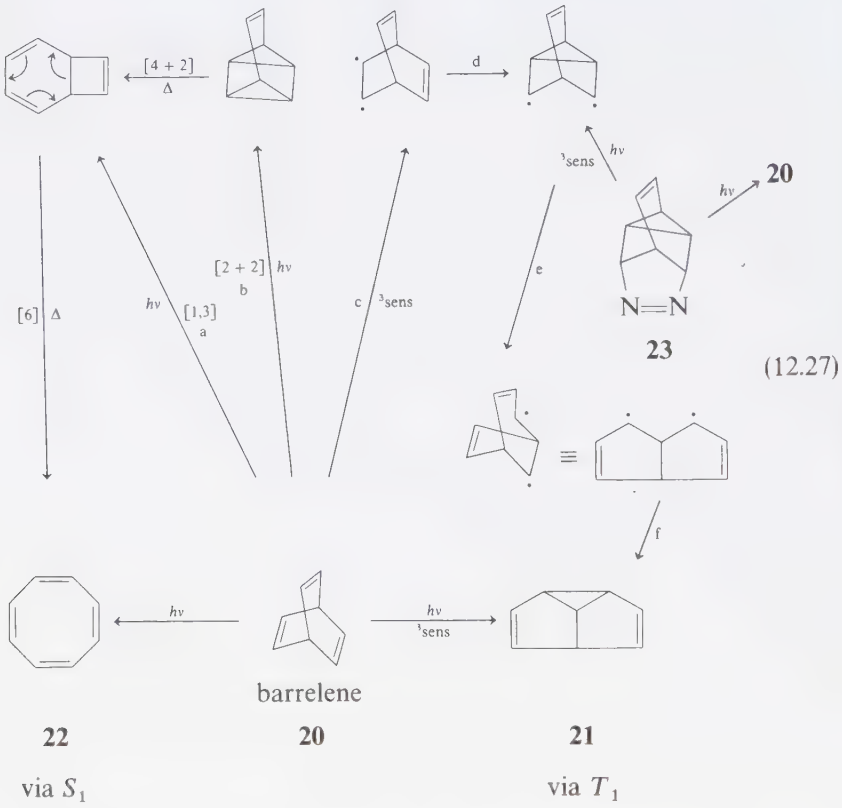

(12.27)

The pathway to cyclooctatetraene in the direct irradiation of **20** is not known. Two allowed pathways are shown in Eq. 12.27: (a) a primary photochemical [1,3] shift of **20** to produce bicyclooctatriene, which then undergoes a thermal ring opening to product; and (b) a primary photochemical [2 + 2] cycloaddition followed by thermal reverse [4 + 2] to yield the bicyclooctriene.

The biradical pathway c → d → e → f in the triplet reaction to form **21** from **20** is supported by deuterium labeling experiments and the observation that photosensitized decomposition of the azo compound **23**[39] yields **21** exclusively (Eq. 12.27). The photosensitized decomposition of **23** is expected to lead to a triplet diradical which is identical in structure to that postulated along the pathway from **20** to **21**.

An aromatic ring system may replace one of its double-bond components in a di-π-methane isomerization.[40] For example, triplet-sensitized isomerization of benzonorbornadienes to tetracyclic compound **25** occurs via an efficient ($\Phi \sim 0.5$) [1,2] sigmatropic rearrangement (Eq. 12.28). Labeling experiments (**24**, X = D →

25, X = D) demonstrate the absence of a hydrogen shift during this rearrangement. Direct excitation of **24** does not result in formation of **25**; in fact, **24** is recovered after extensive direct excitation.

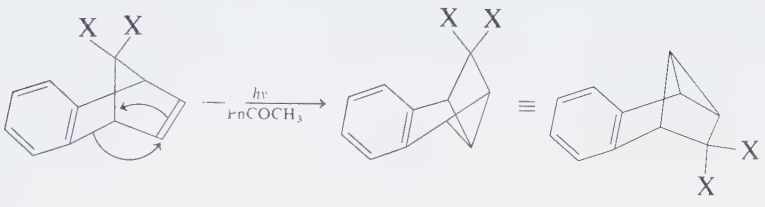

24 **25**

(12.28)

The inertness of structures such as **24** to direct excitation may be due to the occurrence of a [2 + 2] cycloaddition of S_1 to produce a highly strained quadricyclane derivative **26** which thermally reverts to the starting structure (Eq. 12.29):

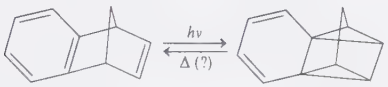

24 **26**

(12.29)

Support of the intermediacy of a quadricyclane structure such as **26** is available from the photoreactions of 7-heteroatom-substituted norbornadienes[41,42]. For example, irradiation of 7-aza (or 7-oxa) benzonorbornadienes (e.g., **27**) results in formation of azapines (or oxepines—Eq. 12.30), whereas triplet sensitization results in [1,2] sigmatropic isomerization. Evidently, the 7-aza (and 7-oxa) quadricyclanes undergo a reverse [2 + 4] ring opening which yields an azapine (Eq. 12.30).

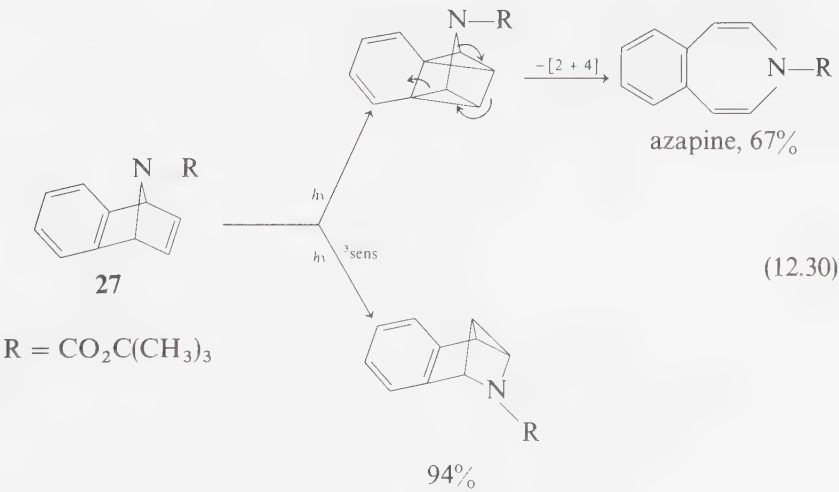

27

$R = CO_2C(CH_3)_3$

(12.30)

An interesting apparent exception the usual di-π-methane rearrangement of benzonorbornenes is found in the photoepimerization of 7-anti-bromobenzonorbornadienes (Eq. 12.31). In fact, this reaction follows the expected course as a primary photochemical pathway; however, the di-π-methane product is thermally unstable and undergoes a rearrangement under very mild conditions to yield the observed product.[43]

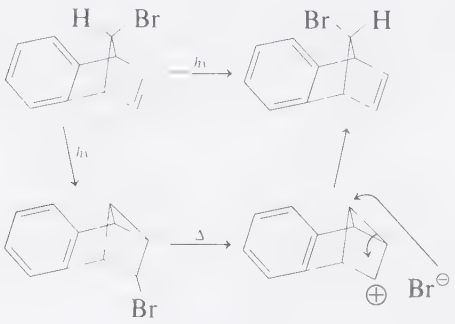

(12.31)

Indirect support for a singlet [2 + 2] reaction in benzonorbornadienes derives from the observation that "benzobarrelene" **28** yields **29** upon direct excitation but yields **30** upon photosensitized excitation.[44] The initial [2 + 2] product would possess a highly strained and labile structure which would be expected to undergo a [2 + 2 + 2] six-electron fragmentation to yield **29**:

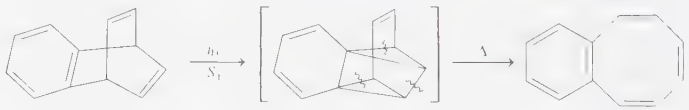

28 **29**

benzobarrelene [2 + 2] product 95%

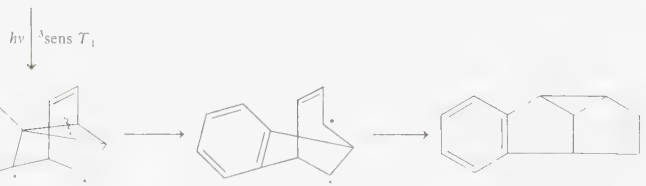

30

99%

(12.32)

Related di-π-methane reactions occur for dibenzobarrelenes,[45] dibenzonorbornadienes,[46] and tribenzobarrelenes.[47]

In some cases, the initial diradicals are diverted to carbenes,[46,48] i.e., a fragmentation rather than a cyclization occurs after the formation of the initial diradical (Eq. 12.33):

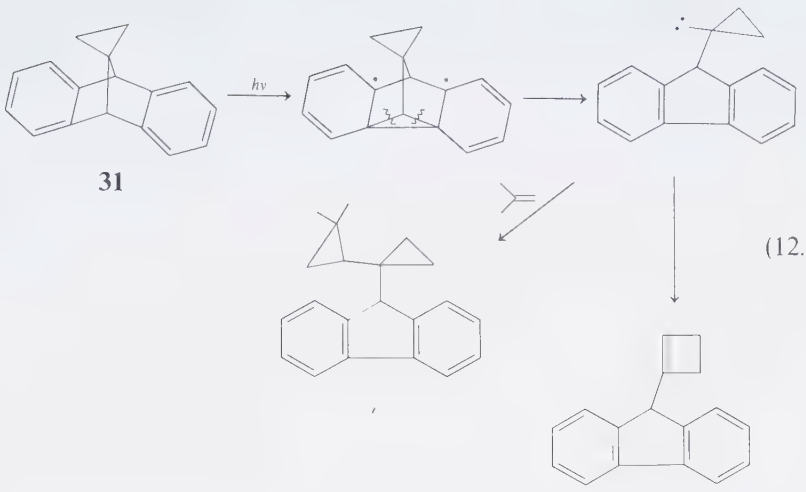

31

(12.33)

12.4 Electrocyclic Reactions

An electrocyclic reaction is a positional isomerization of a special type. The position of π-bonds and σ-bonds (double and single) change during an electrocyclic reaction and (a) a new connectivity of two atoms is made by cyclization along with formation of a new σ-bond, or (b) a connectivity relationship is broken as a ring is opened by cleavage of a σ-bond (Scheme 12.3). An electrocyclic reaction is conveniently defined in terms of a ring closing or ring opening reaction between the termini of a conjugated π system, i.e., an electrocyclic reaction is defined as ring closure or ring opening in which a single bond is formed or is broken between the termini of a linear system containing π electrons. A key idea in electrocyclic reactions is that, like all pericyclic reactions, they involve a cyclic array of interacting orbitals. Electrocyclic reactions may be conveniently classified electronically or structurally in terms of the *ring-closing* reaction, by indicating the number and types of electrons involved in a formal one-step reaction, or by the new ring size formed. Scheme 12.3 shows several examples of this classification.

Selection Rules for Stereospecificity of Concerted Electrocyclic Reactions

The terms *conrotatory* and *disrotatory* are commonly used to describe the motions which occur at the reaction termini during an electrocyclic process. A conrotatory motion is one in which the cis groups rotate in the same sense, and a disrotatory motion is one in which the cis groups rotate in the opposite sense to one another. To clarify these terms consider Figure 12.5, in which the *p*-orbitals at the termini of a polyene undergo an electrocyclic closure. A conrotatory motion causes the lobes of the *p*-orbitals at the termini to rotate *toward* one another whereas a

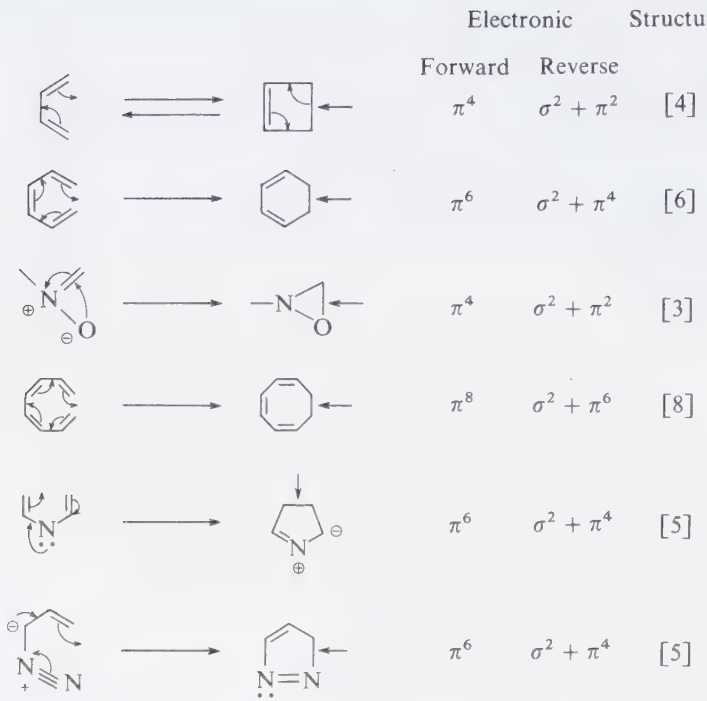

Scheme 12.3

Examples of electrocyclic reactions. The number of curved arrows times two equals the number of electrons involved in the pericyclic reaction. An arrow points to the new σ-bond formed in the closure of the ring. The number in brackets indicates the number of atoms involved in the electrocyclic reaction.

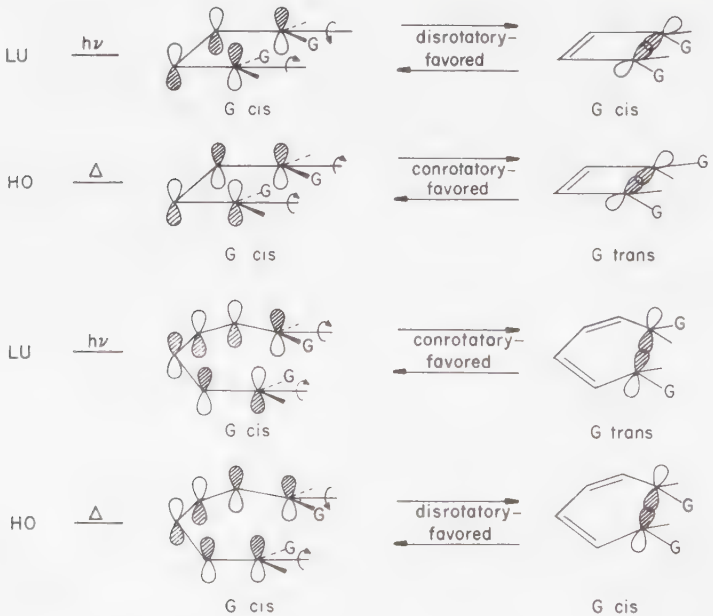

Figure 12.5

Relationship of *HO* and *LU* symmetry to conrotation (inversion) and disrotation (retention) in electrocyclic reactions.

disrotatory motion causes the lobes of the *p*-orbitals to rotate away from one another. For a review of how orbital interactions or correlation diagrams lead to a theoretical rationale of these results the reader is referred to Section 7.6 or any one of a number of excellent texts.[1]

An outstanding feature of electrocyclic reactions is their *stereospecificity*. The following selection rules generally hold for electrocyclic reactions which occur as primary photochemical processes:

> *Rule 1.* The stereochemical pathway of photochemical electrocyclic ring opening is the same as for ring closure.
>
> *Rule 2.* Photochemical electrocyclic reactions proceed via disrotatory pathways when the number of interacting electrons in the cyclic array is 4,8,12, or, in general, $4q$ where q = an integer.
>
> *Rule 3.* Photochemical electrocyclic reactions proceed via conrotatory pathways when the number of interacting electrons is 2,6,10, or, in general $4q + 2$ where $q = 0$ or an integer.

These rules are summarized in Table 12.3, and compared to the selection rules for ground state electrocyclic reactions.

Electrocyclic Reactions of Polyenes and Related Molecules

A remarkable example of the orbital symmetry selection rules for electrocyclic reactions is given by the interconversions of the isomeric polyenes **32** **39** (Eq. 12.34).[49,50] Irradiation of **32** yields the tetraene **33** which possesses one trans double bond as the result of a photochemically allowed conrotatory 6-electron electrocyclic ring opening. Heating of **33** results in formation of **34** via a thermally allowed disrotatory 6-electron electrocyclic ring closure. Irradiation of **33** results in an "allowed" 2-electron trans-cis isomerization to yield **35**, the all-cis tetraene. Heatings of **35** yields **32** via a thermally allowed disrotatory 6-electron electrocyclic ring closure. Irradiation of **35** yields **36** via a photochemically allowed disrotatory 8-electron electrocyclic ring closure. Irradiation of **39** yields **38** via a disrotatory [4] electrocyclic ring closure and irradiation of **37** yields **32** via a disrotatory [4] electrocyclic ring opening. The conversion of **38** to **37** involves an allowed [1,3] sigmatropic rearrangement.

Nearly all electrocyclic ring closures which are true one-step processes occur in S_1 and not in T_1. In order to be concerted in T_1 an electrocyclic reaction either

Table 12.3 Orbital Symmetry Rules for Allowed Concerted Electrocyclic Reactions

Number of electrons	Ground state	Excited state
$4q$ (q = 1, 2, etc.)	Conrotation	Disrotation
$4q + 2$	Disrotation	Conrotation

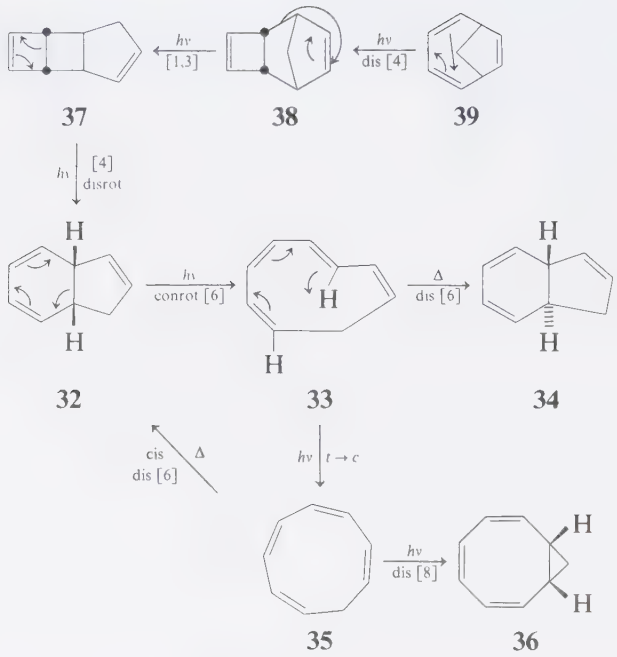

(12.34)

would have to produce a triplet product (high-energy process) or possess a mechanism for efficient intersystem crossing to the ground state of the product (involve very strong spin-orbit coupling). Apparent exceptions to the rule that electrocyclic reactions do not occur efficiently in T should be viewed skeptically. It was reported, for example, that **40**c undergoes triplet photosensitized [4] closure to **41**c[51]. Later it was discovered that **40**c and **40**t are interconverted by triplet sensitizers *without* the occurrence of competing triplet electrocyclic ring closure.[52] However, *direct* excitation of **40**t results specifically in formation of **41**t (4q, $h\nu$, disrotation) and direct excitation of **40**c results specifically in formation of **41**c (4q, $h\nu$, disrotation).

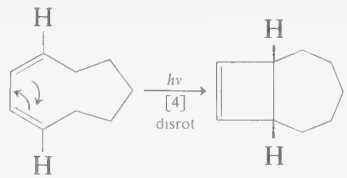

(12.35)

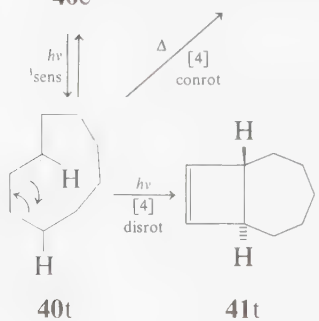

(12.36)

The "photochemical" conversion of **40**c to **41**c under triplet-sensitized conditions is really a two step process: **40**c → **40**t (photochemical) followed by **40**t → **41**c (thermal).

It thus appears that both electrocyclic photoreactions (Eqs. 12.35 and 12.36) are concerted, since both occur stereospecifically. It is of further interest to note that *heating* **40**t results in thermal closure to **41**c ($4q$, Δ, conrotation). Note that a primary photochemical process of **40**c produces a strained ground-state molecule, the *trans*, *cis*-cyclic diene **40**t, which undergoes a thermal reaction to produce the observed product.

Consider the strongly contrasting behavior of the two epimeric compounds ergosterol (**42**t) and isopyrocalciferol (**42**c). The former undergoes [6] electrocyclic ring opening to yield the hexatriene **43**, while the latter undergoes electrocyclic ring closure to yield the cyclobutene **44**.[53]

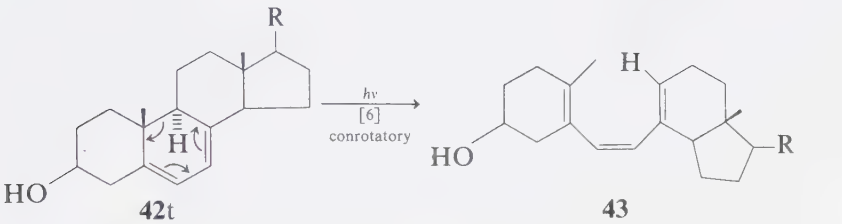

42t ergosterol — **43** previtamin D (12.37)

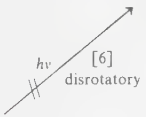

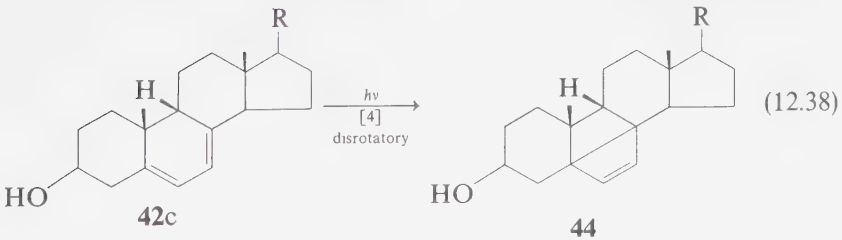

42c isopyrocalciferol — **44** (12.38)

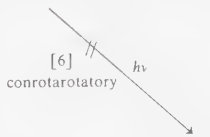

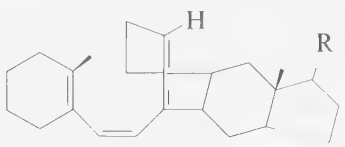

45 a trans cyclohexene (not formed) (12.39)

Since a considerable amount of strain is introduced in the **42**c → **44** transformation, while relief of strain and entropy factors would seem to favor the **42**c → **43** process, it might seem to be mysterious that **42**c ring-closes rather than ring-opens. The mystery is removed when it is realized that the **42**c → **43** transformation involves a disrotation to yield **43** and is therefore forbidden to be concerted. If concerted, the $[4q + 2]$ ring opening is required to occur via a conrotatory pathway and generate trans cyclohexene **45**. The strain energy produced in a butadiene-to-cyclobutene conversion is of the order of 10 kcal/mole, while the energy required to produce a trans double-bond in a six-membered ring may be of the order of 40 kcal/mole. Thus the transition state for the **42**c → **45** conversion is much higher than that for the **42**c → **44** conversion.

We also note that the **42**t → **43** conversion occurs via a conrotatory pathway and is therefore an *allowed* photochemical $4q + 2$ electrocyclic [6] process. Thus, the contrasting "periselectivity" of two epimers is nicely rationalized on the basis of orbital symmetry arguments.

The molecules discussed in Eqs. 12.37, 12.38, and 12.39 are all important in the synthesis of the important family of compounds related to vitamin D.[53]

Prediction of the specific pathway followed by a molecule which has a choice of several allowed-pericyclic reactions (the periselectivity of a reaction) is an interesting challenge. It should be pointed out that the pathway observed may depend on subtle features such as the populations of ground-state conformers in flexible systems; wavelength dependences may thus result.[54]

For example the photochemistry of cis-bicyclo [4.3.0] nona-2,4-diene (**46**) is wavelength-dependent. Irradiation of **46** with 254 nm light generates a photostationary mixture of **46** and the π^6 product **47**. However, irradiation of **46** with longer wavelength light (>300 nm) does not result in formation of **47**. Instead, a new photoproduct, the π^4 product **48** is formed. It may be that conformational factors determine these wavelength-dependent reactions. A conformer in which 1,4 bonding (and thereby π^4 reaction) may absorb selectively at longer wavelengths. In contrast, a conformer for which 1,6 bonding is favored absorbs selectively at shorter wavelengths and the allowed π^6 ring opening becomes the favored reaction pathway.[54]

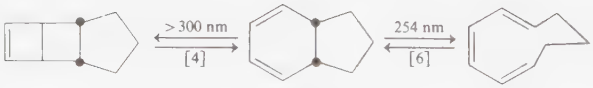

48 **46** **47** (12.40)

Most of the examples of electrocyclic reactions discussed above involve polyenes in cyclic systems. Acyclic polyenes also undergo electrocyclic ring closures.[49] These reactions are also highly stereospecific.[55] Yields are often good to excellent and even highly strained structures can be prepared by this reaction:[56]

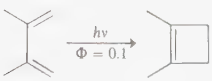

100% (12.41)

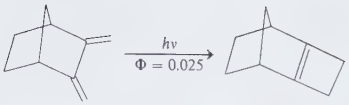

60%

(12.42)

Photovalence Isomerization Reactions of Benzenes; Photochemistry of Benzene Valence Isomers

There are three valence isomers of benzene, i.e., compounds that can be formally derived from benzene by simple reorganization of π and σ bonds. These are: bicyclo-[2.2.0]-hexadiene (commonly called Dewar benzene), benzvalene, and prismane. A fourth structural isomer of benzene, 3,3′-bis-cyclopropenyl, completes the possible $(CH)_6$ isomers (Eq. 12.43).

Benzene Dewar benzene Benzvalene Prismane bis-cyclopropenyl

(12.43)

The photochemistry of benzenes is known to involve Dewar benzenes and benzvalenes.[57] Prismanes are not produced directly from photoexcited benzenes, but result from secondary [2 + 2] cycloaddition of Dewar benzenes.[57] The bis-cyclopropenyl structure does not appear to result from photoexcitation of benzenes, but photoexcitation of bis-cyclopropenyls results in formation of benzenes and benzene isomers.[58,59] All of these photoisomerizations generally involve singlet states and not triplet states.

Excitation of the S_2 state of benzene leads to the formation of Dewar benzene and benzvalene, but excitation of the S_1 state of benzene yields only benzvalene.[60] Quenchers known to efficiently intercept benzene triplets have no effect on these

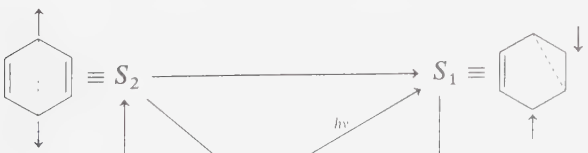

(12.44)

(12.45)

photoisomerizations, thereby attesting to the occurrence of a singlet precursor to the valence isomers. Interestingly, the S_2 state of benzene should have 1,4-bonding characteristics, whereas the S_1 state will possess 1,3-bonding characteristics. Thus, we may interpret the wavelength-dependent photochemical reactions of benzene as shown in Eq. 12.45. From S_2, reaction to form Dewar benzene and internal conversion to S_1 occur. Benzvalene is formed from the latter state.[61]

Ionic reactions are observed when benzene is irradiated in the presence of polar solvents.[62] For example, irradiation of benzene in methanol (Eq. 12.47) leads to formation of the solvent adduct **49**. This adduct could be formed from reaction of methanol with (a) S_1, (b) Z, or (c) benzvalene. Direct reaction of S_1 with methanol is ruled out by the lack of fluorescence quenching of S_1 by methanol.[62] However both Z and benzvalence are permissible intermediates. Benzvalene is known to form **49**, but the same product is expected from attack of methanol on Z. Evidence in favor of the benzvalene addition is available from photoreaction of CH_3OD with benzene.[63] In this case and in the ground-state addition of CH_3OD to benzvalene, exclusive *endo* protonation is observed.

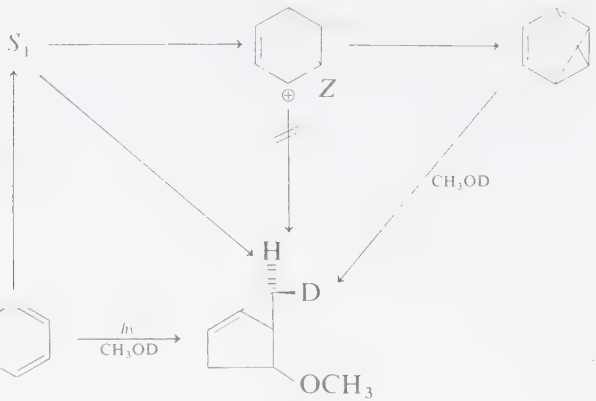

(12.46)

(12.47)

49

The photovalence isomerization reactions of benzenes are complicated by the high reactivity of the products. Each valence isomer is kinetically stable at room temperature but can be easily aromatized by catalysis or photosensitization.[64] As we have seen in the case of benzvalene, reaction of the valence isomer with solvent can also occur. Fulvene is found among the products produced by direct irradiation of benzene but this product has been shown to result from secondary photolysis of benzvalene. Only a low steady-state concentration of benzvalene is achievable by direct irradiation due to benzene triplet-sensitized aromatization of benzvalene.[65]

The possibility of rearomatization of benzvalenes under the reaction conditions provides a mechanism for isomerization of the benzene nucleus and for an apparent reaction inefficiency. For example, the photoisomerization of 1,3,5-trideuterobenzene (**50**) to 1,2,5-trideuterobenzene (**51**) probably occurs via a benzvalene intermediate:[66]

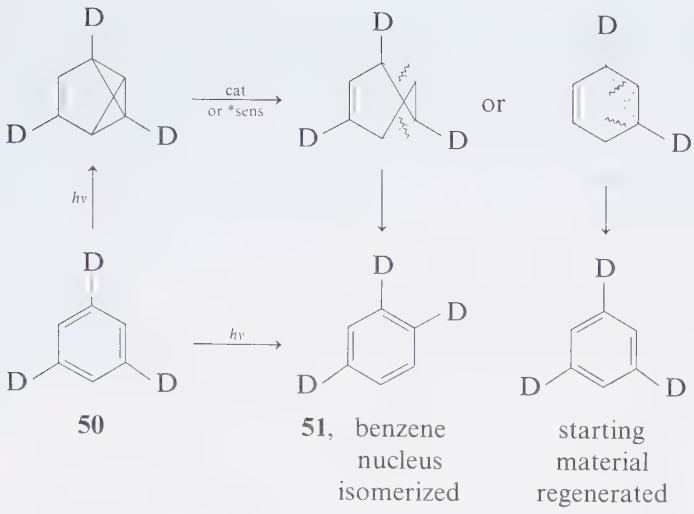

(12.48)

50 **51**, benzene nucleus isomerized; starting material regenerated

The sequence benzene $\xrightarrow{h\nu}$ valence isomer $\xrightarrow[h\nu]{\Delta}$ benzene provides a pathway for "scrambling" or transposing the atoms of a benzene ring.

The major reaction which results from direct excitation of benzvalene is a degenerate [1,3] sigmatropic rearrangement.[64] Deuterium labeling was required to uncover this reaction.

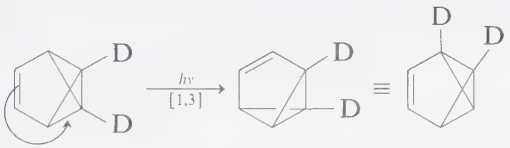

(12.49)

(12.50)

The mechanism of this [1,3] shift may either be concerted, or occur via a Z or ^1D intermediate.

Triplet photosensitized excitation of benzvalene leads to different results, depending on the energy of the sensitizer employed (Eqs. 12.51 and 12.52). It has been proposed that sensitizers are capable of exciting either of two benzvalene triplets (T_2 and T_1).[64] Excitation of the higher energy triplet results in a retrocycloaddition

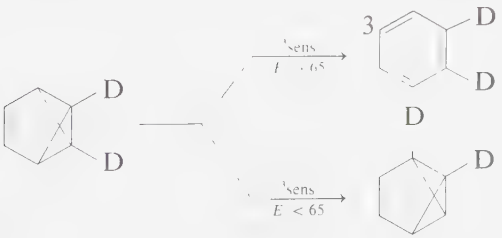

retrocycloaddition via T_2 (12.51)

[1, 3] sigma tropic isomerization via T_1 (12.52)

to produce triplet benzene. Excitation of the lowest-energy triplet results in cleavage of a cyclopropane ring followed by recyclization.

The photochemistry of Dewar benzene reveals that benzene is the major product of direct photolysis. A significant yield of prismane (Eq. 12.53) is also produced via a [2 + 2] cyclization.[65] Triplet sensitization of Dewar benzene yields benzene triplets in an unusual triplet [4] electrocyclic reaction that produces an electronically excited product:

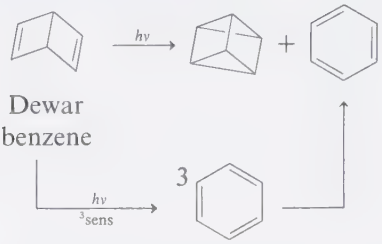

(12.53)

(12.54)

Direct excitation of prismane yields benzene. The triplet photosensitized photochemistry of prismane is interesting in that triplet sensitization yields Dewar benzene as the major product.[67] This result is remarkable in the sense that the diradical presumably produced by sensitization, undergoes only inefficient ring opening to benzene.

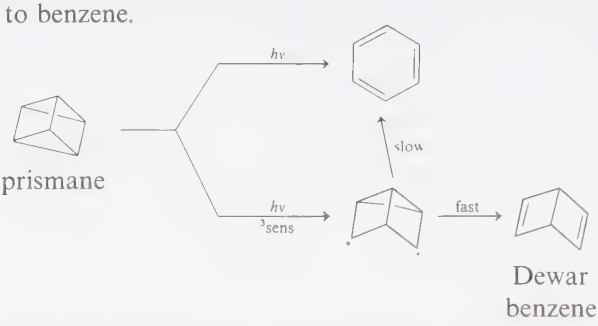

(12.55)

(12.56)

A qualitative surface diagram for the benzene ⇆ Dewar benzene interconversion is shown in Figure 12.6.[61] The degeneracy of the Zero Order benzene molecular orbitals poses some difficulties in generating a Zero Order diagram, so that Figure 12.6 must be considered only as provisional. The S_1 state of benzene is found to correlate (assumption of D_{6h} symmetry) with a very high-energy-excited state of Dewar benzene, whereas an upper excited singlet S_n is found to correlate with the ground state of Dewar benzene (spectroscopic notation, A_1). The crossing of the S_n and S_0 surfaces is only weakly avoided and a substantial energy barrier ($\Delta H^{\ddagger} = 25$ kcal mole) occurs for the highly exothermic ($\Delta H = -60$ kcal mole) conversion of Dewar benzene to benzene.

Treating the Dewar-benzene-to-benzene isomerization as a ground state *forbidden* disrotatory electrocyclic reaction leads to the conclusion that a triplet surface comes close to the S_0 surface near the geometry for the transition state for the forbidden disrotatory ring opening.[68] Indeed, heating of Dewar benzene has been shown to produce (in part) benzene triplet states, i.e., the thermal ring opening is a chemiluminescent reaction (Chapter 14).

In Figure 12.6, reaction pathways along the benzene-Dewar reaction coordinate from S_n, S_1, and T_1 of benzene and from S_0, T_1, S_1, and S_n of Dewar benzene are shown.

S_n of benzene produces Dewar benzene via a pathway analogous to the conventional electrocyclic ring closures, i.e., $S_n \rightarrow$ minimum $\rightarrow S_0$ (benzene) + S_0 (Dewar). S_1 does not correlate with a low-lying state of Dewar benzene and as a result does not proceed along the reaction pathway to Dewar. Instead, S_1 fluoresces, proceeds toward benzvalene (or a Z precursor), or undergoes intersystem crossing to T_1. The latter may possess both an activation and spin-forbidden barrier on its way to Dewar benzene, and mainly undergoes intersystem crossing to S_0.

S_1 and S_n of Dewar benzene undergo ring opening to benzene via the minimum in the Zero Order S_n surface. T_1 undergoes *adiabatic* ring opening to benzene triplet.[67]

Electrocyclic Reactions of Stilbenes and Related Compounds

Irradiation of stilbene and related compounds results in two general photoisomerizations: cis-trans isomerization and [6] electrocyclic ring closure (Eq. 12.57). The electrocyclic reaction occurs only from cis-stilbenes. The [6] product is a dihydrophenanthrene **53** which may be thermally or photochemically converted back to cis-stilbene or may be oxidized by a variety of reagents to phenanthrene.[69] If we treat the cis-stilbene $\rightarrow$ **53** reaction as a concerted π^6 electrocyclic reaction, we predict the stereochemistry of the bridgehead hydrogens of **53** to be trans.

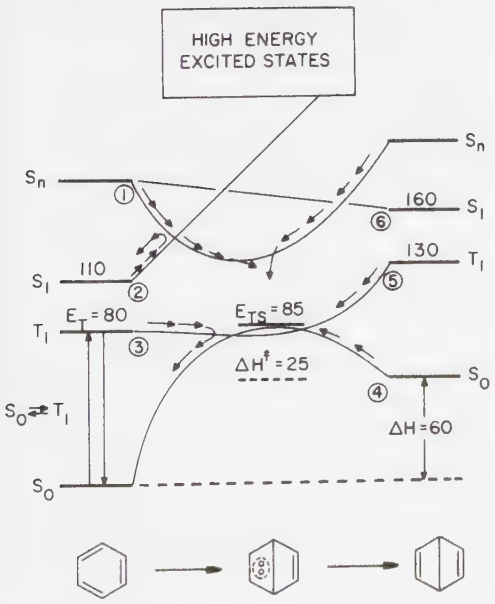

Figure 12.6
Qualitative surface diagram for the interconversion conversion of Dewar benzene and benzene.

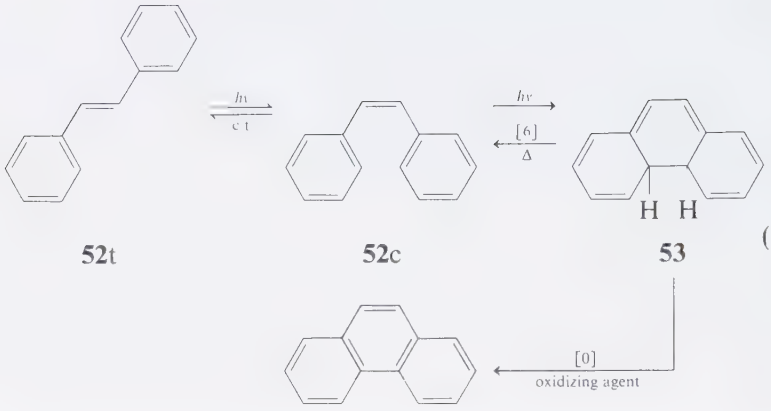

52t **52c** **53** (12.57)

That [6] is very probably a concerted π^6 reaction of S_1 of stilbene is based on the following evidence:[70]

1. The reaction proceeds upon direct excitation but not with triplet sensitization. This excludes T_1 as a candidate for the active state in the electrocyclic reaction.

2. Stilbenes substituted with groups known to enhance intersystem crossing from S_1 to T_1 (e.g., Br, RCO, NO_2) do not undergo the [6] reaction efficiently.

3. Optically active derivatives of **53** have been prepared by photocyclization, a result consistent only with the trans stereochemistry since the cis derivative would not be capable of exhibiting optical activity (Eq. 12.58):[71]

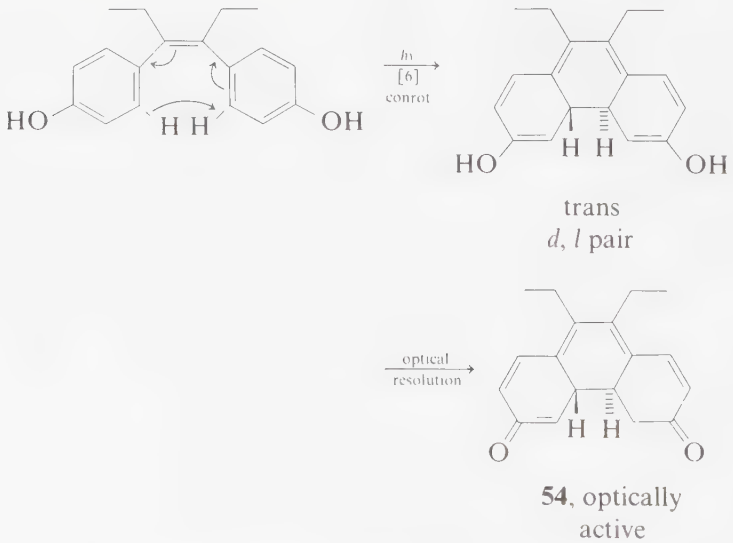

trans
d, *l* pair

54, optically active (12.58)

An interesting example of photochemically-induced optical activity (Eq. 12.59) was achieved by employing circularly polarized light to excite and photocyclize

cis-di-β-naphthyl ethylene (**55**).[72] The latter is chiral due to its helical shape. Circularly polarized light is absorbed in slightly different amounts by each of the enantiomers of **55**, so that one enantiomer is converted more rapidly to product than the other. Of the two stereoisomeric [6] products, only the trans form is capable of exhibiting optical activity. This result thus confirms the preferred trans stereochemistry of the cyclization step. It is interesting to view photons as chiral reagents in this reaction. Optically active products could also be produced by irradiating compounds capable of cyclizing to helicenes in chiral solvents.[73]

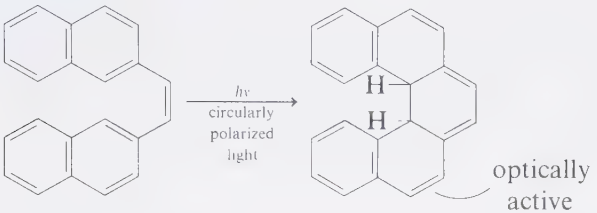

(12.59)

55

A general paradigm which satisfactorily explains the photochemistry of stilbenes with respect to photoisomerizations is: The S_1 state may deactivate by twisting about the central C=C bond or by undergoing conrotatory [6] cyclization. Intersystem crossing to T_1 will compete with these reactions from S_1. Since in T_1 electrocyclic reactions do not occur, in general only cis-trans isomerization is observed. This explains why certain substituted stilbenes do not undergo [6] electrocyclic reactions (i.e., Br, RCO, NO_2, etc.)[70] since these substituents are known to accelerate intersystem crossing.

12.5 Intramolecular Cycloadditions of Conjugated Hydrocarbons

An intramolecular cycloaddition of a conjugated system is a reaction forming two or more rings and for which *two* new σ-bonds are made. As such, these reactions differ in type from electrocyclic reactions in which only *one* new σ-bond is made. Intramolecular cycloaddition may be classified in terms of the π-electron components formally involved in making the new σ-bonds and by the number of atoms contributed to the new rings by the component systems. For example, the intramolecular isomerization of 1,3-butadiene to bicyclobutane (Scheme 12.5) is an intramolecular cycloaddition which involves 2π systems of 2 atoms each.[74] It is thus termed a $\pi^2 + \pi^2$ or $x[2 + 2]$ cycloaddition. We place a label x in the latter classification to serve as a reminder that a "cross" bonding is formally occurring (terminal atom to internal atom) and to contrast the reaction with its counterpart, a "parallel" bonding [2 + 2] which we have defined as an electrocyclic π^4 or [4] reaction. In Scheme 12.4, some examples of intramolecular cycloadditions are given. The rules for classification are derived from identification of the new σ-bonds

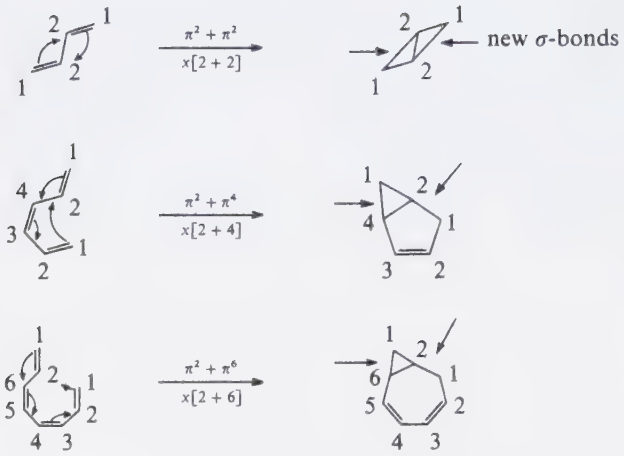

Scheme 12.4

Intramolecular cycloaddition reactions of conjugated systems.

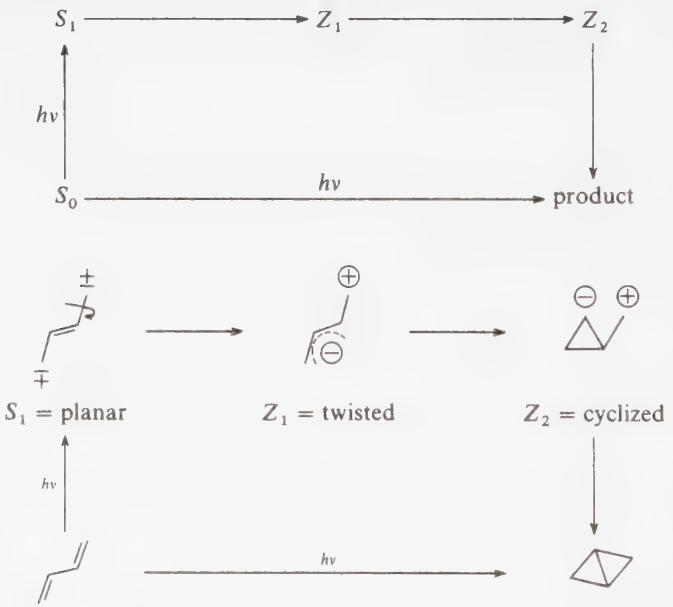

Scheme 12.5

Paradigm for intramolecular cycloadditions initiated in $S_1(\pi, \pi^*)$ states. Top: general description. Bottom: specific example of 1,3-butadiene → bicyclobutane.

being made in the transformation and of the groups participating in the cycloaddition. The numbering system gives the reaction termini involved in making the new σ-bond the number 1 and then counts atoms in the new ring until one reaches the second atom of the new σ-bond. Thus, the isomerization of 1,3,5-hexatriene to bicyclo [3.1.0] hexene is a $\pi^2 + \pi^4$ or $x[2 + 4]$ cycloaddition. Strained σ-bonds may replace π-bonds in these reactions.

Mechanisms of Intramolecular Cycloadditions of Conjugated Systems

Intramolecular cycloadditions of conjugated systems are pericyclic reactions, and as such can be discussed in terms of concerted reactions.[1] However, experimental evidence indicates that in structurally flexible systems these reactions are probably not concerted, in contrast to the situation for photoinduced electrocyclic reactions.[75] Nevertheless, intramolecular cycloadditions commonly occur from singlet states.

For example, excitation of the *s*-trans conformer of 1,3-butadiene is viewed as producing a planar S_1 state which is highly polarizable and which has a tendency to take on zwitterion character.[76] S_1 then transforms by rotation about one of the terminal groups into Z_1, a minimum on the excited singlet-state surface. This species in turn undergoes cyclization to form a dipolar cyclopropyl carbinyl system which then cyclizes to product (Scheme 12.5).

Experimental support for the zwitterion mechanism is available from studies of the stereochemistry of the cyclization of butadienes to bicyclobutanes and the formation of adducts indicative of ionic addition to zwitterion intermediates (in distinction to ionic addition to ground-state bicyclobutanes).[75]

Examples of Intramolecular Cycloadditions of Conjugated Systems

Intramolecular cycloaddition reactions of conjugated polyenes generally must compete with $[n]$ electrocyclic reactions. For example, in the case of 1,3-butadiene, $x[2 + 2]$ cycloaddition must compete with [4] electrocyclic ring closure:[74]

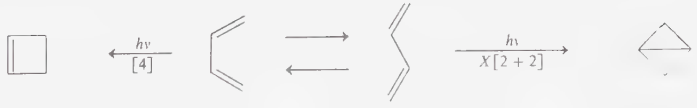

cyclobutene	*s*-cis	*s*-trans	bicyclobutene
30%	(minor)	(major)	10%

(12.60)

From structural considerations, the $x[2 + 2]$ reaction appears to be likely to result from the *s*-trans conformer of 1,3-butadiene, whereas the [4] reaction seems more likely from the *s*-cis conformer. However, even though the major conformer of 1,3-butadiene is the *s*-trans form, the major product from irradiation of 1,3-butadiene is cyclobutene. Evidently, the efficiency of *s*-trans* → bicyclobutane is much less than that of *s*-cis* → cyclobutene.

In methanol as solvent, direct excitation of 1,3-butadiene yields adducts which appear to have trapped the zwitterion, Z:[77]

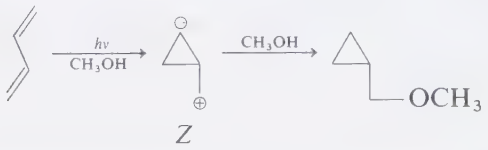

Z (12.61)

It is expected, and found,[74b] that constraint of a 1,3-diene to a *s*-trans conformation completely inhibits the [4] reaction in favor of the $x[2 + 2]$ reaction:

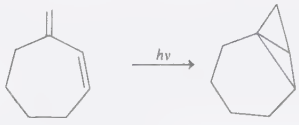

fused *s*-trans (12.62)

12.6 Electrocyclic Reactions and Intramolecular Cycloadditions of Heteroatomic Conjugated Systems

Although the orbital symmetry arguments appear to be valid for hydrocarbon systems, it is not certain whether an unqualified extension to heteroatom systems is warranted. However, if we postulate that π, π^* states of appropriate conjugated chromophores possessing heteroatoms have a tendency to undergo electrocyclic reactions, we find a strong analogy with the hydrocarbon systems.

First of all, formal electrocyclic processes are known for heterocyclic systems (**56** and **57**):

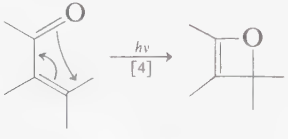

56 (12.63)[78]

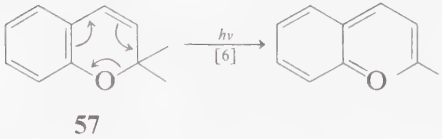

57 (12.64)[79]

In other cases, intermediates expected via analogy to hydrocarbon systems have been proposed. For example,[80] an oxabicyclobutane intermediate **58** "explains" the labeling observed in the photorearrangement of purpurogallin tetramethyl ether (only partial structure is shown):

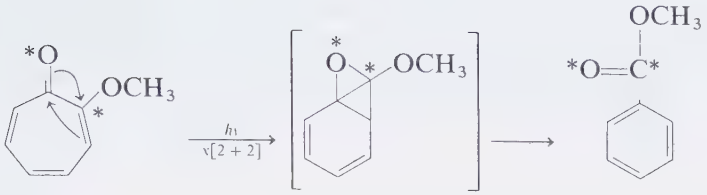

(12.65)

58

The [6] ring opening of spiropyranes (e.g. **57**) is of special practical importance as a photochromic system, i.e., a photoreaction which produces a colored species which thermally reverts to starting material (**59** → **60**). It is of interest that benzophenone sensitizes this reaction, which may be an example of an *adiabatic* triplet photoreaction or one which occurs completely on an excited triplet energy-surface. The lower energy of the product states allow the possibility of such a reaction in this case:[81]

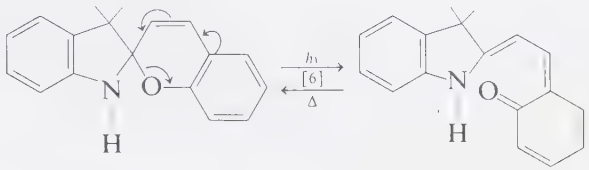

(12.66)

59, colorless **60**, colored

As a second example, the six-electron electrocyclic reaction of diphenyl[82] or divinyl[83] amines results in five-membered ring openings or closures, i.e., [5] reactions. In analogy to the hydrocarbon systems, such reactions should proceed in a conrotatory (inversion) fashion if they are concerted. Indeed, irradiation of diphenyl amines (**61**) leads to cyclized adducts such as **62**:[82]

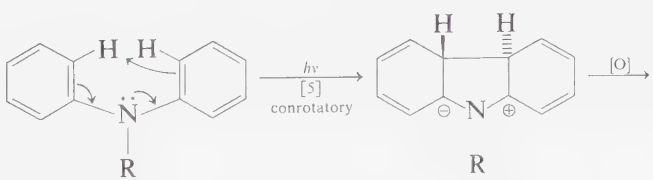

61 **62**

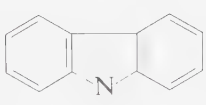

(12.67)

63

The isolated product (**63**) results from a loss of hydrogen, usually by an oxidation of some sort. The cyclized species **62** has been detected spectroscopically and evidence has been put forth which indicates that the conversion of **62** to **63** may involve an adiabatic triplet reaction.[82]

Photochemical electrocyclic reactions of heteroatomic molecules which can be represented by charge separated (zwitterionic) structures are quite common.[84] For example, N-oxides undergo four-electron [3] electrocyclic closure reactions to yield oxaziridines.[85,86] In some cases the oxaziridine is reactive under the conditions of formation:

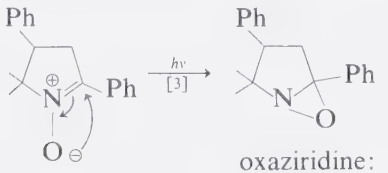

(12.68)[85]

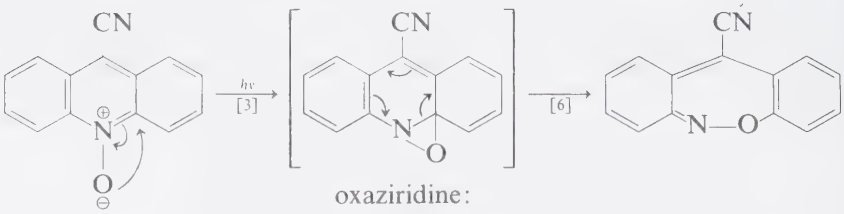

(12.69)

Among the other products commonly observed in the photolysis of N-oxides are pyridines (formal loss of an oxygen atom) and pyrrole-aldehydes:[87]

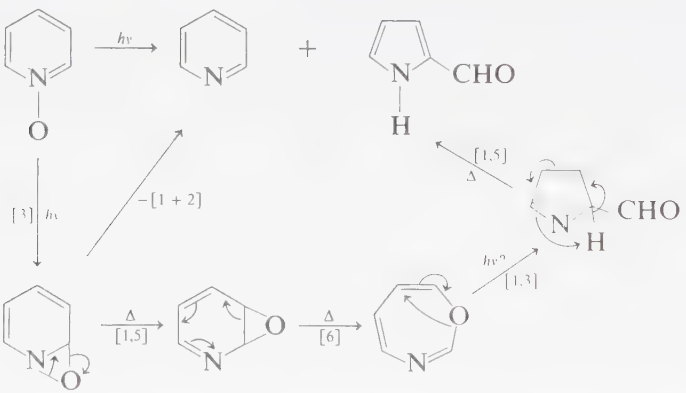

(12.70)

Aromatic heterocycles undergo electrocyclic rearrangements upon direct photochemical excitation, but generally not upon triplet photosensitization.[88] These rearrangements may be unified in terms of the paradigm given in Scheme 12.6. There are two common initial primary processes that convert aromatic heterocyclic singlet states: (a) to bicyclic isomers, via a [4] electrocyclic reaction, or (b) to a cyclopropene, via a [1,3] shift.[89] Subsequent (thermal or photochemical) rearrangements of these primary products then lead to the isolated skeletally rearranged isomers.

Irradiation of numerous aromatic heterocycles such as thiophenes,[90] isoxazoles,[91] indazole,[92] and related compounds[93] results in isomerizations that

can be rationalized in terms of Scheme 12.6 if it is assumed that Dewar or cyclopropenyl intermediates rearrange thermally to produce the isomerized product:

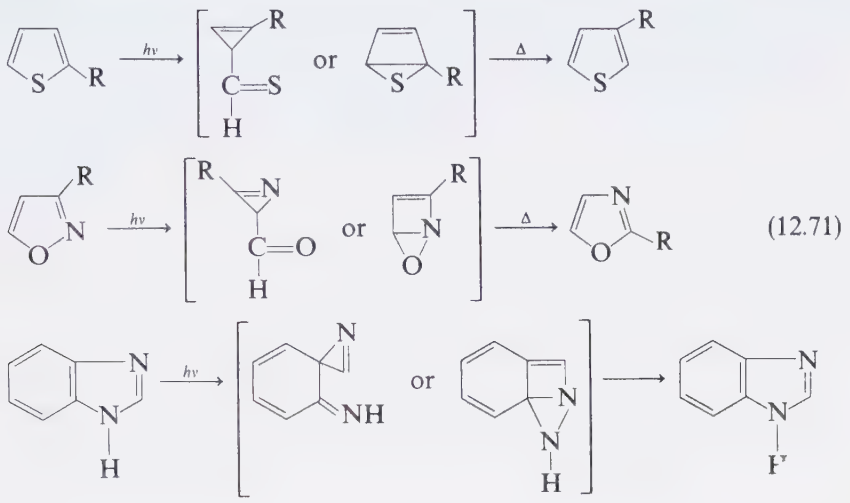

(12.71)

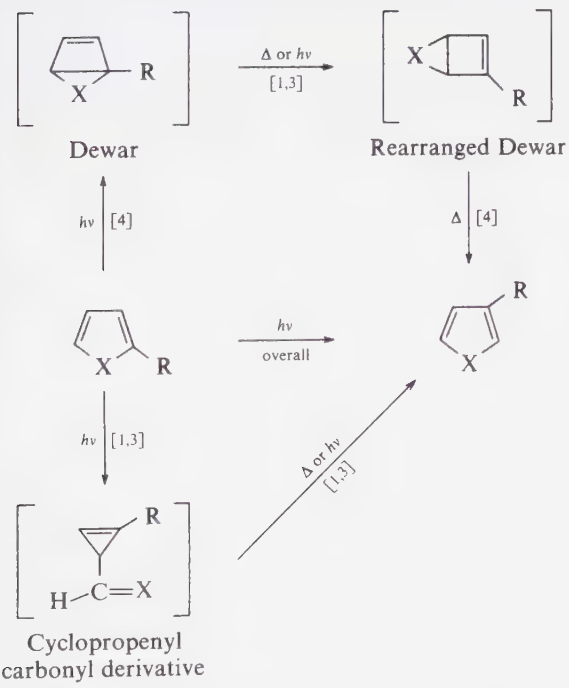

Scheme 12.6

Paradigm for the rearrangements of aromatic heterocycles. The structures in brackets are proposed transient intermediates. The [1,3] rearrangements may be either photochemically or thermally induced, depending on the reactions conditions.

In favorable cases, the primary products can be isolated, e.g., **64**[94] and **65**:

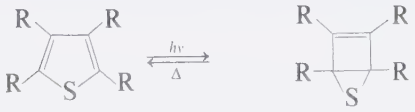

(12.72)

$R = CF_3$ **64**, a Dewar thiophene

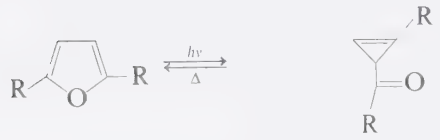

(12.73)

$R = C(CH_3)_3$ **65**, a cyclopropenyl ketone

Irradiation of pyridine, in analogy to aromatic hydrocarbons, produces a Dewar derivative:[95]

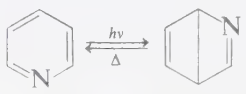

(12.74)

An interesting example of a temperature effect on periselectivity is displayed by azoheterocycles which undergo [4] electrocyclic closure to a diazobicyclopentenes at low temperature and a [5] electrocyclic ring opening at room temperature:[96]

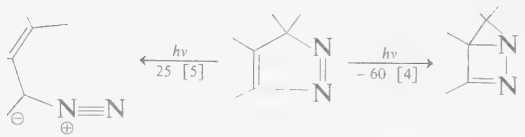

(12.75)

Photorearrangements of 2,4-Cyclohexadienones

2,4-cyclohexadienones undergo two typical rearrangements: an electrocyclic ring opening to a linear ketene[97] and a [1,2] sigmatropic shift[98] to a [3.1.0] bicyclohexene (Scheme 12.7). The [6] ring opening is viewed as an α-cleavage of the n, π^* *singlet* state which leads to a diradical.[99] The latter, by simple twisting about bonds, is converted to the ketene product. Usually the ketenes are not isolated but are trapped by nucleophiles. Their existence is unambiguous, however, since they may be detected spectroscopically.[100] The [1,2] shift appears to be a polar rearrangement of the π, π^* singlet state.[98] The ketene produced by [6] ring opening may also undergo a *thermal* $\pi_s[4 + 2]$ internal cycloaddition to yield a product identical to the [3.1.0] bicyclohexene produced by a direct [1,2] shift.

An elegant synthetic application of the [6] ring opening of 2,4-cyclohexadienones is found in a double-barreled ring opening:[101]

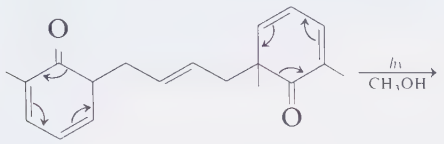

(12.76)

Sigmatropic Isomerization of Cyclic Enones and Dienones

The photoreactions of cyclic enones and dienones have played a special role in the development of synthetic and mechanistic organic photochemistry.[102] These compounds undergo many complex structural rearrangements which appear to be unrelated on a superficial inspection of product structures. A mechanistic analysis has developed, however, which has brought considerable order to the field, although many puzzles still remain to be solved. This serves as a challenge for future researchers.

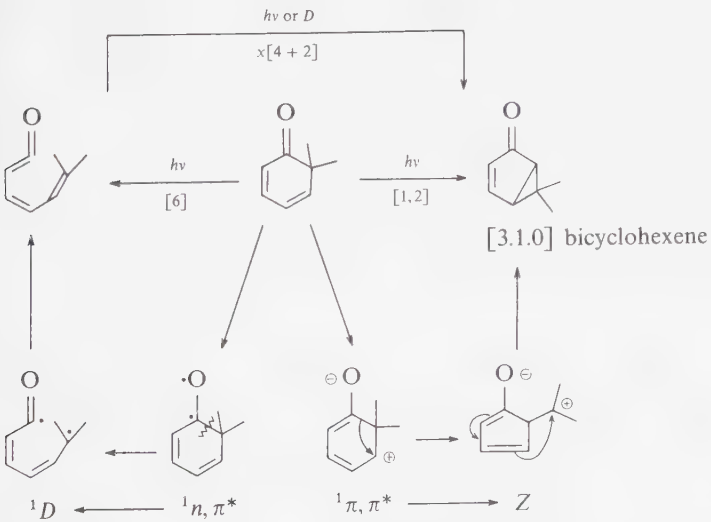

Scheme 12.7

Typical reaction types of 2,4-cyclohexadienones.

We shall consider only five- and six-membered-ring cyclic enones and six-membered cyclic dienones in this section. Four- and three-membered-ring cyclic enones tend to undergo ring fragmentations as primary processes (Section 13.6) and seven- and larger ring enones tend to undergo cis-trans isomerization as primary processes (Section 12.2).

For five-membered-ring enones, there are three important rearrangements we consider as typical:

1. A [1,2] sigmatropic shift to form a cyclobutanone:

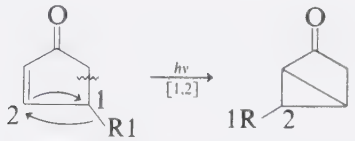

(12.77)[103]

2. A [1,3] sigmatropic shift to form a cyclopropanone:

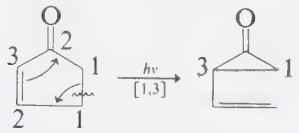

(12.78)[104]

3. A [1,3] shift to form a cyclopropyl ketene:

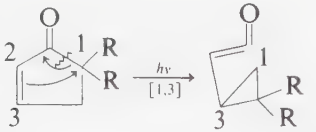

(12.79)[105]

This reaction is favored by radical stabilizing 5,5 substituents, i.e., for R=Ph, reaction 12.79 goes in ~80% yield.

For six-membered-ring enones or cross conjugated dieones, only [1,2] shifts are typical, but two types of 1,2 shifts may occur:

4. A [1,2] shift which contracts the ring from 6 to 5 by rearrangement of the ring atoms and is called a "Type A" rearrangement:

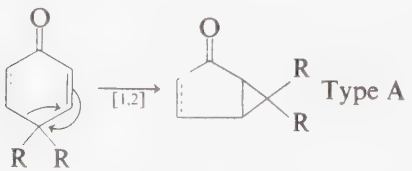

(12.80)[106]

5. A [1,2] shift which contracts the ring from 6 to 5 by migration of a ring substituent, called a "Type B" rearrangement:

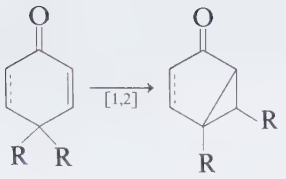

Type B (12.81)[107]

In general the reactions of the six-membered-ring enones and dienones proceed via triplet states.[106] The mechanisms of the cyclopentenone rearrangements are not well-established but bear a formal resemblance to the rearrangements of β,γ-unsaturated enones which undergo triplet [1,2] shifts and singlet [1,3] shifts. A difficulty in setting up a paradigm for the photorearrangements of cyclic enones is the lack of general knowledge of whether T_1 is a n, π^* or a π, π^* state.[98]

As a prototype mechanism consider the following simplified mechanism, which has been postulated for the rearrangement of cross-conjugated cyclohexadienones such as 4,4-diphenyl-2,5-cyclohexadienone:[106]

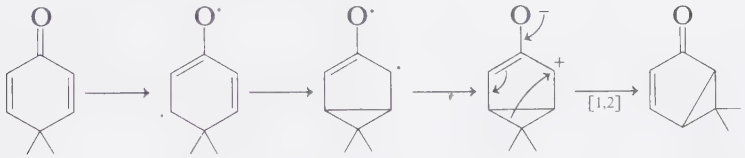

(12.82)

The intermediate Z is the key to understanding the rearrangements of 2,5-cyclohexadienones. Reactions other than the [1,2] rearrangement of Z to the product type shown may compete when certain structural modifications are made Knowledge of such a scheme is also important because it allows a mechanistic shorthand to be used. We may proceed directly to Z from the starting material without always indicating a detailed pathway.

For example, irradiation of the dienone structure such as **66** in acidic media is commonly found to induce rearrangement to cyclopentenones via enols of skeletal structure **67** and/or skeletal structure **68**:[108,109]

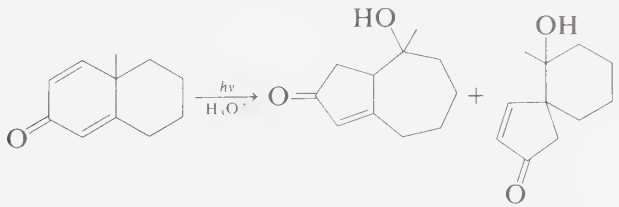

(12.83)

66 **67** **68**

These rearrangements may be viewed as interception by H_2O of the Z intermediate, which, as expected, forms a [1,2] shift product **69** in neutral media. Irradiation of

69 in acidic media does not lead to **67** or **68**:

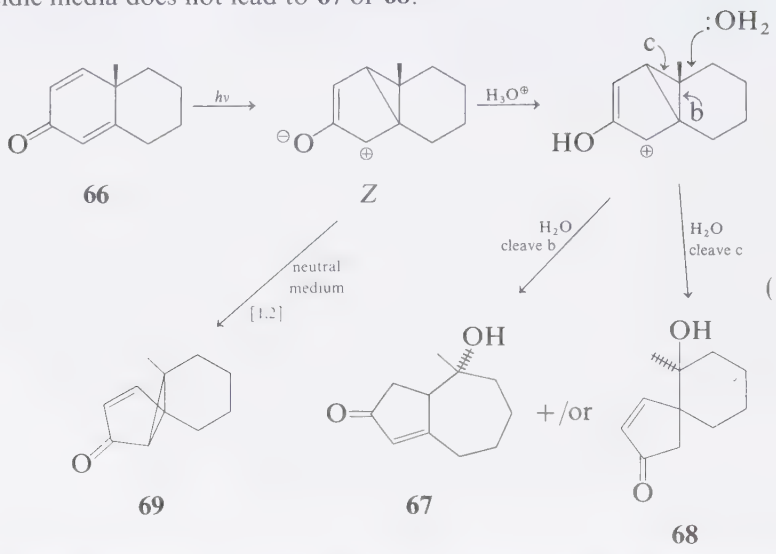

(12.84)

We may view the formation of **67** and **68** from **66** as follows: the usual sequence leading to formation of *Z* occurs, but in acidic media protonation of *Z* occurs competitively with Type A rearrangement. A carbonium ion is produced, which then is attacked by solvent to break either bond b (leading to **67**) or bond c (leading to **68**). In nonacidic solvents, *Z* rearranges to **69** in a normal Type A rearrangement. The enols of **67** and **68** may be formed as initial products and then tautomerize to **67** and **68**.

The intermediacy of a zwitterionic intermediate in the Type A rearrangement of 4,4-diphenylcyclohexadienone **70** has been tested by generation of *Z* via a thermal route:[111]

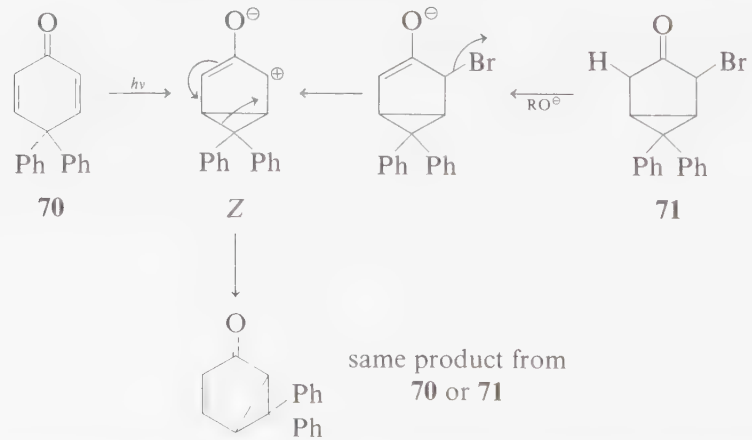

(12.85)

Thus, treatment of the bromoketone **71** with base leads to the same product as is achieved via photoexcitation of **70**.

The [3.2.0] bicyclohexenone produced by Type A rearrangement of 2,5-cyclohexadienones (e.g., **66** → **69**) is prone to undergo secondary photolysis leading to

further rearrangements.[112] In general, the products may be rationalized starting from the postulate that an excited state (e.g., **72**) is produced that can lead to a ring-opened zwitterion **73** which is the ring-opened form of a cyclopropanone **74**:

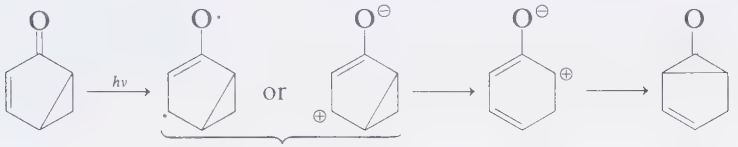

(12.86)

In aprotic media, the zwitterion produced by ring opening may undergo rearrangements, such as the [1,2] rearrangement of **75** into **76**:[109]

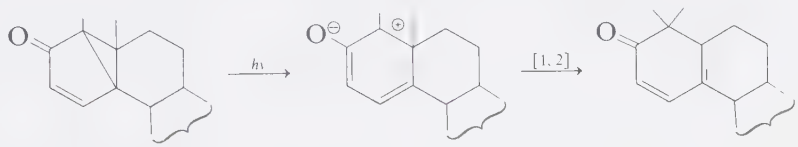

(12.87)

In addition to providing a convenient formalism for rationalizing the pathways of photorearrangements, evidence for zwitterionic structures such as **73** is available from the methods of spectroscopy,[113] alternate syntheses,[114] kinetics[115] and chemical trapping.[115] As an illustration it is found that the [3.2.0] cyclopentenone **77** undergoes photorearrangement in acid solution to **78** and **79** in the ratio of 90% to 10% respectively. Treatment of the bromoketone **81** with base is expected to generate the same zwitterion (**80**) as the photolysis of **77**. Indeed the same product ratio of **78** to **79** is obtained by either photochemical or thermal entry to **80**. In protic media zwitterions such as **80** may be protonated to yield carbonium ions, which are prone to undergo rearrangements and eventual loss of H^+, elimination of an anion, or capture of a nucleophile to yield the observed product:

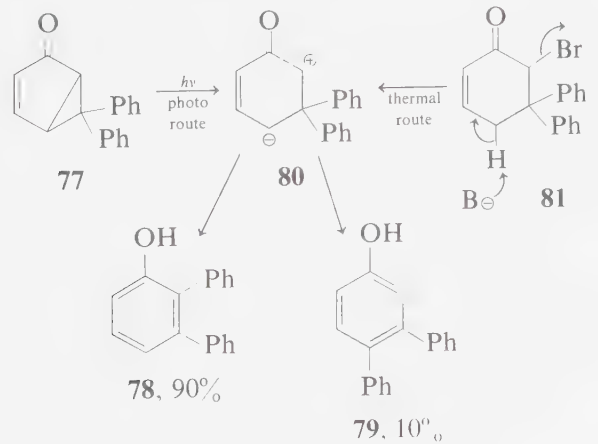

(12.88)

The observation that cyclopropanone **84** (the closed form of zwitterion **83**) is formed upon photolysis of **82** and may be matrix-isolated, lends further credence to the zwitterion hypothesis:[100,112b]

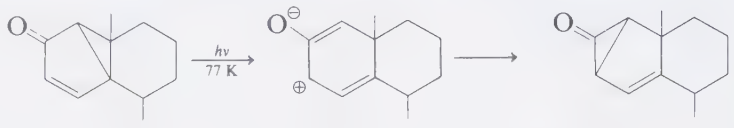

82 **83** **84**, matrix isolated

(12.89)

On another typical rearrangement reaction of [3.2.0] bicyclohexenones, ketenes are produced (e.g., **85** → **86**). This process occurs by breaking the external rather than the internal cyclopropyl bond (**88** → **89**):[98,112]

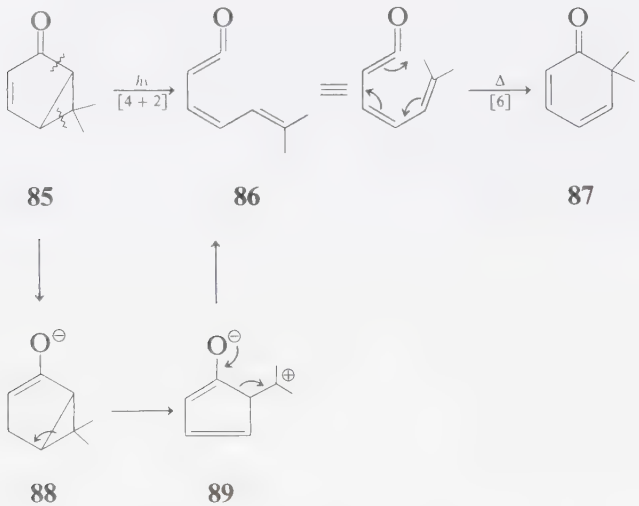

85 **86** **87**

(12.90)

88 **89**

The primary product ketene is often thermally unstable and undergoes a [6] ring closure to a 2,4-cyclohexadienone (e.g., **86** → **87**).

The mechanism of both the Type A and the Type B rearrangements of cyclopentenones and cyclohexenones may be quite different mechanistically from the rearrangements of 2,5-cyclohexadienones. Diradical intermediates appear to be involved in some cases and zwitterions in others. It seems that the nature of the lowest triplet (n, π^* or π, π^*)—both of which are comparable in energy—may determine whether diradicaloid or zwitterionic behavior is observed.

Evidently these two energetically proximate states can be inverted via solvent effects. It has been postulated that for cyclohexenones, the n, π^* state undergoes the Type B rearrangement preferentially and that the π, π^* state undergoes the Type A rearrangement preferentially. For example, irradiation of the cyclohexenone **90** in polar solvents yields the Type A product **91** whereas in nonpolar solvents the

Type B product **92** is produced:[114]

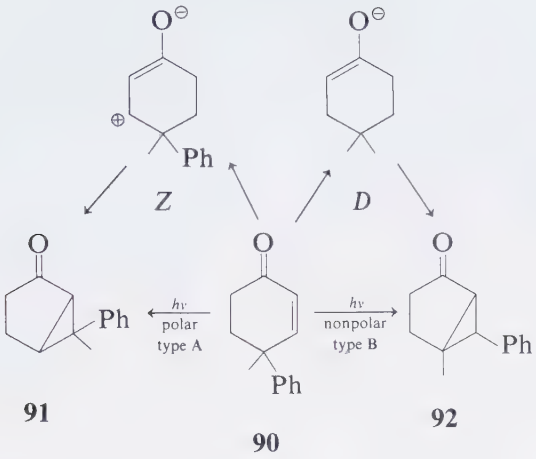

(12.91)

Since π, π^* states are lowered in energy by increasing solvent polarity and n, π^* states are raised in energy by increasing solvent polarity, the differing reactions as a function of solvent are ascribed to state switching.[116]

12.7 Sigmatropic Isomerizations of β,γ-Unsaturated Enones

Direct excitation of numerous β,γ-unsaturated ketones results in rearrangement to isomeric β,γ-unsaturated ketones via a [1,3] sigmatropic rearrangement (Eq. 12.92). Triplet photosensitization, on the other hand, results in rearrangement to isomeric cyclopropyl ketones via a [1,2] sigmatropic rearrangement (Eq. 12.93). The latter reaction is analogous to the di-π-methane rearrangement (Section 12.3) and is termed the "oxa-di-π-methane rearrangement.[117] The mechanisms of photorearrangements of β,γ-unsaturated ketones are discussed in detail in Section 13.3.

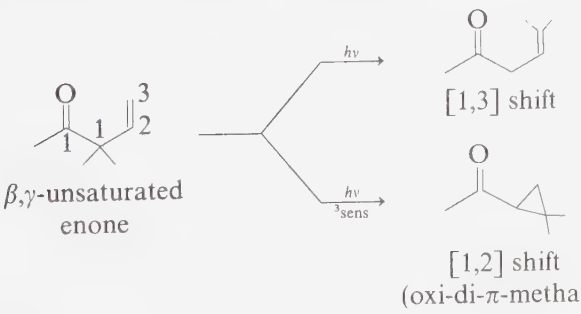

(12.92)

(12.93)

12.8 Summary

Most of the reactions discussed in Chapters 10 and 11 involved the generation of intermediates, usually diradicals, as primary photochemical products. Many of the reactions in this Chapter, however, may be viewed as being concerted from S_1 or concerted after formation of a Z species. Electrocyclic and sigmatropic rearrangements from S_1 are characterized by their stereospecificity, are prototype concerted pericyclic reactions, and obey orbital symmetry selection rules. Cis-trans isomerizations may be viewed as the simplest of pericyclic reactions and the energy surfaces for this reaction serve as prototypes for pericyclic reactions that are forbidden in S_0. The photosensitized cis-trans isomerization of polyenes is an important mechanistic tool in organic photochemistry.

Many apparent "deep-seated" rearrangements may be interpreted as sequences of conventional rearrangements via diradicaloid, zwitterionic, or strained ground state intermediates. Such rearrangements are valuable as a means of synthesizing unusual ring structures. In this chapter we have attempted to systematize and unify many superficially unrelated photoreactions by employing the concept of concerted pericyclic photoreactions, together with the general principles set forth in Chapters 10 and 11.

References

1. Woodward, R. B., and Hoffmann, R., *The Conservation of Orbital Symmetry*, New York: Academic Press, 1970; Gill, G. B., and Willis, M. R., *Pericyclic Reactions*, London: Chapman and Hall, 1974; Gilchrist, T. L., and Storr, R. C., *Organic Reactions and Orbital Symmetry*, Cambridge: Cambridge Press, 1972.
2. Saltiel, J., et al. *Org. Photochem.*, *3*, 1 (1972); For an extensive review of synthetic applications see: Meier, H., *Photochemie I*, in Houben-Weyl, *Methoden der Organische Chemie*, Stuttgart: Gerog Thieme, 1976, p. 189 ff.
3. Crandall, J., and Haseltine, R. P., *J. Am. Chem. Soc.*, *90*, 6251 (1968); Noyori, R., and Kato, M., *Tetrahedron Letters*, 5075 (1968).
4. Marshall, J. A., and Arrington, J. P., *J. Org. Chem.*, *36*, 214 (1971).
5. Turro, N. J., *Photochem. Photobio.*, *9*, 555 (1969).
6. Hammond, G. S., and Saltiel, J., *J. Am. Chem. Soc.*, *85*, 2516 (1963); Herkstroeter, W. G., and Hammond, G. S., *ibid.*, *88*, 4789 (1966).
7. Schenck, G. O., Eggert, H., and Denk, W., *Ann.*, *584*, 176 (1953).
8. Hammond, G. S., et al., *J. Am. Chem. Soc.*, *86*, 3197 (1964).
9. Wettack, F. S., et al., *J. Am. Chem. Soc.*, *92*, 1318 (1970).
10. Barltrop, J. A., and Carless, H. A. J., *J. Am. Chem. Soc.*, *94*, 8761 (1972); Yang, N. C., et al., *ibid.*, *99*, 3023 (1977).
11. Cundall, R., *Prog. Reaction Kinetics*, *2*, 161 (1964).
12. Carless, H. A. J., *J. Chem. Soc., Perkin II*, 834 (1974).

13. Saltiel, J., Metts, L., and Wrighton, M., *J. Am. Chem. Soc.*, *91*, 5684 (1972). For a discussion of the potential-energy surfaces of 1,3-dienes, see Inuzuka, K., and Becker, R. S., *Bull. Chem. Soc. Japan*, *44*, 3323 (1971).

14. Ramamurthy, V., and Liu, R. S. H., *J. Am. Chem. Soc.*, *98*, 2935 (1976).

15. Honig, B., and Ebrey, T. G., *Ann. Rev. Biophys. Bioeng.*, *3*, 151 (1974).

16. For an extended discussion of strain in unsaturated systems, see Zefirov, N. S., and Sakolov, V. I., *Russ. Chem. Rev.*, *36*, 87 (1967); Liebman, J. F., and Greenberg, A., *Chem. Rev.*, *76*, 311 (1976); Mock, W. L., *Tetrahedron Letters*, 475 (1972).

17. (a) Corey, E. J., et al. *J. Am. Chem. Soc.*, *87*, 2054 (1965).
(b) Eaton, P. E., and Liu, K., *J. Am. Chem. Soc.*, *87*, 2052 (1965).
(c) Noyori, R., and Kato, M., *Bull. Chem. Soc. Japan*, *47*, 1460 (1974).

18. Bonneau, R., de Violet, P. F., and Joussot-Dubien, J., *Nouveau J. Chem.*, *1*, 31 (1977).

19. Kropp, P. J., *J. Am. Chem. Soc.*, *88*, 4091 (1966); *ibid.*, *89*, 1126 (1967); *ibid.*, *89*, 5199 (1967).

20. (a) Zimmerman, H. E., Kamm, K. S., Wertheman, D. P., *J. Am. Chem. Soc.*, *97*, 3718 (1975).
(b) Bonneau, R., Joussot-Dubien, J., Salem, L., and Yarwood, A. J., *J. Am. Chem. Soc.*, *98*, 4329 (1976); *Tetrahedron Letters*, 235 (1977).

21. Hutton, R. F., and Steel, C., *J. Am. Chem. Soc.*, *86*, 745 (1964).

22. Fogel, L. D., and Steel, C., *J. Am. Chem. Soc.*, *98*, 4589 (1976), and references therein.

23. See the following papers and references therein: Turro, N. J., Renner, C. A., Waddell, W. H., and Katz, T. J., *J. Am. Chem. Soc.*, *98*, 4320 (1976); Durr, H., and Ruge, B., *Topics Curr. Chem.*, *66*, 55 (1976).

24. Overberger, C. G., Chi, M. S., Pucci, D. G., and Barry, J. A., *Tetrahedron Letters*, 4565 (1972).

25. Gisin, M., and Wirz, J., *Helv. Chim. Acta.*, *59*, 2273 (1976); Pagni, R. M., Burnett, M., and Dodd, J. R., *J. Am. Chem. Soc.*, *99*, 1972 (1977).

26. See: Padwa, A., and Albrecht, F., *J. Am. Chem. Soc.*, *96*, 4849 (1974), and references therein.

27. Cookson, R. C., *Quart. Rev.*, *22*, 423 (1968); Cookson, R. C., Henstock, J., and Hudek, J., *J. Am. Chem. Soc.*, *88*, 1060 (1966); Sharma, M., *ibid.*, *97*, 1153 (1975).

28. Jones, L. B., and Jones, V. K., *Forschrit.*, *13*, 307 (1969); *J. Org. Chem.*, *34*, 1298 (1969).

29. Tezyka, T., Kimura, M., Sato, A., and Mukai, T., *Bull. Chem. Soc. Japan*, *43*, 1120 (1970); ter Borg, A. P., and Klossterziel, *Rec. Trav. Chim.*, *84*, 242 (1965).

30. Kiefer, E. F., and Tanna, C. H., *J. Am. Chem. Soc.*, *91*, 4478 (1969); *Tetrahedron Letters*, 993 (1969).

31. Fields, T. R., and Kropp, P. J., *J. Am. Chem. Soc.*, *96*, 7554 (1974); Inoue, Y., Takamuku, S., and Sakurai, H., *Chem. Comm.*, 577 (1975).

32. Hixon, S. S., Tausta, J. C., and Borovsky, J., *J. Am. Chem. Soc.*, *97*, 3230 (1975); Hixson, S. S., *ibid.*, *97*, 1981 (1975).

33. Palensky, F. J., and Morrison, H. A., *J. Am. Chem. Soc.*, *99*, 3507 (1977); McCullough, J. J., and Yarwood, A. J., *Chem. Comm.*, 485 (1975).

34. General review: Zimmerman, H. E., et al., *Chem. Rev.*, *73*, 531 (1973); *J. Am. Chem. Soc.*, *98*, 540 (1976).

35. Zimmerman, H. E., and Mariano, P. S., *J. Am. Chem. Soc.*, *91*, 1718 (1969).

36. Zimmerman, H. E., and Pratt, A. C., *J. Am. Chem. Soc.*, *92*, 6267 (1970).

37. Zimmerman, H. E., and Epling, G., *J. Am. Chem. Soc.*, *94*, 8749 (1972); Swenton, J. S., Crumrine, A. R., and Walker, T. J., *ibid.*, *92*, 1406 (1970).

38. Zimmerman, H. E., et al., *J. Am. Chem. Soc.*, *91*, 3316 (1969); Zimmerman, H. E., and Iwamura, H., *ibid.*, *92*, 2015 (1970).

39. Zimmerman, H. E., Boettchner, R. J., and Keck, G. E., *J. Am. Chem. Soc.*, *97*, 5635 (1975); *ibid.*, *98*, 7680 (1976).

40. Edman, J. R., *J. Am. Chem. Soc.*, *91*, 7103 (1969).

41. Kaupp, G., Perreten, J., Leute, R., and Pringbach, H., *Chem. Ber.*, *103*, 2288 (1970).

42. Ziegler, G. E., and Hammond, G. S., *J. Am. Chem. Soc.*, *90*, 513 (1968).

43. Cristol, S. J., Ziebarth, T. D., Turro, N. J., Stone, P., and Scribe, P., *J. Am. Chem. Soc.*, *96*, 3016 (1974).

44. Zimmerman, H. E., Givens, R. S., and Pagni, R. M., *J. Am. Chem. Soc.*, *90*, 6096 (1968).

45. Rabideau, P. W., Hamilton, J. B., and Friedman, L., *J. Am. Chem. Soc.*, *90*, 4465 (1968).

46. Ipaktschi, J., *Chem. Ber.*, *105*, 1989 (1972).

47. Turro, N. J., et al., *J. Am. Chem. Soc.*, *91*, 516 (1969); Walsh, T. D., *ibid.*, *91*, 515 (1969).

48. Iwamura, H., and Yoshimura, K., *J. Am. Chem. Soc.*, *96*, 2652 (1974).

49. For an extensive review of photoelectrocyclic reactions, see Meier, H., *Photochemie I*, in Houben-Weyl, *Methoden der Organische Chemie*, Stuttgart: Georg Thieme, 1976, p. 222 ff.

50. For references to reactions in Eq. 12.34 Eberbach, W., *Chem. Ber.*, *108*, 1052 (1975). For further examples see Masamune, S., and Dabby, N., *Acc. Chem. Research*, *5*, 272 (1972).

51. Schumate, K. M., and Fonken, G. J., *J. Am. Chem. Soc.*, *87*, 3996 (1965); *ibid.*, *88*, 1073 (1966); Radlick, P., and Fenical, W., *Tetrahedron Letters*, 4901 (1967).

52. Liu, R. S. H., *J. Am. Chem. Soc.*, *87*, 112 (1967).

53. Sanders, G. M., Pot, J., and Havinga, E., *Fortschr. Chem. Org. Nautrst.*, *27*, 129 (1969); Havinga, E., *Experientia*, *29*, 1181 (1973).

54. Dauben, W. G., and Kellogg, M. S., *J. Am. Chem. Soc.*, *93*, 3805 (1971); Dauben, W. G., et al. *Pure Appl. Chem.*, *33*, 197 (1973); Vroegop, P. J., Lugtenburg, J., and Havinga, E., *Tetrahedron*, *29*, 1393 (1973).

55. Srinivasan, R., *J. Am. Chem. Soc.*, *90*, 4498 (1968).

56. Aue, D., and Reynolds, R. N., *J. Am. Chem. Soc.*, *95*, 2027 (1973).

57. Wilzbach, K. E., and Kaplan, *J. Am. Chem. Soc.*, *87*, 4004 (1965); *J. Am. Chem. Soc.*, *89*, 1030 (1967). Reviews: Scott, L. T., and Jones, M., *Chem. Rev.*, *72*, 181 (1972); Bolesov, I., *Russ. Chem. Rev.*, *37*, 666 (1968).

58. Breslow, R., et al., *J. Am. Chem. Soc.*, *87*, 5139 (1965).

59. Weiss, R., and Kölbl, H., *ibid.*, *97*, 3222, 3224 (1975).

60. Bryce-Smith, D., Gilbert, A., and Robinson, D. A., *Angew. Chem., Inter. Ed. Eng., 10*, 745 (1971), and references therein.

61. For a theoretical analysis see Haller, I., *J. Chem. Phys., 47*, 1117 (1967); Halevi, E. A., *Nouv. J. Chim., 1*, 229 (1977).

62. Kaplan, L., Ransch, D. J., and Wilzbach, K. E., *J. Am. Chem. Soc., 94*, 8638 (1972); *ibid., 88*, 2881 (1966).

63. Katz, T. J., Wang, E. J., and Acton, N., *ibid., 93*, 3782 (1971).

64. Renner, C. R., Katz, T. J., Pouliquen, J., Turro, N. J., and Waddell, W. H., *J. Am. Chem. Soc., 97*, 2568 (1975).

65. Kaplan, L., and Wilzbach, K. E., *J. Am. Chem. Soc., 89*, 1030, 1031 (1966).

66. Wilzbach, K. E., Harkness, A. L., and Kaplan, L., *J. Am. Chem. Soc., 90*, 1116 (1968).

67. Turro, N. J., Ramamurthy, V., and Katz, T. J., *Nouv. J. Chimie, 1*, 363 (1977).

68. Turro, N. J., and Devaquet, A., *J. Am. Chem. Soc., 97*, 3859 (1975).

69. For reviews see Scholy, M., Cietz, F., and Muhlstadt, M., *Z. Chemie, 7*, 329 (1967); Stermitz, F. R., *Organic Photochemistry, I*, ed. Chapman, O. L., New York: Dekker, 1967; Blackburn, E. V., and Timmons, C. J., *Quart. Rev., 23*, 482 (1969); Meier, H., in *Photochemie J.*, Houben-Weyl, *Methoden der Organische Chemie*, Stuttgart: Georg Thieme, 1975, p. 511.

70. Mallory, F. B., Wood, C. S., and Gordon, J. T., *J. Am. Chem. Soc., 86*, 3094 (1964); Muszkat, K. A., and Fischer, E., *J. Chem. Soc., 13*, 662 (1967).

71. Doyle, T. D., Benson, W. R., and Filipescu, N., *J. Am. Chem. Soc., 98*, 3262 (1976); Cuppen, J. H. M., and Laarhoven, W. H., *ibid.*, 5914 (1972).

72. Bernstein, W. J., Calvin, M., and Buchardt, O., *J. Am. Chem. Soc., 95*, 527 (1973); Buchardt, O., *Angew. Chem. Inter. Ed. Eng., 13*, 179 (1974); Moradpour, A., and Tsoucaris, *J. Am. Chem. Soc., 93*, 2353 (1971).

73. Martin, R. H., *Angew. Chem. Inter. Ed. Eng., 13*, 649 (1974); Laarhoven, W. H., and Cuppen, T. J. H. M., *Chem. Comm.*, 47 (1977).

74. (a) Srinivasan, R., *J. Am. Chem. Soc., 85*, 4045 (1963).
(b) Dauben, W. G., and Poulter, *Tetrahedron Letters*, 3021 (1967); *Pure Appl. Chem., 9*, 539 (1964).

75. Dauben, W. G., and Ritscher, J. S., *J. Am. Chem. Soc., 92*, 2925 (1970).

76. Salem, L., et al., *Angew. Chem. Inter. Ed. Eng., 14*, 575 (1975); *J. Am. Chem. Soc., 98*, 5037 (1976).

77. Barltrop, J. A., and Browning, H. E., *Chem. Comm.*, 1481 (1968).

78. Friedrich, L. E., and Schuster, G. B., *J. Am. Chem. Soc., 91*, 7204 (1969).

79. Becker, R. S., Dolan, E., and Balke, D. E., *J. Chem. Phys., 50*, 239 (1969).

80. Chapman, O. L., et al., *J. Am. Chem. Soc., 89*, 3476 (1967).

81. Bercovici, T., and Fischer, E., *J. Am. Chem. Soc., 86*, 5687 (1964): For other examples see: *Photochromism*, ed. Brown, G. H., in *Techniques of Organic Chemistry, III*, New York: Wiley, 1971.

82. Forster, E. W., Grellmann, K. H., and Linschitz, H., *J. Am. Chem. Soc., 95*, 3108 (1973) and references therein; Forster, E. W., and Grellmann, K. H., *Chem. Phys. Letters, 14*, 536 (1972); Shizuka, H., Takayama, Y., Tanaka, I., and Morita, T., *J. Am. Chem. Soc., 92*, 7270 (1970); *ibid., 93*, 5987 (1971).

83. Chapman, O. L., Eian, G. L., Bloom, A., and Clardy, J., *J. Am. Chem. Soc.*, *93*, 2918 (1971).

84. Reviews: *Photochemistry of Heterocyclic Compounds*, ed. Buchardt, O., New York: Wiley, 1976; Vernin, G., et al., *Bull. Soc. Chim. France*, 1743 (1973); Reid, S. T., *Adv. Heterocyclic Chem.*, *11*, 57 (1969).

85. Bopat, J. B., and Black, D. St. C., *Chem. Comm.*, *73*, (1967); Yamada, S., Ishikawa, M., and Kaneko, C., *Chem. Comm.*, 1093 (1972); *Tetrahedron Letters*, 971 (1972); Hecht, S. S., and Greene, F. D., *J. Am. Chem. Soc.*, *89*, 6761 (1967); Splitter, J. S., Su, T. M., Ono, H., Calvin, M., *J. Am. Chem. Soc.*, *93*, 4076 (1971).

86. Tsuchiya, T., Arai, H., and Igeta, H., *Chem. Comm.*, 550 (1972); *Tetrahedron Letters*, *29*, 2747 (1973).

87. Bellamy, F., Barragan, L. G. R., and Streith, J., *Chem. Comm.*, 456 (1971); Streith, J., *Pure Appl. Chem.*, *49*, 305 (1977). See also: Kumler, P. L., and Buchardt, O., *J. Am. Chem. Soc.*, *90*, 5640 (1968); *J. Am. Chem. Soc.*, *95*, 7402 (1973).

88. Van Tamelen, E. E., and Whiteside, T. H., *J. Am. Chem. Soc.*, *93*, 6129 (1971).

89. Singh, B., Zweig, A., and Gallivan, J. B., *J. Am. Chem. Soc.*, *95*, 1199 (1972) and references therein.

90. Kellogg, R. M., Dik, J. K., van Driel, H., and Wynberg, H., *J. Org. Chem.*, *35*, 2737 (1970) and references therein; Review: reference 84, p. 123.

91. Dietliker, K., Gilgen, P., Heimgartner, and Schmid, H., *Helv. Chim. Acta.*, *59*, 2074 (1976), and references therein.

92. Heinzelmann, W., Marky, M., and Gilgen, P., *Helv. Chim. Acta.*, *59*, 1528 (1976).

93. Review: Lablache-Combier, A., and Remy, M. A., *Bull. Soc. Chim. France*, 679 (1971).

94. Kobayshi, Y., Kumadaki, I., Ohsawa, A., and Ardo, A., *J. Am. Chem. Soc.*, *99*, 7350 (1977).

95. Wilzbach, K. E., and Rausch, D. J., *J. Am. Chem. Soc.*, *92*, 2178 (1970); Ogata, Y., and Takagi, K., *ibid.*, *96*, 5933 (1974).

96. Closs, G. L., Boll, W. A., and Dev., V., *J. Am. Chem. Soc.*, *90*, 173 (1968).

97. Quinkert, G., *Pure Appl. Chem.*, *33*, 285 (1973); *Angew. Chem.*, *11*, 1072 (1972).

98. Griffiths, J., and Hart, H., *J. Am. Chem. Soc.*, *90*, 5296 (1968); *ibid.*, *90*, 3297 (1968); Murray, R. K., and Hart, H., *J. Org. Chem.*, *35*, 1535 (1970).

99. Dauben, W. G., Salem, L., and Turro, N. J., *Acc. Chem. Research*, *8*, 41 (1975).

100. Chapman, O. L., and Lassila, J. D., *J. Am. Chem. Soc.*, *90*, 2449 (1968).

101. Quinkert, G., *Chimia*, *31*, 225 (1977).

102. Reviews: Kropp, P. J., *Org. Photochem.*, *1*, 1 (1967); Schaffner, K., *Adv. Photochem.*, *3*, 81 (1966).

103. Zimmerman, H. E., and Little, R. D., *J. Am. Chem. Soc.*, *96*, 4623 (1974); Matsuura, T., and Ogura, K., *Chem. Comm.*, 1247 (1967).

104. Barber, L. L., Chapman, O. L., and Lassila, J. D., *J. Am. Chem. Soc.*, *91*, 3664 (1969).

105. Agosta, W. C., and Smith, A. B., *Tetrahedron Letters*, 4517 (1969).

106. Zimmerman, H. E., and Schuster, D. I., *J. Am. Chem. Soc.*, *84*, 4527 (1962); Zimmerman, H. E., and Swenton, J. S., *ibid.*, *89*, 906 (1967); Zimmerman, H. E., *Pure Appl. Chem.*, *9*, 493 (1964).

107. Zimmerman, H. E., et al., *J. Am. Chem. Soc.*, *88*, 159, 1968 (1966); Chapman, O. L., et al., *Tetrahedron Letters*, 2049 (1963); Dauben, W. G., Shaffer, G. W., and Vietmeyer, N. D., *J. Org. Chem.*, *33*, 4060 (1968).

108. Kropp, P. J., *J. Am. Chem. Soc.*, *86*, 4053 (1964); *J. Org. Chem.*, *29*, 3110 (1964); Kropp, P. J., and Erman, E. F., *J. Am. Chem. Soc.*, *95*, 2456 (1963).

109. Fisch, M. H., and Richards, J. H., *J. Am. Chem. Soc.*, *90*, 1547, 1553 (1968); Chapman, O. L., and Englert, L. F., *ibid.*, *95*, 3028 (1963).

110. Dauben, W. G., Spitzer, W. A., and Kellogg, M. S., *J. Am. Chem. Soc.*, *93*, 3672 (1971).

111. Zimmerman, H. E., Crumrine, D. S., Döpp, D., and Huyffer, P. S., *J. Am. Chem. Soc.*, *91*, 434 (1969).

112. (a) Zimmerman, H. E., Keese, R., Nasielski, J., and Swenton, J. S., *J. Am. Chem. Soc.*, *88*, 4895 (1966).
(b) Chapman, O. L., Clardy, J. C., McDowell, T. L., and Wright, H. E., *J. Am. Chem. Soc.*, *95*, 5086 (1973).

113. Fisch, M. H., *Chem. Comm.*, 1472 (1973).

114. Zimmerman, H. E., and Epling, G. A., *J. Am. Chem. Soc.*, *94*, 3245 (1972).

115. Schuster, D. I., and Liu, K. C., *J. Am. Chem. Soc.*, *93*, 6711 (1971); Schuster, D. I., and Abraitys, V. Y., *Chem. Comm.*, 419 (1969).

116. Dauben, W. G., Spitzer, W. A., and Kellogg, M. S., *J. Am. Chem. Soc.*, *93*, 3674 (1971).

117. Review of the photochemistry of β,γ-unsaturated enones: Houk, K., *Chem. Rev.*, *76*, 1 (1976); Dauben, W. G., Loder, G., and Jpastski, J., *Topics in Current Chemistry*, *54*, 23 (1975).

13

Photofragmentation Reactions

13.1 Photofragmentations and Photoeliminations

A number of photoreactions are initiated by the cleavage of a sigma bond(s) and result in net rearrangement, fragmentation, or elimination of a small molecule (e.g., N_2, CO, CO_2, etc.). Pericyclic fragmentation reactions, such as concerted electrocyclic ring openings, were discussed in Chapter 12. Pericyclic retrocycloadditions are discussed in Section 13.5.

Classification of Photochemical Cleavage Reactions

In this chapter we will consider processes which possess the common mechanistic step of requiring a photochemical cleavage of a sigma bond as a key feature of the reaction. In particular, we will consider reactions for which sigma bond cleavage is probably a primary photochemical process. These reactions may be classified as:

1. *Homolytic cleavage*, in which the sigma bond is cleaved to produce a radical pair or a diradical.

2. *Heterolytic cleavage*, in which the sigma bond is cleaved to produce an ion pair or a zwitterion.

The distinction between a radical pair and a diradical, like that between an ion pair and a zwitterion, is arbitrary and not meant to imply a different inherent chemical reactivity. However, the actual reactions of diradicals and zwitterions are often *intramolecular*, and it is helpful to keep this in mind in our classification.

There are certain molecules (e.g., diazo compounds, azides) for which cleavage of a formal sigma bond produces a *molecule* (e.g., N_2) and a diradical or zwitterion.

The products expected for α-cleavage of n, π^* and π, π^* states in terms of primary product formation are analogous to those discussed in previous chapters for additions, rearrangements, etc. As before, $n, \pi^* \rightarrow D$ and $^3\pi, \pi^* \rightarrow D$ transformations are expected to be common and *general*. In addition, $^1\pi, \pi^* \rightarrow Z$ reactions are possible and *relatively common*, because fragmentations are unimolecular and

may be initiated by single bond cleavage (a process that can be competitive with other paths of deactivation of $^1\pi, \pi^*$ states).

Examples of Reactions Resulting from a Primary Photochemical Cleavage Reaction

A wide variety of isolated products may result from any one of a number of primary photochemical σ-bond cleavages. A common feature of these reactions is cleavage of a relatively weak σ-bond followed by secondary thermal reactions such as loss of a small molecule (CO, CO_2, N_2) to generate a highly energetic diradical, zwitterion, or fully bonded, but strained, molecule. Often these species may be generated and matrix isolated at very low temperatures.

For example, benzyne (Eq. 13.1), α-lactones (Eq. 13.2), and cyclobutadiene (Eq. 13.3) have been generated and matrix isolated by irradiation of cyclic esters at 77 K. The loss of the small, stable molecule CO_2 provides a driving force for these reactions.

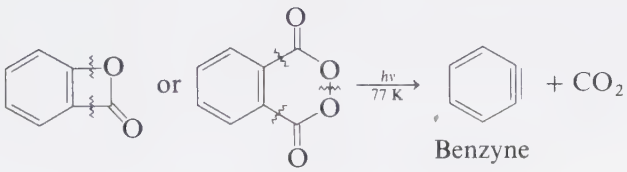

Benzyne (13.1)[1]

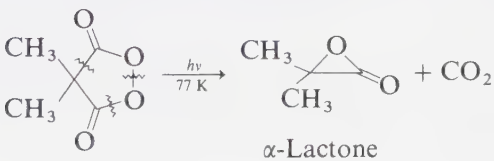

α-Lactone (13.2)[2]

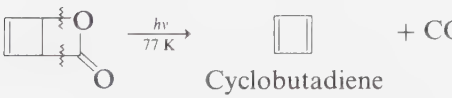

Cyclobutadiene (13.3)[3]

Similarly, carbenes, nitrenes, diradicals, trimethylenemethanes, and 1,3-zwitterions have been prepared and matrix isolated (Eqs. 13.4–13.8) via low temperature photolysis:

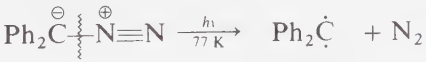

Carbene (13.4)[4]

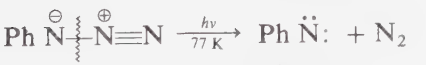

Nitrene (13.5)[5]

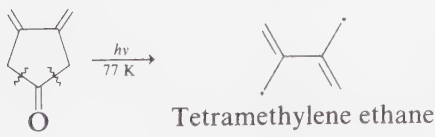

Tetramethylene ethane (13.6)[6]

(13.7)[7]

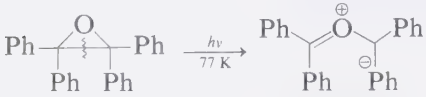

Zwitterions

(13.8)[8]

13.2 Homolytic α-Cleavage of Ketones; An Alkoxy Radical Model

From a consideration of orbital interactions and correlation diagrams, it appears that homolytic α-cleavage of the n, π^* states of ketones (a so-called "Type I" reaction) is initiated by the electrophilic half-filled n-orbital (Section 7.3).[9] If this is correct, we may postulate that the alkoxy radical $R_3C\dot{O}$, which possesses a half-filled oxygen orbital, may serve as a model for α-cleavage from the n, π^* states of ketones.

Indeed, alkoxy radicals undergo a homolytic α-cleavage reaction:[10]

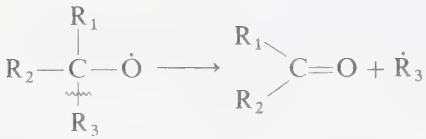

(13.9)

From the chemistry of alkoxy radicals it has been established that the group that fragments is usually the one which corresponds to the most stable radical.[11] In turn, this corresponds to cleavage of the weakest α-bond to the radical center. In the case of unstrained ketones, the more stable the diradical or radical pair derived from α-cleavage, the weaker the fragmenting bond. In the case of strained (usually small-ring) ketones, diradical stability determines the α-bond which cleaves (regioselectivity), but release of strain determines the rate constant of α-cleavage.[12]

We can now postulate that for an n, π^* state of a given multiplicity, (a) the α-cleavage which produces the most stable radical pair occurs faster, (b) for different molecules of similar structure the more stable the radical pair produced by α-cleavage, the faster is the absolute rate constant for reaction, and (c) for cleavages which produce radicals of comparable stability, the greater the relief strain the faster the rate of cleavage.

Since radical stability generally correlates with bond energy, we may apply this rule with our knowledge of *bond dissociation energies*. For example, since a typical triplet energy of an n, π^* state is ~70 kcal/mole, the strong (80–90 kcal/mole)

OC—CH_3 and OC—Ph bonds undergo inefficient α-cleavage, whereas the relatively weak (< 70 kcal/mole) OC—CH_2Ph and OC—$C(CH_3)_3$ bonds undergo efficient α-cleavage from $T(n, \pi^*)$ states at room temperature. Intermediate behavior is expected from ketones whose bond strengths are between 70 and 80 kcal/mole.

We may use the oxy model as a rough guide for reactivity relationships. It is found that *A* (Eq. 13.10) cleaves to lose CH_3 about 10^7 times *slower* than *B* (Eq. 13.11) cleaves to lose $\dot{C}(CH_3)_3$:[13]

$$A\ (CH_3)_3C\dot{O} \rightarrow \dot{C}H_3 + (CH_3)_2CO \qquad k \sim 10^2\ \text{sec}^{-1} \quad (13.10)$$

$$B\ (CH_3)_3C(CH_3)_2C\dot{O} \rightarrow (CH_3)_3\dot{C} + (CH_3)_2CO \qquad k \sim 10^9\ \text{sec}^{-1} \quad (13.11)$$

For example, acetone and benzophenone are relatively stable toward formation of products from α-cleavage, whereas methyl tert-butyl ketone and phenyl tert-butyl ketone yield α-cleavage products efficiently. These results are understandable in terms of the above rule because of the radical stability order $\dot{C}_6H_5 < \dot{C}H_3 \ll \dot{C}(CH_3)_3$. Thus, the *rate* of α-cleavage of t-butyl ketones should be much faster than that for acetone and benzophenone. The rule also allows us to predict that methyl tert-butyl ketone and phenyl tert-butyl ketone will cleave the OC-tert butyl bond preferentially to the OC-CH_3 or OC-C_6H_5 bond.

In cyclic systems, the reactivity pattern of ring opening of alkoxy radicals follows that expected for the *relief of ring strain.*

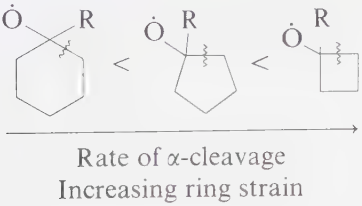

Alkoxy radicals (13.12)

It can be seen from a comparison of Eqs. 13.12 and 13.13 that the reactivity of (n, π^*) states is qualitatively similar to that of alkoxy radicals.

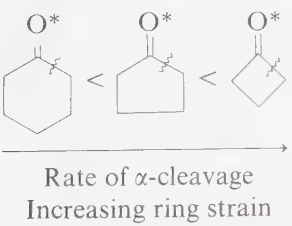

n, π^* states (13.13)

Finally, polar effects are known to affect the reactivity of cleavage of alkoxy radicals to yield $\dot{R}'$. The polar effect is quantified by the Hammett ρ constant, which is a measure of the sensitivity of a reaction rate constant (for a series of substituent changes at a functional group undergoing a given reaction by a similar

mechanism) to polar effects.[14] The value of ρ is -1.7 for α-cleavage of alkoxy radicals[11] and ρ is -1.1 for α-cleavage of n, π^* states.[15]

Some General Results for the Photochemical α-Cleavage of Ketones

The experimental evidence for a homolytic α-cleavage primary photochemical process of ketones is substantial. In addition to the consistency of product structures and structure reactivity relationships with this postulate, direct spectroscopic identification has been reported for both the acyl and the alkyl radicals produced by α-cleavage. For example, irradiation of methyl tert-butyl ketone in the cavity of an ESR spectrometer results in direct observation of the ESR signal of the $CH_3\dot{C}O$ and $(CH_3)_3\dot{C}$ radicals.[16] In addition, CIDNP studies (Eq. 13.14) provide further support that acyl and alkyl radicals are produced:[16,17]

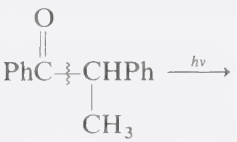

$$\xrightarrow{h\nu} \quad \mathrm{PhC\dot{O}} + \mathrm{CH_3\dot{C}HPh} \qquad (13.14)$$

Detected by CIDNP of products

As mentioned in the preceding section, the reactivity-structure profile for α-cleavage is also consistent with the notion of a homolytic α-cleavage, i.e., this postulate explains the parallelism between the reactivity of alkoxy radicals and n, π^* states toward α-cleavage and the basis for the regioselectivity of cleavage of an unsymmetrical ketone (see Table 13.1 for examples).

However, the following reactivity patterns are not explained in an obvious fashion by the postulation of a homolytic cleavage and most stable radical pair:

1. For the same multiplicity, the rate constant for α-cleavage of $n, \pi^* \gg \pi, \pi^*$. For example, phenyl tert-butyl ketone ($T_1 = n, \pi^*$) undergoes relatively rapid and efficient α-cleavage, but 4-phenyl-phenyl tert-butyl ketone ($T_1 = \pi, \pi^*$) is stable toward cleavage:[18]

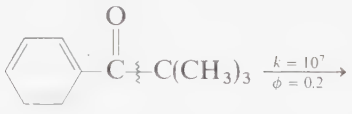

$$\xrightarrow[\phi = 0.2]{k = 10^7} \qquad \cdot\mathrm{C(CH_3)_3} \qquad (13.15)$$

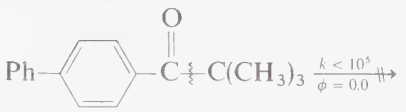

$$\xrightarrow[\phi = 0.0]{k < 10^5} \qquad \cdot\mathrm{C(CH_3)_3} \qquad (13.16)$$

2. For the same structure and electronic configuration, the rate constant for α-cleavage of $^3(n, \pi^*) \gg {}^1(n, \pi^*)$ for saturated ketones.[19] For example, the rate constant for α-cleavage of $S_1(n, \pi^*)$ of tetramethyl cyclopentanone is at least 10^2 times slower than the rate constant for α-cleavage of $T_1(n, \pi^*)$ of the same

compound:[20]

$$S_1(n, \pi^*) \xrightarrow{k < 10^8} {}^1D \tag{13.17}$$

$$T_1(n, \pi^*) \xrightarrow{k > 10^{10}} {}^3D \tag{13.18}$$

3. For the same electronic and spin configuration, dialkyl ketones (RCOR) undergo α-cleavage to RĊO and Ṙ radicals faster than the analogous aryl alkyl ketone (ArCOR). For example, the rate constant for $T_1(n, \pi^*)$-initiated α-cleavage of methyl tert-butyl ketone is about 10^3 times faster than that for

Table 13.1 Quantum Yields and Rate Constants for α-cleavage

	$\phi(S_1)$	$\phi(T_1)$	$k(S_1)$	$k(T_1)$	Reference
$CH_3COC(CH_3)_3$	0.18	0.33	$<10^8$	$>10^9$	a
Cyclobutanone	~0.3	—	$>10^9$	—	b
Cyclopentanone	—	~0.2	$<10^8$	2×10^8	c
2-methylcyclopentanone	—	~0.3	$<10^8$	2×10^9	c
2,2,5,5-tetramethylcyclo-pentanone	—	~0.6	$<10^8$	$>10^{10}$	c
Cyclohexanone	—	~0.2	$<10^8$	2×10^7	c
2-methylcyclohexanone	—	~0.3	$<10^8$	3×10^8	c
2,2-dimethylcyclohexanone	—	~0.4	$<10^8$	2×10^9	c
$PhCOCH_2Ph$	—	~0.4	—	2×10^6	d
$PhCOCH(CH_3)Ph$	—	~0.4	—	3×10^7	d
$PhCOC(CH_3)_2Ph$	—	~0.4	—	1×10^8	d
$PhCOC(CH_3)_3$	—	~0.3	—	1×10^7	e
$4\text{-}CH_3O\text{-}C_6H_4COC(CH_3)_3$	—	~0.1	—	7×10^5	e
$4\text{-}C_6H_5\text{-}C_6H_4COC(CH_3)_3$	—	<0.001	—	$<10^5$	e
$PhCH_2COCH_2Ph$	—	0.7	—	$>10^{10}$	f
$PhCOCH_2Ph$	—	~0.4	—	10^6	g
$PhCOCHPhOCOCH_3$	—	~0.3	—	5×10^7	g
$PhCOCHPhOCH_3$	—	~0.4	—	$>10^{10}$	g
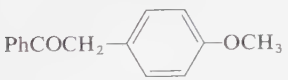	—	~0.2	—	~10^7	h
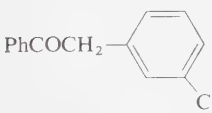	—	~0.1	—	~10^5	h

a. Yang, N. C., Feit, E. D., Hui, M. J., Turro, N. J., and Dalton, J. C., *J. Am. Chem. Soc.*, *92*, 6974 (1970).
b. Hemminger, J. C., Rusbult, C. F., and Lee, E. K. C., *J. Am. Chem. Soc.*, *93*, 1867 (1971).
c. Wagner, P. J., and Spoerke, R. W., *J. Am. Chem. Soc.*, *91*, 4437 (1969); Dalton, J. C., et al., *ibid.*, *93*, 7213 (1971)
d. Heine, H. G., et al., *J. Org. Chem.*, *39*, 691 (1974).
e. Lewis, F. D., and Magyar, J. G., *J. Org. Chem.*, *37*, 2102 (1972).
f. Engel, P. S., *J. Am. Chem. Soc.*, *92*, 6074 (1970).
g. Lewis, F. D., et al., *J. Am. Chem. Soc.*, *97*, 1519 (1975).
h. Lewis, F. D., *J. Org. Chem.*, *40*, 488 (1975).

phenyl tert-butyl ketone:

$$CH_3C(=O)C(CH_3)_3 \xrightarrow{k \sim 10^{10}} CH_3\dot{C}O + \dot{C}(CH_3)_3 \qquad (13.19)^{21}$$

$$PhC(=O)C(CH_3)_3 \xrightarrow{k \sim 10^{7}} Ph\dot{C}O + \dot{C}(CH_3)_3 \qquad (13.20)^{18}$$

$$T_1(n, \pi^*) \longrightarrow {}^3D$$

4. The *activation* energy for α-cleavage from $T_1(n, \pi^*)$ is considerably less than that for α-cleavage of $S_1(n, \pi^*)$. For example, for acetone it is found that $E_a(T_1)$ is ~6 kcal/mole whereas $E_a(S_1)$ is ~17 kcal/mole.[22] Although this result is

$$\begin{array}{lll} CH_3C(=O)CH_3 & \longrightarrow & CH_3\dot{C}=O + \dot{C}H_3 \\ S_1(n, \pi^*) & & E_a \sim 17 \text{ kcal/mole} \\ T_1(n, \pi^*) & & E_a \sim 6 \text{ kcal/mole} \end{array} \qquad (13.21)$$

generally in line with the much faster rate constant for α-cleavage of $T_1(n, \pi^*)$ relative to $S_1(n, \pi^*)$ mentioned above, the magnitude of the activation energy for simple α-cleavage is somewhat in doubt, and requires further study.[22b]

5. The rate constant for α-cleavage of cyclic ketones (from a given n, π^* state) increases with ring strain. For example (Table 13.1), the rate of α-cleavage of cyclobutanone in $S_1(n, \pi^*)$ is at least 10 times faster than the rate of α-cleavage of cyclopentanone in $S_1(n, \pi^*)$.[23]

Products from Photoinduced α-Cleavage of Dialkyl and Alkyl Aryl Ketones

The most common reactions derived from radical pairs produced from α-cleavage of dialkyl and alkyl aryl ketones are radical recombination, disproportionation, and decarbonylation. In the last case a *new* pair of radicals is formed and may themselves undergo radical recombination or disproportionation. If free radicals result from the original cage-radical pair, they may be trapped by appropriate radical scavengers. The recombination reaction of the primary radical pair is manifested by quantum yields for cleavage products which are less than unity, even under circumstances such that kinetic analysis indicates that the quantum yield of the α-cleavage step is unity.[18a] For example, the cleavage of phenyl tert-butyl ketone into benzaldehyde and isobutylene proceeds via a primary α-cleavage of $T_1(n, \pi^*)$ into a caged triplet benzoyl and tert-butyl radical pair. These radicals escape from their initial cage and become free radicals in solution. The radical-radical disproportionation of benzoyl and tert-butyl radicals leads to the observed products benzaldehyde and isobutylene and recombination regenerates the starting ketone. The decay constant for triplet phenyl tert-butyl

ketone is about 10^3 that of acetophenone, suggesting that every triplet of the former ketone undergoes cleavage. However, the quantum yield of benzaldehyde formation is only about 20%. The reaction inefficiency is explained by a secondary radical-radical combination reaction to regenerate the starting material.

Further support for the recombination pathway is found in the observation that under irradiation the optically active ketone **1** undergoes both disproportionation *and* racemization.[24] Interestingly, the sum of the quantum yields for disproportionation and for racemization adds up to about 0.75. The reaction inefficiency may be due to cage combination before substantial rotation of the radical pair. If this interpretation is correct, then intersystem crossing in the radical cage must be competitive with the rotation of the caged radical pair and diffusion out of the solvent cage:

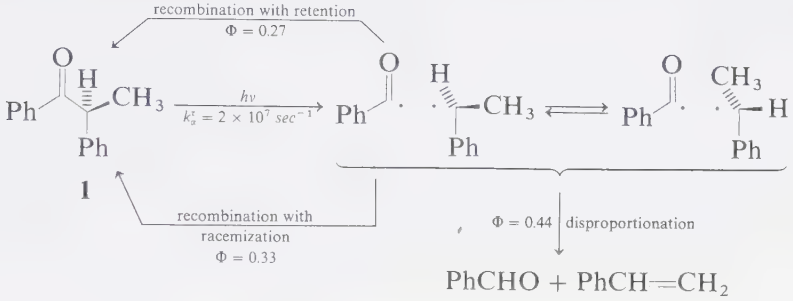

(13.22)

The products resulting from α-cleavage of cyclic ketones are analogous to those resulting from α-cleavage of acyclic ketones, i.e., combination, disproportionation, and decarbonylation.[20] For example, irradiation of cyclopentanones and cyclohexanones results in formation of disproportionation products. Cyclization may regenerate the starting material or result in formation of epimers:[25]

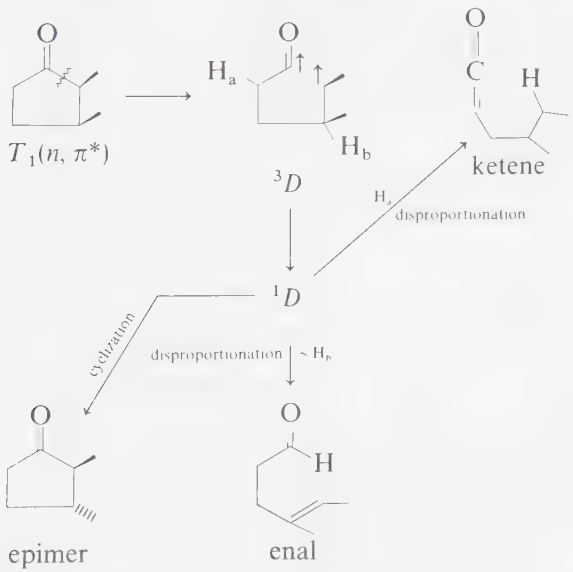

(13.23)

For structures in which one of the two disproportionation processes is blocked, the formation of ketene or enal product may be synthetically useful:[26]

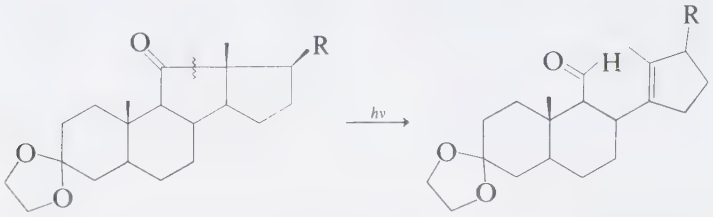

(13.24)

The third typical reaction of acyl alkyl radical pairs is decarbonylation of the acyl fragment.[27] This reaction generally does not compete with recombination and disproportionation unless the radical produced by decarbonylation is exceptionally stable (i.e., an allyl or tert-butyl radical). For example, irradiation of methyl tert-butyl ketone results mainly in formation of acetaldehyde and isobutylene (disproportionation products), whereas irradiation of di-tert-butyl ketone results mainly in formation of decarbonylation products.[16,21]

The observation that **2** yields a statistical mixture of products derived from $PhC\dot{H}_2$ and $Ph_2C\dot{H}$ radicals provides good evidence that the α-cleavage and decarbonylation steps are sequential and that truly "free" radicals are involved.[28]

$$\underset{\mathbf{2}}{PhCH_2CO\text{-}CHPh_2} \longrightarrow PhCH_2\dot{C}O + \dot{C}HPh_2$$

$$\xrightarrow[-CO]{} \underset{\text{Free radicals}}{PhC\dot{H}_2 + Ph_2C\dot{H}} \longrightarrow \underset{25\%}{PhCH_2CH_2Ph} + \underset{50\%}{PhCH_2CHPh_2} + \underset{25\%}{Ph_2CHCHPh_2}$$

Statistical mixture of coupling products (13.25)

If the acyl or alkyl fragments produced by α-cleavage are capable of rearrangements (e.g., of the cyclopropyl carbinyl → allyl type)[29] this process may compete with other reactions of the diradical.[30] A synthetic application of this idea is given in the ring expansion of **3** to **4** which involves two sequences of α-cleavage, ring opening, and cyclization.[31]

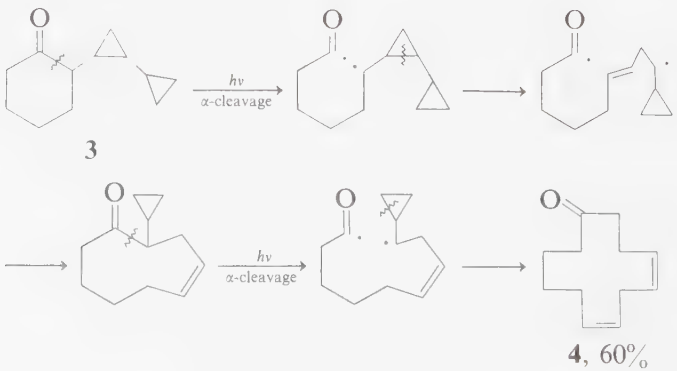

3

4, 60%

(13.26)

The Photochemical Reactions of Cyclobutanones

The photochemistry of cyclobutanone and its derivatives is dominated by the primary photochemical process of α-cleavage.[32] In contrast to other alkanones, cyclobutanones undergo efficient α-cleavage from $S_1(n, \pi^*)$ to product a *singlet* 1,4-acyl-alkyl diradical, ^1D. These reactions generally result from this diradical: (a) decarbonylation, (b) cycloelimination, and (c) oxacarbene formation:[33]

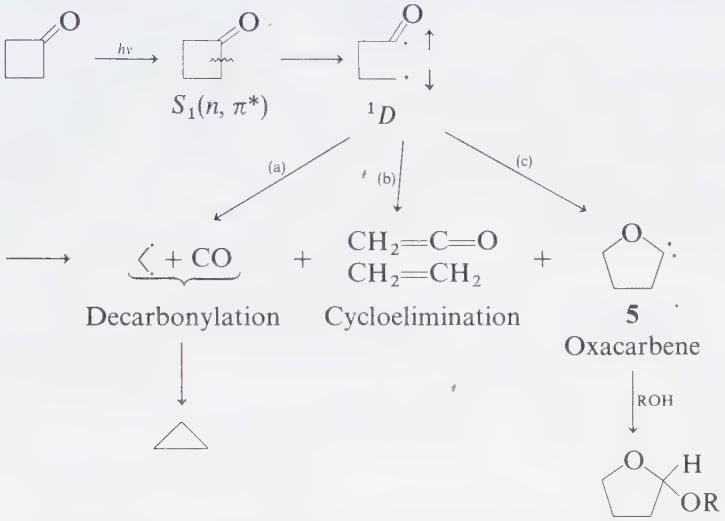

(13.27)

Decarbonylation of ^1D produces a 1,3-diradical which may generally cyclize (Eqs. 13.28 and 13.29). The oxacarbene intermediate derived from ^1D has been trapped by alcohols (Eq. 13.30):

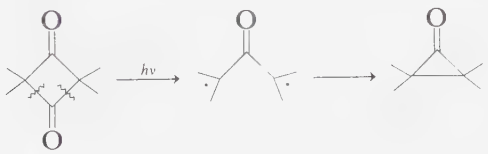

(13.28)[34]

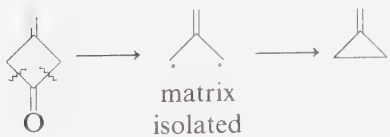

(13.29)[35]

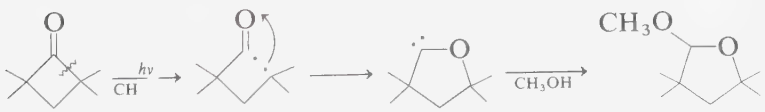

(13.30)[36]

It appears that the α-cleavage reactions of cyclobutanones generally proceed via a $S_1(n, \pi^*) \rightarrow {}^1D$ primary process.[32] From Eq. 13.27 it is clear that the fate

of ^1D is very different from that of the 1, *n* diradical produced from photolysis of cyclopentanones and cyclohexanones. The latter cyclanones undergo α-cleavage predominantly via a $T_1(n, \pi^*) \rightarrow {}^3D$ process, and mainly yield disproportionation products (Eq. 13.23). Another important difference between cyclobutanone photochemistry and that of larger cyclanones is the observation of *stereospecificity* in reaction products. For example, the ethyl alkoxy cyclobutanone **6** undergoes stereospecific decarbonylation to yield **7**, cycloelimination to yield **8**, and oxacarbene formation to yield **9** (Eq. 13.31):

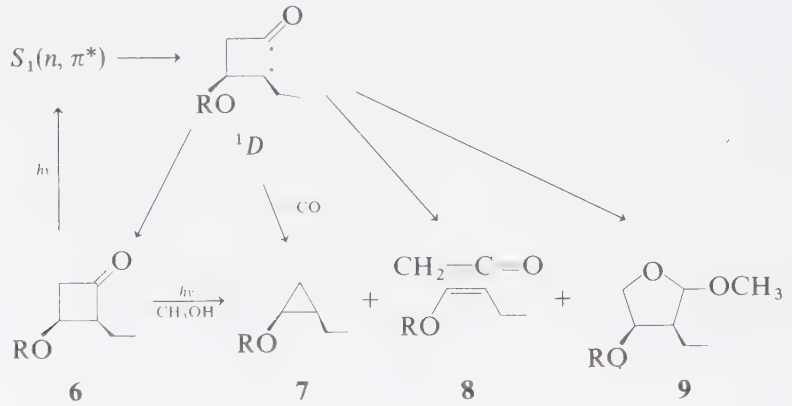

6 **7** **8** **9**

(13.31)[37]

The stereospecificity observed in the reactions listed in Eq. 13.31 is a manifestation of a general rule for cis-1,4-carbon singlet diradicals: The stabilizing reactions of a cis-1,4-carbon singlet diradical (cyclization, fragmentation, etc.) are *stereospecific* with respect to loss of stereochemistry at the reaction termini.

Use of Salem Correlation Diagrams to Understand the Unique Photochemistry of Cyclobutanones

The contrasting nature of the products from photochemical α-cleavage of cyclobutanones compared to the products of other alkanones (e.g., cyclohexanones) can be rationalized in terms of a unique surface reaction pathway for this small-ring ketone.[38] Consider the following differences between the photoreactivities of cyclobutanone, (**CB**) and cyclohexanone, (**CH**) in condensed phases:

1. **CB** undergoes α-cleavage reactions mainly from the singlet *n*, π* excited state whereas **CH** cleaves exclusively from the triplet *n*, π* state.

2. The singlet *n*, π* of **CB** yields fragmentation (ketene and olefin), cyclization (oxacarbene), or decarbonylation (cyclopropane and CO) products, whereas the triplet of **CH** undergoes only disproportionation reactions.

3. The photochemical activity of **CB** persists even at very low temperatures (77 K), a condition under which **CH** is photostable.

Although the concept of "ring strain" may explain the faster rate of α-cleavage of cyclobutanone, this concept does not explain how the "memory" of ring strain can persist after the ring is cleaved to influence the formation of products.

The state correlation diagram (Salem diagram)[40] for α-cleavage of cyclobutanone (Fig. 13.1) is qualitatively equivalent to that for α-cleavage of acetone or cyclohexanone (Fig. 13.2), but is quantitatively different.[38] For acetone the pathway allowed by orbital symmetry (formation of linear acyl fragment) is thermochemically forbidden, i.e., the energy of the linear-acyl-radical pair is high relative to the energy of the initial n, π^* state. In cyclobutanone, however, the release of ring strain drops the energy of the bent and the linear diradical products by ~25 kcal/mole. As a result, the orbital symmetry-allowed pathway to the linear diradical product becomes thermochemically allowed, since the energy of n, π^* states is comparable for all cyclanones. The symmetry-imposed barrier remains for the bent acyl pathway.

The intriguing features of cyclobutanone photochemistry are explained by the Salem diagram given in Figure 13.1. The loss of CO from a bent acyl radical of

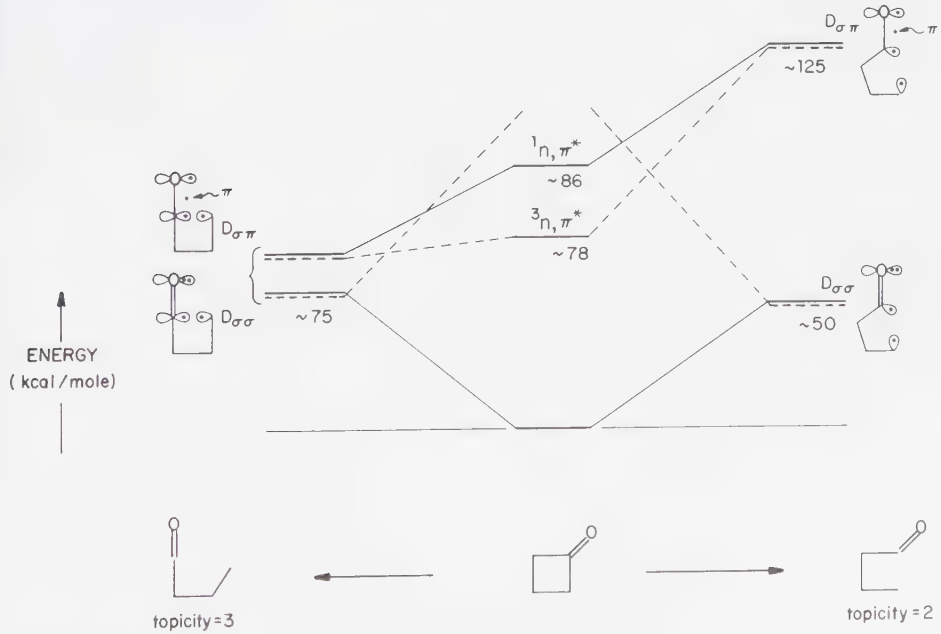

Figure 13.1
Surface correlation diagram for the symmetry-forbidden ditopic (right) and the symmetry-allowed tritopic (left) α-cleavage reactions of cyclobutanone.

the type $RCH_2\dot{C}O$ is known to require an activation energy of ~14 kcal/mole.[16,41] Since cyclobutanone undergoes photochemical loss of CO even at 77 K (conditions in which reactions having activation energies of greater than 2–3 kcal/mole are completely quenched), an equilibrated $\dot{C}H_2CH_2CH_2\dot{C}O$ radical (E_a for loss of CO expected to be ~14 kcal/mole, based on data for $RCH_2\dot{C}O$) cannot be involved in the decarbonylation.

From the Salem diagram, it can be seen that the linear pathway should be followed for cyclobutanone. From spectroscopic data for the $H\dot{C}O$ radical, the linear form is expected to be close to the transition state for thermal decarbonylation.[42] If the linear form is produced as predicted from the Salem diagram, it is formed in an electronically excited state, so that the reaction linear $\dot{C}H_2CH_2CH_2—\dot{C}{=}O \rightarrow \dot{C}H_2CH_2\dot{C}H_2 + CO$ is a photochemical primary process of the first excited state of the bent radical. The equilibrated linear radical thus corresponds to the thermally relaxed first excited state of the bent radical. The former will possess the same energy as the continuous vibrational levels that correspond to the products of decarbonylation. Thus, a radiationless transition will cause the linear acyl radical to fly apart to $\dot{C}H_2CH_2\dot{C}H_2 + CO$.

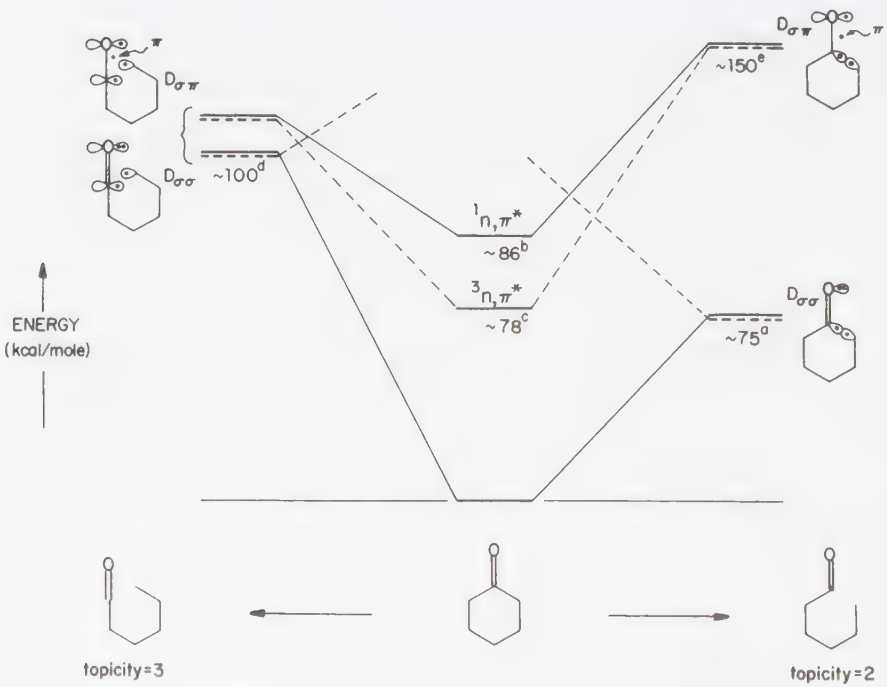

Figure 13.2

Surface correlation diagram for the symmetry "forbidden" ditopic (right) and the symmetry "allowed" tritopic (left) α-cleavage reactions of cyclohexanone.

It is important to note that the other common products of cyclobutanone photolysis (ketene/olefin and oxacarbene) may also be rationalized in terms of the linearization of the acyl radical during cleavage.

13.3 Sigmatropic Rearrangements of β,γ-Unsaturated Ketones Initiated by α-Cleavage

In contrast to the sigmatropic rearrangements of π, π^* states, which may be concerted if the number of electrons and the stereochemistry of the rearrangement conforms to the orbital symmetry rules, we expect sigmatropic shifts of n, π^* states to proceed directly to diradical intermediates. One of the most common examples of a sigmatropic shift from an n, π^* state is a [1,3] acyl shift, which occurs when β,γ-unsaturated carbonyls or aryl esters are photoexcited.[43]

From the chemical structure point of view these reactions are unified by a notion of a 1,3-migration (Eqs. 13.32 and 13.33). The reaction can be extended conceptually via the "vinylogous principle" to include [1,5], [1,7], [i, j = odd] shifts.

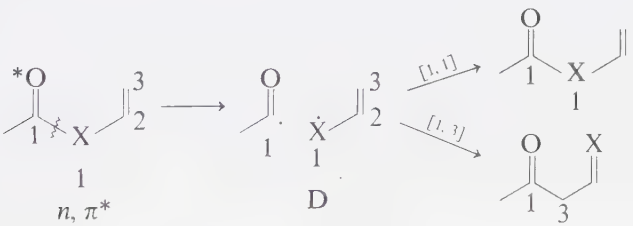

(13.32)

(13.33)

These reactions, which were discussed in Chapter 12 under sigmatropic rearrangement, are included in this chapter because of their mechanistic kinship to α-cleavage of saturated carbonyl compounds. Indeed, it seems that the primary photochemical process for both the n, π^* states of saturated ketones and the n, π^* states of β,γ-unsaturated ketones are of the same *genre*.

Examples of [1,3] Sigmatropic Shifts of β, γ-Unsaturated Carbonyl Compounds

If the n, π^* states of β,γ-unsaturated carbonyl compounds do indeed enter a primary process which is an α-cleavage followed by a [1,3] shift, then the reactions competing with rearrangement should be those expected of acyl: X–C–C radical pairs. This is indeed the case. For example, irradiation of **10** leads to **11**a via a [1,3] shift and to **11**b via a competing disproportionation, and irradiation

of **12** leads to **13** via a [1,3] shift and to radical coupling products.[44,45] The proportions of [1,3] and radical products are a sensitive function of structure.[45,46]

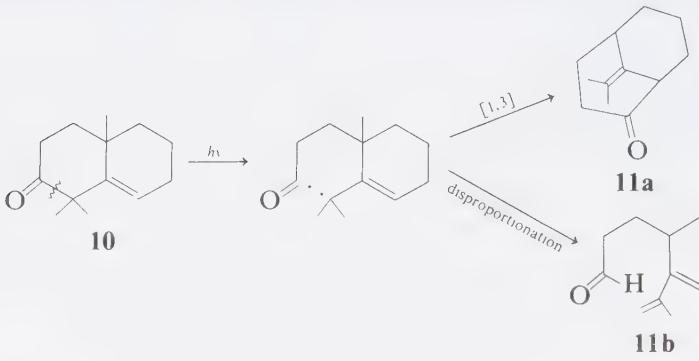

10 **11a** **11b** (13.34)[44] (13.35)

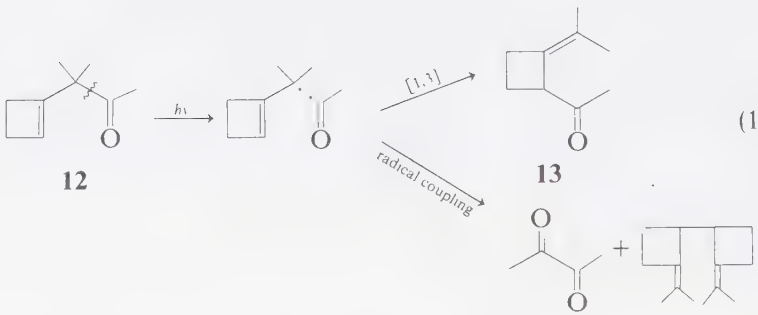

12 **13** (13.36)[45]

In addition to the competing reactions derived from α-cleavage, the [1,3] sigmatropic shift is sometimes accompanied by a [1,2] sigmatropic shift or oxy-di-π-methane rearrangement (Section 12.6). In general, the [1,2] shift is triplet sensitized whereas the [1,3] shift occurs upon direct excitation. From the standpoint of synthesis, this dichotomy is an excellent means of obtaining good yields of both [1,3] and [1,2] shift products from the same molecule. For example, direct excitation of **14** yields **15** in good yield, while triplet sensitized excitation of **14** yields **16** in good yield:

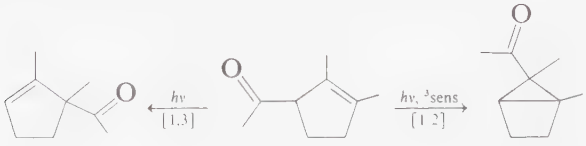

15 **14** **16** (13.37)[47]

The α-Cleavage Reactions of Esters and Amides; The Photo-Fries Rearrangement and Related Reactions[42]

A competition between [1,3] shift (the so-called photo-Fries reaction) and formation of products derived from homolytic α-cleavage and the [1,3] and [1,5]

photorearrangement of aryl esters and aromatic compounds of the general formula, **17**, of carboxylic acids and their derivatives is given by:[43b]

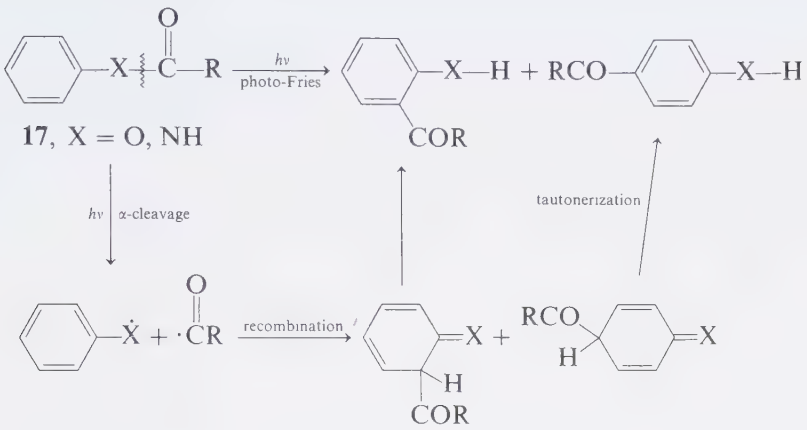

(13.38)

A radical mechanism has been confirmed in the case of the photo-Fries rearrangement (**17**, X = O). For example, PhȮ radicals and a transient cyclohexadienone have been detected by flash spectroscopy.[48] Products resulting from a shift to the meta position are rarely observed in the photo-Fries and related reactions.

A clever application of an intramolecular photo-Fries has been devised to generate paracyclophanes. In this case (Eq. 13.39), migration to the ortho position is "blocked" by a pair of methyl groups, thereby forcing exclusive rearrangement to the para position.[49]

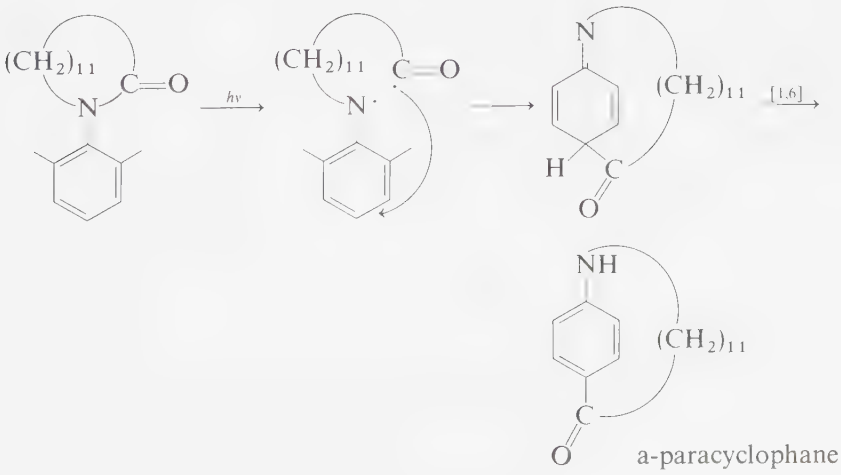

(13.39)

Decarboxylation of esters (the analogue of decarbonylation of ketones) may also occur.[50a] The OC —C, rather than the OC—O ester bond is α-cleaved:

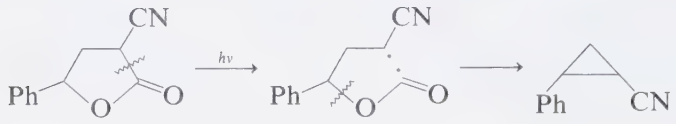

(13.40)

Mechanisms of [1,3] and [1,2] Sigmatropic Shifts of β,γ-Unsaturated Carbonyl Compounds

As a general rule, [1,3] shifts occur when β,γ-unsaturated carbonyl compounds are excited directly, whereas [1,2] shifts require photosensitized excitation.[43] In the case of the photo-Fries rearrangement the [1,3] shift is believed to occur from $S_1(n, \pi^*)$.[51,52] The major argument rests on an inverse correlation between fluorescence yields and yields of photo-Fries product.[48] In this case no [1,2] shift product is observed. It has been proposed that a general mechanism for the photo-Fries involves homolytic cleavage of the ArO-COR bond in $S_1(n, \pi^*)$ to form a singlet diradical pair which then undergoes the [1,3] shift or become free radicals by diffusion out of the solvent cage.[43]

The photolysis of **18** results in the observation of CIDNP. From the net polarization measurements, and from the ESR parameters for benzoyl radical and phenoxy radical, it was deduced that a singlet precursor radical pair is responsible for the CIDNP.[52] These observations confirm both the homolytic nature of the primary step in the photo-Fries and the probable singlet character of the excited state precursor to the radical pair.

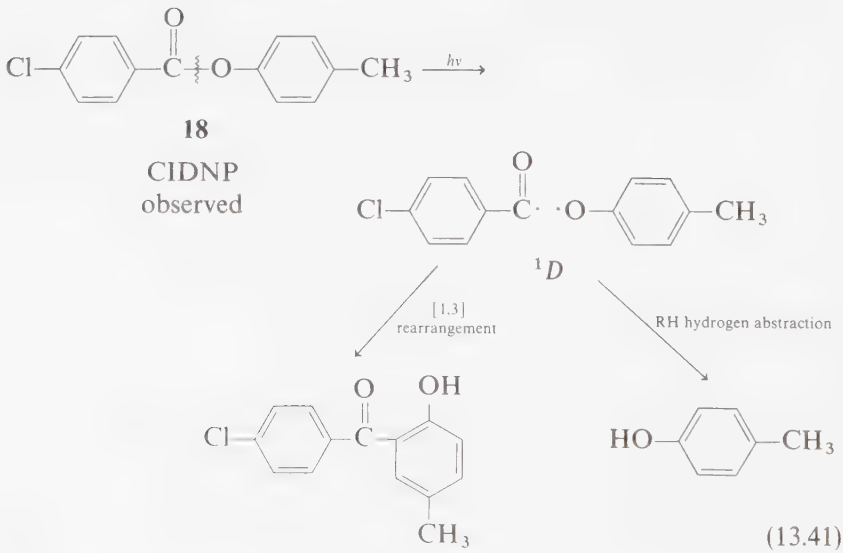

(13.41)

When viewed as the result of a primary α-cleavage, the [1,3] sigmatropic rearrangement of β, γ-unsaturated ketones could result from either an initial $S_1(n, \pi^*) \rightarrow {}^1D$ or a $T_2(n, \pi^*) \rightarrow {}^3D$ process. The possibilities are listed in Figure 13.3. The observations that the [1,3] shift generally (a) occurs via direct excitation, (b) does not occur via triplet sensitization, and (c) cannot be quenched by triplet-specific quenchers, have been used to support the $S_1(n, \pi^*) \rightarrow {}^1D \rightarrow [1,3]$ pathway. However, these observations would also be consistent with a $T_2(n, \pi^*) \rightarrow {}^3D \rightarrow [1,3]$ pathway *if* (a) the rate constant for $T_2 \rightarrow T_1$ internal conversion were slower than the $T_2 \rightarrow {}^3D$ process, (b) triplet sensitizers preferentially transferred to $T_1(\pi, \pi^*)$ rather than $T_2(n, \pi^*)$, and (c) T_2 were too short-lived to be quenched by triplet specific quenchers.[53] Further, the overall process ${}^3D \rightarrow [1,3]$ product must be fast enough to compete with loss of stereochemistry, since the rearrangement is generally stereospecific.

This rather extensive set of restrictions evidently can be satisfied in some cases. This conclusion is based on observations that fluorescence from $S_1(n, \pi^*)$ is observed from both β,γ-enones, which are reactive toward, and β,γ-unsaturated enones, which are unreactive toward [1,3] acyl shifts.[53,54] In fact, alkyl substitutions, which are expected to increase the rate of a $S_1(n, \pi^*) \rightarrow {}^1D$ process, sometimes *increase* the lifetime of $S_1(n, \pi^*)$, by slowing down $S_1(n, \pi^*) \rightarrow T$ intersystem crossing.[55]

Thus, the $S_1(n, \pi^*) \rightarrow T_2(n, \pi^*) \rightarrow {}^3D \rightarrow [1,3]$ pathway appears to be a viable one for at least some β,γ-unsaturated enones. The preferential sensitization of $T_1(\pi, \pi^*)$ can be explained as a kinetic effect, i.e., faster transfer to $T_1(\pi, \pi^*)$ which may result from a thermochemical barrier or electronic barrier to excitation of T_2 relative to T_1. In order to avoid efficient quenching, the lifetime of $T_2(n, \pi^*)$

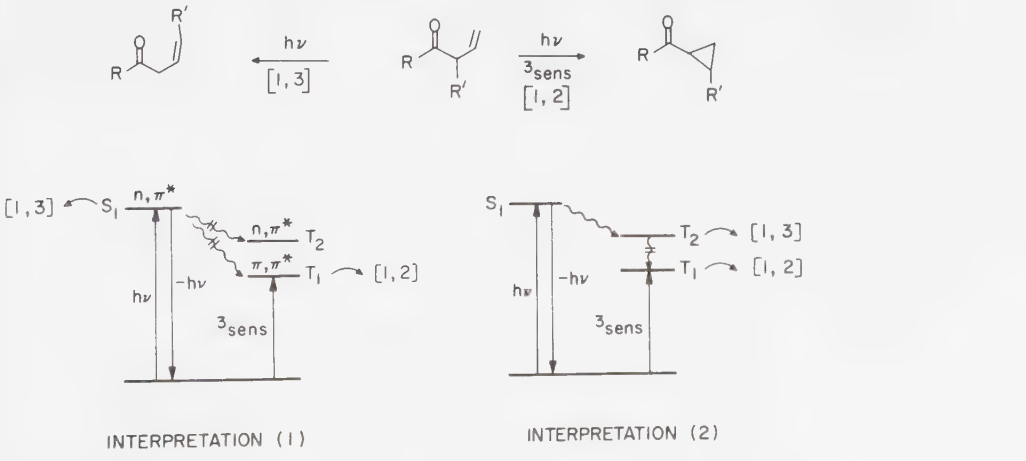

Figure 13.3

Two possible interpretations of the different behavior of β, γ-unsaturated carbonyl compounds under direct and triplet photosensitized excitation.

must be of the order of 10^{-10} sec or less, and the lifetime of T_2 must be determined by α-cleavage. Such a fast rate suggests a different cleavage pathway from that followed by aryl ketones (see Table 13.1).

13.4 Photoelimination Reactions of Azo Compounds

The lowest-energy electronic transition of many azo compounds, like that of many ketones, is characterized as being $n \rightarrow \pi^*$.[56] A reaction analogous to α-cleavage of the n, π^* states of ketones also occurs with azo compounds. However, there is a major difference in products derived from α-cleavage of carbonyl compounds and azo compounds. The dominant reaction from the diradical intermediate is usually the loss of a molecule of N_2 followed by reactions of the resulting radical pair, i.e., coupling and disproportionation.[57] In the case of acyclic azo compounds, the formation of free alkyl radicals generally competes with radical reactions in the solvent cage. It appears that the cleavage of the carbon-nitrogen bond occurs stepwise but that loss of N_2 from $R\dot{N}_2$ is fast relative to diffusion of $\dot{R}$ and $R\dot{N}_2$ out of the solvent cage.[58]

In general, the basis for the difference in products from α-cleavage of azo compounds relative to the α-cleavage of ketones derives from the greater exothermicity and associated lower activation energy of the $R{-}\dot{N}_2 \rightarrow \dot{R} + N_2$ process relative to the $R{-}\dot{C}O \rightarrow \dot{R} + CO$ process. Indeed, products derived from reaction of the $R{-}\dot{N}_2$ fragment are exceedingly rare, although evidence for the occurrence of a two-step elimination of nitrogen is available from CIDNP experiments[59] and labeling experiments.[58]

Examples of Elimination of Nitrogen from Cyclic Azo Alkanes

Qualitatively, acyclic and cyclic azo compounds behave similarly, since elimination of nitrogen is a general photochemical process for both classes of structures. Quantitatively, however, acyclic azo compounds may behave quite differently from cyclic azo compounds, and it is clear that these acyclic azo compounds possess mechanisms for the elimination of nitrogen which are not available to cyclic azo compounds. Photochemical elimination of N_2 from cyclic azo compounds produces 1,*n* diradicals. If *n* is 8 or less, the intramolecular reactions of disproportionation, cyclization, or fragmentation usually determine the product structure.

Of the three processes, disproportionation is not encountered as commonly as cyclization and cleavage in cyclic systems. The rarity of disproportionation products may be understood if singlet cis-1,*n* diradicals ($n \leq 6$) are produced by photolysis of cyclic azo compounds, since such radicals appear to react in their initial conformations, i.e., cleavage and or cyclization are faster than bond rotations (required for disproportionation) about the free radical termini.

Thus, the photochemical loss of N_2 from **19** or **20** (Eq. 13.42), yields cyclopropanes in a stereospecific reaction. In contrast, thermolyses of **19** and **20** result in nonstereospecific cyclizations.

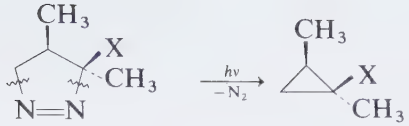

19 (X = CO_2CH_3) 70% (13.42)[60]

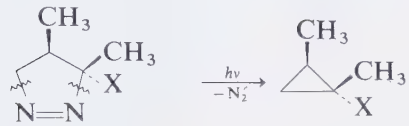

20 (X = CO_2CH_3) 75% (13.43)[60]

As another example, the photolysis of the cyclic azo compound **21** results in loss of N_2 and competing cyclization and cleavage of the presumed intermediate diradical:

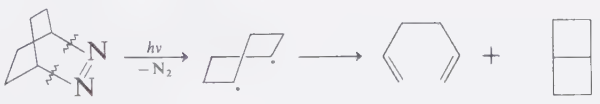

21 cleavage product cyclization product (13.44)[61]

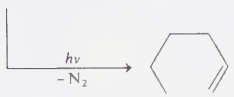

disproportionation, not formed

Of the two diradical reaction pathways, cyclization has found the greatest use in syntheses. In particular, photochemical extrusion of N_2 from cyclic azo com-compounds followed by cyclization has proven a valuable (but not universally reliable) method of synthesizing unusual small rings and polycyclic structures.[57] The formations of cyclopropanes (Eq. 13.45) and cyclobutanes (Eq. 13.46) are examples:

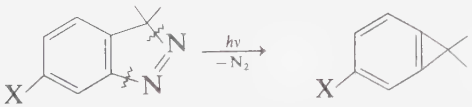

X = CO_2CH_3 Benzocyclopropane (13.45)[62]

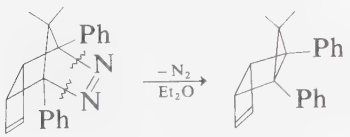

100% (13.46)[63]

As mentioned in Section 13.1, for certain compounds the photoelimination of N_2 occurs even at very low temperatures (e.g., 77 K). As a result, the diradicals produced from loss of N_2 can be matrix-isolated and detected spectroscopically, i.e., via ESR and optical spectroscopy.

For example, irradiation of the azo compound **22** (Eq. 13.47) at 77 K produces a diradical pair whose triplet ESR spectrum is readily observed:

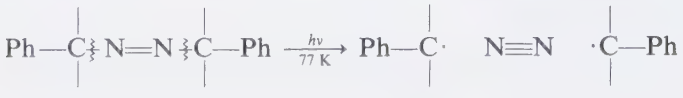

22 **23** ← ~6–7 Å →

Detected by ESR

(13.47)[64]

Recall that from the triplet ESR spectrum a "*D* parameter" (Section 8.11) allows a rough calculation of the "average" distance of separation *R* of two parallel electron spins. An approximate relationship between *D* and *R* is:[65]

$$D\,(\text{cm}^{-1}) \cong 10^{-24}\,R^{-3} \tag{13.48}$$

Photolysis of the azo compound **22** at 77 K in a rigid matrix produces a triplet ESR of the diradical pair produced by loss of N_2. The observed experimental value of $D = 0.011\ \text{cm}^{-1}$ for the diradical **23** allows a value of $R \cong 6 - 7 \times 10^{-8}$ cm = 6–7 Å to be calculated.

Photoelimination of N_2 has been employed to generate and matrix isolate the 1,3 and 1,4 and 1,5 diradicals **24**, **25**, and **26**. From the *D* for **24** ($D = 0.084\ \text{cm}^{-1}$)

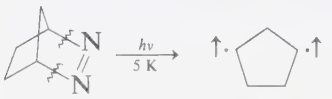

$D = 0.084\ \text{cm}^{-1}$
$R \sim 2$ Å

(13.49)[66]

24
1,3-Diradical

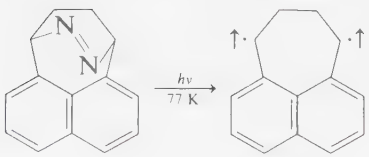

$D = 0.018\ \text{cm}^{-1}$
$R \sim 3$–4 Å

(13.50)[67]

25
1,4-Diradical

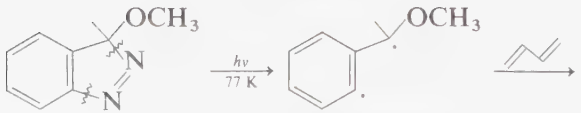

1,3-Diradical
(Trapped)

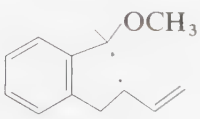

$D = 0.015\ \text{cm}^{-1}$
$R \sim 4$–5 Å

(13.51)[68]

26
1,5-Diradical

and for **26** ($D = 0.015\ cm^{-1}$), the average separation of electrons can be seen to be much larger for **26**. The unpaired spins (electrons) in **25** are both separated by a longer carbon chain and partially delocalized into the naphthalene ring.

The interesting diradical structure, trimethylenemethane has been prepared and matrix-isolated via photoextrusions of N_2 and CO at low temperatures (Eq. 13.7).[8,69] This species is predicted, from simple MO considerations, to possess an orbitally degenerate ground state and should therefore be a triplet, according to Hund's rule.[70] The trimethylene methane diradicals produced from photoextrusion of bicyclic azo compounds of the type **27** (Eq. 13.52) may be detected by their triplet ESR spectra (matrix isolation)[71] and by their *optical* spectra (absorption and emission).[72] Interestingly, the products isolated from photolysis of **27** are dimers of **28**, the intermediate trimethylene methane which may also be trapped by ethylenes (Eq. 13.53 and 13.54).[71]

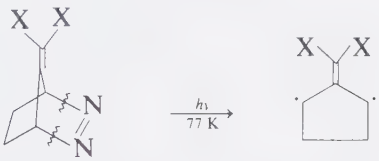

(13.52)[71]

27 (X = CH_3, Ph) **28** Detected by ESR, optical spectroscopy

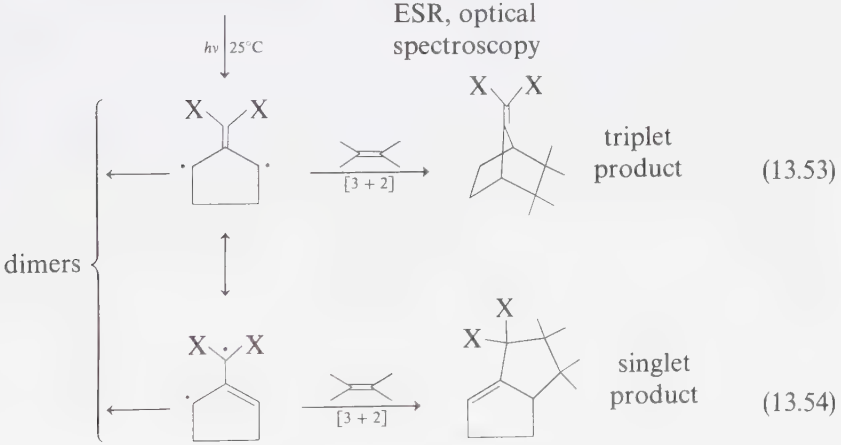

(13.53)

(13.54)

The Mechanisms of Photoextrusion of Nitrogen from Azo Compounds

It appears that for acyclic azo compounds, the elimination of nitrogen does not occur efficiently upon triplet sensitization.[73] A major reaction of some azo compounds which have been excited by triplet photosensitization is trans to cis isomerization:[74]

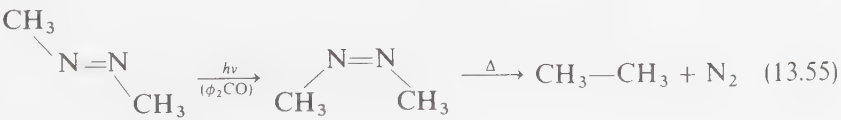

(13.55)

The cis isomer is often thermally unstable with respect to loss of N_2. This sequence (trans → cis → loss of N_2) is possibly the major pathway for elimination of nitrogen from acyclic azoalkanes under triplet photosensitization.

In the case of cyclic azo compounds the situation is different, in that for medium size rings (5, 6, and 7) the trans isomer is very strained and its formation rate is expected to be severely retarded. However, examples of the detection and isolation of a strained trans-cyclic sevenmembered azo compound have been reported[75] (see Section 12.2).

Acyclic azoalkanes are nonfluorescent and nonphosphorescent.[56,73] Although cyclic azoalkanes are nonphosphorescent, some are strongly fluorescent.[73]

Direct irradiation of the azo compound **29** yields the entire array of valence isomers of benzene, but triplet sensitization yields diazacyclooctatetraene as the major product:[76]

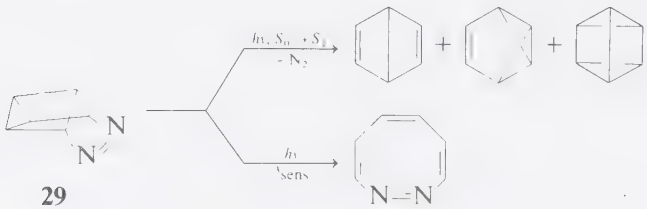

(13.56)

29 **30**

These results are consistent with the postulate that $S_1 \rightarrow T_1$ intersystem crossing is generally *inefficient* in cyclic azo compounds. The observation of different products upon direct excitation and triplet sensitization is termed the *spin-correlation effect*. Two interesting features of the photochemistry of **29** are the observations that (a) at low temperatures, **30** becomes the exclusive product of direct $S_0 \rightarrow S_1$ irradiation, and (b) oxygen appears to enhance the formation of **30** in the direct $S_0 \rightarrow S_1$ excitation of **29**. The loss of N_2 occurs from $S_1(n, \pi^*)$ in competition with intersystem crossing to $T_1(n, \pi^*)$. Rearrangement to **30** occurs from $T_1(n, \pi^*)$. The α-cleavage which occurs from S_1 requires an activation energy of ~ 5–6 kcal mole, whereas the rate of intersystem crossing to T_1 is temperature-independent.[68] Thus, at low temperature, S_1 undergoes exclusive intersystem crossing and is the only product. That **30** is a product of T_1 is convincingly demonstrated by the observation that direct $S_0 \rightarrow T_1$ excitation leads to formation of **30** at room temperature. The photochemical parameters for **29** are summarized in Figure 13.4. Finally, in the presence of oxygen, the $S_1 \rightarrow T_1$ process is catalyzed by a $S_1 + O_2 \rightarrow T_1 + O_2$ mechanism and again **30** becomes the major product.

A nice example of spin correlation effects[77] on product distributions is found in the photochemical loss of N_2 from **31** (Eq. 13.57). Although nitrogen is lost via both direct and sensitized excitation, the yields of the hydrocarbon products vary considerably, depending on the mode of excitation. It appears that the triplet diradical shows a strong tendency to undergo a di-π-methane-like rearrangement. Apparently, the same diradical is achieved by photosensitization of both **31** and barrelene **32**.[78]

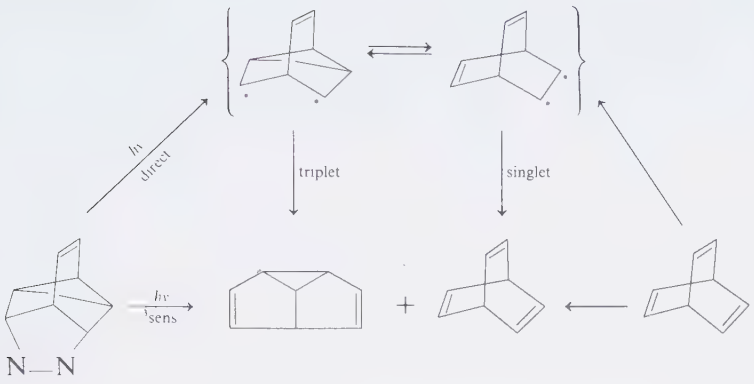

(13.57)

31 **32**

	Semibullvalene	Barrelene	
	100%	0%	← ³sens
hν →	25%	75%	
³sens →	100%	0%	
Δ →	0%	100%	

It is evident that the loss of nitrogen can produce highly strained compounds even when less strained compounds are possible, as in the formation of quadricyclane as the major product from triplet sensitized photoextrusion from azo compounds (**33**a and **33**b). Thermolysis and singlet state reactions of **33**a and **33**b yield norbornadiene as the major product (for a more detailed discussion of this

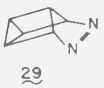

29

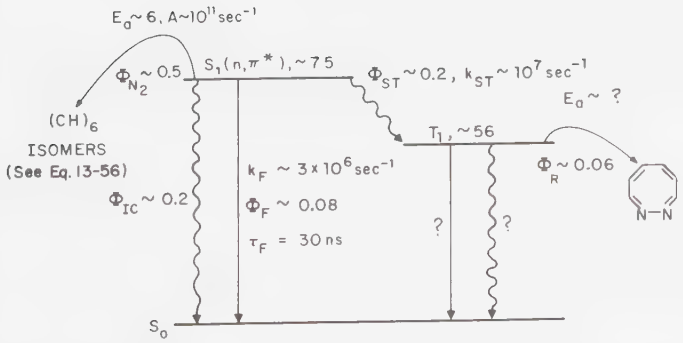

Figure 13.4

Energy diagram summarizing the photochemical parameters for azoalkane **29**.

reaction see Section 11.2):

33a Quadricyclane **33b** (13.58)[59]

The timing of the breaking of the C—N bonds in photoextrusion of nitrogen from azoalkanes has not been established: i.e., it is not known whether the C—N bonds break concertedly or sequentially. It appears that any R—N = N intermediate must undergo "very rapid" loss of N_2. However, in the case of aryl alkyl azocompounds, the alkyl-N bond breaks first and is followed by slower cleavage of the aryl-N bond. The evidence for this conclusion is: (a) photolysis of optically active **34** results in racemization concomitantly with photoextrusion of N_2;[80] (b) CIDNP is observed during photolysis of aryl alkyl azocompounds:[81]

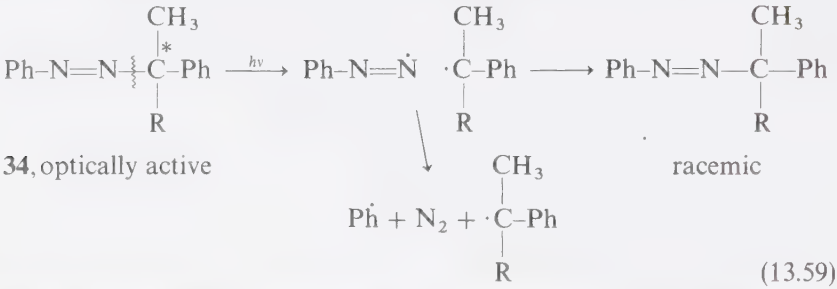

34, optically active racemic (13.59)

A spectacular application of photoextrusion of N_2 is found in the photolysis of dimethyl-s-tetrazine (Eq. 13.60) for which it was shown that *the relative chemical reactivity of triplet sublevels* (T_x, T_y, T_z) *are different*.[82] Photolysis was conducted at 4 K, so that no thermal equilibration of T_x, T_y, and T_z was possible. By using an oriented (crystal) sample, in a high magnetic field, it was possible to excite and to maintain one of the three triplet sublevels. Measurement of the triplet lifetime and analysis of the lifetime as a function of orientation allowed the conclusion that T_x undergoes photolysis more slowly than T_y and T_z.

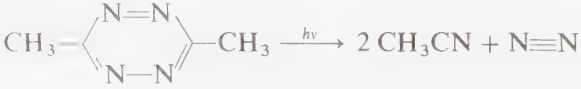

(13.60)

13.5 Photoelimination of Nitrogen from Diazocompounds, Azides, and Related Compounds

The most characteristic photoreaction of diazocompounds and azides is photoelimination of a molecule of N_2 followed by reaction of the resulting *carbene* or *nitrene*.

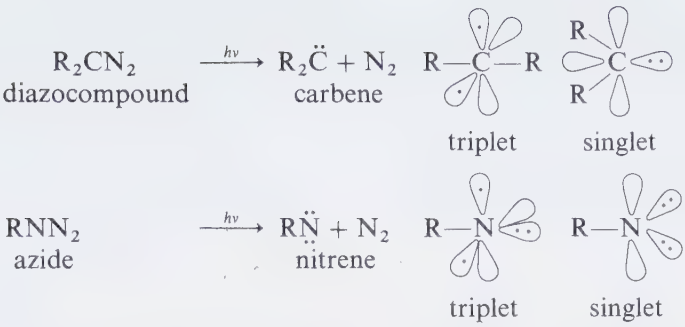

The photochemistry of both diazocompounds and azides are nicely parallel, as are the chemistries of carbenes[83] and nitrenes.[84] From an analysis of the photochemistry of diazo compounds and the reactions of carbenes we may infer the photochemistry of azides and reactions of nitrenes by the use of the *isoelectronic analogy principle*, i.e., since carbenes and nitrenes are isoelectronic species (six valence electrons) their chemistries are expected to be qualitatively similar.

Photochemistry of Diazocompounds and Azides: Carbenes and Nitrenes

In order to understand the photochemistry of diazocompounds, one must understand the chemistry of carbenes, because the most characteristic photoreaction of diazocompounds is loss of nitrogen to form carbenes. Use of the Wigner spin rule (spin conservation in an elemental chemical step) suggests that the following pattern should occur:

$$\begin{aligned} \text{Diazocompound} &\rightarrow \text{carbene} + N_2 \\ S_1 &\rightarrow \text{singlet carbene} \\ T_1 &\rightarrow \text{triplet carbene} \\ S_0 &\rightarrow \text{singlet carbene} \end{aligned} \tag{13.62}$$

An interesting and important general feature of carbenes is the occurrence of two energetically proximate states, a singlet and a triplet state. Let us consider methylene as a prototype for analysis of the electronic structure and chemical reactions of carbenes.[85]

In the extreme cases of sp^2 and sp hybridization of the carbene carbon atom, we predict that the bent form of CH_2 will be a singlet because its orbital occupancy will be $(sp^2)^2$ whereas the orbital occupany for the linear form of CH_2 will be triplet $(p_x)^1(p_z)^1$. For a nitrene, the nuclear shape will be the same, linear for the singlet and triplet, but the orbital configuration will be different, i.e., singlet = $(sp^2)^4(p_z)^0$; triplet = $(sp)^2(p_x)^1(p_z)^1$.

As was the case for 1, *n* diradicals (Eqs. 13.49–13.52), parameters available from ESR spectroscopy (Eq. 13.48) provide a means of evaluating the average distance between the triplet electrons of triplet carbenes and nitrenes. The *D* parameter of triplet ESR provides a measure of the interaction energy of two magnetic dipoles.[86]

On the average, the closer the two dipoles, the larger the value of D. Thus, the D-value for naphthalene is $\sim 0.1\ cm^{-1}$ ($\sim 3 \times 10^{-4}$ kcal/mole); for a nitrene it is $\sim 1.6\ cm^{-1}$ ($\sim 4.5 \times 10^{-3}$ kcal/mole); and for a carbene it is $\sim 0.8\ cm^{-1}$ ($\sim 2.2 \times 10^{-3}$ kcal/mole):

$r \sim 2$Å	$r \sim 1$Å	$r \sim 1$Å
$D \sim 0.1\ cm^{-1}$	$D \sim 0.8\ cm^{-1}$	$D \sim 1.6\ cm^{-1}$
Organic triplet	carbene	nitrene

Mechanisms and Expected Reactions from Photolysis of Diazocompounds and Azides

The typical reactions of singlet carbenes and nitrenes are zwitterionic, whereas the triplet reactions of triplet carbenes are diradicaloid. Thus, in discussing reactions of these species we may employ the resonance structures **35** and **36** as a guide to reactivity and reaction type.

$$\underset{\textbf{35}\text{ singlet}}{R_2C\!\uparrow\!\downarrow} \equiv \underset{\text{zwitterionic}}{R_2\overset{\oplus}{C}\!:\!\ominus} \qquad \underset{\textbf{36}\text{ triplet}}{R_2\overset{\uparrow}{C}\!\uparrow} \equiv \underset{\text{diradicaloid}}{R_2\dot{C}\cdot} \tag{13.63}$$

For example, singlet diphenyl carbene behaves like an electrophile in its reaction with isopropanol in an electron pair (zwitterion) reaction, while triplet diphenyl diazomethane behaves like a diradical in a single electron reaction.[87]

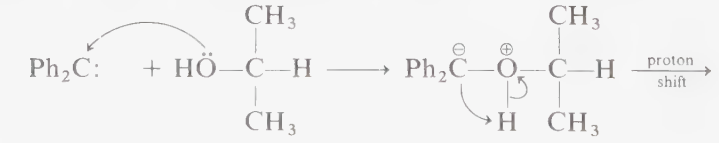

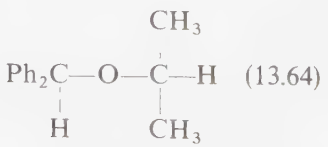

(13.64)

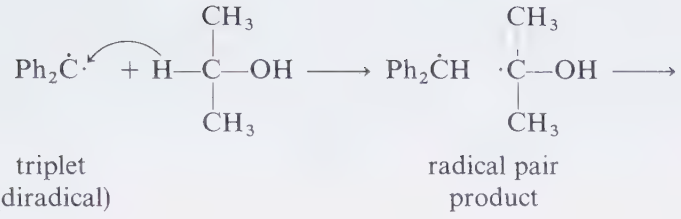

triplet (diradical) — radical pair product

$$Ph_2CH_2 + (CH_3)_2C{=}O \quad (13.65)$$

isolated products

Similarly, the reactions of singlet and triplet nitrenes are expected to be those derived from structures **37** and **38**.

$$\underset{\textbf{37}\text{ singlet}}{R{-}N\!\uparrow\!\downarrow} \equiv \underset{\substack{\text{zwitterionic}\\ \text{a two-electron}\\ \text{reagent}}}{R{-}\overset{\oplus}{N}{:}^{\ominus}} \qquad \underset{\textbf{38}\text{ triplet}}{R{-}\overset{\uparrow}{N}\!\uparrow} \equiv \underset{\substack{\text{diradical}\\ \text{a one-electron}\\ \text{reagent}}}{R{-}\dot{N}\cdot} \quad (13.66)$$

The typical reactions of singlet carbenes are:

1. 1,2 sigmatropic shifts to yield an ethylene
2. Stereospecific insertion into sigma bonds
3. Stereospecific insertion into pi bonds
4. Addition of a nucleophile or (less commonly) an electrophile.

The typical reactions of triplet carbenes are:

1. Atom abstraction reactions to produce radicals
2. Nonstereospecific additions to pi bonds
3. Addition of radicals or radical-like substrates.

Two methods are available to specifically induce reactions of triplet carbenes: (a) use of an inert diluent (or one which promotes singlet-triplet conversion) which allows the singlet carbene to relax to the ground state triplet carbene, and (b) use of a triplet sensitizer to form a triplet precursor which, because of Wigner's spin rule, specifically produces the triplet carbene.[88] The latter method suffers from the restriction that chemical sensitization must be carefully excluded, i.e., the "triplet" sensitizer cannot initiate chemical reactions which then cause carbene-like reactions to occur.

The different chemistries of singlet and triplet carbenes lead to spin correlation effects, as were found for azocompounds. For example, direct irradiation of diazomethane in the presence of cis or trans-2-butene results in stereospecific insertion of $CH_2(\uparrow\downarrow)$, whereas benzophenone-sensitized decomposition of diazomethane leads to nonstereospecific addition of $CH_2(\uparrow\uparrow)$:[88]

(13.67)

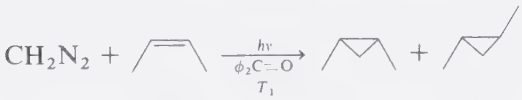

(13.68)

Recall that when radical intermediates are present along reaction pathways, enhanced absorption or emission is observed in the NMR spectra of products (CIDNP). When diazomethane is irradiated in toluene, ethyl benzene is a major product but no CIDNP spectrum of this molecule is observed.[89] The triplet photosensitized decomposition of diazo methane in toluene results in a strong CIDNP spectrum of ethyl benzene. These results are consistent with the formation of ethyl benzene by concerted insertion of singlet CH_2 into a CH-bond in the direct photolysis, and a hydrogen abstraction by triplet CH_2 in the photosensitized case:

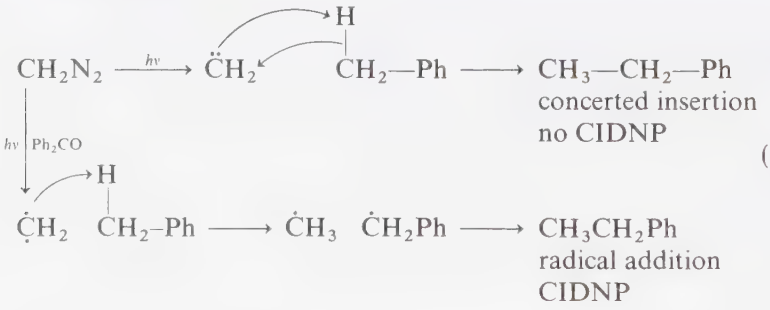

(13.69)

Irradiation of diazoacetophenone **39** in alcohol results in formation of the rearranged ester **40** as the major product. Triplet-sensitized decomposition results in formation of acetophenone as the major product:[90]

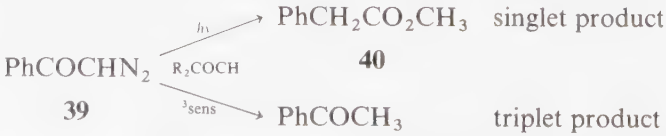

(13.70)

The direct excitation of diazoketones produces a singlet ketocarbene which undergoes a [1,2] rearrangement to a ketene (Wolff rearrangement). The loss of N_2 might be concerted with rearrangement in some cases. The ketene is then attacked by alcohol to form the observed product.[91]

Triplet-sensitized excitation of diazoketones produces a triplet carbene, which cannot undergo rearrangement to the ketene without violation of the Wigner spin

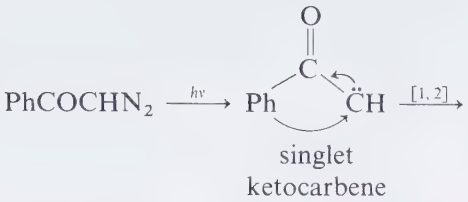

(13.71)

rule. Instead, the triplet carbene abstracts hydrogen atoms from the alcohol solvent to yield ketones (or radical derived products).[90]

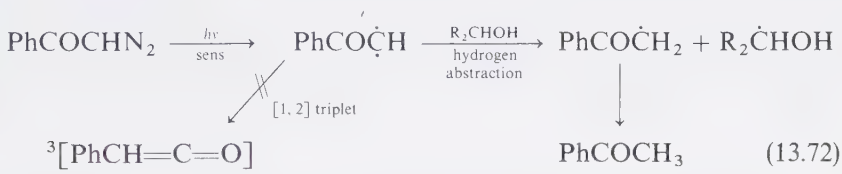

(13.72)

The photolyses of diazocompounds and azides has been used successfully to achieve numerous syntheses that would have been difficult to achieve by conventional thermal methods.[92] For example, the polycyclic ketone **42** is formed upon photolysis of the diazo compound **41**:

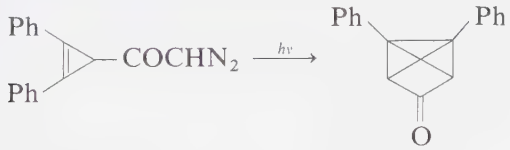

carbene insertion into C=C (13.73)

41 **42**

The photo Wolff rearrangement has been employed successfully to "shrink" rings. A particularly interesting application of this reaction is given by the formation of the propellane **44**, a molecule possessing two carbon atoms whose valences are severely distorted.[93]

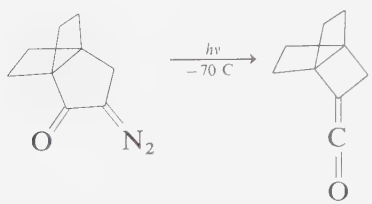

carbene → ketene rearrangement (13.74)

43 **44**

Penicillin precursors and derivatives (β-lactams) have been prepared via cyclization of the carbene produced from photolysis of appropriate α-keto diazo

compounds:[94]

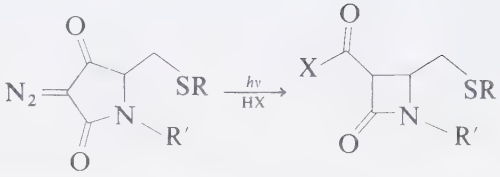

(13.75)

In some circumstances the direct photolysis of α-diazo ketones may lead to an oxiirene intermediate (**45**). Ring opening of the oxiirene is then followed by rearrangement to ketenes or other 1,2 shifts:[95]

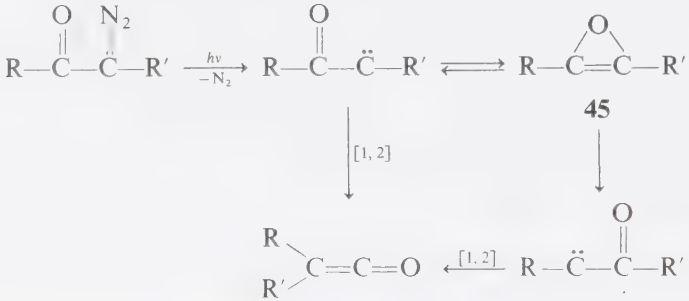

(13.76)

Flash spectroscopic studies of diaryl carbenes have revealed that the dimerization of carbenes occurs at close to the diffusion controlled rate,[96] i.e., for diphenyl carbene, the rate constant for dimerization is 5×10^9 M^{-1} sec^{-1} in benzene at room temperature. Addition reactions of diphenyl carbene are considerably slower, i.e., for addition to 1,3-butadiene and to styrene, the rate constants are 6×10^5 M^{-1} sec^{-1} and 4×10^5 M^{-1} sec^{-1}, respectively.

The formation of and reactions of nitrenes from azides parallel the formation of and reactions of carbenes from diazocompounds.[97] Thus, one need only replace the CR group in R′CR with an isoelectronic N atom and the expected chemistry of RN species is evident:

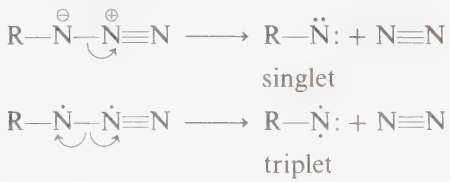

(13.77)

Some examples of synthetic uses of the photoextrusion of N_2 from azides are:

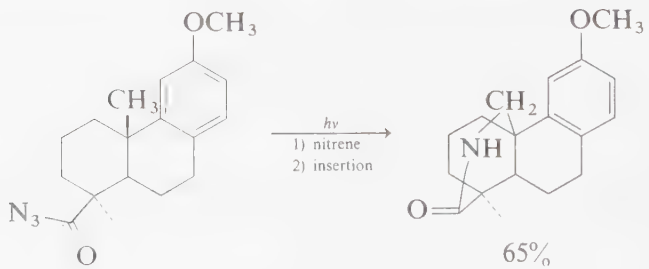

(13.78)[98]

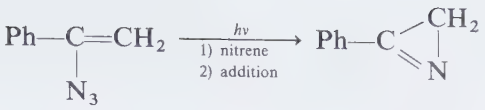

93%

(13.79)[99]

13.6 Photochemical Cleavage of Small Rings

The strain energy locked into small rings may be released by ring opening. This provides a powerful thermodynamic driving force for energy release. Photochemical excitation can initiate the cleavage of small rings if an electronically excited chromophore is contained by the ring or if an excited chromophore nearby overlaps properly with the bonds of the strained ring. For example, the cleavage of three-membered rings is quite commonly observed. The cleavage may be zwitterionic, i.e., $^1(\pi, \pi)^*$, or diradical i.e., (n, π^*) or $^3(\pi, \pi^*)$, in nature.

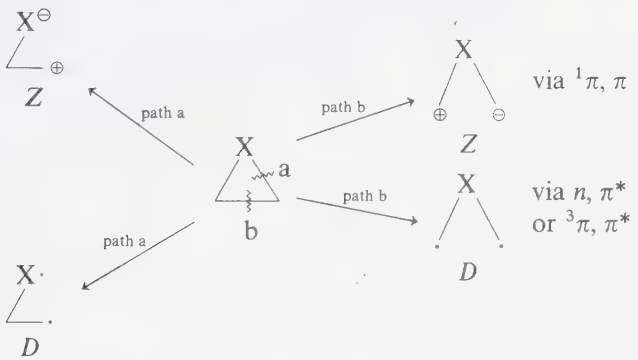

(13.80)

The typical reactions of the *D* and *Z* intermediates produced from photofragmentation of small rings are: (a) a second bond fragmentation, (b) rearrangements, and (c) reclosure of the ring. Bimolecular reactions of the *D* and *Z* intermediates are known but can rarely compete with unimolecular processes (a), (b), and (c).

Homolytic α-cleavage of Cyclopropyl and Epoxyketones

The n, π^* states of conjugated cyclopropyl and epoxyketones commonly undergo homolytic cleavage of a β-bond.[100] This reaction, in contrast to α-cleavage, appears to be initiated by overlap of the π^* orbital with the σ^* orbital associated with the bond undergoing rupture (Fig. 13.5). In general, if two β-bonds are potentially available for cleavage, the bond capable of best overlap with the π^* orbital is cleaved preferentially.[101]

For example, irradiation of **46** yields **47** (Eq. 13.81). Models indicate that in the favored chair conformation in its ground state, the π^* orbit of the n, π^* state overlaps best with the C_1C_7 bond. This is, in fact, the bond that generally breaks.[101]

Structural factors can, however, cause cleavage of the internal bond to be favored. For example, bicyclo-[3.1.0]-hexanones (Section 12.6, Eq. 12.88) undergo photo-β-cleavage of the "internal" cyclopropane bond to yield zwitterionic species.[102]

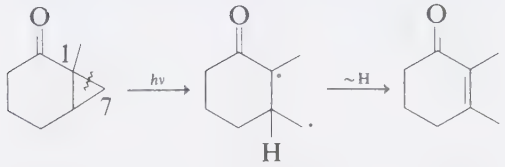

(13.81)

46 **47**

Conjugated cyclopropenyl ketones are occasionally found to undergo photo-β-cleavage. The initial diradical produced is electronically related to a carbene. For example, photolysis of **48**(R = H) in methanol yields the solvent adduct **49** possibly via the sequence shown.[103]

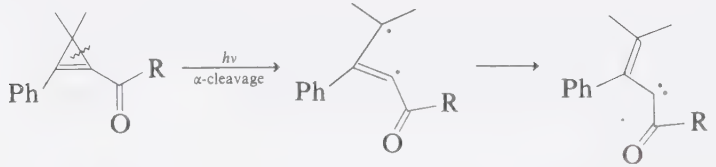

48 ^1D singlet carbene

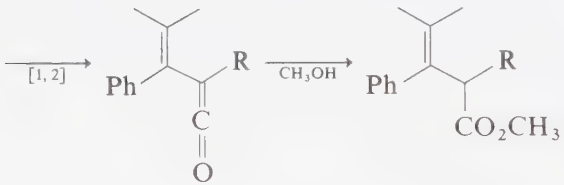

(13.82)

49

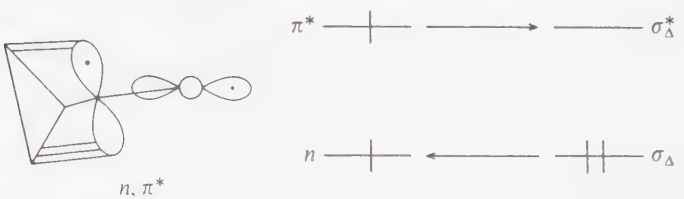

Figure 13.5

Orbital interactions for the β-cleavage of cyclopropyl ketones. Overlap of the π^* orbital and the σ^* (cyclopropane) orbital dominates.

If the π^* orbital indeed assists in cleaving the β-bond of cyclopropanes, cleavage of epoxides should also occur and more easily, since the σ^* epoxide orbital is lower in energy than the corresponding cyclopropyl orbital. Indeed, homolytic cleavage of the β-CO bond of epoxides generally occurs more efficiently than cleavage of the β-CC bond.[104] The reaction products are usually derived from a 1,2 shift to yield a 1,3-diketone, **51**:[105]

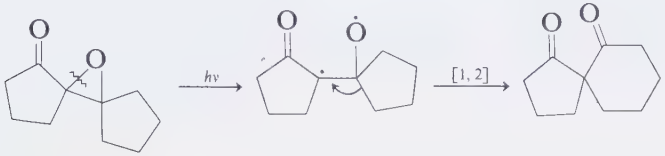

(13.83)

50 **51**

In analogy to the epimerization of cyclic ketones via α-cleavage (Eq. 13.23), epoxyketones may be photoepimerized, presumably via reversible β-cleavage:[106]

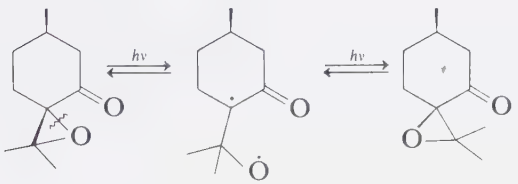

(13.84)

52

In analogy to the "internal" α-cleavage that may occur in the photolysis of bicyclo-[3.1.0]-hexenones, the analogous epoxide (**53**) ring opening to produce a zwitterion (**54**) is known to occur. In this case, the ring open species is detectable spectroscopically and may be trapped chemically:[107]

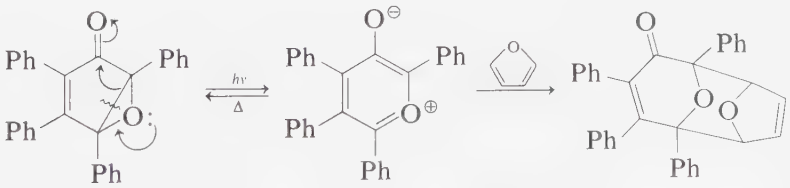

53 **54** (13.85)

β-Elimination of Substituents: Zwitterionic β-Cleavage

Outside of the β-cleavage reactions of small rings, only few examples of the cleavage of other groups are known. Among the better documented examples are the photoinduced β-eliminations of a sulphonyloxy group[108] and of acetoxy groups:[109]

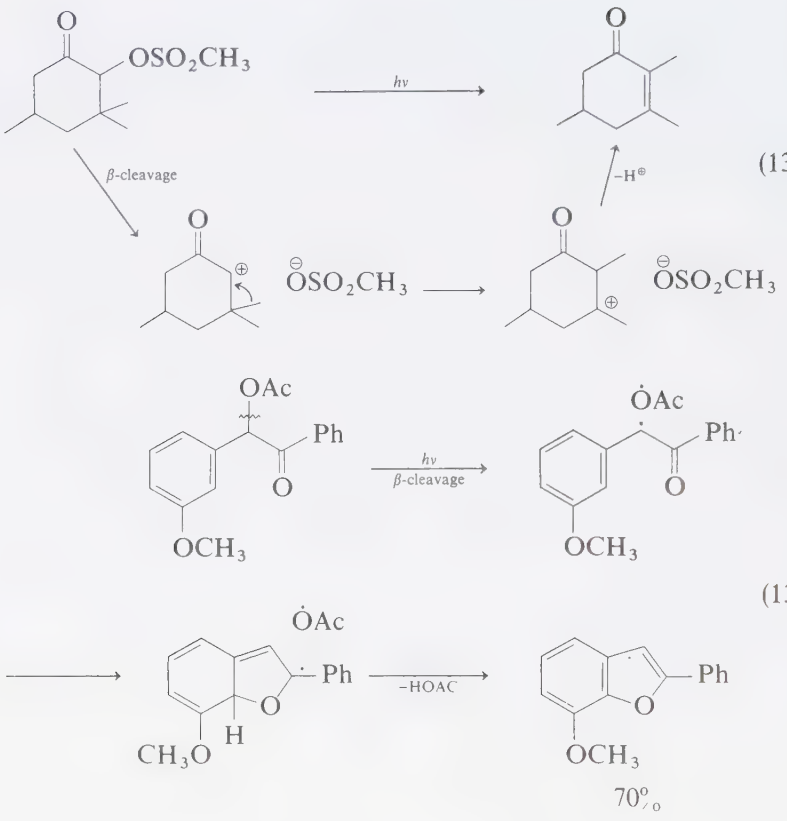

(13.86)

(13.87)

Some photoreactions of α-halocyclic ketones may also be initiated by β-cleavage:[110]

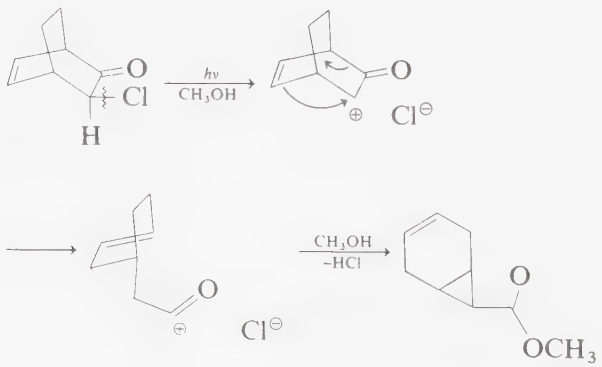

(13.88)

The mechanisms shown in Eqs. 13.85–13.87 are speculative and require experimental support before they can be considered as valid.

Ring-Opening Reactions of Azirines

Direct photoexcitation of azirines results in ring cleavage to produce a 1,3-dipolar zwitterionic species (nitrile ylides), which may be trapped intra- or intermolecularly by a variety of dipolarophiles.[111] The ring opening is formally a [3] four electron electrocyclic process and therefore might be viewed as a concerted photoreaction. However, the initial singlet state for this reaction is generally n, π^* so that ring opening from S_1 must produce an initial D state. This situation is reminiscent of the bent-linear dichotomy of α-cleavage of ketones, except that in this case (a) the linear form is more stable in general than the bent form, and (b) the linear form is more stable as a zwitterion than a diradical.[112]

The n, π^* excitation plays a similar role in the α-cleavage of azirines as it does for ketones. The n electron (originally localized on nitrogen and in the plane of the molecule) becomes dispersed over carbon and nitrogen when it is excited into the π^* orbital, which is located above and below the molecular plane. Consequently, the nitrogen atom becomes electrophilic and is on its way to resembling an aziridinyl cation. The half-filled n orbital (in the molecular plane) will now suck electron density from the C—C bond via overlap with the back lobe of the saturated carbon atom. Cleavage is then facilitated and a diradical is produced. The detailed electronic pathway depends on whether the ring opening occurs with or without linearization. If the bent form is produced (by surmounting an energy barrier) then a bent D intermediate is formed. Simple linearization of this species will produce the lowest-energy diradicaloid, i.e., the linear 1,3-dipolar zwitterion. If linearization occurs along with ring opening, the lowest excited state of Z is produced. Internal conversion or intersystem crossing then leads to Z.

For example, irradiation of the azirene **55** (Eq. 13.89) in the presence of dimethyl fumarate (trans, X = CO_2CH_3) or dimethyl maleate (cis, X = CO_2CH_3) results in stereospecific [3 + 2] cycloaddition. In the absence of a dipolarophile, dimers such as **56** and **57** are obtained,[111] These reactions are not inhibited by standard triplet quenchers, nor are they initiated by standard triplet sensitizers. Thus, they appear to be initiated from $S_1(n, \pi^*)$ states.

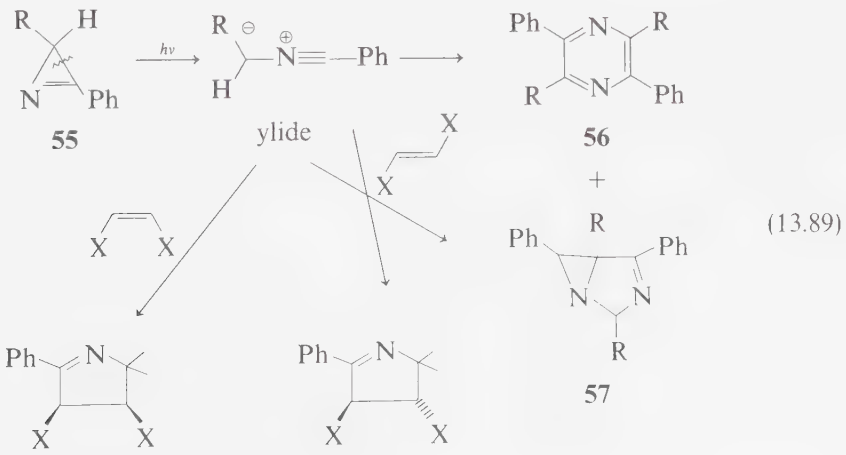

(13.89)

The fragmentation-cycloaddition reactions of azirenes (e.g., **58**) occurs with a wide variety of electron-deficient acceptors and is a synthetically useful reaction for preparation of heterocycles. Even CO_2 is effective, with which oxazolinones **59** are formed:

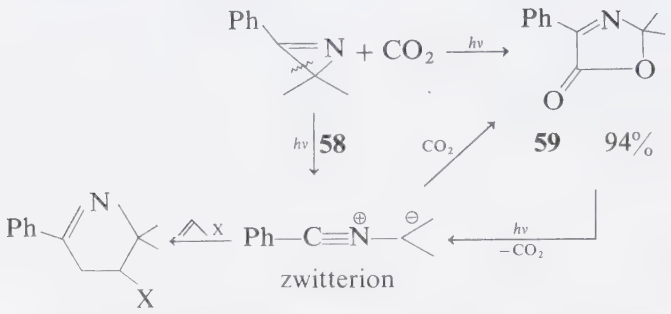

The latter undergo photoextrusion of CO_2 to yield the same nitrile ylide as does photolysis of **58**.

Irradiation of a number of arylazirines in a rigid matrix at −185 C produces an intermediate believed to be the nitrile ylide:[114]

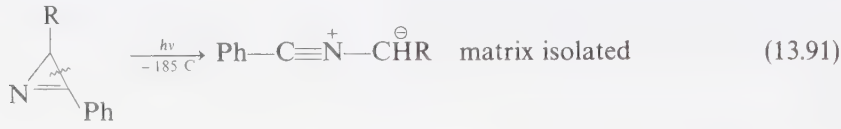

Interestingly, the nitrile ylide undergoes photochemical (electrocyclic) closure to regenerate the azirine, but does not undergo thermal reversion to the azirine.

The photocleavages of small ring compounds appear to singlet reactions. It is not known whether $S_1 \rightarrow {}^1D \rightarrow Z$ or $S_1 \rightarrow Z$ pathways are involved.[112]

Pericyclic Fragmentation Reactions

Pericyclic reactions which result in a net fragmentation may be classified as ring-opening (electrocyclic) and ring-fragmenting (retrocycloadditions). When a single atom component of a ring is extruded, the term *cheleotropic fragmentation* is applied.

Pericyclic fragmentation reactions which are initiated by n, π^* states can be viewed as examples of a $n, \pi^* \rightarrow D$ process, followed by diversion of the diradical to a pericyclic reaction. For example, the ring opening reactions of 2,4-cyclohexadienones proceed from n, π^* singlet states. Although the reaction is formally an electrocyclic ring opening, the mechanism (Section 12.6) is probably α-cleavage to yield a diradical which then rearranges to the ketene product.

In contrast to the [1,2] shifts common to the photochemistry of 4,4-disubstituted cyclohexenones, 4,4-disubstituted cyclopentenones undergo pericyclic fragmenta-

tion rearrangement. For example, irradiation of **60** yields **61** (Eq. 13.89):

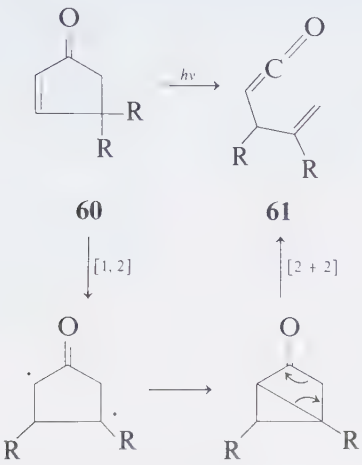

(13.92)[115]

A plausible mechanism for such fragmentation rearrangements involves an initial [1,2] shift to generate a 1,4-diradical, which then cyclizes to a cyclobutanone (detectable by low-temperature IR). The latter then undergoes a retro [2 + 2] cycloaddition to yield a ketene.

Ketenes are also produced in the photolysis of bicyclic dienones. The mechanism of reaction is not established.

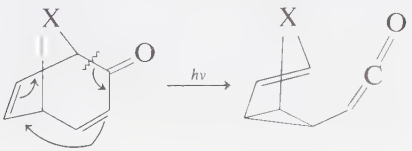

(13.93)[116]

Photoretrocycloaddition Reactions of Small Rings

Four-electron cycloadditions and retrocycloadditions can be allowed to occur in a concerted manner via photoexcitation.[117] Two of the most common types of retrocycloadditions are $[3 \rightarrow 2 + 1]$ and $[4 \rightarrow 2 + 2]$ reactions.

A wide variety of three-membered ring compounds undergo photochemical $[3 \rightarrow 2 + 1]$ retrocycloadditions or cycloeliminations which yield carbenes or nitrenes. In some cases, the yields are excellent. For example, irradiation of either the cyclopropane **62** or the oxirane **63** yields diphenyl carbene.[100,118] The latter has been characterized by chemical trapping and by direct spectroscopic identification:[118]

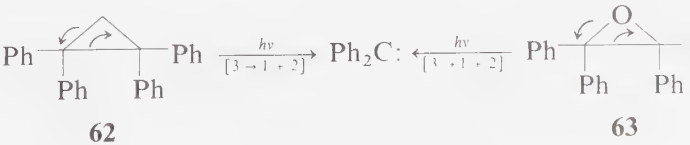

62 63

(13.94)

Photolysis of cyclobutanes and cyclobutenes causes [4 → 2 + 2] retrocycloadditions. For example, photoexcitation of cyclobutene **64** yields **65** and **66** and photoexcitation of **67** yields **68**, both via [4 → 2 + 2] retrocycloadditions:[119]

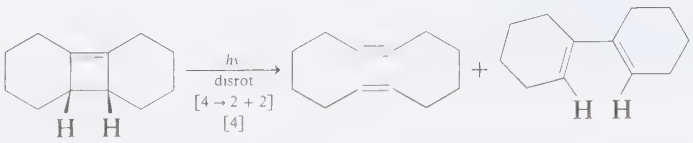

64 **65** (25%) **66**

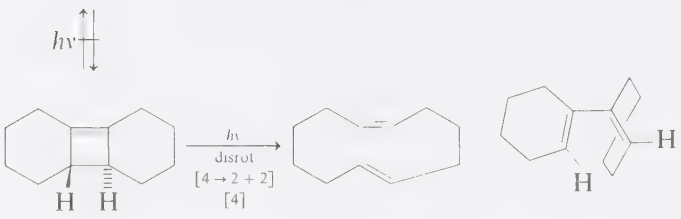

67 **68** (40%) **69** (not formed)

(13.95)

It is interesting that in the case of **64**, the allowed disrotatory [4] electrocyclic ring opening competes with the [4 → 2 + 2] retrocycloaddition to **65**, but for **67** no [4] electrocyclic ring opening is observed. This can be understood in terms of the requirement that the *allowed* [4] ring opening is disrotatory and would produce a *trans*-cyclohexene (**69**). Such a species is too energetic to be produced in competition with the allowed [4 → 2 + 2] retrocycloaddition to **68**.

The photo [4 → 2 + 2] retrocycloaddition reaction has been used to release simple pentalenes from their dimers (Eq. 13.96):[120]

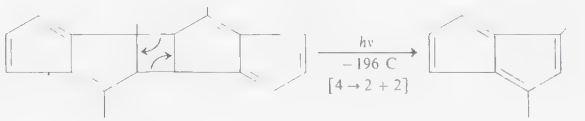

dimer monomer

(13.96)

The fluctional molecule bullvalene **71** was first prepared by a photo [4 → 2 + 2] retrocycloaddition of **70**:[121]

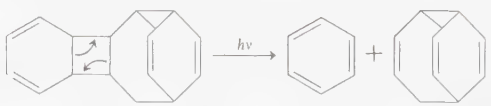

70 **71**, bullvalene

(13.97)

Photoretrocycloadditions of the type [12 → 6 + 6] provide possible examples of allowed pericyclic reactions involving 12 electrons:[122]

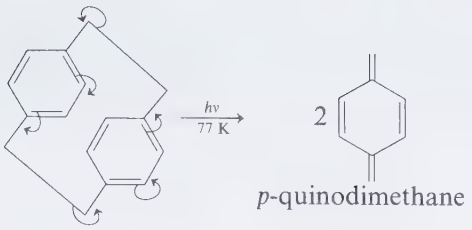

(13.98)

Cyclobutadiene, a reactive intermediate of long-standing theoretical interest to organic chemists,[123] has been prepared and studied by matrix isolation via several different retrocycloaddition reactions:

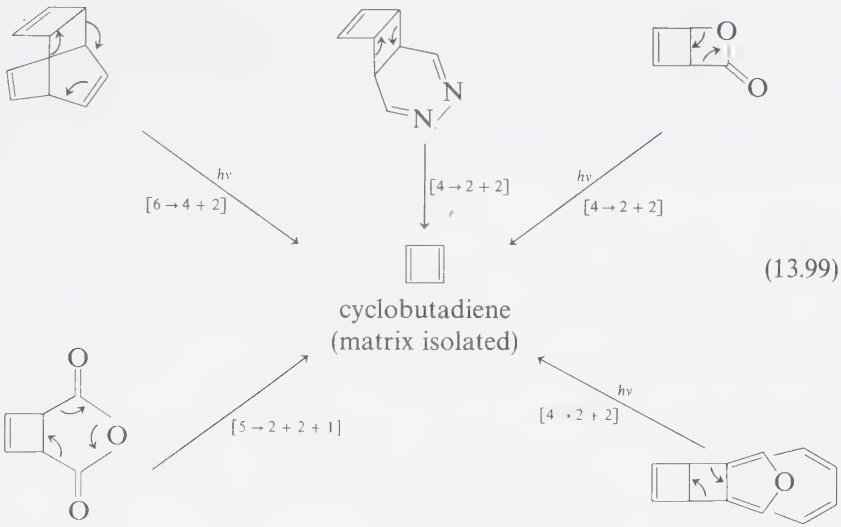

(13.99)

The mechanism of fragmentation of heterocyclic three-membered ring compounds may involve bond cleavages to yield transient species such as 1,3-diradicals or 1,3-zwitterions (Eq. 13.80). In the case of oxiranes, for example, spectroscopic evidence exists for the intermediacy of 1,3-zwitterions in ring-opening reactions.[124] The postulate of such a species allows rationalization of the cleavage which will occur for asymmetric oxiranes. The rule is to consider the more stable zwitterionic structure and then cleave the formal single bond to yield products. Thus, irradiation of **72** yields mainly PhC̈CN with PhC̈H as a minor product:[125]

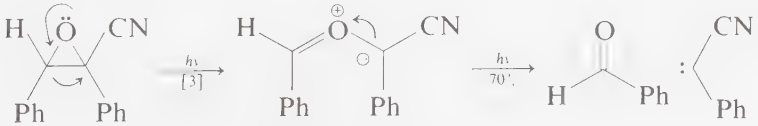

72

(13.100)

Further evidence for the occurrence of intermediates in the photolysis of oxiranes is available from the methods of *alternate synthesis*. As an illustration, the epoxide **73** may be ring-opened to **74** by irradiation at 77 K. The ylide **74** is colored blue and can readily be detected spectroscopically.[126] The same species can be produced by photodecarbonylation of the ketone **75**. An important reaction of the ylide is cleavage to a carbene and carbonyl compound. In systems capable of exhibiting cis-trans isomerization, none is observed. This result is interpreted to imply that cleavage is faster than closure, which would be expected to be a thermal conrotatory process that would effect cis-trans isomerization.[27] The fragmentation of ylides such as **74** to carbenes is (at least in part) a photochemical reaction:[128]

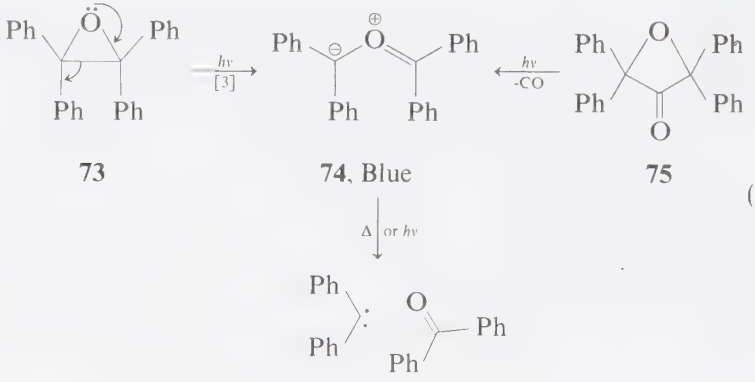

(13.101)

The photochemical ring-opening reactions of oxiranes to zwitterions are formally [3] four-electron *electrocyclic* reactions. If subject to orbital symmetry constraints, favored disrotatory ring opening is anticipated. Spectroscopic evidence, in fact, suggests the symmetry selection rules are obeyed and that only **76** Z and **77** Z are produced from the stereoisomeric stilbene oxides **76** and **77**, respectively.[126]

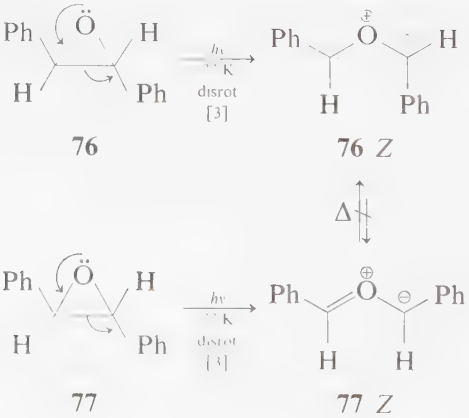

(13.102)

Further support for a concerted [3] is found in the stereospecific photoring opening of aziridine to trapable zwitterionic intermediates.[129]

Evidence for the theoretically expected contrast between singlet (zwitterionic) and triplet (diradical) behavior is found in the contrasting behavior of 1,2-diphenyl cyclopropane upon direct and triplet-sensitized excitation. The cyclopropane **78** undergoes predominantly cis-trans isomerization via a diradical[130] (photosensitization) whereas the singlet (direct excitation) opens to a zwitterion and may be trapped by protic reagents.[131]

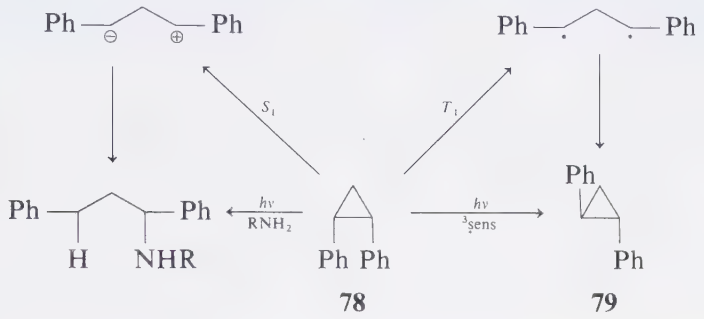

(13.103)

It is found when the conversion of **78** to **79** is effected by optically active sensitizers that **79** is optically active:[132]

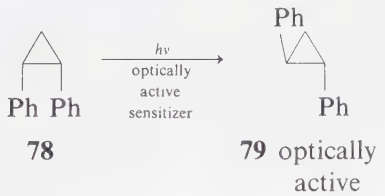

(13.104)

Benzene-sensitized decomposition of the sulfones **80** and **81** results in a [5 → 4 + 1] retrocycloaddition.[133] Interestingly, the reactions are moderately stereospecific, leading to a product expected from *conrotation* (inversion of stereochemistry). Although this result is expected for an *allowed* 6-electron cheleotropic reaction for singlet states, it is interesting that triplet sensitization is required.

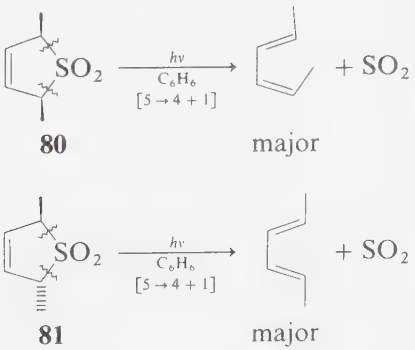

(13.105)

13.7 Miscellaneous α-Cleavage Reactions of Peroxides, Halides, and Nitrites; The Barton Reaction

Aryl halides (especially aryl bromides and iodides) are known to undergo photo-induced homolytic α-cleavage into halogen atoms and aryl radicals.[134] The aryl radicals produced have been used successfully in a number of synthetic sequences. Among the more noteworthy are cyclization eliminations such as the conversion of the iodide **82** to **83** (methyl ester aristolochic acid) and the bromide **84** to **85**:

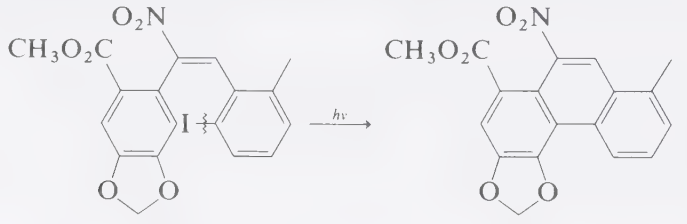

82 **83** (13.106)[135]

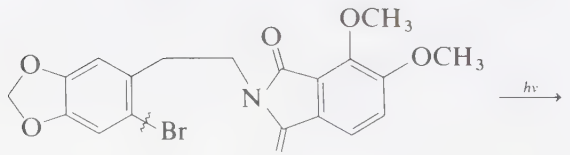

84

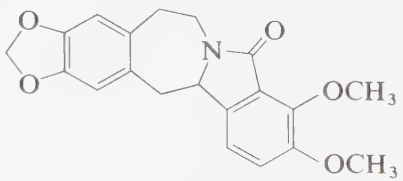

(13.107)[136]

85

Carbonium ions which are difficult to produce by solvolysis of halides (e.g., bridgehead and vinyl carbonium ions) have been generated by photolyses of the corresponding bromide or iodide:

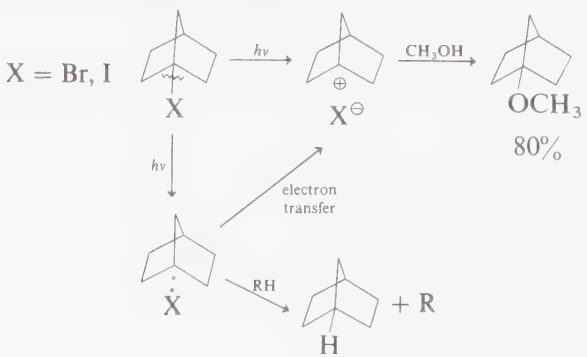

(13.108)[137]

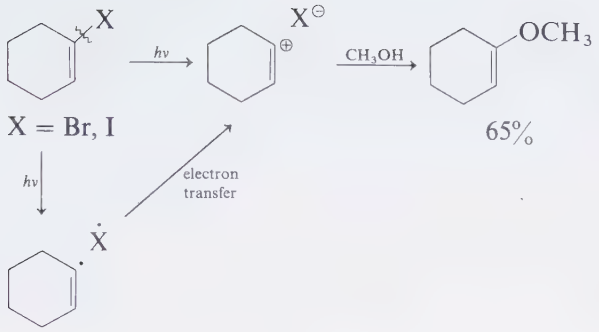

(13.109)[138]

The mechanism involved is thought to be an initial homolytic cleavage of the C—X to yield a diradical pair (Ċ Ẋ) followed by electron transfer to yield an ion pair ($\overset{\oplus}{\text{C}}$ $\overset{\ominus}{\dot{\text{X}}}$), i.e., $S_0 \rightarrow \sigma, \sigma^* \rightarrow D \rightarrow Z$.
Photocleavage of 1,1-dihalides has been employed to generate carbenes:

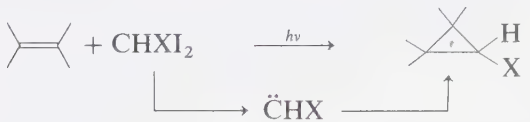

(13.110)[139]

Ozonides and cyclic peroxides, which may seem unlikely candidates for useful photochemical substrates, have in fact proven to be exceedingly useful in several important syntheses, such as the generation of Dewar benzenes and cyclobutadienes:[140]

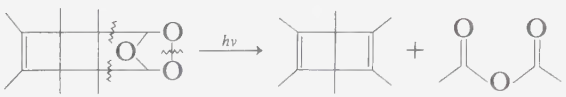

(13.111)

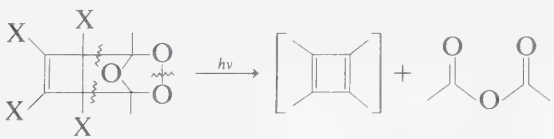

(13.112)

$X = CH_3, Cl$

A Dewar naphthalene has also been prepared by the ozonide photolysis method:[141]

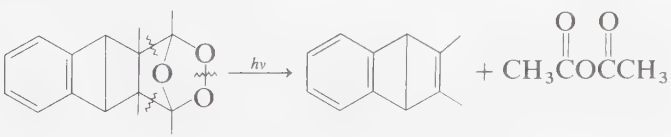

(13.113)

Reaction 13.114 is remarkable in that it seems to involve formation and cyclization of a 1,14-diradical:[142]

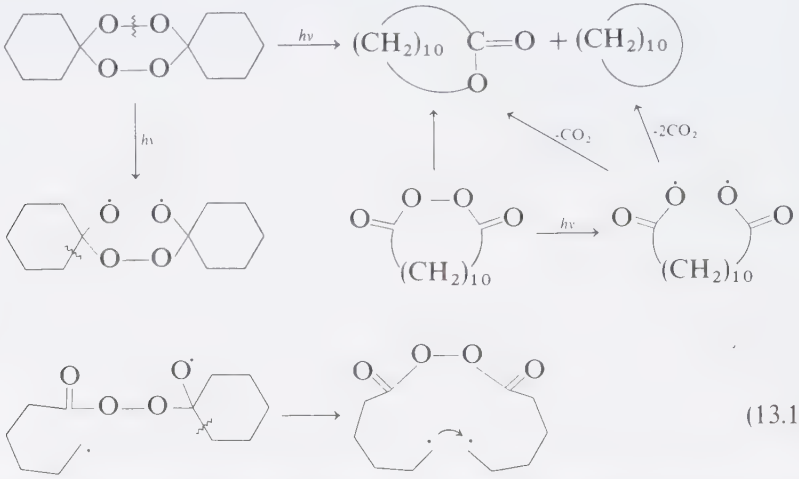

(13.114)

Remarkably, the analogous reaction also works, even with cyclodecanone diperoxides.

The photolysis of cyclic peroxides sometimes results in unusual rearrangement products:

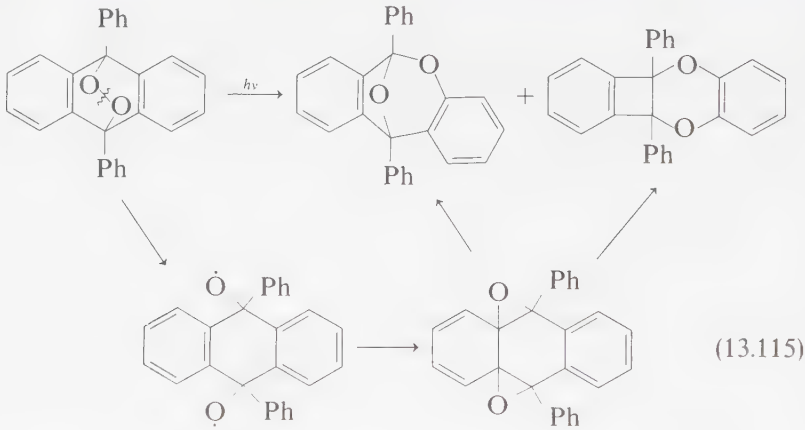

(13.115)[143]

The photolysis of 1,2-dioxetane (a cyclic four-membered ring peroxide) results in cleavage into carbonyl fragments.[121] This reaction is of special interest because one of the carbonyl fragments is produced in the excited state (an adiabatic photoreaction; see Chapter 14):[144]

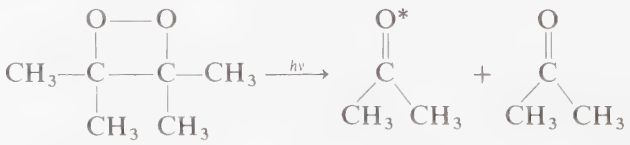

1,2-dioxetane excited product

(13.116)

The photochemistry of organic nitrites is dominated by one primary photochemical process: homolytic cleavage of the RO—NO bond (Barton reaction).[145] The products obtained from this primary process are understandable on the basis of an alkoxy radical as a reaction intermediate. Thus, hydrogen abstraction, addition to unsaturated systems, and fragmentations are all expected (and found) to occur. The latter is an inherent unimolecular process and the former two processes usually tend to occur intramolecularly.

The mechanism of the Barton reaction is believed to involve the following steps:

1. Homolysis of the nitrite
2. Internal hydrogen abstraction by an alkoxy radical
3. Radical coupling
4. Isomerization of a nitroso compound to an oxime.

An outstanding example of the use of nitrite photolysis[146] is the photolysis of **86** to yield cortisone oxime **87**:

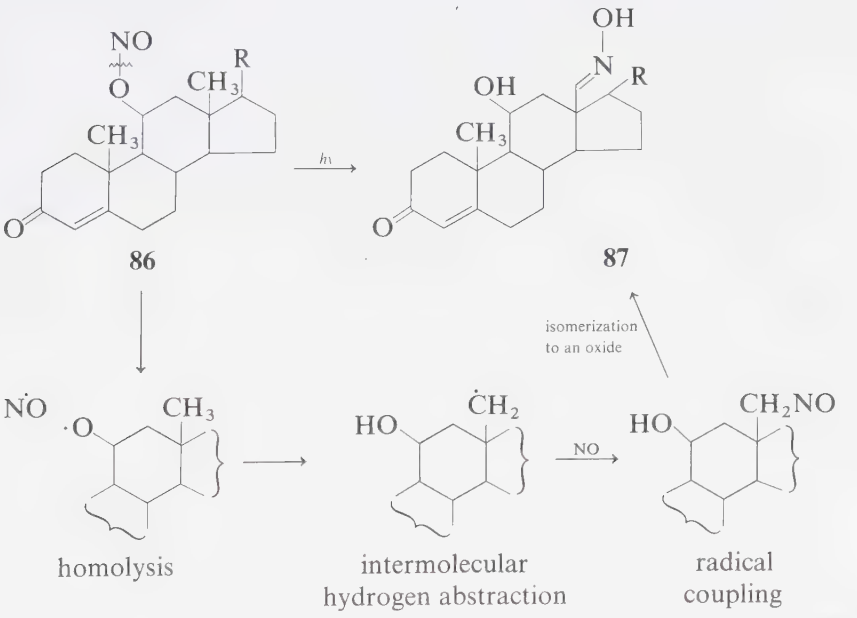

(13.117)[123]

13.8 Summary

Photofragmentations and photoelimination reactions provide a valuable means of generating a variety of reactive diradicals, zwitterions, and strained ground state species. The α-cleavage of a σ-bond attached directly to a chromophore is

a very common primary process for both S_1 and T_1 states. The β-cleavage of a σ-bond is less common but is occasionally encountered.

A major synthetic application of photofragmentations is to prepare reactive intermediates under matrix isolation conditions. A wide variety of important strained or reactive organic molecules have been prepared and studied via this technique.

References

1. Chapman, O. L., et al., *J. Am. Chem. Soc.*, *95*, 6134 (1973).
2. Chapman, O. L., Wojtkowski, P. W., Adam, W., Rodriguez, O., and Rucktaschel, R., *J. Am. Chem. Soc.*, *92*, 1365 (1972); Adam, W., Liu, J.-C., and Rodriguez, O., *J. Org. Chem.*, *38*, 2269 (1973).
3. Chapman, O. L., et al., *J. Am. Chem. Soc.*, *95*, 614 (1973); *ibid.*, *95*, 1337 (1973); Lim, C. Y., and Krantz, A., *Chem. Comm.*, 1111 (1972).
4. Trozzolo, A. M., et al., *J. Am. Chem. Soc.*, *89*, 3357 (1967).
5. Wasserman, E., Smolinsky, G., and Yager, W. A., *J. Am. Chem. Soc.*, *86*, 3166 (1964).
6. Dowd, P., *J. Am. Chem. Soc.*, *92*, 1066 (1970).
7. Dowd, P., *J. Am. Chem. Soc.*, *88*, 2587 (1966).
8. DoMinh, T., Trozzolo, A. M., and Griffin, G. W., *J. Am. Chem. Soc.*, *92*, 1402 (1970).
9. Zimmerman, H. E., *Adv. Photochem.*, *1*, 183 (1963); Kasha, M., in *Light and Life*, eds., McElroy, W. D., and Glass, B., Baltimore, Md. Johns Hopkins Press, 1961, p. 31.
10. Kochi, J., in *Free Radicals*, *Vol. II*, ed. Kochi, J., New York: Wiley, 1973, p. 665.
11. Walling, C., and Clark, R. T., *J. Am. Chem. Soc.*, *96*, 4530 (1974).
12. Walling, C., *Pure Appl. Chem.*, *15*, 69 (1967).
13. Ingold, K. U., in *Free Radicals*, *I*, ed. Kochi, J., New York: Wiley, 1973, p. 37.
14. Rüchardt, C., and Mayer-Ruthardt, I., *Chem. Ber.*, *104*, 593 (1971); Rüchardt, C., and Pantke, R., *ibid.*, *106*, 2542 (1973).
15. Lewis, F. D., et al., *J. Org. Chem.*, *40*, 488 (1975); *J. Am. Chem. Soc.*, *97*, 1519 (1975).
16. Schuh, H., Hamilton, E. J., Paul, H., and Fisher, H., *Helv. Chim. Acta.*, *57*, 2011 (1974); Paul, H., and Fisher, H., *ibid.*, *56*, 1575 (1973); Blank, B., Henne, A., and Fischer, H., *ibid.*, *57*, 920 (1974); Fischer, H., *Pure Appl. Chem.*, *41*, 475 (1975); Laroff, G. P., and Fischer, H., *ibid.*, *56*, 2011 (1973).
17. Muller, K., and Closs, G. L., *J. Am. Chem. Soc.*, *94*, 1002 (1972).
18. (a) Lewis, F. D., and Magyar, M. G., *J. Org. Chem.*, *37*, 2102 (1972).
    (b) For a related example see: Baum, A. A., *J. Am. Chem. Soc.*, *94*, 6866 (1972).
19. Dalton, J. C., et al., *J. Am. Chem. Soc.*, *92*, 2564 (1970).
20. Dalton, J. C., et al., *J. Am. Chem. Soc.*, *93*, 7213 (1971); Wagner, P. J., and Spoerke, R. W., *ibid.*, *91*, 4437 (1969).
21. Yang, N. C., et al., *J. Am. Chem. Soc.*, *92*, 6974 (1970).

22. (a) O'Neal, H. E., and Larson, C. W., *J. Phys. Chem.*, *73*, 1011 (1969).
(b) For other examples of activation energies for α-cleavage see: Mirbach, M. F., Mirbach, M. J., Liu, K. C., and Turro, N. J., *J. Photochem.*, *8*, 299 (1978).
(c) Abuin, E., and Liss, E. A., *J. Photochem.*, *5*, 65 (1975); Encina, M. V., Nogales, A., and Lissi, D. A., *J. Photochem.*, *6*, 75 (1975).
(d) Berger, M., and Steel, C., *J. Am. Chem. Soc.*, *97*, 4817 (1975).
(e) Shortridge, R. G., et al., *ibid.*, *93*, 1863 (1971).

23. Hemminger, J. C., Rusbult, C. F., and Lee, E. K. C., *J. Am. Chem. Soc.*, *93*, 1867 (1971).

24. (a) Lewis, F. D., and Magyar, J. G., *J. Am. Chem. Soc.*, *95*, 5973 (1973).
(b) For related examples see: Heine, H. G., Rosenbranz, H. J., and Rudolph, H., *Angew. Chem. Inter. Ed. Eng.*, *11*, 974 (1972); Heine, H. G., et al., *J. Org. Chem. 39*, 691 (1974).

25. Rickborn, R., Alumbaugh, R. L., and Pritchard, G. O., *Chem. Ind.*, 1951 (1964); *J. Phys. Chem.*, *69*, 3225 (1965); Frey, H. M., and Lister, D. H., *J. Am. Chem. Soc.*, *A*, 627 (1970); Barltrop, J. A., and Coyle, J. D., *Chem. Comm.*, 1081 (1969).

26. Iriarte, J., Schaffner, K., and Jeger, O., *Helv. Chim. Acta.*, *47*, 1244 (1964).

27. Review of the chemistry of acyl radicals: Vinogradov, M. G., and Nikishin, G. I., *Russ. Chem. Rev.*, *40*, 916 (1971).

28. Robbins, W. K., and Eastman, R. H., *J. Am. Chem. Soc.*, *92*, 6076–6077 (1970); see also: Engel, P. S., *ibid.*, *92*, 6074 (1970); Quinkert, G., et al., *Tetrahedron Letters*, 1863 (1963).

29. Maillard, B., Forrest, D., and Ingold, K. U., *J. Am. Chem. Soc.*, *98*, 7024 (1976).

30. Sonoda, A., et al., *Bull. Chem. Soc. Japan*, *45*, 1777 (1972).

31. Carlson, R. G., and Mardis, W. S., *J. Org. Chem.*, *40*, 817 (1975).

32. Reviews of cyclobutanone photochemistry: Morton, D. R., and Turro, N. J., *Adv. Photochem.*, *9*, 197 (1974); Strohrer, W. D., Jacobs, P., Kaiser, K. H., Wiech, G., and Quinkert, G., *Fortschr. Chem. Forsch.*, *46*, 181 (1974).

33. (a) Turro, N. J., and Southam, R., *Tetrahedron Letters*, 545 (1967).
(b) Reviews of oxacarbene formation: Yates, P., *J. Photochem.*, *5*, 91 (1976); Yates, P., and Loutfy, R. O., *Acc. Chem. Research*, *8*, 209 (1975).

34. Turro, N. J., Hammond, W. B., and Leermakers, P. A., *J. Am. Chem. Soc.*, *87*, 2774 (1965); *87*, 2613 (1965).

35. Dowd, P., and Sachdev, K., *J. Am. Chem. Soc.*, *89*, 715 (1967).

36. Morton, D. R., Lee-Ruff, E., Southam. R. M., and Turro, N. J., *J. Am. Chem. Soc.*, *92*, 4349 (1970); Morton, D. R., and Turro, N. J., *ibid.*, *95*, 3947 (1973).

37. Turro, N. J., and McDaniel, D. M., *J. Am. Chem. Soc.*, *92*, 5727 (1970); Quinkert, G., Jacobs, P., and Stoher, W. D., *Angew. Chem., Inter. Ed. Eng.*, *13*, 199 (1974).

38. Turro, N. J., Farneth, W. E., and Devaquet, A., *J. Am. Chem. Soc.*, *98*, 7425 (1976).

39. Thomas, S. G., and Guillory, W. A., *J. Phys. Chem.*, *78*, 1461 (1974).

40. Salem, L., *J. Am. Chem. Soc.*, *96*, 3486 (1974).

41. Shortridge, R. G., and Lee, E. K. C., *J. Phys. Chem.*, *77*, 1936 (1973).

42. Herzberg, G., *Electronic Spectra of Polyatomic Molecules*, Princeton, N. J.; Van Nostrand, 1966, p. 469.

43. Reviews:
(a) *Ketones*: Houk, K. N., *Chem. Rev.*, *76*, 1 (1976); Schaffner, K., *Tetrahedron*, *32*, 641 (1976);
(b) *Esters and Amides*: Bellus, D., *Adv. Photochem.*, *8*, 109 (1973).

44. Paquette, L. A., and Mecham, G. V., *J. Org. Chem.*, *34*, 450 (1969); Furntachi, N., Nakadaira, Y., and Nakanishi, K., *J. Am. Chem. Soc.*, *91*, 1028 (1969).

45. Engel, P. S., and Schnexnaayder, M. A., *J. Am. Chem. Soc.*, *94*, 9252 (1972); *ibid.*, *97*, 145 (1975).

46. Engel, P. S., et al., *J. Am. Chem. Soc.*, *96*, 924 (1974).

47. Bagglioni, E., Schaffner, K., and Jeger, O., *Chem. Comm.*, 1103 (1969); Baggiolini, E., Hamlow, H. P., and Schaffner, K., *J. Am. Chem. Soc.*, *92*, 4096 (1970).

48. Kalmus, C. E., and Hercules, D. N., *J. Am. Chem. Soc.*, *96*, 449 (1974).

49. Fischer, M., *Tetrahedron Letters*, 2281 (1969); *Chem. Ber.*, *102*, 342 (1969).

50. Givens, R. S., and Oettle, W. F., *J. Am. Chem. Soc.*, *93*, 3301 (1971). For other related examples see: Yegev, A., and Mazui, Y., *J. Am. Chem. Soc.*, *87*, 3250 (1965); Chapman, O. L., and McIntosh, *Chem. Comm.*, 383 (1971).

51. Sander, M. R., Hedaya, E., and Trecker, D. J., *J. Am. Chem. Soc.*, *90*, 7249 (1968).

52. Adam, W., de Sanabia, J. A., and Fischer, H., *J. Org. Chem.*, *38*, 2571 (1973); *Chem. Comm.*, 289 (1974).

53. Dalton, J. C., Shen, M., and Snyder, J. J., *J. Am. Chem. Soc.*, *98*, 5023 (1976).

54. Schuster, D., et al., *ibid.*, *98*, 5025 (1976).

55. Waddell, W. H., Turro, N. J., and Farrington, G., *Molec. Photochem.*, *7*, 425 (1976) and references therein.

56. Rau, H., *Angew. Chem. Inter. Ed. Eng.*, *12*, 224 (1973).

57. Review: Strauss, O. P., Lown, J. W., and Gunning, H. E., in *Comprehensive Chemical Kinetics*, eds. Bamford, C. H., and Tippen, C., *Vol. 5*, Amsterdam/New York: Elsevier, 1973, p. 566. Kellogg, R., *Photochemistry of Heterocyclic Compounds*, ed. Buchardt, O., New York: John Wiley, 1976. Durr, H., and Ruge, B., *Topics in Chemistry*, *66*, 53 (1976). Meier, H., and Zeller, K. D., *Angew. Chem. Inter. Ed. Eng.*, *16*, 835 (1977).

58. (a) Lyon, R. K., and Levy, D. H., *J. Am. Chem. Soc.*, *93*, 4290 (1961).
(b) Nadelmen, N., and Martin, J. C., *ibid.*, *98*, 6597 (1976).

59. Porter, N. A., et al., *J. Am. Chem. Soc.*, *94*, 3664 (1972); *Tetrahedron Letters*, 3363 (1975); *J. Am. Chem. Soc.*, *99*, 1264 (1973).

60. Von Auken, V., and Rinehart, K. L., *J. Am. Chem. Soc.*, *84*, 3736 (1962).

61. Cohen, S. G., and Zand, R., *J. Am. Chem. Soc.*, *84*, 586 (1962).

62. Anet, R., and Anet, F. A. L., *J. Am. Chem. Soc.*, *96*, 525 (1964).

63. Paquette, L. A., and Leichter, L. M., *J. Am. Chem. Soc.*, *92*, 1765 (1970).

64. Bartlett, P. D., and McBride, J. M., *Pure Appl. Chem.*, *15*, 89 (1967).

65. Zuchlich, J., *J. Chem. Phys.*, *52*, 3592 (1970).

66. Buchwalter, S. L., and Closs, G. L., *J. Am. Chem. Soc.*, *97*, 3857 (1975).

67. Pagni, R. M., Watson, C. R., Bloor, J. E., and Dodd, J. R., *J. Am. Chem. Soc.*, *96*, 4064 (1974); *ibid.*, *98*, 2551 (1976).

68. Closs, G. L., and Kaplan, L. R., *J. Am. Chem. Soc.*, *91*, 2168 (1969).

69. Dowd, P. *Acc. Chem. Research*, *5*, 242 (1972).

70. Borden, W. S., *Molecular Orbital Theory for Organic Chemists*, Engelwood Cliffs, N.J.: Prentice-Hall, 1975.

71. Berson, J. A., Bushby, R. J., McBride, J. M., and Tremelling, M., *J. Am. Chem. Soc.*, *93*, 1544 (1971); *ibid.*, *98*, 6743 (1976); Berson, et al., *ibid.*, *99*, 2009 (1977); *ibid.*, *96*, 6177 (1974).

72. Turro, N. J., Mirbach, M. J., Harrit, N., Berson, J., and Platz, M. S., *J. Am. Chem. Soc.*, in press.

73. (a) Engel, P. S., and Steel, C., *Acc. Chem. Research*, *6*, 275 (1973).
(b) Engel, P. S., and Shen, L., *Canad. J. Chem.*, *52*, 4040 (1974).
(c) Mirbach, M. J., Liu, K. C., Mirbach, M. F., Cherry, W. R., Turro, N. J., and Engel, P. *J. Am. Chem. Soc.*, in press.

74. Hutton, R. F., and Steel, C., *J. Am. Chem. Soc.*, *86*, 745 (1964); Mill, T., and Stringham, R. S., *Tetrahedron Letters*, 1853 (1969).

75. Overberger, C. G., et al., *Tetrahedron Letters*, 4565 (1972); Gisin, M., and Wirz, J., *Helv. Chim. Acta.*, *59*, 2273 (1976); Pagni, R. M., et al., *J. Am. Chem. Soc.*, *99*, 1972 (1977).

76. Trost, B. M., and Cory, R. M., *J. Am. Chem. Soc.*, *93*, 5573 (1971); Turro, N. J., Renner, C. A., Waddell, W. H., and Katz, T. J., *ibid.*, *98*, 4320 (1976); Katz, T. J., and Acton, N., *ibid.*, *95*, 2738 (1973).

77. Fox, J. R., and Hammond, G. S., *J. Am. Chem. Soc.*, *86*, 4031 (1964); Bartlett, P. D., and Porter, N. A., *ibid.*, *90*, 5317 (1970).

78. Zimmerman, H. E., Boettcher, R. J., Buehler, N. E., and Keck, G. E., *J. Am. Chem. Soc.*, *97*, 5635 (1975).

79. Turro, N. J., Cherry, W. R., Mirbach, M. F., and Mirbach, M. J., *J. Am. Chem. Soc.*, *99*, 7389 (1977).

80. Porter, N. A., and Marnett, L. J., *J. Am. Chem. Soc.*, *95*, 4361 (1973).

81. Porter, N. A., Marnett, L. J., Lochmüller, J., Closs, G. L., and Shobataki, M., *J. Am. Chem. Soc.*, *94*, 3664 (1972). See also Green, J. G., Dubay, G. R., and Porter, N. A., *J. Am. Chem. Soc.*, *99*, 1264 (1977).

82. Dellinger, B., Hochstrasser, R. M., and Smith, A. B., *J. Am. Chem. Soc.*, *99*, 5834 (1977).

83. Reviews of Photochemistry of diazo compounds: Durr, H., and Kober, H., *Topics in Current Chemistry*, *66*, 54 (1976); Durr, H., "Photochemie II," in *Methoden der Organische Chemie*, Sturrgart: Houben-Weyl, Thieme, 1975, p. 1158.

84. Reviews of Photochemistry of azides: Lwowski, W., *Angew. Chem.*, *6*, 897 (1966); Durr, H., *Topics in Current Chemistry*, *66*, 89 (1976); see also Ref. 83.

85. *Carbenes*, *Vols. I* and *II*, eds. Jones, M., and Moss, R., New York: Wiley, 1973.

86. Review: Wasserman, E. W., *Acc. Chem. Research*; Wasserman, E., et al., *J. Am. Chem. Soc.*, *92*, 7491 (1970) and references therein.

87. Bethell, D., Stevens, G., and Tickle, P., *Chem. Comm.*, 792 (1970).

88. Kopecky, K. R., Hammond, G. S., and Leermakers, P. A., *J. Am. Chem. Soc.*, *84*, 1015 (1962).

89. For a discussion of this point see Roth, H. D., and Manion, M. L., *J. Am. Chem. Soc.*, *98*, 3392 (1976).

90. Padwa, A., and Layton, R., *Tetrahedron Letters*, 2167 (1965); Cowan, D. O., Couch M. M., Kopecky, K. R., and Hammond, G. S., *J. Org. Chem.*, *29*, 1922 (1964).

91. For a review of the Wolff rearrangement, see Meier, H., and Zeller, K., *Angew. Chem. Inter. Ed. Eng.*, *14*, 32 (1975); Wentrup, C., *Top. Curr. Chem.*, *62*, 173 (1976).

92. Pomerantz, M., and Witherup, T. H., *J. Am. Chem. Soc.*, *95*, 5977 (1973); Trotter, J., Gibbons, C. S., Nakatsuka, N., and Masamune, S., *J. Am. Chem. Soc.*, *95*, 7508 (1973).

93. Eaton, P. E., and Temme, G. H., *J. Am. Chem. Soc.*, *95*, 7508 (1973).

94. Hlubucek, J. R., and Lowe, G., *Chem. Comm.*, 419 (1974).

95. Csizmadia, I. G., Font, J., Strausz, O. P., *J. Am. Chem. Soc.*, *90*, 7360 (1968); *ibid.*, *95*, 124 (1973); Zeller, K. P., *Angew. Chem. Inter. Ed. Eng.*, *16*, 781 (1977).

96. Closs, G. L., and Rabinow, B. E., *J. Am. Chem. Soc.*, *98*, 8190 (1976).

97. Reviews: Lwowski, W., *Angew. Chem.*, *6*, 897 (1966); Lwowski, L., *Nitrenes*, New York: John Wiley, 1970; Fowler, F. W., *Adv. Heterocycl. Chem.*, *13*, 54 (1971); Labbe, G., and Hassner, A., *Angew. Chem. Inter. Ed. Eng.*, *10*, 98 (1971); Abramovitch, R. A., and Kyba, E. D., in *The Chemistry of the Azido Group*, ed. Patai, S., New York: Interscience, 1971, p. 221; Dürr, H., and Kober, H., *Topics in Current Chemistry*, *66*, 90 (1976).

98. Apsimon, J. W., and Edwards, O. E., *Can. J. Chem.*, *40*, 896 (1962).

99. Hassner, A., and Fowler, F. W., *J. Am. Chem. Soc.*, *90*, 2869 (1968).

100. Griffin, G. W., and Padwa, A., *Photochemistry of Heterocyclic Compounds*, ed. Buchart, O., New York: Wiley, 1976, p. 41.

101. Dauben, W. G., Shaffer, G. W., and Deving, E. J., *J. Am. Chem. Soc.*, *92*, 6273 (1970); *J. Org. Chem.*, *34*, 2512 (1969); Hess, L. D., Jacobson, J. L., Schaffner, K., and Pitts, J. N., *J. Am. Chem. Soc.*, *89*, 3684 (1964).

102. Zimmerman, H. E., and Epling, G. A., *J. Am. Chem. Soc.*, *94*, 7806 (1972) and references therein.

103. Schrader, L., and Hartmann, W., *Tetrahedron Letters*, 3995 (1973).

104. Zimmerman, H. E., et al., *J. Am. Chem. Soc.*, *86*, 947 (1964).

105. Wuthrich, W. J., Siewinski, A., Schaffner, K., and Jeger, O., *Helv. Chim. Acta.*, *56*, 239 (1973).

106. Wehrli, H., Lehmann, C., Keller, P., Bonet, J. J., Schaffner, K., and Jeger, O., *Helv. Chim. Acta.*, *49*, 2218 (1966).

107. Ullman, E. F., *J. Am. Chem. Soc.*, *85*, 3529 (1963); *ibid.*, *86*, 3814 (1964).

108. Schaffner, K., *Pure Appl. Chem.*, *16*, 75 (1968); *21*, 247 (1970).

109. Sheehan, J. C., Wilson, R. M., and Oxford, A. W., *J. Am. Chem. Soc.*, *93*, 7222 (1971).

110. Givens, R. S., Strekowski, L., and Devonshire, R., *J. Am. Chem. Soc.*, *96*, 1631 (1974). Kaplan, B. E., and Hartwig, A. L., *Tetrahedron Letters*, 4855 (1970).

111. Reviews: Padwa, A., et al., *Pure Appl. Chem.*, *33*, 269 (1973); Schmid, H., et al., *ibid.*, *33*, 339 (1973); Padwa, A., *Angew. Chem. Inter. Ed. Eng.*, *15*, 123 (1976).

112. Salem, L., *J. Am. Chem. Soc.*, *96*, 3486 (1974).

113. Padwa, A., and Wetmore, S. I., *J. Am. Chem. Soc.*, *96*, 2414 (1974); *ibid.*, *99*, 1871 (1977).

114. Sieber, W., Gilgen, P., Chaloupka, S., Hansen, H. J., and Schmid, H., *Helv. Chim. Acta.*, *56*, 1679 (1973).

115. Zimmerman, H. E., and Little, R. D., *Chem. Comm.*, 698 (1972); Wolf, S., and Agosta, W. D., *ibid.*, 226 (1972).

116. Chapman, O. L., et al., *J. Am. Chem. Soc.*, *91*, 6856 (1969).

117. Review: Griffin, G. W., *Angew. Chem. Inter. Ed. Eng.*, *10*, 537 (1971).

118. Trozzolo, A. M., et al., *J. Am. Chem. Soc.*, *89*, 3357 (1967).

119. Saltiel, J., and Liu, L. S. N., *J. Am. Chem. Soc.*, *91*, 5404 (1969).

120. Hafner, K., Donges, R., Gocdecke, E., and Kaiser, R., *Angew. Chem. Inter. Ed. Eng.*, *12*, 337 (1973).

121. Schroeder, G., *Angew. Chem.*, *75*, 91, 722 (1963).

122. Kaupp, G., *Angew. Chem. Inter. Ed. Eng.*, 442 (1976).

123. Maier, G., Martan, H. G., and Sayrac, T., *Angew. Chem. Inter. Ed. Eng.*, *15*, 226 (1976) and references therein. For a review of cyclobutadiene: Maier, G., *ibid.*, *13*, 425 (1974).

124. Becker, R. S., et al., *J. Am. Chem. Soc.*, *92*, 1302 (1970); Arnold, D. R., and Kanischly, L. A., *J. Am. Chem. Soc.*, *92*, 1404 (1970).

125. Petrellis, P., et al., *J. Am. Chem. Soc.*, *89*, 1967 (1967).

126. Domink, T., Trozzolo, A. M., and Griffin, G. W., *J. Am. Chem. Soc.*, *92*, 1402 (1970); *ibid.*, *89*, 3357 (1967).

127. Paulson, D. R., Tang, F. Y., and Sloan, R. B., *J. Org. Chem.*, *38*, 3967 (1973).

128. Griffin, G. W., et al., *J. Am. Chem. Soc.*, *98*, 5697 (1976).

129. Hermann, H., Huisgen, R., and Mader, H., *J. Am. Chem. Soc.*, *93*, 1779 (1971); Huisgen, R., Scheer, W., and Huber, H., *ibid.*, *89*, 1753 (1967).

130. Hammond, G. S., Wyatt, P., DeBoer, C. D., and Turro, N. J., *J. Am. Chem. Soc.*, *86*, 2532 (1964); Griffin, G. W., O'Connell, E. J., and Hammond, H. A., *ibid.*, *85*, 1001 (1963).

131. Irving, C. S., et al., *J. Am. Chem. Soc.*, *88*, 5675 (1966); Hixson, S. S., *Chem. Comm.*, 1170 (1972); *J. Am. Chem. Soc.*, *96*, 4872 (1974) and references therein.

132. Hammond, G. S., and Cole, R. S., *J. Am. Chem. Soc.*, *87*, 3256 (1965).

133. Saltiel, J., and Metts, L., *J. Am. Chem. Soc.*, *89*, 2232 (1967).

134. Review: Shama, R. K., and Kharash, *Angew. Chem. Inter. Ed. Eng.*, *7*, 37 (1968).

135. Kupcham, S. M., and Wormser, H. C., *Tetrahedron Letters*, 359 (1965).

136. Bernard, H. W., and Snieckus, V., *ibid.*, 4867 (1971).

137. Kropp, P. J., et al., *J. Am. Chem. Soc.*, *98*, 8135 (1976); Poindexter, G. A., and Kropp, P. J., *J. Am. Chem. Soc.*, *96*, 7142 (1974); *ibid.*, *95*, 5420 (1973).

138. McNeely, S. A., and Kropp, P. J., *ibid.*, *98*, 4319 (1976).

139. Marolewski, T., and Yang, N. C., *J. Am. Chem. Soc.*, *90*, 5644 (1970); *Chem. Comm.*, 1225 (1967); Blomstrom, D. C., Herbig, K., and Simmons, H. E., *J. Am. Chem. Soc.*, *30*, 959 (1965).

140. Story, P. R., Morrison, W. H., and Butler, J. M., *J. Am. Chem. Soc.*, *91*, 2393 (1969); Criegee, R., and Hurber, R., *Chem. Ber.*, *103*, 1862 (1970).

141. Carty, D. T., *Tetrahedron Letters*, 4753 (1969).

142. Story, P., *Adv. Org. Chem.*, *8*, 67 (1972).

143. Rigaudy, J., *Pure Appl. Chem.*, *16*, 169 (1968).

144. Turro, N. J., et al., *J. Am. Chem. Soc.*, *95*, 2035 (1973).

145. Reviews of the Barton Reaction: Nussbaum, A., and Robinson, C. H., *Tetrahedron Letters*, *17*, 35 (1962); Akhtar, A., *Adv. Photochem.*, *2*, 263 (1964).

146. Barton, D. H. R., and Beaton, J. M., *J. Am. Chem. Soc.*, *83*, 750 (1961); *ibid.*, *84*, 1496 (1962).

14

Singlet Oxygen and Chemiluminescent Organic Reactions

14.1 A Conceptual Link Between Photoreactions and Chemiluminescent Organic Reactions

Chemiluminescence occurs when a sizeable fraction of the exothermicity (ΔG) of a chemical reaction is converted into electronic excitation energy (*) of a reaction product, which then emits photons of light ($h\nu$).[1,2] We can describe chemiluminescence as a $\Delta G \rightarrow * \rightarrow h\nu$ sequence (Fig. 14.1). The heart of the sequence is the chemiexcitation ($\Delta G \rightarrow *$) step. The $* \rightarrow h\nu$ process is an ordinary and well-understood luminescence step which serves to announce the presence of an

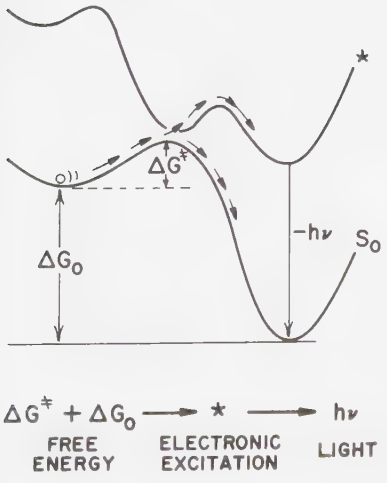

Figure 14.1

Schematic of a chemiluminescent organic reaction. A key elementary step is a transition from a ground surface to an excited state surface. The free energy of a reaction is partially or entirely converted to electronic excitation energy of a product. An important goal is to determine at which nuclear geometries such "surface jumps" may occur and what electronic mechanisms determine the probability of such jumps.

electronically excited state. If we consider photochemistry as a $h\nu \rightarrow * \rightarrow \Delta G$ sequence (Fig. 14.2), it follows that a conceptual link exists between chemiluminescence phenomena (photochemistry in reverse) and photochemical reactions.

Classification of Chemiluminescent Organic Reactions

In terms of potential-energy surfaces, we recognize two major classes of chemiluminescent organic reactions: (a) *nonadiabatic* chemiluminescence, and (b) *adiabatic* chemiluminescence. An adiabatic reaction proceeds entirely on one electronic energy surface (i.e., in one electronic state). A nonadiabatic reaction occurs with a change from one electronic energy surface to another (i.e., from one electronic state to another) as a result of a surface jump at some point along the reaction coordinate.

The essence of many photochemical processes is a change in electronic state. All photoreactions must involve at least one nonadiabatic step, since an electronically excited state eventually results in ground-state products.

With these facts in mind, we can see that the $\Delta G \rightarrow *$ step is generally a nonadiabatic reaction, because the reactant R is in its ground state but the product P^* is in an electronically excited state. The process $R \rightarrow R^* \rightarrow P^* \rightarrow P + h\nu$ is thus an adiabatic chemiluminescence. Adiabatic chemiluminescence is a process in which an electronically excited reactant R^* produces an electronically excited product P^* which then emits light.

It is possible to classify chemiluminescent organic reactions in many ways. Empirically, a classification by *reaction type* has evolved. The majority of chemiluminescent organic reactions require a critical step which involves an oxidation of a substrate with molecular oxygen or its synthetic equivalent. Other important types of chemiluminescent organic reactions are *electron transfer*, *fragmentation*, and *pericyclic rearrangements*.

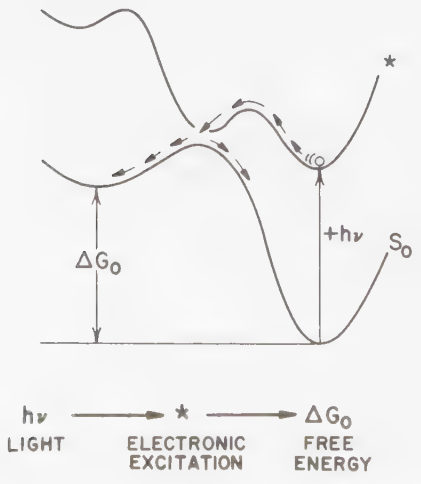

Figure 14.2
Schematic of a typical photochemical organic reaction. Absorption places a molecule on an excited electronic surface. At some critical nuclear geometry a radiationless transition to a ground state surface occurs. An understanding of photoreactions requires knowledge of such geometries and of the electronic mechanisms which determine the probabilities of such "surface jumps."

The oxidation of luminol (Eq. 14.1) represents a classic example of a chemiluminescent organic reaction:[3]

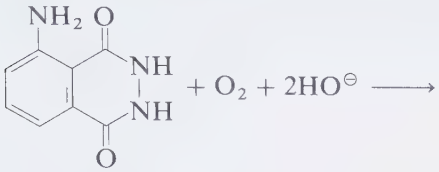

Luminol

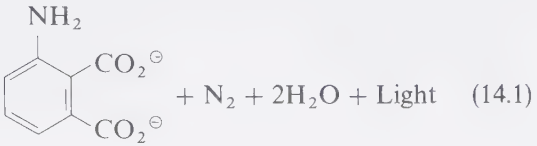

(14.1)

The famous example of firefly (Photinus pyralis) bioluminescence is also believed to involve a key oxidative step:[4]

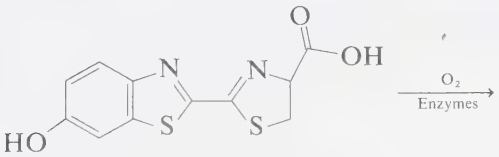

Photinus pyralis

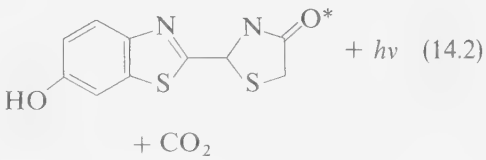

(14.2)

The reaction of the radical anions of organic hydrocarbons with organic cations produces chemiluminescence that corresponds spectrally to the fluorescence of the aromatic hydrocarbon. A typical example is the reaction of the anthracene radical anion and the cation of aromatic amines to yield anthracene, an amine, and light:[5]

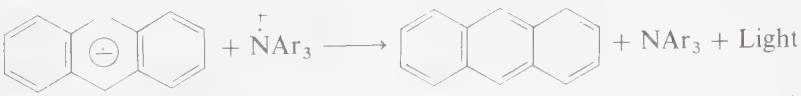

(14.3)

Reports of chemiluminescent pericyclic rearrangements (or reactions) which do not involve oxygen in some form are very rare, an example being the electrocyclic rearrangement of Dewar benzenes to benzenes (Eq. 14.4). In contrast to the previous examples, the emission in this case is too weak for direct measurement.

Energy transfer to a strongly emitting acceptor A is required to increase emission to a measurable value.[6]

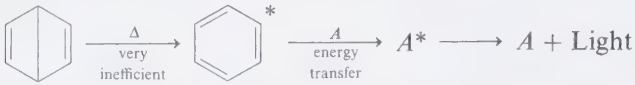

(14.4)

The fragmentation of endoperoxides into singlet molecular oxygen plus a diene equivalent (Eq. 14.5)[7] and the fragmentation of 1,2-dioxetanes into two carbonyl compounds (Eq. 14.6)[8] are generally chemiluminescent and represent classes for which the chemiexcitation step is relatively efficient (10–100%):

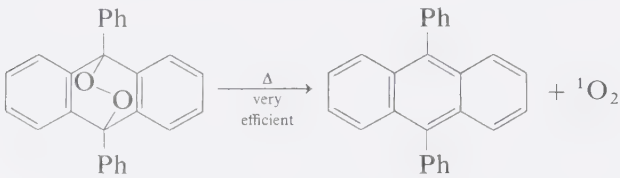

(14.5)

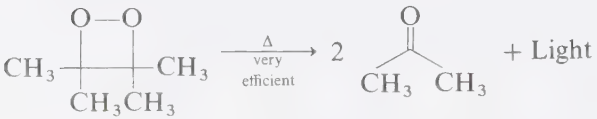

(14.6)

Although *energetics* determines the feasibility of producing an efficient chemiluminescent reaction, *surface dynamics* determines the observed efficiency of exothermic (i.e., $\Delta G + \Delta G^{\ddagger} > E_{P^*}$) chemiluminescent reactions. In general, it appears that the ability to achieve a diradicaloid geometry (Fig. 14.3) enhances the efficiency of surface jumps that correspond to chemiexcitation.

In terms of energy surfaces, the diradicaloid geometry corresponds to a structure for which two or more electronic surfaces tend to merge to a common point

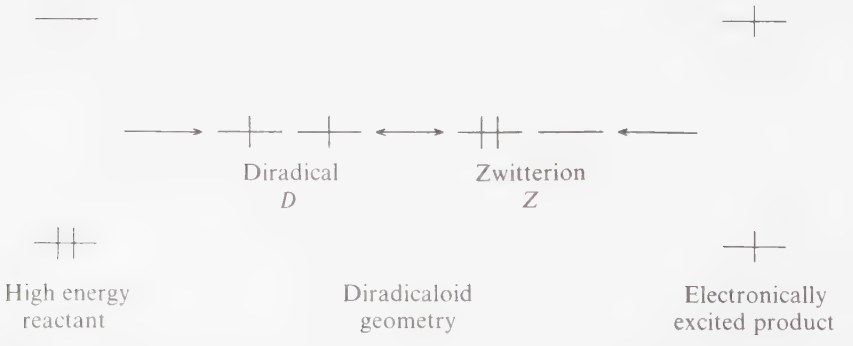

Figure 14.3

Schematic of the conversion: high energy reactant → diradicaloid geometry → electronically excited product, a mechanism for the process $\Delta G \rightarrow ^*$.

(Zero Order surface crossing or surface touching). Such a convergence of surfaces is the most favorable for jumps between surfaces. An important point is that the Zero Order crossing must *not* be strongly avoided, because such a situation would push the two surfaces far apart and reduce the probability of a surface jump.

Molecular Oxygen and Chemiluminescent Organic Reactions

Many of the reported chemiluminescent organic reactions involve molecular oxygen (a ground state triplet termed $^3\Sigma$ oxygen) or an O—O (peroxide) bond in some manner.[1,9] The lowest excited state of molecular oxygen is a singlet state (termed the $^1\Delta$ state of molecular oxygen). The $^1\Delta$ state of oxygen is involved in many chemiluminescent processes. For example, the reaction of $^1\Delta$ oxygen with electron-rich ethylenes sometimes produces cyclic peroxides which undergo chemiluminescent fragmentation reactions:[10]

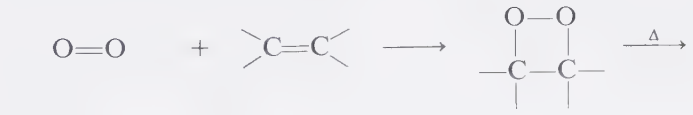

$^1\Delta$ Singlet oxygen — Electron-rich ethylene — Dioxetane

(14.7)

Singlet oxygen is also a primary *product* of certain reactions. For example, it has been shown that $^1\Delta$ is produced when the endo peroxides of anthracenes are thermolyzed (Eq. 14.5).[7]

What are the special features of molecular oxygen or of peroxide bonds that have such a pervasive influence in efficient chemiluminescent reactions? A partial answer is revealed in the *energetics* of reactions involving molecular oxygen and peroxide bonds. For example, the reactions of $^1\Delta$ and $^3\Sigma$ oxygen with simple ethylenes to yield ketones are exothermic by about 100 kcal mole and 80 kcal mole, respectively.[11] Also, cleavage of an O—O bond occurs in many cases and brings the molecule to the diradicaloid geometry required for an effective surface jump (see Fig. 14.3).

14.2 Molecular Oxygen: Ground State ($^3\Sigma$) and Excited Singlet States ($^1\Delta$ and $^1\Sigma$)

Molecular oxygen is an important participant in photochemical processes because of its high chemical energy content, its unique reactivity characteristics, its low-lying excited state, and its ubiquity as an "impurity" in reaction systems. The reactions of the excited states of molecular oxygen are intriguing in their own right.

Two Lewis structures for molecular oxygen (1 and 2) serve as a basis for discussion of its chemistry:

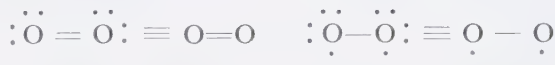

1, electrons paired **2**, electrons unpaired (14.8)

Structure **1**, in which all the electrons are paired, corresponds to a singlet state structure, while structure **2**, in which two electrons are unpaired, may correspond to either a singlet or a triplet state. We expect the chemistries of the states of molecular oxygen corresponding to structures **1** and **2** to be quite different. However, it is not obvious how to correlate structures **1** and **2** to particular electronic states. This correlation is best done in terms of a molecular orbital description of oxygen. The ground state of O_2 is described by the electron configuration:

$$O_2 \rightarrow (\text{core})(\pi_x)^2(\pi_y)^2(\pi_x^*)^1(\pi_y^*)^1 \tag{14.9}$$

Ignoring all but the two highest-energy electrons, we have:

$$O_2 \rightarrow (\pi_x^*)^1(\pi_y^*)^1 \tag{14.10}$$

Schematic descriptions of the π_x^* and π_y^* orbitals of the oxygen molecule are shown in Figure 14.4. Because the π_x^* and π_y^* orbitals are degenerate, and because the ground state of O_2 has two electrons for the occupancy of these orbitals, the ground state of molecular oxygen is predicted (Hund's rule) and found to be a triplet, i.e., for a given degenerate electronic configuration, the state of highest multiplicity lies lowest.

Consider the orbital occupancies of the $(\pi_x^*)(\pi_y^*)$ pair and their corresponding spin states.[12] The four possible orbital occupancies correspond to a lowest energy triplet state and three singlet states:

$$\begin{aligned} T &\rightarrow (\pi_x^*\uparrow)(\pi_y\uparrow) && \text{called } {}^3\Sigma \\ S &\rightarrow (\pi_x^*\downarrow)(\pi_y^*\uparrow) && \text{called } {}^1\Sigma \\ S &\rightarrow (\pi_x^*\uparrow\downarrow)^2 && \text{called } {}^1\Delta_x \\ S &\rightarrow (\pi_y^*\uparrow\downarrow)^2 && \text{called } {}^1\Delta_y \end{aligned} \tag{14.11}$$

These four states have been given spectroscopic notations of ${}^3\Sigma$, ${}^1\Sigma$, ${}^1\Delta_x$, and ${}^1\Delta_y$, respectively. The electron orbital occupancy corresponding to these four states leads to the electronic distributions shown on the right-hand side of Figure 14.4. The two Σ states possess an electronic distribution which is cylindrically symmetric about the bond axis. The Δ states possess an electronic distribution such that two π^* electrons are in one of two mutually perpendicular planes. The π^* electronic distribution of the Δ states is reminiscent of the π electronic distribution of ethylene, except that there is a nodal plane passing through the center of the O –O bond. The ${}^1\Delta_x$ and ${}^1\Delta_y$ states are degenerate in the Zero-Order Approximation. Approach

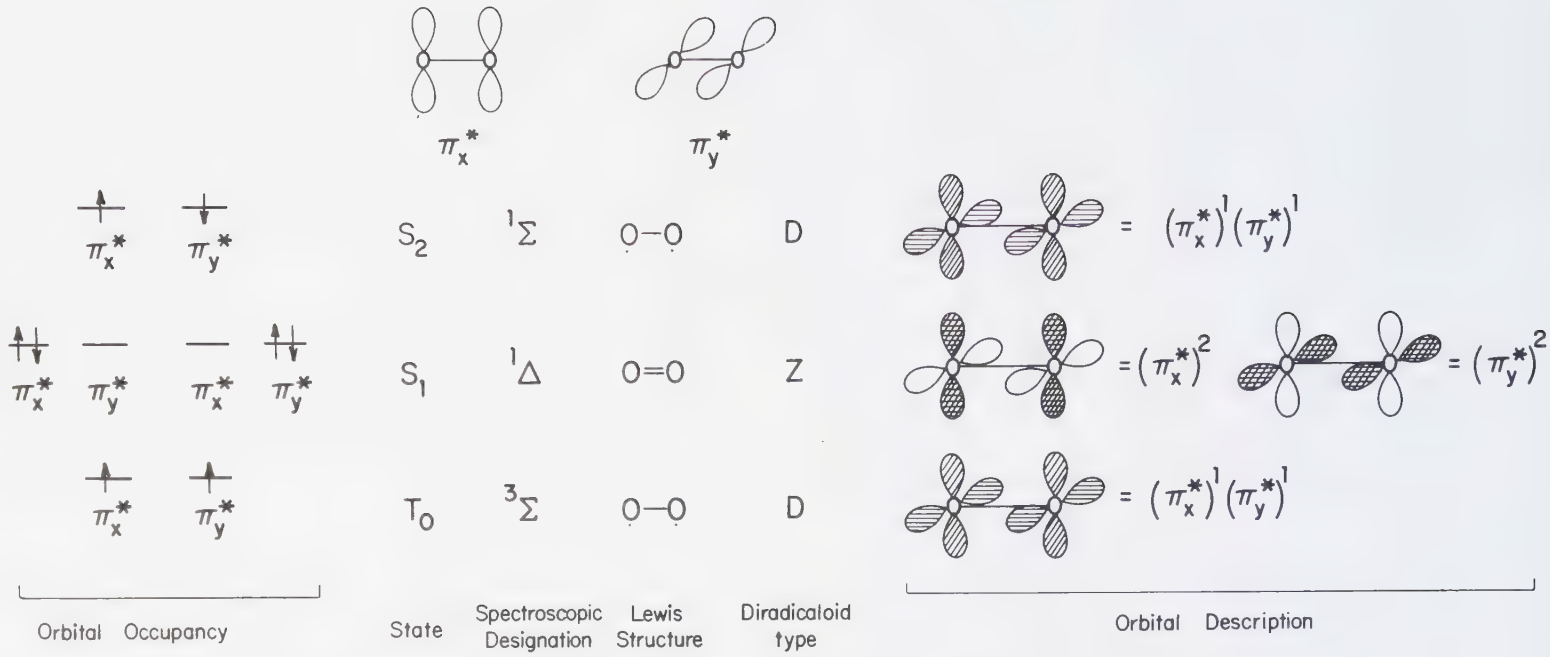

Figure 14.4

A qualitative description of the three lowest electronic orbital configurations and states of molecular oxygen.

of another molecule will cause a splitting of these two states. We shall ignore the degeneracy and refer to S_1 as $^1\Delta$, by which we imply either $^1\Delta_x$ or $^1\Delta_y$. The $^1\Delta$ state of molecular oxygen is generally referred to as "singlet oxygen" by organic chemists.[13]

From the Lewis structures and the orbital descriptions of molecular oxygen we deduce that:

1. The spin-independent chemical reactivity of $^3\Sigma$ and $^1\Sigma$ should be similar, since both possess an identical electronic distribution in Zero Order.

2. The reactions of $^3\Sigma$ and $^1\Sigma$ should be radical-like in character (i.e., they are diradicaloid states).

However, the electron-paired Lewis structure **1** (Eq. 14.8) does not properly reveal the zwitterionic reaction-chain activities of $^1\Delta$ oxygen. The zwitterionic character of this state derives from the wave functions for the $^1\Delta$ state.[12] Perturbation by an attacking reagent will polarize the electronic structure of $^1O_2$ so that it resembles the Lewis structures shown in:

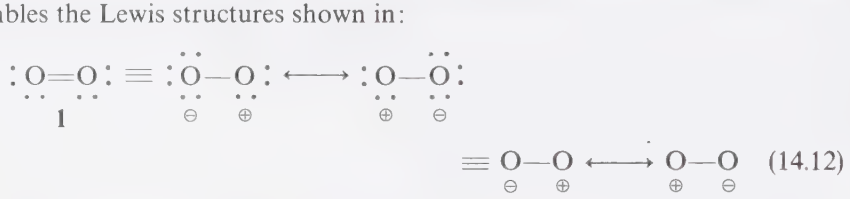

(14.12)

The State Diagram and Potential Energy Curves for Molecular Oxygen: Energetics and Dynamics

The potential energy curves for molecular oxygen are given in Figure 14.5. Due to the very weak electronic coupling between the $^3\Sigma$ and $^1\Delta$ states of oxygen in the "free" molecule, even simple collisions provide significant spin-orbit perturbation mechanisms to mix these two states.[14] As an example of the magnitude of the environment on the probability of the radiative $^3\Sigma \rightarrow {}^1\Delta$ transition (which, incidentally, is a magnetic dipole transition), the oscillator strength of the transition increases by 10^3 upon going from low pressures in the vapor to solution. The pure radiative lifetime of $^1\Delta$ molecular oxygen decreases from the order of tens of minutes to seconds.[15]

Experimentally, the energetic ordering of the lowest electronic states of molecular oxygen is found to be $^3\Sigma < {}^1\Delta$ (22.5 kcal/mole) $< {}^1\Sigma$ (37.5 kcal/mole). The pure radiative lifetimes of $^1\Delta$ and $^1\Sigma$ are quite long; 2.7×10^3 sec and 7.1 sec, respectively.[16] Such long lifetimes are usually not observed under laboratory conditions because at ordinary pressures or in solution, collisional or chemical deactivation of $^1\Delta$ and $^1\Sigma$ occurs efficiently. However, the radiationless conversion of $^1\Delta$ to $^3\Sigma$ is spin-forbidden and might be expected to be quite slow. In fact, in condensed phases the rate of this intersystem crossing process is quite variable.[17] Apparently the $^1\Delta$ state interacts with all solvents in such a manner as to allow intersystem crossing to occur. The longest lifetimes of $^1\Delta$ ($\sim 10^{-3}$ sec) are observed in solvents normally considered to be chemically inert (e.g., fluorinated materials).

The lifetime of the $^1\Sigma$ state in solution is not known, since no direct method for probing its decay has been devised. It would be interesting to see if this state persists long enough to be detected spectroscopically in fluorocarbon solvents. The $^1\Delta$ species can be generated in a number of ways and then be trapped. The disappearance of the trapping agent can be determined spectroscopically, and thus serves as a monitor of $^1\Delta$ oxygen. The lifetime of $^1\Delta$ in various solvents has been measured by this technique; the results are given in Table 14.1.

Methods of Generating Singlet Oxygen

Many methods have been developed for the generation of $^1\Delta$ molecular oxygen. Both thermal and photochemical methods are utilized.[18] Although the direct photoexcitation of molecular oxygen is possible, it is not a practical photochemical method.[19] However, the *triplet* photosensitized production of singlet oxygen is a general and synthetically useful method of generating singlet oxygen (Eqs. 14.13*a* and *b*). Commonly, a strongly absorbing dye (Rose Bengal, methylene blue, etc.) is employed as photosensitizer:[18]

$$\text{Sens} + h\nu \rightarrow {}^1\text{Sens} \rightarrow {}^3\text{Sens} \qquad (14.13a)$$

$${}^3\text{Sens} + {}^3\text{O}_2 \rightarrow \text{Sens} + {}^1\text{O}_2 \qquad (14.13b)$$

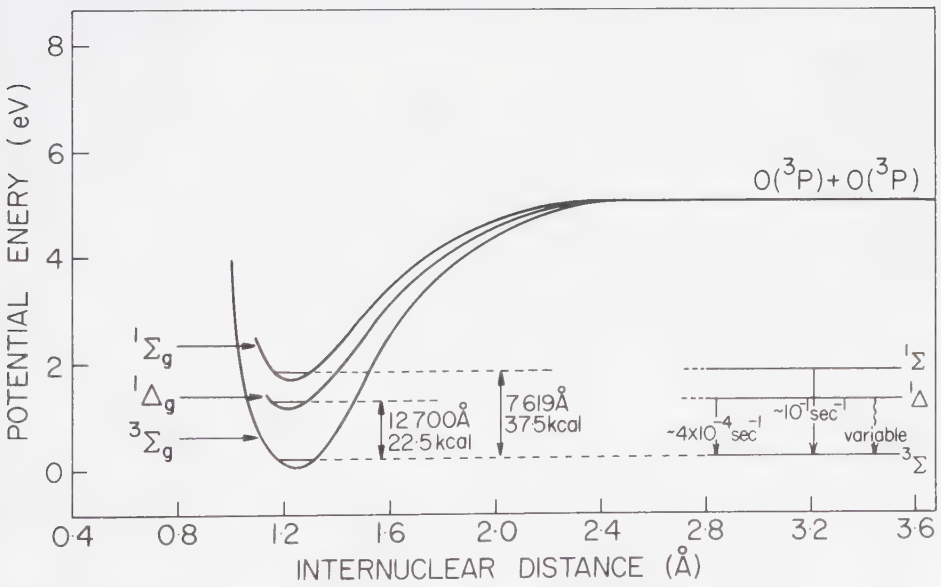

Figure 14.5

Potential energy curves for the three lowest electronic states of molecular oxygen. The energies and inherent radiative lifetimes of the $^1\Delta$ and $^1\Sigma$ states are also listed.

Equation 14.13b represents a *triplet-triplet* annihilation which results in an energy transfer to yield $^1O_2$. This annihilation is depicted in terms of orbitals in Figure 14.6. It is generally assumed that an electron exchange mechanism operates in the triplet-photosensitized formation of singlet oxygen. A range of ^{3}sens interactions with $^3\Sigma$ may operate in any given case. Thus, mechanisms varying from weak overlap and a simple collisional energy exchange to an electron transfer or diradical formation via bonding may occur:

Electron exchange

$$^3\text{Sens}\text{-----}^3O_2 \rightarrow \text{Sens} + {}^1O_2 \tag{14.14}$$

Electron transfer

$$\left\{\begin{array}{rl} {}^3\text{Sens} + {}^3O_2 \rightarrow & \text{Sens}^+ + O_2^- \ (D_\pm) \quad (14.15) \\ \rightarrow & \text{Sens} + {}^1O_2 \quad (14.16) \end{array}\right.$$

Diradical formation

$$\left\{\begin{array}{rl} {}^3\text{Sens} + {}^3O_2 \rightarrow & \dot{\text{S}}\text{ens} - \text{O} - \dot{\text{O}} \ (D) \quad (14.17) \\ \rightarrow & \text{Sens} + {}^1O_2 \quad (14.18) \end{array}\right.$$

These photochemical mechanisms for generating $^1O_2$ are radical-like in nature, since the key interactions involve diradicaloid structures. The thermal generation of singlet oxygen usually involves two electron (zwitterionic) processes. This

Table 14.1 Lifetime of Singlet Molecular Oxygen ($^1\Delta$) in Various Solvents at Room Temperature

Solvent	τ (in μ sec)	Reference (see below)
H_2O	2	1
$HCON(CH_3)_2$	7	6
CH_3OH	7	1
EtOH	10	5, 6
$CH_3CH_3CH_2Br$	10	7
D_2O	20	2
C_6H_{12}	16	5
C_6H_6	24	1
$(CH_3)_2CO$	25	1
$(CD_3)_2CO$	25	1
CH_3CN	30	5
$CHCl_3$	60	3
CS_2	200	1
$CDCl_3$	300	3
C_6F_6	600	3
CCl_4	700	5
CF_3Cl (Freon 11)	1,000	3
Vapor (1 atm)	80,000	4
Radiative (zero pressure)	2,700,000,000	4

1. Merkel, P. B., and Kearns, D. R., *J. Am. Chem. Soc.*, *94*, 1029 (1972).
2. Merkel, P. B., Nilsson, R., and Kearns, D. R., *ibid.*, *94*, 1030 (1972).
3. Long, C. A., and Kearns, D. R., *ibid.*, *97*, 2018 (1975).
4. Badger, R. M., Wright, A. C., and Whitlock, R. F., *J. Chem. Phys.*, *43*, 4345 (1965); see also Wayne, R. P., *Adv. Photochem.*, *7*, 400 (1969); Gleason, W. S., et al., *J. Am. Chem. Soc.*, *92*, 2068 (1970).
5. Merkel, P. B., and Kearns, D. B., *J. Am. Chem. Soc.*, *94*, 7244 (1972).
6. Adams, D. R., and Wilkinson, F., *J. Chem. Soc. Faraday, Trans II*, *68*, 586 (1972).
7. Wilkinson, F., *Singlet Oxygen Reactions with Polymers*, New York: John Wiley, 1978, p. 27.

means that $^1\Delta$ (a zwitterion structure, see Eq. 14.12) is the product to be expected from thermal generation of $^1O_2$. Of the many thermal reactions that have been found to generate $^1O_2$, the more synthetically useful examples involve decomposition of phosphite ozonides (Eq. 14.19)[20] or endoperoxides (Eq. 14.20).[7,21]

$$(RO)_3PO_3 \xrightarrow{\Delta} (RO)_3PO + {}^1O_2 \tag{14.19}$$

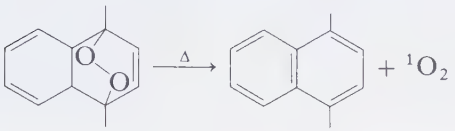

(14.20)

Notice that these reactions are *chemiluminescent* reactions because $^1O_2$ is an electronically excited product. Indeed, reactions such as 14.20 (and 14.5) are experimentally found to be chemiluminescent.

Quenching of Excited Singlet and Triplet States by Molecular Oxygen

Ground state molecular oxygen is a general and efficient quencher of the S_1 and T_1 states of organic molecules.[22,23] With few exceptions, the rate constant for quenching is within an order of magnitude of the diffusional quenching constant (see Table 14.2). The quenching mechanism may be physical or chemical in nature. The two most common chemical mechanisms are probably diradicaloid electron

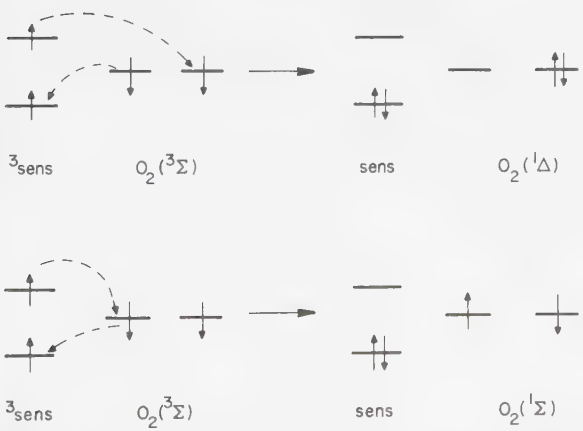

Figure 14.6

Molecular orbital description of the triplet-sensitized generation of singlet oxygen. An electron exchange mechanism is assumed. The diagrams do not correctly display the spin statistics of the process. Only one out of nine possible triplet-triplet spin combinations is correct for formation of singlet products. If special dephasing or spin flipping mechanisms are operative, the spin statistics do not apply.

transfer and addition:

$$\text{Electron transfer} \quad M^* + O{-}O \rightarrow M^+ + O_2^{\cdot -} \qquad D_{\pm} \qquad (14.21)$$

$$\text{Diradical formation} \quad M^* + O{-}O \rightarrow \dot{M}{-}O{-}\dot{O} \qquad D \qquad (14.22)$$

Physical quenching mechanisms include exciplex formation and energy transfer (e.g., Eq. 14.14).

From Table 14.2 some important generalizations may be made:

1. In general, quenching of S_1 of aromatic hydrocarbons occurs at close to the diffusional rate.

2. Quenching of T_1 of aromatic hydrocarbons usually occurs within an order of magnitude of the diffusional rate, but is consistently slower than quenching of S_1.

3. Some n, π^* states are only weakly quenched by $^3O_2$, but others are efficiently quenched.

The k_q value should depend on the electron donor properties of the quenchee (i.e., be related to its ionization potential).[24] Such behavior has been observed experimentally. For example, the quenching of substituted benzenes by molecular oxygen is only slightly dependent on molecular structure when the ionization potential of the aromatic molecule is *less* than ~ 9 eV. When the quenchee ionization potential is greater than this value, k_q falls off.

Experimentally, it is found that quenching of the *singlet* states of aromatic hydrocarbons by oxygen occurs at a comparable rate even when the S_1–T_1

Table 14.2 Rate Constants for Quenching of Excited Singlet and Triplet States by Molecular Ground-State Oxygen

Compound	Singlet quenching (M^{-1} sec^{-1})	Triplet quenching (M^{-1} sec^{-1})	Reference
Benzene	2×10^{10}	—	1, 2
Naphthalene	3×10^{10}	—	1, 2
Anthracene	3×10^{10}	3×10^{9}	1, 2
Pyrene	3×10^{10}	2×10^{9}	1, 2
Perylene	2×10^{10}	—	2
Acetophenone	—	3×10^{9}	3
Benzophenone	—	1×10^{9}	3
Benzil	—	1×10^{9}	3
Hexafluoracetone	8×10^{7}	4×10^{8}	4
Diaza-Bicyclo[2.2.2]octene	1×10^{10}	—	5
2-Acetylnaphthalene	—	2×10^{8}	6
4-Phenylbenzophenone	—	8×10^{7}	6

1. Kearns, D., *Chem. Rev.*, *91*, 395 (1971).
2. Gijzman, O. L. J., et al., *Faraday Trans. II*, *70 708* (1973).
3. Carbon tetrachloride at 25 . Merkel, P. B., and Kearns, D., *J. Chem. Phys.*, *58*, 398 (1973).
4. Vapor phase measurement. Ware, W., and Lee, S. K., *J. Chem. Phys.*, *49*, 217 (1968).
5. Liu, C. K., unpublished results.
6. Morina, V. F., and Sveshnikova, E. B., *Opt. Spectroscopy*, *34*, 359 (1973)

energy gap of the aromatic is smaller than the $^3\Sigma$–$^1\Delta$ energy gap of oxygen (anthracene [$\Delta E \sim 34$ kcal/mole], $k_q \sim 3 \times 10^{10}$ M^{-1} sec^{-1}, triphenylene [$\Delta E \sim$ 15 kcal/mole], $k_q \sim 2 \times 10^{10}$ M^{-1} sec^{-1}). Thus, a $S_1 + O_2(^3\Sigma) \rightarrow T + O_2(^1\Delta)$ energy transfer cannot be a general requirement for quenching.[25] There is evidence that in the vapor phase, singlet quenching does not yield $^1\Delta$ oxygen; on the other hand, the *triplet* state of the donor *is* produced by the quenching.[26] Thus, quenching of singlet state by $O_2(^3\Sigma)$ amounts to catalyzed intersystem crossing:[27]

$$\underset{\text{crossing}}{\overset{\text{Oxygen catalyzed intersystem}}{}} \quad S_1 + O_2(^3\Sigma) \rightarrow T + O_2(^3\Sigma) \tag{14.23}$$

An interesting feature of diffusional quenching by $^3O_2$ is that this diatomic diffuses considerably faster than most organic molecules. For example, in benzene near room temperature, oxygen diffuses two to three times faster than anthracene.[28] Another important practical feature of quenching by molecular oxygen is its low solubility in most organic solvents $[O_2] \sim 10^{-2}$ M at 760 mm O_2. Since concentrations of O_2 greater than 10^{-2} M are not obtainable unless external pressures greater than 760 mm of O_2 are applied, if $k_q \sim 10^{10}$ M^{-1} sec^{-1}, then $k_q[O_2] \lesssim 10^8$ sec^{-1} at ordinary pressures. Thus, S_1 or T_1 states with decay rates on the order of 10^8–10^9 sec^{-1} will not be efficiently quenched in air-saturated solutions and will be only moderately quenched in oxygen-saturated solutions.

On the other end of the dynamic spectrum, if $[O_2] \sim 10^{-6}$ M (a value corresponding to "degassing" by saturation with nitrogen) then the maximal $k_q[O_2]$ of $\sim 10^4$ sec^{-1} will be sufficient to strongly quench triplets whose decay rates are smaller than 10^3 sec^{-1}. Since it is experimentally impractical to routinely achieve $[O_2] \sim 10^{-7}$ M, it is clear that the lifetime of triplets in solution will not exceed $\sim 10^{-3}$ sec if they are efficiently quenched by oxygen.

Chemistry of Molecular Oxygen

The Zero Order orbital descriptions of $^3\Sigma$ and $^1\Delta$ are the starting points for a description of the effect of any perturbation which destroys the Zero Order cylindrical symmetry of the oxygen molecule, e.g., the approach of a reactive molecule (see Fig. 14.4). In general, the effect of such a perturbation mixes the Zero Order $^1\Sigma$ state with the $^1\Delta$ state, and generally causes the latter to become lower in energy. Thus, the $^3\Sigma$ and $^1\Delta$ descriptions are useful descriptions for the behavior of molecular oxygen at the initial stages of a reaction.

Most of the known general reactions of $^1\Delta$ oxygen may be classified as one of three types:[18,29]

1. Hydrogen abstraction and addition (the *ene* reaction):

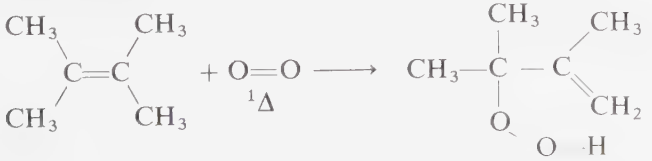

(14.24)[30]

An allylic hydroperoxide

2. [2 + 2] and [4 + 2] cycloaddition reactions:

$$O{=}O + CH_3CH_2OCH{=}CHOCH_2CH_3 \xrightarrow[[2+2]]{} \underset{CH_3CH_2OCH—CHOCH_2CH_3}{\overset{O—O}{|\quad|}} \quad (14.25)^{31}$$

$^1\Delta$

a 1,2-dioxetane

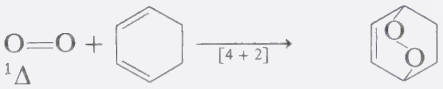

(14.26)[32]

An endo-peroxide

3. Oxygenation:

$$R—S—R + O{=}O \rightarrow R_2SO \quad (14.27)^{33}$$

In general, the mechanisms of these reactions are not known, although the ene reaction and formation of 1,2-dioxetanes exhibit many of the characteristics associated with concerted reactions. In general, the rates of the reactions of $^1\Delta$ increase as the ionization potential of the substrate decreases. This suggests that a charge transfer character (substrate electron donor-$^1\Delta$ electron acceptor) generally occurs at the initial stages of reaction.

The data in Table 14.3, which surveys the rate constants for quenching of $^3O_2$ by various substrates, confirms the postulate that charge transfer interactions are most important in determining the reactivities of quenchers toward deactivation of $^1O_2$.[34] Although many electronic effects must be operating, a general tendency toward low ionization potential → large k_q is evident.

According to quantitative MO calculations, the most favored geometry for initial interaction of $O_2(^1\Delta)$ with C=C bonds has been proposed to be a single-atom, end-on interaction.[35] Continuation of this interaction could lead to

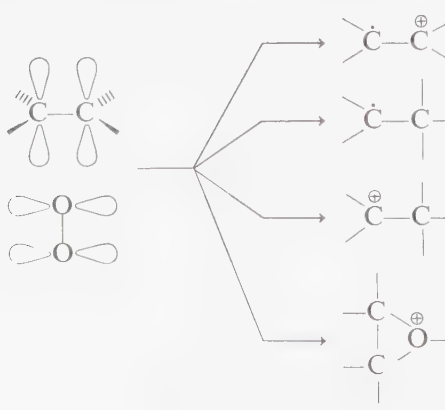

Superoxide formation (14.28)

Diradical (14.29)

Zwitterion (14.30)

Perepoxide (14.31)

(a) transfer of an electron to form a $D_{\pm}$ pair (Eq. 14.28), (b) addition to form a diradical D (Eq. 14.29), (c) addition to form a zwitterion (Eq. 14.30), or (d) addition to form a perepoxide (Eq. 14.31). The mechanism that actually occurs depends strongly on the substrate structure. Also, it is possible that when the substrate is a nonpolar species, a *concerted* reaction leading directly to products such as those given in Eqs. 24–27 may result. For example, the ene reaction of $^1\Delta$ with alkyl ethylenes appears generally to be a concerted reaction,[18] as does the [4 + 2] cycloaddition of $^1\Delta$ to 1,3-dienes.

Table 14.3 Rate Constants for Quenching of $^1\Delta$ Oxygen by Various Singlet Oxygen Quenchers

Quencher	k_q (M^{-1} sec^{-1})	Reference
CF_2ClCCl_2F	$<10^2$	1
Cyclohexene (C_6H_{10})	4×10^3	2
1,4-Dimethylnaphthalene	1×10^4	5
CH_3CH_2I	2×10^4	9
$CH_3CH_2NH_2$	3×10^4	3
$O_2(^3\Sigma)$	6×10^4	4
Cyclopentene (C_5H_8)	7×10^4	2
Anthracene	1×10^5	5
D_2O	1×10^5	6
$CH_3CH_2CH_2NH_2$	2×10^5	3
Diphenylanthracene	1×10^6	5
H_2O	1×10^6	6
Trimethylethylene	2×10^6	2
$(CH_3CH_2)_3N$	2×10^6	3
2,5-Dimethyl-2,4-hexadiene	2×6	6
1,3-Cyclohexadiene	4×10^6	11
$CH_3CH_2SCH_2CH_3$	6×10^6	12
1,3-Cyclopentadiene	1×10^7	7
9,10-Dimethyoxyanthracene	1×10^7	5
Tetramethylethylene	$\sim 5 \times 10^7$ (1×10^6)	2, 10
1,4-Diazabicyclooctane (DABCO)	3×10^7	8
Rubrene	4×10^7	5
I^-	8×10^7	12
Nickel (II) chelates	3×10^8	9
α-Terpinene	3×10^8	12
2,5-Dimethylfuran	4×10^8 (2×10^7)	6, 10
1,3-Diphenylisobenzofuran	1×10^9	1
Pentacene	4×10^9	5
β-Carotene	1×10^{10}	8

1. Matheson, I. B. C., Lee, J., Yamanashi, R. S., and Wolbarsht, M. L., *J. Am. Chem. Soc.*, *96*, 3343 (1974).
2. Ashford, R. D., and Ogryzlo, E. A., *ibid.*, *97*, 3604 (1975); Monroe, B., *J. Phys. Chem.*, *82*, 15 (1978).
3. Matheson, I. B. C., and Lee, N., *J. Am. Chem. Soc.*, *94*, 3310 (1972); Monroe, B., *J. Phys. Chem.*, *81*, 1861 (1977).
4. Stevens, B., *Acc. Chem. Research*, *6*, 90 (1973).
5. Stevens, B., Perez, S. R., and Ore, J. A., *J. Am. Chem. Soc.*, *96*, 6846 (1974).
6. Merkel, P. B., and Kearns, D. B., *J. Am. Chem. Soc.*, *94*, 7244 (1972).
7. Furukowa, K., Gray, E. W., and Lgryzlo, E. A., *Ann. N.Y. Acad. Sci.*, *171*, 175 (1970).
8. Carlsson, D. J., Suprunchuk, T., and Miles, D. M., *Can. J. Chem.*, *52*, 3728 (1974).
9. Wilkinson, F., *Singlet Oxygen Reactions with Polymers*, New York: John Wiley, 1978, p. 27. For a large compilation of quenching constants for singlet oxygen by metal complexes, see Ziweig, A., and Henderson, W. A., *J. Polymer Sci.*, *13*, 717 (1975).
10. Value in parenthesis refers to gas phase values of k_q.
11. Calculations from data in Higgins, R., Foote, C. S., and Cheng, H., *Adv. Chem. Ser.*, *77*, 102 (1968).
12. Gollnick, K., *Singlet Oxygen Reactions in Polymers*, New York: John Wiley, 1978, p. 111.

14.3 Chemiluminescence of 1,2-Dioxetanes and Endo Peroxides

Numerous dioxetanes and dioxetanones, once believed to be only fleeting intermediates and too unstable to be isolated, have now been prepared.[36] Many are isolable and quite stable at room temperature and one (bis adamantylidene adamantane dioxetane) is stable beyond 150 °.[31] The activation parameters of a number of dioxetanes are in the range of 25 ± 5 kcal/mole.[36] As a typical example, tetramethyl-1,2-dioxetane (TMD) is a yellow solid (it exists as beautiful long needles) at room temperature.[8] It melts at 78 °C and, if cooled quickly, resolidifies. Upon continued heating, TMD is converted quantitatively to acetone with $E_a \sim$ 28 kcal/mole. Studies (described below) indicate that thermolyses of all 1,2-dioxetanes display two important chemiluminescent properties (Section 14.10): (a) they cleave quantitatively into two carbonyl fragments, one of which is electronically excited ($\phi^* \sim 100$ to 1%); (b) the directly produced excited fragment is predominantly triplet rather than singlet ($\phi_T^*/\phi_S^* \sim 10$ to 1000). Thus, thermolyses of dioxetanes display two unusual and remarkable features: excited states are produced in high yields, and a spin-forbidden pathway is favored over a spin-allowed pathway.

The decomposition of endo-peroxides (Eqs. 14.5 and 14.20) are often chemiluminescent due to emission from aggregates of singlet oxygen or from the aromatic chromophore.[37,38]

Experimental Methods for Analyzing the Chemiluminescent Reactions of Cyclic Peroxides

All 1,2-dioxetanes and most endo-peroxides of aromatic compounds prepared to date are either chemiluminescent or capable of inducing the luminescence of an additive. Thus, a $\Delta H \rightarrow *$ step is common to the thermolysis of these compounds. What are the structural features and mechanistic details of these thermolyses? What makes the peroxide's ring system such a common ingredient in chemiluminescent systems? In other words, what qualities of these thermolyses allow the $\Delta H \rightarrow *$ to occur and do so efficiently? Why do the thermolyses of simple 1,2-dioxetanes produce triplets selectively, whereas the thermolyses of endo-peroxides produce singlet O_2 selectively? Before seeking answers to these questions, let us review some important aspects of the theory of chemiluminescence reactions.[39]

Consider the reactions:

	Rate	
$R \rightarrow P^*$	$k_1[R]$	(14.32)
$P^* \rightarrow P + h\nu$	$k_*[P^*]$	(14.33)
$R \rightarrow$ "dark" reactions	$k_d[R]$	(14.34)
$P^* \rightarrow$ "dark" reactions	$k_d'[P^*]$	(14.35)

The fundamental experimental parameter in chemiluminescence studies is the *intensity* of luminescence, I, the units of which are moles of photons per second per liter. The key equation which relates the value of the measured quantity I to microscopic quantities is:

$$I = k_1[R]\phi_*\phi_e \tag{14.36}$$

i.e., the measured intensity (I) equals the total rate of decomposition of $R(k_1[R])$ times the probability (ϕ_*) that decomposition of molecules of R will produce an excited molecule, times the probability (ϕ_e) that an excited molecule will emit a photon. Thus, the macroscopic observation of light emission provides information on the microscopic transition state for decomposition of R (via k_1).

If a quencher molecule (Q) is added to the solution of R, I will drop to a new value I^Q because some of the excited molecules (P^*) have been quenched *before* they can emit. The difference between I and I^Q is simply a measure of the effectiveness of Q as a quencher of P^*, and on the microscopic level is a reflection of the competition between all of the normal unimolecular decay paths of P^* (which include light emission) and the new bimolecular decay path introduced by adding Q:

		Rate	
Quenching of P^* by Q	$P^* + Q \rightarrow A + P^*$	$k_q[Q][P^*]$	(14.37)

The Stern-Volmer relationship (Eq. 14.39) provides a quantitative connection between the measured values of I and I^Q, the quencher concentration $[Q]$, and the rate constant k_* (defined as τ_*^{-1} the inverse of the lifetime of P^*).

$$\frac{I}{I^Q} = 1 + k_q[Q]/k_* \qquad \text{Stern-Volmer relationships} \tag{14.38}$$

$$\frac{I}{I^Q} = 1 + k_q\tau_*[Q] \tag{14.39}$$

A linear plot of I/I^Q versus $[Q]$ confirms the simple competition of Eq. 14.37 and the unimolecular decay of P^*, and the slope of this plot is equal to $k_q\tau_*$. It should be noted that I^Q is less than I, according to Eq. (14.36), not because the rate ($k_1[R]$) or the excitation probability has changed, but because ϕ_e, the probability of emission, drops to a smaller value, ϕ_e^Q due to the occurrence of Eq. 14.37.

The *efficiency* of a chemiluminescent reaction (ϕ_{CL}) is simply the probability that an excited state will form times the probability that the latter will emit:

$$\phi_{CL} = \phi_*\phi_e \tag{14.40}$$

If the key intermediate R is itself produced in a reaction from a prior reagent R', then the efficiency of chemiluminescence starting from R' must include the

efficiency (ϕ_R) of the R' to R conversion:

$$\phi_{CL} = \phi_R \phi_* \phi_e \tag{14.41}$$

In many chemiluminescent reactions emission is not observed from the primary product of the chemiexcitation step P^*, but instead from A^*, a species capable of accepting energy from P^* and then emitting. In this case (called *indirect* chemiluminescence, in contrast with *direct* chemiluminescence from P^*) the efficiency of energy transfer (ϕ_{ET}) to produce A^* and the efficiency of emission (ϕ_e^A) from A^* replace the emission efficiency in Eq. 14.41:

$$\phi_{CL} = \phi_R \phi_* \phi_{ET} \phi_e^A \tag{14.42}$$

The fact that Eq. 14.42 contains *four* probabilities would lead us to expect that complicated chemical sequences are not likely candidates for efficient chemiluminescent reactions. Thus, we expect high efficiency only in systems corresponding to Eq. 14.40. This is generally correct, but some important exceptions occur.

The most efficient chemiluminescent system reported to date is the bioluminescence of the firefly.[4] Bioluminescence requires a lumophore, and enzymes which mediate the key chemiexcitation step.[2] The enzyme associated with the lumophore is called *luciferin*. The enzyme which "triggers" the chemiluminescent reaction is called *luciferase*. Commonly, molecular oxygen is also required. In the case of the firely luciferin-luciferase system, a quantum yield of $\phi_{CL} = 1.0$ has been measured. A peroxylactone is believed to be a key intermediate:

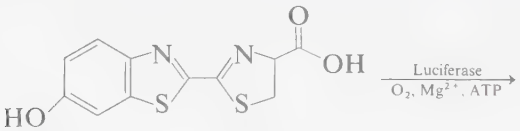

Lumophore of firefly

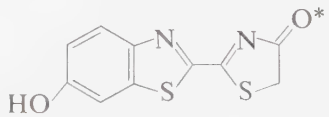

$\Phi_{CL} = 1.0$

(14.43)

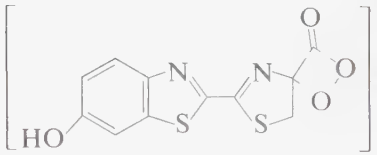

Peroxylactone intermediate

(14.44)

The most efficient "synthetic" chemiluminescent system ($\phi_{CL} \sim 0.25$) involves a multistep sequence for which the reaction of H_2O_2 and an oxalate ester produces

a reactive intermediate, believed to be a cyclic peroxy dione (Eq. 14.46). The decomposition of the latter is catalyzed by various energy acceptors which are responsible for the observed emission. The mechanism of catalysis appears to be of a charge-transfer type, possibly an initial electron transfer followed by retransfer of an electron within a radical ion pair to produce an excited state (see Eq. 14.3).[40]

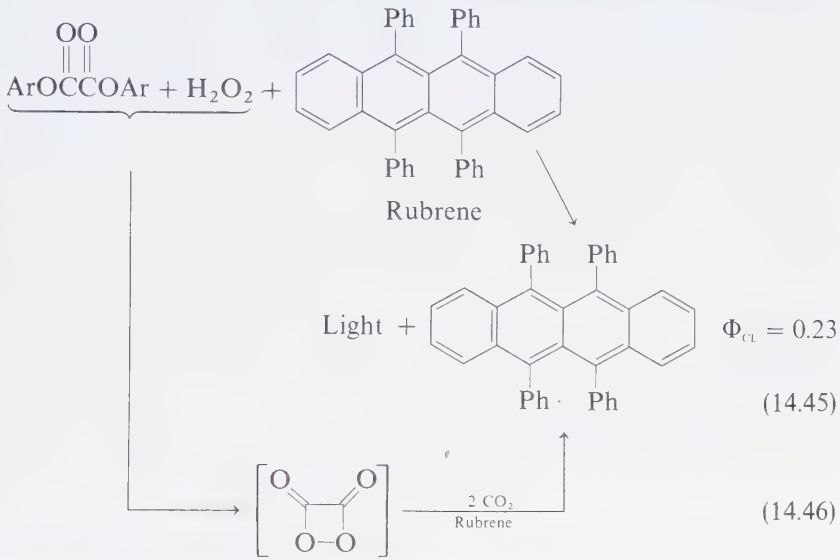

Thermolysis of 1,2-dioxetanes: A Model System

We shall employ tetramethyl-1,2-dioxetane (TMD) as a model system to discuss chemiluminescent organic reactions.[41] The thermolysis of TMD yields acetone in quantitative yield (Eq. 14.47). The thermolysis is clearly First Order and the activation enthalpy in acetonitrile is $\Delta H^{\ddagger} \sim 27$ kcal mole. The enthalpy of reaction (ΔH_0) in solution is ~ 63 kcal/mole.[42]

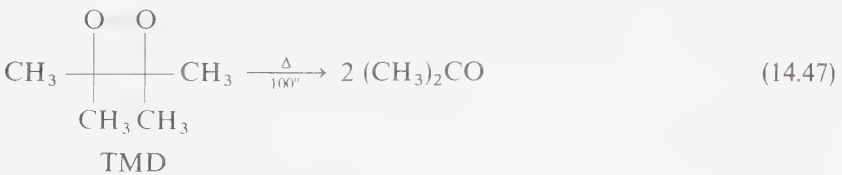

Figure 14.7 compares the reaction energetics to the state energy diagram of acetone. It can be seen that the sum $\Delta H_0 + \Delta H^{\ddagger}$ is greater than the energy required to populate *either* $S_1(n, \pi^*)$ or $T_1(n, \pi^*)$ of acetone. We say that the reactions TMD $\rightarrow {}^1(n, \pi^*)$ and/or ${}^3(n, \pi^*)$ are *energy-sufficient*, i.e., both products may be formed exothermically from the transition state for thermolysis.

Experimentally, one must seek to measure the primary efficiency of formation of $S_1(n, \pi^*)$ and $T_1(n, \pi^*)$ from TMD. This can be done by direct methods in which *chemiluminescence* emission from acetone-excited states is measured quantitatively

and compared to *photoexcited* emission. In effect, the number of fluorescence photons and phosphorescence photons may be titrated or measured quantitatively. From a knowledge of the fluorescence and phosphorescence quantum yields and other photochemistry of acetone, the primary excitation yields of acetone singlets (^1A) and triplets (^3A) may be derived.

The primary yield of ^1A and ^3A from thermolysis of TMD was first measured by chemical titration of acetone-excited states with trans-dicyanoethylene (t-DCE).[43] The latter reagent has been shown to react with ^1A to yield only an oxetane and to react with ^3A to yield only *cis*-dicyanoethylene (c-DCE). Thermolysis of TMD in the presence of t-DCE, and extrapolation of the yield of oxetane, and of c-DCE to infinite concentration of t-DCE, allow the determination of the primary yield of ^1A, i.e., $^1\phi_*$ and the primary yield of ^3A, i.e., $^3\phi_*$:

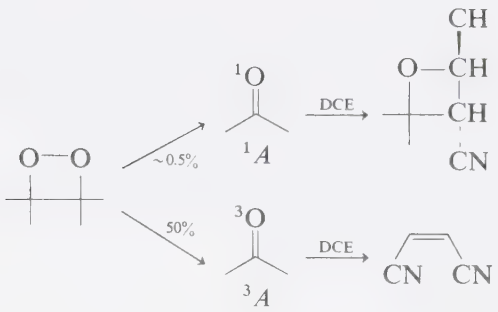

(14.48)

(14.49)

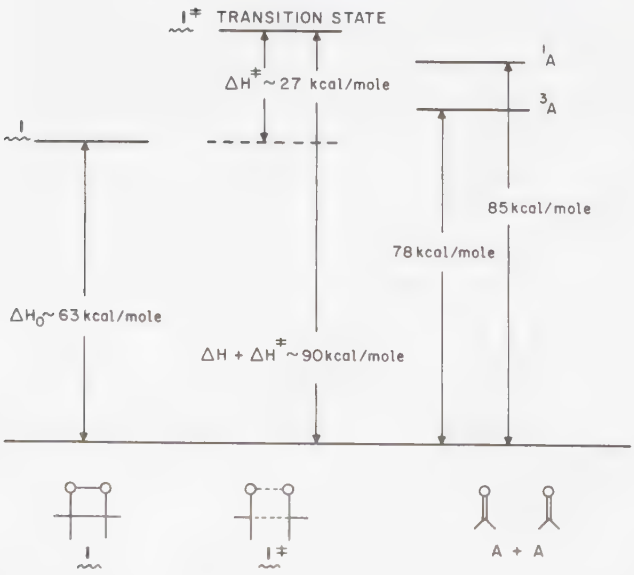

Figure 14.7
Thermochemistry of tetramethyl-1,2-dioxetane.

Remarkably, the experimental result is that ${}^1\phi_* \simeq 0.5\%$ and ${}^3\phi_* \simeq 50\%$. A chemiluminescence photon titration leads to the same conclusion: the predominant primary path in decomposition of TMD is the selective and efficient generation of ${}^3A$, i.e., an electronically nonadiabatic, spin-forbidden pericyclic fragmentation has occurred.

A simple, striking, and convincing experimental demonstration of the above conclusion was possible. The chemiluminescence of TMD consists of both acetone fluorescence (Eq. 14.50) and phosphorescence (Eq. 14.51):

$$ {}^1A \rightarrow A + h\nu_f \tag{14.50} $$

$$ {}^3A \rightarrow A + h\nu_p \tag{14.51} $$

The latter is very sensitive to quenching by O_2, whereas the former (because of the much shorter lifetime of the excited species) is not. Deaeration of a solution of TMD by simple nitrogen purging results in chemiluminescence which is essentially pure acetone *phosphorescence* ($\lambda^p_{max} = 430$ nm).[44] If air is admitted to the initially deaerated solution, the chemiluminescence intensity immediately drops to about 1% of pure acetone *fluorescence*. Photoexcitation of acetone (deaerated solutions) results in nearly pure *fluorescence*. Thus, when TMD is decomposed, ${}^3A$ must be produced directly and *not* via ${}^1A$, otherwise the ratio of fluorescence to phosphorescence would be the same in both chemiexcitation and photoexcitation.

Mechanism of The Chemiluminescence Thermolysis of 1,2-Dioxetanes. Chemiexcitation Mechanisms (The $\Delta H \rightarrow {}^*$ Step)

A central question which can be asked of all photoreactions is, "At which nuclear structure during the reaction does the electronic deexcitation or electronic relaxation occur?" This question is important because the rates of photoreactions—and hence the efficiencies and yields of photoproducts—depend on the rate of electronic relaxation. More specifically, it is important to establish at which nuclear structure or geometry deexcitation is possible and what factors determine the probabilities of deexcitation when these structures are achieved. The same kinds of questions can be asked about a reaction involving chemiexcitation. At what point does electronic excitation occur? What are the nuclear geometries for which chemiexcitation is possible, and what determines the efficiency of chemiexcitation when these geometries are achieved? In both these cases we are fundamentally concerned with how electronic excitation energy is converted into nuclear motion and chemical energy and vice versa. What are the structural features which might determine the rates of the $\Delta H \rightarrow {}^*$ step in thermolysis of TMD?

A simple qualitative model to analyze the chemiexcitation step in the thermolyses of dioxetanes is shown in Figure 14.8. The key four-atom array of the dioxetane ring is assumed to cleave in a more or less planar fashion. This allows us to formulate reaction 14.47 as *electronically forbidden* for the ground state of TMD. This means we expect a high-energy symmetry-imposed (Zero Order) barrier on the ground-state surface. We know from Chapter 7 that a triplet of TMD (symmetrical with respect to the reaction plane) will connect with a ${}^3(\pi, \pi^*)$

of acetone via a surface touching which will occur near the transition state for the concerted cleavage of TMD.

Since the lowest excited states of acetone are n, π^* we must determine with which states of TMD they correlate. Experimentally, TMD is found to possess a weak absorption near 280 nm.[41] Evidently TMD possesses a singlet state (probably of the $\pi \rightarrow \sigma^*$ type) whose symmetry with respect to the reaction plane is antisymmetrical, i.e., this state will correlate directly to the n, π^* state of acetone. The appropriate correlations of the states of TMD and acetone are shown in the top portion of Figure 14.9.[46] Note that the correlation of the π, π^* state with the n, π^* states implies an *obligatory* surface crossing of both the S_1 and T_1 states with S_0. A weak avoiding of S_0 and S_1 is also expected.

The center of the surface diagram corresponds to the (forbidden) transition state for concerted cleavage. To the left of center, the O—O bond has lengthened and a diradical structure is expected to occur near the Zero Order surface crossings of S_1 and T_1 with S_0. This diradicaloid structure should resemble an alkoxy radical and as such should possess substantial spin-orbit coupling, thereby causing an *avoiding* of the S_0 and T_1 surfaces near the diradicaloid geometry. To the right of center, the carbon-carbon bond begins to break, the odd electrons originally localized on oxygen begin to delocalize into π and π^* orbitals, and the magnitude of the spin-orbit coupling decreases. In addition, the fragments are beginning to move rapidly apart. Thus, the Zero Order crossings of S_0 and T_1 and of S_0 and S_1 which occur to the right of center of the surface diagram probably exist in a First-Order analysis also.

If we now follow a representative point along the ground state surface, we see that it will climb in energy until it reaches the diradicaloid geometry. A "switch

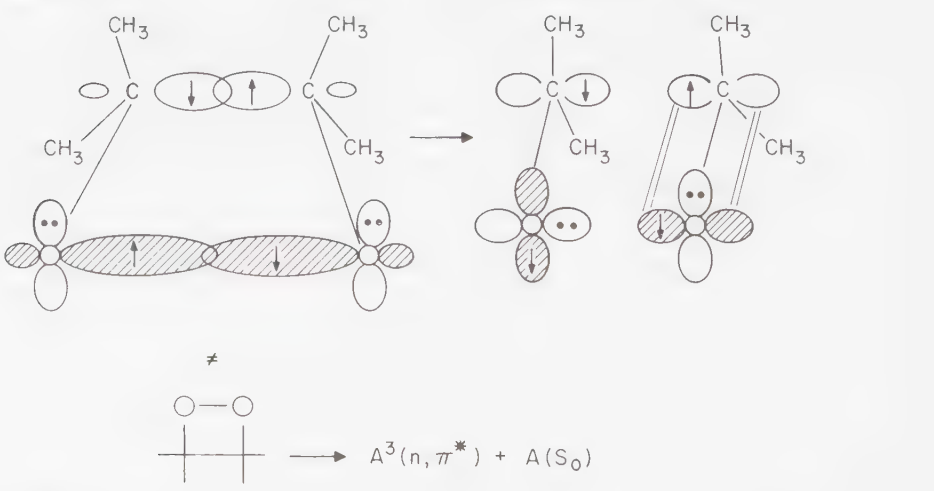

Figure 14.8

Orbital basis for the unusual preference of 1,2-dioxetanes to cleave to triplet fragments.

of states" corresponding to a spin flip or jump to the triplet surface occurs and the point starts down the triplet surface. The point proceeds past the crossing of the triplet and S_0 surfaces to $T_1(n, \pi^*)$, and produces acetone triplets.

In order to visualize in greater detail what is happening electronically when the representative point is near the diradicaloid structure, consider the lower portion of Figure 14.9 top, which shows schematically the diradicaloid structure, in which the O—O bond is severely stretched and the C—C bond is significantly weakened. Now contrast the electronic structure of this transition state (TS) with the electronic structure of the products, an acetone ground state molecule and a n, π^* state. We see that in going from $TS \rightarrow n, \pi^*$ state, electric charge must be moved

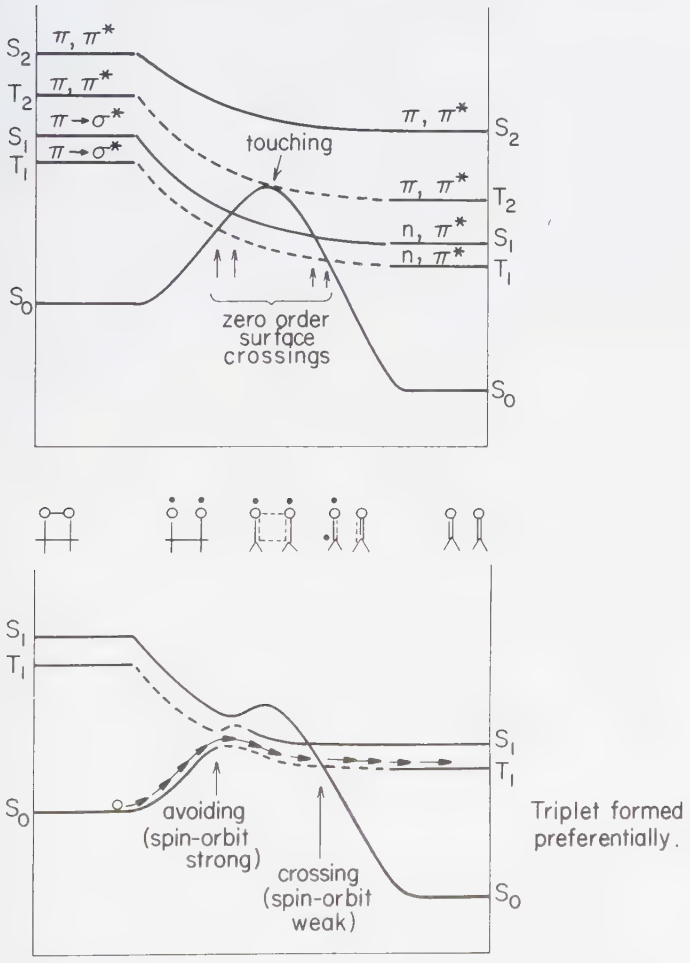

Figure 14.9

Top: Zero Order surface correlation of the decomposition of TMD into acetone.
Bottom: Working surface correlation for the decomposition of TMD into acetone.

from a region above and below the original molecular plane of the four-membered ring into a region *in* the original molecular plane (Figure 14.8). This movement of charge can be described in terms of an electronic transition from a p_x-orbital (perpendicular to the molecular plane) into a p_z-orbital (in the molecular plane). Furthermore, according to this picture, the "business end" of the major electronic change is localized on the left-hand oxygen atom. From the concepts discussed in Chapters 3 and 5 we expect that a $p_x \rightarrow p_z$ electronic transition would result in an enormous facilitation of the rate of spin flipping. Recall that the physical reason for this derives from the generation of a strong magnetic field and an electron jump from one orbital into another at right angles to the originally occupied orbital, i.e., when spin and orbital momentum can be coupled or exchanged, spin selection rules break down and spin flips become allowed. This coupling of electron spin momentum with electron angular momentum is the key mechanism for singlet $\rightleftarrows$ triplet process in organic molecules.

In order to appreciate the effect of spin-orbital coupling we need only review the $n_o \rightarrow \pi^*_{co}$ transition of ketones. This process is electronically analogous to the $p_x(\pi_o) \rightarrow p_z(\sigma^*_o)$ transition shown in Figure 14.8. The inherent probability of absorption or emission from an n, π^* triplet is about 10^3 times greater than that from a π, π^* triplet. In the latter case no $p_x \rightarrow p_z$ transition is possible.

Furthermore, since the $p_x \rightarrow p_z$ transition is more or less localized on the oxygen atom, it is understandable that energy is concentrated on the carbonyl group, since this is exactly what happens when a carbonyl function undergoes a $n \rightarrow \pi^*$ excitation or $\pi^* \rightarrow n$ relaxation. For example, from analysis of the n, π^* absorption and emission spectra of carbonyl compounds, it is concluded that electronic excitation is highly localized on the C O function. Interestingly, the C—O bond length, the dipole moment, the shape of the ring carbon, and energy content of TMD are more similar to those of $^*A$ than to A.

Thus, a model based on the ideas of molecular spectroscopy allows a rather interesting description and interpretation of the mechanism of thermolysis of TMD. This model combines the notion of the key electronic reorganization involved in the TMD $\rightarrow {}^*A + A$ process with spin-orbit coupling, which allows rationalization of the high yield of ^3A from TMD. This model also suggests significant coupling of the O –O bond breaking with the C C bond breaking. Thus, should certain choreographical sequences of the molecule (which are most effective in inducing spin-orbital coupling) be inhibited, we expect the reaction rate as well as the efficiency and selectivity of the chemiexcitation step, to be strongly affected.

Thermolysis of Dewar Benzenes

Dewar benzene (Eq. 14.4) undergoes a chemiluminescent electrocyclic rearrangement to benzene triplet. In contrast to TMD, this reaction possesses a very low chemiluminescence efficiency. What is the reason for the low efficiency of formation of T_1? Examination of a wide range of Dewar benzenes indicates that energy insufficiency is probably not it.[47] A clue to the mechanism is provided by the observation that chlorinated Dewar benzenes show *higher* chemiexcitation

efficiencies than the parent compound.[6] This result implies that a heavy-atom effect on intersystem crossing may be operating, and that the low efficiency of Eq. 14.4 is due to the very weak spin-orbit coupling inherent in hydrocarbon systems.

Consider Figure 14.10 which shows the archetype surface diagram for a forbidden pericyclic reaction, modified to accommodate the state diagram of the Dewar benzene → benzene system.[46] The representative point starts off on a "pure singlet" surface. Near the geometry of the transition state for the ground state electrocyclic ring opening, a "near" surface touching of the S_0 and T_1 surfaces is expected. The touching is only weakly avoided because it involves states of different spin multiplicity and because hydrocarbons possess no good mechanism to mix or split singlet and triplet states.

A qualitative argument shows why the molecule prefers to go "over the top" and then down to S_0 of benzene in preference to "sliding over" to T_1 of benzene. The time the representative point spends about r_c (the "critical nuclear geometry" that corresponds to the "touching") is on the order of the lifetime of a transition state, i.e., $\sim 10^{-12}$ sec. If we consider the time of intersystem crossing of benzene ($S_1 \rightarrow T_1$) as a rough guide to the time ($1/k_{si}$) it might take for intersystem crossing, a value of $\sim 10^{-7}$ sec is obtained. Thus, we see that only a small fraction of transition state structures near r_c (about 1 in 10^5) will undergo intersystem crossing to T_1, in agreement with the low experimental efficiency of Eq. 14.4.

Thermolyses of Endo-Peroxides: Concerted Spin-Allowed Pericyclic Fragmentation

The endo peroxides of naphthalenes[21] and anthracenes[7] generally undergo thermolysis to yield the parent aromatic compound and molecular oxygen. In

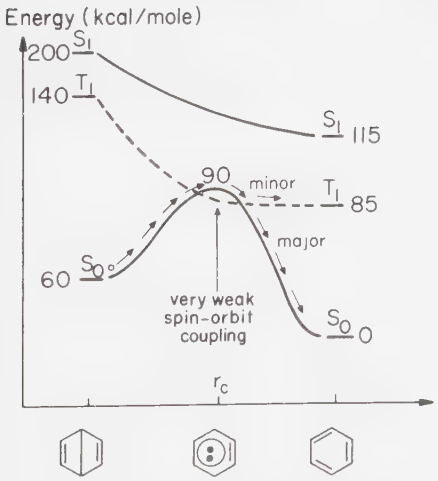

Figure 14.10
Schematic surface description of the Dewar benzene to benzene rearrangement.

most case studies, chemical trapping experiments and chemiluminescence experiments indicate that $^1O_2$ is a primary product of the thermolysis (Eq. 14.5):

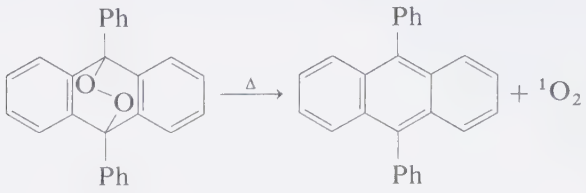

(14.52)

DAP

For example, heating 9,10-diphenylanthracene peroxide (DAP) in the presence of tetramethyl ethylene results in formation of an allylic hydroperoxide, the product expected from $^1O_2$.[7]

The heat of reaction of DAP → DPA + $O_2(^3\Sigma)$ may be estimated from the application of the principle of microscopic reversibility and the use of spectroscopic data and activation parameters. The reaction of $O_2(^1\Delta)$ and DPA possesses an activation energy of about 5 kcal mole. From the spectroscopic value of 23 kcal/mole for the $^3\Sigma \rightarrow {}^1\Delta$ transition energy we can locate the transition state for the DPA + $O_2(^1\Delta)$ reaction at 5 + 23 = 28 kcal mole above DPA + $O_2(^3\Sigma)$. The activation energy for DAP → DPA + $O_2(^1\Delta)$ is 33 kcal/mole. If the addition and fragmentation reactions are related by microscopic reversibility, they share a common transition state. Therefore, the energy of DAP (which is ~33 kcal mole below the transition state) must be 5 kcal mole lower than that of $O_2(^3\Sigma)$ + DPA (which is ~28 kcal mole below the common transition state). In effect the reaction DAP → DPA + $O_2(^3\Sigma)$ is essentially thermoneutral. However, most of the activation energy for decomposition of DAP is stored in the primary product $O_2(^1\Delta)$.

The question arises as to the reason for the contrast between the selective formation of triplets when simple dioxetanes are decomposed thermally and the selective formation of singlets when endo peroxides are decomposed thermally.

From a state correlation diagram based on the assumption of a plane of symmetry in the transition state, the lowest DPA + $O_2(^3\Sigma)$ state is found to attempt to correlate with an *excited* triplet state of DAP (see Fig. 14.11). In First Order, avoiding will occur and the correlation will ultimately be with a lower triplet state of DAP. The DPA + $O_2(^1\Delta)$ state, however, correlates directly to ground state DAP, i.e., the DPA + $O_2(^1\Delta) \rightleftarrows$ DAP interconversion is an electronically allowed reaction.

The correlation diagram for the addition of O_2 to 1,3-dienes provides the following qualitative information concerning the thermolysis of endo peroxides and addition of molecular oxygen to 1,3-dienes:

1. $O_2(^3\Sigma)$ is not expected to add to dienes because the interaction of this state with a ground state 1,3-diene correlates endothermically with a high energy triplet state of DAP.

2. The reaction does not proceed via a diradicaloid intermediate so that there is no structure which favors spin-orbit coupling along the assumed reaction coordinate (i.e., an Ar—O—Ȯ structure does not occur).

3. $O_2(^1\Delta)$ is expected (and found) to undergo [4 + 2] cycloaddition to 1,3-dienes with low activation energy, because a ground state diene and $O_2(^1\Delta)$ correlate directly to the endo peroxide product.

4. The thermolysis of endo peroxides requires substantial activation unless the heat of reaction for endo peroxide → 1,3-diene + $O_2(^3\Sigma)$ reaction is substantially exothermic (i.e., $\Delta H^{\ddagger} > 23$ kcal/mole), because $\Delta H^{\ddagger}$ mainly represents the energy needed to climb the energy surface to form $O_2(^1\Delta)$.

5. Because of the poor spin-orbit coupling along the reaction coordinates, there is little chance for intersystem crossing in either direction. Therefore, for the assumed reaction coordinate, both addition and chemiluminescent fragmentation are highly efficient (i.e., "quenching" to DPA + $O_2(^3\Sigma)$ is not important).

6. The addition-chemiluminescent fragmentation is a Diels-Alder analogue.

In the same way that 1,2-dioxetanes may be viewed as a "shelf-stable" form of the n, π^* states of carbonyl compounds, endo peroxides are a form of "stored" $O_2(^1\Delta)$. The excited state is released from its "masked" state by simple heating.

14.4 Applications of Chemiexcitation to Photochemical Problems

The ability to use chemical energy to generate electronically excited states provides a means of studying "photochemical" processes without the need of an initiating photon absorption. One can think of such systems as "photochemistry in the

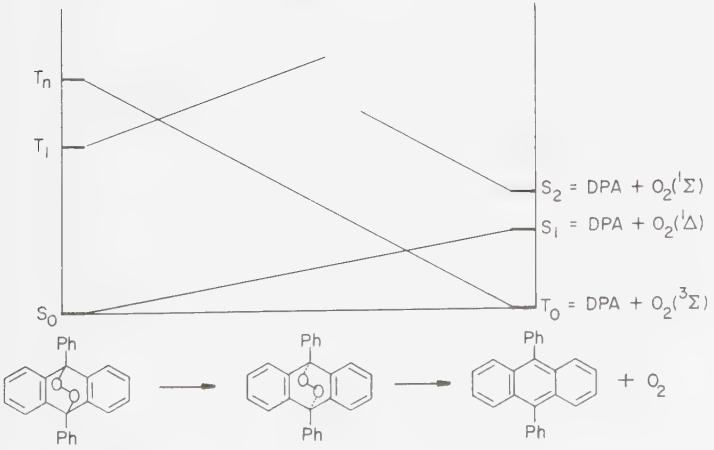

Figure 14.11
State correlation diagram for decomposition of an endo peroxide.

dark."[48] There are several important practical differences between photochemical processes initiated by light and those initiated by chemical energy release:

1. For systems excited by absorption of photons, the rate of generation of excited states depends on the extinction coefficient (ε) of various chromophores, and the selectivity (orbital, vibrational, and spin) of generation of excited states depends on the relative magnitudes of ε.

2. For systems excited by chemical reaction, the generation rate of excited states depends on the rate constants for the various steps leading up to the formation of the excited species, and the selectivity of generation of excited states depends on the bonds being made or broken during the chemiexcitation step.

3. In chemiexcitation processes, the law of energy conservation exerts a controlling influence over the "efficiency" of excited state production. Only *energy sufficient* processes have an a priori high probability of proceeding with high efficiency. In excitation by light, the law of conservation of energy is met by adjusting the photon's energy to match the energy gap required for an orbital jump.

The differing methods for producing excited states may result in differing selection rules for excited state formation. The selection rules for photon absorption are determined mainly by the interaction of the electric vector of a light wave with the higher-energy electrons of a molecule. The selection rules for chemiexcitation are determined by the surfaces traversed by the molecule as the nuclear geometry proceeds along the reaction coordinate, i.e., by the surface connection leading from the starting ground state to excited states of product. Furthermore, when a surface "jump" is required, the detailed pathway on the surface depends on the rate of movement of the nuclei through the array of nuclear configurations that correspond to the crossing region. Mixing mechanisms must be available to remove Zero Order crossings in this crucial region.

For example, in 1,2-dioxetanes there is good spin-orbit coupling in the region of the surface crossing of S_0 and the triplet surface which leads to the $^3(n, \pi^*)$ state of acetone. As a result, the selection rule for exciting a product state is that the spin-forbidden process is strongly favored.

In endo peroxides, there is no good intersystem crossing mechanism along the reaction coordinate. A singlet product is therefore obligatory.

A number of novel types of experiments can be performed by taking advantage of the special selection rules for chemiexcitation. Since chemiexcitation is insensitive to extinction coefficients, an electronically excited molecule may be produced under environmental conditions that would be impossible via photoexcitation, i.e., in a solution of a strong competitive absorber. "Photochemistry in the dark" may be utilized in a number of ways. Photoreactions may be initiated by direct formation of reactive excited states via chemiexcitation, or by indirect formation of reactive excited states via energy transfer from excited molecules produced by chemiexcitation.

For example, decomposition of 1,2-dioxetanes such as **3**, **5**, and **7** result in electronically excited carbonyl fragments, which then undergo their expected photochemical reactions:

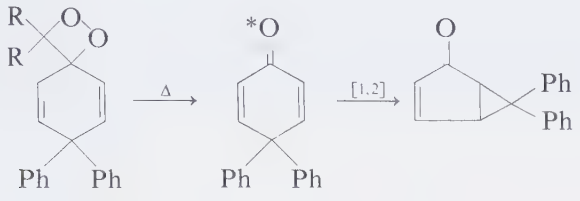

3 **4** (14.53)[49]

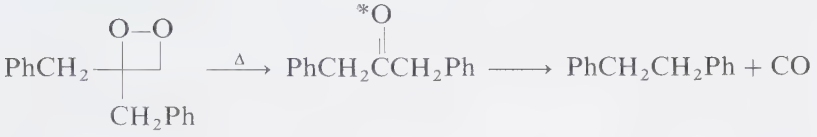

5 **6** (14.54)[50]

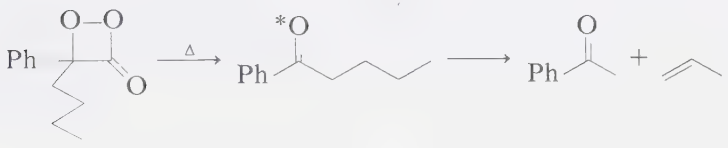

7 **8** (14.55)[51]

Chemiexciation of carbonyl groups has been employed to study energy transfer processes. Because triplets are produced with high selectivity and since the acceptor extinction coefficient is not pertinent to chemiexcitation, an ideal situation is set up for studying triplet-to-singlet energy transfer.

Utilization of Chemiluminescence to Study Organic Reaction Mechanisms

Because of the high sensitivity of devices that measure chemiluminescence, exceedingly low concentrations of chemiluminescent intermediates can be detected. This feature allows the detection of chemiluminescent reaction intermediates, even in cases in which conventional methods of analysis fail to detect their presence.

For example, the thermolysis of 3,3-dimethyl-bis-cyclopropenyl, **9**, to xylenes has been shown to involve a Dewar benzene. Detection of the latter was possible via its chemiluminescence characteristics:[52]

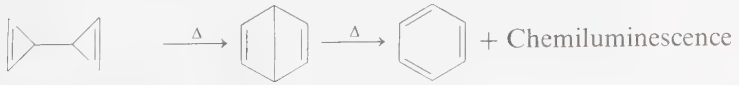

9 (3,3′-dimethyl) (14.56)

The thermal fragmentation of the polycyclic azo compound, **10**, also involves an initial loss of nitrogen to form Dewar benzenes. The latter are unstable under the reaction conditions and undergo chemiluminescent ring openings:[53]

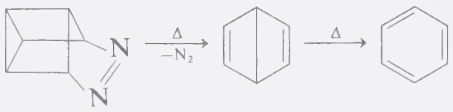

+ Chemiluminescence (14.57)

10

14.5 Adiabatic Photoreactions: Examples of Chemiluminescent Photoreactions

Most photoreactions do not produce primary products in an electronically excited state. The adiabatic passage of an electronically excited reactant R^* to an electronically excited product P^* is termed an *adiabatic* photoreaction (Fig. 14.12). Since P^* possesses the potential of light emission, such reactions can also be termed *chemiluminescent photoreactions*.[53] Such processes are well known. For instance, the formation and dissociation of excimers and exciplexes are examples of *reversible* adiabatic photoreactions:[54]

$$M^* + M \rightleftarrows M\overset{*}{-\!-\!-\!-}M \tag{14.58}$$

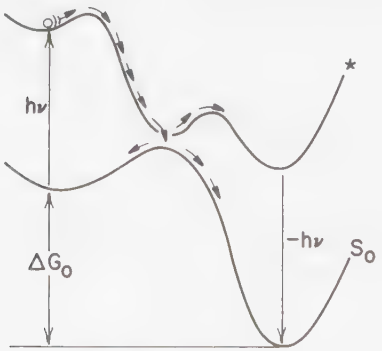

ADIABATIC PHOTOCHEMISTRY hν′ → * → hν
NON-ADIABATIC PHOTOCHEMISTRY hν → * → ΔG
CHEMILUMINESCENCE ΔG → * → hν

Figure 14.12
Schematic surface description of an adiabatic photoreaction.

The reversible loss and addition of protons to electronically excited bases is another commonly encountered adiabatic photoreaction:[54]

$$A—H^* \rightleftarrows {}^*A^- + H^+ \tag{14.59}$$

Less commonly encountered are examples of adiabatic photoreactions which involve substantial bond-making or nuclear reorganizations. Two classes of chemiluminescent photoreactions have been found to have a fairly general scope:

1. Photoinitiated electrocyclic ring openings.
2. Photoinitiated pericyclic fragmentations.

Both naphthvalene, **11**[55], and Dewar naphthalene, **12**[56], undergo adiabatic photo-ring opening to electronically excited naphthalene:

Photolysis of 1,2-dioxetanes results in the formation of electronically excited ketone products.[55] Triplet sensitization also effects the decomposition of 1,2-dioxetanes and formation of triplet ketone products.[57] From the surface diagram (see Fig. 14.9) for decomposition of 1,2-dioxetanes, these results may be interpreted as follows. Direct photoexcitation of dioxetanes causes rapid cleavage of the 0—0 bond. The molecule then proceeds along the excited surface to produce electronically excited products (Eq. 14.61). The high yields of electronically excited fragments may reflect a "dynamic" effect in which the nuclei are moving so fast that they are carried rapidly through the geometries at which surface crossings occur.

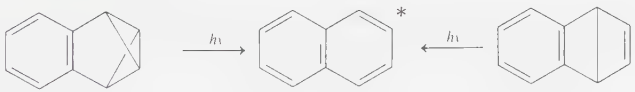

(14.60)

11 Nephthvalene **12**

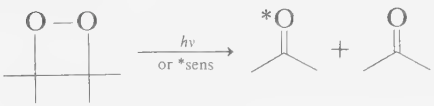

(14.61)

14.6 "Red Light to Blue Light" Experiments and "Uphill" Photosensitization

Direct photoexcitation or photosensitization of dioxetanes produces electronically excited ketone products.[55,57] In some respects, these two methods are related to *biphotonic* processes, since direct photoexcitation involves the collision of a dioxetane (a pseudo-excited state) with a photon, and photosensitization involves the collision of a dioxetane with an electronically excited molecule. A biphotonic process possesses an unusual energetic feature in that the total energy available in a biphotonic interaction can be considerably greater than that of an originally

absorbed photon. This means that absorbed *red* light can produce emitted *blue* light in the sense that electronically excited products emit "to the blue" of the energy of absorbed photons. This also means that "uphill" photosensitization is possible in the sense that a low-energy sensitizer may be capable of sensitizing the formation of a high-energy carbonyl fragment. Let S be a low-energy sensitizer and A be the carbonyl fragment produced by decomposition of a dioxetane, D. The following process represents the key steps in an "uphill" sensitization:

$$S + h\nu \rightarrow S^* \tag{14.62}$$

$$S^* + D \rightarrow S + A^* + A \tag{14.63}$$

If the triplet energy of S, $E_3(S) < 78$ kcal mole (the approximate energy of $^*A$), then Eq. 14.63 represents an uphill photosensitization, since more energy is available from ^3A than from the absorbed photon. What is the lowest energy of S^* which could effect eq. 14.63 efficiently? As long as $E_3(S)$ plus the reaction enthalpy and activation enthalpy is greater than $E_3(A)$, reaction 14.63 is exothermic i.e., in principle, it can proceed with negligible activation energy. Since the reaction enthalpy plus available thermal energy at room temperature is 70 kcal/mole for Eq. 14.63, we conclude that $E_3(S)$ can be as low as 10 kcal/mole and still efficiently effect the reaction. This is a rather remarkable possibility since 10 kcal/mole corresponds to light of wavelength equal to 2600 nm (3850 cm^{-1}) (i.e., infrared light). Since A^* emission occurs in the 400–450 nm region, this hypothetical process would correspond to an uphill photosensitization in which infrared light is transformed into blue light.

A rather convincing experimental verification of the notion of an uphill photosensitization is demonstrated by a thioketone ($E_3 = 40$ kcal/mole) photosensitized decomposition of valerophenone ($E_3 = 74$ kcal/mole) in the presence of tetramethyl-1,2-dioxetane (TMD).[58]

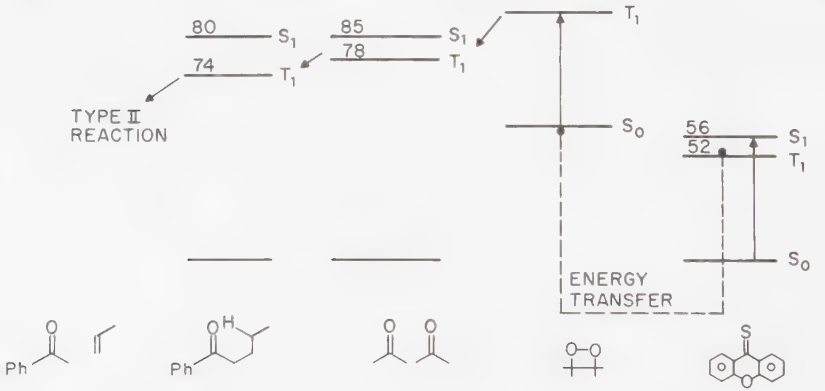

Figure 14.13

Energy diagram for "uphill" sensitization reaction assisted by tetramethyl-1,2-dioxetane.

Figure 14.13 will serve to guide our thinking in the microscopic interpretation of this unusual observation. Experimentally, one can selectively photoexcite a thioketone in the presence of a large excess of valerophenone. However, no sensitized decomposition of valerophenone is observed under these conditions because the energy transfer from thioketone (*I*) to valerophenone (*V*) is endothermic by nearly 20 kcal/mole, which is too large an amount of thermal energy to be picked up during the lifetime of the sensitizer. However, with TMD as a relay, photosensitization of valerophenone photochemistry is readily and efficiently achieved. Demonstration of this effect was possible by using Type II reaction of valerophenone as a probe for electronically excited molecules. This reaction is known to proceed exclusively via the valerophenone triplet, which possesses an energy content of about 74 kcal/mole in excess of its ground state. These results mean that an excited state of the thioketone has sensitized formation of excited acetone which in turn transfers its excitation to valerophenone which rapidly cleaves in a Type II process (Fig. 14.13).

Thus, a molecule of high energy content may be used as an excited state equivalent in a sensitization relay which eventuates in generation of an electronically excited state whose energy is well to the *blue* of an initially absorbed photon. In effect, we are dealing with a "two-quantum" process in which one of the quanta is masked in the chemical energy of the dioxetane. Acetone is an effective sensitizer in many photochemical and photobiological systems. It is of special interest to organic chemists and to biochemists since it can generate excited acetone molecules employing long-wavelength excitation and very mild conditions.

14.7 Interplay of Organic Photochemistry and Chemiluminescent Organic Reactions

The material discussed in this chapter shows how organic photochemistry and chemiluminescent organic reactions may be tied together conceptually via the use of energy surfaces. The theories of radiative and radiationless processes, of critical geometries for jumps between energy surfaces, electronic energy transfer, and spin-orbit coupling are of central importance for both photochemical and chemiluminescent reactions. Knowledge of one discipline can be profitably employed to understand and design experiments in the other discipline.

References

1. Reviews of chemiluminescent organic reactions:
   (a) Gundermann, K., *Topics in Current Chemistry*, *46*, 63 (1974);
   (b) McCapra, F., *Prog. Org. Chem.*, *8*, 231 (1971);
   (c) McCapra, F., *Pure Applied Chem.*, *24*, 611 (1970); White, E. H., et al., *Angew. Chem.*, *13*, 229 (1974).

2. Review of bioluminescence:
(a) Adam, W., *J. Chem. Ed.*, *52*, 138 (1975) and references therein;
(b) Hastings, J. W., *Ann. Rev. Biochem.*, *37*, 597 (1968).

3. White, E. H., and Roswell, D. F., *Acc. Chem. Res.*, *3*, 54 (1970).

4. Hopkins, T. A., Seliger, H. H., White, E. H., and Cass, M. W., *J. Am. Chem. Soc.*, *89*, 7148 (1967).

5. Weller, A., and Zachariasse, K., *Chem. Phys. Letters*, *10*, 590 (1971).

6. Lechtken, P., Breslow, R., Schmidt, A. H., and Turro, N. J., *J. Am. Chem. Soc.*, *95*, 3025 (1973).

7. Wasserman, H. H., Schaffer, J. R., and Cooper, J. L., *J. Am. Chem. Soc.*, *94*, 4991 (1972).

8. Turro, N. J., and Lechtken, P., *J. Am. Chem. Soc.*, *95*, 264 (1973); Kopecky, K. R., and Mumford, C., *Canad. J. Chem.*, *47*, 709 (1969).

9. Vassilev, R. F., *Prog. Reaction Kinetics*, *4*, 305 (1967); Wilson, T., and Hastings, J. W., *Photophysiology*, *5*, 49 (1970).

10. Bogan, D. J., Sheinson, R. S., Gann, R. G., and Williams, F. W., *J. Am. Chem. Soc.*, *97*, 2560 (1975).

11. Richardson, W. H., and O'Neil, H. E., *J. Am. Chem. Soc.*, *94*, 8665 (1972); *ibid.*, *92*, 6553 (1970); correction *ibid.*, *93*, 1828 (1971).

12. Salem, L., *Pure Appl. Chem.*, *33*, 317 (1973).

13. Reviews of singlet oxygen chemistry: Foote, C. S., *Acc. Chem. Research*, *1*, 104 (1968); Schaap, A. P., *Singlet Molecular Oxygen*, (a series of reprints with editorial comment), Strausburg: Dowden, Huchinson, and Ross, 1976.

14. Lanhoff, S. R., *J. Chem. Phys.*, 61, 1708 (1974); Merkel, P. B., and Kearns, D. R., *J. Am. Chem. Soc.*, *94*, 7244 (1972).

15. Wayne, J. P., *Adv. Photochem.*, *7*, 311 (1970); Kasha, M., and Khan, A. U., *Amm. N.Y. Acad. Sci.*, *171*, 5 (1970).

16. Badger, R. M., Wright, A. C., and Whitlock, R. F., *J. Chem. Phys.*, *43*, 4345 (1965).

17. Merkel, P. B., and Kearns, D. R., *J. Am. Chem. Soc.*, *94*, 1030, 7244 (1972).

18. Denney, R. W., and Nickon, A., *Org. React.*, *20*, 133 (1973).

19. Matheson, I. B. C., et al., *J. Am. Chem. Soc.*, *96*, 3343 (1974) and references therein.

20. Murray, R. W., and Kaplan, M. L., *J. Am. Chem. Soc.*, *91*, 5358 (1969); *ibid.*, *90*, 527 (1968).

21. Schafer-Ridder, M., Brocker, U., and Vogel, E., *Angew. Chem. Int. Ed. Eng.*, *15*, 228 (1976); Wasserman, H. H., and Larsen, D. L., *Chem. Comm.*, 253 (1972).

22. Birks, J. B., *Photophysics of Aromatic Molecules*, New York: John Wiley, 1970, p. 509.

23. (a) Kawaoka, K., Khan, A. U., and Kearns, D. R., *J. Chem. Phys.*, *46*, 1842 (1967);
(b) Gijzeman, O. L. J., Kaufman, F., and Porter, G., *Faraday Trans, II*, *69*, 708 (1973).

24. Brown, R. G., and Phillips, D., *Trans. Faraday Soc. II*, *70*, 630 (1974).

25. Parmenter, C. S., and Rau, N. D., *J. Chem. Phys.*, *41*, 2242 (1969).

26. Potashnik, R., Goldschmidt, D. R., and Ottolenghi, M., *Chem. Phys. Letters*, *9*, 424 (1971).

27. For an example of O_2 catalyzed $S_1 \rightarrow T_1$ conversions, see Turro, N. J., et al., *J. Am. Chem. Soc.*, *98*, 4320 (1976).

28. Ware, W. R., *J. Phys. Chem.*, *65*, 455 (1962).

29. Gollnick, K., *Adv. Photochem.*, *6*, 1 (1968); Review: Gollnick, K., and Schenck, G. O., in *1,4-Cycloaddition Reactions*, ed. Hamer, J., New York: Academic Press, 1967, p. 255.

30. Schenck, G. O., *Angew. Chem.*, *64*, 12 (1952).

31. (a) Bartlett, P. D., and Schaap, A. P., *J. Am. Chem. Soc.*, *92*, 3223 (1970).
(b) Wieringa, J. H., Staating, J., Wynberg, H., and Adam, W., *Tetrahedron Letters*, 169 (1972).

32. Schenck, G. O., and Dunlap, D. E., *Angew. Chem.*, *68*, 248 (1956).

33. Foote, C. S., et al., *Am. N.Y. Acad. Sci.*, *171*, 139 (1970): Foote, C. S., and Peters, J. W., *J. Am. Chem. Soc.*, *93*, 3795 (1971).

34. For a comprehensive review of quenching of singlet oxygen, see Shlyapintokh, V., and Ivanov, V. B., *Russ. Chem. Rev.*, *45*, 99 (1976).

35. Kearns, D. R., *Chem. Rev.*, *71*, 395 (1971); Dewar, M. J. S., Griffin, A. C., Thiel, W., and Turchi, I. J., *J. Am. Chem. Soc.*, *97*, 4439 (1975); Inagaki, S., and Fukui, K., *ibid.*, *97*, 7480 (1975).

36. Lee, D.C.-S., and Wilson, T., in *Chemiluminescence and Bioluminescence*, eds. Cormier, M. J., et al., New York: Plenum Press, 1973, p. 265; Kopecky, K. R., et al., *Can. J. Chem.*, *53*, 1104 (1975); White, E. H., et al., *J. Am. Chem. Soc.*, *95*, 7050 (1973); Adam, A., *Adv. Heterocyclic Chem.*, *21*, 437 (1977); Wilson, T., *International Review of Science, Physical Chemistry Series Two, Vol. 9*, London: Butterworth, 1976, p. 265.

37. Rigaudy, J., *Pure Applied Chem.*, *16*, 169 (1968).

38. Wilson, T., *Photochem. Photobio.*, *16*, 169 (1968) and references therein.

39. Vassilev, R. F., *Russ. Chem. Rev.*, *39*, 529 (1970).

40. Rauhut, M., *Acc. Chem. Research*, *2*, 80 (1969); Schuster, G. B., and Schmidt, S. P., *J. Am. Chem. Soc.*, *100*, 1966 (1978); *ibid.*, *99*, 6107 (1977).

41. Turro, N. J., et al., *Acc. Chem. Research*, *7*, 97 (1974); Turro, N. J., and Lechtken, P., *Pure Applied Chem.*, *33*, 363 (1973).

42. Lechtken, P., and Hohne, G., *Angew. Chem. Int. Ed. Eng.*, *12*, 772 (1972).

43. Turro, N. J., and Lechtken, P., *J. Am. Chem. Soc.*, *94*, 2886 (1972).

44. Turro, N. J., Steinmetzer, H. C., and Yekta, A., *J. Am. Chem. Soc.*, *95*, 6468 (1973).

45. Turro, N. J., et al., *J. Am. Chem. Soc.*, *96*, 1627 (1974).

46. Turro, N. J., and Devaquet, A., *J. Am. Chem., Soc.*, *97*, 3859 (1975).

47. Turro, N. J., et al., *J. Am. Chem. Soc.*, *96*, 6797 (1974).

48. White, E. H., Wildes, P. D., Weicko, J., Doshan, H., and Wei, C. C., *J. Am. Chem. Soc.*, *95*, 7050 (1973).

49. Zimmerman, H. E., Keck, G. E., and Pflederer, J. L., *J. Am. Chem. Soc.*, *98*, 5574 (1976).

50. Darling, T. R., and Foote, C. S., *J. Am. Chem. Soc.*, *96*, 1625 (1974).

51. Ito, Y., Chow, M. F., and Turro, N. J., unpublished results.

52. Turro, N. J., Schuster, G. B., Bergman, R. G., Shea, K. J., and Davis, J. H., *J. Am. Chem. Soc.*, *97*, 4758 (1975).

52. Turro, N. J., Renner, C. A., Waddell, W. H., and Katz, T. J., *ibid.*, *98*, 4320 (1976).

54. Forster, T., *Pure Appl. Chem.*, *24*, 443 (1970).

55. Forster, T., *Angew. Chem. Inter. Ed. Eng.*, *8*, 333 (1969).

56. Turro, N. J., Lyons, A., Hautala, R. R., Carnahan, E., and Katz, T. J., *J. Am. Chem. Soc.*, *95*, 2035 (1973).

57. Carr, R. V., Kim, B., McVey, J., Yang, N. C., Gerhartz, W., and Michl, J., *Chem. Phys. Letters*, *39*, 57 (1976).

58. Turro, N. J., et al., *J. Am. Chem. Soc.*, *96*, 1936 (1974).

59. Turro, N. J., and Lechtken, P., *Tetrahedron Letters*, 565 (1973); Turro, N. J., Brewer, D., Farneth, W., and Ramamurthy, V., *Nouv. J. Chim.*, *2*, 85 (1978).

Epilogue

It is hoped that this text will meet its goal of providing a unifying intellectual basis for understanding the processes involved in the photochemistry of organic molecules. The author has attempted to break down systems to be analyzed into their components (the qualitative kinds of structures), their compositions (the number of each kind of structure), their constitution (the connections between structures), and their configurations (the "shape" of a structure). The idea of molecular structure and energy surfaces provides a very general and powerful means of tracking a molecule during reactions, monitoring the reaction energetics, and revealing reaction pathways and critical geometries for surface jumps. The dynamics of photochemical processes can be understood by further decomposing molecular structure into its electronic, vibrational, and spin components. The latter serve as a basis to generate molecular states, to evaluate orbital interactions, and to construct state diagrams. Molecular dynamics or the time dependence of interchange of molecular structure can be readily visualized in terms of state diagrams which are used to examine prototype photochemical reactions from n, π^* and π, π^* states. The very useful notion of Z and D intermediates provides a broad and powerful basis for analyzing photochemical reactions of organic molecules. The number and kinds of fundamentally different photoreactions are few and readily interrelated.

The text was written with the intention of putting forth very broad and general principles of chemistry and scientific thinking and reinforcing these principles with numerous examples and useful tabulations of data. These general principles, which are termed topological ideas, provide a qualitative framework which reveals all of the important connectivity relationships between the components of the system under study. It is hoped that the student was able to absorb the broader aspects of the material in addition to the more factual material.

In conclusion, it has been my goal to make an impact on the teaching of organic photochemistry by giving students a stimulating, coherent view of molecular processes in terms of readily visualizable structural, energetic, and dynamic concepts. The following quotation (made in response to the proposal that it is unimportant and/or impossible to provide an intuitive or pictorial context for the basic concepts of quantum mechanics) epitomizes my attitude and attempts to interpret molecular photochemistry in a manner that is both exciting and concrete:

> "I am certain that the human mind would not be fully satisfied with a universe in which all phenomena were governed by mathematical processes that are perfectly coherent but completely abstract and impossible to visualize. Are we not then in a wonderland? When deprived of all possibility of intellectualization—that is, of interpreting geometrically a given process—the human brain will seek to create, even in the face of conspicuous deficiencies, through appropriate interpretation, an intuitive rationalization of the process. The alternative is submergence into a resigned incomprehension, which repetition will transform to apathetic acceptance."

The author invites comments and criticism from readers as to the effectiveness of the approach espoused in the text.

Index

MODERN MOLECULAR PHOTOCHEMISTRY

by Nicholas J. Turro

"This book is so thorough in its coverage of organic molecular photochemistry, both in basic theory and in detailed examples useful for all kinds of photochemistry, that it can be used as a basic textbook in an introductory course for undergraduate and graduate students."

—Melvin Calvin, University of California, Berkeley
from a review in *American Scientist*

ALSO AVAILABLE FROM UNIVERSITY SCIENCE BOOKS

INTERPRETING SPECTRA OF ORGANIC MOLECULES
by Thomas N. Sorrell. 175 pages, 7″ x 9″, paperback,
$22.50 U.S. (ISBN 0-935702-59-8)

"Succeeds very well . . . an exemplary job of showing how to integrate information from different spectroscopic techniques."

—*Nature*, March 1989

REACTIONS AND SYNTHESES IN THE ORGANIC CHEMISTRY LABORATORY
by L. F. Tietze and T. Eicher. 593 pages, 8½″ x 11″, paperback,
$56.00 U.S. (ISBN 0-935702-50-4)

"This excellent book will become an essential presence in all organic chemistry laboratories. Its only real competitor is Vogel."

—*The Times Higher Education Supplement*, April 28, 1989

ONE-DIMENSIONAL AND TWO-DIMENSIONAL NMR SPECTRA BY MODERN PULSE TECHNIQUES
Koji Nakanishi, editor. 234 pages, 7¼″ x 10¼″, paperback,
$38.50 U.S. (ISBN 0-935702-63-6)

"Very useful and unique. The only available source of clear cut examples of modern pulse techniques."

Universit
20 Edgeh
Mill Valley
Fax: (415)